

2013

## Depositional history of the Trinity-Tiger Shoals region : a transgressed delta complex of the middle Holocene Mississippi Delta

Clint Hoyt Edrington  
*Louisiana State University and Agricultural and Mechanical College*

Follow this and additional works at: [https://digitalcommons.lsu.edu/gradschool\\_dissertations](https://digitalcommons.lsu.edu/gradschool_dissertations)



Part of the [Oceanography and Atmospheric Sciences and Meteorology Commons](#)

---

### Recommended Citation

Edrington, Clint Hoyt, "Depositional history of the Trinity-Tiger Shoals region : a transgressed delta complex of the middle Holocene Mississippi Delta" (2013). *LSU Doctoral Dissertations*. 2213.  
[https://digitalcommons.lsu.edu/gradschool\\_dissertations/2213](https://digitalcommons.lsu.edu/gradschool_dissertations/2213)

This Dissertation is brought to you for free and open access by the Graduate School at LSU Digital Commons. It has been accepted for inclusion in LSU Doctoral Dissertations by an authorized graduate school editor of LSU Digital Commons. For more information, please contact [gradetd@lsu.edu](mailto:gradetd@lsu.edu).



DEPOSITIONAL HISTORY OF THE TRINITY-TIGER SHOALS REGION:  
A TRANSGRESSED DELTA COMPLEX OF THE MIDDLE HOLOCENE  
MISSISSIPPI DELTA

A Dissertation

Submitted to the Graduate Faculty of the  
Louisiana State University and  
Agricultural and Mechanical College  
in partial fulfillment of the  
requirements for the degree of  
Doctor of Philosophy

in

The Department of Oceanography and Coastal Sciences

by

Clint H Edrington

B.S., University of New Orleans, 2005

M.S., Louisiana State University, 2008

May 2013

To Mom and Dad, for believing in me through all these years.

## **ACKNOWLEDGMENTS**

I want to thank my major adviser, Dr. Harry Roberts, for his example, guidance, and friendship. I learned a great deal about sedimentology under Harry's mentorship, from the study area of this research to the Wax Lake Delta. Since the beginning, I recognized my good fortune in having the opportunity of working with Harry, and it has truly been a great experience. For their efforts and contributions, I would also like to thank the remainder of my committee, including Drs. Mike Blum, Alan Brown, James Coleman, Kanchan Maiti, Jeff Nunn (Minor Chair), and Ron Malone (Dean's Representative).

This research was funded through the Minerals Management Service (now BOEM) and the Louisiana Department of Natural Resources. Mr. Syed Khalil (LA DNR) played an instrumental role in securing funding for this research, and his efforts are greatly appreciated. Additional project funding was provided through student research grants; granting organizations and corporations include the American Association of Petroleum Geologists, Gulf Coast Association of Geological Societies, Geological Society of America, and ExxonMobil. The Department of Oceanography and Coastal Sciences also provided me with teaching assistantships during part of my study; these opportunities are greatly appreciated.

A special thanks goes to the Coastal Studies Field Support Group, including Chris Cleaver, Floyd De Mers, Darren Depew, Charlie Sibley, Eddie Weeks, and Walker Winas. Data collection, and thus this dissertation, could not have happened without their professional assistance. Furthermore, I express my sincere appreciation to Floyd De Mers for his exceptional assistance in the lab, which was only matched by his unselfishness.

Many other individuals from LSU also generously aided this research. I am grateful to Dr. Sophie Warny, who provided materials and (most importantly!) foram-picking undergraduate

students looking for research experience. Undergraduate students who helped pick forams include Jessee Landreneau, Jessica Martinez, and Chris Murley; their individual efforts are appreciated. I am also grateful to Dr. Barun Sen Gupta, Lorene Smith, and Dr. Barry Kohl (Tulane) for providing materials and guidance for picking forams. Dr. Juan Lorenzo allowed access to the subsurface lab (Department of Geology and Geophysics), which was very helpful in manipulating the geophysical data.

The Weeks family is greatly appreciated for providing our research group their camp in Cypremort Point, Louisiana. Their camp greatly simplified the logistics of our field operations.

Drs. Mark Kulp (UNO) and Mead Allison (Tulane) provided additional data. Although the data they provided were not used in this dissertation, these data did provide insight.

Finally, and most certainly not least, I thank my family and friends for providing encouragement, support, and inspiration throughout my study, and an outlet when I needed to break away from it.

## TABLE OF CONTENTS

ACKNOWLEDGMENTS .....	iii
ABSTRACT.....	vii
INTRODUCTION .....	1
Opposing Views.....	4
Research Objectives.....	9
Study Area .....	13
BACKGROUND .....	14
Setting .....	14
Holocene Geologic Framework: The Delta Cycle.....	20
Depositional Environments and Facies Associations of the Mississippi Delta .....	32
Acoustic Data and Its Analysis .....	49
Previous Work .....	55
METHODOLOGY .....	59
R/V Coastal Profiler.....	59
Navigation.....	59
Geophysical Surveying .....	60
Vibracoring .....	60
GEOTEK Multi-Sensor Core Logger .....	63
Imaging .....	64
Sand-Mud Ratios/Grain-Size Analysis of the Sand Fraction .....	65
Graphic Logging .....	66
X-Ray Radiography .....	70
AMS Radiocarbon Dating.....	72
Acoustic Data Manipulation .....	74
Data Analysis, Integration, and Interpretation .....	75
RESULTS .....	77
Acoustic Facies .....	77
Lithofacies.....	89
DISCUSSION .....	114
The Regressive Component .....	114
The Transgressive Component .....	133
The Atchafalaya Regressive Component.....	158
Framework within the Sequence-Stratigraphic Model .....	159
The Prevailing Model Contrasted with this Study: Incompatible Differences .....	161
CONCLUSION.....	168
Suggested Areas for Further Research.....	173

REFERENCES CITED.....	178
APPENDIX 1: CROSS SECTIONS .....	193
APPENDIX 2: GRAPHIC LOGS.....	253
APPENDIX 3: CORE IMAGES.....	313
APPENDIX 4: X-RAY RADIOGRAPHS.....	373
APPENDIX 5: CROSS SECTIONS OF THE REGRESSIVE COMPONENT .....	394
APPENDIX 6: AMS RADIOCARBON DATES.....	402
APPENDIX 7: GRAIN SIZE ANALYSES OF THE SAND FRACTION.....	404
VITA.....	886

## ABSTRACT

The Holocene Mississippi River Delta is arguably the world's most thoroughly researched deltaic system. However, much of this research has occurred predominantly within the present-day subaerial delta, whereas comparatively little research has been attempted down-dip within the offshore, more difficult-to-reach parts. This study advances our understanding of the Holocene delta by examining deltaic sediments within the Trinity-Tiger Shoals Complex region, located ~ 30 – 40 km offshore of central Louisiana. Specifically, this study addresses two questions. Which delta complex prograded into this offshore region? Do the overlying transgressive deposits reflect that predicted by the prevailing transgressive depositional systems model? To answer these questions, this study uses an integrated data set consisting of ~ 1,350 km of high-resolution subbottom sonar profiles and various sedimentological data gleaned from 60 vibracores, including 22 AMS radiocarbon dates.

Results from this study depict an intricate stacking arrangement of 12 distinct depositional units. Near the base of the stratigraphic framework above antecedent topography are the remnants of a middle Holocene Mississippi Delta complex. Prodelta and delta-front facies along with the partially-preserved southwest trending distributary system that fed these depositional environments are recognized. Furthermore, analysis of the regressive component reveals an offsetting, overlapping, and stacked arrangement of four delta lobes and one subdelta. Five AMS radiocarbon dates (~ 4,820 yr BP to 5,980 yr BP) measured from these regressive sediments confirm a Maringouin Delta Complex origin.

A ~ 4,000 yr hiatus ensued following the abandonment of the Maringouin Delta Complex, as indicated by 17 AMS radiocarbon dates measured from the overlying transgressive component. During this hiatus, erosional shoreface retreat produced a prominent ravinement

surface along the entire top boundary of the Maringouin Delta. It was not until ~ 1,000 yr BP that significant amounts of sediments began migrating into the study area from the east, which have remained, at least for the time being, mostly preserved. Among these recent post-Maringouin depositional units are a detached down-drift subaqueous delta related to the Lafourche Delta Complex as well as the most-recent sandy deposits of Trinity Shoal and an unnamed shoal. This new understanding of post-Maringouin deposition is considered incompatible with the prevailing transgressive depositional systems model, particularly stage 3 of that model.



## INTRODUCTION

The depositional history of the Holocene Mississippi River Delta is written in its preserved stratigraphic record. However, our realization of its history is hindered by formidable logistics in accessing that record, particularly for the early stages of Holocene delta development. For instance, the Maringouin and Teche Delta Complexes, the two oldest delta complexes recognized within the Mississippi Delta (Fig. 1), formed during the early-to-middle Holocene when a still-rising sea level was ~ 6 – 3 meters below present-day level (Törnqvist et al., 2006; Milliken et al., 2008). Each was later abandoned and subsequently inundated as sea level continued to rise into the late Holocene. Consequently, a succession of deltas now resides offshore along Louisiana's inner-continental shelf (Coleman, 1988; Roberts, 1997). As one can imagine, conducting research within the marine environment is fraught with challenges. For that reason, research on the offshore portions of the Maringouin and Teche Delta Complexes has been restricted in comparison with research conducted on the Mississippi Delta's more conveniently accessible, subaerial counterpart. Nevertheless, if the appropriate technology is employed, such as used during this research, one can perhaps more thoroughly demonstrate the stratigraphic record of the offshore portion of the Mississippi Delta.

Despite inherent challenges, the Holocene Mississippi Delta remains arguably the world's most studied deltaic system. However, there are some glaring discrepancies in our understanding of its geochronology, particularly for those offshore delta complexes mentioned above. For instance, there is consensus within the literature that large sand shoals along Louisiana's inner-continental shelf represent the transgressed shoreline expression of early-to-middle Holocene delta complexes that long ago submerged following abandonment. The Trinity-Tiger Shoals Complex, positioned offshore of west-central Louisiana, is thought to be

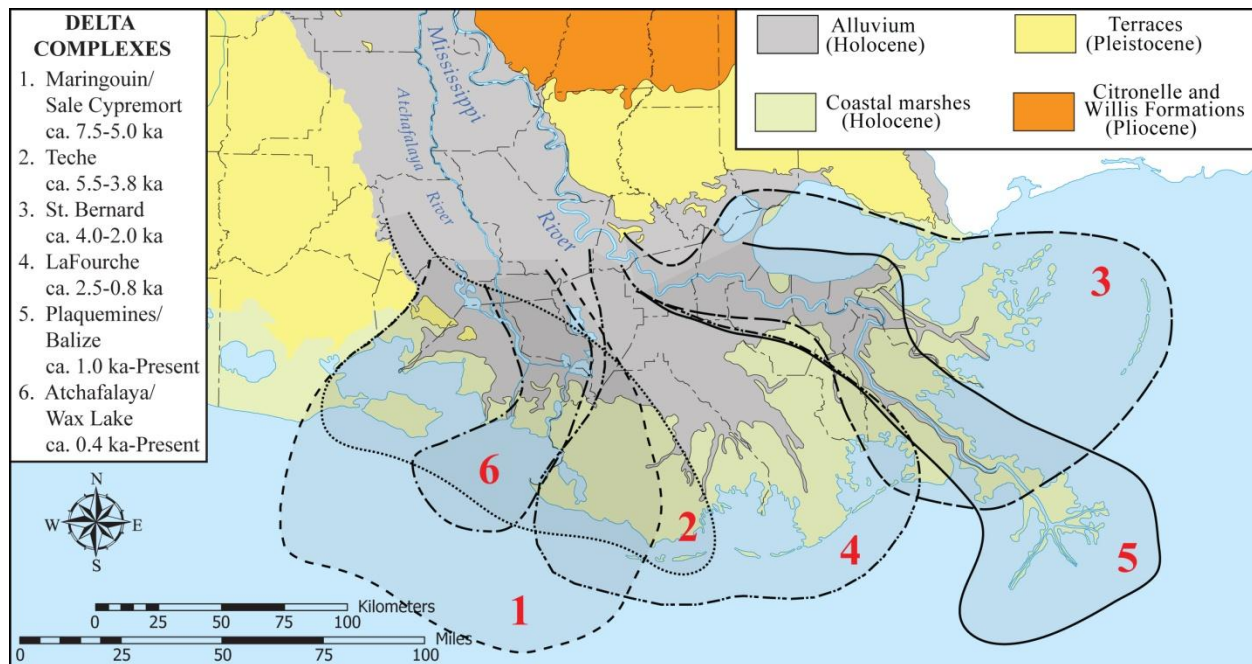


Figure 1. The Holocene Mississippi Delta Plain as it is observed today. Also outlined are the six major delta complexes that comprise it. The geochronologic order of the delta complexes is in the upper left. After Frazier (1967) and Roberts (1997). Base map is from [www.lgs.lsu.edu](http://www.lgs.lsu.edu).

one such set of marine sand lithosomes (Fig. 2). There is discrepancy within the literature, however, as to which delta complex Trinity Shoal represents. (Besides acknowledging its existence, note that the literature essentially ignores Tiger Shoal, and so for the moment Tiger Shoal is ignored. The evolution of Tiger Shoal will be discussed later in this dissertation.) One view argues that Trinity Shoal is the transgressed shoreline expression of the Maringouin Delta Complex based on Trinity Shoal's geographic position and their interpretation of its correlation to a stillstand in an overall rising relative sea level. An opposing view contends a Teche origin based on Trinity Shoal's sedimentology and their conflicting interpretation of its correlation to a later stillstand. Neither argument, however, is based on radiocarbon dating or chronostratigraphic correlations.

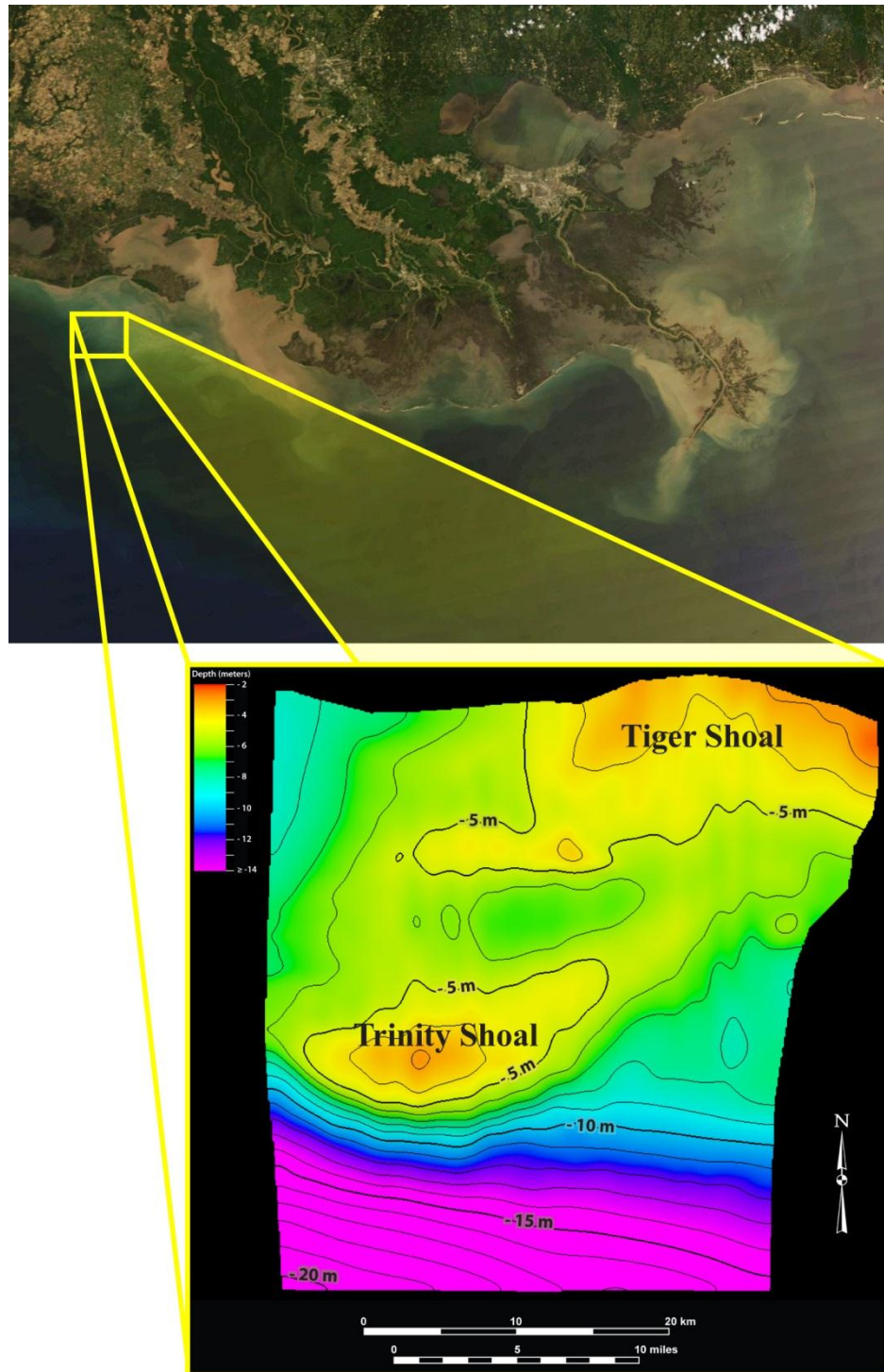


Figure 2. The relative position of the Trinity-Tiger Shoals Complex area in relation to the modern Mississippi Delta Plain, as indicated by the yellow box. Inset is a bathymetric map of the study area. MODIS (Moderate Resolution Imaging Spectroradiometer) Satellite image of the Mississippi Delta Plain was taken from the Louisiana State University Earth Scan Laboratory ([www.esl.lsu.edu](http://www.esl.lsu.edu)).

## **Opposing Views**

Early research (Van Lopik, 1955; Frazier, 1967; 1974) associated Trinity Shoal with the Maringouin Delta Complex based on its geographic position: Trinity Shoal lies ~ 40 km offshore of west-central Louisiana at the seaward terminus of what is believed to be the Maringouin Delta Complex. Hence, Trinity Shoal is thought to partially represent the relict shoreline of the Maringouin Delta. Yet linking this proposed Trinity Shoal-Maringouin Delta Complex system to a Maringouin-Mississippi River system up-dip within the mainland is not absolute. Intuition would suggest that perhaps Bayou Sale' and/or Bayou Cypremort gave rise to the Maringouin Delta (Fig. 3). Although both were responsible for prograding separate delta lobes within the western region of the Holocene Mississippi Delta, both are also known to have been major distributaries of the Teche-Mississippi River system (delta lobes 2 and 4, respectively, of the Frazier (1967) geochronologic model). Furthermore, as Van Lopik (1955) describes, the subaerial levees of these distributaries are much smaller than levees of former Mississippi River courses, as they exhibit narrow, steeply sloping profiles. Such steep profiles reflect a distributary's attempt to maintain comparable levee height with the larger, broader levees of the main stream (Van Lopik, 1955). Thus, Van Lopik (1955) contends that these distributaries of the Teche-Mississippi River could not have been responsible for constructing the large offshore delta complex believed to be represented by Trinity Shoal.

Van Lopik (1955), however, presents some geomorphic evidence suggesting much broader levee ridges occur within the Bayou Sale' region. (Note that this evidence is mostly buried). In fact, two broad-levee distributaries are thought to diverge from a similar broad-levee channel beneath the present-day Bayou Sale', implying that the steep, narrow subaerial levees of Bayou Sale' overlie older, much broader levee deposits. Van Lopik (1955) shows similar



Figure 3. Locations of Bayou Sale' and Bayou Cypremort. Yellow box indicates the region of the Trinity-Tiger Shoals Complex. MODIS (Moderate Resolution Imaging Spectroradiometer) Satellite image of the Mississippi Delta Plain was taken from the Louisiana State University Earth Scan Laboratory ([www.esl.lsu.edu](http://www.esl.lsu.edu)).

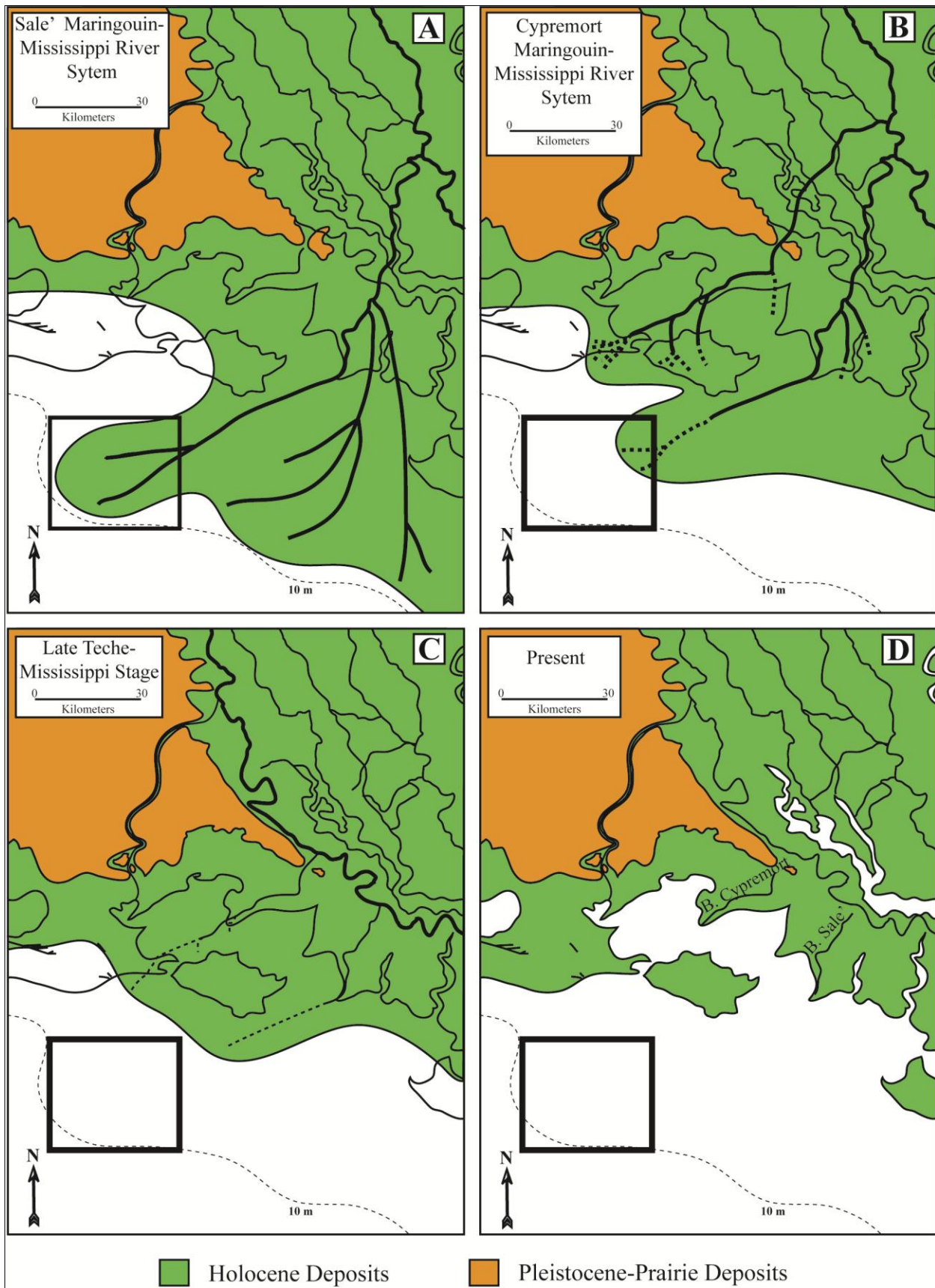
geomorphic evidence indicating this earlier Sale' system continues (although bisected) north of the present-day Bayou Teche ridge. Cultural evidence (i.e. Native American artifacts) indicates that these older, broader levees were inhabited by pre-Tchefuncte cultures. (Note that the Tchefuncte culture is associated with the Teche Delta Complex.) Because associated levees are large, Van Lopik (1955) contends that the Sale' system of the pre-Teche-Mississippi River was much more significant than the Bayou Sale' distributary of the Teche-Mississippi River. Because associated levees appear old (based on their cross-cutting relationship with the Teche-Mississippi River and cultural evidence), Van Lopik (1955) contends that the Sale' of the pre-Tech-Mississippi River was a primary channel of the Maringouin-Mississippi River system. Thus, Van Lopik (1955) argues that this Sale' Maringouin-Mississippi River system had to have been responsible for building the extensive delta complex that now resides offshore of west-central Louisiana. His interpretations are presented in Figure 4. A similar Maringouin-Mississippi River scenario was demonstrated to have occurred for the Cypremort system

following the Sale', but on a much smaller scale. Hence, the Cypremort of the Maringouin-Mississippi River system is not thought to have prograded a delta lobe as far basinward as did the Sale' of the Maringouin-Mississippi River system. Van Lopik (1955) also contends that the older, larger Sale' and Cypremort levee systems were later breached and reoccupied as distributaries by, first, the combined Red-Arkansas River followed later by the Teche-Mississippi River after it diverted into the Red-Arkansas River's course.

Researchers (Frazier, 1967; 1974; Suter et al., 1987) have also emphasized the coupling and timing of the Trinity-Shoal paleo-shoreline to a temporary stillstand within the northern Gulf of Mexico's overall rising Holocene relative sea-level trend. Hence, their premise implies an episodic, or stair-stepping, rise in Holocene relative sea level. Frazier (1974) placed Trinity Shoal at the ~ 16 m isobath, which he argues correlates to a stillstand that occurred between 10,000 to 7,500 yr BP. In other words, his relative sea-level curve estimates that sea level along the northern Gulf of Mexico was ~ 16 m below present-day level between 10,000 to 7,500 yr BP. Because this time interval corresponds more closely with the Maringouin Delta Complex, Frazier (1967; 1974) proposed that the Maringouin Delta Complex prograded consequent to this stillstand. As sea-level rise resumed, the Maringouin Delta was eventually inundated, leaving behind the reworked, transgressive shoreline supposedly reflected by the position and shape of Trinity Shoal.

Figure 4. A) The Sale' of the Maringouin-Mississippi River system, which Van Lopik (1955) contends is responsible for the extensive offshore deltaic deposits as depicted here. B) The Cypremort of the Maringouin-Mississippi River system occurred after the Sale' but on a smaller scale. C) The Teche-Mississippi River system, with its active Sale' and Cypremort distributaries depicted. D) The present-day Bayou Sale' and Bayou Cypremort. Note that the black square encloses the region of the Trinity-Tiger Shoals Complex. Modified from Van Lopik (1955).





Penland et al. (1989) similarly followed the logic of Frazier (1974). However, they appropriately placed the base of Trinity Shoal near the ~ 10 m isobath, a position that instead correlates to a temporary stillstand which they argue occurred between 6,000 to 4,000 yr BP. In contrast with previous research, Penland et al. (1989) contend Trinity Shoal is the transgressed shoreline expression of the Sale'-Cypremort Delta Complex, which they maintain constructed during this stillstand. Penland et al. (1989) did not explicitly state whether they intended the Maringouin Delta Complex or the Teche Delta Complex when they inferred the Sale'-Cypremort Delta Complex, although the names Sale'-Cypremort and Maringouin have been used interchangeably by others in the past (Coleman, 1966; 1988; Roberts, 1997). However, recognize that Penland et al. (1989) correlated Trinity Shoal to a flooding event that occurred ~ 4,000 yr BP, a time which marks the onset of transgression for the Teche Delta Complex (Fig. 1). Furthermore, Penland et al. (1989) associate Trinity Shoal with the late Holocene Mississippi Delta Plain, a term that Penland et al. (1987) used to distinguish the combined Maringouin-Teche Delta Complexes. (Note that Penland et al., (1987) separate the Holocene Mississippi Delta Plain, as originally described by Fisk (1944), Frazier (1967), among many others, into two separate delta plains: 1) the late Holocene Mississippi Delta Plain, which includes the Maringouin and Teche Delta Complexes, and 2) the modern Mississippi Delta Plain, which includes all post-Teche delta complexes.) Likewise, Penland et al. (1990) and Pope et al. (1991) associate Trinity Shoal with Penland et al.'s (1987) late Holocene Mississippi Delta Plain, but they clearly assert that Trinity Shoal is a transgressive remnant of the Teche Delta Complex.

An additional form of reasoning based on sedimentology lends support to the hypothesis that Trinity Shoal is the transgressed shoreline expression of the Teche Delta Complex, not the Maringouin. As with Trinity Shoal, Penland et al. (1989) associate Ship Shoal with their so-



called late Holocene Mississippi Delta Plain. (Note that Ship Shoal is a separate sand shoal of similar dimensions as Trinity Shoal, approximately 120 km to the east of Trinity Shoal, and likewise positioned along the 10 m isobath.) Hence, both Trinity Shoal and Ship Shoal are a part of their combined Maringouin-Teche Delta Plain. Ship Shoal is thought to be a completely reworked marine sand body (i.e. no preserved barrier-island facies; Penland et al., 1986; 1989), whereas Trinity Shoal, in contrast, is thought to retain much of its original barrier-island core (Penland et al., 1989; 1990; Pope et al., 1991). Working under the presumption that the older a shoal is the longer it has been exposed to marine-reworking processes, researchers (Penland et al., 1985; 1988) judge Ship Shoal to be considerably older than Trinity Shoal. Thus, they correlate the completely reworked Ship Shoal with the older Maringouin Delta Complex, whereas they correlate the relatively well-preserved Trinity Shoal with the more recent Teche Delta Complex.

Note that similar discrepancies are found with regard to Ship Shoal as well. In addition to those researchers mentioned above, Frazier (1967; 1974) also links Ship Shoal to the Maringouin Delta Complex. Penland et al. (1987), however, associate Ship Shoal with the Teche Delta Complex, as they find no stratigraphic evidence for the existence of the Maringouin Delta Complex within the surrounding region of Ship Shoal. Clearly, there is confusion within the literature for not only which delta complex Trinity Shoal represents, but also with regard to the depositional history of the early-to-middle Holocene Mississippi Delta as a whole.

## **Research Objectives**

The Mississippi Delta is without question one of the world's best studied deltaic systems. However, as the preceding discussion reveals, our understanding of its depositional history during the early-to-middle Holocene is not clear. The first objective of this research addresses

this confusion by asking (and answering) two straight forward questions. (1) Are the preserved, regressive sediments within the region of the Trinity-Tiger Shoals Complex genetically linked to the Maringouin Delta Complex or the Teche? (2) Alternatively, are regressive sediments genetically linked to both? In other words, did both delta complexes prograde as far basinward as the bounds of the study area, implying that the Teche stacks stratigraphically atop of the Maringouin?

A number of past studies, especially more recent ones (e.g. Penland et al., 1989), direct a considerable amount of attention to the offshore sand shoals along Louisiana's inter-continental shelf for explaining the depositional history of the Maringouin and Teche Delta Complexes. Their premise, which is longstanding, is that these sand shoals represent the transgressed shoreline expression of the now-submerged delta complexes. The second objective of this study challenges the prevailing, three-stage transgressive depositional systems model for abandoned delta complexes. Particularly, this study challenges the culmination of this model as depicted by its final stage (stage 3). To do so, this study asks (and answers) the following question. Does the succession of preserved transgressive facies now overlying the regressive component within the Trinity-Tiger Shoals Complex region reflect that predicted by the transgressive depositional systems model?

To meet these objectives, this study evaluated the sedimentology, stratigraphy, and depositional history of the Trinity-Tiger Shoals Complex region. To do so, various field and lab methods were employed. Two separate geophysical surveys gathered a total of ~ 1,350 km of high-resolution subbottom sonar profiles (chirp sonar). Both surveys were followed by coring campaigns from which 60 total vibracores were extracted. Cores were logged using a GEOTEK core logger, photographed with a high-resolution scanning digital camera, and described

lithologically. In addition, 21 select cores were X-ray radiographed to enhance lithologic descriptions. Sand-mud ratios were established for 293 sediment samples, and grain-size analysis was conducted on the sand fraction of 242 of these samples. Furthermore, 22 discrete samples were AMS radiocarbon dated. All geophysical, sedimentological, and geochronologic data were integrated using Petrel<sup>TM</sup> software. Results include the differentiation of 12 acoustic-facies units and 12 lithofacies units. With exceptions, each lithofacies unit complements a corresponding acoustic-facies unit. One acoustic-facies unit distinguishes the antecedent topography, one distinguishes the relict regressive component, one distinguishes the distributary channel system associated with the relict regressive component, eight distinguish the transgressive component, and one distinguishes the most recent, present-day regressive component. The resulting facies architecture is illustrated by 60 cross sections and 60 lithologs. Furthermore, the regressive component is separated into four major delta lobes and one subdelta, and this specific part of the facies architecture is also illustrated by an additional 29 cross sections. Interpretations show that the relict regressive sediments within the Trinity-Tiger Shoals region are the remains of the Maringouin Delta's most southwestern extent. Interpretations also show that preserved transgressive sediments do not reflect that predicted by the prevailing transgressive depositional systems model, but instead indicate sedimentation dominated by a suite of marine processes occurring over relatively recent times.

Current understanding of the Holocene Mississippi Delta's geochronology is based mostly on work conducted within the subaerial part of the delta, whereas work conducted within the subaqueous part has lagged behind in influence. As noted above, this is consequent to logistical challenges in accessing offshore deposits. Thus, the geochronologic model of earlier delta complexes (i.e. the Maringouin and Teche) is less thoroughly defined than it is for later

delta complexes (i.e. post-Teche). There should be no surprise then that discrepancies exist within the literature with regard to the Mississippi Delta's early-to-middle Holocene depositional history. This study actually accessed the offshore, middle Holocene Mississippi Delta. Although it is not the first to do so, it is the first to clearly differentiate the depositional trends and clearly define the depositional history (based on AMS radiocarbon dating) of the more basinward part of the Maringouin Delta Complex, specifically within the Trinity-Tiger Shoals region. In doing so, this study has clarified some of the lingering confusion regarding the Mississippi Delta's early-to-middle Holocene geochronology.

This study has probably had more of an impact, however, not in its analysis of the regressive component, but rather in its scrutiny of the transgressive component. The prevailing, three-stage transgressive depositional systems model for abandoned delta complexes (Penland and Boyd, 1981; 1985 and Penland et al., 1985; 1988) is built upon a substantial amount of work conducted within different parts of the transgressive Mississippi Delta Plain, and it dominates our understanding of transgressive evolution within the delta. Working in the Trinity-Tiger Shoals region, this study accessed that part of the transgressed Mississippi Delta Plain used to define (along with Ship Shoal) the final stage (stage 3) of the transgressive depositional systems model. However, unlike previous studies conducted within the Trinity-Tiger Shoals region, the findings from this research are incompatible with the final stage of the prevailing model. This study does not argue that transgression as outlined in the transgressive depositional systems model does not occur (there is overwhelming evidence that it does), but it finds that affiliated deposits are not preserved, at least not within the Trinity-Tiger Shoals Complex region. Consequences are significant for geologists working in the ancient stratigraphic record, as they

are not just interested in the evolution of depositional systems but also in what actually gets preserved.

## **Study Area**

The Trinity-Tiger Shoals Complex region is located along the inner-continental shelf of the northern Gulf of Mexico, positioned approximately 30 – 40 km offshore of west-central Louisiana, USA. The study area for this research partially encloses this shoal complex, with areal grid dimensions of approximately 34 km (east-west) by 38 km (north-south). Water depths within the study area range from less than 4 m in shoal areas to greater than 20 m in the southernmost part. As expanded upon later, low-energy marine conditions dominate for much of the year. Such conditions are interrupted, however, during the passage of high-energy extratropical and tropical cyclones. As Figure 2 reveals, the most pronounced bathymetric features within the study area are the designated shoals, especially Trinity Shoal. However, the reader should recognize, as results from this research show, that these features are just one part in a complex history of deltaic deposition.

## BACKGROUND

### Setting

Significant fluvial deposition has been occurring along northern Gulf of Mexico since the Cretaceous, but it was not until the Miocene that the major extrabasinal, primary axis for fluvial sediment input shifted to the Mississippi embayment, a position that persists today (Winker, 1982; Galloway et al., 2000, Galloway, 2005). The late Neogene was marked by Pliocene tectonic rejuvenation of the Rockies and Plio-Pleistocene glaciation in the midcontinent, which resulted in rejuvenation of sediment sources and development of the present-day integrated Mississippi River drainage basin as a continental-scale system (Winker, 1982; Galloway et al., 2000, Galloway, 2005). Today, this drainage basin covers 3,344,560 km<sup>2</sup>, including ~ 70% of the continental United States and the lower portions of two Canadian provinces (Coleman, 1988; Roberts, 1997).

The Mississippi River's mean annual high- and low-water flow rates are ~ 23,500 m<sup>3</sup> s<sup>-1</sup> and ~ 7,000 m<sup>3</sup> s<sup>-1</sup>, respectively (measured between 1961 – 2004; Nittrouer et al., 2008). Average annual flow rate down the controlled Atchafalaya distributary is ~ 6,500 m<sup>3</sup> s<sup>-1</sup> (Roberts, 1997). Considering the similar character of all Holocene Mississippi River meander belts presently exposed in the Lower Mississippi Valley, these values are presumed an approximate representative of the river's annual flooding-nonflooding discharge cycle throughout the Holocene (Roberts, 1997). Prior to the 20<sup>th</sup> Century (i.e. before major control structures such as dams and levees were emplaced), the Mississippi-River system is estimated to have transported ~ 400 – 500 million metric tons of suspended sediment annually to the Louisiana coast (Kesel et al., 1992; Meade and Moody, 2010). Bedload flux is estimated to have been as high as 30% of total sediment load (Kesel, 1992). Furthermore, approximately 230 –

290 million tons of pre-20<sup>th</sup> Century sediment is estimated to have been trapped annually within the Mississippi River's alluvial valley and delta (Blum and Roberts, 2009). For comparison, mean suspended sediment load for the present-day Mississippi-Atchafalaya River system is ~ 205 million tons annually (Blum and Roberts, 2009), whereas bedload, measured only from the Mississippi River below the Atchafalaya River diversion, is ~ 2.5% of total suspended discharge (Nitttrouer et al., 2008).

The Mississippi River delivers its sediment load to the low-gradient northern Gulf of Mexico, a receiving basin that is characterized by relatively low-energy marine conditions (Coleman, 1988; Roberts, 1997). Accordingly, it has constructed the Holocene Mississippi Delta Plain, which presently encompasses ~ 25,000 km<sup>2</sup> of coastal Louisiana (Fig. 1; Blum and Roberts, 2012). Deltas of all sizes within the Mississippi Delta Plain display an overall elongate to lobate morphology and are considered the quintessential river-dominated delta type (Galloway, 1975; Coleman and Wright, 1975; Bhattacharya, 2006). Despite the relatively static basin into which the Holocene Mississippi Delta has built, the delta has and continues to persist in a constant state of flux, with rising relative sea level and various marine-reworking processes continuously working against it. The magnitude of change that these destructive processes can impose has been magnified since the early 20<sup>th</sup> century due to an anthropogenic reduction of sediment input into the system. Consequently, the Mississippi Delta has experienced a net loss of almost 5,000 km<sup>2</sup> of land area since 1932 (Couvillion et al., 2011).

### Rising Relative Sea Level

Eustatic sea level rose sharply out of the last glacial maximum, reached a level of approximately 5 m below present level by ca. 6 kyr BP, and has since risen slowly to its current level (Fairbanks, 1989; Chappell and Polach, 1991; Bard et al., 1996). Of course the Holocene

sea-level record of the Mississippi Delta region records this eustatic component, but it also includes cumulative subsidence caused by various processes that operate over different spatial and temporal scales (Kulp, 2000). Processes relevant to Holocene regional subsidence trends may include glacio-hydro-isostasy (Mitrovica and Milne, 2002), sedimentary loading (Kulp, 2000; Ivins et al., 2007; Hutton and Syvitski, 2008), and shallow sediment compaction (Roberts et al., 1994; Meckel et al., 2006; 2007). Hence, resolving the history of Holocene relative sea-level (RSL) rise (i.e. eustatic change and/or subsidence) within the Mississippi Delta is difficult and has led to several hypotheses that remain contentiously debated (Törnqvist et al., 2006; Blum et al., 2008; Donnelly and Giosan, 2008; among many others).

Resolving this debate is beyond the scope of this research. Instead, this study utilizes a composite Holocene RSL curve established by Milliken et al. (2008) for the greater northern Gulf of Mexico, which includes data points obtained from the Holocene-Pleistocene contact underlying the Mississippi Delta (Fig. 5). Evidence supporting this recognition includes additional Gulf of Mexico data from the Suwannee River Delta and adjacent areas of northwest peninsular Florida that likewise document a gradual rise in Holocene RSL (Wright et al., 2005). Furthermore, an extensive compilation of data from the Caribbean (Toscano and Macintyre, 2003) records a smooth, asymptotic rise in Holocene RSL over the last 4 kyr, which closely corresponds to that of the northern Gulf of Mexico as estimated by Milliken et al. (2008). The significance of this last finding from the peripheral region of the Gulf of Mexico, which is considered tectonically stable during the Holocene, implies that tectonic subsidence along the northern Gulf of Mexico over the last 4 kyr was a minor component of total RSL rise (Milliken et al., 2008).



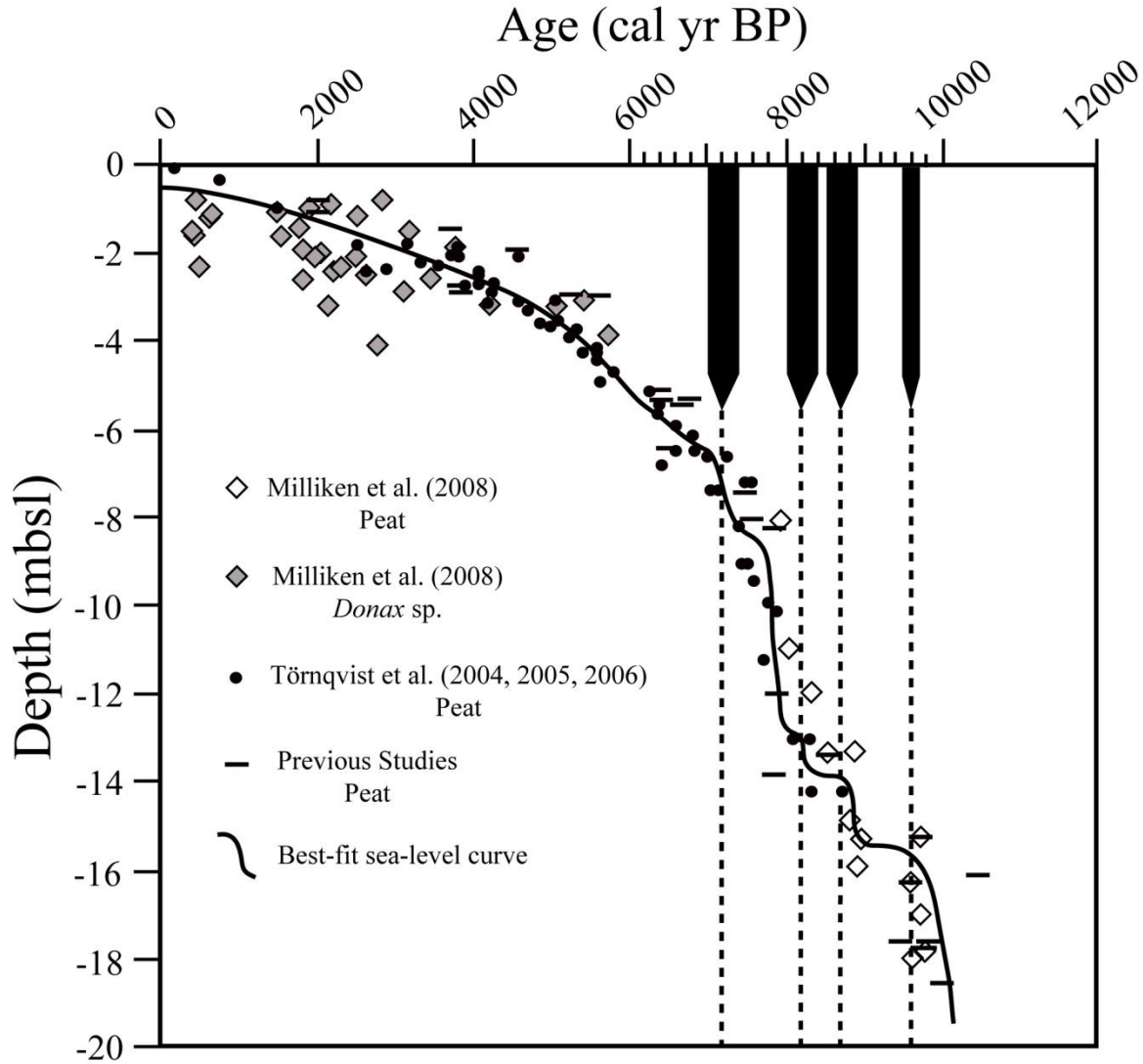


Figure 5. A regional Holocene RSL curve for the northern Gulf of Mexico (mbsl – meters below sea level). The RSL curve tracks a smooth, asymptotic rise between  $\sim 7$  kyr BP to present, whereas RSL rise appears more episodic during the early Holocene. Black arrows mark the flooding events interpreted to have occurred in estuaries studied by Milliken et al. (2008); width of arrows indicates the uncertainty in timing of flooding events. Modified from Milliken et al. (2008).

The Milliken Holocene RSL curve (Fig. 5) is applied broadly to the northern Gulf of Mexico, and thus it does not account for subsidence processes that are rather unique to the Mississippi Delta, most notably the compaction of thick Holocene sediments. For time scales relevant to the Holocene, shallow-sediment compaction is the dominant mechanism driving land-

surface subsidence within the delta (Törnqvist et al., 2008). Long-term (i.e. century to millennium) compaction rates generally increase with increasing Holocene sediment thickness (Roberts et al., 1994). Superimposed upon this trend are the effects of gradational stacking patterns of different lithofacies, with certain lithofacies, such as peats, prodelta clays, and bay clays, more prone to compaction than others (Keucher et al., 1993; Keucher, 1994; Roberts et al., 1994). Numerically modeled compaction rates are estimated, generally, from -0.7 mm/yr to -2.2 mm/yr and rarely exceed -5.0 mm/yr (Meckel et al., 2006; 2007). Locally, however, particularly within the shelf-margin Balize Delta lobe where accumulation rates are high and the basal prodelta clays are thick, compaction rates may be extreme (Fisk and McFarlan, 1954). Deep-seated faulting is not thought to significantly contribute to overall, regional subsidence trends within the delta during the Holocene (Törnqvist et al., 2006; Edrington et al., 2008), although fault-induced subsidence can be locally significant, especially in the more basinward parts of the delta (Kuecher, 2001; Roberts et al., 2008). Furthermore, active salt-tectonic processes may also be significant on the continental shelf where the most basinward sediments of the early-to-middle Holocene Mississippi Delta reside (Berryhill, 1986).

#### Marine-Reworking Processes

A low-energy shoreface-to-shelf environment dominated by infrequent, high-energy storms exists offshore of coastal Louisiana. During fair-weather conditions, prevailing winds, and thus wind-driven waves, are predominantly from the southeast (Jaffe et al., 1997; Georgiou et al., 2005). Significant deep-water wave height is approximately 1 m, with a mean wave period ranging between approximately 4.5 – 6.0 seconds (Jaffe et al., 1997; Georgiou et al., 2005). Wave height decreases towards the shore, however, as substantial dissipation and refraction occur during the advancement of waves across the shallow shelf (Pepper and Stone, 2004). The

prevailing wind stress also drives wind-driven coastal currents generally westward along the west-central Louisiana coast (Cochrane and Kelly, 1986; Murray, 1997). Lastly, tides are mixed diurnal (Crout and Hamiter, 1981), have a tidal range of approximately 40 cm, and thus produce only weak tidal currents (Jaffe et al., 1997; Wright et al., 1997).

Interrupting the prevailing, low-energy conditions of the northern Gulf of Mexico are the occurrences of high-energy extratropical and tropical cyclones. Every winter, 20 – 30 extratropical cyclones, or cold fronts, pass over the Louisiana coast (Roberts et al., 1987; Roberts et al., 1989). Each passage may be summarized in three stages: pre-frontal, frontal passage, and post-frontal (Roberts et al., 1987; Roberts et al., 1989). During the pre-frontal phase (~ 2 – 3 day duration), warm, strong, long-fetched winds blow out of the south towards the oncoming front (Roberts et al., 1987; Roberts et al., 1989). As the front passes, air pressure drops and a relatively short period of erratic, vertical winds transpires (Roberts et al., 1987; Roberts et al., 1989). After the front passes, the post-frontal phase (~ 2 – 3 day duration) ensues, which is characterized by cold, northerly winds that are even stronger than those of the pre-frontal phase (Roberts et al., 1987; Roberts et al., 1989). The increased shear velocities and bottom currents along the lower shoreface and shelf that accompany such a high-energy event permit the entrainment and transport of sands that generally does not occur during fair-weather conditions (Crout and Hamiter, 1981; Adams et al., 1982; Wright et al., 1997; Pepper and Stone, 2004).

Tropical cyclones (i.e. hurricanes and tropical storms) are, on the other hand, even less frequent. They typically strike coastal Louisiana during the warm summer months approximately every other year, or at least they did so during the 20<sup>th</sup> Century (Stone et al., 1997). Wind velocities associated with hurricanes are significantly greater than those of typical cold fronts, and as such they generate significantly greater shear velocities and currents (Stone et

al., 1997). Although the less energetic but more frequent cold fronts dominate physical changes within some parts of the delta (e.g. progradation along the chenier plain; Roberts et al., 1987; Roberts et al., 1989), hurricanes can have a much more profound impact on other parts, particularly the sandier parts that evolve during the transgressive phase of delta building (Kahn and Roberts, 1982; Stone et al., 1997; Fearnley et al., 2009).

### **Holocene Geologic Framework: The Delta Cycle**

During the last glacial period, eustatic sea level (ESL) lowered as ice sheets expanded across the continents. By the end of the last glacial maximum (ca. 21 ka), ESL was at the shelf margin, ~120 m below present (Peltier and Fairbanks, 2006). This drop in base level, coupled with intermittent glacial outwash, induced fluvial entrenchment of the Lower Mississippi Valley (Fisk, 1944; Fisk and McFarlan, 1955; Autin et al., 1991; Saucier, 1994; Blum and Törnqvist, 2000). Upon deglaciation, ESL rise incrementally inundated the northern Gulf of Mexico's continental shelf, eventually flooding parts of the Mississippi River's Pleistocene alluvial valley (Fisk and McFarlan, 1955). These two post-glacial parameters, rising ESL and the incised Mississippi River valley, fundamentally influenced the timing of Holocene Mississippi Delta Plain evolution. It was not until ca. 7.5 ka, after the deceleration of ESL rise and sufficient sediment infilling of the incised valley, that the Holocene Mississippi River's first delta complex, the Maringouin, prograded out onto the continental shelf (Frazier, 1967; 1974; Fig. 1).

#### **Regressive Phase**

Delta building within the Mississippi Delta is an inherently cyclical process, consisting of a fluvial-dominated regressive phase, or constructive phase, and a marine-dominated transgressive phase, or destructive phase (Fisk, 1944; Fisk and McFarlan, 1955; Kolb and Van Lopik, 1958). During the regressive phase, a sufficient quantity of sediment is supplied to the

receiving basin via the main channel and its distributaries such that sediment deposition overwhelms the ability of marine processes to remove or redistribute that sediment (Scruton, 1960). Consequently, the delta's shoreline advances seaward as sediment infills the available accommodation (Fig. 6). As the delta's shoreline continues to prograde, accommodation within the alluvial valley is likewise filled by aggradation. The expanding fluvial-deltaic system ultimately becomes overextended, loses its gradient advantage, and thus becomes unstable as 1) the elevation difference between the top of the channel levee and the adjacent floodplain increases and 2) the cross-valley slope and down-channel slope ratio increases (Törnqvist and Bridge, 2002; Jerolmack, 2009). Up-stream avulsion will follow as the river seeks a more direct, hydraulically efficient route to the sea. This process of stream abandonment, which is responsible for the spatial shift of individual deltaic depocenters, is termed delta switching (Fisk, 1944; Fisk and McFarlan, 1955; Kolb and Van Lopik, 1958). Such an event is thought to have occurred ca. 5.5 ka when the Mississippi River shifted out of the Maringouin system and began forming the Teche Delta Complex (Fig. 1; Roberts, 1997). This process of progradation-avulsion, progradation-avulsion has persisted into the present.

Delta switching also occurs over a range of temporal and spatial scales, producing an aggregation of deltaic depositional features that offset, overlap, and stack over a range of temporal and spatial scales: hence the phrase "deltas within deltas" (Roberts, 1997). At the top of the Mississippi Delta hierarchy, in both a spatial and temporal sense, is the all-encompassing delta plain. Figure 1 displays the Holocene delta plain as it is observed today, as well as the evolutionary history of the six major delta complexes that comprise it. These delta complexes are defined and distinguished from one another by their respective association with a single major (paleo-) Mississippi River channel (i.e. trunk channel). This understanding defines the

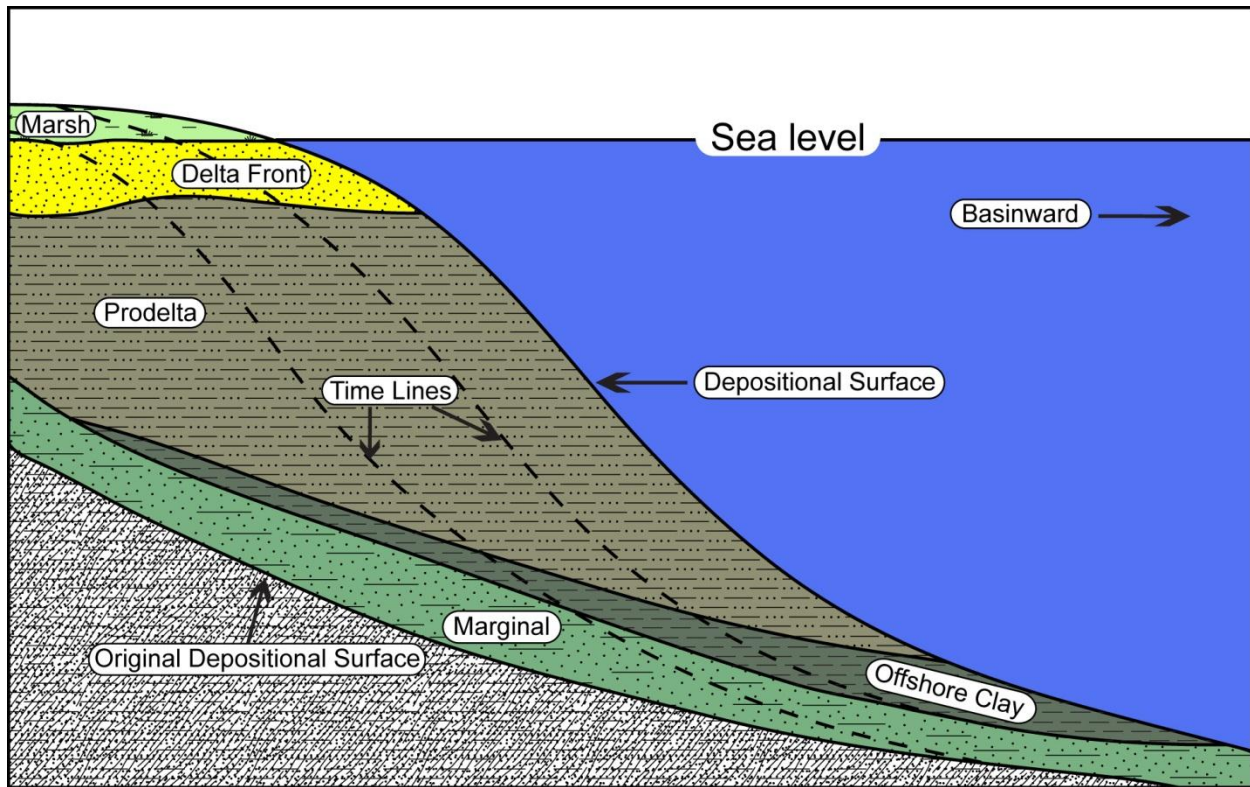


Figure 6. Idealized schematic cross section of a prograding delta. Note the dashed time lines, which indicate paleo-depositional surfaces that successively migrate basinward. Modified from Scruton (1960).

delta's geochronologic order. Constituting a delta complex may be several individual delta lobes, each an outgrowth of a major distributary. Frazier (1967) identified a total of 16 delta lobes within the Mississippi Delta, all of which were determined within the Teche, St. Bernard, Lafourche, and Plaquemines-Balize Delta Complexes. None were identified within the Maringouin Delta Complex as radiocarbon-age control was too sparse and offshore data were largely not available. The Atchafalaya Delta Complex, on the other hand, is still an embryonic, bay-head delta (Roberts et al., 1980; Van Heerden and Roberts, 1988). Constituting delta lobes are subdeltas and smaller-order crevasse splays, which build into shallow, interdistributary bays after secondary channels scour through the natural levees of major distributaries (Fig. 7; Welder, 1959; Coleman and Gagliano, 1964).



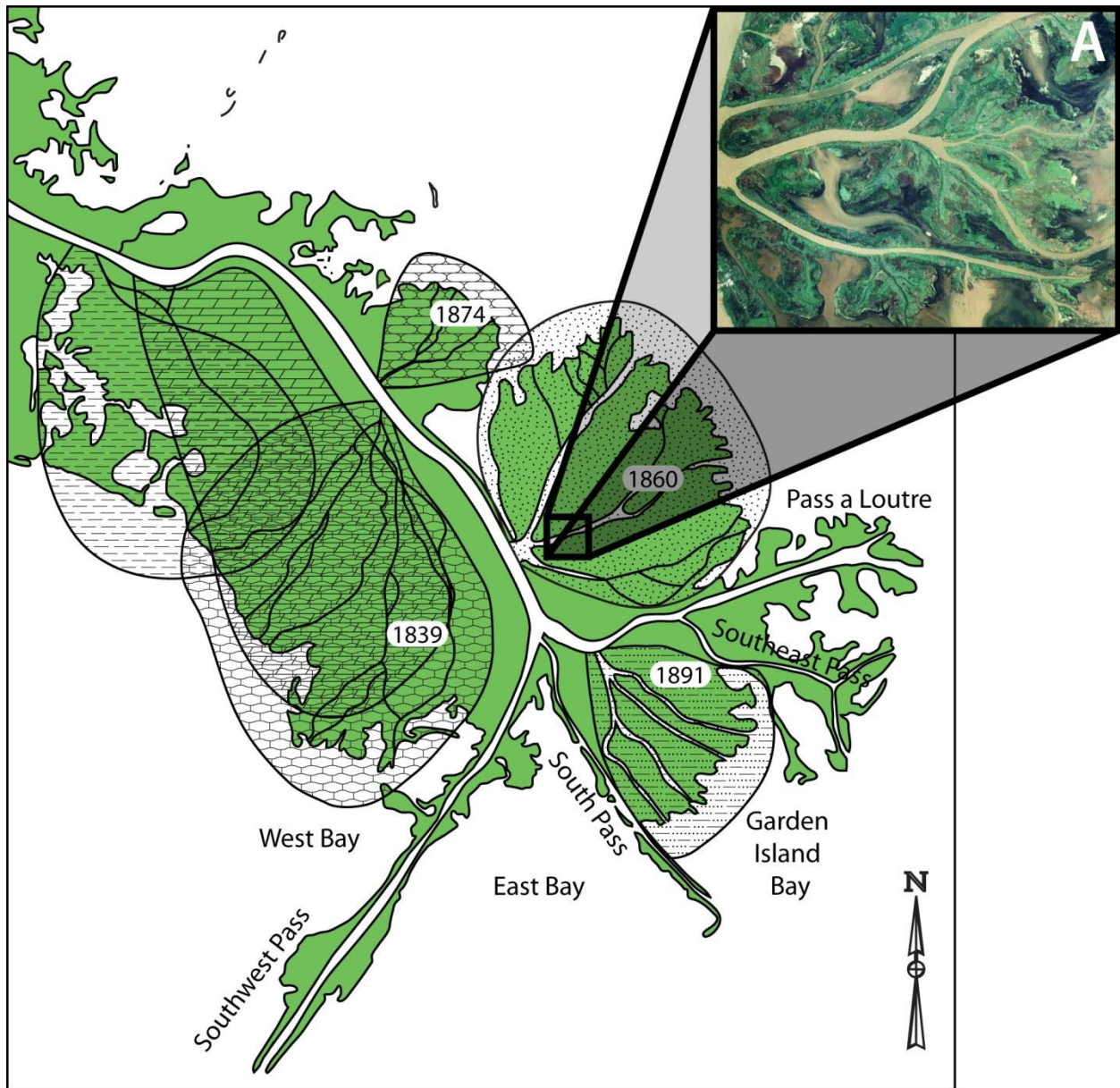


Figure 7. The modern Balize Mississippi Delta lobe. At least six subdeltas that comprise this delta lobe are delineated. Inset A is a crevasse splay flanking a channel within a higher-order subdelta. Modified from Coleman and Gagliano (1964).

### Transgressive Phase

In addition to shifting the depocenter to a new location within the delta plain, up-dip avulsion also initiates the transgressive phase of the now-older delta, although not necessarily immediately. Both channels, new and old, share the flow and sediment load initially, but as the

new course begins capturing a greater percentage of the total, the previously active delta begins yielding to rising RSL and marine-reworking processes (Coleman, 1988; Roberts, 1997).

#### “The Prevailing Model for Transgression of Abandoned Deltas”

Early research evidently recognized the destructive phase of deltas that followed stream abandonment (e.g. Scruton, 1960; Coleman and Gagliano, 1964). However, much of our current, organized understanding of transgression within the Mississippi Delta comes from more recent, improved offshore data sets not available to early workers. These data have been concisely summarized by Penland and Boyd (1981; 1985) and Penland et al. (1985; 1988). Their model, known as the transgressive depositional systems model and which still prevails today, partitions transgression of deltas into three stages: Stage 1, erosional headland with flanking spits and barrier islands; Stage 2, barrier island arc detached from the mainland; Stage 3, inner-shelf shoals (Fig. 8). The following discussion describes each stage of the transgressive depositional systems model. The following discussion also draws heavily from Penland and Boyd (1981; 1985) and Penland et al. (1985; 1988). For the sake of brevity and avoiding redundancy, they will not be cited again. However, the reader should recognize them as the ultimate source for this discussion. Additional works will be cited where appropriate.

The transgressive evolution of a delta is first perceived by an erosional headland with flanking spits and barrier islands fronting restricted interdistributary bays (Stage 1; Fig. 8). An example of Stage 1 is the eroding Caminada-Moreau headland, which is associated with the relatively recent Lafourche Delta (Gerdes, 1985; Fig. 9). Subsidence and the recurring wave energy impacting the coastal zone (and the littoral-to-shoreface currents this sets up) drives shoreface retreat, reworking and redistributing the sands of the Caminada-Moreau beach-ridge plain and the Lafourche distributaries laterally by longshore transport. The Caminada Pass Spit



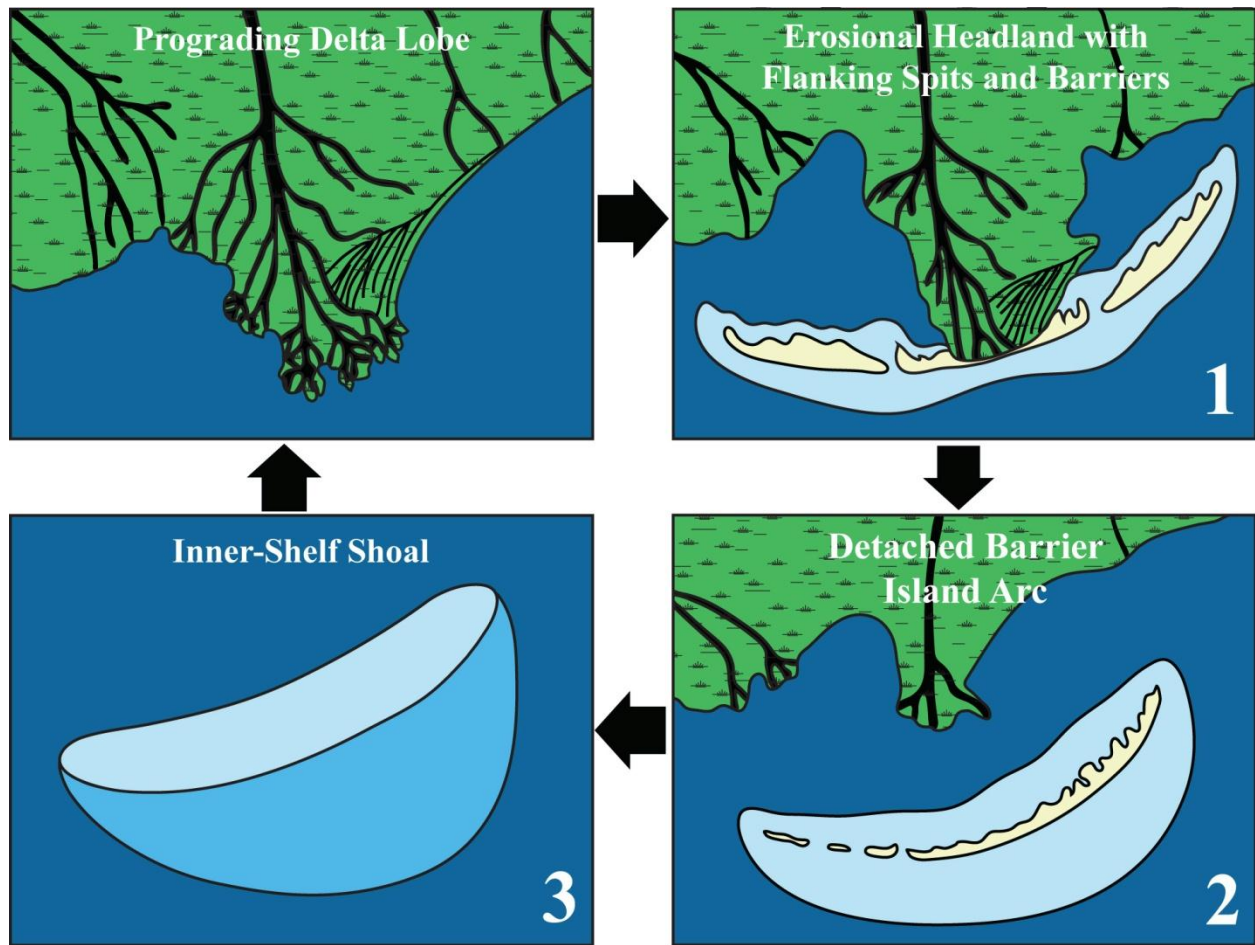


Figure 8. The evolution of a transgressing delta lobe, depicted graphically as a 3-stage process. Transgression begins with Stage 1, an erosional headland with flanking spits and barriers. In Stage 2, barriers detach from the mainland and coalesce into an island arc. Ultimately, the barrier-island arc succumbs to relative sea-level rise and marine-reworking processes, transforming into a Stage 3 submarine sand shoal. Modified from Penland et al. (1988).

and the Lafourche Spit are both byproducts, accreting downdrift in divergent directions away from the sediment source of the erosional headland. Likewise, Grand Isle and the Timbalier Islands also formed by downdrift accretion but are detached from the headland (and each other in the case of the East Timbalier Islands) by tidal inlets. These flanking barriers have since migrated laterally across the Caminada Bay (now a part of the greater Barataria Bay) and Timbalier Bay, respectively, restricting tidal-flow exchange between these bays and the Gulf of Mexico. Due to persistent subsidence and subsequent wetland loss within the surrounding back-

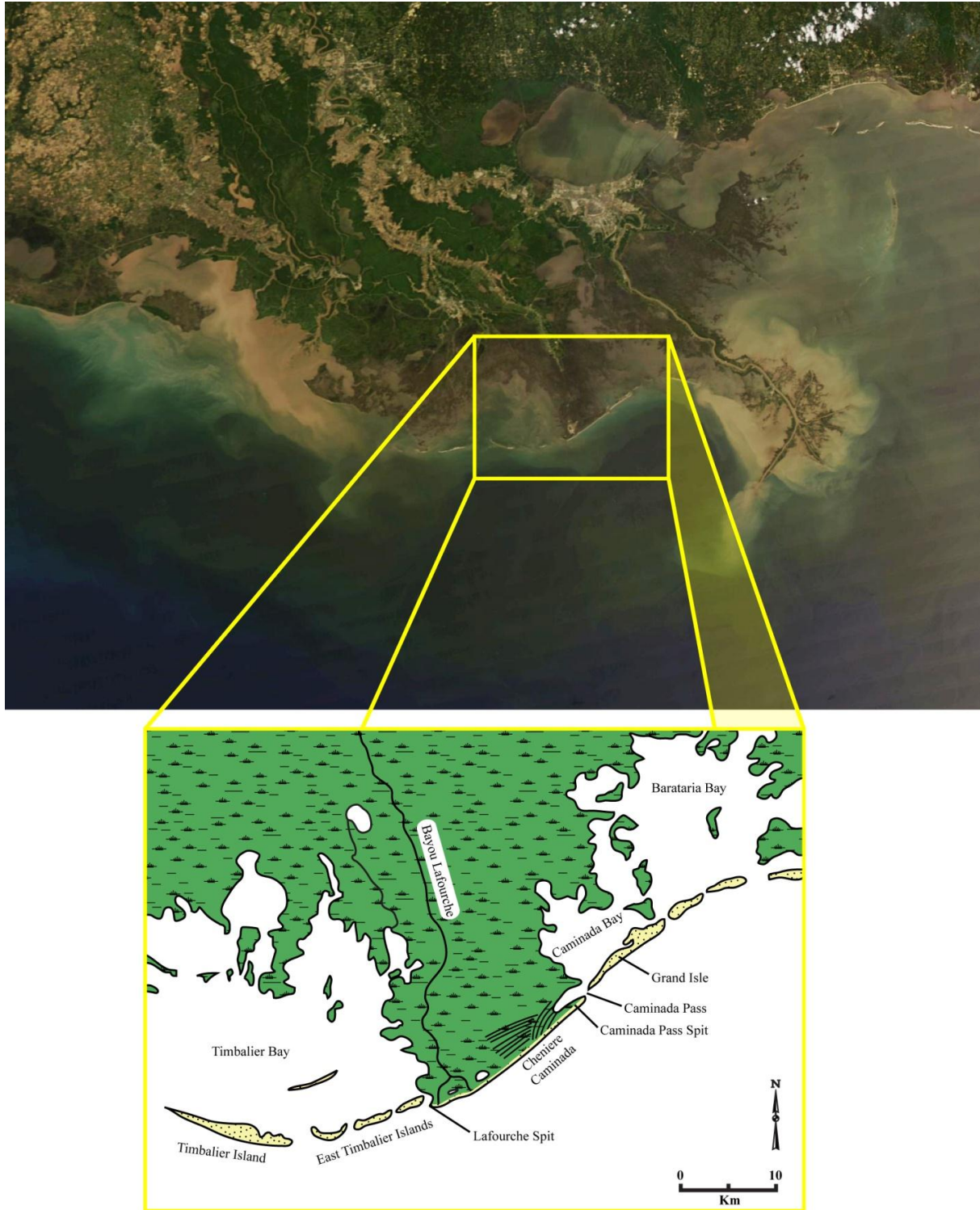


Figure 9. Stage 1 of the delta's three-stage transgressive model: the Caminada-Moreau headland. Note flanking spits, barrier islands, back-barrier bays, and tidal inlets. MODIS (Moderate Resolution Imaging Spectroradiometer) Satellite image of the Mississippi Delta Plain was taken from the Louisiana State University Earth Scan Laboratory ([www.esl.lsu.edu](http://www.esl.lsu.edu)). Inset is modified from Penland and Boyd, 1985.

-barrier delta, the interdistributary bays continuously enlarge, causing a correlated increase in the tidal prism. Consequently, these processes, together with the destructive impacts of infrequent but catastrophic tropical cyclones, promote degradation of the barriers: preexisting tidal inlets and their associated ebb-tidal deltas equilibrate by enlarging, additional tidal inlets form, and the shoreline migrates landward (List et al., 1997; Kulp et al., 2003; Stone et al., 2003; FitzGerald et al., 2007; Miner et al., 2007).

As transgression progresses, a detached barrier-island arc will eventually develop as the back-barrier headland submerges under subsidence (Stage 2; Fig. 8). Accordingly, interdistributary bays coalesce, resulting in a large intradeltaic lagoon separating the barrier-island arc from the mainland. The Isles Dernieres, which is associated with the Caillou headland of the early Lafourche Delta Complex (Kulp et al., 2005), represents the early transition from flanking spits and barriers of Stage 1 to the now-detached Stage 2 barrier-island arc (Fig. 10). This transition has also been historically documented, as Figure 10 depicts. Note that in just 125 years, the cumulative impacts of major storms have significantly reduced the extent of the subaerial barrier-island arc. Furthermore, while the island arc has retreated landward during this time interval, it has been outpaced by the mainland shoreline, and today more than seven kilometers of open water separates the two.

The Chandeleur barrier-island arc is another Stage 2 example (Fig. 11), but it is much older (a product of the St. Bernard Delta Complex) and in a more advanced stage of evolution than is the Isles Dernieres. Most of the tidal exchange between the Chandeleur and Breton Sounds and the Gulf of Mexico now occurs around the margins of the island arc, whereas tidal inlets play a minimal role. During major storms, sands are transported both landward as storm overwash and offshore onto the shoreface and inner-shelf (Boyd and Penland, 1981; Kahn and



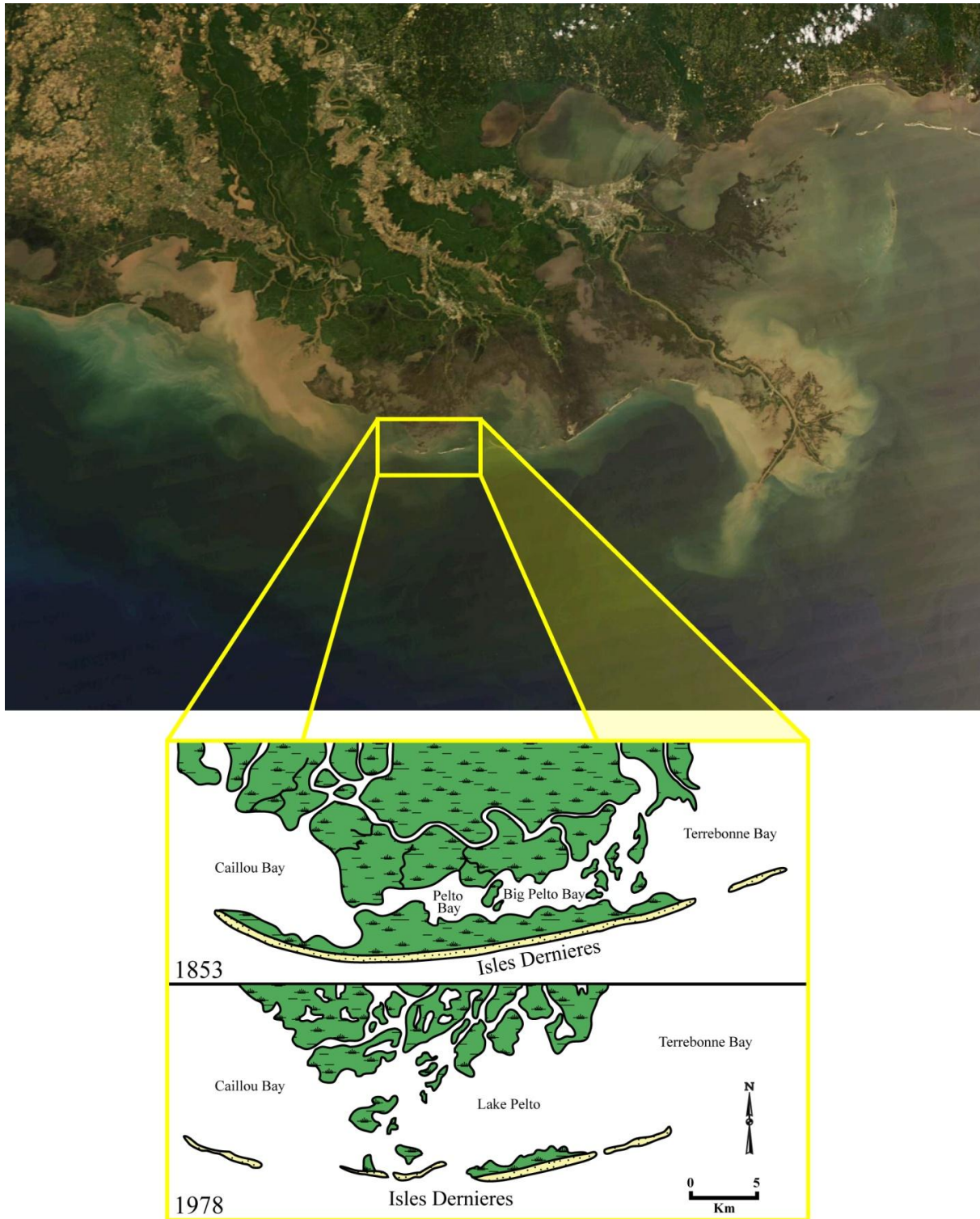


Figure 10. Stage 2 of the delta's three-stage transgressive model: the Isles Dernieres. Note the drastic changes in the barrier-island complex and the coalescing of the back-barrier lagoon in just 125 years. MODIS (Moderate Resolution Imaging Spectroradiometer) Satellite image of the Mississippi Delta Plain was taken from the Louisiana State University Earth Scan Laboratory ([www.esl.lsu.edu](http://www.esl.lsu.edu)). Inset is modified from Penland and Boyd (1985).



Figure 11. Stage 2 of the delta's three-stage transgressive model: the Chandeleur Islands. MODIS (Moderate Resolution Imaging Spectroradiometer) Satellite image of the Mississippi Delta Plain was taken from the Louisiana State University Earth Scan Laboratory ([www.esl.lsu.edu](http://www.esl.lsu.edu)).

Roberts, 1982). Thus, recurring major storms continually drive the barrier system landward while also steadily depleting it of its finite sand resource. Although the island arc recovers during the non-hurricane interval of constructive, fair-weather hydrodynamics, it generally does not recover to its pre-storm condition (McBride and Byrnes, 1997; Fearnley et al., 2009). Furthermore, recent research (Miner et al., 2009) documents the significance of down-drift spit accretion into deep-water sinks at the margins of the island arc, where sands are effectively removed from the littoral system. Landward migration and rising relative sea level eventually remove the island arc from its original sand source, i.e. the channel sands and distributary mouth bar deposits that were deposited basinward within the now underlying delta (Suter et al., 1988; Roberts, 1997).

Recurring destruction from storm impacts, a depleting supply of sand, and long-term relative sea-level rise ultimately overcomes the ability of the diminished barrier-island arc to

remain subaerial, and translation into a Stage 3 subaqueous, inner-shelf sand shoal ensues (Fig 8). The southern Chandeleurs are thought to be in the early transitional phase of inner-shelf shoal conversion, where only a sliver of one island, Breton Island, has recovered since the most recent stormy period (i.e. Hurricanes Georges, 1998; Isidore, 2002; Ivan, 2004; and Katrina, 2005) (Fearnley et al., 2009).

Isolated, older, and more evolved shoals on the inner shelf include Trinity and Ship Shoals (Fig. 12). These shore-parallel sand bodies are approximately 6 – 8 m thick, on the order of 30 – 50 km long by 5 – 10 km wide, and reside near the 10 m isobath, shoaling up to a 3 – 4 m depth at their crests. A thin, broad sand sheet overlying distant, truncated barrier-island, tidal-inlet, and lagoonal deposits is thought to extend seaward from the base of each shoal, marking the retreat path of the once-subaerial barrier-island arcs, now subaqueous sand shoals (Penland and Suter, 1983). Ship Shoal's lengthwise asymmetry, with its steep side facing landward, suggests that it is migrating landward in a northwest direction (Penland et al., 1986). Just within the last 100 years, for instance, it is estimated to have migrated approximately 1 km (Roberts, 2012). Shoal migration is thought to occur by erosion on the seaward-side slope with deposition on the landward-side. Eventually, persistent migration completely reworks the original barrier-island facies into an entirely marine sand body. Such is interpreted for Ship Shoal, which is thought to have since migrated across, and now lie atop of, the lagoonal deposits that formed previously behind the once-subaerial Ship barrier-island arc (Penland et al., 1986; 1989). Similarly, Trinity Shoal is judged to be migrating landward. In contrast with Ship Shoal, however, Trinity Shoal is argued to be composed of a thin (1 – 2 m), reworked marine sand layer overlying the shoal's core of original barrier-island facies, including tidal inlets, tidal deltas, recurved spits, washover sands, and even aeolian deposits (Penland et al., 1989; 1990; Pope et



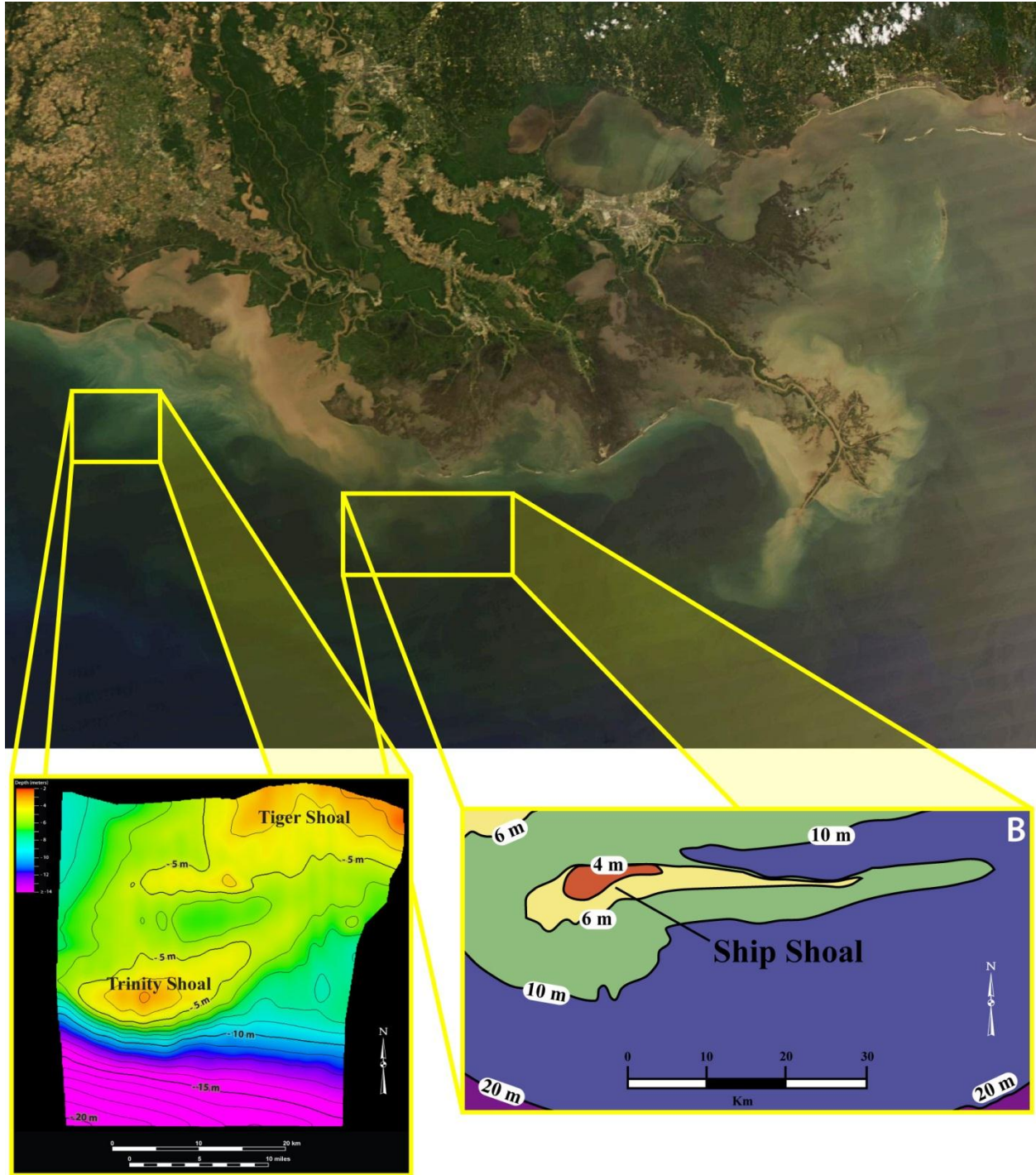


Figure 12. Locations of Trinity Shoal and Ship Shoal along the inner-continental shelf. Inset A is a bathymetric map of the Trinity-Tiger Shoals region generated during this study. Inset B is modified from Penland et al. (1986). MODIS (Moderate Resolution Imaging Spectroradiometer) Satellite image of the Mississippi Delta Plain was taken from the Louisiana State University Earth Scan Laboratory ([www.esl.lsu.edu](http://www.esl.lsu.edu)).

al., 1991). The presumption is that Ship Shoal is much older than Trinity Shoal and therefore has experienced more reworking. This interpretation appears to have inspired the more recent conceptual understanding (e.g. Penland et al., 1985; 1988) that Ship Shoal originated from the Maringouin Delta Complex, whereas Trinity Shoal emanated from the Teche.

### **Depositional Environments and Facies Associations of the Mississippi Delta**

To meet the objectives of this dissertation, the bulk of this research essentially scrutinized the various deltaic depositional environments (both regressive and transgressive) preserved within the Trinity-Tiger Shoals region. Many of these depositional environments were sampled by vibracoring, and are thus directly observable. All preserved depositional environments are presumably recorded in the geophysical data. In order to correctly interpret the subsurface from the lithological and geophysical data sets, a thorough understanding of the depositional patterns of deltas, how the various resulting depositional environments relate to one another, and how to identify those environments within a given data set is imperative. The following discussion gives a detailed account of these environments of deposition, particularly in regards to their lithofacies. A section towards the end will discuss acoustic facies and the unique attributes associated with deltas.

#### **The Concept of Facies**

The term facies, from the Latin word for outward appearance, is defined as a body of rock (or unlithified sediment) with a specified combination of lithology and sedimentary and biological structures that impart an appearance (i.e. facies) markedly different from bodies of rock (or unlithified sediment) above, below, and/or laterally adjacent (Walker, 1992; Reading and Levell, 1996). In theory, a facies should reflect the process(es) and environment under which sedimentation occurred (Walker, 1992; 2006; Reading and Levell, 1996). If examined in



isolation, however, interpretations of individual facies are severely limited (Walker, 1992; 2006; Reading and Levell, 1996). For example, a cross-bedded, quartz-sand lithofacies can form in marine, fluvial, and aeolian environments. If, however, this lithofacies is found positioned 1) conformably above a lithofacies characterized by muddy sediments reworked intensely by animal burrowing and 2) conformably beneath a lithofacies characterized by parallel-to-cross stratified sands reworked by both animal and root burrowing, then one could conceivably make the first-order interpretation of a shoreface environment positioned between offshore-shelf and barrier environments, respectively. It is only through an understanding of relationships between one facies and its neighbor(s) that an environmental interpretation can be made (Walker, 1992; 2006; Reading and Levell, 1996). Accordingly, genetically related facies are grouped into a facies association, which by definition implies an environmental relationship (Walker, 1992; 2006; Reading and Levell, 1996).

Individual facies within a facies association gradually transition into their laterally-adjacent neighbors (Walker, 1992; 2006; Reading and Levell, 1996). Likewise, a gradual transition of facies may be observed in the vertical direction as well (Walker, 1992; 2006; Reading and Levell, 1996). This concept of vertical facies succession was first described by Johannes Walther in his Law of the Correlation of Facies, which states that a facies conformably above another also accumulated alongside it laterally (Middleton, 1973). If, however, the contact between adjacent facies is sharp and/or erosional, this may signify a fundamental change in the depositional environment, including the passage of any number of depositional environments whose products were subsequently removed (Walker, 1992; 2006; Reading and Levell, 1996). Such sharp breaks between facies are referred to as bounding discontinuities and are used to separate stratigraphic sequences (Walker, 1992; 2006; Reading and Levell, 1996).

### Depositional Patterns of Delta Building

There are two model types of delta complexes recognized within the Holocene Mississippi Delta Plain. The deep-water model is exemplified by the modern Birdfoot Delta, which is currently building near the shelf edge. The shoal-water model is embodied by every other delta complex, all of which formed by prograding out onto the shallow-water, inner-continental shelf (Fig. 13; Fisk, 1955; Gould, 1970). River-mouth processes of the deep-water delta are dominated by outflow buoyancy, whereas river-mouth processes of shoal-water deltas are dominated by turbulent bed friction (Wright, 1977). These processes cause respective deltas to form different depositional patterns and, consequently, construct different stratigraphic frameworks (Wright, 1977). In shoal-water deltas, sands transported to the distal ends of an extensive, highly-bifurcating network of distributaries amalgamate to form a widely semi-continuous sand body that fronts the perimeter of the delta (Fisk, 1955; Gould, 1970). As the delta builds farther basinward, a semi-continuous sheet of sand, called the delta-front sheet sand, advances across the underlying, finer-grained facies (Fisk, 1955; Gould, 1970). In contrast, sands transported within the modern Birdfoot Delta are deposited at the distal ends of only a few straight, digit-like distributaries. Due to subsidence in the very thick, underlying clayey sediments, thick sands on the order of 70 m may accumulate at the mouth bars (Fisk, 1955; Gould, 1970). Progradation of the Birdfoot Delta has led to the development of thick, elongated bodies of sand, called bar fingers, with large interdistributary troughs separating them (Fisk, 1955; Gould, 1970).

Despite contrasts among delta complexes, sediment dispersal at the river mouth can generally be described by the same sediment-fractionation processes. As less dense fluvial water debouches out over the more dense Gulf waters, the coarse-grained bed load and sands in

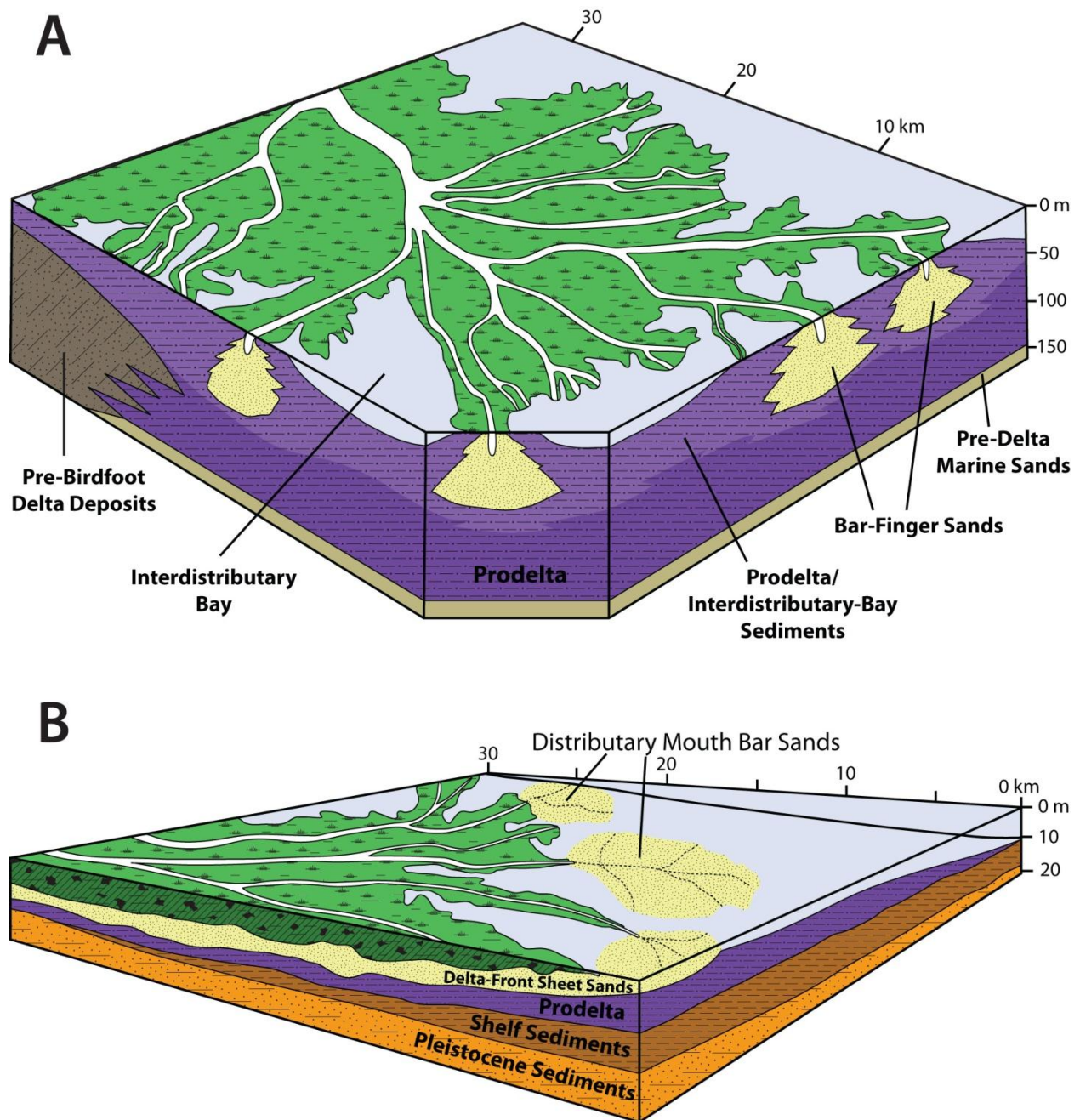


Figure. 13. A) The deep-water, or shelf-edge, delta. Note the elongated, digit-like bar-finger sands. Modified from Fisk et al., 1954. B) The shoal-water, or inner-shelf, delta. In contrast with the bar-finger sands of the deep-water delta, note the semi-continuous delta-front sheet sand. Modified from Gould, 1970.

suspension settle out and are deposited just seaward of the river mouths in the distributary mouth-bar and upper delta-front environments (Scruton, 1960; Coleman, 1981). Finer sediments

may also accumulate in the distributary mouth bar but are subsequently removed by marine-reworking processes, leaving only a predominantly clean, well-sorted sandy mouth-bar deposit (Coleman, 1981). Finer sediments in suspension are largely carried farther basinward where further fractionation by settling occurs. The resulting depositional surface is expressed as a basinward fining succession of facies, from the coarser-grained distributary mouth bar and delta fronts facies to the finest-grained, most basinward prodelta facies (Fig. 6; Scruton, 1960; Coleman, 1981). As the deltaic system progrades and the depositional surface shifts basinward, these facies likewise prograde. Thus, progradation produces the coarsening-upward succession of facies characteristic of all deltas (Scruton, 1960; Coleman, 1981).

#### Major Depositional Environments of the Mississippi Delta

The various environments of deposition found within the Mississippi Delta region are divided, and discussed herein, into two categories: those that form during the regressive phase and those that form during the transgressive phase. Furthermore, depositional environments of the regressive phase are divided further (*sensu* Coleman, 1981): those that constitute the subaqueous delta (i.e. those that accumulate below sea level) and those that constitute the subaerial delta (i.e. those that accumulated near or above sea level). Depositional environments of the subaqueous delta include the prodelta, delta front, distributary mouth bar, and subaqueous natural levee. As for the subaerial delta, this study is only concerned with the lower delta plain (Coleman and Prior, 1982). Depositional environments of the subaerial, lower delta plain include channels, natural levee or overbank splays, interdistributary bays, subdeltas or bay fills, and marshes. Depositional environments comprising the transgressive phase may include lagoonal, overwash, backshore-dune, foreshore, shoreface, tidal inlets, tidal deltas, shoal base, shoal front, shoal crest, and sand sheet (i.e. retreat path).

### “Regressive Phase: The Subaqueous Delta”

The basal and most seaward depositional environment of the regressive delta is the prodelta (Fig. 14; also Fig. 6). The prodelta facies is characterized as a blanket of clays deposited from suspension, with broad lateral continuity and low lithologic variation (Roberts, 1980; Coleman, 1982). Deposits of the prodelta may vary considerably in thickness, approaching 100 m within the deep-water birdfoot delta (Fisk et al., 1954) to less than 1 m within parts of the Atchafalaya bayhead delta (Roberts et al., 1980). Parallel laminations are the dominant primary structures, although unlithified prodelta sediments may appear as massive, structureless clays unless viewed with an X-ray radiograph. In the most seaward, basal portions of the prodelta, parallel laminations are generally very thin and less frequent, whereas in the shallower, more landward portions of the prodelta, silty parallel laminations become thicker and more common with even cross-laminated and current-ripple primary structures occasionally encountered (Coleman and Gagliano, 1965; Coleman, 1981; Coleman and Prior, 1982; Roberts, 1998). As the depositional rate is relatively high, bioturbation of sediments is generally low, although intensity may increase locally (Coleman and Gagliano, 1965; Roberts et al., 1980; Coleman, 1981; Coleman and Prior, 1982). The degree of bioturbation generally increases towards the seaward and basal margins of the prodelta. Ultimately, the prodelta grades into a bay or shelf facies where clay sediments accumulate under much slower rates of deposition, and which are thus significantly reworked by bioturbation (Coleman and Gagliano, 1965; Roberts et al., 1980; Coleman, 1981; Coleman and Prior, 1982; Roberts, 1998).

Lying above and landward of the prodelta facies is the delta front facies (Fig. 14; also Fig. 6). (The delta front is also referred to as distal bar, delta platform, or delta fringe. This



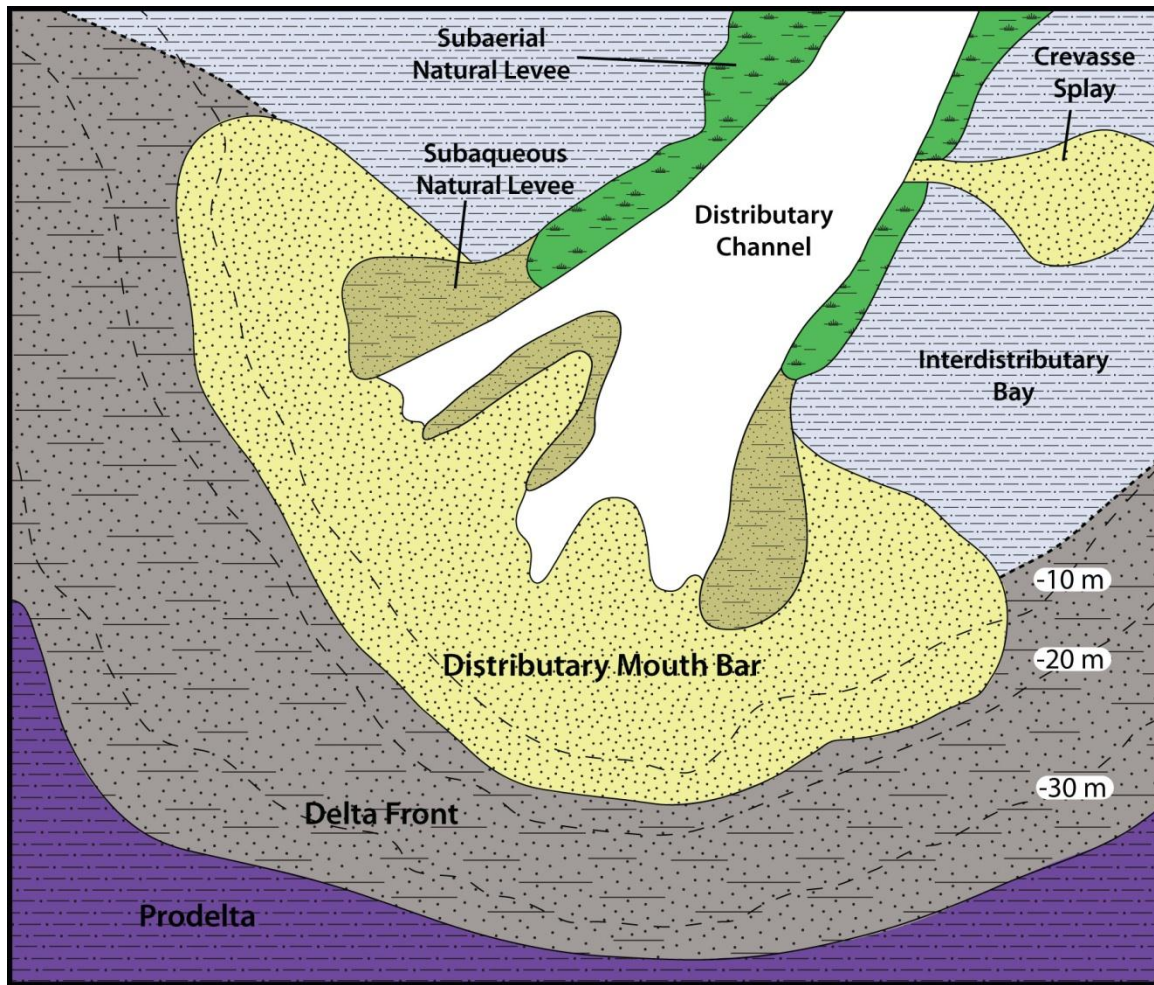


Figure 14. An idealized plan-view schematic of the major depositional environments, or facies, associated with the prograding Mississippi Delta. Modified from Coleman, 1981.

dissertation follows the terminology of Coleman, 1981). Compared with the other subaqueous deltaic environments, the delta front has the steepest depositional slope, although even the slope of the deep-water Mississippi Birdfoot Delta rarely exceeds 0.5 to 0.75 degrees (Coleman, 1981; Coleman and Prior, 1982). The delta front is distinguished from the prodelta by higher sedimentation rates, coarser sediments, and a greater influence from current and wave processes. In the lower, more seaward parts of the delta front, sediments are characterized by parallel and lenticular laminated silts and clays, with occasional thin layers of sand (Coleman and Gagliano, 1965; Roberts et al., 1980; Coleman, 1981; Coleman and Prior, 1982). In the shallower, more

landward parts of the delta front (i.e. closer to channel mouths), sediments become coarser, alternating between interlaminated silts and clays and interbedded silts and silty sands (Coleman and Gagliano, 1965; Roberts et al., 1980; Coleman, 1981; Coleman and Prior, 1982). The shallower, more landward parts of the delta front are also subjected to greater influences from both unidirectional and oscillatory currents associated with river flood stages and waves, respectively (Coleman and Gagliano, 1965; Roberts et al., 1980; Coleman, 1981; Coleman and Prior, 1982). Thus, various primary structures such as small-scale cross laminations, scour and fill, current ripples, and erosional truncation are more common (Coleman and Gagliano, 1965; Roberts et al., 1980; Coleman, 1981; Coleman and Prior, 1982). In spite of high depositional rates, burrowing may occur due to diluted salinities and nutrient-laden currents, but it is generally more prevalent in the lower parts of the delta front (Coleman and Gagliano, 1965; Coleman, 1981; Coleman and Prior, 1982).

Lying above and landward of the delta front facies is the distributary mouth bar facies (Fig. 14). The distributary mouth bar is also adjacent to the seaward limit of the channel mouth(s). Here, the delta's coarsest sediments accumulate very rapidly in consequent to the drastic reduction of the stream's velocity and, thus, carrying capacity as the stream debouches beyond the confines of its channel and into the receiving basin (Coleman et al., 1964; Coleman and Gagliano, 1965; Roberts et al., 1980; Coleman, 1981; Coleman and Prior, 1982). Hence, distributary mouth bar sediments within the Mississippi Delta are predominantly fine sands and coarse silts. Any finer sediments that accumulate are mostly reworked and removed by constant marine processes and fluvial currents. These same hydrodynamic processes also give rise to the primary sedimentary structures that dominate the distributary mouth bar facies: thin, multi-directional, trough-cross laminations and current-ripple drift (Coleman et al., 1964; Coleman and

Gagliano, 1965; Roberts et al., 1980; Coleman, 1981; Coleman and Prior, 1982). Although less common (but diagnostic), gas-heave structures may form as gas from underlying sediments is expelled through the distributary mouth bar (Coleman et al., 1964; Coleman and Gagliano, 1965). In the upper portions of the distributary mouth bar, laminations or thin beds of plant debris may also occur. Such strata originate from degraded, river-borne organics (e.g. degraded logs and sticks) discharged into the nearshore zone where they can be ground down further into even finer organic particles, or “coffee grinds”, by wave energy (Coleman and Gagliano, 1965; Coleman, 1981; Coleman and Prior, 1982).

The subaqueous natural levee facies is essentially an extension of the subaerial natural levee facies (discussed below) into the shallow marine environment (Fig. 14). As the stream debouches into the receiving basin, the subaqueous natural levee aggrades at the outer perimeters in response to the reduced current velocity (Coleman and Gagliano, 1965; Coleman, 1981). However, its basinward extent is rather limited. For example, the subaqueous natural levees associated with Johnson’s Pass, a small distributary in the modern Birdfoot Delta, extend basinward no farther than ~ 1.2 km before completely grading into the distributary mouth bar facies (Coleman et al., 1964). The dominant lithology of the subaqueous natural levee is very-fine sand and silt, with thin clay or organic-debris laminations occasionally encountered (Coleman et al., 1964; Coleman and Gagliano, 1965; Coleman, 1981). Similar to the distributary mouth bar environment, the subaqueous natural levee is subjected to the same reworking and winnowing processes. Thus, current related structures are dominant, and include wave ripples, parallel laminations, and other complex forms of cross laminations (Coleman et al., 1964; Coleman and Gagliano, 1965; Coleman, 1981).



### “Regressive Phase: The Subaerial Delta”

The distributary channel is the conduit for which a portion of the overall discharge and sediment load of the parent river system is dispersed into the receiving basin (Fig. 14; Coleman et al., 1964; Coleman and Gagliano, 1965; Coleman, 1981; Coleman and Prior, 1982). Distributary channels range in size, from as large as the main river itself to as small as 2 – 3 m wide and ~ 1 m thick (Coleman, 1981). Near its base, channel fill reflects the fluvial processes under which the distributary operates. Poorly-sorted channel sands and silts, characterized by cross-laminations, current ripple laminations, scour and fill, erosional truncations, and slump-type structures, are interbedded with an abundance of organic debris and sporadic clay layers that escape erosion (Coleman et al., 1964; Coleman and Gagliano, 1965; Coleman, 1981; Coleman and Prior, 1982). After the channel is abandoned, the active influx of water and sediment is severely suppressed. In time, the remaining accommodation of the channel will largely fill with highly bioturbated, poorly-sorted silts, clays, and organic debris (Coleman, 1981; Coleman and Prior, 1982).

Subaerial natural levees are areas of slightly higher elevation that border and confine the channel (Fig. 14; Coleman et al., 1964; Coleman and Gagliano, 1965; Coleman, 1981; Coleman and Prior, 1982). During annual floods, channel flow may overtop the subaerial natural levees and in some places may even cause small crevasses splays to emerge (Coleman, 1981; Coleman and Prior, 1982). Individual crevasses may remain active for a year to several years as they aggrade the subaerial natural levee (Coleman, 1981; Coleman and Prior, 1982). This process is intermittent along the river and its distributaries and is partially responsible for the deposition and, thus, buildup of the subaerial natural levee to flood-stage level (Coleman, 1981; Coleman and Prior, 1982). The subaerial natural levee is largely characterized by very-fine sand and silt

strata with sporadic organic and clay laminations. Primary sedimentary structures within the coarse strata may include current ripples and a variety of cross laminations (Coleman et al., 1964; Coleman and Gagliano, 1965; Coleman, 1981; Coleman and Prior, 1982). In some respects, subaerial natural levee facies resembles the subaqueous natural levee and the delta front facies. However, it can be readily distinguished by the burrowing of both plant and animals, which can be intense (Coleman et al., 1964; Coleman and Gagliano, 1965; Coleman, 1981).

Interdistributary bays are largely shallow, open bodies of brackish-to-marine water surrounded by distributary systems and/or marsh and typically open to the sea or connected to it by tidal channels (Fig. 14; Coleman et al., 1964; Coleman and Gagliano, 1965; Coleman, 1981; Coleman and Prior, 1982). The lithology is primarily comprised of fine-grained sediments originally carried into the bays during river floods or from abnormal high tides caused by storms (Coleman et al., 1964; Coleman and Gagliano, 1965; Coleman, 1981). Lenticular laminations, a product of wave reworking, are the most common primary sedimentary structure (Coleman et al., 1964; Coleman and Gagliano, 1965; Coleman, 1981; Coleman and Prior, 1982). Current-induced parallel laminations, current ripples, and scour and fill structures are occasionally encountered and likely formed by tidal currents or during flooding of the Mississippi River (Coleman et al., 1964; Coleman and Gagliano, 1965; Coleman, 1981; Coleman and Prior, 1982). However, the preservation potential of primary sedimentary structures is low, as bioturbation in this environment is generally intense (Coleman et al., 1964; Coleman and Gagliano, 1965; Coleman, 1981; Coleman and Prior, 1982).

As discussed above, crevasse splays occasionally break through the subaerial natural levee. Rather than aggrading the levee and shutting off after a year or so, a crevasse splay may instead gradually increase its discharge and sediment load and eventually extend itself farther

basinward into the accommodation of the interdistributary bay via a complex network of highly-bifurcating channels (Fig. 14; Welder, 1959; Coleman and Gagliano, 1964). Bay-fill crevasses are essentially mini deltas, exhibiting the same coarsening-upward succession of facies as described above for the subaqueous delta (Coleman and Gagliano, 1964; Coleman, 1981; Coleman and Prior, 1982). Deposition within a bay fill eventually terminates, however, and it ultimately submerges under marine waters due to subsidence (Coleman and Gagliano, 1964; Coleman, 1981; Coleman and Prior, 1982). The newly converted bay environment may later be filled by another bay-fill crevasse, resulting in the stacking pattern of successive bay-fill deposits (Coleman and Gagliano, 1964; Brooks et al., 1995).

Capping a complete deltaic sequence is the marsh environment (Fig. 14). Marshes of the Mississippi Delta range from fresh to brackish to salt (Coleman et al., 1964; Coleman and Gagliano, 1965; Coleman, 1981). As for sedimentology, they are most notable for their accumulation and preservation of organic materials under anoxic conditions (Coleman et al., 1964; Coleman and Gagliano, 1965; Coleman, 1981; Coleman and Prior, 1982). Soils of salt- and brackish-water marshes (i.e. near the coast) are, however, generally more clay-rich than are soils of fresh-water marshes, as the latter tends to preserve more organics (Hatton et al., 1983). For the most part, bioturbation completely obliterates any previously formed primary sedimentary structures (Coleman et al., 1964; Coleman and Gagliano, 1965; Coleman, 1981; Coleman and Prior, 1982).

#### “Transgressive Phase”

The complete transgressive component consists of lagoonal deposits underlying either a core barrier-island complex or a fully marine sand body (Penland and Boyd, 1981; 1985; Penland et al., 1985; 1988). The two alternatives are a function of the degree of reworking of the

original barrier island facies, which itself is a function of time (Penland et al., 1986; 1989; 1990). As discussed above, an example of each is thought to be Trinity Shoal and Ship Shoal, respectively. The following discussion will first describe the vertical succession of facies with preserved barrier-island depositional environments followed by a description of the more evolved transgressive sequence associated with a fully marine sand body.

The lagoonal facies is the lowermost depositional environment in a vertical succession of transgressive facies, lying unconformably above the regressive component (Fig. 15; Van Heerden et al., 1985; Penland et al., 1986). This facies may in fact be transitional, as a brackish-water, restricted interdistributary bay environment may occur at the very base before transitioning vertically into a more saline, lagoonal environment (Penland et al., 1986). The existence of brackish-water carbonate shell reefs (e.g. *Rangia* sp. and *Crassostrea* sp.) is the only major distinguishing aspect (Penland et al., 1986). The lagoonal environment generally consists of fine-grained sediments that slowly accumulate in a biologically active, shallow-water environment (Van Heerden et al., 1985; Penland et al., 1986). Primary sedimentary structures including parallel laminations, starved ripples, and asymmetrical ripple laminations may occur (the latter two under storm conditions), but their preservation potential is generally very low owing to animal burrowing (Penland, et al., 1986). As such, this facies is characterized as a highly-bioturbated, silty-clay unit with scattered sand lenses and shell fragments, and both vertical and horizontal burrows are commonly filled with sand and shell (Van Heerden et al., 1985; Penland et al., 1986).

Building atop of the lagoonal environment are overwash deposits (also called washover deposits), which form by the overtopping or breaching of a barrier island during the passage of a

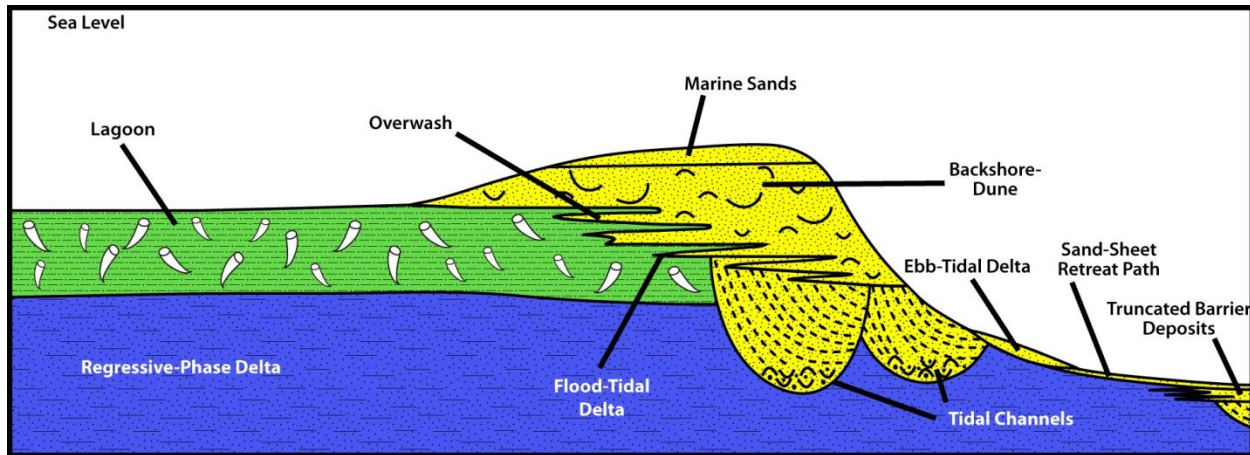


Figure 15. An idealized schematic cross section of a Stage 3 subaqueous, inner-shelf sand shoal. Here, much of the original barrier-island's facies are preserved. Modified from Penland et al., 1990.

tropical cyclone (Fig. 15; Boyd and Penland, 1981; Kahn and Roberts, 1982). This facies is first perceived by the interfingering of thin, coarse-grained overwash deposits within the thicker, fine-grained lagoonal deposits (Van Heerden et al., 1985). In a vertical sense, individual overwash deposits within this facies become thicker towards the surface at the expense of fine-grained lagoonal sediments as the barrier island continues to migrate landwards (Van Heerden et al., 1985). Overall, overwash deposits are predominantly sand (Van Heerden et al., 1985; Flocks et al., 2009). Cross laminations may form, but bioturbation is generally intense and, thus, preservation is low (Van Heerden et al., 1985). Furthermore and in addition to animal burrowing, root burrowing may occur near the top of the overwash facies, indicating back-barrier aquatic plant growth (Van Heerden et al., 1985).

Stratigraphically above the overwash facies is the backshore-dune facies (Fig. 15). This environment is primarily subaerial, and as such is dominated by wind-generated depositional processes (Reinson, 1984). Wind-winnowed, clean-sand deposits are characterized by multidirectional, parallel-to-cross stratified structures, with trough-cross strata also common

(Reinson, 1984; Van Heerden et al., 1985). However, bioturbation, particularly that associated with plant-root growth, may be intensive (Reinson, 1984; Van Heerden et al., 1985). Small paleosol horizons, another element associated with biological activity, may also occur (Reinson, 1984; Van Heerden et al., 1985).

A barrier island may also be crosscut by several tidal channels (Fig. 15). Sandy sediments accumulate within the tidal channel as the channel migrates laterally in the direction of longshore sediment transport, resulting in a facies that is largely characterized by an erosional base, large-scale planar-to-trough cross beds within the bottom section, and grain size and primary sedimentary structures both fining upwards (Reinson, 1992). Primary sedimentary structures are also bidirectional, a consequent of ebb- and flood-tidal currents (Reinson, 1992). Fundamentally related to tidal channels are tidal deltas. The flood-tidal delta forms landward of the barrier island, whereas the ebb-tidal delta forms seaward. Deposits of tidal deltas display textures and primary sedimentary structures similar to deposits of the tidal-channel fill (Reinson, 1984).

Seaward and immediately adjacent to the backshore environment is the foreshore. This part of the barrier island forms within the intertidal zone and is dominated by the swash and backwash of breaking waves (Reinson, 1984; Walker and Plint, 1992). Sand deposits generally display low-angle planar laminations (Reinson, 1984; Walker and Plint, 1992). The foreshore environment transitions basinward into the sandy shoreface environment, which forms between the low-tide mark and the fair-weather wave base (Reinson, 1984; Walker and Plint, 1992). The shoreface is associated with combined wind-driven and oscillatory (wave) fair-weather currents, which commonly produce combined-flow, fair-weather primary sedimentary structures such as symmetrical ripples (Walker and Plint, 1992). However, in a storm-dominated, sandy shoreface

environment, such as those adjacent to Louisiana's barrier islands, fair-weather sedimentary structures are commonly obliterated and replaced with storm-generated hummocky cross strata (Walker and Plint, 1992).

Note that the discussion above on both foreshore and shoreface facies is not in the context of vertical succession of facies. Instead, these facies are discussed in the context of lateral succession. The reason for this digression is that these environments, as well as the backshore-dune environment, are subjected to extensive reworking during transgression, and it is generally only the lagoonal and overwash deposits that stand a chance of being preserved during transgression (Reinson, 1992). Therefore, in order for the complete suite of barrier-complex facies to be preserved, their burial prior to significant reworking is required. If Trinity Shoal is comprised of its original barrier-island core as many researchers contend (see Penland et al., 1989; 1990; Pope et al., 1991), then this scenario would be playing out today as the newly activated, prograding Atchafalaya Delta Complex builds basinward across Trinity Shoal and the inner-continental shelf.

The continual landward migration, and the reworking that such migration implies, ultimately converts the submerged barrier-island complex into a fully marine sand shoal (Penland and Boyd, 1981; 1985; Penland et al., 1985; 1988). The shoal-base facies represents the advancing edge of the landward-migrating fully marine sand body, which is thought to lie unconformably atop of lagoonal muds associated with the former back-barrier environment (Fig. 16; Penland et al., 1986). (Note that the following discussion is based on work conducted at Ship Shoal, but is considered an analogue for all fully-evolved marine sand shoals associated with the Mississippi Delta; Penland and Boyd, 1981; 1985 and Penland et al., 1985; 1988.) The contact between the shoal base and lagoonal muds is relatively sharp (~ 5 – 15 cm; Penland et

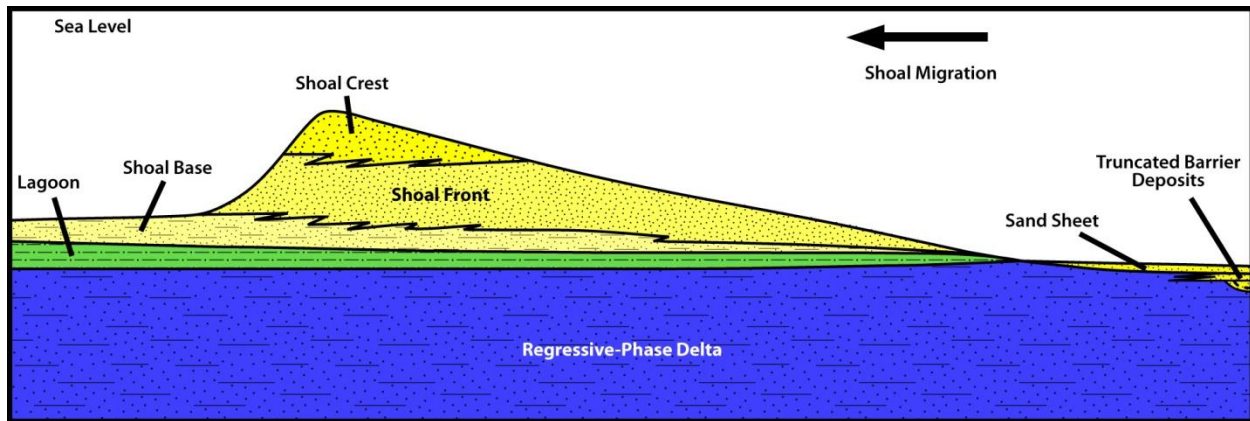


Figure 16. An idealized schematic cross section of a Stage 3 subaqueous, inner-shelf sand shoal. In contrast with Figure 12, all original barrier-island facies have been reworked into a fully-marine lithosome. Modified from Penland et al., 1986 and Kulp et al., 2001.

al., 1986), in contrast with the interfingering of washover sands and lagoonal muds found in the lower parts of the washover facies as described above. The shoal-base facies is characterized by the interlayering of highly-burrowed silty clays and lenticular- to wavy-layered, poorly sorted, very-fine sands (Penland et al., 1986).

Migrating atop of the shoal base is the shoal-front facies (Fig. 16). This facies is composed of moderately sorted, predominantly fine sand derived from erosion of the shoal crest and ramp (Penland et al., 1986). Whole and reworked shells are also scattered throughout (Penland et al., 1986). Horizontal and cross laminations occur, but the facies largely appears massive owing to intensive bioturbation (Penland et al., 1986).

Migrating atop of the shoal front and extending into the zone of active fair-weather processes is the shoal-crest facies (Fig. 16; Penland et al., 1986). This facies consists of clean, moderately sorted fine sand (Penland et al., 1986). Note that fine sands of the shoal crest are coarser than those of the shoal front. Hence, there is a coarsening upward of grain size, from the very-fine sands associated with the shoal base to the fine sands of the shoal front and crest. Graded layers of sand and shell approximately 10 – 50 cm thick are supposedly common in the



shoal crest and are interpreted as storm beds (Penland et al., 1986). Individual storm beds are characterized by a sharp, erosional base of sand and shell, which transitions upwards into parallel and cross laminations (Penland et al., 1986). In turn, sedimentary structures transition upwards into medium-scale trough cross-beds (Penland et al., 1986). Lastly, individual storm beds are capped by symmetrical ripple laminations, which reflect deposition in fair-weather oscillatory wave conditions (Penland et al., 1986). Burrowing is common in the shoal crest but is generally less intensive than what occurs at the shoal base and shoal front (Penland et al., 1986).

Extending seaward from the shoal complex (as well as from a transgressing, subaerial barrier island for that matter) and marking its retreat path is the sand-sheet facies (Fig. 16; also Fig. 15). (Note that the shoal ramp environment of Figure 16 is not discussed by Penland et al., (1986) or any other work, except only to say that it is a source of sand for other parts of the shoal complex.) Shoal migration and the dispersal of sand from storms account for the deposition and accumulation of the sand sheet (Penland and Suter, 1983; Penland and Boyd, 1985; Penland et al., 1986). Seaward dipping, graded bedding and parallel- to cross-laminations occur, but they are likely obscured by burrowing (Penland and Boyd, 1985; Penland and Suter, 1986; Penland et al., 1986). Basinward from the shoal, the sand sheet overlies truncated barrier-island and tidal-channel facies that mark the former positions of Stages 1 and 2 barrier-island shorelines (Penland and Boyd, 1981; 1985; Penland et al., 1985; 1988; also Penland and Suter, 1983).

### **Acoustic Data and Its Analysis**

Acoustic-reflection profiles, or subbottom profiles, are gathered in the marine environment by transmitting an acoustic signal through the water column into the underlying sediments and then measuring the duration of time between the pulse transmission and the arrival

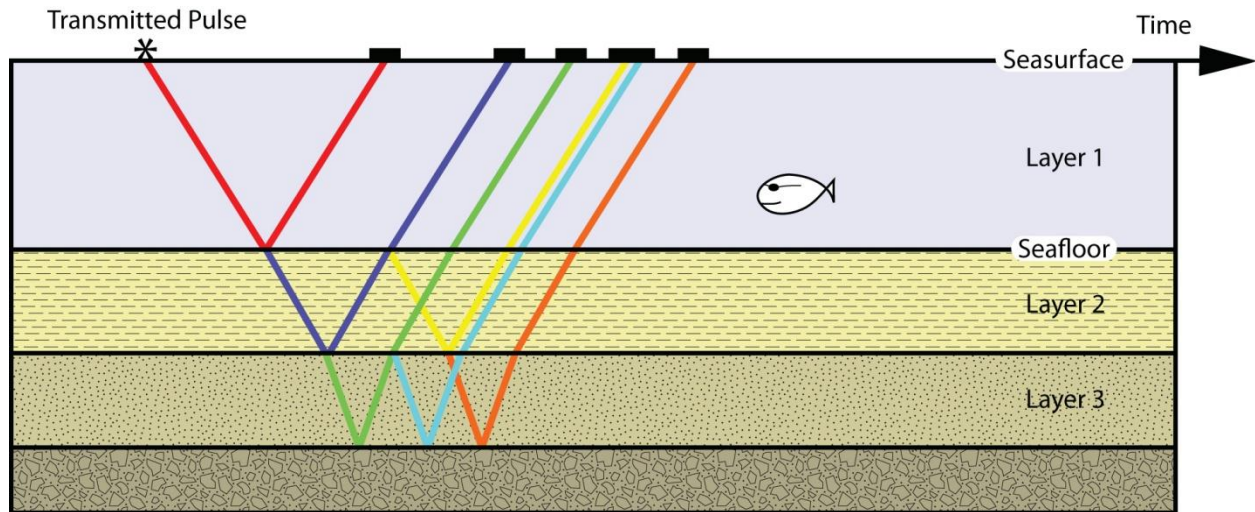


Figure 17. An idealized schematic subbottom profile depicting the paths (among many others) taken by certain rays (i.e. acoustic energy) through the water column and underlying strata. The horizontal axis indicates the duration of time between the pulse transmission and the arrival of the reflected signals. After Stevenson et al., 2001.

of the reflected signals (Fig. 17; Quinn et al., 1997). Acoustic reflections occur at interfaces (e.g. bedding contacts and unconformities) separating layers of contrasting density and/or compressional wave velocity (Cant, 1992; Quinn et al., 1997; Liner, 2004). For a given layer, the product of these two parameters is referred to as its acoustic impedance. The greater the contrast in impedance between adjacent layers, the larger the reflection's amplitude will be (Cant, 1992; Quinn et al., 1997; Liner, 2004). In contrast, if an interface separates layers with similar impedance, then very little if any energy will be reflected, and the interface will go undetected (Cant, 1992; Quinn et al., 1997; Liner, 2004). Note that only a portion (the exact portion is dependent on the contrast in impedance) of the acoustic energy is reflected at a given surface, while the remainder is transmitted deeper (Liner, 2004). Accordingly, deeper, subsequent surfaces separating layers of contrasting impedance will successively reflect portions of transmitted acoustic energy (Cant, 1992; Liner, 2004).

As with sedimentological data, facies analysis can also be applied to acoustic data. Acoustic-facies analysis involves the characterization and interpretation of acoustic reflection parameters, including their configuration, continuity, amplitude, frequency, and interval velocity (Mitchum et al., 1977). Acoustic reflectors with similar parameters are grouped into three-dimensional acoustic-facies units, so that each unit's reflection parameters differ from those of adjacent units (Mitchum et al., 1977). The external boundaries of each acoustic-facies unit may be obvious and easily identified from a series of reflectors that terminate against a common reflector or from a conformable reflector that bounds a particular configuration (Mitchum et al., 1977). Figure 18 displays various types of reflection terminations, each a function of stratal terminations. If instead a gradational change in the reflection parameters is observed, then an arbitrary boundary is placed (Mitchum et al., 1977). Note that reflection terminations are discussed by Mitchum et al. (1977) on the scale of seismic sequences (i.e. depositional sequences or system tracts), but the same principles can be applied, and are so within this study, on a finer scale of acoustic resolution (i.e. parasequence). Likewise, this same reasoning applies to the following discussion.

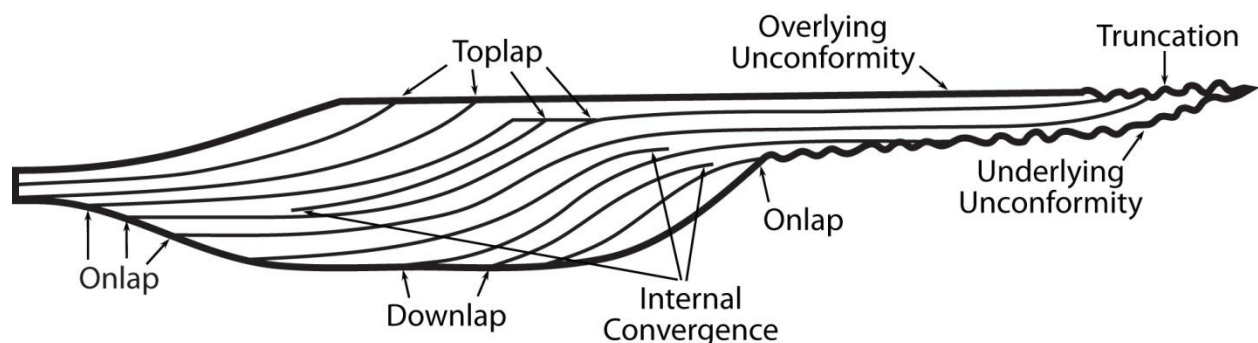


Figure 18. An idealized seismic sequence depicting various types of reflection terminations. Modified from Mitchum et al., 1977.

The overall style of an acoustic-facies unit is defined by its external form and its internal reflection configuration, the latter being the most apparent and readily analyzed reflection parameter (Mitchum et al., 1977). Figures 19 and 20 depict various external forms and reflection-configuration patterns, respectively, that may be observed from analyzing acoustic data from various geological settings. The configuration of reflectors imparts the gross stratigraphic patterns of a particular unit, whereas the external form reveals the unit's three-dimensional sedimentary structure (Mitchum et al., 1977). Lending to reflection-configuration patterns and the stratigraphic interpretation they impart are: (a) reflection continuity, which conveys the continuity of strata, or lack thereof, (b) frequency, which reveals the spacing of reflectors as measured in time or depth, and (c) amplitude, which imparts the contrast in impedance between adjacent layers (Mitchum et al., 1977). By defining three-dimensional associations among separate, genetically related acoustic-facies units, the depositional environment, depositional processes, and estimates of lithology can be interpreted (Mitchum et al., 1977).

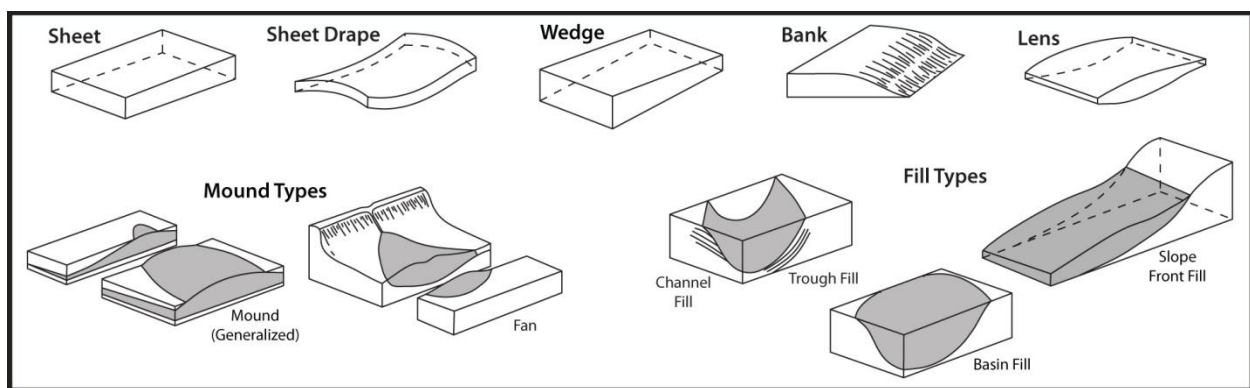


Figure 19. Some of the various types of external forms that may characterize different acoustic-facies units. Modified from Mitchum et al., 1977.

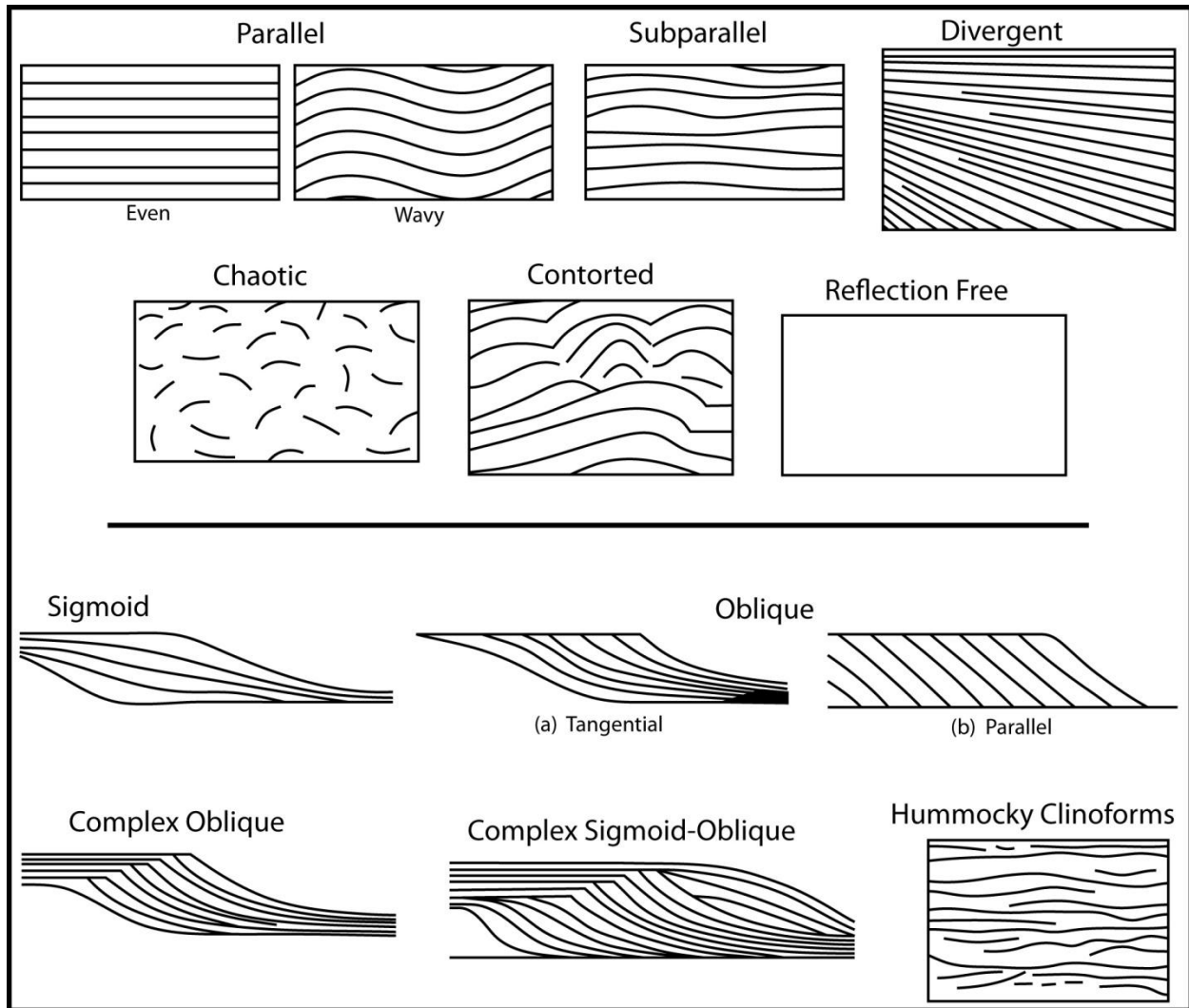


Figure 20. Some of the various types of reflection-configuration patterns. The bottom half are associated with strata that form by way of progradation. For the Complex Oblique and Complex Sigmoid-Oblique reflection-configuration patterns, note that this study follows the terminology of Berg, 1982. Modified from Mitchum et al., 1977 and Berg, 1982.

The representative acoustic-reflection pattern for a high-energy, fluvial-dominated delta is the tangential-oblique progradational-configuration pattern, which is generally bounded by a fan-shaped external form (Figs. 19 and 20; Sangree and Widmier, 1977; Berg, 1982). The tangential-oblique reflection-configuration pattern is characterized by clinoforms that terminate updip by toplap and downdip by downlap (Sangree and Widmier, 1977; Berg, 1982). The coarser-grained delta plain and delta front is coincident with the upper, more horizontal part of

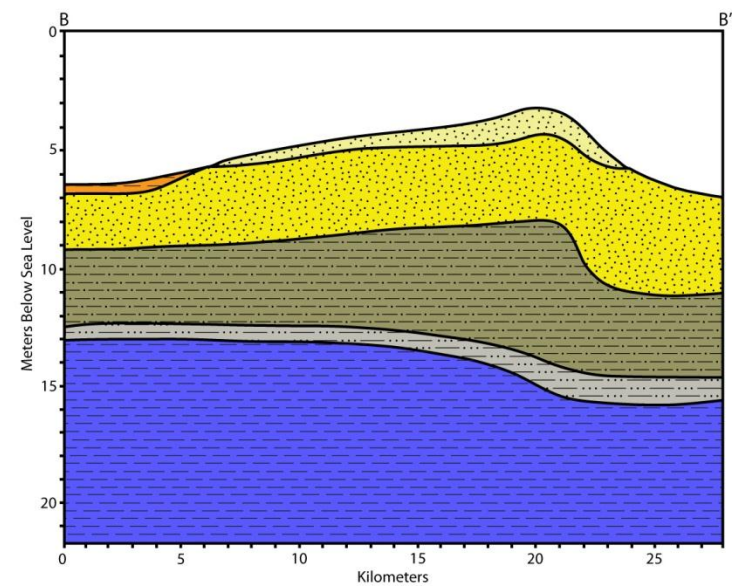
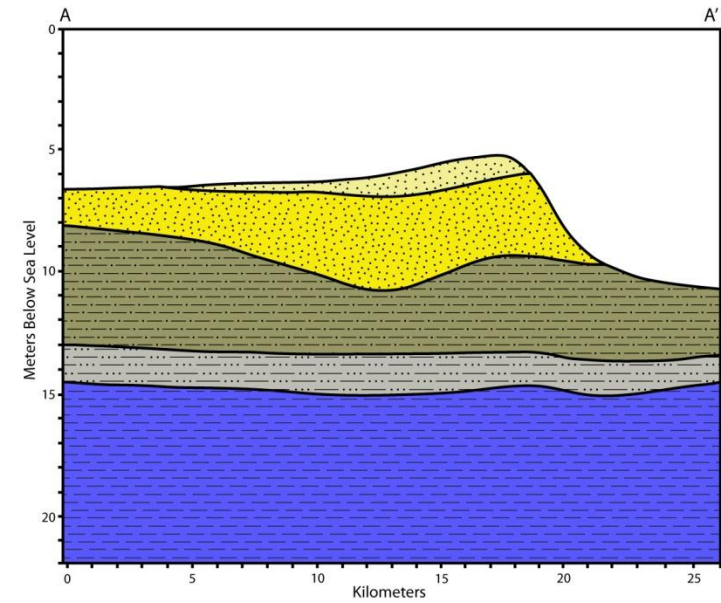
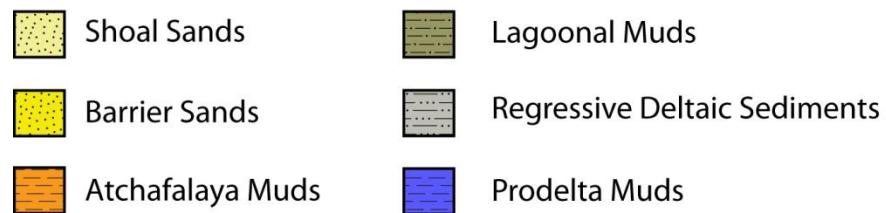
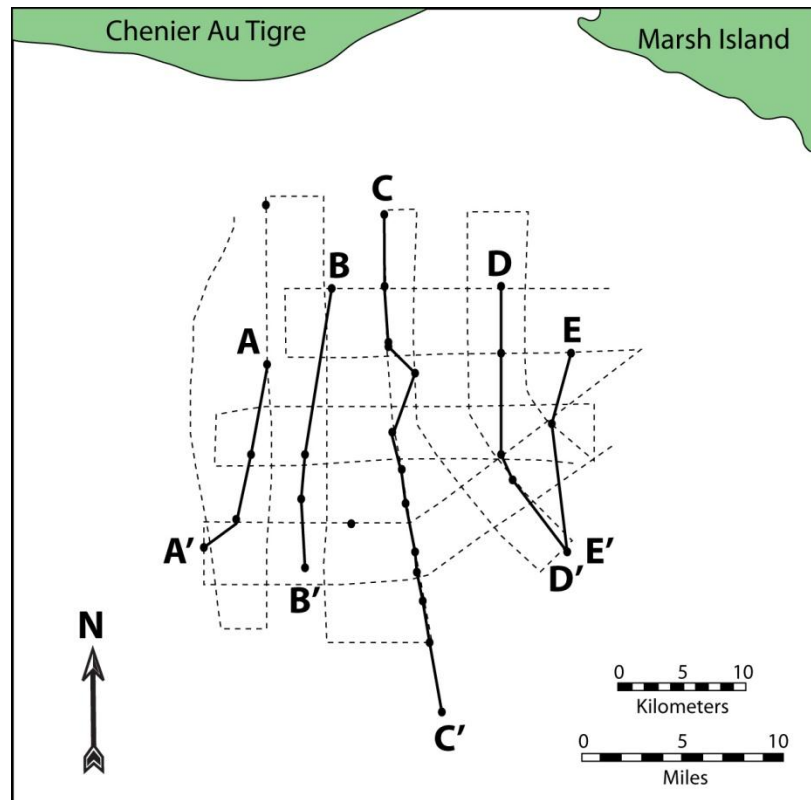
the reflection pattern (i.e. the topset and upper parts of the foreset), whereas the middle-to-lower parts reflect the prodelta clays (i.e. middle-to-lower parts of the foreset and bottomset; Sangree and Widmier, 1977; Berg, 1982). Other reflection parameters such as continuity, frequency, and amplitude may vary depending on the position in the tangential-oblique configuration (Sangree and Widmier, 1977). In contrast, the sigmoidal reflection-configuration pattern is characterized by S-shaped clinoforms that are concordant with the top of the unit but terminate downdip by downlap (Fig. 20; Sangree and Widmier, 1977; Berg, 1982). Sigmoidal reflectors are typically highly continuous and display moderate-to-high amplitude. Although frequency is typically uniform along depositional strike, it is variable along dip, broadening in the middle clinoform zone where the thicker beds are found (Sangree and Widmier, 1977). The sigmoidal reflection-configuration pattern generally represents a relatively low-energy regime where little or no sand is present (Berg, 1982). However, it is often found adjacent to the high-energy, tangential-oblique pattern (Berg, 1982). Where these two different types of progradational reflection-configuration patterns are observed overlapping one another within the same acoustic sequence, they may be combined into a single reflection-configuration pattern termed complex sigmoid-oblique (Fig. 20; Berg, 1982). (For the complex oblique and complex sigmoid-oblique reflection-configuration patterns (Fig. 20), note that this study follows the terminology of Berg, 1982, which is different from Mitchum et al., 1977). Within a deltaic setting, the complex sigmoid-oblique reflection-configuration pattern suggests delta-lobe switching (i.e. switching from a high-energy, fluvial dominated regime to a relatively low-energy, adjacent marine regime, or vice versa; Berg, 1982).

## Previous Work

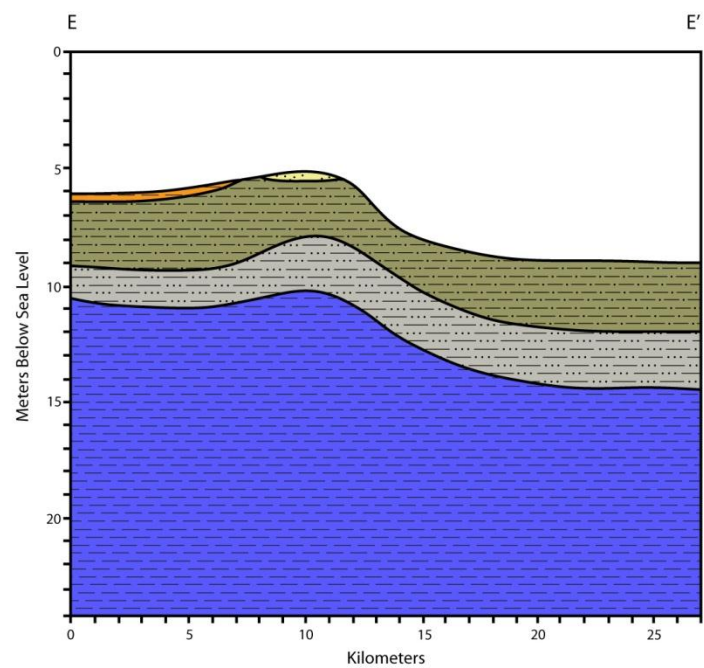
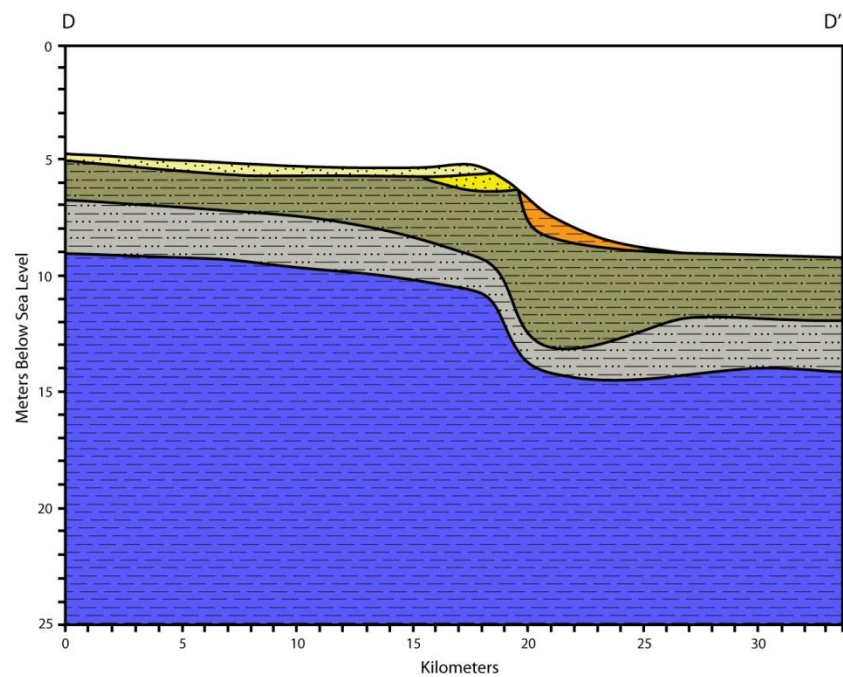
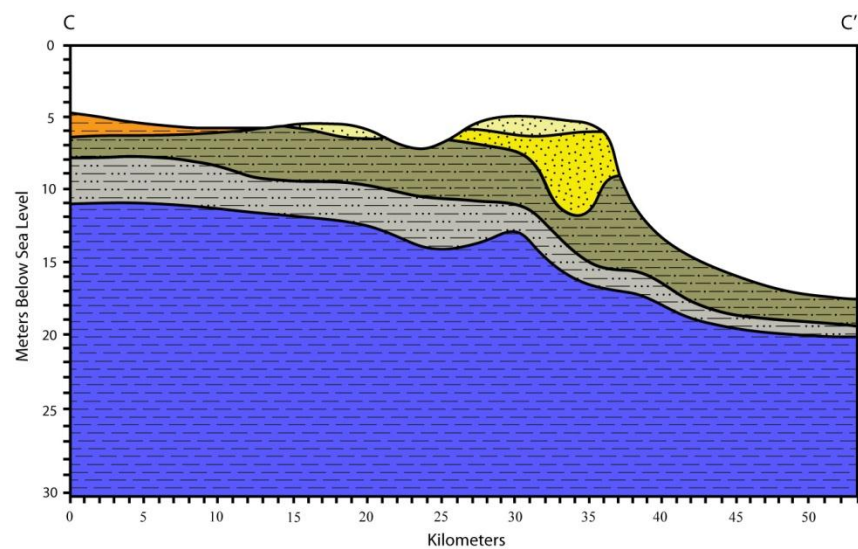
Previous work (Penland et al., 1990; Pope et al., 1991) within the Trinity-Tiger Shoals region was conducted in the mid-1980s as part of a cooperative sand-resource study among the Minerals Management Service, the U.S. Geological Survey, and the Louisiana Geological Survey. Approximately 800 km of high-resolution acoustic profiles and 30 vibracores were gathered and integrated for regional interpretation. However, the acoustic data were not published, and the vibracore data were only presented as percent-sand logs. Nevertheless, they did produce a series of geological cross sections and a regional sand-body isopach map of the study area.

Five north-south cross sections from Penland et al. (1990) and Pope et al. (1991) are depicted in Figure 21. They identified six separate facies. These facies include the regressive depositional environments of the prodelta, the “regressive deltaic sediments” (their inclusive term for the combined delta-front and distributary-channel environments) and the recent Atchafalaya muds, as well as the transgressive depositional environments of the shoal sands, barrier-island sands (including the various subenvironments of the barrier island as discussed previously), and lagoonal muds. For all five transects, they interpret an extensive blanket of lagoonal muds extending out of the study area in both the seaward and landward directions, a transect that is greater than 50 km. This interpretation implies that a once-subaerial Trinity barrier island existed at least 20 km basinward of its present location (refer to C-C’ of Figure 21). Furthermore, they do not distinguish a separate sand lithosome north of Trinity Shoal but instead

Figure 21. Five north-south cross sections illustrating the subsurface of the Trinity-Tiger Shoals region, as interpreted by Penland et al. (1990) and Pope et al. (1991). A base map indicating the location and trend of each cross section is also included. Dashed lines and black dots along the base map represent the acoustic survey tract lines and vibracore locations, respectively, that were used to generate cross sections. Modified from the above authors.







interpret an undivided barrier-shoal complex. Their sand-body isopach map augments this interpretation (Fig. 22). This interpretation suggests a Trinity Shoal-Barrier system larger than 35 km long by 32 km wide.

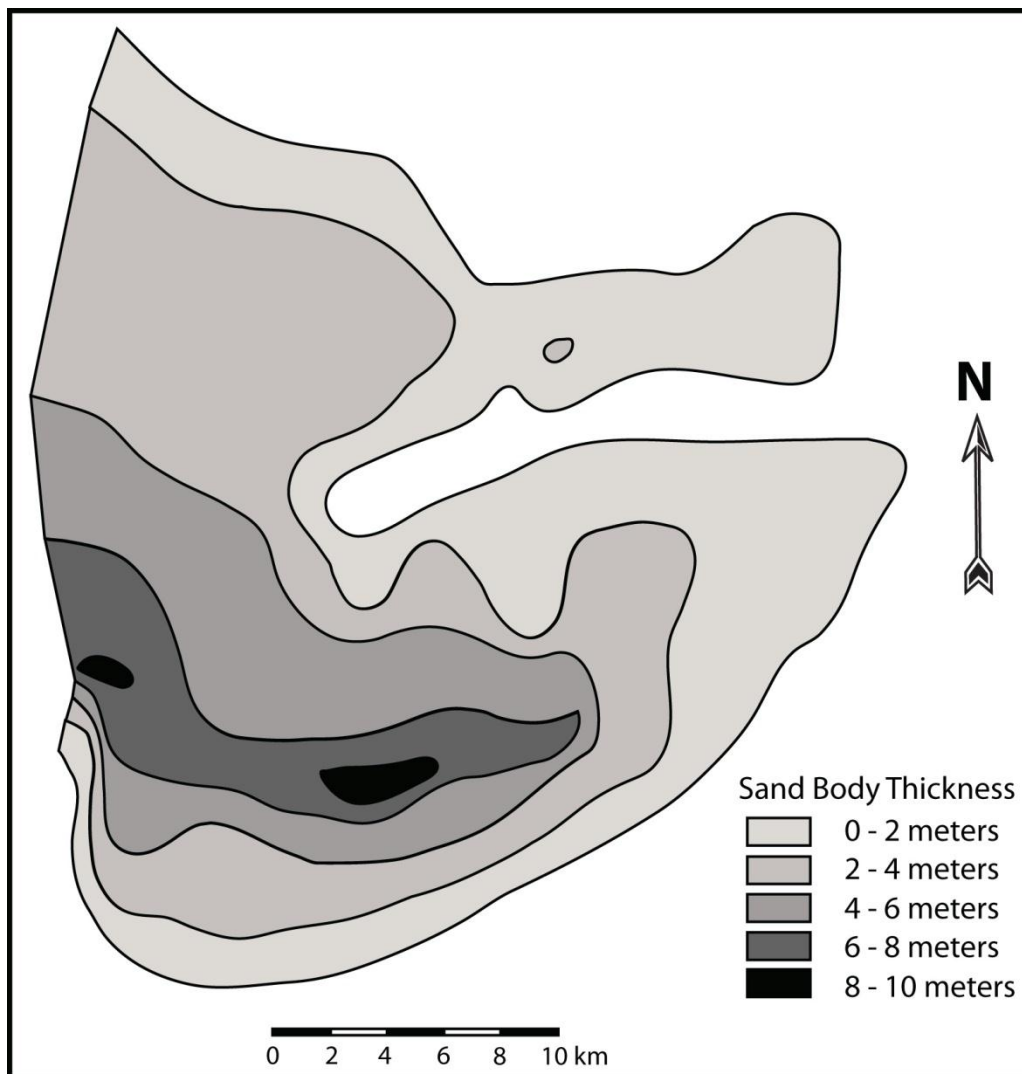


Figure 22. An isopach map of the Trinity-Tiger Shoals region, as interpreted by Penland et al. (1990) and Pope et al. (1991). See the above authors for the exact location of the isopach map relative to the survey grid displayed in Figure 21. Modified from the above authors.

## METHODOLOGY

### R/V Coastal Profiler

All field-data collection occurred on the R/V Coastal Profiler, a Lafitte Skiff with an overall length of 12.5 m and a beam of 5.2 m (Fig. 23). The vessel was custom built for Coastal Studies Institute (CSI) for the purpose of shallow-water geophysical surveying and vibracoring. An EdgeTech SB512i towfish was towed from the port side approximately 0.5 – 0.75 m beneath the water surface, and a fathometer was attached along the starboard side at a fixed depth of 0.5 m. Vibracoring occurred from the stern.



Figure 23. The R/V Coastal Profiler. This vessel was used for geophysical surveying and vibracoring.

### Navigation

Accurate geographical coordinates are essential for data integration. Navigation data were acquired using a C&C Technologies GPS receiver system utilizing SatLoc3 differential

GPS that produces sub-meter accuracy. Navigational data were delivered in real time and incorporated into the chirp sonar subbottom digital data set. The GPS-fix data were sent to the data acquisition systems at a rate of one fix per second. Navigational control was maintained on an IBM compatible PC running HYPACK 2010® navigational software. A navigational chart with a plot of the survey plan was displayed along with the vessel's position, orientation, course, and speed. Similar GPS location data were acquired at each vibracore site.

### **Geophysical Surveying**

High-resolution subbottom profiles were gathered using an EdgeTech SB512i towfish, a chirp sonar system that uses a linearly swept, frequency modulated pulse to penetrate the subsurface (Fig. 24). Insonification was performed at a frequency range of 2 – 12 kHz with a sweep duration of 20 msec. Acquired data were processed in real time using EdgeTech's DISCOVER subbottom software and saved in the industry standard SEG-Y format. Navigation data from differential GPS were also retained for each shotpoint within the SEG-Y data. Geophysical surveying was carried out in water depths ranging from ~ 3.5 to 20 m (Fig. 25) and at a cruising speed of ~ 5 knots.

The initial geophysical survey (2007) collected ~ 1,150 km of subbottom profiles: 42 north-south profiles, with a spacing interval of ~ 0.9 km, and 11 east-west profiles, with a spacing interval of ~ 2.3 km, were gathered (Fig. 25). A second survey (2010) collected an additional ~ 200 km of profiles, and in doing so extended the subbottom coverage further west and south. Geophysical data were imported into Petrel<sup>TM</sup> software for interpretation.

### **Vibracoring**

Sediments were sampled using a marine vibracoring system custom built for CSI by SEAS Vibracoring Systems of Australia. The assembled vibracorer consists of a watertight,



Figure 24. The EdgeTech SB512i towfish being deployed from a davit on the R/V Coastal Profiler. The towfish was towed approximately 0.5 – 0.75 m beneath the water surface.

steel head with two 3-phase electric motors within, a relatively lightweight tubular aluminum tower with three legs, and the core barrel encased within the tower and secured to the motor head at the top (Fig. 26). Core barrels used in this study were made from 7.6 cm diameter aluminum tubing cut to 4.5 m lengths.

Following the mapping of major acoustic reflectors using Petrel<sup>TM</sup> software, generated surfaces were used to guide the selection of vibracoring sites. The motivation was to penetrate these surfaces in as many locations as possible so as to integrate core data with geophysical data and, afterward, extrapolate stratigraphic and geologic interpretations across the study area. In 2008, 46 vibracores were extracted (Fig 25). Once on board, cores were immediately cut into 1.5 m sections, capped, and labeled for future analyses. A second coring campaign followed in 2010 when 14 additional cores were collected to augment incomplete core data (i.e. short cores)



collected in 2008, as well as to cover additional areas where ground-truthing data were desired.

Table 1 lists the identification numbers and geographic locations of all vibracores collected.

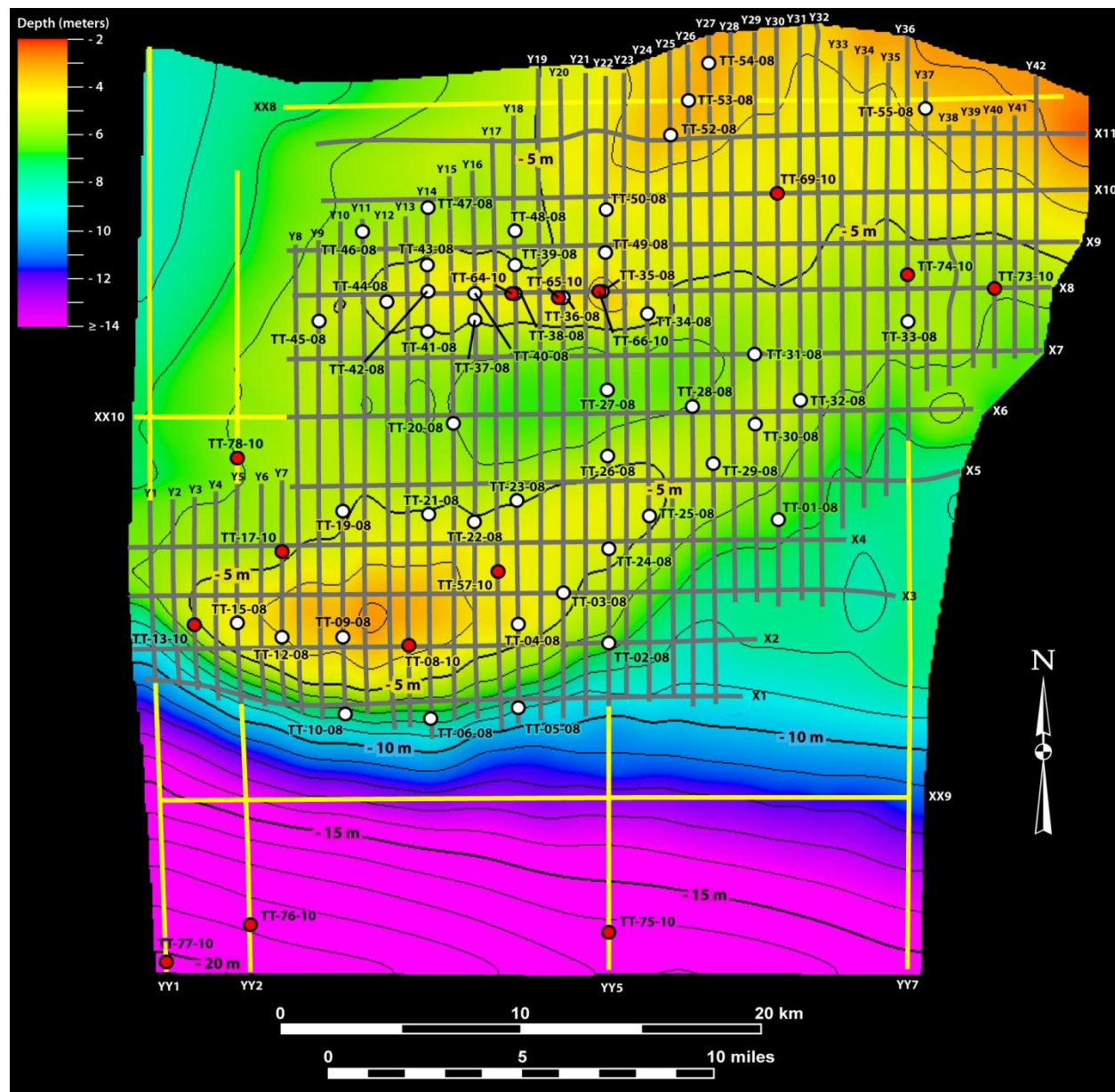


Figure 25. The geophysical survey grid of the Trinity-Tiger Shoals region along which high-resolution acoustic data were collected. Dark grid lines indicate profiles gathered in 2007, whereas yellow grid lines indicate profiles gathered in 2010. Names and relative positions of vibracores collected are also shown. White circles indicate cores acquired in 2008, whereas red circles indicate cores acquired in 2010. The survey grid and core positions are superimposed upon the study's bathymetric map.

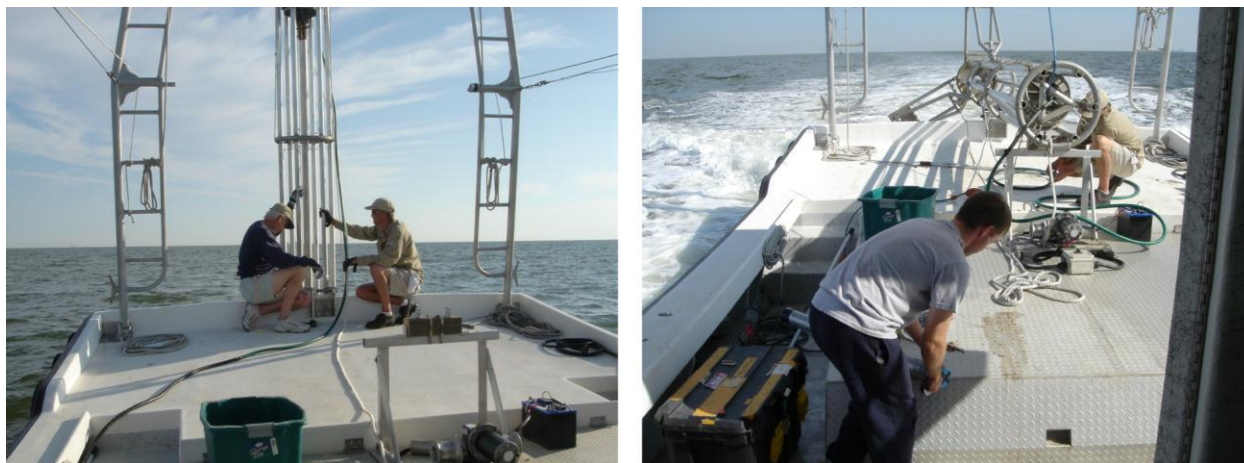


Figure 26. (A) The marine vibracoring system being lowered from the stern of the R/V Coastal Profiler. (B) As seen here, cores are brought onboard, cut into 1.5 m sections, capped, and labeled.

### **GEOTEK Multi-Sensor Core Logger**

Cores were first processed using a GEOTEK Multi-Sensor Core Logger (MSCL) (Fig. 27). The MSCL uses a conveyor system to push an un-split core section past a set of stationary sensors that operate simultaneously in a nondestructive fashion. The sensor configuration used in this study included (a) a pair of ultrasonic transducers that measure compressional (P) wave velocity and (b) a gamma ray source ( $^{137}\text{Cs}$ ) and detector that measure the attenuation of gamma rays, which in turn is used to calculate bulk density. Measurements were obtained incrementally every 1 cm at 5 second intervals. The MSCL log profiles were generated for both compressional wave velocity and bulk density data. Impedance logs (a product of velocity and density) were also generated. As both compressional wave velocity and bulk density measurements are sensitive to changes in lithology, they were used later as an aid in lithologic descriptions. Sensor calibrations were conducted in the standard set by Best and Gunn (1999). See Schultheiss and McPhail (1989), Schultheiss and Weaver (1992), and Gunn and Best (1998) for a detailed description of the MSCL, its sensors, and operating intricacies.

Table 1.  
Geographic Coordinates of Vibracores in Decimal Degrees

<b>Vibracore</b>	<b>Latitude</b>	<b>Longitude</b>		<b>Vibracore</b>	<b>Latitude</b>	<b>Longitude</b>
TT-01-08	29.23892	-92.08697		TT-36-08	29.32184	-92.17962
TT-02-08	29.19278	-92.16083		TT-37-08	29.31444	-92.21732
TT-03-08	29.21300	-92.18014		TT-38-08	29.32334	-92.19961
TT-04-08	29.20082	-92.19955		TT-39-08	29.33462	-92.19965
TT-05-08	29.16924	-92.19938		TT-40-08	29.32454	-92.21744
TT-06-08	29.16533	-92.23716		TT-41-08	29.31015	-92.23724
TT-08-10	29.19252	-92.24605		TT-42-08	29.32518	-92.23689
TT-09-08	29.19589	-92.27375		TT-43-08	29.33496	-92.23698
TT-10-08	29.16853	-92.27346		TT-44-08	29.32114	-92.25467
TT-12-08	29.19618	-92.29966		TT-45-08	29.31391	-92.28336
TT-13-10	29.20128	-92.33783		TT-46-08	29.34788	-92.26471
TT-15-08	29.20148	-92.31827		TT-47-08	29.35644	-92.23680
TT-17-10	29.22751	-92.30008		TT-48-08	29.34781	-92.19959
TT-19-08	29.24300	-92.27391		TT-49-08	29.33973	-92.16071
TT-20-08	29.27659	-92.22664		TT-50-08	29.35538	-92.16046
TT-21-08	29.24195	-92.23698		TT-52-08	29.38222	-92.13276
TT-22-08	29.23901	-92.21818		TT-53-08	29.39510	-92.12484
TT-23-08	29.24661	-92.19936		TT-54-08	29.40927	-92.11652
TT-24-08	29.22933	-92.16075		TT-55-08	29.39216	-92.02358
TT-25-08	29.24072	-92.14270		TT-57-10	29.22047	-92.20717
TT-26-08	29.26352	-92.16067		TT-64-10	29.32313	-92.19998
TT-27-08	29.28799	-92.16049		TT-65-10	29.3222	-92.18258
TT-28-08	29.28086	-92.12433		TT-66-10	29.32415	-92.16417
TT-29-08	29.26038	-92.11538		TT-69-10	29.36098	-92.08709
TT-30-08	29.27443	-92.09688		TT-73-10	29.3248	-91.9939
TT-31-08	29.30128	-92.09709		TT-74-10	29.33022	-92.03137
TT-32-08	29.28365	-92.07793		TT-75-10	29.08238	-92.16112
TT-33-08	29.31280	-92.03136		TT-76-10	29.08458	-92.31857
TT-34-08	29.31612	-92.14284		TT-77-10	29.0689	-92.35607
TT-35-08	29.32444	-92.16243		TT-78-10	29.26332	-92.31943

## Imaging

After geophysical logging was completed, cores were cut into halves. One half was immediately archived in cold storage, whereas the other half was used for imaging, describing, and sampling. A newly opened core was allowed to air dry for ~ 24 hours before imaging, as sedimentary structures were found to be visually enhanced in slightly desiccated sediments.





Figure 27. The GEOTEK Multi-Sensor Core Logger.

Core images were acquired using the GEOTEK MSCL, which is also equipped with a high-resolution scanning digital camera. See Bouma (1969) for an extensive discussion on the methods for opening and handling cores.

### **Sand-Mud Ratios/Grain-Size Analysis of the Sand Fraction**

Discrete sediments were sampled from individual cores at approximately 50 cm intervals to determine sand-mud ratios and the mean grain size of the sand fraction. The sand and mud fractions were separated by wet-sieving on a 63  $\mu\text{m}$  sieve. Separated fractions were then oven-dried, and dry-sample, percent sand-mud ratios were subsequently determined. Note that biogenic carbonates and other organic matter were not removed chemically nor was the weight of salt within samples determined. However, salt was removed during the washing process, macroscopic bivalve shells and other biogenic debris were manually removed from the sand fraction after drying, and much of the organic matter was manually removed from the fine fraction after drying. Despite the relative crudeness, the methodology used to determine sand-

mud ratios as described above is deemed adequate for the scope of this study. In total, dry-sample, percent sand-mud ratios were determined for 293 samples.

The sand fraction was then dry-sieved at 0.25 ( $\phi$ ) sieve intervals using a Gilson SS-3 sieve shaker. Table 2 depicts the standard subdivisions of sand-sized grain particles that were used in this study. Sands retained on individual sieves were weighed and resulting data were entered into SediGraph 5100 software for analyses. SediGraph software reports several statistics that describe the central tendency of a sample, including mean, mode, median, standard deviation, skewness, and kurtosis. In addition, it generates a particle-size table and a mass frequency vs. diameter histogram for each sample. Note that particle diameters are reported in micrometers ( $\mu\text{m}$ ). See Table 2 for a sieve, micron, phi, or class conversion. Refer to Poppe et al. (2000) for a more extensive discussion on methods used for determining sand-mud ratios and conducting grain-size analysis.

### **Graphic Logging**

The lithology and stratification observed within each core were described. The grain-size nomenclature of Folk (1974) was used to classify sediments on the basis of the sand-mud ratio. Nomenclature includes sand (a sand-mud ratio  $\geq 9:1$ ), muddy sand (a sand-mud ratio 1:1 to 9:1), sandy mud (a sand-mud ratio 1:9 to 1:1), and mud (a sand-mud ratio  $\leq 1:9$ ). The sand fraction was further subdivided by the standard Wentworth grades of very-coarse sand, coarse sand, medium sand, fine sand, and very-fine sand (Table 2). This subdivision was guided by the mean particle diameter determined from grain-size analysis (as discussed above). Constituents of the mud fraction include silt and clay. Folk (1974) subdivides the mud fraction by the following: material containing  $\geq 67\%$  silt is termed silt; material containing  $\geq 67\%$  clay is termed clay; intermediate mixtures are termed mud. Determining the relative proportions of each

Table 2.  
Grain-Size Conversion Data for the Sand Fraction

Sieve Mesh #	Millimeters	Microns	Phi ( $\phi$ )	Wentworth Size Class
12	1.68	1680	-0.75	Very- Coarse Sand
14	1.41	1410	-0.5	
16	1.19	1190	-0.25	
18	1.00	1000	0.0	
20	0.84	840	0.25	Coarse Sand
25	0.71	710	0.5	
30	0.59	590	0.75	
35	0.50	500	1.0	
40	0.42	420	1.25	Medium Sand
45	0.35	350	1.5	
50	0.30	300	1.75	
60	0.25	250	2.0	
70	0.21	210	2.25	Fine Sand
80	0.177	177	2.5	
100	0.149	149	2.75	
120	0.125	125	3.0	
140	0.105	105	3.25	Very-Fine Sand
170	0.088	88	3.5	
200	0.074	74	3.75	
230	0.0625	62.5	4.0	

constituent by lab analysis was not attempted. However, if the mud fraction was visually determined to be obviously dominated by silt or clay, then the appropriate description was applied. If not, the broad term of “mud” was applied.

Stratification refers to the layering of sediments either parallel to the original dip of the unit or at an angle to it (McKee and Weir, 1953; Allen, 1982). Descriptions of strata within cores may include the bounding surfaces of stratified units, the apparent shape of stratified units, and the primary sedimentary structures within stratified units. Various types of primary structures may occur, and the reader is referred to Coleman and Gagliano (1965) for detailed illustrations and descriptions (see also Pettijohn and Potter (1964) and Allen (1982)). This study also followed the approach of Moore and Scruton (1957) and subdivided strata into four basic

types (Fig. 28). Subdivisions are generalized and directly correlated to the degree of bioturbation. Note that the terms bed and lamina refer to stratum thickness: a stratum greater than 1 cm in thickness is termed bed, whereas a stratum less than or equal to 1 cm in thickness is termed lamina (McKee and Weir, 1953).

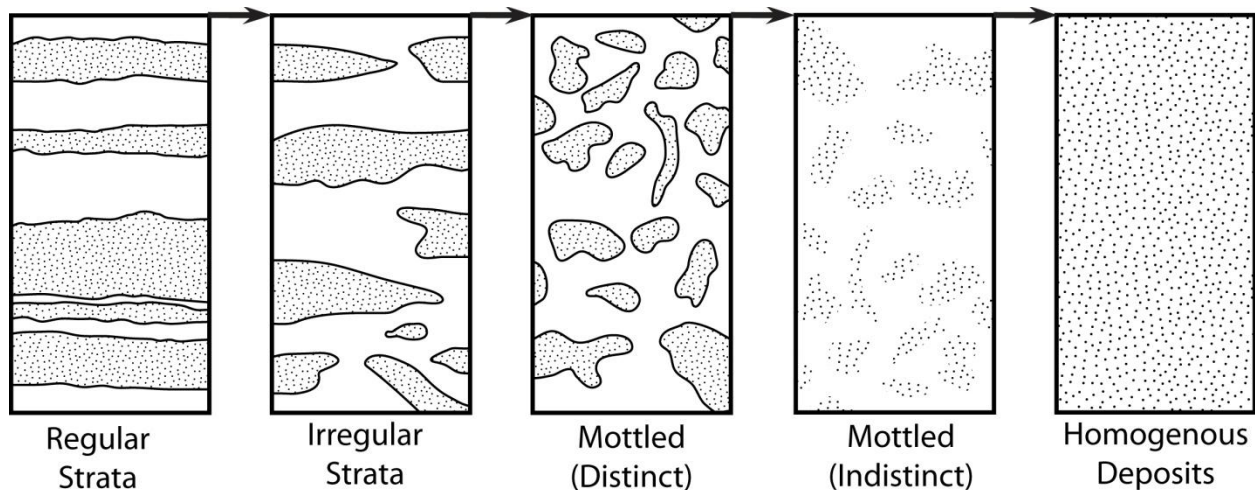


Figure 28. Four basic types of strata, including regular, irregular, mottled (distinct and indistinct), and homogenous. Modified from Moore and Scruton (1957).

Secondary sedimentary structures, particularly the degree of bioturbation, were also distinguished. There is a direct correlation between increasing sedimentation rates and decreasing bioturbation intensity, as increased sedimentation makes it difficult for dwellings to be constructed and permanently maintained at the seafloor, reduces concentration of food particles per unit volume of sediment at the seafloor, and can rapidly bury sedimentary material to depths where even the deepest penetrating deposit feeders cannot reach (MacEachern et al., 2005). Other variables that would affect burrowing organisms, and thus the degree of bioturbation, within a deltaic environment include reduced bottom-water oxygenation, salinity variations, storm and fair-weather waves, and substrate consistencies (e.g. fluid mud versus sand)

(MacEachern et al., 2005). Bioturbation intensity was measured in select cores according to the bioturbation index, as described by Bann et al. (2004) (Fig. 29). Film-negative X-ray radiographs (discussed below) were used extensively for assessing the bioturbation index. A detailed analysis of ichnology, including the identification of ichnospecies, ichnogenera, or ethology, was not attempted.

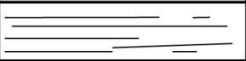






Grade	Classification	Visual Representation
0	Bioturbation absent	
1	Sparse bioturbation, bedding distinct, few discrete traces	
2	Uncommon bioturbation, bedding distinct, low trace density	
3	Moderate bioturbation, bedding boundaries sharp, traces discrete, overlap rare	
4	Common bioturbation, bedding boundaries indistinct, high trace density with overlap common	
5	Abundant bioturbation, bedding completely disturbed (just visible)	
6	Complete bioturbation, total biogenic homogenization of sediment	

Figure 29. Graphic classification of the bioturbation index. Seven grades are distinguished based on the intensity of bioturbation. Modified from Bann et al. (2004).

Lithologic and stratigraphic observations were transferred to graphic form using Adobe Illustrator. Graphic logs may include any number of various common sedimentary and biogenic symbols to aid the reader (Fig. 30). In addition, several forms of additional details are included: (1) lithofacies codes, as outlined by Folk (1974) and Farrell et al. (2012), are used herein to


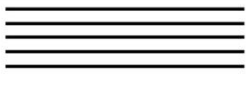



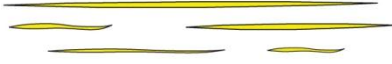





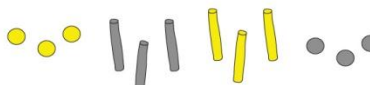
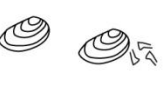
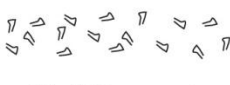

Key Sedimentary and Biogenic Symbols			
Sedimentary Structures			
	Cross Strata	Parallel Strata	Convoluted Strata
Contacts			
	Wavy Bedding	Mud Inclusions	Lenticular Sands
Contacts			
	Sharp	Gradual Transition	Gradual Transition Burrowed
Miscellaneous			
	Scoured	Sharp Burrowed	
Miscellaneous			
	Undifferentiated Burrowing	Undifferentiated Shell	Shell Fragments (hash)
Miscellaneous			
	Plant Fragments		

Figure 30. Key Symbols for sedimentary and biogenic structures. After Bouma (1962) and Farrell et al. (in press).

transcribe graphic descriptions (Fig. 31); (2) lithofacies and corresponding acoustic-facies identification designate which depositional environment sediments correlate to; (3) percent sand (i.e. sand-mud ratios) and if applicable the mean grain size of the sand fraction are indicated at the subbottom depth from which the sample was obtained; (4) if applicable, the degree of bioturbation is indicated by the bioturbation index (Fig. 29); (5) if applicable, the subbottom depth from which an AMS radiocarbon date was obtained is indicated.

### X-Ray Radiography

As used in this study, a radiograph is a “shadow picture,” or film negative, of a sediment slab that has been placed between film and an overhead X-ray point source (Hamblin, 1962; Bouma, 1969). On the X-ray radiograph film negative, the resulting darker regions of the

<b>Lithofacies Codes</b>					
Texture		Attribute		Examples	
Code	Description	Code	Description	Code	Description
S	sand	m	Massive	S m	massive sand
M	mud	b	Burrowed	S x-lam	cross-laminated sand
mS	muddy sand	lam	Laminated	S b	burrowed sand
sM	sandy mud	x-lam	cross laminated	(m) S	slightly muddy sand
(s)	slightly sandy	org	plant debris	(s) M	slightly sandy mud
(m)	slightly muddy	reg	regular strata	S/M	interbedded sand and mud strata; sand is dominant
Z	silt	ireg	irregular strata	mS mot	mottled muddy sand
C	clay	mot	Mottled	loc mot	locally mottled
/	interbedded	loc	Locally	S/M ireg	irregular, interbedded sand and mud strata

Figure 31. Lithofacies codes used to transcribe graphic descriptions. Modified from Farrell et al. (2012).

radiograph represent the more penetrable (less dense) parts of the sample, whereas the lighter regions represent the less penetrable (more dense) parts (Hamblin, 1962; Bouma, 1969). The radiograph is used to enhance primary and secondary structures within sediments that may be difficult to discriminate visually, including sediments that may otherwise appear to be “structureless”, or massive (Hamblin, 1962).

The X-ray radiography imaging technique was conducted over the entire length of 21 separate cores. Sediments within these select cores represent most of the major facies within the study area. One-centimeter thick vertical slabs of sediments were sliced from cores using a CSI fabricated resting block and steel wire. Individual sediment slabs were placed upon 25.4 x 30.5 cm Fuji Film IX 100 Envelopak industrial X-ray film and X-rayed using a Hewlett Packard

Faxitron 43855A X-ray system. System parameters include a focal-film distance of 61 cm, kilovoltage of 50 kVp, milliamperage of 3 mA, and an exposure time that varied from 40 – 110 seconds. See Hamblin (1962) and Bouma (1969) for a more detailed discussion on the techniques used in X-ray radiography.

### **AMS Radiocarbon Dating**

Establishing the geochronology of sediments within the Trinity-Tiger Shoals region is dependent upon accurately identifying and age-constraining all depositional units. The latter was partially accomplished by accelerator mass spectrometry (AMS) radiocarbon dating. Discrete sediments sampled for AMS radiocarbon dating included thin shell layers (consisting of disarticulated, but unbroken shells) and foraminifera from preferential muds. A thin shell layer is thought to represent deposition from a single, high-energy event such as a tropical cyclone. Such an event size-sorts and transports shells from their habitat of origin to their place of deposition but does not appreciably alter their preexisting taphonomic signature (e.g. degree of abrasion, fragmentation, and dissolution; Davies et al., 1989). Rather, most taphonomic alterations are thought to occur at the shell's habitat of origin and, accordingly, reflect the measure of time that the shell spent at or near the sea-bottom surface within its habitat of origin (Davies et al., 1989). This study targeted macroscopic *Mulinia lateralis* shells for dating, as the shells of this species were by far the most abundant in the subsurface. Considering that all chosen shells were unbroken (but disarticulated) and revealed little other taphonomic alterations, it is believed that shells used for AMS radiocarbon dating had a relatively short postmortem residence time in the taphonomically active zone before being sequestered in the stratigraphic record. Therefore, the time of deposition of a stratigraphic unit in which a given dated shell layer resides should closely correlate with the age in which the shells formed.



Foraminifera were targeted within those lithofacies that required dating but did not contain shell-event layers. Beta Analytic suggests a minimum of 10 mg of foraminifera for a single AMS radiocarbon date. To obtain the suggested mass of foraminifera, an approximately 10 cm vertical section of core sediment was sampled and washed over a 63  $\mu\text{m}$  sieve. The sand fraction, which was retained on the sieve, was then poured over filter paper to remove excess water and allowed to air dry overnight. Upon transferring the sand fraction to a picking tray, an optical microscope (50X magnification) was used to individually pick and transfer foraminifera to a separate glass vial for storage.

Samples were sent to Beta Analytic for AMS radiocarbon dating. Conventional radiocarbon ages (years BP) are determined based on the parameters and methods described by Stuiver and Polach (1977), signifying the use of 1950 as the base year, the use of the Libby  $^{14}\text{C}$  half-life (5,568 yr), accounting for isotopic fractionation by normalization of  $\delta^{13}\text{C}$  to -25‰, using oxalic acid as a standard, and assuming constant  $^{14}\text{C}$  atmospheric levels. Levels of atmospheric  $^{14}\text{C}$  are known to have fluctuated in the past. Therefore, necessary corrections based on the terrestrial dendrochronologic-calibrated INTCAL04 data set were made in order to convert conventional radiocarbon ages to calendar years (Reimer et al., 2004). However, all dated samples are marine carbonates and as such were further corrected to account for the global  $^{14}\text{C}$  reservoir effect of the ocean's upper mixed layer (Hughen et al., 2004). The MARINE04 database was used to perform this correction. Note that an additional marine correction may be applied to account for regional offsets from the global ocean's  $^{14}\text{C}$  age (Stuiver and Braziunas, 1993; Hughen et al., 2004). However, a regional  $^{14}\text{C}$  offset as a consequence of the Mississippi River is not known and is therefore not applied. Regional corrections have been determined elsewhere along the northern Gulf of Mexico but, notably, only within drowned river-valley

estuaries (Milliken et al., 2008; Simms et al., 2008). Sediment samples from this study were most likely influenced at their time of formation by brackish to open-marine environments. All corrections were performed by Beta Analytic. See Talma and Vogel (1993) for a further discussion on the mathematics used to calibrate  $^{14}\text{C}$  dates.

## **Acoustic Data Manipulation**

### Conversion of Coordinates

Petrel<sup>TM</sup> (version 2008.1) software was used to integrate the acoustic and vibracore data sets gathered during this study. By default, the EdgeTech chirp sonar system records coordinates within the trace headers of each SEG-Y file in geographic arcsecond units, whereas Petrel<sup>TM</sup> software handles only SEG-Y files with UTM coordinate units. Therefore, prior to importing the acoustic data, coordinates within the trace headers were converted to UTM units. First, Seismic Unix, an open source seismic utilities package, was used to transfer the shot coordinates of each SEG-Y file into a text file. Coordinates were then converted to Latitude/Longitude using Excel. This conversion is simple since an arcsecond is 1/3600 of one degree. Afterward, the Corpscon6 program, furnished online by the US Army Corps of Engineers, converted coordinates from geographic Latitude/Longitude units to UTM units (NAD83 UTM15, m). Seismic Unix was then used again to replace the geographic coordinates within the trace headers of each SEG-Y file with the newly-converted UTM units (NAD83 UTM15, m). Afterward, acoustic data were imported into Petrel<sup>TM</sup>.

### Depth Conversion

The z-axis domain for acoustic data is inherently in time (i.e. the measured time duration between acoustic transmission and the arrival of the reflected signals). For the purpose of this study, acoustic data needed to be converted to true depth. A time-to-depth conversion within

Petrel<sup>TM</sup> was accomplished by first constructing a velocity model for the study area. Parameters for this model included an assumed water-column velocity of 1,500 m/s (Turgut et al., 2006; Bull et al., 2005; among many others) and a sediment-column velocity of 1,550 m/s. It is recognized that the velocity of sound within sediment varies with sediment type. For example, sound velocity within high-porosity muddy sediments may be as low as ~ 1,480 m/s (less than water) or as high as ~1,680 m/s within low-porosity very-fine sands (Jackson and Richardson, 2007; note that the sand fraction within the Trinity-Tiger Shoals region is dominated by very-fine sands). Intermediate velocities range from as low as ~ 1,510 m/s within muddy sands to as high as ~1,650 m/s within sandy muds (Jackson and Richardson, 2007). Thus, as both the grain size of sediments and their respective sand-mud ratios vary spatially, acoustic velocities will vary accordingly. Nevertheless, this study used 1,550 m/s as a conservative, ubiquitous representative of sound velocity for the sediment column. It is also recognized that sound velocity will generally increase with depth. However, because of signal attenuation and a shallow water-bottom multiple throughout the study area, generally only the upper ~ 20 – 30 m of the subsurface is accessible to observation. Consequently, the effect of velocity increasing with depth is minimal. Based on this velocity model, all acoustic data were depth converted and subsequently combined with the core data set.

### **Data Analysis, Integration, and Interpretation**

Major acoustic reflectors were first mapped throughout the acoustic dataset. Petrel's<sup>TM</sup> three-dimensional capabilities permit one to work with multiple subbottom profiles at the same time, thus facilitating consistent interpretations among separate profiles. The “loop-tying” technique, as described by Bradley (1985), was followed to further assure consistency. Acoustic-facies units were then distinguished following the approach of Mitchum et al. (1977)

(refer to Figs. 18 – 20; see also Sangree and Widmier, 1977 and Berg, 1982). Most acoustic-facies units were penetrated with cores. Thus, most acoustic-facies units are associated with a corresponding lithofacies unit. Sedimentological attributes that may define a lithofacies include, for example, mean grain size, stratification, primary structures, secondary structures, and bounding surfaces (e.g. Reading and Levell, 1996). Note that there was no attempt to define biofacies. However, lithofacies descriptions may include relative proportions of shell content (e.g. scattered shell hash). Data used to define each lithofacies were acquired by the various methods described previously. The integration of these two fundamental approaches (i.e. the acoustic-facies and lithofacies approaches) for characterizing the subsurface enabled the interpretation of depositional environments and the processes that led to their deposition. By adding the geochronologic dataset, the depositional history of the Trinity-Tiger Shoals region was established.

## **RESULTS**

### **Acoustic Facies**

Based on the interpretations of acoustic-facies boundaries, twelve separate acoustic-facies units (AFU) were distinguished in the Trinity-Tiger Shoals region. The reflection parameters that characterize each acoustic-facies unit are described in the following discussion, and include each unit's internal reflection configuration pattern and its overall reflection amplitude, continuity, and frequency patterns. Note that frequency within this context refers to the spacing between successive reflectors, ranging from narrow to broad. The termination of reflections at unit boundaries and the external form of each unit are also described. The reader should also note that all acoustic-facies descriptions follow the fundamentals and terminology of Mitchum et al. (1977), Sangree and Widmier (1977), and Berg (1982). A more detailed discussion on the characterization and interpretation of acoustic facies can be found in the Background section, including Figures 18 – 20. In addition to the more extensive discussion that follows, a concise summary of the attributes of each acoustic-facies unit can be found in Table 3.

This section refers extensively to the cross sections found in Appendix 1. For the sake of brevity, cross sections will not be included as individual figures in this section, but instead the reader should refer to Appendix 1. Cross sections that trend east to west, beginning with X1, are introduced first in Appendix 1 followed by cross sections that trend north to south, beginning with Y1. For a map-view location of cross sections, refer to Figure 25. Each individual cross section along with associated interpretations is presented as follows. The raw, non-interpreted subbottom profile is displayed at the top along with the profile's identification (e.g. X1), an arrow indicating the direction of north or west, depth and distance scales, the degree of vertical exaggeration, and the positions of intersecting subbottom profiles. The middle cross section

displays the boundaries of the separate acoustic-facies units encountered along a given transect. If observed, note that a few prominent internal reflectors associated with individual acoustic-facies units are outlined, so as to illustrate (and thus aide the reader) the configuration pattern of reflectors. It is impractical to depict all reflectors, and the reader should be aware that there may be many reflectors between outlined reflectors. On the other hand, there may be few, if any reflectors between those outlined. Also indicated, where applicable, are the water-bottom multiple, gas-charged sediments, the locations and approximate subbottom extent of vibracores, and the subbottom position of samples from which AMS radiocarbon dates were measured. The bottom cross section is essentially the same as the middle cross section, except that each acoustic-facies unit is identified (e.g. AFU1) and color coded to enhance visualization. Note that the persistent water-bottom multiple, in many places gas-charged sediments, and in a few places the attenuation of the acoustic signal prevent the full observation and interpretation of the subsurface, most particular for AFU1. Nevertheless, more than sufficient data exist to meet the objectives of this dissertation.

Although this author strived for complete objectivity during the research of this dissertation, observations and descriptions are slightly subjective, as they are based on this author's understanding of the literature and experience (this study). Nevertheless, knowledge of the vertical resolution of chirp sonar, insight gathered from the literature, and an understanding of the geological framework, descriptions herein are considered defensible. Furthermore, consistency has been maintained throughout this study.

Table 3.  
Acoustic Facies Unit Attributes

Acoustic Facies Unit	External Form	Reflection Terminations at Boundaries	Reflection Parameters			
			Configuration	Amplitude	Continuity	Frequency
AFU1	Fan	Erosionally truncated along top boundary; apparent downlap along bottom boundary where bottom boundary is discerned	Complex sigmoid-oblique	Variable, from low to high	Variable, from low to high  Notably much higher in the very west and south	Variable, from narrow to broad  Breadth between cycles increases substantially in the very south
AFU2	Lens to sheet-like	Indiscernible	High degree of acoustic scatter	Variable, from low to high	Mostly indiscernible	Indiscernible
AFU3	Lens	Toplap along top boundary; apparent downlap along bottom boundary	Divergent, with reflectors dipping and converging to the southwest; high degree of acoustic scatter also observed	Moderate to high	Low to moderate (where observed)	Narrow to moderate (decreasing in direction of convergence)
AFU4	Lens	Erosional truncation to reflection-free along the top boundary; where observed, reflectors onlap along the northern bottom boundary and approach apparent downlap along the southern bottom boundary	Largely reflection free with some prominent parallel to diverging reflectors observed dipping and converging to the southwest	Variable, from low to high	Moderate to high (where observed)	Narrow to moderate (slightly decreasing in direction of convergence)
AFU5	Wedge	Mostly Indiscernible  Exception is in the very south and west where reflectors tolap along the top boundary. The termination of these reflectors along the bottom boundary is not observed	High degree of acoustic scatter  Exception is in the very south and west where divergent reflectors dip and converge to the southwest	Low to high	Mostly Indiscernible  Exception: high in the very south and west	Mostly Indiscernible  Exception: narrow to broad in the very south and west (decreasing in the direction of convergence)

(Table 3 continued)

Acoustic Facies Unit	External Form	Reflection Terminations at Boundaries	Reflection Parameters			
			Configuration	Amplitude	Continuity	Frequency
AFU6	Mounded to sheet-like	Not applicable	Predominantly reflection free	Not applicable	Not applicable	Not applicable
AFU7	Mounded	Not applicable	Predominantly reflection free	Not applicable	Not applicable	Not applicable
AFU8	Mounded to sheet-like	Indiscernible	High degree of acoustic scatter; some parts are reflection free	Generally low to moderate	Indiscernible	Indiscernible
AFU9	Wedge	Where reflectors are observed, their terminations along the top boundary are not discerned; terminations along bottom boundary apparently downlap	Predominantly reflection free in northern part with a few isolated reflectors; acoustic scatter predominant in southern part	Low to moderate where reflectors are observed	Low to moderate where reflectors are observed	Narrow where reflectors are observed
AFU10	Channel fill	Indiscernible	Chaotic to high degree of acoustic scatter to reflection free	Variable, from low to high (not applicable to reflection-free channel-fill areas)	Indiscernible (not applicable to reflection-free channel-fill areas)	Indiscernible (not applicable to reflection-free channel-fill areas)
AFU11	Indiscernible	Terminations along the top boundary are mostly indiscernible although some reflectors appear truncated; terminations along the bottom boundary are indiscernible	Reflection free to sub-parallel to contorted	Variable, from low to high	Low to moderate, occasionally highly continuous	Variable, from narrow to broad
AFU12	Sheet	Indiscernible	High degree of acoustic scatter	Largely moderate	Indiscernible	Indiscernible



## AFU1

The AFU1 is found throughout the entire study area. It is characterized by progradational reflection-configuration patterns that are easily distinguished if viewed along dip (i.e. east-west). Locally, hummocky clinoforms are observed proximal to a separate acoustic-facies unit, AFU10, that incises into AFU1. The tangential-oblique reflection-configuration pattern defines the AFU1 at least as far south as the latitude of subbottom profile X4, with subparallel clinoforms dipping to the west (e.g. see cross section X11). It is difficult to discern the reflection configuration pattern of AFU1 immediately south of subbottom profile X3 (i.e. subbottom profiles X2 and X1), as most of AFU1 in this region is masked by the water-bottom multiple and gas-charged sediments. However, in subbottom profile XX9, which is located farther south in relatively deep water and therefore less affected by the water-bottom multiple, AFU1 is clearly defined by the sigmoidal reflection-configuration pattern. Hence, a transition in the dominant reflection-configuration pattern from tangential oblique to sigmoidal occurs between subbottom profiles X4 and XX9. Subparallel clinoforms in the sigmoidal zone also dip to the west but are distinguished by a thickening of their middle segments. Clinoforms discerned along subbottom profile XX9 are also locally contorted. Considering the tangential-oblique and sigmoidal subfacies together, the overall reflection-configuration pattern of AFU1 is defined by the complex sigmoid-oblique pattern (Berg, 1982).

Along strike (i.e. north-south), distinct sets of subparallel clinoforms are observed dipping either north or south. Particularly, this is observed in the eastern section of the study area where AFU1 is not as extensively masked by the water-bottom multiple or gas-charged sediments (e.g. see cross section YY7). Along-strike clinoforms in the most southern parts of the study area (e.g. see cross section YY5 and the most southern extent of cross section YY7) also

display highly contorted clinoforms, even more so than is observed along dip (i.e. east-west) in subbottom profile XX9.

The top boundary of AFU1 is easily distinguished. Although reflectors in the most northern section of the study area appear concordant with the top boundary if viewed along strike (i.e. north-south), dip profiles (i.e. east-west) clearly confirm that reflectors are truncated along the top boundary. One could make the case for toplap in the very northwest (e.g. see cross section XX8), but based on interpretations discussed later, the entire AFU1 is considered erosionally truncated. Progressing south, erosional truncation along the top boundary is clearly observed, even if viewed along strike (e.g. see cross section Y27). The bottom boundary of AFU1 is mostly indiscernible as consequent to the water-bottom multiple and gas-charged sediments, or as in a few places because of acoustic-signal attenuation. However, in the very northwestern and southwestern parts of the study area, clinoforms appear to approach downlap (or apparent downlap). Such bottom-boundary terminations are expected for tangential-oblique and sigmoidal reflection-configuration patterns (Mitchum et al., 1977; Sangree and Widmier, 1977; Berg, 1982).

As a whole, the continuity of reflectors within AFU1 ranges from low to high, but is notably highest in the very west (e.g. cross section YY2) and very south (e.g. cross section XX9). The frequency of reflectors ranges from narrow to broad, and like continuity, a distinction in frequency is noted in the very west (e.g. cross section YY2) and very south (e.g. cross section XX9) where the breadth between cycles increases substantially. Note that this increase in continuity and breadth occurs within the sigmoidal zone. Amplitude is also variable, ranging from low to high. Several aspects make observing the external form of AFU1 difficult: (a) the acoustic facies extends out of the study area in all directions, (b) the bottom boundary is

largely obscured due to the water-bottom multiple and gas-charged sediments, or because of acoustic-signal attenuation, and (c) all of the top boundary has been erosionally truncated. Nevertheless, it appears that the external form is defined as fan-shaped, which is characteristic of progradational reflection-configuration patterns (Sangree and Widmier, 1977). Furthermore, because the bottom boundary is largely obscured, it is difficult to judge the thickness of AFU1. In the southern part of the study area, however, where water depths are greatest and thus the water-bottom multiple is deepest, AFU1 may be as thick as 10+ m (e.g. see cross section YY5)

### AFU2

The AFU2 resides stratigraphically atop of AFU1 in the northern part of the study area (e.g. see cross sections X10 and Y27). This lens- to sheet-like unit may be as thick as ~ 2.5 m in its central section but generally thins away in all directions. It tapers away to the west and south, whereas it extends beyond the study area to the north and east. The AFU2 partially underlies AFU4, AFU5, AFU8, AFU9, and AFU12. Elsewhere, it forms part of the seabed. The AFU2 is characterized by a high degree of acoustic scatter, with amplitude ranging from low to high. Other reflection parameters are for the most part indiscernible, although slightly continuous reflectors are observed in the central, most northern part of this acoustic facies.

### AFU3

In the southeastern part of the study area and also lying stratigraphically atop of AFU1 is AFU3 (e.g. see cross section X5). The lens-shaped AFU3 may be as thick as 2 m but generally tapers off in all directions from its central section. However, its eastern boundary is not directly observed. Internal reflectors of AFU3 can be difficult to distinguish because of the high degree of acoustic scatter. Where reflectors are observed (which are most apparent in the northern and eastern part of the unit), their configuration is recognized as divergent, in which they dip and

converge towards the southwest. Reflectors are also characterized by toplap along the top boundary and appear to approach apparent downlap along the bottom boundary. Furthermore, observed reflectors express low to moderate continuity, generally moderate to high amplitude, and narrow to moderate frequency that decreases in the direction of convergence (i.e. southwestward).

#### AFU4

The AFU4 spans a large part of the study area. Depending on where it is observed within the grid of data, it may stratigraphically lie atop of AFUs 1, 2, and/or 3. Although the reflection-configuration pattern of AFU4 is predominantly reflection free, a few prominent reflectors are observed. Where observed, parallel to diverging reflectors dip and slightly converge to the southwest (e.g. see cross sections X6 and Y26). In the eastern and most western parts of the unit, it appears that erosional truncation, as opposed to toplap, occurs. Elsewhere, the top boundary is largely reflection free. In the central to eastern parts of AFU4, reflectors onlap along the bottom boundary's northern perimeter, whereas they approach apparent downlap along the bottom boundary's southern perimeter. Observed reflectors generally express moderate to high continuity, low to high amplitude, and narrow to moderate frequency that slightly decreases in the direction of convergence (i.e. southwestward). The external form of AFU4 is lens-shaped, and like its internal reflectors, it dips to the southwest. The AFU4 may be as thick as 5+ m, but like other lens-shaped units, it tapers towards its boundaries.

#### AFU5

The wedge-shaped AFU5 overlies most of AFU4 and the southern and western parts of AFU1 (e.g. see cross section X2). The AFU5 generally thickens to the west, and may be as thick as 9 m in its southwestern section. Those parts of AFU5 that can be observed are largely

characterized by a high degree of acoustic scatter, and accordingly, reflection continuity, frequency, and terminations at boundaries are indiscernible. However, two exceptions to this characterization exist. First, that part of AFU5 that lies directly beneath AFU6 (discussed below) generally is reflection free. (The AFU6 is a thick sand shoal and therefore wipes out the signal of the low-powered chirp.) The other exception is in the very southern and western parts of the unit where concave-up, diverging reflectors dip and converge to the southwest (e.g. cross sections XX9 and YY1). These reflectors generally exhibit high continuity, low to high amplitude, and narrow to broad frequency, with breadth between reflectors decreasing in the direction of convergence (i.e. southwestward). Reflectors tolap along the top boundary only in the very southern part of the unit (see cross section XX9; note that the top boundary here is the seabed). Elsewhere, they transition upwards into the top part of the unit that, like most parts of AFU5, is predominantly indiscernible because of the high degree of acoustic scatter. The termination of these reflectors along the bottom boundary is not directly observed, as the study area does not extend far enough south or west. Based on the trajectories of the reflectors, however, they most likely downlap in those directions.

#### AFU6

The AFU6 lies stratigraphically above AFU5 in the central part of the study area (e.g. see cross sections X2 and Y14). By volume, most of this unit is located within its southern-southwestern parts where thickness may be as great as 6 – 7 m. From this thick, core region, AFU6 extends and tapers off to the north, spanning the northeast to slightly northwest quadrants (e.g. see cross sections X6 and Y9). Thus, the external form of AFU6 is mounded in its southern-southwestern core, with sheet-like forms extending north along its northern perimeter. The AFU6 is predominantly reflection free, although acoustic scatter is observed where this unit

tapers to its perimeters. Consequently, reflection continuity, amplitude, frequency, and terminations at boundaries are for the most part not applicable to this facies' description. Also, note that the seabed forms the upper boundary of this unit.

#### AFU7

Similar to AFU6 but located farther to the north, AFU7 lies stratigraphically above AFU5 (e.g. see cross section X8). Also like AFU6, AFU7 is predominantly reflection free (although it is characterized by more acoustic scatter in its very western section where it appears to weld to AFU6). Consequently, reflection amplitude, continuity, frequency, and terminations at boundaries are for the most part not applicable to AFU7's description. In contrast to AFU6, the mounded AFU7 is approximately geometrically symmetrical along its central east-west axis, with a maximum thickness of ~ 2+ m. As with AFU6, the seabed forms the upper boundary of AFU7.

#### AFU8

Uniquely, AFU8 is actually comprised of two separated units, albeit they are very proximal to one another. The AFU8 occurs within the northern region of the study area and primarily overlies AFU2, but also portions of AFU4, AFU7, and AFU12 (e.g. see cross section X10). Although some parts reveal a reflection-free configuration pattern, AFU8 is for the most part characterized by acoustic scatter. The amplitude of reflectors is generally low to moderate, but sometimes is observed as high. On the other hand, reflection continuity, frequency, and terminations at boundaries are indiscernible. Thickness is generally  $\leq 1$  m, but locally may thicken to 2+ m. The external form varies from sheet-like to mounded. To a large degree, the top boundary is the seabed.

### AFU9

The wedge-shaped AFU9 is located in the northeastern part of the study area overlying AFU2 (e.g. see cross sections X11 and Y39). It is predominantly reflection free within its northern part but becomes more associated with acoustic scatter in its southern reach. Although the northern part is generally reflection free, a few isolated reflectors are observed. They are characterized by low to moderate amplitude, low to moderate continuity, and narrow breadth between cycles. Terminations along the top boundary, which is also the seabed, were not discerned, but reflectors appear to apparently downlap along the bottom boundary. The AFU9 may approach 1.5 m thickness in its northeastern part, but is typically much thinner. In fact, AFU9 tapers away to the west and south.

### AFU10

The reflection-configuration pattern of AFU10 is variable. It is largely recognized as chaotic (with some reflectors being recognizable) or is associated with a high degree of acoustic scatter (having no recognizable reflection pattern). In a few instances, however, AFU10 is distinguished by a reflection-free configuration pattern. Amplitude of reflectors is also variable, ranging from low to high. In contrast, reflection terminations at boundaries are largely indiscernible, as is reflection continuity and frequency. The external form of AFU10 is identified as channel fill, and it is found within (i.e. incises into) AFU1. Figure 32 displays examples of AFU10 taken from subbottom profiles X9 and Y25.

### AFU11

The AFU11 is observed in the most southwestern part of the study area underlying AFU1 (e.g. see cross sections XX9 and YY2). The reflection-configuration pattern of AFU11 is

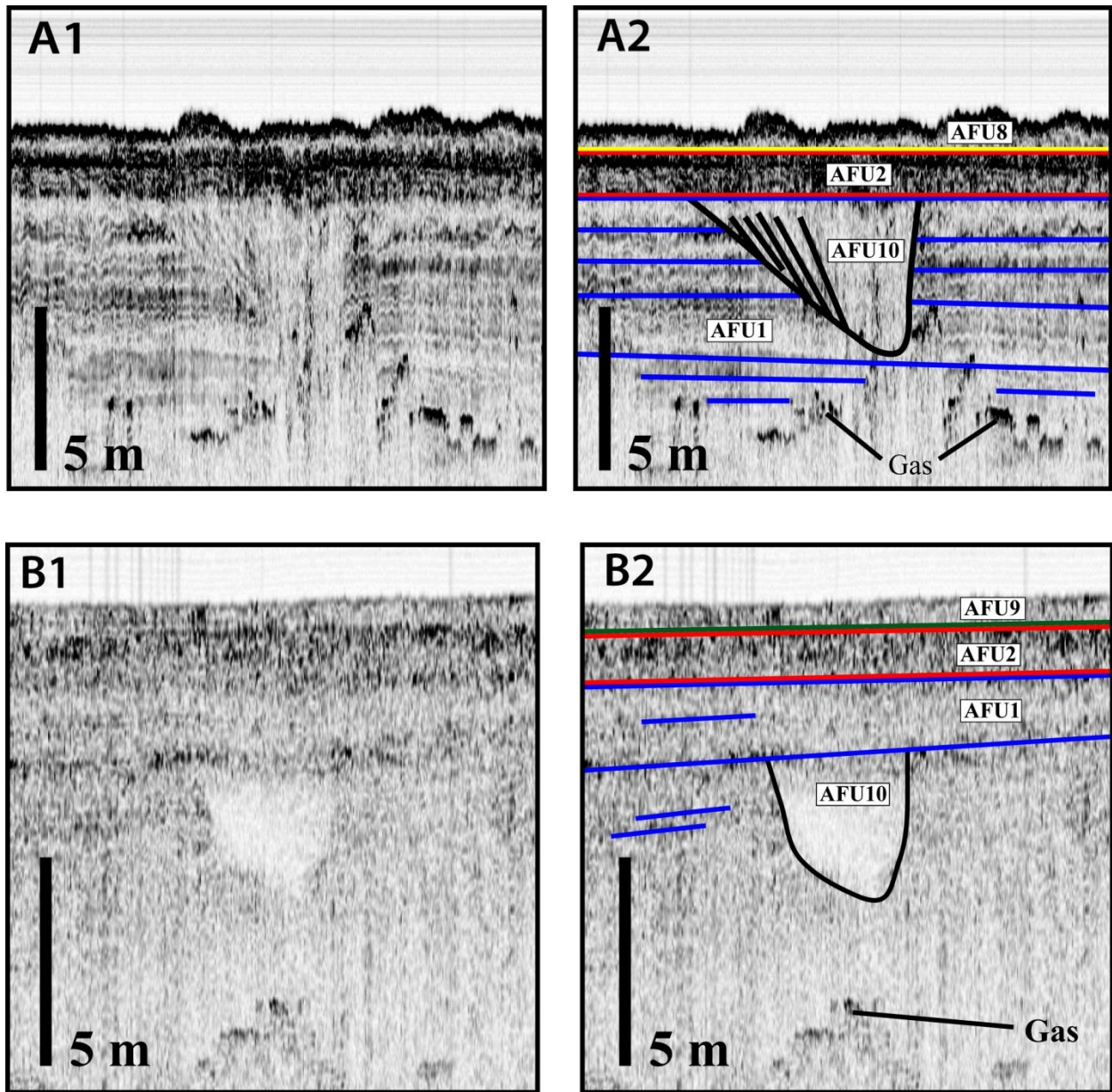


Figure 32. A1) An example of AFU10 taken from subbottom profile Y25. Note the chaotic channel-fill configuration. A2) The same example of AFU10 as seen in A1, with surrounding acoustic-facies units and gas-charged sediments delineated. Vertical exaggeration is 100x. B1) A second example of AFU10 taken from subbottom profile X9. Note that this channel-fill configuration is largely reflection free. B2) The same example of AFU10 as seen in B1, with surrounding acoustic-facies units and gas-charged sediments delineated. Vertical exaggeration is 50x.

variable, ranging from reflection free to sub-parallel to contorted. Where reflectors are observed, frequency ranges from narrow to broad, whereas amplitude ranges from low to high. Reflection



continuity is generally low to moderate with the occasional highly continuous reflector. Some reflectors appear truncated along the top boundary, but for the most part terminations are indiscernible. The bottom boundary is obscured, and so terminations along this boundary are not observed. Therefore, true maximum thickness of AFU11 cannot be measured. Based on what is observable within this data set, however, maximum thickness of AFU11 is at least 14 m. There is insufficient data coverage to make an assessment on AFU11's external form.

### AFU12

The AFU12 is located in the northern section of the study area. It may partially underlie limited portions of AFU8 and AFU9, but for the most part its top boundary forms part of the seabed (e.g. see cross section X11). The AFU12 is characterized by a high-degree of acoustic scatter, whereas amplitude is largely moderate. All other reflection parameters are indiscernible. This unit is generally thin ( $\leq 1$  m) and has a sheet-like external form.

### **Lithofacies**

Twelve separate lithofacies units (LFU) were identified in the Trinity-Tiger Shoals region. Each of these lithofacies units complements a corresponding acoustic-facies unit (e.g. LFU4 corresponds with AFU4). Exceptions exist: (1) two lithofacies units, LFU1A and LFU1B, correspond with different parts of AFU1 and (2) two lithofacies units, LFU10A and LFU10B, correspond with different parts of AFU10. However, note that LFU10A and LFU10B do not represent the complete AFU10. Also, note that no lithofacies unit complements AFU11 or AFU12, as cores do not penetrate these acoustic-facies units.

The following discussion is based on lithological data gleaned from cores. Attributes that characterize each lithofacies unit are described within this discussion, including each unit's siliciclastic grain size, primary sedimentary structures, degree of bioturbation (i.e. secondary

sedimentary structures), stratal and unit boundaries, among several others. For the sake of brevity, usually only one visualization (i.e. figure) highlighting aspects of each lithofacies unit is presented where each respective lithofacies unit is discussed. However, the reader should also continually refer to the graphic logs, core images, and X-ray radiographs found in Appendixes 2, 3, and 4, respectively, as cores have been described and documented within these Appendixes in great detail. Again, note that lithofacies units and corresponding acoustic-facies units are indicated on the graphic logs, and the reader should use the graphic logs to reference corresponding zones in the cores images and X-ray radiographs. Also, note again that percent-sand (i.e. sand-mud ratios) and the mean grain size of the sand fraction were measured from discrete core samples, and this information is incorporated into the graphic logs. For further statistical calculations of the sand fraction, the reader should refer to Appendix 7. Cores that penetrate individual lithofacies units are indicated in the descriptions below. In many cases, there may be a large number of cores that penetrate an individual lithofacies unit, and for the sake of brevity, associated cores are written as the following example depicts: TT-01-, -02-, -03-, -04-08 and TT-75-, -76-, -77-, -78-10. Note that this example represents the abbreviated form for cores TT-01-08, TT-02-08, TT-03-08, TT-04-08, TT-75-10, TT-76-10, TT-77-10, and TT-78-10. Refer to Figure 25 for the location of cores and Appendix 1 for the subbottom extent of cores. In addition to the more extensive discussion that follows, a concise summary of the attributes of each lithofacies unit can be found in Table 4.

#### LFU1A

The LFU1A is characterized by interlaminated to interbedded silty-clay and silt to sandy-silt sediments (Fig. 33). Silty clays typically dominate the sediment column (i.e. > 50%), but in many cases, particularly towards the top of the unit, sandy silts become dominate. Primary

Table 4.  
Lithofacies Unit Attributes

Lithofacies Unit	Lithology		Degree of Bioturbation	Internal Strata Boundaries	Top Boundary of Unit	Additional Characteristic(s)
LFU1A	<p>Interlaminated to interbedded silty clays and silts to sandy silts; silty clays dominate</p> <p>General coarsening upwards</p> <p>Primary sedimentary structures observed within coarse sediment beds include parallel laminations, cross laminations, lenticular laminations, flaser laminations, and both unidirectional and oscillatory ripple laminations</p>		<p>Sparse to uncommon</p> <p>May be severe locally</p>	Typically distinct; occasional burrowing may alter; normal grading characterizes some thicker silt beds and so may appear gradational	<p>Generally Sharp</p> <p>Bioturbation may be severe in some places</p>	<p>Siderite banding</p> <p>Occasional strata of particulate plant organics</p>
LFU1B	<p>Clays to silty clays dominate; silt to sandy-silt strata also occur</p> <p>Primary sedimentary structures are largely parallel strata; lenticular silt lenses and cross laminations occasionally encountered</p>		Scarce to moderate	Distinct to gradational	Indiscernible (severe bioturbation)	Siderite banding
LFU2	Eastern Section	<p>Interlaminated to interbedded muddy-sand and sandy-mud strata; sand fraction dominates</p> <p>Grain size of sand fraction ranges very-fine to medium; bimodal to trimodal</p> <p>Sediments predominantly mottled</p>	Abundant to complete	Indiscernible	Sharp to gradational	Shell material makes up considerable portion of sediment column
	Central to Western Section	Transitions east to west from thick sandy beds separated by occasional thin muddy bed, to interlaminated to interbedded sands and muds	Highly variable, from absent to complete	Distinct to indiscernible	Sharp to gradational	Shell beds (~ 3 cm thick) found throughout

(Table 4 continued)

<b>Lithofacies Unit</b>	<b>Lithology</b>		<b>Degree of Bioturbation</b>	<b>Internal Strata Boundaries</b>	<b>Top Boundary of Unit</b>	<b>Additional Characteristic(s)</b>
LFU2 (cont.)	Central to Western Section (cont.)	Grain size of sand fraction ranges very-fine to medium; bimodal to trimodal; sands fine to the east  Primary sedimentary structures within sandy beds typically parallel to cross laminations	(cont.)	(cont.)	(cont.)	(cont.)
LFU3	Muddy sediments punctuated with interlaminated to interbedded sand and silt strata  Primary sedimentary structures observed include lenticular laminations and cross laminations (only in northern part of unit; no preservation in southern part)		Moderate in northern part of unit; abundant to complete in southern part	Distinct to normal gradation in northern part of unit; Nonexistent in southern part	Gradational in northern part of unit; seabed forms top boundary of southern part	Shell lag at base of unit
LFU4	Overwhelmingly clay sediments, but with interlaminated to interbedded silts and sands within  Cross laminations observed within rare interbedded sands		Sparse to moderate	Subtle	Varies from gradational to sharp to clearly erosional; may also form part of the seabed	The vast majority of laminations are only discerned with X-ray radiographs  Siderite banding in rare instances
LFU5	Interlaminated to interbedded sandy muds and muddy sands; silts replace sand-dominated strata in southern part of unit  Parallel to cross laminations observed in southern part of unit; primary structures are not preserved elsewhere		Typically at least moderate to complete	Largely reworked by bioturbation	Gradational; may also form part of the seabed	Shell beds (~ 3 cm thick) occasionally encountered
LFU6	Almost entirely sand  Primary sedimentary structures are difficult to discern: appear massive to cross laminated		Varies from scarce to abundant	Gradational where recognized	Forms part of the seabed	

(Table 4 continued)

<b>Lithofacies Unit</b>	<b>Lithology</b>	<b>Degree of Bioturbation</b>	<b>Internal Strata Boundaries</b>	<b>Top Boundary of Unit</b>	<b>Additional Characteristic(s)</b>
LFU7	Sand to slightly muddy sand Preservation of primary sedimentary structures is poor	Typically abundant to complete	Largely reworked by bioturbation	Forms part of the seabed; gradational elsewhere	Significant shell content in eastern half of unit
LFU8	Predominantly comprised of shell Sand-sized clastic sediments also present	Not discerned	NA	Forms part of the seabed	Sands range in size from very-fine to medium; sands are bimodal to trimodal
LFU9	Predominantly clay with interlaminated to interbedded silts	Generally uncommon	Generally distinct	Forms part of the seabed	Interlaminated silts and beds are only discerned with X-ray radiographs  High water content  May overlie a shell lag
LFU10A	Bed-scale sands dominate, with interlaminated to interbedded sands and muds also prevalent  Sands generally fine upwards, from fine to very-fine sands  Primary sedimentary structures encountered include parallel laminations, cross laminations, trough-cross laminations, and multi-directional current ripples	Generally absent	Generally distinct but may also be distorted; scouring occasionally observed	Gradational	Distortion of strata occasionally encountered  Large amounts of particulate plant organics

(Table 4 continued)

<b>Lithofacies Unit</b>	<b>Lithology</b>	<b>Degree of Bioturbation</b>	<b>Internal Strata Boundaries</b>	<b>Top Boundary of Unit</b>	<b>Additional Characteristic(s)</b>
LFU10B	Interlaminated to interbedded sandy silts and silty clays Primary sedimentary structures include parallel to lenticular laminations	Uncommon to abundant	Generally distinct, although burrowing can alter the boundary	Heavily burrowed	Distortion of strata occasionally encountered  Siderite banding

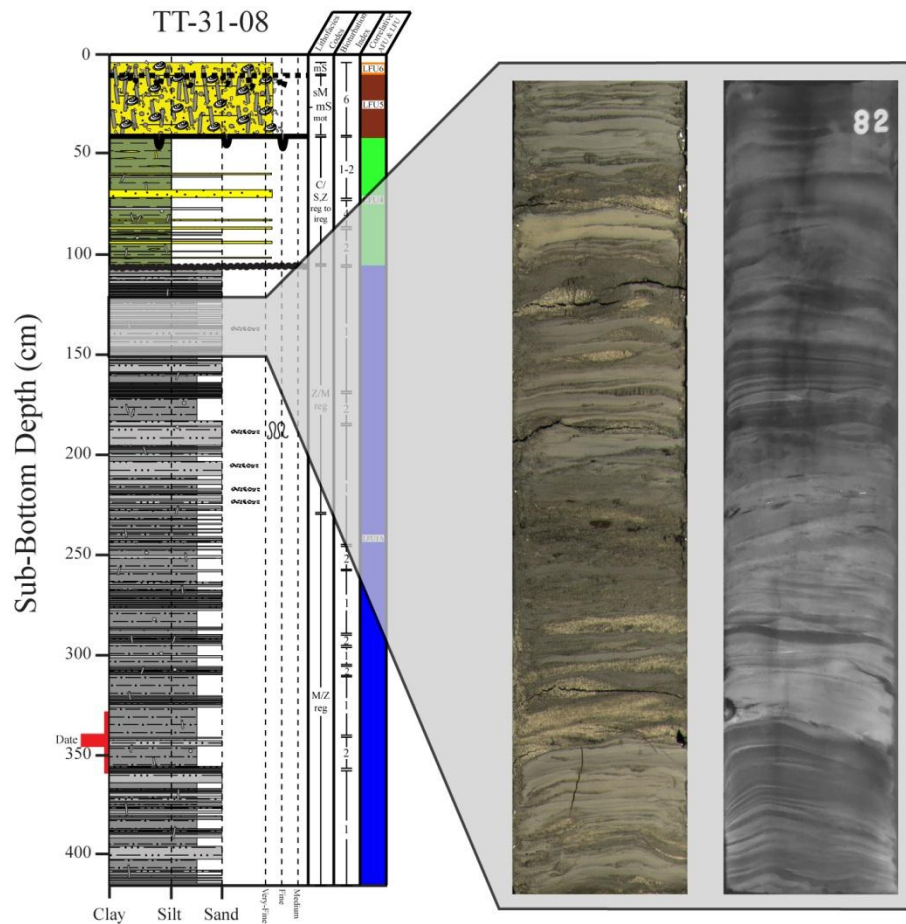


Figure 33. A single example of LFU1A, as observed from vibracore TT-31-08. For a more thorough visual review of LFU1A, refer also to the graphic logs, images, and X-ray radiographs (Appendixes 2, 3, and 4, respectively) of all cores associated with LFU1A, as indicated in the text.

sedimentary structures observed include parallel laminations, cross laminations, lenticular laminations, flaser laminations, and both unidirectional (current) and oscillatory (wave) ripple laminations. Bioturbation is generally sparse to uncommon but may become severe locally. Hence, most strata are classified as regular to irregular. The boundaries separating individual layers are typically distinct, although occasional burrowing can alter them. In contrast, normal grading is at times observed in some of the thicker silty beds, which may precipitate a more transitional boundary with its overlying neighbor. Although not abundant, strata dominated by particulate plant organics (i.e. “coffee grinds”) are encountered occasionally, whereas shell

carbonates are rarely encountered. The top boundary of LFU1A is generally sharp. In some cores, however, bioturbation is severe at the top of the unit, and thus the contact between LFU1A and the overlying unit may appear gradational. One aspect characteristic of LFU1A (as well as to LFU10B and to a lesser degree LFU1B and LFU4) is the moderate greenish-yellow to grayish-yellow colored silty-clay laminations and thin beds that occasionally occur in an otherwise pale-olive, silty-clay fraction (Fig. 34). Such peculiar strata most likely reflect siderite banding, suggesting porewaters of fine-grained sediments were initially relatively low in salinity (Bailey et al., 1998). Cores that penetrate LFU1A include TT-01-, -31-, -32-, -33-, -47-, -48-08, and TT-69-, -73-, -75-10. For additional visual accounts to the above descriptions, refer to the graphic logs, images, and X-ray radiographs of these cores (Appendixes 2, 3, and 4, respectively).



Figure 34. An approximately 10 cm section of core cropped from vibracore TT-69-10. Note the single, moderate greenish-yellow to grayish-yellow colored, very-thin bed within an otherwise pale-olive, silty-clay fraction. Such peculiar stratum most likely reflects siderite banding (Bailey et al., 1998).



## LFU1B

Clay to silty-clay sediments dominate LFU1B, although silt to sandy-silt laminae- to bed-scale strata occur (Fig. 35). Primary sedimentary structures observed are largely parallel strata, with lenticular silt lenses and cross-laminations occasionally encountered. The occasional silt bed generally shows normal grading, which may lead to a rather gradational contact with its upper neighboring unit. Elsewhere, contacts between internal strata are distinct if burrowing does not alter the boundaries, but bioturbation is generally scarce to moderate. However,

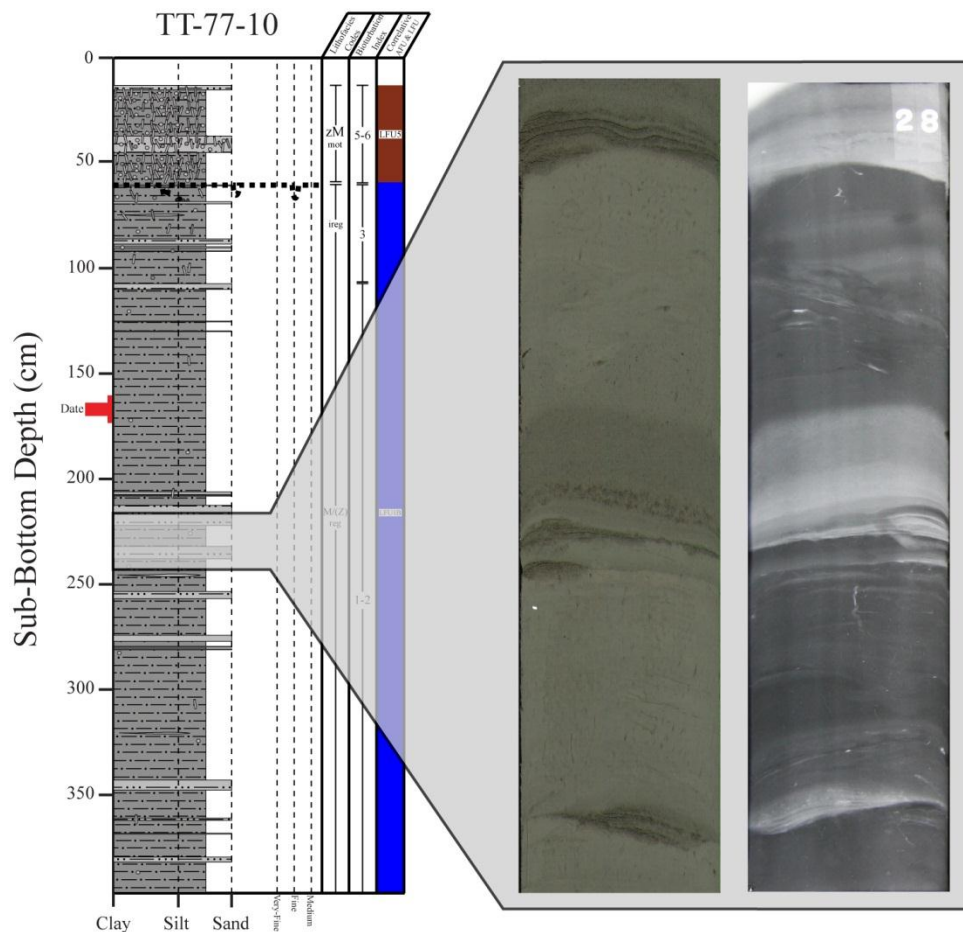


Figure 35. A single example of LFU1B, as observed from vibracore TT-77-10. For a more thorough visual review of LFU1B, refer also to the graphic logs, images, and X-ray radiographs (Appendixes 2, 3, and 4, respectively) of all cores associated with LFU1B, as indicated in the text.

bioturbation increases substantially near LFU1B's top boundary (primarily within the overlying LFU5). Consequently, the precise contact between LFU1B and the overlying LFU5 is indiscernible. Slightly greenish-yellow to grayish-yellow colored laminations (i.e. siderite banding) are encountered occasionally, but they are not as distinct as observed within LFU1A or LFU10B. Organics are for the most part absent. Cores that penetrate LFU1B include TT-76-10 and TT-77-10. For additional visual accounts to the above descriptions, refer to the graphic logs, images, and X-ray radiographs of these cores (Appendixes 2, 3, and 4, respectively).

## LFU2

The LFU2 is the most transitional of all lithofacies units. In its eastern section, the LFU2 is generally characterized by interlaminated to interbedded muddy-sand and sandy-mud strata, with the sand fraction dominating the sediment column (Fig. 36). Bioturbation, however, is abundant to complete and largely obliterates strata boundaries and any internal primary sedimentary structures. Consequently, sediments are predominantly mottled, although very-irregular strata are occasionally observed. The grain size of the sand fraction ranges from very-fine to medium, and is often bimodal to even trimodal. Note that a consistent vertical trend is not observed. Shell material (both whole and hash) makes up a considerable portion of the eastern section of LFU2 and in fact, as seen in core TT-73-10, may dominate the sediment column. Where LFU2 underlies LFU9, the contact is sharp (see core TT-55-08) to gradational (see core TT-73-10). Cores that penetrate the eastern section of LFU2 include TT-33-, -55-08 and TT-73-, -74-10. For additional visual accounts to the above descriptions, refer to the graphic logs, images, and X-ray radiographs of these cores (Appendixes 2, 3, and 4, respectively).

Within its central to western parts, LFU2 transitions east to west from predominantly sandy beds separated by an occasional relatively-thin muddy bed to interlaminated to

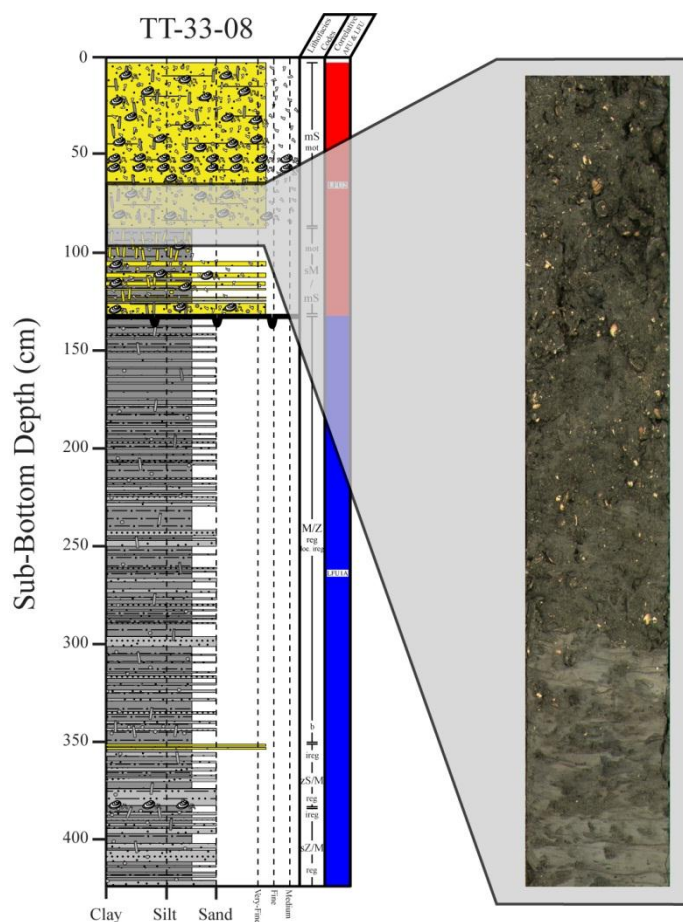


Figure 36. A single example of the eastern section of LFU2, as observed from vibracore TT-33-08. This core was not X-rayed. For a more thorough visual review of LFU2's eastern section, refer also to the graphic logs, images, and X-ray radiographs (Appendixes 2, 3, and 4, respectively) of all cores associated with LFU2's eastern section, as indicated in the text.

interbedded sands and muds (Fig. 37). Primary sedimentary structures observed within the sandy beds of the central to western parts LFU2 are typically parallel to cross laminations. Bioturbation is variable, and thus, for example, a highly bioturbated massive sand may underlie a regular, interlaminated sand-mud section. The sand fraction within this part of LFU2 generally coarsens upwards from very-fine sands (which are dominant) up through possibly fine- to medium-sized grains. Similar to its eastern section, such coarser sands are typically associated with bimodal to even trimodal samples. Fine- to medium-sized sands (i.e. the coarser sands), however, are not found beyond LFU2's central section, suggesting a fining of sands to the west.

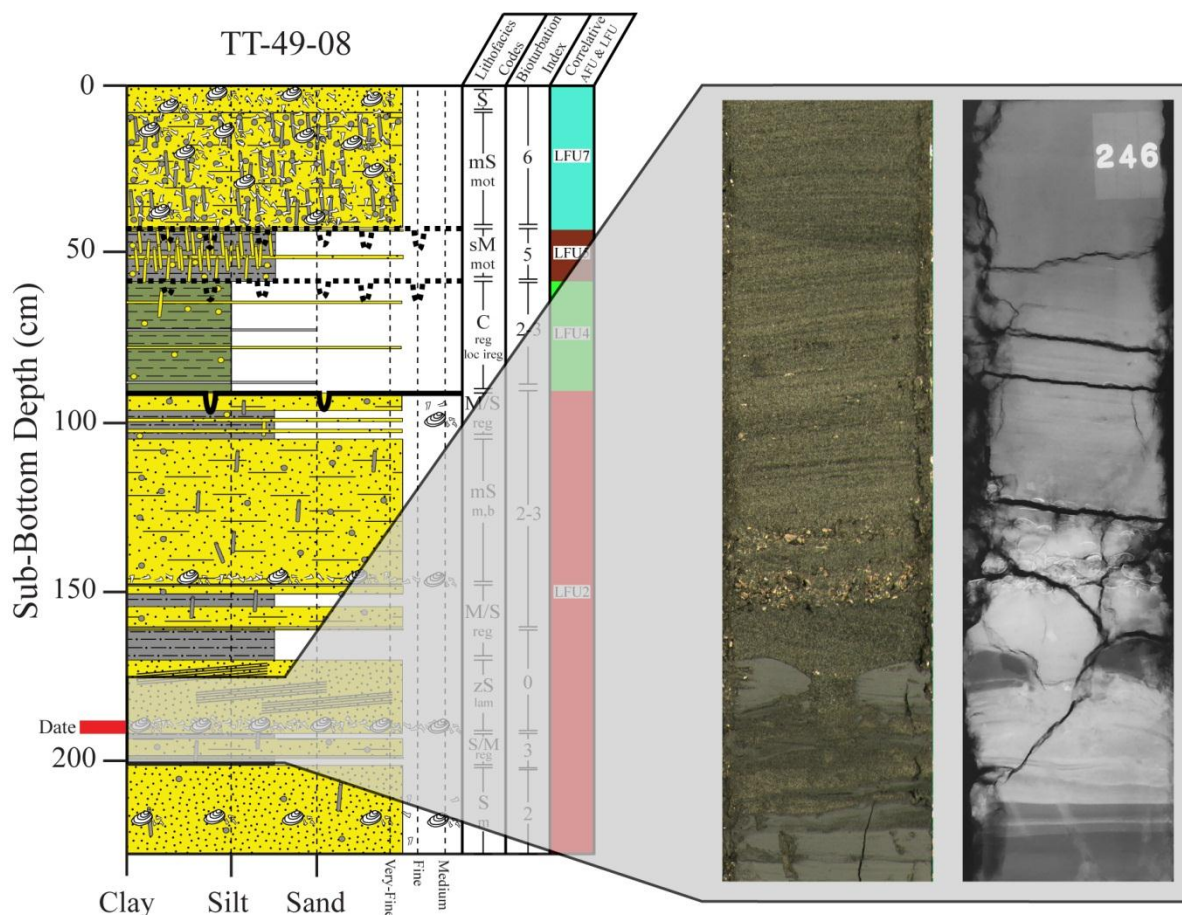


Figure 37. A single example of the central to western parts of LFU2, as observed from vibracore TT-49-08. For a more thorough visual review of LFU2's central to western parts, refer also to the graphic logs, images, and X-ray radiographs (Appendixes 2, 3, and 4, respectively) of all cores associated with LFU2's central to western parts, as indicated in the text.

Shell event layers, typically 2 – 4 cm thick, are also found throughout this part of LFU2. Directly beneath these event layers is usually a scour surface. Shell layers may also be found concentrated at the interface between LFU2 and the underlying LFU1A (see cores TT-47-08 and TT-69-10), and likely represent lag deposits between the two units. Furthermore, the upper sediments of LFU2 that directly underlie LFU8 typically consist of very high concentrations of shell material (both whole and fragments). Consequently, LFU2 grades into the overlying LFU8, which itself is predominantly shell. In contrast, a sharp contact generally occurs at the top of LFU2 where it directly underlies LFU4, although bioturbation may partially obscure this

distinction. Cores that penetrate LFU2's central to western parts include TT-39-, -46-, -47-, -48-, -49-, -50-, -52-, -53-08, and TT-66-, -69-10. For additional visual accounts to the above descriptions, refer to the graphic logs, images, and X-ray radiographs of these cores (Appendixes 2, 3, and 4, respectively).

### LFU3

The LFU3 is dominated by muddy sediments punctuated with interlaminated to interbedded sand and silt strata (Fig. 38). Lenticular laminations are observed, but rare. In the northern part of LFU3 (see cores TT-01-08 and TT-32-08), these intermittent strata are generally sand dominated, whereas in the southern part (see TT-75-10) silt predominates. Cross laminations and in many cases normal grading are observed within the thicker sand beds. Bioturbation is generally moderate in the northern part of LFU3 but becomes abundant to complete in the southern part. Hence, primary sedimentary structures within the southern part of LFU3 are largely non-existent, and instead they are replaced by secondary, mottled structures. In the northern part of LFU3, the top boundary is moderately burrowed and grades into the overlying fine-grained LFU4. In contrast, the seabed forms the top boundary in the southern part. In the northern part of LFU3, internal boundaries between strata may be distinct, depending on the degree of normal gradation into overlying strata and the local degree of bioturbation. Internal boundaries between strata are largely nonexistent in the southern part of LFU3. Carbonate shells are generally rare and occur sporadically, but occasionally they are found concentrated. In the northern part, the base of LFU3 is characterized by a slight concentration of shell material, and seems to suggest a lag deposit. Cores that penetrate LFU3 include TT-01-08, TT-32-08, and TT-75-10. For additional visual accounts to the above descriptions, refer to the

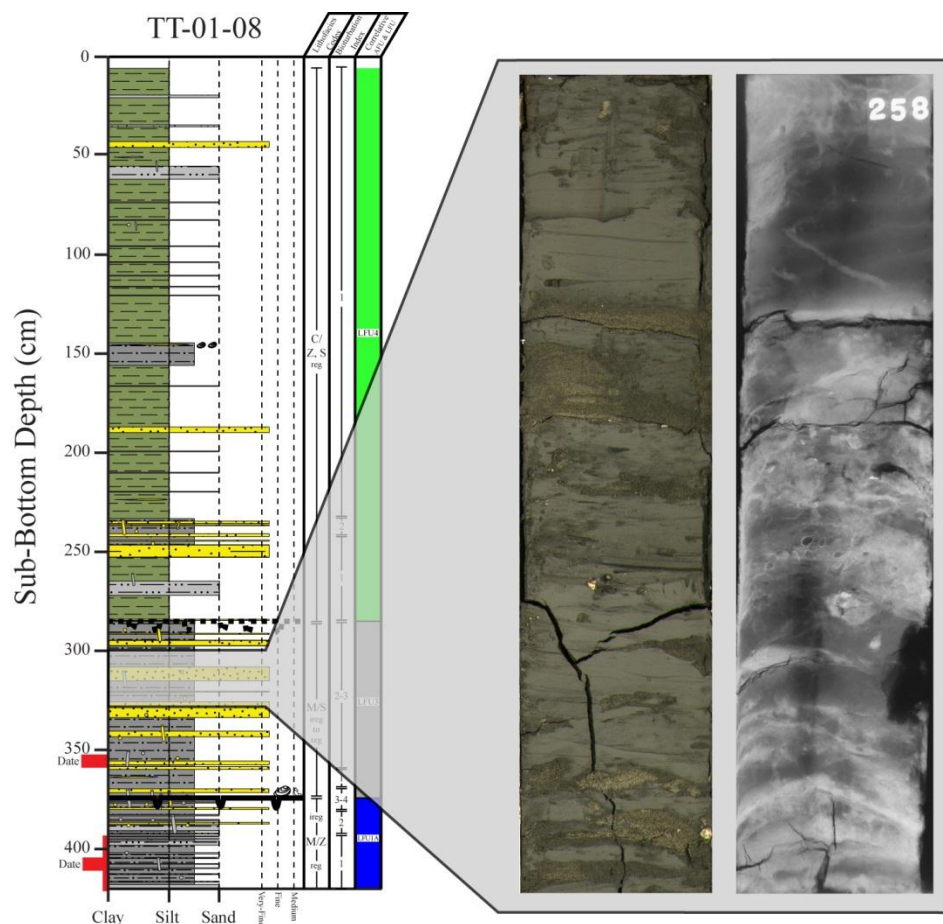


Figure 38. A single example of LFU3, as observed from vibracore TT-01-08. For a more thorough visual review of LFU3, refer also to the graphic logs, images, and X-ray radiographs (Appendixes 2, 3, and 4, respectively) of all cores associated with LFU3, as indicated in the text.

graphic logs, images, and X-ray radiographs of these cores (Appendixes 2, 3, and 4, respectively).

#### LFU4

The LFU4 is overwhelmingly comprised of clay sediment (Fig. 39). Within this clay core are interlaminated to interbedded silts and sands, with frequencies (i.e. spacing between successive coarse-grained strata) that vary across the lithofacies. Although a few are readily apparent with the naked eye, the vast majority of laminations are subtle and only discernible with the aid of X-ray radiographs. Cross laminations may also be observed within the rare, coarser-



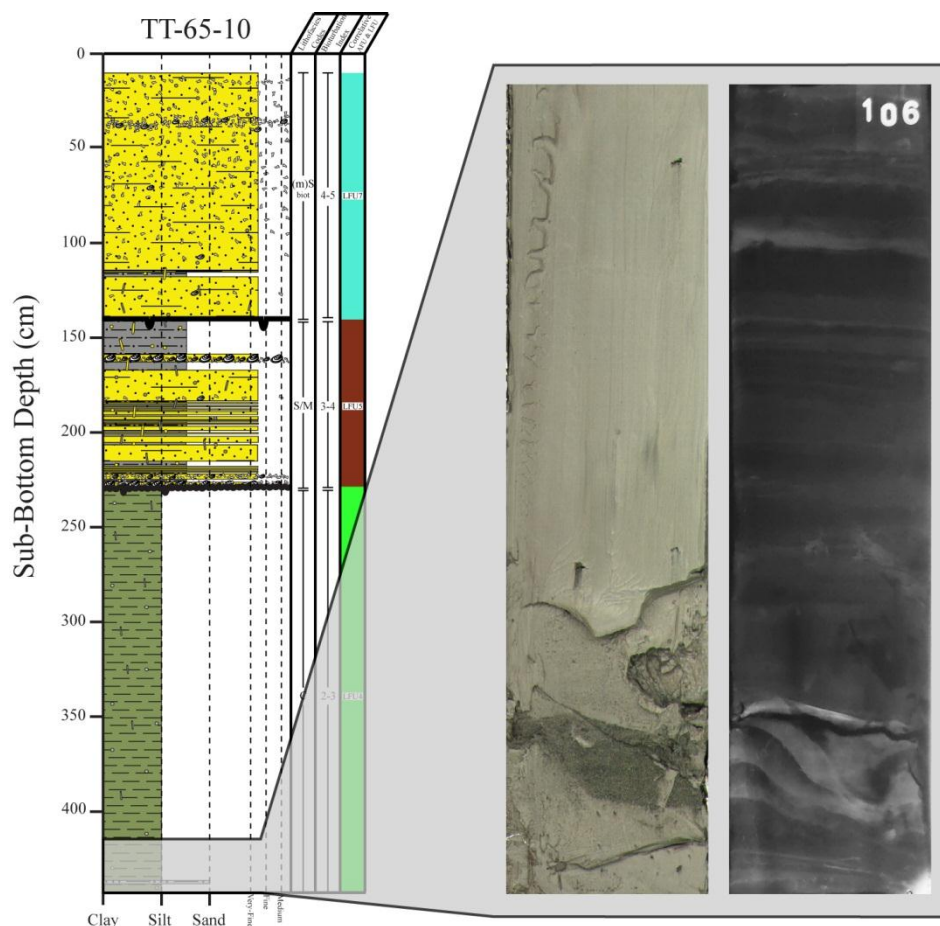


Figure 39. A single example of LFU4, as observed from vibracore TT-65-10. For a more thorough visual review of LFU4, refer also to the graphic logs, images, and X-ray radiographs (Appendixes 2, 3, and 4, respectively) of all cores associated with LFU4, as indicated in the text.

sediment beds, which themselves may directly overlie a shell layer and an associated scour surface. Bioturbation within LFU4 ranges from sparse to moderate, and so preservation of primary sedimentary structures is generally good. Despite such a low degree of bioturbation, the top boundary of most individual laminations appears subtle, apparently because the coarser laminations grade into the dominating clay sediments. The top boundary of LFU4 itself, however, is inconsistent, varying from gradational to sharp to clearly erosional. In other places, LFU4's top boundary represents the seabed. The color of the clay sediment within LFU4 is generally pale to grayish olive, but in rare instances includes slightly greenish-yellow to grayish-

yellow colored laminations (i.e. siderite banding). However, these deviant-colored laminations are much more infrequent and inconspicuous in LFU4 than observed in LFU1A and LFU10B. Instead, they are more in line with what was observed in LFU1B. Cores that penetrate LFU4 include TT-01-, -20-, -25-, -26-, -27-, -28-, -30-, -31-, -32-, -37-, -39-, -40-, -41-, -42-, -43-, -44-, -46-, -47-, -48-, -49-08, and TT-64-, -65-, -66-10. For additional visual accounts to the above descriptions, refer to the graphic logs, images, and X-ray radiographs of these cores (Appendixes 2, 3, and 4, respectively).

### LFU5

The LFU5 is characterized by interlaminated to interbedded sandy muds and muddy sands, although shell beds (~ 3 cm thickness) are occasionally encountered (Fig. 40). The exception is in the most southern part of the study area (see TT-76-10 and TT-77-10) where sandy silts replace sand-dominated strata. Muds typically dominate the sediment column. However, sands, all of which are within the very-fine sand fraction, make up a considerable percentage and in some places dominate (see TT-02-08, TT-05-08, and TT-78-10). Where observed, boundaries demarcating individual strata are generally distinct, although normal grading within coarse strata is occasionally encountered. However, bioturbation largely reworks strata boundaries. Bioturbation intensity may vary from sparse to complete within a single core but, with exceptions, is typically at least moderate. Thus, strata are largely irregular to mottled, although regular strata are not uncommon. Consequently, preservation of primary sedimentary structures is generally poor. By far the best exception is seen in core TT-02-08 where parallel to cross laminations are observed within thick, and in some cases inclined, sand beds (see also TT-05-08, TT-06-08, and TT-78-10). Within its southern and northern parts, LFU5 gradationally transitions upwards into LFU6 and LFU7, respectively. Elsewhere, the top of LFU5 forms the



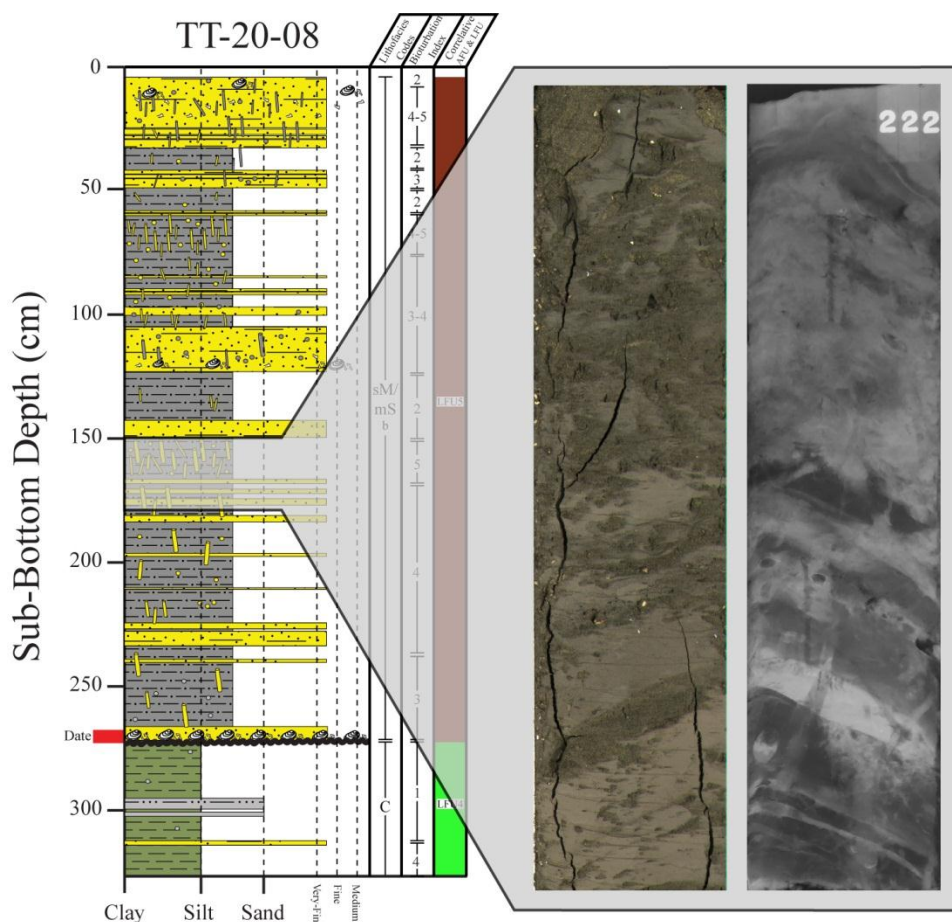


Figure 40. A single example of LFU5, as observed from vibracore TT-20-08. For a more thorough visual review of LFU5, refer also to the graphic logs, images, and X-ray radiographs (Appendixes 2, 3, and 4, respectively) of all cores associated with LFU5, as indicated in the text.

seabed, except in the very northeast where it underlies AFU12 (again, note that AFU12 does not have a corresponding lithofacies). Sediments within LFU5's southern parts are typically devoid of shell material. Within its northern parts, particularly in the vicinity of LFU7, shell material, especially shell hash, noticeably increases in concentration. Cores that penetrate LFU5 include TT-02-, -03-, -05-, -06-, -10-, -19-, -20-, -21-, -22-, -23-, -25-, -26-, -27-, -28-, -30-, -31-, -32-, -37-, -39-, -40-, -41-, -42-, -43-, -44-, -45-, -46-, -47-, -48-, -49-08 and TT-64-, -65-, -66-, -76-, -77-, -78-10. For additional visual accounts to the above descriptions, refer to the graphic logs, images, and X-ray radiographs of these cores (Appendixes 2, 3, and 4, respectively).

## LFU6

The LFU6 is overwhelmingly comprised of very-fine sand, although it becomes slightly muddy along its perimeters, particularly within its large, tapering northern section (Fig. 41). In many instances, it is difficult to discern primary sedimentary structures within LFU6 even if examining this lithofacies using X-ray radiographs. A lack of internal structures may be due to the fact that sediments are largely homogenous, very-fine sands, or it could be the result of complete mixing caused by burrowing organisms. Also, it cannot be ruled out that sands were homogenized during the vibracoring process. Where the cause for homogenization cannot be resolved, such sands are simply considered massive. Nevertheless, many cores display cross laminations that are readily apparent. These primary structures may be observed visually or sometimes only from X-ray radiographs. The boundaries of individual laminations, particularly as observed in X-ray radiographs, are generally undefined, as they appear to be highly gradational. On the other hand, many cores display burrowing, from sparse and uncommon where primary sedimentary structures are preserved to common and abundant where they are not. Sands within the central, thicker part of LFU6 are generally devoid of shell material, with perhaps minute amounts of hash or larger shell fragments. Shell content increases along the perimeters of LFU6, particularly within its large, tapering northern sections. Moreover, shell event layers are also occasionally recognized here, and in many cases are reworked by burrowing. Lastly, the top of LFU6 forms part of the seabed. Cores that penetrate LFU6 include TT-02-, -03-, -04-, -05-, -06-, -09-, -10-, -12-, -15-, -19-, -21-, -22-, -23-, -24-, -25-, -26-, -28-, -29-, -30-, -31-, -32-, -45-08 and TT-08-, -13-, -17-, -57-10. For additional visual accounts to the above descriptions, refer to the graphic logs, images, and X-ray radiographs of these cores (Appendixes 2, 3, and 4, respectively).

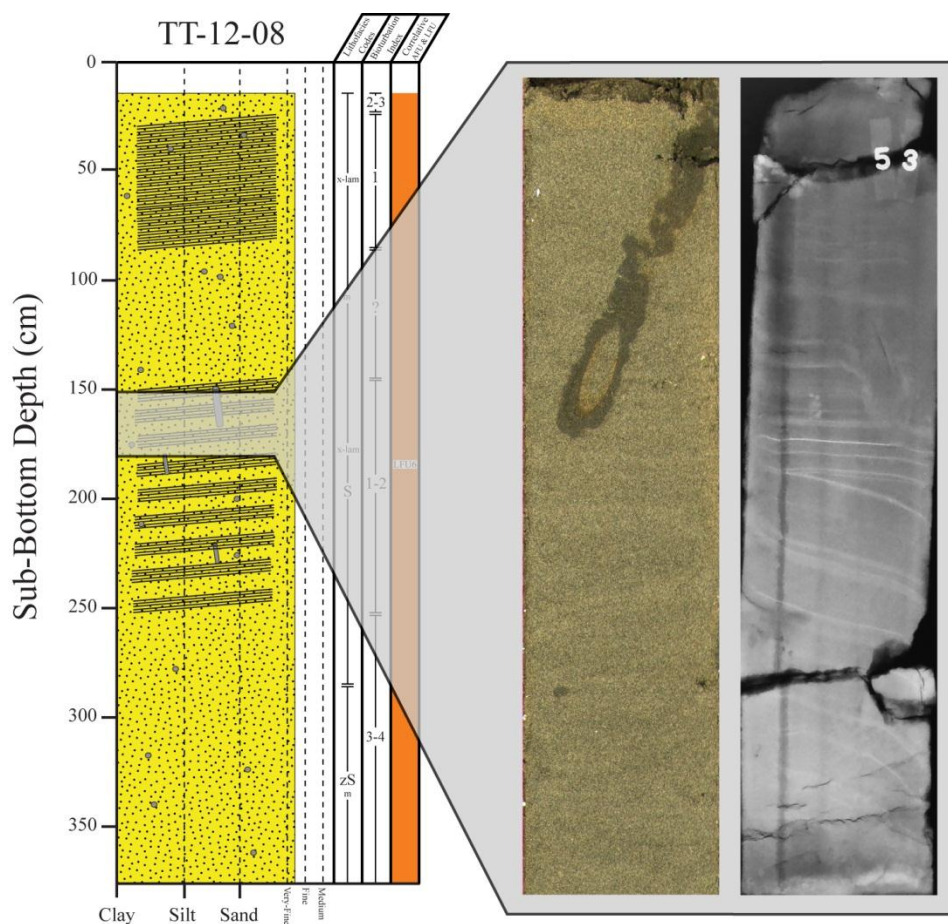


Figure 41. A single example of LFU6, as observed from vibracore TT-12-08. For a more thorough visual review of LFU6, refer also to the graphic logs, images, and X-ray radiographs (Appendixes 2, 3, and 4, respectively) of all cores associated with LFU6, as indicated in the text.

### LFU7

The LFU7 is predominantly comprised of sand to slightly-muddy sand sediment (Fig. 42). It displays a principally dark-colored hue, which suggests a muddy character at first glance. However, sand-mud ratios determined from several dark-colored samples clearly show that much of this sediment is sand (i.e. sand:mud ratio > 90%; Folk, 1974). Other samples with essentially the same hue were measured as muddy sand (i.e. sand:mud ratio < 90% sand; Folk, 1974). Hence, the color of the sandy sediment within LFU7 can be diagnostically misleading. Bioturbation is generally intense, and therefore stratification and other primary sedimentary

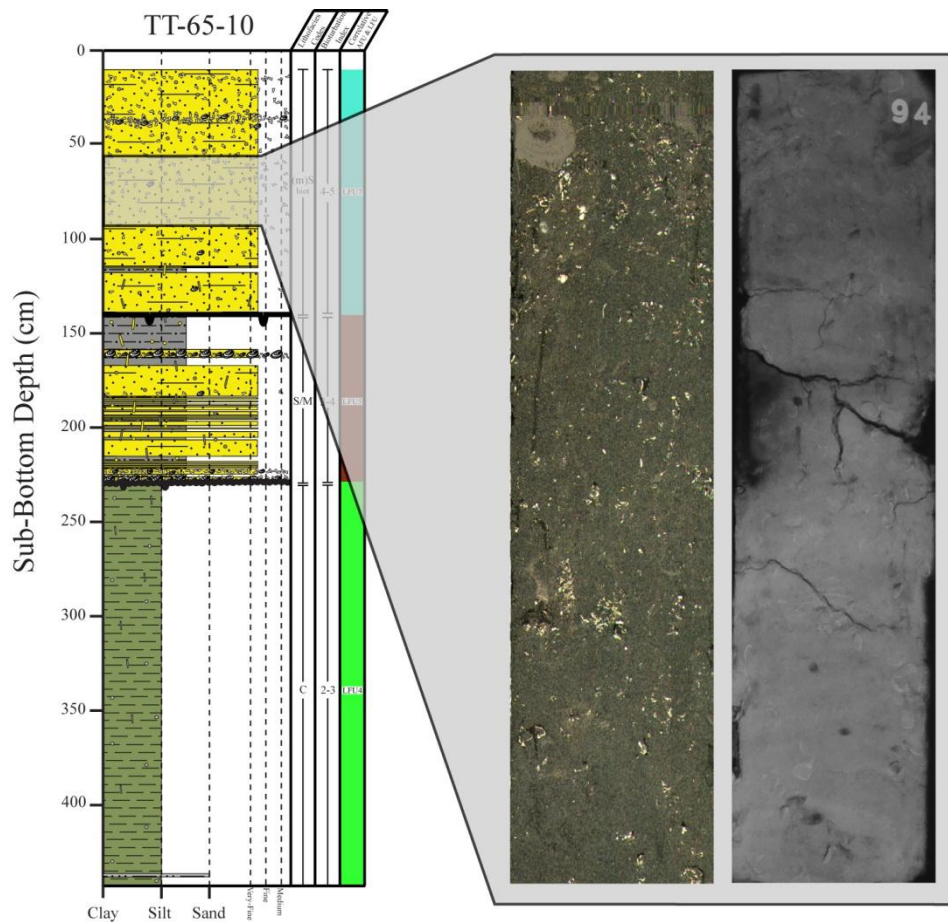


Figure 42. A single example of LFU7, as observed from vibracore TT-65-10. For a more thorough visual review of LFU7, refer also to the graphic logs, images, and X-ray radiographs (Appendixes 2, 3, and 4, respectively) of all cores associated with LFU7, as indicated in the text.

structures are for the most part not preserved. It is not believed that these deposits are instead massive in consequent to homogenous sediment deposition, as an exception to the above observation is found in the most western section of this lithofacies (see cores TT-41-08 and TT-44-08). Here, laminated to cross-laminated sands occur, although partially burrowed, in the lower half of LFU7. The lower half transitions upwards into the upper half where all primary sedimentary structures have been obliterated by bioturbation. The LFU7 also consists of a significant amount of shell (both whole and fragment), particularly within the eastern half of the unit. Although still relatively prominent, the shell component in the western half makes up much

less of the sediment column's total percentage. For the most part, LFU7 crops out at the seabed, except in the very east where it lies beneath, and grades into, LFU8 (see cross section Y22 and vibracore TT-66-10). Cores that penetrate LFU7 include TT-37-, -39-, -40-, -41-, -42-, -43-, -44-, -49-08 and TT-64-, -65-, -66-10. For additional visual accounts to the above descriptions, refer to the graphic logs, images, and X-ray radiographs of these cores (Appendixes 2, 3, and 4, respectively).

### LFU8

The LFU8 is predominantly comprised of shell material with the dominant species (fossil) represented by the marine bivalve *Mulinia lateralis* (Laurie Anderson, personal communication, 2012; Fig. 43). Clastic sediments, largely sand-sized grains, are also present. Sands may range in size from very-fine to medium and are commonly characterized as bimodal to even trimodal. The top of LFU8 forms part of the seabed. Cores that penetrate LFU8 include TT-34-, -35-, -50-, -52-, -53-, -54-08, TT-66-10, and TT-69-10. For additional visual accounts to the above descriptions, refer to the graphic logs and images of these cores (Appendixes 2 and 3, respectively). Attempts to X-ray LFU8 proved futile.

### LFU9

The LFU9 is predominantly comprised of clay sediment that is a light-brown color (Fig. 44). Interlaminated to interbedded silts are observed within the clay core but are only visualized with the aid of an X-ray radiograph. Boundaries separating the silt strata and the clay core are also generally distinct. Bioturbation is largely uncommon, and so the preservation of stratification is generally good. Although not measured in the lab, LFU9 appears to have a high water content. Shell material is generally scarce to absent, but LFU9 does overlie, or at least it does so within the two cores examined, a shell-lag deposit. The top boundary of LFU9 forms



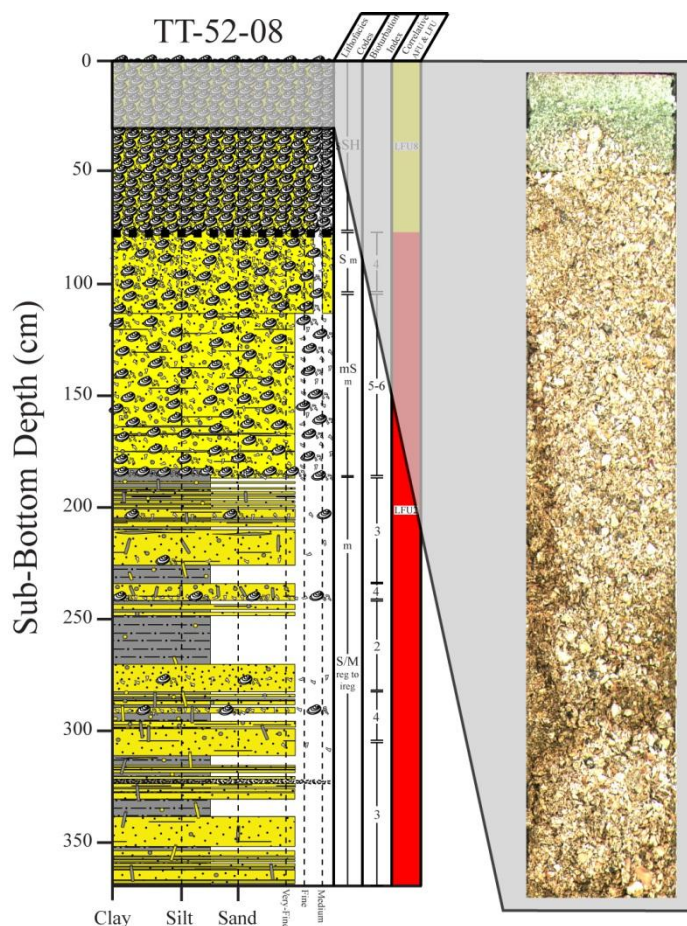


Figure 43. A single example of LFU8, as observed from vibracore TT-52-08. Note that this facies was not X-rayed. For a more thorough visual review of LFU8, refer also to the graphic logs and images (Appendixes 2 and 3, respectively) of all cores associated with LFU8, as indicated in the text.

part of the seabed. Cores that penetrate LFU9 include TT-55-08 and TT-73-10. For additional visual accounts to the above descriptions, refer to the graphic logs, images, and X-ray radiographs of these cores (Appendixes 2, 3, and 4, respectively).

### LFU10A

The LFU10A is dominated by bed-scale sands, with interlaminated to interbedded sands and muds also prevalent (Fig. 45). Both strata and the size of sand grains appear to fine upwards, from fine sands upwards into very-fine sands (at least so within core TT-74-10).

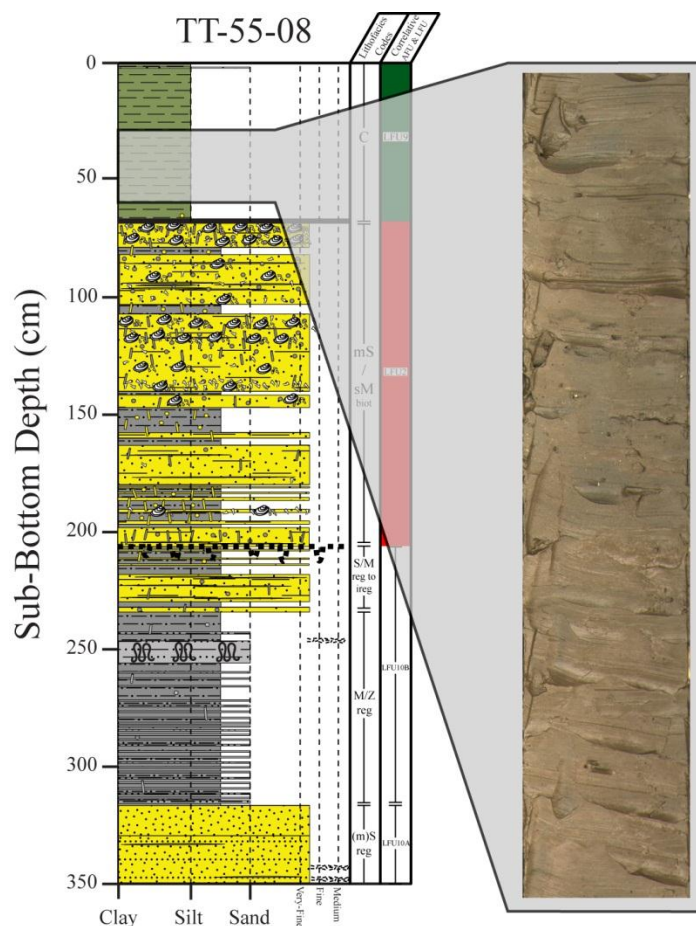


Figure 44. A single example of LFU9, as observed from vibracore TT-55-08. Note that this facies was not X-rayed. For a more thorough visual review of LFU9, refer also to the graphic logs and images (Appendixes 2 and 3, respectively) of all cores associated with LFU9, as indicated in the text.

Various types of primary sedimentary structures are present, including parallel laminations, cross laminations, trough-cross laminations, and multi-directional current ripples. Boundaries separating individual strata are generally distinct, although scouring along boundaries is occasionally recognized. Distortion of strata is also occasionally encountered, whereas bioturbation is generally absent. The LFU10A may also be characterized by large amounts of particulate plant organics (i.e. “coffee grinds”), particularly as seen within core TT-74-10. The LFU10A gradually transitions upwards into LFU10B. Cores that penetrate LFU10A include TT-

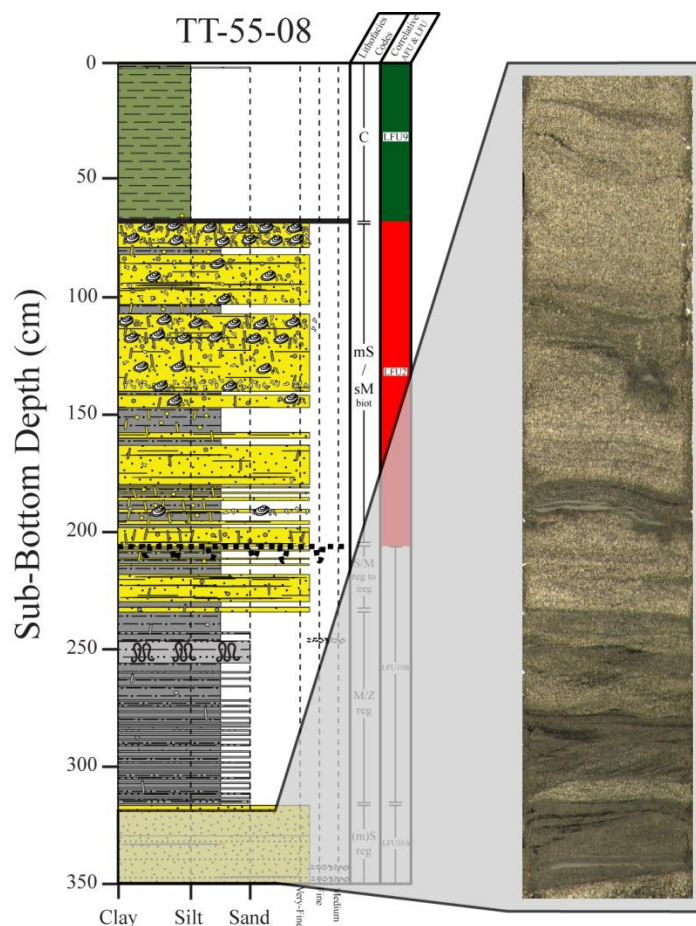


Figure 45. A single example of LFU10A, as observed from vibracore TT-55-08. Note that this facies was not X-rayed. For a more thorough visual review of LFU10A, refer also to the graphic logs and images (Appendixes 2 and 3, respectively) of all cores associated with LFU10A, as indicated in the text.

55-08 and TT-74-10. For additional visual accounts to the above descriptions, refer to the graphic logs and images of these cores (Appendixes 2 and 3, respectively).

### LFU10B

The LFU10B lies stratigraphically above LFU10A. The LFU10B is largely similar in description to LFU1A. For instance, LFU10B is dominated by interlaminated to interbedded, sandy-silt and silty-clay sediments (Fig. 46). However, sediments within LFU10B are predominantly coarser and do not display the variety of primary sedimentary structures as seen in



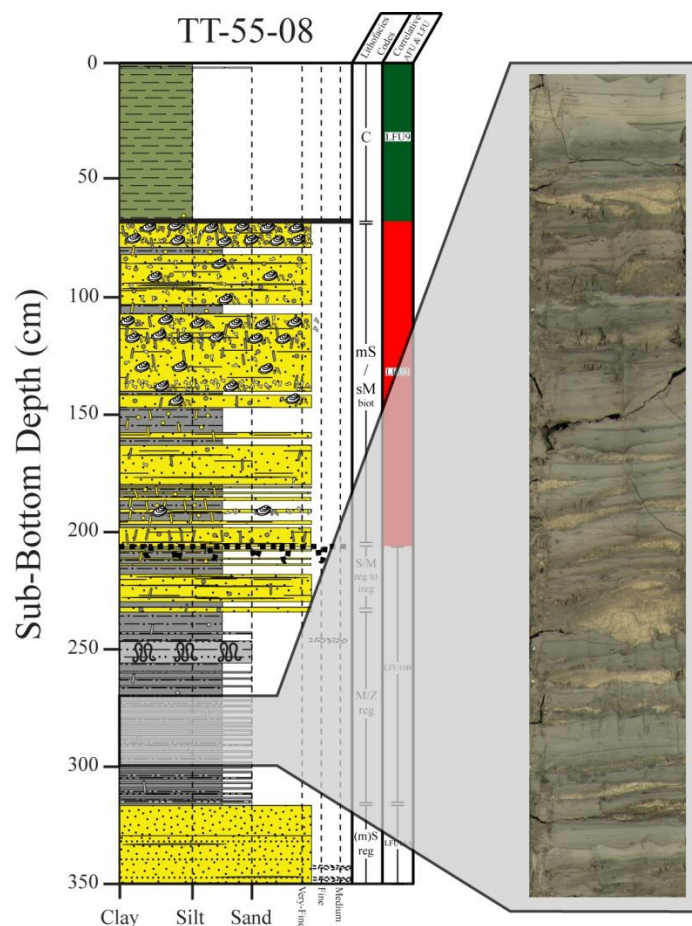


Figure 46. A single example of LFU10B, as observed from vibracore TT-55-08. Note that this facies was not X-rayed. For a more thorough visual review of LFU10B, refer also to the graphic logs and images (Appendixes 2 and 3, respectively) of all cores associated with LFU10B, as indicated in the text.

LFU1A. The LFU10B also occasionally displays moderate greenish-yellow to grayish-yellow colored laminations (i.e. siderite banding) within its overall pale-olive clay fraction. Bioturbation is recognized as uncommon to abundant, with molted beds occasionally observed. This unit's top boundary is heavily burrowed, and so it appears to gradually transition into the overlying LFU2 (although interpretations discussed later would imply a relatively distinct top boundary for LFU10B). Cores that penetrate LFU10B include TT-55-08 and TT-74-10. For additional visual accounts to the above descriptions, refer to the graphic logs and images of these cores (Appendixes 2 and 3, respectively).

## **DISCUSSION**

The depositional model of the Trinity-Tiger Shoals region established from this study was developed largely through the integration of the acoustic and lithological data sets characterized in the preceding Results section. Incorporating the AMS radiocarbon data set (i.e. geochronology) completed the model. The following discussion begins with the interpretations drawn from the regressive component of the delta and then shifts upwards stratigraphically into the transgressive component. Afterward, the discussion considers where both regressive and transgressive sediments fit within a sequence-stratigraphic framework. The discussion then examines the prevailing transgressive depositional systems model which has long been used to explain transgressive deposition within the Mississippi Delta, including the Trinity-Tiger Shoals region. The discussion closes by contrasting this model with interpretations derived herein.

### **The Regressive Component**

The AFU1, and all that it encompasses, constitutes the regressive component of a portion of a once-active Mississippi Delta complex. The most convincing features of evidence supporting this interpretation are AFU1's progradational reflection-configuration patterns, especially the set of tangential-oblique patterns observed over large parts of the study area. Observations at the local scale (e.g. cross section XX8 near its intersection with cross section Y19, Appendix 1) reveal strongly dipping clinoforms along depositional dip (east-west) and horizontal- to moderately-dipping clinoforms along depositional strike (north-south). Such diverging views between dip and strike profiles are not incompatible but in fact express the fundamental architecture of progradational reflection-configuration patterns associated with individual fluvial-dominated delta lobes (Fig. 47; Mitchum et al., 1977; Sangree and Widmier, 1977; Berg, 1982). Corroborating this interpretation are complementing lithofacies units. Note

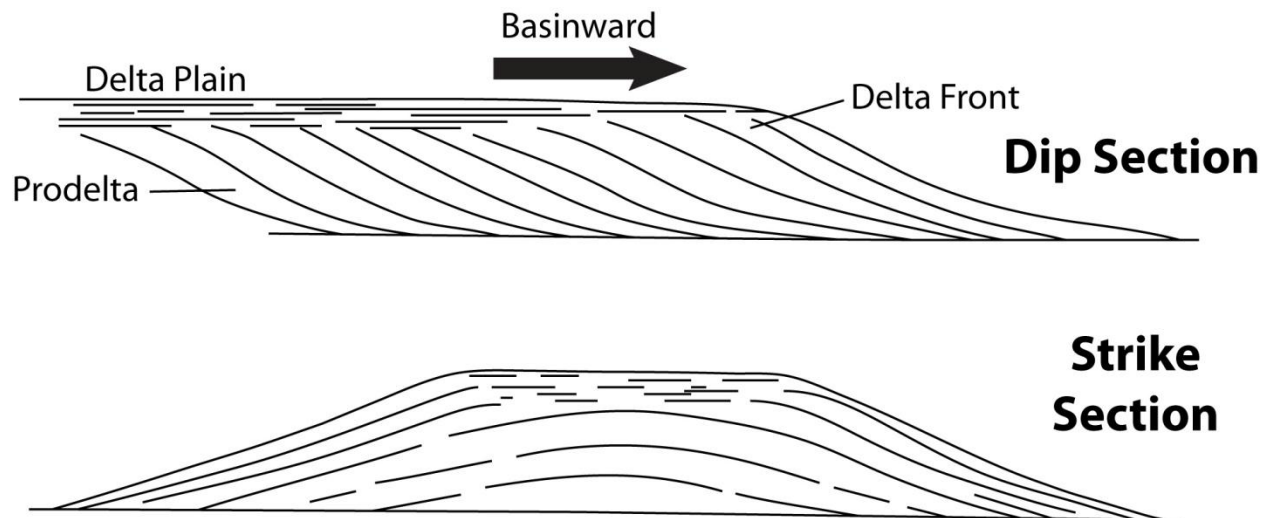


Figure 47. Contrasting dip and strike profiles from an idealized prograding, fluvial-dominated delta lobe. Modified from Berg, 1982.

that the upper part of the clinoform zone (i.e. the topset and upper parts of the foreset) associated with a fluvial-dominated delta lobe corresponds with the delta front and other proximal depositional environments, whereas the lower part of the clinoform zone (i.e. middle-to-lower parts of the foreset and the bottomset) corresponds with the prodelta environment (Fig. 47; Sangree and Widmier, 1977; Berg, 1982). The LFU1A, associated with the upper part of the clinoform zone, represents the delta-front environment, whereas LFU1B, associated with the lower part of the clinoform zone, represents the prodelta environment. Note that only two cores (TT-76-10 and TT-77-10) penetrate LFU1B, and they do so only within the bottomset strata of a detached, down-drift subaqueous delta lobe (the stratigraphic framework is discussed in more detail below). Nevertheless, the prodelta of a down-drift subaqueous delta lobe is considered more-or-less equivalent to the prodelta of the more tangential-oblique-like delta lobes observed elsewhere within the study area, and so LFU1B is considered representative of the prodelta facies.

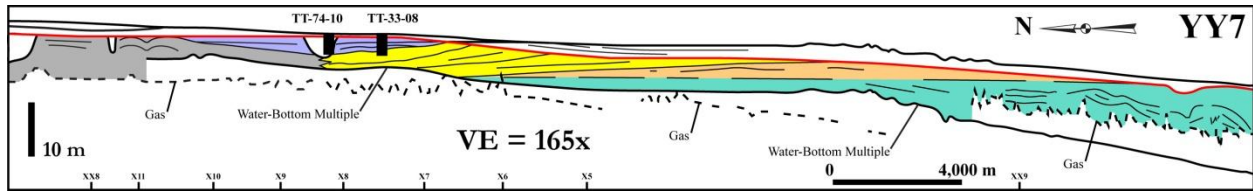


Figure 48. An offsetting, overlapping, and stacked arrangement of deltas. Here along the north-south cross section of YY7, four major delta lobes and one subdelta are distinguished. Refer to Figure 25 for cross section location.

Observations of the regressive component at the regional scale (i.e. the scale of the study area) reveal an offsetting, overlapping, and stacked arrangement of deltas (Fig. 48). Such a “deltas within deltas” arrangement is the fundamental architecture of a Mississippi Delta-type delta complex (Roberts, 1997). Partial elements of this delta complex that are preserved and herein distinguished include four major delta lobes and one subdelta. The areal bounds of these separate deltaic units are interpreted as shown in Figure 49. Note that the four delta lobes and one subdelta are color coded, and from this point onward they are referred to by their respective color. The distributary system that fed part of this region of the delta complex is also partially preserved, but, with one exception, only in the northern part of the study area (Fig. 49). Elsewhere, it has been removed by transgressive ravinement. The distributary system is identified within the acoustic data set as AFU10. Based on the overall reflection-configuration patterns perceived within each deltaic unit coupled with the generally west-southwest trend of the preserved distributary system, the deltaic system is interpreted to have largely prograded from the east-northeast to the west-southwest. Variances from this generalization, particularly as related to the orange delta lobe, are discussed below. Obviously, more subdeltas should exist, as they are building blocks for the delta lobe (Coleman and Gagliano, 1964; Roberts, 1997). However, further delineation was not possible owing to the partial removal of the top portion of

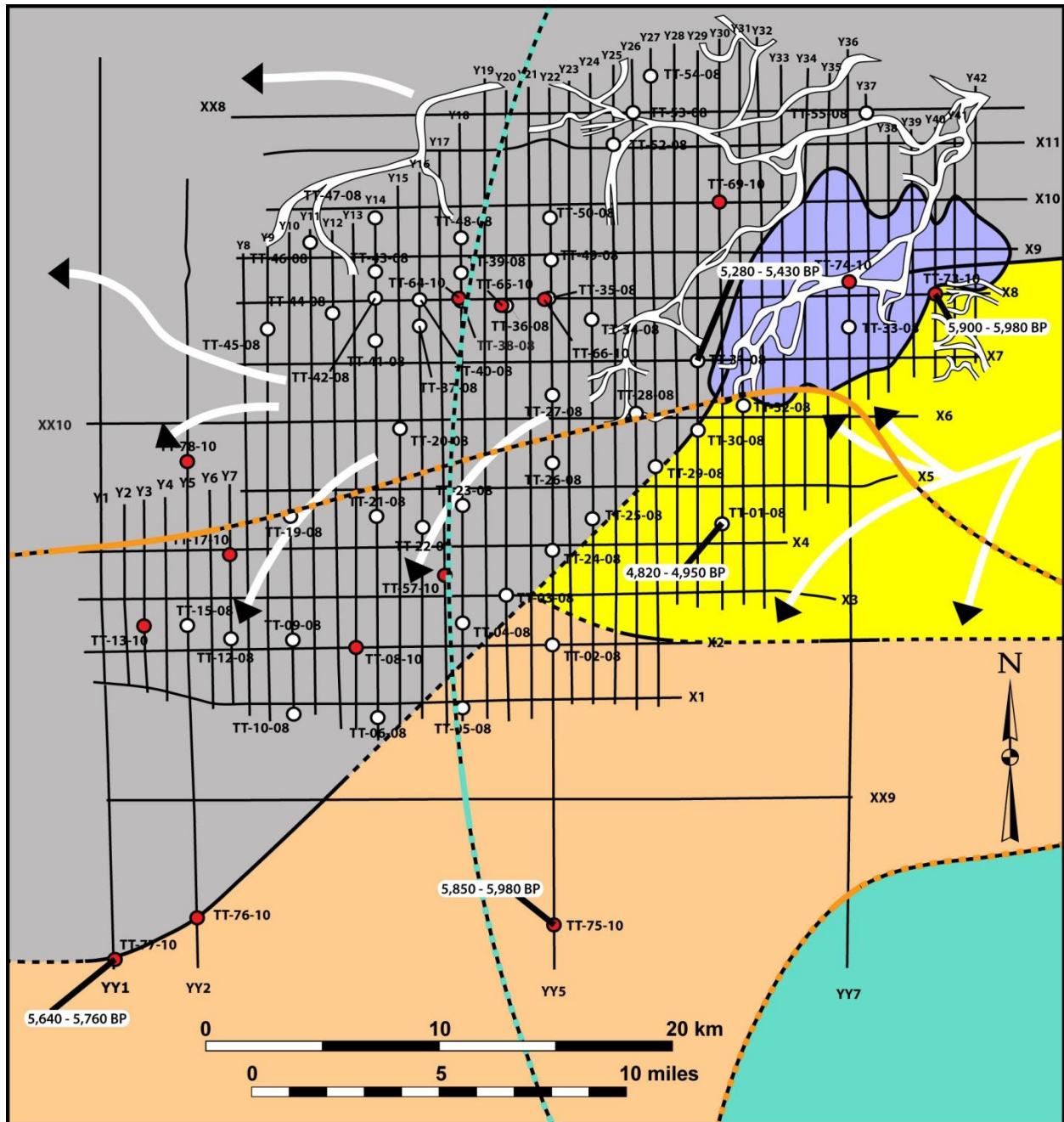


Figure 49. The four delta lobes and one subdelta differentiated within the study area. Each deltaic unit is recognized here by their respective color. Those parts of the distributary system that are preserved are also indicated. Elsewhere, generalized depositional trends are indicated by arrows. Dashed lines indicate the estimated boundaries of what is preserved of the respected deltaic units; solid lines indicate boundary positions of greater confidence, typically where deltaic units are directly observed in cross sections. Note that the orange and green delta lobes lie stratigraphically beneath the other deltaic units, and so their estimated boundaries are indicated by colored-dashed lines (e.g. the green and black dashed line indicates the boundary of the green delta lobe). The peculiar trend of the orange delta lobe's boundary in the southeastern part of the study area is a consequence of erosional truncation.

the delta complex by transgressive ravinement, in addition to acoustic masking brought on by the water-bottom multiple and gas-charged sediments.

### Depositional Patterns

The depositional patterns of the regressive component and the resulting stratigraphic framework are best depicted through illustration, and the reader should familiarize himself/herself with Appendix 5 before proceeding. Appendix 5 consists of a series of cross sections that analyze only the regressive component, and the following discussion draws from this appendix almost entirely. Cross section locations are illustrated in Figure 49. In some instances, references will also be made to Appendix 1, and these references will be noted in the text. However, unless otherwise noted, the reader should refer to the cross sections in Appendix 5. Beginning this discussion with cross section YY7, which extends nearly the entire north-to-south length of the study area, the partial remnants of the four major delta lobes and one subdelta are identified. The green-colored delta lobe is at the base of the regressive component. The orange delta lobe is stratigraphically above, followed by the gray-colored delta lobe to the north, the yellow-colored delta lobe to its south, and the blue-colored subdelta nested between and atop of the gray and yellow delta lobes. Note that only the southern and northern halves of the gray and yellow delta lobes are observed, respectively. The exact position of the boundary that separates these two delta lobes is slightly arbitrary, as the two appear to have regularly overlapped during their more-or-less contemporaneous progradational phase. Nevertheless, a boundary separating the two lobes is estimated based on the position and inclination of their respective internal reflectors. In many cases, the boundary is also associated with hummocky clinoforms, which are indicative of interfingering strata (Mitchum et al., 1977). Beginning with cross section Y42 and moving westward, the boundary between the gray and yellow delta lobes

is perceived to shift progressively southward, a mere reflection of the overall west-to-southwest trend of the deltaic system.

#### “The Green Delta Lobe”

Although subbottom coverage of the green delta lobe is sparse, it is estimated to extend the entire north-to-south length of the study area, as indicated in Figure 49 (e.g. cross sections Y42 and YY7; again, refer to cross sections in Appendix 5 during this and the following discussion unless stated otherwise). Its westward extent is directly revealed only in cross section XX9, which appears to show the green delta lobe terminating down-dip against the antecedent topography of AFU11 (also, see cross section XX9 in Appendix 1). However, the exact point of termination is obscured by the water-bottom multiple. Again, the green delta lobe lies at the base of the regressive component, and the quality of the acoustic data is relatively poor due to attenuation. Nevertheless, a small portion of its tangential-oblique reflection-configuration pattern is recognized, and suggests progradation was largely east-to-west. Likewise, only a small portion of its distributary system is recognized in the northeastern part of the study area (Fig. 49). Elsewhere, it is not discernible. It is plausible, however, that the distributary system extended towards the southern part of the study area considering the substantial deltaic mass that exists there.

#### “The Orange Delta Lobe”

The orange delta lobe encompasses a significant portion of the southern half of the study area, as is indicated in Figure 49. In contrast with the three other delta lobes and one subdelta, which are each characterized by the tangential-oblique reflection-configuration pattern, the orange delta lobe is defined by the sigmoidal reflection-configuration pattern (e.g. cross section XX9). The sigmoidal acoustic facies generally represents a relatively low-energy environment,

and in a deltaic setting, this acoustic-facies type likely represents an interlobe area that received mostly fine-grained clastics (Berg, 1982). The orange delta lobe's upper strata have also been significantly truncated by transgressive ravinement (e.g. cross sections XX9 and YY5). Furthermore, an associated distributary system is not recognized. However, a missing distributary system is not thought to be consequent to transgressive ravinement, but instead is believed to have never existed within the study area. Based on the above conditions, the orange delta lobe is interpreted as a detached, down-drift subaqueous delta physically decoupled from the subaerial delta lobe(s) from which it derived its sediment. Perhaps the most compelling piece of evidence to support this interpretation comes from the geometry of the orange subaqueous delta (e.g. cross section XX9). Internally, it consists of the sigmoidal reflection-configuration pattern, whereas its external form reveals a thick, central sequence that thins to the east, north, and west. Hence, there is not an immediate, local sediment source from any of these directions.

Along the modern coastline of west Louisiana, it is well established that muds discharging out of the Atchafalaya River and beyond the Atchafalaya Bay are transported predominantly westward along the inner shelf by the prevailing coastal current (Wells and Kemp, 1981; Huh et al., 1991; Roberts, 1998; Walker and Hammack, 2000; Bentley, 2003). It is also well established that such muds are currently forming a detached, down-drift subaqueous delta along the shoreface adjacent to the eastern chenier plain (Roberts et al., 2002; Draut et al., 2005). With this in mind, it is interpreted here that at one time muds were discharging out of a distributary system associated with a separate subaerial delta lobe(s) located well beyond the eastern boundary of the study area (but still within the confines of the same delta complex) and were subsequently transported westward along the paleo-inner shelf in a fashion similar to that observed today along the coastline of west Louisiana. A significant portion of these muds were



ultimately deposited within the study area atop of the southern part of the green delta lobe, forming the orange subaqueous delta. The resulting stratigraphic framework of the orange subaqueous delta, which is most clearly recognized along the dip-profile of cross section XX9, reflects the classic topset, foreset, and bottomset sigmoidal-shaped pattern, a pattern that suggests progradation was from east to west.

Considering the vast area over which the orange subaqueous delta prograded, subbottom coverage is rather limited. Nevertheless, some estimates of its areal bounds can be made (Fig. 49). As cross section XX9 indicates, the orange subaqueous delta onlaps the green delta lobe in the east. Despite significant erosional truncation along its top boundary in this region, preserved clinoforms of the orange subaqueous delta suggest that the upper-most foreset and topset strata once extended considerably farther east than the longitude of cross section YY7 and likely beyond the eastern boundary of the study area. This interpretation is certainly conceivable considering that the mud stream that built the orange subaqueous delta was transported into the study area from the east. Cross section XX9 (also, cross sections YY1 and YY2) also reveals that the sigmoidal clinoform package of the orange delta lobe tapers away to the west. Based on the low-angle, westward-thinning trend of bottomset strata, the orange subaqueous delta likely extends as far west as the western limit of the study area, but likely not much farther. Likewise, the orange subaqueous delta tapers away to the north in this western part of the study area. This latter interpretation is based simply on the trend of the orange subaqueous delta's northward-thinning bottomset strata as recognized in cross sections YY1 and YY2. In the eastern part of the study area, specifically as observed along the north-to-south cross section of YY7, the orange subaqueous delta also tapers away to the north. In contrast, clinoforms appear to thicken towards

the south (cross sections YY1, YY2, and YY5), suggesting that the southern boundary of the orange subaqueous delta extends well beyond the southern boundary of the study area.

#### “The Gray Delta Lobe”

The gray delta lobe extends the entire east-west length of the study area, mostly within the northern half (Fig. 49). However, only portions of the gray delta lobe’s distributary system are preserved as far west as the longitude of acoustic line Y10. Despite this lack of preservation, the distributary system, along with the delta front and other proximal depositional environments, are interpreted to have continued building within the northern part of the gray delta lobe as far west as the longitude of acoustic line YY1. (This interpretation is in contrast with an alternative scenario of only a progressively thinning prodelta environment extending westward from the longitude of acoustic line Y10.) Evidence supporting this interpretation includes the tangential-oblique reflection-configuration patterns that clearly extend beyond the western limits of cross sections X9, X10, X11, and XX8 (here, refer to cross sections in Appendix 1; again, note that the delta-front, i.e. LFU1A, and associated depositional environments correspond with the upper parts of the clinoform zone. Also, note that the water-bottom multiple obstructs observation south of cross section X9). Furthermore, and in spite of significant erosional truncation along its top boundary, preserved clinoforms within both cross sections YY1 and YY2 observed north of the latitude of cross section XX10 indicate the partial strike-view of a fluvial-dominated delta lobe (see Fig. 47 for the idealized architecture of a fluvial-dominated delta lobe.) The prodelta environment, forming the base of the delta lobe, presumably extends much farther west than the longitude of acoustic line YY1. Generalized depositional trends for the northern part of the gray delta lobe are depicted as arrows in Figure 49.

Delta-building trends within the southern part of the gray delta lobe are more difficult to discern because of acoustic masking brought on by the water-bottom multiple and gas-charged sediments (significant masking begins with cross section Y27 but becomes much more inhibiting to the immediate west). Nevertheless, low-angle basinward-thinning clinoforms associated with the gray delta lobe are observed in the southwestern portion of the study area (cross sections XX9, YY1, and YY2). These strata are interpreted as the basinward extension of the prodelta environment associated with a distributary system positioned farther updip. Note, however, that a single channel is recognized in the very southern part of the gray delta lobe in cross section YY1. This single point of evidence suggests the gray delta lobe's distributary system extended at least this far basinward. Generalized depositional trends for the southern part of the gray delta lobe are depicted as arrows in Figure 49.

#### “The Yellow Delta Lobe”

In contrast with the above discussion, there is no evidence to suggest that the yellow delta lobe prograded as far westward as did the gray delta lobe. In fact, the yellow delta lobe is not observed west of cross section Y26. This lack of observation is partially consequent to acoustic masking brought on by the water-bottom multiple and gas-charged sediments, but it is also partially consequent to the removal of a significant portion of the yellow delta lobe during transgressive ravinement. Furthermore, except for two channels that are differentiated along cross section X6 (refer to Appendix 1), transgressive ravinement has also essentially removed the yellow delta lobe's distributary system. Despite these constraints, some interpretations on depositional trends can be made.

Focusing first on cross section YY7, which includes the most complete strike-view of what is preserved of the yellow delta lobe, note that a partially preserved set of clinoforms is

observed dipping to the north before ultimately interfingering, and thus terminating, with a contemporaneous set of clinoforms associated with the gray delta lobe. Essentially, the yellow delta lobe's northward-dipping set of clinoforms is a mirror image of the southward dipping set of the gray delta lobe (cross section YY7). However, the major distributary that sourced the gray delta lobe's clinoforms is recognized within the subsurface, whereas the major distributary that sourced yellow delta lobe's clinoforms is not. Nevertheless, considering the geometry of what is preserved of the yellow delta lobe together with what is considered the idealized architecture of a fluvial-dominated delta lobe (Fig. 47), it appears that the central part (i.e. from where clinoforms dip either north or south) of the yellow delta lobe along the north-to-south transect of cross section YY7 would have been positioned at the approximate latitude of cross section X4 (see Fig. 49 for a map view). Hence, a major distributary of the yellow delta lobe is interpreted to have prograded across this position. As its northern and western boundaries are relatively well defined (i.e. they are known to merge with the gray delta lobe), the only significant accommodation available for the yellow delta lobe to have built into would have been basinward towards the south-southwest. Thus, the yellow delta lobe is believed to have continued prograding farther basinward towards the south and/or southwest. Note that the southern-southwestern boundary of the yellow delta lobe as estimated in Figure 49 marks the basinward extent of what is presently preserved of the yellow delta lobe. Considering the significant portion of the yellow delta lobe that was removed by transgressive ravinement, it is believed that this delta most likely prograded farther basinward than this position. However, this interpretation is presently unresolvable. Generalized depositional trends for the yellow delta lobe are depicted as arrows in Figure 49.

### “The Blue Subdelta”

The blue subdelta occurs in the northeastern part of the study area, where it is positioned between and atop of the gray and yellow delta lobes (compensational stacking; Fig. 49). Its internal reflection-configuration pattern, specifically the downlapping of its internal reflectors onto the underlying gray and yellow delta lobes, differentiates it (e.g. cross section YY7). The blue subdelta's sediment source appears to be affiliated with the distributary system of the gray delta lobe, based on interpretations within the subbottom data set (Fig. 49 for a map view). It likely originated as a small crevasse splay that would have developed during flooding stage as over-topping waters scoured down through the natural levee and into the adjacent interdistributary bay (see Welder, 1959; Coleman and Gagliano, 1964). Through successive flooding events, it gradually enlarged its own emerging distributary system, progressively infilled the interdistributary bay (i.e. accommodation), and ultimately evolved into the subdelta that is partially preserved today. Its depositional trend, as the course of its dominant distributary system implies, is to the southwest, which is similar to the depositional trends of the delta lobes beneath it. The blue subdelta is not observed west of cross section Y30, although it is estimated to have prograded beyond this longitude. All preexisting deposits of the blue subdelta west of the longitude of acoustic line Y30 were removed by transgressive ravinement.

### Geochronology

Five AMS radiocarbon dates were measured from the regressive component, with ages ranging from as young 4,820 yr BP to as old as 5,980 yr BP (Fig. 49; also Appendixes 2, 5, and 6). Note that all dates discussed here and throughout the remainder of this text are in calendar years. Two of these five dates were measured from the orange delta lobe, two from the yellow delta lobe, and one from the gray delta lobe. Neither the green delta lobe nor the blue subdelta

was AMS radiocarbon dated. As a group, the five measured ages fall within the durational scale of a Mississippi Delta-type delta complex (~ 1,000 – 2,000 years; Frazier, 1967; Roberts, 1997). Based on these five AMS radiocarbon dates together with the current large-scale geochronologic model of the Holocene Mississippi Delta (Fig. 1), which again is based mostly on work conducted updip within the subaerial part of the delta, this study interprets regressive sediments within the Trinity-Tiger Shoals region as the remains of what was once the most southwestern extent of the shoal-water Maringouin Delta Complex. Furthermore, this study finds that the Teche Delta Complex did not prograde across and basinward of the Maringouin Delta and into the study area as an alternative hypothesis would suggest.

Below the delta-complex scale (i.e. at the spatial and temporal scales of delta lobes and subdeltas), the geochronologic model of the study area is difficult to resolve, particularly because of poor preservation in some areas, but also because of signal attenuation and acoustic masking brought on by the water-bottom multiple and gas-charged sediments. Moreover, additional age constraints are always desired. Nevertheless, some generalizations for the development of the Maringouin Delta Complex within the region of the study area can be made based on the five age constraints, together with the stratigraphic principle of superposition.

Note that progradation within the boundaries of the Maringouin Delta Complex certainly occurred in many places contemporaneously to some degree. The following discussion, however, focuses on where the dominant locus/loci of deposition occurred within the study area. Obviously, the green delta lobe constructed first, as it resides at the base of the regressive component (at least that which can be observed). In fact, at the green delta lobe's shallowest position (i.e. at or very near its paleo-subaerial surface), it lies beneath at least ~ 2 m of later-Maringouin deltaic sediment (e.g. see cross section Y42 in Appendix 5). The "later-Maringouin

Delta” refers here to those Maringouin deltaic units that followed the green delta lobe (e.g. the yellow delta lobe). This value is clearly an underestimate since transgressive ravinement removed much of the upper parts of the later-Maringouin Delta, and was likely at least double this value originally. In other words, at least 4 m of sediment originally separated the paleo-subaerial surface of the green delta lobe from the paleo-subaerial surface of the gray and yellow delta lobes. This 4+ m of accommodation was created by rising relative sea level (RSL). The two most important contributing processes would have most certainly been shallow-sediment compaction and eustatic sea-level rise.

As discussed in the Background section, previous researchers (Törnqvist et al., 2006; Milliken et al., 2008) measure a smooth, asymptotic rise in RSL along the northern Gulf of Mexico during the middle-to-late Holocene (see Fig 5). However, their measurements do not record, and thus their resulting RSL curves do not reflect, the high rates of shallow-sediment compaction that are rather unique to the thick Holocene Mississippi Delta. Instead, they record relatively low compaction rates unique to their sample areas, which are superimposed upon a smooth rise in eustatic sea level. In contrast, other researchers (Frazier, 1974; Penland et al., 1989) argue that stillstands (i.e. pauses) occurred during the overall rise in Holocene eustatic sea level, which they in turn argue allowed early-to-middle Holocene Mississippi Delta complexes to prograde across the shelf.

If using the maximum rate of sediment compaction within the Mississippi Delta Plain (~ 5 mm/yr) as determined numerically by Meckel et al. (2006; 2007), at least 800 years would have to transpire before 4 m of compaction would occur. If using a more modest, yet still high, rate of compaction at ~ 2.2 mm/yr (Meckel et al., 2006; 2007), then ~ 1,800 years would have to transpire before 4 m of compaction occurred. It is recognized, however, that deltas building atop

of the green delta would have exacerbated compaction of the underlying green delta. Regardless of the true compaction rate(s), it is nevertheless clear that accommodation was created above the green delta prior to the building of the later-Maringouin deltaic units, and compaction-induced subsidence certainly contributed to the creation of this accommodation.

It is not believed, however, that the green delta lobe is very much older than the deltaic units that lie stratigraphically above it. This interpretation is based principally on the fact that the green delta lobe is not significantly reworked, as would be expected if it were to have been left exposed to open marine processes for ~ 800 – 1,800 years following abandonment (a duration of time that would be required to create 4 m of accommodation through compaction alone; i.e. during a stillstand). Instead, the green delta lobe is believed to have been buried soon after by other Maringouin delta lobes and thus remains modestly preserved. The phrase “soon after” is used here in the relative sense, as there is evidence that some appreciable time transpired before progradation resumed in the study area following abandonment of the green delta lobe. For instance, local distortion of the green delta lobe’s top boundary is recognized in the northeastern part of the study area. Part of what is interpreted as distortion within this region may not in fact be real, but instead may reflect transgressive shell beds that developed atop of the green delta lobe following delta-lobe switching (cross section X7, Appendix 1). Perhaps these shell beds are similar (but on a much smaller scale) to those observed in the transgressive component as discussed later (specifically, LFU8/AFU8). However, distortion observed elsewhere within this region suggests local uplift, perhaps consequent to salt diapirism induced by the recent increase in overburden (i.e. progradation of the green delta lobe; cross section Y39, Appendix 5; Berryhill, 1986). In contrast, distortion of strata is not recognized within the yellow



delta lobe directly overlying the uplifted area (cross section Y39, Appendix 5), suggesting that a minor hiatus separates the green delta lobe from at least the yellow, gray, and blue deltaic units.

If at least 4 m of accommodation above the green delta lobe was created prior to progradation of later-Maringouin deltas, and if the hiatus between the green delta lobe and overlying deltas was relatively minor (i.e. < 800 – 1800 years required by sediment compaction alone), then eustatic sea-level rise would have had a significant impact in creating accommodation. In other words, eustatic sea level rose rapidly following the abandonment of the green delta lobe, as opposed to a still stand within the overall rising Holocene sea-level trend. Evidence supporting a rapid rise in sea level following the abandonment of the green delta lobe is recognized from the green delta lobe's distributary system, which in many instances is associated with a reflection-free configuration pattern (Fig. 32, B1 and B2). Again, channel fill within the delta is typically characterized by highly bioturbated, poorly-sorted silts, clays, and organic debris (Coleman, 1981; Coleman and Prior, 1982), which is expected to be expressed in acoustic data by a chaotic reflection-configuration pattern and/or a very high degree of acoustic scatter. Such channel-fill configuration patterns are observed in the gray and blue delta's distributary systems (Fig. 32, A1 and A2). In contrast, a reflection-free configuration pattern would imply the infilling of channels with homogenous sediments. Note that the reflection-free channels depicted in Figure 32 are not thought to be consequent to gas-charged sediments, as acoustic wipeout does not exist beneath channels. Instead, the local reflection patterns beneath these channels are readily apparent. Based on the above evidence, the following, plausible scenario is hypothesized. Following abandonment, the green delta lobe underwent rapid inundation due to sediment compaction and rising eustatic sea level. The homogenous sediment-filled channels characterizing parts of the green delta lobe's distributary system may represent an

initial lack of infilling due to this rapid inundation. It was not until fine-grained sediments associated with the muddy, subaqueous orange delta began arriving soon after that the unfilled channels of the green delta lobe began filling with fine-grained sediments.

As the locus of deposition within the Maringouin Delta Complex shifted to the east following the abandonment of the green delta lobe, it is believed that muds originating from the east were later transported into the study area by the prevailing, westward-directed coastal current, which in turn constructed the orange subaqueous delta. The orange subaqueous delta prograded within the study area until approximately 5,600 yr BP, as the AMS radiocarbon date measured from vibracore TT-77-10 indicates (Fig. 49). Note that the date measured from vibracore TT-77-10, which is positioned at the most basinward reach of the orange subaqueous delta's bottomset strata, is considered a fair time constraint for the termination of the orange subaqueous delta.

Following deposition of the orange subaqueous delta, the locus of deposition shifted again back to the west as evidenced by the gray and yellow delta lobes. As discussed above, the gray and yellow delta lobes prograded more or less simultaneously at first, a judgment based on their regular overlapping, or interfingering, of one another along their boundary. Progradation of these two lobes was also initially contemporaneous with the orange subaqueous delta, as the AMS radiocarbon date from vibracore TT-73-10 suggests. Following the abandonment of the orange subaqueous delta, the gray and yellow delta lobes continued building basinward, however. Although a lack of evidence prevents the confirmation of this hypothesis, it appears that the gray delta lobe ultimately captured the bulk of the flow and sediment load to the detriment of the yellow delta lobe. Subsequently, the gray delta lobe built beyond the western

boundary of the study area and across the top of much of the orange subaqueous delta (Fig. 49; cross sections XX9, YY1, and YY2, Appendix 5).

As discussed above, the blue subdelta infilled the interdistributary bay that had developed along the axis of the boundary (i.e. bathymetric low) separating the gray and yellow delta lobes in the northeastern part of the study area. Interdistributary bays are generally dominated by fine-grained sediments but are also associated with wave-induced lenticular strata, shell remains, and intense bioturbation (Coleman et al., 1964; Coleman and Gagliano, 1964; Coleman, 1981; Coleman and Prior, 1982). The interdistributary-bay environment forming the base of the blue subdelta is recognized as a thin, minor concentration of shell material overlying a relatively thin section of bioturbated, sandy-mud sediments (see the 381-388 cm subbottom depth interval in vibracore TT-33-08, Appendixes 2-3). This relatively thin section of clastic sediment and shell does not appear to be the quintessential expression of an interdistributary-bay environment. Thus, it is interpreted that the interdistributary bay was not long lasting, as progradation of the blue subdelta must have occurred on the very heels of progradation of the gray and yellow delta lobes.

#### Lithofacies Units 10A and 10B

As mentioned previously, AFU10 represents the distributary system of the Maringouin Delta Complex. Two attempts to sample this acoustic facies were made with vibracores TT-55-08 and TT-74-10. Although bed-scale sands associated with plant-organic debris and various primary structures (see the LFU10A description in the Results section) are observed at the base of both cores, these sediments are not interpreted as channel sands. If they were in fact channel sands, then channel fill, which is characterized by highly bioturbated, poorly-sorted silts, clays, and organic debris, would ensue following channel abandonment (see Coleman, 1981; Coleman

and Prior, 1982). Instead, largely regular-to-irregular (with the occasional molted exception), interlaminated-to-interbedded sandy-silt and silty-clay deposits overly the sandy unit (see the LFU10B description in the Results section). Based on this vertical succession of facies, the sandy unit (i.e. LFU10A) at the base of both cores is interpreted as a distributary mouth bar environment, whereas deposits that overly it (i.e. LFU10B) are interpreted as a subaqueous natural-levee environment. Although LFU10A and LFU10B do not represent a channel environment, such a vertical succession of lithofacies is expected to be found very proximal to the channel nevertheless. Note that LFU10B, if not observed in the above context, could also have been interpreted as the upper parts of the delta-front environment. Also, note that no attempt was made to core channels with reflection-free configuration patterns. Such channels are found only within the green delta lobe and are at depths beyond the reach of the vibracoring system.

#### What Is Not Preserved

In light of the above discussion, it is worth noting what is not preserved in the Maringouin Delta. If my interpretations are correct, that LFU10A and LFU10B represent the distributary mouth-bar and subaqueous natural-levee facies, respectively, then a complete vertical succession of facies would transition upwards into a subaerial natural levee facies capped by a marsh facies. However, neither the subaerial natural levee facies nor the marsh facies is observed in vibracores TT-55-08 and TT-74-10, the two cores from which LFU10A and LFU10B were identified. In fact, neither the subaerial natural levee facies nor the marsh facies is observed anywhere within the Maringouin Delta. This lack of preservation is consequent to the significant amount of erosion that the Maringouin Delta endured during transgression, which resulted in the removal of both of these upper-most deltaic facies.

### Antecedent Topography

The AFU11, identified in the southwestern part of the study area, is recognized as the antecedent topography (at least that part which can be observed) over which the Maringouin Delta Complex prograded. Sufficient evidence is unavailable to judge whether AFU11 is of deltaic origin or not. Nevertheless, from observations along cross section XX9 (Appendix 1), its external form slopes from west to east before being lost to the water-bottom multiple. Therefore, if AFU11 were of deltaic origin, its sediment source would have likely emanated from the north, in contrast with the more western trend that is recognized within the overlying Maringouin Delta. The AFU11 is also characterized by channel incision, which lends support to the deltaic-origin hypothesis. However, it cannot be ruled out, given the lack of strong evidence, that the incised top of the AFU11 represents the Pleistocene Prairie surface. Regardless, based on the relatively deep stratigraphic position of the AFU11, it is believed to be of pre-Maringouin Delta age.

Where AFU11 is observed in the very southwestern part of the study area, its topography likely played a minimum role in the depositional patterns of the Maringouin Delta, other than providing a surface on which the orange subaqueous delta's bottomset strata downlaps. Farther north, however, it may have had more of an influence on the western parts of the gray delta lobe, although data are not available to make such an interpretation.

### **The Transgressive Component**

The Maringouin Delta Complex advanced basinward across the Louisiana shelf until, through the process of delta switching, the Mississippi River shifted its depocenter to the east and began forming the Teche Delta Complex (Fig. 1). Upon this switch, the Maringouin Delta entered the transgressive phase as marine erosional processes and rising relative sea level overwhelmed its ever-decreasing supply of sediment. The shoreface of the Maringouin Delta

responded over the long term by adjusting its equilibrium profile through the process of erosional shoreface retreat (Fig. 50; Swift, 1975; Demarest and Kraft, 1987; Nummedal and Swift, 1987; Cattaneo and Steel, 2003). This process transferred the Maringouin Delta's shoreface profile landward (and upward where transient barriers may have once existed), resulting in a transgressive ravinement surface that is now characterized by bedding truncation below, in many places a lag deposit above, and a sharp change in facies across (see Swift, 1975; Demarest and Kraft, 1987; Nummedal and Swift, 1987; Cattaneo and Steel, 2003).

The transgressive ravinement surface, as observed throughout the entire study area, scours down into and truncates the top portion of the entire Maringouin Delta Complex, with severity increasing basinward (Appendixes 1 and 5; note that the red line along the top boundary of the regressive component in Appendix 5 highlights the transgressive ravinement surface). Such an extensive degree of erosional truncation implies a relatively long period of scouring that, in addition, removed any barrier and lagoonal facies that may have developed during earlier stages of transgression. The resulting discontinuity is properly recognized using AMS radiocarbon dating. In vibracore TT-01-08, for example, an AMS radiocarbon date in the very top part of the Maringouin Delta is approximately 4,900 yr BP, whereas an AMS radiocarbon date near the base of the overlying transgressive component is approximately 1,000 yr BP (cross section Y30 in Appendix 1; also Appendixes 2 and 6). Most other AMS radiocarbon dates measured from the transgressive component are at least as young, if not younger, than 1,000 yr BP. Only AFU2/LFU2 is measured older at ~ 1,600 yr BP. However, this depositional unit is a transgressive lag, and this date should be used with caution. Thus, there appears to be an approximately 4,000 year discontinuity between the Maringouin Delta Complex and what is preserved of the overlying transgressive component.

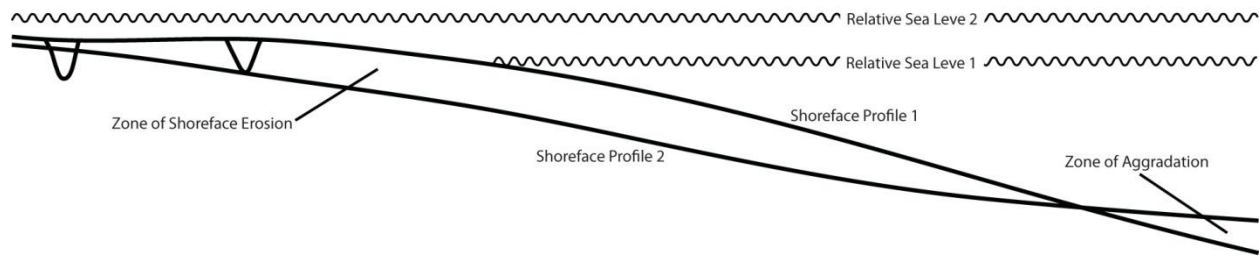


Figure 50. A simplified depiction of erosional shoreface retreat on the Maringouin Delta during transgression. Shoreface Profile 1 corresponds with the original shoreface, whereas Shoreface Profile 2 corresponds with the resulting transgressive ravinement surface. After Swift, 1975.

During an idealized period of erosional shoreface retreat, equilibrium of the concave-up shoreface profile is also partially maintained by deposition on the lower shoreface and shelf. This region of deposition is the zone of aggradation, as depicted in Figure 50. These deposits are commonly recognized as sandy sheet-like storm beds that onlap the ravinement surface (Swift, 1975; Demarest and Kraft, 1987; Nummedal and Swift, 1987; Cattaneo and Steel, 2003). Appropriately, they are also referred to as “healing-phase” deposits, in the sense that they “heal” the bathymetric profile which generally has a gradient that is too steep (i.e. out of equilibrium) following scouring (Cattaneo and Steel, 2003; Catuneanu, 2006). However, healing-phase deposits are not recognized within the bounds of the study area (at least not of any significance) even though much of the transgressed Maringouin Delta’s paleo-shoreface profile clearly reveals a steep gradient (e.g. the southern half of cross section Y30, Appendix 1). The implication is that while the sediment-starved Maringouin Delta was undergoing erosional shoreface retreat, the width of the zone of net erosion was extensive, and therefore the zone of net deposition must have been farther offshore and/or “down storm-current” (see Demarest and Kraft, 1987). In other words, sediment eroded by storm currents from the paleo-shoreface of the Maringouin Delta was largely removed from the proximate region. Instead, more recent sediments are

preserved immediately above the Maringouin Delta's paleo-shoreface as, for example, vibracore TT-01-08 and the AMS radiocarbon dates obtained from it suggest (see preceding paragraph).

In brief, the truncated Maringouin Delta Complex eventually submerged under rising relative sea level, but of course it was still subjected to marine erosional processes, particularly during high-energy storms. Moreover, storm-induced currents continually removed any ephemeral sediment that may have been deposited atop of the ravinement surface during times of fair weather (excluding the development of storm-derived lag deposits). It was not until approximately 1,000 yr BP that significant amounts of sediments began migrating into the study area from the east, upon which they were deposited and have since accumulated. These recent sediments are, at least for the time being, preserved. Although data gathered during this research does not allow for the direct observation of sediment transport, two distinct shelf processes are believed herein responsible for this relatively recent introduction of sediment into the study area. One is the well-documented, prevailing, westward wind-driven coastal currents that characterize the west-central Louisiana coast, especially when amplified by seasonal cold-front passages. These currents are believed to account for most of the fine-sediment fraction. The second shelf process believed responsible for the recent introduction of sediment into the study area is the poorly-documented, alongshore, westward-directed combined-flow currents that accompany the periodic passage of high-energy tropical cyclones. These periodic, high-velocity storm-induced currents are believed to account for most of the long-term mobilization and transport of the coarse-sediment fraction. The following discussion begins by explaining how both of these processes likely operated and influenced deposition within the study area, and then ends with an interpretation of the depositional history of the resulting transgressive component.



### The Lafourche Mud Stream

The down-drift response of Louisiana's shoreline and continental shelf to the burgeoning Atchafalaya Delta serves as a modern analogue for interpreting the vast amount of fine-grained sediments that accumulated within the study area after the Maringouin Delta's transgression. Fine-grained sediments that discharge out of the Atchafalaya River and advect beyond the Atchafalaya Bay may flocculate and settle seaward of their source, forming the muddy, sigmoidal-shaped progradational clinoforms recognized today along the Atchafalaya shelf (Fig. 51; Allison and Neill, 2003; Neill and Allison, 2005). This subaqueous delta is in fact westward skewed, as a majority of the Atchafalaya-derived muds are transported along the inner shelf to the west by the prevailing coastal current, especially when amplified by the pre-frontal phase of seasonal cold-front passages (Fig. 51; Wells and Kemp, 1981; Huh et al., 1991; Roberts, 1998; Walker and Hammack, 2000; Bentley, 2003). Accordingly, the Atchafalaya mud stream is delivering significant volumes of muddy sediment to the down-drift inner shelf adjacent to the eastern chenier plain, which has instigated a similar, seaward-dipping progradational response as seen to the east (Roberts et al., 2002; Draut et al., 2005).

Despite its fine-grained character, the sedimentology of the down-drift Atchafalaya subaqueous delta reflects depositional processes that occur over relatively short time intervals. Working along the inner-continental shelf adjacent to the eastern chenier plain, Rotondo (2004) (also Roberts et al., 2002; Rotondo and Bentley, 2003) recognized discrete depositional units within the shallow subsurface, each characterized by a silt-enriched basal layer(s) that generally grades into an overlying, thicker clay deposit (Fig. 52A). The basal layer(s) is interpreted as a storm event(s), whereas the clay-rich sediments are associated with Spring-flooding discharge from the Atchafalaya River. Deep, long cores reveal stacked accretions of similar depositional

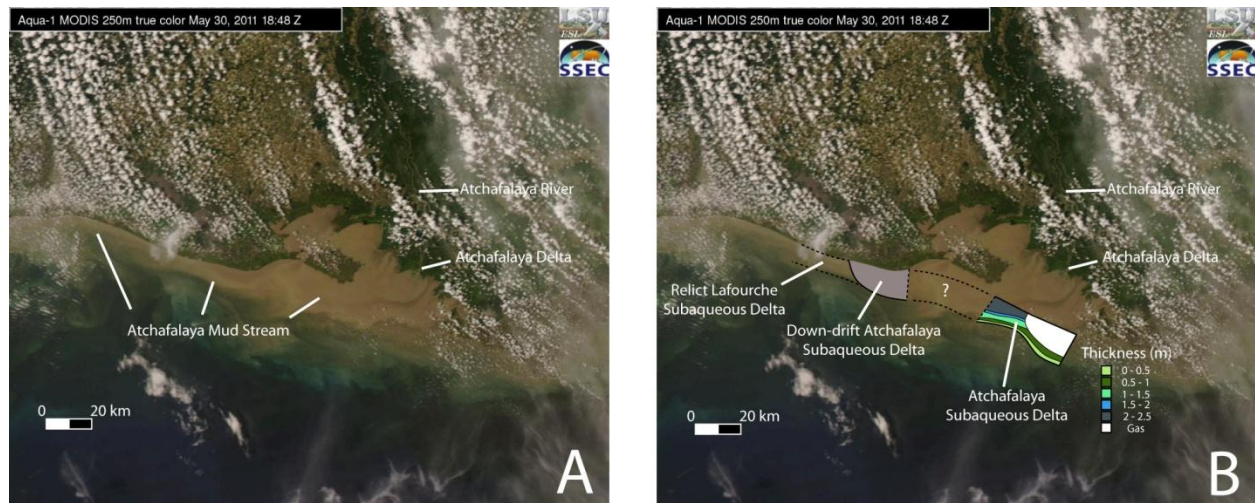


Figure 51. A) The Atchafalaya mud stream, sourced from the Atchafalaya River, flowing westward along the inner shelf adjacent to the Louisiana chenier plain. B) The decoupled Atchafalaya subaqueous delta and its down-drift counterpart. Just west of the down-drift Atchafalaya subaqueous delta is part of the truncated Lafourche subaqueous delta. After Draut et al., 2005 and Neill and Allison, 2005. MODIS (Moderate Resolution Imaging Spectroradiometer) Satellite image was taken from the Louisiana State University Earth Scan Laboratory ([www.esl.lsu.edu](http://www.esl.lsu.edu)).

units, suggesting that the cyclic interplay of largely cold fronts and Atchafalaya-flood sediment is disproportionately preserved in the stratigraphic record (Fig. 52B; Roberts et al., 2002; Rotondo and Bentley, 2003; Rotondo, 2004).

The same set of processes that are now creating the down-drift Atchafalaya subaqueous delta also once created a down-drift subaqueous delta associated with the Lafourche Delta Complex. The Lafourche Delta began constructing along the central part of Louisiana's coast approximately 2,500 yr BP (Fig. 53); it is recognized that some researchers suggest a later beginning (see Törnqvist et al, 1996). Presumably, the Lafourche Delta spent the better part of its early history infilling accommodation. Accommodation included that associated with regional base level (which had since inundated both of the relict Maringouin and Teche Delta Complexes to the west of the Lafourche Delta) and that perpetuated by the high rates of subsidence associated with prograding over the incised Mississippi River Alluvial Valley (Fisk,

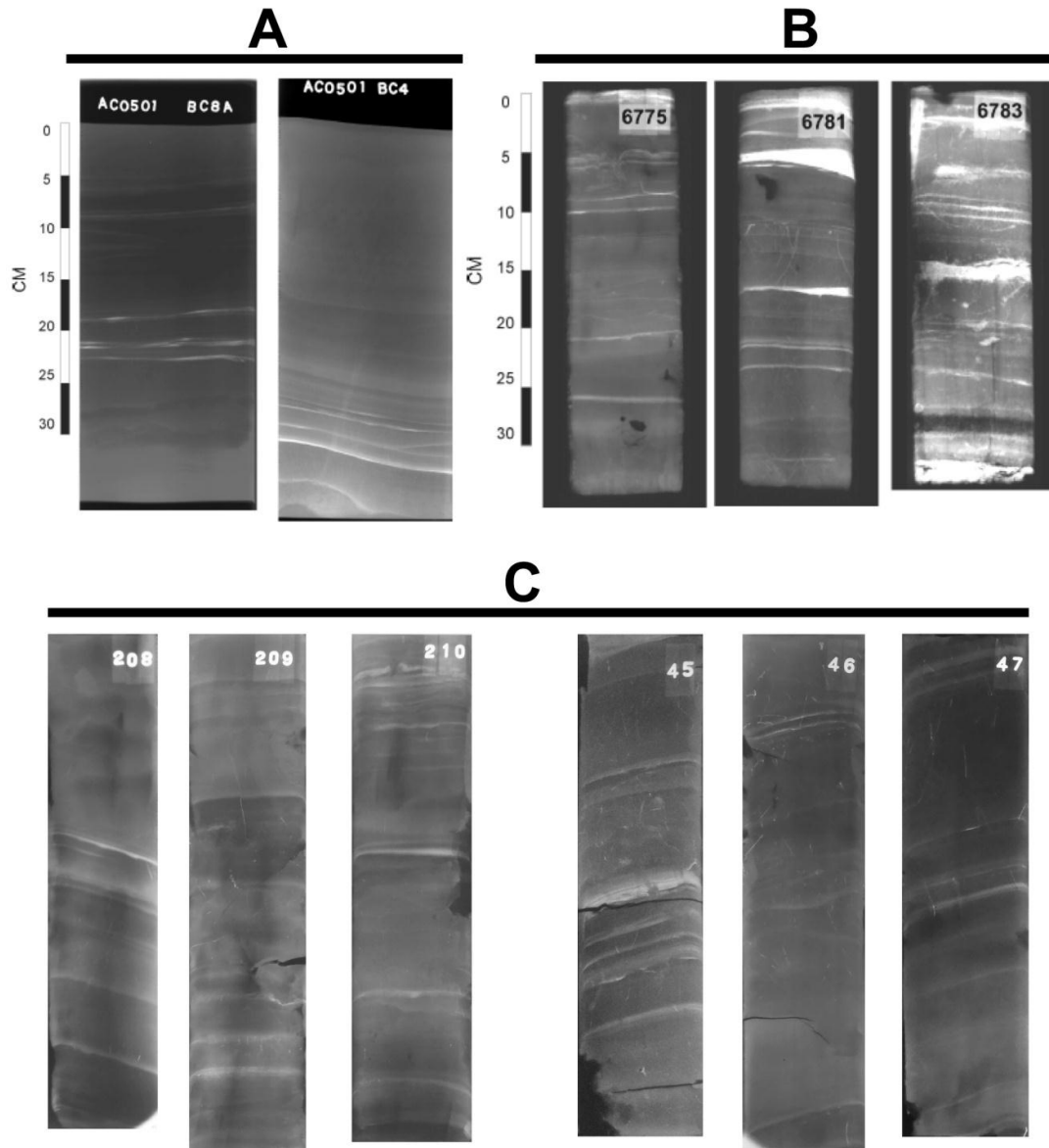


Figure 52. A) X-ray radiographs of the upper-most sediment column from the Atchafalaya subaqueous delta (box cores BC8A and BC4). Note that the lighter regions indicate silt-enriched strata, whereas the darker regions indicate clay-rich strata. B) X-ray radiographs from a single onshore vibracore, adjacent to the Atchafalaya subaqueous delta. Samples were obtained at the subsurface positions of 30 – 60 cm, 180 – 210 cm, and 240 – 270 cm, respectively. Both A and B were taken from Roberts et al. (2002). See Figure 1 of Roberts et al. (2002) for core locations. C) X-ray radiographs from vibracores TT-27-08 and TT-25-08, this study. The subsurface depth intervals of X-ray radiographs 208, 209, and 210 (TT-27-08) are approximately 120 – 150 cm, 150 – 180 cm, and 180 – 210 cm, respectively. The subsurface depth intervals of X-ray radiographs 45, 46, and 47 (TT-25-08) are approximately 328 – 356 cm, 356 – 384 cm, and 384 – 408 cm, respectively. Sediments represented in X-ray radiographs of C are from LFU4, and are remarkably comparable to sediments represented in A and B, above. See Figure 25 for locations of vibracores TT-25-08 and TT-27-08.

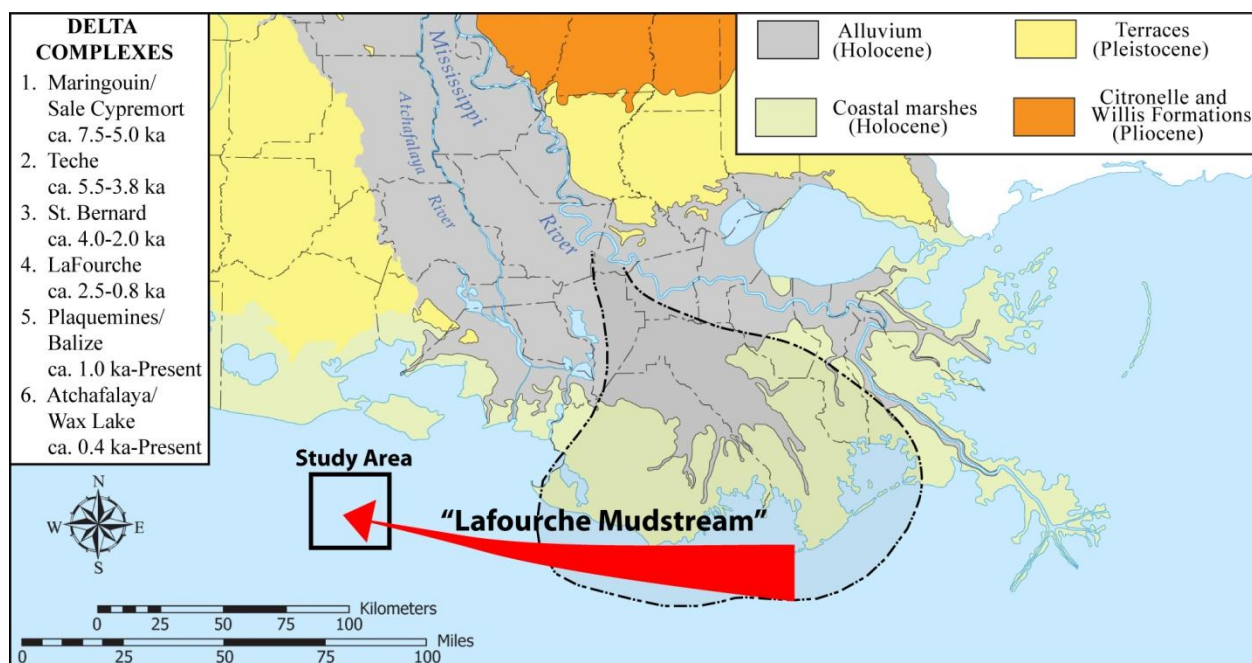


Figure 53. The Mississippi Delta Plain, with the approximate boundary of the Lafourche Delta Complex highlighted. Originating from the Lafourche Delta, the “Lafourche mudstream” flowed westward, introducing fine-grained sediments into the Trinity-Tiger Shoals study area.

1944; Roberts et al., 1994). Eventually, the Lafourche Delta prograded as far basinward as the latitude of the Trinity-Tiger Shoals study area. From this basinward position, it is argued here that a “Lafourche mud stream”, analogous to that associated with the present-day Atchafalaya system, began transporting fine-grained sediments originating from the Lafourche Delta westward into the study area (Fig 53).

The AFU4 and LFU4 (Appendixes 1 and 2) represent the quintessential part of the Lafourche subaqueous delta that prograded into the study area. As discussed previously, LFU4 is predominantly comprised of a clay-sediment core with interlaminated silty strata, along with sparse-to-moderate bioturbation. As Figure 52C illustrates, LFU4 is remarkably comparable to the lithofacies distinguished today in the down-drift Atchafalaya subaqueous delta. On the other hand, AFU4 is less indicative of the sigmoidal reflection configuration pattern that is observed in the Atchafalaya subaqueous delta (see Roberts et al., 2002; Allison and Neill, 2003; Draut et al.,

2005; Neill and Allison, 2005). This inconsistency is in part consequent to the top portion (i.e. topset) of AFU4 having been partially removed by erosion. There are also relatively too few internal reflectors within AFU4 to make a straightforward judgment. Nevertheless, close inspection reveals very subtle thickening (i.e. broadening of frequency) of clinoforms within the foreset zone of AFU4. Based on the general orientation of converging clinoforms within AFU4, it appears that the Lafourche subaqueous delta prograded towards the southwest. This orientation of AFU4's clinoform package is similar to the westward-skewed, shore-oblique pattern of the down-drift Atchafalaya subaqueous delta recognized along the inner shelf adjacent to the eastern chenier plain (Draut et al., 2005) and is most likely consequent to the westward flow of the Lafourche mud stream. Furthermore, just west of the down-drift Atchafalaya subaqueous delta (Fig. 51) a truncated sigmoidal clinoform package also outcrops along the eastern chenier plain shelf, which Draut et al. (2005) contend is part of a relict Lafourche subaqueous delta. Its truncated geometry and estimated age are remarkably similar to AFU4.

The interpretation of AFU4/LFU4 as a relic of the down-drift Lafourche subaqueous delta is further supported by AMS radiocarbon dating. Three dates were measured from AFU4/LFU4, ranging in age from approximately 500 yr BP to less than 1,000 yr BP (Appendixes 1, 2, and 6). This time duration corresponds with the final progradational stage of the Lafourche Delta Complex, a time when the Lafourche had prograded to its maximum southern extent near the latitude of the Trinity-Tiger Shoals study area (Fig. 53). (Note that after an up-dip avulsion (e.g. a shift from the Lafourche to the Plaquemine-Belize system), both the new and old delta complexes share the flow and sediment load initially (Roberts, 1997), which explains the most recent ages.) The time duration of AFU4/LFU4 also corresponds with the late pre-Atchafalaya chenier plain chronology, a sequence of progradational mudflats and

transgressive ridges that are thought to mostly coincide with delta lobe switching that occurred only within the Lafourche Delta Complex itself (Penland and Suter, 1989).

### Sand-Shoal Migration

The transport of sand-sized sediment along the lower shoreface and shelf of the low-energy northern Gulf of Mexico occurs largely during storm events (Crout and Hamiter, 1981; Morton, 1981; Pepper and Stone, 2004). Despite the seasonal, regular recurrence interval of 20 – 30 cold-front passages per year (Roberts et al., 1987; Roberts et al., 1989), it is the less-frequent but much more energetic passages of tropical cyclones, however, that disproportionately dominate the transport of sand and the resulting sedimentary record.

Prior to and during the passage of a tropical cyclone, powerful winds augmented with a substantial drop in atmospheric pressure generate coastal setup (or storm surge) along the shoreline, where water levels can elevate on the order of several meters (Swift et al., 1986; Wright et al., 1986; Duke, 1990; Walker and Plint, 1992). The resulting offshore-directed sea-surface slope creates an onshore-offshore horizontal pressure gradient that drives bottom water offshore (Fig. 54A; Swift et al., 1986; Wright et al., 1986; Duke, 1990; Walker and Plint, 1992). In the northern hemisphere, this flow is progressively deflected to the right (i.e. to the west along the northern Gulf of Mexico) by the Coriolis force. Equilibrium is ultimately reached between the offshore-directed pressure-gradient force and the landward-directed Coriolis force, resulting in a maximized shore-parallel geostrophic flow that persists for as long as the pressure gradient persists (Fig. 54B; Swift et al., 1986; Wright et al., 1986; Duke, 1990; Walker and Plint, 1992). This force-balance setup is adequate for describing the core region of non-shearing flow. For that part of the flow proximal to the seafloor, however, a significant frictional force is introduced, causing the near-bottom flow to veer slightly offshore from its shore-parallel

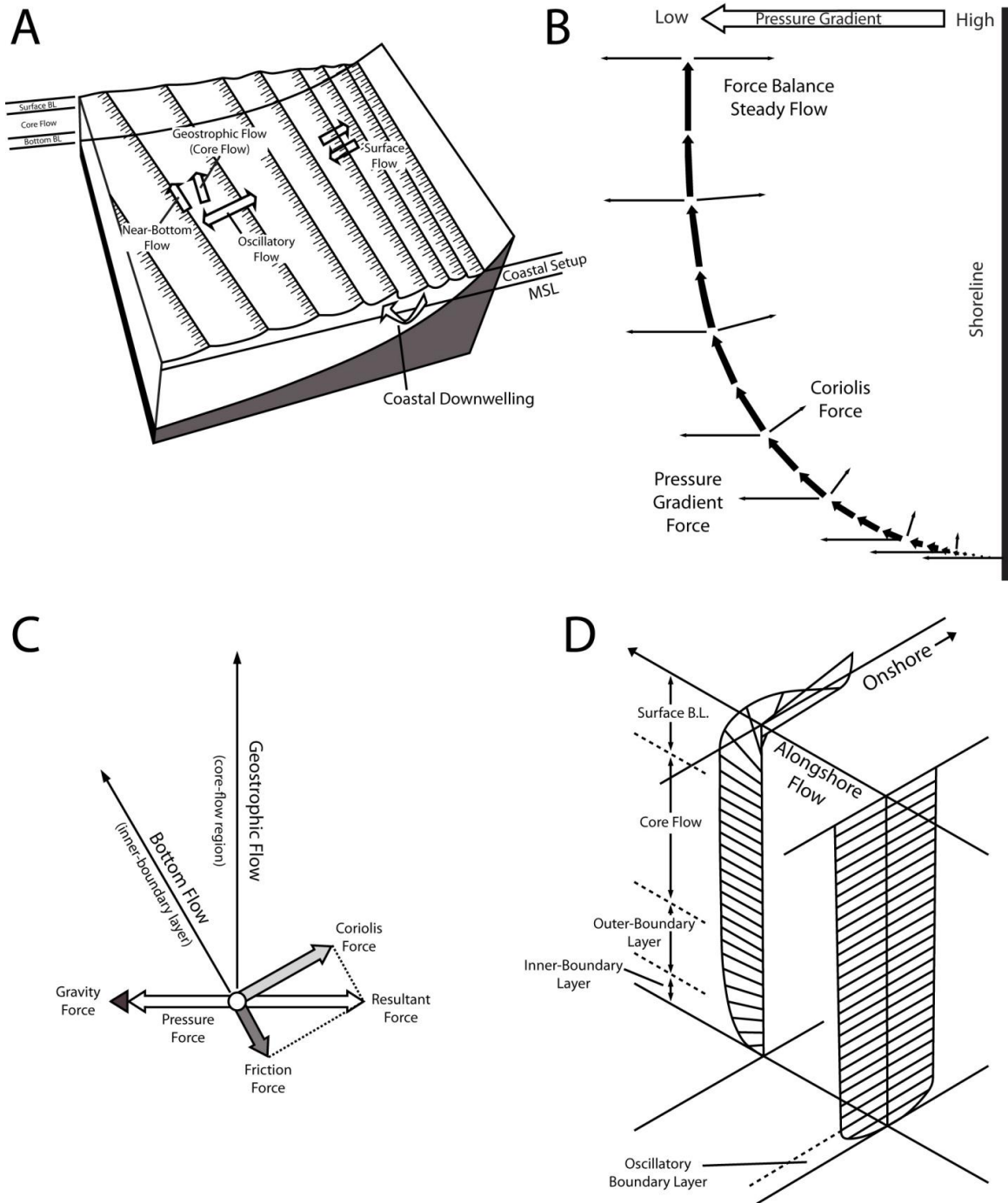


Figure 54. A) The continental-shelf water column broken down into a three-layer flow system. Water pushed onshore during coastal setup is returned offshore by coastal downwelling. B) Downwelling water is deflected to the right in the northern hemisphere by the Coriolis force. Equilibrium between the pressure gradient force and Coriolis force results in a shore-parallel geostrophic flow. C) Balance of forces within the near-bottom flow. The bottom flow deviates offshore with respect to the geostrophic flow due to the frictional force at the seafloor. D) Superimposition of wave-induced oscillatory motions and the unidirectional near-bottom flow. Modified from Duke, 1990.



tendency (Fig. 54C; Swift et al., 1986; Duke, 1990). Note that a gravity force directed parallel to the horizontal pressure-gradient force is also included within the force balance, but it is considered rather miniscule on gently sloping surfaces such as the continental shelf of the northern Gulf of Mexico (Duke, 1990).

Major storms are also associated with the intense oscillatory motions of waves, which in fact dominate fluid motion near the seafloor (Swift et al., 1986; Wright et al., 1986; Duke, 1990; Walker and Plint, 1992). Within the inner-boundary layer (a relatively thin layer immediately adjacent to the seafloor), unidirectional near-bottom flow is superimposed upon wave-induced oscillatory motions, and the resulting combined-flow current (i.e. unidirectional near-bottom flow combined with oscillatory motions) greatly enhances shear stress along the seafloor and, thus, the capacity to transport sand (Fig. 54D; Swift et al., 1986; Wright et al., 1986; Duke, 1990; Walker and Plint, 1992). Based on the above discussion, one would expect the net transport of bed-load sediment to be slightly-oblique offshore relative to the alongshore-flow direction. This has practically been the observation from studies conducted along the middle Atlantic shelf after the passage of extratropical cyclones, although net transport of bedload is essentially alongshore (Swift et al., 1986; Wright et al., 1986). However, migrating seafloor geomorphology (e.g. ripples, dunes, and sand waves) is typically larger than the scale of the thin inner-boundary layer and therefore disrupts the near-bottom combined flow during major storms (Duke, 1990). This disruption causes turbulent eddies to shed from the crest of ripples and suspend “clouds” of sand high above the seafloor, well above the inner-boundary layer and into the outer-boundary layer and even the lower parts of the core-flow region (Fig. 54D; Swift et al., 1986; Duke, 1990). High ratios of suspended load to bed load are supported by such highly turbulent bottom flows (Swift et al., 1986). Thus, the time-averaged transport of sand during the passage of tropical

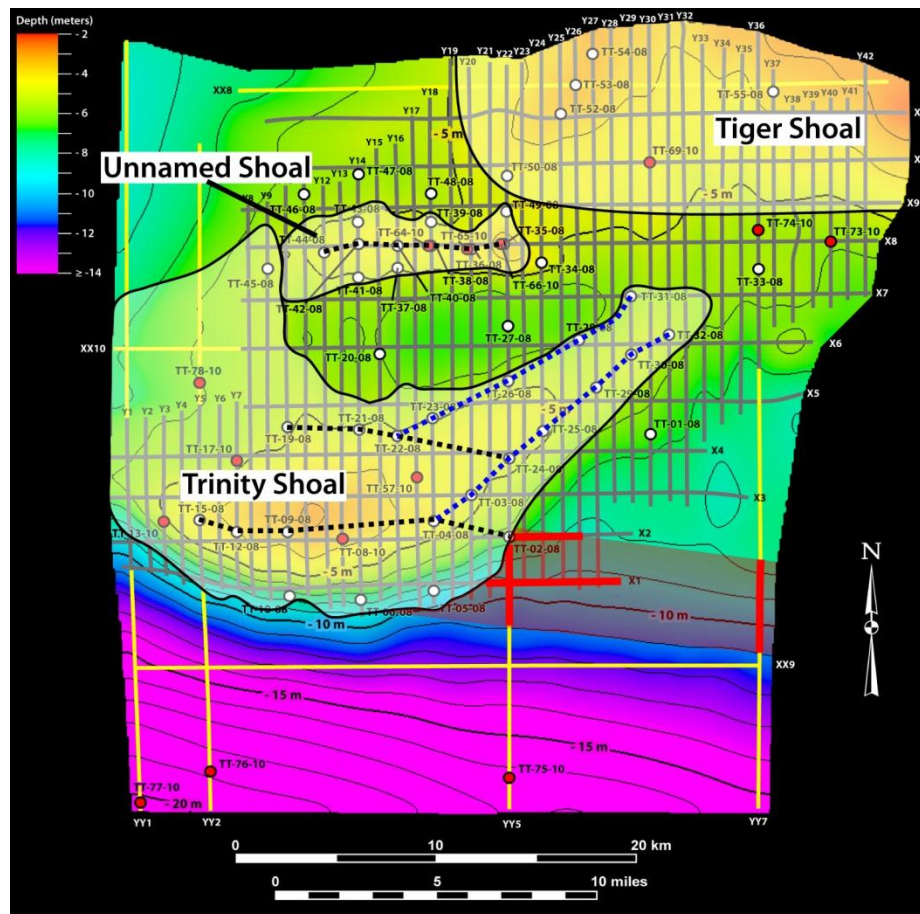


cyclones along the northern Gulf of Mexico should occur predominately within the outer-boundary layer and lower core-flow region of the water column, which is directed in the approximate alongshore direction of geostrophic flow (i.e. to the west along the northern Gulf of Mexico).

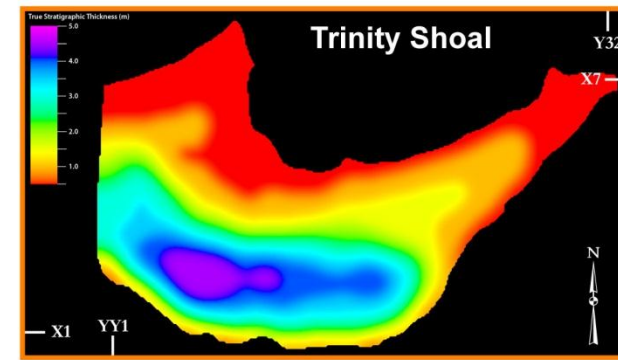
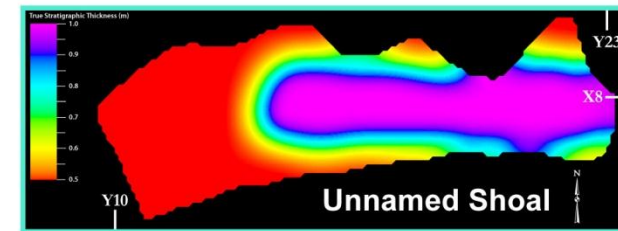
Three separate “shoals” are recognized within the study area. Two of these are actually distinct sand lithosomes and are expressed as AFU6/LFU6 and AFU7/LFU7 (Appendixes 1 and 2). Respectively, these facies represent Trinity Shoal and a hitherto unnamed shoal. In light of the above discussion, these sand bodies are interpreted to have migrated into the study area from the east. Several derivations of evidence manifest this generally westward-directed alongshore migration pattern, including geochronologic constraints, seafloor geomorphology, and the mean grain-size trends of their respective sand fractions. This evidence is discussed in the following paragraphs. In contrast, the third shoal, labeled Tiger Shoal by early researchers (e.g. Van Lopik, 1955), is not a sand lithosome but is essentially just a shallow-water area in the northern part of the study area. Tiger Shoal resides in shallow waters partially because preservation of the Maringouin Delta Complex is greatest here, as transgressive ravinement was more operative to the south (e.g. cross section Y28 in Appendix 1). Thus, the Maringouin Delta “shoals” in the Tiger Shoal area. Moreover, additional depositional units within the Tiger Shoal area have since accumulated atop of the Maringouin Delta, including AFU2/LFU2, AFU8/LFU8, AFU9/LFU9/ and AFU12, and this deposition has further decreased water depths (e.g. cross section Y34, Appendix 1). Figure 55 indicates the approximate dimensions of each shoal.

#### “Geochronologic Constraints”

Both Trinity Shoal and the unnamed shoal outcrop at the seafloor, and so each represent the most recent deposits within their respected regions of the study area. Both shoals also lie



A



B

Figure 55. Approximate dimensions of Trinity Shoal, Tiger Shoal, and the unnamed shoal. A) Plan-view extent of each shoal. Note that Trinity Shoal and the unnamed shoal actually weld together as their boundaries indicate. Tiger Shoal is essentially a shallow region of the study area, and its boundary is simply approximated. Dashed black and blue lines indicate transects noted within text. Red lines drawn along acoustic lines X1, X2, Y22, YY5, and YY7 indicate the region of irregular seafloor geomorphology. The red shaded region suggests the dominant pathway of sand-sediment transport as related to Trinity Shoal. B) Isopach maps (i.e. thickness maps) of Trinity Shoal and the unnamed shoal. Isopach maps are not to scale with respect to one another.

stratigraphically above the Lafourche subaqueous delta which, as established above, prograded into the study area between approximately 1,000 yr BP to 500 yr BP. Note that a transitional facies (AFU5/LFU5) separates the underlying Lafourche subaqueous delta from the overlying shoals (e.g. cross section Y18, Appendix 1). However, AFU5/LFU5's depositional duration closely corresponds with the underlying Lafourche subaqueous delta as indicated by the seven AMS radiocarbon dates measured from it (Appendixes 1, 2, and 6). In other words, very little time transpired between the so-called transitional facies of AFU5/LFU5 and the underlying Lafourche subaqueous delta. Considering the above time constraint, it is recognized that an extremely large volume of sandy sediment, especially regarding Trinity Shoal, appeared within the study area in just a very short time period. It is interpreted here that only the repetitive passages of tropical cyclones operating over 100-year time scales could accomplish such a task. For context, a tropical cyclone struck the Louisiana coast about every other year during the 20<sup>th</sup> century (Stone et al., 1997). Again, the time-averaged transport of sand along the continental shelf during the passage of a tropical cyclone is thought to be directed in the approximate alongshore direction of storm-induced geostrophic flow, which is in the westward direction along the northern Gulf of Mexico. Thus, both Trinity Shoal and the unnamed shoal migrated into the study area from the east.

#### “Seafloor Geomorphology”

The seafloor geomorphology also provides evidence that sands migrated into the study area from the east, specifically in respect to Trinity Shoal. A portion of the seafloor along subbottom profile YY7 just north of where subbottom profile XX9 intersects it appears highly irregular (Appendix 1; also Fig. 55A for a map-view location of irregular seafloor). Such seafloor geomorphology is known to be associated with sandy sediments (e.g. see Trinity Shoal's

seafloor geomorphology in cross sections X3 and YY2, Appendix 1) and most likely represents the remnants of migrating sand waves and dunes mobilized during the passage of tropical cyclones. (It is recognized that shell-wave bedforms, analogous to sand waves, are also associated with the same storm-induced seafloor-geomorphologic expression, as AFU8 reveals; e.g. cross section Y25 in Appendix 1.) A comparable irregular seafloor is also observed more proximal to Trinity Shoal along its eastern flank as portions of subbottom profiles X1, X2, Y22, and YY5 reveal (Appendix 1; also Fig. 55A). Vibracore TT-02-08 actually penetrates this region of the study area and reveals 10-50 cm thick sand beds, with well-preserved internal parallel-to-cross laminations, interbedded with bioturbated muds (Appendixes 2 and 3; also Fig. 55A for a map-view location). Although dune-scale structures cannot be resolved within a 7.6 cm diameter core, the sedimentology identified from vibracore TT-02-08 suggests hummocky cross stratification (Walker and Plint, 1992). Such structures are known to constitute dunes that migrate during storm-induced geostrophic flows (Walker and Plint, 1992). This region of irregular seafloor geomorphology (shaded red in Fig. 55A) is interpreted as the wake of Trinity Shoal, suggesting that this has been the dominant pathway for which sands have migrated into the present-day Trinity-Shoal location.

#### “Mean Grain-Size Trends”

Although geostatistical analyses were not attempted, qualitative observations of mean grain-size trends calculated from sands within Trinity Shoal and the unnamed shoal indicate a general fining of sands in the westward direction. One conflicting trend is recognized within Trinity Shoal, however, and is discussed below. The westward-fining trend is most convincing within the unnamed shoal where vibracore locations are relatively close to one another. The reader can observe this trend by following a transect that begins with vibracore TT-35-08 and

ends with vibracore TT-44-08 (black dashed line in Fig. 55A; Appendixes 2 and 7). Note that the unnamed shoal includes some heterogeneity in its sand fraction, as the mean grain size ranges from very-fine to medium sand and in some cases is bimodal to even trimodal. However, all heterogeneity is found in the unnamed shoal's most eastern section (vibracores TT-35-08 and TT-49-08, Appendixes 2 and 7) and likely reflects sediments derived from multiple sources (Folk, 1974). Particularly, the coarsest sands are thought to be sourced from the relatively-local region of the underlying Maringouin Delta and conceivably emanate from its reworked channels and/or distributary mouth bars. West of the unnamed shoal's most eastern section, the sand fraction is comprised entirely of very-fine sand. Finer sands have moved farther "downcurrent" (i.e. alongshore) by selective sorting (Folk, 1974), and thus the east-to-west fining trend of the unnamed shoal.

In contrast with the unnamed shoal, two diverging trends are recognized within Trinity Shoal. In congruence with the above observations, an overall fining of sands in the westward direction can be distinguished by following two transects: (1) beginning at vibracore TT-02-08 and ending at vibracore TT-15-08 and (2) beginning at vibracore TT-24-08 and ending at vibracore TT-19-08 (black dashed lines in Fig. 55A; Appendixes 2 and 7). No apparent trend is distinguished along Trinity Shoal's most southern perimeter (vibracores TT-05-, -06-, -10-08 in Appendixes 2 and 7). A second fining trend is observed oriented in a southwestward direction. The reader can observe this trend by also following two transects: (1) beginning at vibracore TT-32-08 and ending at vibracore TT-04-08 and (2) beginning at vibracore TT-31-08 and ending at vibracore TT-22-08 (blue dashed lines in Fig. 55A; Appendixes 2 and 7). Note that the mean grain size of sands within Trinity Shoal is entirely very-fine sand, although sands do approach the fine-sand size within Trinity Shoal's northeastern section (vibracores TT-25-, -28-, -29-, -30-,

-32-08, Appendixes 2 and 7). Also, note that Trinity Shoal interfaces with AFU2/LFU2, and therefore possibly reworked Maringouin sediments, in its coarser, most northeastern section. However, it is readily apparent west of the longitude of cross section Y28 (Appendix 1) that this northeastern protrusion of Trinity Shoal (Fig. 55A for a map view) becomes largely isolated from a local supplementary Maringouin source. Nevertheless, this study recognizes the likely local Maringouin influence in this northeastern part of Trinity Shoal, which may account for the northeast-to-southwest trend in grain size described above. The overwhelming majority of the westward-fining, very-fine sands of Trinity Shoal are, however, interpreted as being derived from a westward-streaming source originating from well outside the eastern boundary of the study area.

#### The Depositional Model of the Transgressive Component

From the above discussion, it is established that the Maringouin Delta Complex, at least that part which exists within the study area, entered its transgressive phase ~ 5,000 yr BP following abandonment by the Mississippi River. The Maringouin Delta was subsequently left exposed to and eventually overwhelmed by rising relative sea level and marine-erosional processes, which ultimately produced the prominent transgressive ravinement surface observed today. It is also established that preservation of accumulated sediments above this surface within the study area was relatively minimal until approximately 1,000 yr BP when sediments began migrating into the study area from the east (the transgressive lag deposits withstanding). The following discussion begins by describing the development of the transgressive lag, and then addresses the sequence of depositional events that have since occurred within the transgressive component of the Maringouin Delta. Unless otherwise indicated, the reader should continually refer to Appendix 1 for graphic illustration to this discussion.

The AFU2/LFU2 is the first major “transgressive” depositional unit to emerge (and remain preserved) atop of the ravinement surface, and predictably, it is interpreted as a transgressive lag deposit. The AFU2/LFU2 transgressive lag accumulated in the northern part of the study area above where the Maringouin Delta, including its sand-prone depositional environments of distributary channels and mouth bars, is relatively well preserved. As discussed above, transgressive ravinement was much more significant in the middle-to-southern parts of the study area in comparison with the north (e.g. Y30, Appendix 1). Subsequent to an initially severe period of transgressive ravinement following abandonment, it is interpreted that these sand-prone depositional environments have since been reworked continually by storm waves and currents, resulting in the formation of a significant lag deposit, up to ~ 2.5 m thickness (e.g. X9, Appendix 1). Note that minor lag deposits (i.e. ~ 2 – 3 cm of reworked sands and perhaps some shell material) may cap the ravinement surface in the middle part of the study area (e.g. TT-01-, -31-, -32-08, Appendixes 2 and 3; also, see the stratigraphic framework in the area from where these cores penetrate the subsurface in cross sections Y30, Y29, and Y31, Appendix 1). However, such minor lag deposits are considered relatively insignificant in comparison, and are thus not correlated with the AFU2/LFU2 transgressive lag to the north. Furthermore, note that lag deposits are not distinguished atop of the ravinement surface in the southern part of the study area where underlying Maringouin-Delta strata are prodelta muds (e.g. vibracores TT-75-, -76-, -77-10, Appendixes 2 and 3; also, see the stratigraphic framework in the area from where these cores penetrate the subsurface in cross sections YY5, YY2, and YY1, Appendix 1).

Lag deposits commonly display lateral variations in thickness and lithofacies (Hwang and Heller, 2002), and such is the case for the AFU2/LFU2 transgressive lag. A relatively thin package (i.e. ~ 1 m) of predominantly mottled, muddy sand with a considerable amount of shell

material occurs in the eastern section of the AFU2/LFU2 lag (e.g. Y40, Appendix 1; also vibracore TT-73-10, Appendixes 2 and 3). A significant portion of the mud fraction was likely sourced from the Lafourche mud stream and mixed into the lag through animal burrowing. To some degree, modern Atchafalaya muds probably also make up a portion of the mud fraction. In contrast, the AFU2/LFU2 lag thickens considerably in its central section (up to ~ 2.5 m) before it tapers away to the west (e.g. X9 and Y22, Appendix 1). This thickening section of the AFU2/LFU2 lag correlates with that part of the lag's lithofacies that is largely dominated by the sand fraction, where parallel to cross laminated sands are commonly observed (e.g. vibracores TT-49-08 and TT-50-08, Appendixes 2 and 3; also cross section Y22, Appendix 1). Although inconclusive, it is speculated that the sand fraction of the AFU2/LFU2 lag migrated westward in a fashion similar to Trinity Shoal and the unnamed shoal. Hence the westward-skewed thickening into cleaner sands.

It is perhaps not appropriate to date a transgressive lag considering that, by definition, it is a reworked sediment deposit. Nevertheless, two AMS radiocarbon dates were measured from the AFU2/LFU2 transgressive lag, specifically within its central section where sands predominate. One date measured between 1,570 yr BP – 1,710 yr BP (vibracore TT-49-08, Appendixes 2 and 6), whereas the other measured between 640 yr BP – 720 yr BP (vibracore TT-50-08, Appendixes 2 and 6). Note that the locations of the vibracores from which these dates were measured are relatively close to one another (Fig. 25). Two shell-lag deposits positioned stratigraphically at the interface between the AFU2/LFU2 lag and the overlying Lafourche subaqueous delta (AFU4/LFU4) were also AMS radiocarbon dated. One date measured between 1,340 yr BP – 1,520 yr BP (vibracore TT-46-08, Appendixes 2 and 6), whereas the other measured between 1,250 yr BP – 1,370 yr BP (vibracore TT-66-10, Appendixes 2 and 6). It



appears that the oldest date (1,570 yr BP – 1,710 yr BP, from vibracore TT-49-08) measured from within the central section of the AFU2/LFU2 transgressive lag is more representative of the lag considering that: (1) the shell layer from which this date is measured lies at the base of a ~ 30 cm sand bed with very-well preserved internal primary structures (i.e. no disturbance from burrowing, Appendixes 2 and 3), and (2) the two shell-lag deposits at the top of the AFU2/LFU2 lag are both slightly younger. Note that both of the dates measured from the shell-lag deposits are older than the youngest date measured from within the AFU2/LFU2 lag. Thus, it is possible that the youngest date (640 yr BP – 720 yr BP, vibracore TT-50-08) was contaminated by burrowing: note that there are a few pronounced burrows within the sediment column above the sample site (Appendixes 2 and 3). Despite the reasoning outlined above, the AMS radiocarbon dates measured from the AFU2/LFU2 transgressive lag should be viewed with caution.

Early Lafourche mud-stream deposits are also recognized farther basinward within AFU3/LFU3, with this facies also being positioned immediately atop of the ravinement surface. One could make a legitimate argument that the AFU3/LFU3 is simply a part of the adjacent, overlying down-drift Lafourche subaqueous delta (AFU4/LFU4). The LFU3's character, however, produces a corresponding acoustic facies (AFU3) that contrasts with AFU4. Therefore, these the two units have been separated. The LFU3 contains considerably more sandy strata within its mud core than does the overlying LFU4, implying a relatively low depositional rate of Lafourche sediments (compared to that seen in LFU4). The sandy sediments were likely derived from the same westward-streaming sand source from which the overlying AFU5/LFU5 and Trinity Shoal (AFU6/LFU6) sands were derived, which may explain why internal reflectors within LFU3 dip and converge to the southwest. During the time of AFU3/LFU3 deposition, however, the sand source must have been distant as muds still dominate the sediment column and

continue to do so into the overlying LFU4. One AMS radiocarbon date measured from AFU3/LFU3 suggests that sediments were deposited as early as ~ 1,000 yr BP.

The influx of muddy sediments increased substantially as the Lafourche mud stream intensified, which likely initiated following a delta-lobe switch within the “up-current” Lafourche Delta Complex. As discussed above, the result was the progradation of the down-drift Lafourche subaqueous delta (AFU4/LFU4). Based on AMS radiocarbon dating, the subaqueous delta began building within the study area as early as ~ 900 yr BP (probably earlier based on the discussion below) and continued to do so at least as late as ~ 500 yr BP.

Very little time must have transpired before the greater amount of advancing sands of Trinity Shoal and the unnamed shoal began migrating into the study area from the east, and for a time an appreciable amount of sand deposition was contemporaneous with deposition of the Lafourche muds. This part of the facies succession is expressed by AFU5/LFU5, which accordingly is characterized by interlaminated-to-interbedded sands and muds. Note that AFU5/LFU5 is considered a “transitional” facies between the underlying down-drift Lafourche subaqueous delta and the overlying sandy shoals. In this regard, AFU5/LFU5 could be divided into two separate “transitional” facies: one associated with Trinity Shoal and one associated with the unnamed shoal. This point is best illustrated in cross sections Y19 – Y23 (Appendix 1), from which one can clearly see the development of two separate parts of AFU5/LFU5. However, west of cross section Y19, their individuality quickly becomes less distinct. Therefore, for the sake of simplicity, all of the “transitional” deposits are incorporated into AFU5/LFU5. This facies began to develop as early as ~ 1,000 yr BP as indicated by AMS radiocarbon dating.

Note that AFU3/LFU3, the down-drift Lafourche subaqueous delta (AFU4/LFU4), and AFU5/LFU5 were each AMS radiocarbon dated as old as ~ 1,000 yr BP. At first glance this may

appear conflicting, as it is fundamentally understood through the principle of superposition that strata successively become older in the downward direction. Any apparent conflict, however, is simply a consequent of dates obtained from different geographic locales. (In hindsight, perhaps this study should have obtained a core in the eastern part of the study area that penetrated each facies, and then have dated each.) Nevertheless, it is glaringly apparent from AMS radiocarbon dating that large volumes of sediments from multiple sources were rapidly migrating into the study area from the east in an almost coincident fashion. Vibracores TT-01-08 and TT-25-08, which are positioned ~ 6 km apart along more or less the same latitude, illuminate this observation (Appendix 2; also cross sections Y24 and Y30, Appendix 1 and Fig. 25 for core locations). In vibracore TT-01-08, an AMS radiocarbon date from AFU3/LFU3 was measured between 940 yr BP – 1,070 yr BP. Approximately 6 km to the west in core TT-25-08, one date was obtained from the top of AFU4/LFU4, whereas another date was obtained from the base of the overlying AFU5/LFU5. The interface separating these two facies is therefore very well constrained. Dates were measured between 800 yr BP – 960 yr BP and 920 – 1,070 yr BP, respectively. Based on these dates, the overlying AFU5/LFU5 appears slightly older than the underlying AFU4/LFU4. This discrepancy does not appear to be a result of biogenic mixing, based on observations of vibracore TT-25-08 (Appendix 2 and 3). However, this difference may be the result of the overlapping of the normal-distribution curves around their respective means. Furthermore, the down-drift Lafourche subaqueous delta (AFU4/LFU4) is comprised of aggregates of seasonal deposits, and individual deposits are considered instantaneous over the time scale relevant to this study. Therefore, the date measured from AFU4/LFU4 is considered most accurate. In contrast, the date obtained from AFU5/LFU5 was measured from a shell-event layer. Again, only well-preserved shells were used for dating, which signify minimum time

spent in the taphonomically active zone before being sequestered into the stratigraphic record. However, shells spending 100 – 200 years within the taphonomically active zone is not unreasonable and is probably as precise as one can expect. Thus, dates measured from vibracore TT-25-08 are not considered here to violate the principle of superposition. Along this single ~ 6 km east-west transect between vibracores TT-01-08 and TT-25-08, it is estimated based on AMS radiocarbon age control that within 200 – 300 years this part of the study area had transitioned through the “AFU3/LFU3 – AFU4/LFU4 – AFU5/LFU5” facies succession. Furthermore, one can observe from other AMS radiocarbon dates (Appendixes 1, 2, and 6) that each facies becomes progressively “younger” towards the west, which is interpreted to reflect the westward transport of sediment.

The Mississippi River eventually switched its principal course from the Lafourche to the Plaquemines/Belize system (Fig. 1). As stressed previously, delta switching is not necessarily immediate but rather a gradual process (Roberts, 1997). By as early as ~ 500 yr BP, however, it appears that the Lafourche mud stream had ceased as the transgressing Lafourche Delta Complex fully succumbed to abandonment. Even though Lafourche muds were no longer being supplied to the study area, the westward-streaming supply of sand from the east continued unabated and has since constructed Trinity Shoal and the unnamed shoal during this very short subsequent time period. The source of sand that has and likely continues to feed the development of the unnamed shoal appears to be the AFU2/LFU2 transgressive lag. From observing cross section X8 (Appendix 1), for example, the western part of the AFU2/LFU2 transgressive lag is evidently preserved within the stratigraphic record, as it is now buried by overlying strata. Therefore, the AFU2/LFU2 transgressive lag can no longer migrate westward. However, it appears that sands have since been shedding from the crest of the central section of the AFU2/LFU2 transgressive

lag, and that these westward migrating sands have since constructed the unnamed shoal (cross section X8, Appendix 1). On the other hand, very little can be demonstrated in regards to Trinity Shoal's sand source, other than saying that it ultimately originated from beyond the eastern bounds of the study area. Considering the volume of Trinity Shoal, it can be hypothesized that the sands are derived from a major reworked headland and barrier island chain. However, Trinity Shoal is interpreted to have evolved under conditions that ultimately disagree with the three-staged transgressive depositional systems model (Penland and Boyd, 1981; 1985 and Penland et al., 1985; 1988), as discussed later.

Although not considered important to the overall depositional model compared to those facies described above, two additional facies are distinguished within the transgressive component. These facies are AFU8/LFU8 and AFU12. First, AFU8/LFU8 is a composite concentration of shell material, with *Mulinia lateralis* being the dominant bivalve (Laurie Anderson, personal communication, 2012; also Kidwell, 1991). This facies is found atop of AFU2/LFU2 in some of the shallowest parts of the study area (e.g. X10, Appendix 1). Whether or not AFU8/LFU8 formed through taphonomic feedback is beyond the scope of this research. However, its development in this shallow-water location is likely no coincidence. Recurring storms have most likely winnowed away any fine-grained sediment, continually leaving only shell and sand sediments behind. Furthermore, major storms have also left their mark on AFU8/LFU8's seafloor geomorphology, which appears highly irregular similar to that seen in the form of sand waves farther south. The subordinate sand fraction of AFU8/LFU8 ranges in particle size from very-fine to medium sand and in some cases may be bimodal to even trimodal. As was interpreted for parts of the AFU2/LFU2 lag and the unnamed shoal, at least the coarsest sands probably originated from the relatively local region of the underlying Maringouin Delta.

The AFU12 is also found in the northern part of the study area. In short, this acoustic-facies unit includes those parts of the near-surface sediment column that are not represented by the other transgressive facies and for which no further distinction can be made. Although not a single core penetrated this acoustic-facies unit, its corresponding lithofacies is most likely comprised of highly-bioturbated sandy muds. Probable mud sources include the Lafourche Delta Complex as well as the recently active Atchafalaya Delta. Note that AFU12's boundary with AFU5/LFU5 is transitional, and the boundaries displayed in Appendix 1 are rather arbitrary (cross sections Y15-Y20). Nevertheless, its acoustic facies is distinct from that of AFU5, and so a separation of units is justified.

### **The Atchafalaya Regressive Component**

Prograding over the northeastern part of the Maringouin Delta's transgressive component is AFU9/LFU9 (e.g. cross section X11, Appendix 1; TT-55-08, Appendixes 2 – 3). Both AFU9 and LFU9 are remarkably similar in character to that observed in the Lafourche subaqueous delta (AFU4/LFU4). For instance, LFU9 is characterized by a clay-dominated core with well-preserved interlaminated-to-interbedded silts that are only observed with the aid of an X-ray radiograph, whereas AFU9 exhibits a mostly reflection-free facies (at least within its northern section) with a few isolated reflectors that apparently downlap along its bottom boundary. In contrast with LFU4, sediments of LFU9 appear to have a high water content, suggesting recent deposition. It is interpreted that AFU9/LFU9 represents the leading edge of the present-day decoupled Atchafalaya subaqueous delta, which is stratigraphically correlated to its updip counterpart (Fig 51B). Future progradation of the Atchafalaya Delta over Holocene time scales will commit the Maringouin Delta and its overlying transgressive component to the stratigraphic record.

## **Framework within the Sequence-Stratigraphic Model**

### Parasequences

The regressive phase of the Maringouin Delta represents a typical coarsening upward parasequence bounded at the top by a flooding surface, or discontinuity, that formed consequent to rising relative sea level and the autocyclic termination of its sediment supply (Van Wagoner et al., 1990; Catuneanu, 2006; Catuneanu et al., 2009). In the case of this study, the flooding surface corresponds with a transgressive ravinement surface. Situated atop of the flooding surface in the northern, shallower part of the study area is typically ~ 1 – 2 m of sediments that have largely been reworked by physical and biological processes. These sediments are at least partially derived from reworked Maringouin strata and appear to grade down into the underlying Maringouin Delta (e.g. cross section Y36 and vibracore TT-33-08, Appendixes 1, 2, and 3). These sediments were defined previously as the AFU2/LFU2 transgressive lag and represent a “second type” of lag deposit (*sensu* Van Wagoner et al., 1990). In contrast, in the middle-to-southern, deeper parts of the study area, the flooding surface is comparatively sharp (e.g. cross section Y31 and vibracore TT-32-08, Appendixes 1, 2, and 3). Overlying the flooding surface instead are more recent sediments that clearly represent deposition in relatively deeper-water environments. In other words, the vertical succession of facies in the middle-to-southern, deeper parts of the study area indicates an abrupt increase in water depth across the flooding surface.

The present-day progradation of the Atchafalaya subaqueous delta over the Maringouin Delta's transgressive component signifies a new parasequence within the study area. The Atchafalaya-Delta parasequence, as observed within the study area, actually begins immediately atop of the flooding surface that marks the top of the Maringouin-Delta parasequence (*sensu* Van Wagoner et al., 1990). Thus, the entire transgressive component of the Maringouin Delta is

considered the basal component of the Atchafalaya-Delta parasequence. Note that a separate flooding surface does not bound the top of the down-drift Lafourche subaqueous delta (AFU4/LFU4) within the study area, but in fact the vertical succession of facies within the Maringouin Delta's transgressive component continues to shoal upward. A significant implication to this reality is that the down-drift Lafourche subaqueous delta, which is genetically linked to the regressive phase of a separate parasequence (i.e. the Lafourche-Delta parasequence), is incorporated within the Atchafalaya-Delta parasequence.

### Systems Tracts

In a larger sense, the Maringouin-Delta parasequence is part of a succession of genetically-related backstepping parasequences that successively onlap the underlying Type-1 sequence boundary (i.e. the Pleistocene Prairie surface; Boyd et al., 1989). This retrogradational parasequence set defines the transgressive systems tract (Van Wagoner et al., 1990). Whether or not the Maringouin Delta directly overlies the Type-1 sequence boundary within the study area is not convincingly resolvable. In fact, it is only within the very southwest section of the study area that the antecedent topography of AFU11 is recognized (e.g. cross section XX9, Appendix 1). The data suggest that AFU11 is of pre-Maringouin Delta age, but it is unclear whether the AFU11 is of Holocene age or older. It is possible that the top of AFU11 is in fact the Pleistocene Prairie surface.

The Teche Delta Complex, which followed the Maringouin, is positioned at the top of the transgressive systems tract (Fig. 1; Boyd et al., 1989). It is assumed that the stacking pattern of parasequences within the Holocene Mississippi Delta shifted in character from retrogradational to aggradational at the approximate time when the Mississippi River avulsed out of the Teche system and began building the St. Bernard Delta Complex. Aggradation of parasequences



generally characterizes the early highstand systems tract (Van Wagoner et al., 1990), although the highstand systems tract of the Holocene Mississippi Delta appears to have quickly transitioned into its current pattern of progradational parasequences (Boyd et al., 1989). The most recent progradational parasequence, the Atchafalaya, is currently downlapping the flooding surface that bounds the top of the Maringouin Delta Complex. In this sense, the flooding surface bounding the top of the Maringouin Delta, at least within the boundary of the study area, defines the maximum flooding surface (Van Wagoner et al., 1990).

### **The Prevailing Model Contrasted with this Study: Incompatible Differences**

As discussed in the Background section, the large-scale sand shoals that presently reside along Louisiana's continental shelf are thought to represent the final evolutionary stage (stage 3) of the 3-stage transgressive depositional systems model (Penland and others; Figs. 8 and 12). The precursors to these subaqueous sand shoals are thought to have been once-subaerial barrier islands (stage 2). The transformation of an offshore sand body from subaerial to subaqueous form has been described by Penland et al. (1988) as a process they term "transgressive submergence" (Fig. 56). This process, they argue, operates when relative sea-level rise is rapid enough to inundate barrier islands, while marine processes continually drive transgression and shoreface retreat. Such conditions are sustained within the Mississippi Delta due to its high subsidence rates (which drive relative sea-level rise in the delta today), limited supply of sandy sediment, and the low-gradient, storm-dominated shelf upon which the delta builds (Penland et al., 1988). Refer to the Background section for a more thorough review of the prevailing, transgressive depositional systems model, which again has long been used to explain the delta cycle's complete transgressive phase.

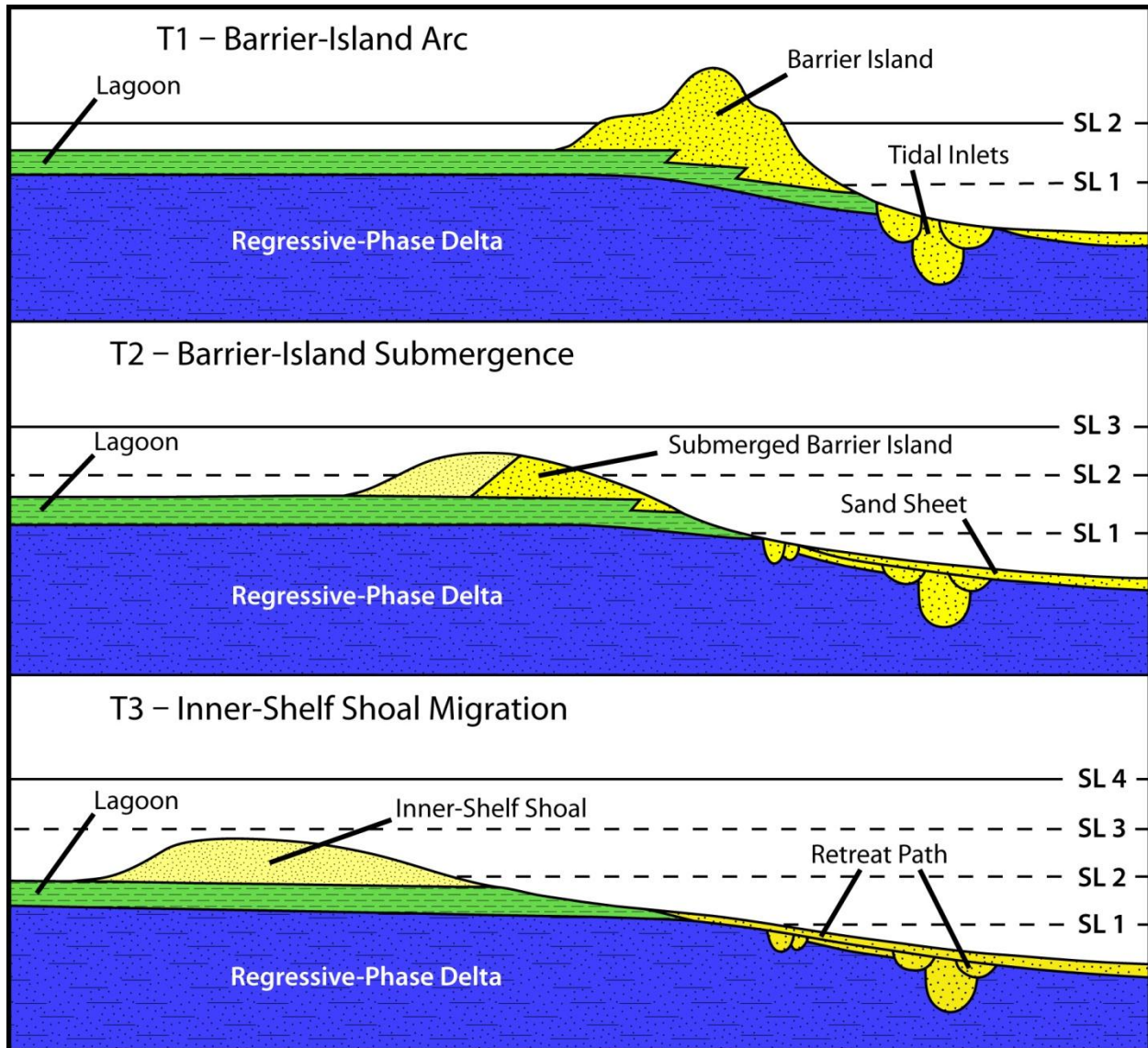


Figure 56. The transgressive-submergence process. In this idealized set of cross sections, a subaerial barrier island (T1) is inundated under rising relative sea level (T2) and ultimately reworked into a completely marine sand body (T3) as the sand shoal migrates landward. Modified from Penland et al. (1988).

Previous research (Penland et al., 1989; 1990; Pope et al., 1991) contends that Trinity Shoal is in a relatively early stage of transgressive submergence. That is, they argue that much of Trinity Shoal's original barrier-island facies is still preserved with only a thin (1-2 m), reworked marine sand layer capping the lithosome (Fig. 15 for an idealized schematic cross

section). This argument is derived from a data set similar to the one gathered during this study: acoustic subbottom profiles and vibrocores. From this data set, researchers expanded their interpretations of Trinity Shoal to include the greater Trinity-Tiger Shoals region, as construed by a series of north-south cross sections that the reader can observe in Figure 21. They depict Trinity Shoal stratigraphically above lagoonal sediments, which presumably accumulated behind the once-subaerial Trinity barrier island prior to the barrier migrating landward atop of them. Note that lagoonal sediments extend at least 20 km farther basinward than present-day Trinity Shoal (cross section C-C' in Fig. 21), implying that the once-subaerial Trinity barrier island migrated landward from a position at least as far basinward as this latitude. Ultimately, the Trinity barrier island was inundated during transgressive submergence, but apparently it has remained relatively stationary since that time as most of its original barrier-island facies is claimed to be preserved.

The relatively well-preserved Trinity Shoal, as the above model contends, stands in stark contrast with Ship Shoal, which is thought to be a completely reworked marine sand body without any original barrier-island facies preserved (Penland et al., 1986; 1989). Based on this understanding, researchers (Penland et al., 1985; 1988) argue that Trinity Shoal and Ship Shoal are the transgressed shoreline expressions of the Teche and Maringouin Delta Complexes, respectively. Again, this interpretation is not based on radiocarbon dating but instead is based on the perceived degree of reworking of the original, once-subaerial barrier islands: Trinity Shoal is largely comprised of its original barrier-island facies and so is considered younger (i.e. of Teche origin), whereas Ship Shoal has been completely reworked and, thus, is considered older (i.e. of Maringouin origin). The cross sections of Figure 21 portray the previous researchers'

interpretation of the unconformable stratigraphic relationship between Trinity Shoal and other transgressive sediments with what they contend as the underlying Teche Delta Complex.

The results and interpretations compiled during this dissertation are incompatible with the prevailing transgressive depositional systems model described in the preceding paragraphs. Particularly, stage 3 of the transgressive depositional systems model does not correctly explain what is actually observed within the Trinity-Tiger Shoals region. First, the regressive component is recognized as part of the Maringouin Delta Complex, not the Teche. This understanding is based on detailed mapping of the subsurface integrated with five AMS radiocarbon dates. Second, this study recognizes two distinct shoal bodies (Trinity Shoal and the unnamed shoal; Fig. 55A) that formed independently from one another, not a single, indiscriminate barrier-island complex as the previous model suggests (Figs. 21 and 22). If these two separate sand bodies had originally developed as subaerial barrier islands, and had they migrated landwards in unison following the cessation of the Maringouin Delta as the transgressive-submergence process predicates, one would have a difficult time explaining how a separate barrier island (i.e. the unnamed shoal) evolved behind the seaward-positioned Trinity barrier island. Furthermore, one would have an even more difficult time explaining how this separate barrier island (i.e. the unnamed shoal) evolved atop of Trinity's associated thick, back-barrier lagoonal muds. Third, regardless of the second point, neither barrier-island nor lagoonal environments are preserved within the study area. Instead, a prominent transgressive ravinement surface is recognized as having scoured down into the upper parts of the Maringouin Delta, removing in the process any transgressive sediments that presumably accumulated during the early stages of transgression. Fourth, in contrast, deposits that presently reside stratigraphically above the ravinement surface did not begin accumulating (and remain preserved) until ~ 4,000 years after the cessation of the

Maringouin Delta, a significant hiatus over Holocene time scales. It is recognized that the transformation from a Stage 1 erosional headland with flanking spits and barrier islands to a Stage 2 detached barrier-island arc with an associated back-barrier lagoon is not instantaneous (Fig. 8; Penland et al., 1988). However, the transitional process occurs within a time scale of centuries, not millennia. Fifth, there is no evidence suggesting that a barrier-island retreat path exists basinward of Trinity Shoal. As the previous model implies, the once-subaerial Trinity barrier island would have migrated landward from a position at least 20 km basinward from its current position (Fig. 21), leaving in its wake truncated tidal-inlet scars and deltas, the basal portions of the barrier island itself, and a thin sand sheet capping everything (Fig. 56; Penland and Suter, 1983; Penland et al., 1988). Assuming that a subaerial barrier island(s) did once exist in the region of the study area and assuming that it did undergo erosional shoreface retreat, its retreat path is likewise not preserved for the same reason that neither barrier-island nor lagoonal environments are preserved. Again, only more recent deposits presently reside stratigraphically above the ravinement surface. Cross section XX9 (Appendix 1), which would undoubtedly envelop any proposed retreat path (particularly as observed along strike view), best illustrates this final point.

Considering the extensive amount of research that has been carried out within modern transgressive settings, particularly deltaic-transgressive settings such as the various ones observed within the Mississippi Delta but also, for example, transgressive barrier islands observed elsewhere, the rationale for employing the transgressive depositional systems model to explain the evolution of Trinity Shoal and neighboring transgressive sediments is not incomprehensible. For the sake of argument, one could ignore for a moment the evidence outlined in the preceding paragraph and make the case, as Penland et al. (1990) and Pope et al.

(1991) did previously, that AFU4/LFU4 represents a lagoonal facies, AFU5/LFU5 represents an overwash facies associated with the paleo-Trinity barrier island, and AFU6/LFU6 represents all other barrier-island facies thought to exist within the paleo-Trinity barrier island (including tidal inlets and deltas, recurved spit(s) and even aeolian environments). One could make these arguments because there are similarities between respective facies. However, there are distinguishable differences, and the following, brief discussion is an attempt to refute these claims.

First, a lagoonal facies and AFU4/LFU4 are both characterized by fine-grained sediments. However, a lagoonal setting is for the most part a slow accumulating, biologically active environment, and the preservation potential of primary structures is generally very low due to bioturbation (Van Heerdan et al., 1985; Penland et al, 1986). In contrast, the clay core of AFU4/LFU4 includes generally well-preserved interlaminated-to-interbedded silts and sands, with a minimum of animal-burrowed, secondary structures. Second, an overwash facies and AFU5/LFU5 are both characterized by interbedded sands and muds. However, the overwash facies generally displays a thickening of individual sand beds at the expense of lagoonal muds towards the top of section (Van Heerdan et al., 1985), whereas such a trend is not very readily apparent in LFU5. Furthermore, although both facies generally show reworking by burrowing animals, the top part of the overwash facies may also be characterized by root burrowing (Van Heerdan et al., 1985). Root burrows are readily distinguished in an X-ray radiograph (Harry Roberts, personal communication, 2012). Of the 35 cores that penetrate LFU5, 15 were X-rayed (see LFU5 in the Results section). There is no evidence for root burrowing within any of the 35 LFU5-penetrating cores, including the 15 that were X-rayed. Third, a barrier-island facies and LFU6 are both largely comprised of clean sand. Although a suite of primary sedimentary

structures including multidirectional parallel-to-cross strata and trough-cross strata are associated with a backshore-dune environment (Reinson, 1984; Van Heerdan et al., 1985), only cross laminations are observed within LFU6. However, note that it is difficult if not hopeless to discern bed-scale features such as trough-cross bedding in a 7.6 cm diameter core. Furthermore, as discussed in the Results section, it is difficult in many cases to discern primary sedimentary structures in LFU6 due to homogeneity of sands, bioturbation, or both. Regardless, the backshore-dune environment is characterized by root burrowing (Reinson, 1984; Van Heerdan et al., 1985), and such secondary structures are not observed in LFU6, not even in the 7 LFU6-penetrating cores that were X-ray radiographed (see LFU6 in Results section).

In light of the above discussion, ample evidence demonstrates that the prevailing transgressive depositional systems model as advocated by Penland et al. (1988; also, Penland and Boyd, 1981; 1985; Penland et al., 1985; Fig. 8) does not adequately explain the post-Maringouin depositional history, at least as observed within the study area. Instead, an alternative, more rigorous depositional model is presented in this dissertation, as outlined earlier in the section titled The Transgressive Component. One final set of points is emphasized here. The three-stage transgressive depositional systems model established for the Mississippi Delta's transgressive phase (Penland and Boyd, 1981; 1985; Penland et al., 1985; 1988) is not invalid, as there is overwhelming evidence for its validity in describing the various transgressive settings displayed in the modern, highstand Mississippi Delta Plain. Furthermore, it is not argued that the Maringouin Delta, including that part within the bounds of the study area, did not undergo all three stages of this transgressive model. However, it is argued that any associated deposits that may have once accumulated within the study area during any one of these three stages have not been preserved in the stratigraphic record.

## CONCLUSION

Sand lithosomes of the Trinity-Tiger Shoals Complex, particularly Trinity Shoal, have long been thought to express the transgressed shoreline of a now-submerged, early-to-middle Holocene Mississippi Delta complex. However, confusion has persisted within the literature with regard to which delta complex is actually represented by this shoal complex. Early research argued for the Maringouin Delta Complex, whereas more recent studies suggested the Teche. Arguments have been largely based on indirect evidence, such as sea-level interpretations, sand-body geometry, and geographic relationships. More recently, acoustic and lithological data gathered from the region were also included into the argument. Nevertheless, no part of this argument has hitherto been based on AMS radiocarbon dating, be it measured from within the region or correlated into it from outside.

The first objective of this research addressed this lack of detail. Specifically, the question asked was whether the regressive component within the Trinity-Tiger Shoals region was genetically linked to the Maringouin Delta Complex or the Teche. Alternatively, this research recognized the possibility that perhaps both delta complexes prograded into the region, which would imply that the Teche Delta Complex resides stratigraphically atop of the Maringouin. The first objective was approached, as was the second objective discussed below, using an integrated data set consisting of ~ 1,350 km of high-resolution subbottom sonar profiles and various sedimentological data gleaned from 60 vibracores. This latter part of the data set included 22 discrete samples that were AMS radiocarbon dated. For formulating interpretations, this research relied extensively on concepts derived by others including our understanding of the various depositional processes and resulting depositional environments (i.e. facies) of the Mississippi Delta (e.g. Coleman, 1981; Penland and Boyd, 1985; Van Heerden et al., 1985;



Roberts, 1997), as well as how to recognize these environments from an acoustic data set by their reflection parameters (e.g. Mitchum et al., 1977; Berg, 1982). Altogether, 12 acoustic-facies units and 12 lithofacies units were differentiated.

Analysis of the regressive component reveals an offsetting, overlapping, and stacked arrangement of four delta lobes and one subdelta. Three of these delta lobes and the one subdelta reflect the tangential-oblique reflection-configuration pattern that characterizes the typical fluvial-dominated delta. Progradation of these deltas occurred predominantly along an east-northeast to west-southwest trend. The distributary system that fed these deltas is also partially preserved, but, with one exception, only within the northern part of the study area. Elsewhere, the distributary system was removed by transgressive ravinement that subsequently followed abandonment. In contrast, the one other delta lobe reflects the sigmoidal reflection-configuration pattern, which defines, at least in this case, a detached, down-drift subaqueous delta. Progradation of the subaqueous delta was predominantly east to west in accordance with the prevailing westward-directed coastal current. A distributary system associated with a separate subaerial delta lobe(s) located beyond the up-drift, eastern boundary of the study area is believed to have sourced this down-drift subaqueous delta. Five AMS radiocarbon dates were measured from three of the above mentioned delta lobes, with ages ranging from as young 4,820 yr BP to as old as 5,980 yr BP. Collectively, this age control confirms that in fact the Maringouin Delta Complex constructed within this most-basinward position of the middle Holocene Mississippi Delta. Evidence also confirms that the Teche Delta Complex did not prograde across the Maringouin Delta within the bounds of the study area, as suggested by an alternative hypothesis.

Unlike the confusion that once surrounded the regressive component as outlined above, there has been no substantial disagreement within the literature with regard to the sandy,

transgressed shoreline expression of deltas. Up to this point, all research has recognized the inner-shelf sand shoals to be the end products of abandoned, reworked deltas. The complete transgressive phase of abandoned deltas has been concisely defined by the prevailing, three-stage transgressive depositional systems model (Fig. 8). Among other things, this model predicates that barrier islands ultimately submerge under rising relative sea level, while marine process continually drive the sand lithosome landward, both before and after inundation. Without discrepancy, the transgressive depositional systems model presumes a coarsening upward succession of transgressive facies, with a once-subaerial barrier island facies or, alternatively, a completely reworked marine-sand facies residing stratigraphically atop of the once back-barrier lagoonal facies. The dominant variable of this model appears to be the shoal's age: more recent shoals are believed to retain much of their original barrier-island facies, whereas older shoals are thought to be completely reworked.

The second objective of this research challenged the prevailing transgressive depositional systems model, particularly the culmination of this model as depicted by its final stage (stage 3). Specifically, the question asked was whether the succession of preserved transgressive facies that now overly the Maringouin Delta Complex within the Trinity-Tiger Shoals region reflect that predicted by this model. This question was approached using the same data set as summarized above, and concepts derived by others were drawn upon extensively. Analysis of the transgressive component reveals a complex facies architecture, with eight separate facies identified. As a whole, the transgressive component overlies a prominent transgressive ravinement surface recognized as having scoured down into the upper parts of the entire underlying Maringouin Delta Complex. Thus, any transgressive sediments that presumably accumulated during the early stages of transgression are interpreted to have been removed by

erosion. Instead, a ~ 4,000 yr hiatus, as revealed by AMS radiocarbon dating, separates the transgressive component from the underlying regressive component (seventeen AMS radiocarbon dates were measured from the transgressive component). It was not until ~ 1,000 yr BP that significant amounts of sediments began migrating into the study area from the east, which have remained, at least for the time being, mostly preserved. Among the resulting depositional units is a detached down-drift subaqueous delta, which is interpreted to have been sourced from the Lafourche Delta Complex via a Lafourche mud stream transported westward by the prevailing westward-directed coastal current (analogous to the present-day Atchafalaya mud stream). Following the abandonment of the Lafourche Delta Complex, its mud stream eventually terminated. However, the westward streaming supply of sand, which is interpreted herein to be predominantly controlled over century timescales by the alongshore, westward directed combined flows that accompany periodic passages of high-energy tropical cyclones, has continued unabated. In turn, this continual influx of sand has led to the development of Trinity Shoal and the hitherto unnamed shoal. Tiger Shoal, on the other hand, is essentially a shallow-water part of the study area on account of greater preservation of the Maringouin Delta Complex within this area, with overlying deposits further decreasing water depths. The Atchafalaya Delta is currently prograding across the northeastern part of the study area. Further progradation will ultimately commit the Maringouin Delta Complex and its overlying transgressive component to the stratigraphic record.

The depositional model of the Trinity-Tiger Shoals region established during this research conflicts sharply with previous interpretations made within the region (Penland et al., 1989; 1990; Pope et al., 1991.) Previous interpretations contend that Trinity Shoal is a submerged, yet more-or-less preserved barrier island overlying its associated back-barrier

lagoonal deposits. These previous interpretations were also used to corroborate the final stage (stage 3) of the transgressive depositional systems model, as advocated by Penland and Boyd (1981; 1985) and Penland et al. (1985; 1988). However, transgressive deposits that are presumed to have accumulated during the early stages of transgression (e.g. the back-barrier lagoon, the barrier-island, and the barrier-island retreat path) are not recognized by this dissertation within the bounds of the study area. To the contrary, such deposits are interpreted to have been removed by transgressive ravinement. Only more recent deposits, as outlined previously, are preserved. From this understanding, the depositional model developed herein is considered incompatible with that predicted by the prevailing transgressive depositional systems model. Note that results derived from this study do not imply that the various forms of transgression as described by the transgressive depositional systems model did not occur to some degree at one time. This study does argue, however, that any affiliated deposits are not preserved, at least not within the Trinity-Tiger Shoals study area. Thus, this study essentially amends the prevailing model by adding to it what could be described a stage 4: complete obliteration of stage 3 (particularly the back-barrier lagoonal facies) by transgressive ravinement.

It is worth noting that working within the transgressive component was by far the most difficult aspect of this research. Difficulties were partially consequent to the transgressive component's complex facies architecture. However, they were equally, if not more so consequent to the fact that this research began by "looking" for the idealized succession of facies predicted by the transgressive depositional systems model. Conceptual models, such as the transgressive depositional systems model, become powerful and sometimes difficult to question when they become as widely accepted in the community as this one. It was only after (painstakingly) analyzing the various data sets gathered during this research, differentiating these

data (i.e. the subsurface) into appropriate depositional units, properly interpreting those depositional units with the aid of an extensive literature review, and then augmenting those interpretations with AMS radiocarbon dating that the depositional history of the transgressive component, as this research understands it, emerged.

### **Suggested Areas for Further Research**

This study has clearly shown that using the transgressive depositional systems model, particularly stage 3, to explain the stacking pattern of preserved transgressive sediments within the Trinity-Tiger Shoals region is not correct. However, this study also recognizes the uniqueness of the Trinity-Tiger Shoals region. For instance, this region is positioned within the most western part of the transgressed Maringouin Delta Complex, and is therefore down drift to and perhaps older than all other depocenters of the Holocene Mississippi Delta. Therefore, this study advises caution in applying the depositional model derived during this research to other regions identified elsewhere along central Louisiana's inner-continental shelf where shoal complexes exist.

Nevertheless, in spite of its uniqueness, there are broad similarities recognized herein between the facies architecture of the Trinity-Tiger Shoals region, as distinguished during this research, and the facies architecture of other regions where shoal complexes exist. These other shoal complexes include Ship Shoal and an unnamed shoal complex located ~ 50 – 60 km east of Trinity Shoal (this latter, unnamed shoal complex is not to be confused with the now-differentiated, unnamed shoal within the Trinity-Tiger Shoals Complex). For instance, all shoal complexes along central Louisiana's inner-continental shelf overlie either the Maringouin Delta Complex or the Teche. As discussed above, both delta complexes reside within the transgressive systems tract of the Holocene Mississippi Delta, and thus were exposed to erosional shoreface

retreat for a considerable period following their abandonment. In the case of the Trinity-Tiger Shoals region, a significant hiatus ensued upon the abandonment of the Maringouin Delta Complex, which was accompanied by severe erosional truncation. Only within the last ~ 1,000 years was this hiatus terminated by significant sediment deposition. Should not other parts of the Maringouin and Teche Delta Complexes reflect similar conditions? Principally, should they not also reflect a long period of erosional truncation that would have scoured down into the upper parts of the once-prograding deltas, removing in the process any transgressive sediments (e.g. barrier islands, shoals, and lagoonal muds) that presumably accumulated during the early stages of transgression? This study suggests they should. Thus, the transgressive component within regions where other shoal complexes exist may also reflect a similar sequence of deposits as recognized within the transgressive component of the Trinity-Tiger Shoals region. If true, then one has to ask whether the transgressive depositional systems model, particularly stage 3, applies to any shoal complex identified along central Louisiana's inner-continental shelf. Further research within the regions of Ship Shoal and the unnamed shoal complex should address these questions.

Previous researchers (e.g. Penland et al., 1988; Penland et al. 1989) developed the final stage of the transgressive depositional systems model based largely on their interpretations of the different facies architectures within both the Trinity Shoal region and the Ship Shoal region. The fact that there are severe, irreconcilable differences between the findings of this dissertation and the findings from previous studies carried out in the Trinity-Tiger Shoals region is enough alone to suggest a reevaluation of the Ship Shoal region. Particularly, new research should reevaluate those sediments beneath Ship Shoal that have previously been interpreted as a lagoonal facies,

and determine whether they are instead associated with the Lafourche Delta as AFU4/LFU4 was found to be within the Trinity-Tiger Shoals region.

Other than its recognition, there has been practically no research conducted within the region of the unnamed shoal complex. Again, this unnamed shoal complex is ~ 50 – 60 km east of Trinity Shoal, and resides at approximately the same latitude and depth. Most intriguing, the unnamed shoal and the strata beneath it display a similar succession of acoustic facies as seen in the Trinity-Tiger Shoals region (see line A-A' in Allison and Neill, 2003; their Figs. 1 and 5). At the base of this succession of acoustic facies is an acoustic-facies unit that is predominantly reflection free. Above this unit is an acoustic-facies unit characterized by a high degree of acoustic scatter, and above this unit and at the top of the succession is a mostly reflection-free acoustic-facies unit. Again, this succession of acoustic facies is remarkably similar to what is observed within the Trinity-Tiger Shoals region. For instance, the AFU4 (i.e. the detached, down-drift subaqueous delta of Lafourche origin) appears to correspond with the basal, reflection-free acoustic-facies unit. Overlying AFU4 in the Trinity-Tiger Shoals region is AFU5 (i.e. the transitional facies), which appears to correspond with the middle acoustic-facies unit characterized by a high degree of acoustic scatter. The AFU6 (i.e. Trinity Shoal) appears to correspond with the mostly reflection-free acoustic-facies unit at the top of the succession. The significance of these relationships, if true, is that the unnamed sand shoal within this region resides stratigraphically above relatively recently deposited Lafourche muds, not back-barrier lagoonal muds. A future research program, employing the same methodology used in this dissertation, could settle these issues.

Resolving the questions outlined above would also allow for the assessment of other outstanding questions that have emerged during this research.

- Previous research recognized Lafourche muds both within and immediately offshore of the Louisiana Chenier Plain (Penland and Suter , 1998; Draut et al., 2005). However, this study is the first to identify a significant muddy depositional unit (AFU4/LFU4) along central Louisiana's inner-continental shelf as part of a detached, down-drift subaqueous delta of Lafourche origin. Are deposits previously interpreted as lagoonal muds in the Ship Shoal region (and presumably the region of the unnamed shoal) instead associated with the Lafourche Delta Complex? Answering this question would allow further assessment of a previously underappreciated, inner-shelf depositional phenomenon: the down-drift Lafourche subaqueous delta.
- Further research within the Ship Shoal region should also verify which delta complex resides beneath the transgressive sediments. As noted previously, there is confusion within the literature with regard to which delta complex underlies Ship Shoal. Several studies suggest the Maringouin Delta Complex (e.g. Frazier, 1967; Penland et al., 1989), whereas Penland et al. (1987 – a study stated to have been based on 500 km of high-resolution subbottom profiles, 368 vibracores, and 158 radiocarbon dates) contend the Teche. Likewise, a study within the region of the unnamed shoal should also address the depositional history of the underlying regressive component. New geochronologic constraints, combined with the results from this dissertation, would further advance our understanding of the middle Holocene Mississippi Delta. Such an understanding would also allow one to address the final question below.
- This study interprets that the sands of Trinity Shoal migrated into their present-day position from beyond the eastern boundary of the study area. Intuition would suggest that the sand source originated from a reworked headland within the more eastern parts of the Maringouin



Delta. However, the eastern part of the Teche Delta Complex is thought by some to have extended at least as far basinward as the latitude of the Trinity-Tiger Shoals Complex (Fig. 1). If true, the Teche Delta Complex, to some degree, would have constructed atop of the eastern part of the Maringouin Delta Complex. Could sands derived from the reworked portions of the Teche Delta comprise Trinity Shoal? Such a (plausible) scenario would be in stark contrast with prevailing thought, as it is generally accepted that offshore sand shoals, derived from reworked regressive sediments, overlie the delta complex from which they were sourced.

## REFERENCES CITED

- Adams, C.E., Jr., J.T. Wells, and J.M. Coleman, 1982, Sediment transport on the central Louisiana continental shelf: Implications for the developing Atchafalaya River Delta: *Contributions in Marine Science*, v. 25, p. 133-148.
- Allen, J.R.L., 1982, *Sedimentary Structures: Their Character and Physical Basis*, v. 2. New York: Elsevier Scientific Publishing Company, 663 p.
- Allison, M.A. and C.F. Neill, 2003, Development of a modern subaqueous mud delta on the Atchafalaya shelf, Louisiana. *In*: Scott, E.K., A.H. Bouma, and W.R. Bryant (eds.), *Depositional Processes and Characteristics of Siltstones, Mudstones and Shales*. SEPM, Tulsa, p. 23-34.
- Autin, J.W., Burns, S.F., Miller, B.J., Saucier, R.T., and Snead, J.I., 1991, Quaternary geology of the Lower Mississippi Valley. *In*: Morrison, R.B., (ed.), *Quaternary Nonglacial Geology; Conterminous U.S.* Boulder: Geological Society of America, *The Geology of North America*, v. K-2, p. 547-582.
- Bailey, A.M., H.H. Roberts, and J.H. Blackson, 1998, Early diagenetic minerals and variables influencing their distributions in two long cores (> 40 m), Mississippi River Delta Plain: *Journal of Sedimentary Research*, v. 68, p. 185-197.
- Bann, K.L., C.R. Fielding, J.A. MacEachern, and S.C. Tye, 2004, Differentiation of estuarine and offshore marine deposits using integrated ichnology and sedimentology: Permian Pebble Beach Formation, Sydney Basin, Australia. *In*: McIlroy, D., (ed.), *The Application of Ichnology to Paleoenvironmental and Stratigraphic Analysis: Lyell Meeting 2003*, The Geological Society of London, Special Publication 228, p. 179-211.
- Bard, E., B. Hamelin, M. Arnold, L. Montaggioni, G. Cabioch, G. Faure, and F. Rougerie, 1996, Deglacial sea-level record from Tahiti corals and the timing of global meltwater discharge: *Nature*, v. 382, p. 241-244.
- Bentley, S.J., Sr., 2003, Wave-current dispersal of fine-grained fluvial sediments across continental shelves: the significance of hyperpycnal plumes: *In*: Scott, E.K., A.H. Bouma, and W.R. Bryant (eds.), *Depositional Processes and Characteristics of Siltstones, Mudstones and Shales*. SEPM, Tulsa, p. 35-48.
- Berg, O.R., 1982, Seismic detection and evaluation of delta and turbidite sequences: their application to the exploration for the subtle trap: *American Association of Petroleum Geologists*, v. 66, p. 57-75.
- Berryhill, H.L., Jr., 1987, Diapirism and faulting, continental shelf and upper continental slope off southwestern Louisiana. *In*: Berryhill, H.L., Jr., J.R. Suter, and N.S. Hardin, (eds.), *Late Quaternary Facies and Structure, Northern Gulf of Mexico: Interpretation from Seismic Data*, AAPG Studies in Geology No. 23, p. 191-224.

- Best, A.I. and D.E. Gunn, 1999, Calibration of marine sediment core loggers for quantitative acoustic impedance studies: *Marine Geology*, v. 160, p. 137-146.
- Bhattacharya, J.P., 2006, Deltas. *In*: Walker, R.G., and H. Posamentier, (eds.), *Facies Models Revisited*, SEPM Special Publication No 84, p. 237-292.
- Blum, M.D. and Roberts, 2009, Drowning of the Mississippi Delta due to insufficient sediment supply and global sea-level rise: *Nature Geoscience*, v. 2, p. 488-491.
- Blum, M.D. and H.H. Roberts, 2012, The Mississippi Delta region: Past, present, and future: *Annual Review of Earth and Planetary Sciences*, v. 40, p. 655-683.
- Blum, M.D., J.H. Tomkin, A. Purcell, and R.R. Lancaster, 2008, Ups and downs of the Mississippi Delta: *Geology*, v. 36, p. 675-678.
- Blum, M.D. and T.E. Törnqvist, 2000, Fluvial response to climate and sea-level change: A review and a look forward: *Sedimentology*, v. 47, p. 2-48.
- Boyd, R. and S. Penland, 1981, Washover of deltaic barriers on the Louisiana coast: *Transactions – Gulf Coast Association of Geological Societies*, v. 31, p. 243-248.
- Boyd, R., J. Suter, and S. Penland, 1989, Sequence stratigraphy of the Mississippi Delta: *Transactions – Gulf Coast Association of Geological Societies*, v. 39, p. 331-340.
- Bradley, M.E., 1985, *Practical Seismic Interpretation*. Boston: International Human Resources Development Corporation, 266 p.
- Brooks, G.R., J.L. Kindinger, S. Penland, S.J. Williams, and R.A. McBride, 1995, East Louisiana Continental Shelf Sediments: A product of delta reworking: *Journal of Coastal Research*, v. 11, p. 1026-1036.
- Bouma, A.H., 1962, *Sedimentology of Some Flysch Deposits*. Amsterdam/New York: Elsevier Publishing Company, 168 p.
- Bouma, A.H., 1969, *Methods for the Study of Sedimentary Structures*. New York: Wiley-Interscience, 458 p.
- Bull, J.M., M. Gutowski, J.K. Dix, T.J. Henstock, P.Hogarth, T.G. Leighton, and P.R. White, 2005, Design of a 3D chirp sub-bottom imaging system: *Marine Geophysical Researches*, v. 26, p. 157-169.
- Cant, J.D., 1992, Subsurface Facies Analysis. *In*: Walker, R.G. and N.P. James, (eds.), *Facies Models: Response to Sea Level Change*: Geological Association of Canada, p. 27-45.
- Cattaneo, A. and R.J. Steel, 2003, Transgressive deposits: A review of their variability: *Earth-*

- Science Reviews, v. 62, p. 187-228.
- Catuneanu, O., 2006, Principles of Sequence Stratigraphy. Amsterdam: Elsevier, p. 375.
- Catuneanu, O., et al., 2009, Towards the standardization of sequence stratigraphy: Earth-Science Reviews, v. 92, p. 1-33.
- Chappell, J. and H. Polach, 1991, Post-glacial sea-level rise from a coral record at Huon Peninsula, Papua New Guinea: Nature, v. 349, p. 147-149.
- Cochrane, J.D. and F.J. Kelly, 1986, Low-frequency circulation on the Texas-Louisiana continental shelf: Journal of Geophysical Research, v. 91, p. 10,645-10659.
- Coleman, J.M., 1966, Recent coastal sedimentation: central Louisiana coast: Louisiana State University, Coastal Studies Institute Technical Report No. 17, 73 p.
- Coleman, J.M., 1981, Deltas: Processes of Deposition and Models for Exploration, 2<sup>nd</sup> ed.: Minneapolis, Burgess Publishing Company, 124 p.
- Coleman, J.M., 1988, Dynamic changes and processes in the Mississippi River Delta: Geological Society of America Bulletin, v. 100, p. 999-1015.
- Coleman, J.M. and S.M. Gagliano, 1964, Cyclic sedimentation in the Mississippi River Delta Plain: Transactions – Gulf Coast Association of Geological Societies, v. 14, p. 67-80.
- Coleman, J.M. and S.M. Gagliano, 1965, Sedimentary structures: Mississippi River Deltaic Plain. In: Middleton, G.V., (ed.), Primary Sedimentary Structures and Their Hydrodynamic Interpretation, SEPM Special Publication No. 12, p. 133-148.
- Coleman, J.M., S.M. Gagliano, and J.E. Webb, 1964, Minor sedimentary structures in a prograding distributary: Marine Geology, v. 1, p. 240-258.
- Coleman, J.M. and D.B. Prior, 1982, Deltaic environments of deposition. In: Scholle, P.A. and D.R. Spearing, (eds.), Sandstone Depositional Environments: American Association of Petroleum Geologists, Memoir 31, p. 139-178.
- Coleman, J.M. and L.D. Wright, 1975, Modern river deltas: variability of processes and sand bodies. In: Broussard, M.L., (ed.), Deltas: Models for Exploration: Houston, Houston Geological Society, p. 99-149.
- Crout, R.L. and R.D. Hamiter, 1981, Response of bottom waters on the west Louisiana shelf to transient wind events and resulting sediment transport: Transactions – Gulf Coast Association of Geological Societies, v. 31, p. 273-278.
- Couvillion, B.R., J.A. Barras, G.D. Steyer, W. Sleavin, M. Fischer, H. Beck, N. Trahan, B. Griffin, and D. Heckman, 2011, Land area change in coastal Louisiana from 1932 to

- 2010: U.S. Geological Survey Scientific Investigations Map 3164, scale 1:265,000, 12 p. pamphlet.
- Davies, D.J., E.N. Powell, and R.J. Stanton, 1989, Taphonomic signature as a function of environmental process: shells and shell beds in a hurricane-influenced inlet on the Texas coast: *Palaeogeography, Palaeoclimatology, Palaeoecology*, v. 72, p. 317-356.
- Demarest, J.M. and J.C. Kraft, 1987, Stratigraphic record of Quaternary sea levels: Implications for more ancient strata. *In*: Nummedal, D., O.H. Pilkey, and S.D. Howard (eds.), *Sea-Level Fluctuation and Coastal Evolution: SEPM Special Publication*, v. 41, p. 223-239.
- Donnelly, J.P. and L. Giosan, 2008, Tempestuous highs and lows in the Gulf of Mexico: *Geology*, v. 36, p. 751-752.
- Draut, A.E., G.C. Kineke, D.W. Velasco, M.A. Allison, and R.J. Prime, 2005, Influence of the Atchafalaya River on recent evolution of the chenier-plain inner continental shelf, northern Gulf of Mexico: *Continental Shelf Research*, v. 25, p. 91-112.
- Duke, W.L., 1990, Geostrophic circulation or shallow marine turbidity currents? The dilemma of paleoflow patterns in storm-influenced prograding shoreline systems: *Journal of Sedimentary Petrology*, v. 60, p. 870-883.
- Edrington, C.H., M.D. Blum, J.A. Nunn, and J.S. Hanor, 2008, Long-term subsidence and compaction rates: A new model for the Michoud area, south Louisiana: *Transactions – Gulf Coast Association of Geological Societies*, v. 58, p. 261-272.
- Fairbanks, R.G., 1989, A 17,000-year glacio-eustatic sea level record: Influence of glacial melting rates on the Younger Dryas event and deep-ocean circulation: *Nature*, v. 342, p. 637-642.
- Farrell, K.M., B.W. Harris, D.J. Mallinson, S.J. Culver, S.R. Riggs, J. Pierson, J.M. Self-Trail, and J.C. Lautier, 2012, Standardizing texture and facies codes for a process-based classification of clastic sediment and rock: *Journal of Sedimentary Research*, v. 82, p. 364-378.
- Farrell, K.M., B.W. Harris, D.J. Mallinson, S.J. Culver, S.R. Riggs, J.F. Wehmiller, J. Pierson, J.M. Self-Trail, and J.C. Lautier, in review, A method of graphic logging for interpreting process-generated stratigraphic sequences: with analog shelf examples from the Atlantic Coastal Plain Province, U.S.A.: *Journal of Sedimentary Research*.
- Fearnley, S., M. Miner, M. Kulp, C. Bohling, L. Martinez, and S. Penland, 2009, Chapter A. Hurricane impact and recovery shoreline change analysis and historical island configuration: 1700s to 2005. *In*: Lavoie, D. (ed.), *Sand resources, regional geology, and coastal processes of the Chandeleur Islands coastal system—an evaluation of the Breton National Wildlife Refuge*: U.S. Geological Survey Scientific Investigations Report 2009–5252, p. 7-26.

- Fisk, H.N., 1944, Geologic investigations of the alluvial valley of the lower Mississippi River: Vicksburg, Mississippi, U.S. Army Corp of Engineers, Mississippi River commission, 78 p.
- Fisk, H.N., 1955, Sand facies of recent Mississippi Delta deposits: 4<sup>th</sup> World Petroleum Congress, Proceedings, Section I, p. 377-398.
- Fisk, H.N., E. McFarlan, Jr., C.R. Kolb, and L.J. Wilbert, Jr., 1954, Sedimentary framework of the modern Mississippi Delta: *Journal of Sedimentary Petrology*, v. 24, p. 76-99.
- Fisk, H.N. and E. McFarlan, Jr., 1955, Late Quaternary deltaic deposits of the Mississippi River. *In*: Poldervaart, A., (ed.), *Crust of the earth: Geological Society of America Special Paper* 62, p. 279-302.
- FitzGerald, D.M., M.A. Kulp, Z. Huges, I. Georgiou, M.D. Miner, S. Penland, and N. Howes, 2007, Impacts of rising sea level to backbarrier wetlands, tidal inlets, and barrier islands: Barataria Coast, Louisiana. *In*: *Proc Coastal Sediments 07*, American Society of Civil Engineers, p. 1179-1192.
- Flocks, J., D. Twichell, J. Sanford, E. Pendleton, and W. Baldwin, 2009, Chapter F. Sediment sampling analysis to define quality of sand resources. *In*: Lavoie, D. (ed.), *Sand resources, regional geology, and coastal processes of the Chandeleur Islands coastal system—an evaluation of the Breton National Wildlife Refuge: U.S. Geological Survey Scientific Investigations Report 2009–5252*, p. 99-124.
- Folk, R.L., 1974, *Petrology of Sedimentary Rocks*. Austin: Hemphill Publishing Company, 182 p.
- Frazier, D.E., 1967, Recent deltaic deposits of the Mississippi River: Their development and chronology: *Gulf Coast Association of Geological Societies Transactions*, v. 17, p. 287-315.
- Frazier, D.E., 1974, Depositional-episodes: Their relationship to the Quaternary stratigraphic framework in the northwestern portion of the Gulf Basin: Bureau of Economic Geology, The University of Texas at Austin, *Geological Circular*, v. 74, no. 1, p. 1-28.
- Galloway, W.E., 1975, Process framework for describing the morphologic and stratigraphic evolution of deltaic depositional systems. *In*: Broussard, M.L., (ed.), *Deltas: Models for Exploration: Houston, Houston Geological Society*, p. 87-98.
- Galloway, W.E., 2005, Gulf of Mexico basin depositional record of Cenozoic North American drainage basin evolution: *Special Publications International Association Sedimentation*, v. 35, p. 409-423.
- Galloway, W.E., Ganey-Curry, P.E., Li, X., and Buffler, R.T., 2000, Cenozoic depositional

- history of the Gulf of Mexico basin: American Association of Petroleum Geologists Bulletin, v. 84, p. 1743-1774.
- Georgiou, I.Y., D.M. FitzGerald, and G.W. Stone, 2005, The impact of physical processes along the Louisiana coast: Journal of Coastal Research, v. 44, p. 72-89.
- Gerdes, R.G., 1985, The Caminada-Moreau beach ridge plain. *In*: Penland, S. and R. Boyd (eds.), Transgressive Depositional Environments of the Mississippi River Delta Plain, Louisiana Geological Survey Guidebook Series No. 3, p. 127-140.
- Gould, H.R., 1970, The Mississippi Delta Complex. *In*: Morgan, J.P. (ed.), Deltaic Sedimentation: Modern and Ancient: Society of Economic Paleontologists and Mineralogists (SEPM) Special Publication No. 15, p. 3-30.
- Gunn, D.E. and A.I. Best, 1998, A new automated nondestructive system for high resolution multi-sensor core logging of open sediment cores: Geo-Marine Letters, v. 18, p. 70-77.
- Hamblin, W.M.K., 1962, X-ray radiography in the study of structures in homogeneous sediments: Journal of Sedimentary Petrology, v. 32, p. 201-210.
- Hatton, R.S., R.D. DeLaune, W.H. Patrick, Jr., 1983, Sedimentation, accretion, and subsidence in marshes of Barataria Basin, Louisiana: Limnology and Oceanography, v. 28, p. 494-502.
- Hughen, K.A., M.G.L. Baillie, E. Bard, J.W. Beck, C.J.H. Bertand, P.G. Blackwell, C.E. Buck, G.S. Burr, K.B. Cutler, P.E. Damon, R.L. Edwards, R.G. Fairbanks, M. Friedrich, T.P. Guilderson, B. Kromer, G. McCormac, S. Manning, C.B. Ramsey, P.J. Reimer, R.W. Reimer, S. Remmele, J.R. Southon, M. Stuiver, S. Talamo, F.W. Taylor, J. van der Plicht, C.E. Weyhenmeyer, 2004b, Marine04 Marine radiocarbon age calibration, 0–26 ka BP: Radiocarbon v. 46, p. 1059–1086.
- Huh, O.K., H.H. Roberts, L.J. Rouse, and D.A. Rickman, 1991, Fine grain sediment transport and deposition in the Atchafalaya and Chenier Plain sedimentary system. American Society of Civil Engineers Proceedings from Coastal Sediments '91, p. 817-830.
- Hutton, E.W.H. and J.P.M. Syvitski, 2008, Sedflux 2.0: An advanced process-response model that generates three-dimensional stratigraphy: Computers and Geosciences, v. 34, p. 1319-1337.
- Hwang, I.-G. and P.L. Heller, 2002, Anatomy of a transgressive lag: Panther Tongue Sandstone, Star Point Formation, central Utah: Sedimentology, v. 49, p. 977-999.
- Ivins, E.R., R.K. Dokka, and R.G. Blom, 2007, Post-glacial sediment load and subsidence in coastal Louisiana: Geophysical Research Letters, v. 34, p. 5.

- Jackson, D. R. and M. D. Richardson, 2007, High-frequency seafloor acoustics. New York: Springer Science, 616 p.
- Jaffe, B.E., J.H. List, and A.H. Sallenger, Jr., Massive sediment bypassing on the lower shoreface offshore of a wide tidal inlet – Cat Island Pass, Louisiana: *Marine Geology*, v. 136, p. 131-149.
- Jerolmack, D.J., 2009, Conceptual framework for assessing the response of delta channel networks to Holocene sea level rise: *Quaternary Science Reviews*, v. 28, p. 1786-1800.
- Kahn, J.H. and H.H. Roberts, 1982, Variations in storm response along a microtidal transgressive barrier island arc: *Sedimentary Geology*, v. 33, p. 129-146.
- Kesel, R.H., E.G. Yodis, and D.J. McCraw, 1992, An approximation of the sediment budget of the Lower Mississippi River prior to major human modification: *Earth Surface Processes and Landforms*, v. 17, p. 711-722.
- Kidwell, S.M., 1991, The stratigraphy of shell concentrations. *In*: Allison, P.A. and D.E.G. Briggs (eds.), *In Taphonomy, Releasing the Data Locked in the Fossil Record*. New York: Plenum Press, p. 211-290.
- Kolb, C.R. and J.R. Van Lopik, 1958, Geology of the Mississippi Delta Plain – southeastern Louisiana: U.S. Army Corps of Engineers, Waterways Experiment Station, Technical Report 2, 482 p.
- Kuecher, G.J., 1994, Geologic framework and consolidation settlement potential of the Lafourche Delta, topstratum valley fill sequence: implications for wetland loss in Terrebonne and Lafourche parishes, Louisiana [Ph.D. dissertation]: Baton Rouge, Louisiana, Louisiana State University, 346 p.
- Kuecher, G.J., N. Chandra, H.H. Roberts, J.H. Suhayda, S.J. Williams, S.P. Penland, and W.J. Autin, 1993, Consolidation settlement potential in south Louisiana: Coastal Zone '93, Proceeding from the 8<sup>th</sup> Symposium on Coastal and Ocean Management p. 1197-1214.
- Kuecher, G.J., H.H. Roberts, M.D. Thompson, and I. Mathews, 2001, Evidence for active growth faulting in the Terrebonne Delta Plain, south Louisiana: Implications for wetland loss and the vertical migration of petroleum: *Environmental Geosciences*, v. 8, p. 77-94.
- Kulp, M., 2000, Holocene stratigraphy, history, and subsidence: Mississippi River Delta region, north-central Gulf of Mexico [Ph.D. dissertation]: Lexington, Kentucky, University of Kentucky, 336 p.
- Kulp, M., D. FitzGerald, and S. Penland, 2005, Sand-rich lithosomes of the Holocene Mississippi River Delta Plain. *In*: Liviu, G. and J.P. Bhattacharya (eds.), *River Deltas: Concepts, Models, and Examples: Society of Sedimentary Geology (SEPM) Special Publication No. 83*, p. 279-293.



- Kulp, M., D. FitzGerald, S. Penland, and J. Motti, 2003, Evolution and stratigraphy of a recent flood tidal delta: Raccoon Pass, Timbalier Islands Louisiana: Transactions – Gulf Coast Association of Geological Societies, v. 53, p. 422-433.
- Kulp, M., S. Penland, and K. Ramsey, 2001, Ship Shoal: Sand resource synthesis report. Prepared by the Coastal Research Laboratory at the University of New Orleans and Submitted to Lee Wilson and Associates, 70 p. + Appendixes.
- Liner, C.L., 2004, Elements of 3D Seismology 2<sup>nd</sup> Edition. Tulsa: PennWell, 608 p.
- List, J.H., B.E. Jaffe, A.H. Sallenger, Jr., and M.E. Hansen, 1997, Bathymetric comparisons adjacent to the Louisiana barrier islands: Processes of large-scale change: Journal of Coastal Research, v. 13, p. 670-678.
- MacEachern, J.A., K.L. Bann, J.P. Bhattacharya, and C.D. Howell, 2005, Ichnology of deltas: Organism responses to the dynamic interplay of rivers, waves, storms and tides. *In*: Giosan, L. and J.P. Bhattacharya, (eds.), River Deltas: Concepts, Models, and Examples: SEPM, Special Publication 83, p. 49-85.
- McBride, R.A. and M.R. Byrnes, 1997, Regional variations in shore response along barrier island systems of the Mississippi River Delta Plain: Historical change and future prediction: Journal of Coastal Research, v. 13, p. 628-655.
- McKee, E.D. and G.W. Weir, 1953, Terminology for stratification and cross-stratification in sedimentary rocks: Geological Society of America Bulletin, v. 64, p. 381-390.
- Meade, R.H. and J.A. Moody, 2010, Causes for the decline of suspended-sediment discharge in the Mississippi River system, 1940-2007: Hydrological Processes, v. 24, p. 35-49.
- Meckel, T.A., U.S. ten Brink, and S.J. Williams, 2006, Current subsidence rates due to compaction of Holocene sediments in southern Louisiana: Geophysical Research Letters, v. 33, 5 p.
- Meckel, T.A., U.S. ten Brink, and S.J. Williams, 2007, Sediment compaction rates and subsidence in deltaic plains: numerical constraints and stratigraphic influences: Basin Research, v. 19, p. 19-31.
- Middleton, G.V, 1973, Johannes Walther's Law of the Correlation of Facies: Geological Society of America Bulletin, v. 84, p. 979-988.
- Milliken, K.T., J.B. Anderson, and A.B. Rodriguez, 2008, A new composite Holocene sea-level curve for the northern Gulf of Mexico. *In*: Anderson, J.B. and A.B. Rodriguez (eds.), Response of Upper Gulf Coast Estuaries to Holocene Climate Change and Sea-Level Rise: Geological Society of America Special Paper 443, p. 1-11.

- Miner, M.D., D.M. FitzGerald, and M.A. Kulp, 2007, 1880 to 2005 morphologic evolution of a transgressive tidal inlet, Little Pass Timbalier, Louisiana. *In: Proc Coastal Sediments 07*, American Society of Civil Engineers, p. 1165-1178.
- Miner, M.D., M. Kulp, H.D. Weathers, and J. Flocks, 2009, Historical (1869-2007) sea floor evolution and sediment dynamics along the Chandeleur Islands. *In: Lavoie, D. (ed.), Sand resources, regional geology, and coastal processes of the Chandeleur Islands coastal system—an evaluation of the Breton National Wildlife Refuge: U.S. Geological Survey Scientific Investigations Report 2009–5252*, p. 47-74.
- Mitchum, R.M., P.R. Vail, and J.B. Sangree, 1977, Seismic stratigraphy and global changes of sea level, Part 6: Stratigraphic interpretation of seismic reflection patterns in depositional sequences. *In: Payton, C.E., (ed.), Seismic Stratigraphy – Applications to Hydrocarbon Exploration*, Memoir 26, American Association of Petroleum Geologists, p. 117-133.
- Mitrovica, J.X. and G.A. Milne, 2002, On the origin of late Holocene sea-level highstands within equatorial ocean basins: *Quaternary Science Reviews*, v. 21, p. 2179-2190.
- Morton, R.A., 1981, Formation of storm deposits by wind-forced currents in the Gulf of Mexico and the North Sea. *In: Nio, S.D. (ed.), Holocene Marine Sedimentation in the North Sea Basin: International Association of Sedimentologists Special Publication No. 5*, p. 385-396.
- Murray, S.P., 1997, An observational study of the Mississippi-Atchafalaya coastal plume: Final report. OCS Study MMS 98-0040. U.S. Dept. of the Interior, Minerals Mgmt. Service, Gulf of Mexico OCS Region, New Orleans, LA, 513 p.
- Neill, C.F. and M.A. Allison, 2005, Subaqueous deltaic formation on the Atchafalaya shelf, Louisiana: *Marine Geology*, v. 214, p. 411-430.
- Nittrouer, J.A., M.A. Allison, R. Campanella, 2008, Bedform transport rates for the lowermost Mississippi River: *Journal of Geophysical Research*, v. 113: F03004, doi:10.1029/2007JF000795
- Nummedal, D. and D.J.P. Swift, 1987, Transgressive stratigraphy at sequence-bounding unconformities: Some principles derived from Holocene and Cretaceous examples. *In: Nummedal, D., O.H. Pilkey, and S.D. Howard (eds.), Sea-Level Fluctuation and Coastal Evolution: SEPM Special Publication*, v. 41, p. 241-260.
- Peltier, W.R. and R.G. Fairbanks, 2006, Global glacial ice volume and Last Glacial Maximum duration from an extended Barbados sea level record: *Quaternary Science Reviews*, v. 25, p. 3322-3337.
- Penland, S. and R. Boyd, 1981, Shoreline changes on the Louisiana barrier coast: *IEEE Oceans*, v. 81, p. 209-219.

- Penland, S. and R. Boyd, 1985, Mississippi Delta barrier shoreline development. *In*: Penland, S. and R. Boyd (eds.), Transgressive Depositional Environments of the Mississippi River Delta Plain, Louisiana Geological Survey Guidebook Series No. 3, p. 53-121.
- Penland, S., R. Boyd, and J.R. Suter, 1988, Transgressive depositional systems of the Mississippi Delta Plain: A model for barrier shoreline and shelf sand development: *Journal of Sedimentary Petrology*, v. 58, p. 932-949.
- Penland, S., D.L. Pope, R.A. McBride, J.R. Suter, and C.G. Groat, 1990, Assessment of sand resources in the Trinity Shoal area, Louisiana continental shelf: Louisiana Geological Survey, Cooperative Agreement Submitted to U.S. Minerals Management Service No. 14-12-0001-30387, 46 p.
- Penland, S. and J.R. Suter, 1983, Transgressive coastal facies preserved in barrier island arc retreat paths in the Mississippi Delta Plain: *Transactions – Gulf Coast Association of Geological Societies*, v. 33, p. 367-382.
- Penland, S. and J.R. Suter, 1989, The geomorphology of the Mississippi River Chenier Plain: *Marine Geology*, v. 90, p. 231-258.
- Penland, S., J.R. Suter, and R. Boyd, 1985, Barrier island arcs along abandoned Mississippi River Deltas: *Marine Geology*, v. 63, p. 197-233.
- Penland, S., J.R. Suter, and R.A. McBride, 1987, Delta plain development and sea level history in the Terrebonne coastal region, Louisiana: *American Society of Civil Engineers, Coastal Sediments*, p. 1689-1705.
- Penland, S., J.R. Suter, R.A. McBride, S.J. Williams, J.L. Kindinger, and R. Boyd, 1989, Holocene sand shoals offshore of the Mississippi River Delta Plain: *Transactions – Gulf Coast Association of Geological Societies*, v. 39, p. 471-480.
- Penland, S., J.R. Suter, and T.F. Moslow, 1986, Inner-shelf shoal sedimentary facies and sequences: Ship Shoal, northern Gulf of Mexico. *In*: Moslow, T.F. and E.G. Rhodes (eds.), *Modern and Ancient Shelf Clastics: A Core Workshop*, Society of Economic Paleontologists and Mineralogists Core Workshop No. 9, Tulsa, OK, p. 73-123.
- Pepper, D.A. and G.W. Stone, 2004, Hydrodynamic and sedimentary responses to two contrasting winter storms on the inner shelf of the northern Gulf of Mexico: *Marine Geology*, v. 210, p. 43-62.
- Pettijohn, F.J. and P.E. Potter, 1964, *Atlas and glossary of primary sedimentary structures*. Berlin: Springer-Verlag, 370 p.
- Pope, D. L., S. Penland, J. R. Suter, and R. McBride, 1991, Holocene Geologic Framework of the Trinity Shoal Region, Louisiana Continental Shelf: GCSSEPM Foundation 12<sup>th</sup> Annual Research Conference Proceedings, p. 191-201.

- Poppe, L.J., A.H. Eliason, J.J. Fredericks, R.R. Rendigs, D. Blackwood, and Polloni, C.F., 2000. Grain-size analysis of marine sediments: methodology and data processing. U.S. Geological Survey Open-File Report 00-358, online at: <http://pubs.usgs.gov/of/2000/of00-358/text/chapter1.htm>
- Quinn, R., J.M. Bull, J.K. Dix, and J.R. Adams, 1997, The Mary Rose site – geophysical evidence for palaeo-scour marks: *The International Journal of Nautical Archaeology*, v. 26, p. 3-16.
- Reading, H.G. and Levell, B.K., 1996, Controls on the sedimentary rock record. *In*: Reading, H.G., (ed.), *Sedimentary Environments: Processes, Facies and Stratigraphy*: Blackwell, Oxford, p. 5-36.
- Reimer, P.J., M.G.L. Baillie, E. Bard, A. Bayliss, J.W. Beck, C.J.H. Bertrand, P.G. Blackwell, C.E. Buck, G.S. Burr, K.B. Cutler, P.E. Damon, R.L. Edwards, R.G. Fairbanks, M. Friedrich, T.P. Guilderson, A.G. Hogg, K.A. Hughen, B. Kromer, G. McCormac, S. Manning, C.B. Ramsey, R.W. Reimer, S. Remmele, J.R. Southon, M. Stuiver, S. Talamo, F.W. Taylor, J. van der Plicht, C.E. Weyhenmeyer, 2004, IntCal04 Terrestrial radiocarbon age calibration, 0–26 ka BP: *Radiocarbon* v. 46, p. 1029–1058.
- Reinson, G.E., 1984, Barrier-island and associated strand-plain systems. *In*: Walker, R.G., (ed.), *Facies Models: Geological Association of Canada, Geoscience Canada Reprint Series 1*, p. 119-140.
- Reinson, G.E., 1992, Transgressive barrier island and estuarine systems. *In*: Walker, R.G. and N.P. James, (eds.), *Facies Models: Response to Sea Level Change: Geological Association of Canada*, p. 179-194.
- Roberts, H.H., 1997, Dynamic changes of the Holocene Mississippi River Delta plain: the delta cycle: *Journal of Coastal Research*, v. 13, p. 605-627.
- Roberts, H.H., 1998, Delta switching: Early responses to the Atchafalaya River diversion: *Journal of Coastal Research*, v. 14, p. 882-899.
- Roberts, H.H., 2012, Sand resources of western Ship Shoal (Ship Shoal Blocks 84, 85, 98, and 99). A report submitted to the Coastal Protection and Restoration Authority of Louisiana, 51 p.
- Roberts, H.H., R.D. Adams, and R.H.W. Cunningham, 1980, Evolution of the sand-dominate subaerial phase, Atchafalaya Delta, Louisiana, *The American Association of Petroleum Geologists Bulletin*, v. 64, p. 264-279.
- Roberts, H.H., A. Bailey, and G.J. Kuecher, 1994, Subsidence in the Mississippi River Delta –

- important influences of valley filling by cyclic deposition, primary consolidation phenomena, and early diagenesis: Transactions – Gulf Coast Association of Geological Societies, v. 44, p. 619-629.
- Roberts, H.H., S.J. Bentley, J.M. Coleman, S.A. Hsu, O.K. Huh, K.A., M. Inoue, L.J. Rouse, Jr., A. Sheremet, G.W. Stone, N.D. Walker, S. Welsh, and W.J. Wiseman, Jr., 2002, Geological framework and sedimentology of recent mud deposition on the eastern chenier plain coast and adjacent inner shelf, western Louisiana: Transactions – Gulf Coast Association of Geological Societies, v. 52, p. 849-859.
- Roberts, H.H., O.K. Huh, S.A. Hsu, L.J. Rouse Jr., and D. Rickman, 1987, Impact of cold-front passages on geomorphic evolution and sediment dynamics of the complex Louisiana coast: American Society of Civil Engineers, Proceedings Coastal Sediment '87, p. 1950-1963.
- Roberts, H.H., O.K. Huh, S.A. Hsu, L.J. Rouse Jr., and D. Rickman, 1989, Winter storm impacts on the Chenier Plain coast of southwestern Louisiana: Transactions – Gulf Coast Association of Geological Societies, v. 39, p. 515-522.
- Roberts, H.H., R.A. Morton, and A. Freeman, 2008, A high-resolution seismic assessment of faulting in the Louisiana Coastal Plain: Transactions – Gulf Coast Association of Geological Societies, v. 58, p. 733-745.
- Rotondo, K.A., 2004, Transport and deposition of fluid mud event layers along the western Louisiana inner shelf: M.S. thesis, Louisiana State University, Baton Rouge, 83 p.
- Rotondo, K.A. and S.J. Bentley, 2003, Deposition and resuspension of fluid mud on the western Louisiana inner shelf: Transactions – Gulf Coast Association of Geological Societies, v. 53, p. 722-731.
- Sangree, J.B. and J.M. Widmier, 1977, Seismic stratigraphy and global changes of sea level, Part 9: Seismic interpretation of clastic depositional facies. *In*: Payton, C.E., (ed.), Seismic Stratigraphy – Applications to Hydrocarbon Exploration, Memoir 26, American Association of Petroleum Geologists, p. 165-184.
- Saucier, 1994, Geomorphology and Quaternary geologic history of the lower Mississippi valley: United States Army Engineer Waterways Experiment Station, Vicksburg, Mississippi, v. 1, 364 p.
- Schultheiss, P.J. and S.D. McPhail, 1989, An automated P-wave logger for recording fine-scale compressional wave velocity structures in sediments. *In*: Ruddiman, W., M. Sarnthein, et al. (eds.), Proceedings of the Ocean Drilling Program, Scientific Results, v. 108, p. 407-413.
- Schultheiss, P.J. and P.P.E. Weaver, 1992, Multi-sensor core logging for science and industry: Proceedings Oceans 92, Mastering the Oceans Through Technology, p. 608-613.

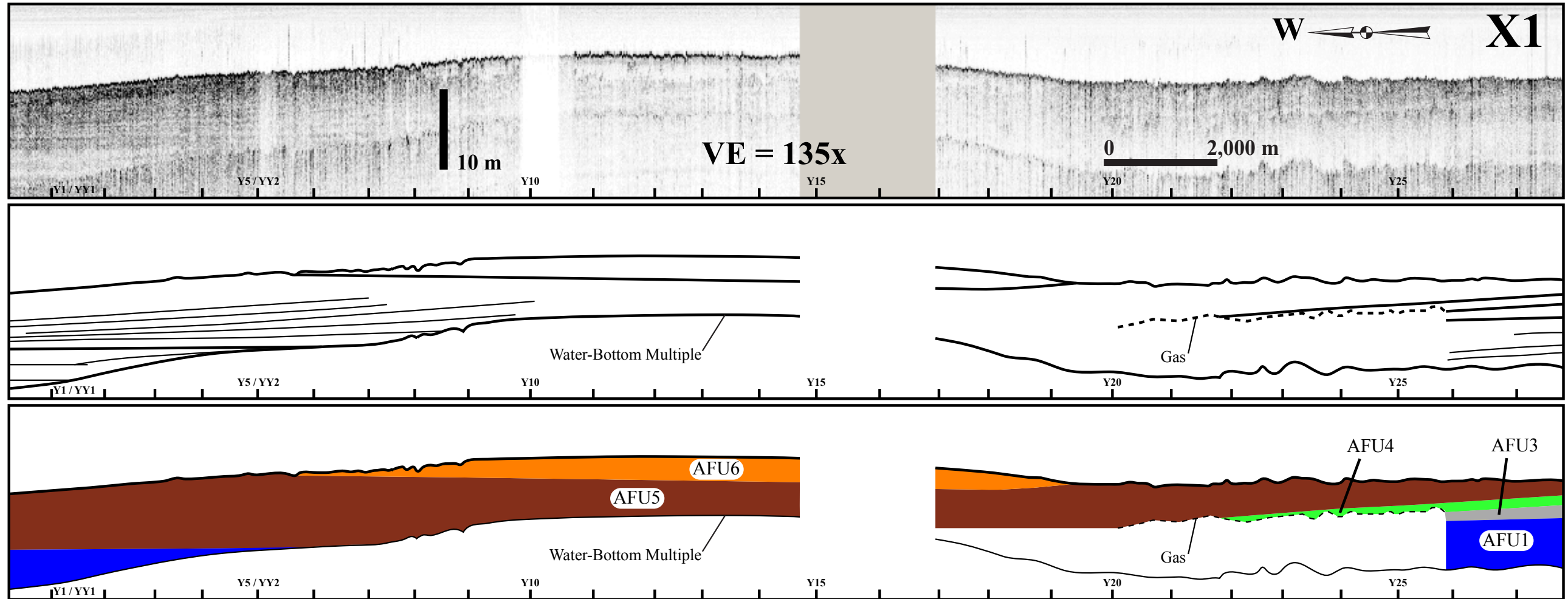
- Scruton, P.C., 1960, Delta building and the deltaic sequence. *In*: Shepard, F.P. et al., (eds.), Recent Sediments, northwest Gulf of Mexico. Tulsa: American Association of Petroleum Geologists, p. 82-102.
- Simms, A.R., J.B. Anderson, K.T. Milliken, and A.B. Rodriguez, 2008, Mechanisms controlling environmental change within an estuary: Corpus Christi Bay, Texas, USA. *In*: Anderson, J.B. and A.B. Rodriguez (eds.), Response of Upper Gulf Coast Estuaries to Holocene Climate Change and Sea-Level Rise: Geological Society of America Special Paper 443, p. 121-146.
- Stevenson, I.R., P. Nicholson, L.M. Linnett, and S. Morrison, 2001, A method for the analysis of chirp signals insonifying layered media for sub-bottom profiling, IEEE Oceans, p. 2608-2615.
- Stone, G.W., J.M. Grymes III, J.R. Dingler, and D.A. Pepper, 1997, Overview and significance of hurricanes on the Louisiana Coast, U.S.A.: Journal of Coastal Research, v. 13, p. 656-669.
- Stone, G.W., A. Sheremet, X. Zhang, Q. He, B. Liu, and B. Strong, 2003, Land fall of two tropical systems seven days apart along southcentral Louisiana, USA, Proceedings Coastal Sediment '03, 14 p.
- Stuiver, M. and T.F. Braziunas, 1993, Modeling atmospheric  $^{14}\text{C}$  influences and  $^{14}\text{C}$  ages of marine samples to 10,000 BC: Radiocarbon, v. 35, p. 137-189.
- Stuiver, M. and H.A. Polach, 1977, Discussion: Reporting  $^{14}\text{C}$  data: Radiocarbon, v. 19, p. 355-363.
- Suter, J.R., H.L. Berryhill, and S. Penland, 1987, Late Quaternary sea-level fluctuations and depositional sequences, southwest Louisiana continental shelf. *In*: Nummedal, D., et al., (eds.), Sea-Level Fluctuation and Coastal Evolution. Tulsa: Society of Economic Paleontologists and Mineralogists, 41, p. 199-219.
- Suter, J.R., S. Penland, S.J. Williams, and J.L. Kindinger, 1988, Transgressive evolution of the Chandeleur Islands, Louisiana: Transactions – Gulf Coast Association of Geological Societies, v. 38, p. 315-322.
- Swift, D.J.P., 1975, Barrier-island genesis: Evidence from the central Atlantic shelf, eastern U.S.A.: Sedimentary Geology, v. 14, p. 1-43.
- Swift, D.J.P., G. Han, and C.E. Vincent, 1986, Fluid processes and sea-floor response on a modern storm-dominated shelf: Middle Atlantic shelf of North America. Part I: The storm-current regime. *In*: Knight, R.J. and J.R. McLean (eds.), Shelf Sands and Sandstones. Canadian Society of Petroleum Geologists, Memoir II, p. 99-119.

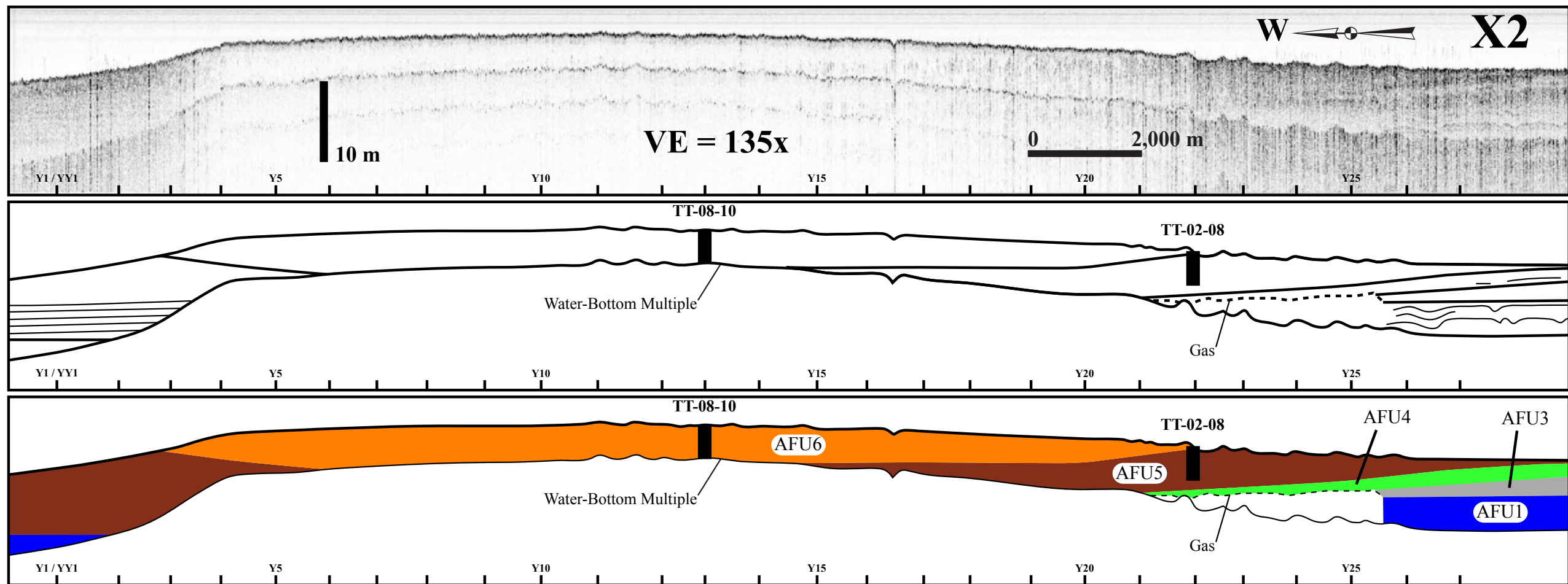
- Talma, A.S. and J.C. Vogel, 1993, A simplified approach to calibrating  $^{14}\text{C}$  dates: Radiocarbon, v. 35, p. 317-322.
- Törnqvist, T.E., S.J. Bick, K. van der Borg, and A.F.M. de Jong, 2006, How stable is the Mississippi Delta?: Geology, v. 34, p. 697-700.
- Törnqvist, T.E. and J.S. Bridge, 2002, Spatial variation of overbank aggradation rate and its influence on avulsion frequency: Sedimentology, v. 49, p. 891-905.
- Törnqvist, T.E., T.R. Kidder, W.J. Autin, K. van der Borg, A.F.M. de Jong, C.J.W. Klerks, E.M.A. Snijders, J.E.A. Storms, R.L. van Dam, M.C. Wiemann, 1996, A revised chronology for Mississippi River subdeltas: Science, v. 273, 1693-1696.
- Törnqvist, T.E., D.J. Wallace, J.E.A. Storms, J. Wallinga, R.L. Van Dam, M. Blaauw, M.S. Derksen, C.J.W. Klerks, C. Meijneken, and E.M.A. Snijders, 2008, Mississippi Delta subsidence primarily caused by compaction of Holocene strata: Nature Geoscience, v. 1, p. 173-176.
- Toscano, M.A. and I.G. Macintyre, 2003, Corrected western Atlantic sea-level curve for the last 11,000 years based on calibrated  $^{14}\text{C}$  dates from *Acropora palmata* framework and intertidal mangrove peat: Coral Reefs, v. 22, p. 257-270.
- Turgut, A., M. McCord, J. Newcomb, and R. Fisher, 2002, Chirp sonar sediment characterization at the northern Gulf of Mexico littoral acoustic demonstration center experimental site: Proceedings Oceans 02, p. 2248-2252.
- Van Heerden, I.L. and H.H. Roberts, 1988, Facies development of Atchafalaya Delta, Louisiana: A modern bayhead delta: The American Association of Petroleum Geologists Bulletin, v. 72, p. 439-453.
- Van Heerden, I.L., S. Penland, and R. Boyd, 1985, A transgressive stratigraphic sequence from the central Chandeleur Islands, Louisiana. In: Penland, S. and R. Boyd (eds.), Transgressive Depositional Environments of the Mississippi River Delta Plain, Louisiana Geological Survey Guidebook Series No. 3, p. 189-201.
- Van Lopik, J.R., 1955, Recent geology and geomorphic history of central coastal Louisiana: Louisiana State University, Coastal Studies Institute Technical Report No. 7, 89 p.
- Van Wagoner, J.C., R.M. Mitchum, K.M. Campion, and V.D. Rahmanian, 1990, Siliciclastic sequence stratigraphy in well logs, cores and outcrops: Concepts for high-resolution correlation of time and facies: American Association of Petroleum Geologists Methods in Exploration Series, No. 7, 55 p.
- Walker, N.D. and A.B. Hammack, 2000, Impacts of winter storms on circulation and sediment transport: Atchafalaya-Vermillion Bay region, Louisiana, U.S.A.: Journal of Coastal Research, v. 16, p. 996-1010.

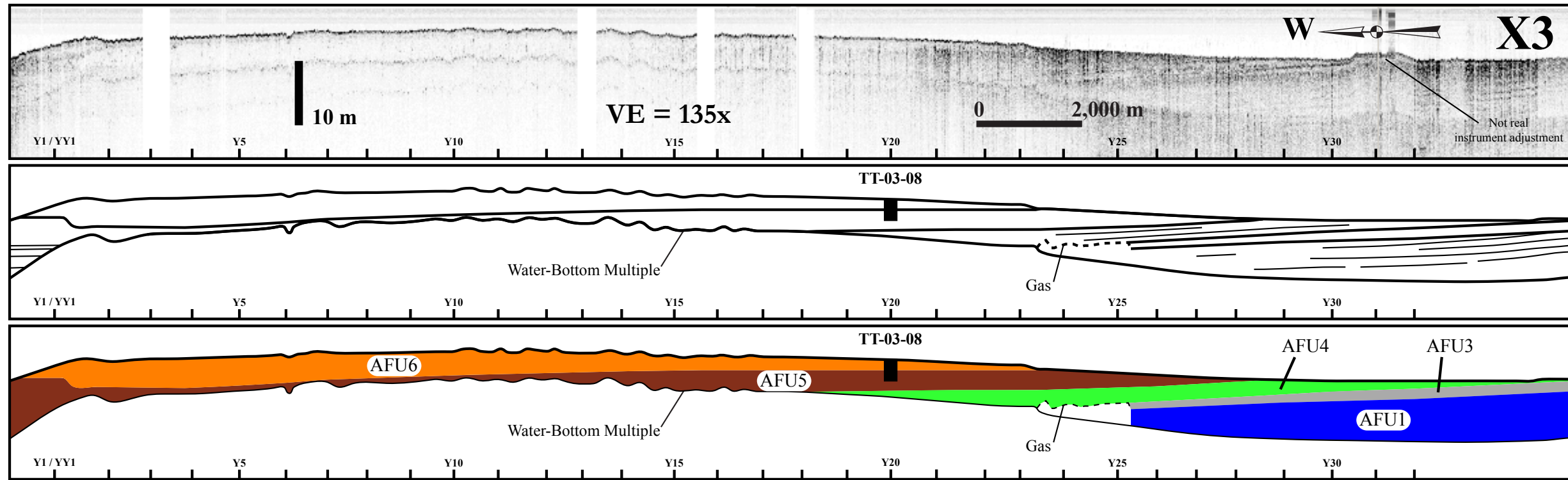
- Walker, R.G., 1992, Facies, facies models and modern stratigraphic concepts. *In*: Walker, R.G. and James, N.P., (eds.), *Facies Models: Response to Sea-Level Change: Geological Association of Canada*, p. 1-14.
- Walker, R.G., 2006, Facies Models Revisited. *In*: Walker, R.G., and H. Posamentier, (eds.), *Facies Models Revisited*, SEPM Special Publication No 84, p. 1-17.
- Walker, R.G. and A.G. Plint, 1992, Wave- and storm-dominated shallow marine systems. *In*: Walker, R.G. and James, N.P., (eds.), *Facies Models: Response to Sea-Level Change: Geological Association of Canada*, p. 219-238.
- Welder, F.A., 1959, Processes of deltaic sedimentation in the lower Mississippi River: Louisiana State University, Coastal Studies Institute Technical Report No. 12, 90 p.
- Wells, J.T. and G.P. Kemp, 1981, Atchafalaya mud stream and recent mudflat progradation: Louisiana Chenier Plain: *Gulf Coast Association of Geological Societies*, v. 31, p. 409-416.
- Winker, C.D., 1982, Cenozoic shelf margins, northwestern Gulf of Mexico: *Transactions – Gulf Coast Associations of Petroleum Geologists*, v. 32, p. 427-448.
- Wright, L.D., J.D. Boon, III, M.O. Green, and J.H. List, 1986, Response of the mid shoreface of the southern Mid-Atlantic Bight to a “northeaster”: *Geo-Marine Letters*, v. 6, p. 153-160.
- Wright, L.D., C.R. Sherwood, and R.W. Sternberg, 1997, Field measurements of fairweather bottom boundary layer processes and sediment suspension on the Louisiana inner continental shelf: *Marine Geology*, v. 140, p. 329-345.
- Wright, E.E., A.C. Hine, S.L. Goodbred, and S.D. Locker, 2005, The effect of sea-level and climate change on the development of a mixed siliciclastic-carbonate, deltaic coastline: Suwannee River, Florida, U.S.A.: *Journal of Sedimentary Research*, v. 75, p. 621-635.

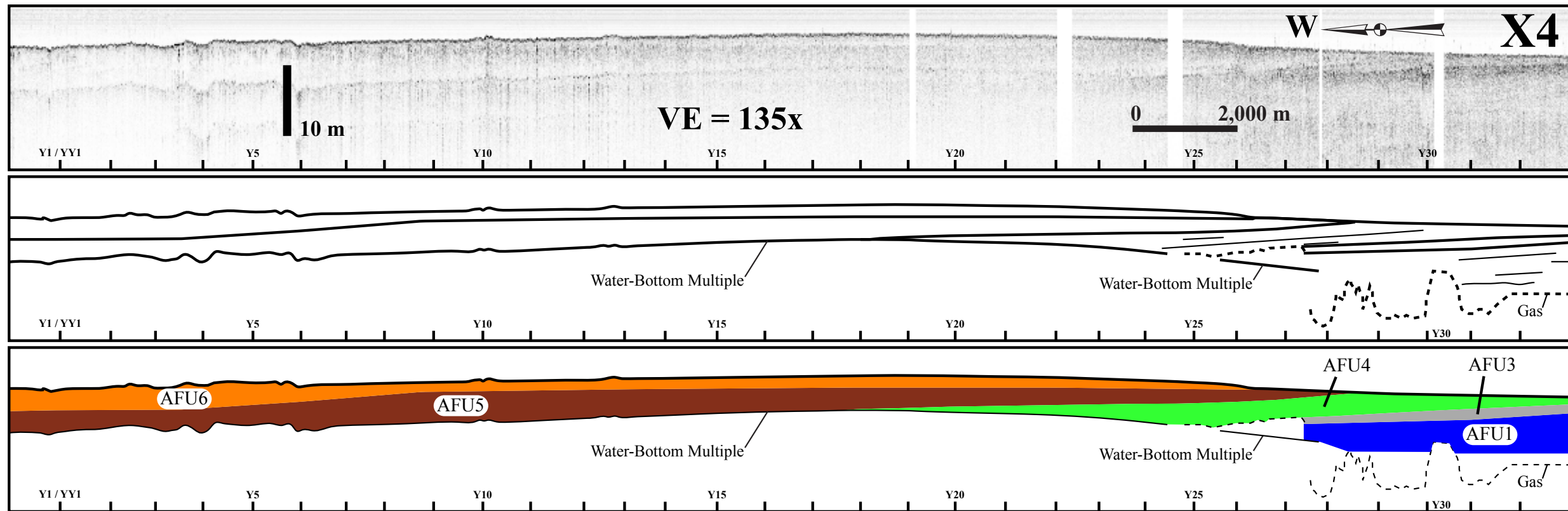


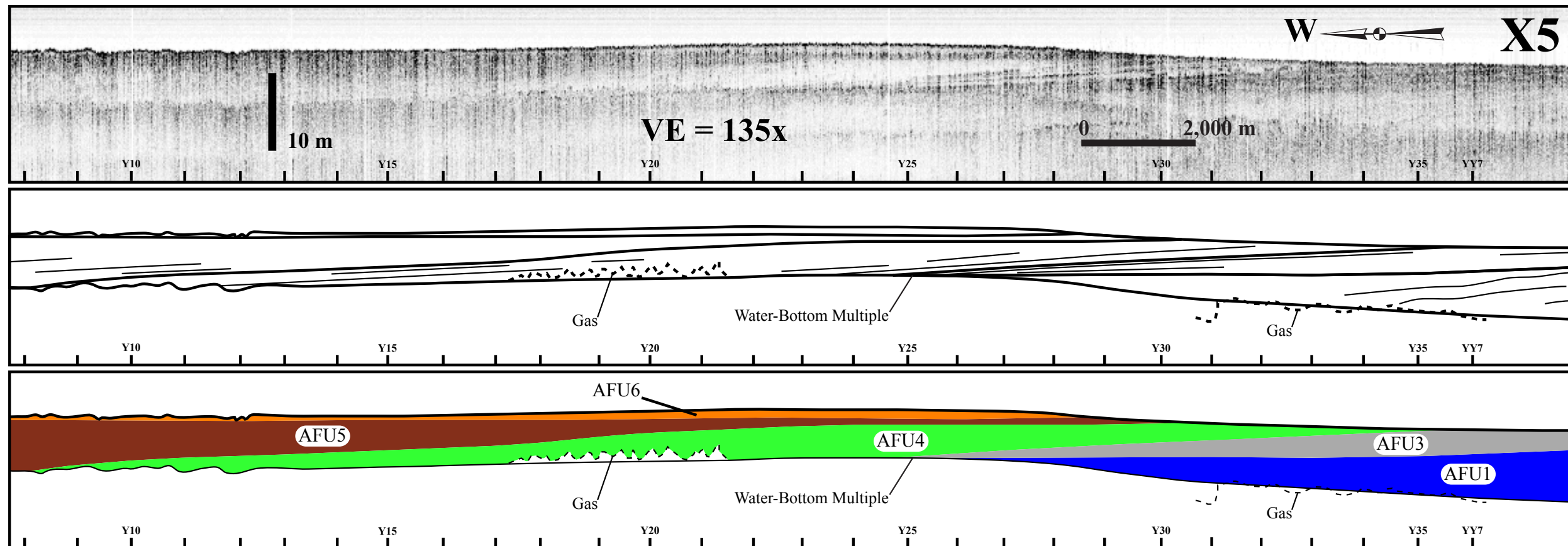
# APPENDIX 1: CROSS SECTIONS



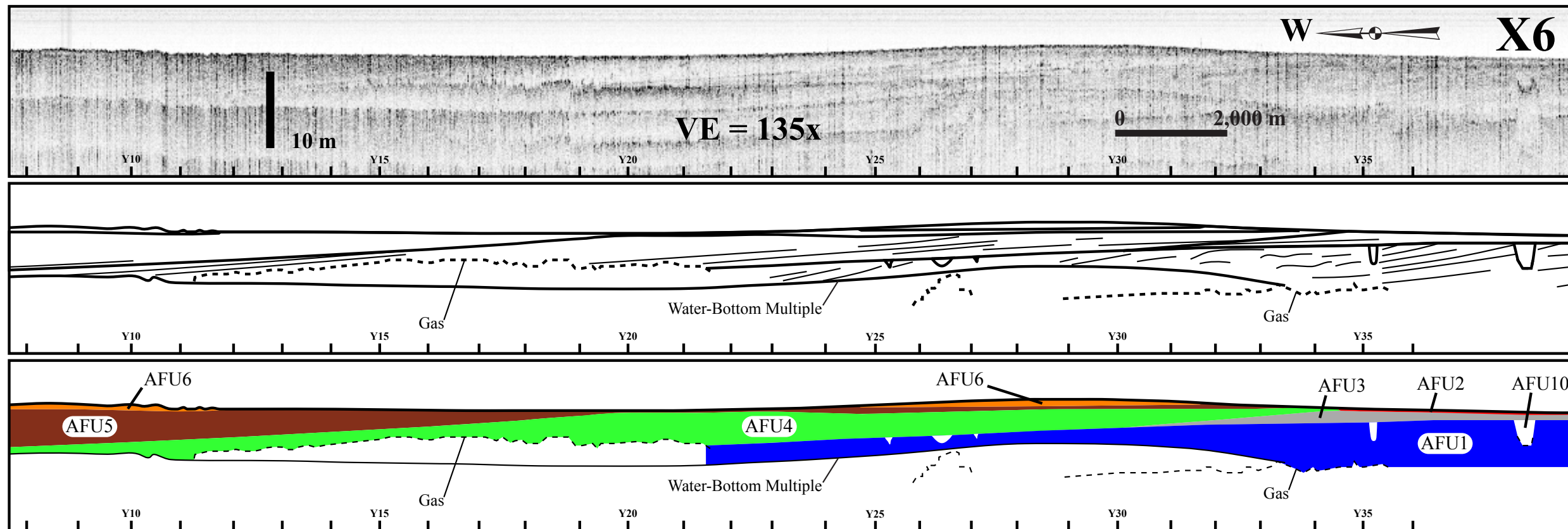


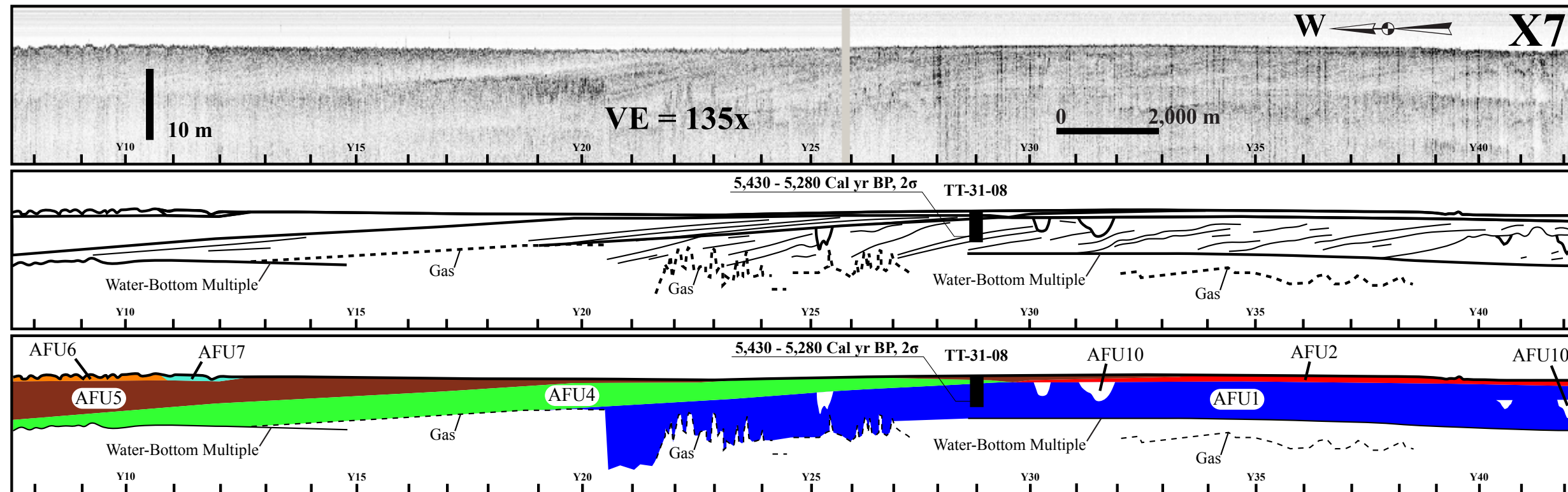


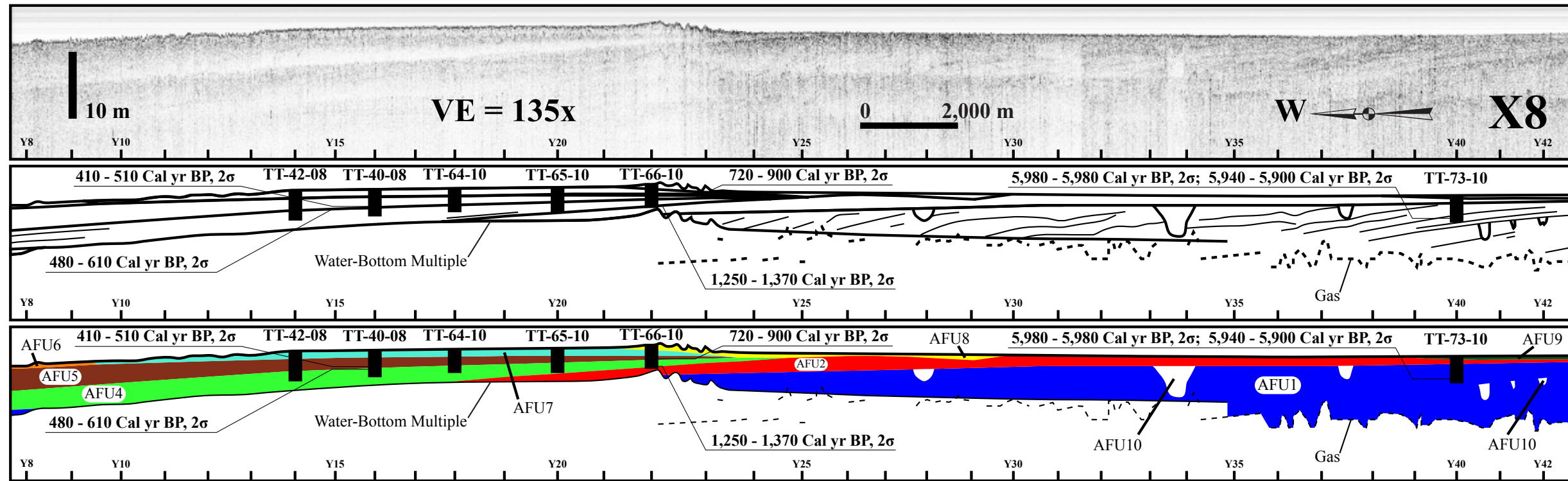




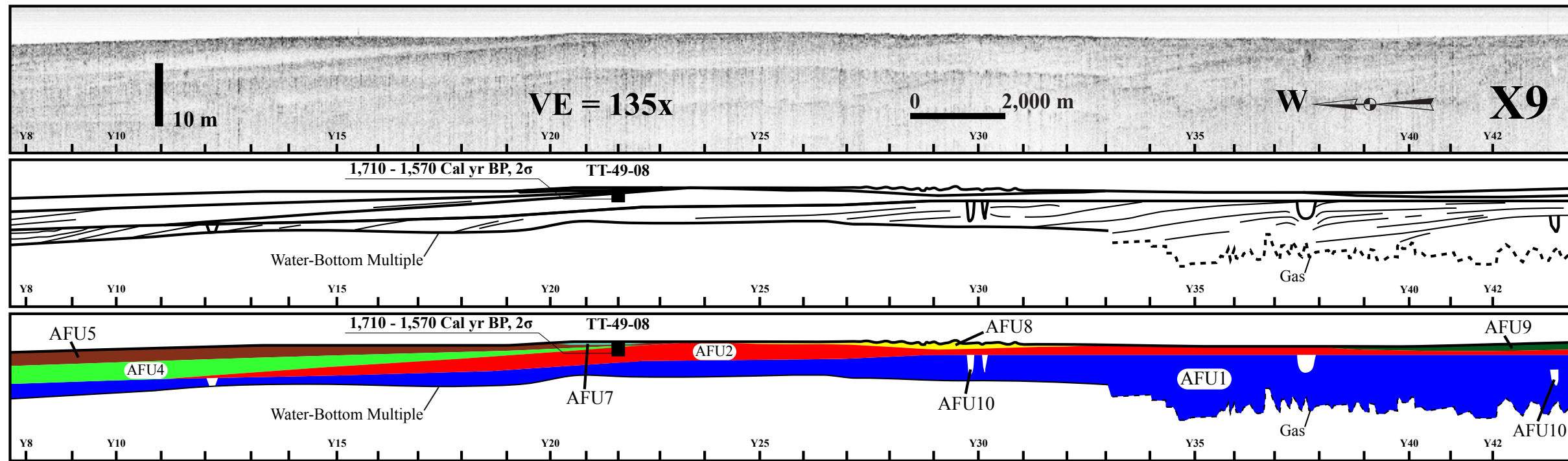


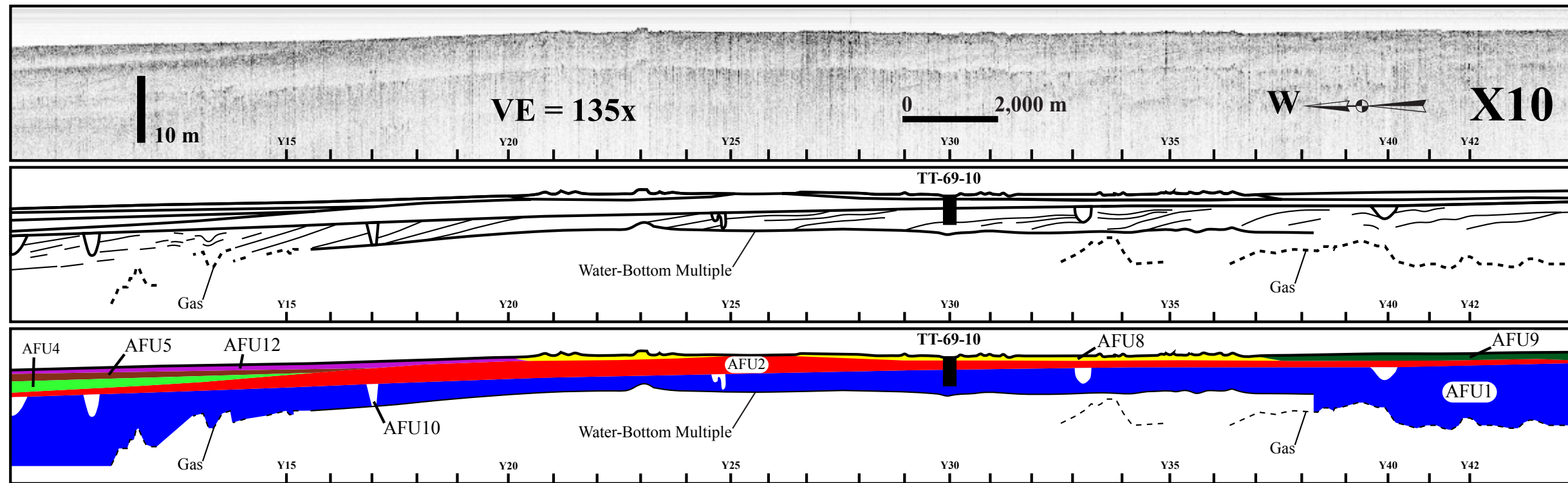


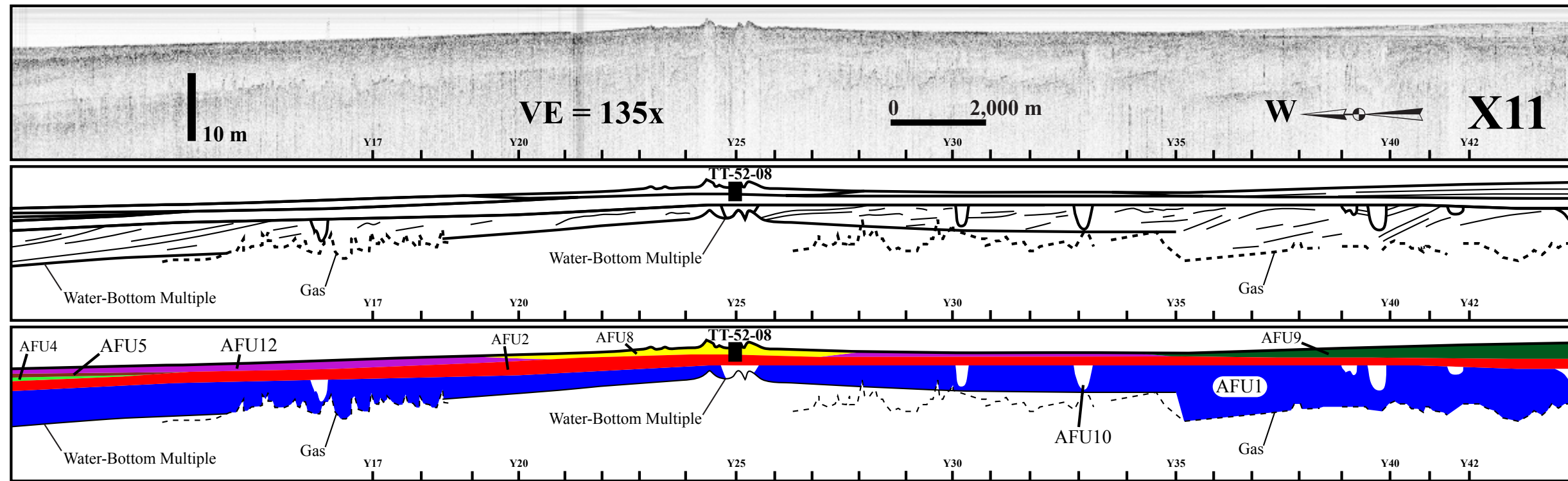


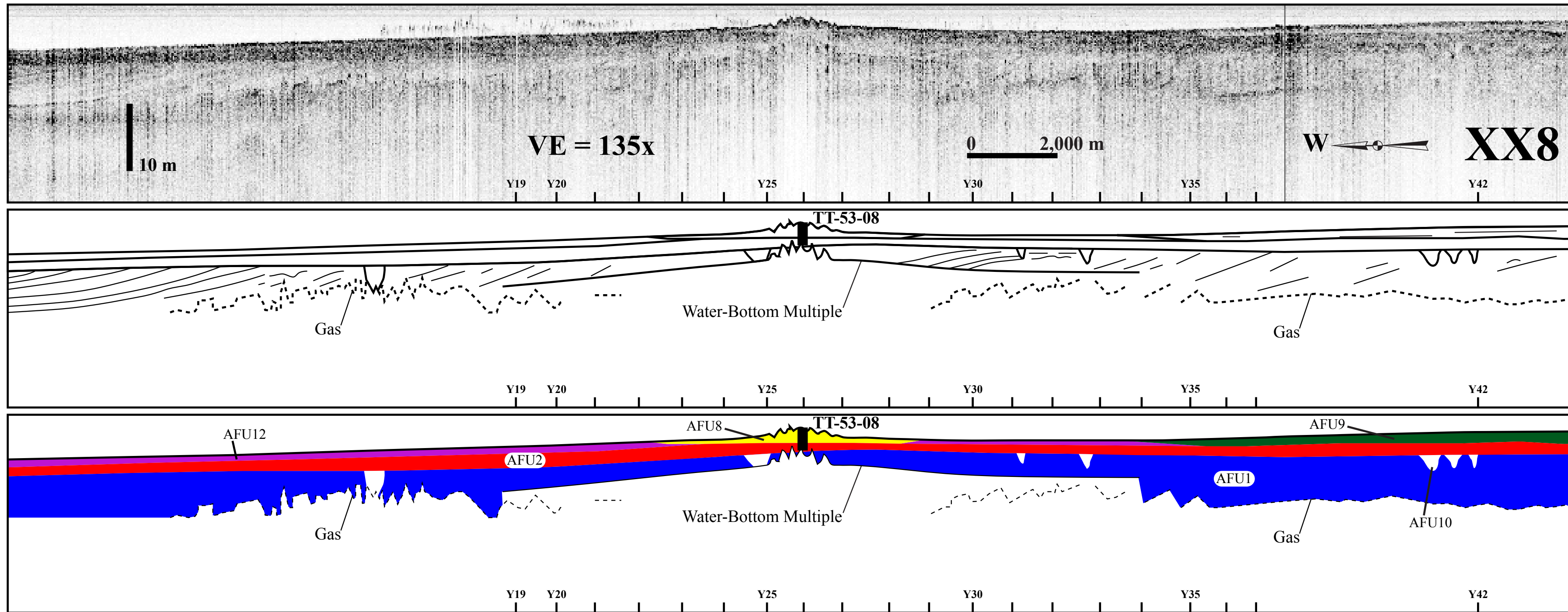


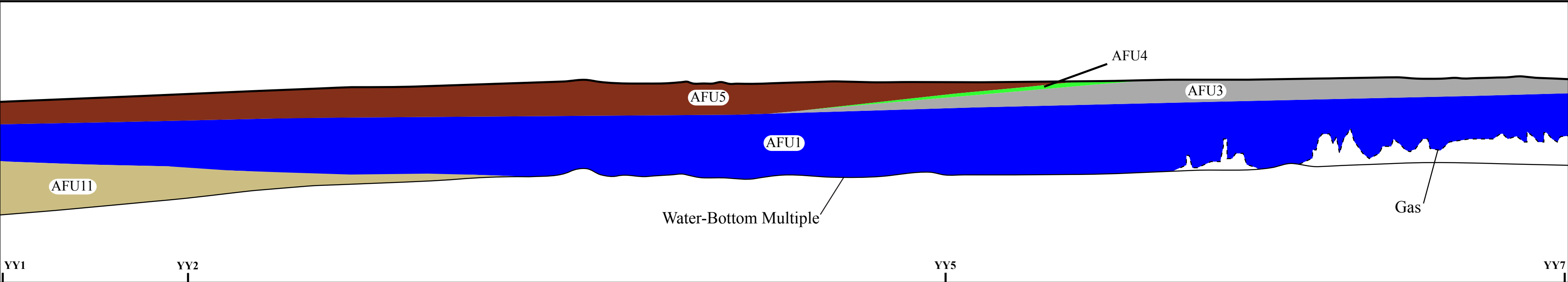
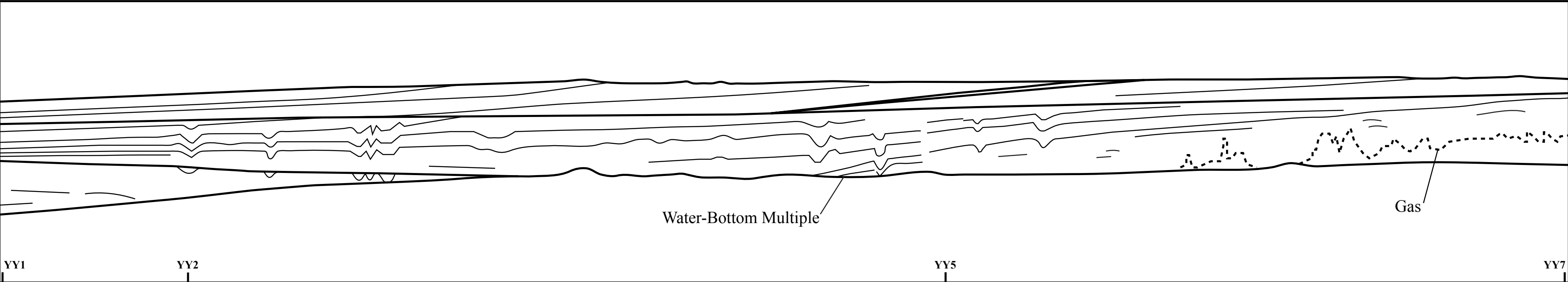
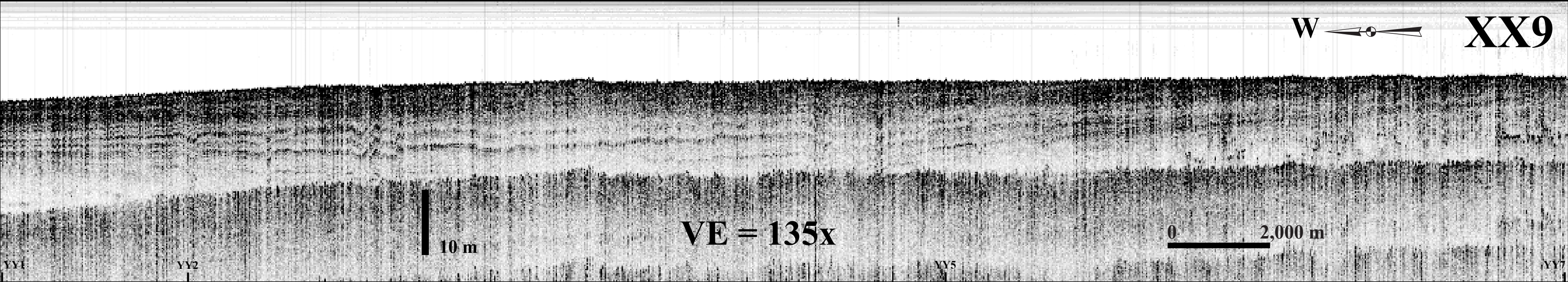




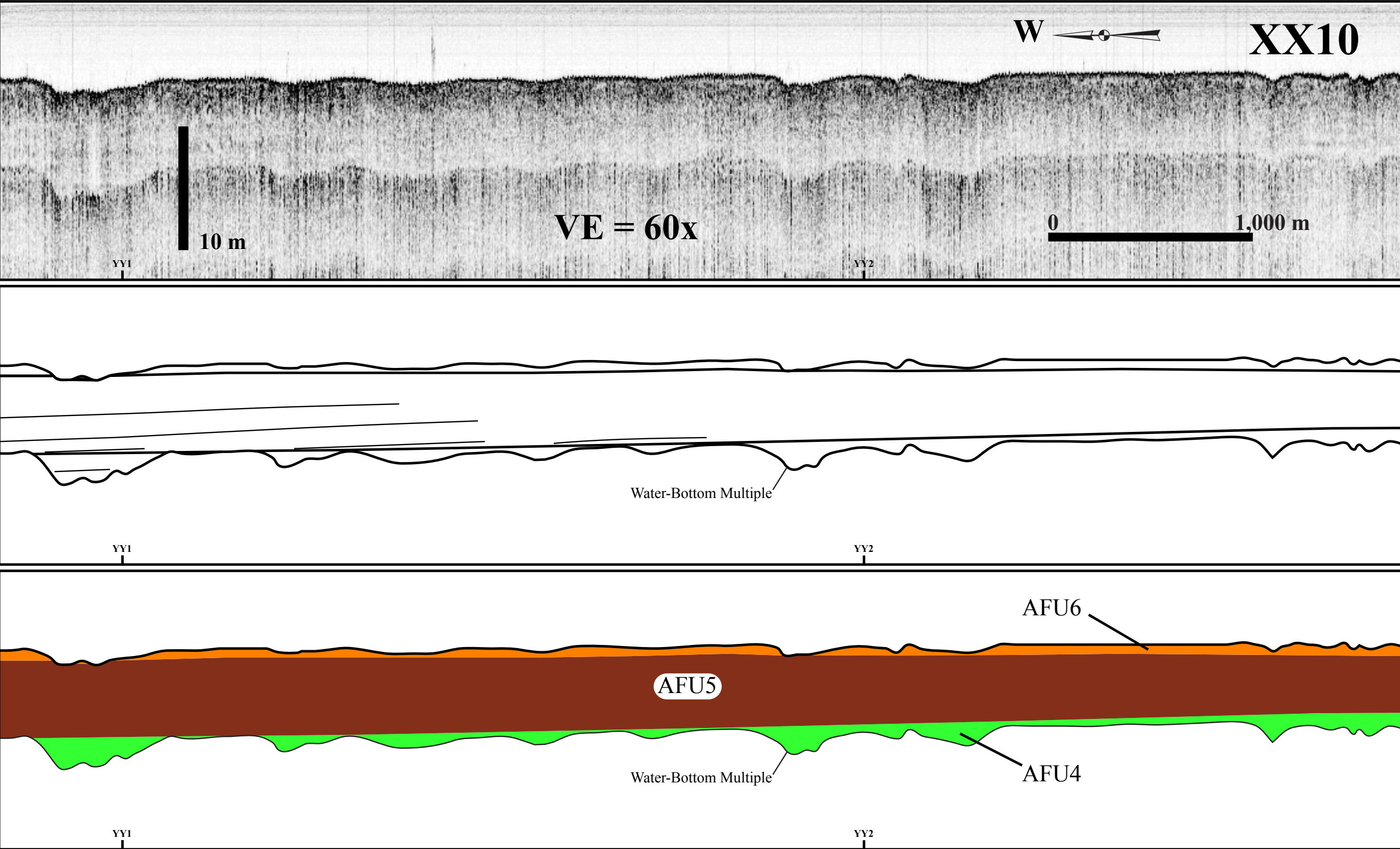


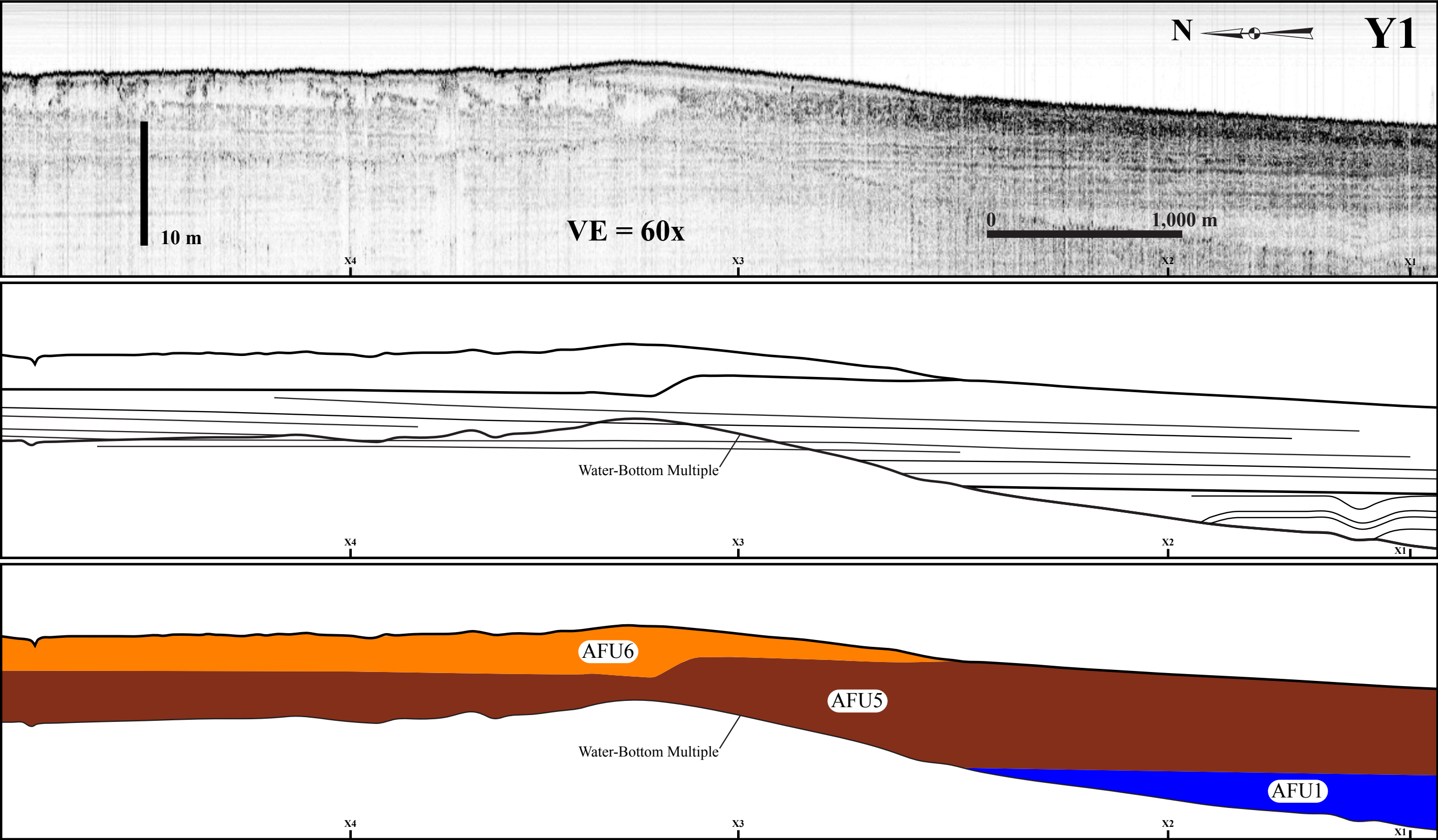




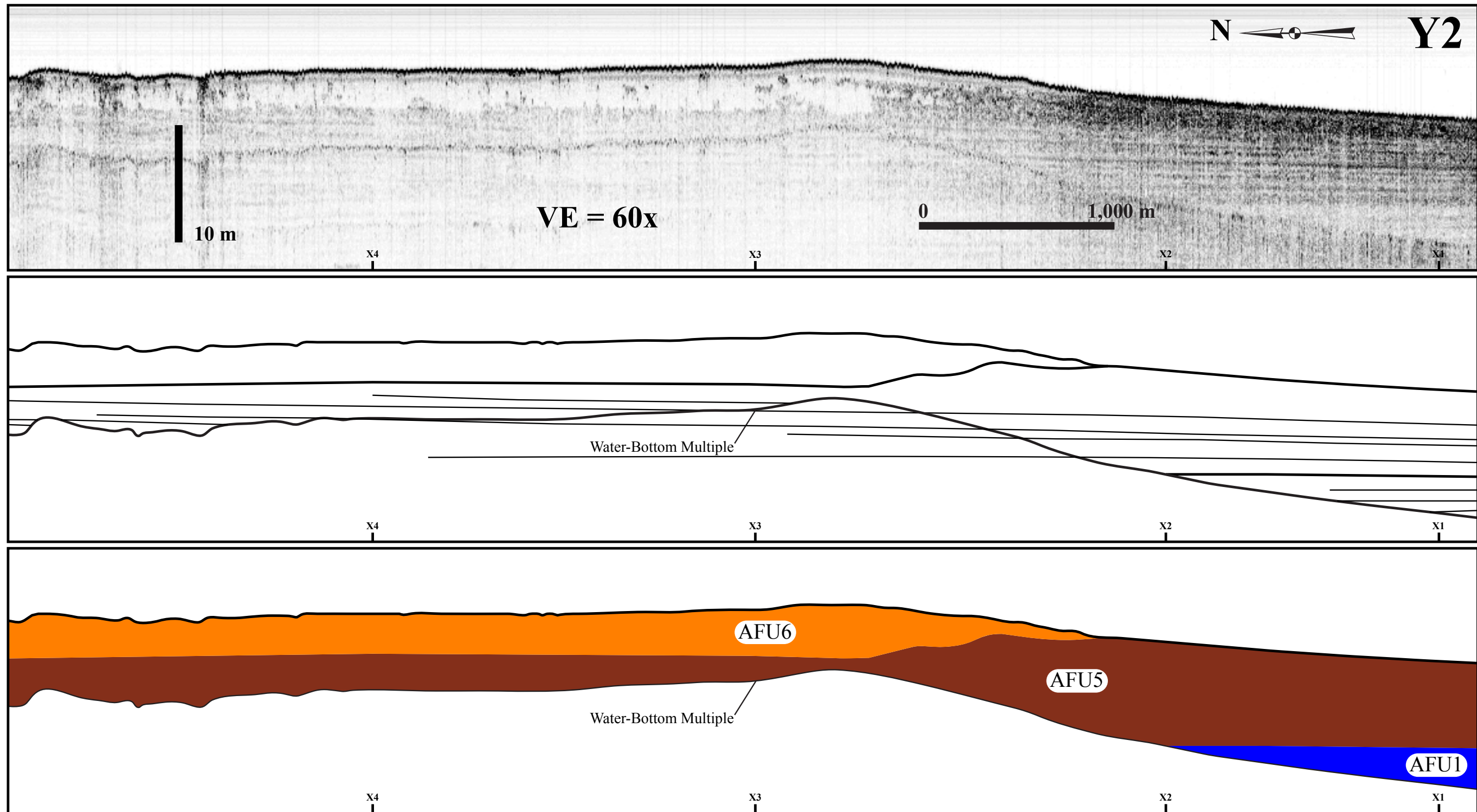




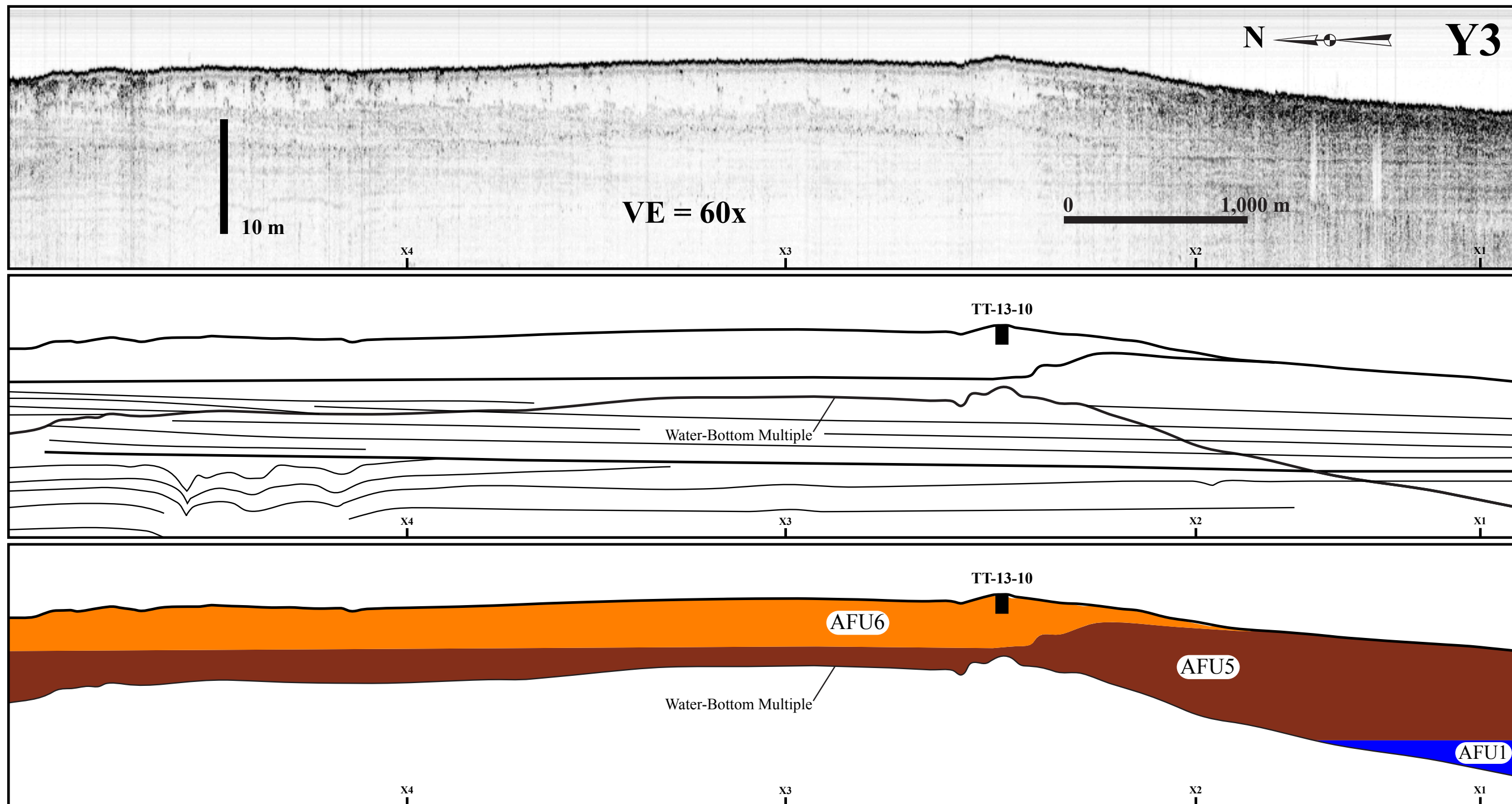


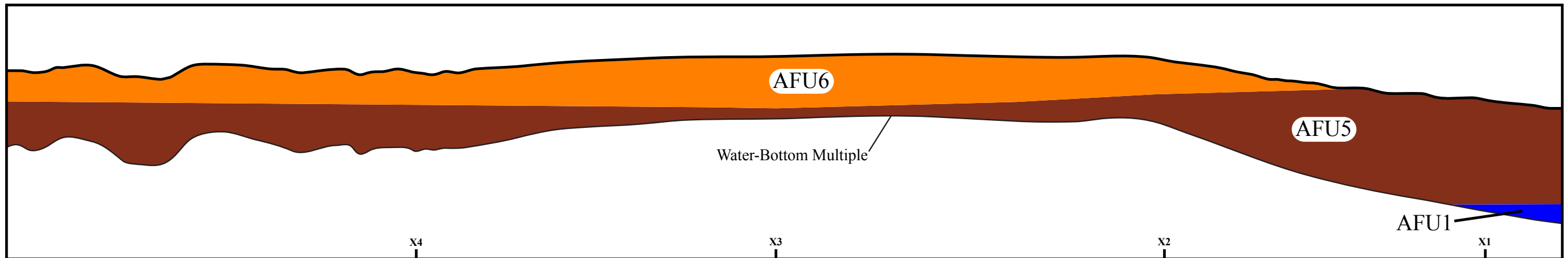
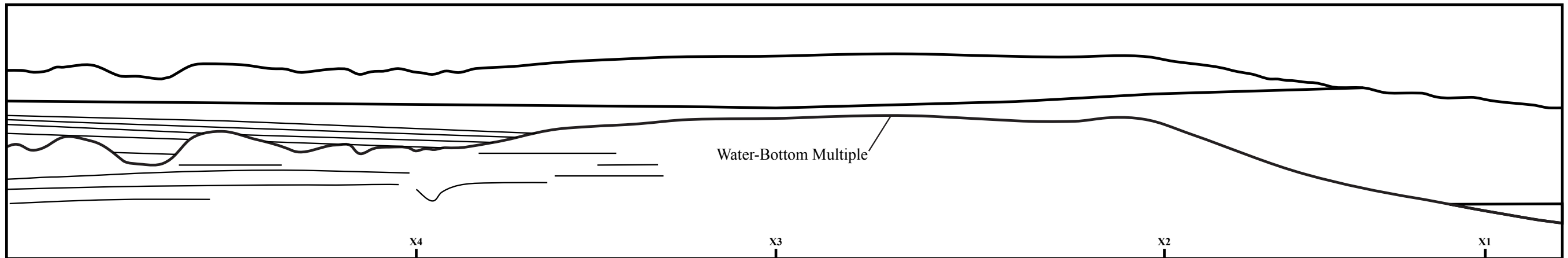
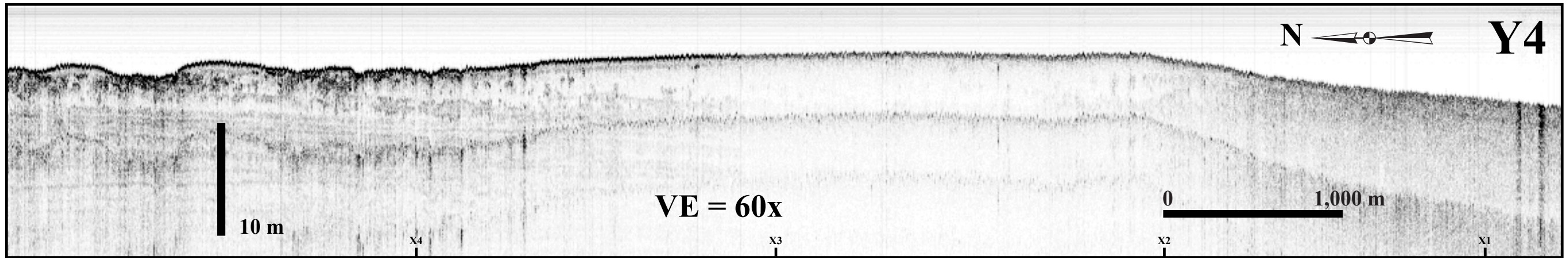


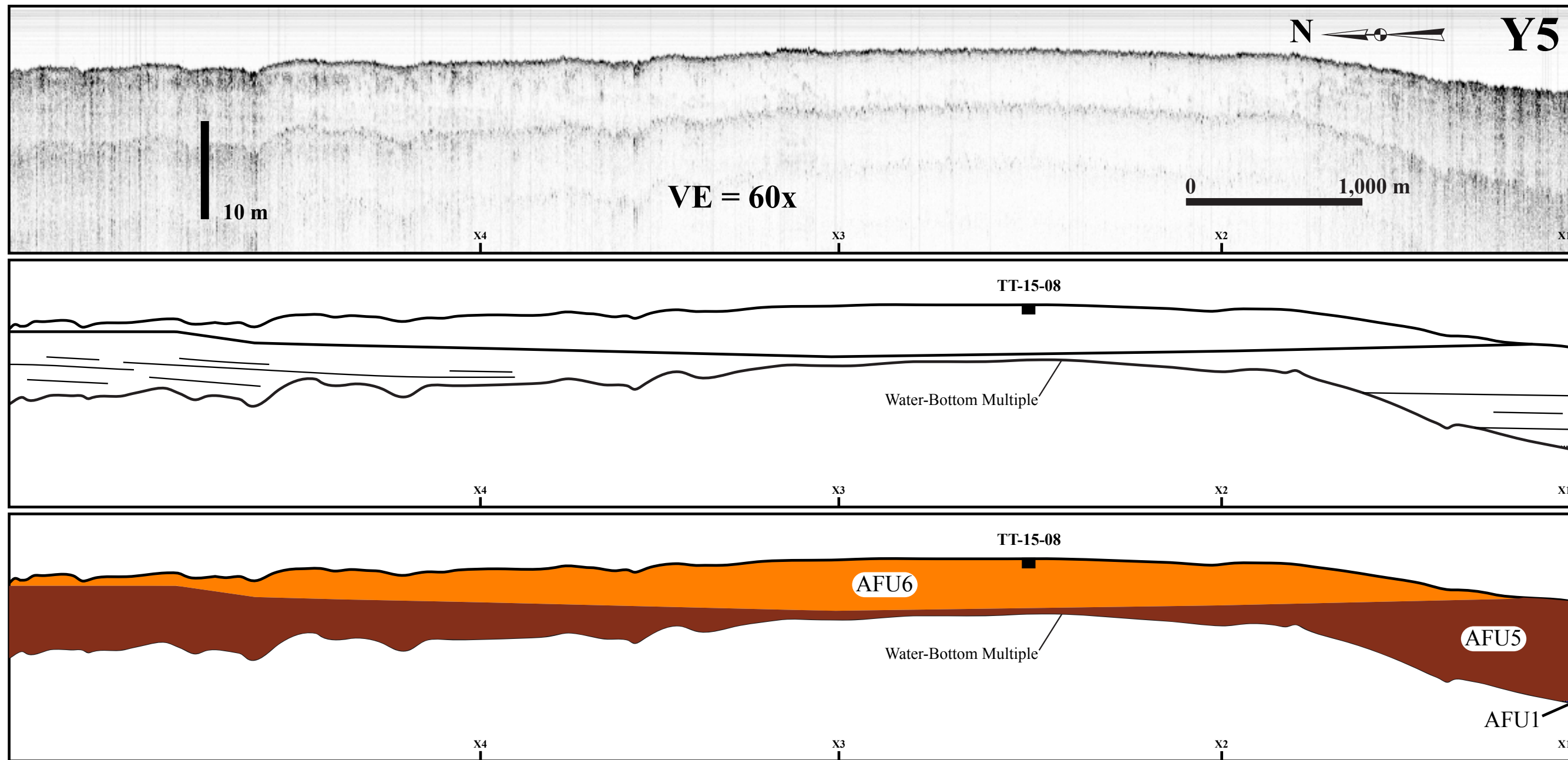


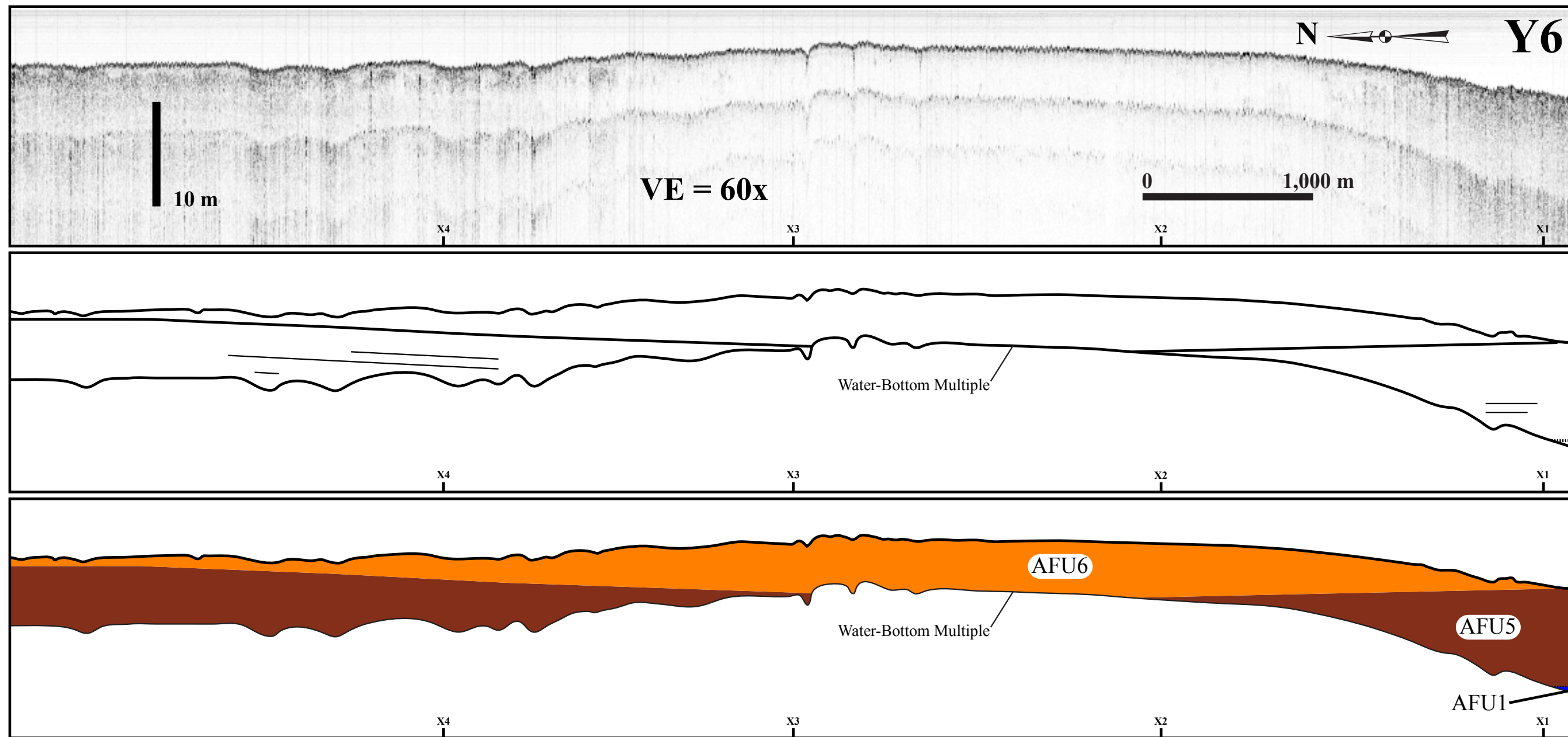




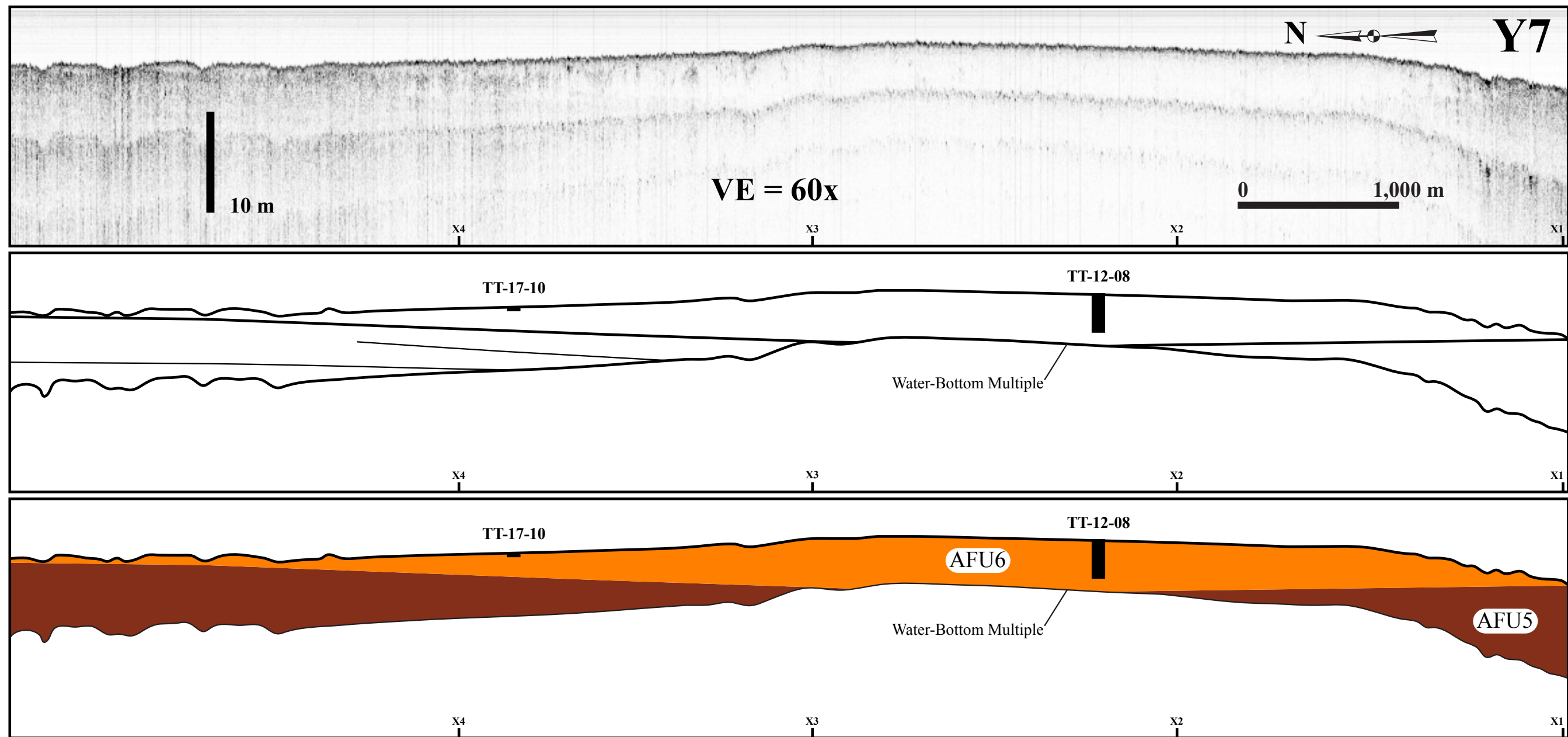


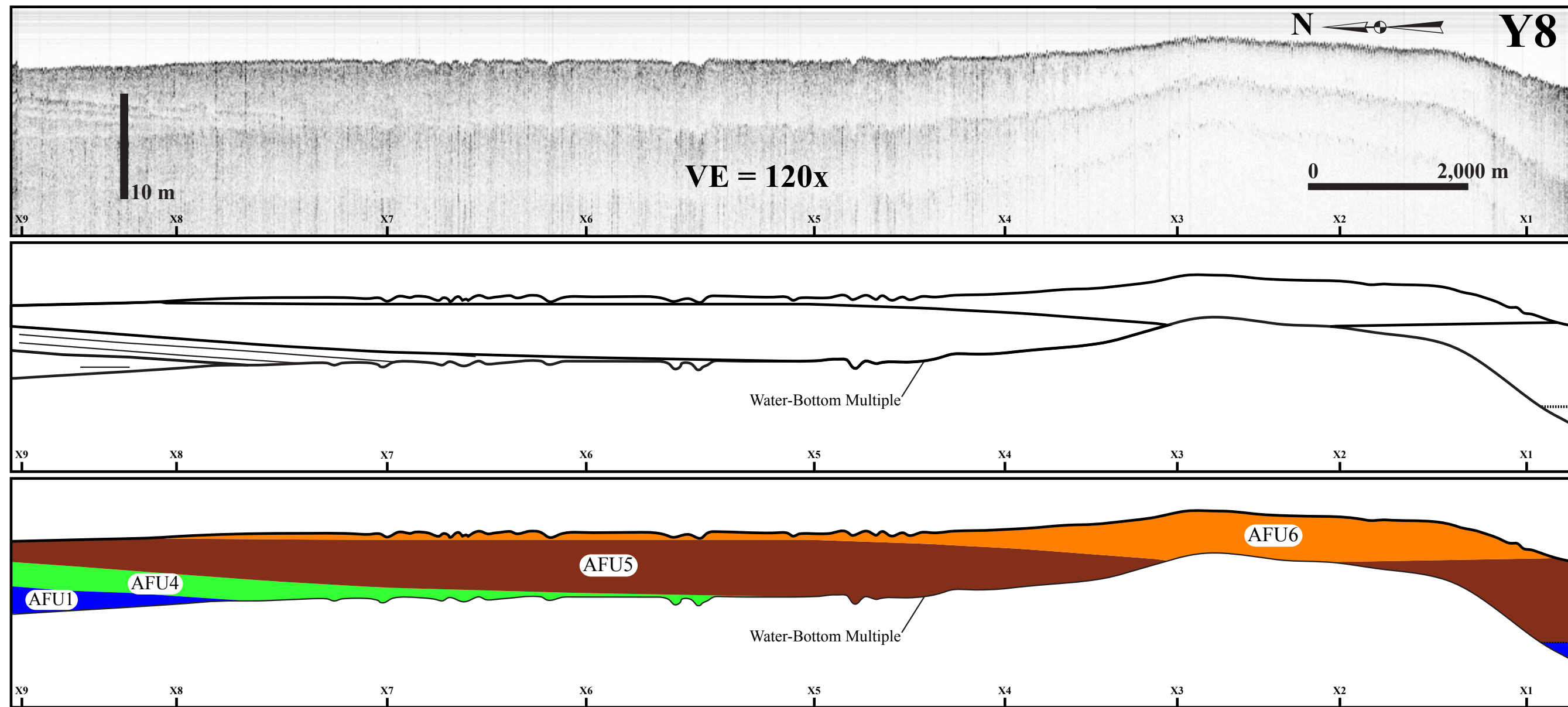


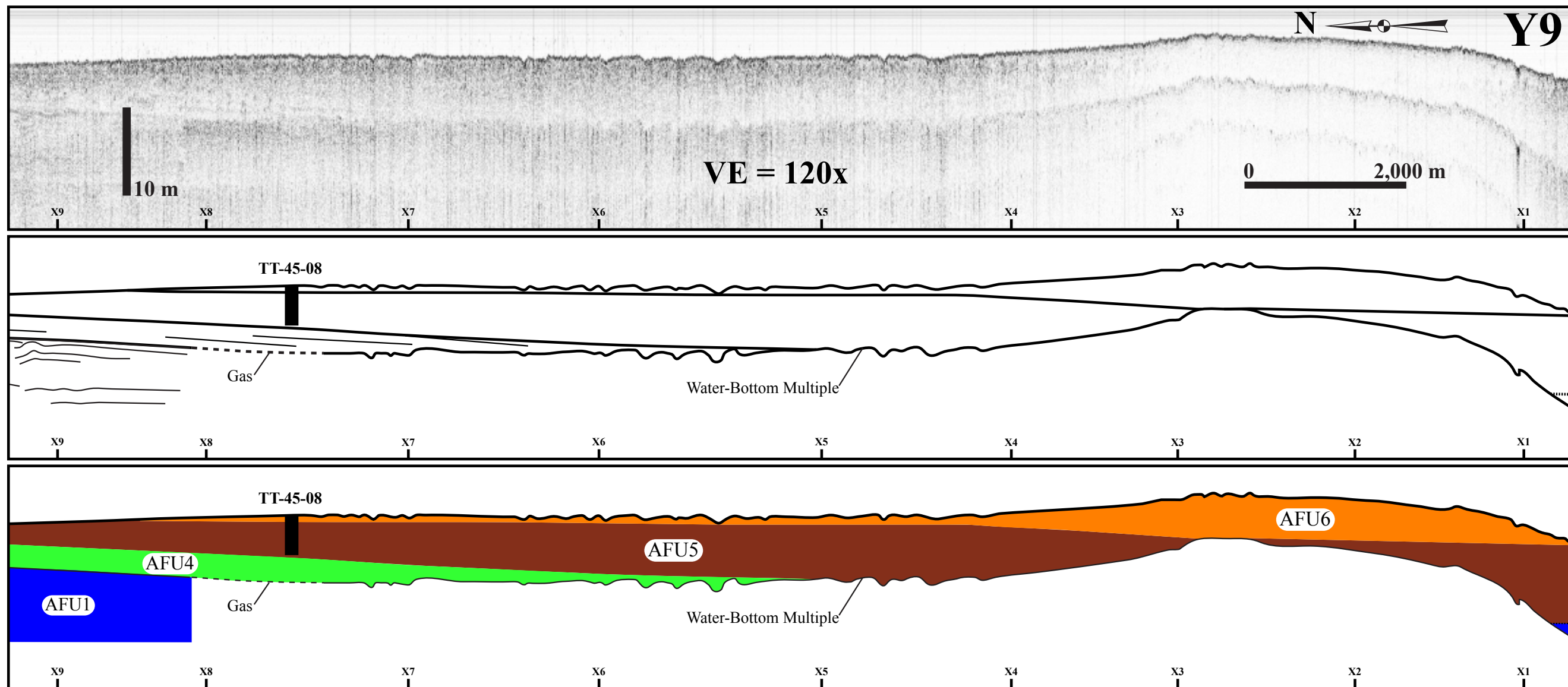


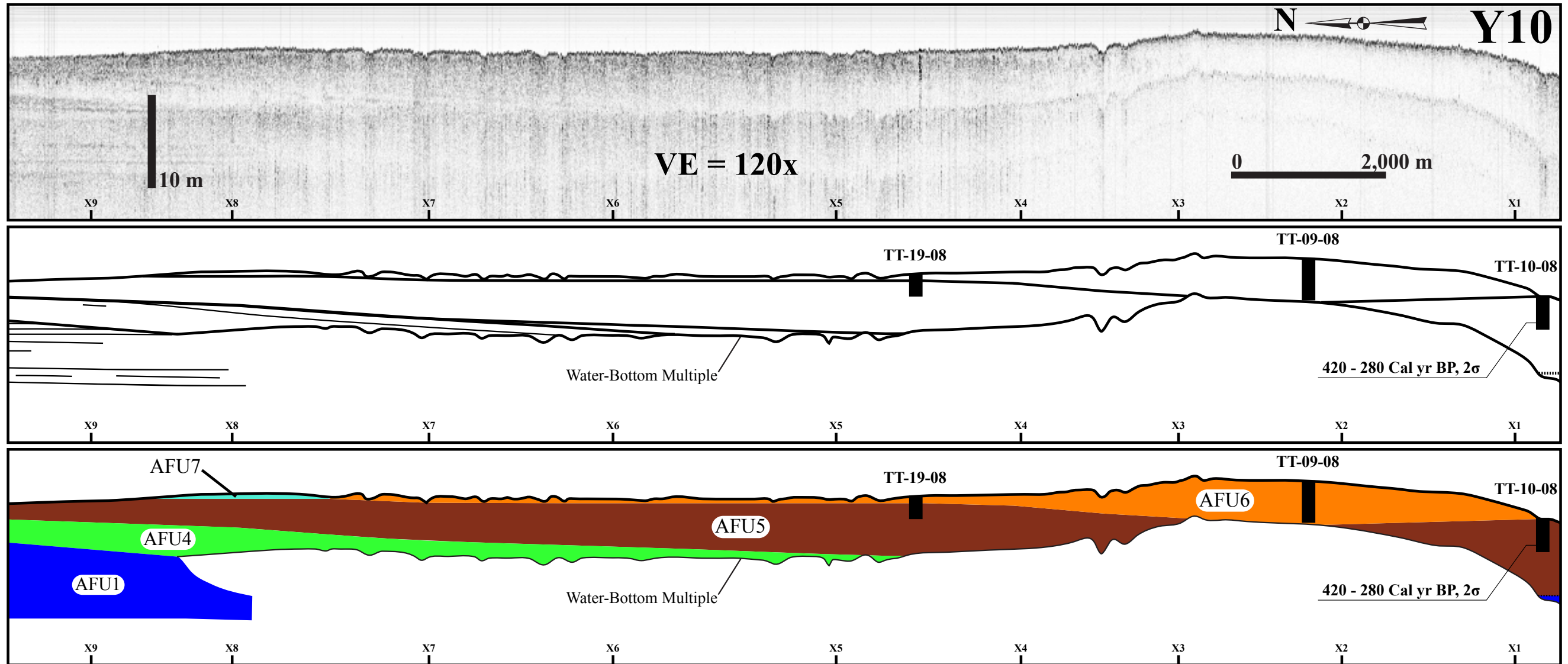




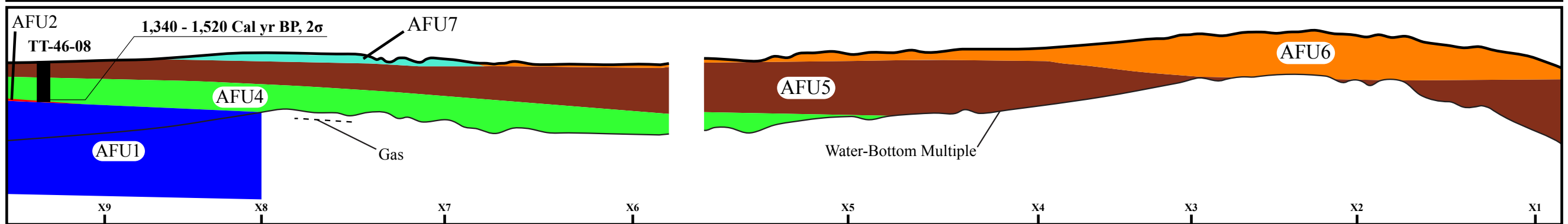
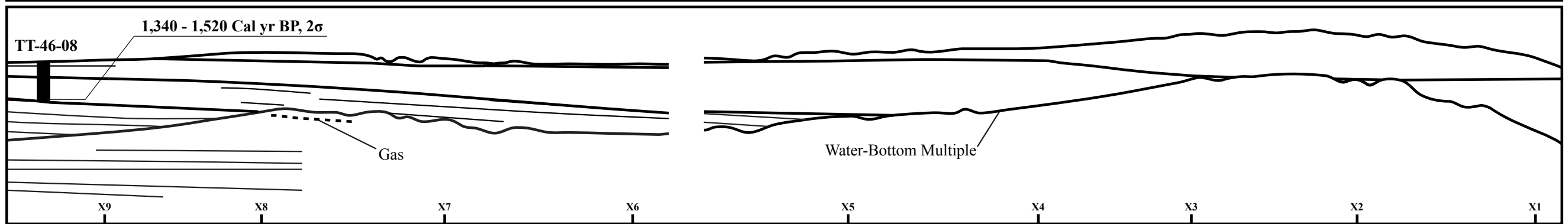
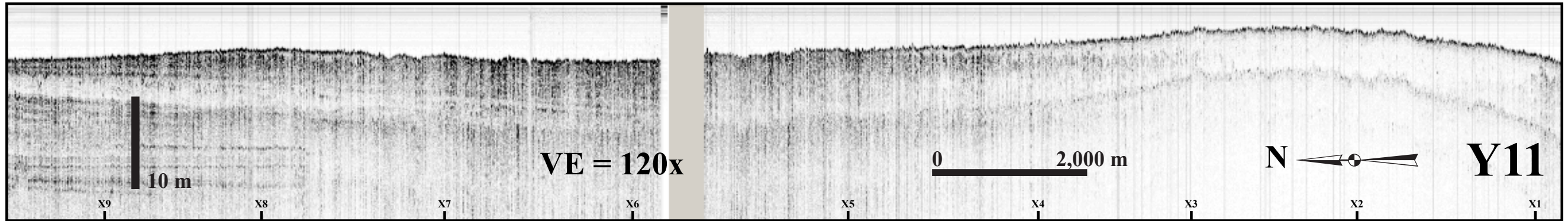


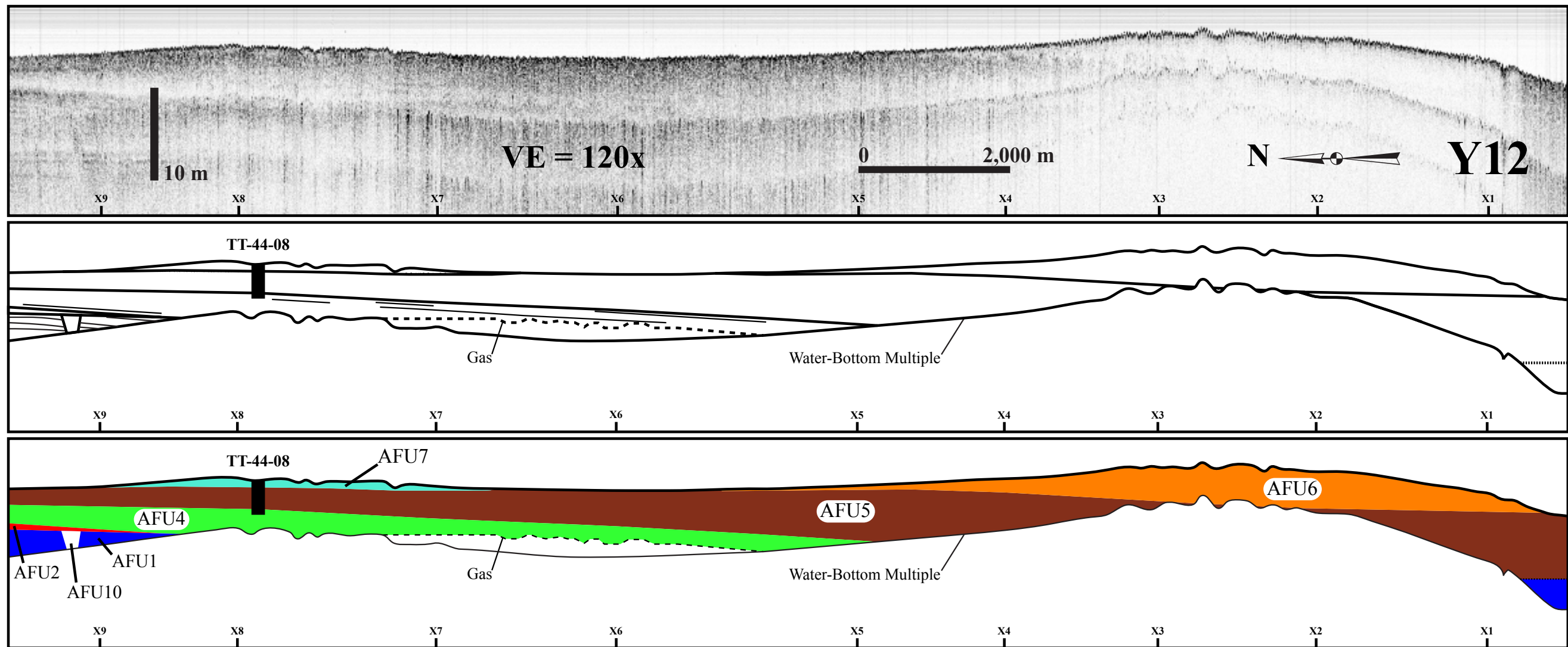


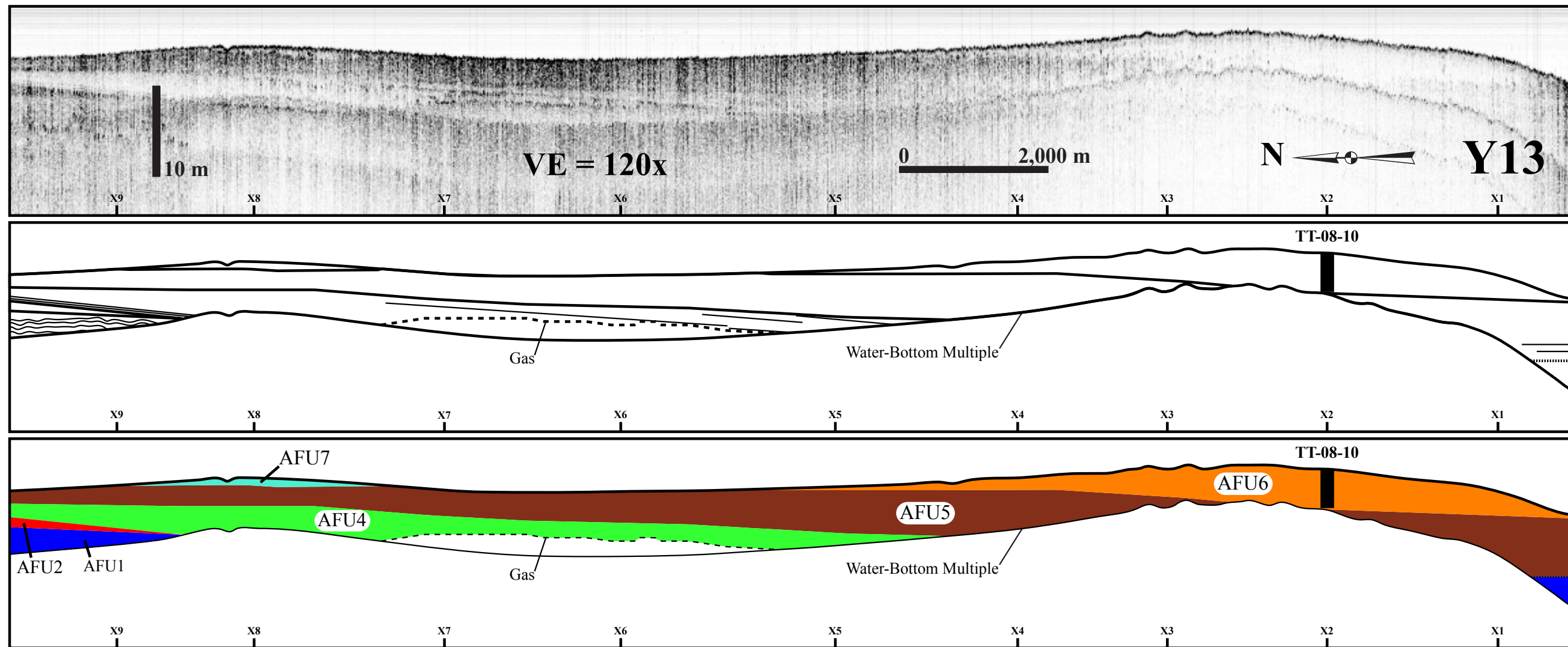


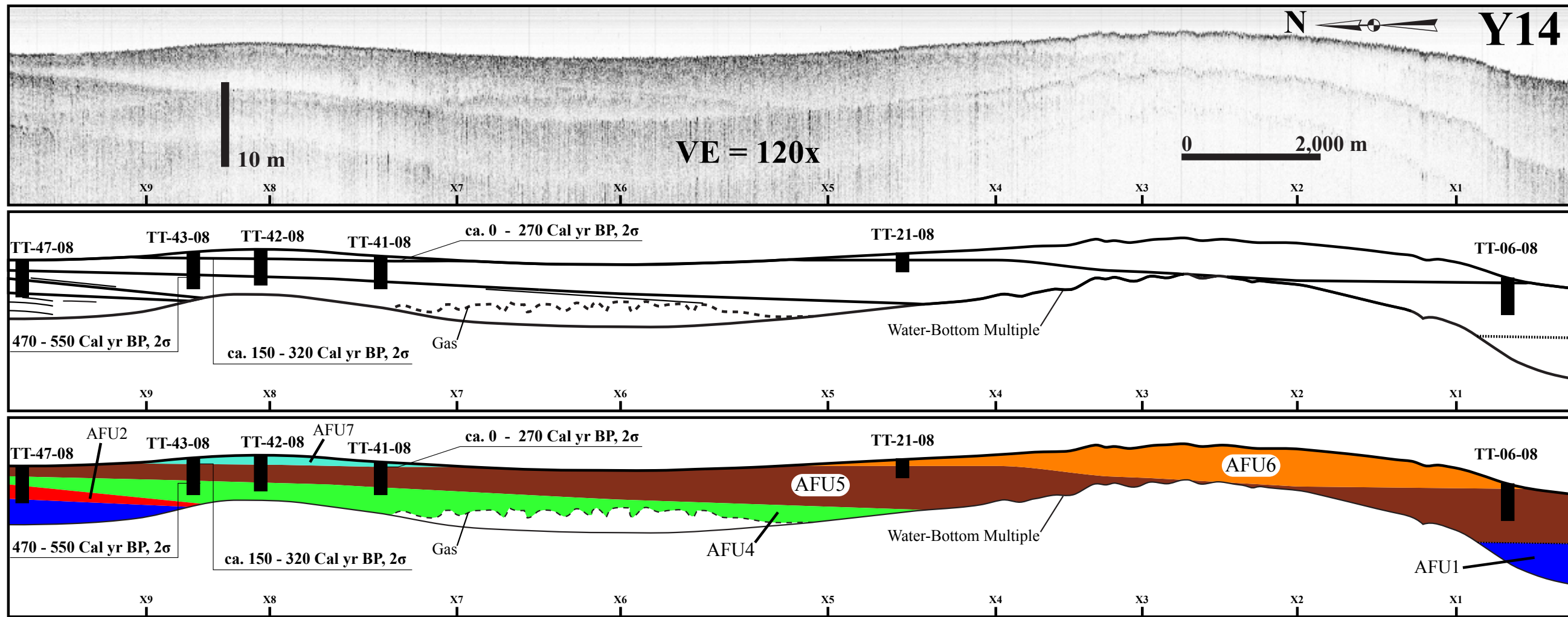




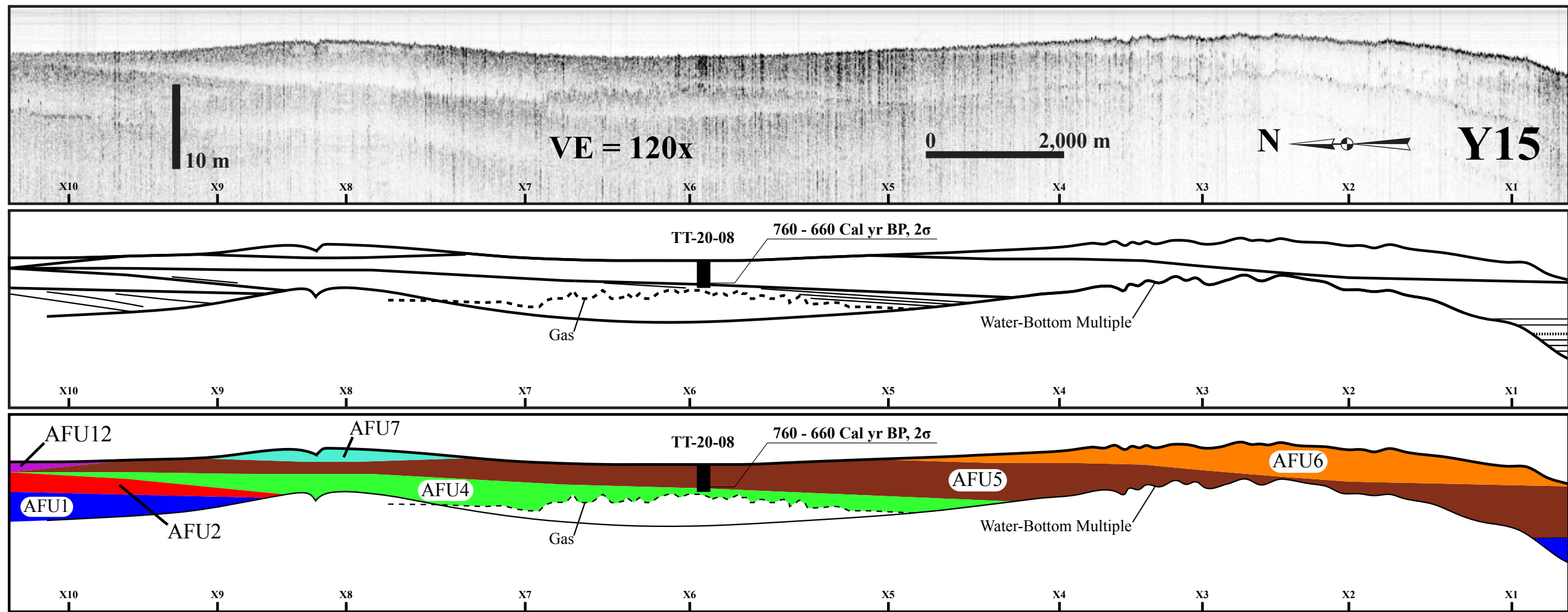


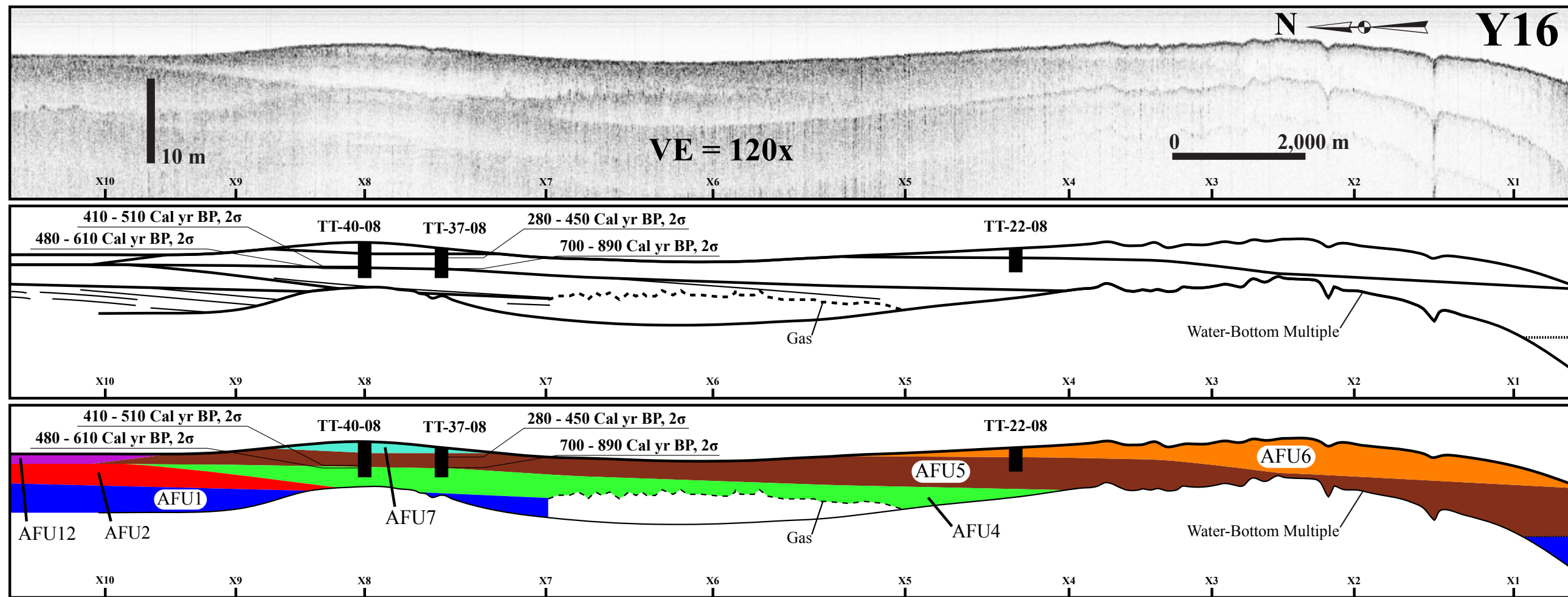


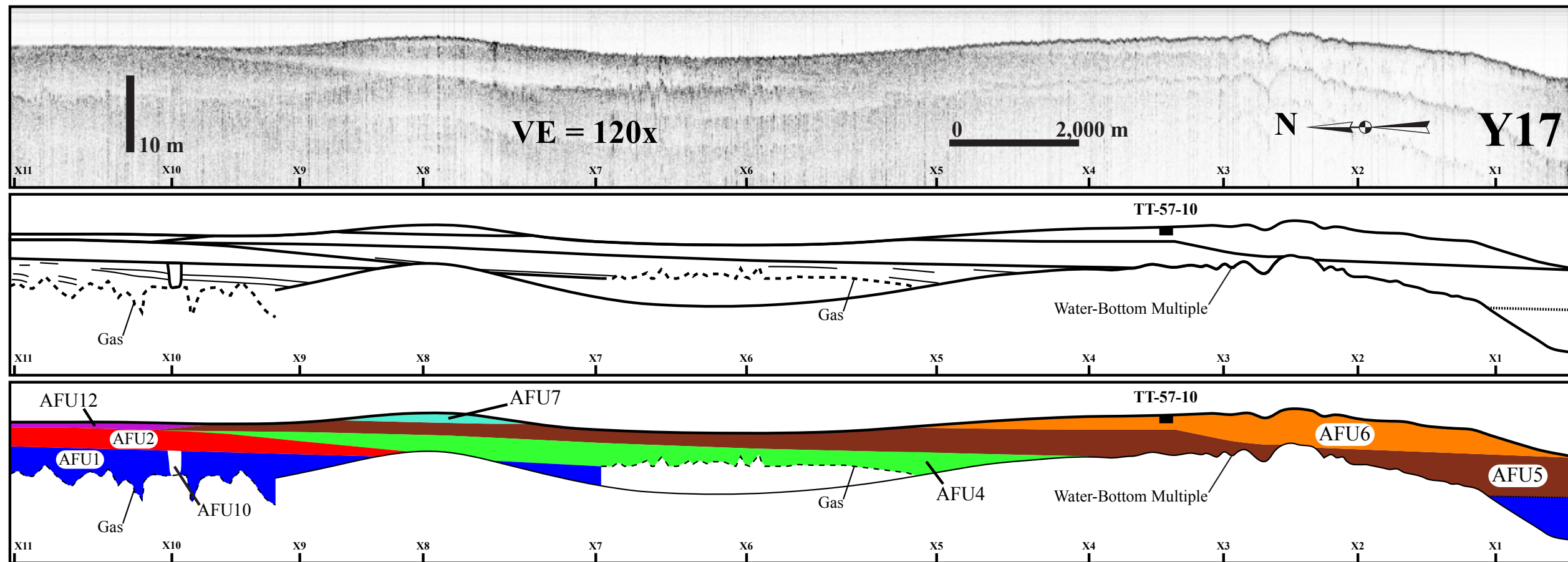


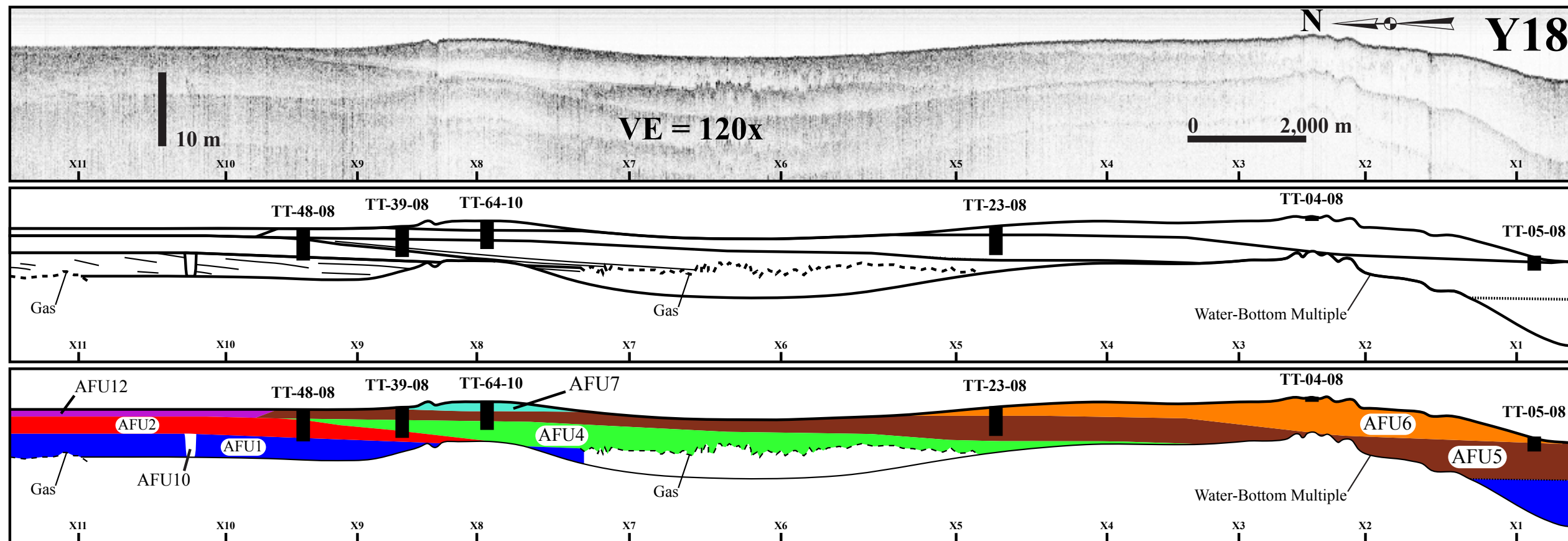




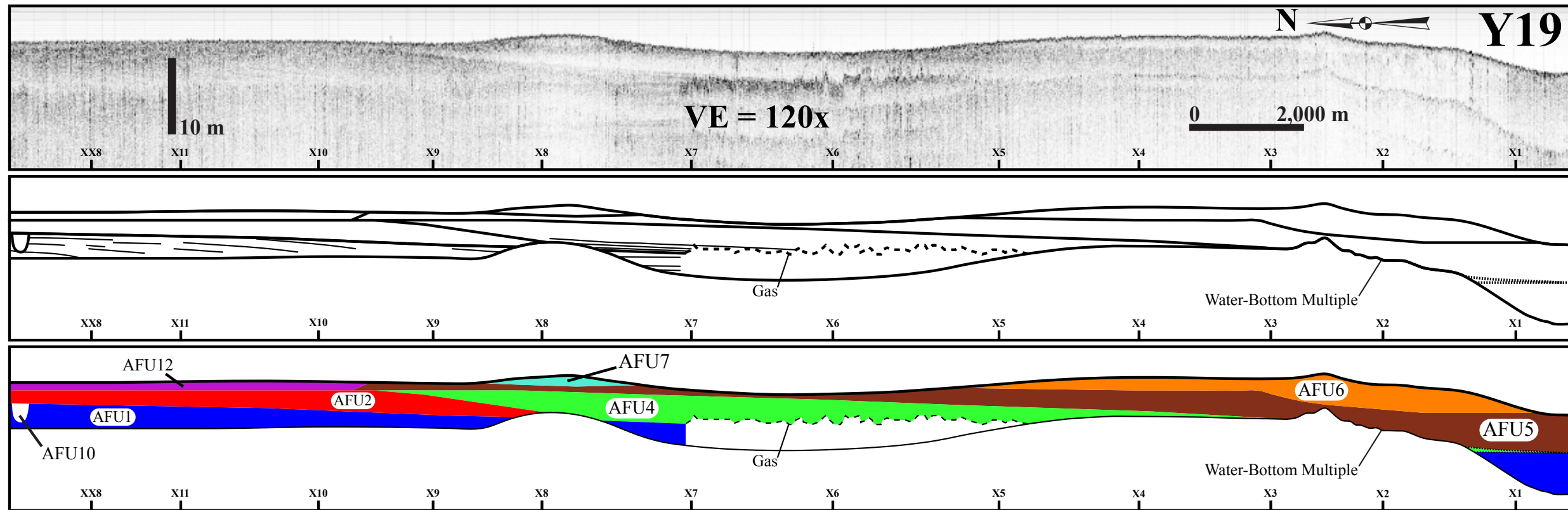


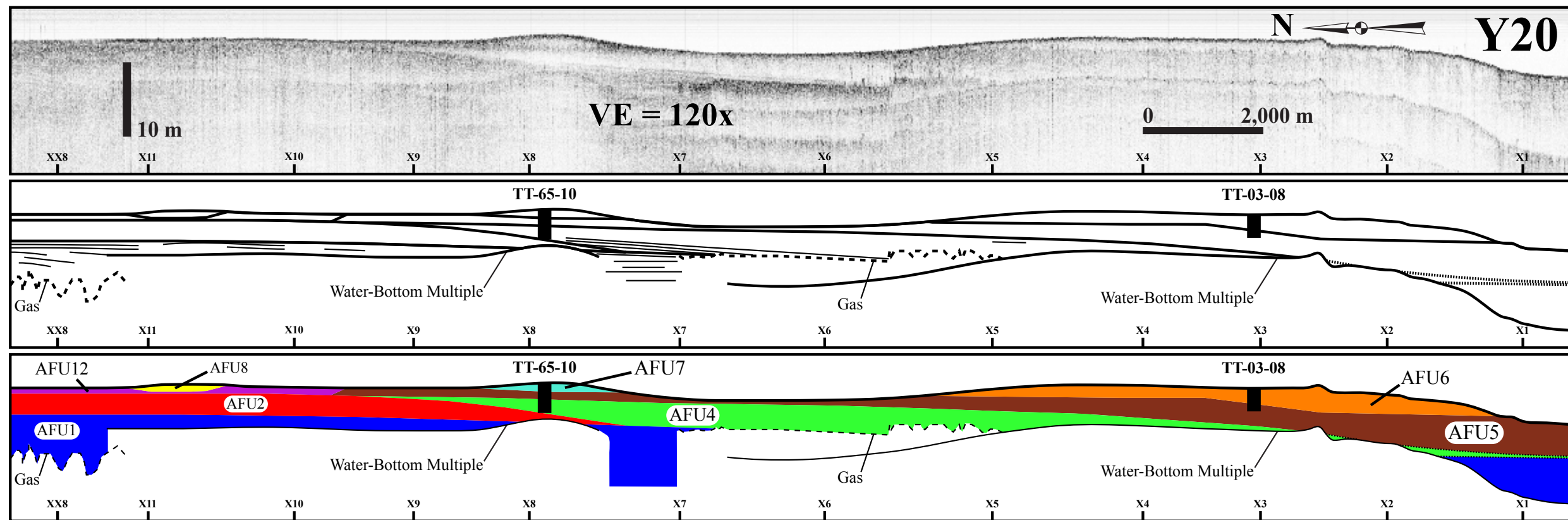


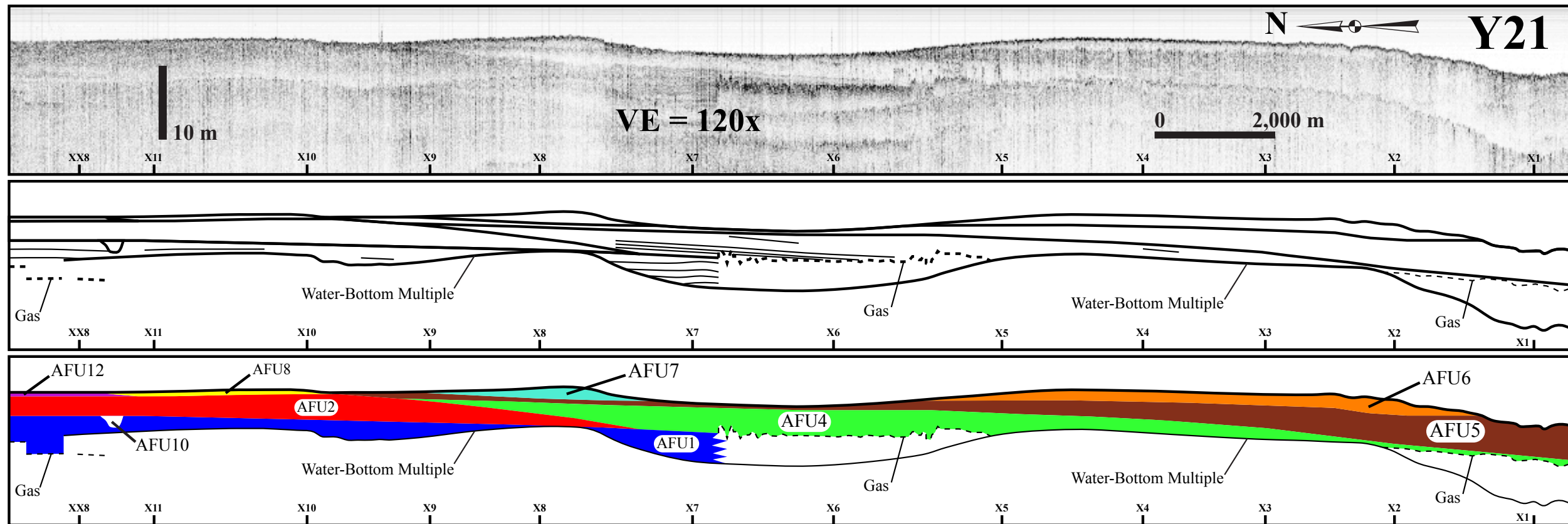


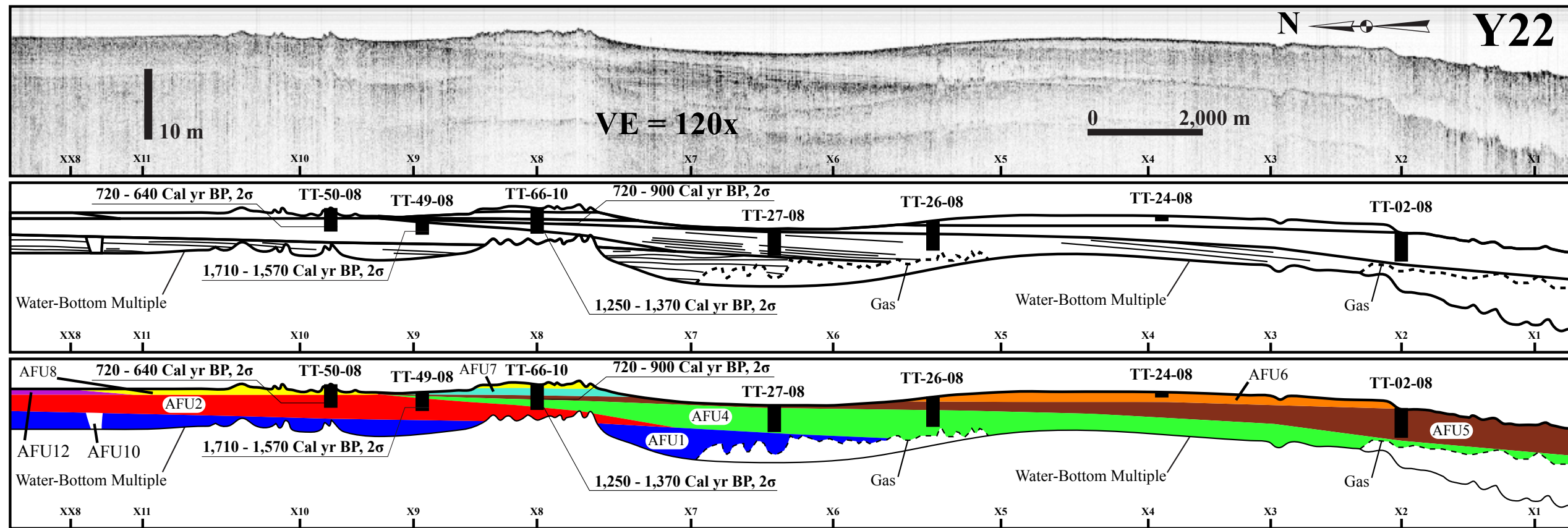


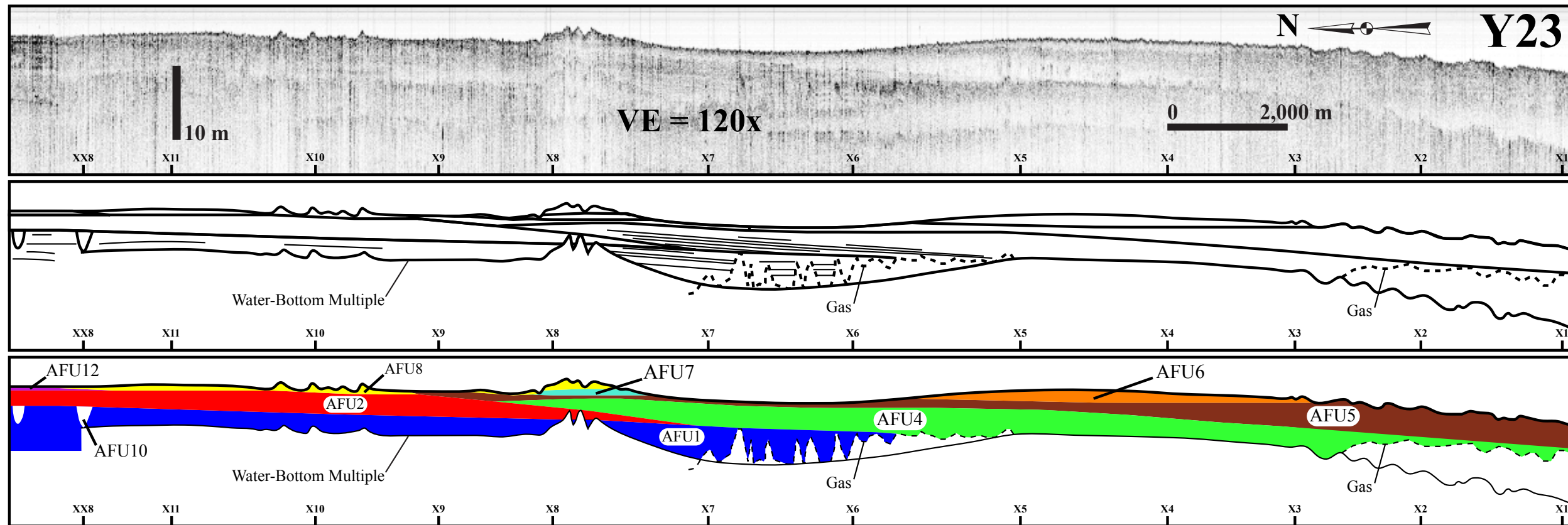




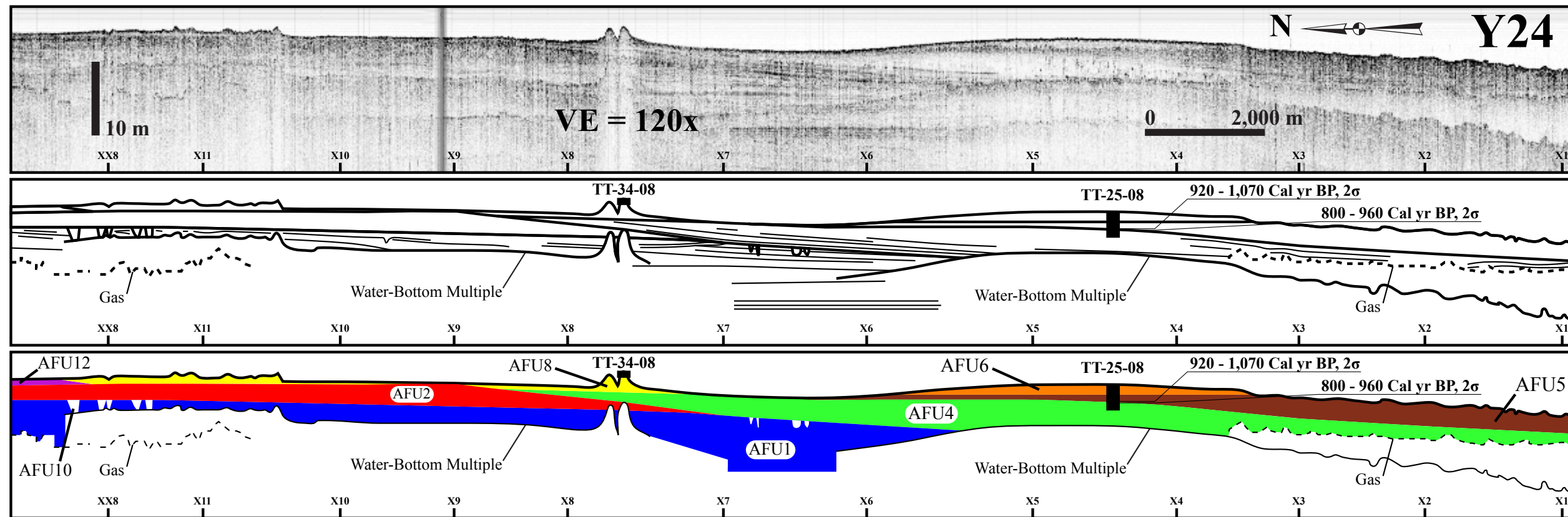


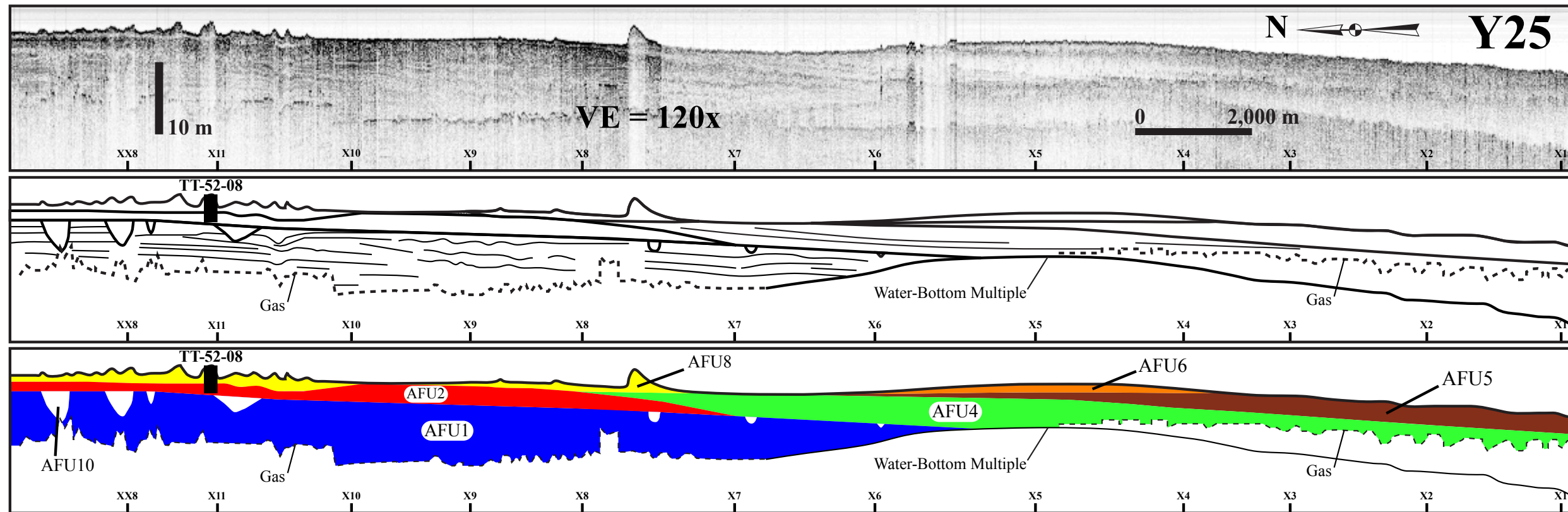


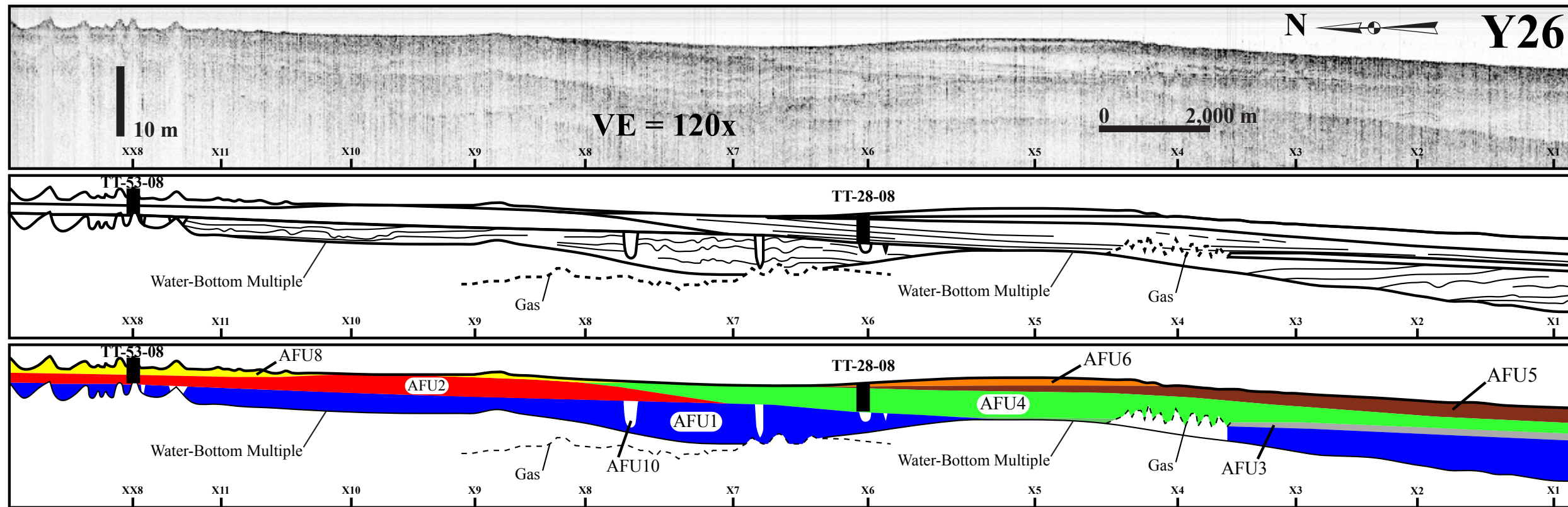




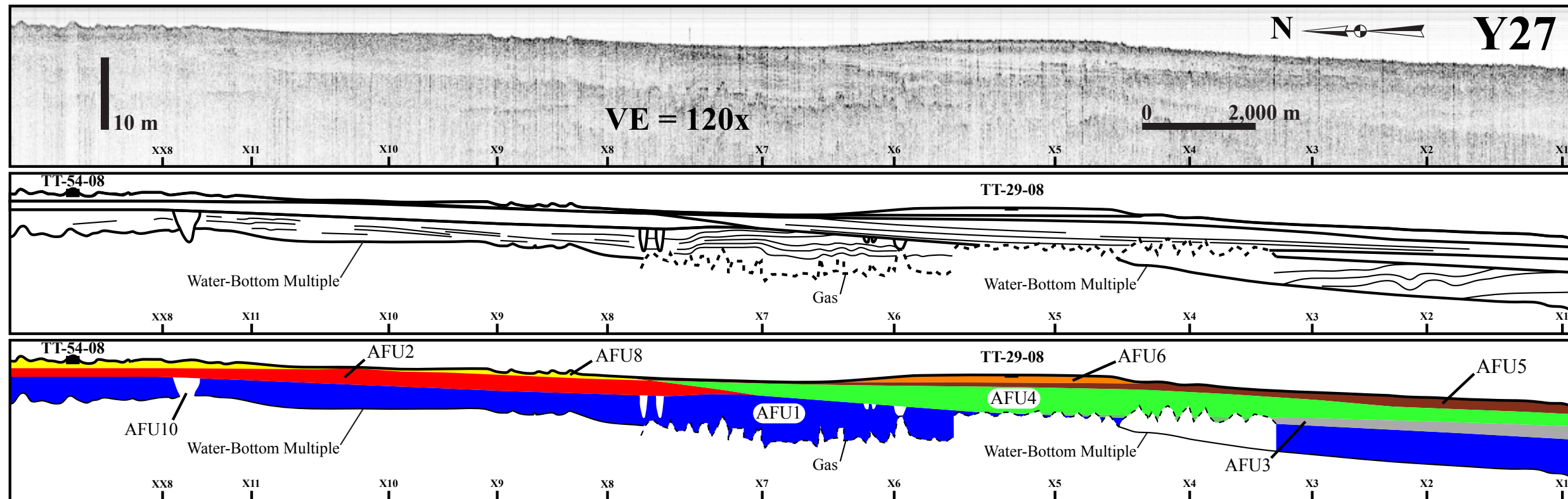


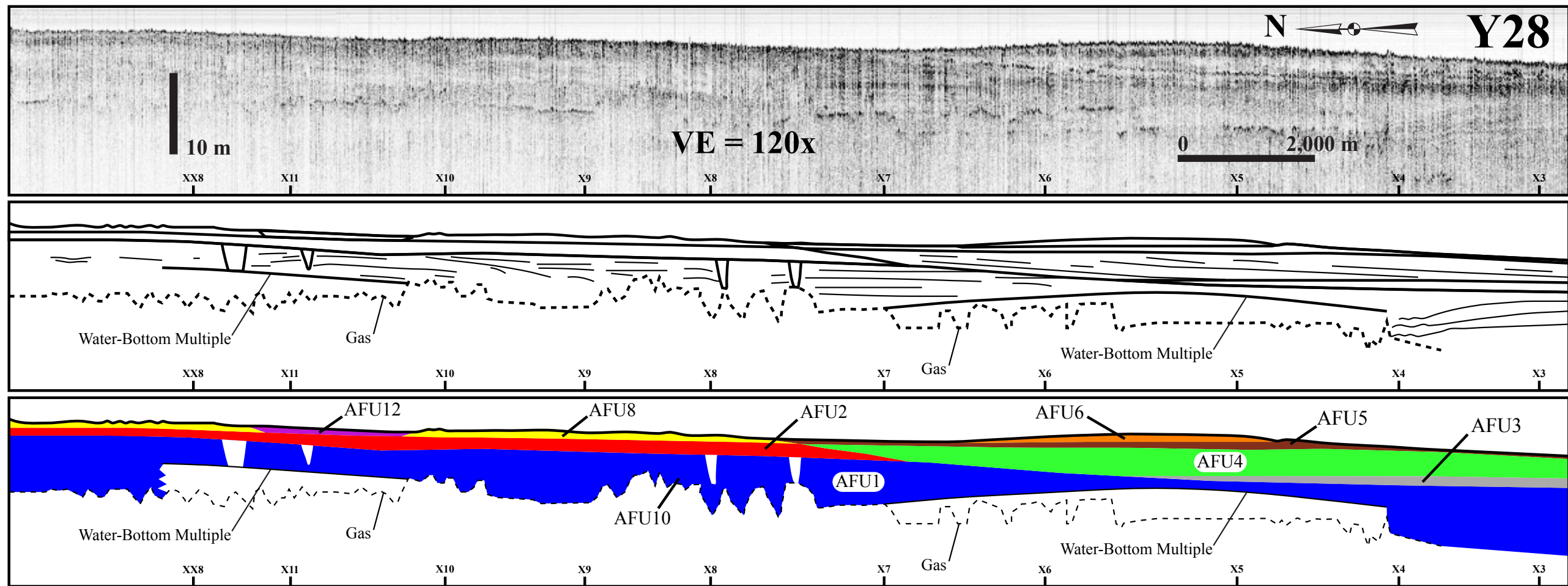


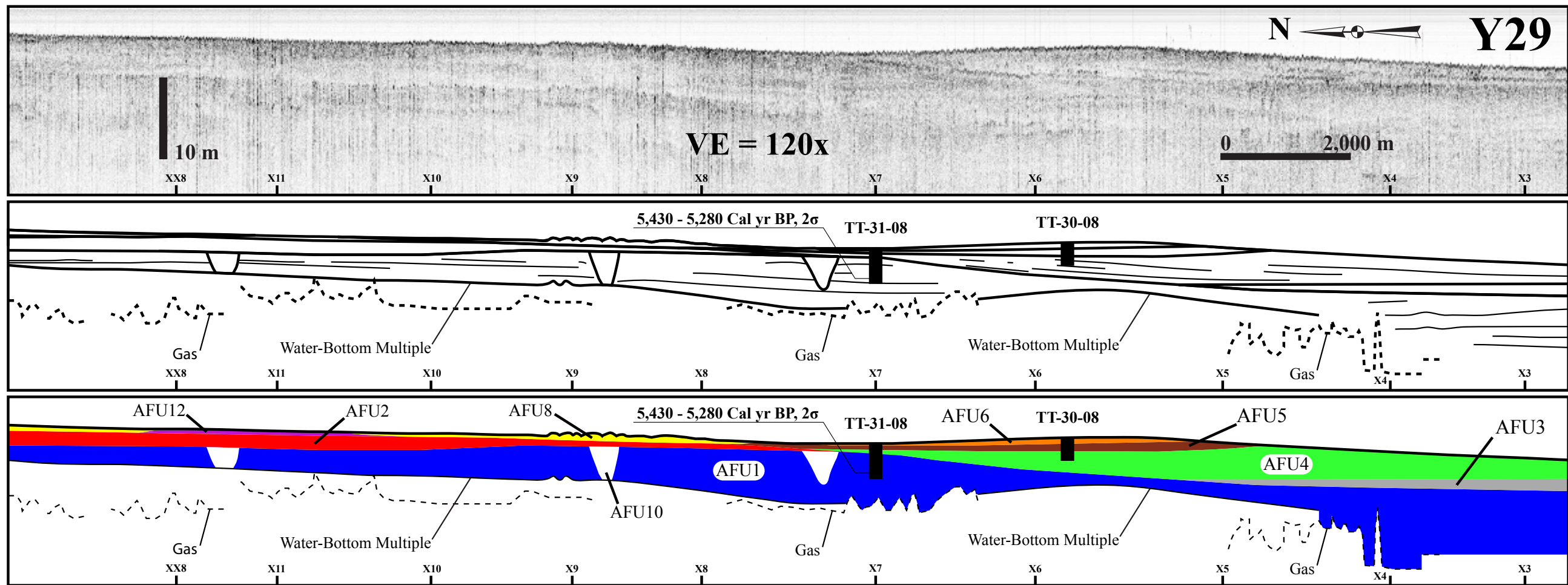


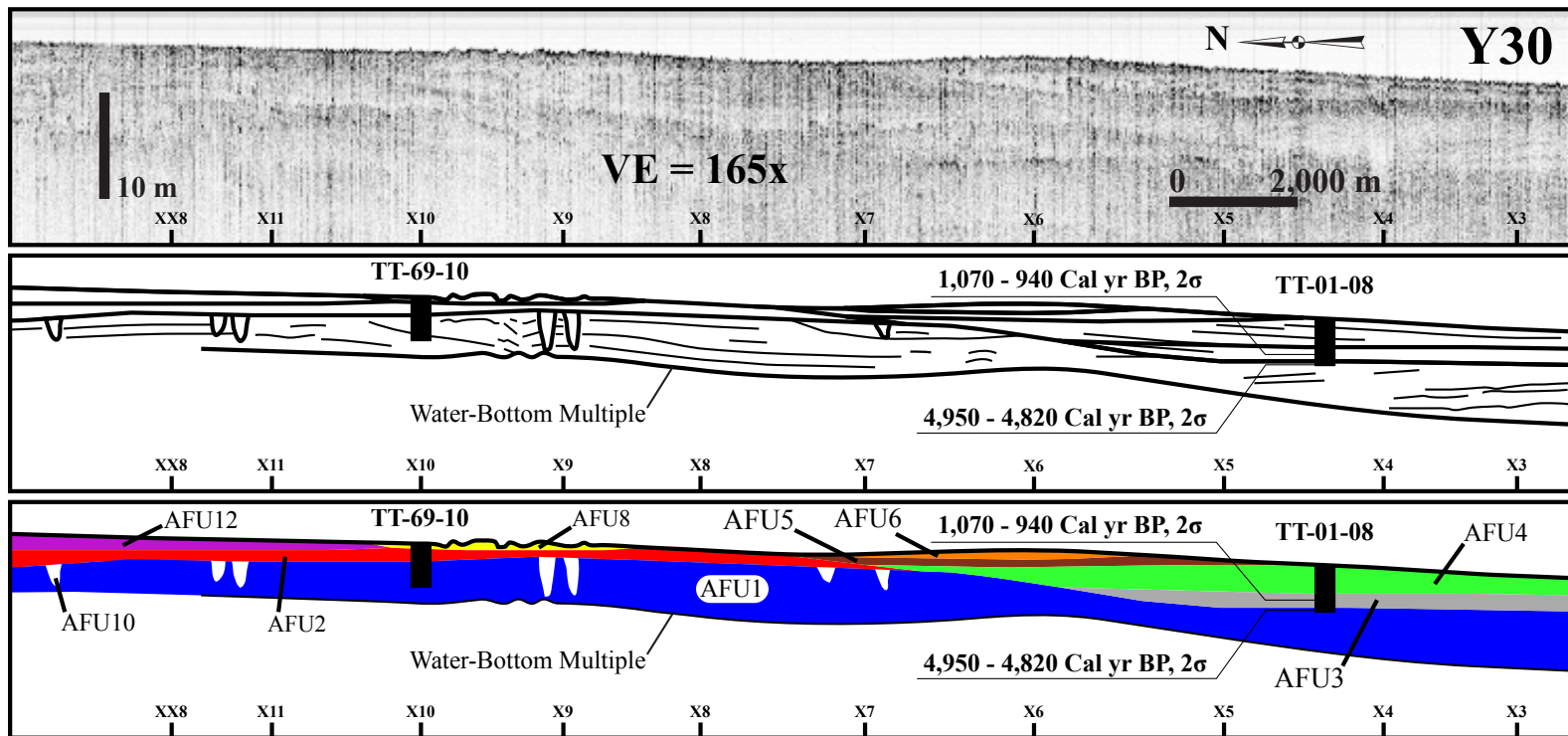




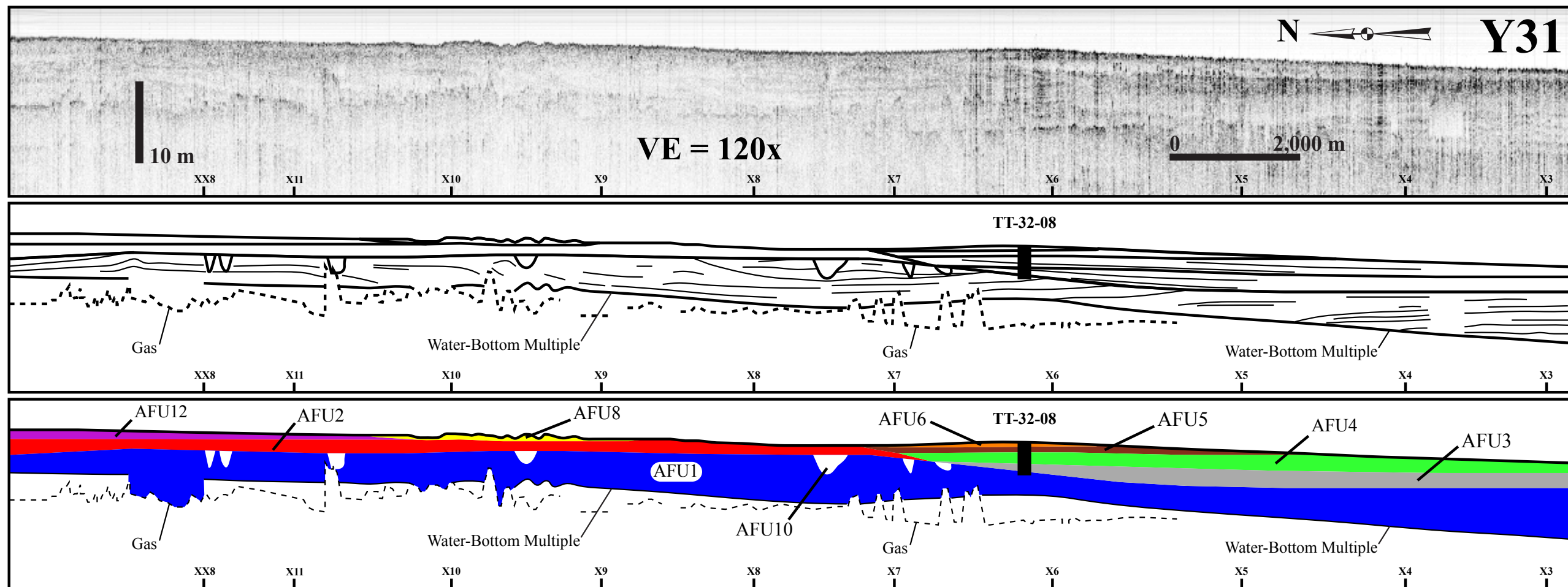


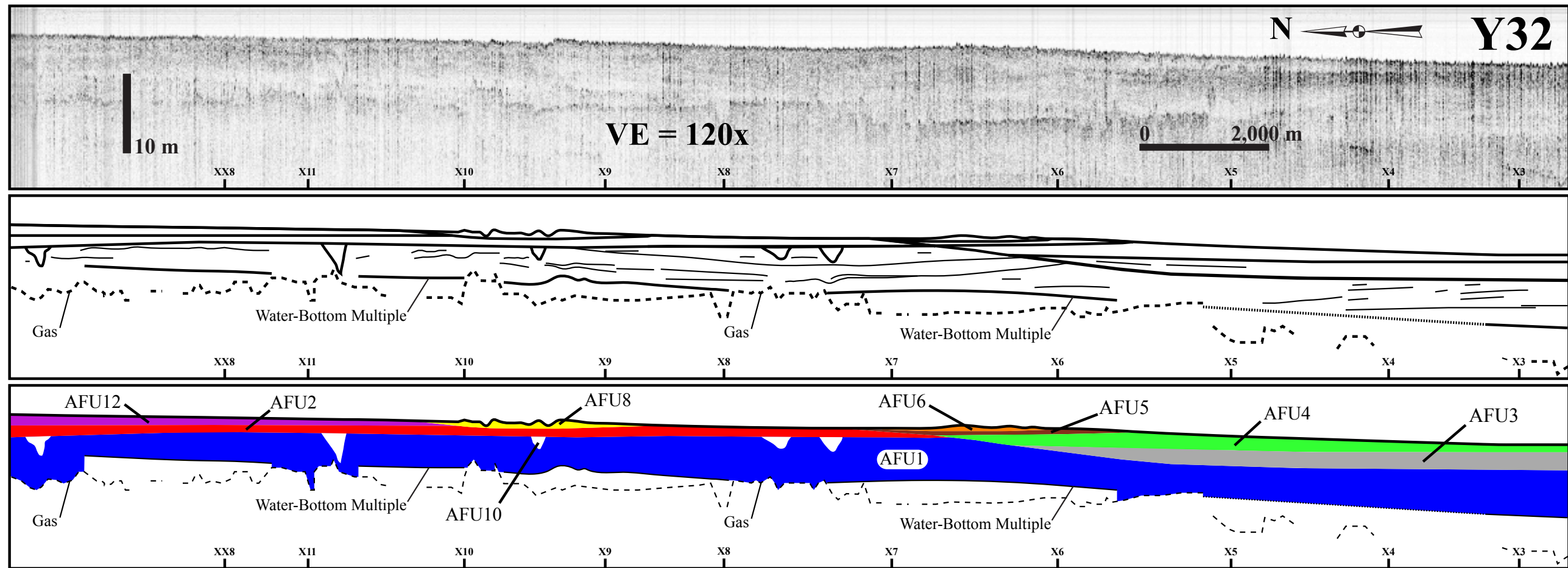




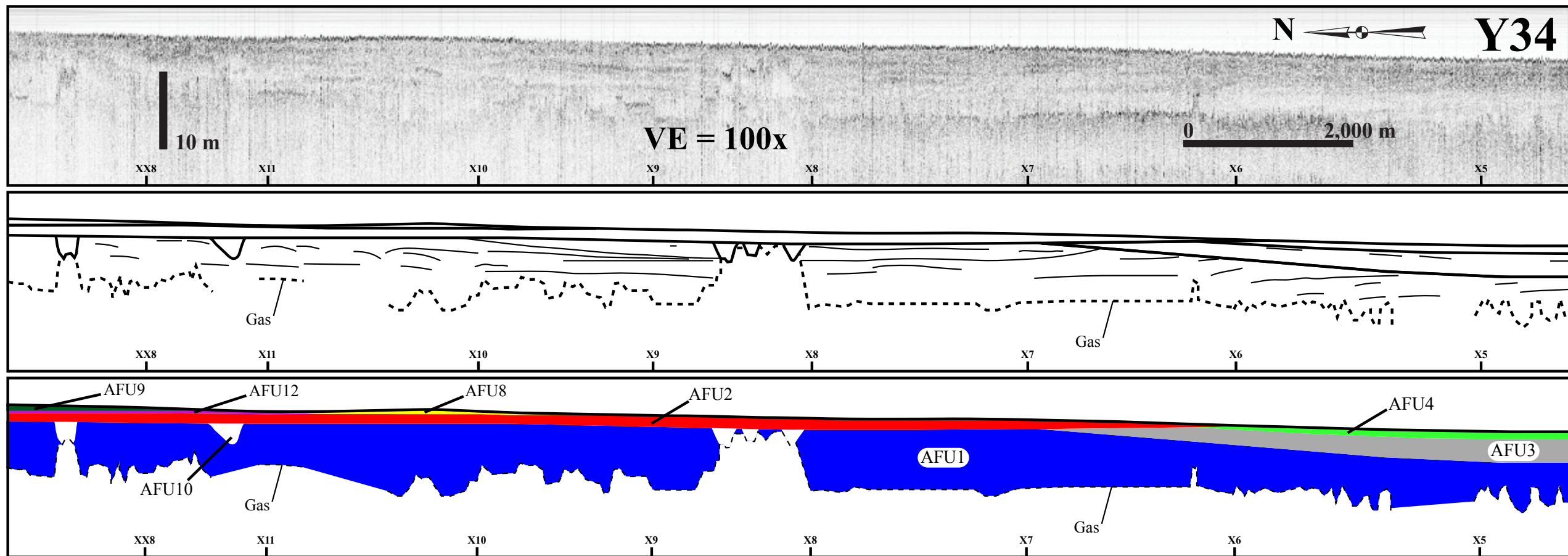




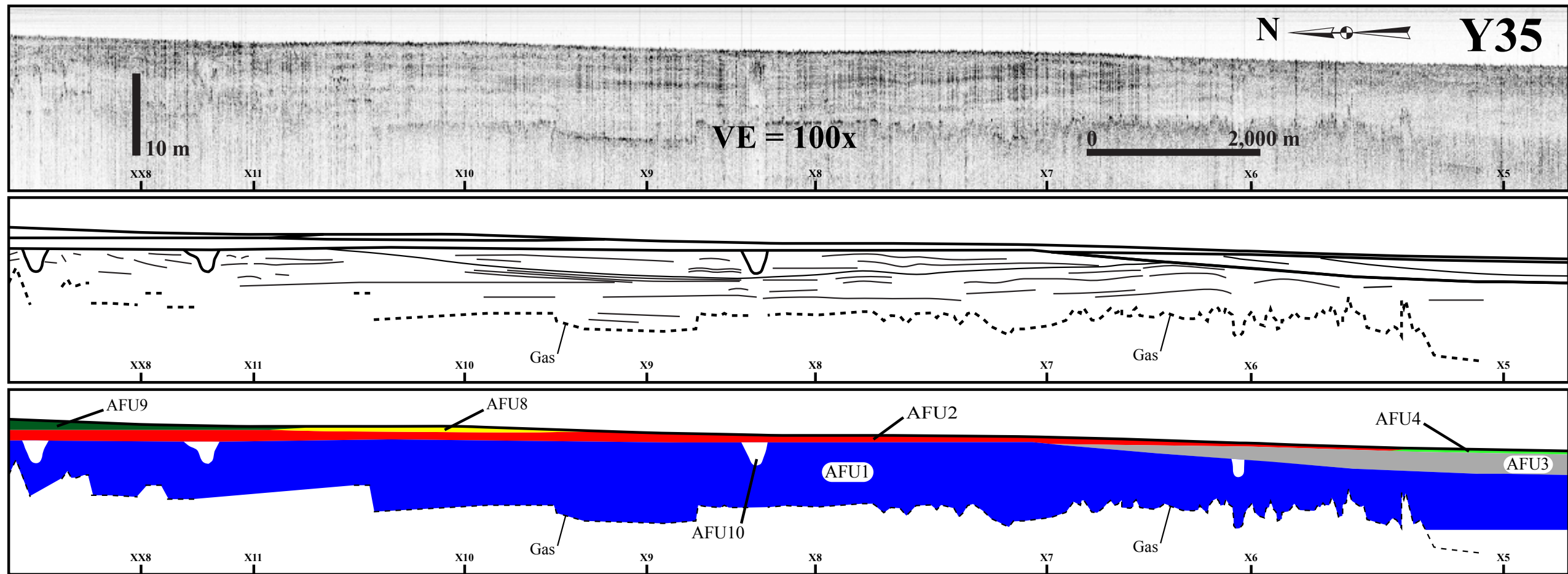


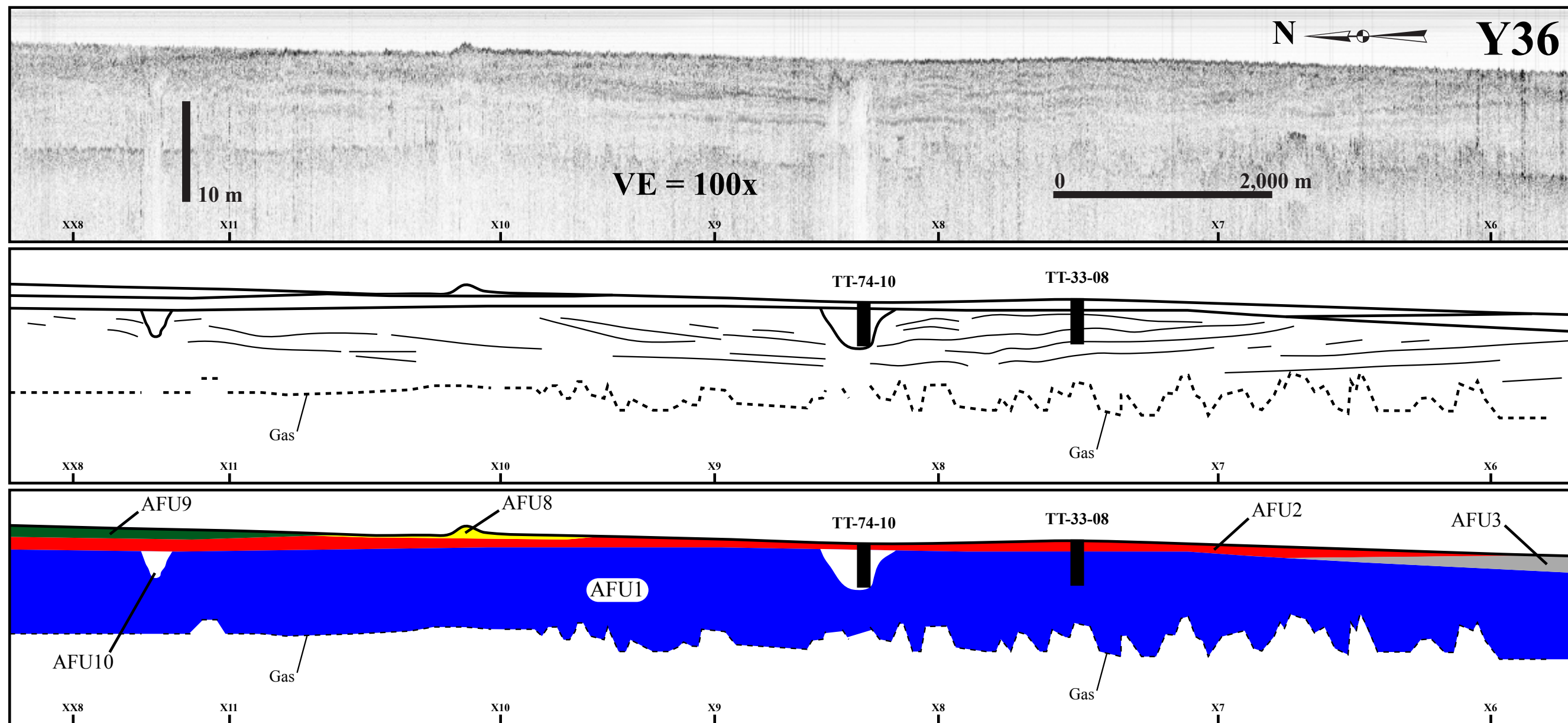


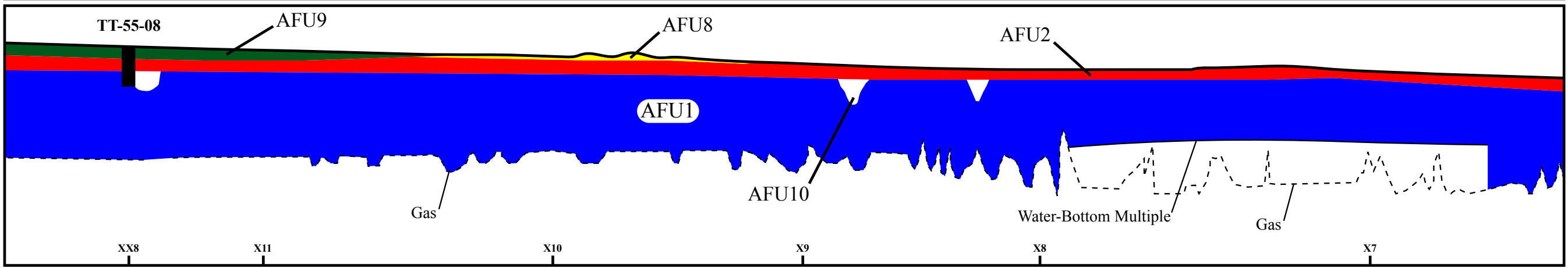
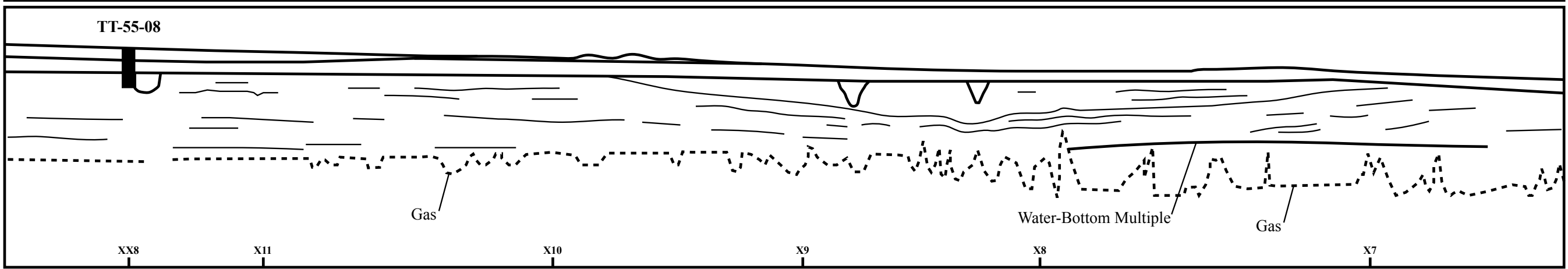
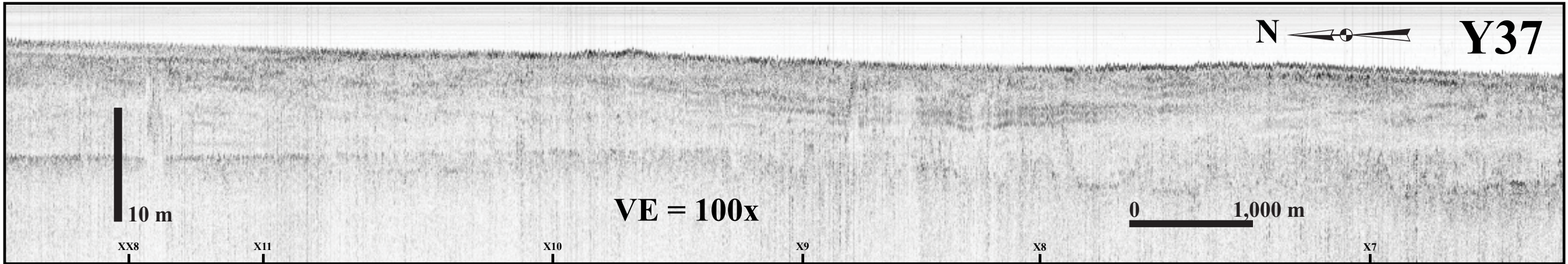




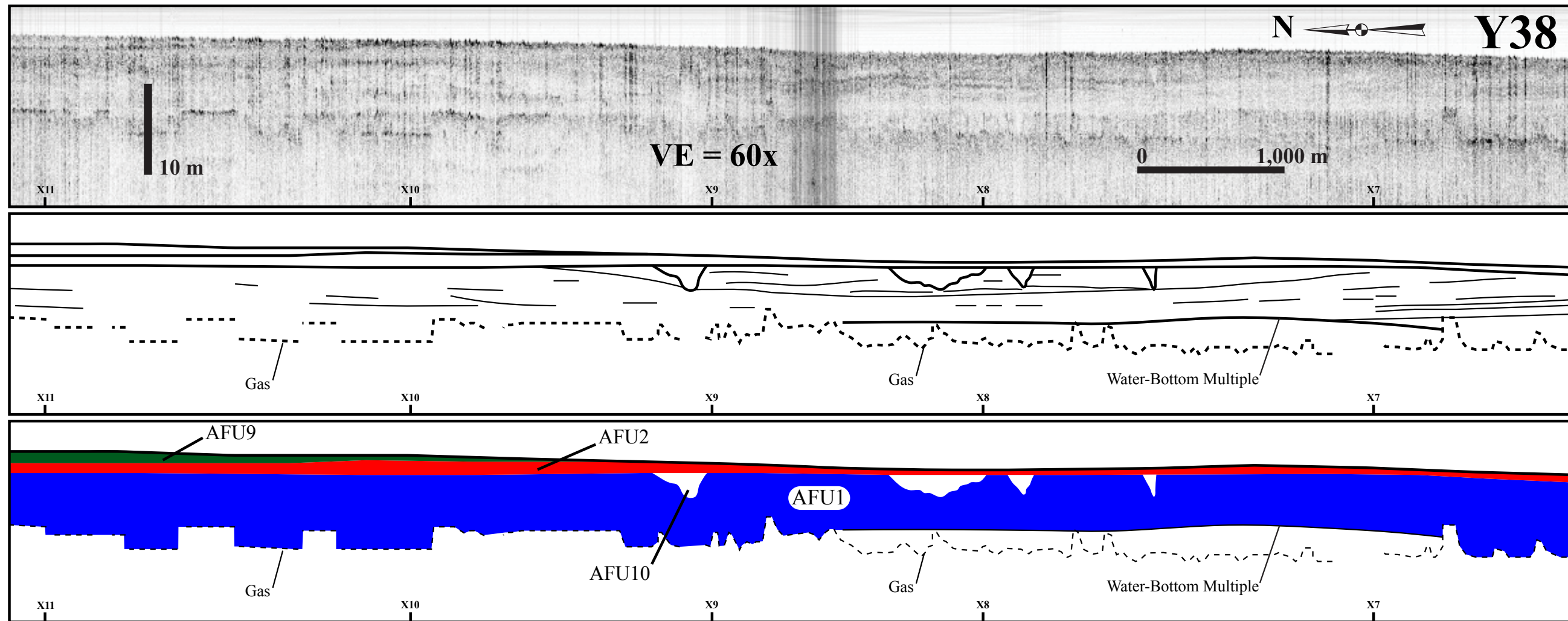


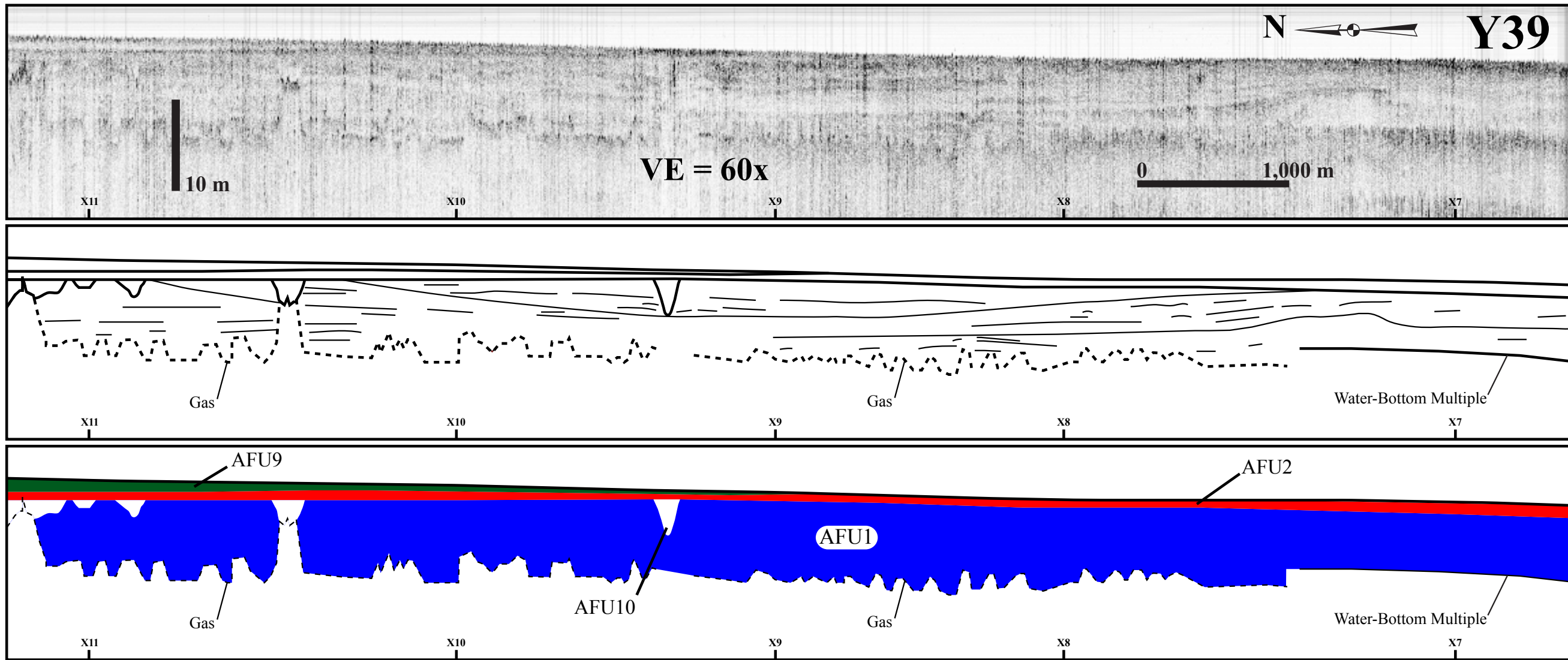


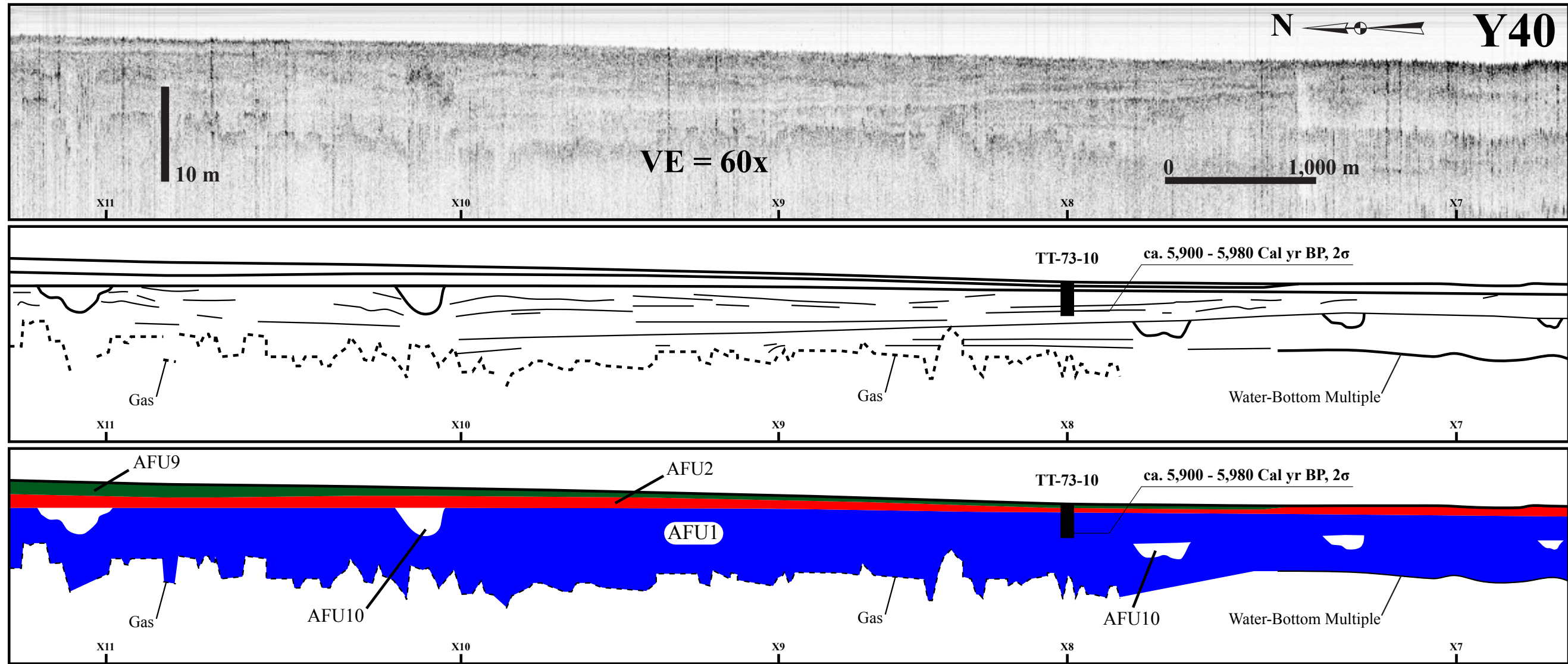




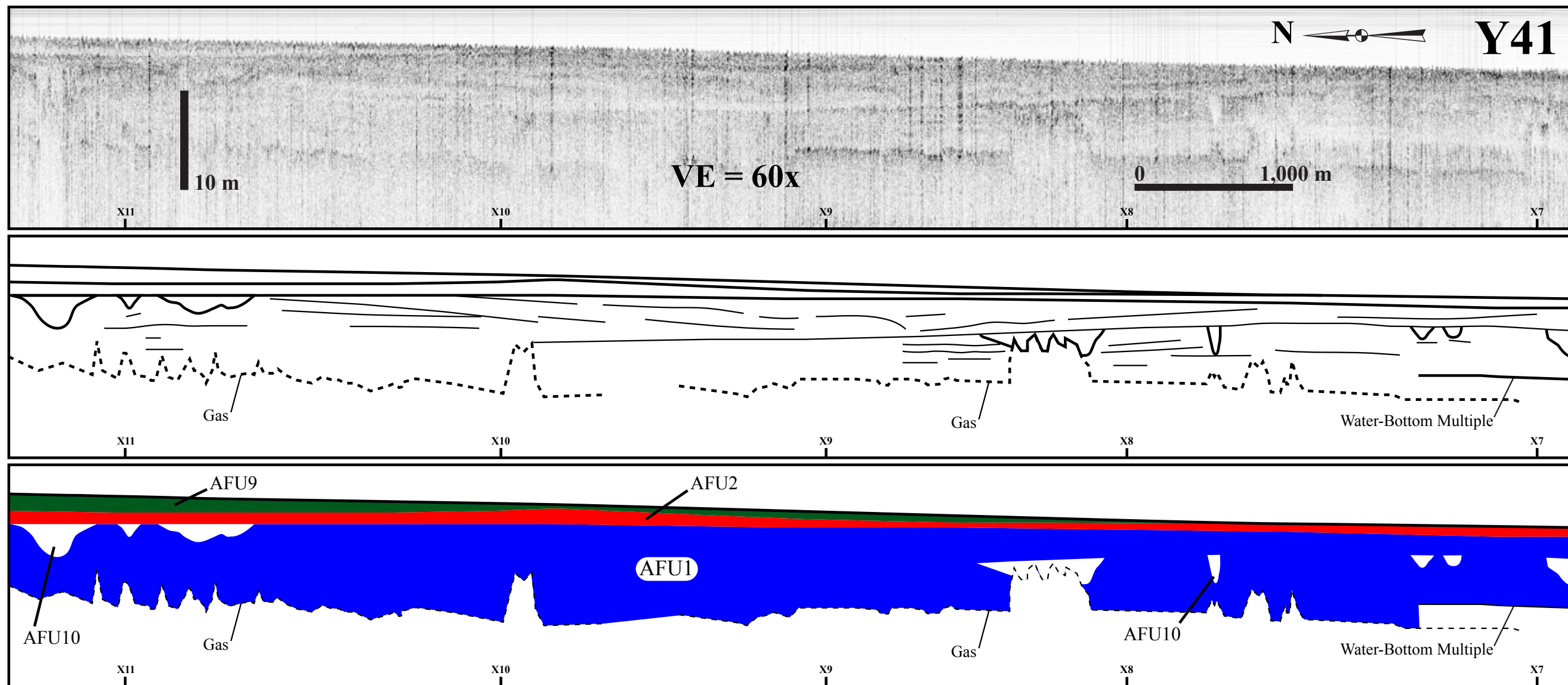


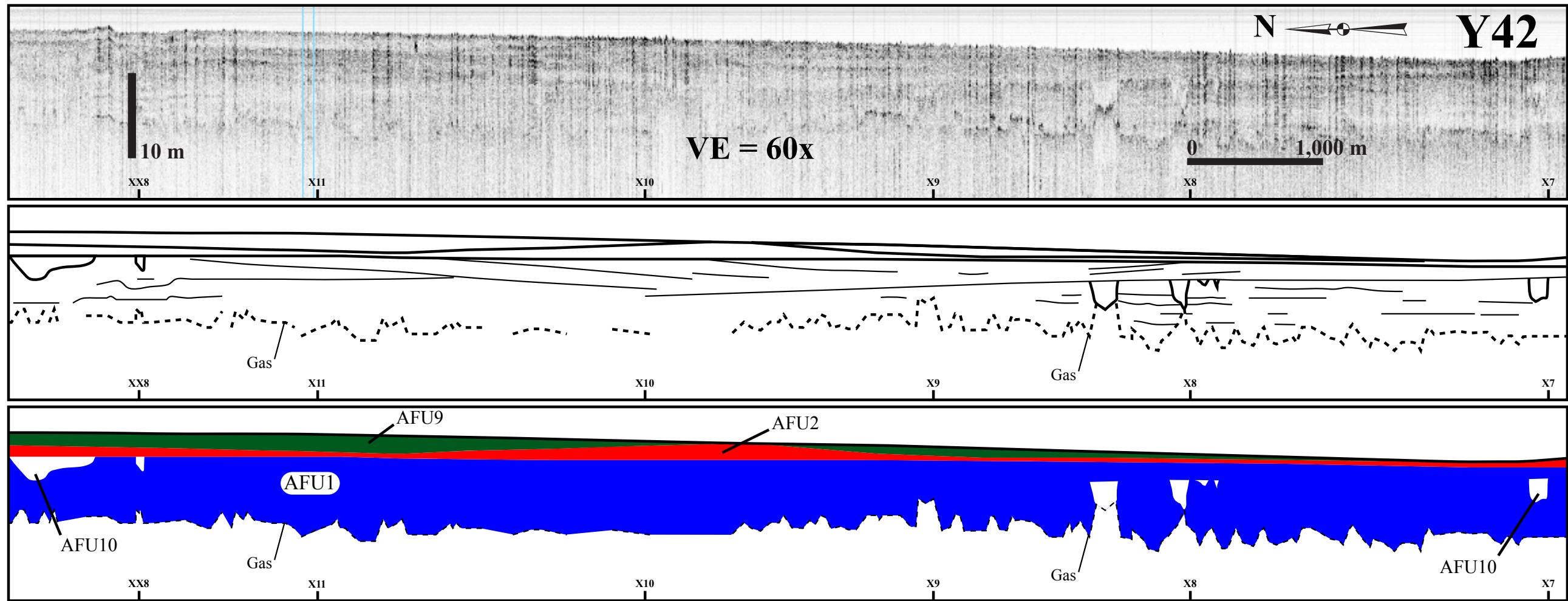




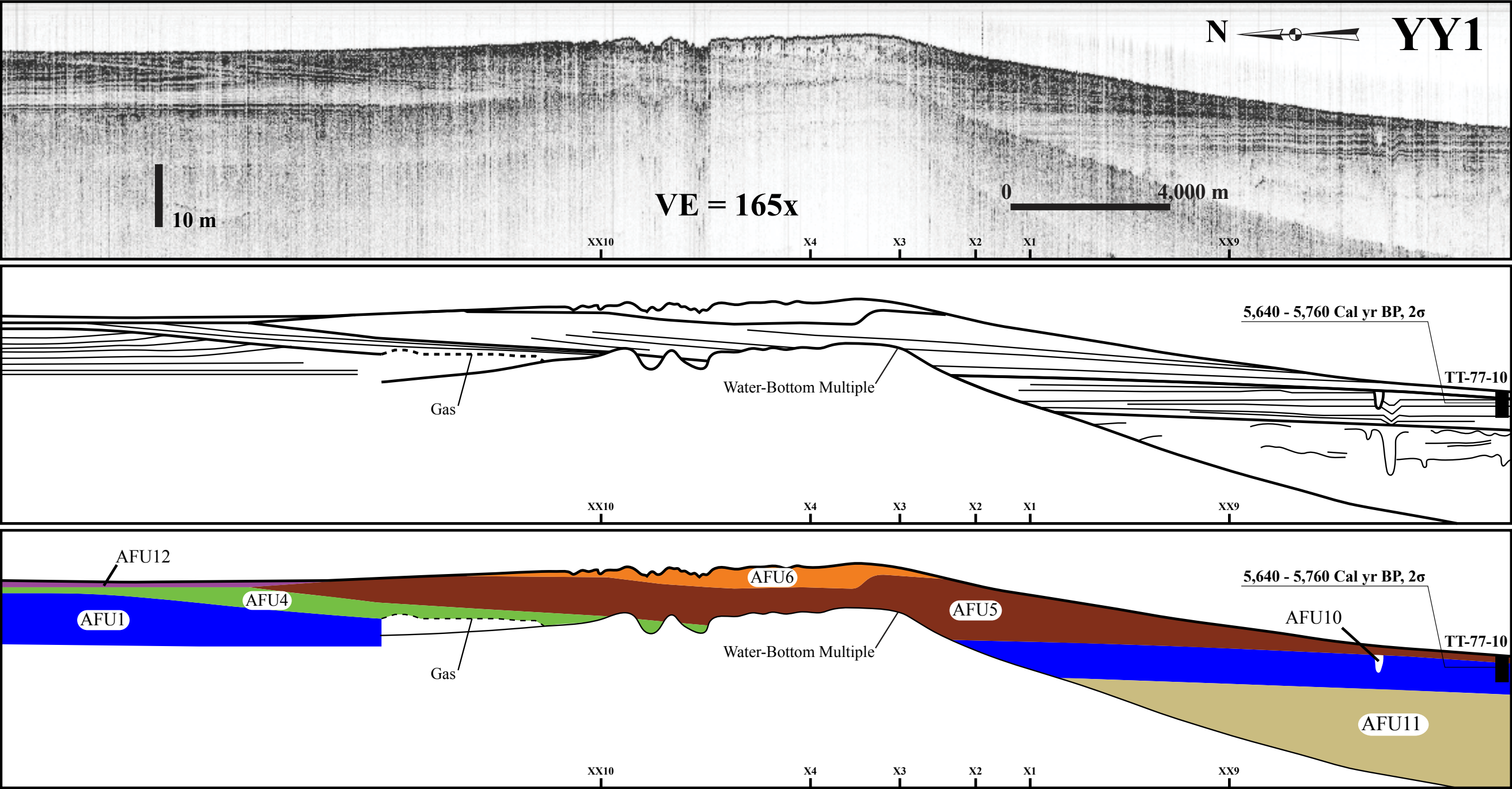


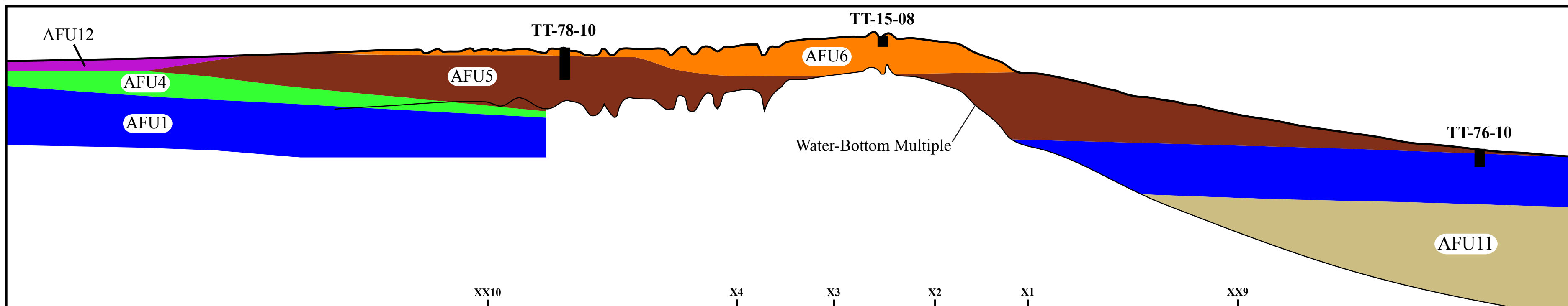
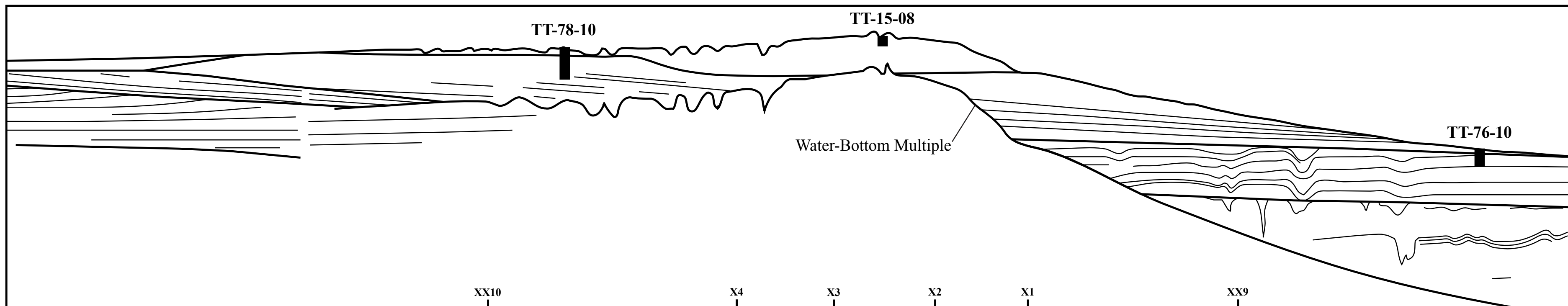
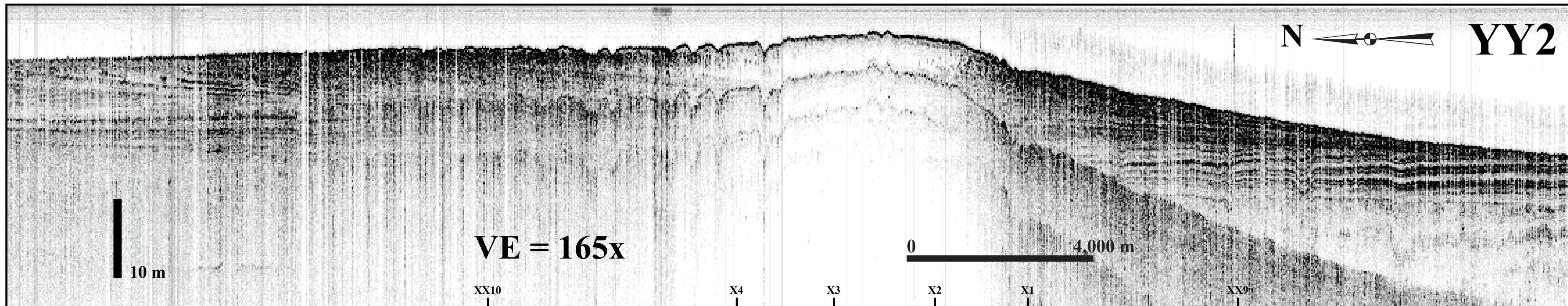




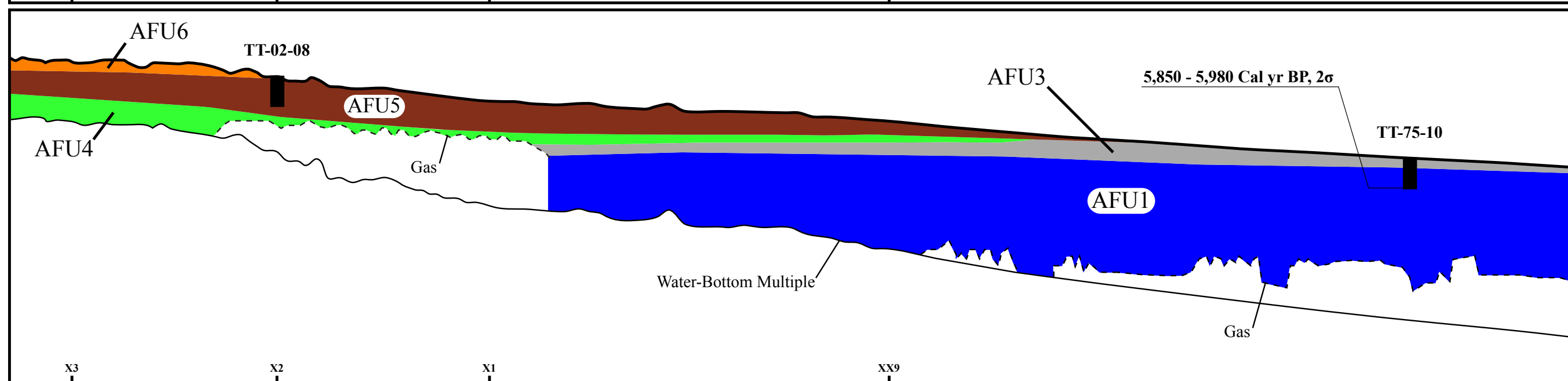
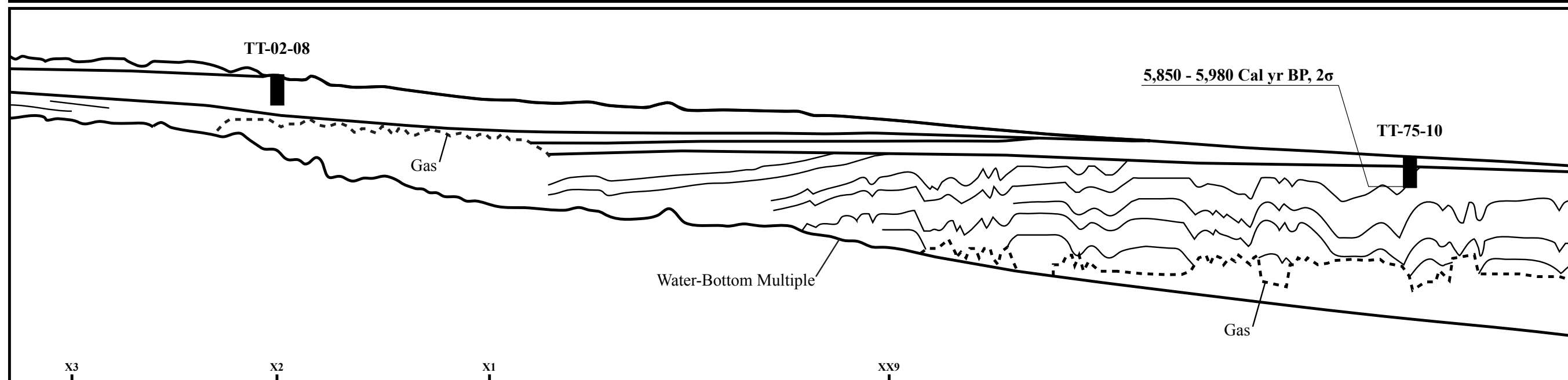
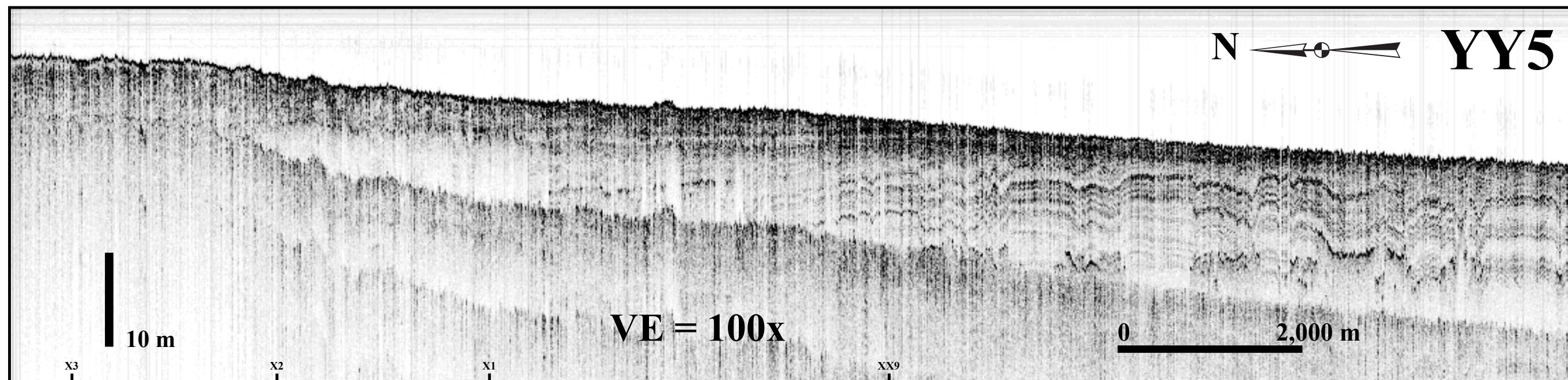


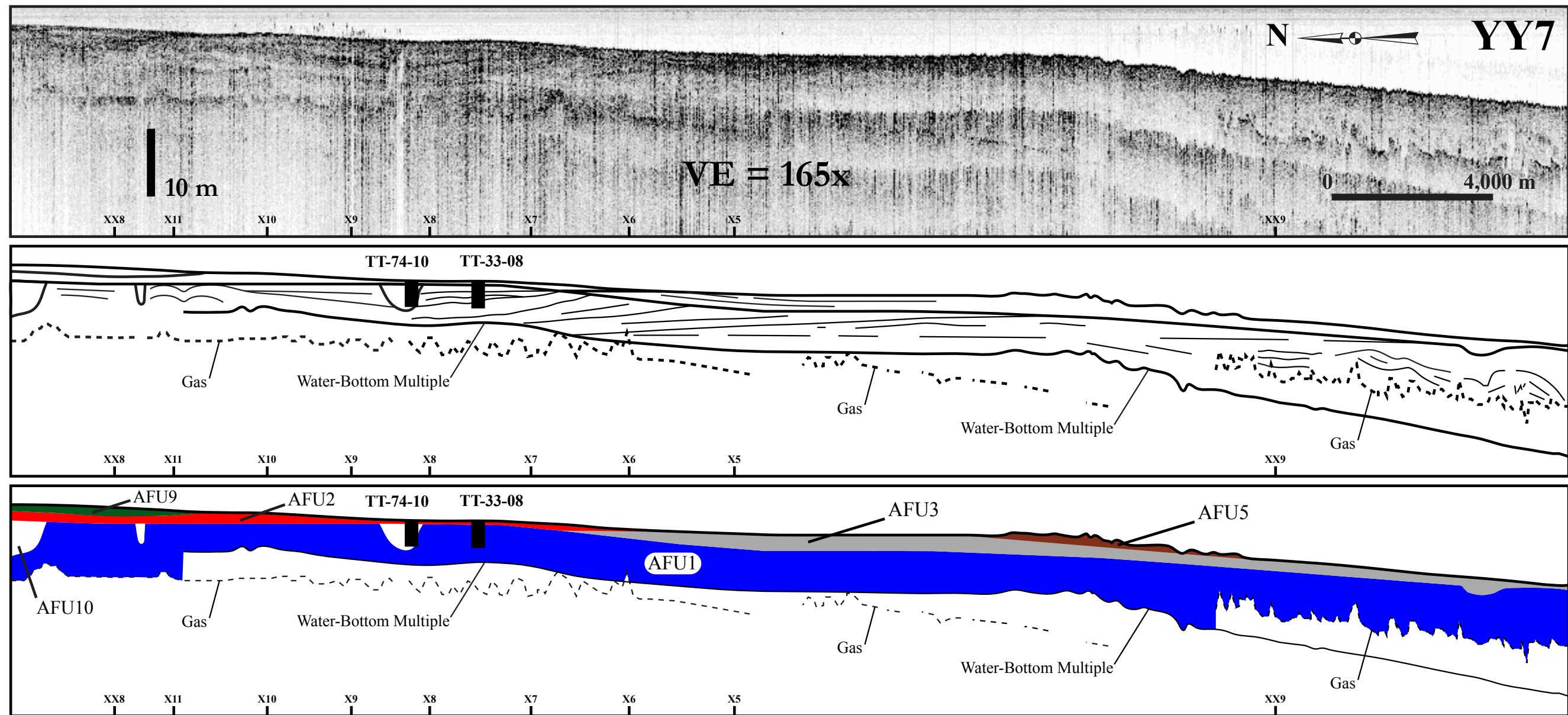






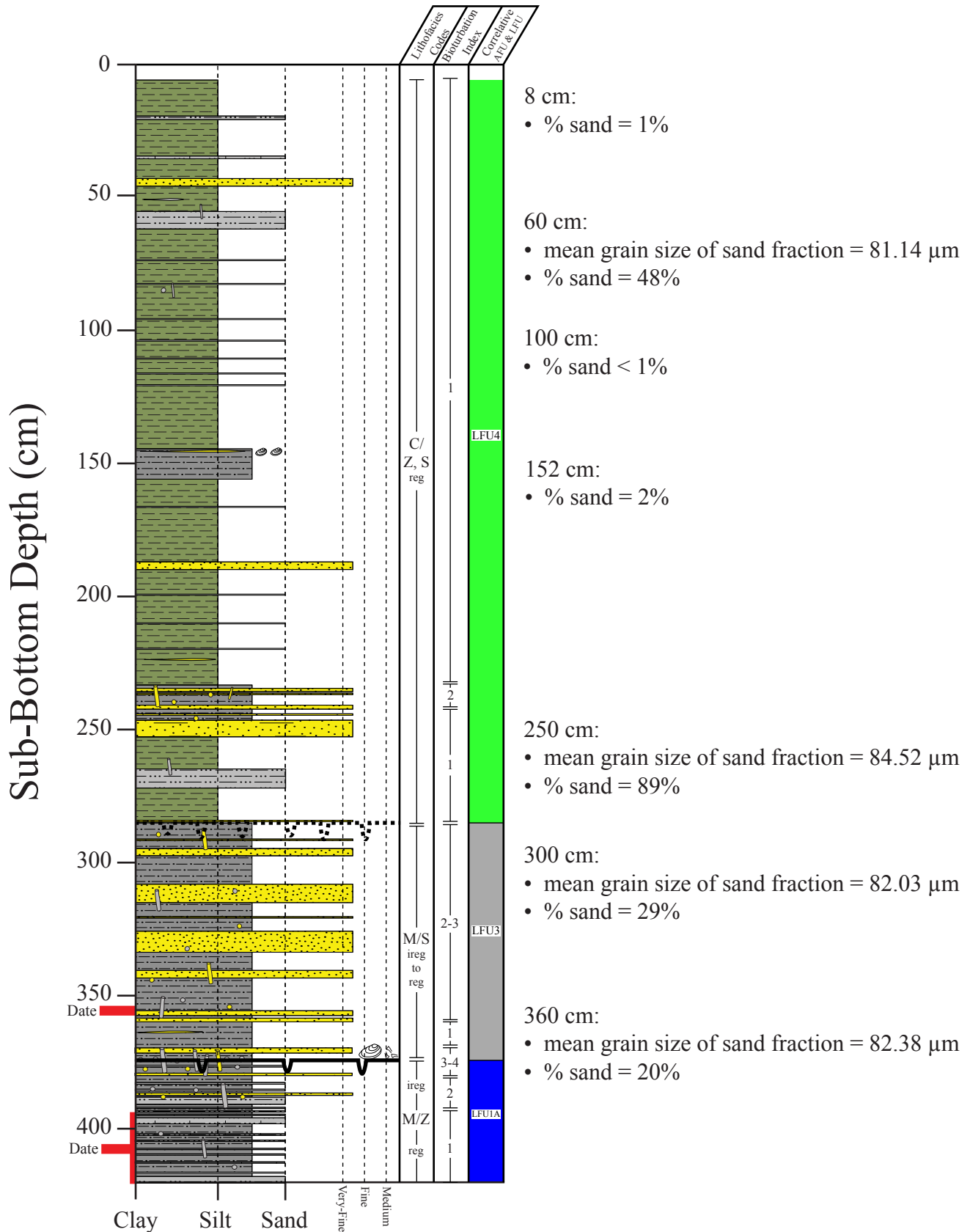




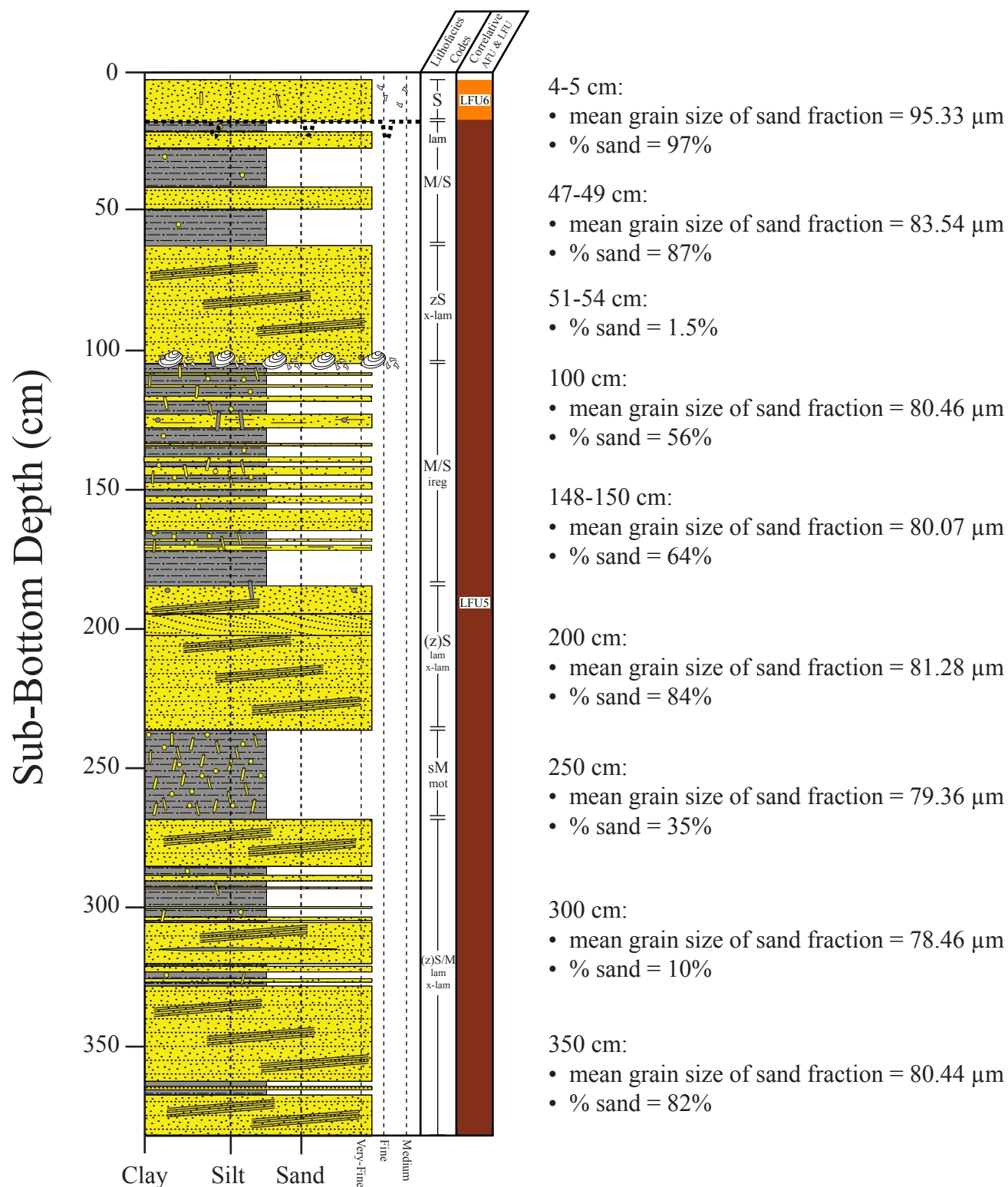




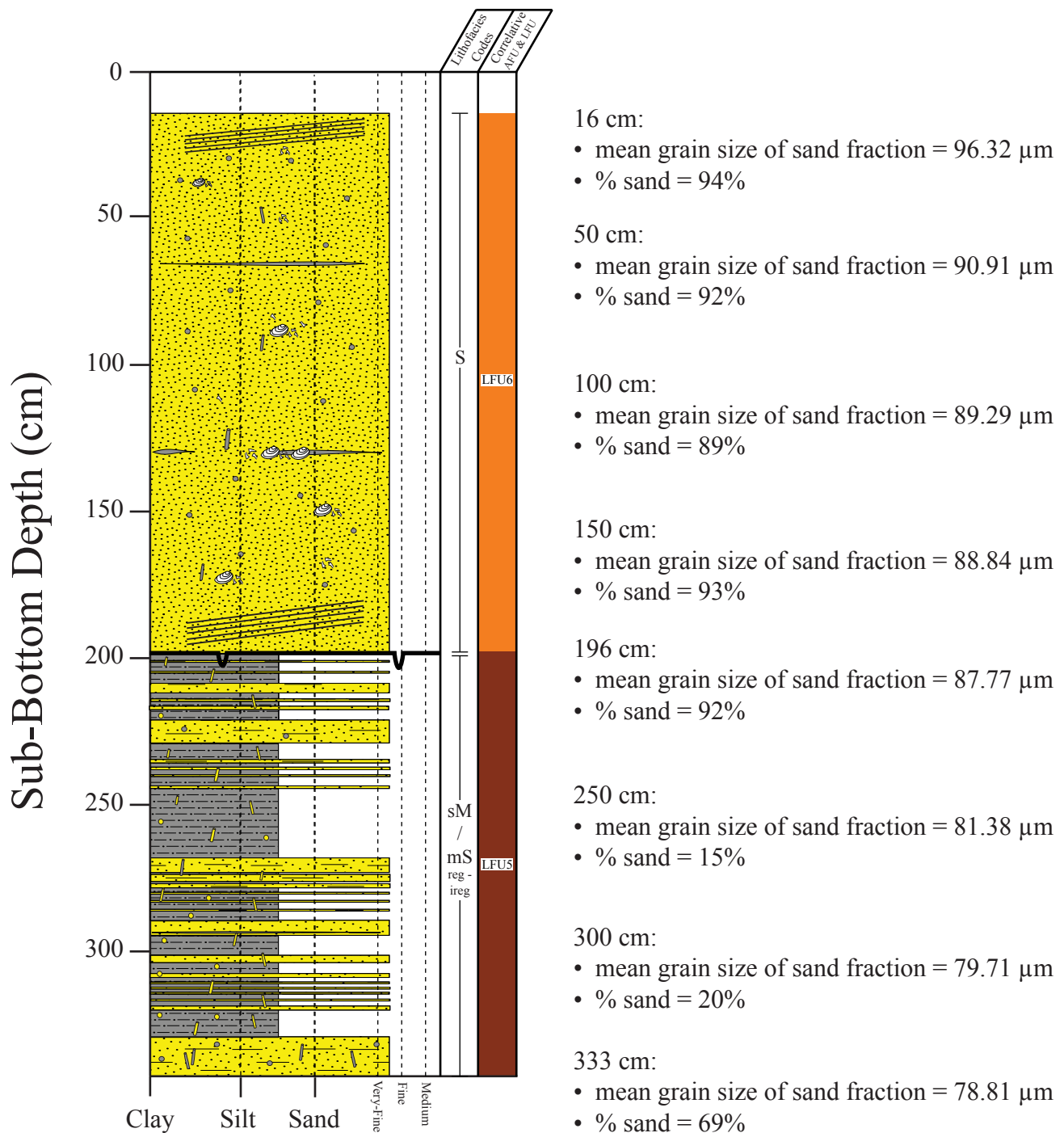
# Trinity-Tiger Shoals Project Vibracore TT-01-08



# Trinity-Tiger Shoals Project Vibracore TT-02-08

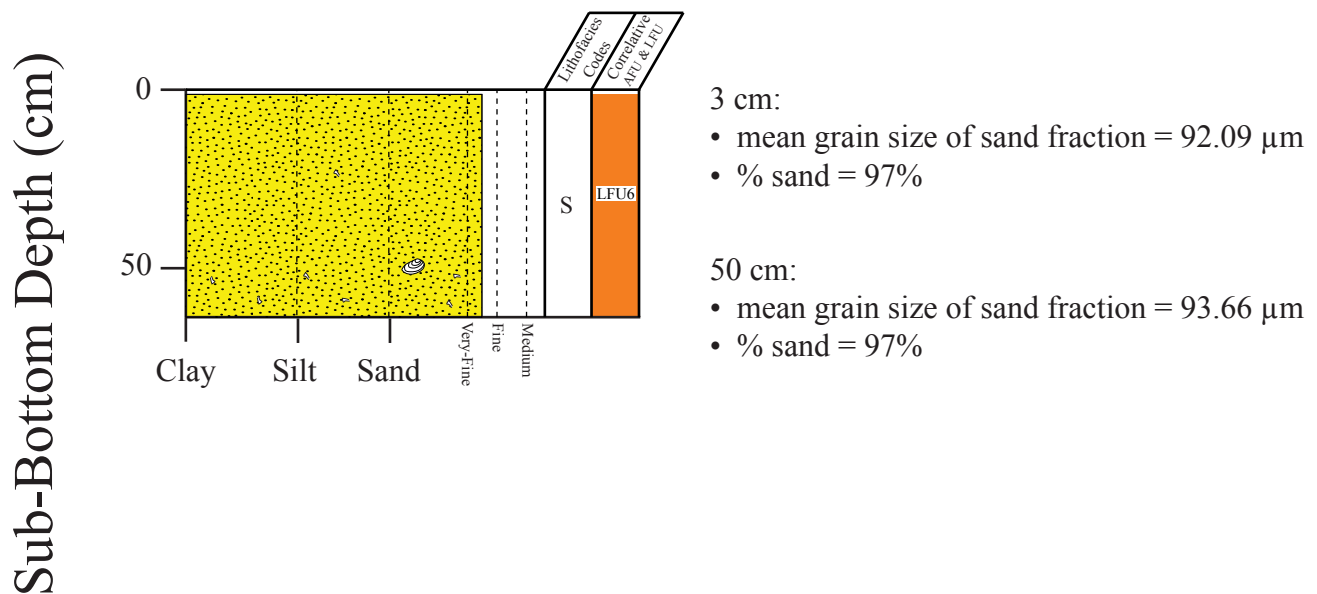


# Trinity-Tiger Shoals Project Vibracore TT-03-08

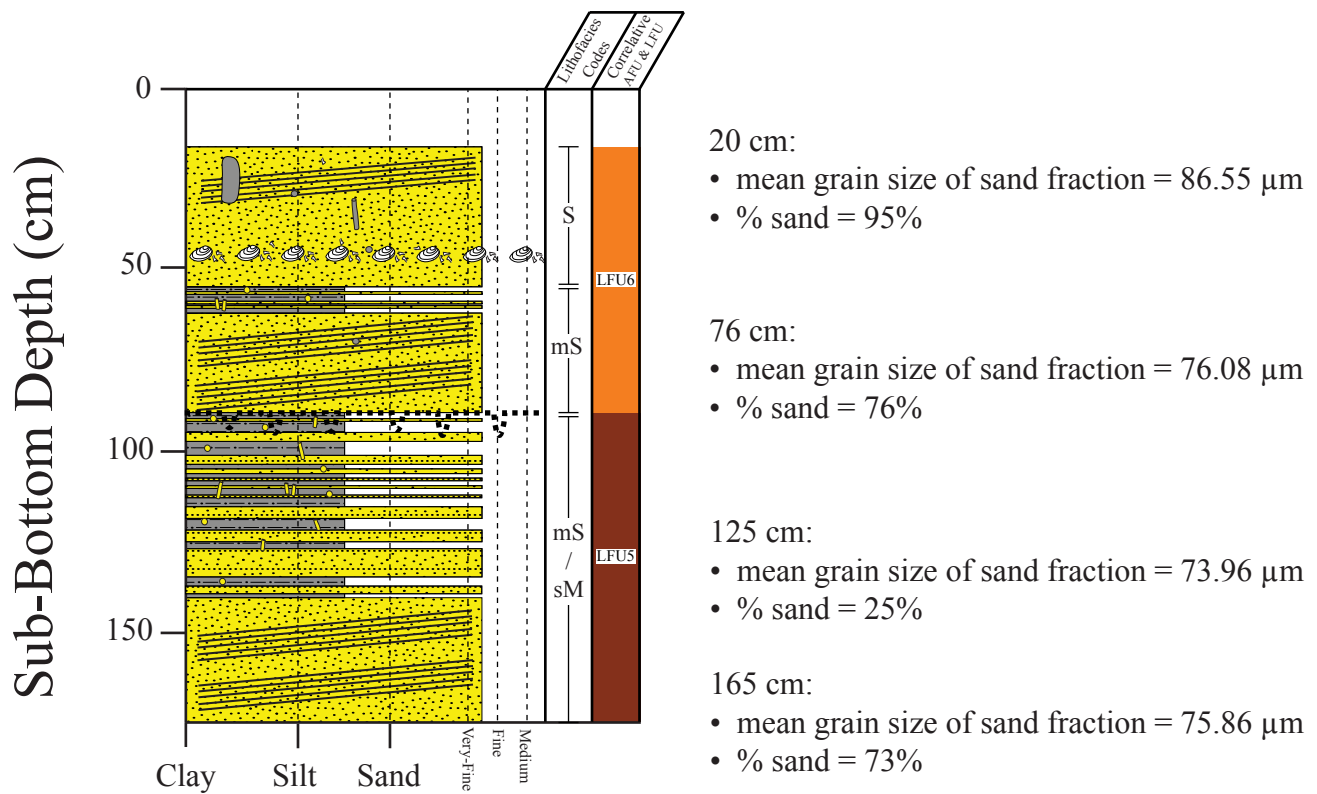




# Trinity-Tiger Shoals Project Vibracore TT-04-08

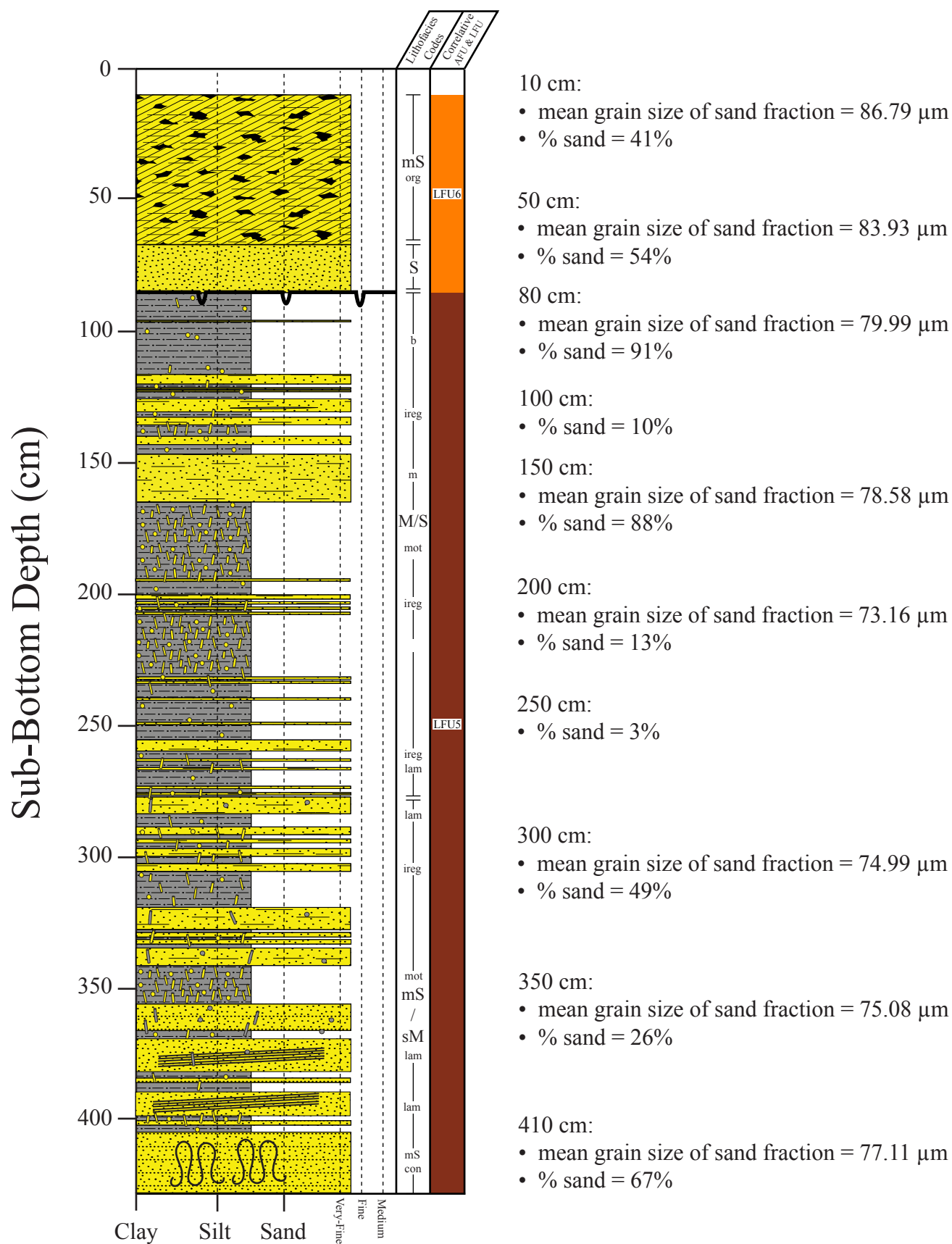


# Trinity-Tiger Shoals Project Vibracore TT-05-08

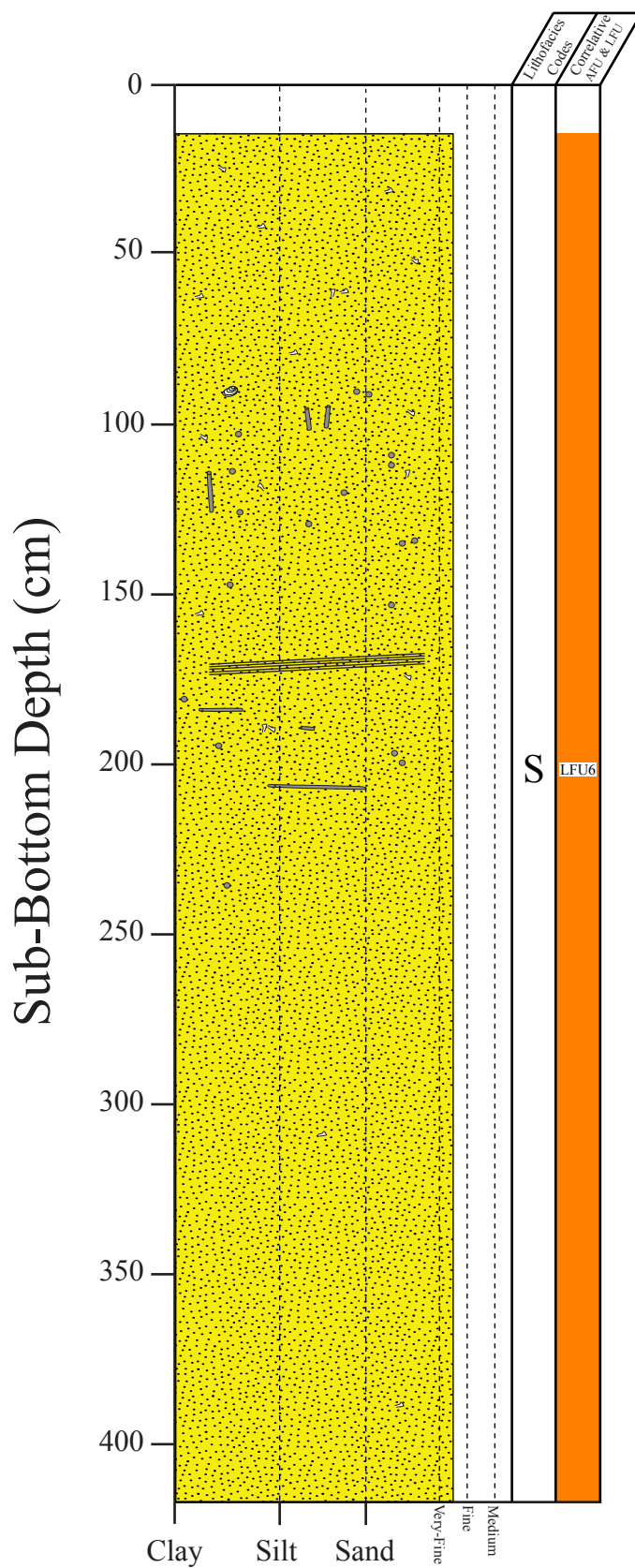


# Trinity-Tiger Shoals Project Vibracore

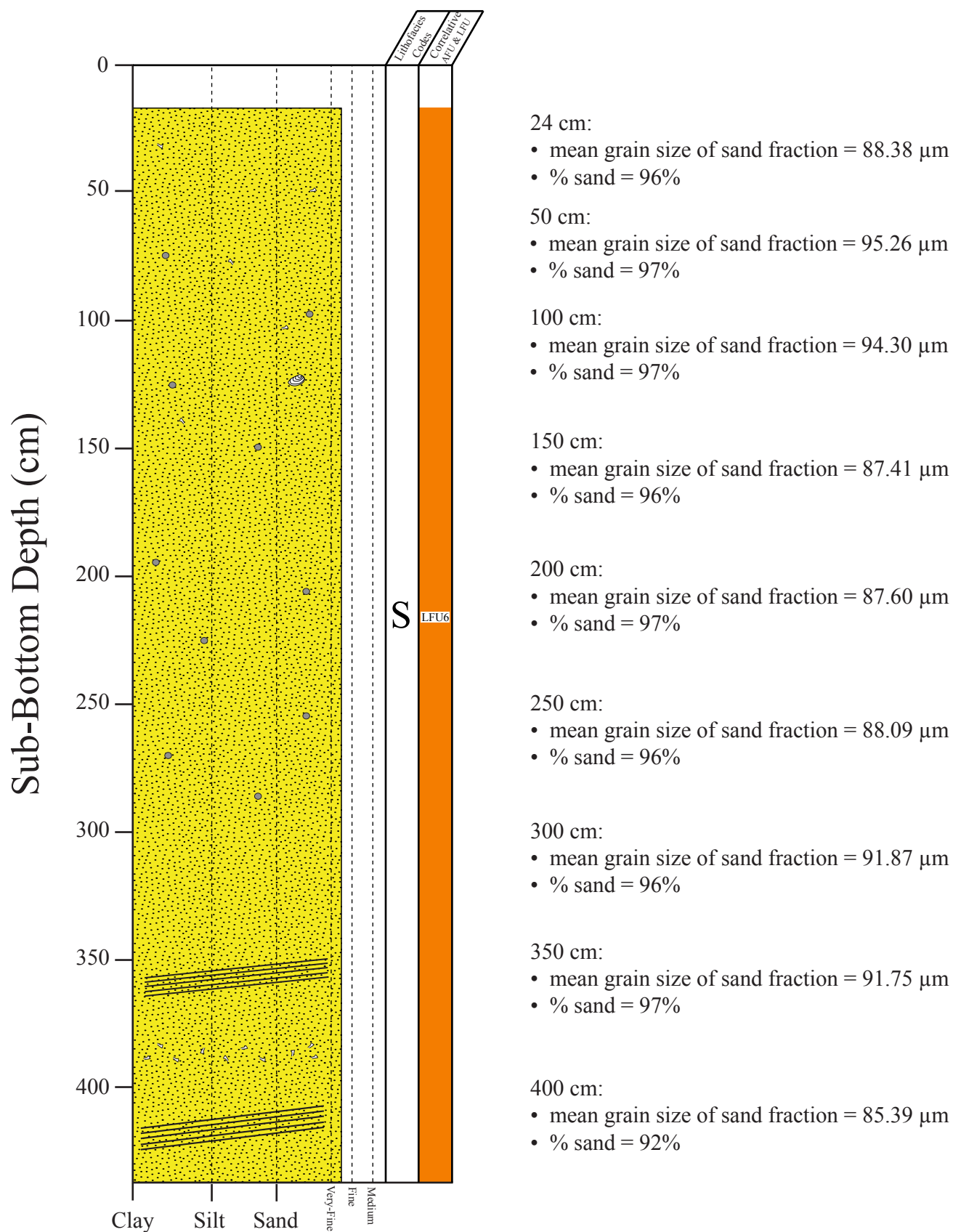
## TT-06-08



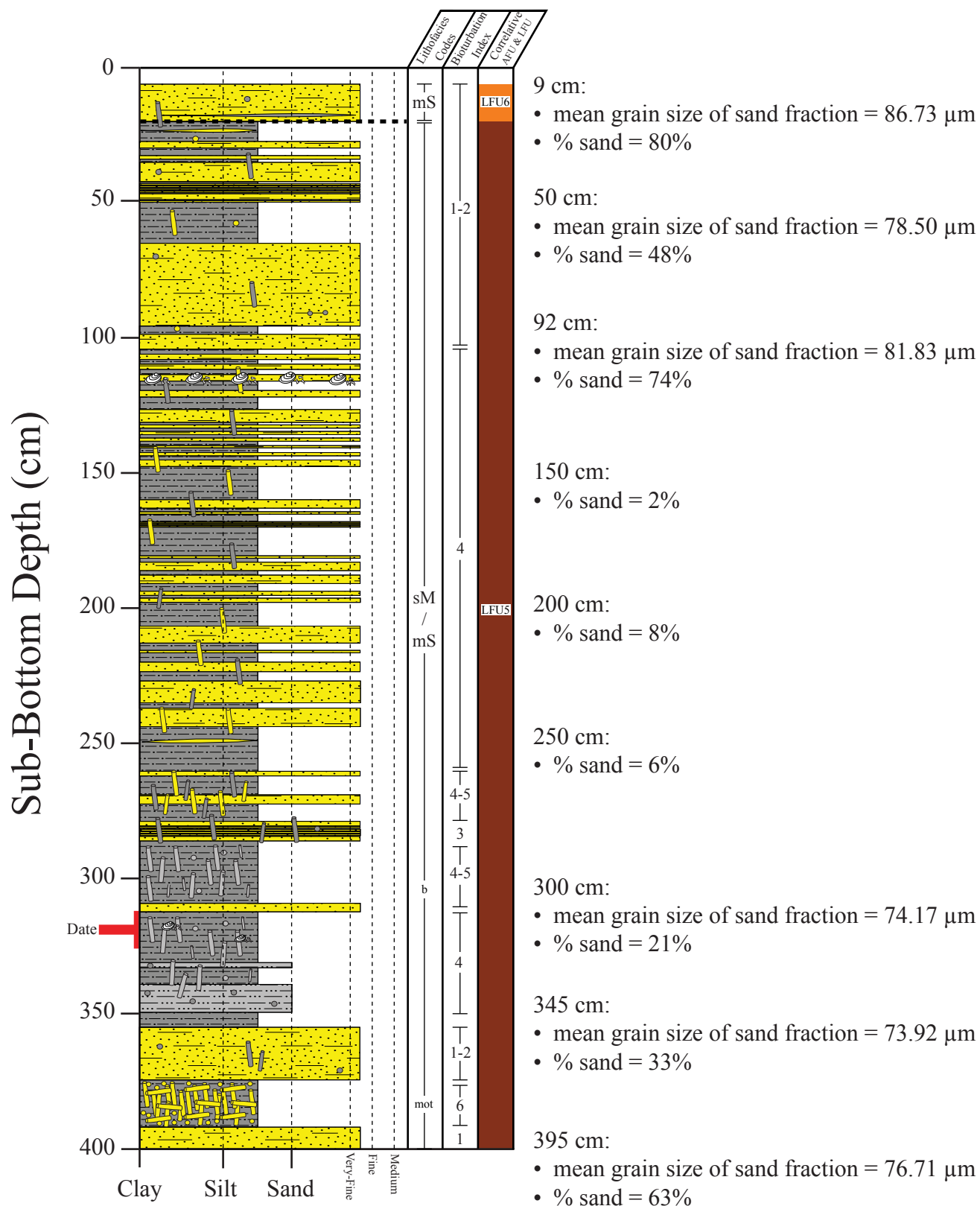
# Trinity-Tiger Shoals Project Vibracore TT-08-10



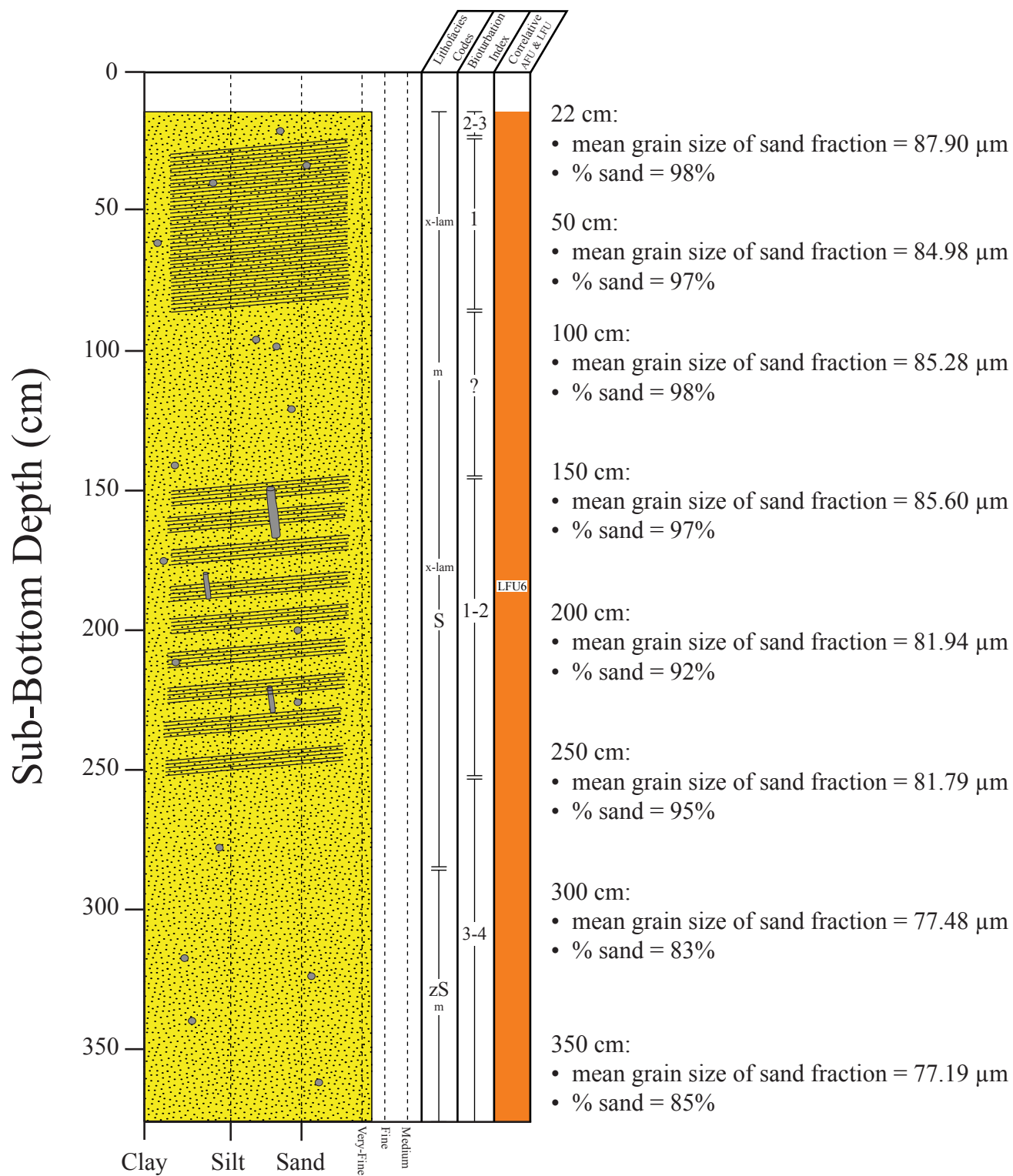
# Trinity-Tiger Shoals Project Vibracore TT-09-10



# Trinity-Tiger Shoals Project Vibracore TT-10-08

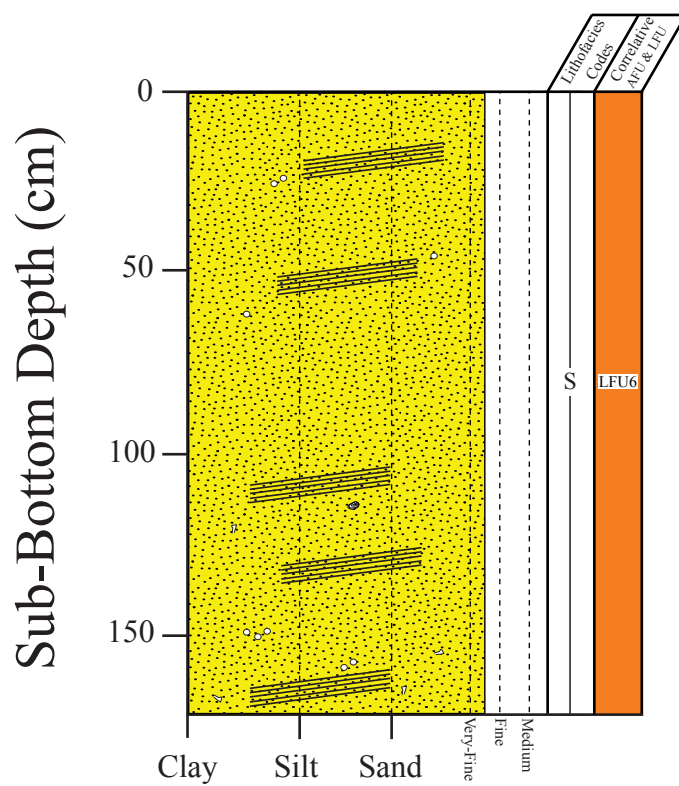


# Trinity-Tiger Shoals Project Vibracore TT-12-08

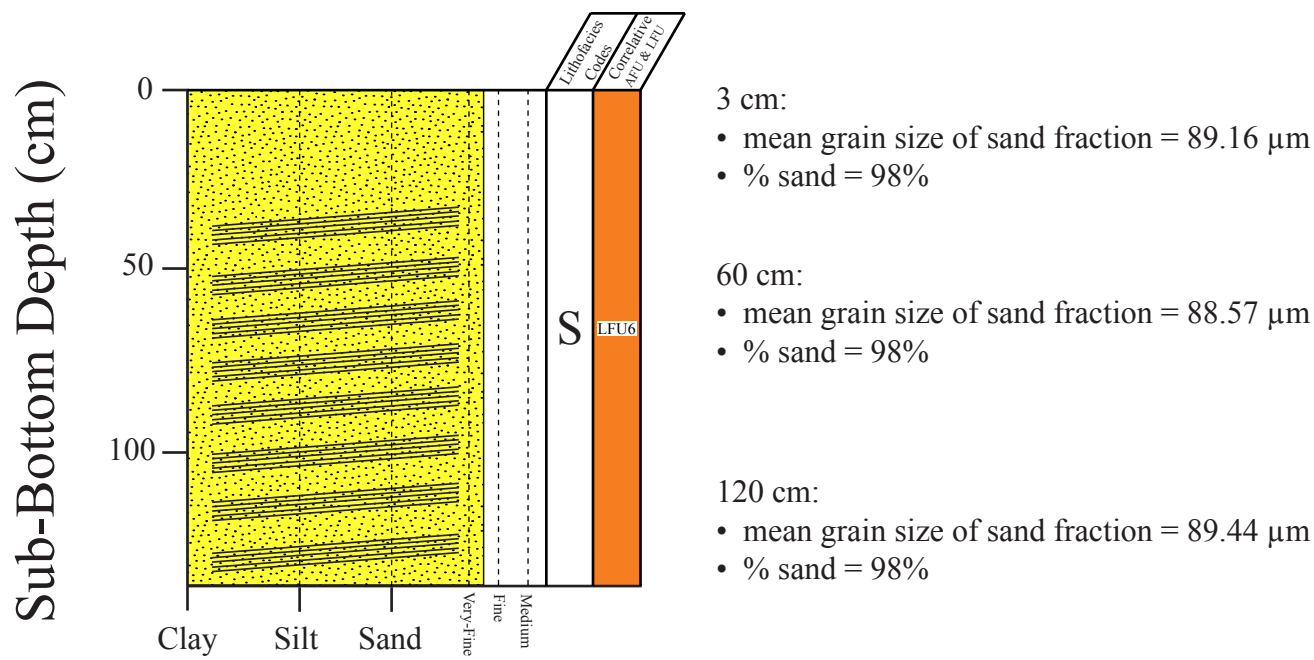




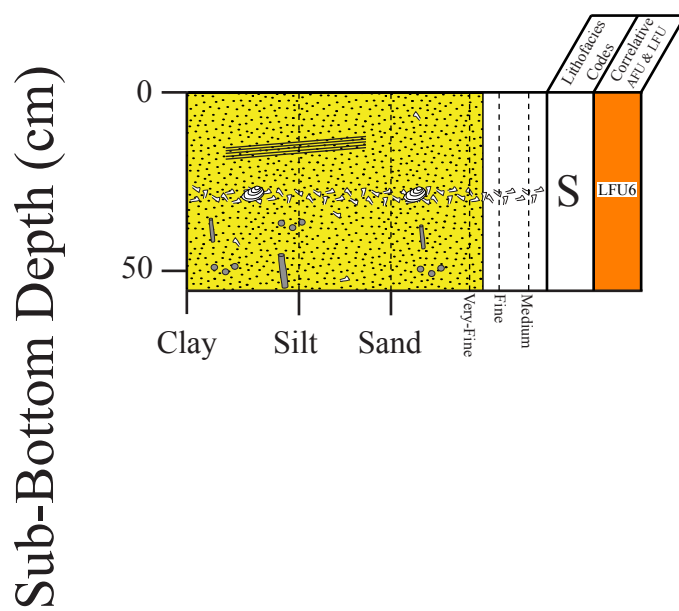
# Trinity-Tiger Shoals Project Vibracore TT-13-10



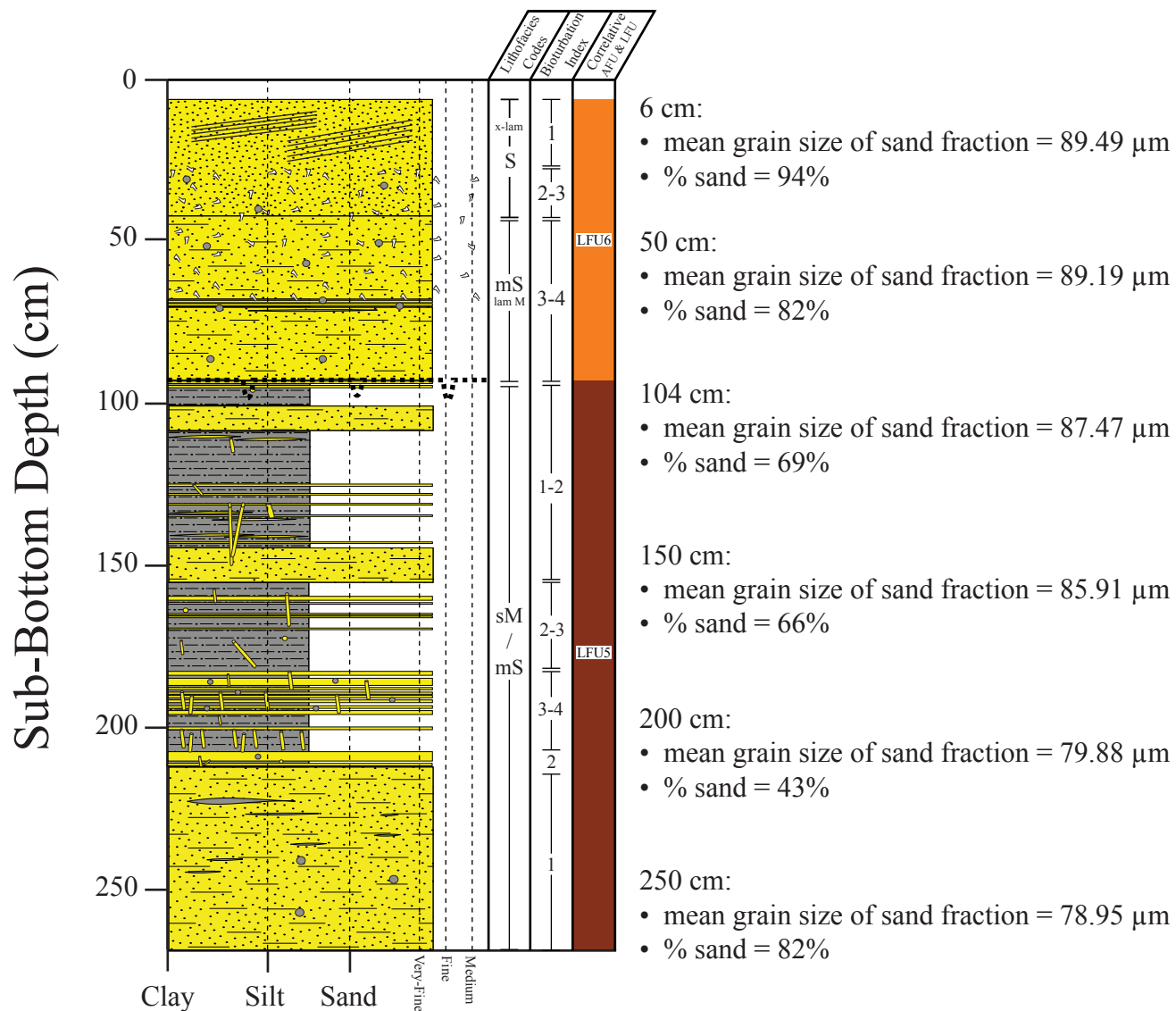
Trinity-Tiger Shoals Project Vibracore  
TT-15-08



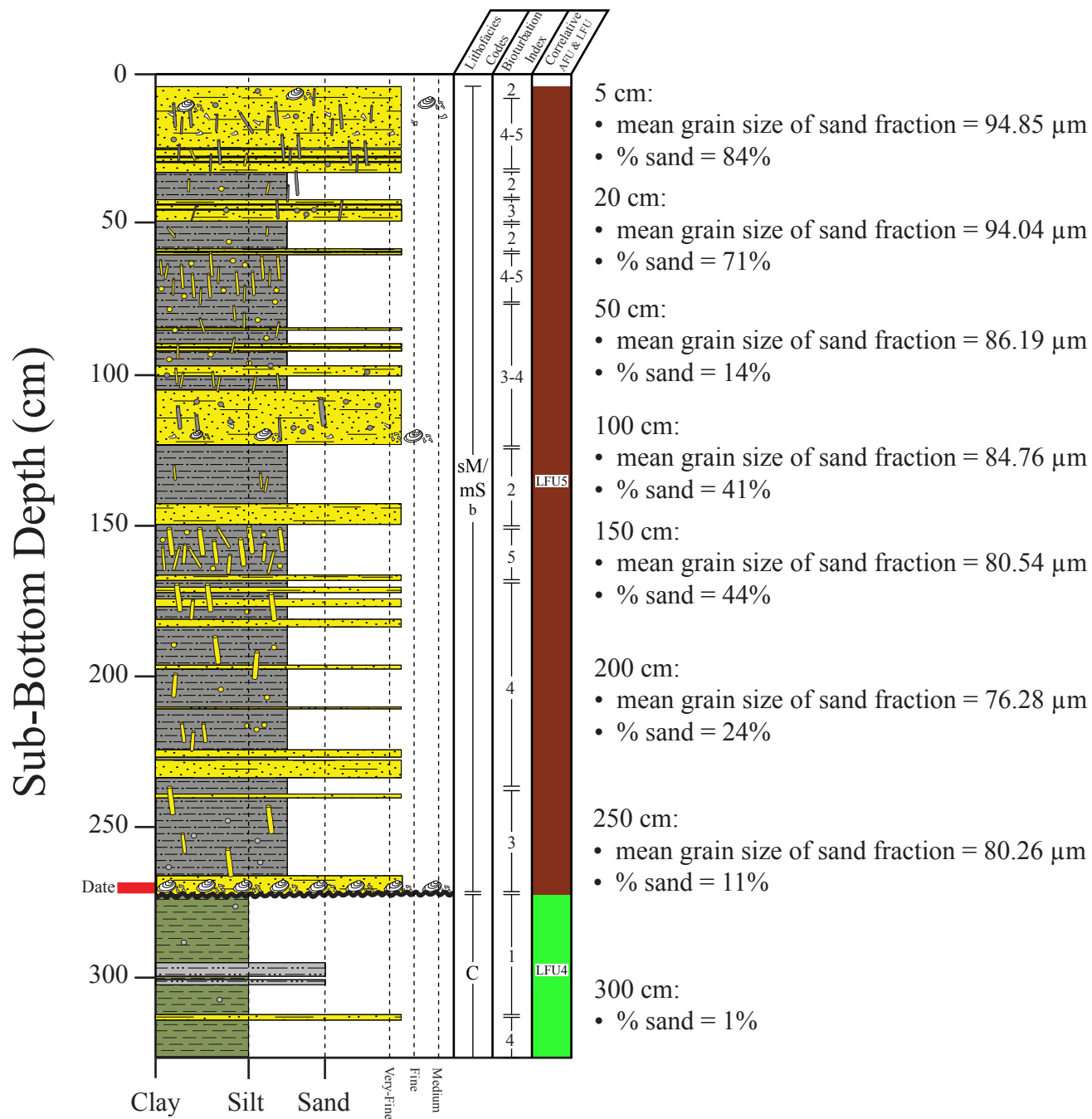
# Trinity-Tiger Shoals Project Vibracore TT-17-10



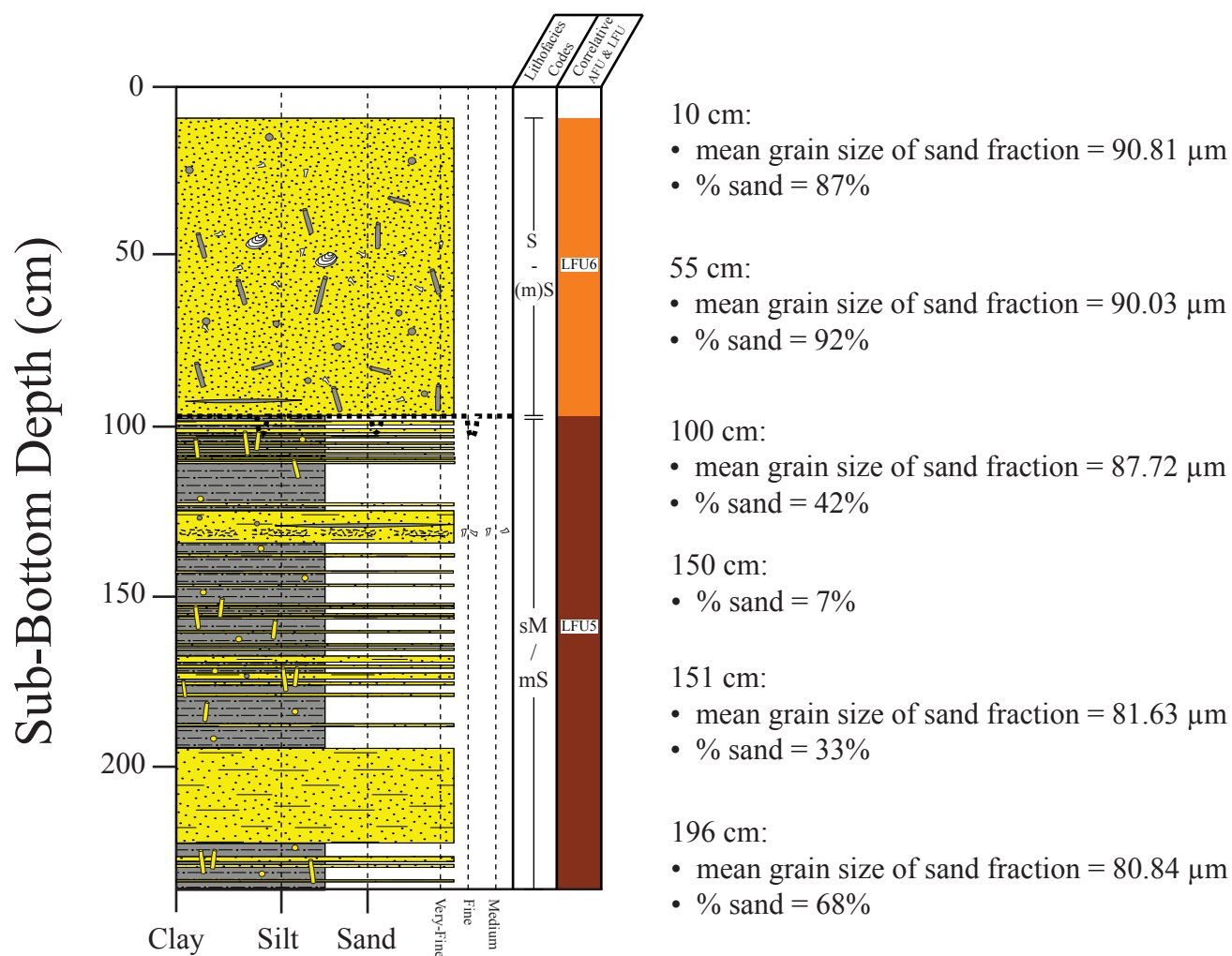
# Trinity-Tiger Shoals Project Vibracore TT-19-08



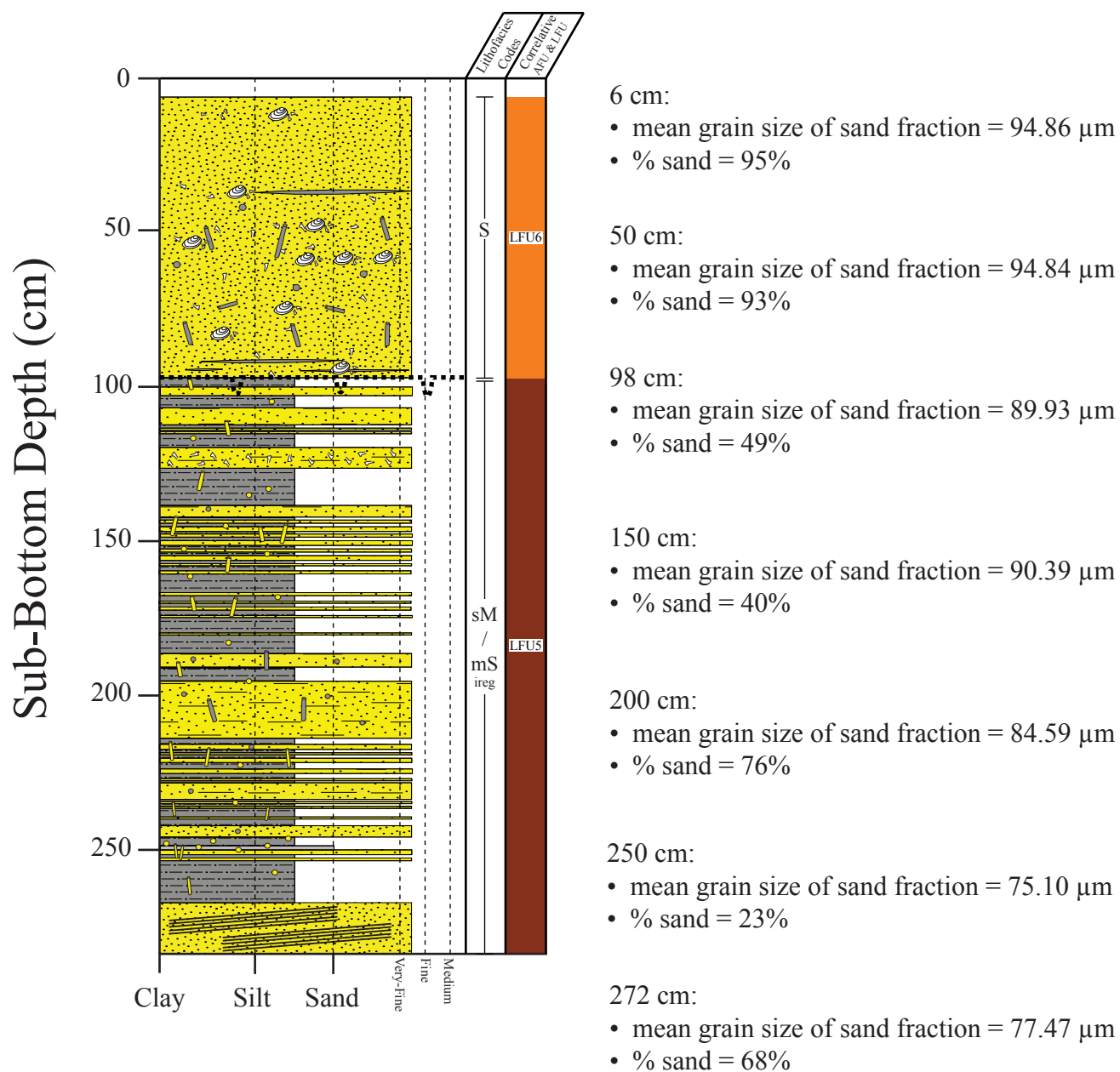
# Trinity-Tiger Shoals Project Vibracore TT-20-08



# Trinity-Tiger Shoals Project Vibracore TT-21-08

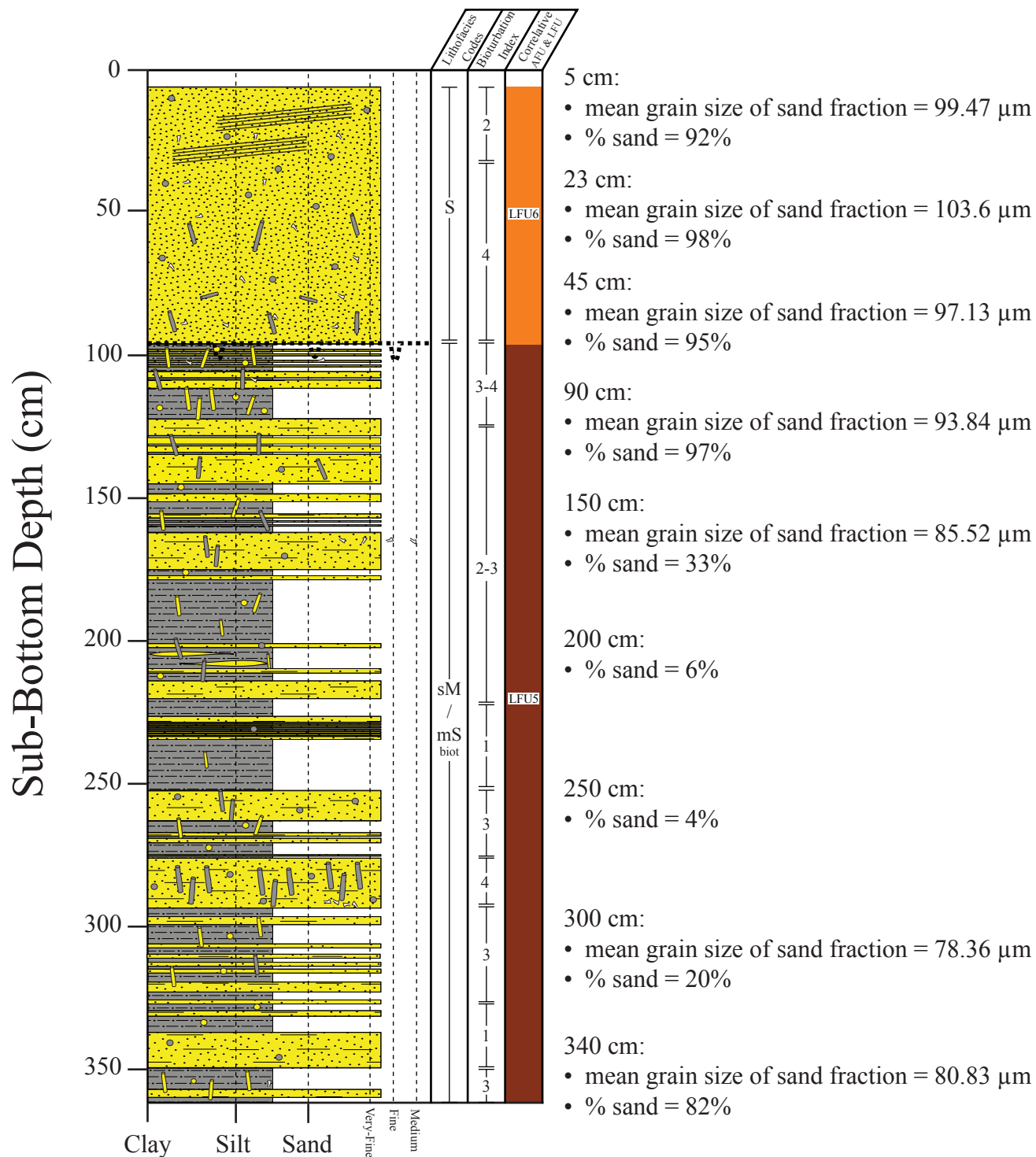


# Trinity-Tiger Shoals Project Vibracore TT-22-08

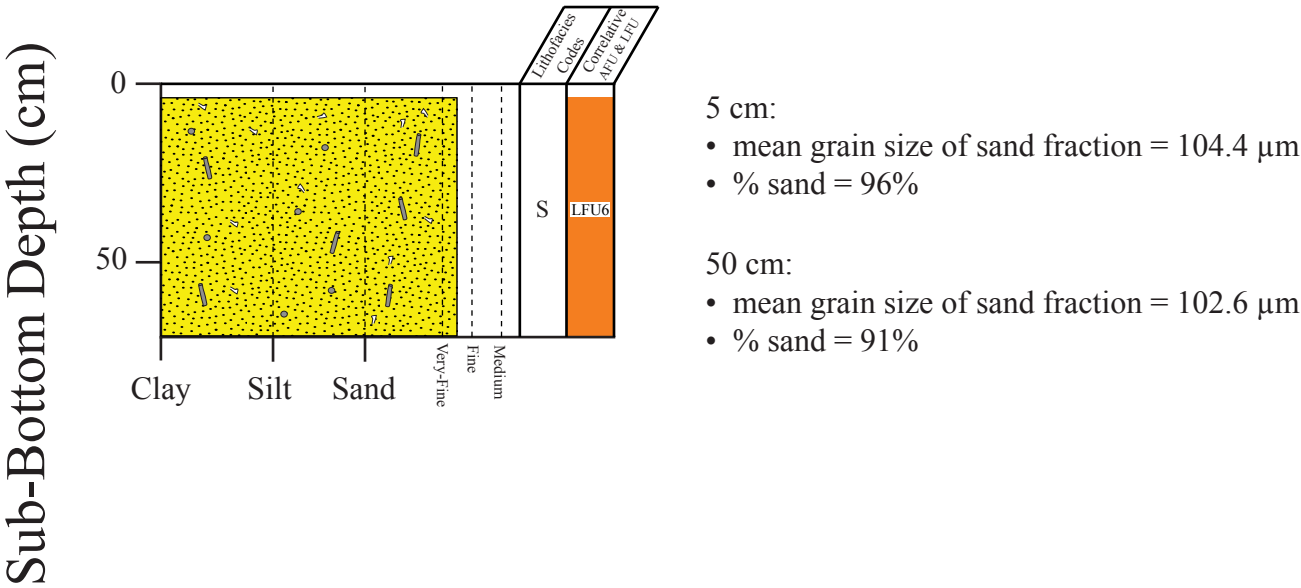




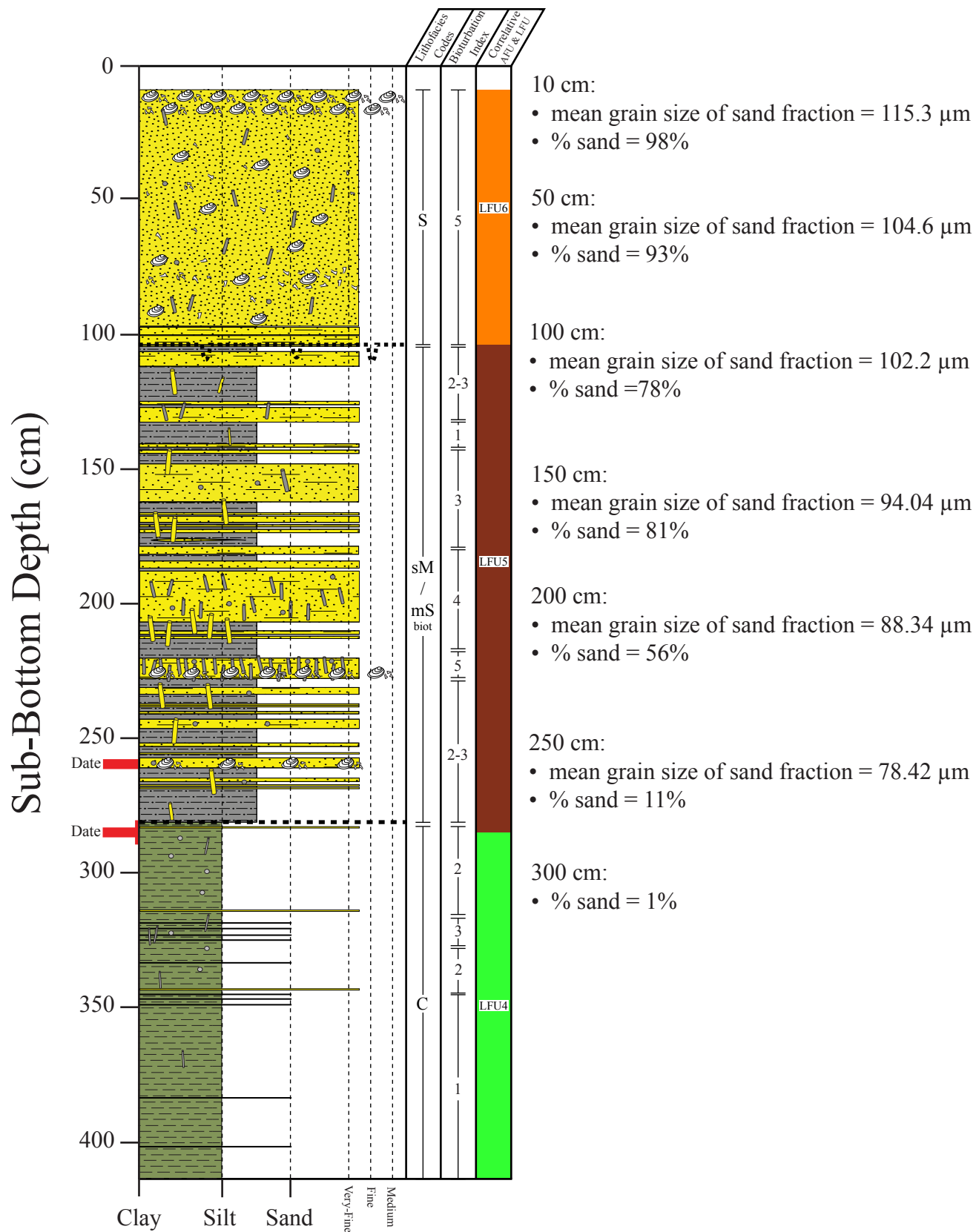
# Trinity-Tiger Shoals Project Vibracore TT-23-08



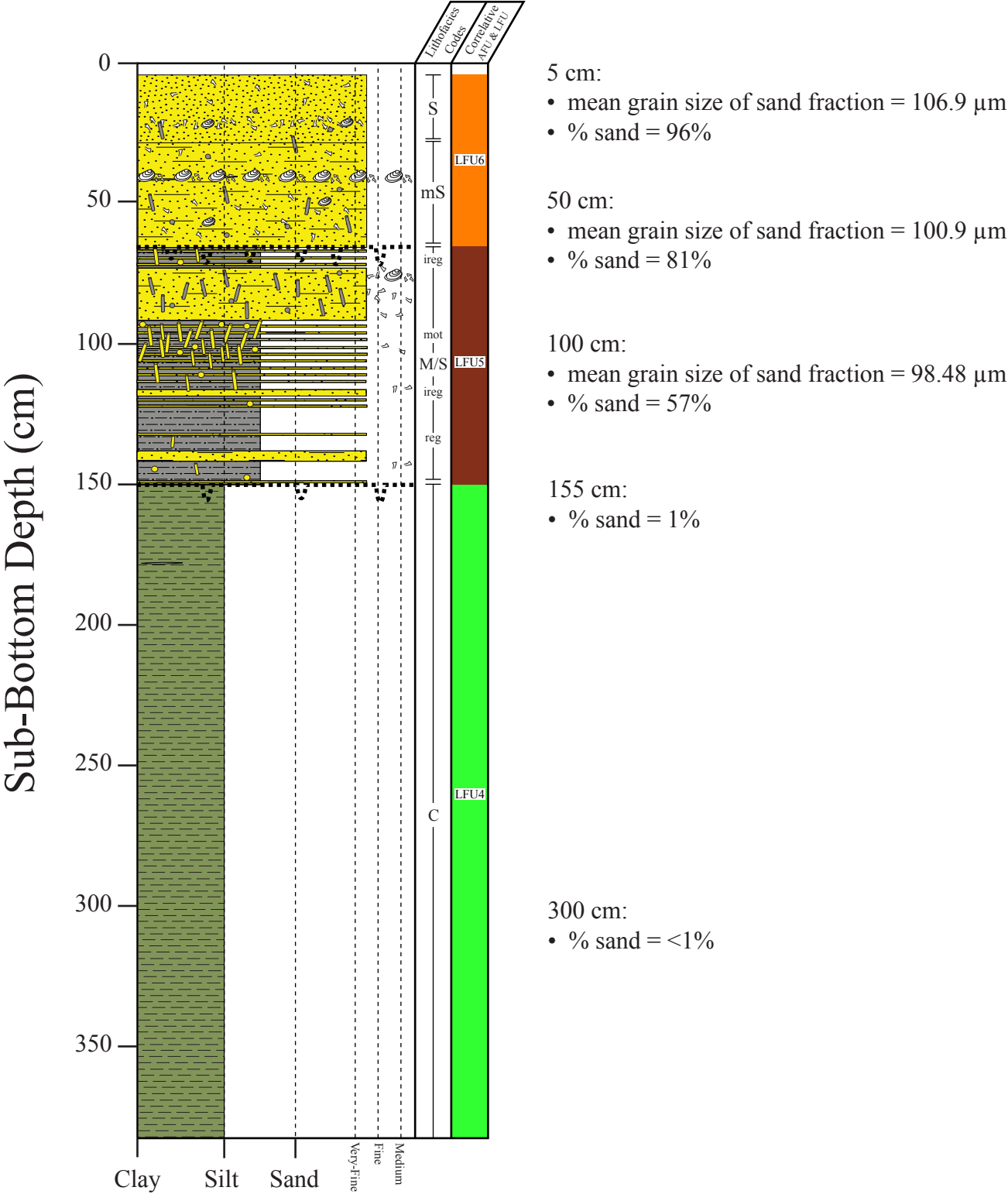
Trinity-Tiger Shoals Project Vibracore  
TT-24-08



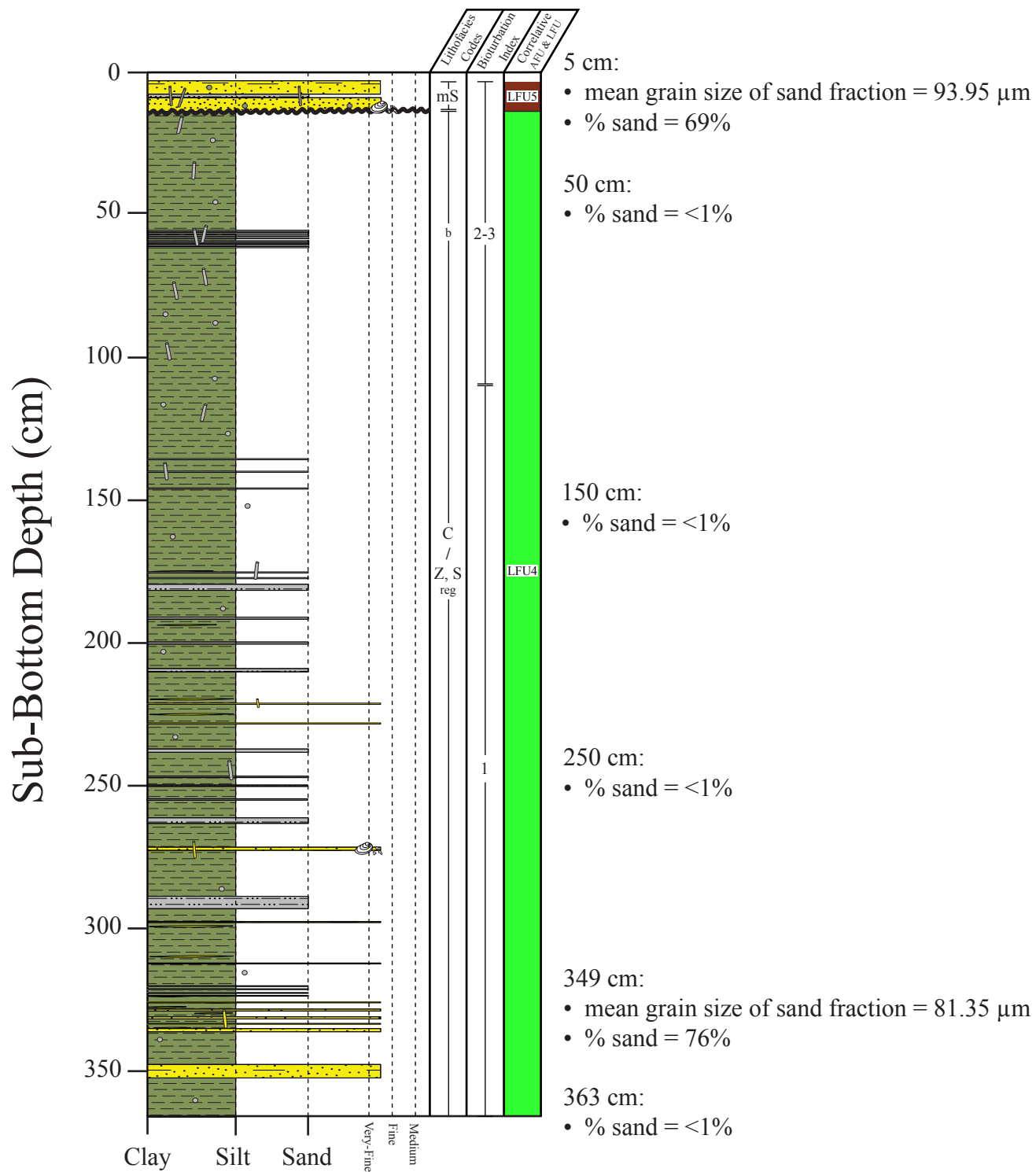
# Trinity-Tiger Shoals Project Vibracore TT-25-08



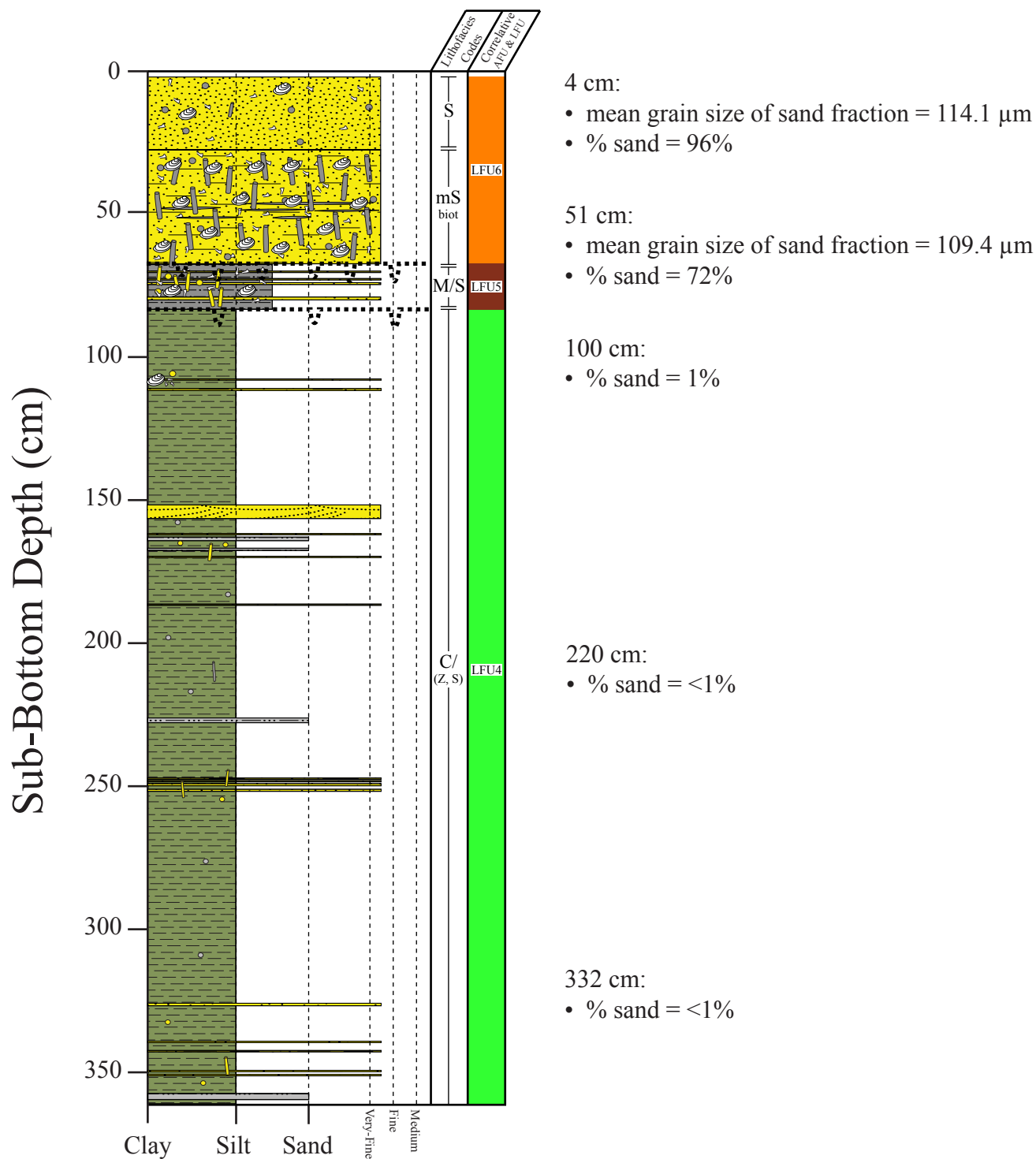
# Trinity-Tiger Shoals Project Vibracore TT-26-08



# Trinity-Tiger Shoals Project Vibracore TT-27-08

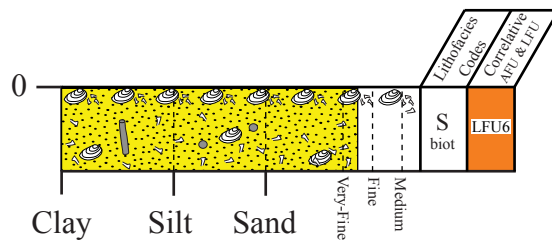


# Trinity-Tiger Shoals Project Vibracore TT-28-08



Sub-Bottom Depth (cm)

## Trinity-Tiger Shoals Project Vibracore TT-29-08



2 cm:

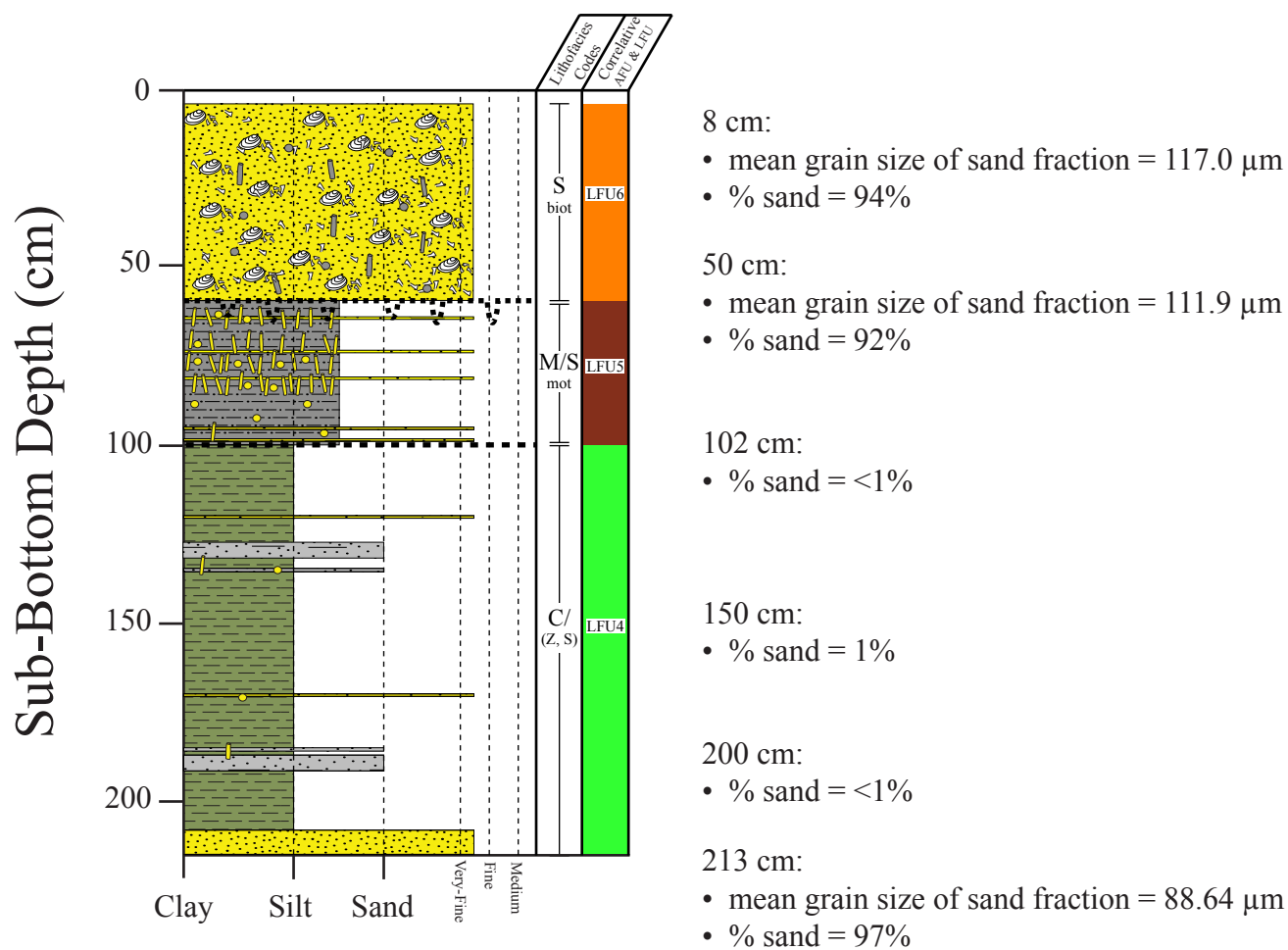
- mean grain size of sand fraction = 120.5  $\mu\text{m}$
- % sand = 93%

20 cm:

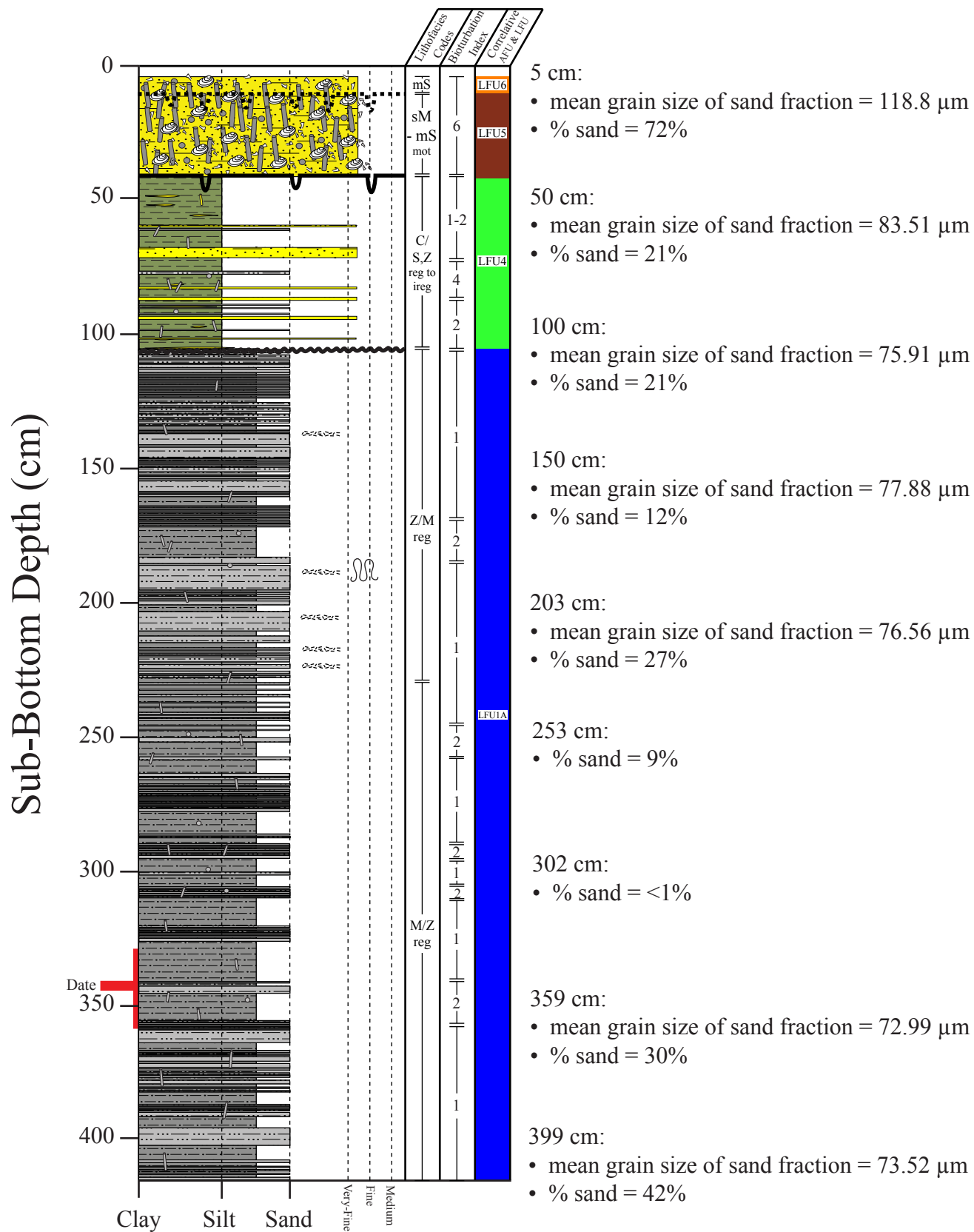
- mean grain size of sand fraction = 111.9  $\mu\text{m}$
- % sand = 96%



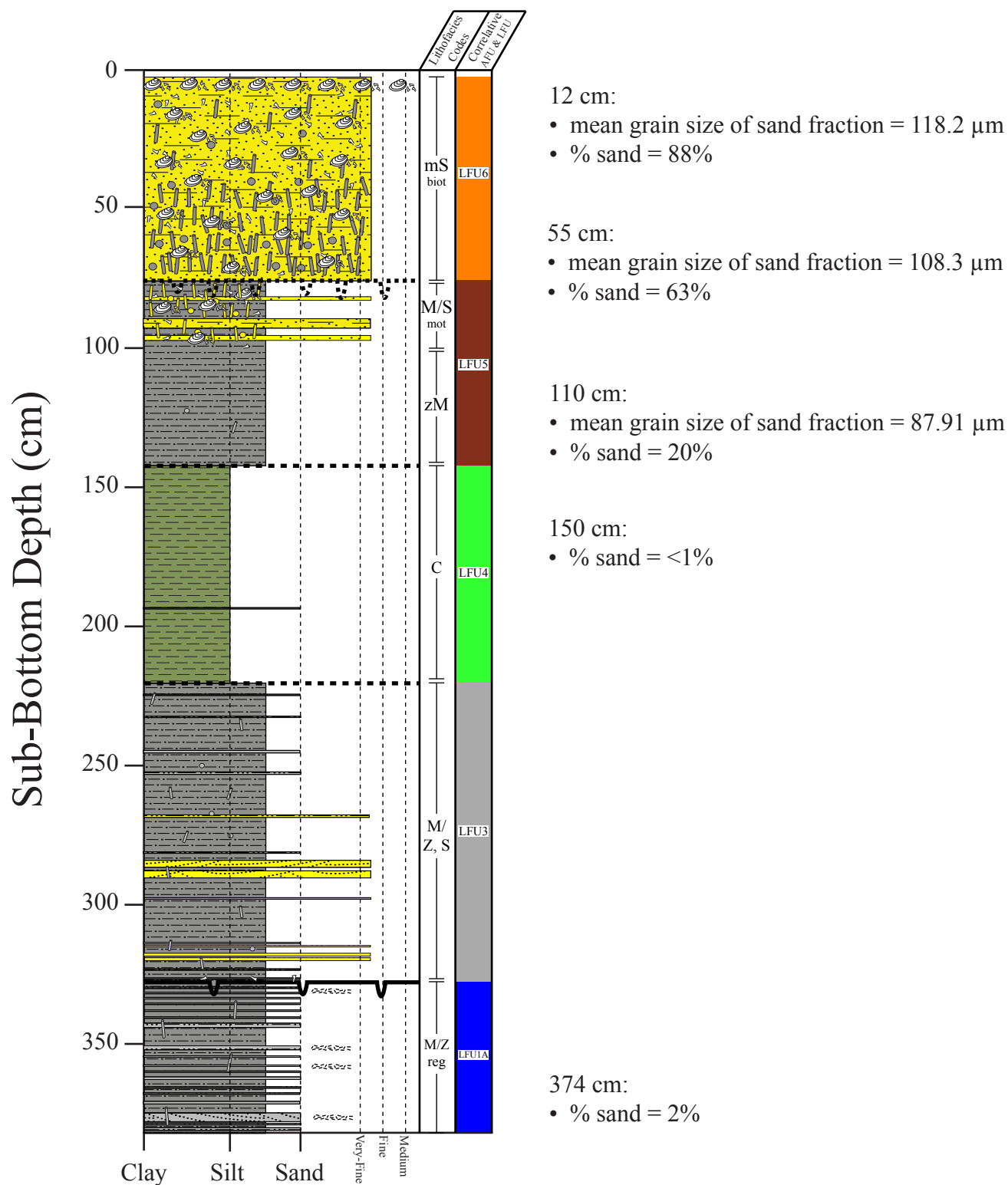
# Trinity-Tiger Shoals Project Vibracore TT-30-08



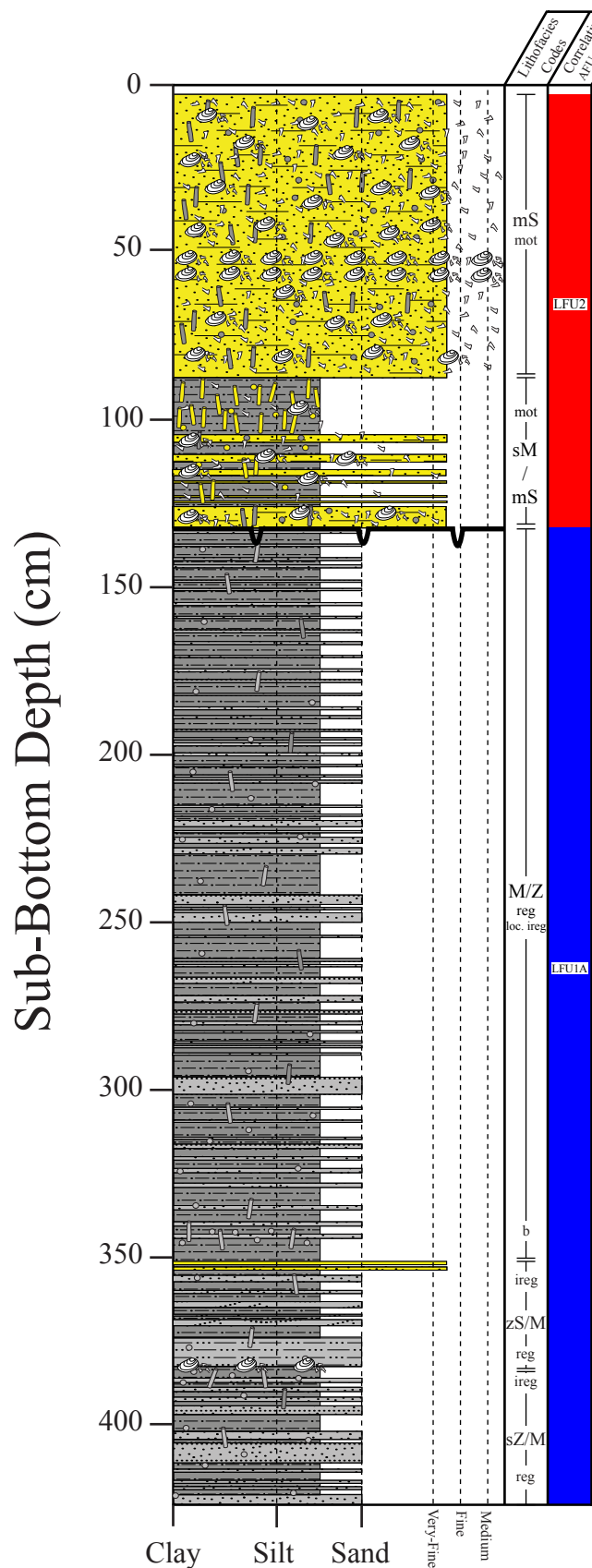
# Trinity-Tiger Shoals Project Vibracore TT-31-08



# Trinity-Tiger Shoals Project Vibracore TT-32-08



# Trinity-Tiger Shoals Project Vibracore TT-33-08



4 cm:

- mean grain size of sand fraction = 130.9  $\mu\text{m}$
- % sand = 68%

50 cm:

Trimodal grain size:

- mean grain size of sand fraction = 132.4  $\mu\text{m}$ 
  - 65% (% of distribution)
- mean grain size of sand fraction = 231.2  $\mu\text{m}$ 
  - 20% (% of distribution)
- mean grain size of sand fraction = 352.7  $\mu\text{m}$ 
  - 27.8% (% of distribution)
- % sand = 85%

100 cm:

Bimodal grain size:

- mean grain size of sand fraction = 74.99  $\mu\text{m}$ 
  - 46.4% (% of distribution)
- mean grain size of sand fraction = 114.1  $\mu\text{m}$ 
  - 74.2% (% of distribution)
- % sand = 13%

150 cm:

- mean grain size of sand fraction = 93.91  $\mu\text{m}$
- % sand = 22%

200 cm:

- % sand = 8%

248 cm:

- % sand = 2%

300 cm:

- % sand = 1%

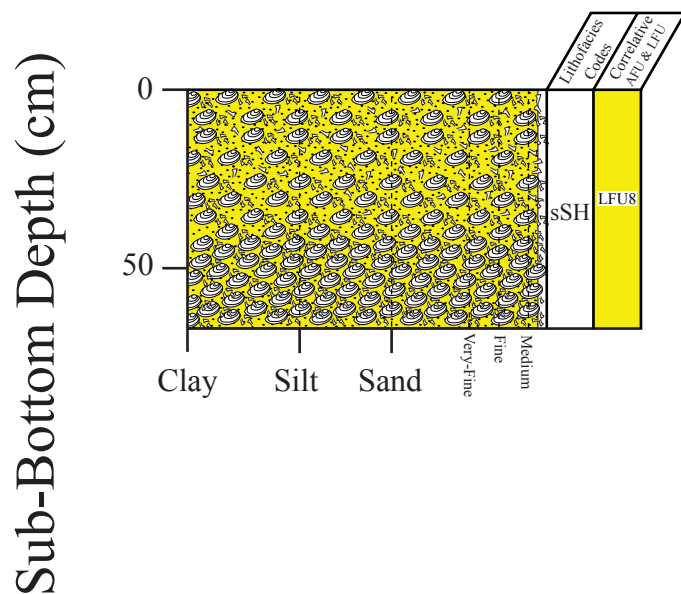
351 cm:

- mean grain size of sand fraction = 81.64  $\mu\text{m}$
- % sand = 48%

406 cm:

- mean grain size of sand fraction = 71.25  $\mu\text{m}$
- % sand = 16%

## Trinity-Tiger Shoals Project Vibracore TT-34-08



0 cm:

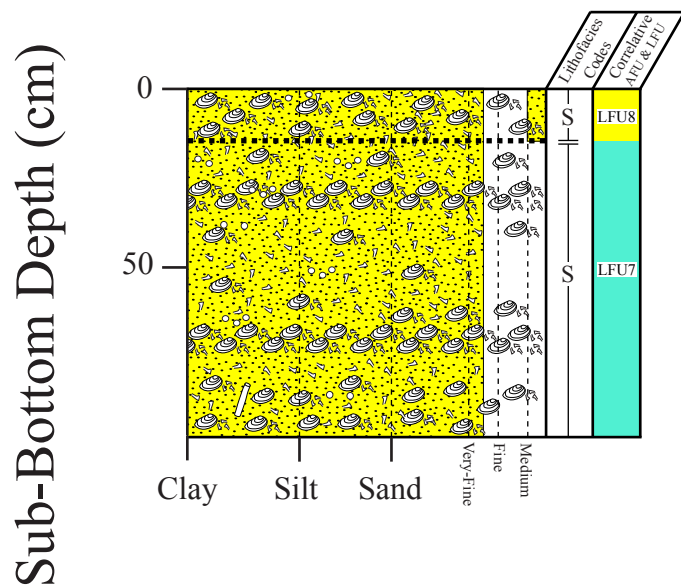
Bimodal grain size:

- mean grain size of sand fraction = 127.3  $\mu\text{m}$ 
  - 17% (% of distribution)
- mean grain size of sand fraction = 316.2  $\mu\text{m}$ 
  - 86% (% of distribution)
- % sand = >99%

50 cm:

- mean grain size of sand fraction = 334.9  $\mu\text{m}$
- % sand = >99%

# Trinity-Tiger Shoals Project Vibracore TT-35-08



0 cm:

Bimodal grain size:

- mean grain size of sand fraction = 123.1  $\mu\text{m}$ 
  - 81% (% of distribution)
- mean grain size of sand fraction = 301.4  $\mu\text{m}$ 
  - 21% (% of distribution)
- % sand = 99%

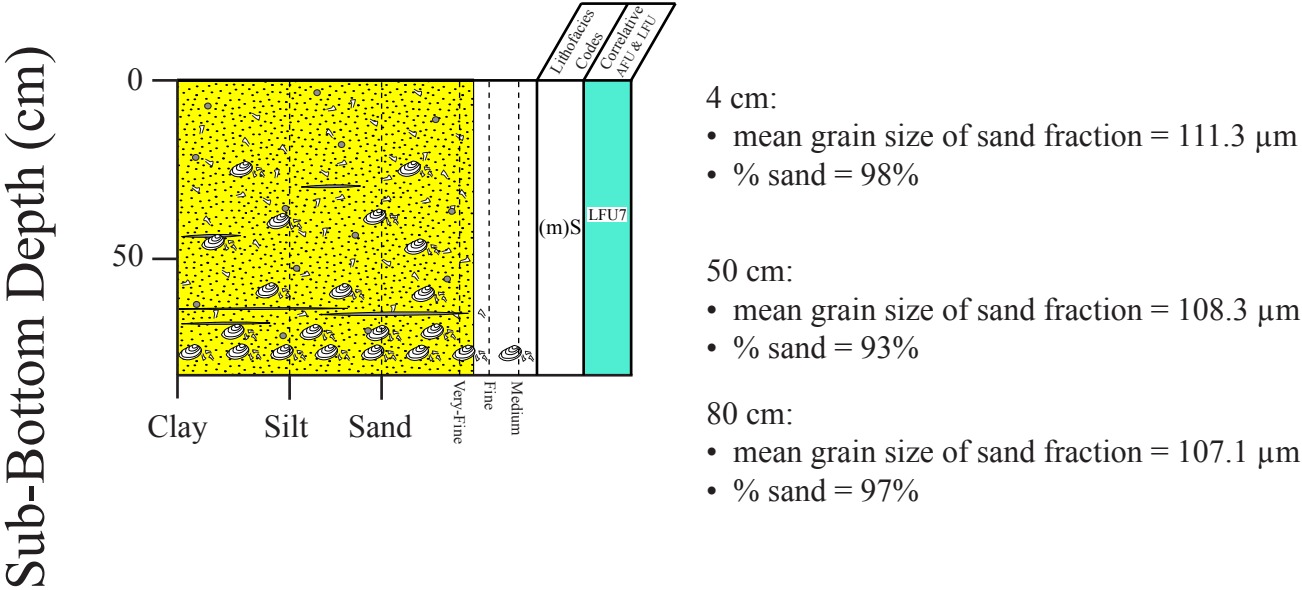
50 cm:

- mean grain size of sand fraction = 116.0  $\mu\text{m}$
- % sand = 98%

94 cm:

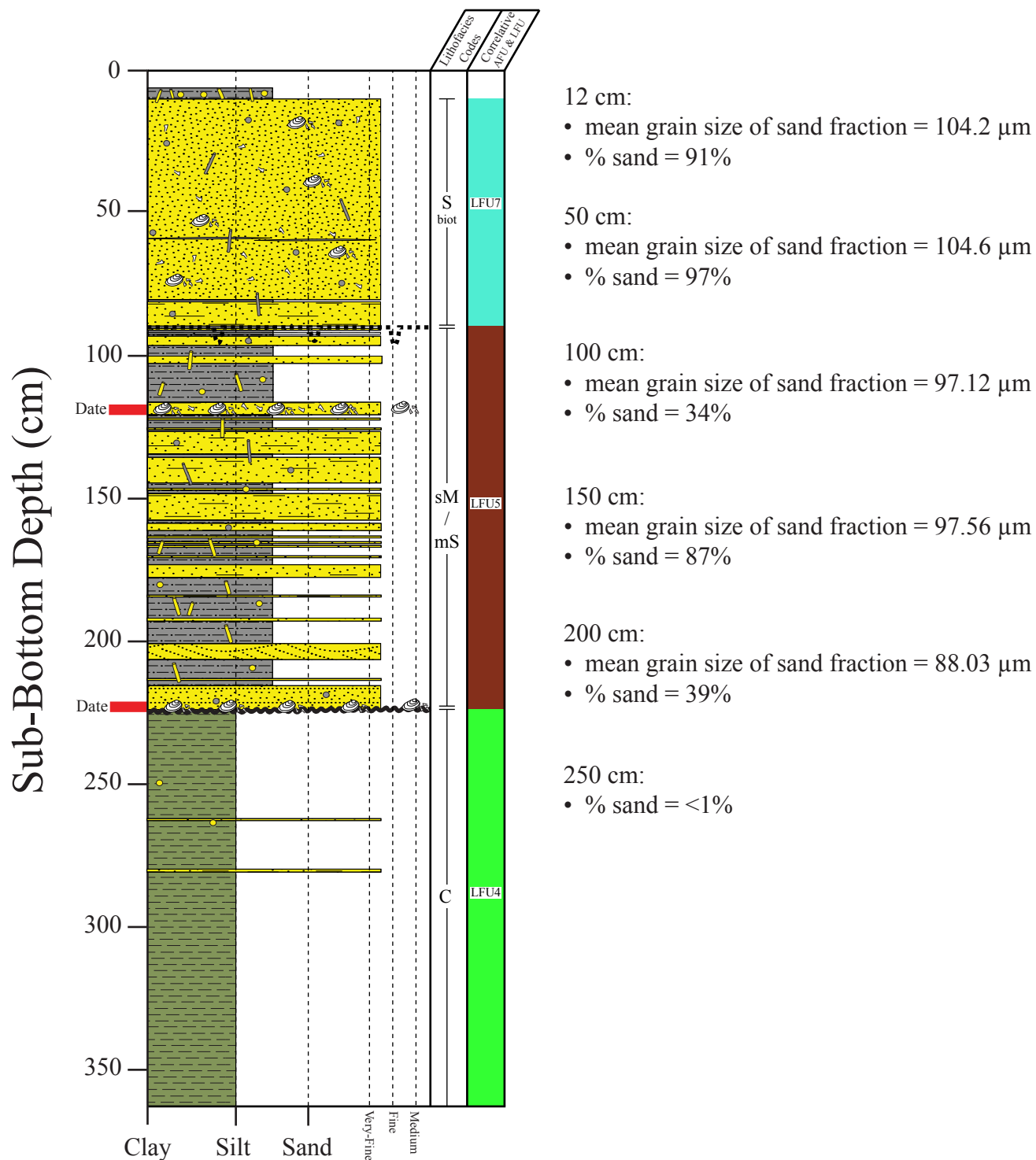
- mean grain size of sand fraction = 115.4  $\mu\text{m}$
- % sand = 97%

# Trinity-Tiger Shoals Project Vibracore TT-36-08

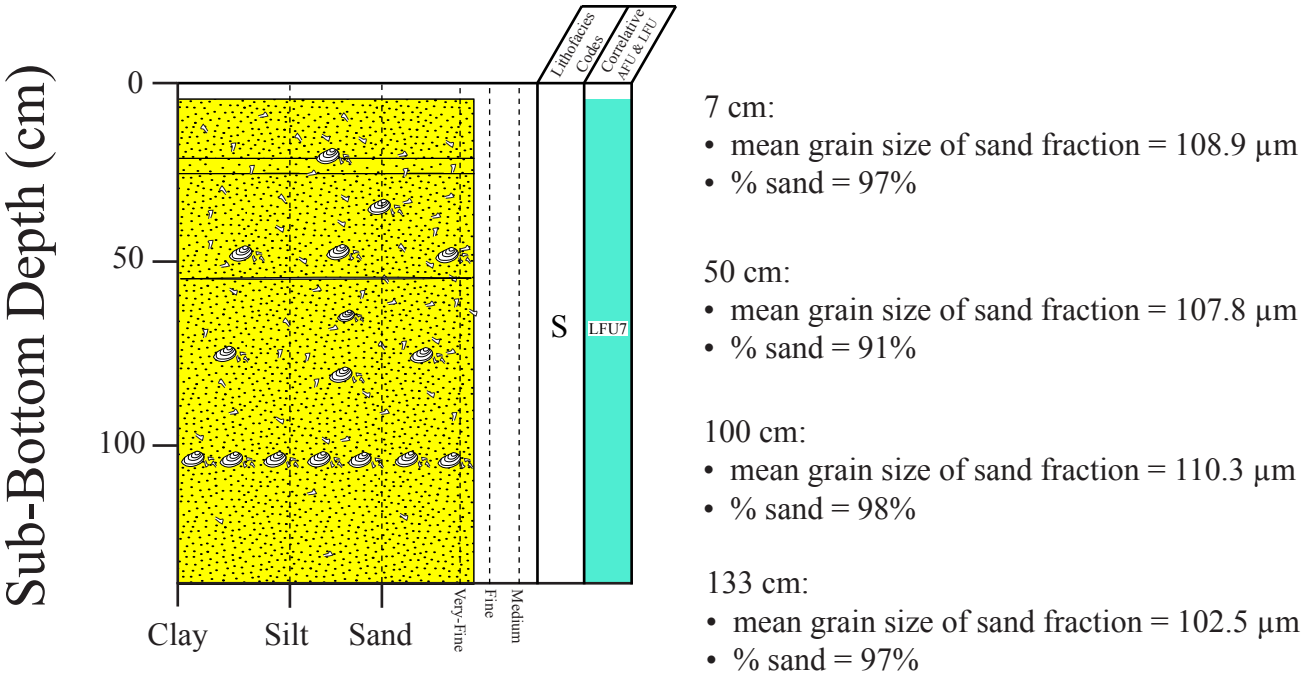




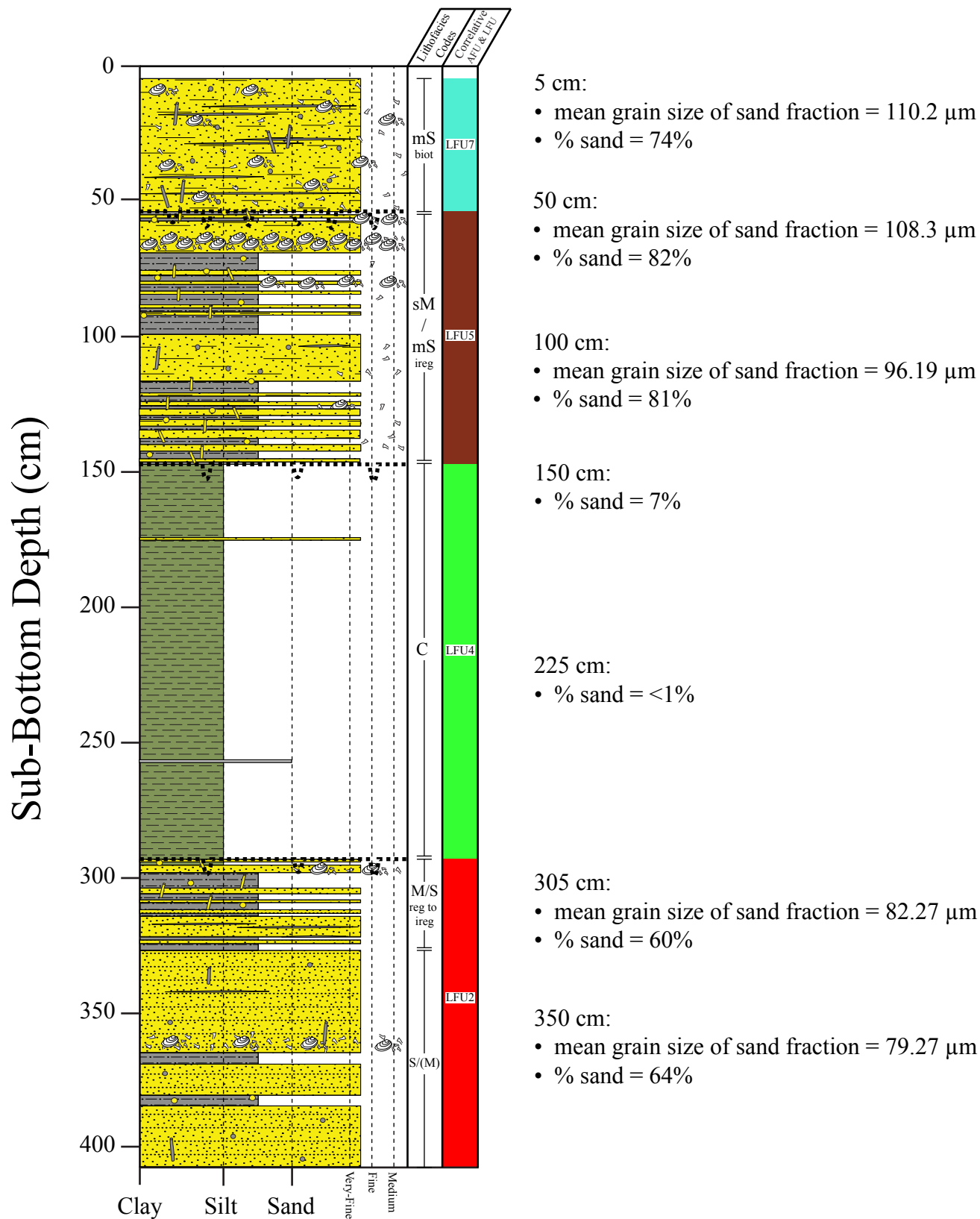
# Trinity-Tiger Shoals Project Vibracore TT-37-08



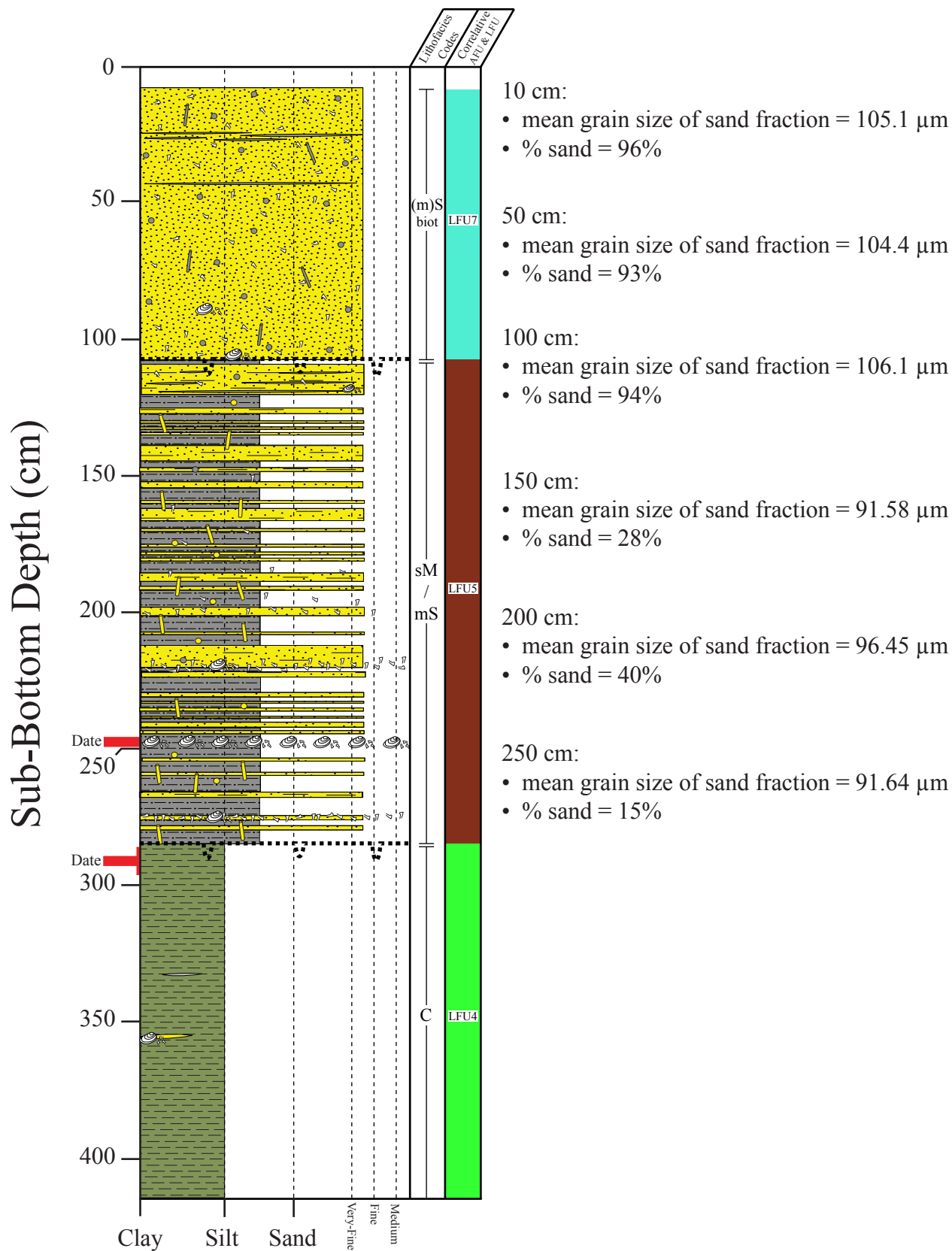
# Trinity-Tiger Shoals Project Vibracore TT-38-08



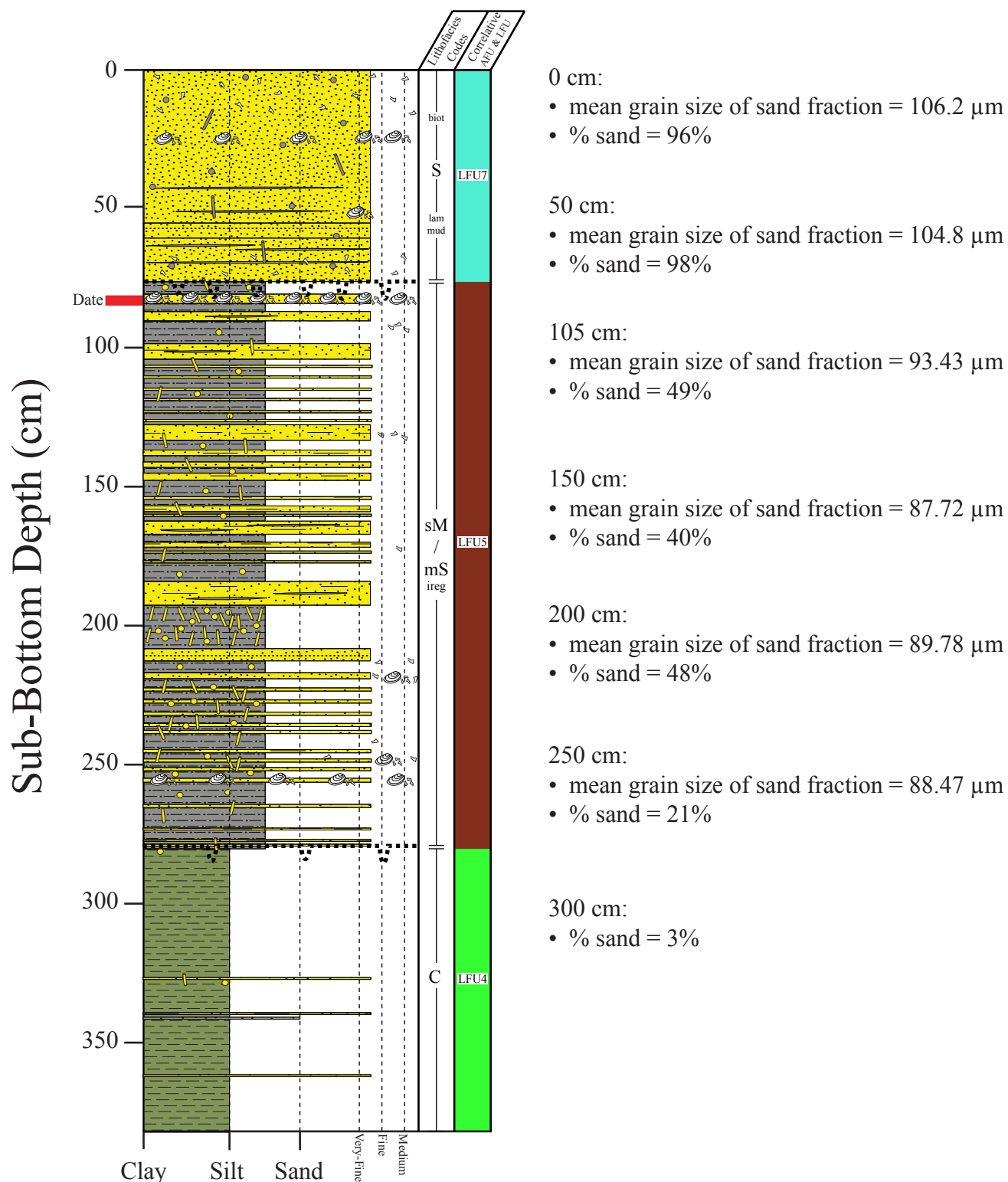
# Trinity-Tiger Shoals Project Vibracore TT-39-08



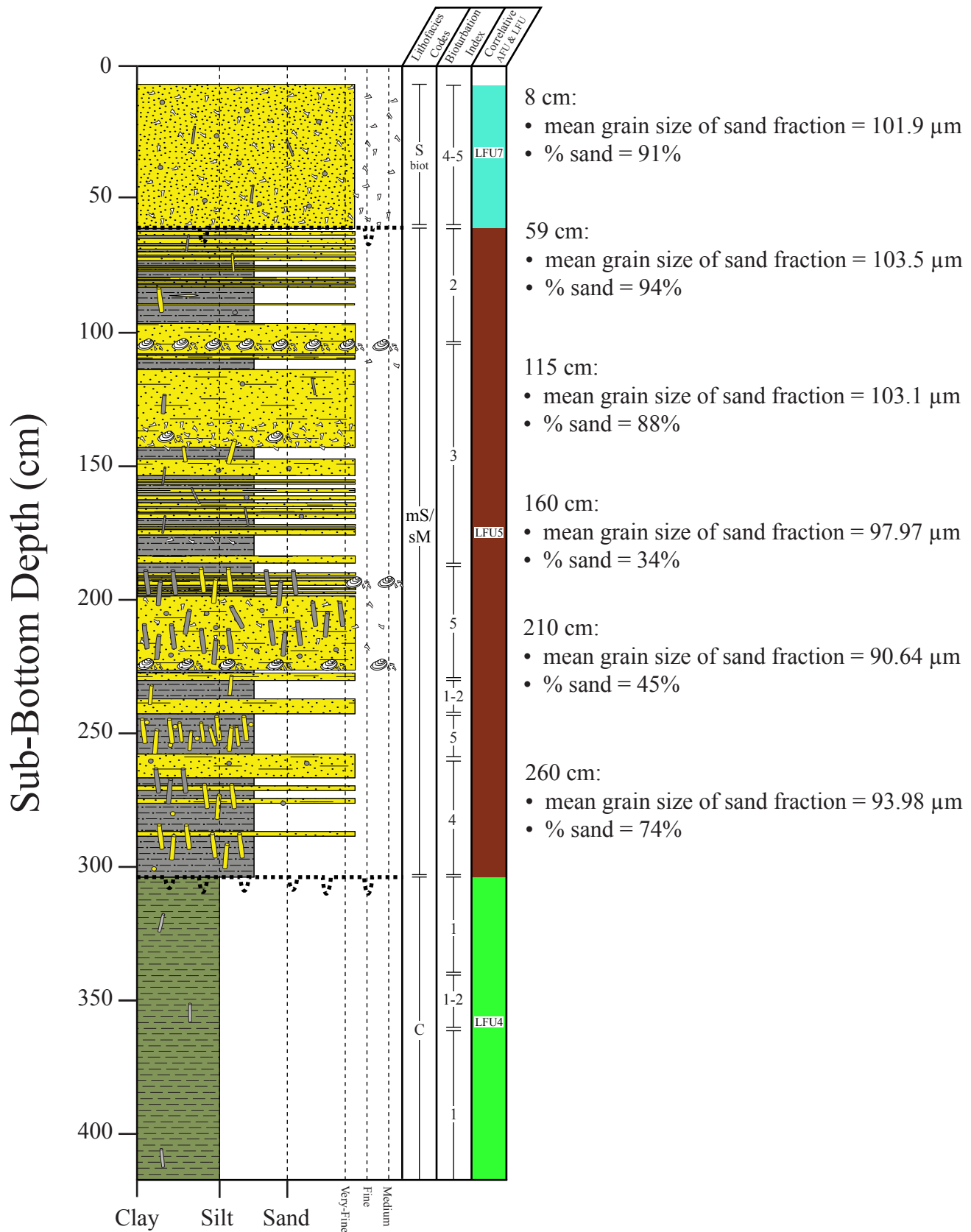
# Trinity-Tiger Shoals Project Vibracore TT-40-08



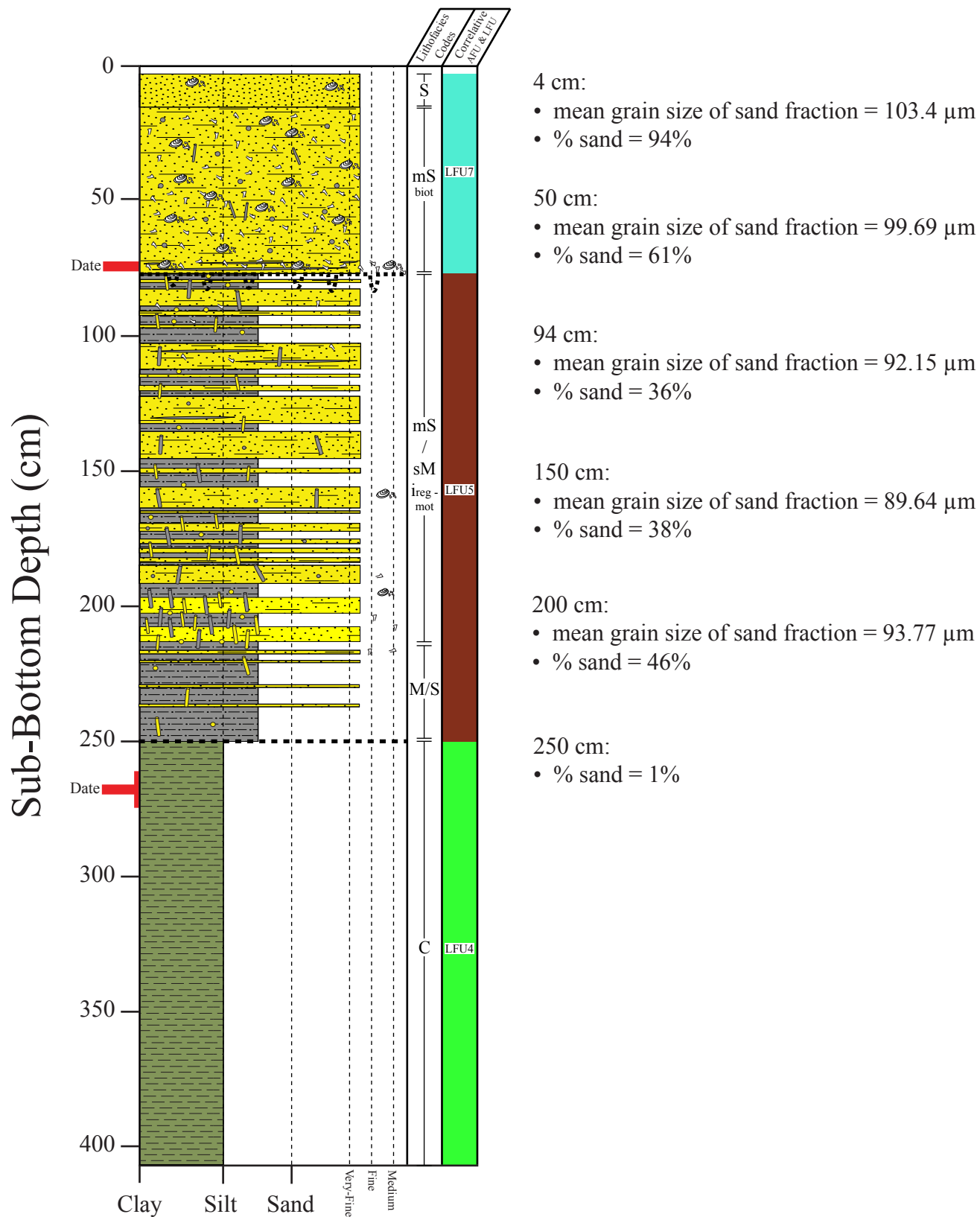
# Trinity-Tiger Shoals Project Vibracore TT-41-08



# Trinity-Tiger Shoals Project Vibracore TT-42-08

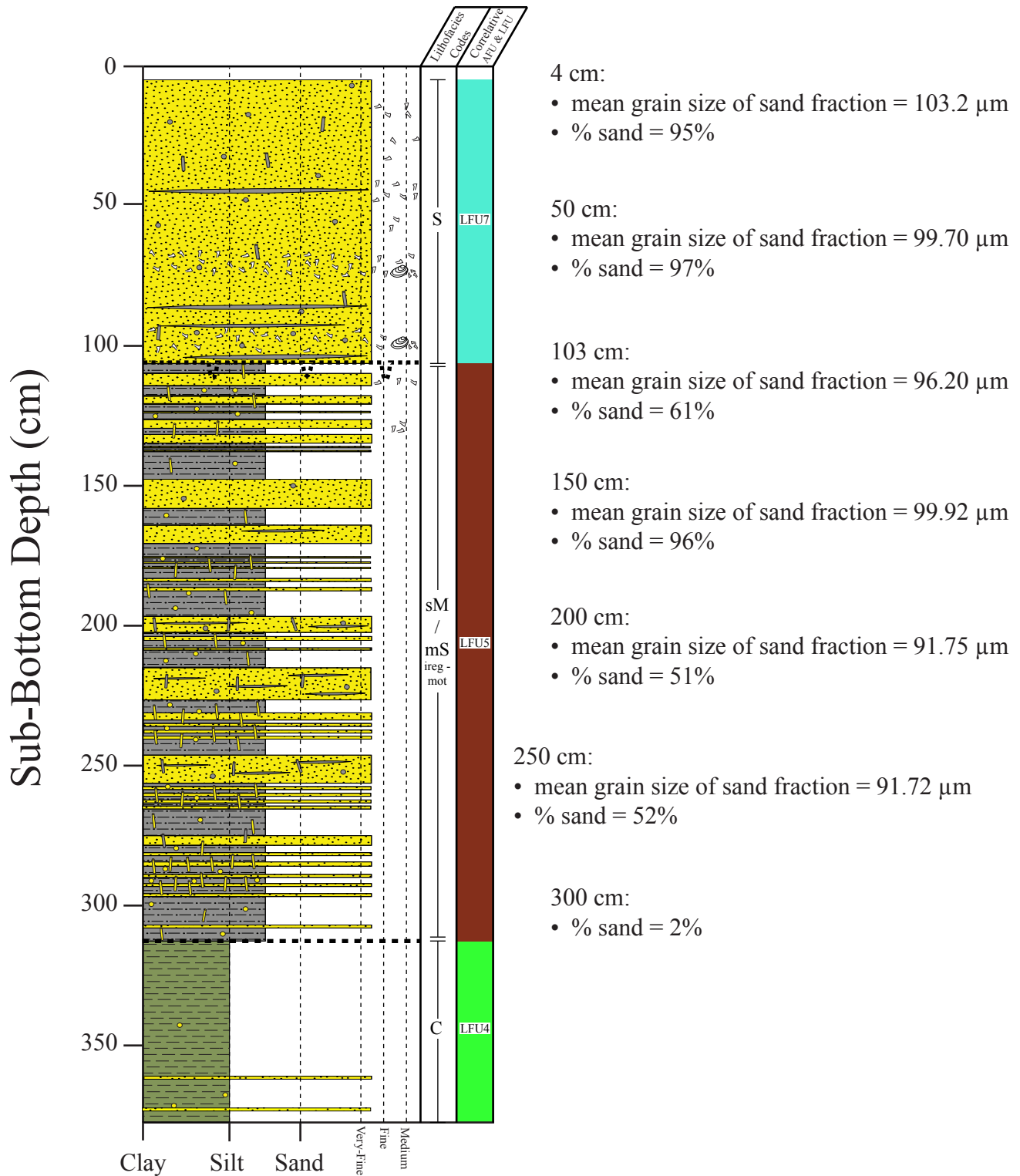


# Trinity-Tiger Shoals Project Vibracore TT-43-08

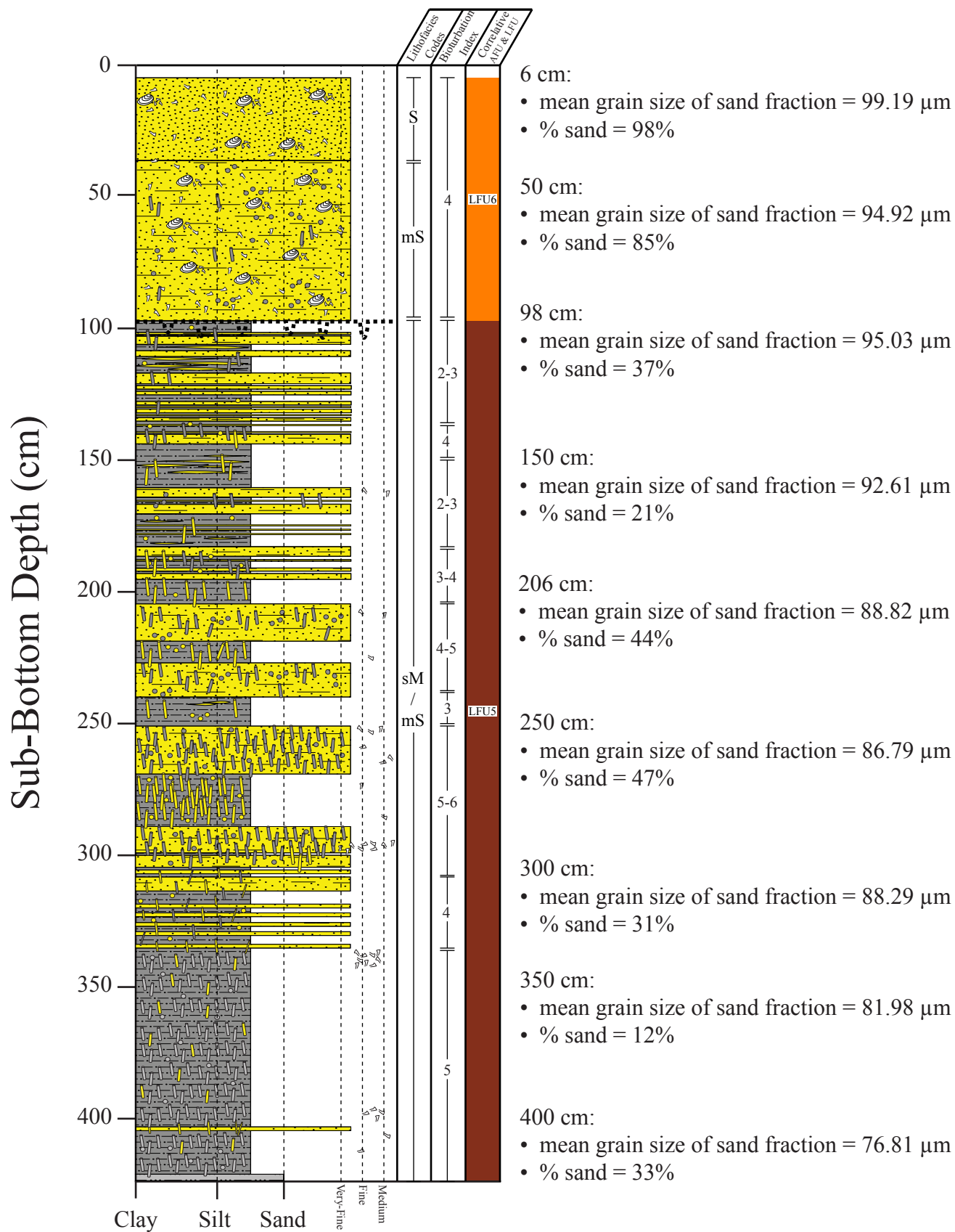




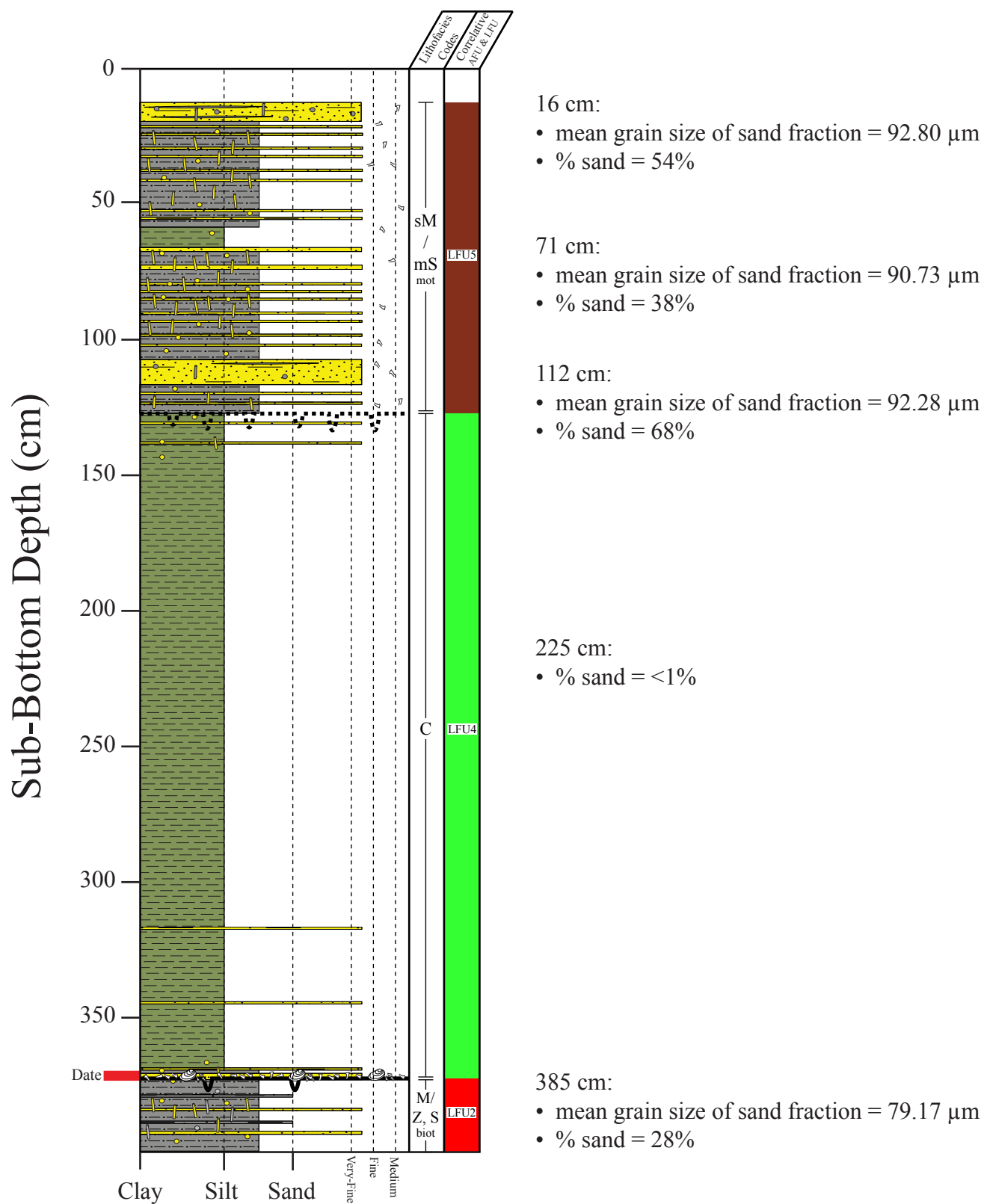
# Trinity-Tiger Shoals Project Vibracore TT-44-08



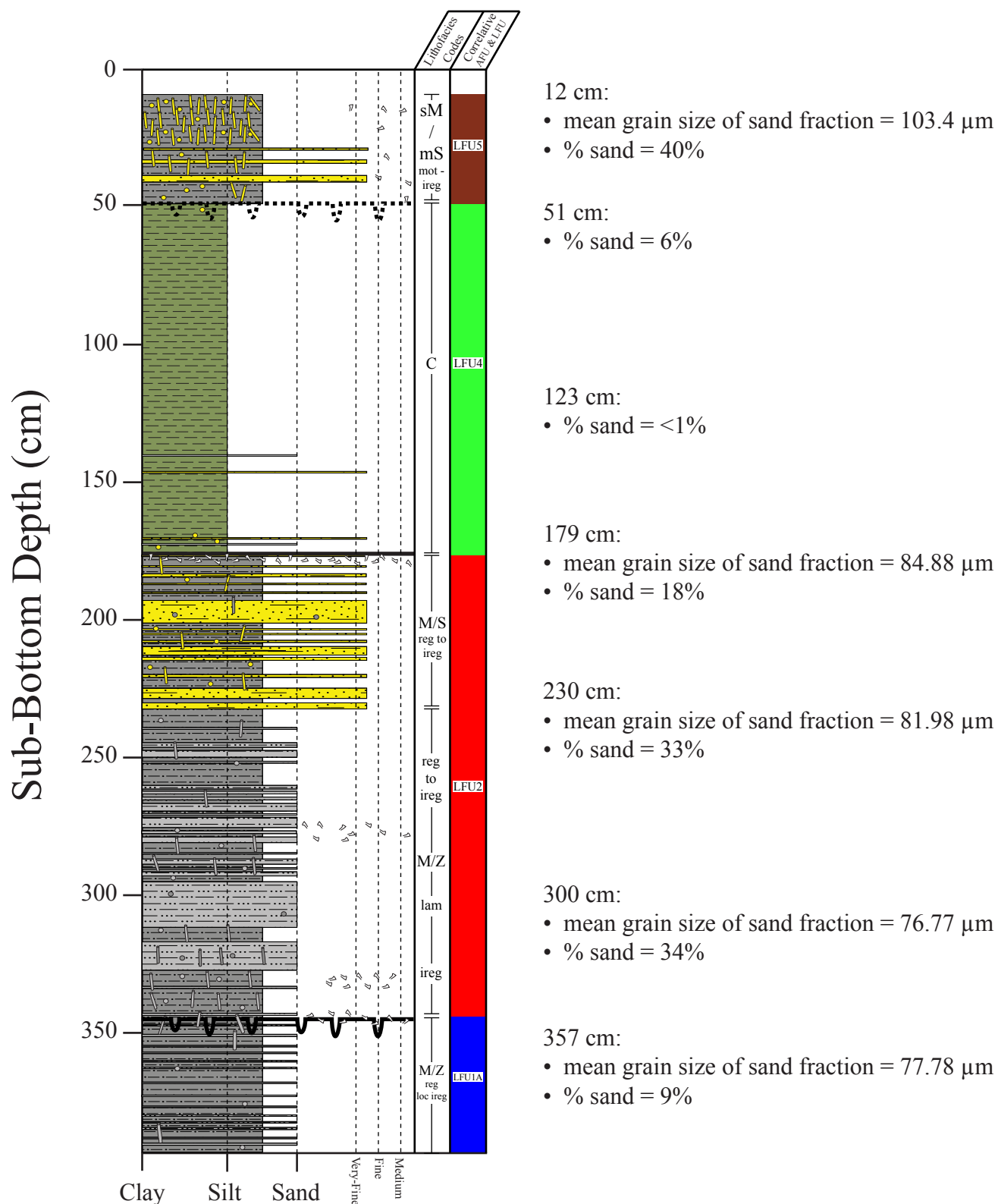
# Trinity-Tiger Shoals Project Vibracore TT-45-08



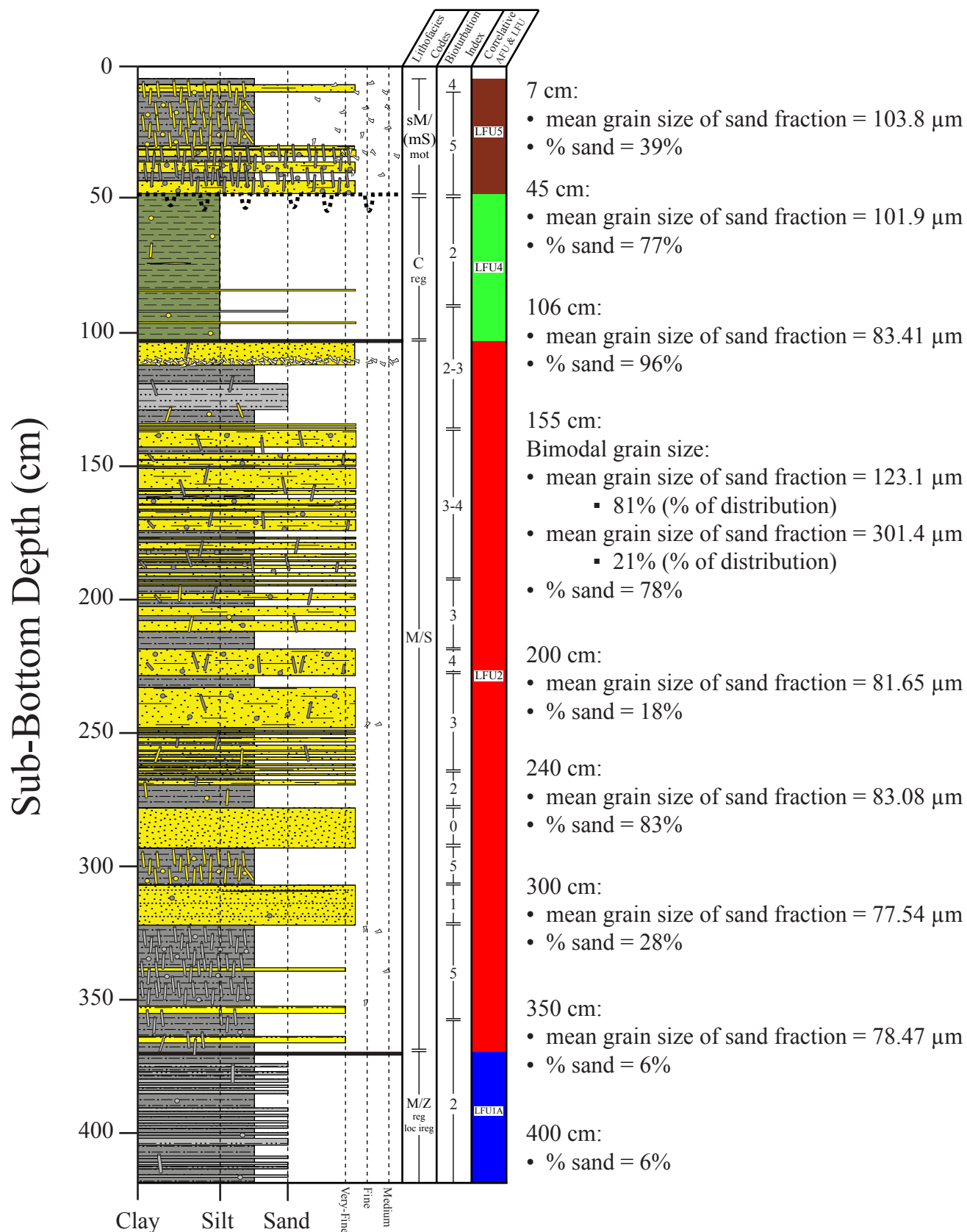
# Trinity-Tiger Shoals Project Vibracore TT-46-08



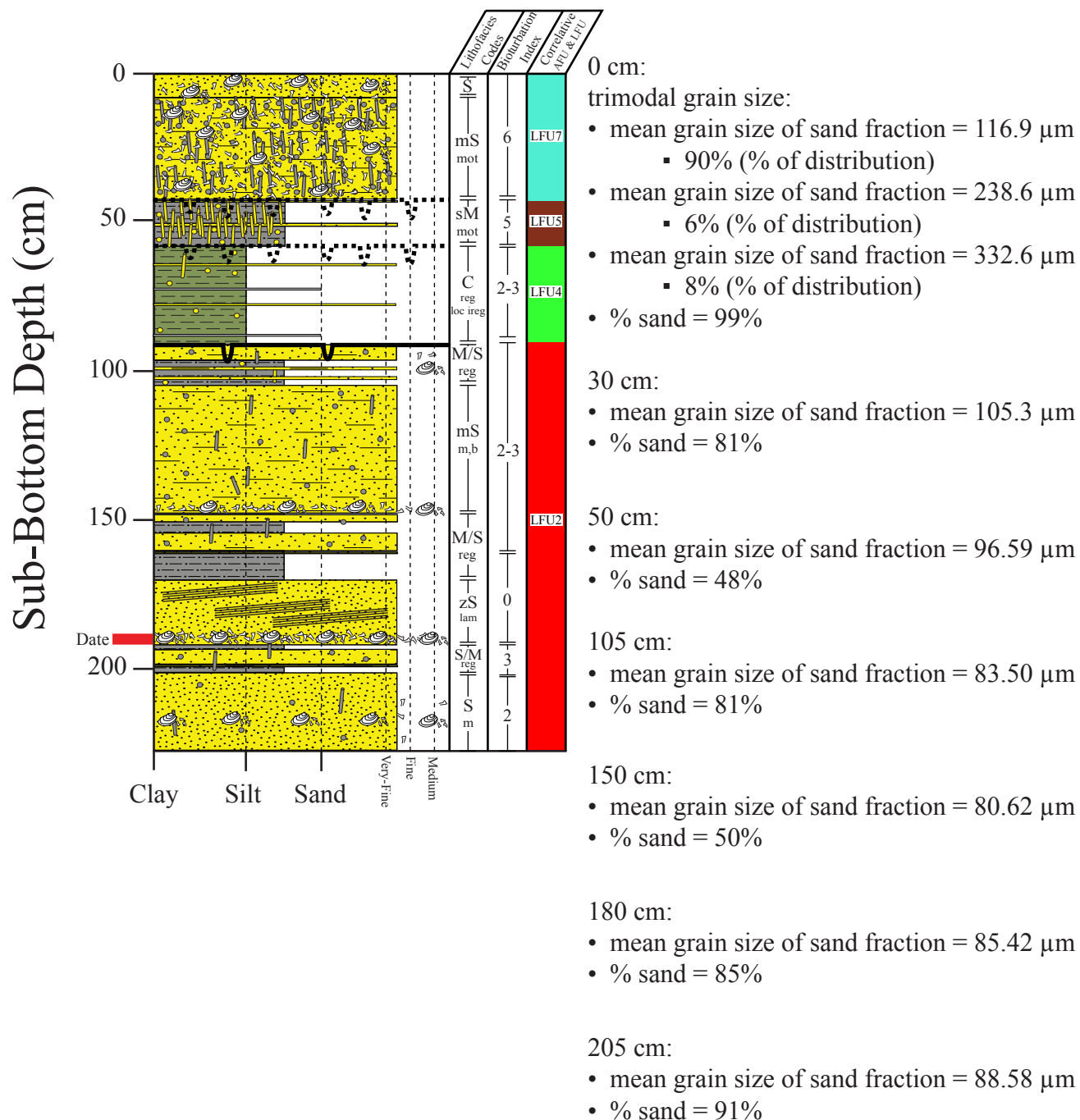
# Trinity-Tiger Shoals Project Vibracore TT-47-08



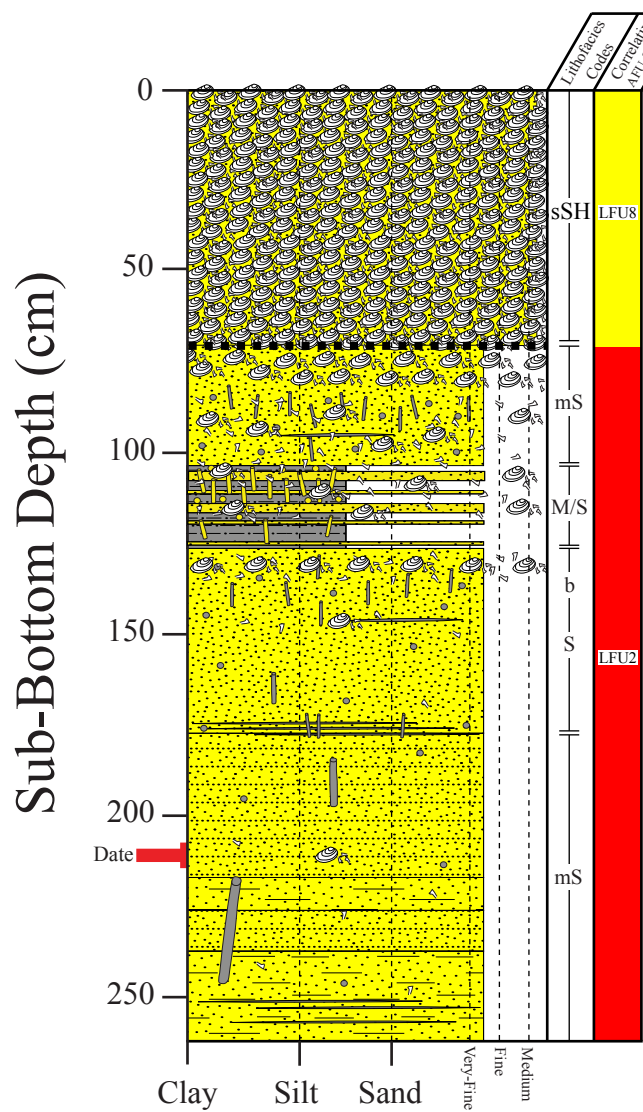
# Trinity-Tiger Shoals Project Vibracore TT-48-08



# Trinity-Tiger Shoals Project Vibracore TT-49-08



# Trinity-Tiger Shoals Project Vibracore TT-50-08



0 cm:

Bimodal grain size:

- mean grain size of sand fraction = 139.5  $\mu\text{m}$ 
  - 12% (% of distribution)
- mean grain size of sand fraction = 291.9  $\mu\text{m}$ 
  - 92% (% of distribution)
- % sand = >99%

50 cm:

Bimodal grain size:

- mean grain size of sand fraction = 149.3  $\mu\text{m}$ 
  - 35% (% of distribution)
- mean grain size of sand fraction = 296.9  $\mu\text{m}$ 
  - 71% (% of distribution)
- % sand = >99%

100 cm:

- mean grain size of sand fraction = 115.0  $\mu\text{m}$
- % sand = 95%

157 cm:

- mean grain size of sand fraction = 87.22  $\mu\text{m}$
- % sand = 91%

200 cm:

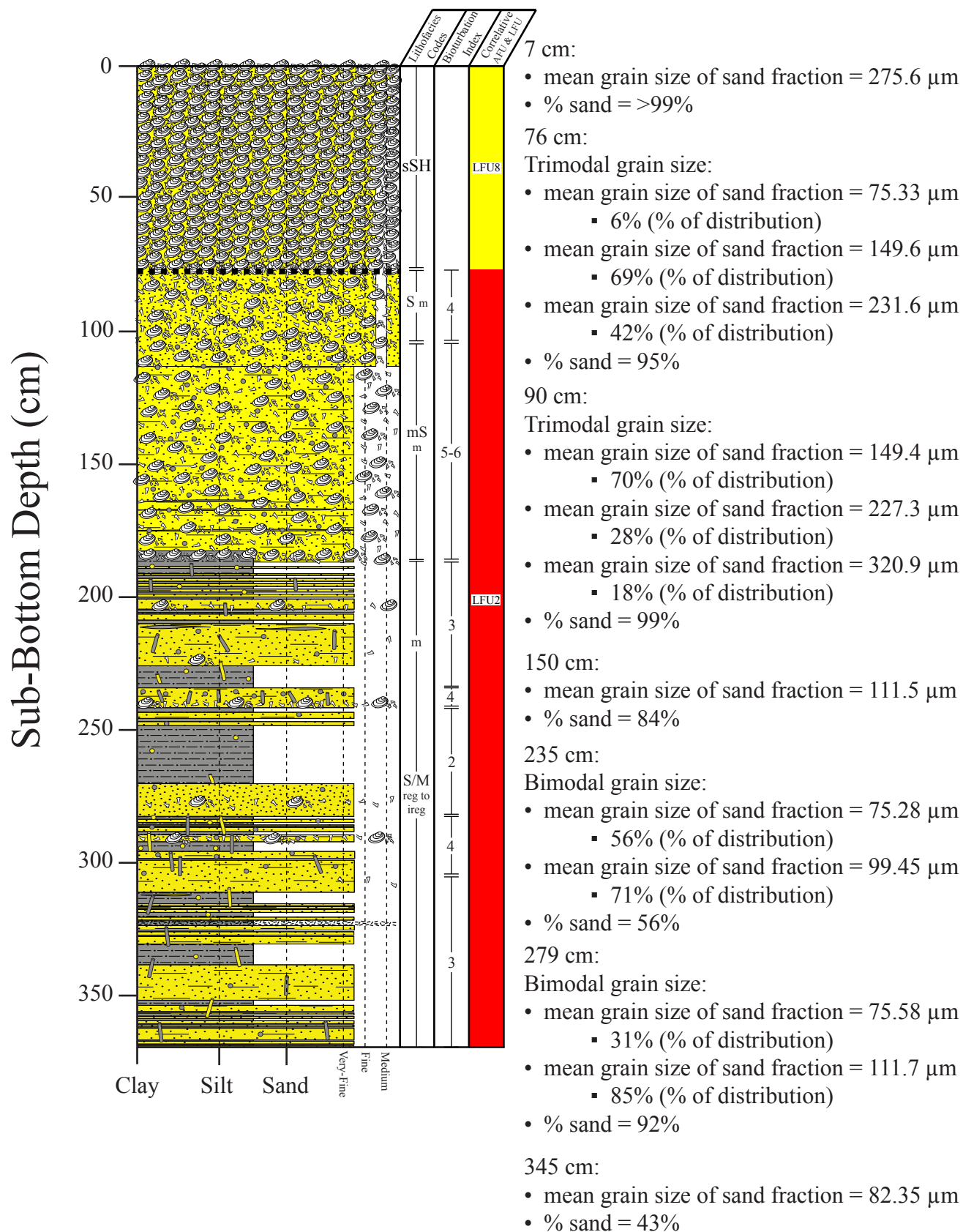
- mean grain size of sand fraction = 83.58  $\mu\text{m}$
- % sand = 71%

248 cm:

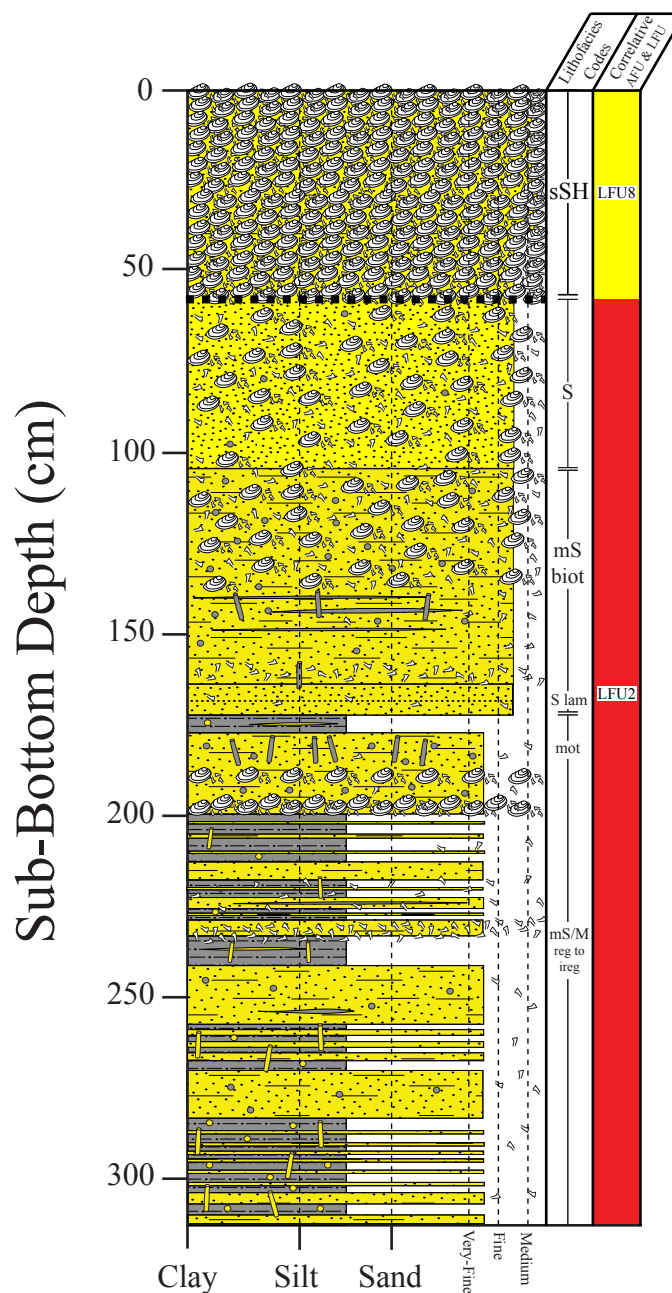
- mean grain size of sand fraction = 81.44  $\mu\text{m}$
- % sand = 81%



# Trinity-Tiger Shoals Project Vibracore TT-52-08



# Trinity-Tiger Shoals Project Vibracore TT-53-08



7 cm:

- mean grain size of sand fraction = 308.0  $\mu\text{m}$
- % sand = 99%

52 cm:

- mean grain size of sand fraction = 152.2  $\mu\text{m}$
- % sand = 98%

100 cm:

- mean grain size of sand fraction = 170.2  $\mu\text{m}$
- % sand = 98%

165 cm:

- mean grain size of sand fraction = 130.0  $\mu\text{m}$
- % sand = 94%

265 cm:

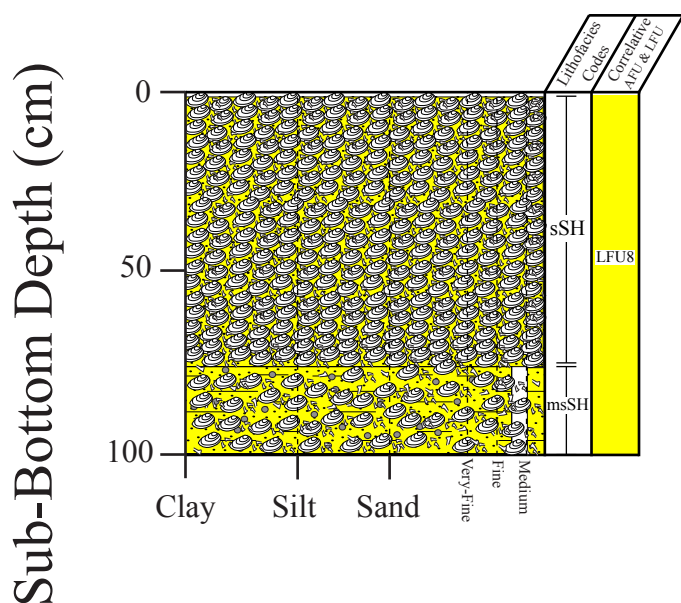
Bimodal grain size:

- mean grain size of sand fraction = 73.78  $\mu\text{m}$ 
  - 55% (% of distribution)
- mean grain size of sand fraction = 104.7  $\mu\text{m}$ 
  - 66% (% of distribution)
- % sand = 50%

310 cm:

- mean grain size of sand fraction = 80.42  $\mu\text{m}$
- % sand = 31%

## Trinity-Tiger Shoals Project Vibracore TT-54-08



3 cm:

- mean grain size of sand fraction = 317.9  $\mu\text{m}$
- % sand = 99%

56 cm:

Trimodal grain size:

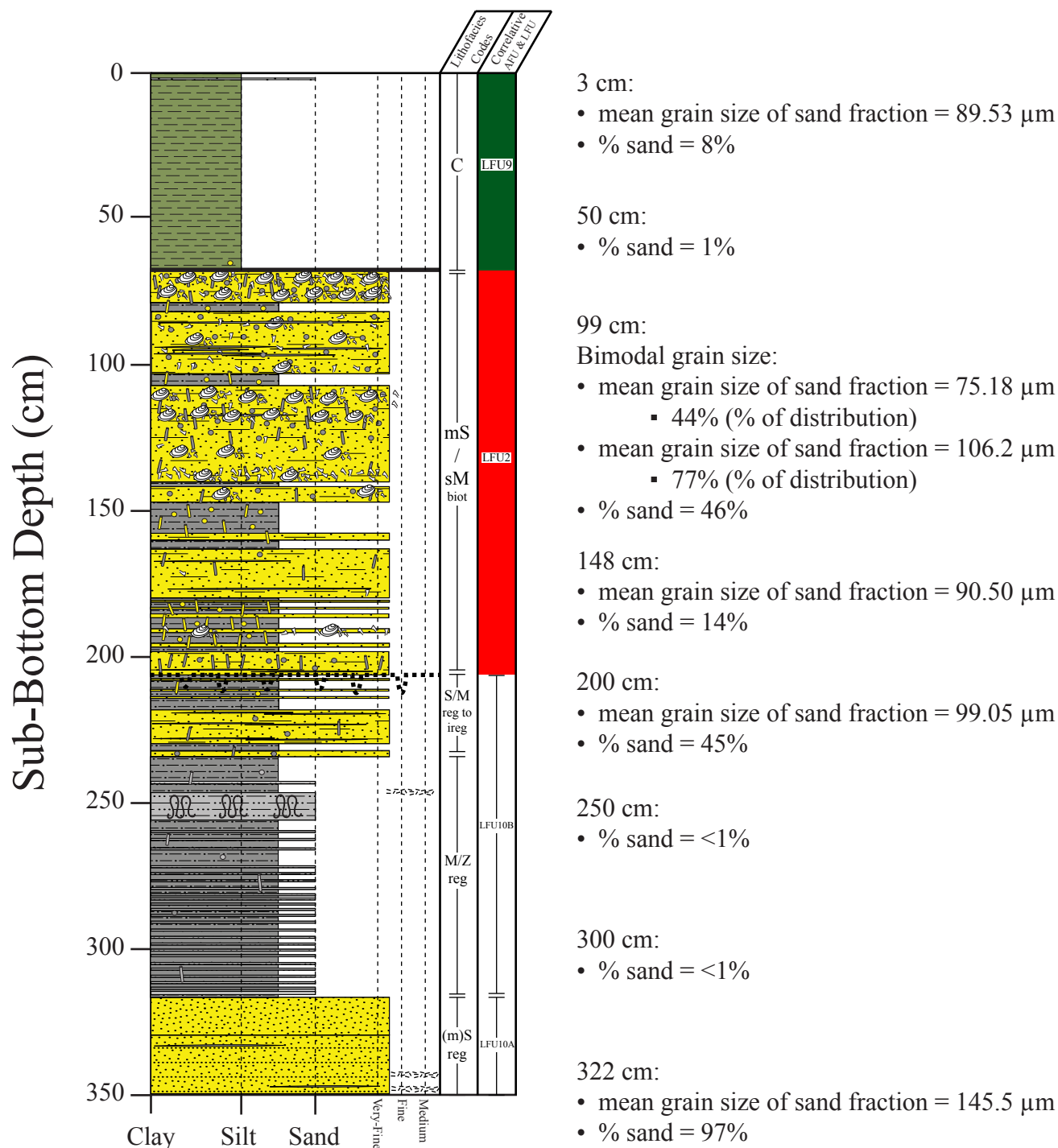
- mean grain size of sand fraction = 156.8  $\mu\text{m}$ 
  - 52% (% of distribution)
- mean grain size of sand fraction = 263.9  $\mu\text{m}$ 
  - 55% (% of distribution)
- mean grain size of sand fraction = 534.4  $\mu\text{m}$ 
  - 7% (% of distribution)
- % sand = 98%

100 cm:

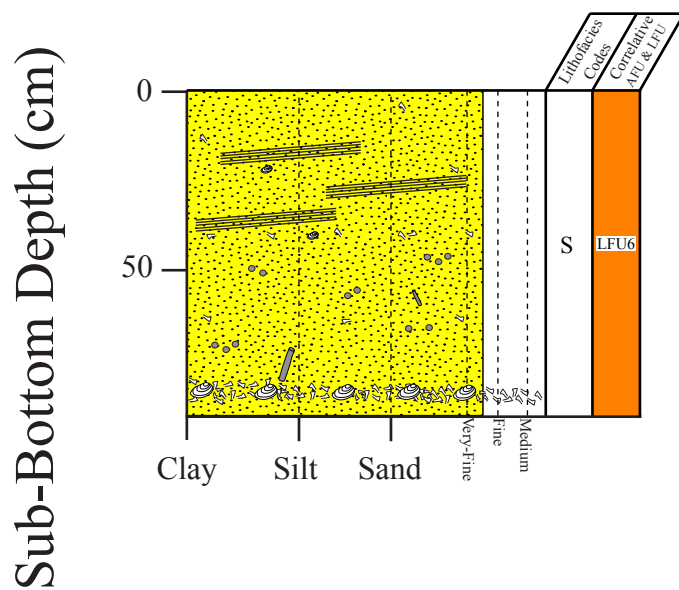
Bimodal grain size:

- mean grain size of sand fraction = 127.9  $\mu\text{m}$ 
  - 91% (% of distribution)
- mean grain size of sand fraction = 268.1  $\mu\text{m}$ 
  - 11% (% of distribution)
- % sand = 77%

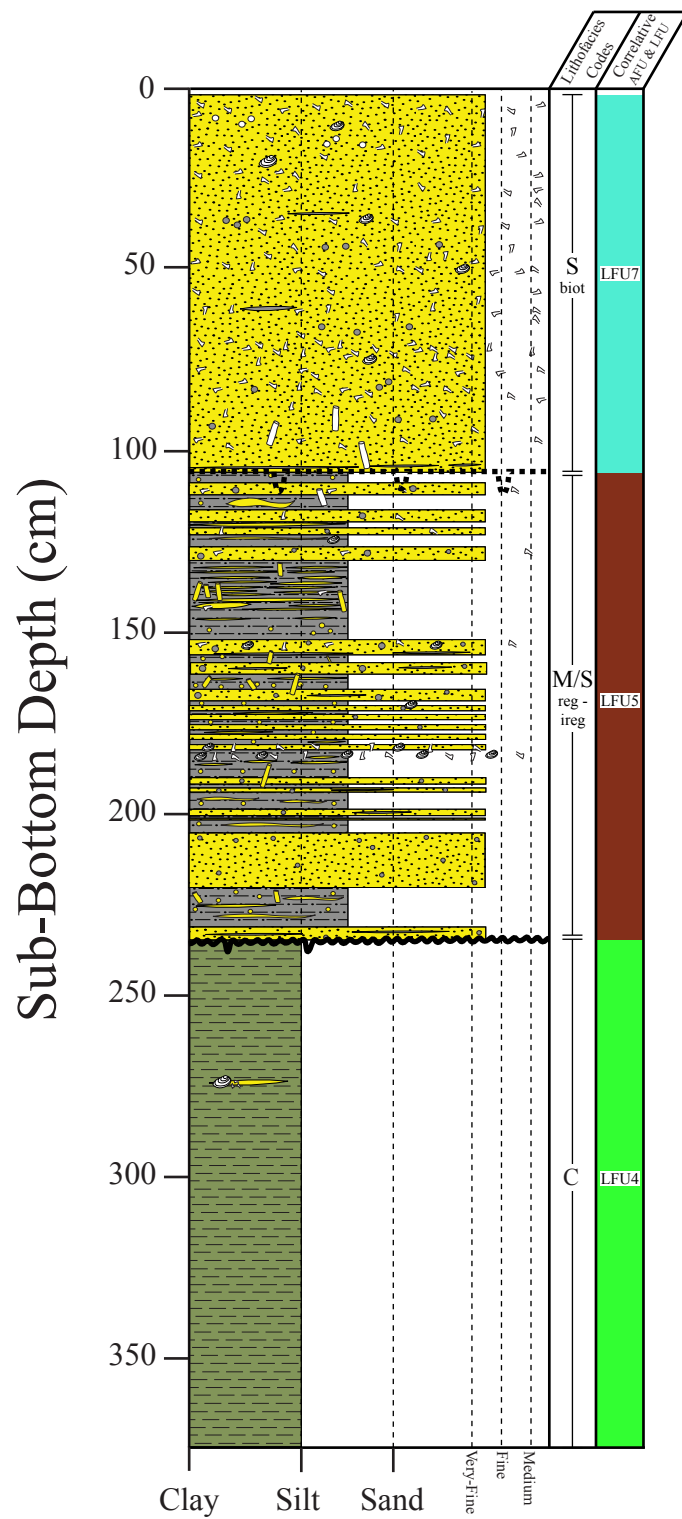
# Trinity-Tiger Shoals Project Vibracore TT-55-08



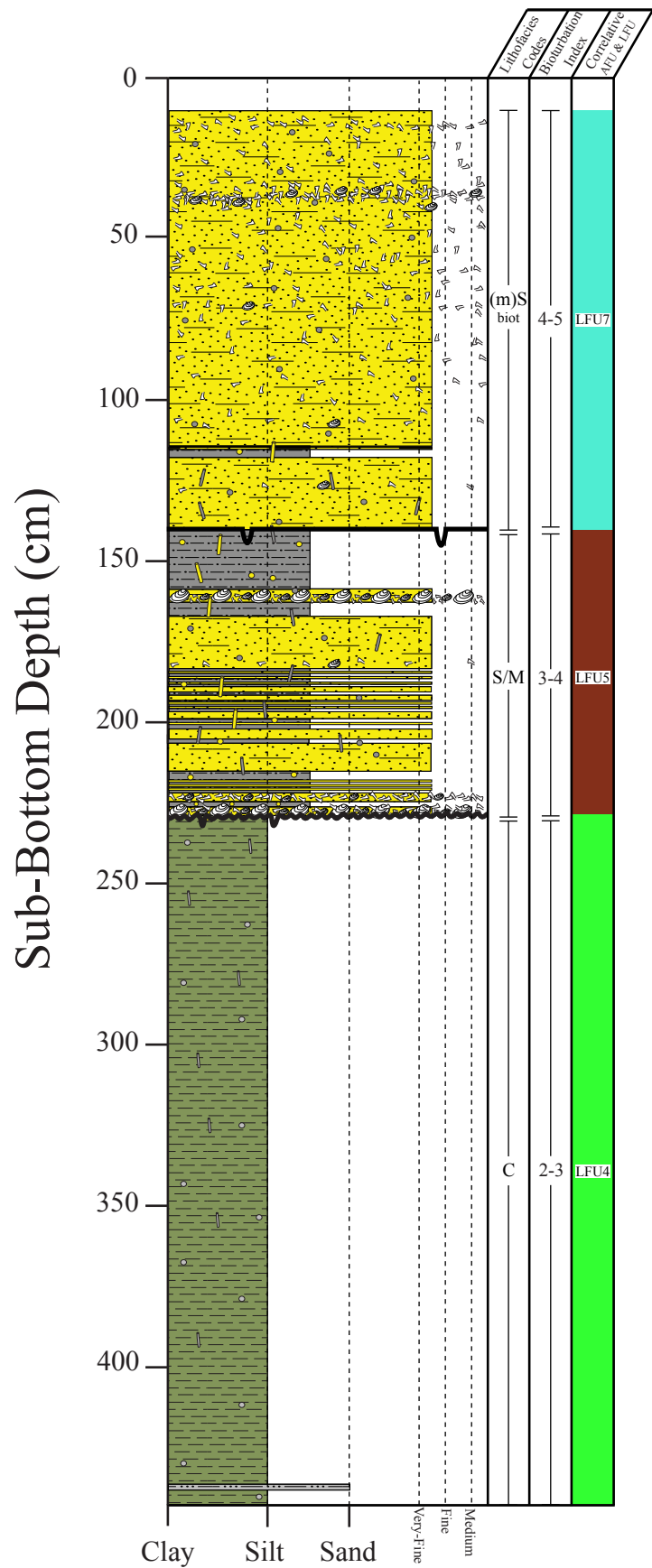
# Trinity-Tiger Shoals Project Vibracore TT-57-10



# Trinity-Tiger Shoals Project Vibracore TT-64-10

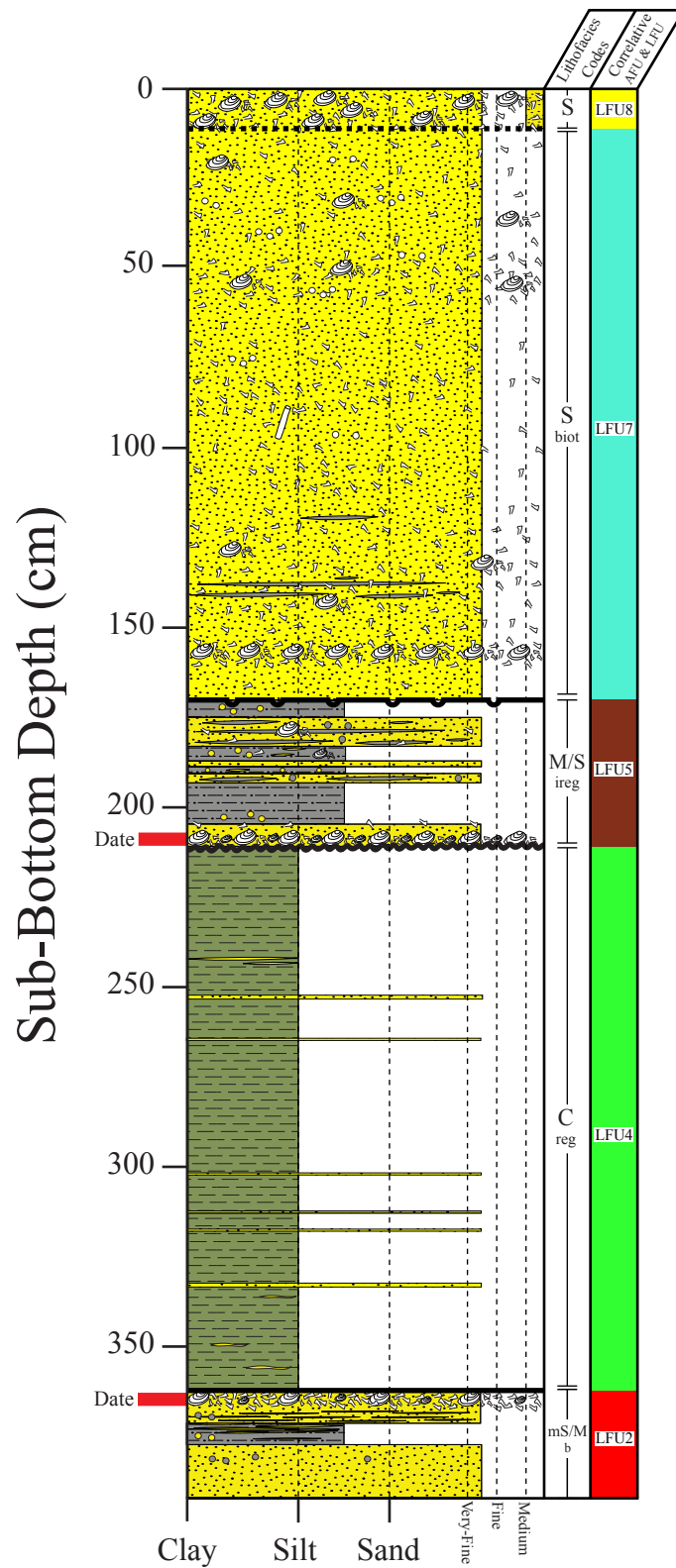


# Trinity-Tiger Shoals Project Vibracore TT-65-10

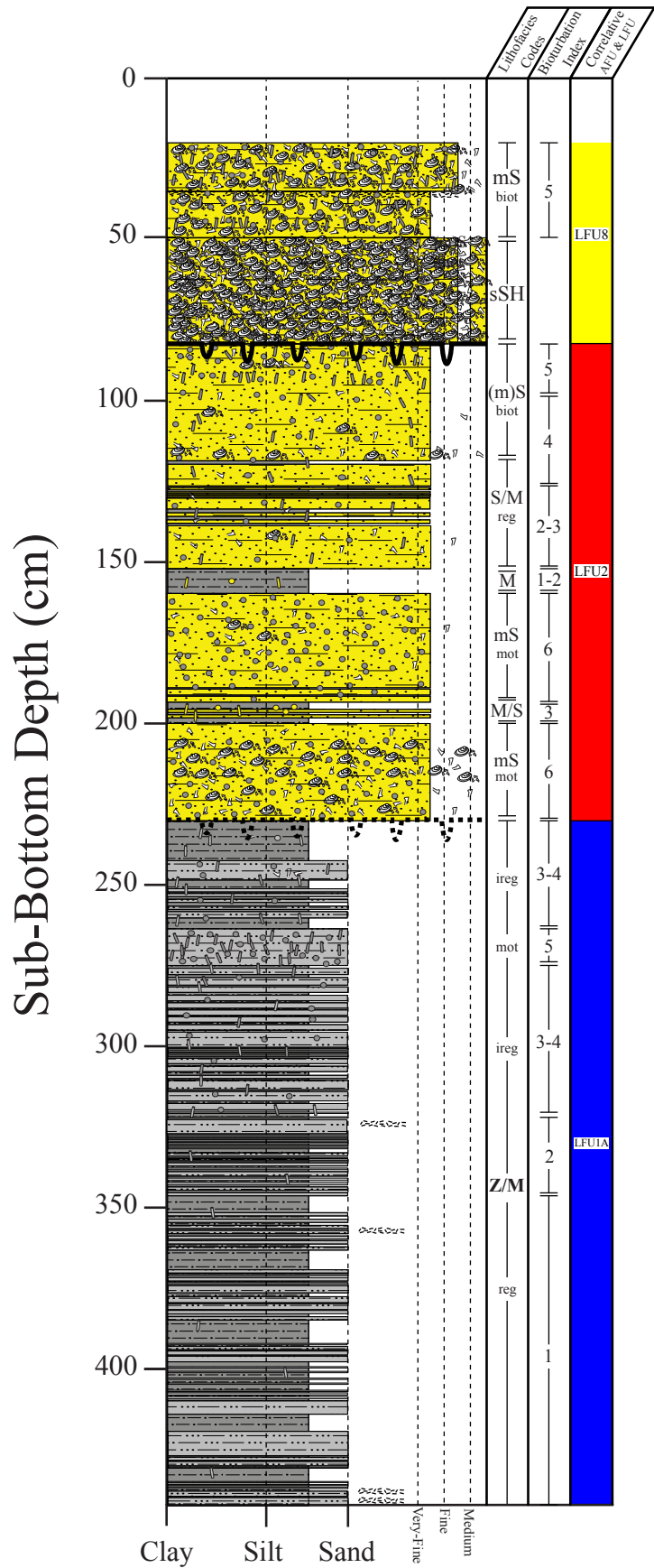




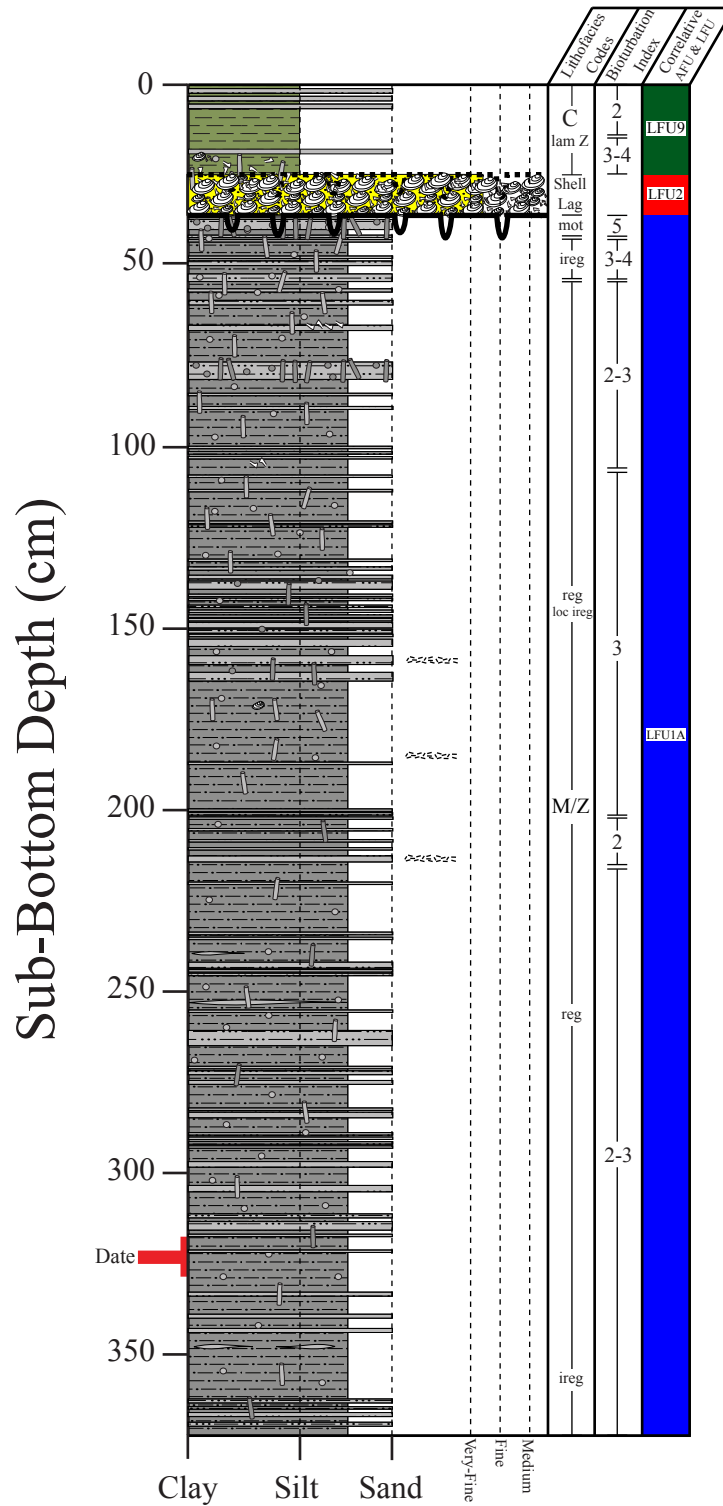
# Trinity-Tiger Shoals Project Vibracore TT-66-10



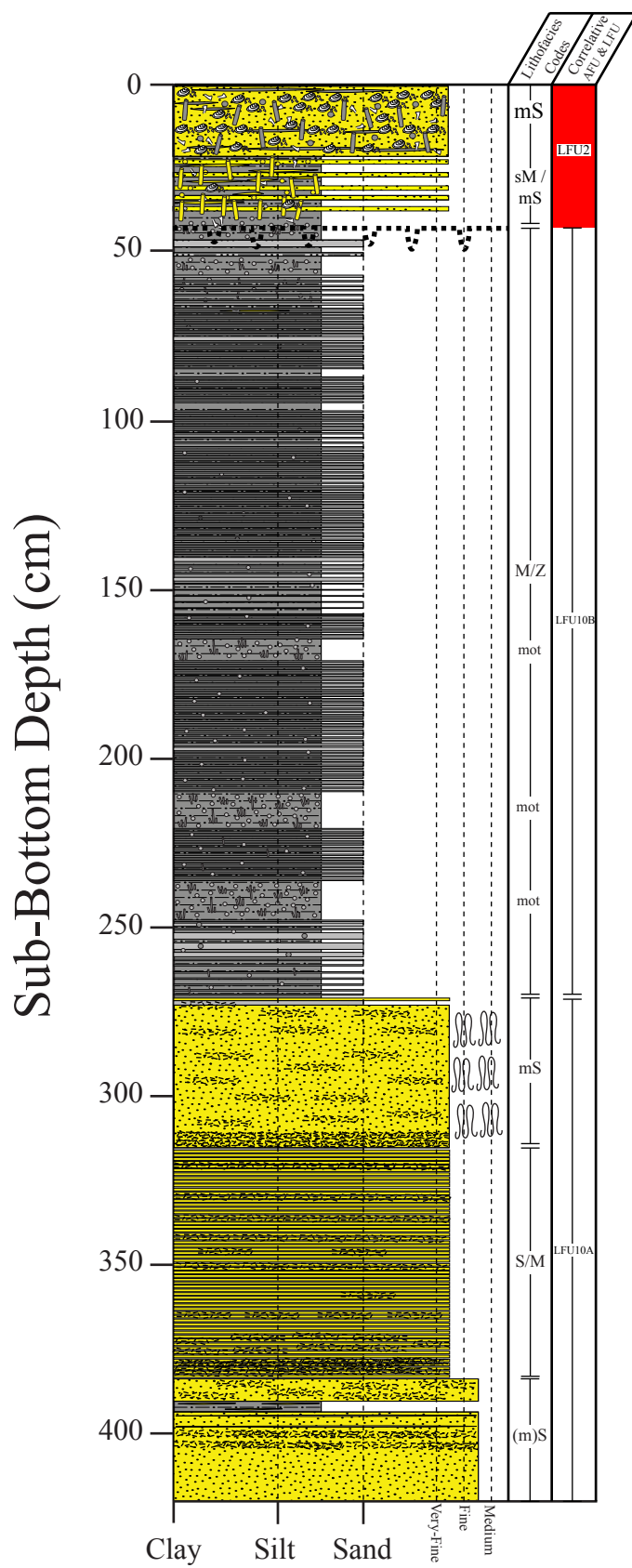
# Trinity-Tiger Shoals Project Vibracore TT-69-10



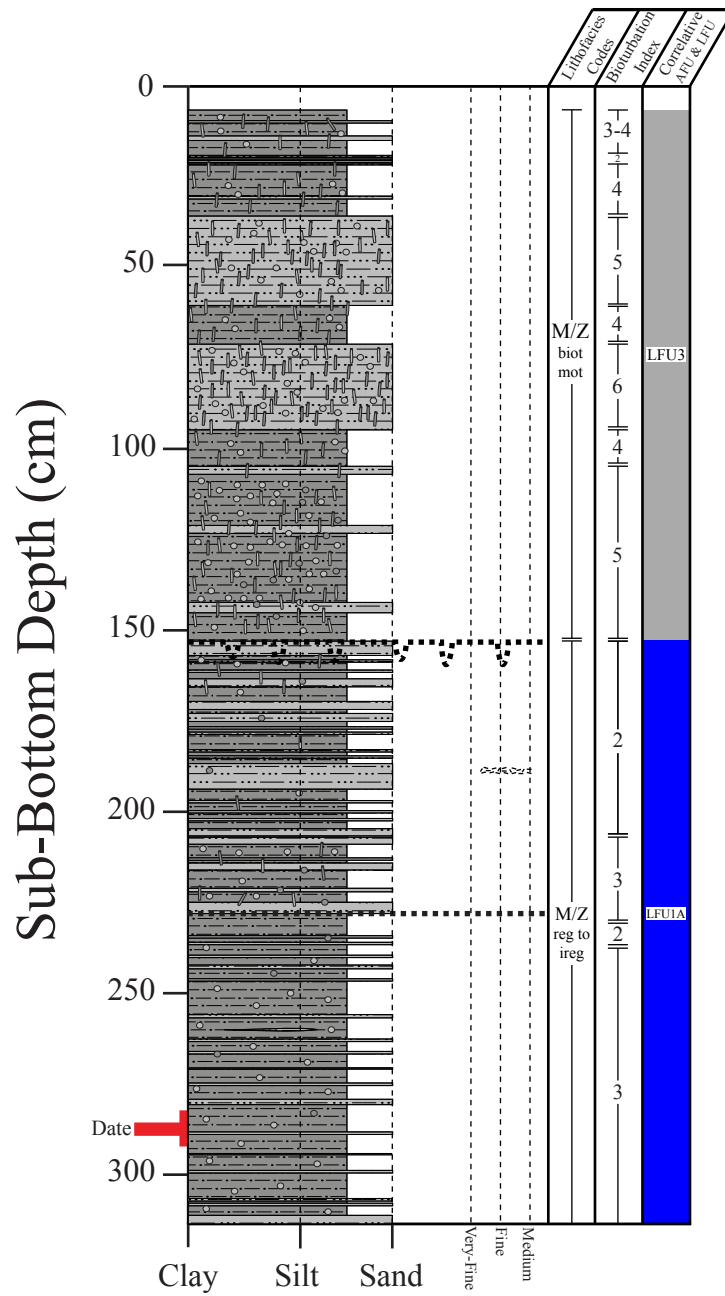
# Trinity-Tiger Shoals Project Vibracore TT-73-10



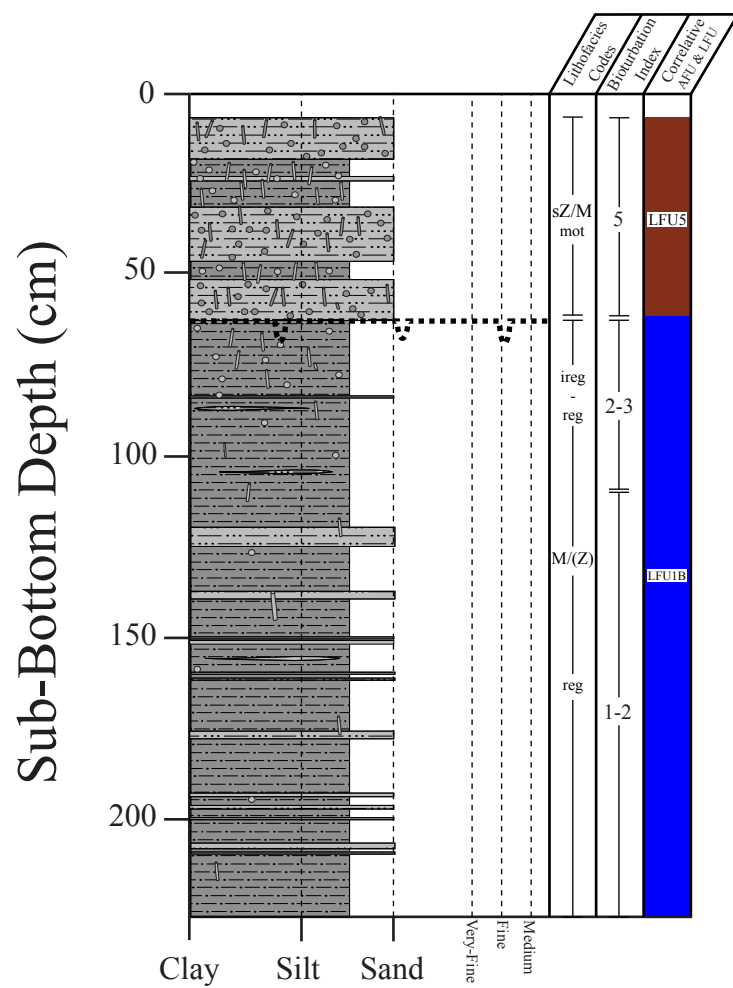
# Trinity-Tiger Shoals Project Vibracore TT-74-10



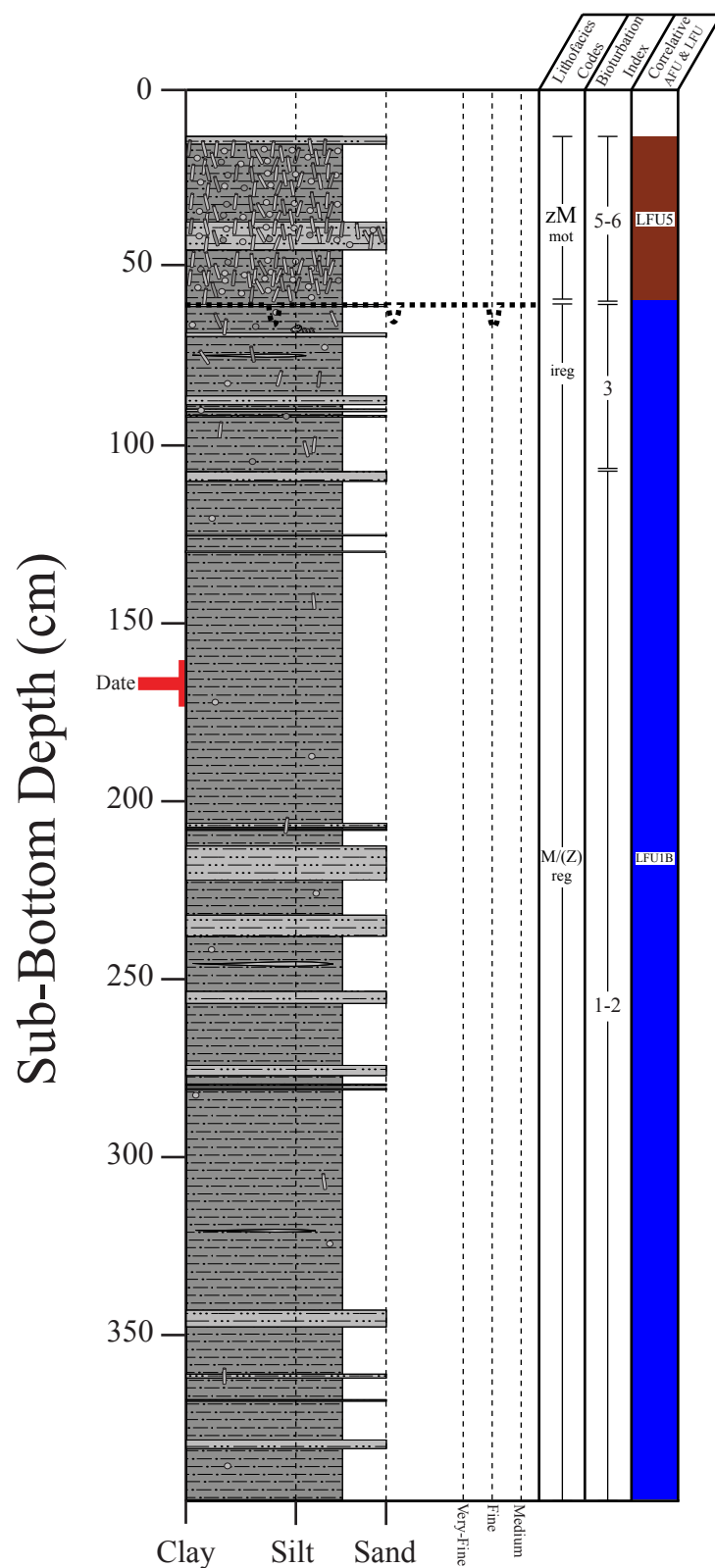
# Trinity-Tiger Shoals Project Vibracore TT-75-10



# Trinity-Tiger Shoals Project Vibracore TT-76-10

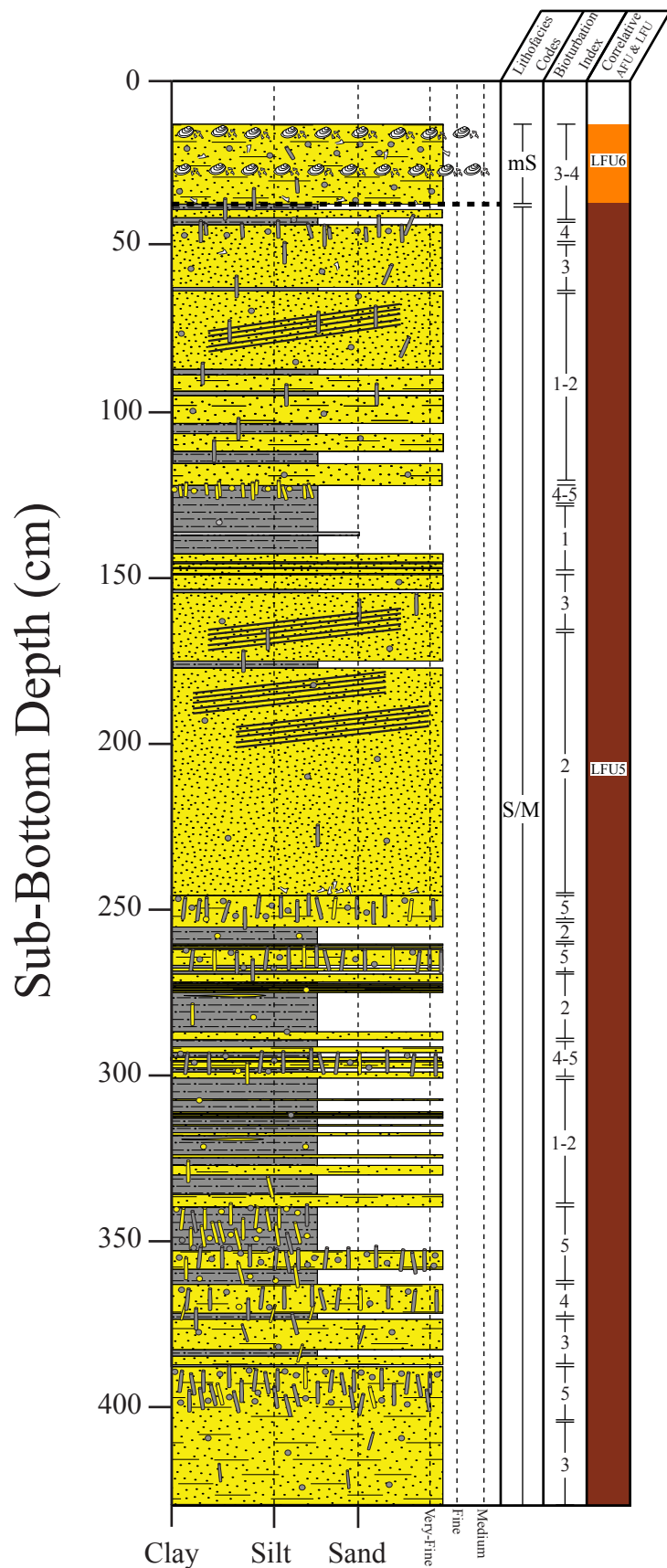


# Trinity-Tiger Shoals Project Vibracore TT-77-10

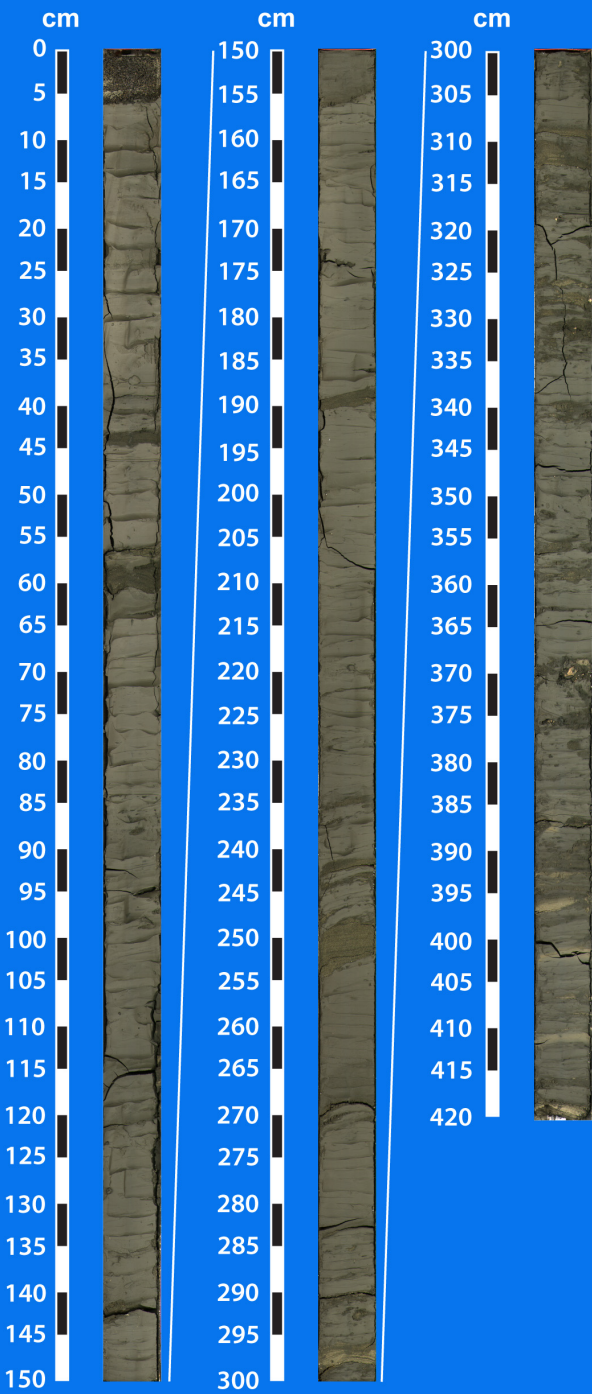




# Trinity-Tiger Shoals Project Vibracore TT-78-10

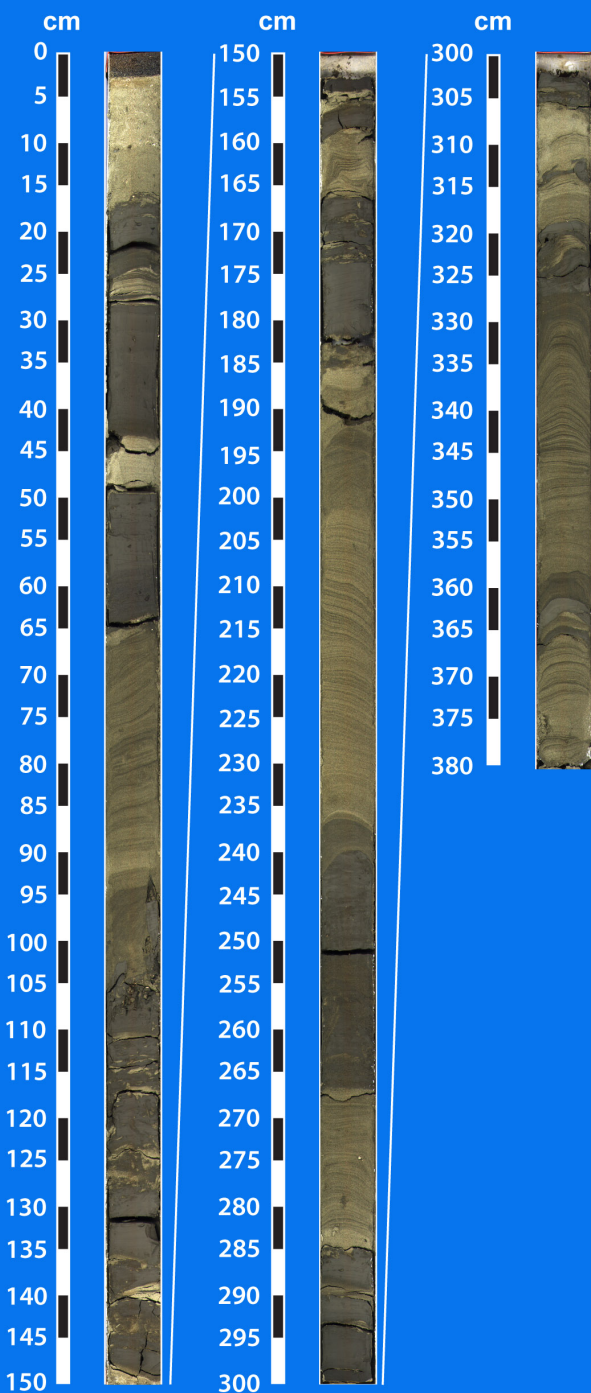


Trinity-Tiger Shoals Complex  
TT-01-08



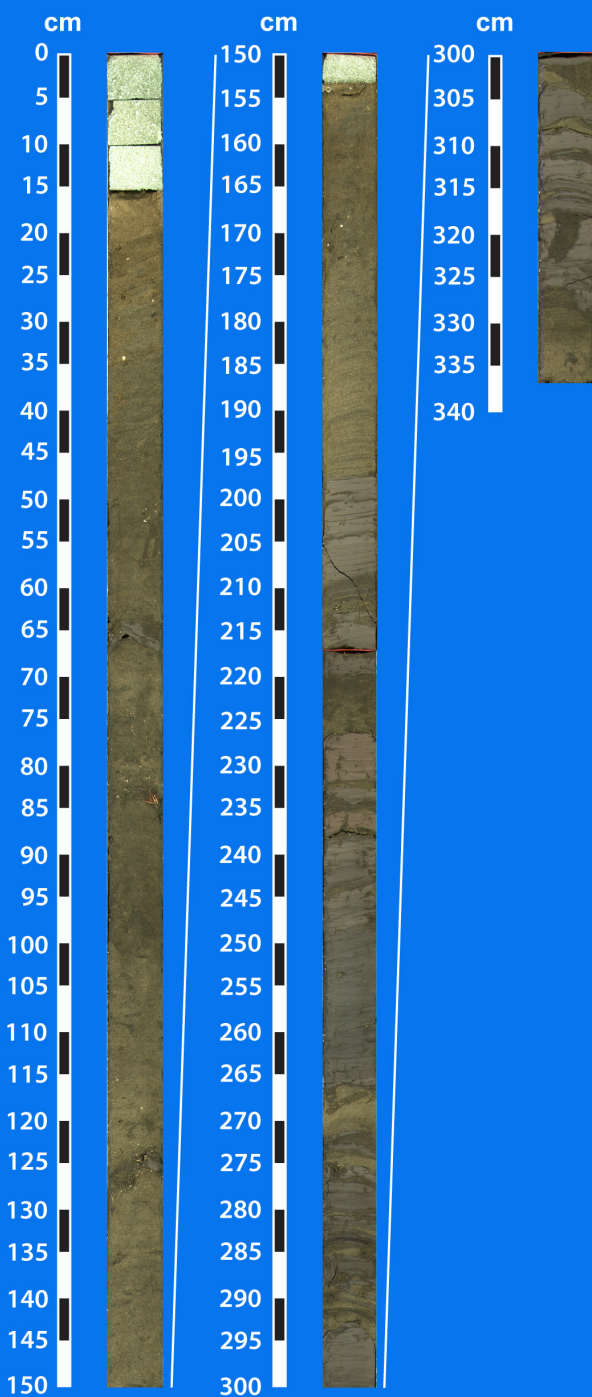
# Trinity-Tiger Shoals Complex

## TT-02-08



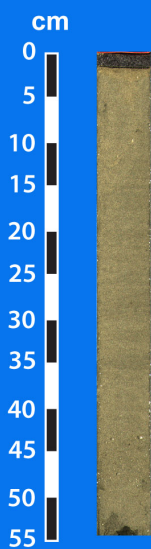
# Trinity-Tiger Shoals Complex

## TT-03-08



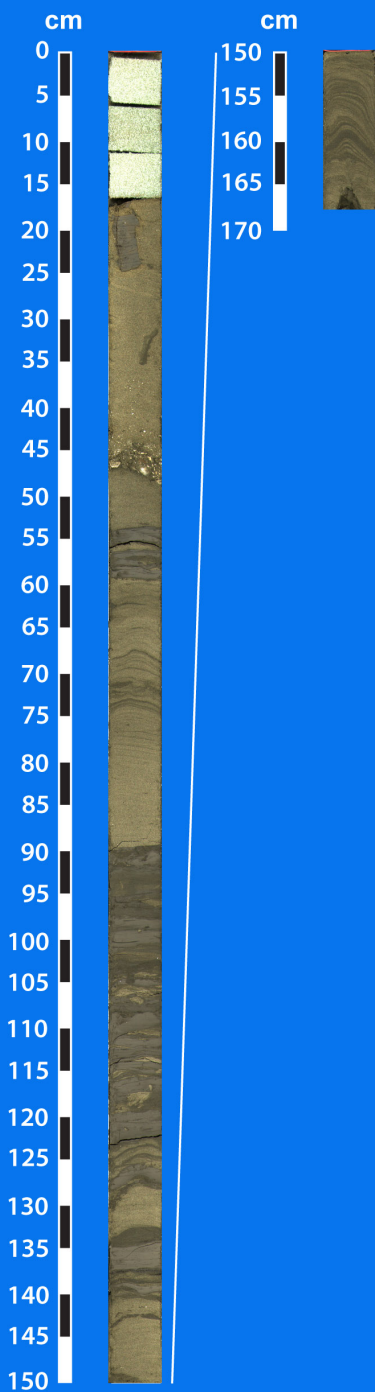
# Trinity-Tiger Shoals Complex

## TT-04-08



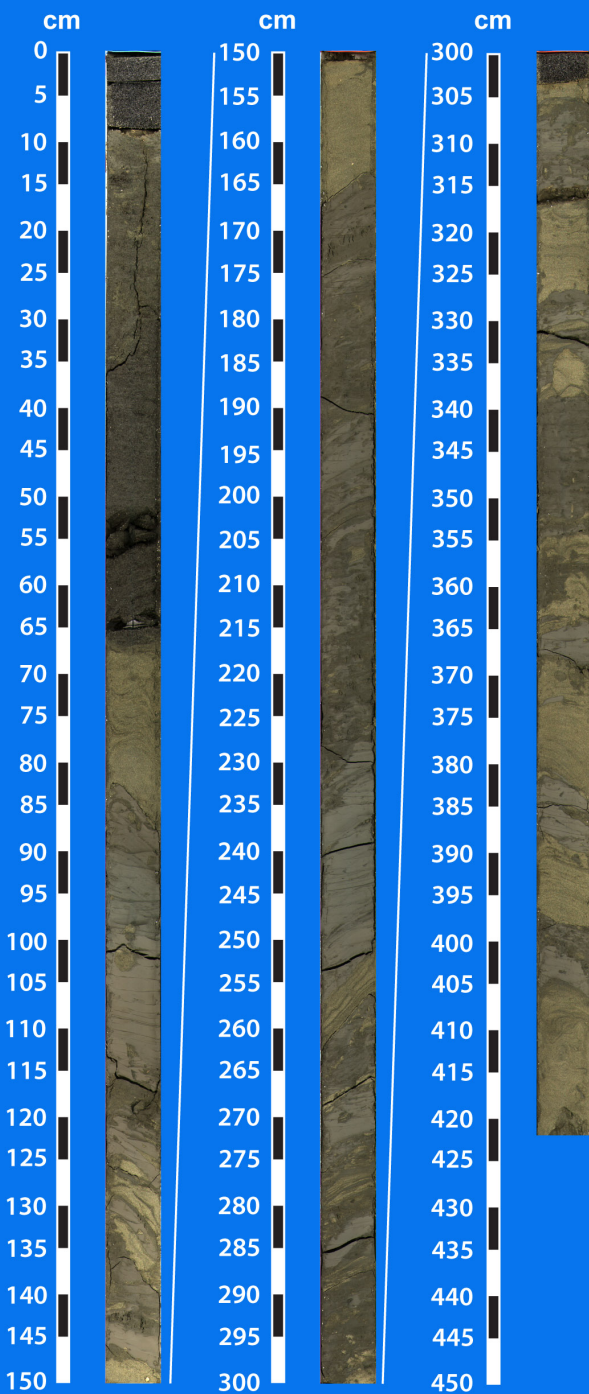
# Trinity-Tiger Shoals Complex

## TT-05-08



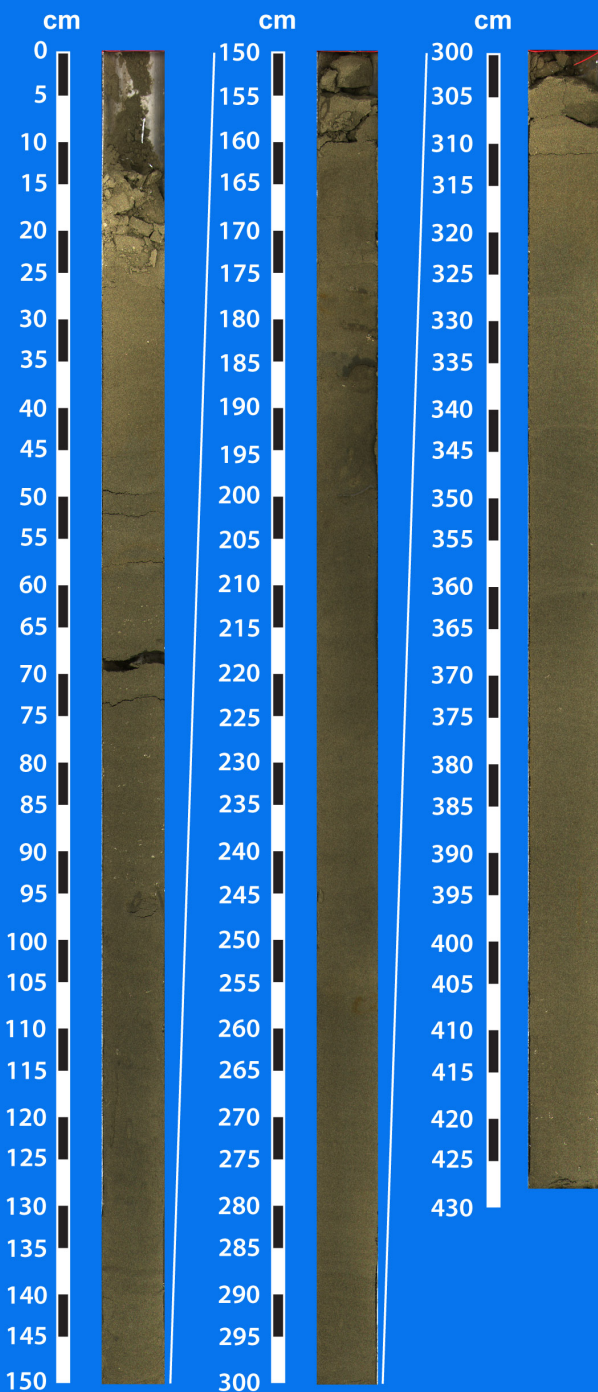
# Trinity-Tiger Shoals Complex

## TT-06-08



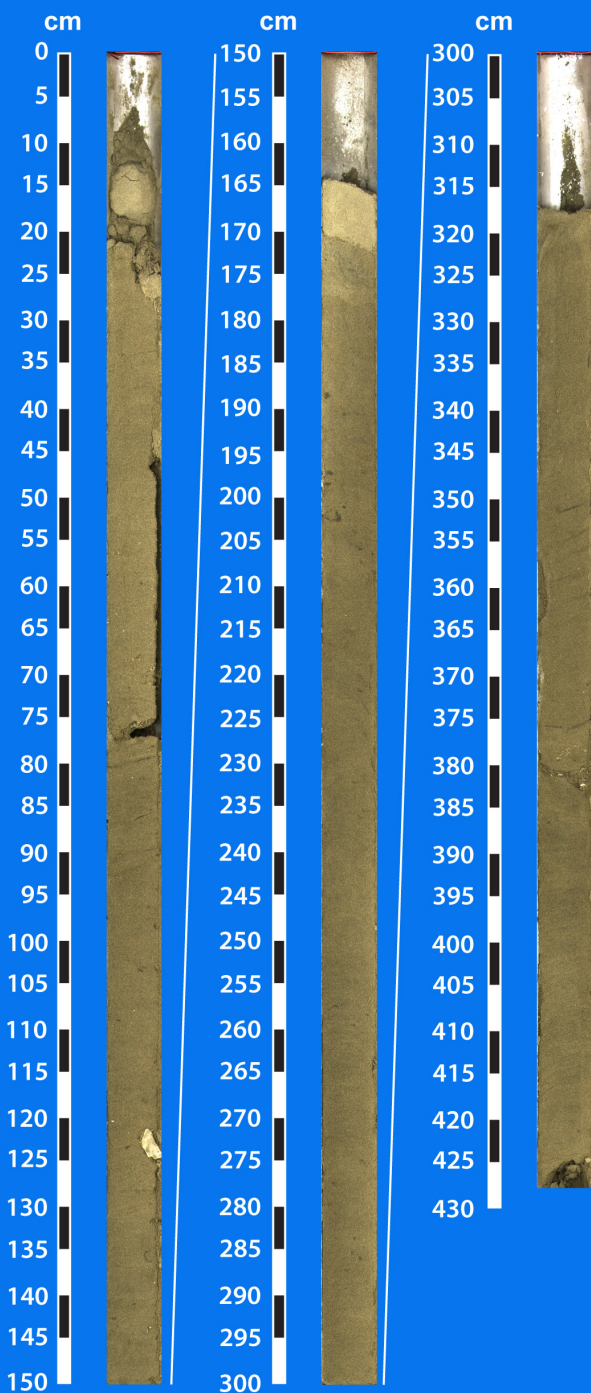


# Trinity-Tiger Shoals Complex TT-08-10

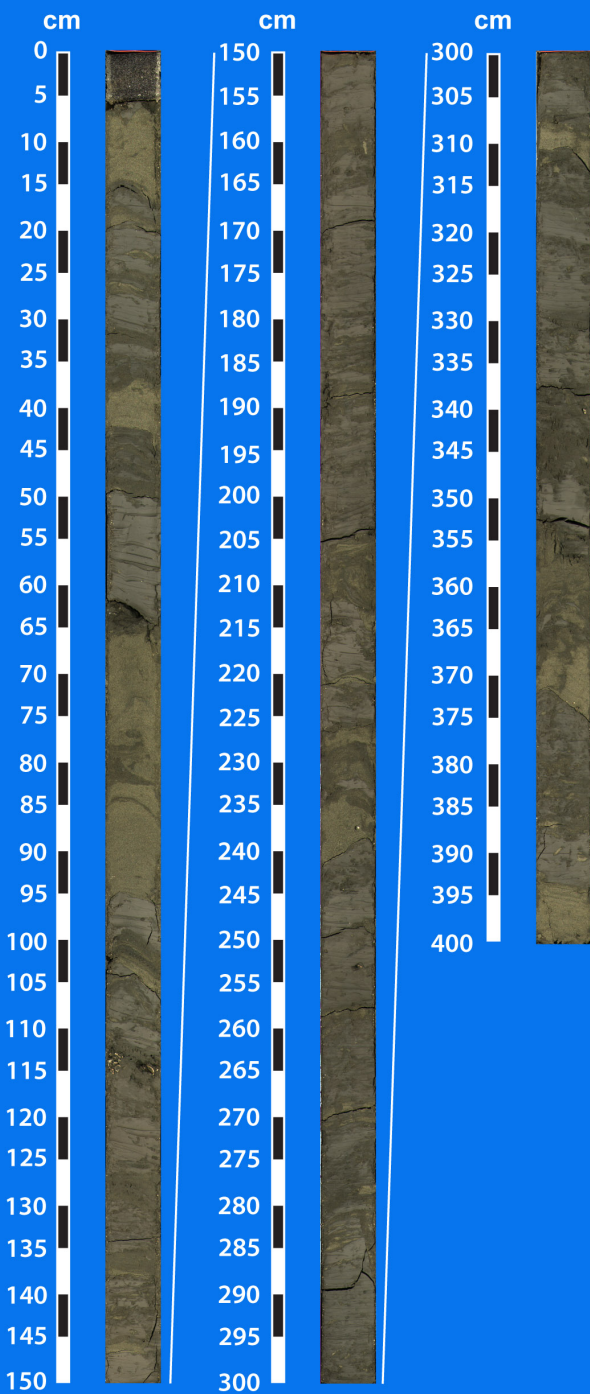


# Trinity-Tiger Shoals Complex

## TT-09-08



# Trinity-Tiger Shoals Complex TT-10-08



# Trinity-Tiger Shoals Complex

## TT-12-08



# Trinity-Tiger Shoals Complex

## TT-13-10

cm

0  
5  
10  
15  
20  
25  
30  
35  
40  
45  
50  
55  
60  
65  
70  
75  
80  
85  
90  
95  
100  
105  
110  
115  
120  
125  
130  
135  
140  
145  
150



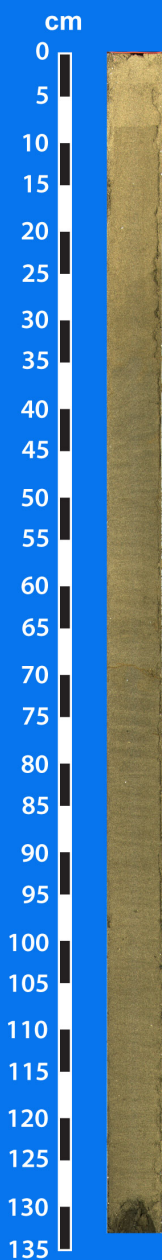
cm

150  
155  
160  
165  
170  
175



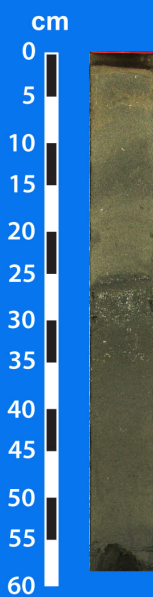
# Trinity-Tiger Shoals Complex

## TT-15-08



# Trinity-Tiger Shoals Complex

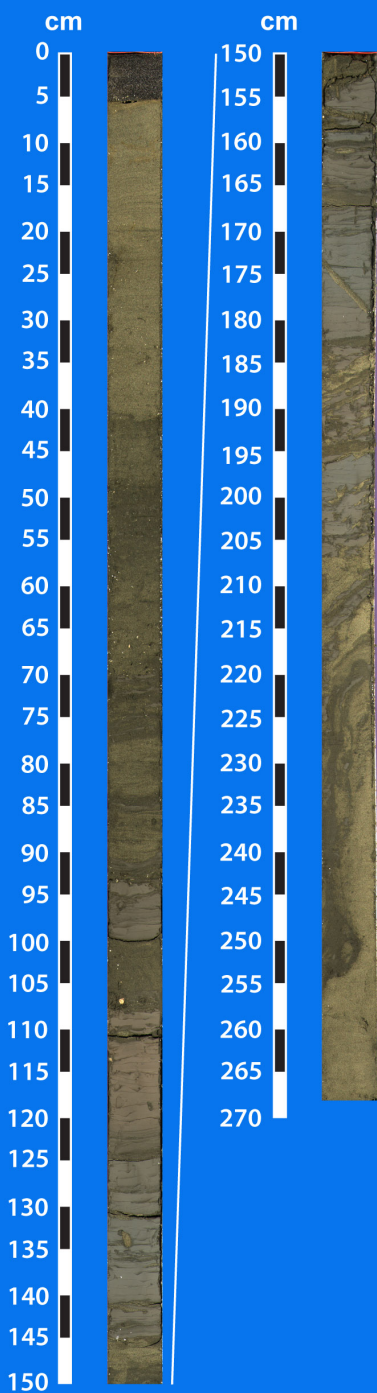
## TT-17-10





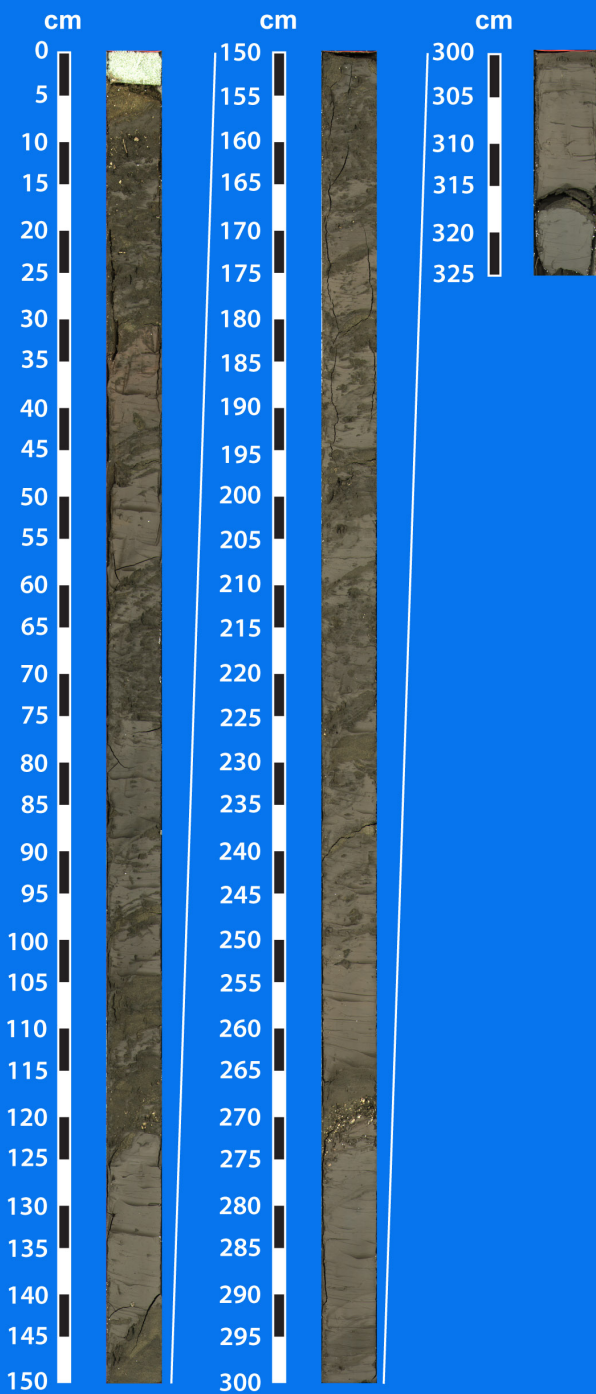
# Trinity-Tiger Shoals Complex

## TT-19-08



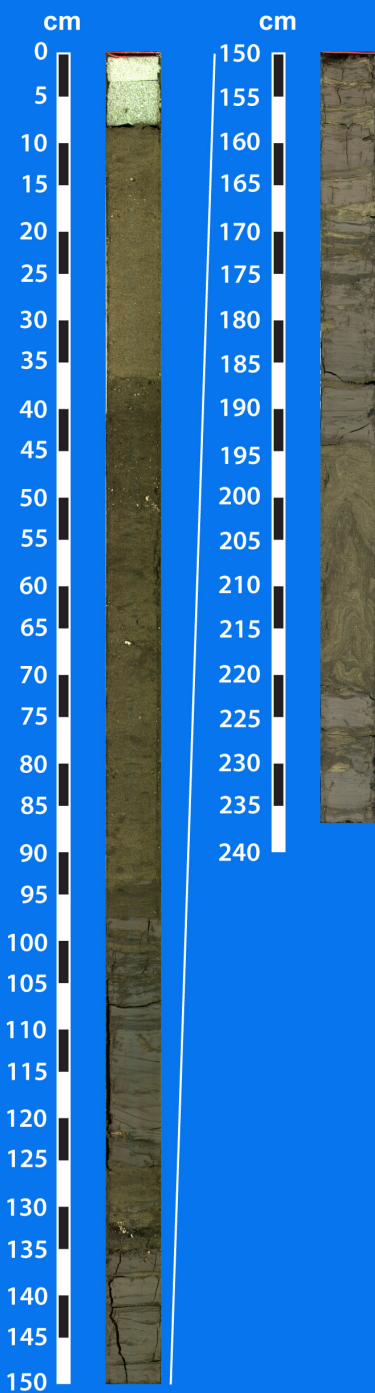
# Trinity-Tiger Shoals Complex

## TT-20-08



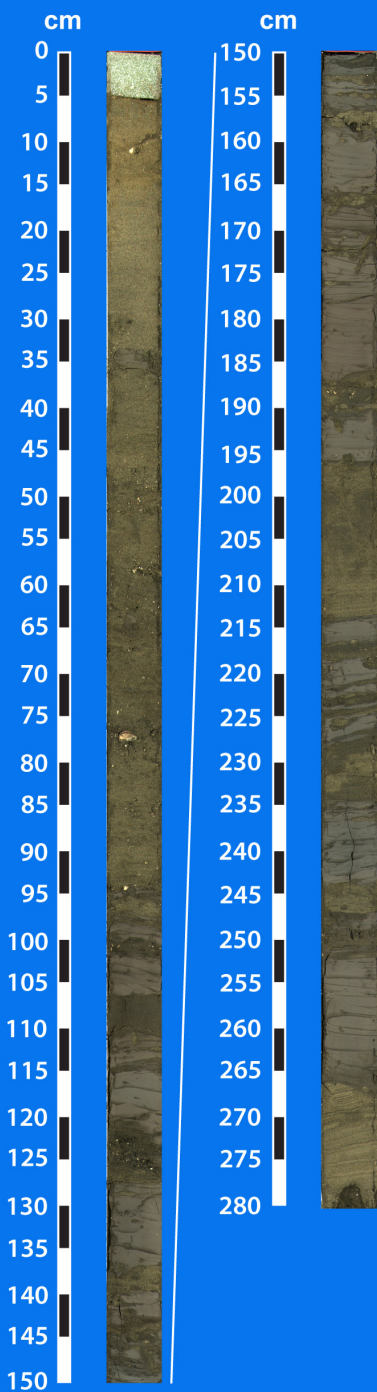
# Trinity-Tiger Shoals Complex

## TT-21-08



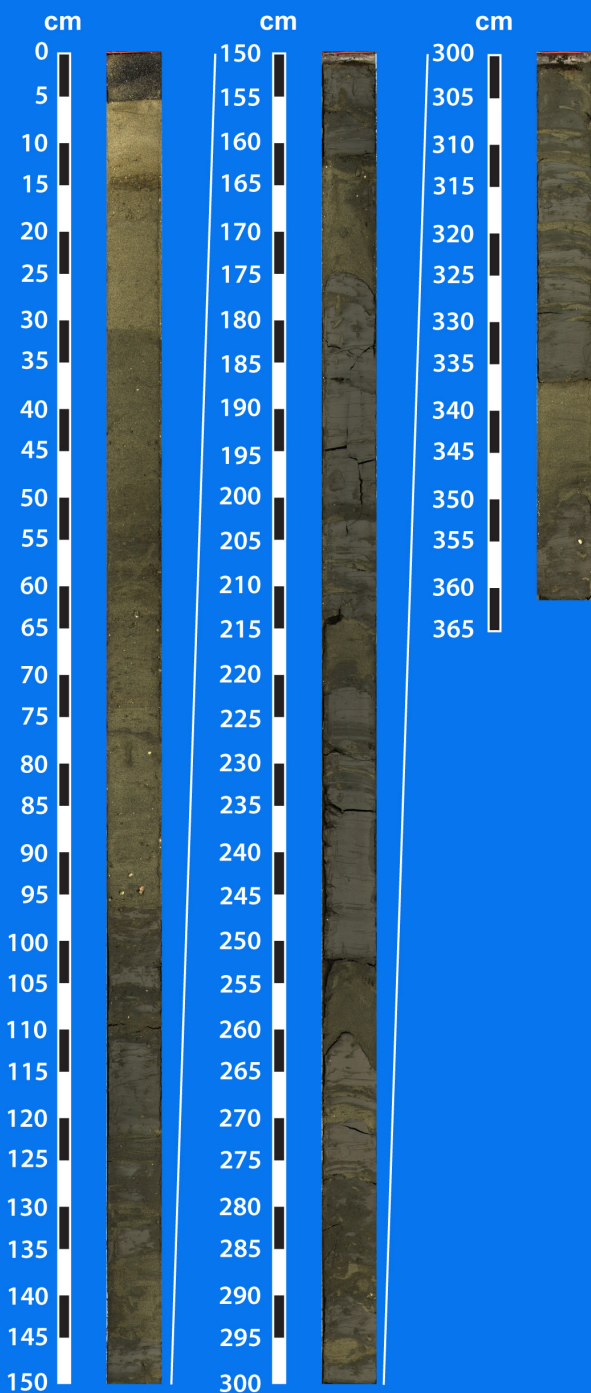
# Trinity-Tiger Shoals Complex

## TT-22-08



# Trinity-Tiger Shoals Complex

## TT-23-08



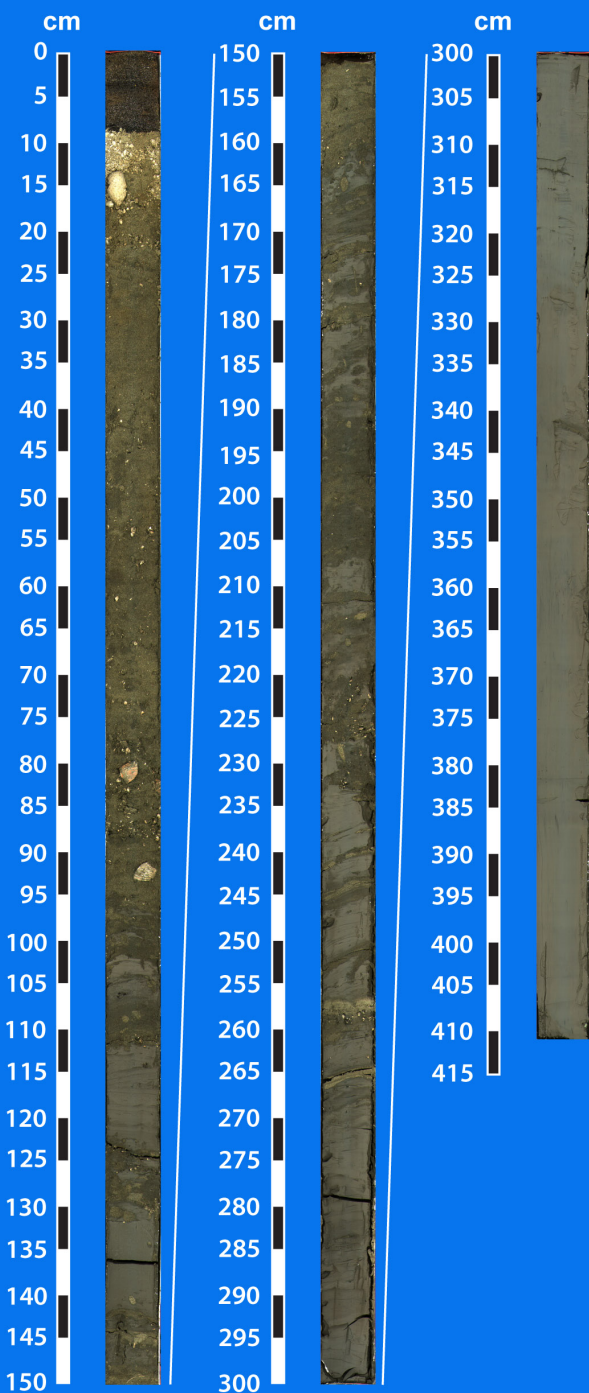
# Trinity-Tiger Shoals Complex

## TT-24-08



# Trinity-Tiger Shoals Complex

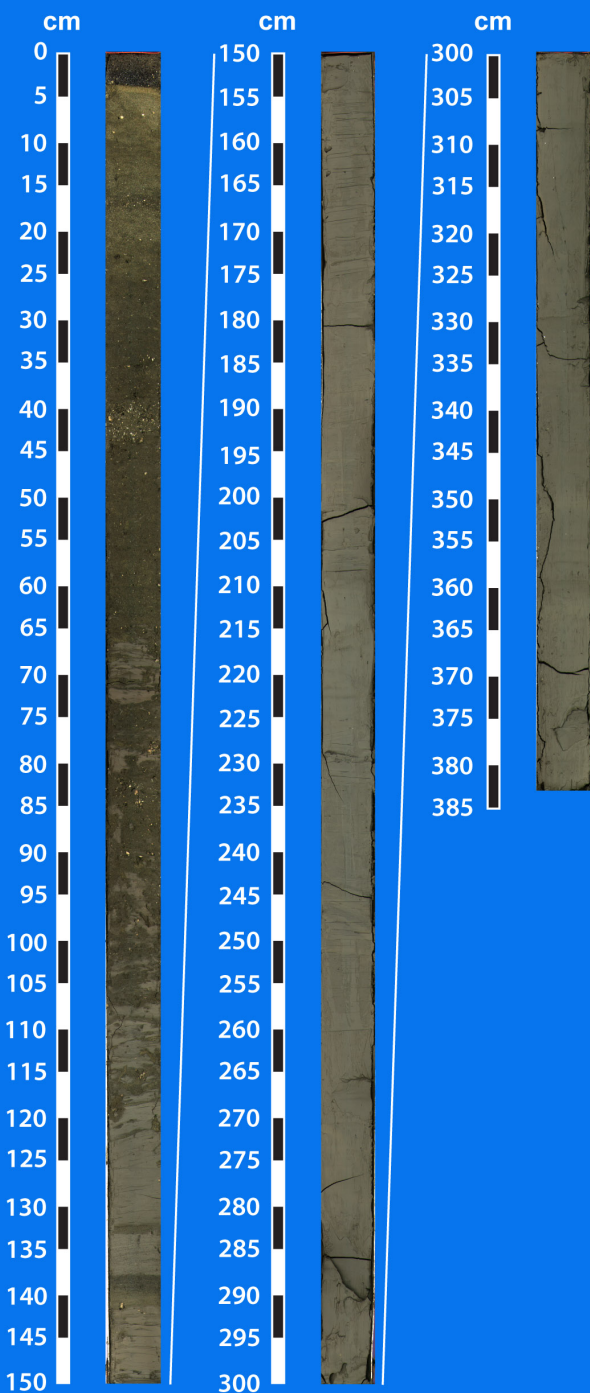
## TT-25-08



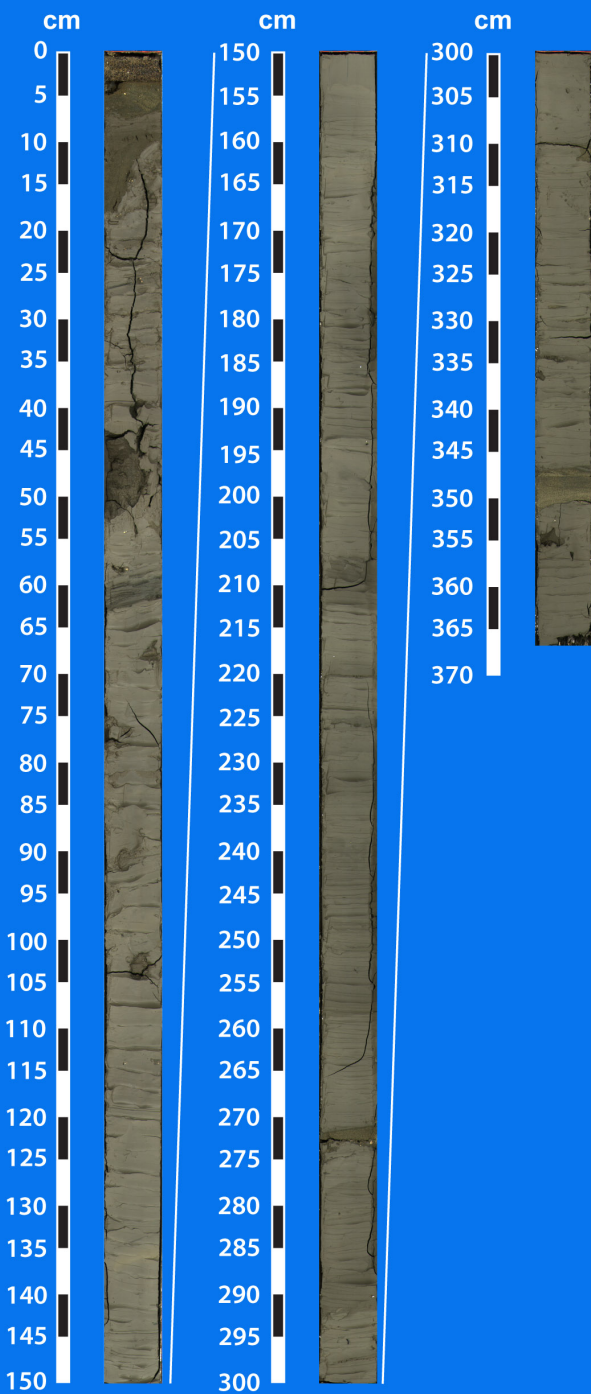


# Trinity-Tiger Shoals Complex

## TT-26-08

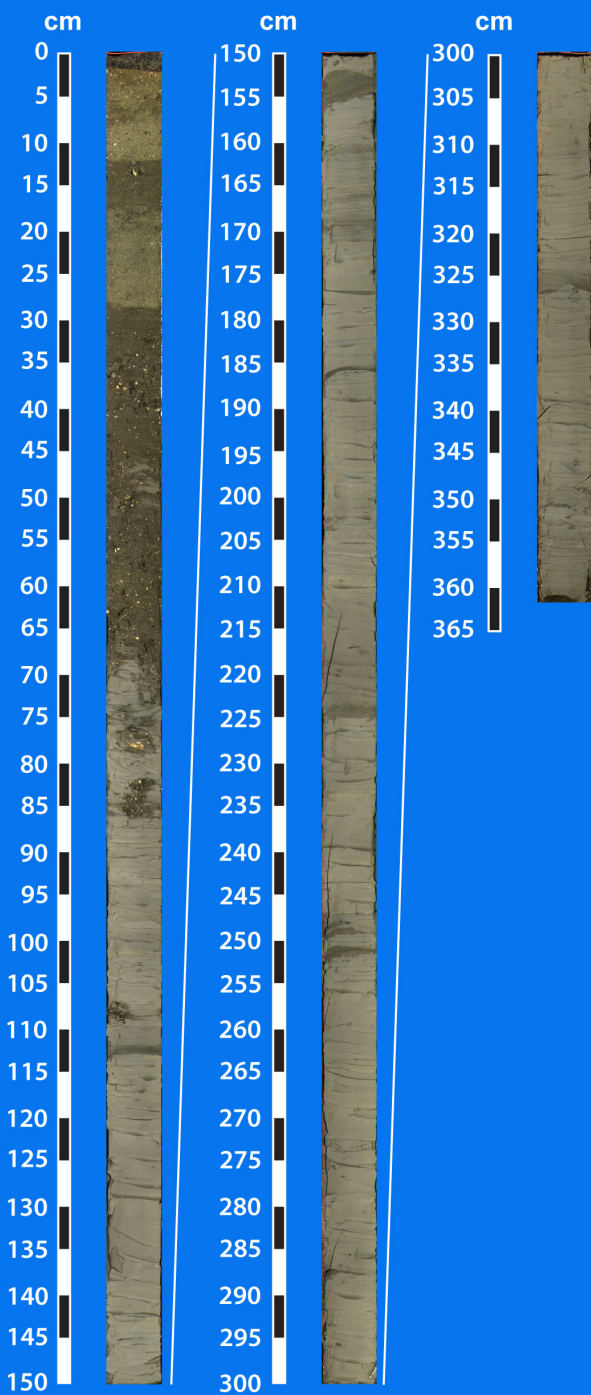


# Trinity-Tiger Shoals Complex TT-27-08



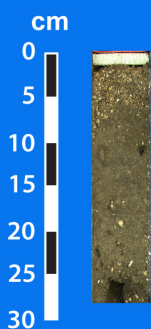
# Trinity-Tiger Shoals Complex

## TT-28-08



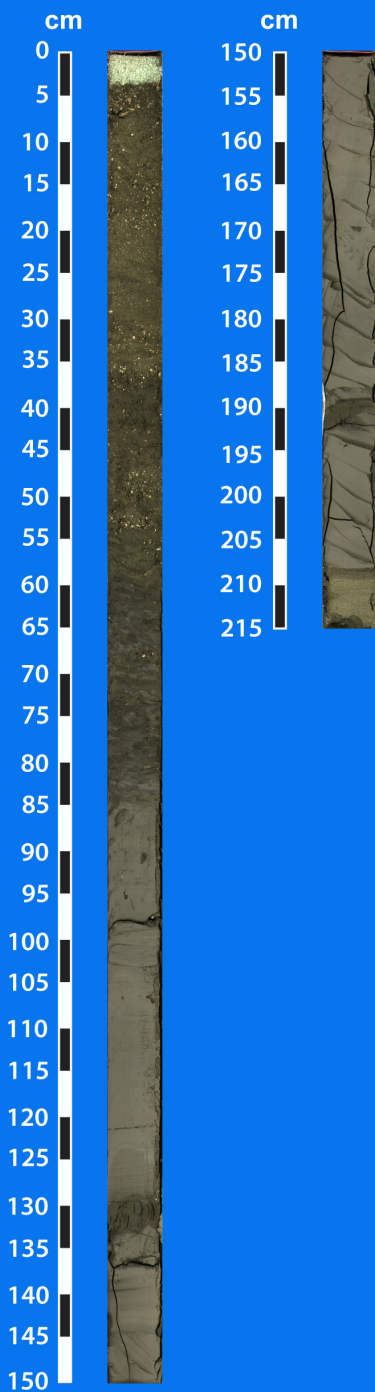
# Trinity-Tiger Shoals Complex

## TT-29-08



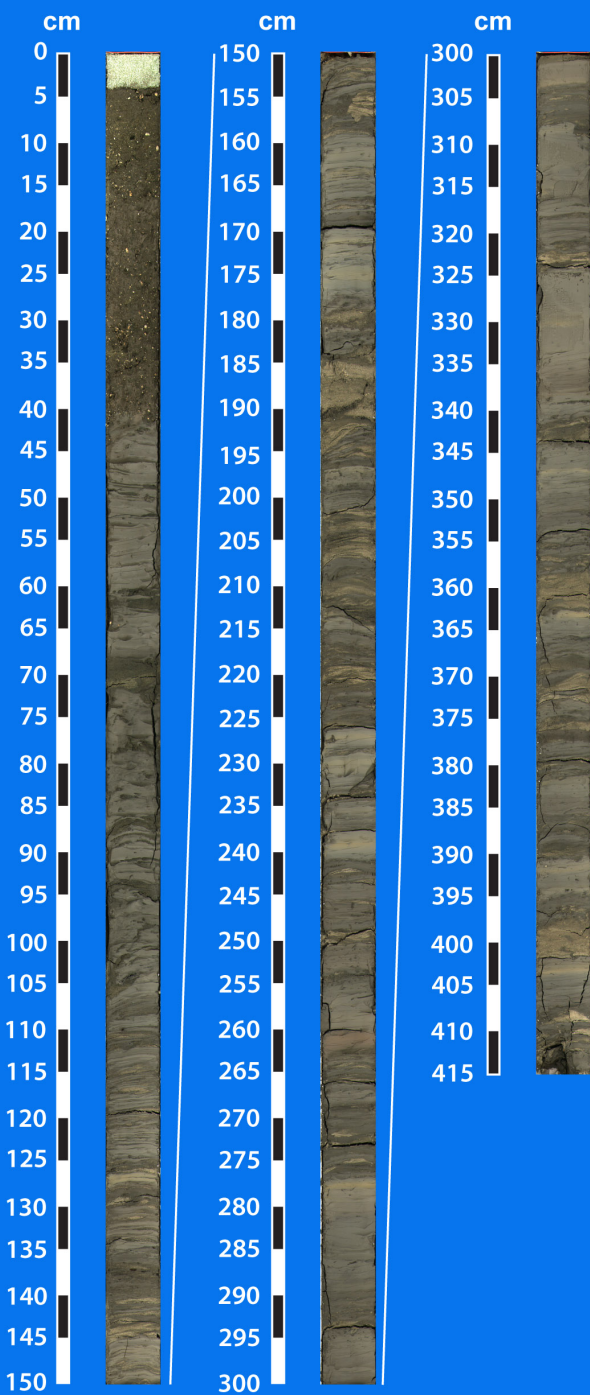
# Trinity-Tiger Shoals Complex

## TT-30-08



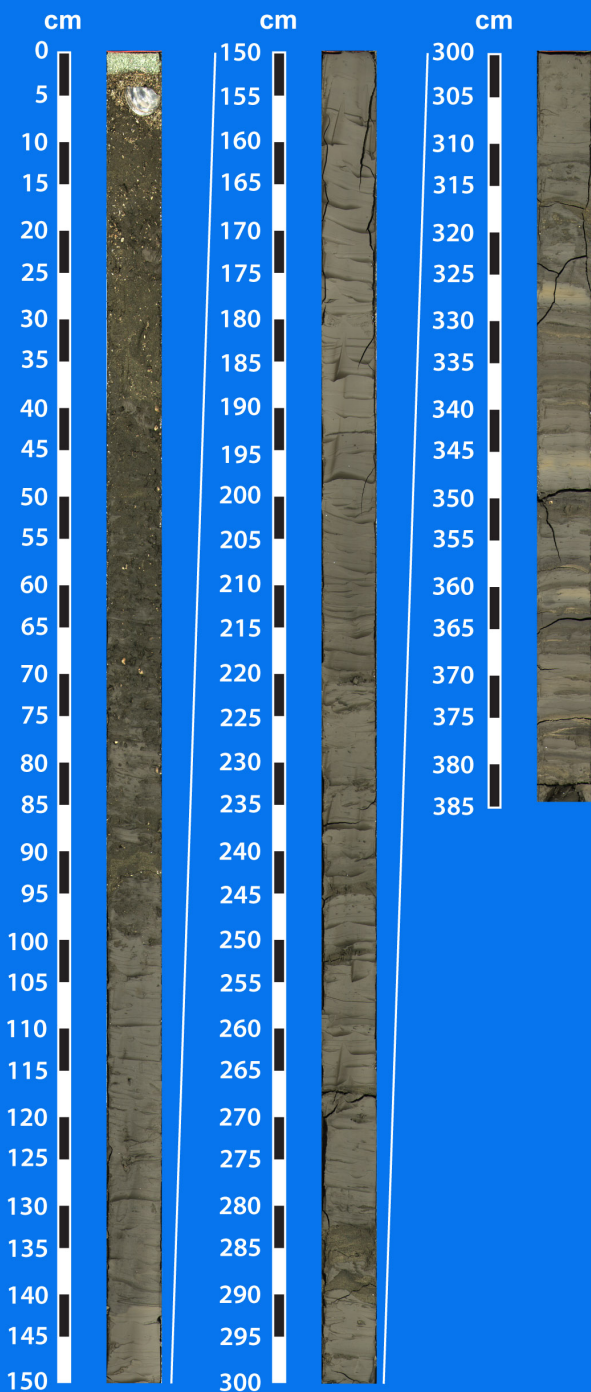
# Trinity-Tiger Shoals Complex

## TT-31-08



# Trinity-Tiger Shoals Complex

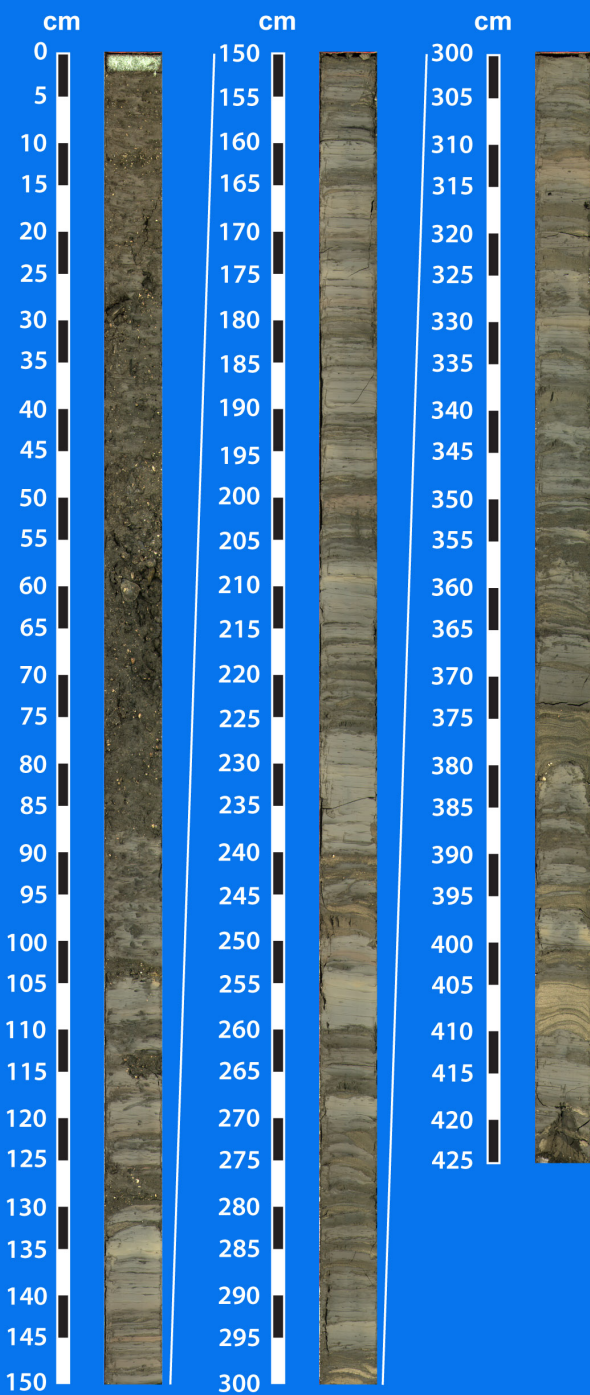
## TT-32-08





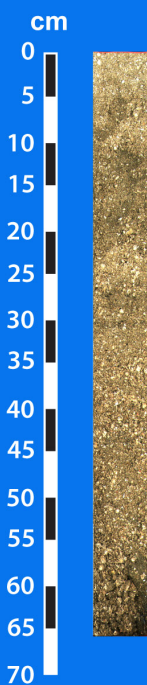
# Trinity-Tiger Shoals Complex

## TT-33-08



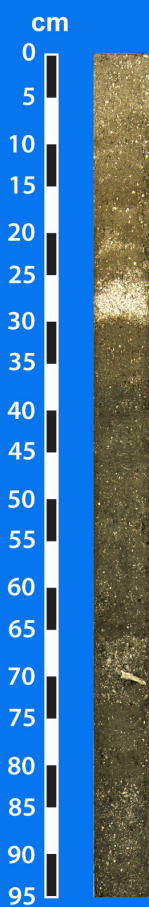
# Trinity-Tiger Shoals Complex

## TT-34-08



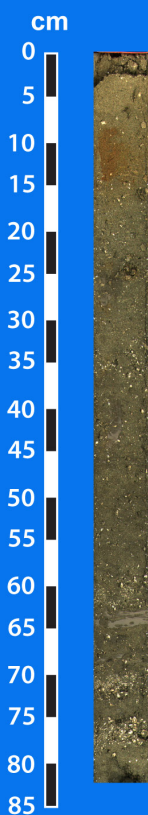
# Trinity-Tiger Shoals Complex

## TT-35-08



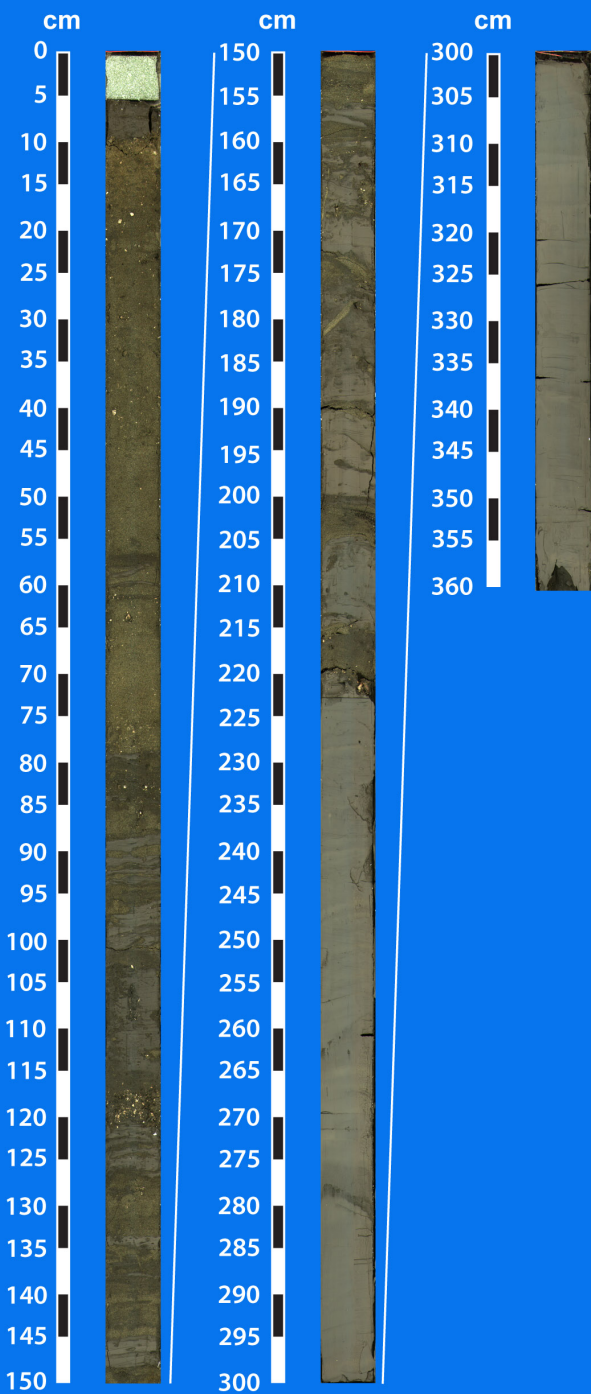
# Trinity-Tiger Shoals Complex

## TT-36-08



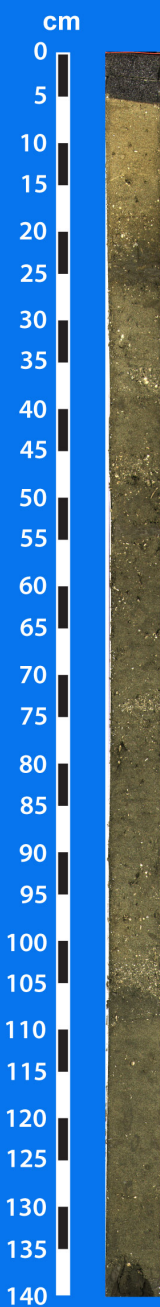
# Trinity-Tiger Shoals Complex

## TT-37-08



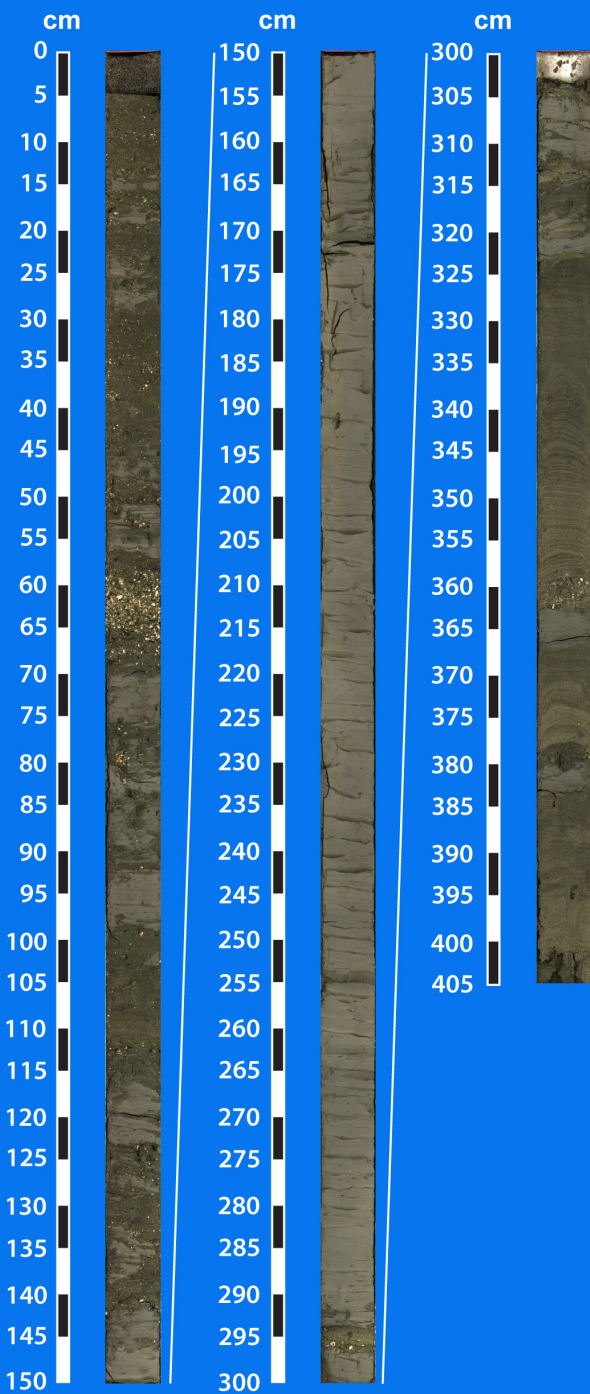
# Trinity-Tiger Shoals Complex

## TT-38-08



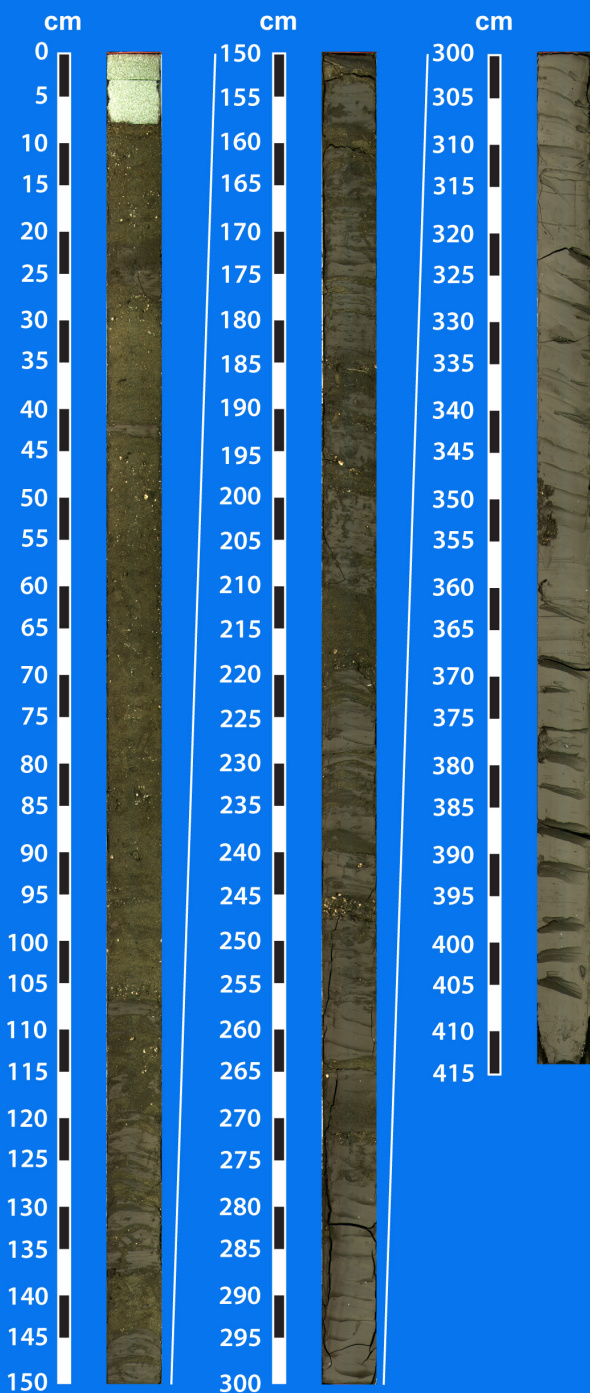
# Trinity-Tiger Shoals Complex

## TT-39-08



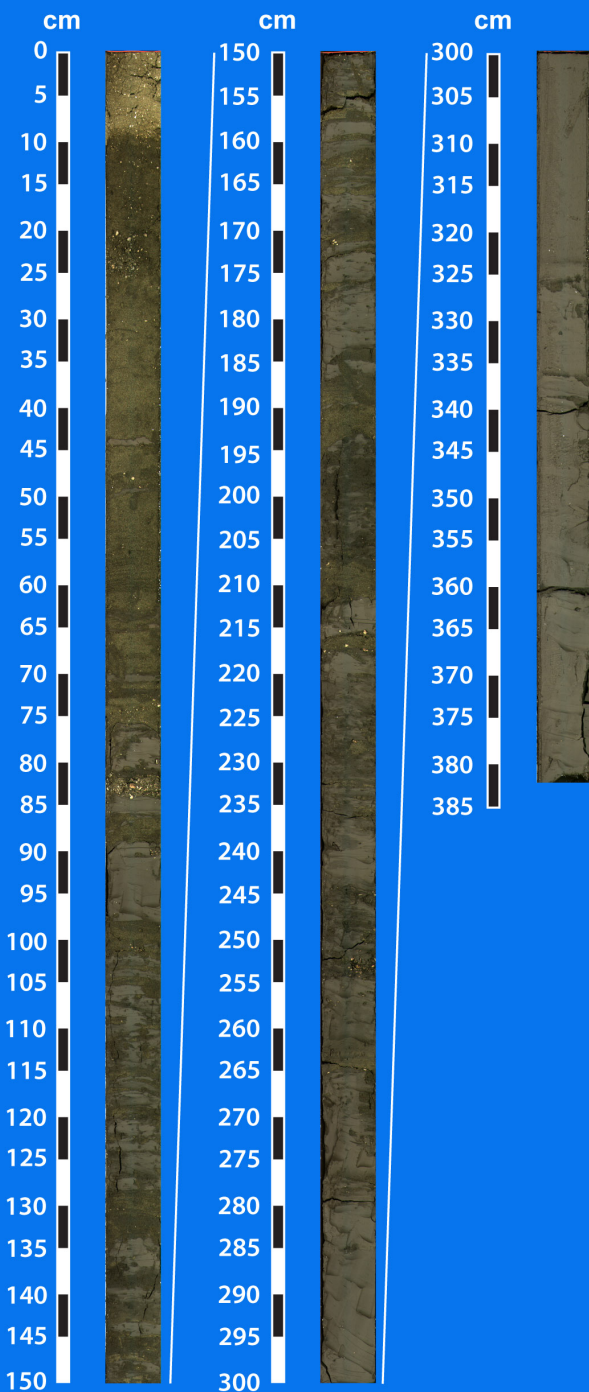


# Trinity-Tiger Shoals Complex TT-40-08



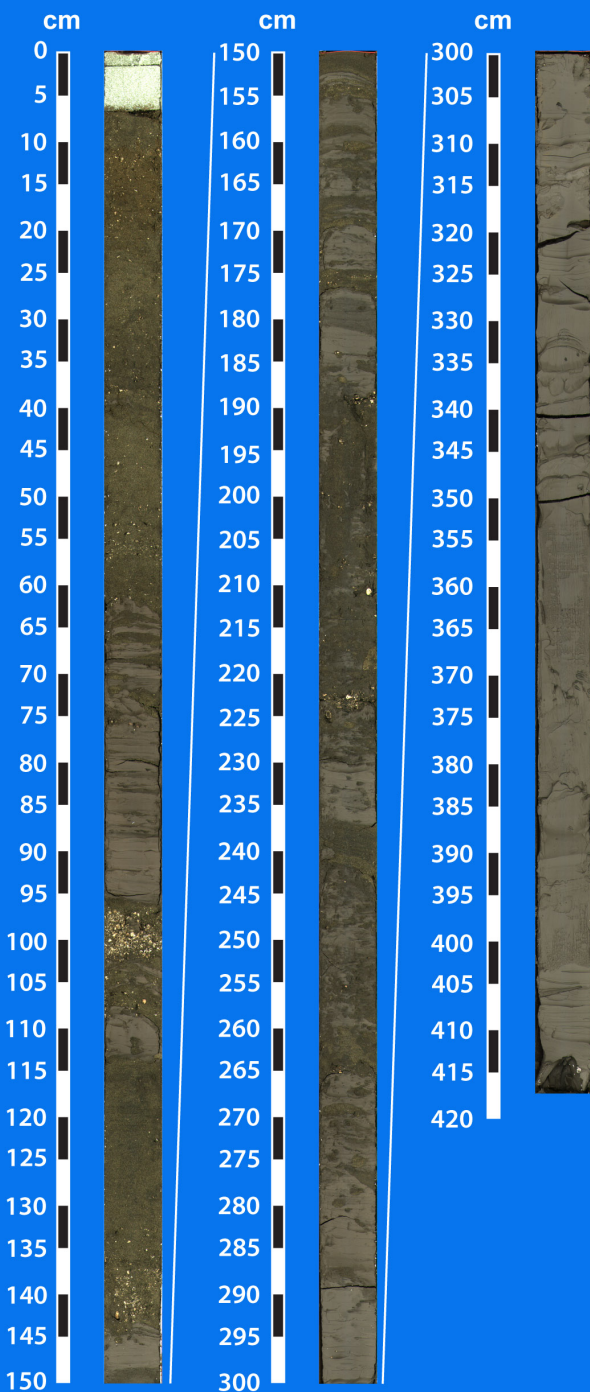
# Trinity-Tiger Shoals Complex

## TT-41-08



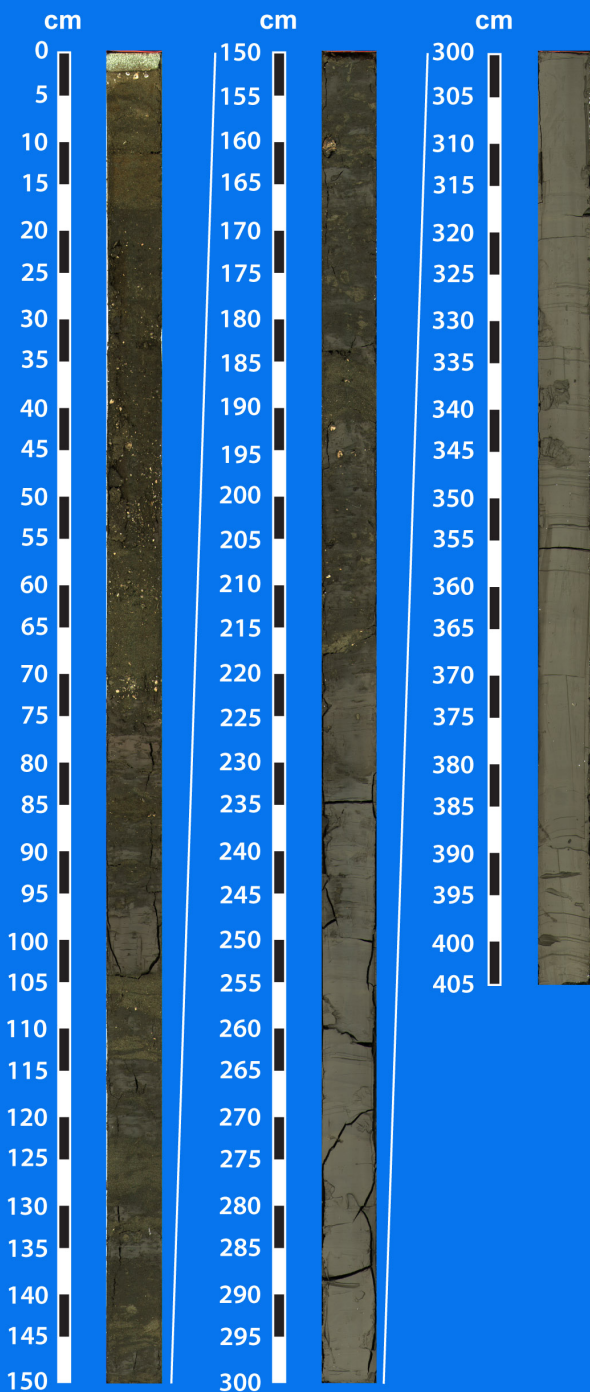
# Trinity-Tiger Shoals Complex

## TT-42-08



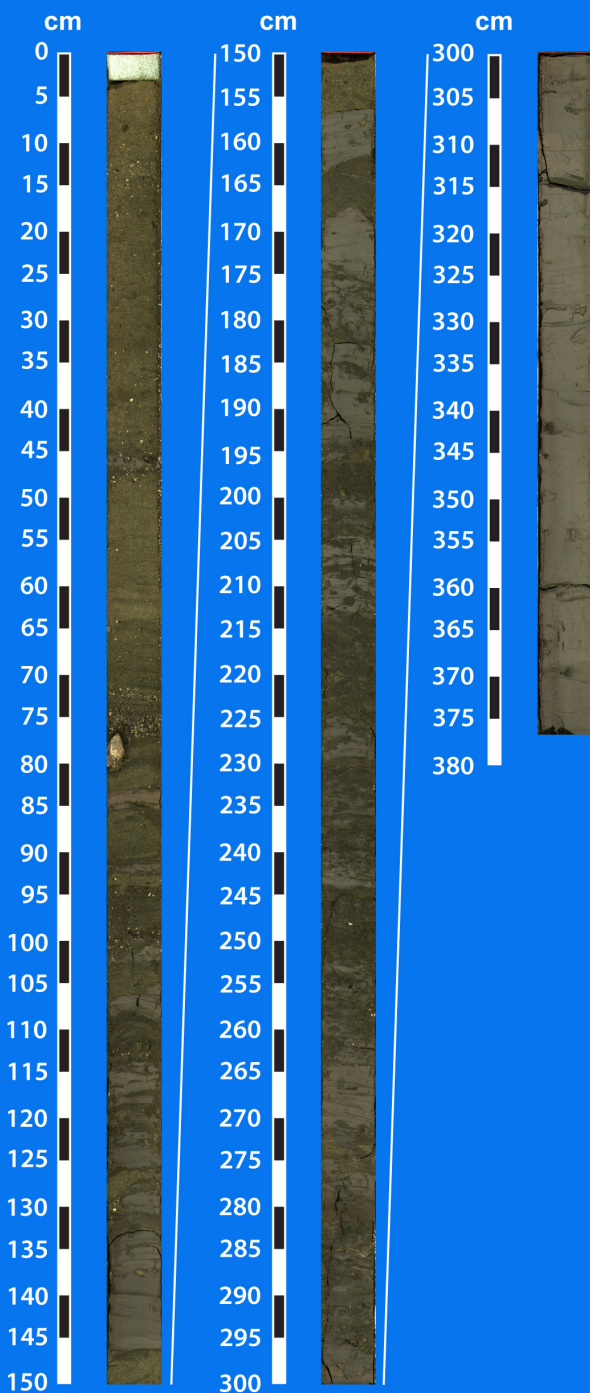
# Trinity-Tiger Shoals Complex

## TT-43-08



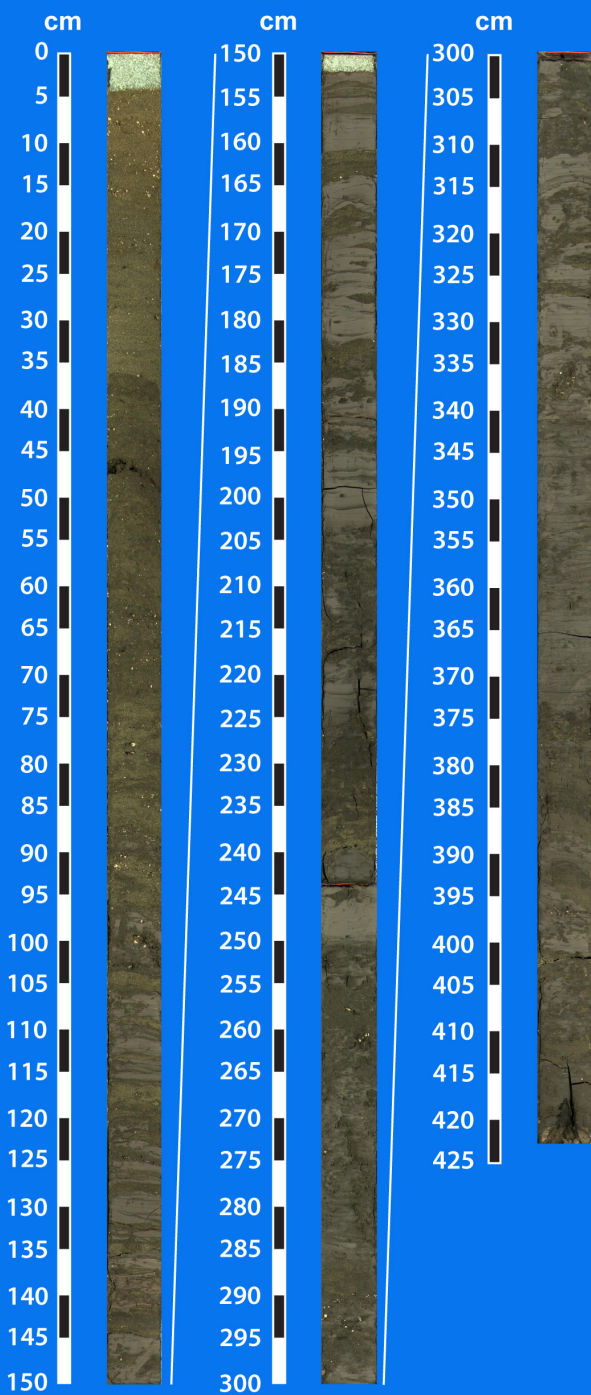
# Trinity-Tiger Shoals Complex

## TT-44-08



# Trinity-Tiger Shoals Complex

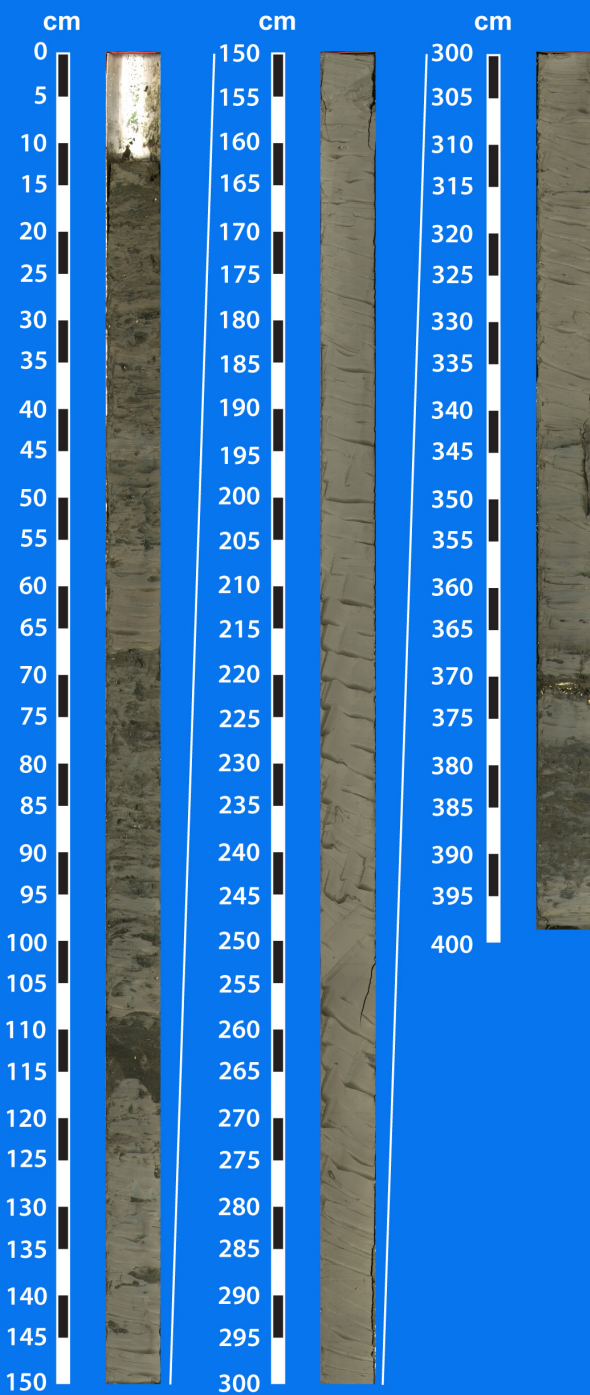
## TT-45-08





# Trinity-Tiger Shoals Complex

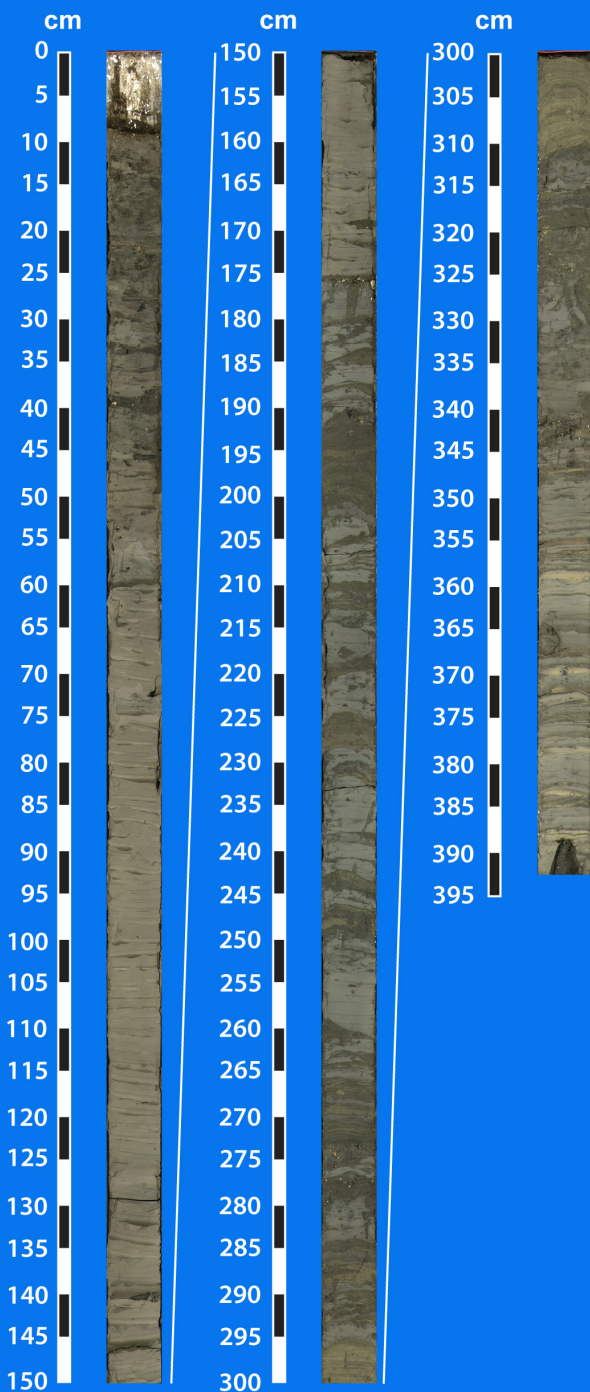
## TT-46-08





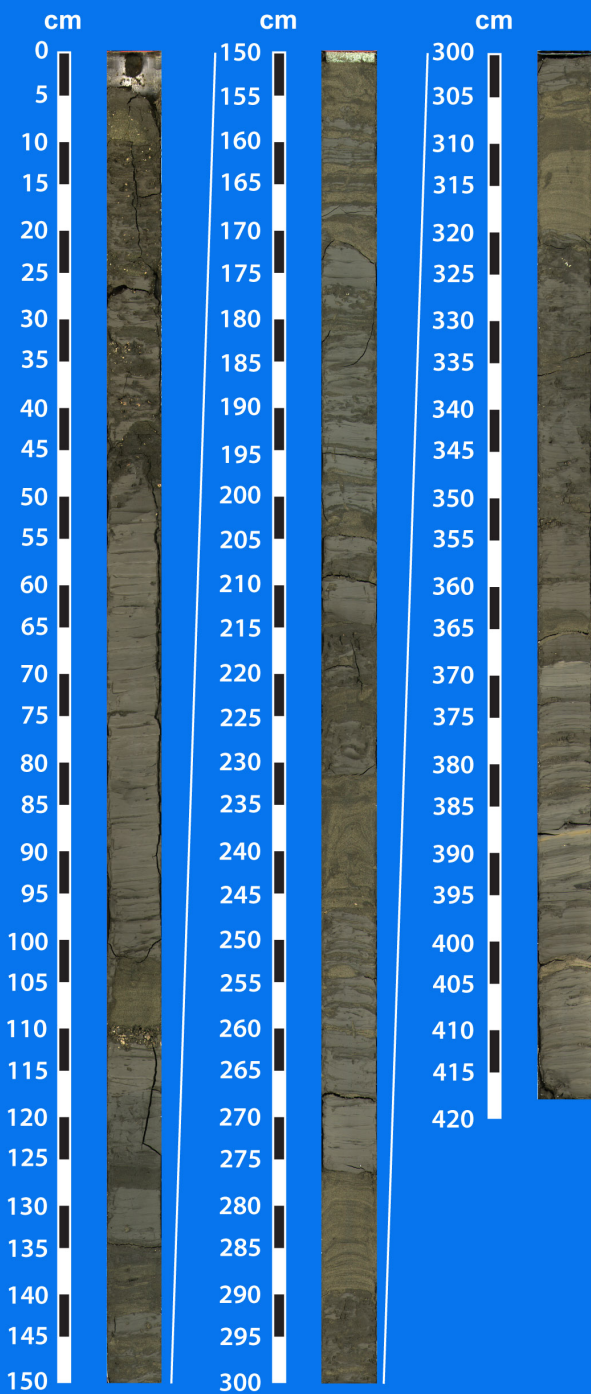
# Trinity-Tiger Shoals Complex

## TT-47-08



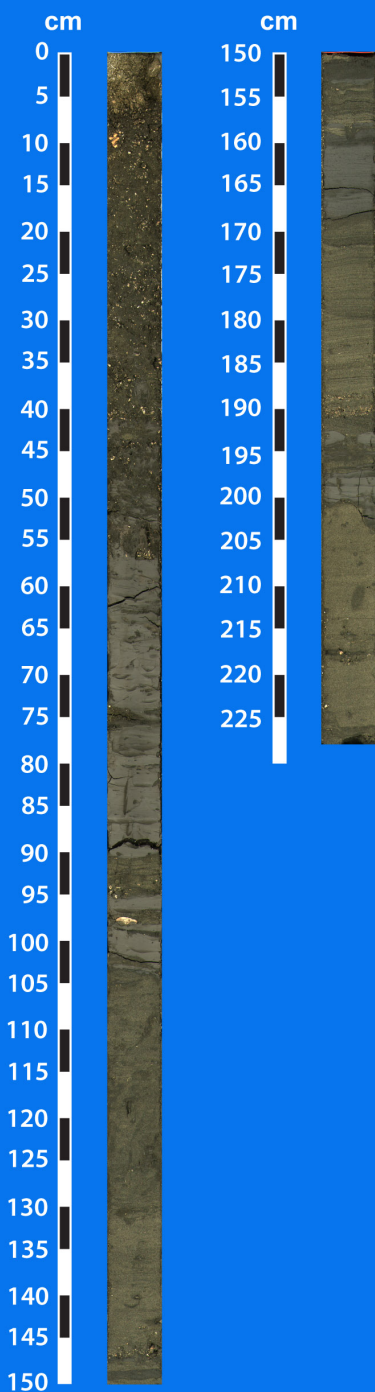
# Trinity-Tiger Shoals Complex

## TT-48-08



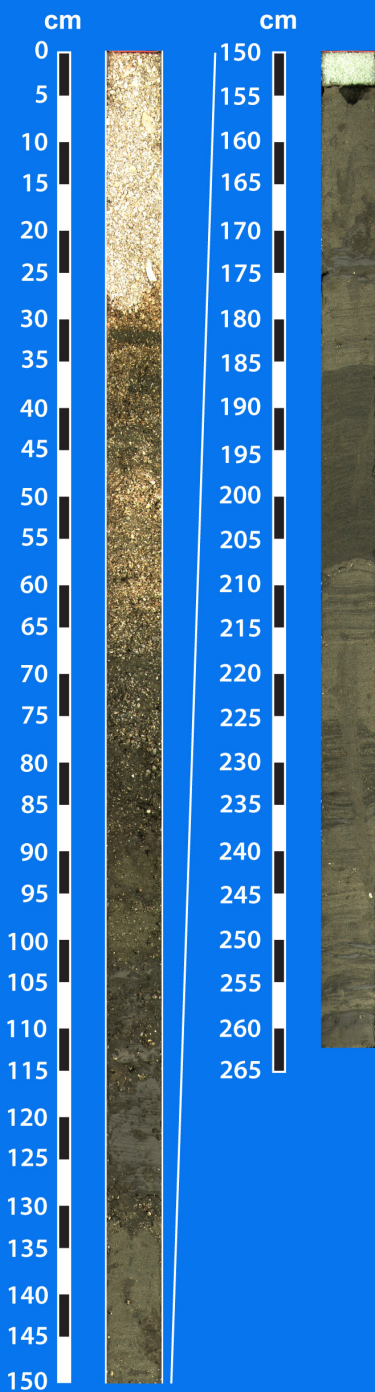
# Trinity-Tiger Shoals Complex

## TT-49-08



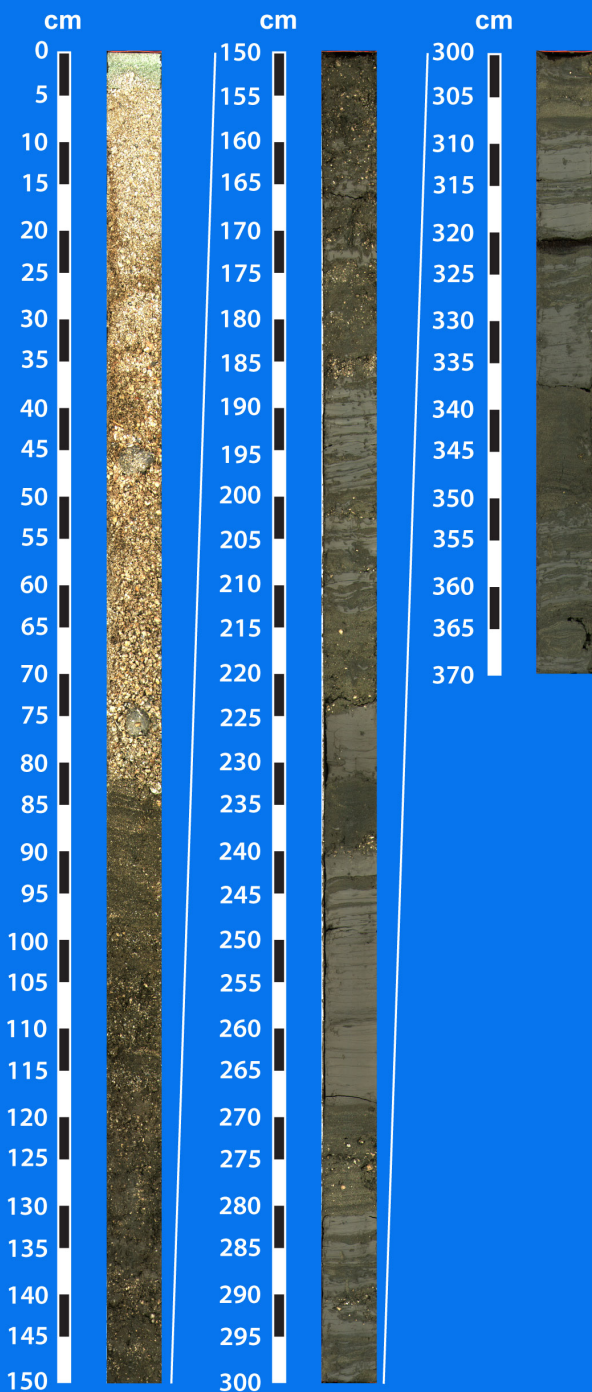
# Trinity-Tiger Shoals Complex

## TT-50-08

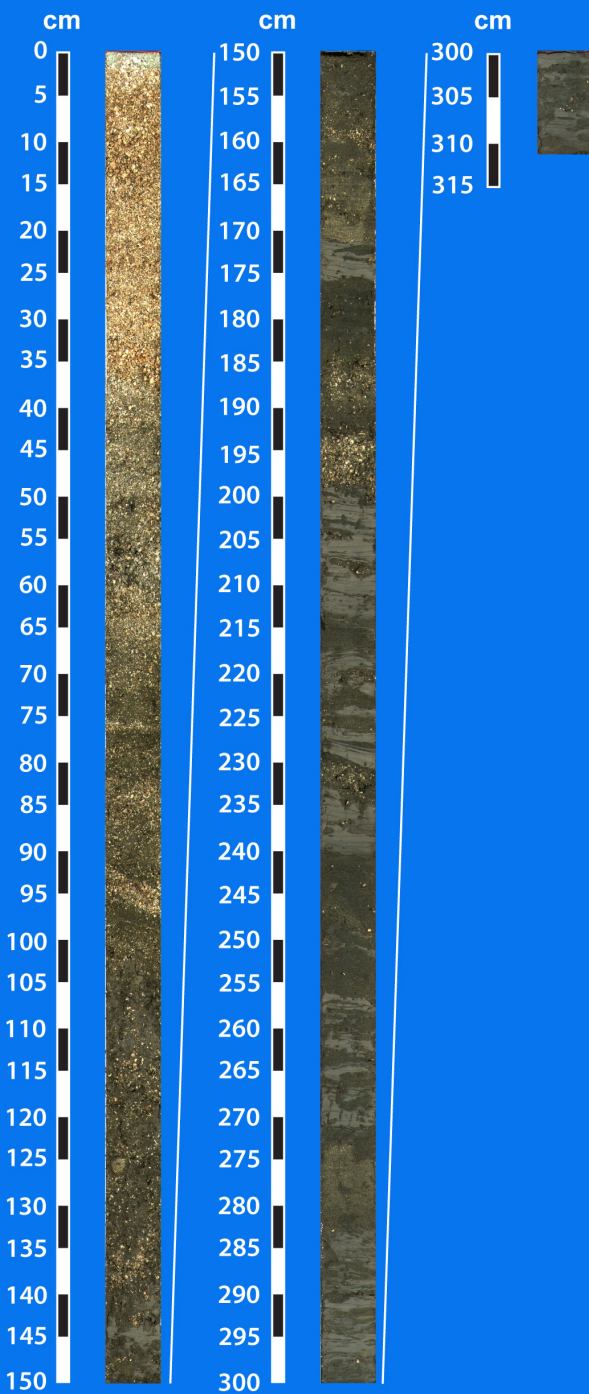


# Trinity-Tiger Shoals Complex

## TT-52-08



# Trinity-Tiger Shoals Complex TT-53-08



# Trinity-Tiger Shoals Complex

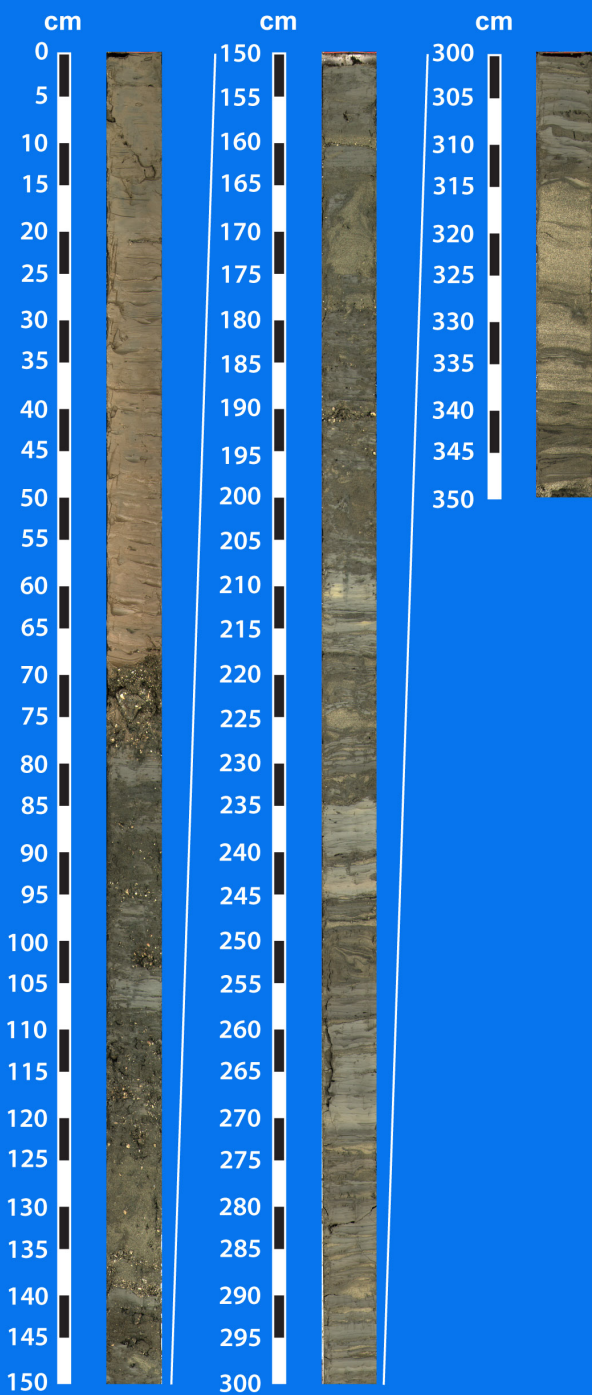
## TT-54-08





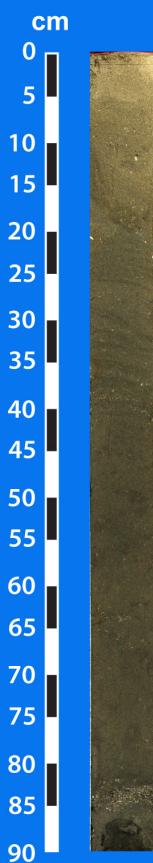
# Trinity-Tiger Shoals Complex

## TT-55-08

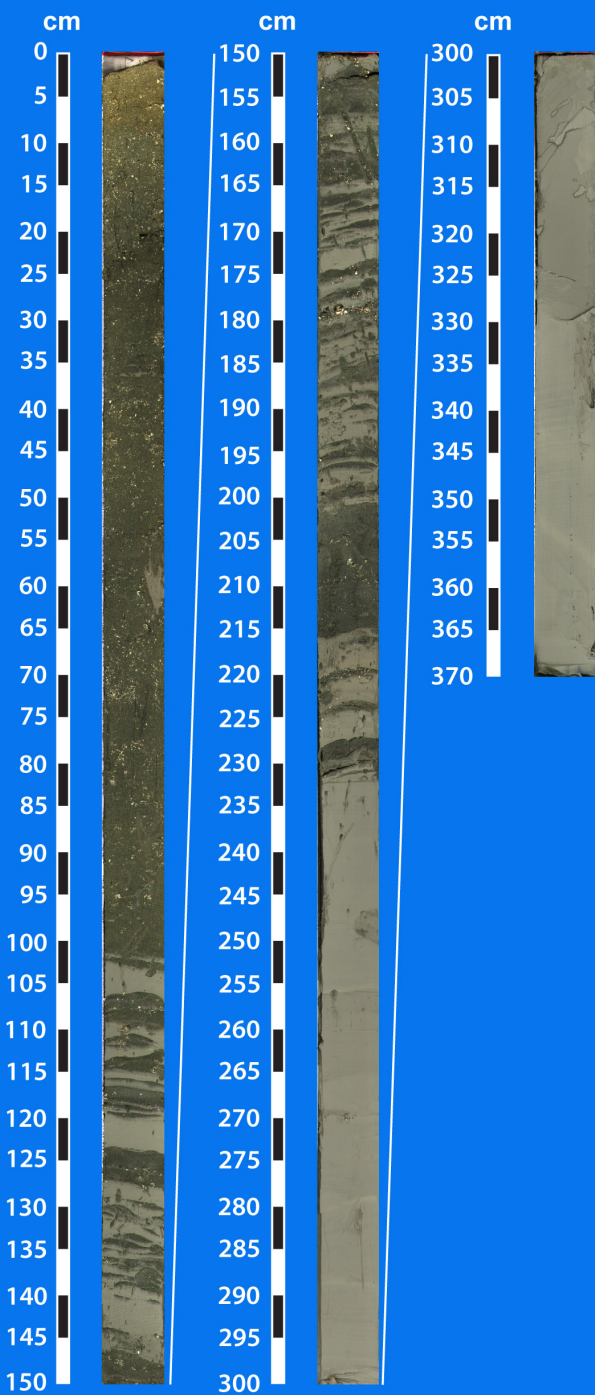


# Trinity-Tiger Shoals Complex

## TT-57-10

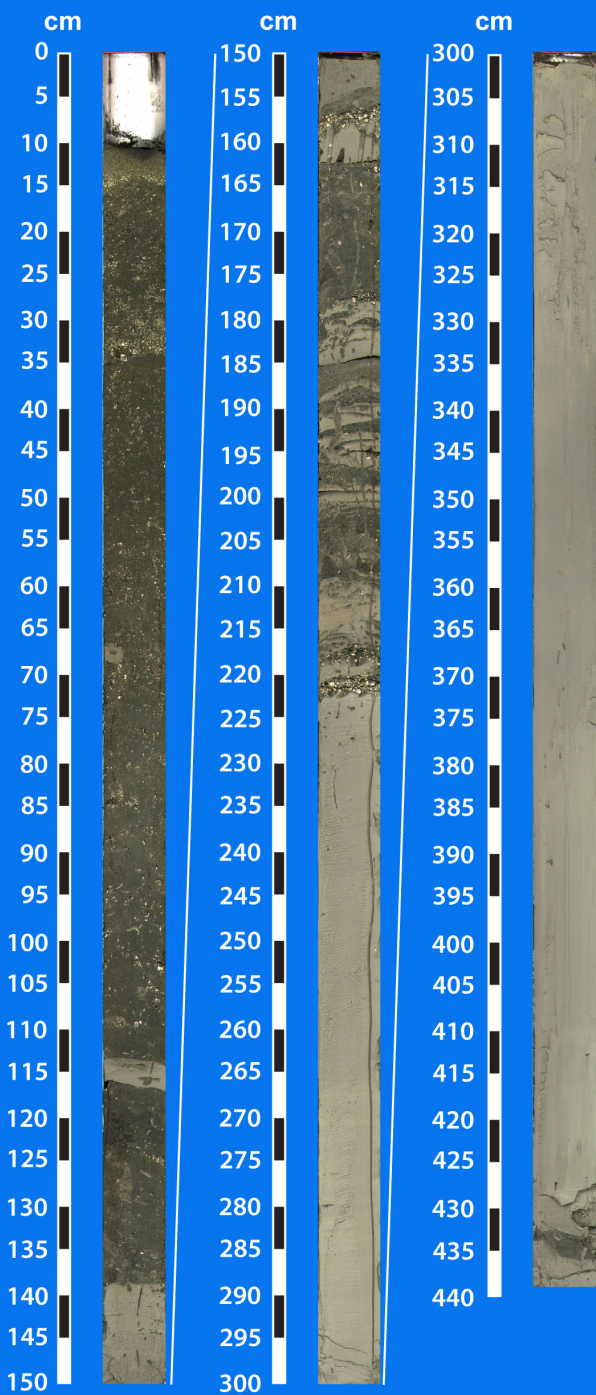


# Trinity-Tiger Shoals Complex TT-64-10



# Trinity-Tiger Shoals Complex

## TT-65-10



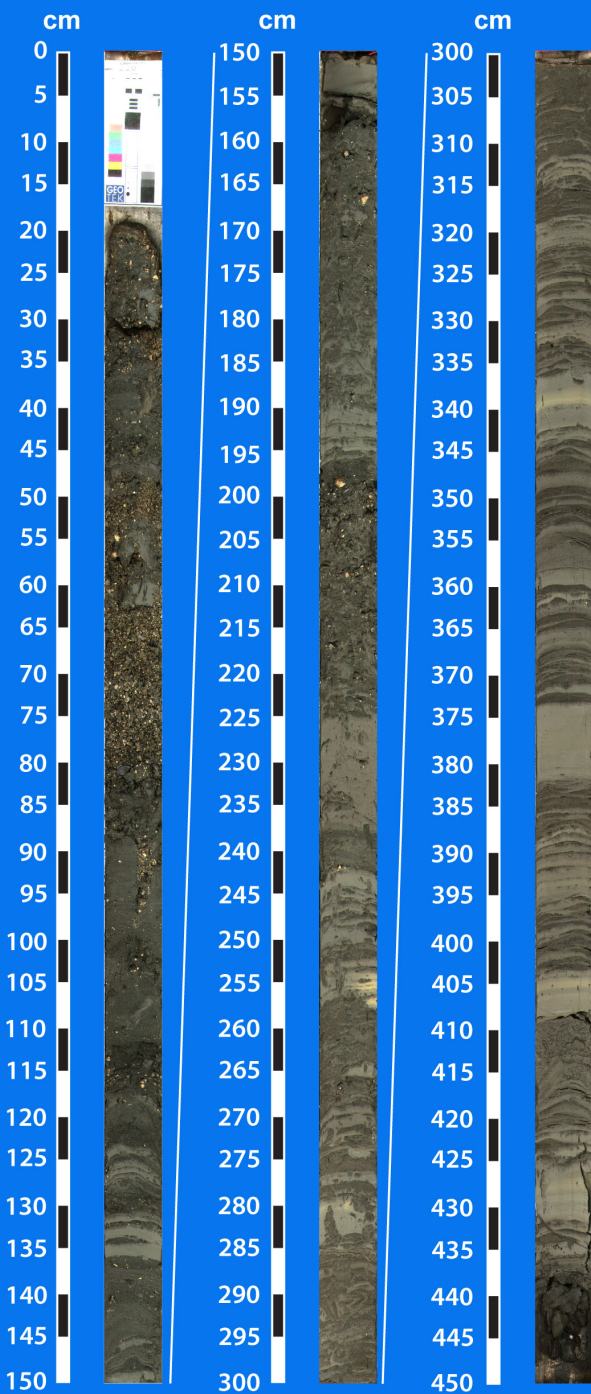
# Trinity-Tiger Shoals Complex

## TT-66-10



# Trinity-Tiger Shoals Complex

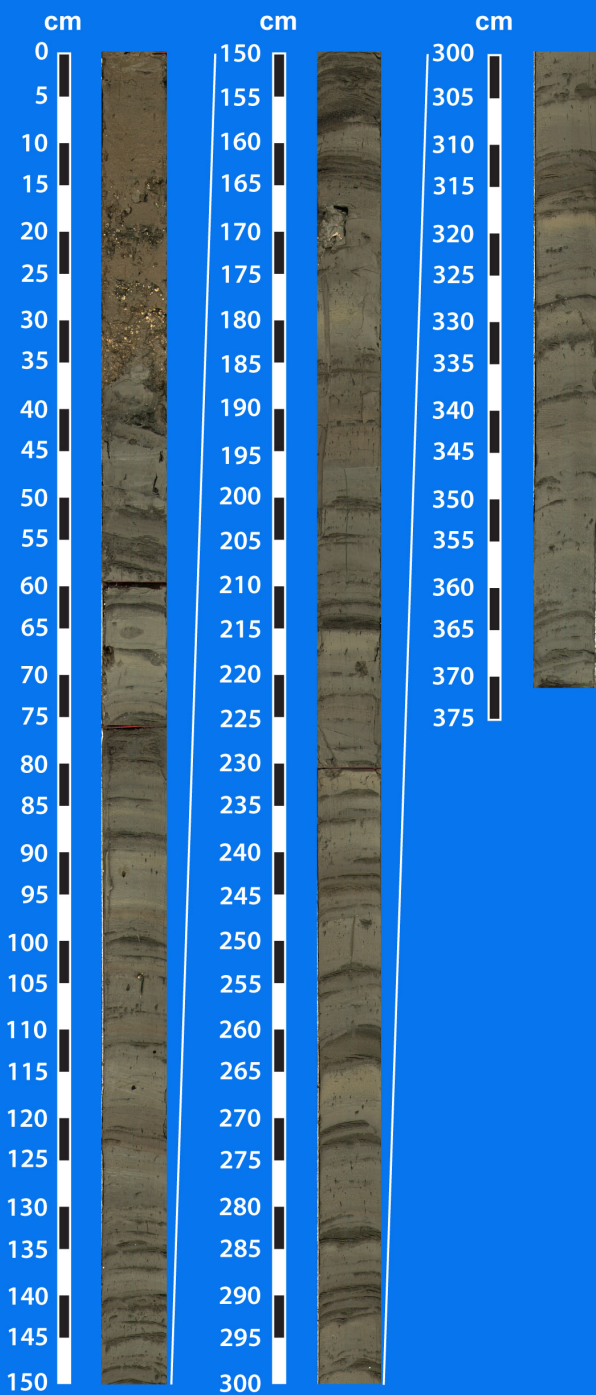
## TT-69-10





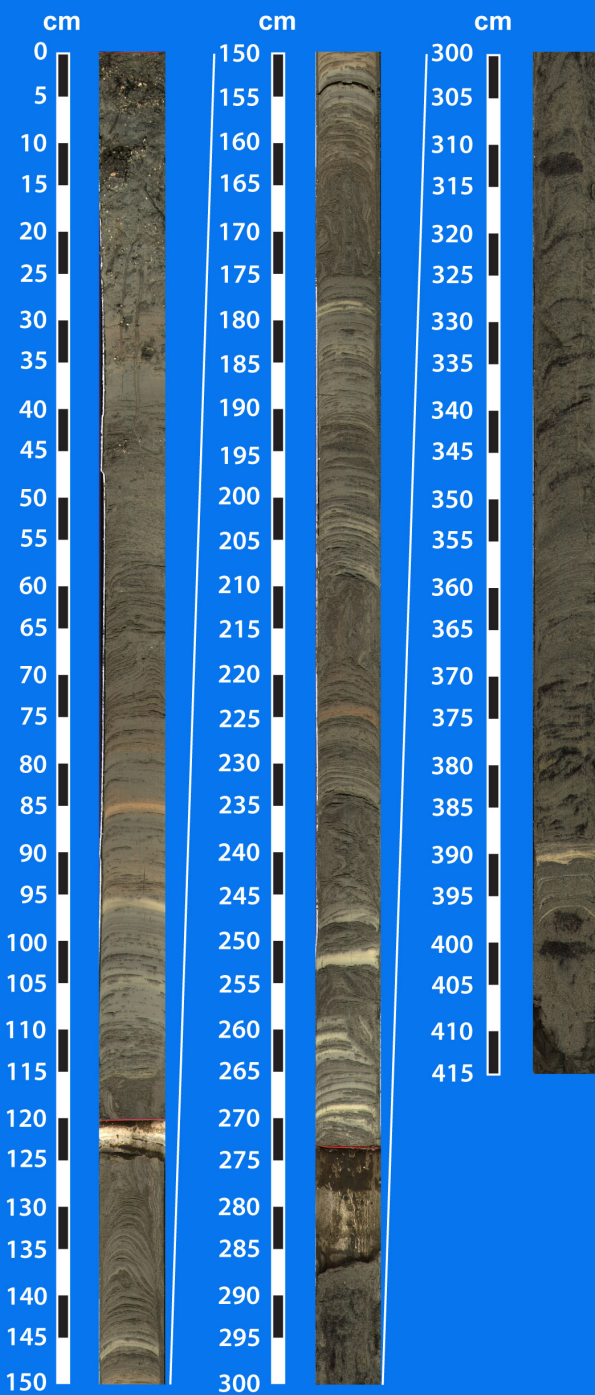
# Trinity-Tiger Shoals Complex

## TT-73-10

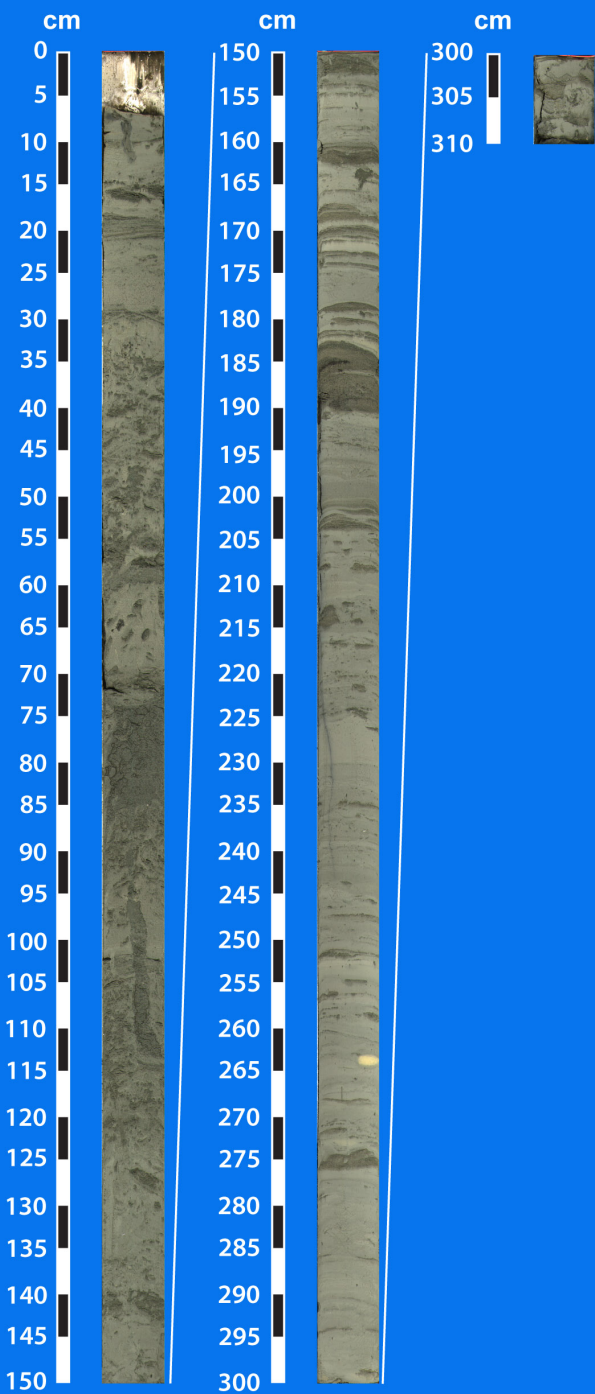




# Trinity-Tiger Shoals Complex TT-74-10



# Trinity-Tiger Shoals Complex TT-75-10



# Trinity-Tiger Shoals Complex

## TT-76-10

cm

0  
5  
10  
15  
20  
25  
30  
35  
40  
45  
50  
55  
60  
65  
70  
75  
80  
85  
90  
95  
100  
105  
110  
115  
120  
125  
130  
135  
140  
145  
150

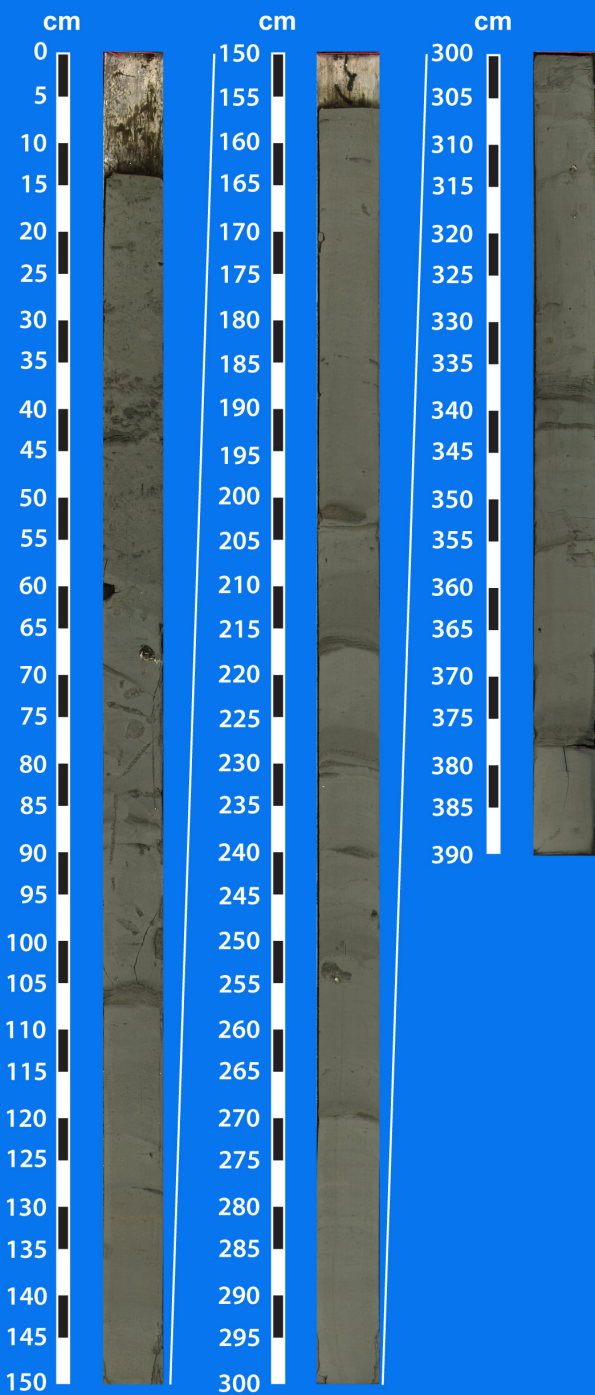


cm

150  
155  
160  
165  
170  
175  
180  
185  
190  
195  
200  
205  
210  
215  
220  
225  
230  
235  
240

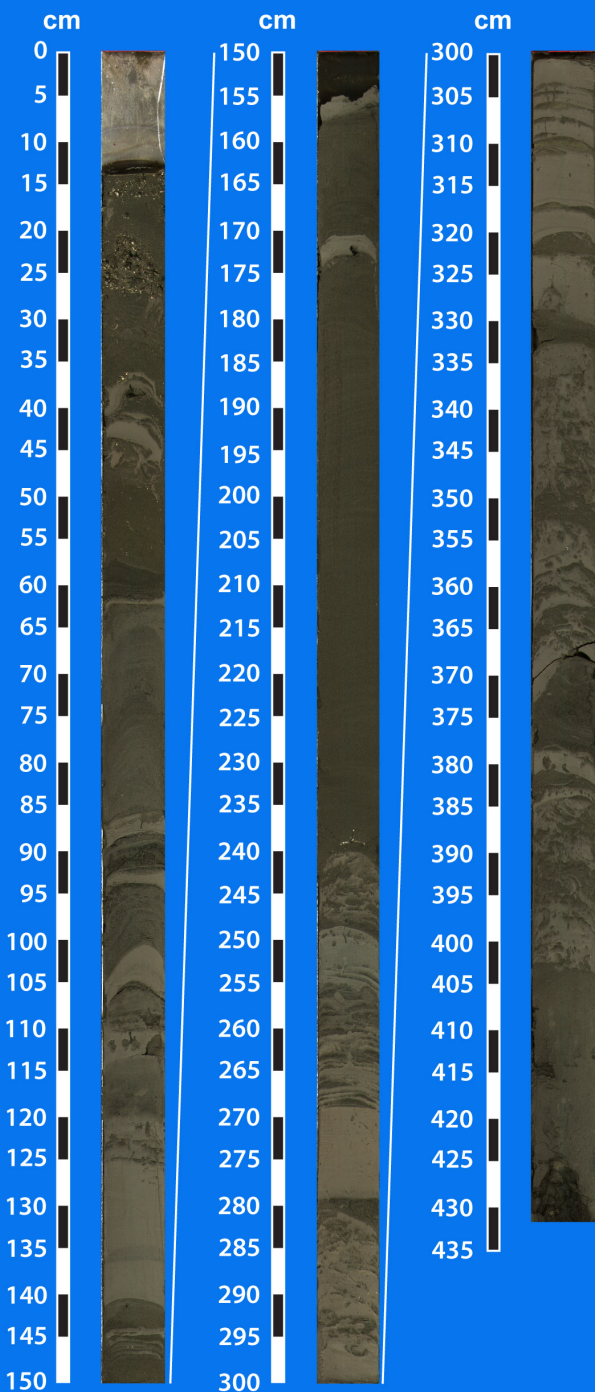


# Trinity-Tiger Shoals Complex TT-77-10

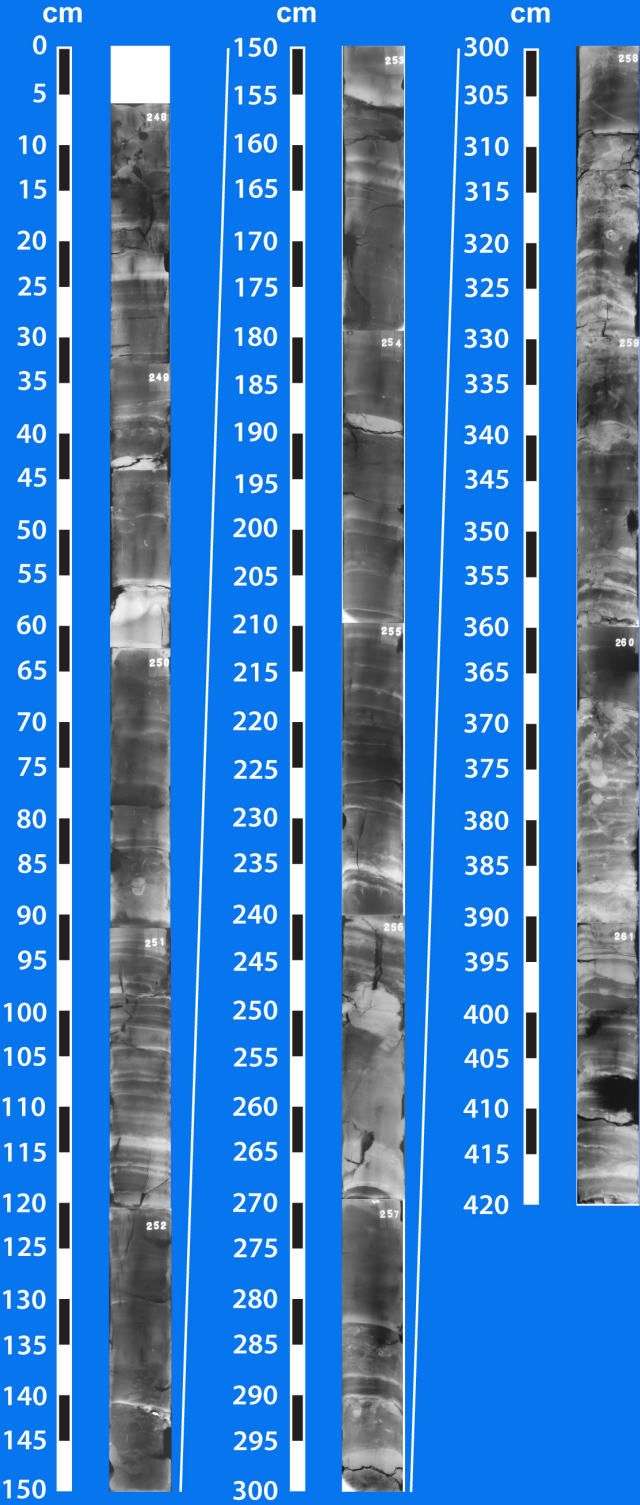


# Trinity-Tiger Shoals Complex

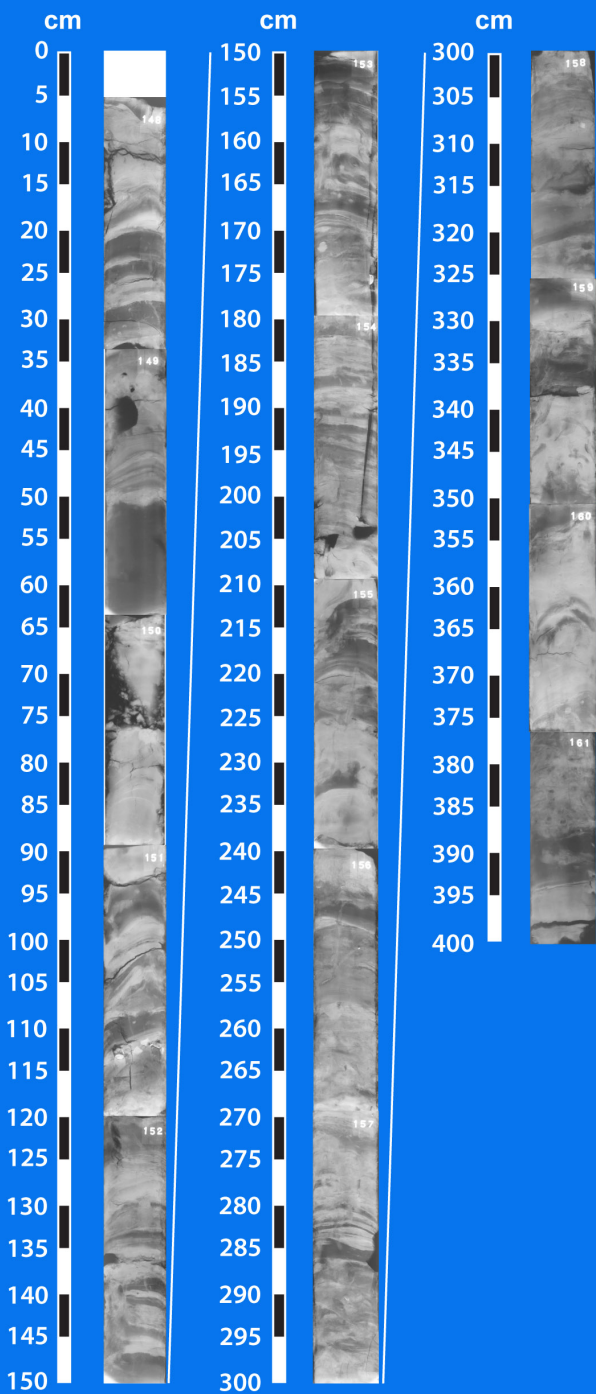
## TT-78-10



Trinity-Tiger Shoals Complex  
TT-01-08



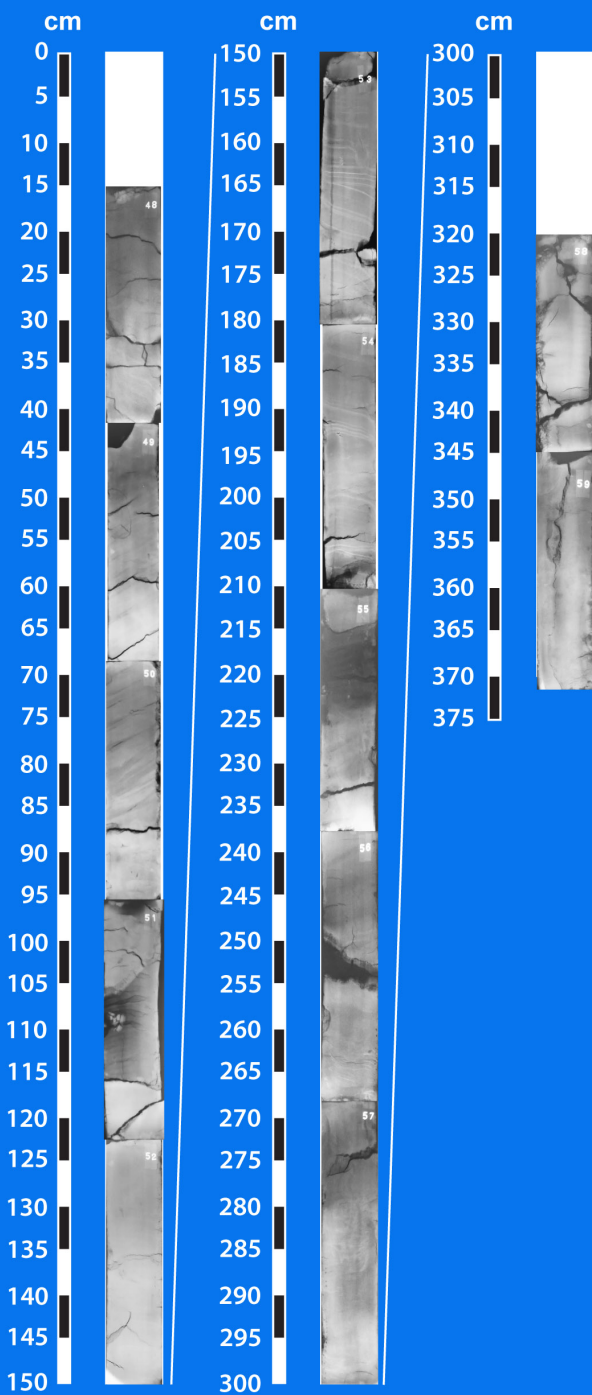
# Trinity-Tiger Shoals Complex TT-10-08



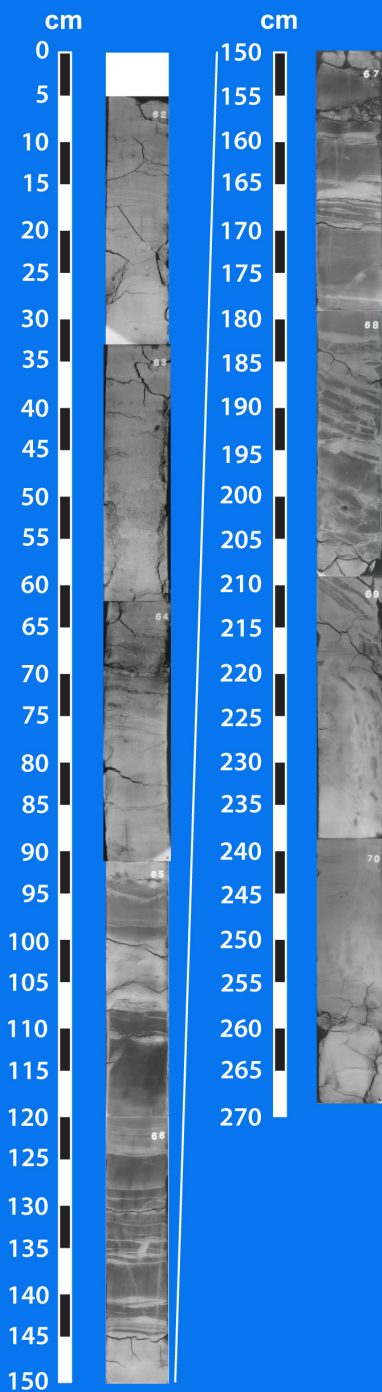


# Trinity-Tiger Shoals Complex

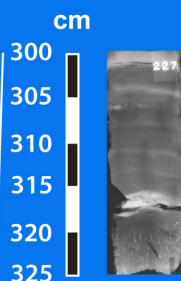
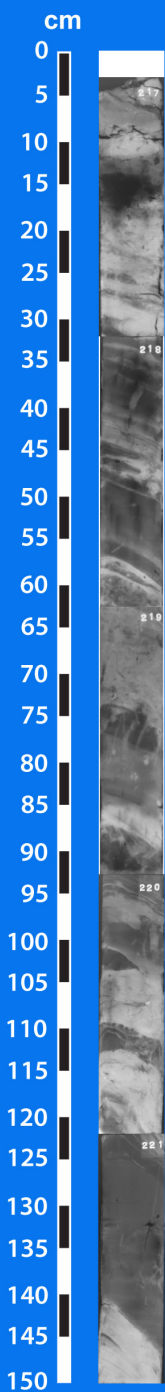
## TT-12-08



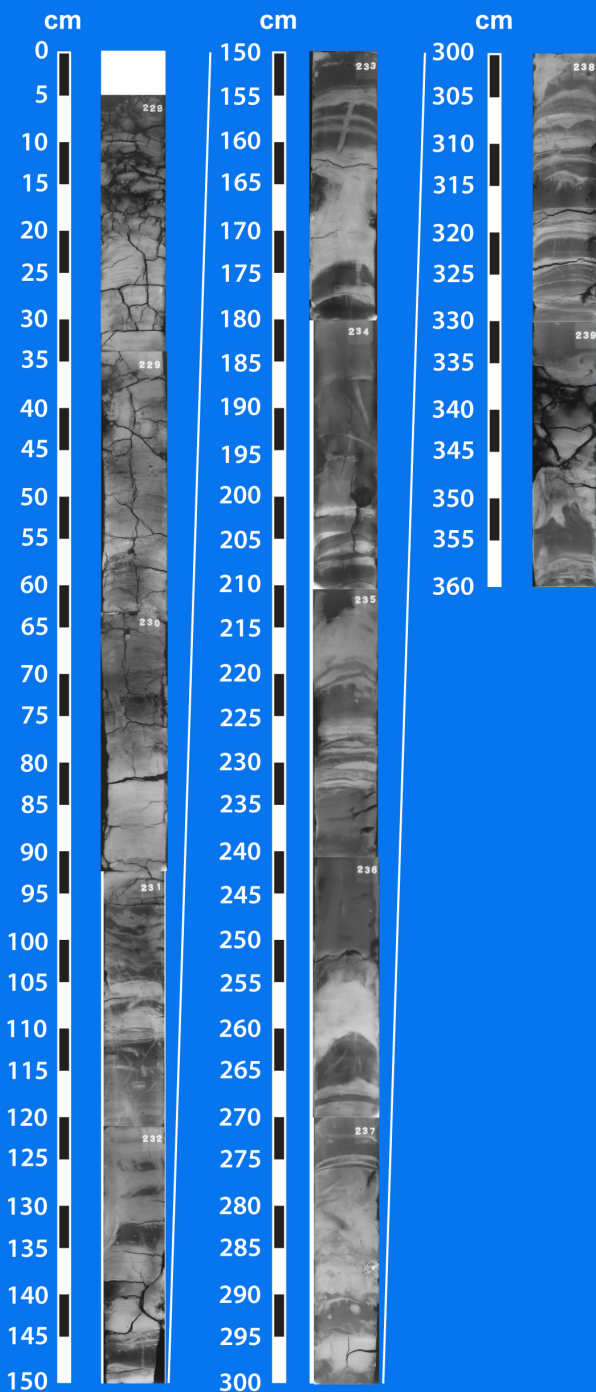
# Trinity-Tiger Shoals Complex TT-19-08



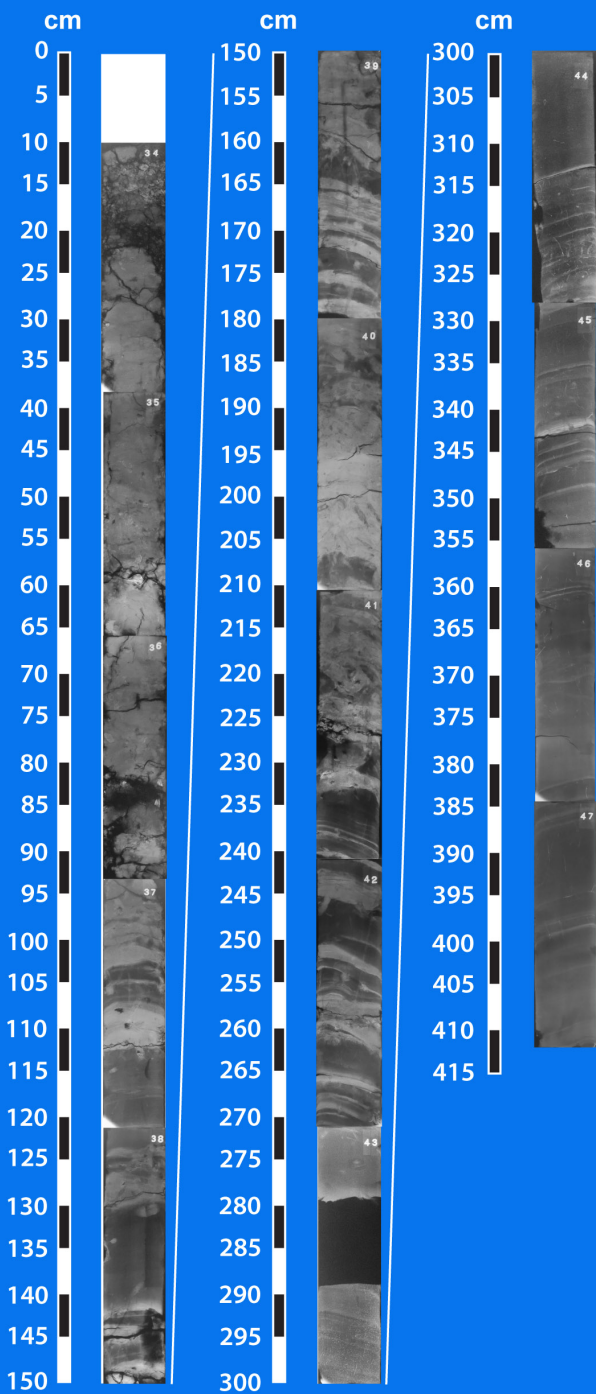
# Trinity-Tiger Shoals Complex TT-20-08



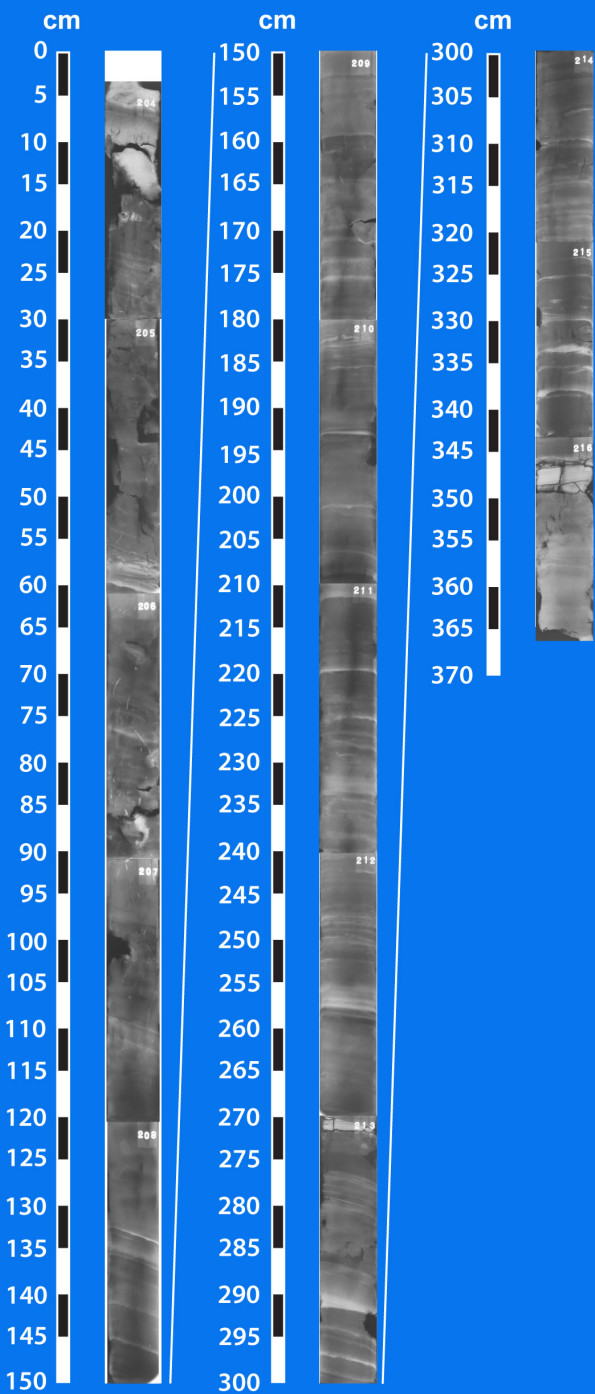
# Trinity-Tiger Shoals Complex TT-23-08



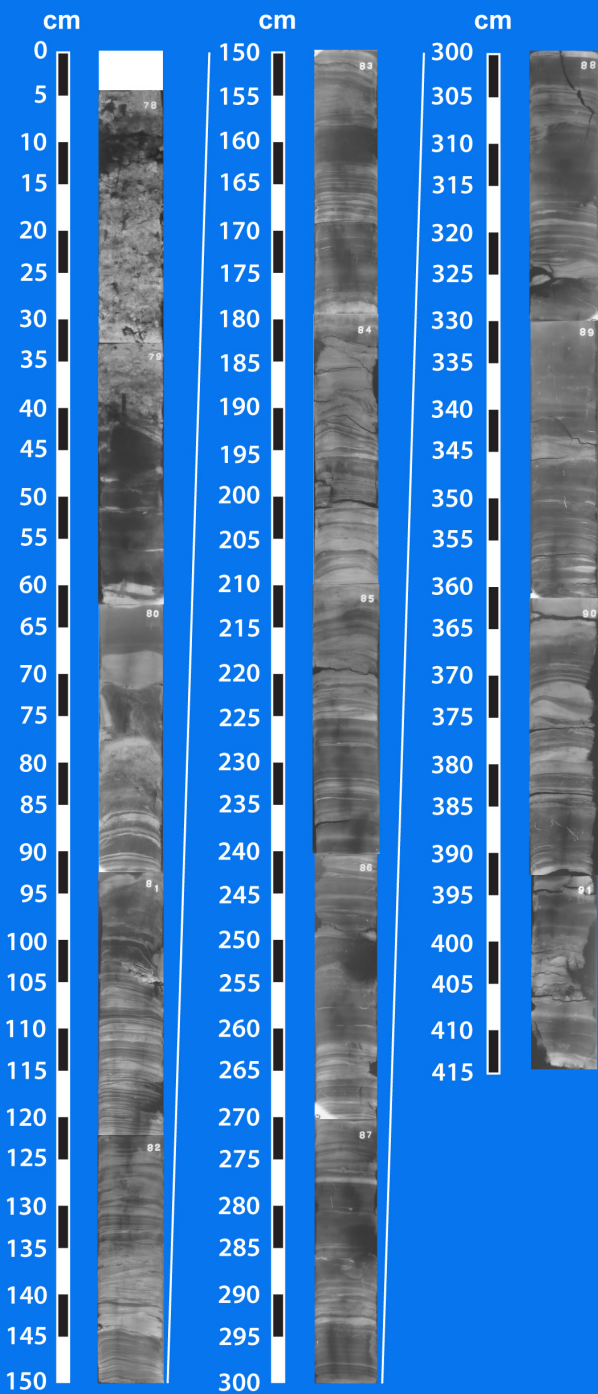
# Trinity-Tiger Shoals Complex TT-25-08



# Trinity-Tiger Shoals Complex TT-27-08

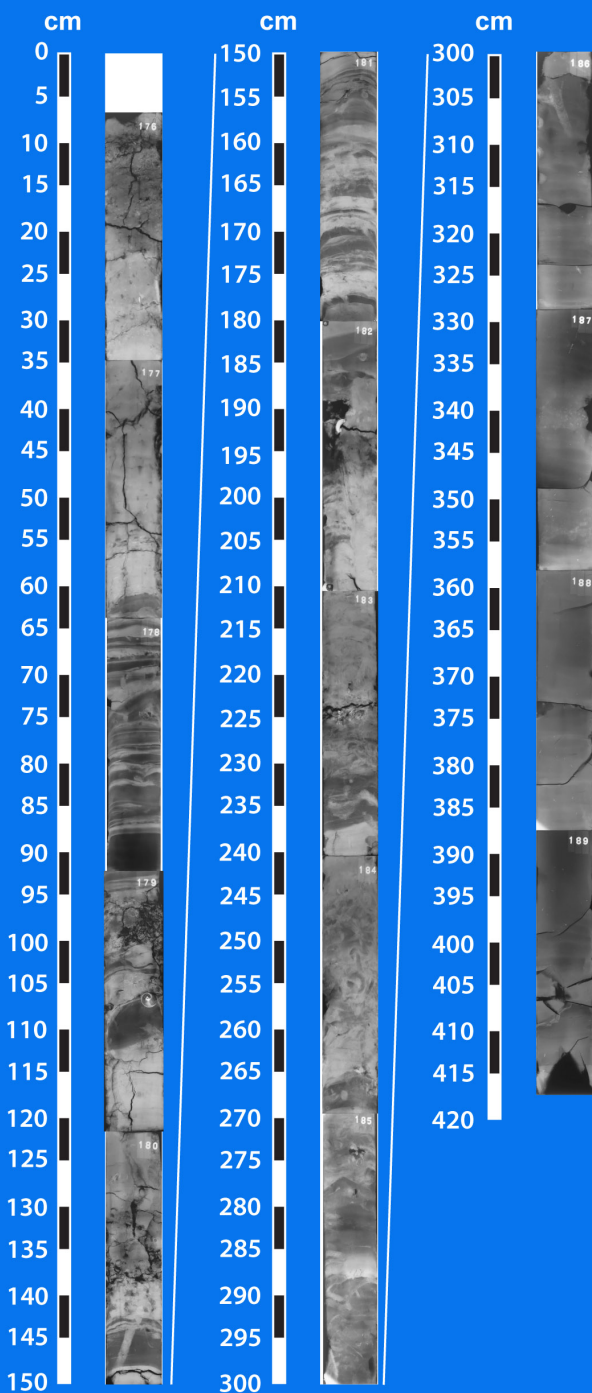


# Trinity-Tiger Shoals Complex TT-31-08



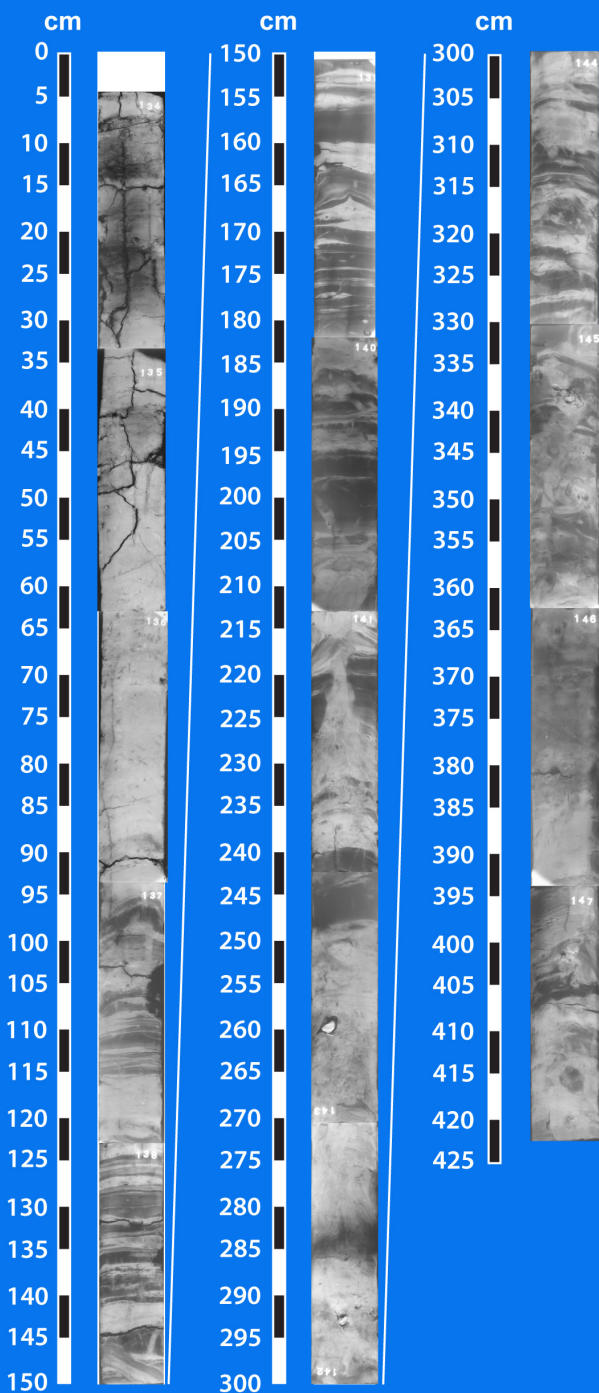


# Trinity-Tiger Shoals Complex TT-42-08



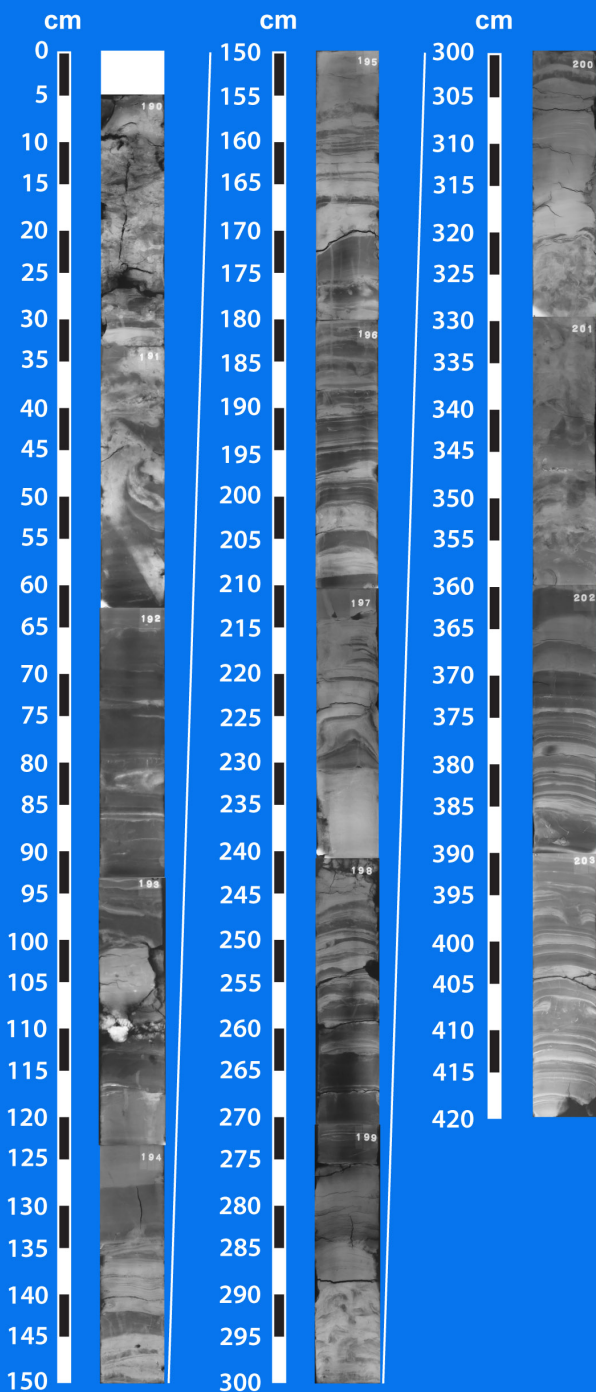
# Trinity-Tiger Shoals Complex

## TT-45-08



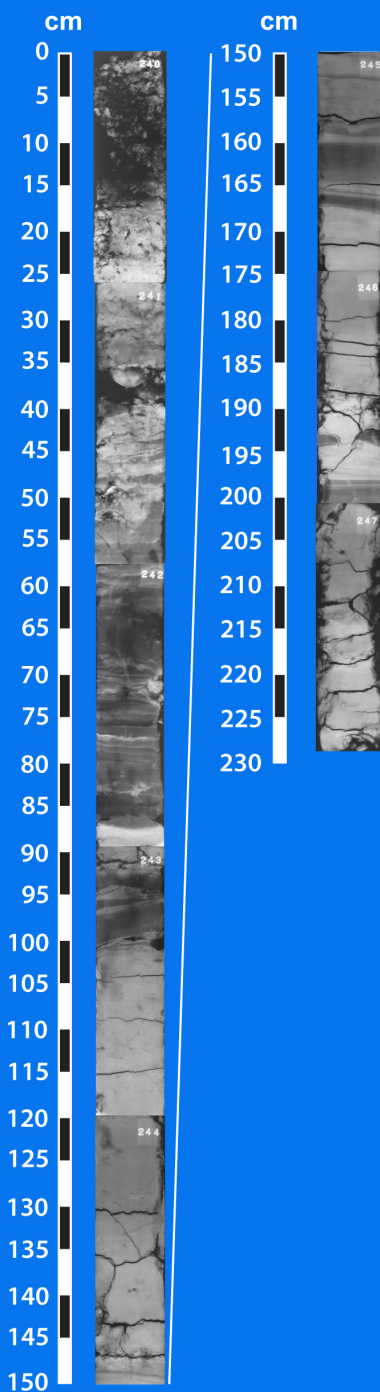
# Trinity-Tiger Shoals Complex

## TT-48-08

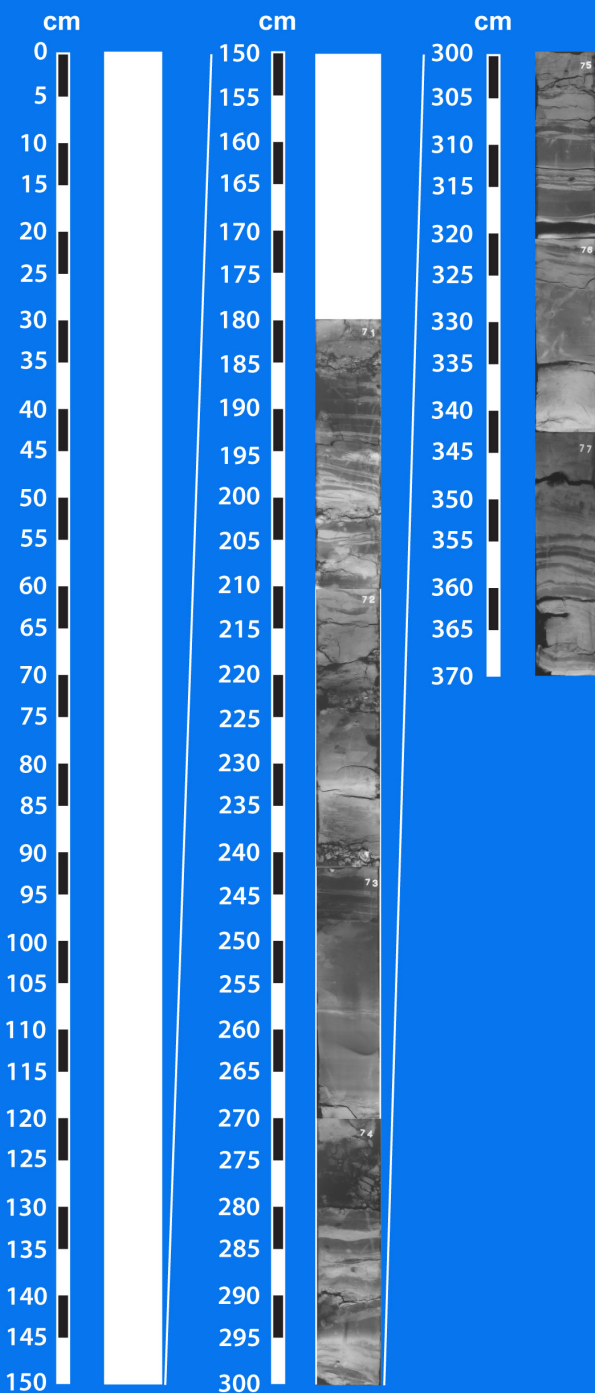


# Trinity-Tiger Shoals Complex

## TT-49-08

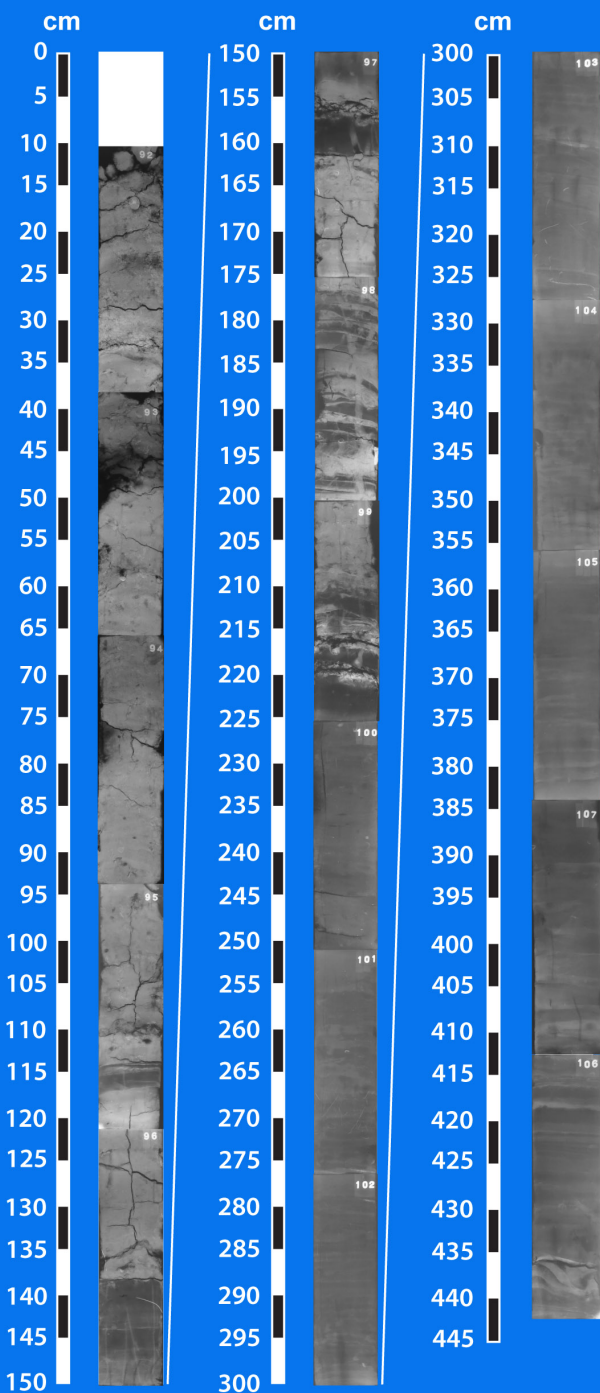


# Trinity-Tiger Shoals Complex TT-52-08

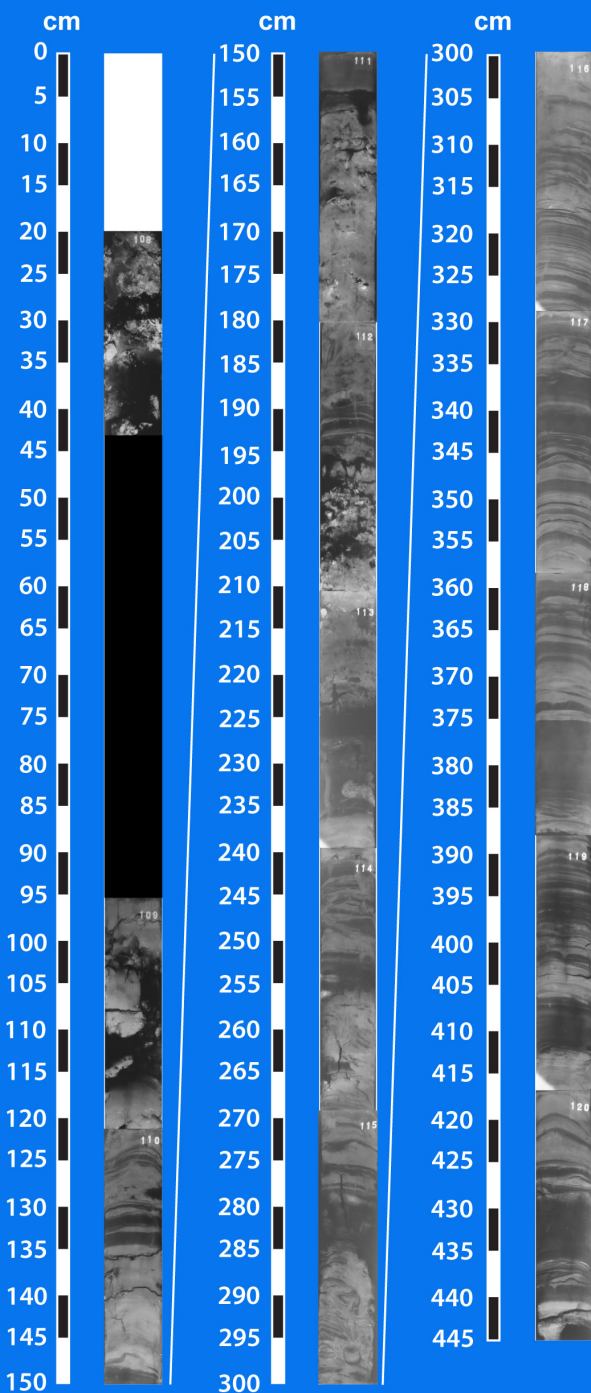


# Trinity-Tiger Shoals Complex

## TT-65-10

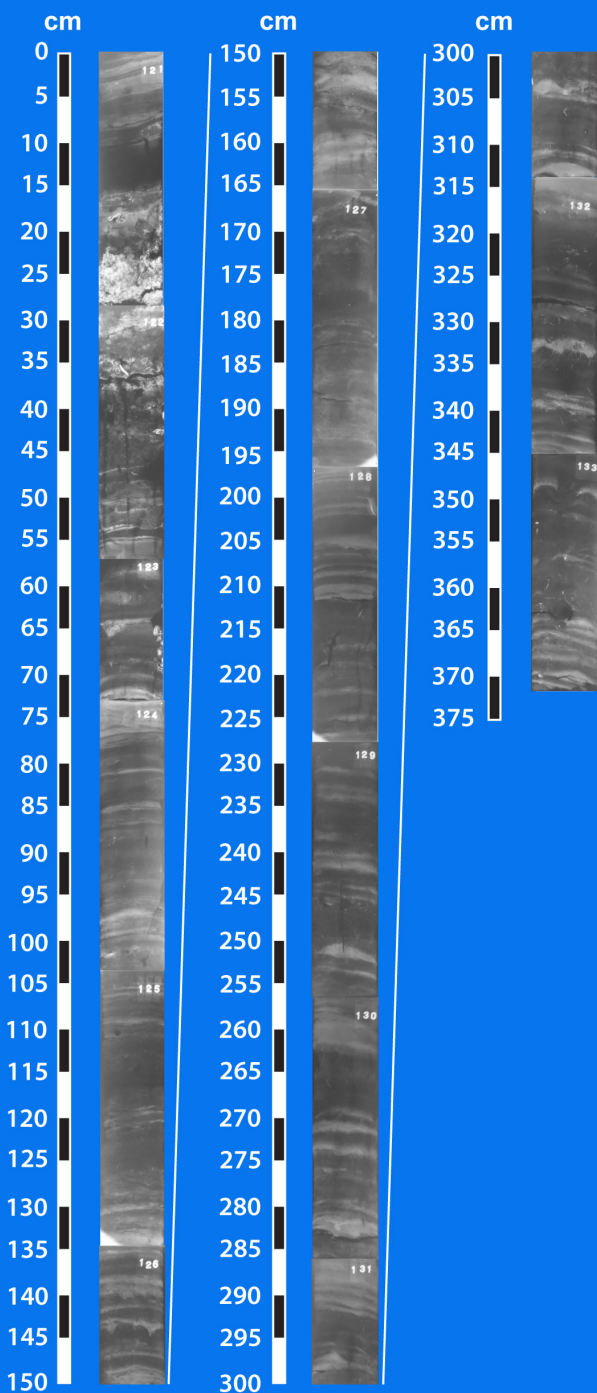


# Trinity-Tiger Shoals Complex TT-69-10

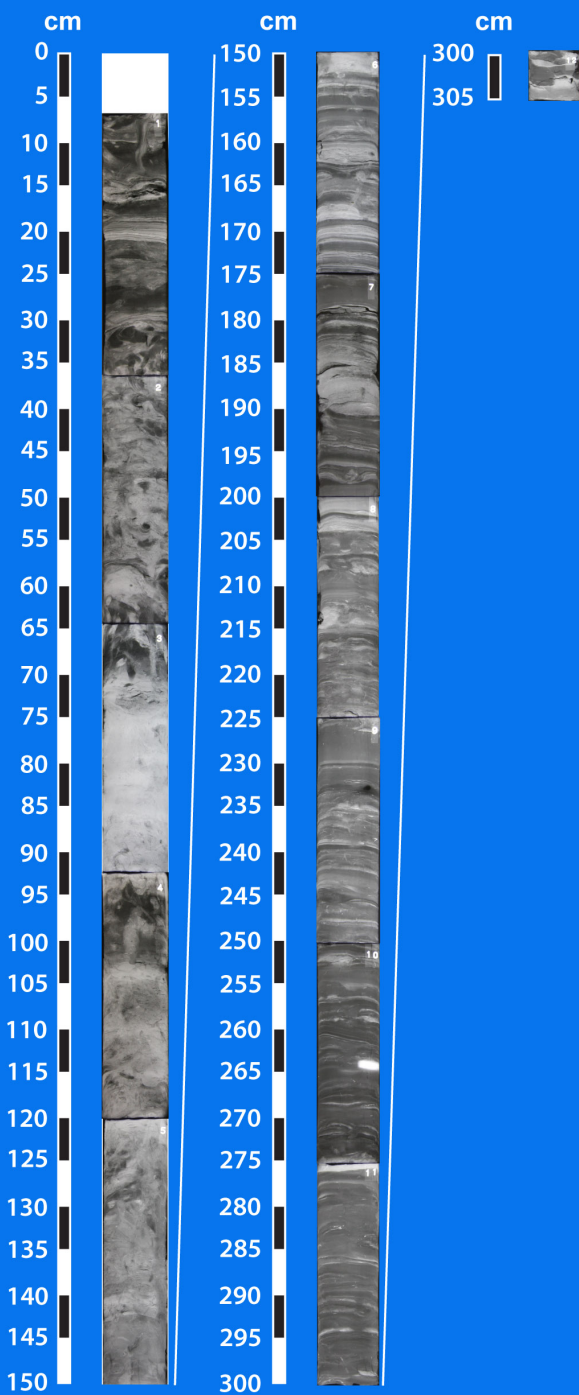




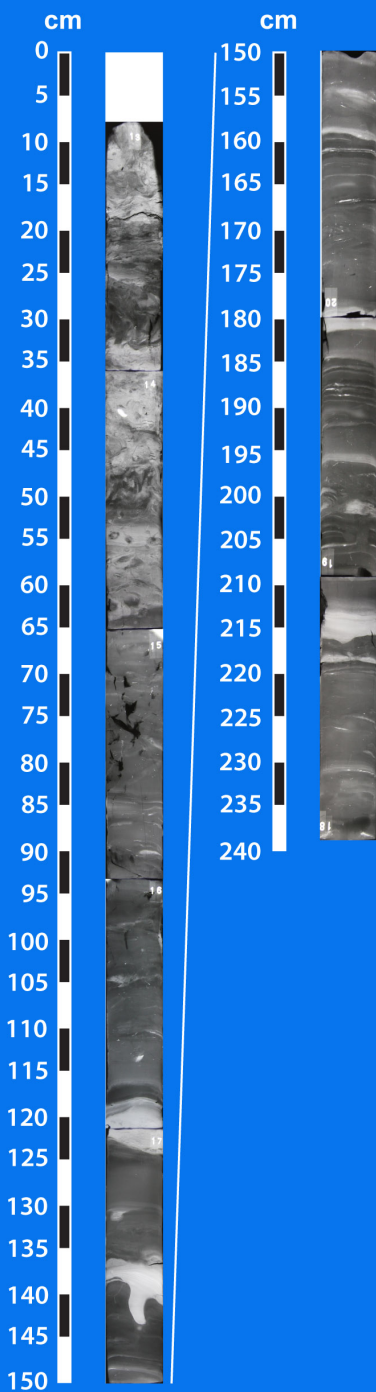
# Trinity-Tiger Shoals Complex TT-73-10



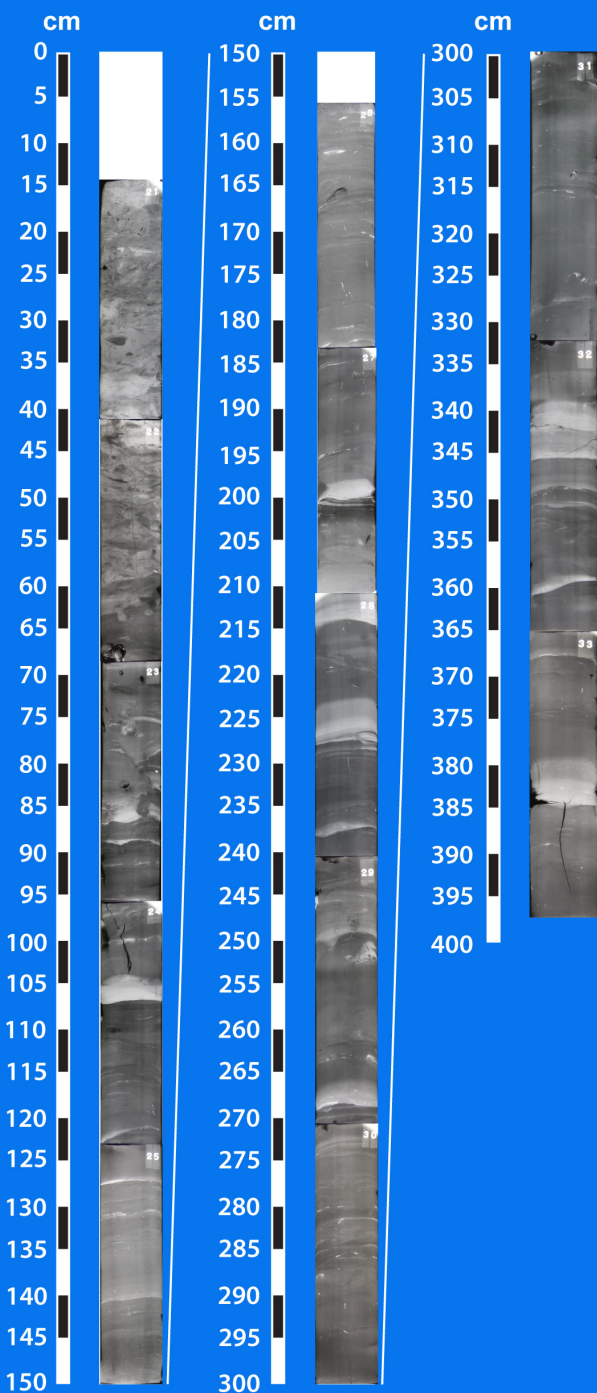
# Trinity-Tiger Shoals Complex TT-75-10



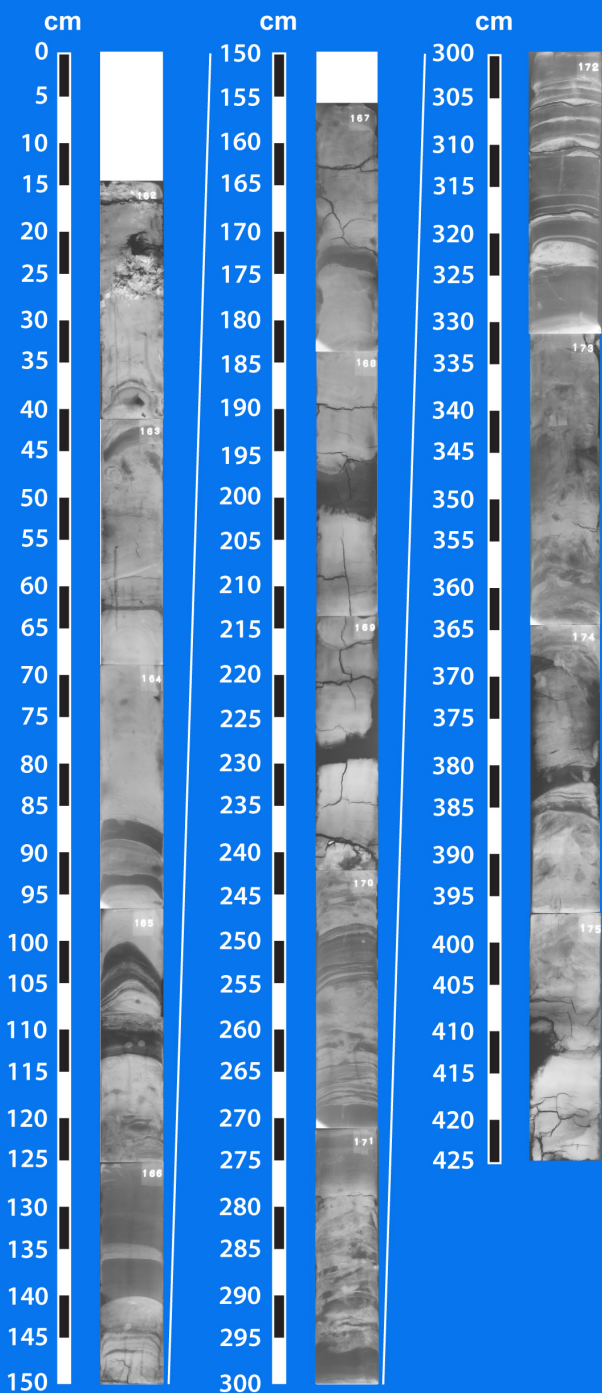
# Trinity-Tiger Shoals Complex TT-76-10

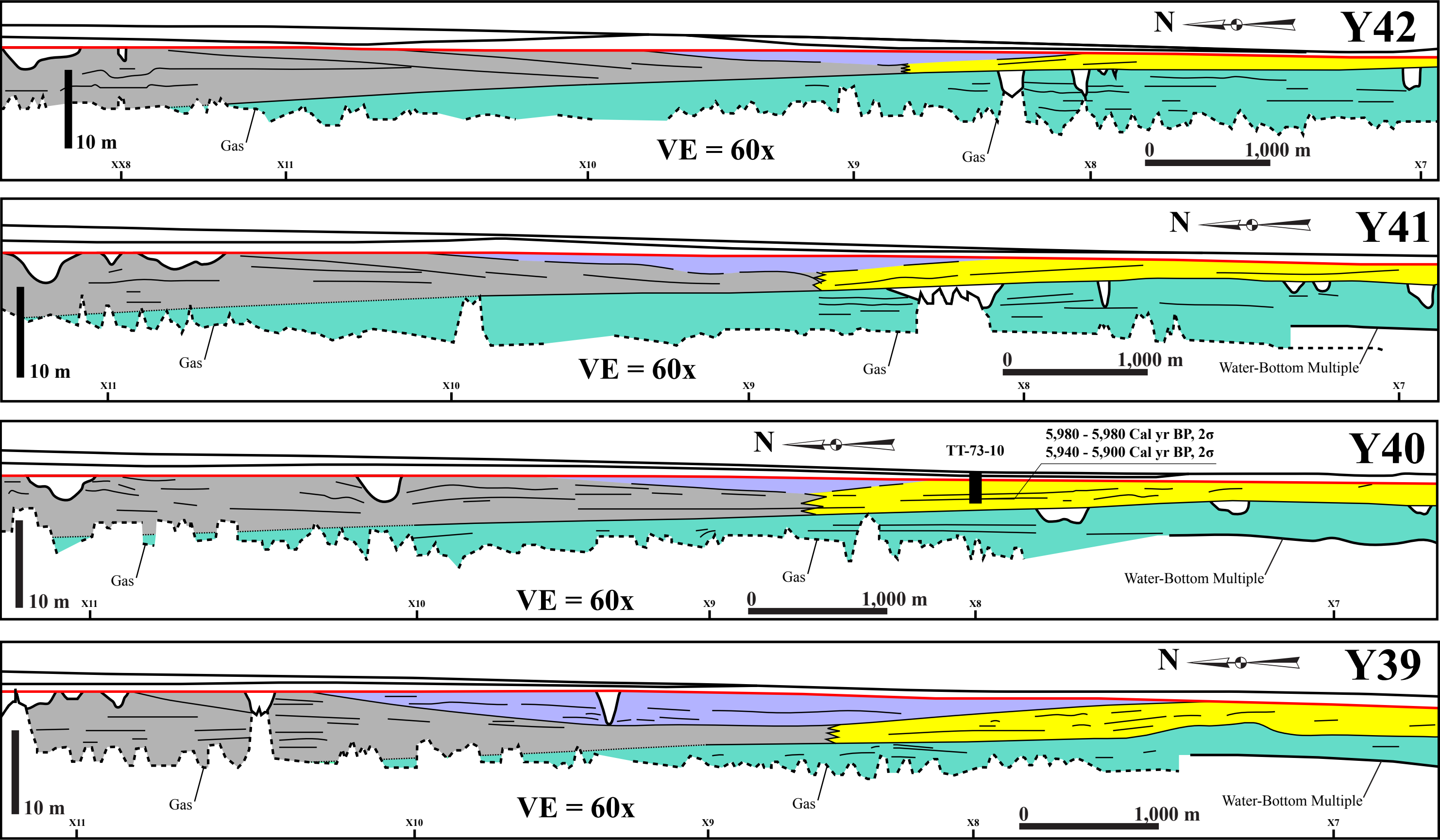


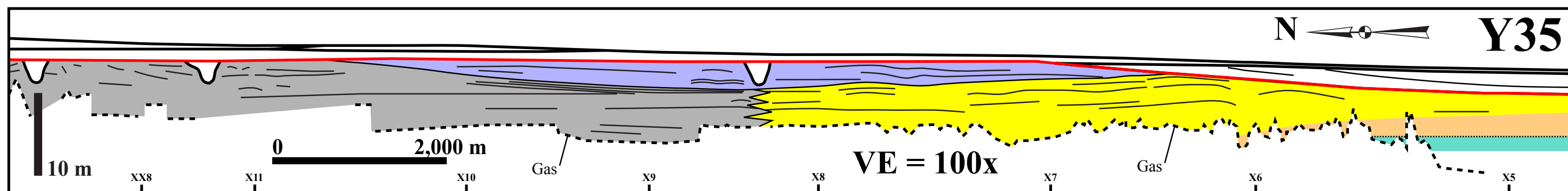
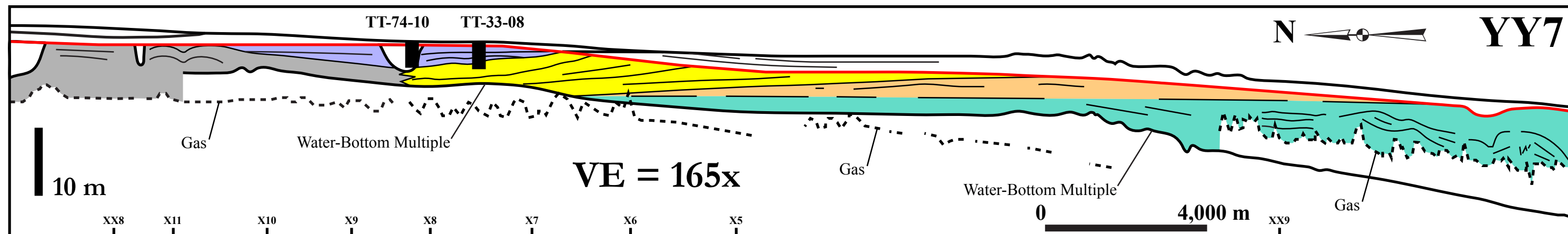
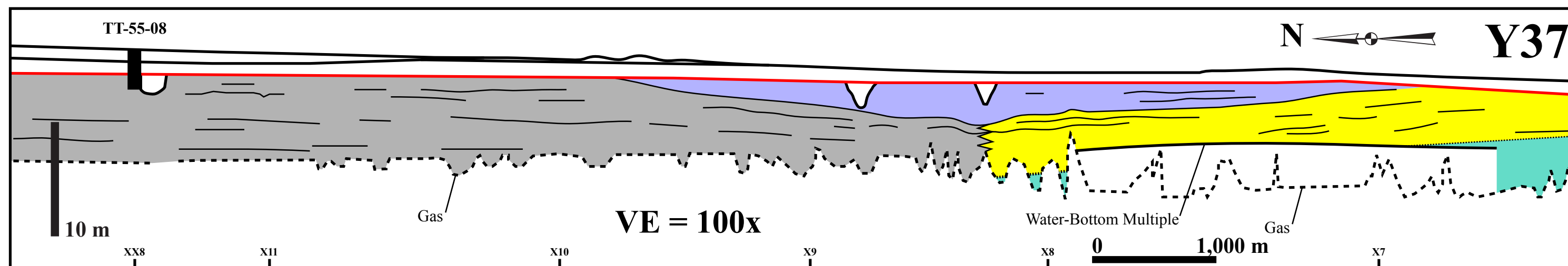
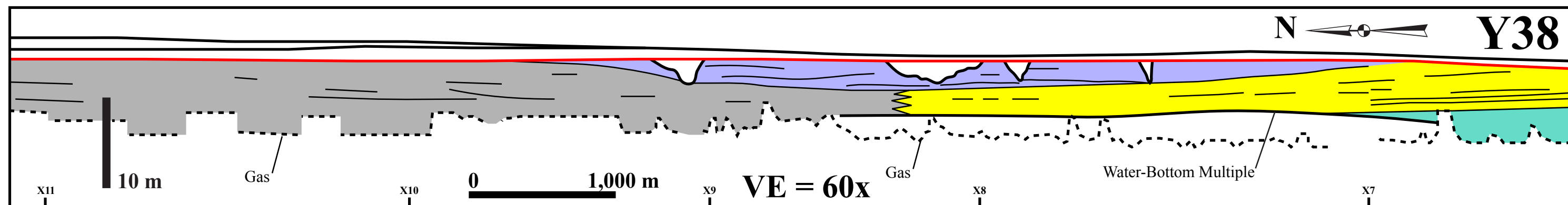
# Trinity-Tiger Shoals Complex TT-77-10



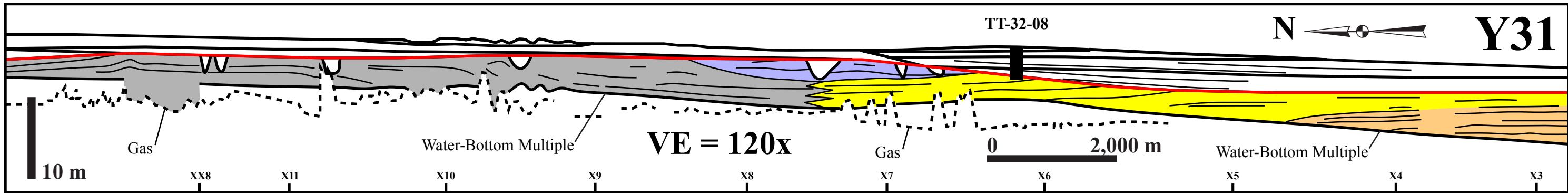
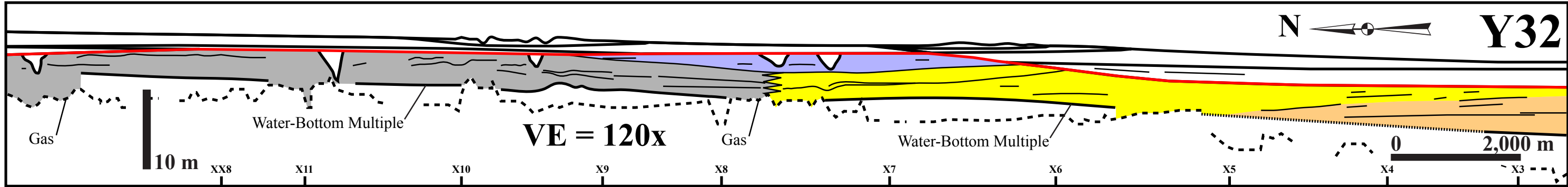
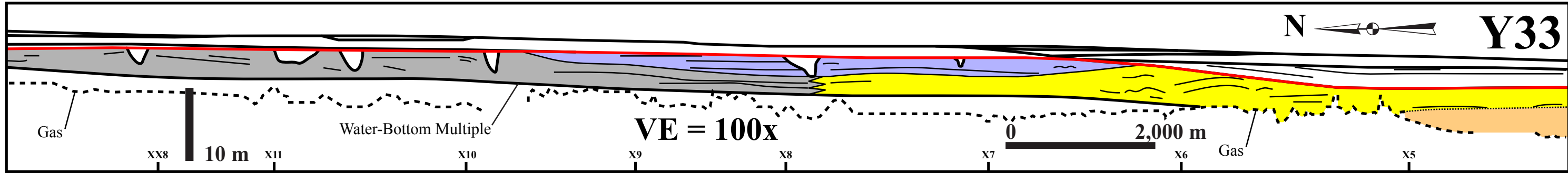
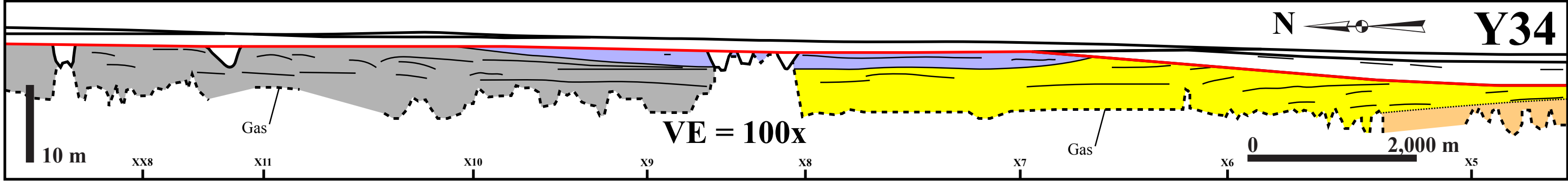
# Trinity-Tiger Shoals Complex TT-78-10

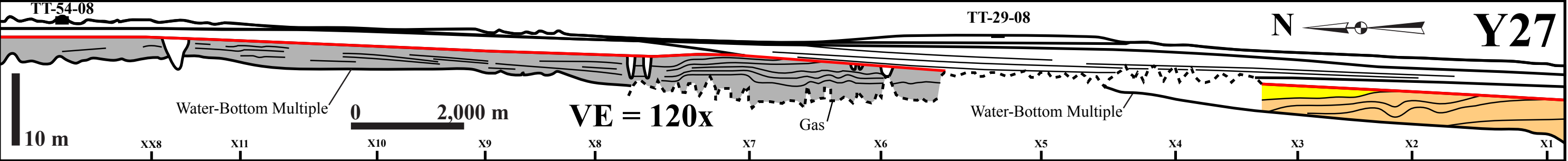
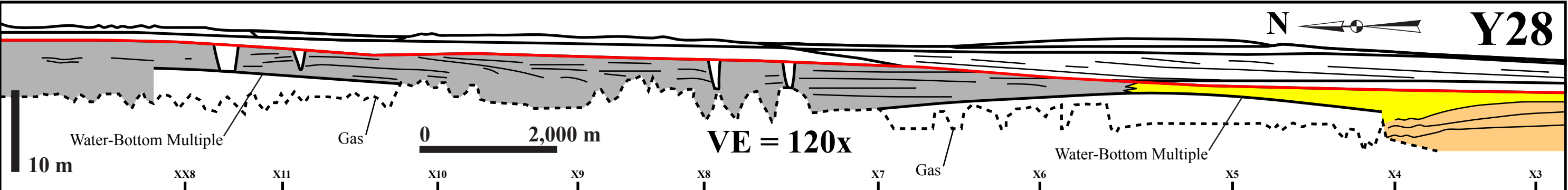
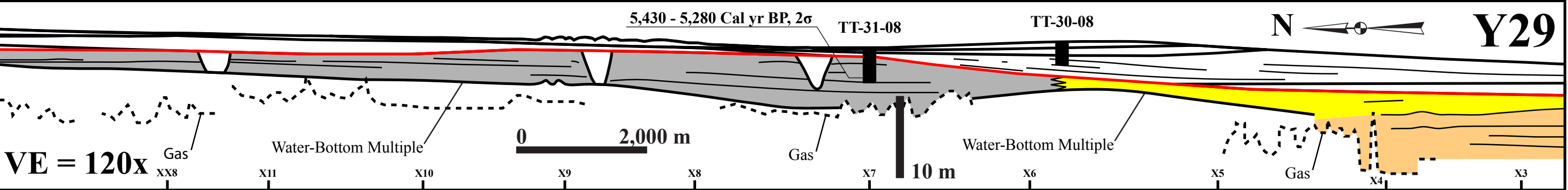
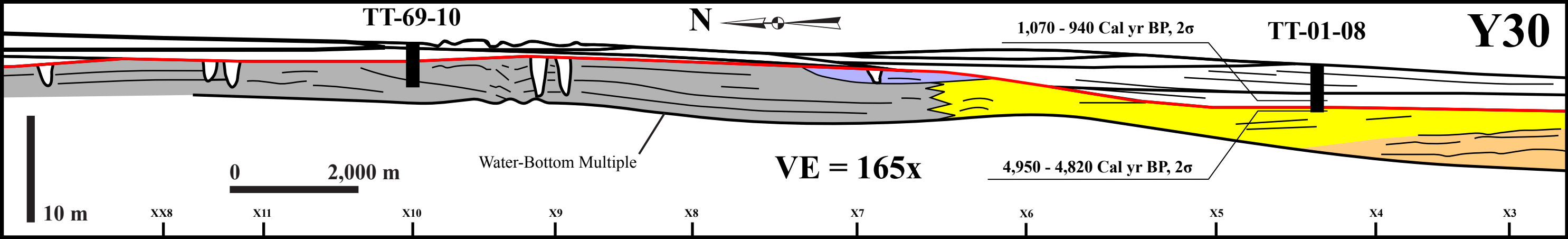


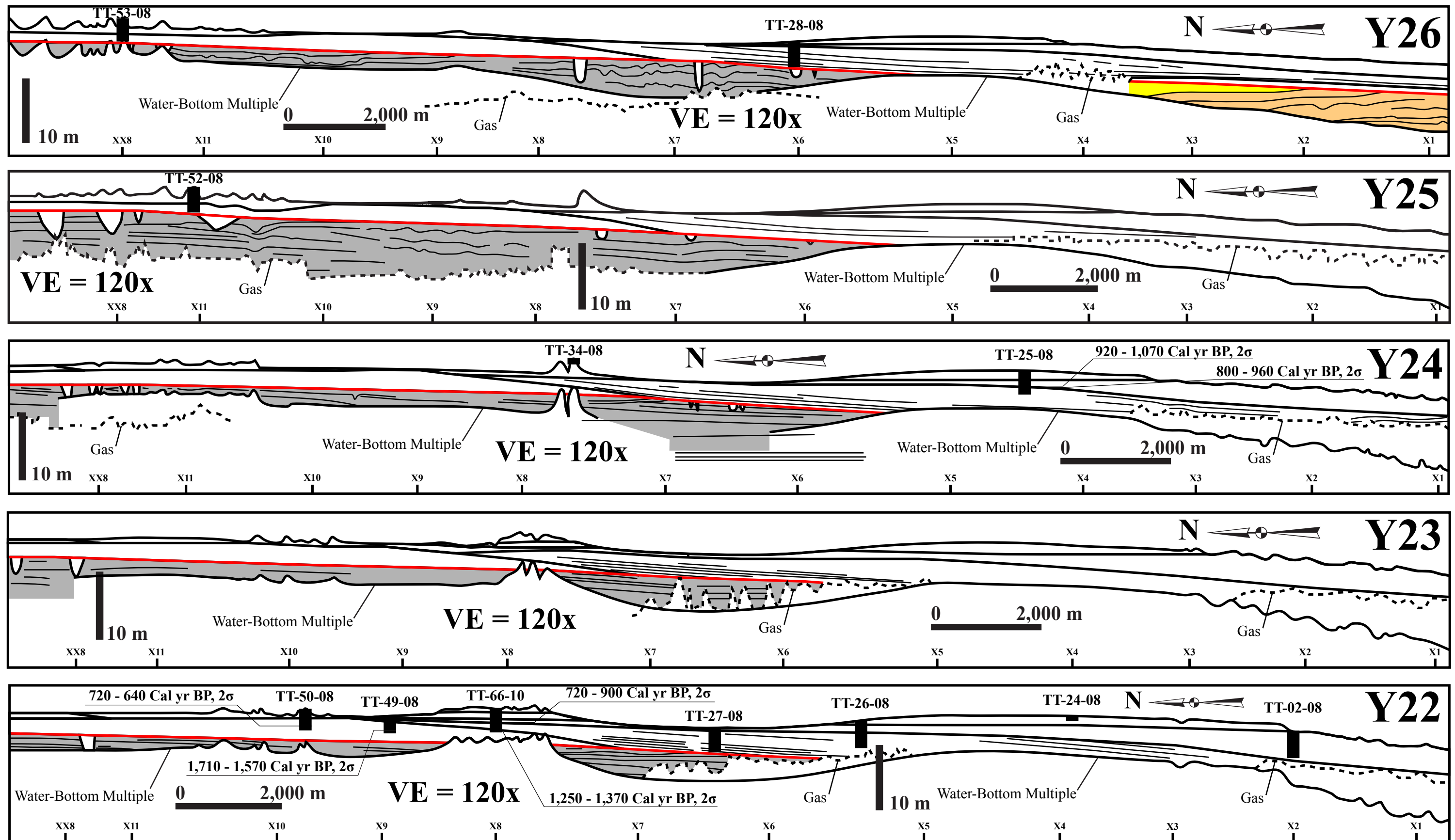


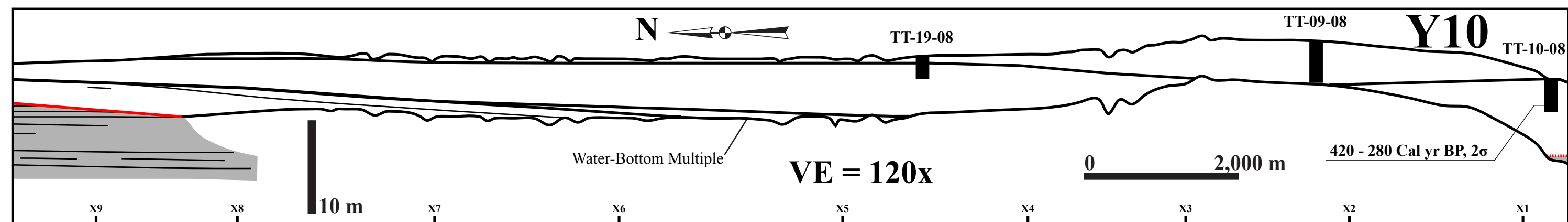
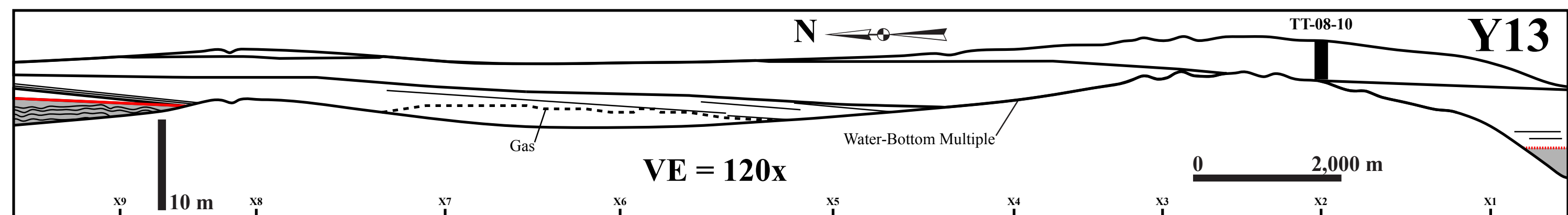
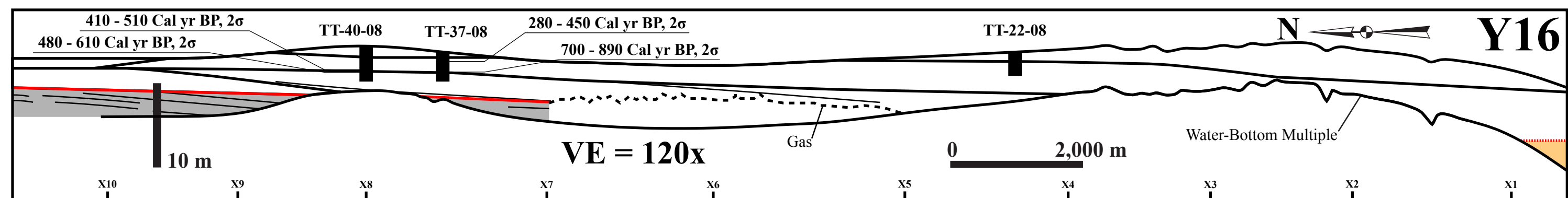
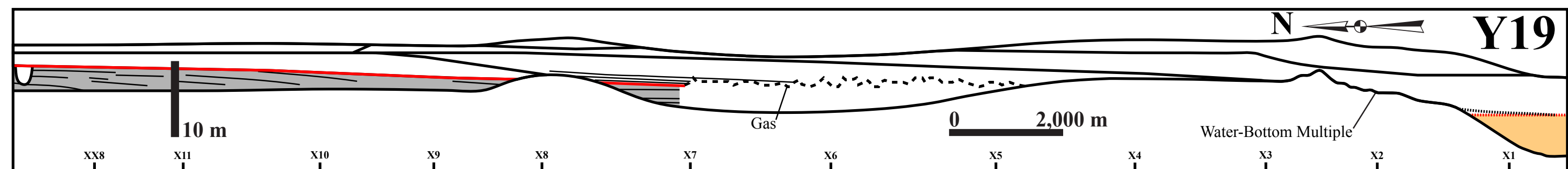


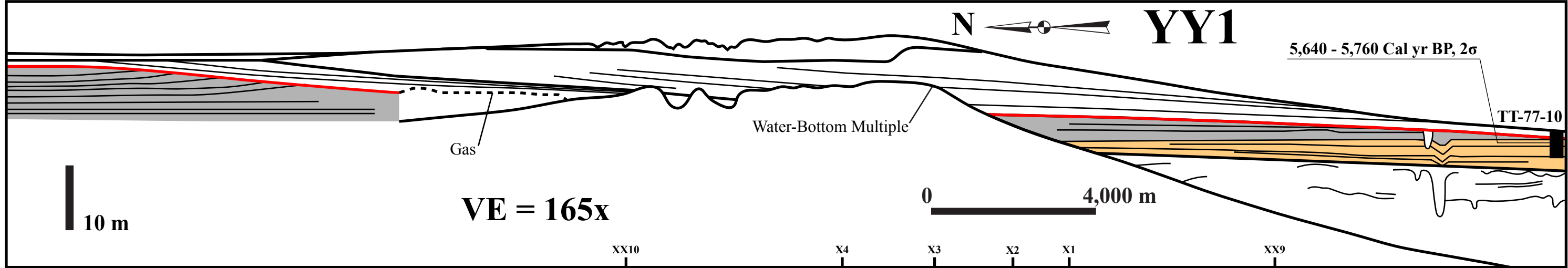
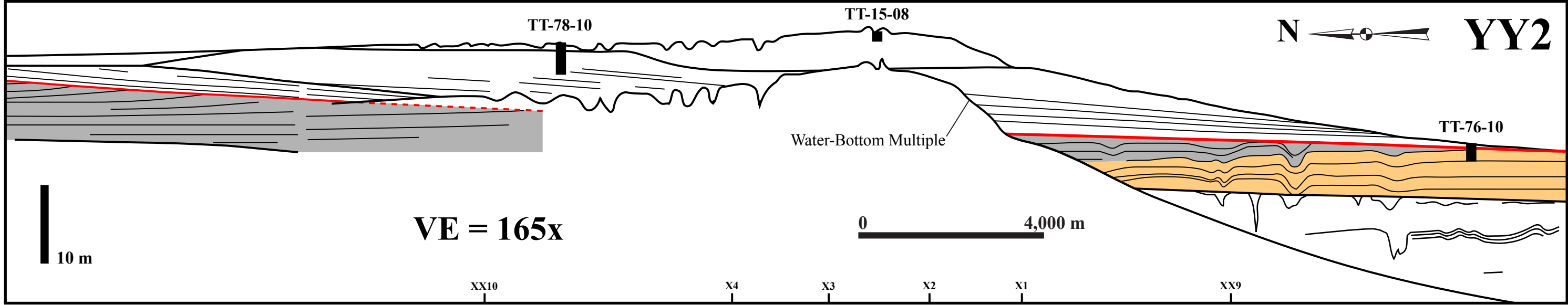


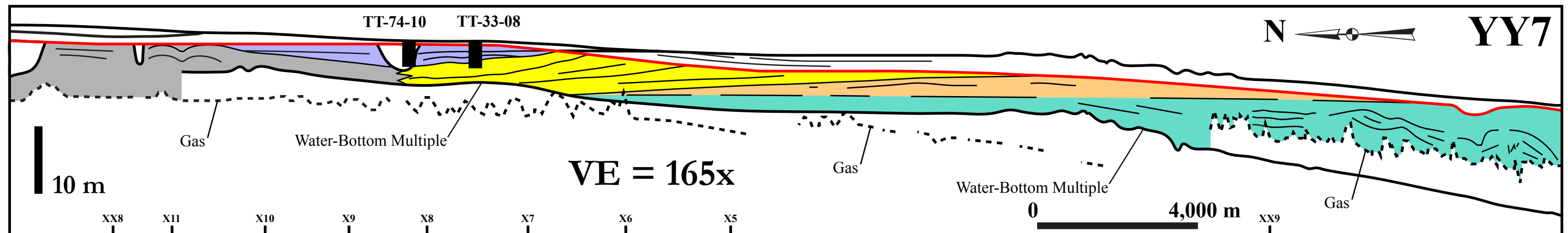
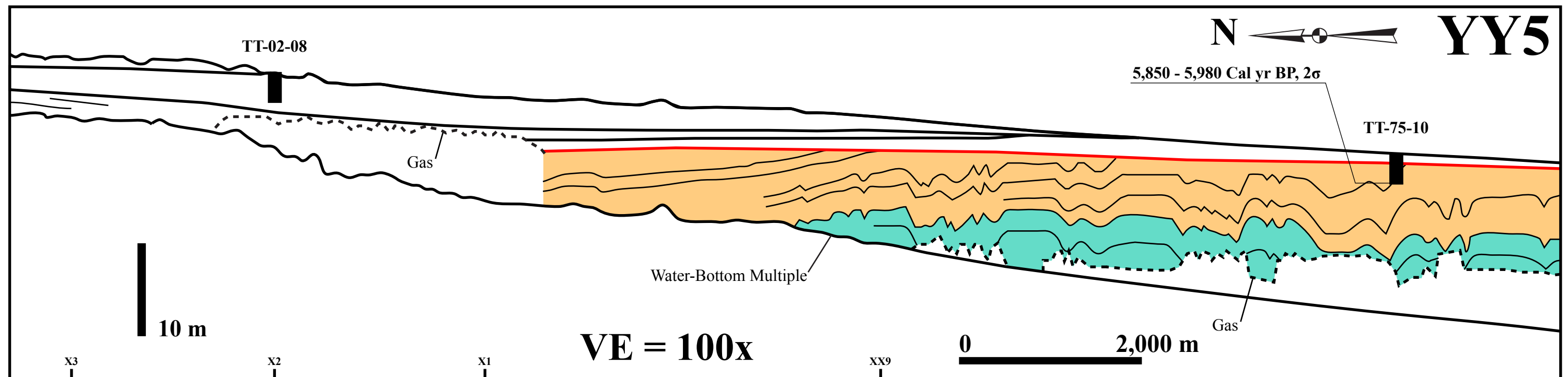
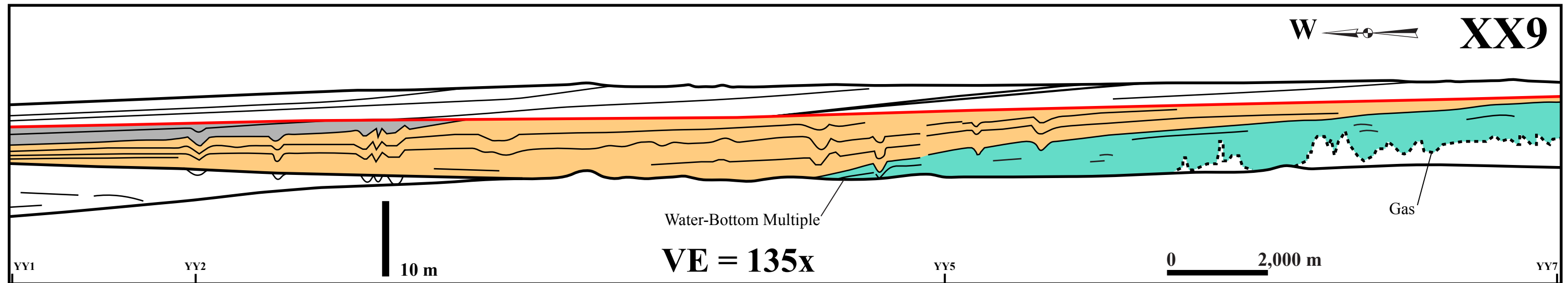












## APPENDIX 6: AMS RADIOCARBON DATES

Sample Name	Lab Code	Sub-Bottom Depth	Material	$^{13}\text{C}/^{12}\text{C}$ Ratio (‰)	Conventional $^{14}\text{C}$ Age (yr BP, 1 $\sigma$ )	Calibration Age (Cal yr BP, 2 $\sigma$ )		Corresponding Facies	Corresponding Sub-Bottom Profile
						Lower	Upper		
TT-01-08 A	Beta – 318848	355 cm	Shell	-1.8	1,470 $\pm$ 30	940	1,070	AFU3/LFU3	Y30
TT-01-08 B	Beta – 317227	395-420 cm	Foraminifera	-2.9	4,670 $\pm$ 30	4,820	4,950	AFU1/LFU1	Y30
TT-10-08	Beta – 318849	313-325 cm	Shell	-1.0	700 $\pm$ 30	280	420	AFU5/LFU5	Y10
TT-20-08	Beta – 317228	270-272 cm	Shell	-0.8	1,170 $\pm$ 30	660	760	AFU5/LFU5	Y15
TT-25-08 A	Beta – 275842	258-260 cm	Shell	-0.9	1,450 $\pm$ 40	920	1,070	AFU5/LFU5	Y24
TT-25-08 B	Beta – 281448	279-289 cm	Foraminifera	-2.4	1,350 $\pm$ 40	800	960	AFU4/LFU4	Y24
TT-31-08	Beta – 317229	329-358 cm	Foraminifera	-5.7	5,000 $\pm$ 30	5,280	5,430	AFU1/LFU1	Y29
TT-37-08 A	Beta – 289518	118-120 cm	Shell	-1.8	720 $\pm$ 40	280	450	AFU5/LFU5	Y16
TT-37-08 B	Beta – 289519	220-222 cm	Shell	-2.2	1,250 $\pm$ 40	700	890	AFU5/LFU5	Y16
TT-40-08 A	Beta – 275843	245-248 cm	Shell	-2.0	830 $\pm$ 40	410	510	AFU5/LFU5	Y16
TT-40-08 B	Beta – 281449	285-296 cm	Foraminifera	-3.5	930 $\pm$ 40	480	610	AFU4/LFU4	Y16
TT-41-08	Beta – 289520	82-84 cm	Shell	-1.9	540 $\pm$ 40	60 0	270 10	AFU7/LFU7	Y14
TT-43-08 A	Beta – 275844	70-72 cm	Shell	-1.7	620 $\pm$ 40	220 200 150	320 210 160	AFU7/LFU7	Y14
TT-43-08 B	Beta – 281450	260-272 cm	Foraminifera	-1.7	900 $\pm$ 40	470	550	AFU4/LFU4	Y14
TT-46-08	Beta – 289521	369-371 cm	Shell	+0.3	1,890 $\pm$ 40	1,340	1,520	Lag (Atop of AFU2/LFU2)	Y11
TT-49-08	Beta – 317230	188-190 cm	Shell	+0.9	2,080 $\pm$ 30	1,570	1,710	AFU2/LFU2	Y22
TT-50-08	Beta – 317231	207-214 cm	Shell	-2.2	1,130 $\pm$ 30	640	720	AFU2/LFU2	Y22



Sample Name	Lab Code	Sub-Bottom Depth	Material	$^{13}\text{C}/^{12}\text{C}$ Ratio (‰)	Conventional $^{14}\text{C}$ Age (yr BP, 1 $\sigma$ )	Calibration Age (Cal yr BP, 2 $\sigma$ )		Corresponding Facies	Corresponding Sub-Bottom Profile
						Lower	Upper		
TT-66-10 A	Beta – 289522	189-192 cm	Shell	-1.4	1,270 $\pm$ 40	720	900	AFU5/LFU5	Y22
TT-66-10 B	Beta – 289523	341-343 cm	Shell	-3.1	1,760 $\pm$ 40	1,250	1,370	Lag (Atop of AFU2/LFU2)	Y22
TT-73-10	Beta – 317232	316-328 cm	Foraminifera	-9.1	5,150 $\pm$ 30	5,980 5,900	5,980 5,940	AFU1/LFU1	Y40
TT-75-10	Beta – 304047	282-292 cm	Foraminifera	-5.9	5,520 $\pm$ 40	5,850	5,980	AFU1/LFU1	YY5
TT-77-10	Beta – 304048	160-173 cm	Foraminifera	-7.0	5,350 $\pm$ 30	5,640	5,760	AFU1/LFU1	YY1

# APPENDIX 7: GRAIN SIZE ANALYSES OF THE SAND FRACTION

Sunday, January 03, 2010  
1:32 PM

## Micromeritics

WIN5100 V2.03

Page 1

Sample: TT-01-08 60 cm  
Operator: Clint Edrington  
Submitter: Clint Edrington  
File Name: C:\EDRING~1\TIGER&~1\SANDFR~1\TT-01-08\01\_60CM.SMP  
Material/Liquid: silicate mud/water/Water

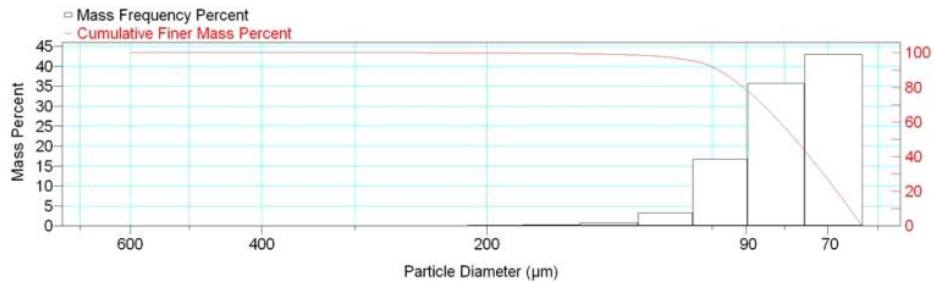
Reported: 01/03/10 13:32:37  
Liquid Visc: 0.7225 cp

Sample Density: 2.650 g/cm<sup>3</sup>  
Liquid Density: 0.9941 g/cm<sup>3</sup>

## Report by Size Class

High Diameter (µm)	Low Diameter (µm)	Average Diameter (µm)	Cumulative Mass Finer (Percent)	Mass Frequency (Percent)
710.0	600.0	652.7	100.0	0.0
600.0	500.0	547.7	100.0	0.0
500.0	425.0	461.0	100.0	0.0
425.0	355.0	388.4	100.0	0.0
355.0	300.0	326.3	100.0	0.0
300.0	250.0	273.9	100.0	0.0
250.0	212.0	230.2	99.9	0.1
212.0	180.0	195.3	99.7	0.2
180.0	150.0	164.3	99.4	0.3
150.0	125.0	136.9	98.6	0.8
125.0	106.0	115.1	95.3	3.3
106.0	90.00	97.67	78.6	16.7
90.00	75.00	82.16	42.9	35.7
75.00	63.00	68.74	0.0	42.9

Mass Frequency vs Diameter



## Summary Report

Full scale pump speed: 3  
Bubble detection: Medium  
Starting Size: 63.00 µm  
Ending Size: 0.50 µm

Stir time: 30 secs  
Stir speed: Low  
Probe time: 30 secs

Sample: TT-01-08 60 cm  
 Operator: Clint Edrington  
 Submitter: Clint Edrington  
 File Name: C:\EDRING~1\TIGER&~1\SANDFR~1\TT-01-08\01\_60CM.SMP  
 Material/Liquid: silicate mud/water/Water

Reported: 01/03/10 13:32:37  
 Liquid Visc: 0.7225 cp

Sample Density: 2.650 g/cm<sup>3</sup>  
 Liquid Density: 0.9941 g/cm<sup>3</sup>

## Summary Report

Parameter 1 0.000

Parameter 2 0.000

Parameter 3 0.000

## Mass Distribution Arithmetic Statistics

Mean	81.14	Std. Dev.	15.62
Median	77.42	Coef. Var.	0.193
Mode	68.74	Skewness	2.791
		Kurtosis	15.837

## Selected Percentiles

Percent Finer	Diameter (µm)
100.0	651.9
80.0	90.80
60.0	81.21
40.0	74.06
20.0	68.08

## Selected Sizes

Diameter (µm)	Percent Finer
500.0	100.0
250.0	100.0
125.0	98.6
88.00	74.9
63.00	0.0

Peak Number	% of Dist. *	Mean	Mode	Median	Standard Deviation	Skewness	Kurtosis
1	100.0	81.14	68.74	77.42	15.62	2.791	15.837

\* Peaks must comprise at least 5.00 % of the distribution.

# Micromeritics

WIN5100 V2.03

Page 1

Sample: TT-01-08 250 cm  
Operator: Clint Edrington  
Submitter: Clint Edrington  
File Name: C:\EDRING~1\TIGER&~1\SANDFR~1\TT-01-08\01\_250CM.SMP  
Material/Liquid: silicate mud/water/Water

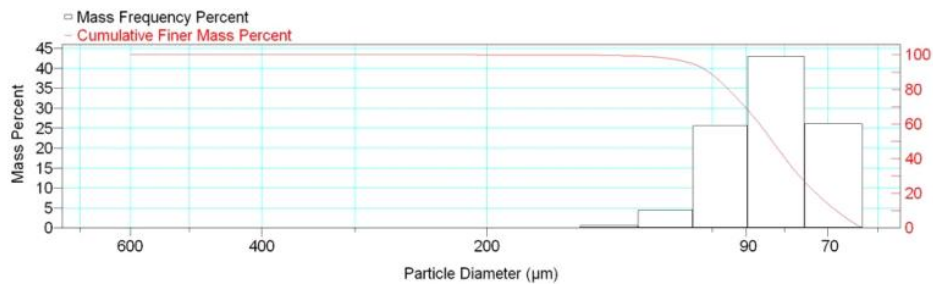
Reported: 01/03/10 13:39:58  
Liquid Visc: 0.7225 cp

Sample Density: 2.650 g/cm<sup>3</sup>  
Liquid Density: 0.9941 g/cm<sup>3</sup>

## Report by Size Class

High Diameter (μm)	Low Diameter (μm)	Average Diameter (μm)	Cumulative Mass Finer (Percent)	Mass Frequency (Percent)
710.0	600.0	652.7	100.0	0.0
600.0	500.0	547.7	100.0	0.0
500.0	425.0	461.0	100.0	0.0
425.0	355.0	388.4	100.0	0.0
355.0	300.0	326.3	100.0	0.0
300.0	250.0	273.9	100.0	0.0
250.0	212.0	230.2	100.0	0.0
212.0	180.0	195.3	99.9	0.1
180.0	150.0	164.3	99.8	0.1
150.0	125.0	136.9	99.2	0.6
125.0	106.0	115.1	94.7	4.5
106.0	90.00	97.67	69.1	25.6
90.00	75.00	82.16	26.1	43.0
75.00	63.00	68.74	0.0	26.1

Mass Frequency vs Diameter



## Summary Report

Full scale pump speed: 3  
Bubble detection: Medium  
Starting Size: 63.00 μm  
Ending Size: 0.50 μm

Stir time: 30 secs  
Stir speed: Low  
Probe time: 30 secs

Sample: TT-01-08 250 cm  
 Operator: Clint Edrington  
 Submitter: Clint Edrington  
 File Name: C:\EDRING~1\TIGER&~1\SANDFR~1\TT-01-08\01\_250CM.SMP  
 Material/Liquid: silicate mud/water/Water

Reported: 01/03/10 13:39:58  
 Liquid Visc: 0.7225 cp

Sample Density: 2.650 g/cm<sup>3</sup>  
 Liquid Density: 0.9941 g/cm<sup>3</sup>

## Summary Report

Parameter 1 0.000

Parameter 2 0.000

Parameter 3 0.000

## Mass Distribution Arithmetic Statistics

Mean	84.63	Std. Dev.	13.74
Median	83.01	Coef. Var.	0.162
Mode	82.16	Skewness	1.351
		Kurtosis	5.359

## Selected Percentiles

Percent Finer	Diameter (µm)
100.0	600.3
80.0	95.05
60.0	86.41
40.0	79.78
20.0	72.58

## Selected Sizes

Diameter (µm)	Percent Finer
500.0	100.0
250.0	100.0
125.0	99.2
88.00	64.2
63.00	0.0

Peak Number	% of Dist. *	Mean	Mode	Median	Standard Deviation	Skewness	Kurtosis
1	99.9	84.52	82.16	82.99	13.30	0.940	1.772

\* Peaks must comprise at least 5.00 % of the distribution.

# Micromeritics

WIN5100 V2.03

Page 1

Sample: TT-01-08 300 cm  
Operator: Clint Edrington  
Submitter: Clint Edrington  
File Name: C:\EDRING~1\TIGER&~1\SANDFR~1\TT-01-08\01\_300CM.SMP  
Material/Liquid: silicate mud/water/Water

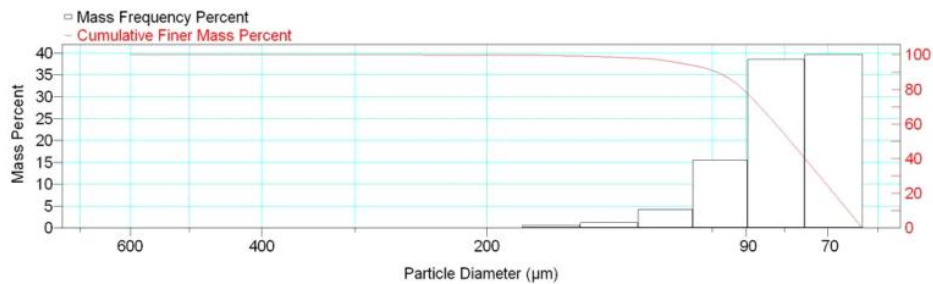
Reported: 01/03/10 13:44:15  
Liquid Visc: 0.7225 cp

Sample Density: 2.650 g/cm<sup>3</sup>  
Liquid Density: 0.9941 g/cm<sup>3</sup>

## Report by Size Class

High Diameter (µm)	Low Diameter (µm)	Average Diameter (µm)	Cumulative Mass Finer (Percent)	Mass Frequency (Percent)
710.0	600.0	652.7	100.0	0.0
600.0	500.0	547.7	100.0	0.0
500.0	425.0	461.0	100.0	0.0
425.0	355.0	388.4	100.0	0.0
355.0	300.0	326.3	100.0	0.0
300.0	250.0	273.9	100.0	0.0
250.0	212.0	230.2	99.9	0.1
212.0	180.0	195.3	99.8	0.1
180.0	150.0	164.3	99.2	0.6
150.0	125.0	136.9	98.0	1.2
125.0	106.0	115.1	93.8	4.2
106.0	90.00	97.67	78.3	15.5
90.00	75.00	82.16	39.7	38.6
75.00	63.00	68.74	0.0	39.7

Mass Frequency vs Diameter



## Summary Report

Full scale pump speed: 3  
Bubble detection: Medium  
Starting Size: 63.00 µm  
Ending Size: 0.50 µm

Stir time: 30 secs  
Stir speed: Low  
Probe time: 30 secs

Sample: TT-01-08 300 cm  
 Operator: Clint Edrington  
 Submitter: Clint Edrington  
 File Name: C:\EDRING~1\TIGER&~1\SANDFR~1\TT-01-08\01\_300CM.SMP  
 Material/Liquid: silicate mud/water/Water

Reported: 01/03/10 13:44:15  
 Liquid Visc: 0.7225 cp

Sample Density: 2.650 g/cm<sup>3</sup>  
 Liquid Density: 0.9941 g/cm<sup>3</sup>

## Summary Report

Parameter 1 0.000

Parameter 2 0.000

Parameter 3 0.000

## Mass Distribution Arithmetic Statistics

Mean	82.03	Std. Dev.	16.30
Median	78.53	Coef. Var.	0.199
Mode	68.74	Skewness	2.591
		Kurtosis	12.635

## Selected Percentiles

Percent Finer	Diameter (µm)
100.0	651.9
80.0	90.84
60.0	82.23
40.0	75.10
20.0	68.72

## Selected Sizes

Diameter (µm)	Percent Finer
500.0	100.0
250.0	100.0
125.0	98.0
88.00	74.0
63.00	0.0

Peak Number	% of Dist. *	Mean	Mode	Median	Standard Deviation	Skewness	Kurtosis
1	100.0	82.03	68.74	78.53	16.30	2.591	12.635

\* Peaks must comprise at least 5.00 % of the distribution.



# Micromeritics

WIN5100 V2.03

Page 1

Sample: TT-01-08 360 cm  
Operator: Clint Edrington  
Submitter: Clint Edrington  
File Name: C:\EDRING~1\TIGER&~1\SANDFR~1\TT-01-08\01\_360CM.SMP  
Material/Liquid: silicate mud/water/Water

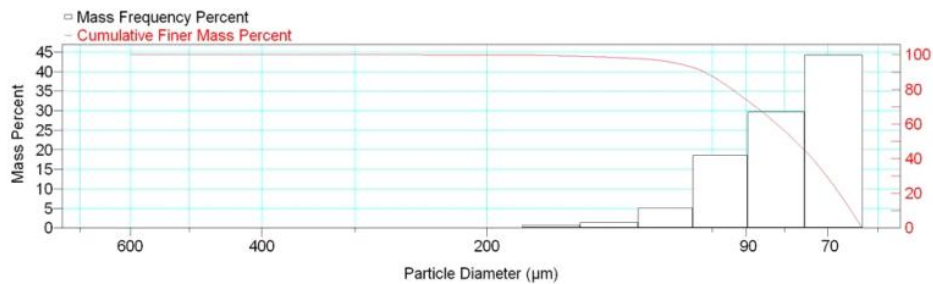
Reported: 01/03/10 13:47:17  
Liquid Visc: 0.7225 cp

Sample Density: 2.650 g/cm<sup>3</sup>  
Liquid Density: 0.9941 g/cm<sup>3</sup>

## Report by Size Class

High Diameter (µm)	Low Diameter (µm)	Average Diameter (µm)	Cumulative Mass Finer (Percent)	Mass Frequency (Percent)
710.0	600.0	652.7	100.0	0.0
600.0	500.0	547.7	100.0	0.0
500.0	425.0	461.0	100.0	0.0
425.0	355.0	388.4	100.0	0.0
355.0	300.0	326.3	100.0	0.0
300.0	250.0	273.9	100.0	0.0
250.0	212.0	230.2	99.9	0.1
212.0	180.0	195.3	99.8	0.1
180.0	150.0	164.3	99.1	0.7
150.0	125.0	136.9	97.7	1.4
125.0	106.0	115.1	92.6	5.1
106.0	90.00	97.67	74.0	18.6
90.00	75.00	82.16	44.3	29.7
75.00	63.00	68.74	0.0	44.3

Mass Frequency vs Diameter



## Summary Report

Full scale pump speed: 3  
Bubble detection: Medium  
Starting Size: 63.00 µm  
Ending Size: 0.50 µm

Stir time: 30 secs  
Stir speed: Low  
Probe time: 30 secs

Sample: TT-01-08 360 cm  
 Operator: Clint Edrington  
 Submitter: Clint Edrington  
 File Name: C:\EDRING~1\TIGER&~1\SANDFR~1\TT-01-08\01\_360CM.SMP  
 Material/Liquid: silicate mud/water/Water

Reported: 01/03/10 13:47:17  
 Liquid Visc: 0.7225 cp

Sample Density: 2.650 g/cm<sup>3</sup>  
 Liquid Density: 0.9941 g/cm<sup>3</sup>

## Summary Report

Parameter 1 0.000

Parameter 2 0.000

Parameter 3 0.000

## Mass Distribution Arithmetic Statistics

Mean	82.38	Std. Dev.	17.43
Median	77.30	Coef. Var.	0.212
Mode	68.74	Skewness	2.289
		Kurtosis	9.606

## Selected Percentiles

Percent Finer	Diameter (µm)
100.0	651.9
80.0	94.02
60.0	81.92
40.0	73.43
20.0	67.59

## Selected Sizes

Diameter (µm)	Percent Finer
500.0	100.0
250.0	100.0
125.0	97.7
88.00	70.9
63.00	0.0

Peak Number	% of Dist. *	Mean	Mode	Median	Standard Deviation	Skewness	Kurtosis
1	100.0	82.38	68.74	77.30	17.43	2.289	9.606

\* Peaks must comprise at least 5.00 % of the distribution.

# Micromeritics

WIN5100 V2.03

Page 1

Sample: TT-02-08 4-5 cm  
Operator: Clint Edrington  
Submitter: Clint Edrington  
File Name: C:\EDRING~1\TIGER&~1\SANDFR~1\TT-02-08\02\_4-5CM.SMP  
Material/Liquid: silicate mud/water/Water

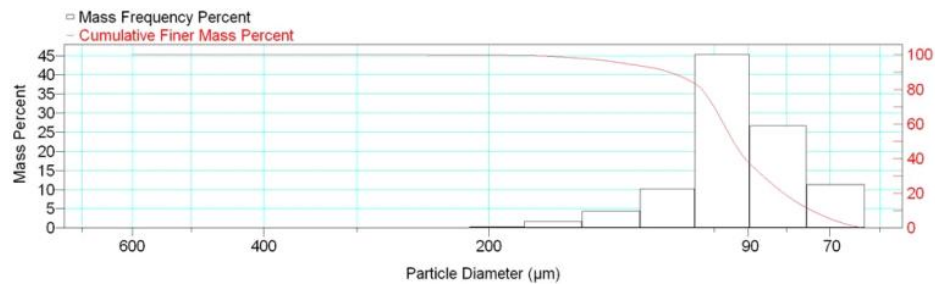
Reported: 01/03/10 13:52:38  
Liquid Visc: 0.7225 cp

Sample Density: 2.650 g/cm<sup>3</sup>  
Liquid Density: 0.9941 g/cm<sup>3</sup>

## Report by Size Class

High Diameter (μm)	Low Diameter (μm)	Average Diameter (μm)	Cumulative Mass Finer (Percent)	Mass Frequency (Percent)
710.0	600.0	652.7	100.0	0.0
600.0	500.0	547.7	100.0	0.0
500.0	425.0	461.0	100.0	0.0
425.0	355.0	388.4	100.0	0.0
355.0	300.0	326.3	100.0	0.0
300.0	250.0	273.9	100.0	0.0
250.0	212.0	230.2	99.9	0.1
212.0	180.0	195.3	99.6	0.3
180.0	150.0	164.3	97.9	1.7
150.0	125.0	136.9	93.5	4.4
125.0	106.0	115.1	83.3	10.2
106.0	90.00	97.67	38.0	45.3
90.00	75.00	82.16	11.3	26.7
75.00	63.00	68.74	0.0	11.3

Mass Frequency vs Diameter



## Summary Report

Full scale pump speed: 3  
Bubble detection: Medium  
Starting Size: 63.00 μm  
Ending Size: 0.50 μm

Stir time: 30 secs  
Stir speed: Low  
Probe time: 30 secs

Sample: TT-02-08 4-5 cm  
 Operator: Clint Edrington  
 Submitter: Clint Edrington  
 File Name: C:\EDRING~1\TIGER&~1\SANDFR~1\TT-02-08\02\_4-5CM.SMP  
 Material/Liquid: silicate mud/water/Water

Reported: 01/03/10 13:52:38  
 Liquid Visc: 0.7225 cp

Sample Density: 2.650 g/cm<sup>3</sup>  
 Liquid Density: 0.9941 g/cm<sup>3</sup>

## Summary Report

Parameter 1 0.000

Parameter 2 0.000

Parameter 3 0.000

## Mass Distribution Arithmetic Statistics

Mean	95.33	Std. Dev.	19.34
Median	94.23	Coef. Var.	0.203
Mode	97.67	Skewness	1.697
		Kurtosis	5.789

## Selected Percentiles

Percent Finer	Diameter (µm)
100.0	651.9
80.0	103.8
60.0	97.07
40.0	90.89
20.0	80.65

## Selected Sizes

Diameter (µm)	Percent Finer
500.0	100.0
250.0	100.0
125.0	93.5
88.00	34.0
63.00	0.0

Peak Number	% of Dist. *	Mean	Mode	Median	Standard Deviation	Skewness	Kurtosis
1	100.0	95.33	97.67	94.23	19.34	1.697	5.789

\* Peaks must comprise at least 5.00 % of the distribution.

Micromeritics

WIN5100 V2.03

Page 1

Sample: TT-02-08 47-49 cm  
Operator: Clint Edrington  
Submitter: Clint Edrington  
File Name: C:\EDRING~1\TIGER&~1\SANDFR~1\TT-02-08\02\_47-CM.SMP  
Material/Liquid: silicate mud/water/Water

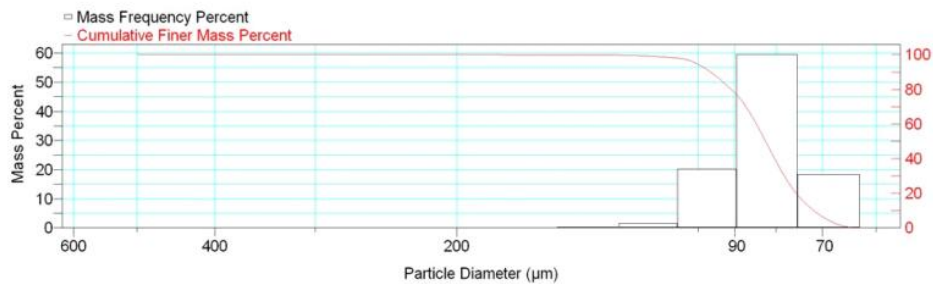
Reported: 01/03/10 13:56:17  
Liquid Visc: 0.7225 cp

Sample Density: 2.650 g/cm<sup>3</sup>  
Liquid Density: 0.9941 g/cm<sup>3</sup>

Report by Size Class

High Diameter ( $\mu\text{m}$ )	Low Diameter ( $\mu\text{m}$ )	Average Diameter ( $\mu\text{m}$ )	Cumulative Mass Finer (Percent)	Mass Frequency (Percent)
600.0	500.0	547.7	100.0	0.0
500.0	425.0	461.0	100.0	0.0
425.0	355.0	388.4	100.0	0.0
355.0	300.0	326.3	100.0	0.0
300.0	250.0	273.9	100.0	0.0
250.0	212.0	230.2	100.0	0.0
212.0	180.0	195.3	100.0	0.0
180.0	150.0	164.3	99.9	0.1
150.0	125.0	136.9	99.7	0.2
125.0	106.0	115.1	98.1	1.6
106.0	90.00	97.67	77.9	20.2
90.00	75.00	82.16	18.4	59.5
75.00	63.00	68.74	0.0	18.4

Mass Frequency vs Diameter



Summary Report

Full scale pump speed: 3  
Bubble detection: Medium  
Starting Size: 63.00  $\mu\text{m}$   
Ending Size: 0.50  $\mu\text{m}$

Stir time: 30 secs  
Stir speed: Low  
Probe time: 30 secs

Parameter 1 0.000

Parameter 2 0.000

Parameter 3 0.000

Sample: TT-02-08 47-49 cm  
 Operator: Clint Edrington  
 Submitter: Clint Edrington  
 File Name: C:\EDRING~1\TIGER&~1\SANDFR~1\TT-02-08\02\_47-CM.SMP  
 Material/Liquid: silicate mud/water/Water

Reported: 01/03/10 13:56:17      Sample Density: 2.650 g/cm<sup>3</sup>  
 Liquid Visc: 0.7225 cp      Liquid Density: 0.9941 g/cm<sup>3</sup>

## Summary Report

Mass Distribution Arithmetic Statistics			
Mean	83.54	Std. Dev.	10.49
Median	82.42	Coef. Var.	0.126
Mode	82.16	Skewness	1.133
		Kurtosis	4.575

Selected Percentiles		Selected Sizes	
Percent Finer	Diameter (µm)	Diameter (µm)	Percent Finer
100.0	553.2	500.0	100.0
80.0	91.00	250.0	100.0
60.0	84.63	125.0	99.7
40.0	80.30	88.00	72.6
20.0	75.52	63.00	0.0

Peak Number	% of Dist.*	Mean	Mode	Median	Standard Deviation	Skewness	Kurtosis
1	100.0	83.54	82.16	82.42	10.49	1.133	4.575

\* Peaks must comprise at least 5.00 % of the distribution.

Micromeritics

WIN5100 V2.03

Page 1

Sample: TT-02-08 100 cm  
Operator: Clint Edrington  
Submitter: Clint Edrington  
File Name: C:\EDRING~1\TIGER&~1\SANDFR~1\TT-02-08\02\_100CM.SMP  
Material/Liquid: silicate mud/water/Water

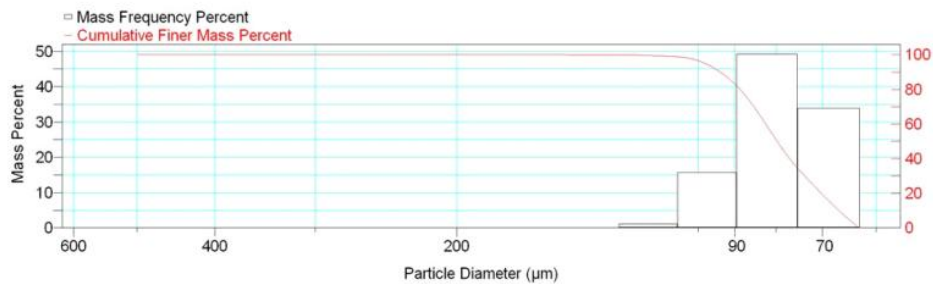
Reported: 01/03/10 13:59:53  
Liquid Visc: 0.7225 cp

Sample Density: 2.650 g/cm<sup>3</sup>  
Liquid Density: 0.9941 g/cm<sup>3</sup>

Report by Size Class

High Diameter ( $\mu\text{m}$ )	Low Diameter ( $\mu\text{m}$ )	Average Diameter ( $\mu\text{m}$ )	Cumulative Mass Finer (Percent)	Mass Frequency (Percent)
600.0	500.0	547.7	100.0	0.0
500.0	425.0	461.0	100.0	0.0
425.0	355.0	388.4	100.0	0.0
355.0	300.0	326.3	100.0	0.0
300.0	250.0	273.9	100.0	0.0
250.0	212.0	230.2	100.0	0.0
212.0	180.0	195.3	100.0	0.0
180.0	150.0	164.3	100.0	0.0
150.0	125.0	136.9	99.9	0.1
125.0	106.0	115.1	98.8	1.1
106.0	90.00	97.67	83.1	15.7
90.00	75.00	82.16	33.9	49.2
75.00	63.00	68.74	0.0	33.9

Mass Frequency vs Diameter



Summary Report

Full scale pump speed: 3  
Bubble detection: Medium  
Starting Size: 63.00  $\mu\text{m}$   
Ending Size: 0.50  $\mu\text{m}$

Stir time: 30 secs  
Stir speed: Low  
Probe time: 30 secs

Parameter 1 0.000

Parameter 2 0.000

Parameter 3 0.000

Sample: TT-02-08 100 cm  
 Operator: Clint Edrington  
 Submitter: Clint Edrington  
 File Name: C:\EDRING~1\TIGER&~1\SANDFR~1\TT-02-08\02\_100CM.SMP  
 Material/Liquid: silicate mud/water/Water

Reported: 01/03/10 13:59:53      Sample Density: 2.650 g/cm<sup>3</sup>  
 Liquid Visc: 0.7225 cp      Liquid Density: 0.9941 g/cm<sup>3</sup>

## Summary Report

## Mass Distribution Arithmetic Statistics

Mean	80.46	Std. Dev.	10.53
Median	79.71	Coef. Var.	0.131
Mode	82.16	Skewness	0.766
		Kurtosis	0.756

## Selected Percentiles

Percent Finer	Diameter (µm)
100.0	505.0
80.0	88.66
60.0	82.40
40.0	76.93
20.0	70.24

## Selected Sizes

Diameter (µm)	Percent Finer
500.0	100.0
250.0	100.0
125.0	99.9
88.00	78.3
63.00	0.0

Peak Number	% of Dist.*	Mean	Mode	Median	Standard Deviation	Skewness	Kurtosis
1	100.0	80.46	82.16	79.71	10.53	0.766	0.756

\* Peaks must comprise at least 5.00 % of the distribution.



Micromeritics

WIN5100 V2.03

Page 1

Sample: TT-02-08 148-150 cm  
Operator: Clint Edrington  
Submitter: Clint Edrington  
File Name: C:\EDRING~1\TIGER&~1\SANDFR~1\TT-02-08\02\_148CM.SMP  
Material/Liquid: silicate mud/water/Water

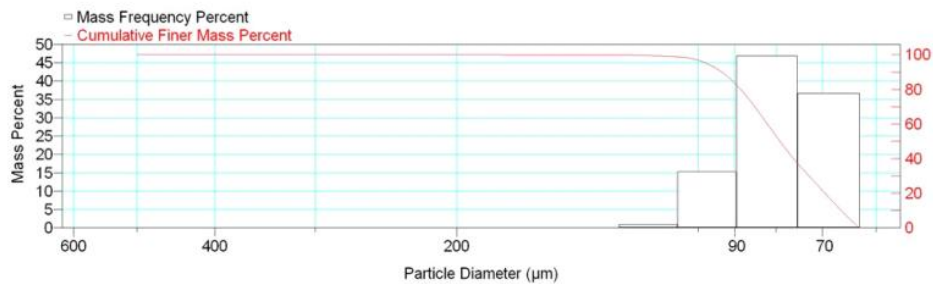
Reported: 01/03/10 14:03:04  
Liquid Visc: 0.7225 cp

Sample Density: 2.650 g/cm<sup>3</sup>  
Liquid Density: 0.9941 g/cm<sup>3</sup>

Report by Size Class

High Diameter ( $\mu\text{m}$ )	Low Diameter ( $\mu\text{m}$ )	Average Diameter ( $\mu\text{m}$ )	Cumulative Mass Finer (Percent)	Mass Frequency (Percent)
600.0	500.0	547.7	100.0	0.0
500.0	425.0	461.0	100.0	0.0
425.0	355.0	388.4	100.0	0.0
355.0	300.0	326.3	100.0	0.0
300.0	250.0	273.9	100.0	0.0
250.0	212.0	230.2	100.0	0.0
212.0	180.0	195.3	100.0	0.0
180.0	150.0	164.3	99.9	0.1
150.0	125.0	136.9	99.8	0.1
125.0	106.0	115.1	98.8	1.0
106.0	90.00	97.67	83.5	15.3
90.00	75.00	82.16	36.7	46.8
75.00	63.00	68.74	0.0	36.7

Mass Frequency vs Diameter



Summary Report

Full scale pump speed: 3  
Bubble detection: Medium  
Starting Size: 63.00  $\mu\text{m}$   
Ending Size: 0.50  $\mu\text{m}$

Stir time: 30 secs  
Stir speed: Low  
Probe time: 30 secs

Parameter 1 0.000

Parameter 2 0.000

Parameter 3 0.000

Sample: TT-02-08 148-150 cm  
 Operator: Clint Edrington  
 Submitter: Clint Edrington  
 File Name: C:\EDRING~1\TIGER&~1\SANDFR~1\TT-02-08\02\_148CM.SMP  
 Material/Liquid: silicate mud/water/Water

Reported: 01/03/10 14:03:04      Sample Density: 2.650 g/cm<sup>3</sup>  
 Liquid Visc: 0.7225 cp      Liquid Density: 0.9941 g/cm<sup>3</sup>

## Summary Report

Mass Distribution Arithmetic Statistics			
Mean	80.07	Std. Dev.	10.92
Median	79.09	Coef. Var.	0.136
Mode	82.16	Skewness	1.165
		Kurtosis	3.803

Selected Percentiles		Selected Sizes	
Percent Finer	Diameter (µm)	Diameter (µm)	Percent Finer
100.0	553.2	500.0	100.0
80.0	88.53	250.0	100.0
60.0	81.99	125.0	99.8
40.0	76.08	88.00	78.6
20.0	69.50	63.00	0.0

Peak Number	% of Dist.*	Mean	Mode	Median	Standard Deviation	Skewness	Kurtosis
1	100.0	80.07	82.16	79.09	10.92	1.165	3.803

\* Peaks must comprise at least 5.00 % of the distribution.

Micromeritics

WIN5100 V2.03

Page 1

Sample: TT-02-08 200 cm  
Operator: Clint Edrington  
Submitter: Clint Edrington  
File Name: C:\EDRING~1\TIGER&~1\SANDFR~1\TT-02-08\02\_200CM.SMP  
Material/Liquid: silicate mud/water/Water

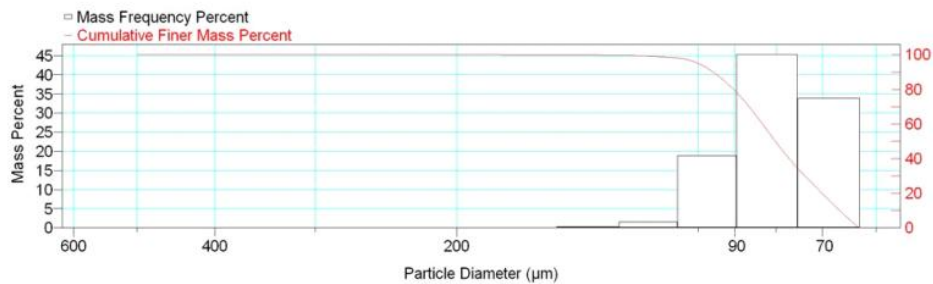
Reported: 01/03/10 14:05:48  
Liquid Visc: 0.7225 cp

Sample Density: 2.650 g/cm<sup>3</sup>  
Liquid Density: 0.9941 g/cm<sup>3</sup>

Report by Size Class

High Diameter (µm)	Low Diameter (µm)	Average Diameter (µm)	Cumulative Mass Finer (Percent)	Mass Frequency (Percent)
600.0	500.0	547.7	100.0	0.0
500.0	425.0	461.0	100.0	0.0
425.0	355.0	388.4	100.0	0.0
355.0	300.0	326.3	100.0	0.0
300.0	250.0	273.9	100.0	0.0
250.0	212.0	230.2	100.0	0.0
212.0	180.0	195.3	100.0	0.0
180.0	150.0	164.3	99.9	0.1
150.0	125.0	136.9	99.6	0.3
125.0	106.0	115.1	98.1	1.5
106.0	90.00	97.67	79.2	18.9
90.00	75.00	82.16	33.9	45.3
75.00	63.00	68.74	0.0	33.9

Mass Frequency vs Diameter



Summary Report

Full scale pump speed: 3  
Bubble detection: Medium  
Starting Size: 63.00 µm  
Ending Size: 0.50 µm

Stir time: 30 secs  
Stir speed: Low  
Probe time: 30 secs

Parameter 1 0.000

Parameter 2 0.000

Parameter 3 0.000

Sample: TT-02-08 200 cm  
 Operator: Clint Edrington  
 Submitter: Clint Edrington  
 File Name: C:\EDRING~1\TIGER&~1\SANDFR~1\TT-02-08\02\_200CM.SMP  
 Material/Liquid: silicate mud/water/Water

Reported: 01/03/10 14:05:48      Sample Density: 2.650 g/cm<sup>3</sup>  
 Liquid Visc: 0.7225 cp      Liquid Density: 0.9941 g/cm<sup>3</sup>

## Summary Report

## Mass Distribution Arithmetic Statistics

Mean	81.28	Std. Dev.	11.74
Median	80.13	Coef. Var.	0.144
Mode	82.16	Skewness	1.133
		Kurtosis	3.212

## Selected Percentiles

Percent Finer	Diameter (µm)
100.0	553.2
80.0	90.36
60.0	83.18
40.0	77.05
20.0	70.12

## Selected Sizes

Diameter (µm)	Percent Finer
500.0	100.0
250.0	100.0
125.0	99.6
88.00	74.3
63.00	0.0

Peak Number	% of Dist.*	Mean	Mode	Median	Standard Deviation	Skewness	Kurtosis
1	100.0	81.28	82.16	80.13	11.74	1.133	3.212

\* Peaks must comprise at least 5.00 % of the distribution.

# Micromeritics

WIN5100 V2.03

Page 1

Sample: TT-02-08 250 cm  
Operator: Clint Edrington  
Submitter: Clint Edrington  
File Name: C:\EDRING~1\TIGER&~1\SANDFR~1\TT-02-08\02\_250CM.SMP  
Material/Liquid: silicate mud/water/Water

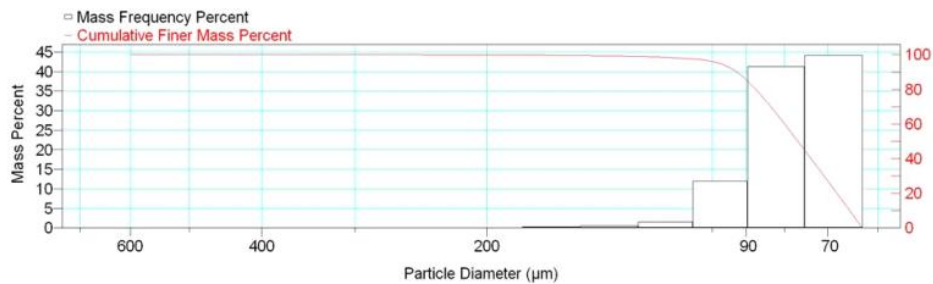
Reported: 01/03/10 14:09:34  
Liquid Visc: 0.7225 cp

Sample Density: 2.650 g/cm<sup>3</sup>  
Liquid Density: 0.9941 g/cm<sup>3</sup>

## Report by Size Class

High Diameter (μm)	Low Diameter (μm)	Average Diameter (μm)	Cumulative Mass Finer (Percent)	Mass Frequency (Percent)
710.0	600.0	652.7	100.0	0.0
600.0	500.0	547.7	100.0	0.0
500.0	425.0	461.0	100.0	0.0
425.0	355.0	388.4	100.0	0.0
355.0	300.0	326.3	100.0	0.0
300.0	250.0	273.9	100.0	0.0
250.0	212.0	230.2	99.9	0.1
212.0	180.0	195.3	99.8	0.1
180.0	150.0	164.3	99.5	0.3
150.0	125.0	136.9	99.0	0.5
125.0	106.0	115.1	97.5	1.5
106.0	90.00	97.67	85.5	12.0
90.00	75.00	82.16	44.2	41.3
75.00	63.00	68.74	0.0	44.2

Mass Frequency vs Diameter



## Summary Report

Full scale pump speed: 3  
Bubble detection: Medium  
Starting Size: 63.00 μm  
Ending Size: 0.50 μm

Stir time: 30 secs  
Stir speed: Low  
Probe time: 30 secs

Sample: TT-02-08 250 cm  
 Operator: Clint Edrington  
 Submitter: Clint Edrington  
 File Name: C:\EDRING~1\TIGER&~1\SANDFR~1\TT-02-08\02\_250CM.SMP  
 Material/Liquid: silicate mud/water/Water

Reported: 01/03/10 14:09:34  
 Liquid Visc: 0.7225 cp

Sample Density: 2.650 g/cm<sup>3</sup>  
 Liquid Density: 0.9941 g/cm<sup>3</sup>

## Summary Report

Parameter 1 0.000

Parameter 2 0.000

Parameter 3 0.000

## Mass Distribution Arithmetic Statistics

Mean	79.36	Std. Dev.	13.67
Median	76.77	Coef. Var.	0.172
Mode	68.74	Skewness	3.398
		Kurtosis	24.286

## Selected Percentiles

Percent Finer	Diameter (µm)
100.0	651.9
80.0	87.45
60.0	79.96
40.0	73.75
20.0	68.06

## Selected Sizes

Diameter (µm)	Percent Finer
500.0	100.0
250.0	100.0
125.0	99.0
88.00	81.2
63.00	0.0

Peak Number	% of Dist. *	Mean	Mode	Median	Standard Deviation	Skewness	Kurtosis
1	100.0	79.36	68.74	76.77	13.67	3.398	24.286

\* Peaks must comprise at least 5.00 % of the distribution.

# Micromeritics

WIN5100 V2.03

Page 1

Sample: TT-02-08 300 cm  
Operator: Clint Edrington  
Submitter: Clint Edrington  
File Name: C:\EDRING~1\TIGER&~1\SANDFR~1\TT-02-08\02\_300CM.SMP  
Material/Liquid: silicate mud/water/Water

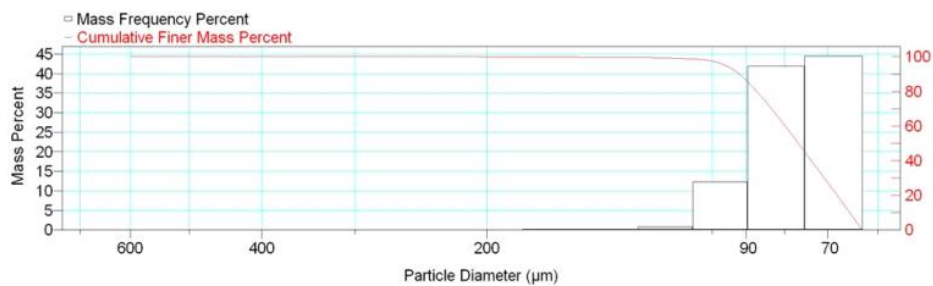
Reported: 01/03/10 14:12:35  
Liquid Visc: 0.7225 cp

Sample Density: 2.650 g/cm<sup>3</sup>  
Liquid Density: 0.9941 g/cm<sup>3</sup>

## Report by Size Class

High Diameter (μm)	Low Diameter (μm)	Average Diameter (μm)	Cumulative Mass Finer (Percent)	Mass Frequency (Percent)
710.0	600.0	652.7	100.0	0.0
600.0	500.0	547.7	100.0	0.0
500.0	425.0	461.0	100.0	0.0
425.0	355.0	388.4	100.0	0.0
355.0	300.0	326.3	100.0	0.0
300.0	250.0	273.9	100.0	0.0
250.0	212.0	230.2	100.0	0.0
212.0	180.0	195.3	99.9	0.1
180.0	150.0	164.3	99.7	0.2
150.0	125.0	136.9	99.5	0.2
125.0	106.0	115.1	98.7	0.8
106.0	90.00	97.67	86.4	12.3
90.00	75.00	82.16	44.5	41.9
75.00	63.00	68.74	0.0	44.5

Mass Frequency vs Diameter



## Summary Report

Full scale pump speed: 3  
Bubble detection: Medium  
Starting Size: 63.00 μm  
Ending Size: 0.50 μm

Stir time: 30 secs  
Stir speed: Low  
Probe time: 30 secs

Sample: TT-02-08 300 cm  
 Operator: Clint Edrington  
 Submitter: Clint Edrington  
 File Name: C:\EDRING~1\TIGER&~1\SANDFR~1\TT-02-08\02\_300CM.SMP  
 Material/Liquid: silicate mud/water/Water

Reported: 01/03/10 14:12:35  
 Liquid Visc: 0.7225 cp

Sample Density: 2.650 g/cm<sup>3</sup>  
 Liquid Density: 0.9941 g/cm<sup>3</sup>

## Summary Report

Parameter 1 0.000

Parameter 2 0.000

Parameter 3 0.000

## Mass Distribution Arithmetic Statistics

Mean	78.75	Std. Dev.	11.79
Median	76.66	Coef. Var.	0.150
Mode	68.74	Skewness	2.452
		Kurtosis	15.054

## Selected Percentiles

Percent Finer	Diameter (µm)
100.0	600.3
80.0	87.15
60.0	79.83
40.0	73.67
20.0	68.04

## Selected Sizes

Diameter (µm)	Percent Finer
500.0	100.0
250.0	100.0
125.0	99.5
88.00	82.0
63.00	0.0

Peak Number	% of Dist. *	Mean	Mode	Median	Standard Deviation	Skewness	Kurtosis
1	99.7	78.46	68.74	76.62	10.54	1.096	1.764

\* Peaks must comprise at least 5.00 % of the distribution.



Micromeritics

WIN5100 V2.03

Page 1

Sample: TT-02-08 350 cm  
Operator: Clint Edrington  
Submitter: Clint Edrington  
File Name: C:\EDRING~1\TIGER&~1\SANDFR~1\TT-02-08\02\_350CM.SMP  
Material/Liquid: silicate mud/water/Water

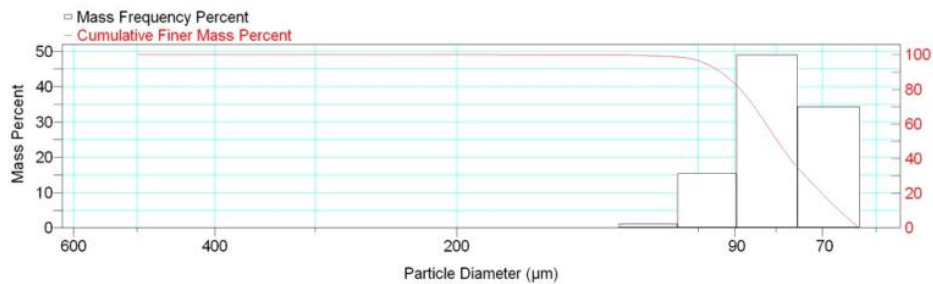
Reported: 01/03/10 14:15:16  
Liquid Visc: 0.7225 cp

Sample Density: 2.650 g/cm<sup>3</sup>  
Liquid Density: 0.9941 g/cm<sup>3</sup>

Report by Size Class

High Diameter ( $\mu\text{m}$ )	Low Diameter ( $\mu\text{m}$ )	Average Diameter ( $\mu\text{m}$ )	Cumulative Mass Finer (Percent)	Mass Frequency (Percent)
600.0	500.0	547.7	100.0	0.0
500.0	425.0	461.0	100.0	0.0
425.0	355.0	388.4	100.0	0.0
355.0	300.0	326.3	100.0	0.0
300.0	250.0	273.9	100.0	0.0
250.0	212.0	230.2	100.0	0.0
212.0	180.0	195.3	100.0	0.0
180.0	150.0	164.3	99.9	0.1
150.0	125.0	136.9	99.8	0.1
125.0	106.0	115.1	98.7	1.1
106.0	90.00	97.67	83.3	15.4
90.00	75.00	82.16	34.3	49.0
75.00	63.00	68.74	0.0	34.3

Mass Frequency vs Diameter



Summary Report

Full scale pump speed: 3  
Bubble detection: Medium  
Starting Size: 63.00  $\mu\text{m}$   
Ending Size: 0.50  $\mu\text{m}$

Stir time: 30 secs  
Stir speed: Low  
Probe time: 30 secs

Parameter 1 0.000

Parameter 2 0.000

Parameter 3 0.000

Sample: TT-02-08 350 cm  
 Operator: Clint Edrington  
 Submitter: Clint Edrington  
 File Name: C:\EDRING~1\TIGER&~1\SANDFR~1\TT-02-08\02\_350CM.SMP  
 Material/Liquid: silicate mud/water/Water

Reported: 01/03/10 14:15:16  
 Liquid Visc: 0.7225 cp

Sample Density: 2.650 g/cm<sup>3</sup>  
 Liquid Density: 0.9941 g/cm<sup>3</sup>

## Summary Report

## Mass Distribution Arithmetic Statistics

Mean	80.44	Std. Dev.	10.84
Median	79.61	Coef. Var.	0.135
Mode	82.16	Skewness	1.152
		Kurtosis	3.911

## Selected Percentiles

Percent Finer	Diameter (µm)
100.0	553.2
80.0	88.58
60.0	82.31
40.0	76.81
20.0	70.13

## Selected Sizes

Diameter (µm)	Percent Finer
500.0	100.0
250.0	100.0
125.0	99.8
88.00	78.5
63.00	0.0

Peak Number	% of Dist.*	Mean	Mode	Median	Standard Deviation	Skewness	Kurtosis
1	100.0	80.44	82.16	79.61	10.84	1.152	3.911

\* Peaks must comprise at least 5.00 % of the distribution.

# Micromeritics

WIN5100 V2.03

Page 1

Sample: TT-03-08 16 cm  
Operator: Clint Edrington  
Submitter: Clint Edrington  
File Name: C:\EDRING~1\TIGER&~1\SANDFR~1\TT-03-08\03\_16CM.SMP  
Material/Liquid: silicate mud/water/Water

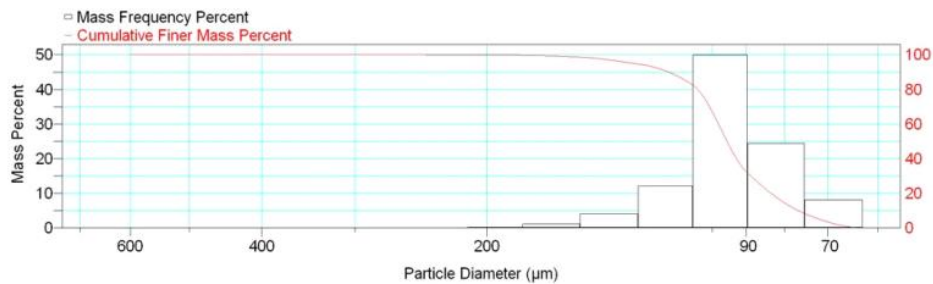
Reported: 01/03/10 14:20:11  
Liquid Visc: 0.7225 cp

Sample Density: 2.650 g/cm<sup>3</sup>  
Liquid Density: 0.9941 g/cm<sup>3</sup>

## Report by Size Class

High Diameter (μm)	Low Diameter (μm)	Average Diameter (μm)	Cumulative Mass Finer (Percent)	Mass Frequency (Percent)
710.0	600.0	652.7	100.0	0.0
600.0	500.0	547.7	100.0	0.0
500.0	425.0	461.0	100.0	0.0
425.0	355.0	388.4	100.0	0.0
355.0	300.0	326.3	100.0	0.0
300.0	250.0	273.9	100.0	0.0
250.0	212.0	230.2	99.9	0.1
212.0	180.0	195.3	99.7	0.2
180.0	150.0	164.3	98.6	1.1
150.0	125.0	136.9	94.5	4.1
125.0	106.0	115.1	82.4	12.1
106.0	90.00	97.67	32.5	49.9
90.00	75.00	82.16	8.1	24.4
75.00	63.00	68.74	0.0	8.1

Mass Frequency vs Diameter



## Summary Report

Full scale pump speed: 3  
Bubble detection: Medium  
Starting Size: 63.00 μm  
Ending Size: 0.50 μm

Stir time: 30 secs  
Stir speed: Low  
Probe time: 30 secs

Sample: TT-03-08 16 cm  
 Operator: Clint Edrington  
 Submitter: Clint Edrington  
 File Name: C:\EDRING~1\TIGER&~1\SANDFR~1\TT-03-08\03\_16CM.SMP  
 Material/Liquid: silicate mud/water/Water

Reported: 01/03/10 14:20:11  
 Liquid Visc: 0.7225 cp

Sample Density: 2.650 g/cm<sup>3</sup>  
 Liquid Density: 0.9941 g/cm<sup>3</sup>

## Summary Report

Parameter 1 0.000

Parameter 2 0.000

Parameter 3 0.000

## Mass Distribution Arithmetic Statistics

Mean	96.32	Std. Dev.	17.61
Median	95.49	Coef. Var.	0.183
Mode	97.67	Skewness	1.639
		Kurtosis	6.686

## Selected Percentiles

Percent Finer	Diameter (µm)
100.0	651.9
80.0	104.5
60.0	98.04
40.0	92.75
20.0	83.39

## Selected Sizes

Diameter (µm)	Percent Finer
500.0	100.0
250.0	100.0
125.0	94.5
88.00	28.5
63.00	0.0

Peak Number	% of Dist. *	Mean	Mode	Median	Standard Deviation	Skewness	Kurtosis
1	100.0	96.32	97.67	95.49	17.61	1.639	6.686

\* Peaks must comprise at least 5.00 % of the distribution.

# Micromeritics

WIN5100 V2.03

Page 1

Sample: TT-03-08 50 cm  
Operator: Clint Edrington  
Submitter: Clint Edrington  
File Name: C:\EDRING~1\TIGER&~1\SANDFR~1\TT-03-08\03\_50CM.SMP  
Material/Liquid: silicate mud/water/Water

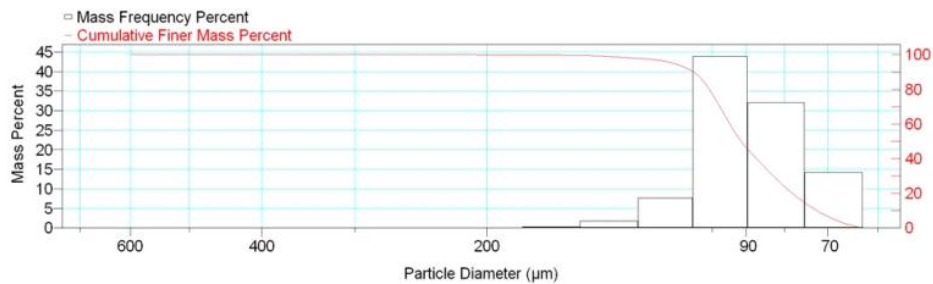
Reported: 01/03/10 14:23:11  
Liquid Visc: 0.7225 cp

Sample Density: 2.650 g/cm<sup>3</sup>  
Liquid Density: 0.9941 g/cm<sup>3</sup>

## Report by Size Class

High Diameter (µm)	Low Diameter (µm)	Average Diameter (µm)	Cumulative Mass Finer (Percent)	Mass Frequency (Percent)
710.0	600.0	652.7	100.0	0.0
600.0	500.0	547.7	100.0	0.0
500.0	425.0	461.0	100.0	0.0
425.0	355.0	388.4	100.0	0.0
355.0	300.0	326.3	100.0	0.0
300.0	250.0	273.9	100.0	0.0
250.0	212.0	230.2	100.0	0.0
212.0	180.0	195.3	99.9	0.1
180.0	150.0	164.3	99.6	0.3
150.0	125.0	136.9	97.8	1.8
125.0	106.0	115.1	90.2	7.6
106.0	90.00	97.67	46.3	43.9
90.00	75.00	82.16	14.2	32.1
75.00	63.00	68.74	0.0	14.2

Mass Frequency vs Diameter



## Summary Report

Full scale pump speed: 3  
Bubble detection: Medium  
Starting Size: 63.00 µm  
Ending Size: 0.50 µm

Stir time: 30 secs  
Stir speed: Low  
Probe time: 30 secs

Sample: TT-03-08 50 cm  
 Operator: Clint Edrington  
 Submitter: Clint Edrington  
 File Name: C:\EDRING~1\TIGER&~1\SANDFR~1\TT-03-08\03\_50CM.SMP  
 Material/Liquid: silicate mud/water/Water

Reported: 01/03/10 14:23:11  
 Liquid Visc: 0.7225 cp

Sample Density: 2.650 g/cm<sup>3</sup>  
 Liquid Density: 0.9941 g/cm<sup>3</sup>

## Summary Report

Parameter 1 0.000

Parameter 2 0.000

Parameter 3 0.000

## Mass Distribution Arithmetic Statistics

Mean	90.91	Std. Dev.	14.97
Median	91.46	Coef. Var.	0.165
Mode	97.67	Skewness	1.051
		Kurtosis	3.964

## Selected Percentiles

Percent Finer	Diameter (µm)
100.0	600.3
80.0	100.8
60.0	94.66
40.0	87.23
20.0	78.10

## Selected Sizes

Diameter (µm)	Percent Finer
500.0	100.0
250.0	100.0
125.0	97.8
88.00	41.8
63.00	0.0

Peak Number	% of Dist. *	Mean	Mode	Median	Standard Deviation	Skewness	Kurtosis
1	100.0	90.91	97.67	91.46	14.97	1.051	3.964

\* Peaks must comprise at least 5.00 % of the distribution.

Micromeritics

WIN5100 V2.03

Page 1

Sample: TT-03-08 100 cm  
Operator: Clint Edrington  
Submitter: Clint Edrington  
File Name: C:\EDRING~1\TIGER&~1\SANDFR~1\TT-03-08\03\_100CM.SMP  
Material/Liquid: silicate mud/water/Water

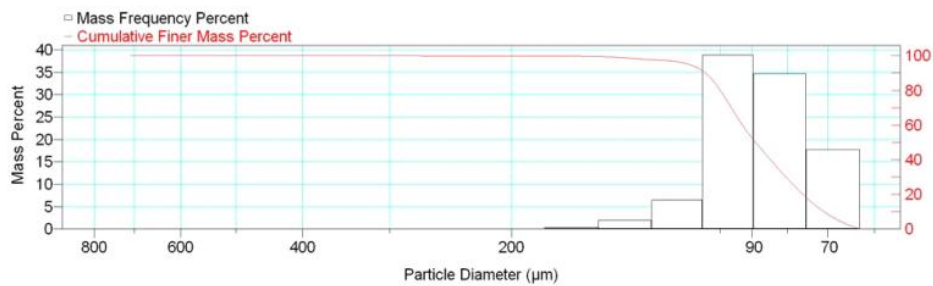
Reported: 01/03/10 14:26:21  
Liquid Visc: 0.7225 cp

Sample Density: 2.650 g/cm<sup>3</sup>  
Liquid Density: 0.9941 g/cm<sup>3</sup>

Report by Size Class

High Diameter ( $\mu\text{m}$ )	Low Diameter ( $\mu\text{m}$ )	Average Diameter ( $\mu\text{m}$ )	Cumulative Mass Finer (Percent)	Mass Frequency (Percent)
850.0	710.0	776.9	100.0	0.0
710.0	600.0	652.7	100.0	0.0
600.0	500.0	547.7	100.0	0.0
500.0	425.0	461.0	100.0	0.0
425.0	355.0	388.4	100.0	0.0
355.0	300.0	326.3	100.0	0.0
300.0	250.0	273.9	99.9	0.1
250.0	212.0	230.2	99.9	0.0
212.0	180.0	195.3	99.9	0.0
180.0	150.0	164.3	99.5	0.4
150.0	125.0	136.9	97.6	1.9
125.0	106.0	115.1	91.2	6.4
106.0	90.00	97.67	52.4	38.8
90.00	75.00	82.16	17.7	34.7
75.00	63.00	68.74	0.0	17.7

Mass Frequency vs Diameter



Summary Report

Full scale pump speed: 3  
Bubble detection: Medium  
Starting Size: 63.00  $\mu\text{m}$   
Ending Size: 0.50  $\mu\text{m}$

Stir time: 30 secs  
Stir speed: Low  
Probe time: 30 secs

Sample: TT-03-08 100 cm  
 Operator: Clint Edrington  
 Submitter: Clint Edrington  
 File Name: C:\EDRING~1\TIGER&~1\SANDFR~1\TT-03-08\03\_100CM.SMP  
 Material/Liquid: silicate mud/water/Water

Reported: 01/03/10 14:26:21  
 Liquid Visc: 0.7225 cp

Sample Density: 2.650 g/cm<sup>3</sup>  
 Liquid Density: 0.9941 g/cm<sup>3</sup>

## Summary Report

Parameter 1	0.000	Parameter 2	0.000	Parameter 3	0.000		
Mass Distribution Arithmetic Statistics							
Mean	89.47	Std. Dev.	16.19				
Median	88.95	Coef. Var.	0.181				
Mode	97.67	Skewness	2.253				
		Kurtosis	17.990				
Selected Percentiles			Selected Sizes				
Percent Finer	Diameter (µm)		Diameter (µm)	Percent Finer			
100.0	714.1		500.0	100.0			
80.0	100.0		250.0	99.9			
60.0	92.95		125.0	97.6			
40.0	84.68		88.00	47.8			
20.0	76.06		63.00	0.0			
Peak Number	% of Dist.*	Mean	Mode	Median	Standard Deviation	Skewness	Kurtosis
1	99.9	89.29	97.67	88.93	15.11	0.991	2.526

\* Peaks must comprise at least 5.00 % of the distribution.



# Micromeritics

WIN5100 V2.03

Page 1

Sample: TT-03-08 150 cm  
Operator: Clint Edrington  
Submitter: Clint Edrington  
File Name: C:\EDRING~1\TIGER&~1\SANDFR~1\TT-03-08\03\_150CM.SMP  
Material/Liquid: silicate mud/water/Water

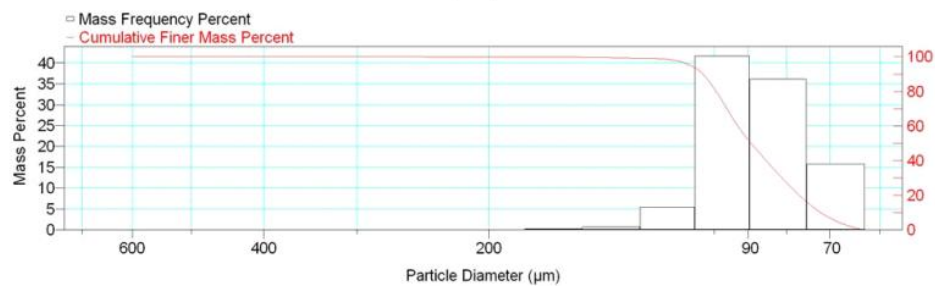
Reported: 01/03/10 14:28:57  
Liquid Visc: 0.7225 cp

Sample Density: 2.650 g/cm<sup>3</sup>  
Liquid Density: 0.9941 g/cm<sup>3</sup>

## Report by Size Class

High Diameter (µm)	Low Diameter (µm)	Average Diameter (µm)	Cumulative Mass Finer (Percent)	Mass Frequency (Percent)
710.0	600.0	652.7	100.0	0.0
600.0	500.0	547.7	100.0	0.0
500.0	425.0	461.0	100.0	0.0
425.0	355.0	388.4	100.0	0.0
355.0	300.0	326.3	100.0	0.0
300.0	250.0	273.9	100.0	0.0
250.0	212.0	230.2	99.9	0.1
212.0	180.0	195.3	99.9	0.0
180.0	150.0	164.3	99.7	0.2
150.0	125.0	136.9	99.0	0.7
125.0	106.0	115.1	93.6	5.4
106.0	90.00	97.67	51.9	41.7
90.00	75.00	82.16	15.8	36.1
75.00	63.00	68.74	0.0	15.8

Mass Frequency vs Diameter



## Summary Report

Full scale pump speed: 3  
Bubble detection: Medium  
Starting Size: 63.00 µm  
Ending Size: 0.50 µm

Stir time: 30 secs  
Stir speed: Low  
Probe time: 30 secs

Sample: TT-03-08 150 cm  
 Operator: Clint Edrington  
 Submitter: Clint Edrington  
 File Name: C:\EDRING~1\TIGER&~1\SANDFR~1\TT-03-08\03\_150CM.SMP  
 Material/Liquid: silicate mud/water/Water

Reported: 01/03/10 14:28:57  
 Liquid Visc: 0.7225 cp

Sample Density: 2.650 g/cm<sup>3</sup>  
 Liquid Density: 0.9941 g/cm<sup>3</sup>

## Summary Report

Parameter 1 0.000

Parameter 2 0.000

Parameter 3 0.000

## Mass Distribution Arithmetic Statistics

Mean	88.98	Std. Dev.	14.05
Median	89.21	Coef. Var.	0.158
Mode	97.67	Skewness	1.535
		Kurtosis	11.235

## Selected Percentiles

Percent Finer	Diameter (µm)
100.0	651.9
80.0	99.36
60.0	92.93
40.0	85.15
20.0	76.90

## Selected Sizes

Diameter (µm)	Percent Finer
500.0	100.0
250.0	100.0
125.0	99.0
88.00	47.0
63.00	0.0

Peak Number	% of Dist. *	Mean	Mode	Median	Standard Deviation	Skewness	Kurtosis
1	99.9	88.84	97.67	89.19	13.32	0.640	1.991

\* Peaks must comprise at least 5.00 % of the distribution.

Micromeritics

WIN5100 V2.03

Page 1

Sample: TT-03-08 196 cm  
Operator: Clint Edrington  
Submitter: Clint Edrington  
File Name: C:\EDRING~1\TIGER&~1\SANDFR~1\TT-03-08\03\_196CM.SMP  
Material/Liquid: silicate mud/water/Water

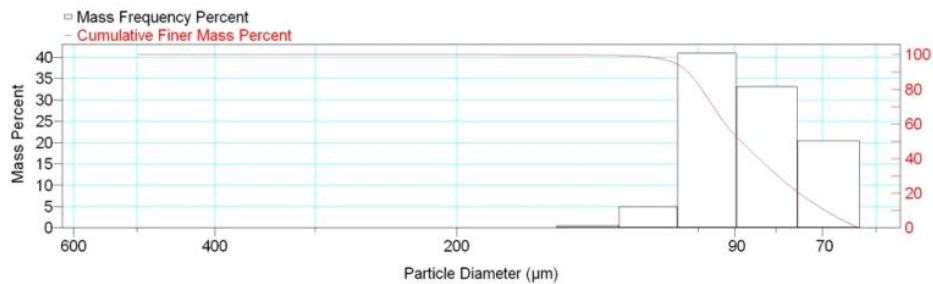
Reported: 01/03/10 14:32:02  
Liquid Visc: 0.7225 cp

Sample Density: 2.650 g/cm<sup>3</sup>  
Liquid Density: 0.9941 g/cm<sup>3</sup>

Report by Size Class

High Diameter (μm)	Low Diameter (μm)	Average Diameter (μm)	Cumulative Mass Finer (Percent)	Mass Frequency (Percent)
600.0	500.0	547.7	100.0	0.0
500.0	425.0	461.0	100.0	0.0
425.0	355.0	388.4	100.0	0.0
355.0	300.0	326.3	100.0	0.0
300.0	250.0	273.9	100.0	0.0
250.0	212.0	230.2	100.0	0.0
212.0	180.0	195.3	100.0	0.0
180.0	150.0	164.3	99.9	0.1
150.0	125.0	136.9	99.4	0.5
125.0	106.0	115.1	94.4	5.0
106.0	90.00	97.67	53.5	40.9
90.00	75.00	82.16	20.4	33.1
75.00	63.00	68.74	0.0	20.4

Mass Frequency vs Diameter



Summary Report

Full scale pump speed: 3  
Bubble detection: Medium  
Starting Size: 63.00 μm  
Ending Size: 0.50 μm

Stir time: 30 secs  
Stir speed: Low  
Probe time: 30 secs

Parameter 1 0.000

Parameter 2 0.000

Parameter 3 0.000

Sample: TT-03-08 196 cm  
 Operator: Clint Edrington  
 Submitter: Clint Edrington  
 File Name: C:\EDRING~1\TIGER&~1\SANDFR~1\TT-03-08\03\_196CM.SMP  
 Material/Liquid: silicate mud/water/Water

Reported: 01/03/10 14:32:02      Sample Density: 2.650 g/cm<sup>3</sup>  
 Liquid Visc: 0.7225 cp      Liquid Density: 0.9941 g/cm<sup>3</sup>

## Summary Report

## Mass Distribution Arithmetic Statistics

Mean	87.77	Std. Dev.	13.41
Median	88.42	Coef. Var.	0.153
Mode	97.67	Skewness	0.414
		Kurtosis	0.792

## Selected Percentiles

Percent Finer	Diameter (µm)
100.0	553.2
80.0	98.98
60.0	92.52
40.0	83.99
20.0	74.80

## Selected Sizes

Diameter (µm)	Percent Finer
500.0	100.0
250.0	100.0
125.0	99.4
88.00	49.1
63.00	0.0

Peak Number	% of Dist.*	Mean	Mode	Median	Standard Deviation	Skewness	Kurtosis
1	100.0	87.77	97.67	88.42	13.41	0.414	0.792

\* Peaks must comprise at least 5.00 % of the distribution.

Micromeritics

WIN5100 V2.03

Page 1

Sample: TT-03-08 250 cm  
Operator: Clint Edrington  
Submitter: Clint Edrington  
File Name: C:\EDRING~1\TIGER&~1\SANDFR~1\TT-03-08\03\_250CM.SMP  
Material/Liquid: silicate mud/water/Water

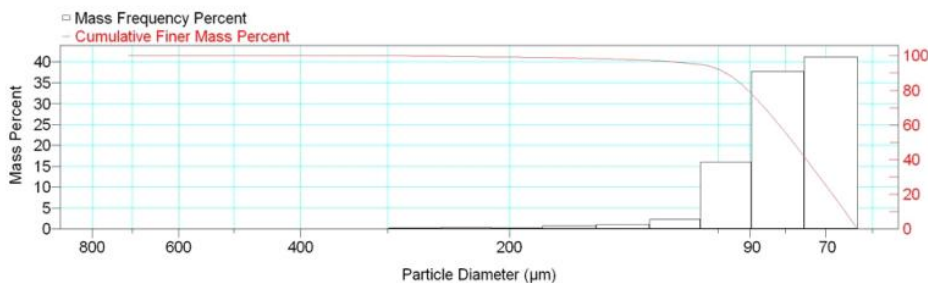
Reported: 01/03/10 14:34:59  
Liquid Visc: 0.7225 cp

Sample Density: 2.650 g/cm<sup>3</sup>  
Liquid Density: 0.9941 g/cm<sup>3</sup>

Report by Size Class

High Diameter ( $\mu\text{m}$ )	Low Diameter ( $\mu\text{m}$ )	Average Diameter ( $\mu\text{m}$ )	Cumulative Mass Finer (Percent)	Mass Frequency (Percent)
850.0	710.0	776.9	100.0	0.0
710.0	600.0	652.7	100.0	0.0
600.0	500.0	547.7	100.0	0.0
500.0	425.0	461.0	100.0	0.0
425.0	355.0	388.4	100.0	0.0
355.0	300.0	326.3	100.0	0.0
300.0	250.0	273.9	99.7	0.3
250.0	212.0	230.2	99.3	0.4
212.0	180.0	195.3	99.0	0.3
180.0	150.0	164.3	98.3	0.7
150.0	125.0	136.9	97.2	1.1
125.0	106.0	115.1	94.9	2.3
106.0	90.00	97.67	78.9	16.0
90.00	75.00	82.16	41.2	37.7
75.00	63.00	68.74	0.0	41.2

Mass Frequency vs Diameter



Summary Report

Full scale pump speed: 3  
Bubble detection: Medium  
Starting Size: 63.00  $\mu\text{m}$   
Ending Size: 0.50  $\mu\text{m}$

Stir time: 30 secs  
Stir speed: Low  
Probe time: 30 secs

Sample: TT-03-08 250 cm  
 Operator: Clint Edrington  
 Submitter: Clint Edrington  
 File Name: C:\EDRING~1\TIGER&~1\SANDFR~1\TT-03-08\03\_250CM.SMP  
 Material/Liquid: silicate mud/water/Water

Reported: 01/03/10 14:34:59  
 Liquid Visc: 0.7225 cp

Sample Density: 2.650 g/cm<sup>3</sup>  
 Liquid Density: 0.9941 g/cm<sup>3</sup>

## Summary Report

Parameter 1	0.000	Parameter 2	0.000	Parameter 3	0.000		
Mass Distribution Arithmetic Statistics							
Mean	82.55	Std. Dev.		21.31			
Median	77.98	Coef. Var.		0.258			
Mode	68.74	Skewness		4.551			
		Kurtosis		30.280			
Selected Percentiles			Selected Sizes				
Percent Finer	Diameter (µm)		Diameter (µm)	Percent Finer			
100.0	714.1		500.0	100.0			
80.0	90.57		250.0	99.7			
60.0	81.68		125.0	97.2			
40.0	74.61		88.00	74.8			
20.0	68.43		63.00	0.0			
Peak Number	% of Dist.*	Mean	Mode	Median	Standard Deviation	Skewness	Kurtosis
1	99.3	81.38	68.74	77.86	16.05	2.695	12.082

\* Peaks must comprise at least 5.00 % of the distribution.

Micromeritics

WIN5100 V2.03

Page 1

Sample: TT-03-08 300 cm  
Operator: Clint Edrington  
Submitter: Clint Edrington  
File Name: C:\EDRING~1\TIGER&~1\SANDFR~1\TT-03-08\03\_300CM.SMP  
Material/Liquid: silicate mud/water/Water

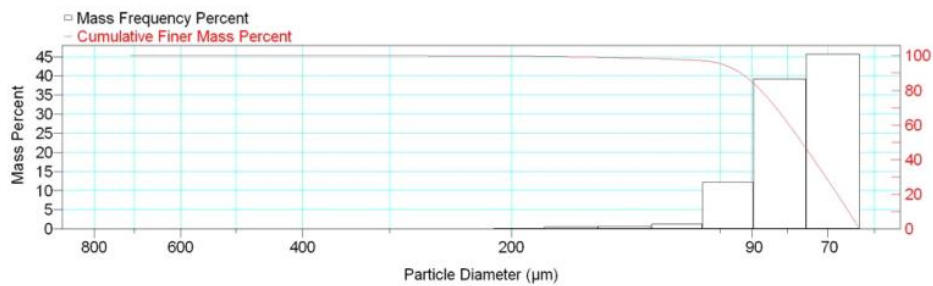
Reported: 01/03/10 14:38:23  
Liquid Visc: 0.7225 cp

Sample Density: 2.650 g/cm<sup>3</sup>  
Liquid Density: 0.9941 g/cm<sup>3</sup>

Report by Size Class

High Diameter ( $\mu\text{m}$ )	Low Diameter ( $\mu\text{m}$ )	Average Diameter ( $\mu\text{m}$ )	Cumulative Mass Finer (Percent)	Mass Frequency (Percent)
850.0	710.0	776.9	100.0	0.0
710.0	600.0	652.7	100.0	0.0
600.0	500.0	547.7	100.0	0.0
500.0	425.0	461.0	100.0	0.0
425.0	355.0	388.4	100.0	0.0
355.0	300.0	326.3	100.0	0.0
300.0	250.0	273.9	99.9	0.1
250.0	212.0	230.2	99.8	0.1
212.0	180.0	195.3	99.6	0.2
180.0	150.0	164.3	99.1	0.5
150.0	125.0	136.9	98.4	0.7
125.0	106.0	115.1	97.1	1.3
106.0	90.00	97.67	84.9	12.2
90.00	75.00	82.16	45.7	39.2
75.00	63.00	68.74	0.0	45.7

Mass Frequency vs Diameter



Summary Report

Full scale pump speed: 3  
Bubble detection: Medium  
Starting Size: 63.00  $\mu\text{m}$   
Ending Size: 0.50  $\mu\text{m}$

Stir time: 30 secs  
Stir speed: Low  
Probe time: 30 secs

Sample: TT-03-08 300 cm  
 Operator: Clint Edrington  
 Submitter: Clint Edrington  
 File Name: C:\EDRING~1\TIGER&~1\SANDFR~1\TT-03-08\03\_300CM.SMP  
 Material/Liquid: silicate mud/water/Water

Reported: 01/03/10 14:38:23  
 Liquid Visc: 0.7225 cp

Sample Density: 2.650 g/cm<sup>3</sup>  
 Liquid Density: 0.9941 g/cm<sup>3</sup>

## Summary Report

Parameter 1	0.000	Parameter 2	0.000	Parameter 3	0.000		
Mass Distribution Arithmetic Statistics							
Mean	79.71	Std. Dev.		16.09			
Median	76.31	Coef. Var.		0.202			
Mode	68.74	Skewness		4.527			
		Kurtosis		36.753			
Selected Percentiles			Selected Sizes				
Percent Finer	Diameter (µm)		Diameter (µm)	Percent Finer			
100.0	714.1		500.0	100.0			
80.0	87.43		250.0	99.9			
60.0	79.53		125.0	98.4			
40.0	73.31		88.00	81.2			
20.0	67.79		63.00	0.0			
Peak Number	% of Dist.*	Mean	Mode	Median	Standard Deviation	Skewness	Kurtosis
1	100.0	79.71	68.74	76.31	16.09	4.527	36.753

\* Peaks must comprise at least 5.00 % of the distribution.



# Micromeritics

WIN5100 V2.03

Page 1

Sample: TT-03-08 333 cm  
Operator: Clint Edrington  
Submitter: Clint Edrington  
File Name: C:\EDRING~1\TIGER&~1\SANDFR~1\TT-03-08\03\_333CM.SMP  
Material/Liquid: silicate mud/water/Water

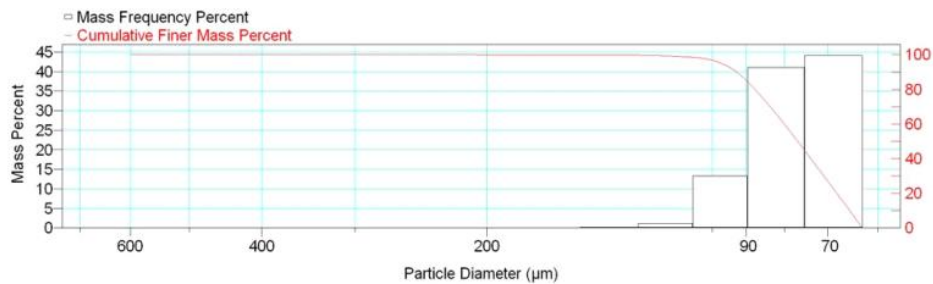
Reported: 01/03/10 14:40:32  
Liquid Visc: 0.7225 cp

Sample Density: 2.650 g/cm<sup>3</sup>  
Liquid Density: 0.9941 g/cm<sup>3</sup>

## Report by Size Class

High Diameter (μm)	Low Diameter (μm)	Average Diameter (μm)	Cumulative Mass Finer (Percent)	Mass Frequency (Percent)
710.0	600.0	652.7	100.0	0.0
600.0	500.0	547.7	100.0	0.0
500.0	425.0	461.0	100.0	0.0
425.0	355.0	388.4	100.0	0.0
355.0	300.0	326.3	100.0	0.0
300.0	250.0	273.9	100.0	0.0
250.0	212.0	230.2	100.0	0.0
212.0	180.0	195.3	99.9	0.1
180.0	150.0	164.3	99.9	0.0
150.0	125.0	136.9	99.7	0.2
125.0	106.0	115.1	98.5	1.2
106.0	90.00	97.67	85.2	13.3
90.00	75.00	82.16	44.1	41.1
75.00	63.00	68.74	0.0	44.1

Mass Frequency vs Diameter



## Summary Report

Full scale pump speed: 3  
Bubble detection: Medium  
Starting Size: 63.00 μm  
Ending Size: 0.50 μm

Stir time: 30 secs  
Stir speed: Low  
Probe time: 30 secs

Sample: TT-03-08 333 cm  
 Operator: Clint Edrington  
 Submitter: Clint Edrington  
 File Name: C:\EDRING~1\TIGER&~1\SANDFR~1\TT-03-08\03\_333CM.SMP  
 Material/Liquid: silicate mud/water/Water

Reported: 01/03/10 14:40:32  
 Liquid Visc: 0.7225 cp

Sample Density: 2.650 g/cm<sup>3</sup>  
 Liquid Density: 0.9941 g/cm<sup>3</sup>

## Summary Report

Parameter 1 0.000

Parameter 2 0.000

Parameter 3 0.000

## Mass Distribution Arithmetic Statistics

Mean	78.92	Std. Dev.	11.52
Median	76.81	Coef. Var.	0.146
Mode	68.74	Skewness	1.936
		Kurtosis	11.073

## Selected Percentiles

Percent Finer	Diameter (µm)
100.0	600.3
80.0	87.62
60.0	80.05
40.0	73.77
20.0	68.07

## Selected Sizes

Diameter (µm)	Percent Finer
500.0	100.0
250.0	100.0
125.0	99.7
88.00	80.9
63.00	0.0

Peak Number	% of Dist. *	Mean	Mode	Median	Standard Deviation	Skewness	Kurtosis
1	99.9	78.81	68.74	76.80	10.92	1.095	1.575

\* Peaks must comprise at least 5.00 % of the distribution.

# Micromeritics

WIN5100 V2.03

Page 1

Sample: TT-04-08 3 cm  
Operator: Clint Edrington  
Submitter: Clint Edrington  
File Name: C:\EDRING~1\TIGER&~1\SANDFR~1\TT-04-08\04\_3CM.SMP  
Material/Liquid: silicate mud/water/Water

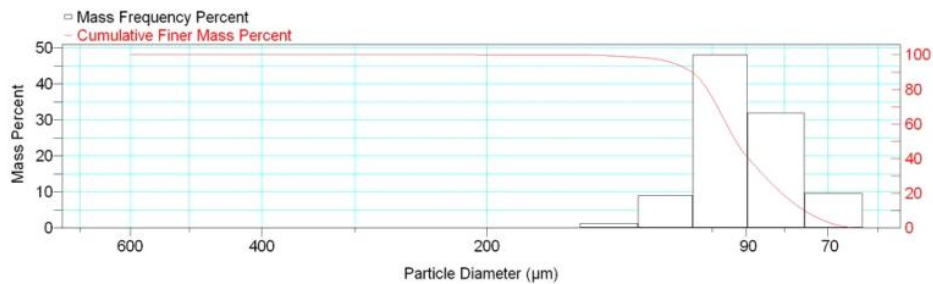
Reported: 01/03/10 14:51:54  
Liquid Visc: 0.7225 cp

Sample Density: 2.650 g/cm<sup>3</sup>  
Liquid Density: 0.9941 g/cm<sup>3</sup>

## Report by Size Class

High Diameter (μm)	Low Diameter (μm)	Average Diameter (μm)	Cumulative Mass Finer (Percent)	Mass Frequency (Percent)
710.0	600.0	652.7	100.0	0.0
600.0	500.0	547.7	100.0	0.0
500.0	425.0	461.0	100.0	0.0
425.0	355.0	388.4	100.0	0.0
355.0	300.0	326.3	100.0	0.0
300.0	250.0	273.9	100.0	0.0
250.0	212.0	230.2	100.0	0.0
212.0	180.0	195.3	99.9	0.1
180.0	150.0	164.3	99.8	0.1
150.0	125.0	136.9	98.5	1.3
125.0	106.0	115.1	89.5	9.0
106.0	90.00	97.67	41.5	48.0
90.00	75.00	82.16	9.6	31.9
75.00	63.00	68.74	0.0	9.6

Mass Frequency vs Diameter



## Summary Report

Full scale pump speed: 3  
Bubble detection: Medium  
Starting Size: 63.00 μm  
Ending Size: 0.50 μm

Stir time: 30 secs  
Stir speed: Low  
Probe time: 30 secs

Sample: TT-04-08 3 cm  
 Operator: Clint Edrington  
 Submitter: Clint Edrington  
 File Name: C:\EDRING~1\TIGER&~1\SANDFR~1\TT-04-08\04\_3CM.SMP  
 Material/Liquid: silicate mud/water/Water

Reported: 01/03/10 14:51:54  
 Liquid Visc: 0.7225 cp

Sample Density: 2.650 g/cm<sup>3</sup>  
 Liquid Density: 0.9941 g/cm<sup>3</sup>

## Summary Report

Parameter 1 0.000

Parameter 2 0.000

Parameter 3 0.000

## Mass Distribution Arithmetic Statistics

Mean	92.19	Std. Dev.	13.73
Median	92.89	Coef. Var.	0.149
Mode	97.67	Skewness	0.866
		Kurtosis	4.036

## Selected Percentiles

Percent Finer	Diameter (µm)
100.0	600.3
80.0	101.5
60.0	95.68
40.0	89.37
20.0	80.62

## Selected Sizes

Diameter (µm)	Percent Finer
500.0	100.0
250.0	100.0
125.0	98.5
88.00	36.7
63.00	0.0

Peak Number	% of Dist. *	Mean	Mode	Median	Standard Deviation	Skewness	Kurtosis
1	99.9	92.09	97.67	92.88	13.34	0.505	1.334

\* Peaks must comprise at least 5.00 % of the distribution.

# Micromeritics

WIN5100 V2.03

Page 1

Sample: TT-04-08 50 cm  
Operator: Clint Edrington  
Submitter: Clint Edrington  
File Name: C:\EDRING~1\TIGER&~1\SANDFR~1\TT-04-08\04\_50CM.SMP  
Material/Liquid: silicate mud/water/Water

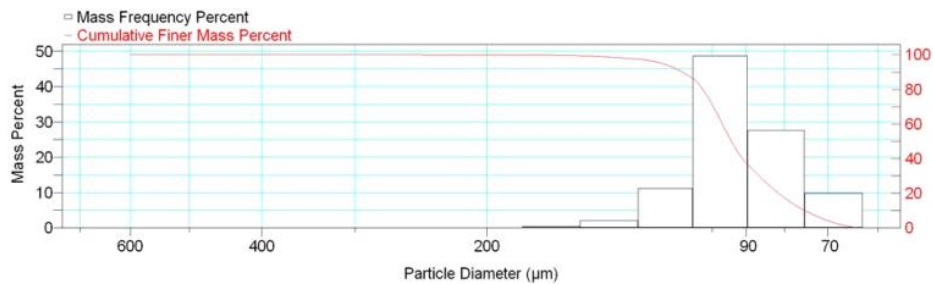
Reported: 01/03/10 14:55:33  
Liquid Visc: 0.7225 cp

Sample Density: 2.650 g/cm<sup>3</sup>  
Liquid Density: 0.9941 g/cm<sup>3</sup>

## Report by Size Class

High Diameter (μm)	Low Diameter (μm)	Average Diameter (μm)	Cumulative Mass Finer (Percent)	Mass Frequency (Percent)
710.0	600.0	652.7	100.0	0.0
600.0	500.0	547.7	100.0	0.0
500.0	425.0	461.0	100.0	0.0
425.0	355.0	388.4	100.0	0.0
355.0	300.0	326.3	100.0	0.0
300.0	250.0	273.9	100.0	0.0
250.0	212.0	230.2	99.9	0.1
212.0	180.0	195.3	99.9	0.0
180.0	150.0	164.3	99.4	0.5
150.0	125.0	136.9	97.3	2.1
125.0	106.0	115.1	86.1	11.2
106.0	90.00	97.67	37.4	48.7
90.00	75.00	82.16	9.8	27.6
75.00	63.00	68.74	0.0	9.8

Mass Frequency vs Diameter



## Summary Report

Full scale pump speed: 3  
Bubble detection: Medium  
Starting Size: 63.00 μm  
Ending Size: 0.50 μm

Stir time: 30 secs  
Stir speed: Low  
Probe time: 30 secs

Sample: TT-04-08 50 cm  
 Operator: Clint Edrington  
 Submitter: Clint Edrington  
 File Name: C:\EDRING~1\TIGER&~1\SANDFR~1\TT-04-08\04\_50CM.SMP  
 Material/Liquid: silicate mud/water/Water

Reported: 01/03/10 14:55:33  
 Liquid Visc: 0.7225 cp

Sample Density: 2.650 g/cm<sup>3</sup>  
 Liquid Density: 0.9941 g/cm<sup>3</sup>

## Summary Report

Parameter 1 0.000

Parameter 2 0.000

Parameter 3 0.000

## Mass Distribution Arithmetic Statistics

Mean	93.80	Std. Dev.	15.48
Median	94.19	Coef. Var.	0.165
Mode	97.67	Skewness	1.378
		Kurtosis	7.614

## Selected Percentiles

Percent Finer	Diameter (µm)
100.0	651.9
80.0	102.9
60.0	96.87
40.0	91.07
20.0	81.46

## Selected Sizes

Diameter (µm)	Percent Finer
500.0	100.0
250.0	100.0
125.0	97.3
88.00	33.1
63.00	0.0

Peak Number	% of Dist. *	Mean	Mode	Median	Standard Deviation	Skewness	Kurtosis
1	99.9	93.66	97.67	94.17	14.87	0.810	2.413

\* Peaks must comprise at least 5.00 % of the distribution.

Micromeritics

WIN5100 V2.03

Page 1

Sample: TT-05-08 20 cm  
Operator: Clint Edrington  
Submitter: Clint Edrington  
File Name: C:\EDRING~1\TIGER&~1\SANDFR~1\TT-05-08\05\_20CM.SMP  
Material/Liquid: silicate mud/water/Water

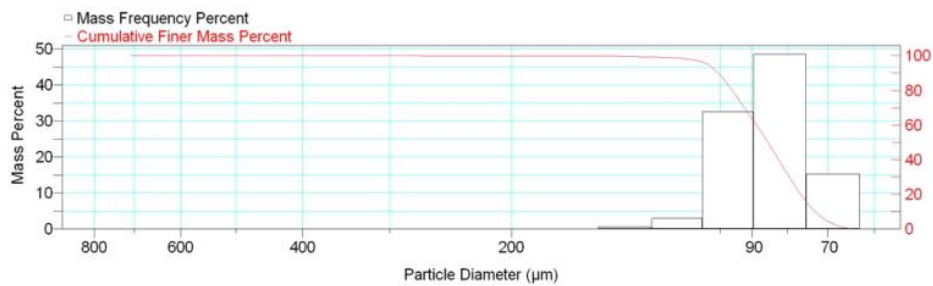
Reported: 01/03/10 14:59:04  
Liquid Visc: 0.7225 cp

Sample Density: 2.650 g/cm<sup>3</sup>  
Liquid Density: 0.9941 g/cm<sup>3</sup>

Report by Size Class

High Diameter ( $\mu\text{m}$ )	Low Diameter ( $\mu\text{m}$ )	Average Diameter ( $\mu\text{m}$ )	Cumulative Mass Finer (Percent)	Mass Frequency (Percent)
850.0	710.0	776.9	100.0	0.0
710.0	600.0	652.7	100.0	0.0
600.0	500.0	547.7	100.0	0.0
500.0	425.0	461.0	100.0	0.0
425.0	355.0	388.4	100.0	0.0
355.0	300.0	326.3	100.0	0.0
300.0	250.0	273.9	99.9	0.1
250.0	212.0	230.2	99.9	0.0
212.0	180.0	195.3	99.9	0.0
180.0	150.0	164.3	99.8	0.1
150.0	125.0	136.9	99.2	0.6
125.0	106.0	115.1	96.3	2.9
106.0	90.00	97.67	63.7	32.6
90.00	75.00	82.16	15.2	48.5
75.00	63.00	68.74	0.0	15.2

Mass Frequency vs Diameter



Summary Report

Full scale pump speed: 3  
Bubble detection: Medium  
Starting Size: 63.00  $\mu\text{m}$   
Ending Size: 0.50  $\mu\text{m}$

Stir time: 30 secs  
Stir speed: Low  
Probe time: 30 secs

Sample: TT-05-08 20 cm  
 Operator: Clint Edrington  
 Submitter: Clint Edrington  
 File Name: C:\EDRING~1\TIGER&~1\SANDFR~1\TT-05-08\05\_20CM.SMP  
 Material/Liquid: silicate mud/water/Water

Reported: 01/03/10 14:59:04  
 Liquid Visc: 0.7225 cp

Sample Density: 2.650 g/cm<sup>3</sup>  
 Liquid Density: 0.9941 g/cm<sup>3</sup>

## Summary Report

Parameter 1	0.000	Parameter 2	0.000	Parameter 3	0.000		
Mass Distribution Arithmetic Statistics							
Mean	86.73	Std. Dev.		13.34			
Median	85.37	Coef. Var.		0.154			
Mode	82.16	Skewness		3.345			
		Kurtosis		39.349			
Selected Percentiles			Selected Sizes				
Percent Finer	Diameter (µm)		Diameter (µm)	Percent Finer			
100.0	714.1		500.0	100.0			
80.0	96.13		250.0	99.9			
60.0	88.63		125.0	99.2			
40.0	82.42		88.00	58.2			
20.0	76.57		63.00	0.0			
Peak Number	% of Dist.*	Mean	Mode	Median	Standard Deviation	Skewness	Kurtosis
1	99.9	86.55	82.16	85.35	11.96	0.857	2.631

\* Peaks must comprise at least 5.00 % of the distribution.



# Micromeritics

WIN5100 V2.03

Page 1

Sample: TT-05-08 76 cm  
Operator: Clint Edrington  
Submitter: Clint Edrington  
File Name: C:\EDRING~1\TIGER&~1\SANDFR~1\TT-05-08\05\_76CM.SMP  
Material/Liquid: silicate mud/water/Water

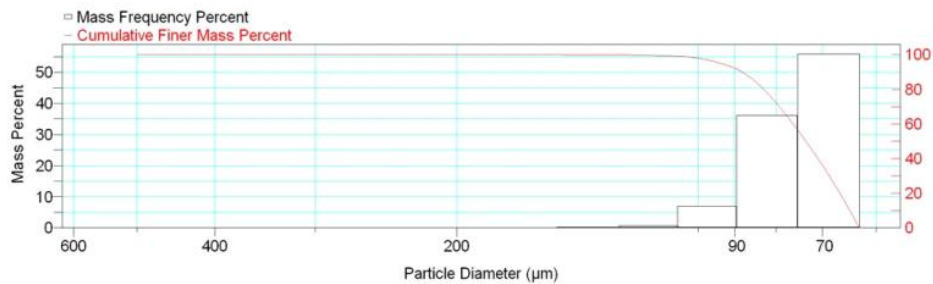
Reported: 01/03/10 15:01:41  
Liquid Visc: 0.7225 cp

Sample Density: 2.650 g/cm<sup>3</sup>  
Liquid Density: 0.9941 g/cm<sup>3</sup>

## Report by Size Class

High Diameter (μm)	Low Diameter (μm)	Average Diameter (μm)	Cumulative Mass Finer (Percent)	Mass Frequency (Percent)
600.0	500.0	547.7	100.0	0.0
500.0	425.0	461.0	100.0	0.0
425.0	355.0	388.4	100.0	0.0
355.0	300.0	326.3	100.0	0.0
300.0	250.0	273.9	100.0	0.0
250.0	212.0	230.2	100.0	0.0
212.0	180.0	195.3	100.0	0.0
180.0	150.0	164.3	100.0	0.0
150.0	125.0	136.9	99.8	0.2
125.0	106.0	115.1	99.1	0.7
106.0	90.00	97.67	92.1	7.0
90.00	75.00	82.16	55.9	36.2
75.00	63.00	68.74	0.0	55.9

Mass Frequency vs Diameter



## Summary Report

Full scale pump speed: 3  
Bubble detection: Medium  
Starting Size: 63.00 μm  
Ending Size: 0.50 μm

Stir time: 30 secs  
Stir speed: Low  
Probe time: 30 secs

Parameter 1 0.000

Parameter 2 0.000

Parameter 3 0.000

Sample: TT-05-08 76 cm  
 Operator: Clint Edrington  
 Submitter: Clint Edrington  
 File Name: C:\EDRING~1\TIGER&~1\SANDFR~1\TT-05-08\05\_76CM.SMP  
 Material/Liquid: silicate mud/water/Water

Reported: 01/03/10 15:01:41  
 Liquid Visc: 0.7225 cp

Sample Density: 2.650 g/cm<sup>3</sup>  
 Liquid Density: 0.9941 g/cm<sup>3</sup>

## Summary Report

Mass Distribution Arithmetic Statistics			
Mean	76.08	Std. Dev.	9.706
Median	73.40	Coef. Var.	0.128
Mode	68.74	Skewness	1.565
		Kurtosis	3.871

Selected Percentiles		Selected Sizes	
Percent Finer	Diameter (µm)	Diameter (µm)	Percent Finer
100.0	505.0	500.0	100.0
80.0	82.85	250.0	100.0
60.0	76.17	125.0	99.8
40.0	70.90	88.00	89.8
20.0	66.59	63.00	0.0

Peak Number	% of Dist.*	Mean	Mode	Median	Standard Deviation	Skewness	Kurtosis
1	100.0	76.08	68.74	73.40	9.706	1.565	3.871

\* Peaks must comprise at least 5.00 % of the distribution.

# Micromeritics

WIN5100 V2.03

Page 1

Sample: TT-05-08 125 cm  
Operator: Clint Edrington  
Submitter: Clint Edrington  
File Name: C:\EDRING~1\TIGER&~1\SANDFR~1\TT-05-08\05\_125CM.SMP  
Material/Liquid: silicate mud/water/Water

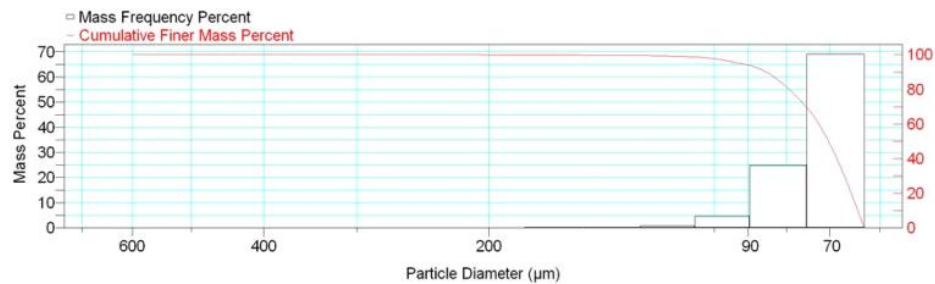
Reported: 01/03/10 15:04:11  
Liquid Visc: 0.7225 cp

Sample Density: 2.650 g/cm<sup>3</sup>  
Liquid Density: 0.9941 g/cm<sup>3</sup>

## Report by Size Class

High Diameter (µm)	Low Diameter (µm)	Average Diameter (µm)	Cumulative Mass Finer (Percent)	Mass Frequency (Percent)
710.0	600.0	652.7	100.0	0.0
600.0	500.0	547.7	100.0	0.0
500.0	425.0	461.0	100.0	0.0
425.0	355.0	388.4	100.0	0.0
355.0	300.0	326.3	100.0	0.0
300.0	250.0	273.9	100.0	0.0
250.0	212.0	230.2	100.0	0.0
212.0	180.0	195.3	99.9	0.1
180.0	150.0	164.3	99.7	0.2
150.0	125.0	136.9	99.5	0.2
125.0	106.0	115.1	98.7	0.8
106.0	90.00	97.67	94.0	4.7
90.00	75.00	82.16	69.1	24.9
75.00	63.00	68.74	0.0	69.1

Mass Frequency vs Diameter



## Summary Report

Full scale pump speed: 3  
Bubble detection: Medium  
Starting Size: 63.00 µm  
Ending Size: 0.50 µm

Stir time: 30 secs  
Stir speed: Low  
Probe time: 30 secs

Sample: TT-05-08 125 cm  
 Operator: Clint Edrington  
 Submitter: Clint Edrington  
 File Name: C:\EDRING~1\TIGER&~1\SANDFR~1\TT-05-08\05\_125CM.SMP  
 Material/Liquid: silicate mud/water/Water

Reported: 01/03/10 15:04:11  
 Liquid Visc: 0.7225 cp

Sample Density: 2.650 g/cm<sup>3</sup>  
 Liquid Density: 0.9941 g/cm<sup>3</sup>

## Summary Report

Parameter 1 0.000

Parameter 2 0.000

Parameter 3 0.000

## Mass Distribution Arithmetic Statistics

Mean	74.27	Std. Dev.	10.70
Median	70.28	Coef. Var.	0.144
Mode	68.74	Skewness	3.987
		Kurtosis	28.704

## Selected Percentiles

Percent Finer	Diameter (µm)
100.0	600.3
80.0	79.33
60.0	72.41
40.0	68.51
20.0	65.54

## Selected Sizes

Diameter (µm)	Percent Finer
500.0	100.0
250.0	100.0
125.0	99.5
88.00	92.8
63.00	0.0

Peak Number	% of Dist. *	Mean	Mode	Median	Standard Deviation	Skewness	Kurtosis
1	99.7	73.96	68.74	70.25	9.150	2.254	7.138

\* Peaks must comprise at least 5.00 % of the distribution.

Micromeritics

WIN5100 V2.03

Page 1

Sample: TT-05-08 165 cm  
Operator: Clint Edrington  
Submitter: Clint Edrington  
File Name: C:\EDRING~1\TIGER&~1\SANDFR~1\TT-05-08\05\_165CM.SMP  
Material/Liquid: silicate mud/water/Water

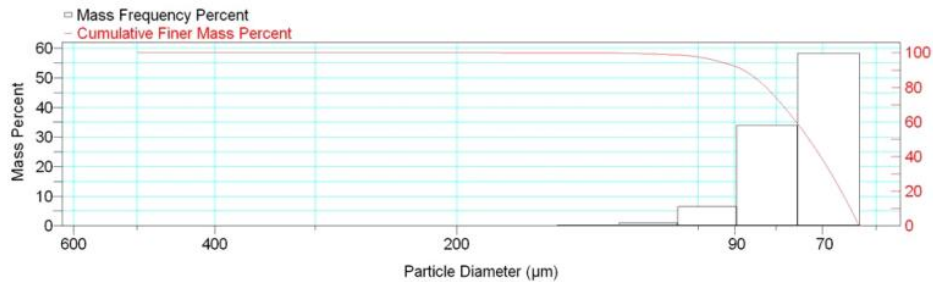
Reported: 01/03/10 15:06:37  
Liquid Visc: 0.7225 cp

Sample Density: 2.650 g/cm<sup>3</sup>  
Liquid Density: 0.9941 g/cm<sup>3</sup>

Report by Size Class

High Diameter ( $\mu\text{m}$ )	Low Diameter ( $\mu\text{m}$ )	Average Diameter ( $\mu\text{m}$ )	Cumulative Mass Finer (Percent)	Mass Frequency (Percent)
600.0	500.0	547.7	100.0	0.0
500.0	425.0	461.0	100.0	0.0
425.0	355.0	388.4	100.0	0.0
355.0	300.0	326.3	100.0	0.0
300.0	250.0	273.9	100.0	0.0
250.0	212.0	230.2	100.0	0.0
212.0	180.0	195.3	100.0	0.0
180.0	150.0	164.3	99.9	0.1
150.0	125.0	136.9	99.7	0.2
125.0	106.0	115.1	98.7	1.0
106.0	90.00	97.67	92.2	6.5
90.00	75.00	82.16	58.3	33.9
75.00	63.00	68.74	0.0	58.3

Mass Frequency vs Diameter



Summary Report

Full scale pump speed: 3  
Bubble detection: Medium  
Starting Size: 63.00  $\mu\text{m}$   
Ending Size: 0.50  $\mu\text{m}$

Stir time: 30 secs  
Stir speed: Low  
Probe time: 30 secs

Parameter 1 0.000

Parameter 2 0.000

Parameter 3 0.000

Sample: TT-05-08 165 cm  
 Operator: Clint Edrington  
 Submitter: Clint Edrington  
 File Name: C:\EDRING~1\TIGER&~1\SANDFR~1\TT-05-08\05\_165CM.SMP  
 Material/Liquid: silicate mud/water/Water

Reported: 01/03/10 15:06:37  
 Liquid Visc: 0.7225 cp

Sample Density: 2.650 g/cm<sup>3</sup>  
 Liquid Density: 0.9941 g/cm<sup>3</sup>

## Summary Report

## Mass Distribution Arithmetic Statistics

Mean	75.86	Std. Dev.	10.23
Median	72.75	Coef. Var.	0.135
Mode	68.74	Skewness	2.149
		Kurtosis	8.828

## Selected Percentiles

Percent Finer	Diameter (µm)
100.0	553.2
80.0	82.31
60.0	75.49
40.0	70.37
20.0	66.34

## Selected Sizes

Diameter (µm)	Percent Finer
500.0	100.0
250.0	100.0
125.0	99.7
88.00	90.3
63.00	0.0

Peak Number	% of Dist.*	Mean	Mode	Median	Standard Deviation	Skewness	Kurtosis
1	100.0	75.86	68.74	72.75	10.23	2.149	8.828

\* Peaks must comprise at least 5.00 % of the distribution.

Micromeritics

WIN5100 V2.03

Page 1

Sample: TT-06-08 10 cm  
Operator: Clint Edrington  
Submitter: Clint Edrington  
File Name: C:\EDRING~1\TIGER&~1\SANDFR~1\TT-06-08\06\_10CM.SMP  
Material/Liquid: silicate mud/water/Water

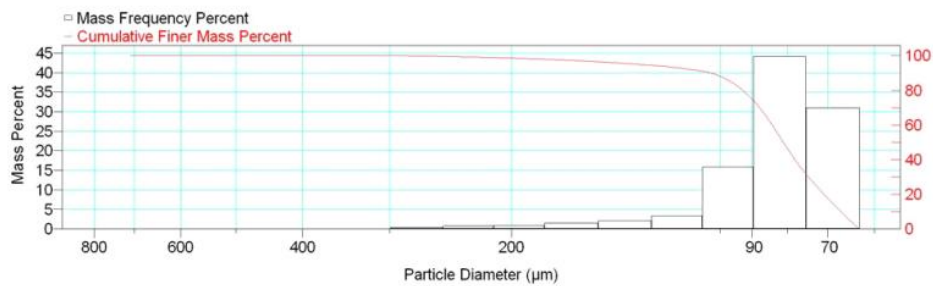
Reported: 01/03/10 15:11:00  
Liquid Visc: 0.7225 cp

Sample Density: 2.650 g/cm<sup>3</sup>  
Liquid Density: 0.9941 g/cm<sup>3</sup>

Report by Size Class

High Diameter ( $\mu\text{m}$ )	Low Diameter ( $\mu\text{m}$ )	Average Diameter ( $\mu\text{m}$ )	Cumulative Mass Finer (Percent)	Mass Frequency (Percent)
850.0	710.0	776.9	100.0	0.0
710.0	600.0	652.7	100.0	0.0
600.0	500.0	547.7	100.0	0.0
500.0	425.0	461.0	100.0	0.0
425.0	355.0	388.4	100.0	0.0
355.0	300.0	326.3	100.0	0.0
300.0	250.0	273.9	99.6	0.4
250.0	212.0	230.2	98.9	0.7
212.0	180.0	195.3	98.0	0.9
180.0	150.0	164.3	96.5	1.5
150.0	125.0	136.9	94.4	2.1
125.0	106.0	115.1	91.0	3.4
106.0	90.00	97.67	75.1	15.9
90.00	75.00	82.16	31.0	44.1
75.00	63.00	68.74	0.0	31.0

Mass Frequency vs Diameter



Summary Report

Full scale pump speed: 3  
Bubble detection: Medium  
Starting Size: 63.00  $\mu\text{m}$   
Ending Size: 0.50  $\mu\text{m}$

Stir time: 30 secs  
Stir speed: Low  
Probe time: 30 secs

Sample: TT-06-08 10 cm  
 Operator: Clint Edrington  
 Submitter: Clint Edrington  
 File Name: C:\EDRING~1\TIGER&~1\SANDFR~1\TT-06-08\06\_10CM.SMP  
 Material/Liquid: silicate mud/water/Water

Reported: 01/03/10 15:11:00  
 Liquid Visc: 0.7225 cp

Sample Density: 2.650 g/cm<sup>3</sup>  
 Liquid Density: 0.9941 g/cm<sup>3</sup>

## Summary Report

Parameter 1	0.000	Parameter 2	0.000	Parameter 3	0.000		
Mass Distribution Arithmetic Statistics							
Mean	86.79	Std. Dev.		26.26			
Median	81.09	Coef. Var.		0.303			
Mode	82.16	Skewness		3.706			
		Kurtosis		17.700			
Selected Percentiles			Selected Sizes				
Percent Finer	Diameter (µm)		Diameter (µm)	Percent Finer			
100.0	714.1		500.0	100.0			
80.0	92.80		250.0	99.6			
60.0	84.18		125.0	94.4			
40.0	78.05		88.00	70.7			
20.0	70.86		63.00	0.0			
Peak Number	% of Dist.*	Mean	Mode	Median	Standard Deviation	Skewness	Kurtosis
1	100.0	86.79	82.16	81.09	26.26	3.706	17.700

\* Peaks must comprise at least 5.00 % of the distribution.



# Micromeritics

WIN5100 V2.03

Page 1

Sample: TT-06-08 50 cm  
Operator: Clint Edrington  
Submitter: Clint Edrington  
File Name: C:\EDRING~1\TIGER&~1\SANDFR~1\TT-06-08\06\_50CM.SMP  
Material/Liquid: silicate mud/water/Water

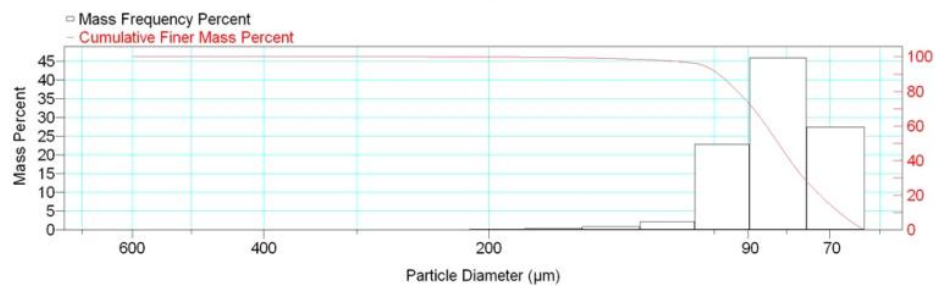
Reported: 01/03/10 15:13:36  
Liquid Visc: 0.7225 cp

Sample Density: 2.650 g/cm<sup>3</sup>  
Liquid Density: 0.9941 g/cm<sup>3</sup>

## Report by Size Class

High Diameter (μm)	Low Diameter (μm)	Average Diameter (μm)	Cumulative Mass Finer (Percent)	Mass Frequency (Percent)
710.0	600.0	652.7	100.0	0.0
600.0	500.0	547.7	100.0	0.0
500.0	425.0	461.0	100.0	0.0
425.0	355.0	388.4	100.0	0.0
355.0	300.0	326.3	100.0	0.0
300.0	250.0	273.9	100.0	0.0
250.0	212.0	230.2	99.9	0.1
212.0	180.0	195.3	99.7	0.2
180.0	150.0	164.3	99.3	0.4
150.0	125.0	136.9	98.4	0.9
125.0	106.0	115.1	96.2	2.2
106.0	90.00	97.67	73.4	22.8
90.00	75.00	82.16	27.5	45.9
75.00	63.00	68.74	0.0	27.5

Mass Frequency vs Diameter



## Summary Report

Full scale pump speed: 3  
Bubble detection: Medium  
Starting Size: 63.00 μm  
Ending Size: 0.50 μm

Stir time: 30 secs  
Stir speed: Low  
Probe time: 30 secs

Sample: TT-06-08 50 cm  
 Operator: Clint Edrington  
 Submitter: Clint Edrington  
 File Name: C:\EDRING~1\TIGER&~1\SANDFR~1\TT-06-08\06\_50CM.SMP  
 Material/Liquid: silicate mud/water/Water

Reported: 01/03/10 15:13:36  
 Liquid Visc: 0.7225 cp

Sample Density: 2.650 g/cm<sup>3</sup>  
 Liquid Density: 0.9941 g/cm<sup>3</sup>

## Summary Report

Parameter 1 0.000

Parameter 2 0.000

Parameter 3 0.000

## Mass Distribution Arithmetic Statistics

Mean	83.93	Std. Dev.	15.06
Median	82.05	Coef. Var.	0.179
Mode	82.16	Skewness	2.815
		Kurtosis	17.389

## Selected Percentiles

Percent Finer	Diameter (µm)
100.0	651.9
80.0	93.03
60.0	85.10
40.0	79.08
20.0	72.12

## Selected Sizes

Diameter (µm)	Percent Finer
500.0	100.0
250.0	100.0
125.0	98.4
88.00	68.4
63.00	0.0

Peak Number	% of Dist. *	Mean	Mode	Median	Standard Deviation	Skewness	Kurtosis
1	100.0	83.93	82.16	82.05	15.06	2.815	17.389

\* Peaks must comprise at least 5.00 % of the distribution.

# Micromeritics

WIN5100 V2.03

Page 1

Sample: TT-06-08 80 cm  
Operator: Clint Edrington  
Submitter: Clint Edrington  
File Name: C:\EDRING~1\TIGER&~1\SANDFR~1\TT-06-08\06\_80CM.SMP  
Material/Liquid: silicate mud/water/Water

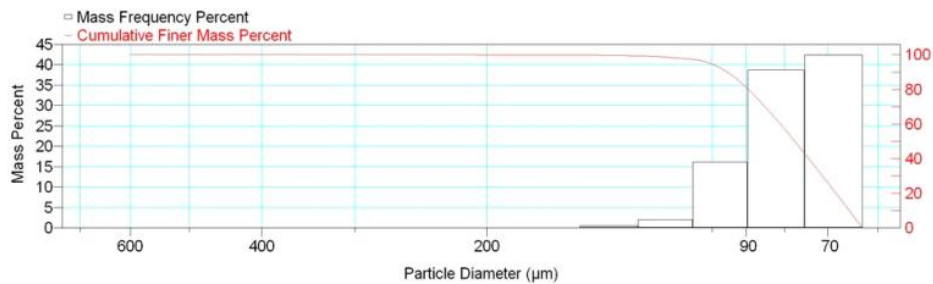
Reported: 01/03/10 15:16:11  
Liquid Visc: 0.7225 cp

Sample Density: 2.650 g/cm<sup>3</sup>  
Liquid Density: 0.9941 g/cm<sup>3</sup>

## Report by Size Class

High Diameter (µm)	Low Diameter (µm)	Average Diameter (µm)	Cumulative Mass Finer (Percent)	Mass Frequency (Percent)
710.0	600.0	652.7	100.0	0.0
600.0	500.0	547.7	100.0	0.0
500.0	425.0	461.0	100.0	0.0
425.0	355.0	388.4	100.0	0.0
355.0	300.0	326.3	100.0	0.0
300.0	250.0	273.9	100.0	0.0
250.0	212.0	230.2	100.0	0.0
212.0	180.0	195.3	99.9	0.1
180.0	150.0	164.3	99.8	0.1
150.0	125.0	136.9	99.3	0.5
125.0	106.0	115.1	97.3	2.0
106.0	90.00	97.67	81.1	16.2
90.00	75.00	82.16	42.4	38.7
75.00	63.00	68.74	0.0	42.4

Mass Frequency vs Diameter



## Summary Report

Full scale pump speed: 3  
Bubble detection: Medium  
Starting Size: 63.00 µm  
Ending Size: 0.50 µm

Stir time: 30 secs  
Stir speed: Low  
Probe time: 30 secs

Sample: TT-06-08 80 cm  
 Operator: Clint Edrington  
 Submitter: Clint Edrington  
 File Name: C:\EDRING~1\TIGER&~1\SANDFR~1\TT-06-08\06\_80CM.SMP  
 Material/Liquid: silicate mud/water/Water

Reported: 01/03/10 15:16:11  
 Liquid Visc: 0.7225 cp

Sample Density: 2.650 g/cm<sup>3</sup>  
 Liquid Density: 0.9941 g/cm<sup>3</sup>

## Summary Report

Parameter 1 0.000

Parameter 2 0.000

Parameter 3 0.000

## Mass Distribution Arithmetic Statistics

Mean	80.11	Std. Dev.	12.94
Median	77.49	Coef. Var.	0.162
Mode	68.74	Skewness	1.920
		Kurtosis	8.817

## Selected Percentiles

Percent Finer	Diameter (µm)
100.0	600.3
80.0	89.46
60.0	81.03
40.0	74.24
20.0	68.26

## Selected Sizes

Diameter (µm)	Percent Finer
500.0	100.0
250.0	100.0
125.0	99.3
88.00	76.9
63.00	0.0

Peak Number	% of Dist. *	Mean	Mode	Median	Standard Deviation	Skewness	Kurtosis
1	99.9	79.99	68.74	77.47	12.42	1.401	3.565

\* Peaks must comprise at least 5.00 % of the distribution.

Micromeritics

WIN5100 V2.03

Page 1

Sample: TT-06-08 150 cm  
Operator: Clint Edrington  
Submitter: Clint Edrington  
File Name: C:\EDRING~1\TIGER&~1\SANDFR~1\TT-06-08\06\_150CM.SMP  
Material/Liquid: silicate mud/water/Water

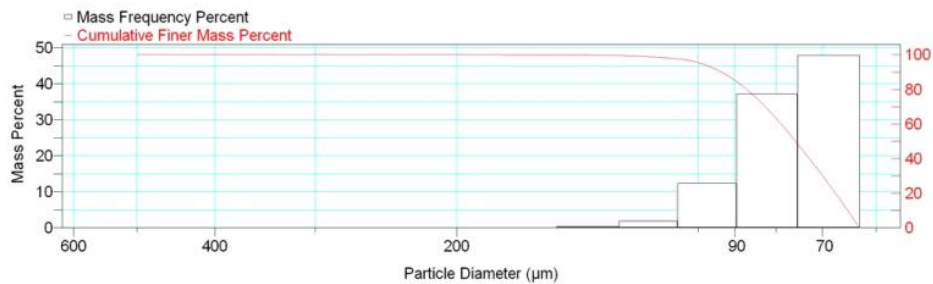
Reported: 01/03/10 15:18:40  
Liquid Visc: 0.7225 cp

Sample Density: 2.650 g/cm<sup>3</sup>  
Liquid Density: 0.9941 g/cm<sup>3</sup>

Report by Size Class

High Diameter ( $\mu\text{m}$ )	Low Diameter ( $\mu\text{m}$ )	Average Diameter ( $\mu\text{m}$ )	Cumulative Mass Finer (Percent)	Mass Frequency (Percent)
600.0	500.0	547.7	100.0	0.0
500.0	425.0	461.0	100.0	0.0
425.0	355.0	388.4	100.0	0.0
355.0	300.0	326.3	100.0	0.0
300.0	250.0	273.9	100.0	0.0
250.0	212.0	230.2	100.0	0.0
212.0	180.0	195.3	100.0	0.0
180.0	150.0	164.3	99.9	0.1
150.0	125.0	136.9	99.5	0.4
125.0	106.0	115.1	97.6	1.9
106.0	90.00	97.67	85.2	12.4
90.00	75.00	82.16	47.9	37.3
75.00	63.00	68.74	0.0	47.9

Mass Frequency vs Diameter



Summary Report

Full scale pump speed: 3  
Bubble detection: Medium  
Starting Size: 63.00  $\mu\text{m}$   
Ending Size: 0.50  $\mu\text{m}$

Stir time: 30 secs  
Stir speed: Low  
Probe time: 30 secs

Parameter 1 0.000

Parameter 2 0.000

Parameter 3 0.000

Sample: TT-06-08 150 cm  
 Operator: Clint Edrington  
 Submitter: Clint Edrington  
 File Name: C:\EDRING~1\TIGER&~1\SANDFR~1\TT-06-08\06\_150CM.SMP  
 Material/Liquid: silicate mud/water/Water

Reported: 01/03/10 15:18:40      Sample Density: 2.650 g/cm<sup>3</sup>  
 Liquid Visc: 0.7225 cp      Liquid Density: 0.9941 g/cm<sup>3</sup>

## Summary Report

Mass Distribution Arithmetic Statistics			
Mean	78.58	Std. Dev.	11.95
Median	75.64	Coef. Var.	0.152
Mode	68.74	Skewness	1.627
		Kurtosis	4.625

Selected Percentiles		Selected Sizes	
Percent Finer	Diameter (µm)	Diameter (µm)	Percent Finer
100.0	553.2	500.0	100.0
80.0	87.00	250.0	100.0
60.0	78.85	125.0	99.5
40.0	72.69	88.00	81.9
20.0	67.44	63.00	0.0

Peak Number	% of Dist.*	Mean	Mode	Median	Standard Deviation	Skewness	Kurtosis
1	100.0	78.58	68.74	75.64	11.95	1.627	4.625

\* Peaks must comprise at least 5.00 % of the distribution.

# Micromeritics

WIN5100 V2.03

Page 1

Sample: TT-06-08 200 cm  
Operator: Clint Edrington  
Submitter: Clint Edrington  
File Name: C:\EDRING~1\TIGER&~1\SANDFR~1\TT-06-08\06\_200CM.SMP  
Material/Liquid: silicate mud/water/Water

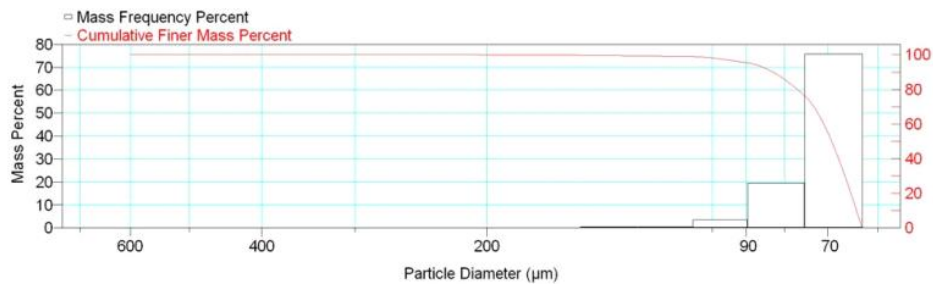
Reported: 01/03/10 15:21:33  
Liquid Visc: 0.7225 cp

Sample Density: 2.650 g/cm<sup>3</sup>  
Liquid Density: 0.9941 g/cm<sup>3</sup>

## Report by Size Class

High Diameter (µm)	Low Diameter (µm)	Average Diameter (µm)	Cumulative Mass Finer (Percent)	Mass Frequency (Percent)
710.0	600.0	652.7	100.0	0.0
600.0	500.0	547.7	100.0	0.0
500.0	425.0	461.0	100.0	0.0
425.0	355.0	388.4	100.0	0.0
355.0	300.0	326.3	100.0	0.0
300.0	250.0	273.9	100.0	0.0
250.0	212.0	230.2	100.0	0.0
212.0	180.0	195.3	99.9	0.1
180.0	150.0	164.3	99.7	0.2
150.0	125.0	136.9	99.3	0.4
125.0	106.0	115.1	98.9	0.4
106.0	90.00	97.67	95.4	3.5
90.00	75.00	82.16	75.8	19.6
75.00	63.00	68.74	0.0	75.8

Mass Frequency vs Diameter



## Summary Report

Full scale pump speed: 3  
Bubble detection: Medium  
Starting Size: 63.00 µm  
Ending Size: 0.50 µm

Stir time: 30 secs  
Stir speed: Low  
Probe time: 30 secs

Sample: TT-06-08 200 cm  
 Operator: Clint Edrington  
 Submitter: Clint Edrington  
 File Name: C:\EDRING~1\TIGER&~1\SANDFR~1\TT-06-08\06\_200CM.SMP  
 Material/Liquid: silicate mud/water/Water

Reported: 01/03/10 15:21:33  
 Liquid Visc: 0.7225 cp

Sample Density: 2.650 g/cm<sup>3</sup>  
 Liquid Density: 0.9941 g/cm<sup>3</sup>

## Summary Report

Parameter 1 0.000

Parameter 2 0.000

Parameter 3 0.000

## Mass Distribution Arithmetic Statistics

Mean	73.16	Std. Dev.	10.32
Median	69.18	Coef. Var.	0.141
Mode	68.74	Skewness	4.786
		Kurtosis	36.954

## Selected Percentiles

Percent Finer	Diameter (µm)
100.0	600.3
80.0	76.90
60.0	70.89
40.0	67.72
20.0	65.21

## Selected Sizes

Diameter (µm)	Percent Finer
500.0	100.0
250.0	100.0
125.0	99.3
88.00	94.6
63.00	0.0

Peak Number	% of Dist. *	Mean	Mode	Median	Standard Deviation	Skewness	Kurtosis
1	100.0	73.16	68.74	69.18	10.32	4.786	36.954

\* Peaks must comprise at least 5.00 % of the distribution.



# Micromeritics

WIN5100 V2.03

Page 1

Sample: TT-06-08 300 cm  
Operator: Clint Edrington  
Submitter: Clint Edrington  
File Name: C:\EDRING~1\TIGER&~1\SANDFR~1\TT-06-08\06\_300CM.SMP  
Material/Liquid: silicate mud/water/Water

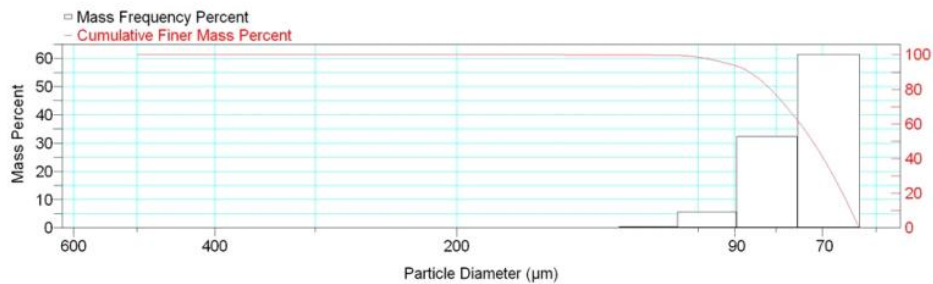
Reported: 01/03/10 15:24:13  
Liquid Visc: 0.7225 cp

Sample Density: 2.650 g/cm<sup>3</sup>  
Liquid Density: 0.9941 g/cm<sup>3</sup>

## Report by Size Class

High Diameter (μm)	Low Diameter (μm)	Average Diameter (μm)	Cumulative Mass Finer (Percent)	Mass Frequency (Percent)
600.0	500.0	547.7	100.0	0.0
500.0	425.0	461.0	100.0	0.0
425.0	355.0	388.4	100.0	0.0
355.0	300.0	326.3	100.0	0.0
300.0	250.0	273.9	100.0	0.0
250.0	212.0	230.2	100.0	0.0
212.0	180.0	195.3	100.0	0.0
180.0	150.0	164.3	100.0	0.0
150.0	125.0	136.9	99.9	0.1
125.0	106.0	115.1	99.5	0.4
106.0	90.00	97.67	93.8	5.7
90.00	75.00	82.16	61.4	32.4
75.00	63.00	68.74	0.0	61.4

Mass Frequency vs Diameter



## Summary Report

Full scale pump speed: 3  
Bubble detection: Medium  
Starting Size: 63.00 μm  
Ending Size: 0.50 μm

Stir time: 30 secs  
Stir speed: Low  
Probe time: 30 secs

Parameter 1 0.000

Parameter 2 0.000

Parameter 3 0.000

Sample: TT-06-08 300 cm  
 Operator: Clint Edrington  
 Submitter: Clint Edrington  
 File Name: C:\EDRING~1\TIGER&~1\SANDFR~1\TT-06-08\06\_300CM.SMP  
 Material/Liquid: silicate mud/water/Water

Reported: 01/03/10 15:24:13  
 Liquid Visc: 0.7225 cp

Sample Density: 2.650 g/cm<sup>3</sup>  
 Liquid Density: 0.9941 g/cm<sup>3</sup>

## Summary Report

## Mass Distribution Arithmetic Statistics

Mean	74.99	Std. Dev.	8.958
Median	72.01	Coef. Var.	0.119
Mode	68.74	Skewness	1.573
		Kurtosis	3.517

## Selected Percentiles

Percent Finer	Diameter (µm)
100.0	505.0
80.0	81.26
60.0	74.60
40.0	69.80
20.0	66.09

## Selected Sizes

Diameter (µm)	Percent Finer
500.0	100.0
250.0	100.0
125.0	99.9
88.00	92.1
63.00	0.0

Peak Number	% of Dist.*	Mean	Mode	Median	Standard Deviation	Skewness	Kurtosis
1	100.0	74.99	68.74	72.01	8.958	1.573	3.517

\* Peaks must comprise at least 5.00 % of the distribution.

Micromeritics

WIN5100 V2.03

Page 1

Sample: TT-06-08 350 cm  
Operator: Clint Edrington  
Submitter: Clint Edrington  
File Name: C:\EDRING~1\TIGER&~1\SANDFR~1\TT-06-08\06\_350CM.SMP  
Material/Liquid: silicate mud/water/Water

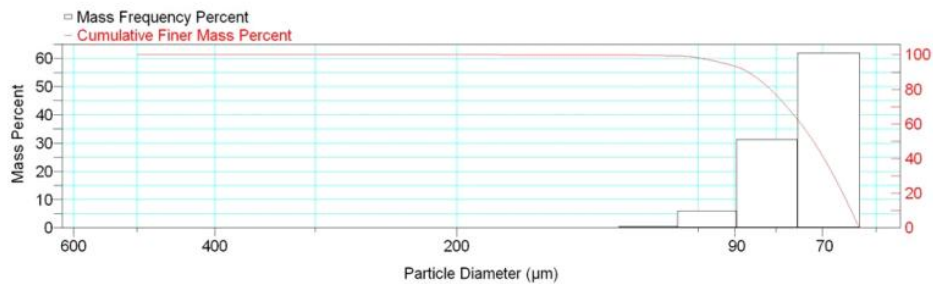
Reported: 01/03/10 15:26:22  
Liquid Visc: 0.7225 cp

Sample Density: 2.650 g/cm<sup>3</sup>  
Liquid Density: 0.9941 g/cm<sup>3</sup>

Report by Size Class

High Diameter ( $\mu\text{m}$ )	Low Diameter ( $\mu\text{m}$ )	Average Diameter ( $\mu\text{m}$ )	Cumulative Mass Finer (Percent)	Mass Frequency (Percent)
600.0	500.0	547.7	100.0	0.0
500.0	425.0	461.0	100.0	0.0
425.0	355.0	388.4	100.0	0.0
355.0	300.0	326.3	100.0	0.0
300.0	250.0	273.9	100.0	0.0
250.0	212.0	230.2	100.0	0.0
212.0	180.0	195.3	100.0	0.0
180.0	150.0	164.3	99.9	0.1
150.0	125.0	136.9	99.8	0.1
125.0	106.0	115.1	99.3	0.5
106.0	90.00	97.67	93.3	6.0
90.00	75.00	82.16	61.9	31.4
75.00	63.00	68.74	0.0	61.9

Mass Frequency vs Diameter



Summary Report

Full scale pump speed: 3  
Bubble detection: Medium  
Starting Size: 63.00  $\mu\text{m}$   
Ending Size: 0.50  $\mu\text{m}$

Stir time: 30 secs  
Stir speed: Low  
Probe time: 30 secs

Parameter 1 0.000

Parameter 2 0.000

Parameter 3 0.000

Sample: TT-06-08 350 cm  
 Operator: Clint Edrington  
 Submitter: Clint Edrington  
 File Name: C:\EDRING~1\TIGER&~1\SANDFR~1\TT-06-08\06\_350CM.SMP  
 Material/Liquid: silicate mud/water/Water

Reported: 01/03/10 15:26:22      Sample Density: 2.650 g/cm<sup>3</sup>  
 Liquid Visc: 0.7225 cp      Liquid Density: 0.9941 g/cm<sup>3</sup>

## Summary Report

## Mass Distribution Arithmetic Statistics

Mean	75.08	Std. Dev.	9.542
Median	71.86	Coef. Var.	0.127
Mode	68.74	Skewness	2.201
		Kurtosis	10.060

## Selected Percentiles

Percent Finer	Diameter (µm)
100.0	553.2
80.0	81.29
60.0	74.44
40.0	69.68
20.0	66.04

## Selected Sizes

Diameter (µm)	Percent Finer
500.0	100.0
250.0	100.0
125.0	99.8
88.00	91.6
63.00	0.0

Peak Number	% of Dist.*	Mean	Mode	Median	Standard Deviation	Skewness	Kurtosis
1	100.0	75.08	68.74	71.86	9.542	2.201	10.060

\* Peaks must comprise at least 5.00 % of the distribution.

Micromeritics

WIN5100 V2.03

Page 1

Sample: TT-06-08 410 cm  
Operator: Clint Edrington  
Submitter: Clint Edrington  
File Name: C:\EDRING~1\TIGER&~1\SANDFR~1\TT-06-08\06\_410CM.SMP  
Material/Liquid: silicate mud/water/Water

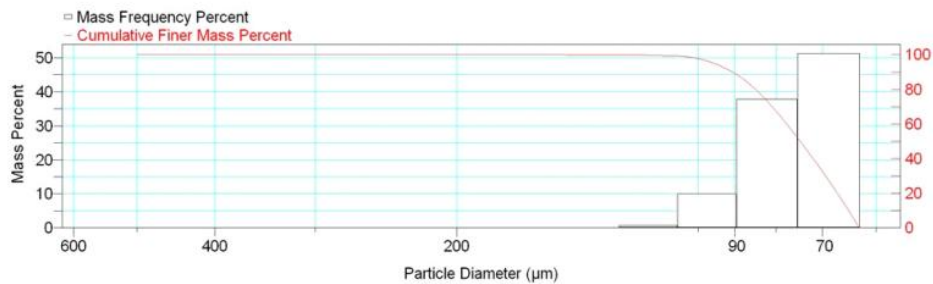
Reported: 01/03/10 15:28:37  
Liquid Visc: 0.7225 cp

Sample Density: 2.650 g/cm<sup>3</sup>  
Liquid Density: 0.9941 g/cm<sup>3</sup>

Report by Size Class

High Diameter ( $\mu$ m)	Low Diameter ( $\mu$ m)	Average Diameter ( $\mu$ m)	Cumulative Mass Finer (Percent)	Mass Frequency (Percent)
600.0	500.0	547.7	100.0	0.0
500.0	425.0	461.0	100.0	0.0
425.0	355.0	388.4	100.0	0.0
355.0	300.0	326.3	100.0	0.0
300.0	250.0	273.9	100.0	0.0
250.0	212.0	230.2	100.0	0.0
212.0	180.0	195.3	100.0	0.0
180.0	150.0	164.3	100.0	0.0
150.0	125.0	136.9	99.9	0.1
125.0	106.0	115.1	99.2	0.7
106.0	90.00	97.67	89.2	10.0
90.00	75.00	82.16	51.3	37.9
75.00	63.00	68.74	0.0	51.3

Mass Frequency vs Diameter



Summary Report

Full scale pump speed: 3  
Bubble detection: Medium  
Starting Size: 63.00  $\mu$ m  
Ending Size: 0.50  $\mu$ m

Stir time: 30 secs  
Stir speed: Low  
Probe time: 30 secs

Parameter 1 0.000

Parameter 2 0.000

Parameter 3 0.000

Sample: TT-06-08 410 cm  
 Operator: Clint Edrington  
 Submitter: Clint Edrington  
 File Name: C:\EDRING~1\TIGER&~1\SANDFR~1\TT-06-08\06\_410CM.SMP  
 Material/Liquid: silicate mud/water/Water

Reported: 01/03/10 15:28:37  
 Liquid Visc: 0.7225 cp

Sample Density: 2.650 g/cm<sup>3</sup>  
 Liquid Density: 0.9941 g/cm<sup>3</sup>

## Summary Report

## Mass Distribution Arithmetic Statistics

Mean	77.11	Std. Dev.	10.08
Median	74.63	Coef. Var.	0.131
Mode	68.74	Skewness	1.187
		Kurtosis	1.656

## Selected Percentiles

Percent Finer	Diameter (µm)
100.0	505.0
80.0	84.83
60.0	77.58
40.0	71.90
20.0	67.07

## Selected Sizes

Diameter (µm)	Percent Finer
500.0	100.0
250.0	100.0
125.0	99.9
88.00	86.2
63.00	0.0

Peak Number	% of Dist.*	Mean	Mode	Median	Standard Deviation	Skewness	Kurtosis
1	100.0	77.11	68.74	74.63	10.08	1.187	1.656

\* Peaks must comprise at least 5.00 % of the distribution.

Micromeritics

WIN5100 V2.03

Page 1

Sample: TT-09-08 23-25 cm  
Operator: Clint Edrington  
Submitter: Clint Edrington  
File Name: C:\EDRING~1\TIGER&~1\SANDFR~1\TT-09-08\09\_23-CM.SMP  
Material/Liquid: silicate mud/water/Water

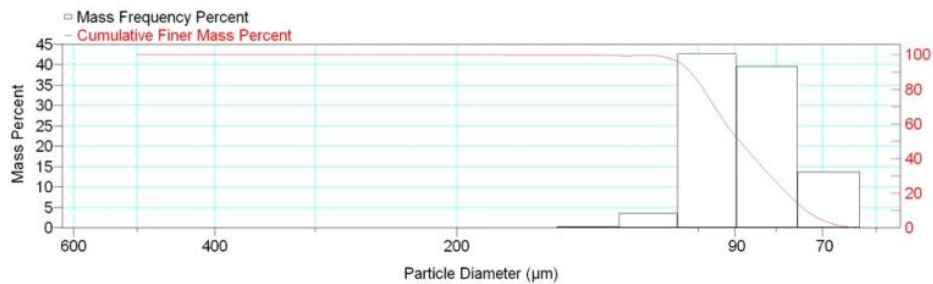
Reported: 01/03/10 15:33:06  
Liquid Visc: 0.7225 cp

Sample Density: 2.650 g/cm<sup>3</sup>  
Liquid Density: 0.9941 g/cm<sup>3</sup>

Report by Size Class

High Diameter (μm)	Low Diameter (μm)	Average Diameter (μm)	Cumulative Mass Finer (Percent)	Mass Frequency (Percent)
600.0	500.0	547.7	100.0	0.0
500.0	425.0	461.0	100.0	0.0
425.0	355.0	388.4	100.0	0.0
355.0	300.0	326.3	100.0	0.0
300.0	250.0	273.9	100.0	0.0
250.0	212.0	230.2	100.0	0.0
212.0	180.0	195.3	100.0	0.0
180.0	150.0	164.3	99.9	0.1
150.0	125.0	136.9	99.6	0.3
125.0	106.0	115.1	96.0	3.6
106.0	90.00	97.67	53.3	42.7
90.00	75.00	82.16	13.7	39.6
75.00	63.00	68.74	0.0	13.7

Mass Frequency vs Diameter



Summary Report

Full scale pump speed: 3  
Bubble detection: Medium  
Starting Size: 63.00 μm  
Ending Size: 0.50 μm

Stir time: 30 secs  
Stir speed: Low  
Probe time: 30 secs

Parameter 1 0.000

Parameter 2 0.000

Parameter 3 0.000

Sample: TT-09-08 23-25 cm  
 Operator: Clint Edrington  
 Submitter: Clint Edrington  
 File Name: C:\EDRING~1\TIGER&~1\SANDFR~1\TT-09-08\09\_23-CM.SMP  
 Material/Liquid: silicate mud/water/Water

Reported: 01/03/10 15:33:06      Sample Density: 2.650 g/cm<sup>3</sup>  
 Liquid Visc: 0.7225 cp      Liquid Density: 0.9941 g/cm<sup>3</sup>

## Summary Report

Mass Distribution Arithmetic Statistics			
Mean	88.38	Std. Dev.	11.98
Median	88.74	Coef. Var.	0.136
Mode	97.67	Skewness	0.395
		Kurtosis	1.483

Selected Percentiles		Selected Sizes	
Percent Finer	Diameter (µm)	Diameter (µm)	Percent Finer
100.0	553.2	500.0	100.0
80.0	98.50	250.0	100.0
60.0	92.32	125.0	99.6
40.0	84.98	88.00	48.1
20.0	77.50	63.00	0.0

Peak Number	% of Dist.*	Mean	Mode	Median	Standard Deviation	Skewness	Kurtosis
1	100.0	88.38	97.67	88.74	11.98	0.395	1.483

\* Peaks must comprise at least 5.00 % of the distribution.



# Micromeritics

WIN5100 V2.03

Page 1

Sample: TT-09-08 50 cm  
Operator: Clint Edrington  
Submitter: Clint Edrington  
File Name: C:\EDRING~1\TIGER&~1\SANDFR~1\TT-09-08\09\_50CM.SMP  
Material/Liquid: silicate mud/water/Water

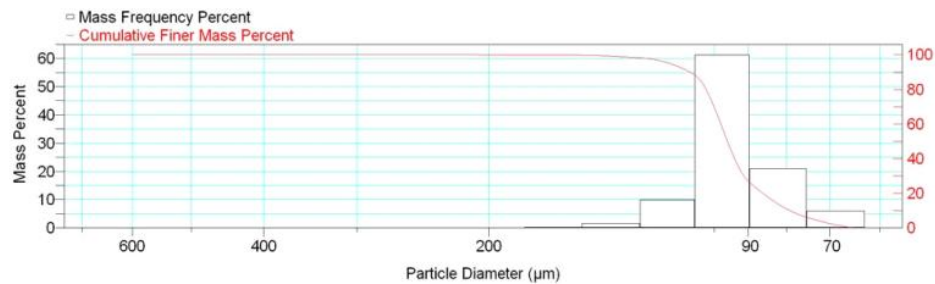
Reported: 01/03/10 15:36:23  
Liquid Visc: 0.7225 cp

Sample Density: 2.650 g/cm<sup>3</sup>  
Liquid Density: 0.9941 g/cm<sup>3</sup>

## Report by Size Class

High Diameter (µm)	Low Diameter (µm)	Average Diameter (µm)	Cumulative Mass Finer (Percent)	Mass Frequency (Percent)
710.0	600.0	652.7	100.0	0.0
600.0	500.0	547.7	100.0	0.0
500.0	425.0	461.0	100.0	0.0
425.0	355.0	388.4	100.0	0.0
355.0	300.0	326.3	100.0	0.0
300.0	250.0	273.9	100.0	0.0
250.0	212.0	230.2	100.0	0.0
212.0	180.0	195.3	99.9	0.1
180.0	150.0	164.3	99.7	0.2
150.0	125.0	136.9	98.1	1.6
125.0	106.0	115.1	88.2	9.9
106.0	90.00	97.67	27.0	61.2
90.00	75.00	82.16	6.0	21.0
75.00	63.00	68.74	0.0	6.0

Mass Frequency vs Diameter



## Summary Report

Full scale pump speed: 3  
Bubble detection: Medium  
Starting Size: 63.00 µm  
Ending Size: 0.50 µm

Stir time: 30 secs  
Stir speed: Low  
Probe time: 30 secs

Sample: TT-09-08 50 cm  
 Operator: Clint Edrington  
 Submitter: Clint Edrington  
 File Name: C:\EDRING~1\TIGER&~1\SANDFR~1\TT-09-08\09\_50CM.SMP  
 Material/Liquid: silicate mud/water/Water

Reported: 01/03/10 15:36:23  
 Liquid Visc: 0.7225 cp

Sample Density: 2.650 g/cm<sup>3</sup>  
 Liquid Density: 0.9941 g/cm<sup>3</sup>

## Summary Report

Parameter 1 0.000

Parameter 2 0.000

Parameter 3 0.000

## Mass Distribution Arithmetic Statistics

Mean	95.26	Std. Dev.	12.97
Median	95.94	Coef. Var.	0.136
Mode	97.67	Skewness	0.921
		Kurtosis	5.675

## Selected Percentiles

Percent Finer	Diameter (µm)
100.0	600.3
80.0	102.5
60.0	97.92
40.0	93.85
20.0	86.07

## Selected Sizes

Diameter (µm)	Percent Finer
500.0	100.0
250.0	100.0
125.0	98.1
88.00	23.3
63.00	0.0

Peak Number	% of Dist. *	Mean	Mode	Median	Standard Deviation	Skewness	Kurtosis
1	100.0	95.26	97.67	95.94	12.97	0.921	5.675

\* Peaks must comprise at least 5.00 % of the distribution.

# Micromeritics

WIN5100 V2.03

Page 1

Sample: TT-09-08 100 cm  
Operator: Clint Edrington  
Submitter: Clint Edrington  
File Name: C:\EDRING~1\TIGER&~1\SANDFR~1\TT-09-08\09\_100CM.SMP  
Material/Liquid: silicate mud/water/Water

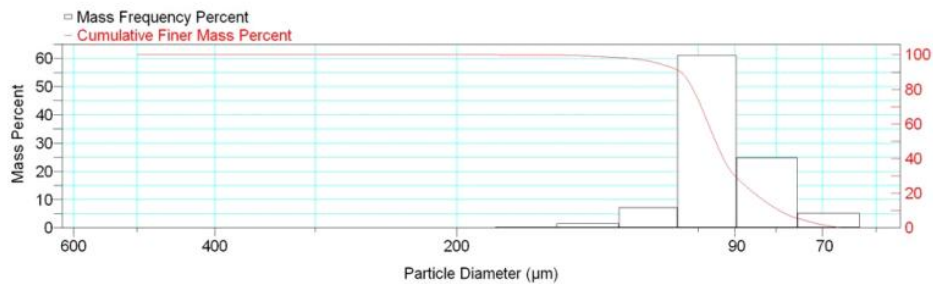
Reported: 01/03/10 15:39:02  
Liquid Visc: 0.7225 cp

Sample Density: 2.650 g/cm<sup>3</sup>  
Liquid Density: 0.9941 g/cm<sup>3</sup>

## Report by Size Class

High Diameter (μm)	Low Diameter (μm)	Average Diameter (μm)	Cumulative Mass Finer (Percent)	Mass Frequency (Percent)
600.0	500.0	547.7	100.0	0.0
500.0	425.0	461.0	100.0	0.0
425.0	355.0	388.4	100.0	0.0
355.0	300.0	326.3	100.0	0.0
300.0	250.0	273.9	100.0	0.0
250.0	212.0	230.2	100.0	0.0
212.0	180.0	195.3	100.0	0.0
180.0	150.0	164.3	99.8	0.2
150.0	125.0	136.9	98.3	1.5
125.0	106.0	115.1	91.1	7.2
106.0	90.00	97.67	30.0	61.1
90.00	75.00	82.16	5.2	24.8
75.00	63.00	68.74	0.0	5.2

Mass Frequency vs Diameter



## Summary Report

Full scale pump speed: 3  
Bubble detection: Medium  
Starting Size: 63.00 μm  
Ending Size: 0.50 μm

Stir time: 30 secs  
Stir speed: Low  
Probe time: 30 secs

Parameter 1 0.000

Parameter 2 0.000

Parameter 3 0.000

Sample: TT-09-08 100 cm  
 Operator: Clint Edrington  
 Submitter: Clint Edrington  
 File Name: C:\EDRING~1\TIGER&~1\SANDFR~1\TT-09-08\09\_100CM.SMP  
 Material/Liquid: silicate mud/water/Water

Reported: 01/03/10 15:39:02      Sample Density: 2.650 g/cm<sup>3</sup>  
 Liquid Visc: 0.7225 cp      Liquid Density: 0.9941 g/cm<sup>3</sup>

## Summary Report

## Mass Distribution Arithmetic Statistics

Mean	94.30	Std. Dev.	12.07
Median	95.15	Coef. Var.	0.128
Mode	97.67	Skewness	0.687
		Kurtosis	3.535

## Selected Percentiles

Percent Finer	Diameter (µm)
100.0	553.2
80.0	101.5
60.0	97.13
40.0	93.00
20.0	85.12

## Selected Sizes

Diameter (µm)	Percent Finer
500.0	100.0
250.0	100.0
125.0	98.3
88.00	25.8
63.00	0.0

Peak Number	% of Dist.*	Mean	Mode	Median	Standard Deviation	Skewness	Kurtosis
1	100.0	94.30	97.67	95.15	12.07	0.687	3.535

\* Peaks must comprise at least 5.00 % of the distribution.

# Micromeritics

WIN5100 V2.03

Page 1

Sample: TT-09-08 150 cm  
Operator: Clint Edrington  
Submitter: Clint Edrington  
File Name: C:\EDRING~1\TIGER&~1\SANDFR~1\TT-09-08\09\_150CM.SMP  
Material/Liquid: silicate mud/water/Water

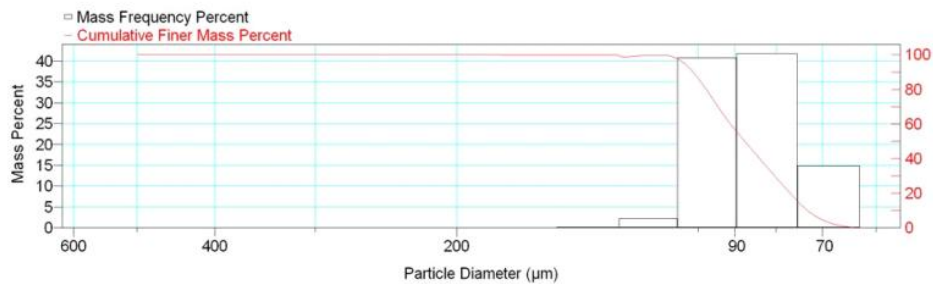
Reported: 01/03/10 15:41:37  
Liquid Visc: 0.7225 cp

Sample Density: 2.650 g/cm<sup>3</sup>  
Liquid Density: 0.9941 g/cm<sup>3</sup>

## Report by Size Class

High Diameter (µm)	Low Diameter (µm)	Average Diameter (µm)	Cumulative Mass Finer (Percent)	Mass Frequency (Percent)
600.0	500.0	547.7	100.0	0.0
500.0	425.0	461.0	100.0	0.0
425.0	355.0	388.4	100.0	0.0
355.0	300.0	326.3	100.0	0.0
300.0	250.0	273.9	100.0	0.0
250.0	212.0	230.2	100.0	0.0
212.0	180.0	195.3	100.0	0.0
180.0	150.0	164.3	99.9	0.1
150.0	125.0	136.9	99.7	0.2
125.0	106.0	115.1	97.5	2.2
106.0	90.00	97.67	56.7	40.8
90.00	75.00	82.16	14.9	41.8
75.00	63.00	68.74	0.0	14.9

Mass Frequency vs Diameter



## Summary Report

Full scale pump speed: 3  
Bubble detection: Medium  
Starting Size: 63.00 µm  
Ending Size: 0.50 µm

Stir time: 30 secs  
Stir speed: Low  
Probe time: 30 secs

Parameter 1 0.000

Parameter 2 0.000

Parameter 3 0.000

Sample: TT-09-08 150 cm  
 Operator: Clint Edrington  
 Submitter: Clint Edrington  
 File Name: C:\EDRING~1\TIGER&~1\SANDFR~1\TT-09-08\09\_150CM.SMP  
 Material/Liquid: silicate mud/water/Water

Reported: 01/03/10 15:41:37      Sample Density: 2.650 g/cm<sup>3</sup>  
 Liquid Visc: 0.7225 cp      Liquid Density: 0.9941 g/cm<sup>3</sup>

## Summary Report

## Mass Distribution Arithmetic Statistics

Mean	87.41	Std. Dev.	11.58
Median	87.49	Coef. Var.	0.133
Mode	82.16	Skewness	0.372
		Kurtosis	1.608

## Selected Percentiles

Percent Finer	Diameter (µm)
100.0	553.2
80.0	97.73
60.0	91.20
40.0	83.86
20.0	76.80

## Selected Sizes

Diameter (µm)	Percent Finer
500.0	100.0
250.0	100.0
125.0	99.7
88.00	51.4
63.00	0.0

Peak Number	% of Dist.*	Mean	Mode	Median	Standard Deviation	Skewness	Kurtosis
1	100.0	87.41	82.16	87.49	11.58	0.372	1.608

\* Peaks must comprise at least 5.00 % of the distribution.

# Micromeritics

WIN5100 V2.03

Page 1

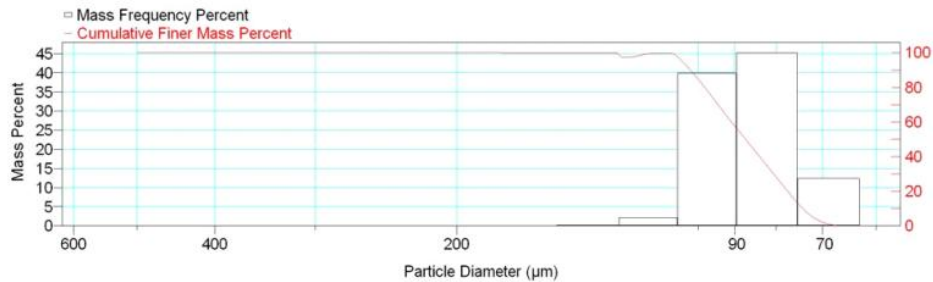
Sample: TT-09-08 200 cm  
Operator: Clint Edrington  
Submitter: Clint Edrington  
File Name: C:\EDRING~1\TIGER&~1\SANDFR~1\TT-09-08\09\_200CM.SMP  
Material/Liquid: silicate mud/water/Water

Reported: 01/03/10 15:43:57  
Liquid Visc: 0.7225 cp  
Sample Density: 2.650 g/cm<sup>3</sup>  
Liquid Density: 0.9941 g/cm<sup>3</sup>

## Report by Size Class

High Diameter (µm)	Low Diameter (µm)	Average Diameter (µm)	Cumulative Mass Finer (Percent)	Mass Frequency (Percent)
600.0	500.0	547.7	100.0	0.0
500.0	425.0	461.0	100.0	0.0
425.0	355.0	388.4	100.0	0.0
355.0	300.0	326.3	100.0	0.0
300.0	250.0	273.9	100.0	0.0
250.0	212.0	230.2	100.0	0.0
212.0	180.0	195.3	100.0	0.0
180.0	150.0	164.3	99.9	0.1
150.0	125.0	136.9	99.7	0.2
125.0	106.0	115.1	97.5	2.2
106.0	90.00	97.67	57.6	39.9
90.00	75.00	82.16	12.4	45.2
75.00	63.00	68.74	0.0	12.4

Mass Frequency vs Diameter



## Summary Report

Full scale pump speed: 3  
Bubble detection: Medium  
Starting Size: 63.00 µm  
Ending Size: 0.50 µm  
Stir time: 30 secs  
Stir speed: Low  
Probe time: 30 secs

Parameter 1 0.000  
Parameter 2 0.000  
Parameter 3 0.000

Sample: TT-09-08 200 cm  
 Operator: Clint Edrington  
 Submitter: Clint Edrington  
 File Name: C:\EDRING~1\TIGER&~1\SANDFR~1\TT-09-08\09\_200CM.SMP  
 Material/Liquid: silicate mud/water/Water

Reported: 01/03/10 15:43:57      Sample Density: 2.650 g/cm<sup>3</sup>  
 Liquid Visc: 0.7225 cp      Liquid Density: 0.9941 g/cm<sup>3</sup>

## Summary Report

## Mass Distribution Arithmetic Statistics

Mean	87.60	Std. Dev.	11.20
Median	87.28	Coef. Var.	0.128
Mode	82.16	Skewness	0.464
		Kurtosis	2.043

## Selected Percentiles

Percent Finer	Diameter (µm)
100.0	553.2
80.0	98.14
60.0	90.87
40.0	83.84
20.0	77.36

## Selected Sizes

Diameter (µm)	Percent Finer
500.0	100.0
250.0	100.0
125.0	99.7
88.00	52.0
63.00	0.0

Peak Number	% of Dist.*	Mean	Mode	Median	Standard Deviation	Skewness	Kurtosis
1	100.0	87.60	82.16	87.28	11.20	0.464	2.043

\* Peaks must comprise at least 5.00 % of the distribution.



Micromeritics

WIN5100 V2.03

Page 1

Sample: TT-09-08 250 cm  
Operator: Clint Edrington  
Submitter: Clint Edrington  
File Name: C:\EDRING~1\TIGER&~1\SANDFR~1\TT-09-08\09\_250CM.SMP  
Material/Liquid: silicate mud/water/Water

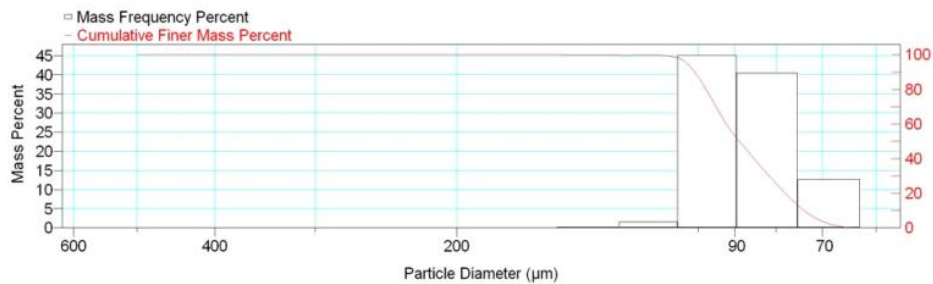
Reported: 01/03/10 15:46:29  
Liquid Visc: 0.7225 cp

Sample Density: 2.650 g/cm<sup>3</sup>  
Liquid Density: 0.9941 g/cm<sup>3</sup>

Report by Size Class

High Diameter ( $\mu\text{m}$ )	Low Diameter ( $\mu\text{m}$ )	Average Diameter ( $\mu\text{m}$ )	Cumulative Mass Finer (Percent)	Mass Frequency (Percent)
600.0	500.0	547.7	100.0	0.0
500.0	425.0	461.0	100.0	0.0
425.0	355.0	388.4	100.0	0.0
355.0	300.0	326.3	100.0	0.0
300.0	250.0	273.9	100.0	0.0
250.0	212.0	230.2	100.0	0.0
212.0	180.0	195.3	100.0	0.0
180.0	150.0	164.3	100.0	0.0
150.0	125.0	136.9	99.8	0.2
125.0	106.0	115.1	98.2	1.6
106.0	90.00	97.67	53.1	45.1
90.00	75.00	82.16	12.7	40.4
75.00	63.00	68.74	0.0	12.7

Mass Frequency vs Diameter



Summary Report

Full scale pump speed: 3  
Bubble detection: Medium  
Starting Size: 63.00  $\mu\text{m}$   
Ending Size: 0.50  $\mu\text{m}$

Stir time: 30 secs  
Stir speed: Low  
Probe time: 30 secs

Parameter 1 0.000

Parameter 2 0.000

Parameter 3 0.000

Sample: TT-09-08 250 cm  
 Operator: Clint Edrington  
 Submitter: Clint Edrington  
 File Name: C:\EDRING~1\TIGER&~1\SANDFR~1\TT-09-08\09\_250CM.SMP  
 Material/Liquid: silicate mud/water/Water

Reported: 01/03/10 15:46:29      Sample Density: 2.650 g/cm<sup>3</sup>  
 Liquid Visc: 0.7225 cp      Liquid Density: 0.9941 g/cm<sup>3</sup>

## Summary Report

## Mass Distribution Arithmetic Statistics

Mean	88.09	Std. Dev.	10.94
Median	88.85	Coef. Var.	0.124
Mode	97.67	Skewness	-0.045
		Kurtosis	-0.064

## Selected Percentiles

Percent Finer	Diameter (µm)
100.0	505.0
80.0	97.78
60.0	92.25
40.0	85.21
20.0	77.88

## Selected Sizes

Diameter (µm)	Percent Finer
500.0	100.0
250.0	100.0
125.0	99.8
88.00	47.7
63.00	0.0

Peak Number	% of Dist.*	Mean	Mode	Median	Standard Deviation	Skewness	Kurtosis
1	100.0	88.09	97.67	88.85	10.94	-0.045	-0.064

\* Peaks must comprise at least 5.00 % of the distribution.

# Micromeritics

WIN5100 V2.03

Page 1

Sample: TT-09-08 300 cm  
Operator: Clint Edrington  
Submitter: Clint Edrington  
File Name: C:\EDRING~1\TIGER&~1\SANDFR~1\TT-09-08\09\_300CM.SMP  
Material/Liquid: silicate mud/water/Water

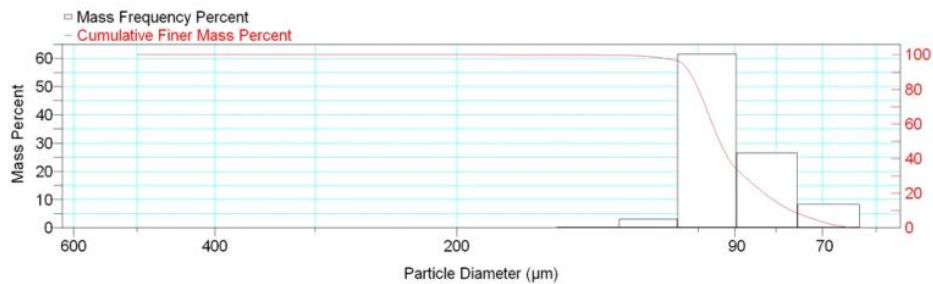
Reported: 01/03/10 15:48:29  
Liquid Visc: 0.7225 cp

Sample Density: 2.650 g/cm<sup>3</sup>  
Liquid Density: 0.9941 g/cm<sup>3</sup>

## Report by Size Class

High Diameter ( $\mu$ m)	Low Diameter ( $\mu$ m)	Average Diameter ( $\mu$ m)	Cumulative Mass Finer (Percent)	Mass Frequency (Percent)
600.0	500.0	547.7	100.0	0.0
500.0	425.0	461.0	100.0	0.0
425.0	355.0	388.4	100.0	0.0
355.0	300.0	326.3	100.0	0.0
300.0	250.0	273.9	100.0	0.0
250.0	212.0	230.2	100.0	0.0
212.0	180.0	195.3	100.0	0.0
180.0	150.0	164.3	99.9	0.1
150.0	125.0	136.9	99.6	0.3
125.0	106.0	115.1	96.5	3.1
106.0	90.00	97.67	34.9	61.6
90.00	75.00	82.16	8.3	26.6
75.00	63.00	68.74	0.0	8.3

Mass Frequency vs Diameter



## Summary Report

Full scale pump speed: 3  
Bubble detection: Medium  
Starting Size: 63.00  $\mu$ m  
Ending Size: 0.50  $\mu$ m

Stir time: 30 secs  
Stir speed: Low  
Probe time: 30 secs

Parameter 1 0.000

Parameter 2 0.000

Parameter 3 0.000

Sample: TT-09-08 300 cm  
 Operator: Clint Edrington  
 Submitter: Clint Edrington  
 File Name: C:\EDRING~1\TIGER&~1\SANDFR~1\TT-09-08\09\_300CM.SMP  
 Material/Liquid: silicate mud/water/Water

Reported: 01/03/10 15:48:29      Sample Density: 2.650 g/cm<sup>3</sup>  
 Liquid Visc: 0.7225 cp      Liquid Density: 0.9941 g/cm<sup>3</sup>

## Summary Report

Mass Distribution Arithmetic Statistics			
Mean	91.87	Std. Dev.	10.88
Median	94.03	Coef. Var.	0.118
Mode	97.67	Skewness	-0.083
		Kurtosis	2.413

Selected Percentiles		Selected Sizes	
Percent Finer	Diameter (µm)	Diameter (µm)	Percent Finer
100.0	553.2	500.0	100.0
80.0	99.96	250.0	100.0
60.0	95.99	125.0	99.6
40.0	91.72	88.00	30.6
20.0	82.75	63.00	0.0

Peak Number	% of Dist.*	Mean	Mode	Median	Standard Deviation	Skewness	Kurtosis
1	100.0	91.87	97.67	94.03	10.88	-0.083	2.413

\* Peaks must comprise at least 5.00 % of the distribution.

Micromeritics

WIN5100 V2.03

Page 1

Sample: TT-09-08 350 cm  
Operator: Clint Edrington  
Submitter: Clint Edrington  
File Name: C:\EDRING~1\TIGER&~1\SANDFR~1\TT-09-08\09\_350CM.SMP  
Material/Liquid: silicate mud/water/Water

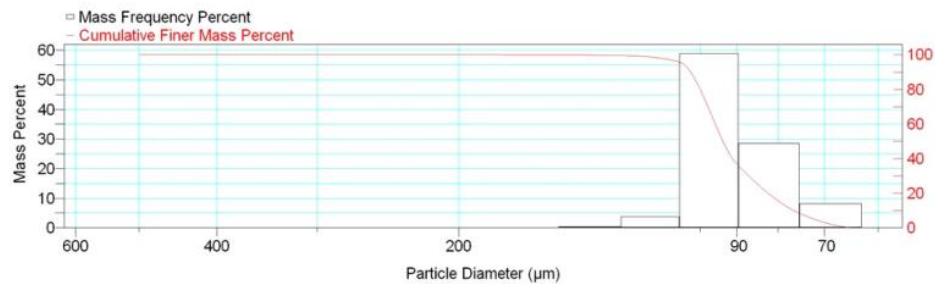
Reported: 01/03/10 15:51:16  
Liquid Visc: 0.7225 cp

Sample Density: 2.650 g/cm<sup>3</sup>  
Liquid Density: 0.9941 g/cm<sup>3</sup>

Report by Size Class

High Diameter ( $\mu\text{m}$ )	Low Diameter ( $\mu\text{m}$ )	Average Diameter ( $\mu\text{m}$ )	Cumulative Mass Finer (Percent)	Mass Frequency (Percent)
600.0	500.0	547.7	100.0	0.0
500.0	425.0	461.0	100.0	0.0
425.0	355.0	388.4	100.0	0.0
355.0	300.0	326.3	100.0	0.0
300.0	250.0	273.9	100.0	0.0
250.0	212.0	230.2	100.0	0.0
212.0	180.0	195.3	100.0	0.0
180.0	150.0	164.3	99.9	0.1
150.0	125.0	136.9	99.5	0.4
125.0	106.0	115.1	95.7	3.8
106.0	90.00	97.67	36.8	58.9
90.00	75.00	82.16	8.2	28.6
75.00	63.00	68.74	0.0	8.2

Mass Frequency vs Diameter



Summary Report

Full scale pump speed: 3  
Bubble detection: Medium  
Starting Size: 63.00  $\mu\text{m}$   
Ending Size: 0.50  $\mu\text{m}$

Stir time: 30 secs  
Stir speed: Low  
Probe time: 30 secs

Parameter 1 0.000

Parameter 2 0.000

Parameter 3 0.000

Sample: TT-09-08 350 cm  
 Operator: Clint Edrington  
 Submitter: Clint Edrington  
 File Name: C:\EDRING~1\TIGER&~1\SANDFR~1\TT-09-08\09\_350CM.SMP  
 Material/Liquid: silicate mud/water/Water

Reported: 01/03/10 15:51:16      Sample Density: 2.650 g/cm<sup>3</sup>  
 Liquid Visc: 0.7225 cp      Liquid Density: 0.9941 g/cm<sup>3</sup>

## Summary Report

## Mass Distribution Arithmetic Statistics

Mean	91.75	Std. Dev.	11.16
Median	93.68	Coef. Var.	0.122
Mode	97.67	Skewness	0.077
		Kurtosis	2.275

## Selected Percentiles

Percent Finer	Diameter (µm)
100.0	553.2
80.0	99.99
60.0	95.77
40.0	91.15
20.0	82.29

## Selected Sizes

Diameter (µm)	Percent Finer
500.0	100.0
250.0	100.0
125.0	99.5
88.00	32.2
63.00	0.0

Peak Number	% of Dist.*	Mean	Mode	Median	Standard Deviation	Skewness	Kurtosis
1	100.0	91.75	97.67	93.68	11.16	0.077	2.275

\* Peaks must comprise at least 5.00 % of the distribution.

# Micromeritics

WIN5100 V2.03

Page 1

Sample: TT-09-08 400 cm  
Operator: Clint Edrington  
Submitter: Clint Edrington  
File Name: C:\EDRING~1\TIGER&~1\SANDFR~1\TT-09-08\09\_400CM.SMP  
Material/Liquid: silicate mud/water/Water

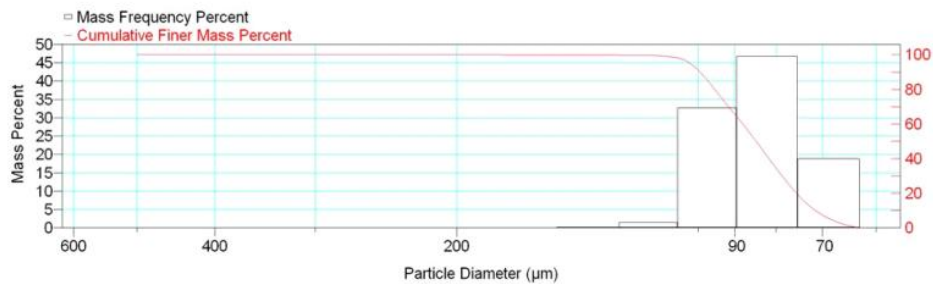
Reported: 01/03/10 15:53:45  
Liquid Visc: 0.7225 cp

Sample Density: 2.650 g/cm<sup>3</sup>  
Liquid Density: 0.9941 g/cm<sup>3</sup>

## Report by Size Class

High Diameter (μm)	Low Diameter (μm)	Average Diameter (μm)	Cumulative Mass Finer (Percent)	Mass Frequency (Percent)
600.0	500.0	547.7	100.0	0.0
500.0	425.0	461.0	100.0	0.0
425.0	355.0	388.4	100.0	0.0
355.0	300.0	326.3	100.0	0.0
300.0	250.0	273.9	100.0	0.0
250.0	212.0	230.2	100.0	0.0
212.0	180.0	195.3	100.0	0.0
180.0	150.0	164.3	99.9	0.1
150.0	125.0	136.9	99.7	0.2
125.0	106.0	115.1	98.2	1.5
106.0	90.00	97.67	65.5	32.7
90.00	75.00	82.16	18.8	46.7
75.00	63.00	68.74	0.0	18.8

Mass Frequency vs Diameter



## Summary Report

Full scale pump speed: 3  
Bubble detection: Medium  
Starting Size: 63.00 μm  
Ending Size: 0.50 μm

Stir time: 30 secs  
Stir speed: Low  
Probe time: 30 secs

Parameter 1 0.000

Parameter 2 0.000

Parameter 3 0.000

Sample: TT-09-08 400 cm  
 Operator: Clint Edrington  
 Submitter: Clint Edrington  
 File Name: C:\EDRING~1\TIGER&~1\SANDFR~1\TT-09-08\09\_400CM.SMP  
 Material/Liquid: silicate mud/water/Water

Reported: 01/03/10 15:53:45      Sample Density: 2.650 g/cm<sup>3</sup>  
 Liquid Visc: 0.7225 cp      Liquid Density: 0.9941 g/cm<sup>3</sup>

## Summary Report

## Mass Distribution Arithmetic Statistics

Mean	85.39	Std. Dev.	11.45
Median	84.68	Coef. Var.	0.134
Mode	82.16	Skewness	0.586
		Kurtosis	2.034

## Selected Percentiles

Percent Finer	Diameter (µm)
100.0	553.2
80.0	95.35
60.0	87.98
40.0	81.62
20.0	75.41

## Selected Sizes

Diameter (µm)	Percent Finer
500.0	100.0
250.0	100.0
125.0	99.7
88.00	60.1
63.00	0.0

Peak Number	% of Dist.*	Mean	Mode	Median	Standard Deviation	Skewness	Kurtosis
1	100.0	85.39	82.16	84.68	11.45	0.586	2.034

\* Peaks must comprise at least 5.00 % of the distribution.



# Micromeritics

WIN5100 V2.03

Page 1

Sample: TT-10-08 9 cm  
Operator: Clint Edrington  
Submitter: Clint Edrington  
File Name: C:\EDRING~1\TIGER&~1\SANDFR~1\TT-10-08\10\_9CM.SMP  
Material/Liquid: silicate mud/water/Water

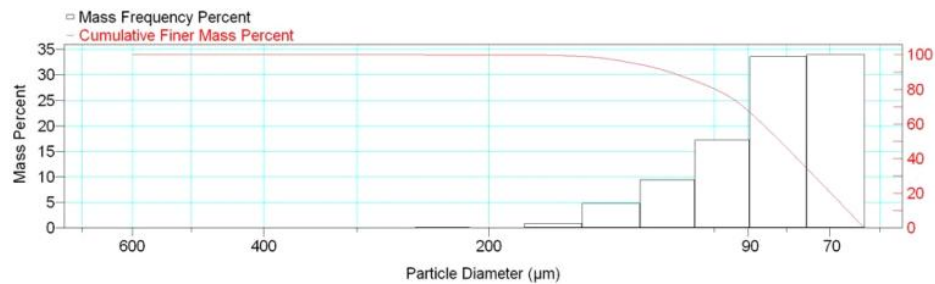
Reported: 01/03/10 15:57:26  
Liquid Visc: 0.7225 cp

Sample Density: 2.650 g/cm<sup>3</sup>  
Liquid Density: 0.9941 g/cm<sup>3</sup>

## Report by Size Class

High Diameter (μm)	Low Diameter (μm)	Average Diameter (μm)	Cumulative Mass Finer (Percent)	Mass Frequency (Percent)
710.0	600.0	652.7	100.0	0.0
600.0	500.0	547.7	100.0	0.0
500.0	425.0	461.0	100.0	0.0
425.0	355.0	388.4	100.0	0.0
355.0	300.0	326.3	100.0	0.0
300.0	250.0	273.9	100.0	0.0
250.0	212.0	230.2	99.9	0.1
212.0	180.0	195.3	99.9	0.0
180.0	150.0	164.3	99.0	0.9
150.0	125.0	136.9	94.2	4.8
125.0	106.0	115.1	84.8	9.4
106.0	90.00	97.67	67.6	17.2
90.00	75.00	82.16	34.0	33.6
75.00	63.00	68.74	0.0	34.0

Mass Frequency vs Diameter



## Summary Report

Full scale pump speed: 3  
Bubble detection: Medium  
Starting Size: 63.00 μm  
Ending Size: 0.50 μm

Stir time: 30 secs  
Stir speed: Low  
Probe time: 30 secs

Sample: TT-10-08 9 cm  
 Operator: Clint Edrington  
 Submitter: Clint Edrington  
 File Name: C:\EDRING~1\TIGER&~1\SANDFR~1\TT-10-08\10\_9CM.SMP  
 Material/Liquid: silicate mud/water/Water

Reported: 01/03/10 15:57:26  
 Liquid Visc: 0.7225 cp

Sample Density: 2.650 g/cm<sup>3</sup>  
 Liquid Density: 0.9941 g/cm<sup>3</sup>

## Summary Report

Parameter 1 0.000

Parameter 2 0.000

Parameter 3 0.000

## Mass Distribution Arithmetic Statistics

Mean	86.88	Std. Dev.	20.23
Median	81.57	Coef. Var.	0.233
Mode	68.74	Skewness	1.621
		Kurtosis	3.848

## Selected Percentiles

Percent Finer	Diameter (µm)
100.0	651.9
80.0	99.56
60.0	86.16
40.0	77.37
20.0	69.76

## Selected Sizes

Diameter (µm)	Percent Finer
500.0	100.0
250.0	100.0
125.0	94.2
88.00	63.7
63.00	0.0

Peak Number	% of Dist. *	Mean	Mode	Median	Standard Deviation	Skewness	Kurtosis
1	99.9	86.73	68.74	81.55	19.72	1.388	1.831

\* Peaks must comprise at least 5.00 % of the distribution.

# Micromeritics

WIN5100 V2.03

Page 1

Sample: TT-10-08 50 cm  
Operator: Clint Edrington  
Submitter: Clint Edrington  
File Name: C:\EDRING~1\TIGER&~1\SANDFR~1\TT-10-08\10\_50CM.SMP  
Material/Liquid: silicate mud/water/Water

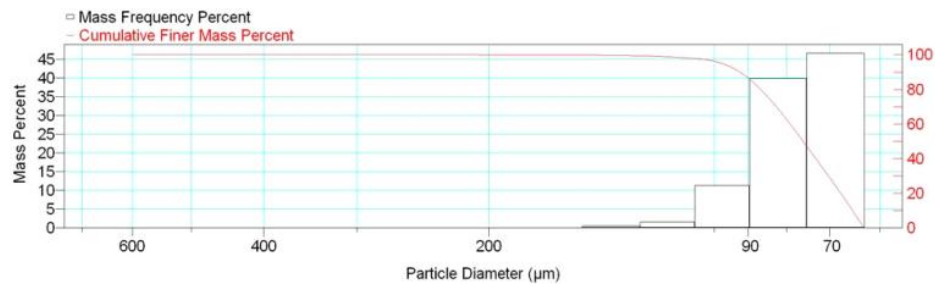
Reported: 01/03/10 16:00:21  
Liquid Visc: 0.7225 cp

Sample Density: 2.650 g/cm<sup>3</sup>  
Liquid Density: 0.9941 g/cm<sup>3</sup>

## Report by Size Class

High Diameter (µm)	Low Diameter (µm)	Average Diameter (µm)	Cumulative Mass Finer (Percent)	Mass Frequency (Percent)
710.0	600.0	652.7	100.0	0.0
600.0	500.0	547.7	100.0	0.0
500.0	425.0	461.0	100.0	0.0
425.0	355.0	388.4	100.0	0.0
355.0	300.0	326.3	100.0	0.0
300.0	250.0	273.9	100.0	0.0
250.0	212.0	230.2	100.0	0.0
212.0	180.0	195.3	99.9	0.1
180.0	150.0	164.3	99.8	0.1
150.0	125.0	136.9	99.3	0.5
125.0	106.0	115.1	97.8	1.5
106.0	90.00	97.67	86.5	11.3
90.00	75.00	82.16	46.6	39.9
75.00	63.00	68.74	0.0	46.6

Mass Frequency vs Diameter



## Summary Report

Full scale pump speed: 3  
Bubble detection: Medium  
Starting Size: 63.00 µm  
Ending Size: 0.50 µm

Stir time: 30 secs  
Stir speed: Low  
Probe time: 30 secs

Sample: TT-10-08 50 cm  
 Operator: Clint Edrington  
 Submitter: Clint Edrington  
 File Name: C:\EDRING~1\TIGER&~1\SANDFR~1\TT-10-08\10\_50CM.SMP  
 Material/Liquid: silicate mud/water/Water

Reported: 01/03/10 16:00:21  
 Liquid Visc: 0.7225 cp

Sample Density: 2.650 g/cm<sup>3</sup>  
 Liquid Density: 0.9941 g/cm<sup>3</sup>

## Summary Report

Parameter 1 0.000

Parameter 2 0.000

Parameter 3 0.000

## Mass Distribution Arithmetic Statistics

Mean	78.62	Std. Dev.	12.23
Median	76.01	Coef. Var.	0.155
Mode	68.74	Skewness	2.347
		Kurtosis	12.370

## Selected Percentiles

Percent Finer	Diameter (µm)
100.0	600.3
80.0	86.64
60.0	79.11
40.0	73.09
20.0	67.69

## Selected Sizes

Diameter (µm)	Percent Finer
500.0	100.0
250.0	100.0
125.0	99.3
88.00	82.8
63.00	0.0

Peak Number	% of Dist. *	Mean	Mode	Median	Standard Deviation	Skewness	Kurtosis
1	99.9	78.50	68.74	75.99	11.66	1.734	5.610

\* Peaks must comprise at least 5.00 % of the distribution.

# Micromeritics

WIN5100 V2.03

Page 1

Sample: TT-10-08 92 cm  
Operator: Clint Edrington  
Submitter: Clint Edrington  
File Name: C:\EDRING~1\TIGER&~1\SANDFR~1\TT-10-08\10\_92CM.SMP  
Material/Liquid: silicate mud/water/Water

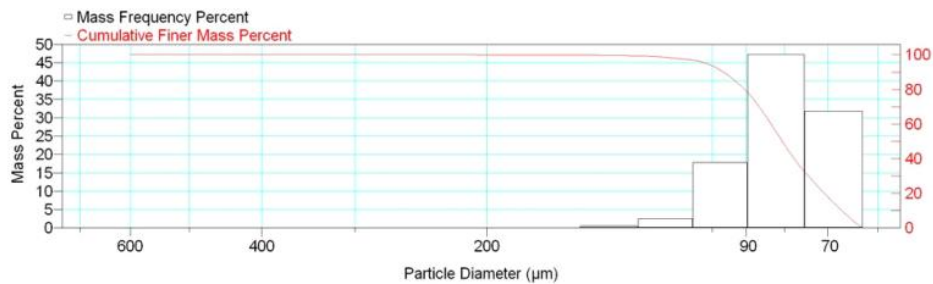
Reported: 01/03/10 16:02:50  
Liquid Visc: 0.7225 cp

Sample Density: 2.650 g/cm<sup>3</sup>  
Liquid Density: 0.9941 g/cm<sup>3</sup>

## Report by Size Class

High Diameter (µm)	Low Diameter (µm)	Average Diameter (µm)	Cumulative Mass Finer (Percent)	Mass Frequency (Percent)
710.0	600.0	652.7	100.0	0.0
600.0	500.0	547.7	100.0	0.0
500.0	425.0	461.0	100.0	0.0
425.0	355.0	388.4	100.0	0.0
355.0	300.0	326.3	100.0	0.0
300.0	250.0	273.9	100.0	0.0
250.0	212.0	230.2	100.0	0.0
212.0	180.0	195.3	99.9	0.1
180.0	150.0	164.3	99.8	0.1
150.0	125.0	136.9	99.3	0.5
125.0	106.0	115.1	96.8	2.5
106.0	90.00	97.67	79.0	17.8
90.00	75.00	82.16	31.8	47.2
75.00	63.00	68.74	0.0	31.8

Mass Frequency vs Diameter



## Summary Report

Full scale pump speed: 3  
Bubble detection: Medium  
Starting Size: 63.00 µm  
Ending Size: 0.50 µm

Stir time: 30 secs  
Stir speed: Low  
Probe time: 30 secs

Sample: TT-10-08 92 cm  
 Operator: Clint Edrington  
 Submitter: Clint Edrington  
 File Name: C:\EDRING~1\TIGER&~1\SANDFR~1\TT-10-08\10\_92CM.SMP  
 Material/Liquid: silicate mud/water/Water

Reported: 01/03/10 16:02:50  
 Liquid Visc: 0.7225 cp

Sample Density: 2.650 g/cm<sup>3</sup>  
 Liquid Density: 0.9941 g/cm<sup>3</sup>

## Summary Report

Parameter 1 0.000

Parameter 2 0.000

Parameter 3 0.000

## Mass Distribution Arithmetic Statistics

Mean	81.95	Std. Dev.	12.72
Median	80.52	Coef. Var.	0.155
Mode	82.16	Skewness	1.808
		Kurtosis	8.766

## Selected Percentiles

Percent Finer	Diameter (µm)
100.0	600.3
80.0	90.48
60.0	83.37
40.0	77.65
20.0	70.75

## Selected Sizes

Diameter (µm)	Percent Finer
500.0	100.0
250.0	100.0
125.0	99.3
88.00	74.2
63.00	0.0

Peak Number	% of Dist. *	Mean	Mode	Median	Standard Deviation	Skewness	Kurtosis
1	99.9	81.83	82.16	80.51	12.21	1.272	3.470

\* Peaks must comprise at least 5.00 % of the distribution.

Micromeritics

WIN5100 V2.03

Page 1

Sample: TT-10-08 300 cm  
Operator: Clint Edrington  
Submitter: Clint Edrington  
File Name: C:\EDRING~1\TIGER&~1\SANDFR~1\TT-10-08\10\_300CM.SMP  
Material/Liquid: silicate mud/water/Water

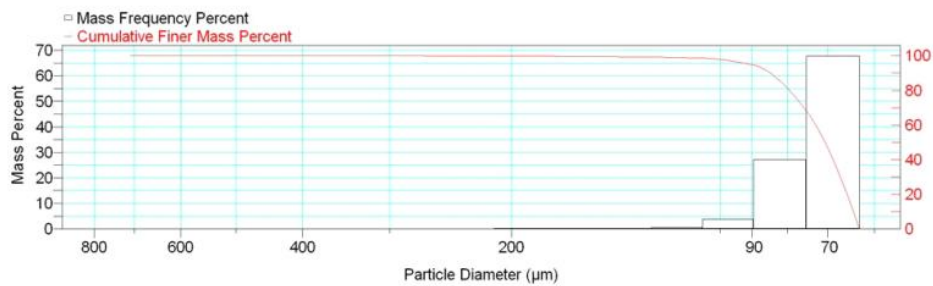
Reported: 01/03/10 16:05:33  
Liquid Visc: 0.7225 cp

Sample Density: 2.650 g/cm<sup>3</sup>  
Liquid Density: 0.9941 g/cm<sup>3</sup>

Report by Size Class

High Diameter ( $\mu\text{m}$ )	Low Diameter ( $\mu\text{m}$ )	Average Diameter ( $\mu\text{m}$ )	Cumulative Mass Finer (Percent)	Mass Frequency (Percent)
850.0	710.0	776.9	100.0	0.0
710.0	600.0	652.7	100.0	0.0
600.0	500.0	547.7	100.0	0.0
500.0	425.0	461.0	100.0	0.0
425.0	355.0	388.4	100.0	0.0
355.0	300.0	326.3	100.0	0.0
300.0	250.0	273.9	99.9	0.1
250.0	212.0	230.2	99.9	0.0
212.0	180.0	195.3	99.7	0.2
180.0	150.0	164.3	99.5	0.2
150.0	125.0	136.9	99.2	0.3
125.0	106.0	115.1	98.6	0.6
106.0	90.00	97.67	94.8	3.8
90.00	75.00	82.16	67.7	27.1
75.00	63.00	68.74	0.0	67.7

Mass Frequency vs Diameter



Summary Report

Full scale pump speed: 3  
Bubble detection: Medium  
Starting Size: 63.00  $\mu\text{m}$   
Ending Size: 0.50  $\mu\text{m}$

Stir time: 30 secs  
Stir speed: Low  
Probe time: 30 secs

Sample: TT-10-08 300 cm  
 Operator: Clint Edrington  
 Submitter: Clint Edrington  
 File Name: C:\EDRING~1\TIGER&~1\SANDFR~1\TT-10-08\10\_300CM.SMP  
 Material/Liquid: silicate mud/water/Water

Reported: 01/03/10 16:05:33  
 Liquid Visc: 0.7225 cp

Sample Density: 2.650 g/cm<sup>3</sup>  
 Liquid Density: 0.9941 g/cm<sup>3</sup>

## Summary Report

Parameter 1	0.000	Parameter 2	0.000	Parameter 3	0.000		
Mass Distribution Arithmetic Statistics							
Mean	74.61	Std. Dev.		12.86			
Median	70.62	Coef. Var.		0.172			
Mode	68.74	Skewness		6.789			
		Kurtosis		77.556			
Selected Percentiles			Selected Sizes				
Percent Finer	Diameter (µm)		Diameter (µm)	Percent Finer			
100.0	714.1		500.0	100.0			
80.0	79.48		250.0	99.9			
60.0	72.83		125.0	99.2			
40.0	68.76		88.00	93.7			
20.0	65.64		63.00	0.0			
Peak Number	% of Dist.*	Mean	Mode	Median	Standard Deviation	Skewness	Kurtosis
1	99.7	74.17	68.74	70.59	9.832	3.317	19.413

\* Peaks must comprise at least 5.00 % of the distribution.



# Micromeritics

WIN5100 V2.03

Page 1

Sample: TT-10-08 345 cm  
Operator: Clint Edrington  
Submitter: Clint Edrington  
File Name: C:\EDRING~1\TIGER&~1\SANDFR~1\TT-10-08\10\_345CM.SMP  
Material/Liquid: silicate mud/water/Water

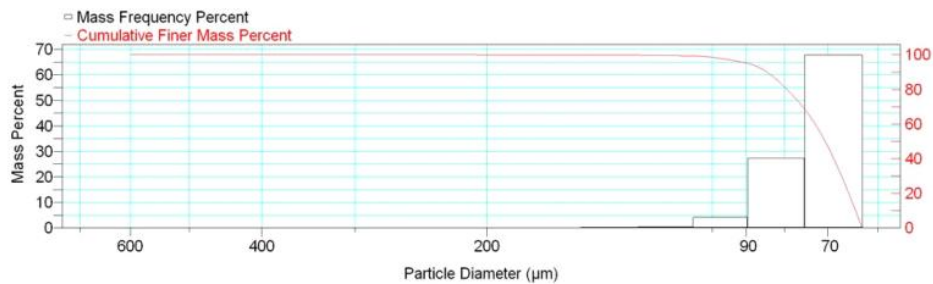
Reported: 01/03/10 16:08:11  
Liquid Visc: 0.7225 cp

Sample Density: 2.650 g/cm<sup>3</sup>  
Liquid Density: 0.9941 g/cm<sup>3</sup>

## Report by Size Class

High Diameter (µm)	Low Diameter (µm)	Average Diameter (µm)	Cumulative Mass Finer (Percent)	Mass Frequency (Percent)
710.0	600.0	652.7	100.0	0.0
600.0	500.0	547.7	100.0	0.0
500.0	425.0	461.0	100.0	0.0
425.0	355.0	388.4	100.0	0.0
355.0	300.0	326.3	100.0	0.0
300.0	250.0	273.9	100.0	0.0
250.0	212.0	230.2	100.0	0.0
212.0	180.0	195.3	99.9	0.1
180.0	150.0	164.3	99.9	0.0
150.0	125.0	136.9	99.7	0.2
125.0	106.0	115.1	99.3	0.4
106.0	90.00	97.67	95.2	4.1
90.00	75.00	82.16	67.9	27.3
75.00	63.00	68.74	0.0	67.9

Mass Frequency vs Diameter



## Summary Report

Full scale pump speed: 3  
Bubble detection: Medium  
Starting Size: 63.00 µm  
Ending Size: 0.50 µm

Stir time: 30 secs  
Stir speed: Low  
Probe time: 30 secs

Sample: TT-10-08 345 cm  
 Operator: Clint Edrington  
 Submitter: Clint Edrington  
 File Name: C:\EDRING~1\TIGER&~1\SANDFR~1\TT-10-08\10\_345CM.SMP  
 Material/Liquid: silicate mud/water/Water

Reported: 01/03/10 16:08:11  
 Liquid Visc: 0.7225 cp

Sample Density: 2.650 g/cm<sup>3</sup>  
 Liquid Density: 0.9941 g/cm<sup>3</sup>

## Summary Report

Parameter 1 0.000

Parameter 2 0.000

Parameter 3 0.000

## Mass Distribution Arithmetic Statistics

Mean	74.04	Std. Dev.	9.452
Median	70.59	Coef. Var.	0.128
Mode	68.74	Skewness	3.726
		Kurtosis	31.292

## Selected Percentiles

Percent Finer	Diameter (µm)
100.0	600.3
80.0	79.38
60.0	72.79
40.0	68.74
20.0	65.64

## Selected Sizes

Diameter (µm)	Percent Finer
500.0	100.0
250.0	100.0
125.0	99.7
88.00	94.0
63.00	0.0

Peak Number	% of Dist. *	Mean	Mode	Median	Standard Deviation	Skewness	Kurtosis
1	99.9	73.92	68.74	70.58	8.642	2.153	7.382

\* Peaks must comprise at least 5.00 % of the distribution.

Micromeritics

WIN5100 V2.03

Page 1

Sample: TT-10-08 395 cm  
Operator: Clint Edrington  
Submitter: Clint Edrington  
File Name: C:\EDRING~1\TIGER&~1\SANDFR~1\TT-10-08\10\_395CM.SMP  
Material/Liquid: silicate mud/water/Water

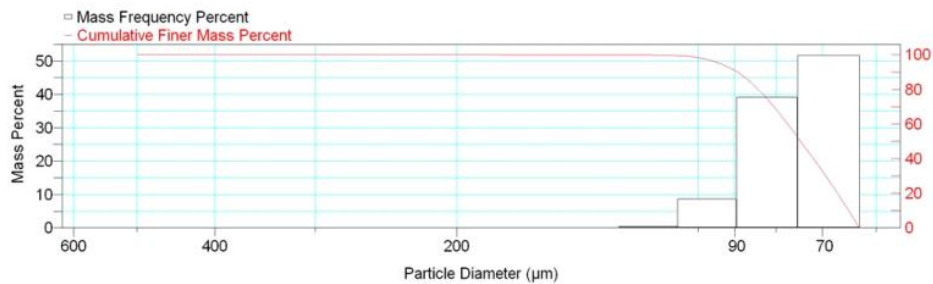
Reported: 01/03/10 16:11:19  
Liquid Visc: 0.7225 cp

Sample Density: 2.650 g/cm<sup>3</sup>  
Liquid Density: 0.9941 g/cm<sup>3</sup>

Report by Size Class

High Diameter ( $\mu\text{m}$ )	Low Diameter ( $\mu\text{m}$ )	Average Diameter ( $\mu\text{m}$ )	Cumulative Mass Finer (Percent)	Mass Frequency (Percent)
600.0	500.0	547.7	100.0	0.0
500.0	425.0	461.0	100.0	0.0
425.0	355.0	388.4	100.0	0.0
355.0	300.0	326.3	100.0	0.0
300.0	250.0	273.9	100.0	0.0
250.0	212.0	230.2	100.0	0.0
212.0	180.0	195.3	100.0	0.0
180.0	150.0	164.3	99.9	0.1
150.0	125.0	136.9	99.9	0.0
125.0	106.0	115.1	99.4	0.5
106.0	90.00	97.67	90.8	8.6
90.00	75.00	82.16	51.7	39.1
75.00	63.00	68.74	0.0	51.7

Mass Frequency vs Diameter



Summary Report

Full scale pump speed: 3  
Bubble detection: Medium  
Starting Size: 63.00  $\mu\text{m}$   
Ending Size: 0.50  $\mu\text{m}$

Stir time: 30 secs  
Stir speed: Low  
Probe time: 30 secs

Parameter 1 0.000

Parameter 2 0.000

Parameter 3 0.000

Sample: TT-10-08 395 cm  
 Operator: Clint Edrington  
 Submitter: Clint Edrington  
 File Name: C:\EDRING~1\TIGER&~1\SANDFR~1\TT-10-08\10\_395CM.SMP  
 Material/Liquid: silicate mud/water/Water

Reported: 01/03/10 16:11:19  
 Liquid Visc: 0.7225 cp

Sample Density: 2.650 g/cm<sup>3</sup>  
 Liquid Density: 0.9941 g/cm<sup>3</sup>

## Summary Report

## Mass Distribution Arithmetic Statistics

Mean	76.80	Std. Dev.	9.864
Median	74.53	Coef. Var.	0.128
Mode	68.74	Skewness	1.586
		Kurtosis	6.324

## Selected Percentiles

Percent Finer	Diameter (µm)
100.0	553.2
80.0	84.17
60.0	77.38
40.0	71.86
20.0	67.07

## Selected Sizes

Diameter (µm)	Percent Finer
500.0	100.0
250.0	100.0
125.0	99.9
88.00	87.9
63.00	0.0

Peak Number	% of Dist.*	Mean	Mode	Median	Standard Deviation	Skewness	Kurtosis
1	99.9	76.71	68.74	74.51	9.472	1.032	0.718

\* Peaks must comprise at least 5.00 % of the distribution.

# Micromeritics

WIN5100 V2.03

Page 1

Sample: TT-12-08 22 cm  
Operator: Clint Edrington  
Submitter: Clint Edrington  
File Name: C:\EDRING~1\TIGER&~1\SANDFR~1\TT-12-08\12\_22CM.SMP  
Material/Liquid: silicate mud/water/Water

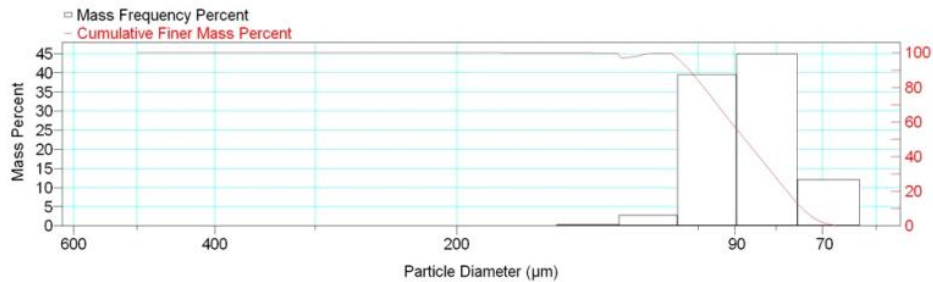
Reported: 01/03/10 17:24:38  
Liquid Visc: 0.7225 cp

Sample Density: 2.650 g/cm<sup>3</sup>  
Liquid Density: 0.9941 g/cm<sup>3</sup>

## Report by Size Class

High Diameter (μm)	Low Diameter (μm)	Average Diameter (μm)	Cumulative Mass Finer (Percent)	Mass Frequency (Percent)
600.0	500.0	547.7	100.0	0.0
500.0	425.0	461.0	100.0	0.0
425.0	355.0	388.4	100.0	0.0
355.0	300.0	326.3	100.0	0.0
300.0	250.0	273.9	100.0	0.0
250.0	212.0	230.2	100.0	0.0
212.0	180.0	195.3	100.0	0.0
180.0	150.0	164.3	99.9	0.1
150.0	125.0	136.9	99.5	0.4
125.0	106.0	115.1	96.7	2.8
106.0	90.00	97.67	57.1	39.6
90.00	75.00	82.16	12.1	45.0
75.00	63.00	68.74	0.0	12.1

Mass Frequency vs Diameter



## Summary Report

Full scale pump speed: 3  
Bubble detection: Medium  
Starting Size: 63.00 μm  
Ending Size: 0.50 μm

Stir time: 30 secs  
Stir speed: Low  
Probe time: 30 secs

Parameter 1 0.000

Parameter 2 0.000

Parameter 3 0.000

Sample: TT-12-08 22 cm  
 Operator: Clint Edrington  
 Submitter: Clint Edrington  
 File Name: C:\EDRING~1\TIGER&~1\SANDFR~1\TT-12-08\12\_22CM.SMP  
 Material/Liquid: silicate mud/water/Water

Reported: 01/03/10 17:24:38  
 Liquid Visc: 0.7225 cp

Sample Density: 2.650 g/cm<sup>3</sup>  
 Liquid Density: 0.9941 g/cm<sup>3</sup>

## Summary Report

## Mass Distribution Arithmetic Statistics

Mean	87.90	Std. Dev.	11.54
Median	87.44	Coef. Var.	0.131
Mode	82.16	Skewness	0.594
		Kurtosis	2.235

## Selected Percentiles

Percent Finer	Diameter (µm)
100.0	553.2
80.0	98.41
60.0	91.06
40.0	83.98
20.0	77.47

## Selected Sizes

Diameter (µm)	Percent Finer
500.0	100.0
250.0	100.0
125.0	99.5
88.00	51.6
63.00	0.0

Peak Number	% of Dist.*	Mean	Mode	Median	Standard Deviation	Skewness	Kurtosis
1	100.0	87.90	82.16	87.44	11.54	0.594	2.235

\* Peaks must comprise at least 5.00 % of the distribution.

# Micromeritics

WIN5100 V2.03

Page 1

Sample: TT-12-08 50 cm  
Operator: Clint Edrington  
Submitter: Clint Edrington  
File Name: C:\EDRING~1\TIGER&~1\SANDFR~1\TT-12-08\12\_50CM.SMP  
Material/Liquid: silicate mud/water/Water

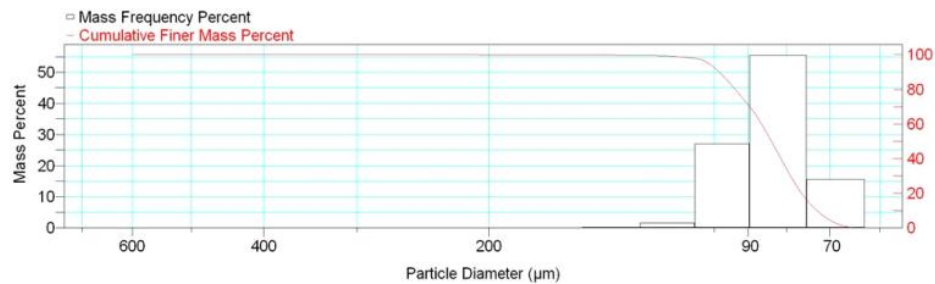
Reported: 01/03/10 17:26:35  
Liquid Visc: 0.7225 cp

Sample Density: 2.650 g/cm<sup>3</sup>  
Liquid Density: 0.9941 g/cm<sup>3</sup>

## Report by Size Class

High Diameter (μm)	Low Diameter (μm)	Average Diameter (μm)	Cumulative Mass Finer (Percent)	Mass Frequency (Percent)
710.0	600.0	652.7	100.0	0.0
600.0	500.0	547.7	100.0	0.0
500.0	425.0	461.0	100.0	0.0
425.0	355.0	388.4	100.0	0.0
355.0	300.0	326.3	100.0	0.0
300.0	250.0	273.9	100.0	0.0
250.0	212.0	230.2	100.0	0.0
212.0	180.0	195.3	99.9	0.1
180.0	150.0	164.3	99.8	0.1
150.0	125.0	136.9	99.6	0.2
125.0	106.0	115.1	98.0	1.6
106.0	90.00	97.67	71.0	27.0
90.00	75.00	82.16	15.6	55.4
75.00	63.00	68.74	0.0	15.6

Mass Frequency vs Diameter



## Summary Report

Full scale pump speed: 3  
Bubble detection: Medium  
Starting Size: 63.00 μm  
Ending Size: 0.50 μm

Stir time: 30 secs  
Stir speed: Low  
Probe time: 30 secs

Sample: TT-12-08 50 cm  
 Operator: Clint Edrington  
 Submitter: Clint Edrington  
 File Name: C:\EDRING~1\TIGER&~1\SANDFR~1\TT-12-08\12\_50CM.SMP  
 Material/Liquid: silicate mud/water/Water

Reported: 01/03/10 17:26:35  
 Liquid Visc: 0.7225 cp

Sample Density: 2.650 g/cm<sup>3</sup>  
 Liquid Density: 0.9941 g/cm<sup>3</sup>

## Summary Report

Parameter 1 0.000

Parameter 2 0.000

Parameter 3 0.000

## Mass Distribution Arithmetic Statistics

Mean	85.09	Std. Dev.	11.29
Median	83.80	Coef. Var.	0.133
Mode	82.16	Skewness	1.663
		Kurtosis	11.321

## Selected Percentiles

Percent Finer	Diameter (µm)
100.0	600.3
80.0	93.67
60.0	86.41
40.0	81.40
20.0	76.37

## Selected Sizes

Diameter (µm)	Percent Finer
500.0	100.0
250.0	100.0
125.0	99.6
88.00	65.4
63.00	0.0

Peak Number	% of Dist. *	Mean	Mode	Median	Standard Deviation	Skewness	Kurtosis
1	99.9	84.98	82.16	83.79	10.74	0.880	3.412

\* Peaks must comprise at least 5.00 % of the distribution.



Micromeritics

WIN5100 V2.03

Page 1

Sample: TT-12-08 100 cm  
Operator: Clint Edrington  
Submitter: Clint Edrington  
File Name: C:\EDRING~1\TIGER&~1\SANDFR~1\TT-12-08\12\_100CM.SMP  
Material/Liquid: silicate mud/water/Water

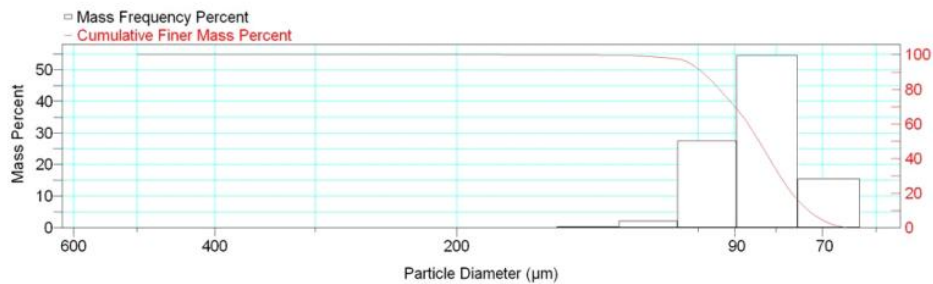
Reported: 01/03/10 17:28:41  
Liquid Visc: 0.7225 cp

Sample Density: 2.650 g/cm<sup>3</sup>  
Liquid Density: 0.9941 g/cm<sup>3</sup>

Report by Size Class

High Diameter (μm)	Low Diameter (μm)	Average Diameter (μm)	Cumulative Mass Finer (Percent)	Mass Frequency (Percent)
600.0	500.0	547.7	100.0	0.0
500.0	425.0	461.0	100.0	0.0
425.0	355.0	388.4	100.0	0.0
355.0	300.0	326.3	100.0	0.0
300.0	250.0	273.9	100.0	0.0
250.0	212.0	230.2	100.0	0.0
212.0	180.0	195.3	100.0	0.0
180.0	150.0	164.3	99.9	0.1
150.0	125.0	136.9	99.6	0.3
125.0	106.0	115.1	97.5	2.1
106.0	90.00	97.67	70.0	27.5
90.00	75.00	82.16	15.5	54.5
75.00	63.00	68.74	0.0	15.5

Mass Frequency vs Diameter



Summary Report

Full scale pump speed: 3  
Bubble detection: Medium  
Starting Size: 63.00 μm  
Ending Size: 0.50 μm

Stir time: 30 secs  
Stir speed: Low  
Probe time: 30 secs

Parameter 1 0.000

Parameter 2 0.000

Parameter 3 0.000

Sample: TT-12-08 100 cm  
 Operator: Clint Edrington  
 Submitter: Clint Edrington  
 File Name: C:\EDRING~1\TIGER&~1\SANDFR~1\TT-12-08\12\_100CM.SMP  
 Material/Liquid: silicate mud/water/Water

Reported: 01/03/10 17:28:41  
 Liquid Visc: 0.7225 cp

Sample Density: 2.650 g/cm<sup>3</sup>  
 Liquid Density: 0.9941 g/cm<sup>3</sup>

## Summary Report

## Mass Distribution Arithmetic Statistics

Mean	85.28	Std. Dev.	11.09
Median	83.98	Coef. Var.	0.130
Mode	82.16	Skewness	0.931
		Kurtosis	3.299

## Selected Percentiles

Percent Finer	Diameter (µm)
100.0	553.2
80.0	94.07
60.0	86.67
40.0	81.52
20.0	76.41

## Selected Sizes

Diameter (µm)	Percent Finer
500.0	100.0
250.0	100.0
125.0	99.6
88.00	64.4
63.00	0.0

Peak Number	% of Dist.*	Mean	Mode	Median	Standard Deviation	Skewness	Kurtosis
1	100.0	85.28	82.16	83.98	11.09	0.931	3.299

\* Peaks must comprise at least 5.00 % of the distribution.

# Micromeritics

WIN5100 V2.03

Page 1

Sample: TT-12-08 150 cm  
Operator: Clint Edrington  
Submitter: Clint Edrington  
File Name: C:\EDRING~1\TIGER&~1\SANDFR~1\TT-12-08\12\_150CM.SMP  
Material/Liquid: silicate mud/water/Water

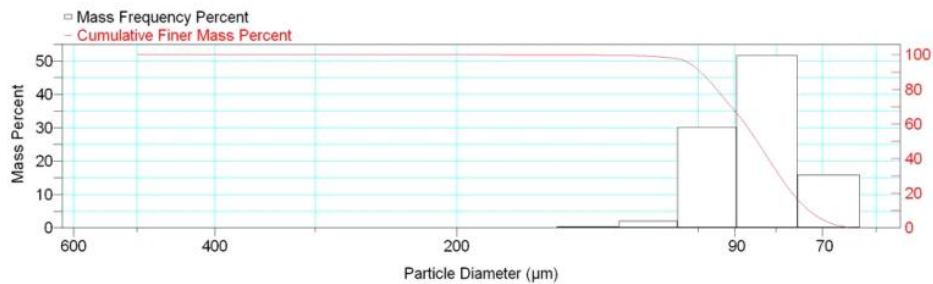
Reported: 01/03/10 17:30:40  
Liquid Visc: 0.7225 cp

Sample Density: 2.650 g/cm<sup>3</sup>  
Liquid Density: 0.9941 g/cm<sup>3</sup>

## Report by Size Class

High Diameter (μm)	Low Diameter (μm)	Average Diameter (μm)	Cumulative Mass Finer (Percent)	Mass Frequency (Percent)
600.0	500.0	547.7	100.0	0.0
500.0	425.0	461.0	100.0	0.0
425.0	355.0	388.4	100.0	0.0
355.0	300.0	326.3	100.0	0.0
300.0	250.0	273.9	100.0	0.0
250.0	212.0	230.2	100.0	0.0
212.0	180.0	195.3	100.0	0.0
180.0	150.0	164.3	99.9	0.1
150.0	125.0	136.9	99.6	0.3
125.0	106.0	115.1	97.6	2.0
106.0	90.00	97.67	67.5	30.1
90.00	75.00	82.16	15.9	51.6
75.00	63.00	68.74	0.0	15.9

Mass Frequency vs Diameter



## Summary Report

Full scale pump speed: 3  
Bubble detection: Medium  
Starting Size: 63.00 μm  
Ending Size: 0.50 μm

Stir time: 30 secs  
Stir speed: Low  
Probe time: 30 secs

Parameter 1 0.000

Parameter 2 0.000

Parameter 3 0.000

Sample: TT-12-08 150 cm  
 Operator: Clint Edrington  
 Submitter: Clint Edrington  
 File Name: C:\EDRING~1\TIGER&~1\SANDFR~1\TT-12-08\12\_150CM.SMP  
 Material/Liquid: silicate mud/water/Water

Reported: 01/03/10 17:30:40      Sample Density: 2.650 g/cm<sup>3</sup>  
 Liquid Visc: 0.7225 cp      Liquid Density: 0.9941 g/cm<sup>3</sup>

## Summary Report

## Mass Distribution Arithmetic Statistics

Mean	85.60	Std. Dev.	11.26
Median	84.46	Coef. Var.	0.131
Mode	82.16	Skewness	0.809
		Kurtosis	2.837

## Selected Percentiles

Percent Finer	Diameter (µm)
100.0	553.2
80.0	94.82
60.0	87.39
40.0	81.79
20.0	76.32

## Selected Sizes

Diameter (µm)	Percent Finer
500.0	100.0
250.0	100.0
125.0	99.6
88.00	61.9
63.00	0.0

Peak Number	% of Dist.*	Mean	Mode	Median	Standard Deviation	Skewness	Kurtosis
1	100.0	85.60	82.16	84.46	11.26	0.809	2.837

\* Peaks must comprise at least 5.00 % of the distribution.

Micromeritics

WIN5100 V2.03

Page 1

Sample: TT-12-08 200 cm  
Operator: Clint Edrington  
Submitter: Clint Edrington  
File Name: C:\EDRING~1\TIGER&~1\SANDFR~1\TT-12-08\12\_200CM.SMP  
Material/Liquid: silicate mud/water/Water

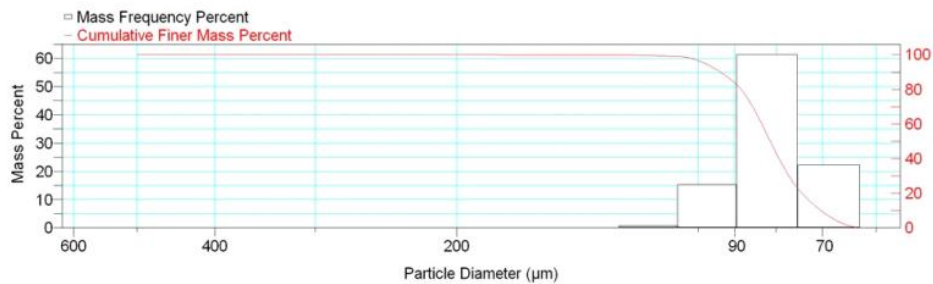
Reported: 01/03/10 17:33:17  
Liquid Visc: 0.7225 cp

Sample Density: 2.650 g/cm<sup>3</sup>  
Liquid Density: 0.9941 g/cm<sup>3</sup>

Report by Size Class

High Diameter ( $\mu\text{m}$ )	Low Diameter ( $\mu\text{m}$ )	Average Diameter ( $\mu\text{m}$ )	Cumulative Mass Finer (Percent)	Mass Frequency (Percent)
600.0	500.0	547.7	100.0	0.0
500.0	425.0	461.0	100.0	0.0
425.0	355.0	388.4	100.0	0.0
355.0	300.0	326.3	100.0	0.0
300.0	250.0	273.9	100.0	0.0
250.0	212.0	230.2	100.0	0.0
212.0	180.0	195.3	100.0	0.0
180.0	150.0	164.3	99.9	0.1
150.0	125.0	136.9	99.8	0.1
125.0	106.0	115.1	99.0	0.8
106.0	90.00	97.67	83.7	15.3
90.00	75.00	82.16	22.3	61.4
75.00	63.00	68.74	0.0	22.3

Mass Frequency vs Diameter



Summary Report

Full scale pump speed: 3  
Bubble detection: Medium  
Starting Size: 63.00  $\mu\text{m}$   
Ending Size: 0.50  $\mu\text{m}$

Stir time: 30 secs  
Stir speed: Low  
Probe time: 30 secs

Parameter 1 0.000

Parameter 2 0.000

Parameter 3 0.000

Sample: TT-12-08 200 cm  
 Operator: Clint Edrington  
 Submitter: Clint Edrington  
 File Name: C:\EDRING~1\TIGER&~1\SANDFR~1\TT-12-08\12\_200CM.SMP  
 Material/Liquid: silicate mud/water/Water

Reported: 01/03/10 17:33:17  
 Liquid Visc: 0.7225 cp

Sample Density: 2.650 g/cm<sup>3</sup>  
 Liquid Density: 0.9941 g/cm<sup>3</sup>

## Summary Report

## Mass Distribution Arithmetic Statistics

Mean	81.94	Std. Dev.	9.766
Median	81.29	Coef. Var.	0.119
Mode	82.16	Skewness	1.181
		Kurtosis	5.907

## Selected Percentiles

Percent Finer	Diameter (µm)
100.0	553.2
80.0	88.41
60.0	83.32
40.0	79.28
20.0	74.22

## Selected Sizes

Diameter (µm)	Percent Finer
500.0	100.0
250.0	100.0
125.0	99.8
88.00	78.8
63.00	0.0

Peak Number	% of Dist.*	Mean	Mode	Median	Standard Deviation	Skewness	Kurtosis
1	100.0	81.94	82.16	81.29	9.766	1.181	5.907

\* Peaks must comprise at least 5.00 % of the distribution.

Micromeritics

WIN5100 V2.03

Page 1

Sample: TT-12-08 250 cm  
Operator: Clint Edrington  
Submitter: Clint Edrington  
File Name: C:\EDRING~1\TIGER&~1\SANDFR~1\TT-12-08\12\_250CM.SMP  
Material/Liquid: silicate mud/water/Water

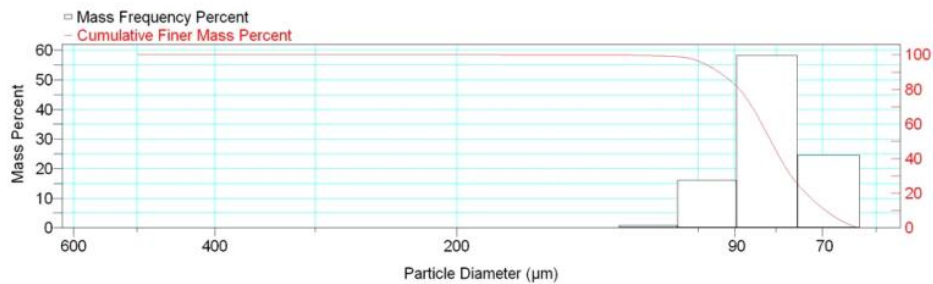
Reported: 01/03/10 17:36:05  
Liquid Visc: 0.7225 cp

Sample Density: 2.650 g/cm<sup>3</sup>  
Liquid Density: 0.9941 g/cm<sup>3</sup>

Report by Size Class

High Diameter ( $\mu\text{m}$ )	Low Diameter ( $\mu\text{m}$ )	Average Diameter ( $\mu\text{m}$ )	Cumulative Mass Finer (Percent)	Mass Frequency (Percent)
600.0	500.0	547.7	100.0	0.0
500.0	425.0	461.0	100.0	0.0
425.0	355.0	388.4	100.0	0.0
355.0	300.0	326.3	100.0	0.0
300.0	250.0	273.9	100.0	0.0
250.0	212.0	230.2	100.0	0.0
212.0	180.0	195.3	100.0	0.0
180.0	150.0	164.3	99.9	0.1
150.0	125.0	136.9	99.8	0.1
125.0	106.0	115.1	98.9	0.9
106.0	90.00	97.67	82.8	16.1
90.00	75.00	82.16	24.6	58.2
75.00	63.00	68.74	0.0	24.6

Mass Frequency vs Diameter



Summary Report

Full scale pump speed: 3  
Bubble detection: Medium  
Starting Size: 63.00  $\mu\text{m}$   
Ending Size: 0.50  $\mu\text{m}$

Stir time: 30 secs  
Stir speed: Low  
Probe time: 30 secs

Parameter 1 0.000

Parameter 2 0.000

Parameter 3 0.000

Sample: TT-12-08 250 cm  
 Operator: Clint Edrington  
 Submitter: Clint Edrington  
 File Name: C:\EDRING~1\TIGER&~1\SANDFR~1\TT-12-08\12\_250CM.SMP  
 Material/Liquid: silicate mud/water/Water

Reported: 01/03/10 17:36:05      Sample Density: 2.650 g/cm<sup>3</sup>  
 Liquid Visc: 0.7225 cp      Liquid Density: 0.9941 g/cm<sup>3</sup>

## Summary Report

## Mass Distribution Arithmetic Statistics

Mean	81.79	Std. Dev.	10.12
Median	81.14	Coef. Var.	0.124
Mode	82.16	Skewness	1.120
		Kurtosis	5.015

## Selected Percentiles

Percent Finer	Diameter (µm)
100.0	553.2
80.0	88.76
60.0	83.31
40.0	78.98
20.0	73.39

## Selected Sizes

Diameter (µm)	Percent Finer
500.0	100.0
250.0	100.0
125.0	99.8
88.00	77.9
63.00	0.0

Peak Number	% of Dist.*	Mean	Mode	Median	Standard Deviation	Skewness	Kurtosis
1	100.0	81.79	82.16	81.14	10.12	1.120	5.015

\* Peaks must comprise at least 5.00 % of the distribution.



Micromeritics

WIN5100 V2.03

Page 1

Sample: TT-12-08 300 cm  
Operator: Clint Edrington  
Submitter: Clint Edrington  
File Name: C:\EDRING~1\TIGER&~1\SANDFR~1\TT-12-08\12\_300CM.SMP  
Material/Liquid: silicate mud/water/Water

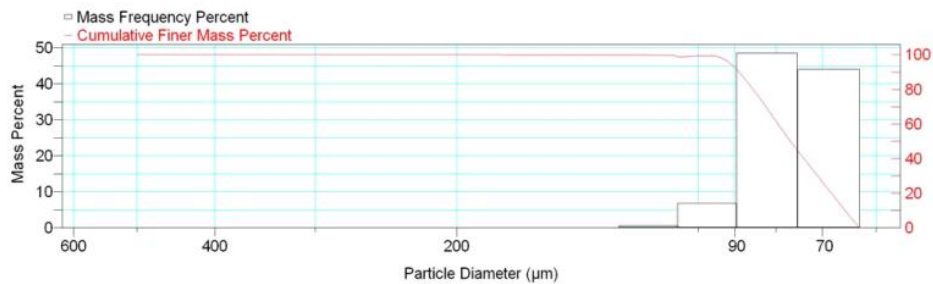
Reported: 01/03/10 17:40:32  
Liquid Visc: 0.7225 cp

Sample Density: 2.650 g/cm<sup>3</sup>  
Liquid Density: 0.9941 g/cm<sup>3</sup>

Report by Size Class

High Diameter ( $\mu\text{m}$ )	Low Diameter ( $\mu\text{m}$ )	Average Diameter ( $\mu\text{m}$ )	Cumulative Mass Finer (Percent)	Mass Frequency (Percent)
600.0	500.0	547.7	100.0	0.0
500.0	425.0	461.0	100.0	0.0
425.0	355.0	388.4	100.0	0.0
355.0	300.0	326.3	100.0	0.0
300.0	250.0	273.9	100.0	0.0
250.0	212.0	230.2	100.0	0.0
212.0	180.0	195.3	100.0	0.0
180.0	150.0	164.3	99.9	0.1
150.0	125.0	136.9	99.9	0.0
125.0	106.0	115.1	99.4	0.5
106.0	90.00	97.67	92.5	6.9
90.00	75.00	82.16	44.0	48.5
75.00	63.00	68.74	0.0	44.0

Mass Frequency vs Diameter



Summary Report

Full scale pump speed: 3  
Bubble detection: Medium  
Starting Size: 63.00  $\mu\text{m}$   
Ending Size: 0.50  $\mu\text{m}$

Stir time: 30 secs  
Stir speed: Low  
Probe time: 30 secs

Parameter 1 0.000

Parameter 2 0.000

Parameter 3 0.000

Sample: TT-12-08 300 cm  
 Operator: Clint Edrington  
 Submitter: Clint Edrington  
 File Name: C:\EDRING~1\TIGER&~1\SANDFR~1\TT-12-08\12\_300CM.SMP  
 Material/Liquid: silicate mud/water/Water

Reported: 01/03/10 17:40:32      Sample Density: 2.650 g/cm<sup>3</sup>  
 Liquid Visc: 0.7225 cp      Liquid Density: 0.9941 g/cm<sup>3</sup>

## Summary Report

Mass Distribution Arithmetic Statistics			
Mean	77.57	Std. Dev.	9.326
Median	76.73	Coef. Var.	0.120
Mode	82.16	Skewness	1.505
		Kurtosis	7.667

Selected Percentiles		Selected Sizes	
Percent Finer	Diameter (µm)	Diameter (µm)	Percent Finer
100.0	553.2	500.0	100.0
80.0	85.42	250.0	100.0
60.0	79.53	125.0	99.9
40.0	73.83	88.00	87.5
20.0	68.24	63.00	0.0

Peak Number	% of Dist.*	Mean	Mode	Median	Standard Deviation	Skewness	Kurtosis
1	99.9	77.48	82.16	76.72	8.918	0.832	0.844

\* Peaks must comprise at least 5.00 % of the distribution.

Micromeritics

WIN5100 V2.03

Page 1

Sample: TT-12-08 350 cm  
Operator: Clint Edrington  
Submitter: Clint Edrington  
File Name: C:\EDRING~1\TIGER&~1\SANDFR~1\TT-12-08\12\_350CM.SMP  
Material/Liquid: silicate mud/water/Water

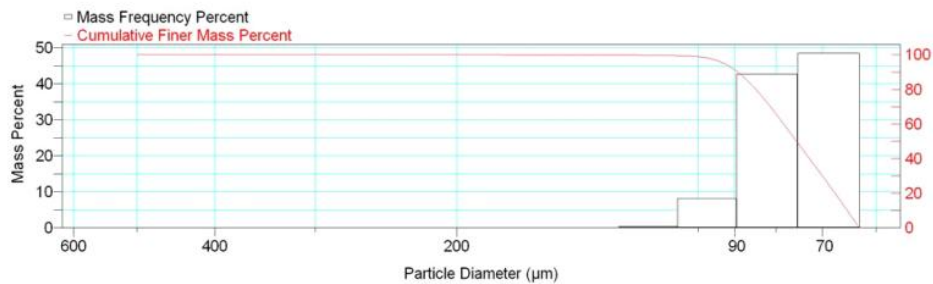
Reported: 01/03/10 17:42:39  
Liquid Visc: 0.7225 cp

Sample Density: 2.650 g/cm<sup>3</sup>  
Liquid Density: 0.9941 g/cm<sup>3</sup>

Report by Size Class

High Diameter ( $\mu$ m)	Low Diameter ( $\mu$ m)	Average Diameter ( $\mu$ m)	Cumulative Mass Finer (Percent)	Mass Frequency (Percent)
600.0	500.0	547.7	100.0	0.0
500.0	425.0	461.0	100.0	0.0
425.0	355.0	388.4	100.0	0.0
355.0	300.0	326.3	100.0	0.0
300.0	250.0	273.9	100.0	0.0
250.0	212.0	230.2	100.0	0.0
212.0	180.0	195.3	100.0	0.0
180.0	150.0	164.3	99.9	0.1
150.0	125.0	136.9	99.8	0.1
125.0	106.0	115.1	99.4	0.4
106.0	90.00	97.67	91.2	8.2
90.00	75.00	82.16	48.5	42.7
75.00	63.00	68.74	0.0	48.5

Mass Frequency vs Diameter



Summary Report

Full scale pump speed: 3  
Bubble detection: Medium  
Starting Size: 63.00  $\mu$ m  
Ending Size: 0.50  $\mu$ m

Stir time: 30 secs  
Stir speed: Low  
Probe time: 30 secs

Parameter 1 0.000

Parameter 2 0.000

Parameter 3 0.000

Sample: TT-12-08 350 cm  
 Operator: Clint Edrington  
 Submitter: Clint Edrington  
 File Name: C:\EDRING~1\TIGER&~1\SANDFR~1\TT-12-08\12\_350CM.SMP  
 Material/Liquid: silicate mud/water/Water

Reported: 01/03/10 17:42:39  
 Liquid Visc: 0.7225 cp

Sample Density: 2.650 g/cm<sup>3</sup>  
 Liquid Density: 0.9941 g/cm<sup>3</sup>

## Summary Report

Mass Distribution Arithmetic Statistics			
Mean	77.19	Std. Dev.	9.823
Median	75.42	Coef. Var.	0.127
Mode	68.74	Skewness	1.642
		Kurtosis	7.288

Selected Percentiles		Selected Sizes	
Percent Finer	Diameter (µm)	Diameter (µm)	Percent Finer
100.0	553.2	500.0	100.0
80.0	84.76	250.0	100.0
60.0	78.25	125.0	99.8
40.0	72.67	88.00	87.5
20.0	67.53	63.00	0.0

Peak Number	% of Dist.*	Mean	Mode	Median	Standard Deviation	Skewness	Kurtosis
1	100.0	77.19	68.74	75.42	9.823	1.642	7.288

\* Peaks must comprise at least 5.00 % of the distribution.

# Micromeritics

WIN5100 V2.03

Page 1

Sample: TT-15-08 3 cm  
Operator: Clint Edrington  
Submitter: Clint Edrington  
File Name: C:\EDRING~1\TIGER&~1\SANDFR~1\TT-15-08\15\_3CM.SMP  
Material/Liquid: silicate mud/water/Water

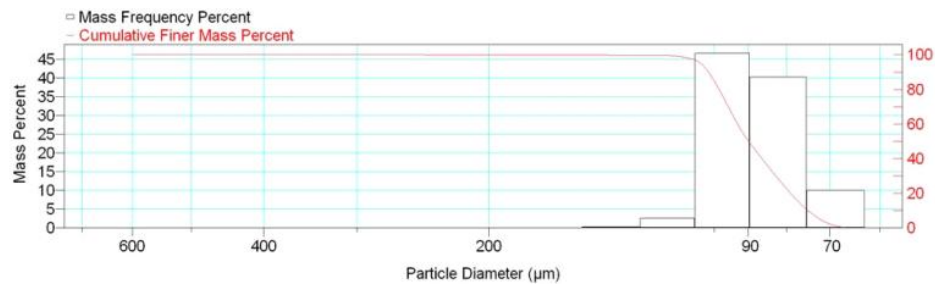
Reported: 01/03/10 17:47:00  
Liquid Visc: 0.7225 cp

Sample Density: 2.650 g/cm<sup>3</sup>  
Liquid Density: 0.9941 g/cm<sup>3</sup>

## Report by Size Class

High Diameter (µm)	Low Diameter (µm)	Average Diameter (µm)	Cumulative Mass Finer (Percent)	Mass Frequency (Percent)
710.0	600.0	652.7	100.0	0.0
600.0	500.0	547.7	100.0	0.0
500.0	425.0	461.0	100.0	0.0
425.0	355.0	388.4	100.0	0.0
355.0	300.0	326.3	100.0	0.0
300.0	250.0	273.9	100.0	0.0
250.0	212.0	230.2	99.9	0.1
212.0	180.0	195.3	99.9	0.0
180.0	150.0	164.3	99.8	0.1
150.0	125.0	136.9	99.5	0.3
125.0	106.0	115.1	96.9	2.6
106.0	90.00	97.67	50.3	46.6
90.00	75.00	82.16	10.0	40.3
75.00	63.00	68.74	0.0	10.0

Mass Frequency vs Diameter



## Summary Report

Full scale pump speed: 3  
Bubble detection: Medium  
Starting Size: 63.00 µm  
Ending Size: 0.50 µm

Stir time: 30 secs  
Stir speed: Low  
Probe time: 30 secs

Sample: TT-15-08 3 cm  
 Operator: Clint Edrington  
 Submitter: Clint Edrington  
 File Name: C:\EDRING~1\TIGER&~1\SANDFR~1\TT-15-08\15\_3CM.SMP  
 Material/Liquid: silicate mud/water/Water

Reported: 01/03/10 17:47:00  
 Liquid Visc: 0.7225 cp

Sample Density: 2.650 g/cm<sup>3</sup>  
 Liquid Density: 0.9941 g/cm<sup>3</sup>

## Summary Report

Parameter 1 0.000

Parameter 2 0.000

Parameter 3 0.000

## Mass Distribution Arithmetic Statistics

Mean	89.30	Std. Dev.	12.05
Median	89.89	Coef. Var.	0.135
Mode	97.67	Skewness	1.859
		Kurtosis	19.521

## Selected Percentiles

Percent Finer	Diameter (µm)
100.0	651.9
80.0	98.44
60.0	93.01
40.0	86.27
20.0	79.00

## Selected Sizes

Diameter (µm)	Percent Finer
500.0	100.0
250.0	100.0
125.0	99.5
88.00	44.8
63.00	0.0

Peak Number	% of Dist. *	Mean	Mode	Median	Standard Deviation	Skewness	Kurtosis
1	99.9	89.16	97.67	89.87	11.20	0.360	2.104

\* Peaks must comprise at least 5.00 % of the distribution.

Micromeritics

WIN5100 V2.03

Page 1

Sample: TT-15-08 60 cm  
Operator: Clint Edrington  
Submitter: Clint Edrington  
File Name: C:\EDRING~1\TIGER&~1\SANDFR~1\TT-15-08\15\_60CM.SMP  
Material/Liquid: silicate mud/water/Water

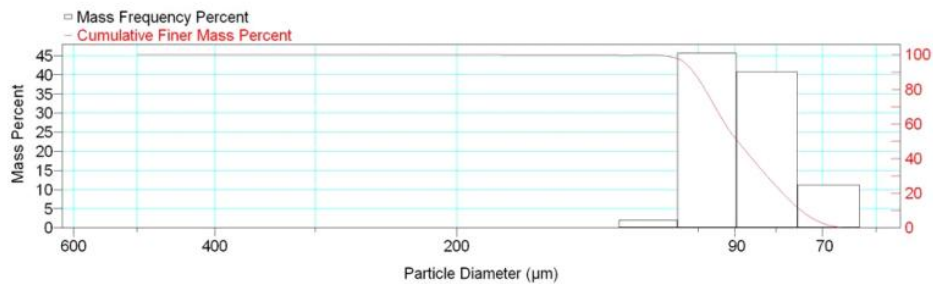
Reported: 01/03/10 17:49:07  
Liquid Visc: 0.7225 cp

Sample Density: 2.650 g/cm<sup>3</sup>  
Liquid Density: 0.9941 g/cm<sup>3</sup>

Report by Size Class

High Diameter ( $\mu$ m)	Low Diameter ( $\mu$ m)	Average Diameter ( $\mu$ m)	Cumulative Mass Finer (Percent)	Mass Frequency (Percent)
600.0	500.0	547.7	100.0	0.0
500.0	425.0	461.0	100.0	0.0
425.0	355.0	388.4	100.0	0.0
355.0	300.0	326.3	100.0	0.0
300.0	250.0	273.9	100.0	0.0
250.0	212.0	230.2	100.0	0.0
212.0	180.0	195.3	100.0	0.0
180.0	150.0	164.3	99.9	0.1
150.0	125.0	136.9	99.8	0.1
125.0	106.0	115.1	97.7	2.1
106.0	90.00	97.67	52.0	45.7
90.00	75.00	82.16	11.2	40.8
75.00	63.00	68.74	0.0	11.2

Mass Frequency vs Diameter



Summary Report

Full scale pump speed: 3  
Bubble detection: Medium  
Starting Size: 63.00  $\mu$ m  
Ending Size: 0.50  $\mu$ m

Stir time: 30 secs  
Stir speed: Low  
Probe time: 30 secs

Parameter 1 0.000

Parameter 2 0.000

Parameter 3 0.000

Sample: TT-15-08 60 cm  
 Operator: Clint Edrington  
 Submitter: Clint Edrington  
 File Name: C:\EDRING~1\TIGER&~1\SANDFR~1\TT-15-08\15\_60CM.SMP  
 Material/Liquid: silicate mud/water/Water

Reported: 01/03/10 17:49:07  
 Liquid Visc: 0.7225 cp

Sample Density: 2.650 g/cm<sup>3</sup>  
 Liquid Density: 0.9941 g/cm<sup>3</sup>

## Summary Report

## Mass Distribution Arithmetic Statistics

Mean	88.57	Std. Dev.	11.03
Median	89.27	Coef. Var.	0.124
Mode	97.67	Skewness	0.226
		Kurtosis	1.734

## Selected Percentiles

Percent Finer	Diameter (µm)
100.0	553.2
80.0	98.07
60.0	92.55
40.0	85.66
20.0	78.44

## Selected Sizes

Diameter (µm)	Percent Finer
500.0	100.0
250.0	100.0
125.0	99.8
88.00	46.5
63.00	0.0

Peak Number	% of Dist.*	Mean	Mode	Median	Standard Deviation	Skewness	Kurtosis
1	100.0	88.57	97.67	89.27	11.03	0.226	1.734

\* Peaks must comprise at least 5.00 % of the distribution.



# Micromeritics

WIN5100 V2.03

Page 1

Sample: TT-15-08 120 cm  
Operator: Clint Edrington  
Submitter: Clint Edrington  
File Name: C:\EDRING~1\TIGER&~1\SANDFR~1\TT-15-08\15\_120CM.SMP  
Material/Liquid: silicate mud/water/Water

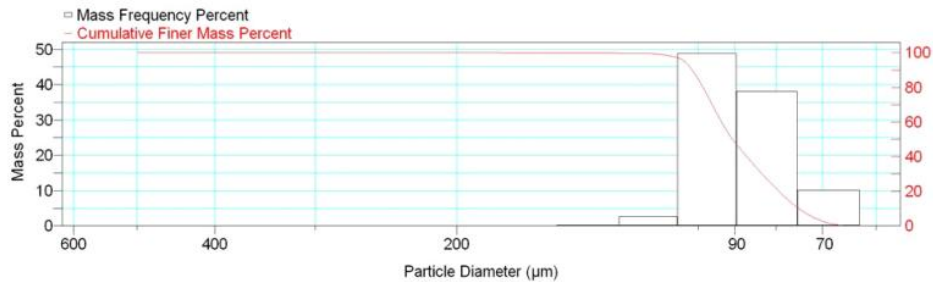
Reported: 01/03/10 17:51:35  
Liquid Visc: 0.7225 cp

Sample Density: 2.650 g/cm<sup>3</sup>  
Liquid Density: 0.9941 g/cm<sup>3</sup>

## Report by Size Class

High Diameter (µm)	Low Diameter (µm)	Average Diameter (µm)	Cumulative Mass Finer (Percent)	Mass Frequency (Percent)
600.0	500.0	547.7	100.0	0.0
500.0	425.0	461.0	100.0	0.0
425.0	355.0	388.4	100.0	0.0
355.0	300.0	326.3	100.0	0.0
300.0	250.0	273.9	100.0	0.0
250.0	212.0	230.2	100.0	0.0
212.0	180.0	195.3	100.0	0.0
180.0	150.0	164.3	99.9	0.1
150.0	125.0	136.9	99.7	0.2
125.0	106.0	115.1	97.1	2.6
106.0	90.00	97.67	48.2	48.9
90.00	75.00	82.16	10.1	38.1
75.00	63.00	68.74	0.0	10.1

Mass Frequency vs Diameter



## Summary Report

Full scale pump speed: 3  
Bubble detection: Medium  
Starting Size: 63.00 µm  
Ending Size: 0.50 µm

Stir time: 30 secs  
Stir speed: Low  
Probe time: 30 secs

Parameter 1 0.000

Parameter 2 0.000

Parameter 3 0.000

Sample: TT-15-08 120 cm  
 Operator: Clint Edrington  
 Submitter: Clint Edrington  
 File Name: C:\EDRING~1\TIGER&~1\SANDFR~1\TT-15-08\15\_120CM.SMP  
 Material/Liquid: silicate mud/water/Water

Reported: 01/03/10 17:51:35  
 Liquid Visc: 0.7225 cp

Sample Density: 2.650 g/cm<sup>3</sup>  
 Liquid Density: 0.9941 g/cm<sup>3</sup>

## Summary Report

## Mass Distribution Arithmetic Statistics

Mean	89.44	Std. Dev.	11.13
Median	90.64	Coef. Var.	0.124
Mode	97.67	Skewness	0.221
		Kurtosis	1.872

## Selected Percentiles

Percent Finer	Diameter (µm)
100.0	553.2
80.0	98.63
60.0	93.51
40.0	86.95
20.0	79.35

## Selected Sizes

Diameter (µm)	Percent Finer
500.0	100.0
250.0	100.0
125.0	99.7
88.00	42.8
63.00	0.0

Peak Number	% of Dist.*	Mean	Mode	Median	Standard Deviation	Skewness	Kurtosis
1	100.0	89.44	97.67	90.64	11.13	0.221	1.872

\* Peaks must comprise at least 5.00 % of the distribution.

# Micromeritics

WIN5100 V2.03

Page 1

Sample: TT-19-08 6 cm  
Operator: Clint Edrington  
Submitter: Clint Edrington  
File Name: C:\EDRING~1\TIGER&~1\SANDFR~1\TT-19-08\19\_6CM.SMP  
Material/Liquid: silicate mud/water/Water

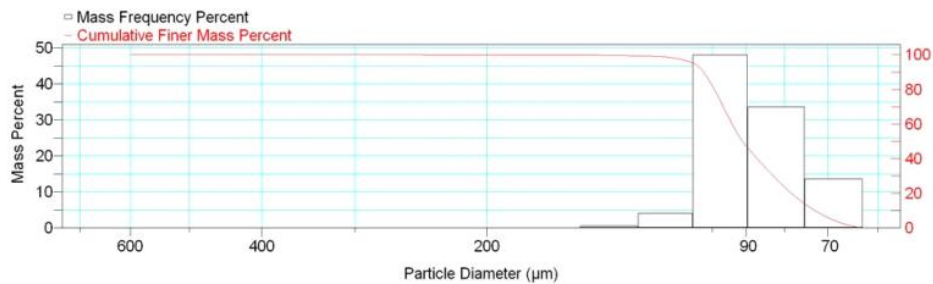
Reported: 01/03/10 17:54:26  
Liquid Visc: 0.7225 cp

Sample Density: 2.650 g/cm<sup>3</sup>  
Liquid Density: 0.9941 g/cm<sup>3</sup>

## Report by Size Class

High Diameter (μm)	Low Diameter (μm)	Average Diameter (μm)	Cumulative Mass Finer (Percent)	Mass Frequency (Percent)
710.0	600.0	652.7	100.0	0.0
600.0	500.0	547.7	100.0	0.0
500.0	425.0	461.0	100.0	0.0
425.0	355.0	388.4	100.0	0.0
355.0	300.0	326.3	100.0	0.0
300.0	250.0	273.9	100.0	0.0
250.0	212.0	230.2	99.9	0.1
212.0	180.0	195.3	99.9	0.0
180.0	150.0	164.3	99.8	0.1
150.0	125.0	136.9	99.3	0.5
125.0	106.0	115.1	95.2	4.1
106.0	90.00	97.67	47.2	48.0
90.00	75.00	82.16	13.6	33.6
75.00	63.00	68.74	0.0	13.6

Mass Frequency vs Diameter



## Summary Report

Full scale pump speed: 3  
Bubble detection: Medium  
Starting Size: 63.00 μm  
Ending Size: 0.50 μm

Stir time: 30 secs  
Stir speed: Low  
Probe time: 30 secs

Sample: TT-19-08 6 cm  
 Operator: Clint Edrington  
 Submitter: Clint Edrington  
 File Name: C:\EDRING~1\TIGER&~1\SANDFR~1\TT-19-08\19\_6CM.SMP  
 Material/Liquid: silicate mud/water/Water

Reported: 01/03/10 17:54:26  
 Liquid Visc: 0.7225 cp

Sample Density: 2.650 g/cm<sup>3</sup>  
 Liquid Density: 0.9941 g/cm<sup>3</sup>

## Summary Report

Parameter 1 0.000

Parameter 2 0.000

Parameter 3 0.000

## Mass Distribution Arithmetic Statistics

Mean	89.64	Std. Dev.	13.13
Median	91.05	Coef. Var.	0.146
Mode	97.67	Skewness	1.445
		Kurtosis	13.603

## Selected Percentiles

Percent Finer	Diameter (µm)
100.0	651.9
80.0	99.28
60.0	94.00
40.0	87.01
20.0	78.33

## Selected Sizes

Diameter (µm)	Percent Finer
500.0	100.0
250.0	100.0
125.0	99.3
88.00	42.4
63.00	0.0

Peak Number	% of Dist. *	Mean	Mode	Median	Standard Deviation	Skewness	Kurtosis
1	99.9	89.49	97.67	91.04	12.36	0.295	1.409

\* Peaks must comprise at least 5.00 % of the distribution.

# Micromeritics

WIN5100 V2.03

Page 1

Sample: TT-19-08 50 cm  
Operator: Clint Edrington  
Submitter: Clint Edrington  
File Name: C:\EDRING~1\TIGER&~1\SANDFR~1\TT-19-08\19\_50CM.SMP  
Material/Liquid: silicate mud/water/Water

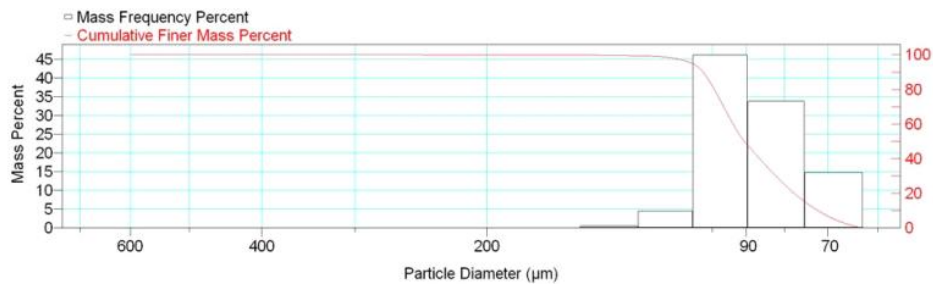
Reported: 01/03/10 17:57:23  
Liquid Visc: 0.7225 cp

Sample Density: 2.650 g/cm<sup>3</sup>  
Liquid Density: 0.9941 g/cm<sup>3</sup>

## Report by Size Class

High Diameter (µm)	Low Diameter (µm)	Average Diameter (µm)	Cumulative Mass Finer (Percent)	Mass Frequency (Percent)
710.0	600.0	652.7	100.0	0.0
600.0	500.0	547.7	100.0	0.0
500.0	425.0	461.0	100.0	0.0
425.0	355.0	388.4	100.0	0.0
355.0	300.0	326.3	100.0	0.0
300.0	250.0	273.9	100.0	0.0
250.0	212.0	230.2	99.9	0.1
212.0	180.0	195.3	99.9	0.0
180.0	150.0	164.3	99.8	0.1
150.0	125.0	136.9	99.3	0.5
125.0	106.0	115.1	94.8	4.5
106.0	90.00	97.67	48.6	46.2
90.00	75.00	82.16	14.8	33.8
75.00	63.00	68.74	0.0	14.8

Mass Frequency vs Diameter



## Summary Report

Full scale pump speed: 3  
Bubble detection: Medium  
Starting Size: 63.00 µm  
Ending Size: 0.50 µm

Stir time: 30 secs  
Stir speed: Low  
Probe time: 30 secs

Sample: TT-19-08 50 cm  
 Operator: Clint Edrington  
 Submitter: Clint Edrington  
 File Name: C:\EDRING~1\TIGER&~1\SANDFR~1\TT-19-08\19\_50CM.SMP  
 Material/Liquid: silicate mud/water/Water

Reported: 01/03/10 17:57:23  
 Liquid Visc: 0.7225 cp

Sample Density: 2.650 g/cm<sup>3</sup>  
 Liquid Density: 0.9941 g/cm<sup>3</sup>

## Summary Report

Parameter 1 0.000

Parameter 2 0.000

Parameter 3 0.000

## Mass Distribution Arithmetic Statistics

Mean	89.33	Std. Dev.	13.38
Median	90.56	Coef. Var.	0.150
Mode	97.67	Skewness	1.412
		Kurtosis	12.634

## Selected Percentiles

Percent Finer	Diameter (µm)
100.0	651.9
80.0	99.28
60.0	93.73
40.0	86.40
20.0	77.67

## Selected Sizes

Diameter (µm)	Percent Finer
500.0	100.0
250.0	100.0
125.0	99.3
88.00	43.8
63.00	0.0

Peak Number	% of Dist. *	Mean	Mode	Median	Standard Deviation	Skewness	Kurtosis
1	99.9	89.19	97.67	90.54	12.62	0.325	1.231

\* Peaks must comprise at least 5.00 % of the distribution.

# Micromeritics

WIN5100 V2.03

Page 1

Sample: TT-19-08 104 cm  
Operator: Clint Edrington  
Submitter: Clint Edrington  
File Name: C:\EDRING~1\TIGER&~1\SANDFR~1\TT-19-08\19\_104CM.SMP  
Material/Liquid: silicate mud/water/Water

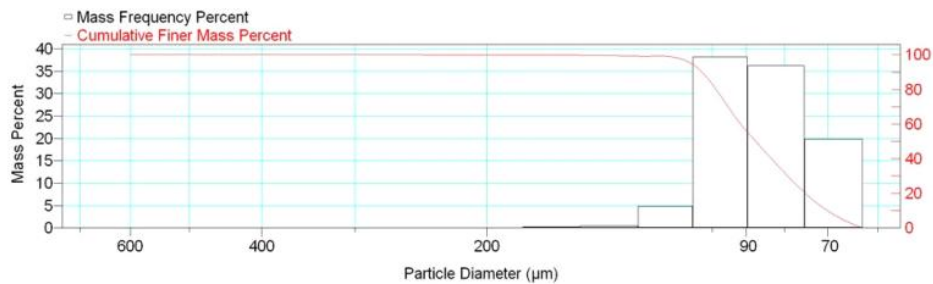
Reported: 01/03/10 17:59:27  
Liquid Visc: 0.7225 cp

Sample Density: 2.650 g/cm<sup>3</sup>  
Liquid Density: 0.9941 g/cm<sup>3</sup>

## Report by Size Class

High Diameter (µm)	Low Diameter (µm)	Average Diameter (µm)	Cumulative Mass Finer (Percent)	Mass Frequency (Percent)
710.0	600.0	652.7	100.0	0.0
600.0	500.0	547.7	100.0	0.0
500.0	425.0	461.0	100.0	0.0
425.0	355.0	388.4	100.0	0.0
355.0	300.0	326.3	100.0	0.0
300.0	250.0	273.9	100.0	0.0
250.0	212.0	230.2	99.9	0.1
212.0	180.0	195.3	99.9	0.0
180.0	150.0	164.3	99.7	0.2
150.0	125.0	136.9	99.2	0.5
125.0	106.0	115.1	94.3	4.9
106.0	90.00	97.67	56.1	38.2
90.00	75.00	82.16	19.9	36.2
75.00	63.00	68.74	0.0	19.9

Mass Frequency vs Diameter



## Summary Report

Full scale pump speed: 3  
Bubble detection: Medium  
Starting Size: 63.00 µm  
Ending Size: 0.50 µm

Stir time: 30 secs  
Stir speed: Low  
Probe time: 30 secs

Sample: TT-19-08 104 cm  
 Operator: Clint Edrington  
 Submitter: Clint Edrington  
 File Name: C:\EDRING~1\TIGER&~1\SANDFR~1\TT-19-08\19\_104CM.SMP  
 Material/Liquid: silicate mud/water/Water

Reported: 01/03/10 17:59:27  
 Liquid Visc: 0.7225 cp

Sample Density: 2.650 g/cm<sup>3</sup>  
 Liquid Density: 0.9941 g/cm<sup>3</sup>

## Summary Report

Parameter 1 0.000

Parameter 2 0.000

Parameter 3 0.000

## Mass Distribution Arithmetic Statistics

Mean	87.62	Std. Dev.	14.20
Median	87.41	Coef. Var.	0.162
Mode	97.67	Skewness	1.541
		Kurtosis	11.016

## Selected Percentiles

Percent Finer	Diameter (µm)
100.0	651.9
80.0	98.77
60.0	91.58
40.0	83.30
20.0	75.04

## Selected Sizes

Diameter (µm)	Percent Finer
500.0	100.0
250.0	100.0
125.0	99.2
88.00	51.4
63.00	0.0

Peak Number	% of Dist. *	Mean	Mode	Median	Standard Deviation	Skewness	Kurtosis
1	99.9	87.47	97.67	87.39	13.47	0.651	1.778

\* Peaks must comprise at least 5.00 % of the distribution.



# Micromeritics

WIN5100 V2.03

Page 1

Sample: TT-19-08 150 cm  
Operator: Clint Edrington  
Submitter: Clint Edrington  
File Name: C:\EDRING~1\TIGER&~1\SANDFR~1\TT-19-08\19\_150CM.SMP  
Material/Liquid: silicate mud/water/Water

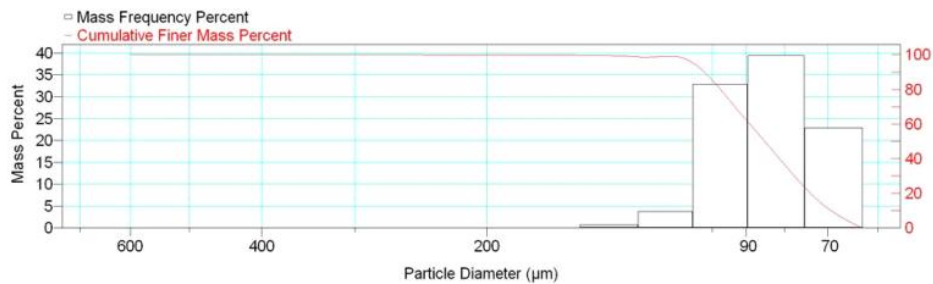
Reported: 01/03/10 18:01:35  
Liquid Visc: 0.7225 cp

Sample Density: 2.650 g/cm<sup>3</sup>  
Liquid Density: 0.9941 g/cm<sup>3</sup>

## Report by Size Class

High Diameter (µm)	Low Diameter (µm)	Average Diameter (µm)	Cumulative Mass Finer (Percent)	Mass Frequency (Percent)
710.0	600.0	652.7	100.0	0.0
600.0	500.0	547.7	100.0	0.0
500.0	425.0	461.0	100.0	0.0
425.0	355.0	388.4	100.0	0.0
355.0	300.0	326.3	100.0	0.0
300.0	250.0	273.9	100.0	0.0
250.0	212.0	230.2	99.9	0.1
212.0	180.0	195.3	99.8	0.1
180.0	150.0	164.3	99.7	0.1
150.0	125.0	136.9	99.0	0.7
125.0	106.0	115.1	95.2	3.8
106.0	90.00	97.67	62.3	32.9
90.00	75.00	82.16	22.9	39.4
75.00	63.00	68.74	0.0	22.9

Mass Frequency vs Diameter



## Summary Report

Full scale pump speed: 3  
Bubble detection: Medium  
Starting Size: 63.00 µm  
Ending Size: 0.50 µm

Stir time: 30 secs  
Stir speed: Low  
Probe time: 30 secs

Sample: TT-19-08 150 cm  
 Operator: Clint Edrington  
 Submitter: Clint Edrington  
 File Name: C:\EDRING~1\TIGER&~1\SANDFR~1\TT-19-08\19\_150CM.SMP  
 Material/Liquid: silicate mud/water/Water

Reported: 01/03/10 18:01:35  
 Liquid Visc: 0.7225 cp

Sample Density: 2.650 g/cm<sup>3</sup>  
 Liquid Density: 0.9941 g/cm<sup>3</sup>

## Summary Report

Parameter 1 0.000

Parameter 2 0.000

Parameter 3 0.000

## Mass Distribution Arithmetic Statistics

Mean	86.17	Std. Dev.	14.43
Median	85.03	Coef. Var.	0.167
Mode	82.16	Skewness	1.955
		Kurtosis	13.398

## Selected Percentiles

Percent Finer	Diameter (µm)
100.0	651.9
80.0	97.42
60.0	89.03
40.0	81.26
20.0	73.89

## Selected Sizes

Diameter (µm)	Percent Finer
500.0	100.0
250.0	100.0
125.0	99.0
88.00	57.5
63.00	0.0

Peak Number	% of Dist. *	Mean	Mode	Median	Standard Deviation	Skewness	Kurtosis
1	99.8	85.91	82.16	84.99	13.26	0.736	1.515

\* Peaks must comprise at least 5.00 % of the distribution.

Micromeritics

WIN5100 V2.03

Page 1

Sample: TT-19-08 200 cm  
Operator: Clint Edrington  
Submitter: Clint Edrington  
File Name: C:\EDRING~1\TIGER&~1\SANDFR~1\TT-19-08\19\_200CM.SMP  
Material/Liquid: silicate mud/water/Water

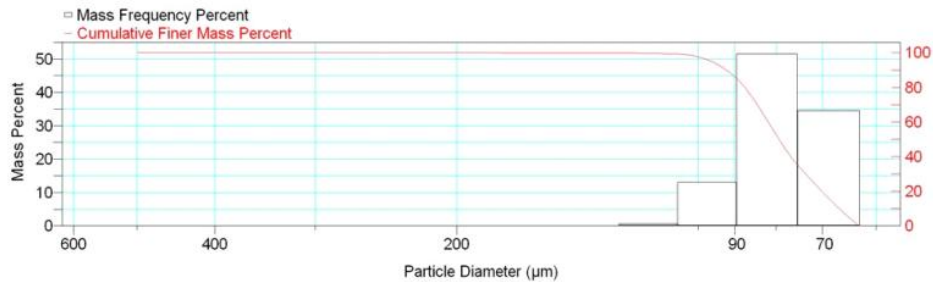
Reported: 01/03/10 18:04:06  
Liquid Visc: 0.7225 cp

Sample Density: 2.650 g/cm<sup>3</sup>  
Liquid Density: 0.9941 g/cm<sup>3</sup>

Report by Size Class

High Diameter ( $\mu$ m)	Low Diameter ( $\mu$ m)	Average Diameter ( $\mu$ m)	Cumulative Mass Finer (Percent)	Mass Frequency (Percent)
600.0	500.0	547.7	100.0	0.0
500.0	425.0	461.0	100.0	0.0
425.0	355.0	388.4	100.0	0.0
355.0	300.0	326.3	100.0	0.0
300.0	250.0	273.9	100.0	0.0
250.0	212.0	230.2	100.0	0.0
212.0	180.0	195.3	100.0	0.0
180.0	150.0	164.3	99.9	0.1
150.0	125.0	136.9	99.8	0.1
125.0	106.0	115.1	99.2	0.6
106.0	90.00	97.67	86.1	13.1
90.00	75.00	82.16	34.6	51.5
75.00	63.00	68.74	0.0	34.6

Mass Frequency vs Diameter



Summary Report

Full scale pump speed: 3  
Bubble detection: Medium  
Starting Size: 63.00  $\mu$ m  
Ending Size: 0.50  $\mu$ m

Stir time: 30 secs  
Stir speed: Low  
Probe time: 30 secs

Parameter 1 0.000

Parameter 2 0.000

Parameter 3 0.000

Sample: TT-19-08 200 cm  
 Operator: Clint Edrington  
 Submitter: Clint Edrington  
 File Name: C:\EDRING~1\TIGER&~1\SANDFR~1\TT-19-08\19\_200CM.SMP  
 Material/Liquid: silicate mud/water/Water

Reported: 01/03/10 18:04:06      Sample Density: 2.650 g/cm<sup>3</sup>  
 Liquid Visc: 0.7225 cp      Liquid Density: 0.9941 g/cm<sup>3</sup>

## Summary Report

Mass Distribution Arithmetic Statistics			
Mean	79.88	Std. Dev.	10.24
Median	79.30	Coef. Var.	0.128
Mode	82.16	Skewness	1.223
		Kurtosis	5.096

Selected Percentiles		Selected Sizes	
Percent Finer	Diameter (µm)	Diameter (µm)	Percent Finer
100.0	553.2	500.0	100.0
80.0	87.48	250.0	100.0
60.0	81.80	125.0	99.8
40.0	76.65	88.00	81.4
20.0	70.14	63.00	0.0

Peak Number	% of Dist.*	Mean	Mode	Median	Standard Deviation	Skewness	Kurtosis
1	100.0	79.88	82.16	79.30	10.24	1.223	5.096

\* Peaks must comprise at least 5.00 % of the distribution.

Micromeritics

WIN5100 V2.03

Page 1

Sample: TT-19-08 250 cm  
Operator: Clint Edrington  
Submitter: Clint Edrington  
File Name: C:\EDRING~1\TIGER&~1\SANDFR~1\TT-19-08\19\_250CM.SMP  
Material/Liquid: silicate mud/water/Water

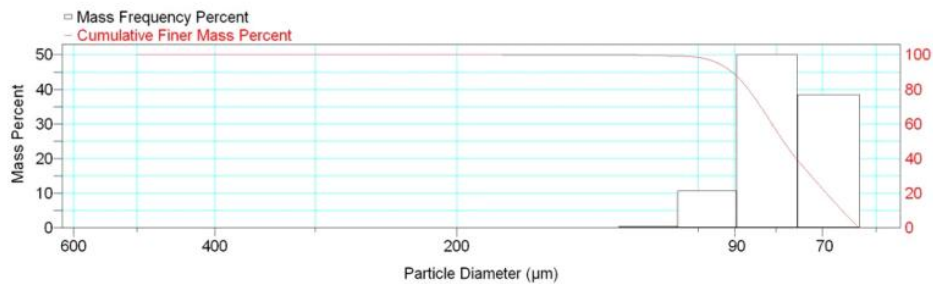
Reported: 01/03/10 18:06:31  
Liquid Visc: 0.7225 cp

Sample Density: 2.650 g/cm<sup>3</sup>  
Liquid Density: 0.9941 g/cm<sup>3</sup>

Report by Size Class

High Diameter ( $\mu\text{m}$ )	Low Diameter ( $\mu\text{m}$ )	Average Diameter ( $\mu\text{m}$ )	Cumulative Mass Finer (Percent)	Mass Frequency (Percent)
600.0	500.0	547.7	100.0	0.0
500.0	425.0	461.0	100.0	0.0
425.0	355.0	388.4	100.0	0.0
355.0	300.0	326.3	100.0	0.0
300.0	250.0	273.9	100.0	0.0
250.0	212.0	230.2	100.0	0.0
212.0	180.0	195.3	100.0	0.0
180.0	150.0	164.3	99.9	0.1
150.0	125.0	136.9	99.8	0.1
125.0	106.0	115.1	99.3	0.5
106.0	90.00	97.67	88.6	10.7
90.00	75.00	82.16	38.5	50.1
75.00	63.00	68.74	0.0	38.5

Mass Frequency vs Diameter



Summary Report

Full scale pump speed: 3  
Bubble detection: Medium  
Starting Size: 63.00  $\mu\text{m}$   
Ending Size: 0.50  $\mu\text{m}$

Stir time: 30 secs  
Stir speed: Low  
Probe time: 30 secs

Parameter 1 0.000

Parameter 2 0.000

Parameter 3 0.000

Sample: TT-19-08 250 cm  
 Operator: Clint Edrington  
 Submitter: Clint Edrington  
 File Name: C:\EDRING~1\TIGER&~1\SANDFR~1\TT-19-08\19\_250CM.SMP  
 Material/Liquid: silicate mud/water/Water

Reported: 01/03/10 18:06:31  
 Liquid Visc: 0.7225 cp

Sample Density: 2.650 g/cm<sup>3</sup>  
 Liquid Density: 0.9941 g/cm<sup>3</sup>

## Summary Report

Mass Distribution Arithmetic Statistics			
Mean	78.95	Std. Dev.	10.000
Median	78.30	Coef. Var.	0.127
Mode	82.16	Skewness	1.361
		Kurtosis	6.033

Selected Percentiles		Selected Sizes	
Percent Finer	Diameter (µm)	Diameter (µm)	Percent Finer
100.0	553.2	500.0	100.0
80.0	86.58	250.0	100.0
60.0	80.90	125.0	99.8
40.0	75.47	88.00	84.0
20.0	69.22	63.00	0.0

Peak Number	% of Dist.*	Mean	Mode	Median	Standard Deviation	Skewness	Kurtosis
1	100.0	78.95	82.16	78.30	10.000	1.361	6.033

\* Peaks must comprise at least 5.00 % of the distribution.

Micromeritics

WIN5100 V2.03

Page 1

Sample: TT-20-08 5 cm  
Operator: Clint Edrington  
Submitter: Clint Edrington  
File Name: C:\EDRING~1\TIGER&~1\SANDFR~1\TT-20-08\20\_5CM.SMP  
Material/Liquid: silicate mud/water/Water

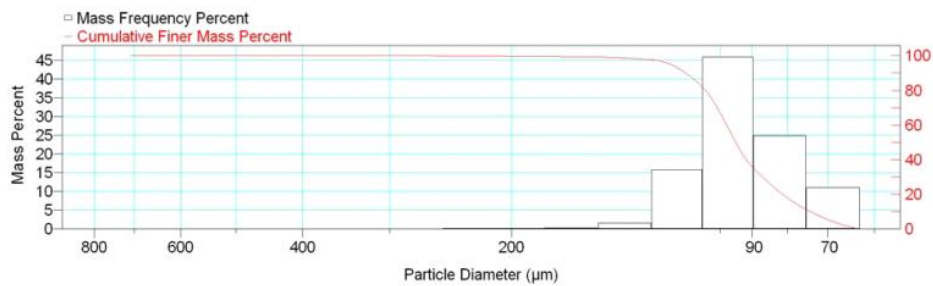
Reported: 01/03/10 18:10:19  
Liquid Visc: 0.7225 cp

Sample Density: 2.650 g/cm<sup>3</sup>  
Liquid Density: 0.9941 g/cm<sup>3</sup>

Report by Size Class

High Diameter ( $\mu\text{m}$ )	Low Diameter ( $\mu\text{m}$ )	Average Diameter ( $\mu\text{m}$ )	Cumulative Mass Finer (Percent)	Mass Frequency (Percent)
850.0	710.0	776.9	100.0	0.0
710.0	600.0	652.7	100.0	0.0
600.0	500.0	547.7	100.0	0.0
500.0	425.0	461.0	100.0	0.0
425.0	355.0	388.4	100.0	0.0
355.0	300.0	326.3	100.0	0.0
300.0	250.0	273.9	99.9	0.1
250.0	212.0	230.2	99.7	0.2
212.0	180.0	195.3	99.5	0.2
180.0	150.0	164.3	99.2	0.3
150.0	125.0	136.9	97.6	1.6
125.0	106.0	115.1	81.8	15.8
106.0	90.00	97.67	35.9	45.9
90.00	75.00	82.16	11.0	24.9
75.00	63.00	68.74	0.0	11.0

Mass Frequency vs Diameter



Summary Report

Full scale pump speed: 3  
Bubble detection: Medium  
Starting Size: 63.00  $\mu\text{m}$   
Ending Size: 0.50  $\mu\text{m}$

Stir time: 30 secs  
Stir speed: Low  
Probe time: 30 secs

Sample: TT-20-08 5 cm  
 Operator: Clint Edrington  
 Submitter: Clint Edrington  
 File Name: C:\EDRING~1\TIGER&~1\SANDFR~1\TT-20-08\20\_5CM.SMP  
 Material/Liquid: silicate mud/water/Water

Reported: 01/03/10 18:10:19  
 Liquid Visc: 0.7225 cp

Sample Density: 2.650 g/cm<sup>3</sup>  
 Liquid Density: 0.9941 g/cm<sup>3</sup>

## Summary Report

Parameter 1	0.000	Parameter 2	0.000	Parameter 3	0.000		
Mass Distribution Arithmetic Statistics							
Mean	94.85	Std. Dev.		17.76			
Median	95.02	Coef. Var.		0.187			
Mode	97.67	Skewness		2.462			
		Kurtosis		18.192			
Selected Percentiles			Selected Sizes				
Percent Finer	Diameter (µm)		Diameter (µm)	Percent Finer			
100.0	714.1		500.0	100.0			
80.0	105.0		250.0	99.9			
60.0	97.94		125.0	97.6			
40.0	91.75		88.00	32.0			
20.0	81.31		63.00	0.0			
Peak Number	% of Dist.*	Mean	Mode	Median	Standard Deviation	Skewness	Kurtosis
1	100.0	94.85	97.67	95.02	17.76	2.462	18.192

\* Peaks must comprise at least 5.00 % of the distribution.



# Micromeritics

WIN5100 V2.03

Page 1

Sample: TT-20-08 15 cm  
Operator: Clint Edrington  
Submitter: Clint Edrington  
File Name: C:\EDRING~1\TIGER&~1\SANDFR~1\TT-20-08\20\_15CM.SMP  
Material/Liquid: silicate mud/water/Water

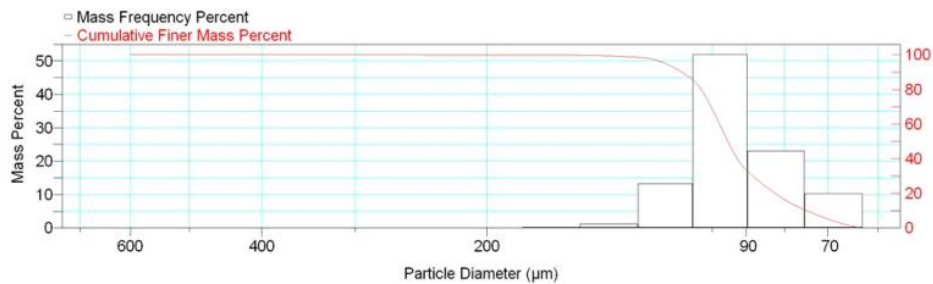
Reported: 01/03/10 18:12:58  
Liquid Visc: 0.7225 cp

Sample Density: 2.650 g/cm<sup>3</sup>  
Liquid Density: 0.9941 g/cm<sup>3</sup>

## Report by Size Class

High Diameter (μm)	Low Diameter (μm)	Average Diameter (μm)	Cumulative Mass Finer (Percent)	Mass Frequency (Percent)
710.0	600.0	652.7	100.0	0.0
600.0	500.0	547.7	100.0	0.0
500.0	425.0	461.0	100.0	0.0
425.0	355.0	388.4	100.0	0.0
355.0	300.0	326.3	100.0	0.0
300.0	250.0	273.9	100.0	0.0
250.0	212.0	230.2	99.9	0.1
212.0	180.0	195.3	99.9	0.0
180.0	150.0	164.3	99.7	0.2
150.0	125.0	136.9	98.5	1.2
125.0	106.0	115.1	85.3	13.2
106.0	90.00	97.67	33.3	52.0
90.00	75.00	82.16	10.2	23.1
75.00	63.00	68.74	0.0	10.2

Mass Frequency vs Diameter



## Summary Report

Full scale pump speed: 3  
Bubble detection: Medium  
Starting Size: 63.00 μm  
Ending Size: 0.50 μm

Stir time: 30 secs  
Stir speed: Low  
Probe time: 30 secs

Sample: TT-20-08 15 cm  
 Operator: Clint Edrington  
 Submitter: Clint Edrington  
 File Name: C:\EDRING~1\TIGER&~1\SANDFR~1\TT-20-08\20\_15CM.SMP  
 Material/Liquid: silicate mud/water/Water

Reported: 01/03/10 18:12:58  
 Liquid Visc: 0.7225 cp

Sample Density: 2.650 g/cm<sup>3</sup>  
 Liquid Density: 0.9941 g/cm<sup>3</sup>

## Summary Report

Parameter 1 0.000

Parameter 2 0.000

Parameter 3 0.000

## Mass Distribution Arithmetic Statistics

Mean	94.18	Std. Dev.	14.62
Median	95.27	Coef. Var.	0.155
Mode	97.67	Skewness	1.055
		Kurtosis	8.021

## Selected Percentiles

Percent Finer	Diameter (µm)
100.0	651.9
80.0	103.4
60.0	97.73
40.0	92.55
20.0	82.39

## Selected Sizes

Diameter (µm)	Percent Finer
500.0	100.0
250.0	100.0
125.0	98.5
88.00	29.6
63.00	0.0

Peak Number	% of Dist. *	Mean	Mode	Median	Standard Deviation	Skewness	Kurtosis
1	99.9	94.04	97.67	95.26	13.98	0.315	1.240

\* Peaks must comprise at least 5.00 % of the distribution.

# Micromeritics

WIN5100 V2.03

Page 1

Sample: TT-20-08 50 cm  
Operator: Clint Edrington  
Submitter: Clint Edrington  
File Name: C:\EDRING~1\TIGER&~1\SANDFR~1\TT-20-08\20\_50CM.SMP  
Material/Liquid: silicate mud/water/Water

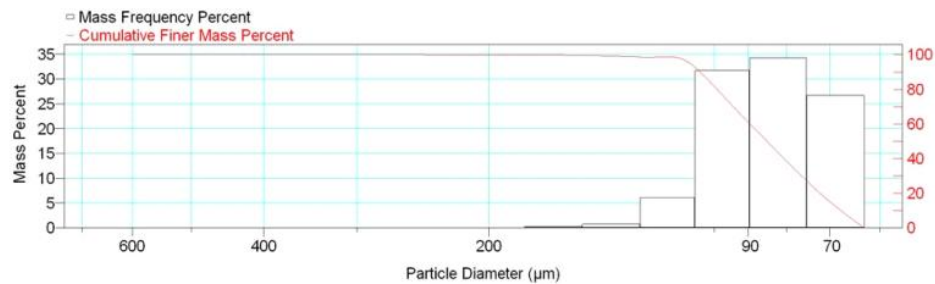
Reported: 01/03/10 18:15:19  
Liquid Visc: 0.7225 cp

Sample Density: 2.650 g/cm<sup>3</sup>  
Liquid Density: 0.9941 g/cm<sup>3</sup>

## Report by Size Class

High Diameter (μm)	Low Diameter (μm)	Average Diameter (μm)	Cumulative Mass Finer (Percent)	Mass Frequency (Percent)
710.0	600.0	652.7	100.0	0.0
600.0	500.0	547.7	100.0	0.0
500.0	425.0	461.0	100.0	0.0
425.0	355.0	388.4	100.0	0.0
355.0	300.0	326.3	100.0	0.0
300.0	250.0	273.9	100.0	0.0
250.0	212.0	230.2	99.9	0.1
212.0	180.0	195.3	99.9	0.0
180.0	150.0	164.3	99.6	0.3
150.0	125.0	136.9	98.8	0.8
125.0	106.0	115.1	92.7	6.1
106.0	90.00	97.67	61.0	31.7
90.00	75.00	82.16	26.7	34.3
75.00	63.00	68.74	0.0	26.7

Mass Frequency vs Diameter



## Summary Report

Full scale pump speed: 3  
Bubble detection: Medium  
Starting Size: 63.00 μm  
Ending Size: 0.50 μm

Stir time: 30 secs  
Stir speed: Low  
Probe time: 30 secs

Sample: TT-20-08 50 cm  
 Operator: Clint Edrington  
 Submitter: Clint Edrington  
 File Name: C:\EDRING~1\TIGER&~1\SANDFR~1\TT-20-08\20\_50CM.SMP  
 Material/Liquid: silicate mud/water/Water

Reported: 01/03/10 18:15:19  
 Liquid Visc: 0.7225 cp

Sample Density: 2.650 g/cm<sup>3</sup>  
 Liquid Density: 0.9941 g/cm<sup>3</sup>

## Summary Report

Parameter 1 0.000

Parameter 2 0.000

Parameter 3 0.000

## Mass Distribution Arithmetic Statistics

Mean	86.34	Std. Dev.	15.47
Median	84.93	Coef. Var.	0.179
Mode	82.16	Skewness	1.586
		Kurtosis	8.604

## Selected Percentiles

Percent Finer	Diameter (µm)
100.0	651.9
80.0	99.04
60.0	89.53
40.0	80.56
20.0	72.17

## Selected Sizes

Diameter (µm)	Percent Finer
500.0	100.0
250.0	100.0
125.0	98.8
88.00	56.7
63.00	0.0

Peak Number	% of Dist. *	Mean	Mode	Median	Standard Deviation	Skewness	Kurtosis
1	99.9	86.19	82.16	84.91	14.79	0.924	1.971

\* Peaks must comprise at least 5.00 % of the distribution.

Micromeritics

WIN5100 V2.03

Page 1

Sample: TT-20-08 100 cm  
Operator: Clint Edrington  
Submitter: Clint Edrington  
File Name: C:\EDRING~1\TIGER&~1\SANDFR~1\TT-20-08\20\_100CM.SMP  
Material/Liquid: silicate mud/water/Water

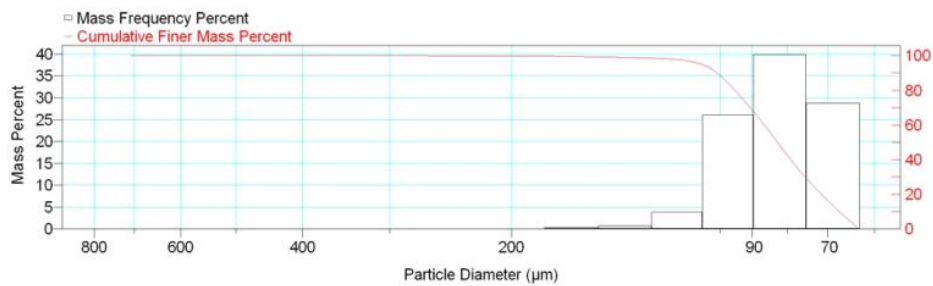
Reported: 01/03/10 18:17:33  
Liquid Visc: 0.7225 cp

Sample Density: 2.650 g/cm<sup>3</sup>  
Liquid Density: 0.9941 g/cm<sup>3</sup>

Report by Size Class

High Diameter ( $\mu\text{m}$ )	Low Diameter ( $\mu\text{m}$ )	Average Diameter ( $\mu\text{m}$ )	Cumulative Mass Finer (Percent)	Mass Frequency (Percent)
850.0	710.0	776.9	100.0	0.0
710.0	600.0	652.7	100.0	0.0
600.0	500.0	547.7	100.0	0.0
500.0	425.0	461.0	100.0	0.0
425.0	355.0	388.4	100.0	0.0
355.0	300.0	326.3	100.0	0.0
300.0	250.0	273.9	99.9	0.1
250.0	212.0	230.2	99.8	0.1
212.0	180.0	195.3	99.7	0.1
180.0	150.0	164.3	99.3	0.4
150.0	125.0	136.9	98.6	0.7
125.0	106.0	115.1	94.8	3.8
106.0	90.00	97.67	68.7	26.1
90.00	75.00	82.16	28.8	39.9
75.00	63.00	68.74	0.0	28.8

Mass Frequency vs Diameter



Summary Report

Full scale pump speed: 3  
Bubble detection: Medium  
Starting Size: 63.00  $\mu\text{m}$   
Ending Size: 0.50  $\mu\text{m}$

Stir time: 30 secs  
Stir speed: Low  
Probe time: 30 secs

Sample: TT-20-08 100 cm  
 Operator: Clint Edrington  
 Submitter: Clint Edrington  
 File Name: C:\EDRING~1\TIGER&~1\SANDFR~1\TT-20-08\20\_100CM.SMP  
 Material/Liquid: silicate mud/water/Water

Reported: 01/03/10 18:17:33  
 Liquid Visc: 0.7225 cp

Sample Density: 2.650 g/cm<sup>3</sup>  
 Liquid Density: 0.9941 g/cm<sup>3</sup>

## Summary Report

Parameter 1	0.000	Parameter 2	0.000	Parameter 3	0.000		
Mass Distribution Arithmetic Statistics							
Mean	84.76	Std. Dev.	16.39				
Median	82.70	Coef. Var.	0.193				
Mode	82.16	Skewness	3.323				
		Kurtosis	26.739				
Selected Percentiles			Selected Sizes				
Percent Finer	Diameter (µm)		Diameter (µm)	Percent Finer			
100.0	714.1		500.0	100.0			
80.0	95.20		250.0	99.9			
60.0	86.41		125.0	98.6			
40.0	79.14		88.00	64.0			
20.0	71.50		63.00	0.0			
Peak Number	% of Dist.*	Mean	Mode	Median	Standard Deviation	Skewness	Kurtosis
1	100.0	84.76	82.16	82.70	16.39	3.323	26.739

\* Peaks must comprise at least 5.00 % of the distribution.

# Micromeritics

WIN5100 V2.03

Page 1

Sample: TT-20-08 150 cm  
Operator: Clint Edrington  
Submitter: Clint Edrington  
File Name: C:\EDRING~1\TIGER&~1\SANDFR~1\TT-20-08\20\_150CM.SMP  
Material/Liquid: silicate mud/water/Water

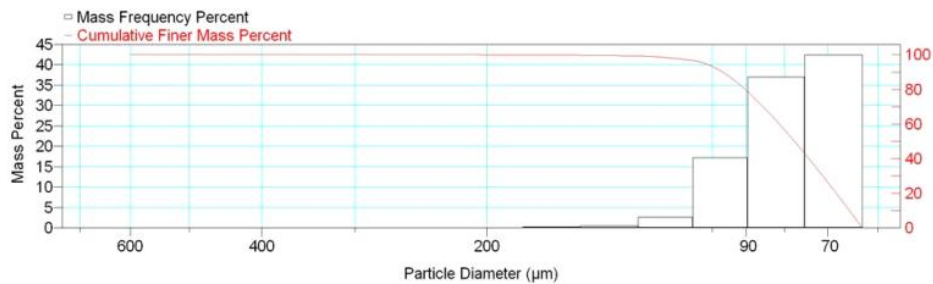
Reported: 01/03/10 18:19:59  
Liquid Visc: 0.7225 cp

Sample Density: 2.650 g/cm<sup>3</sup>  
Liquid Density: 0.9941 g/cm<sup>3</sup>

## Report by Size Class

High Diameter (µm)	Low Diameter (µm)	Average Diameter (µm)	Cumulative Mass Finer (Percent)	Mass Frequency (Percent)
710.0	600.0	652.7	100.0	0.0
600.0	500.0	547.7	100.0	0.0
500.0	425.0	461.0	100.0	0.0
425.0	355.0	388.4	100.0	0.0
355.0	300.0	326.3	100.0	0.0
300.0	250.0	273.9	100.0	0.0
250.0	212.0	230.2	100.0	0.0
212.0	180.0	195.3	99.9	0.1
180.0	150.0	164.3	99.7	0.2
150.0	125.0	136.9	99.2	0.5
125.0	106.0	115.1	96.6	2.6
106.0	90.00	97.67	79.4	17.2
90.00	75.00	82.16	42.4	37.0
75.00	63.00	68.74	0.0	42.4

Mass Frequency vs Diameter



## Summary Report

Full scale pump speed: 3  
Bubble detection: Medium  
Starting Size: 63.00 µm  
Ending Size: 0.50 µm

Stir time: 30 secs  
Stir speed: Low  
Probe time: 30 secs

Sample: TT-20-08 150 cm  
 Operator: Clint Edrington  
 Submitter: Clint Edrington  
 File Name: C:\EDRING~1\TIGER&~1\SANDFR~1\TT-20-08\20\_150CM.SMP  
 Material/Liquid: silicate mud/water/Water

Reported: 01/03/10 18:19:59  
 Liquid Visc: 0.7225 cp

Sample Density: 2.650 g/cm<sup>3</sup>  
 Liquid Density: 0.9941 g/cm<sup>3</sup>

## Summary Report

Parameter 1 0.000

Parameter 2 0.000

Parameter 3 0.000

## Mass Distribution Arithmetic Statistics

Mean	80.54	Std. Dev.	13.59
Median	77.56	Coef. Var.	0.169
Mode	68.74	Skewness	1.923
		Kurtosis	8.224

## Selected Percentiles

Percent Finer	Diameter (µm)
100.0	600.3
80.0	90.32
60.0	81.27
40.0	74.23
20.0	68.20

## Selected Sizes

Diameter (µm)	Percent Finer
500.0	100.0
250.0	100.0
125.0	99.2
88.00	75.4
63.00	0.0

Peak Number	% of Dist. *	Mean	Mode	Median	Standard Deviation	Skewness	Kurtosis
1	100.0	80.54	68.74	77.56	13.59	1.923	8.224

\* Peaks must comprise at least 5.00 % of the distribution.



# Micromeritics

WIN5100 V2.03

Page 1

Sample: TT-20-08 200 cm  
Operator: Clint Edrington  
Submitter: Clint Edrington  
File Name: C:\EDRING~1\TIGER&~1\SANDFR~1\TT-20-08\20\_200CM.SMP  
Material/Liquid: silicate mud/water/Water

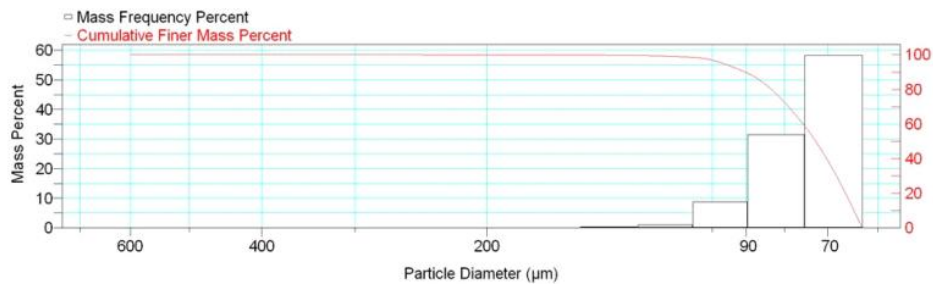
Reported: 01/03/10 18:22:26  
Liquid Visc: 0.7225 cp

Sample Density: 2.650 g/cm<sup>3</sup>  
Liquid Density: 0.9941 g/cm<sup>3</sup>

## Report by Size Class

High Diameter (μm)	Low Diameter (μm)	Average Diameter (μm)	Cumulative Mass Finer (Percent)	Mass Frequency (Percent)
710.0	600.0	652.7	100.0	0.0
600.0	500.0	547.7	100.0	0.0
500.0	425.0	461.0	100.0	0.0
425.0	355.0	388.4	100.0	0.0
355.0	300.0	326.3	100.0	0.0
300.0	250.0	273.9	100.0	0.0
250.0	212.0	230.2	99.9	0.1
212.0	180.0	195.3	99.9	0.0
180.0	150.0	164.3	99.8	0.1
150.0	125.0	136.9	99.5	0.3
125.0	106.0	115.1	98.5	1.0
106.0	90.00	97.67	89.7	8.8
90.00	75.00	82.16	58.2	31.5
75.00	63.00	68.74	0.0	58.2

Mass Frequency vs Diameter



## Summary Report

Full scale pump speed: 3  
Bubble detection: Medium  
Starting Size: 63.00 μm  
Ending Size: 0.50 μm

Stir time: 30 secs  
Stir speed: Low  
Probe time: 30 secs

Sample: TT-20-08 200 cm  
 Operator: Clint Edrington  
 Submitter: Clint Edrington  
 File Name: C:\EDRING~1\TIGER&~1\SANDFR~1\TT-20-08\20\_200CM.SMP  
 Material/Liquid: silicate mud/water/Water

Reported: 01/03/10 18:22:26  
 Liquid Visc: 0.7225 cp

Sample Density: 2.650 g/cm<sup>3</sup>  
 Liquid Density: 0.9941 g/cm<sup>3</sup>

## Summary Report

Parameter 1 0.000

Parameter 2 0.000

Parameter 3 0.000

## Mass Distribution Arithmetic Statistics

Mean	76.44	Std. Dev.	11.91
Median	72.67	Coef. Var.	0.156
Mode	68.74	Skewness	3.668
		Kurtosis	31.901

## Selected Percentiles

Percent Finer	Diameter (µm)
100.0	651.9
80.0	83.31
60.0	75.57
40.0	70.26
20.0	66.29

## Selected Sizes

Diameter (µm)	Percent Finer
500.0	100.0
250.0	100.0
125.0	99.5
88.00	87.6
63.00	0.0

Peak Number	% of Dist. *	Mean	Mode	Median	Standard Deviation	Skewness	Kurtosis
1	99.9	76.28	68.74	72.66	10.87	2.033	7.314

\* Peaks must comprise at least 5.00 % of the distribution.

# Micromeritics

WIN5100 V2.03

Page 1

Sample: TT-20-08 250 cm  
Operator: Clint Edrington  
Submitter: Clint Edrington  
File Name: C:\EDRING~1\TIGER&~1\SANDFR~1\TT-20-08\20\_250CM.SMP  
Material/Liquid: silicate mud/water/Water

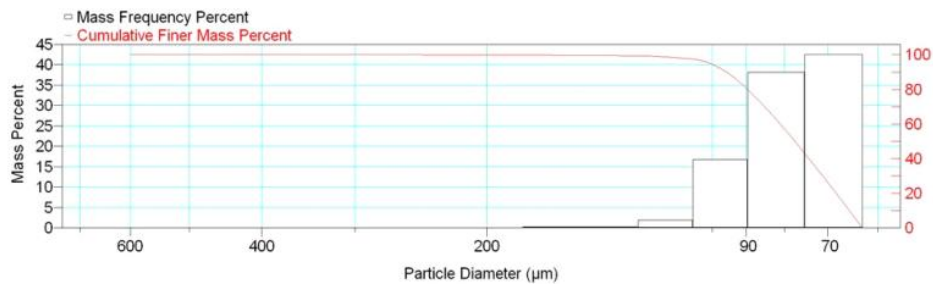
Reported: 01/03/10 18:24:25  
Liquid Visc: 0.7225 cp

Sample Density: 2.650 g/cm<sup>3</sup>  
Liquid Density: 0.9941 g/cm<sup>3</sup>

## Report by Size Class

High Diameter (µm)	Low Diameter (µm)	Average Diameter (µm)	Cumulative Mass Finer (Percent)	Mass Frequency (Percent)
710.0	600.0	652.7	100.0	0.0
600.0	500.0	547.7	100.0	0.0
500.0	425.0	461.0	100.0	0.0
425.0	355.0	388.4	100.0	0.0
355.0	300.0	326.3	100.0	0.0
300.0	250.0	273.9	100.0	0.0
250.0	212.0	230.2	99.9	0.1
212.0	180.0	195.3	99.8	0.1
180.0	150.0	164.3	99.6	0.2
150.0	125.0	136.9	99.3	0.3
125.0	106.0	115.1	97.4	1.9
106.0	90.00	97.67	80.7	16.7
90.00	75.00	82.16	42.5	38.2
75.00	63.00	68.74	0.0	42.5

Mass Frequency vs Diameter



## Summary Report

Full scale pump speed: 3  
Bubble detection: Medium  
Starting Size: 63.00 µm  
Ending Size: 0.50 µm

Stir time: 30 secs  
Stir speed: Low  
Probe time: 30 secs

Sample: TT-20-08 250 cm  
 Operator: Clint Edrington  
 Submitter: Clint Edrington  
 File Name: C:\EDRING~1\TIGER&~1\SANDFR~1\TT-20-08\20\_250CM.SMP  
 Material/Liquid: silicate mud/water/Water

Reported: 01/03/10 18:24:25  
 Liquid Visc: 0.7225 cp

Sample Density: 2.650 g/cm<sup>3</sup>  
 Liquid Density: 0.9941 g/cm<sup>3</sup>

## Summary Report

Parameter 1 0.000

Parameter 2 0.000

Parameter 3 0.000

## Mass Distribution Arithmetic Statistics

Mean	80.26	Std. Dev.	13.82
Median	77.47	Coef. Var.	0.172
Mode	68.74	Skewness	2.905
		Kurtosis	20.648

## Selected Percentiles

Percent Finer	Diameter (µm)
100.0	651.9
80.0	89.65
60.0	81.06
40.0	74.21
20.0	68.23

## Selected Sizes

Diameter (µm)	Percent Finer
500.0	100.0
250.0	100.0
125.0	99.3
88.00	76.6
63.00	0.0

Peak Number	% of Dist. *	Mean	Mode	Median	Standard Deviation	Skewness	Kurtosis
1	100.0	80.26	68.74	77.47	13.82	2.905	20.648

\* Peaks must comprise at least 5.00 % of the distribution.

# Micromeritics

WIN5100 V2.03

Page 1

Sample: TT-21-08 10 cm  
Operator: Clint Edrington  
Submitter: Clint Edrington  
File Name: C:\EDRING~1\TIGER&~1\SANDFR~1\TT-21-08\21\_10CM.SMP  
Material/Liquid: silicate mud/water/Water

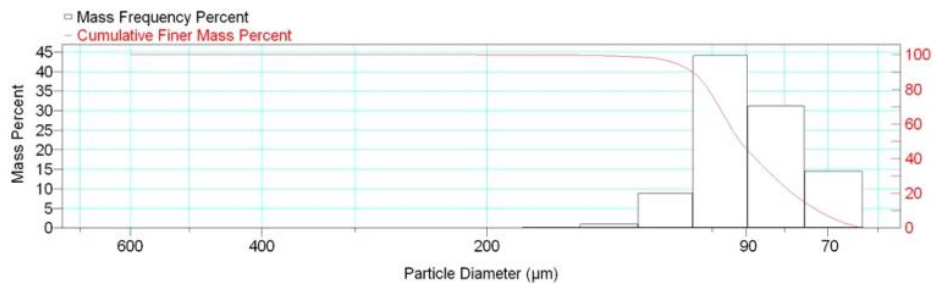
Reported: 01/03/10 18:27:54  
Liquid Visc: 0.7225 cp

Sample Density: 2.650 g/cm<sup>3</sup>  
Liquid Density: 0.9941 g/cm<sup>3</sup>

## Report by Size Class

High Diameter (μm)	Low Diameter (μm)	Average Diameter (μm)	Cumulative Mass Finer (Percent)	Mass Frequency (Percent)
710.0	600.0	652.7	100.0	0.0
600.0	500.0	547.7	100.0	0.0
500.0	425.0	461.0	100.0	0.0
425.0	355.0	388.4	100.0	0.0
355.0	300.0	326.3	100.0	0.0
300.0	250.0	273.9	100.0	0.0
250.0	212.0	230.2	100.0	0.0
212.0	180.0	195.3	99.9	0.1
180.0	150.0	164.3	99.7	0.2
150.0	125.0	136.9	98.7	1.0
125.0	106.0	115.1	89.8	8.9
106.0	90.00	97.67	45.7	44.1
90.00	75.00	82.16	14.5	31.2
75.00	63.00	68.74	0.0	14.5

Mass Frequency vs Diameter



## Summary Report

Full scale pump speed: 3  
Bubble detection: Medium  
Starting Size: 63.00 μm  
Ending Size: 0.50 μm

Stir time: 30 secs  
Stir speed: Low  
Probe time: 30 secs

Sample: TT-21-08 10 cm  
 Operator: Clint Edrington  
 Submitter: Clint Edrington  
 File Name: C:\EDRING~1\TIGER&~1\SANDFR~1\TT-21-08\21\_10CM.SMP  
 Material/Liquid: silicate mud/water/Water

Reported: 01/03/10 18:27:54  
 Liquid Visc: 0.7225 cp

Sample Density: 2.650 g/cm<sup>3</sup>  
 Liquid Density: 0.9941 g/cm<sup>3</sup>

## Summary Report

Parameter 1 0.000

Parameter 2 0.000

Parameter 3 0.000

## Mass Distribution Arithmetic Statistics

Mean	90.81	Std. Dev.	14.50
Median	91.70	Coef. Var.	0.160
Mode	97.67	Skewness	0.844
		Kurtosis	3.583

## Selected Percentiles

Percent Finer	Diameter (µm)
100.0	600.3
80.0	101.2
60.0	94.91
40.0	87.44
20.0	78.05

## Selected Sizes

Diameter (µm)	Percent Finer
500.0	100.0
250.0	100.0
125.0	98.7
88.00	41.2
63.00	0.0

Peak Number	% of Dist. *	Mean	Mode	Median	Standard Deviation	Skewness	Kurtosis
1	100.0	90.81	97.67	91.70	14.50	0.844	3.583

\* Peaks must comprise at least 5.00 % of the distribution.

# Micromeritics

WIN5100 V2.03

Page 1

Sample: TT-21-08 55 cm  
Operator: Clint Edrington  
Submitter: Clint Edrington  
File Name: C:\EDRING~1\TIGER&~1\SANDFR~1\TT-21-08\21\_55CM.SMP  
Material/Liquid: silicate mud/water/Water

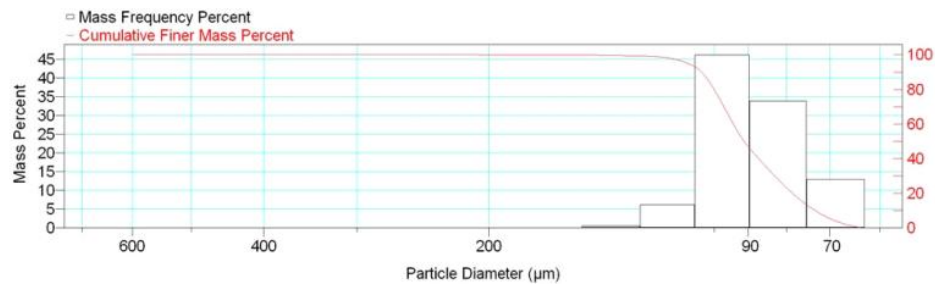
Reported: 01/03/10 18:30:15  
Liquid Visc: 0.7225 cp

Sample Density: 2.650 g/cm<sup>3</sup>  
Liquid Density: 0.9941 g/cm<sup>3</sup>

## Report by Size Class

High Diameter (μm)	Low Diameter (μm)	Average Diameter (μm)	Cumulative Mass Finer (Percent)	Mass Frequency (Percent)
710.0	600.0	652.7	100.0	0.0
600.0	500.0	547.7	100.0	0.0
500.0	425.0	461.0	100.0	0.0
425.0	355.0	388.4	100.0	0.0
355.0	300.0	326.3	100.0	0.0
300.0	250.0	273.9	100.0	0.0
250.0	212.0	230.2	100.0	0.0
212.0	180.0	195.3	99.9	0.1
180.0	150.0	164.3	99.8	0.1
150.0	125.0	136.9	99.2	0.6
125.0	106.0	115.1	93.0	6.2
106.0	90.00	97.67	46.9	46.1
90.00	75.00	82.16	13.0	33.9
75.00	63.00	68.74	0.0	13.0

Mass Frequency vs Diameter



## Summary Report

Full scale pump speed: 3  
Bubble detection: Medium  
Starting Size: 63.00 μm  
Ending Size: 0.50 μm

Stir time: 30 secs  
Stir speed: Low  
Probe time: 30 secs

Sample: TT-21-08 55 cm  
 Operator: Clint Edrington  
 Submitter: Clint Edrington  
 File Name: C:\EDRING~1\TIGER&~1\SANDFR~1\TT-21-08\21\_55CM.SMP  
 Material/Liquid: silicate mud/water/Water

Reported: 01/03/10 18:30:15  
 Liquid Visc: 0.7225 cp

Sample Density: 2.650 g/cm<sup>3</sup>  
 Liquid Density: 0.9941 g/cm<sup>3</sup>

## Summary Report

Parameter 1 0.000

Parameter 2 0.000

Parameter 3 0.000

## Mass Distribution Arithmetic Statistics

Mean	90.13	Std. Dev.	13.25
Median	91.17	Coef. Var.	0.147
Mode	97.67	Skewness	0.819
		Kurtosis	4.643

## Selected Percentiles

Percent Finer	Diameter (µm)
100.0	600.3
80.0	99.98
60.0	94.25
40.0	87.14
20.0	78.55

## Selected Sizes

Diameter (µm)	Percent Finer
500.0	100.0
250.0	100.0
125.0	99.2
88.00	42.1
63.00	0.0

Peak Number	% of Dist. *	Mean	Mode	Median	Standard Deviation	Skewness	Kurtosis
1	99.9	90.03	97.67	91.16	12.84	0.376	1.190

\* Peaks must comprise at least 5.00 % of the distribution.



# Micromeritics

WIN5100 V2.03

Page 1

Sample: TT-21-08 100 cm  
Operator: Clint Edrington  
Submitter: Clint Edrington  
File Name: C:\EDRING~1\TIGER&~1\SANDFR~1\TT-21-08\21\_100CM.SMP  
Material/Liquid: silicate mud/water/Water

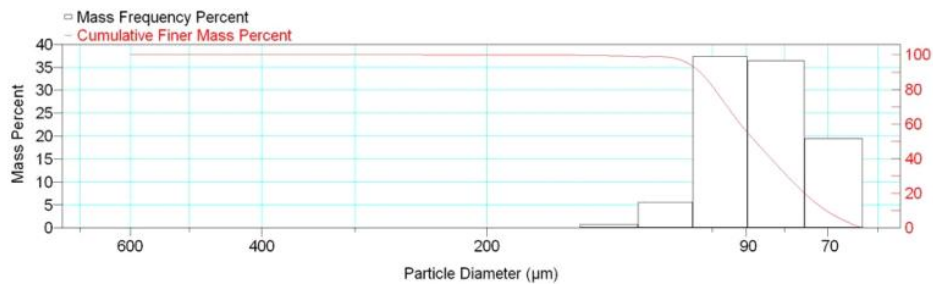
Reported: 01/03/10 18:32:34  
Liquid Visc: 0.7225 cp

Sample Density: 2.650 g/cm<sup>3</sup>  
Liquid Density: 0.9941 g/cm<sup>3</sup>

## Report by Size Class

High Diameter (µm)	Low Diameter (µm)	Average Diameter (µm)	Cumulative Mass Finer (Percent)	Mass Frequency (Percent)
710.0	600.0	652.7	100.0	0.0
600.0	500.0	547.7	100.0	0.0
500.0	425.0	461.0	100.0	0.0
425.0	355.0	388.4	100.0	0.0
355.0	300.0	326.3	100.0	0.0
300.0	250.0	273.9	100.0	0.0
250.0	212.0	230.2	99.9	0.1
212.0	180.0	195.3	99.8	0.1
180.0	150.0	164.3	99.7	0.1
150.0	125.0	136.9	98.9	0.8
125.0	106.0	115.1	93.3	5.6
106.0	90.00	97.67	55.9	37.4
90.00	75.00	82.16	19.5	36.4
75.00	63.00	68.74	0.0	19.5

Mass Frequency vs Diameter



## Summary Report

Full scale pump speed: 3  
Bubble detection: Medium  
Starting Size: 63.00 µm  
Ending Size: 0.50 µm

Stir time: 30 secs  
Stir speed: Low  
Probe time: 30 secs

Sample: TT-21-08 100 cm  
 Operator: Clint Edrington  
 Submitter: Clint Edrington  
 File Name: C:\EDRING~1\TIGER&~1\SANDFR~1\TT-21-08\21\_100CM.SMP  
 Material/Liquid: silicate mud/water/Water

Reported: 01/03/10 18:32:34  
 Liquid Visc: 0.7225 cp

Sample Density: 2.650 g/cm<sup>3</sup>  
 Liquid Density: 0.9941 g/cm<sup>3</sup>

## Summary Report

Parameter 1 0.000

Parameter 2 0.000

Parameter 3 0.000

## Mass Distribution Arithmetic Statistics

Mean	87.97	Std. Dev.	14.75
Median	87.49	Coef. Var.	0.168
Mode	97.67	Skewness	1.714
		Kurtosis	11.421

## Selected Percentiles

Percent Finer	Diameter (µm)
100.0	651.9
80.0	99.17
60.0	91.67
40.0	83.38
20.0	75.21

## Selected Sizes

Diameter (µm)	Percent Finer
500.0	100.0
250.0	100.0
125.0	98.9
88.00	51.2
63.00	0.0

Peak Number	% of Dist. *	Mean	Mode	Median	Standard Deviation	Skewness	Kurtosis
1	99.8	87.72	97.67	87.45	13.64	0.602	1.110

\* Peaks must comprise at least 5.00 % of the distribution.

Micromeritics

WIN5100 V2.03

Page 1

Sample: TT-21-08 151 cm  
Operator: Clint Edrington  
Submitter: Clint Edrington  
File Name: C:\EDRING~1\TIGER&~1\SANDFR~1\TT-21-08\21\_151CM.SMP  
Material/Liquid: silicate mud/water/Water

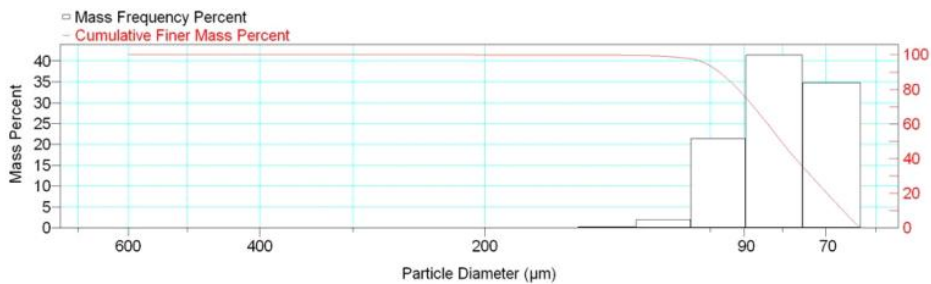
Reported: 01/03/10 18:36:58  
Liquid Visc: 0.7225 cp

Sample Density: 2.650 g/cm<sup>3</sup>  
Liquid Density: 0.9941 g/cm<sup>3</sup>

Report by Size Class

High Diameter (μm)	Low Diameter (μm)	Average Diameter (μm)	Cumulative Mass Finer (Percent)	Mass Frequency (Percent)
710.0	600.0	652.7	100.0	0.0
600.0	500.0	547.7	100.0	0.0
500.0	425.0	461.0	100.0	0.0
425.0	355.0	388.4	100.0	0.0
355.0	300.0	326.3	100.0	0.0
300.0	250.0	273.9	100.0	0.0
250.0	212.0	230.2	100.0	0.0
212.0	180.0	195.3	99.9	0.1
180.0	150.0	164.3	99.9	0.0
150.0	125.0	136.9	99.6	0.3
125.0	106.0	115.1	97.6	2.0
106.0	90.00	97.67	76.2	21.4
90.00	75.00	82.16	34.8	41.4
75.00	63.00	68.74	0.0	34.8

Mass Frequency vs Diameter



Summary Report

Full scale pump speed: 3  
Bubble detection: Medium  
Starting Size: 63.00 μm  
Ending Size: 0.50 μm

Stir time: 30 secs  
Stir speed: Low  
Probe time: 30 secs

Sample: TT-21-08 151 cm  
 Operator: Clint Edrington  
 Submitter: Clint Edrington  
 File Name: C:\EDRING~1\TIGER&~1\SANDFR~1\TT-21-08\21\_151CM.SMP  
 Material/Liquid: silicate mud/water/Water

Reported: 01/03/10 18:36:58  
 Liquid Visc: 0.7225 cp

Sample Density: 2.650 g/cm<sup>3</sup>  
 Liquid Density: 0.9941 g/cm<sup>3</sup>

## Summary Report

Parameter 1 0.000

Parameter 2 0.000

Parameter 3 0.000

## Mass Distribution Arithmetic Statistics

Mean	81.74	Std. Dev.	12.55
Median	80.29	Coef. Var.	0.154
Mode	82.16	Skewness	1.422
		Kurtosis	6.787

## Selected Percentiles

Percent Finer	Diameter (µm)
100.0	600.3
80.0	91.70
60.0	83.76
40.0	76.85
20.0	69.78

## Selected Sizes

Diameter (µm)	Percent Finer
500.0	100.0
250.0	100.0
125.0	99.6
88.00	71.4
63.00	0.0

Peak Number	% of Dist. *	Mean	Mode	Median	Standard Deviation	Skewness	Kurtosis
1	99.9	81.63	82.16	80.27	12.03	0.802	0.676

\* Peaks must comprise at least 5.00 % of the distribution.

# Micromeritics

WIN5100 V2.03

Page 1

Sample: TT-21-08 196 cm  
Operator: Clint Edrington  
Submitter: Clint Edrington  
File Name: C:\EDRING~1\TIGER&~1\SANDFR~1\TT-21-08\21\_196CM.SMP  
Material/Liquid: silicate mud/water/Water

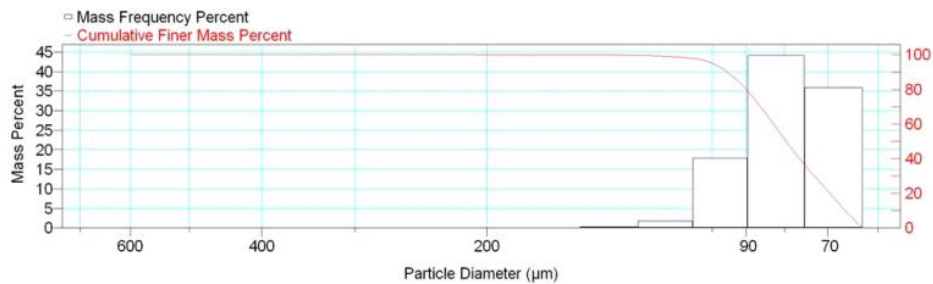
Reported: 01/03/10 18:34:53  
Liquid Visc: 0.7225 cp

Sample Density: 2.650 g/cm<sup>3</sup>  
Liquid Density: 0.9941 g/cm<sup>3</sup>

## Report by Size Class

High Diameter (μm)	Low Diameter (μm)	Average Diameter (μm)	Cumulative Mass Finer (Percent)	Mass Frequency (Percent)
710.0	600.0	652.7	100.0	0.0
600.0	500.0	547.7	100.0	0.0
500.0	425.0	461.0	100.0	0.0
425.0	355.0	388.4	100.0	0.0
355.0	300.0	326.3	100.0	0.0
300.0	250.0	273.9	100.0	0.0
250.0	212.0	230.2	100.0	0.0
212.0	180.0	195.3	99.9	0.1
180.0	150.0	164.3	99.9	0.0
150.0	125.0	136.9	99.6	0.3
125.0	106.0	115.1	97.9	1.7
106.0	90.00	97.67	80.0	17.9
90.00	75.00	82.16	35.9	44.1
75.00	63.00	68.74	0.0	35.9

Mass Frequency vs Diameter



## Summary Report

Full scale pump speed: 3  
Bubble detection: Medium  
Starting Size: 63.00 μm  
Ending Size: 0.50 μm

Stir time: 30 secs  
Stir speed: Low  
Probe time: 30 secs

Sample: TT-21-08 196 cm  
 Operator: Clint Edrington  
 Submitter: Clint Edrington  
 File Name: C:\EDRING~1\TIGER&~1\SANDFR~1\TT-21-08\21\_196CM.SMP  
 Material/Liquid: silicate mud/water/Water

Reported: 01/03/10 18:34:53  
 Liquid Visc: 0.7225 cp

Sample Density: 2.650 g/cm<sup>3</sup>  
 Liquid Density: 0.9941 g/cm<sup>3</sup>

## Summary Report

Parameter 1 0.000

Parameter 2 0.000

Parameter 3 0.000

## Mass Distribution Arithmetic Statistics

Mean	80.96	Std. Dev.	12.11
Median	79.60	Coef. Var.	0.150
Mode	82.16	Skewness	1.625
		Kurtosis	8.443

## Selected Percentiles

Percent Finer	Diameter (µm)
100.0	600.3
80.0	90.00
60.0	82.76
40.0	76.40
20.0	69.60

## Selected Sizes

Diameter (µm)	Percent Finer
500.0	100.0
250.0	100.0
125.0	99.6
88.00	75.1
63.00	0.0

Peak Number	% of Dist. *	Mean	Mode	Median	Standard Deviation	Skewness	Kurtosis
1	99.9	80.84	82.16	79.59	11.56	0.928	1.218

\* Peaks must comprise at least 5.00 % of the distribution.

# Micromeritics

WIN5100 V2.03

Page 1

Sample: TT-22-08 6 cm  
Operator: Clint Edrington  
Submitter: Clint Edrington  
File Name: C:\EDRING~1\TIGER&~1\SANDFR~1\TT-22-08\22\_6CM.SMP  
Material/Liquid: silicate mud/water/Water

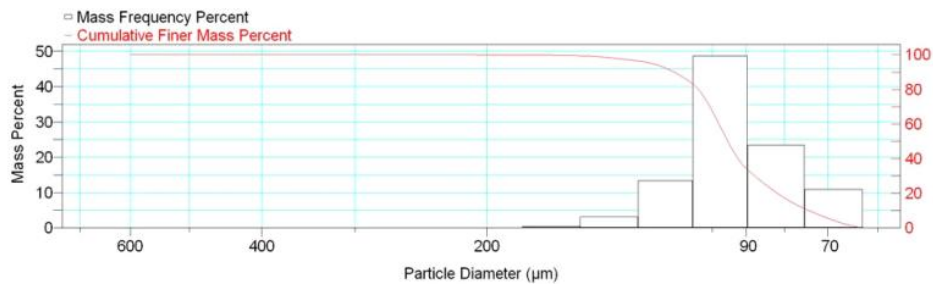
Reported: 01/03/10 19:07:20  
Liquid Visc: 0.7225 cp

Sample Density: 2.650 g/cm<sup>3</sup>  
Liquid Density: 0.9941 g/cm<sup>3</sup>

## Report by Size Class

High Diameter (µm)	Low Diameter (µm)	Average Diameter (µm)	Cumulative Mass Finer (Percent)	Mass Frequency (Percent)
710.0	600.0	652.7	100.0	0.0
600.0	500.0	547.7	100.0	0.0
500.0	425.0	461.0	100.0	0.0
425.0	355.0	388.4	100.0	0.0
355.0	300.0	326.3	100.0	0.0
300.0	250.0	273.9	100.0	0.0
250.0	212.0	230.2	100.0	0.0
212.0	180.0	195.3	99.9	0.1
180.0	150.0	164.3	99.4	0.5
150.0	125.0	136.9	96.3	3.1
125.0	106.0	115.1	83.0	13.3
106.0	90.00	97.67	34.3	48.7
90.00	75.00	82.16	10.9	23.4
75.00	63.00	68.74	0.0	10.9

Mass Frequency vs Diameter



## Summary Report

Full scale pump speed: 3  
Bubble detection: Medium  
Starting Size: 63.00 µm  
Ending Size: 0.50 µm

Stir time: 30 secs  
Stir speed: Low  
Probe time: 30 secs

Sample: TT-22-08 6 cm  
 Operator: Clint Edrington  
 Submitter: Clint Edrington  
 File Name: C:\EDRING~1\TIGER&~1\SANDFR~1\TT-22-08\22\_6CM.SMP  
 Material/Liquid: silicate mud/water/Water

Reported: 01/03/10 19:07:20  
 Liquid Visc: 0.7225 cp

Sample Density: 2.650 g/cm<sup>3</sup>  
 Liquid Density: 0.9941 g/cm<sup>3</sup>

## Summary Report

Parameter 1 0.000

Parameter 2 0.000

Parameter 3 0.000

## Mass Distribution Arithmetic Statistics

Mean	94.86	Std. Dev.	16.11
Median	95.24	Coef. Var.	0.170
Mode	97.67	Skewness	0.883
		Kurtosis	2.857

## Selected Percentiles

Percent Finer	Diameter (µm)
100.0	600.3
80.0	104.3
60.0	97.88
40.0	92.31
20.0	81.76

## Selected Sizes

Diameter (µm)	Percent Finer
500.0	100.0
250.0	100.0
125.0	96.3
88.00	30.6
63.00	0.0

Peak Number	% of Dist. *	Mean	Mode	Median	Standard Deviation	Skewness	Kurtosis
1	100.0	94.86	97.67	95.24	16.11	0.883	2.857

\* Peaks must comprise at least 5.00 % of the distribution.



Micromeritics

WIN5100 V2.03

Page 1

Sample: TT-22-08 50 cm  
Operator: Clint Edrington  
Submitter: Clint Edrington  
File Name: C:\EDRING~1\TIGER&~1\SANDFR~1\TT-22-08\22\_50CM.SMP  
Material/Liquid: silicate mud/water/Water

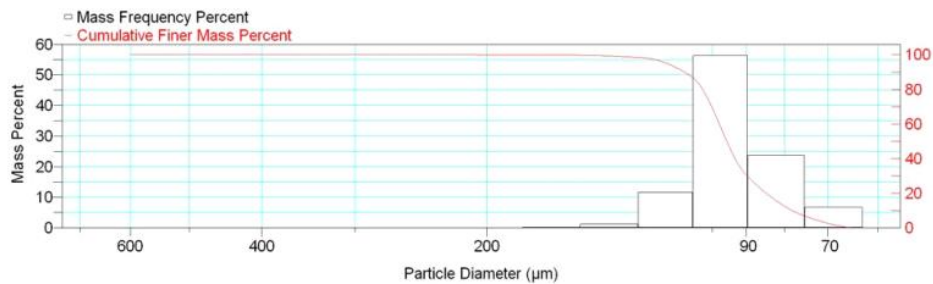
Reported: 01/03/10 19:09:39  
Liquid Visc: 0.7225 cp

Sample Density: 2.650 g/cm<sup>3</sup>  
Liquid Density: 0.9941 g/cm<sup>3</sup>

Report by Size Class

High Diameter (μm)	Low Diameter (μm)	Average Diameter (μm)	Cumulative Mass Finer (Percent)	Mass Frequency (Percent)
710.0	600.0	652.7	100.0	0.0
600.0	500.0	547.7	100.0	0.0
500.0	425.0	461.0	100.0	0.0
425.0	355.0	388.4	100.0	0.0
355.0	300.0	326.3	100.0	0.0
300.0	250.0	273.9	100.0	0.0
250.0	212.0	230.2	100.0	0.0
212.0	180.0	195.3	99.9	0.1
180.0	150.0	164.3	99.7	0.2
150.0	125.0	136.9	98.4	1.3
125.0	106.0	115.1	86.7	11.7
106.0	90.00	97.67	30.4	56.3
90.00	75.00	82.16	6.7	23.7
75.00	63.00	68.74	0.0	6.7

Mass Frequency vs Diameter



Summary Report

Full scale pump speed: 3  
Bubble detection: Medium  
Starting Size: 63.00 μm  
Ending Size: 0.50 μm

Stir time: 30 secs  
Stir speed: Low  
Probe time: 30 secs

Sample: TT-22-08 50 cm  
 Operator: Clint Edrington  
 Submitter: Clint Edrington  
 File Name: C:\EDRING~1\TIGER&~1\SANDFR~1\TT-22-08\22\_50CM.SMP  
 Material/Liquid: silicate mud/water/Water

Reported: 01/03/10 19:09:39  
 Liquid Visc: 0.7225 cp

Sample Density: 2.650 g/cm<sup>3</sup>  
 Liquid Density: 0.9941 g/cm<sup>3</sup>

## Summary Report

Parameter 1 0.000

Parameter 2 0.000

Parameter 3 0.000

## Mass Distribution Arithmetic Statistics

Mean	94.84	Std. Dev.	13.38
Median	95.54	Coef. Var.	0.141
Mode	97.67	Skewness	0.821
		Kurtosis	4.681

## Selected Percentiles

Percent Finer	Diameter (µm)
100.0	600.3
80.0	102.9
60.0	97.77
40.0	93.15
20.0	84.59

## Selected Sizes

Diameter (µm)	Percent Finer
500.0	100.0
250.0	100.0
125.0	98.4
88.00	26.4
63.00	0.0

Peak Number	% of Dist. *	Mean	Mode	Median	Standard Deviation	Skewness	Kurtosis
1	100.0	94.84	97.67	95.54	13.38	0.821	4.681

\* Peaks must comprise at least 5.00 % of the distribution.

# Micromeritics

WIN5100 V2.03

Page 1

Sample: TT-22-08 98 cm  
Operator: Clint Edrington  
Submitter: Clint Edrington  
File Name: C:\EDRING~1\TIGER&~1\SANDFR~1\TT-22-08\22\_98CM.SMP  
Material/Liquid: silicate mud/water/Water

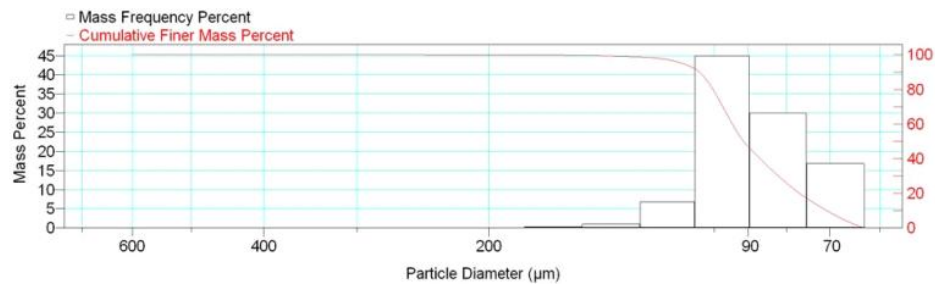
Reported: 01/03/10 19:11:58  
Liquid Visc: 0.7225 cp

Sample Density: 2.650 g/cm<sup>3</sup>  
Liquid Density: 0.9941 g/cm<sup>3</sup>

## Report by Size Class

High Diameter (µm)	Low Diameter (µm)	Average Diameter (µm)	Cumulative Mass Finer (Percent)	Mass Frequency (Percent)
710.0	600.0	652.7	100.0	0.0
600.0	500.0	547.7	100.0	0.0
500.0	425.0	461.0	100.0	0.0
425.0	355.0	388.4	100.0	0.0
355.0	300.0	326.3	100.0	0.0
300.0	250.0	273.9	100.0	0.0
250.0	212.0	230.2	99.9	0.1
212.0	180.0	195.3	99.9	0.0
180.0	150.0	164.3	99.6	0.3
150.0	125.0	136.9	98.6	1.0
125.0	106.0	115.1	91.8	6.8
106.0	90.00	97.67	46.8	45.0
90.00	75.00	82.16	16.8	30.0
75.00	63.00	68.74	0.0	16.8

Mass Frequency vs Diameter



## Summary Report

Full scale pump speed: 3  
Bubble detection: Medium  
Starting Size: 63.00 µm  
Ending Size: 0.50 µm

Stir time: 30 secs  
Stir speed: Low  
Probe time: 30 secs

Sample: TT-22-08 98 cm  
 Operator: Clint Edrington  
 Submitter: Clint Edrington  
 File Name: C:\EDRING~1\TIGER&~1\SANDFR~1\TT-22-08\22\_98CM.SMP  
 Material/Liquid: silicate mud/water/Water

Reported: 01/03/10 19:11:58  
 Liquid Visc: 0.7225 cp

Sample Density: 2.650 g/cm<sup>3</sup>  
 Liquid Density: 0.9941 g/cm<sup>3</sup>

## Summary Report

Parameter 1 0.000

Parameter 2 0.000

Parameter 3 0.000

## Mass Distribution Arithmetic Statistics

Mean	90.07	Std. Dev.	14.90
Median	91.33	Coef. Var.	0.165
Mode	97.67	Skewness	1.359
		Kurtosis	8.959

## Selected Percentiles

Percent Finer	Diameter (µm)
100.0	651.9
80.0	100.4
60.0	94.51
40.0	86.79
20.0	76.87

## Selected Sizes

Diameter (µm)	Percent Finer
500.0	100.0
250.0	100.0
125.0	98.6
88.00	42.6
63.00	0.0

Peak Number	% of Dist. *	Mean	Mode	Median	Standard Deviation	Skewness	Kurtosis
1	99.9	89.93	97.67	91.31	14.23	0.635	1.992

\* Peaks must comprise at least 5.00 % of the distribution.

Micromeritics

WIN5100 V2.03

Page 1

Sample: TT-22-08 150 cm  
Operator: Clint Edrington  
Submitter: Clint Edrington  
File Name: C:\EDRING~1\TIGER&~1\SANDFR~1\TT-22-08\22\_150CM.SMP  
Material/Liquid: silicate mud/water/Water

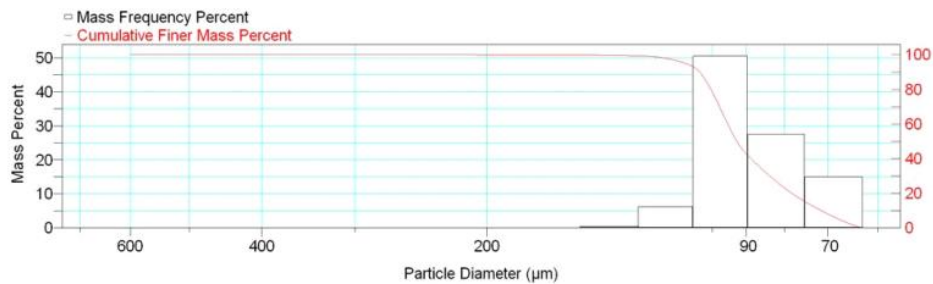
Reported: 01/03/10 19:13:52  
Liquid Visc: 0.7225 cp

Sample Density: 2.650 g/cm<sup>3</sup>  
Liquid Density: 0.9941 g/cm<sup>3</sup>

Report by Size Class

High Diameter ( $\mu\text{m}$ )	Low Diameter ( $\mu\text{m}$ )	Average Diameter ( $\mu\text{m}$ )	Cumulative Mass Finer (Percent)	Mass Frequency (Percent)
710.0	600.0	652.7	100.0	0.0
600.0	500.0	547.7	100.0	0.0
500.0	425.0	461.0	100.0	0.0
425.0	355.0	388.4	100.0	0.0
355.0	300.0	326.3	100.0	0.0
300.0	250.0	273.9	100.0	0.0
250.0	212.0	230.2	100.0	0.0
212.0	180.0	195.3	99.9	0.1
180.0	150.0	164.3	99.8	0.1
150.0	125.0	136.9	99.3	0.5
125.0	106.0	115.1	93.1	6.2
106.0	90.00	97.67	42.6	50.5
90.00	75.00	82.16	15.0	27.6
75.00	63.00	68.74	0.0	15.0

Mass Frequency vs Diameter



Summary Report

Full scale pump speed: 3  
Bubble detection: Medium  
Starting Size: 63.00  $\mu\text{m}$   
Ending Size: 0.50  $\mu\text{m}$

Stir time: 30 secs  
Stir speed: Low  
Probe time: 30 secs

Sample: TT-22-08 150 cm  
 Operator: Clint Edrington  
 Submitter: Clint Edrington  
 File Name: C:\EDRING~1\TIGER&~1\SANDFR~1\TT-22-08\22\_150CM.SMP  
 Material/Liquid: silicate mud/water/Water

Reported: 01/03/10 19:13:52  
 Liquid Visc: 0.7225 cp

Sample Density: 2.650 g/cm<sup>3</sup>  
 Liquid Density: 0.9941 g/cm<sup>3</sup>

## Summary Report

Parameter 1 0.000

Parameter 2 0.000

Parameter 3 0.000

## Mass Distribution Arithmetic Statistics

Mean	90.49	Std. Dev.	13.45
Median	92.65	Coef. Var.	0.149
Mode	97.67	Skewness	0.601
		Kurtosis	4.109

## Selected Percentiles

Percent Finer	Diameter (µm)
100.0	600.3
80.0	100.3
60.0	95.28
40.0	88.71
20.0	78.23

## Selected Sizes

Diameter (µm)	Percent Finer
500.0	100.0
250.0	100.0
125.0	99.3
88.00	38.6
63.00	0.0

Peak Number	% of Dist. *	Mean	Mode	Median	Standard Deviation	Skewness	Kurtosis
1	99.9	90.39	97.67	92.63	13.04	0.164	0.877

\* Peaks must comprise at least 5.00 % of the distribution.

Micromeritics

WIN5100 V2.03

Page 1

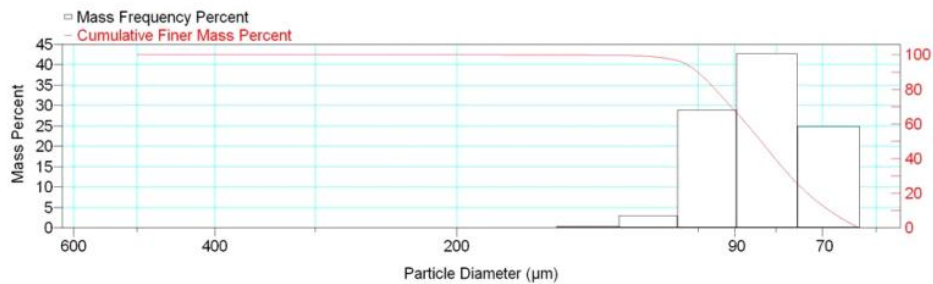
Sample: TT-22-08 200 cm  
Operator: Clint Edrington  
Submitter: Clint Edrington  
File Name: C:\EDRING~1\TIGER&~1\SANDFR~1\TT-22-08\22\_200CM.SMP  
Material/Liquid: silicate mud/water/Water

Reported: 01/03/10 19:15:57  
Liquid Visc: 0.7225 cp  
Sample Density: 2.650 g/cm<sup>3</sup>  
Liquid Density: 0.9941 g/cm<sup>3</sup>

Report by Size Class

High Diameter (μm)	Low Diameter (μm)	Average Diameter (μm)	Cumulative Mass Finer (Percent)	Mass Frequency (Percent)
600.0	500.0	547.7	100.0	0.0
500.0	425.0	461.0	100.0	0.0
425.0	355.0	388.4	100.0	0.0
355.0	300.0	326.3	100.0	0.0
300.0	250.0	273.9	100.0	0.0
250.0	212.0	230.2	100.0	0.0
212.0	180.0	195.3	100.0	0.0
180.0	150.0	164.3	99.9	0.1
150.0	125.0	136.9	99.5	0.4
125.0	106.0	115.1	96.5	3.0
106.0	90.00	97.67	67.6	28.9
90.00	75.00	82.16	24.9	42.7
75.00	63.00	68.74	0.0	24.9

Mass Frequency vs Diameter



Summary Report

Full scale pump speed: 3  
Bubble detection: Medium  
Starting Size: 63.00 μm  
Ending Size: 0.50 μm  
Stir time: 30 secs  
Stir speed: Low  
Probe time: 30 secs

Parameter 1 0.000      Parameter 2 0.000      Parameter 3 0.000

Sample: TT-22-08 200 cm  
 Operator: Clint Edrington  
 Submitter: Clint Edrington  
 File Name: C:\EDRING~1\TIGER&~1\SANDFR~1\TT-22-08\22\_200CM.SMP  
 Material/Liquid: silicate mud/water/Water

Reported: 01/03/10 19:15:57  
 Liquid Visc: 0.7225 cp

Sample Density: 2.650 g/cm<sup>3</sup>  
 Liquid Density: 0.9941 g/cm<sup>3</sup>

## Summary Report

## Mass Distribution Arithmetic Statistics

Mean	84.59	Std. Dev.	12.64
Median	83.52	Coef. Var.	0.149
Mode	82.16	Skewness	0.783
		Kurtosis	1.724

## Selected Percentiles

Percent Finer	Diameter (µm)
100.0	553.2
80.0	95.21
60.0	87.02
40.0	80.21
20.0	73.08

## Selected Sizes

Diameter (µm)	Percent Finer
500.0	100.0
250.0	100.0
125.0	99.5
88.00	62.6
63.00	0.0

Peak Number	% of Dist.*	Mean	Mode	Median	Standard Deviation	Skewness	Kurtosis
1	100.0	84.59	82.16	83.52	12.64	0.783	1.724

\* Peaks must comprise at least 5.00 % of the distribution.



# Micromeritics

WIN5100 V2.03

Page 1

Sample: TT-22-08 250 cm  
Operator: Clint Edrington  
Submitter: Clint Edrington  
File Name: C:\EDRING~1\TIGER&~1\SANDFR~1\TT-22-08\22\_250CM.SMP  
Material/Liquid: silicate mud/water/Water

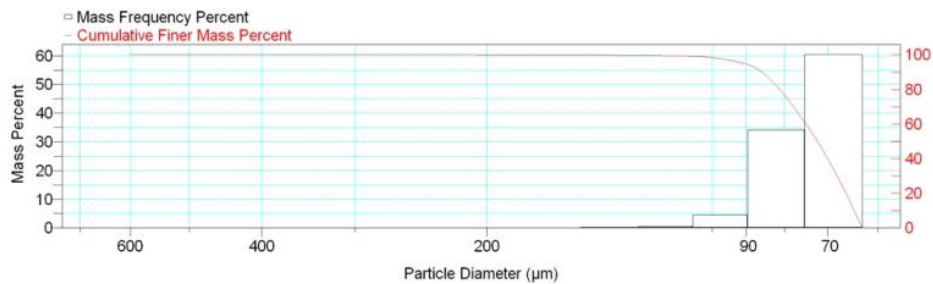
Reported: 01/03/10 19:18:28  
Liquid Visc: 0.7225 cp

Sample Density: 2.650 g/cm<sup>3</sup>  
Liquid Density: 0.9941 g/cm<sup>3</sup>

## Report by Size Class

High Diameter (µm)	Low Diameter (µm)	Average Diameter (µm)	Cumulative Mass Finer (Percent)	Mass Frequency (Percent)
710.0	600.0	652.7	100.0	0.0
600.0	500.0	547.7	100.0	0.0
500.0	425.0	461.0	100.0	0.0
425.0	355.0	388.4	100.0	0.0
355.0	300.0	326.3	100.0	0.0
300.0	250.0	273.9	100.0	0.0
250.0	212.0	230.2	100.0	0.0
212.0	180.0	195.3	99.9	0.1
180.0	150.0	164.3	99.8	0.1
150.0	125.0	136.9	99.6	0.2
125.0	106.0	115.1	99.1	0.5
106.0	90.00	97.67	94.6	4.5
90.00	75.00	82.16	60.4	34.2
75.00	63.00	68.74	0.0	60.4

Mass Frequency vs Diameter



## Summary Report

Full scale pump speed: 3  
Bubble detection: Medium  
Starting Size: 63.00 µm  
Ending Size: 0.50 µm

Stir time: 30 secs  
Stir speed: Low  
Probe time: 30 secs

Sample: TT-22-08 250 cm  
 Operator: Clint Edrington  
 Submitter: Clint Edrington  
 File Name: C:\EDRING~1\TIGER&~1\SANDFR~1\TT-22-08\22\_250CM.SMP  
 Material/Liquid: silicate mud/water/Water

Reported: 01/03/10 19:18:28  
 Liquid Visc: 0.7225 cp

Sample Density: 2.650 g/cm<sup>3</sup>  
 Liquid Density: 0.9941 g/cm<sup>3</sup>

## Summary Report

Parameter 1 0.000

Parameter 2 0.000

Parameter 3 0.000

## Mass Distribution Arithmetic Statistics

Mean	75.22	Std. Dev.	10.12
Median	72.30	Coef. Var.	0.135
Mode	68.74	Skewness	3.555
		Kurtosis	28.070

## Selected Percentiles

Percent Finer	Diameter (µm)
100.0	600.3
80.0	81.19
60.0	74.89
40.0	70.04
20.0	66.20

## Selected Sizes

Diameter (µm)	Percent Finer
500.0	100.0
250.0	100.0
125.0	99.6
88.00	93.0
63.00	0.0

Peak Number	% of Dist. *	Mean	Mode	Median	Standard Deviation	Skewness	Kurtosis
1	99.9	75.10	68.74	72.29	9.387	2.403	12.334

\* Peaks must comprise at least 5.00 % of the distribution.

# Micromeritics

WIN5100 V2.03

Page 1

Sample: TT-22-08 272 cm  
Operator: Clint Edrington  
Submitter: Clint Edrington  
File Name: C:\EDRING~1\TIGER&~1\SANDFR~1\TT-22-08\22\_272CM.SMP  
Material/Liquid: silicate mud/water/Water

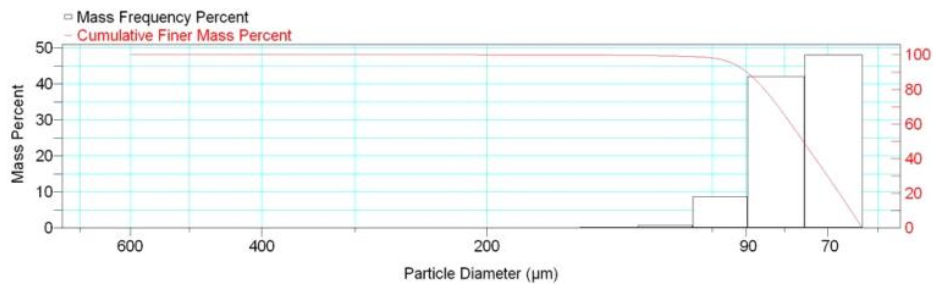
Reported: 01/03/10 19:20:23  
Liquid Visc: 0.7225 cp

Sample Density: 2.650 g/cm<sup>3</sup>  
Liquid Density: 0.9941 g/cm<sup>3</sup>

## Report by Size Class

High Diameter (μm)	Low Diameter (μm)	Average Diameter (μm)	Cumulative Mass Finer (Percent)	Mass Frequency (Percent)
710.0	600.0	652.7	100.0	0.0
600.0	500.0	547.7	100.0	0.0
500.0	425.0	461.0	100.0	0.0
425.0	355.0	388.4	100.0	0.0
355.0	300.0	326.3	100.0	0.0
300.0	250.0	273.9	100.0	0.0
250.0	212.0	230.2	100.0	0.0
212.0	180.0	195.3	99.9	0.1
180.0	150.0	164.3	99.8	0.1
150.0	125.0	136.9	99.6	0.2
125.0	106.0	115.1	98.9	0.7
106.0	90.00	97.67	90.2	8.7
90.00	75.00	82.16	48.1	42.1
75.00	63.00	68.74	0.0	48.1

Mass Frequency vs Diameter



## Summary Report

Full scale pump speed: 3  
Bubble detection: Medium  
Starting Size: 63.00 μm  
Ending Size: 0.50 μm

Stir time: 30 secs  
Stir speed: Low  
Probe time: 30 secs

Sample: TT-22-08 272 cm  
 Operator: Clint Edrington  
 Submitter: Clint Edrington  
 File Name: C:\EDRING~1\TIGER&~1\SANDFR~1\TT-22-08\22\_272CM.SMP  
 Material/Liquid: silicate mud/water/Water

Reported: 01/03/10 19:20:23  
 Liquid Visc: 0.7225 cp

Sample Density: 2.650 g/cm<sup>3</sup>  
 Liquid Density: 0.9941 g/cm<sup>3</sup>

## Summary Report

Parameter 1 0.000

Parameter 2 0.000

Parameter 3 0.000

## Mass Distribution Arithmetic Statistics

Mean	77.59	Std. Dev.	10.95
Median	75.54	Coef. Var.	0.141
Mode	68.74	Skewness	2.656
		Kurtosis	18.223

## Selected Percentiles

Percent Finer	Diameter (µm)
100.0	600.3
80.0	85.10
60.0	78.42
40.0	72.75
20.0	67.56

## Selected Sizes

Diameter (µm)	Percent Finer
500.0	100.0
250.0	100.0
125.0	99.6
88.00	86.6
63.00	0.0

Peak Number	% of Dist. *	Mean	Mode	Median	Standard Deviation	Skewness	Kurtosis
1	99.9	77.47	68.74	75.52	10.30	1.731	7.091

\* Peaks must comprise at least 5.00 % of the distribution.

# Micromeritics

WIN5100 V2.03

Page 1

Sample: TT-23-08 5 cm  
Operator: Clint Edrington  
Submitter: Clint Edrington  
File Name: C:\EDRING~1\TIGER&~1\SANDFR~1\TT-23-08\23\_5CM.SMP  
Material/Liquid: silicate mud/water/Water

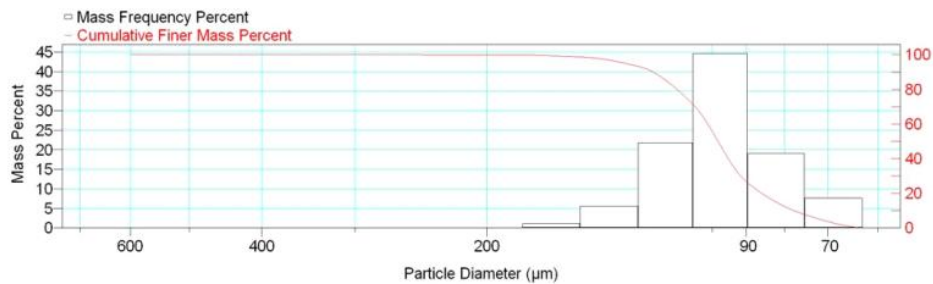
Reported: 01/03/10 19:24:12  
Liquid Visc: 0.7225 cp

Sample Density: 2.650 g/cm<sup>3</sup>  
Liquid Density: 0.9941 g/cm<sup>3</sup>

## Report by Size Class

High Diameter (µm)	Low Diameter (µm)	Average Diameter (µm)	Cumulative Mass Finer (Percent)	Mass Frequency (Percent)
710.0	600.0	652.7	100.0	0.0
600.0	500.0	547.7	100.0	0.0
500.0	425.0	461.0	100.0	0.0
425.0	355.0	388.4	100.0	0.0
355.0	300.0	326.3	100.0	0.0
300.0	250.0	273.9	100.0	0.0
250.0	212.0	230.2	99.9	0.1
212.0	180.0	195.3	99.8	0.1
180.0	150.0	164.3	98.7	1.1
150.0	125.0	136.9	93.1	5.6
125.0	106.0	115.1	71.3	21.8
106.0	90.00	97.67	26.7	44.6
90.00	75.00	82.16	7.6	19.1
75.00	63.00	68.74	0.0	7.6

Mass Frequency vs Diameter



## Summary Report

Full scale pump speed: 3  
Bubble detection: Medium  
Starting Size: 63.00 µm  
Ending Size: 0.50 µm

Stir time: 30 secs  
Stir speed: Low  
Probe time: 30 secs

Sample: TT-23-08 5 cm  
 Operator: Clint Edrington  
 Submitter: Clint Edrington  
 File Name: C:\EDRING~1\TIGER&~1\SANDFR~1\TT-23-08\23\_5CM.SMP  
 Material/Liquid: silicate mud/water/Water

Reported: 01/03/10 19:24:12  
 Liquid Visc: 0.7225 cp

Sample Density: 2.650 g/cm<sup>3</sup>  
 Liquid Density: 0.9941 g/cm<sup>3</sup>

## Summary Report

Parameter 1 0.000

Parameter 2 0.000

Parameter 3 0.000

## Mass Distribution Arithmetic Statistics

Mean	99.47	Std. Dev.	18.30
Median	98.16	Coef. Var.	0.184
Mode	97.67	Skewness	1.092
		Kurtosis	3.949

## Selected Percentiles

Percent Finer	Diameter (µm)
100.0	651.9
80.0	111.4
60.0	101.3
40.0	95.11
20.0	85.83

## Selected Sizes

Diameter (µm)	Percent Finer
500.0	100.0
250.0	100.0
125.0	93.1
88.00	23.4
63.00	0.0

Peak Number	% of Dist. *	Mean	Mode	Median	Standard Deviation	Skewness	Kurtosis
1	100.0	99.47	97.67	98.16	18.30	1.092	3.949

\* Peaks must comprise at least 5.00 % of the distribution.

# Micromeritics

WIN5100 V2.03

Page 1

Sample: TT-23-08 23 cm  
Operator: Clint Edrington  
Submitter: Clint Edrington  
File Name: C:\EDRING~1\TIGER&~1\SANDFR~1\TT-23-08\23\_23CM.SMP  
Material/Liquid: silicate mud/water/Water

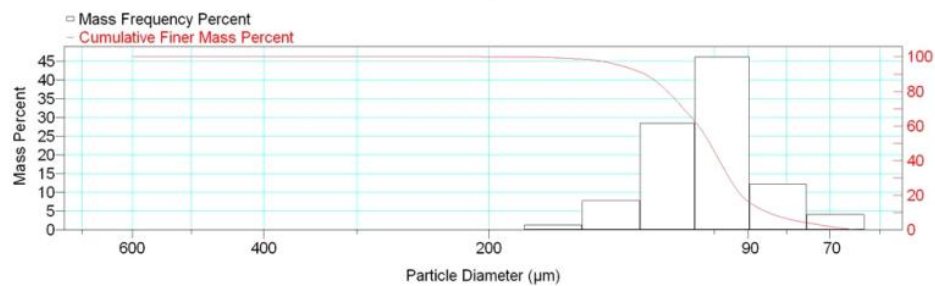
Reported: 01/03/10 19:26:10  
Liquid Visc: 0.7225 cp

Sample Density: 2.650 g/cm<sup>3</sup>  
Liquid Density: 0.9941 g/cm<sup>3</sup>

## Report by Size Class

High Diameter (μm)	Low Diameter (μm)	Average Diameter (μm)	Cumulative Mass Finer (Percent)	Mass Frequency (Percent)
710.0	600.0	652.7	100.0	0.0
600.0	500.0	547.7	100.0	0.0
500.0	425.0	461.0	100.0	0.0
425.0	355.0	388.4	100.0	0.0
355.0	300.0	326.3	100.0	0.0
300.0	250.0	273.9	100.0	0.0
250.0	212.0	230.2	100.0	0.0
212.0	180.0	195.3	99.9	0.1
180.0	150.0	164.3	98.6	1.3
150.0	125.0	136.9	90.8	7.8
125.0	106.0	115.1	62.4	28.4
106.0	90.00	97.67	16.3	46.1
90.00	75.00	82.16	4.1	12.2
75.00	63.00	68.74	0.0	4.1

Mass Frequency vs Diameter



## Summary Report

Full scale pump speed: 3  
Bubble detection: Medium  
Starting Size: 63.00 μm  
Ending Size: 0.50 μm

Stir time: 30 secs  
Stir speed: Low  
Probe time: 30 secs

Sample: TT-23-08 23 cm  
 Operator: Clint Edrington  
 Submitter: Clint Edrington  
 File Name: C:\EDRING~1\TIGER&~1\SANDFR~1\TT-23-08\23\_23CM.SMP  
 Material/Liquid: silicate mud/water/Water

Reported: 01/03/10 19:26:10  
 Liquid Visc: 0.7225 cp

Sample Density: 2.650 g/cm<sup>3</sup>  
 Liquid Density: 0.9941 g/cm<sup>3</sup>

## Summary Report

Parameter 1 0.000

Parameter 2 0.000

Parameter 3 0.000

## Mass Distribution Arithmetic Statistics

Mean	103.6	Std. Dev.	17.40
Median	101.3	Coef. Var.	0.168
Mode	97.67	Skewness	0.758
		Kurtosis	1.759

## Selected Percentiles

Percent Finer	Diameter (µm)
100.0	600.3
80.0	115.4
60.0	104.9
40.0	98.37
20.0	91.94

## Selected Sizes

Diameter (µm)	Percent Finer
500.0	100.0
250.0	100.0
125.0	90.8
88.00	13.7
63.00	0.0

Peak Number	% of Dist. *	Mean	Mode	Median	Standard Deviation	Skewness	Kurtosis
1	100.0	103.6	97.67	101.3	17.40	0.758	1.759

\* Peaks must comprise at least 5.00 % of the distribution.



# Micromeritics

WIN5100 V2.03

Page 1

Sample: TT-23-08 45 cm  
Operator: Clint Edrington  
Submitter: Clint Edrington  
File Name: C:\EDRING~1\TIGER&~1\SANDFR~1\TT-23-08\23\_45CM.SMP  
Material/Liquid: silicate mud/water/Water

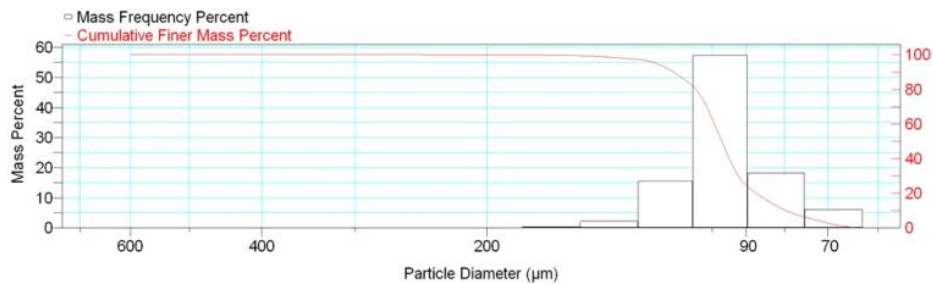
Reported: 01/03/10 19:28:17  
Liquid Visc: 0.7225 cp

Sample Density: 2.650 g/cm<sup>3</sup>  
Liquid Density: 0.9941 g/cm<sup>3</sup>

## Report by Size Class

High Diameter (μm)	Low Diameter (μm)	Average Diameter (μm)	Cumulative Mass Finer (Percent)	Mass Frequency (Percent)
710.0	600.0	652.7	100.0	0.0
600.0	500.0	547.7	100.0	0.0
500.0	425.0	461.0	100.0	0.0
425.0	355.0	388.4	100.0	0.0
355.0	300.0	326.3	100.0	0.0
300.0	250.0	273.9	100.0	0.0
250.0	212.0	230.2	99.9	0.1
212.0	180.0	195.3	99.8	0.1
180.0	150.0	164.3	99.4	0.4
150.0	125.0	136.9	97.2	2.2
125.0	106.0	115.1	81.7	15.5
106.0	90.00	97.67	24.4	57.3
90.00	75.00	82.16	6.1	18.3
75.00	63.00	68.74	0.0	6.1

Mass Frequency vs Diameter



## Summary Report

Full scale pump speed: 3  
Bubble detection: Medium  
Starting Size: 63.00 μm  
Ending Size: 0.50 μm

Stir time: 30 secs  
Stir speed: Low  
Probe time: 30 secs

Sample: TT-23-08 45 cm  
 Operator: Clint Edrington  
 Submitter: Clint Edrington  
 File Name: C:\EDRING~1\TIGER&~1\SANDFR~1\TT-23-08\23\_45CM.SMP  
 Material/Liquid: silicate mud/water/Water

Reported: 01/03/10 19:28:17  
 Liquid Visc: 0.7225 cp

Sample Density: 2.650 g/cm<sup>3</sup>  
 Liquid Density: 0.9941 g/cm<sup>3</sup>

## Summary Report

Parameter 1 0.000

Parameter 2 0.000

Parameter 3 0.000

## Mass Distribution Arithmetic Statistics

Mean	97.13	Std. Dev.	14.86
Median	97.04	Coef. Var.	0.153
Mode	97.67	Skewness	1.462
		Kurtosis	9.489

## Selected Percentiles

Percent Finer	Diameter (µm)
100.0	651.9
80.0	105.0
60.0	99.24
40.0	94.81
20.0	87.27

## Selected Sizes

Diameter (µm)	Percent Finer
500.0	100.0
250.0	100.0
125.0	97.2
88.00	21.1
63.00	0.0

Peak Number	% of Dist. *	Mean	Mode	Median	Standard Deviation	Skewness	Kurtosis
1	100.0	97.13	97.67	97.04	14.86	1.462	9.489

\* Peaks must comprise at least 5.00 % of the distribution.

# Micromeritics

WIN5100 V2.03

Page 1

Sample: TT-23-08 90 cm  
Operator: Clint Edrington  
Submitter: Clint Edrington  
File Name: C:\EDRING~1\TIGER&~1\SANDFR~1\TT-23-08\23\_90CM.SMP  
Material/Liquid: silicate mud/water/Water

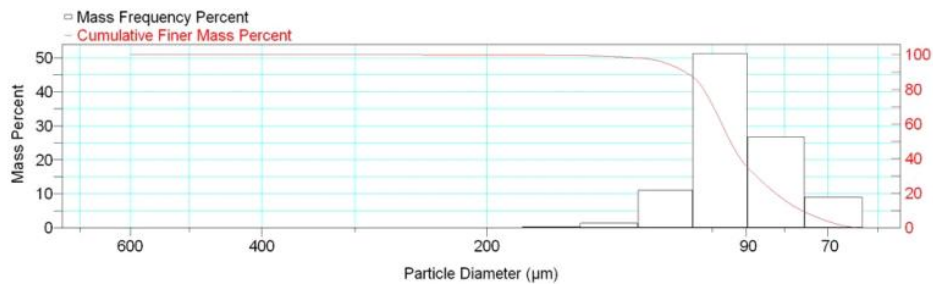
Reported: 01/03/10 19:30:05  
Liquid Visc: 0.7225 cp

Sample Density: 2.650 g/cm<sup>3</sup>  
Liquid Density: 0.9941 g/cm<sup>3</sup>

## Report by Size Class

High Diameter (μm)	Low Diameter (μm)	Average Diameter (μm)	Cumulative Mass Finer (Percent)	Mass Frequency (Percent)
710.0	600.0	652.7	100.0	0.0
600.0	500.0	547.7	100.0	0.0
500.0	425.0	461.0	100.0	0.0
425.0	355.0	388.4	100.0	0.0
355.0	300.0	326.3	100.0	0.0
300.0	250.0	273.9	100.0	0.0
250.0	212.0	230.2	99.9	0.1
212.0	180.0	195.3	99.8	0.1
180.0	150.0	164.3	99.5	0.3
150.0	125.0	136.9	98.1	1.4
125.0	106.0	115.1	87.0	11.1
106.0	90.00	97.67	35.7	51.3
90.00	75.00	82.16	9.0	26.7
75.00	63.00	68.74	0.0	9.0

Mass Frequency vs Diameter



## Summary Report

Full scale pump speed: 3  
Bubble detection: Medium  
Starting Size: 63.00 μm  
Ending Size: 0.50 μm

Stir time: 30 secs  
Stir speed: Low  
Probe time: 30 secs

Sample: TT-23-08 90 cm  
 Operator: Clint Edrington  
 Submitter: Clint Edrington  
 File Name: C:\EDRING~1\TIGER&~1\SANDFR~1\TT-23-08\23\_90CM.SMP  
 Material/Liquid: silicate mud/water/Water

Reported: 01/03/10 19:30:05  
 Liquid Visc: 0.7225 cp

Sample Density: 2.650 g/cm<sup>3</sup>  
 Liquid Density: 0.9941 g/cm<sup>3</sup>

## Summary Report

Parameter 1 0.000

Parameter 2 0.000

Parameter 3 0.000

## Mass Distribution Arithmetic Statistics

Mean	93.84	Std. Dev.	14.86
Median	94.51	Coef. Var.	0.158
Mode	97.67	Skewness	1.525
		Kurtosis	10.097

## Selected Percentiles

Percent Finer	Diameter (µm)
100.0	651.9
80.0	102.6
60.0	97.03
40.0	91.65
20.0	82.21

## Selected Sizes

Diameter (µm)	Percent Finer
500.0	100.0
250.0	100.0
125.0	98.1
88.00	31.5
63.00	0.0

Peak Number	% of Dist. *	Mean	Mode	Median	Standard Deviation	Skewness	Kurtosis
1	100.0	93.84	97.67	94.51	14.86	1.525	10.097

\* Peaks must comprise at least 5.00 % of the distribution.

Micromeritics

WIN5100 V2.03

Page 1

Sample: TT-23-08 150 cm  
Operator: Clint Edrington  
Submitter: Clint Edrington  
File Name: C:\EDRING~1\TIGER&~1\SANDFR~1\TT-23-08\23\_150CM.SMP  
Material/Liquid: silicate mud/water/Water

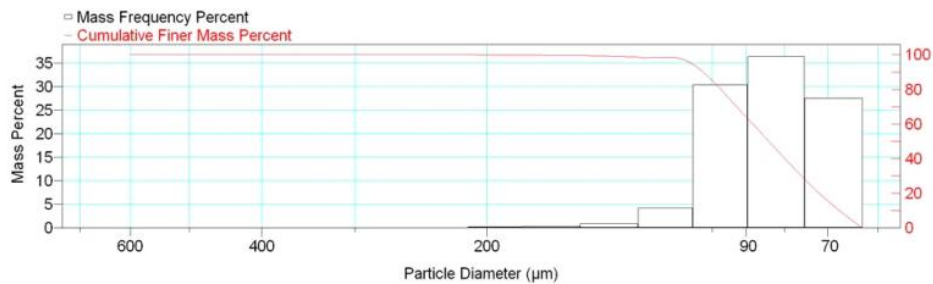
Reported: 01/03/10 19:32:05  
Liquid Visc: 0.7225 cp

Sample Density: 2.650 g/cm<sup>3</sup>  
Liquid Density: 0.9941 g/cm<sup>3</sup>

Report by Size Class

High Diameter (μm)	Low Diameter (μm)	Average Diameter (μm)	Cumulative Mass Finer (Percent)	Mass Frequency (Percent)
710.0	600.0	652.7	100.0	0.0
600.0	500.0	547.7	100.0	0.0
500.0	425.0	461.0	100.0	0.0
425.0	355.0	388.4	100.0	0.0
355.0	300.0	326.3	100.0	0.0
300.0	250.0	273.9	100.0	0.0
250.0	212.0	230.2	100.0	0.0
212.0	180.0	195.3	99.8	0.2
180.0	150.0	164.3	99.5	0.3
150.0	125.0	136.9	98.6	0.9
125.0	106.0	115.1	94.4	4.2
106.0	90.00	97.67	64.0	30.4
90.00	75.00	82.16	27.6	36.4
75.00	63.00	68.74	0.0	27.6

Mass Frequency vs Diameter



Summary Report

Full scale pump speed: 3  
Bubble detection: Medium  
Starting Size: 63.00 μm  
Ending Size: 0.50 μm

Stir time: 30 secs  
Stir speed: Low  
Probe time: 30 secs

Sample: TT-23-08 150 cm  
 Operator: Clint Edrington  
 Submitter: Clint Edrington  
 File Name: C:\EDRING~1\TIGER&~1\SANDFR~1\TT-23-08\23\_150CM.SMP  
 Material/Liquid: silicate mud/water/Water

Reported: 01/03/10 19:32:05  
 Liquid Visc: 0.7225 cp

Sample Density: 2.650 g/cm<sup>3</sup>  
 Liquid Density: 0.9941 g/cm<sup>3</sup>

## Summary Report

Parameter 1 0.000

Parameter 2 0.000

Parameter 3 0.000

## Mass Distribution Arithmetic Statistics

Mean	85.52	Std. Dev.	15.17
Median	83.95	Coef. Var.	0.177
Mode	82.16	Skewness	1.621
		Kurtosis	7.019

## Selected Percentiles

Percent Finer	Diameter (µm)
100.0	600.3
80.0	97.31
60.0	88.20
40.0	79.90
20.0	71.90

## Selected Sizes

Diameter (µm)	Percent Finer
500.0	100.0
250.0	100.0
125.0	98.6
88.00	59.5
63.00	0.0

Peak Number	% of Dist. *	Mean	Mode	Median	Standard Deviation	Skewness	Kurtosis
1	100.0	85.52	82.16	83.95	15.17	1.621	7.019

\* Peaks must comprise at least 5.00 % of the distribution.

# Micromeritics

WIN5100 V2.03

Page 1

Sample: TT-23-08 300 cm  
Operator: Clint Edrington  
Submitter: Clint Edrington  
File Name: C:\EDRING~1\TIGER&~1\SANDFR~1\TT-23-08\23\_300CM.SMP  
Material/Liquid: silicate mud/water/Water

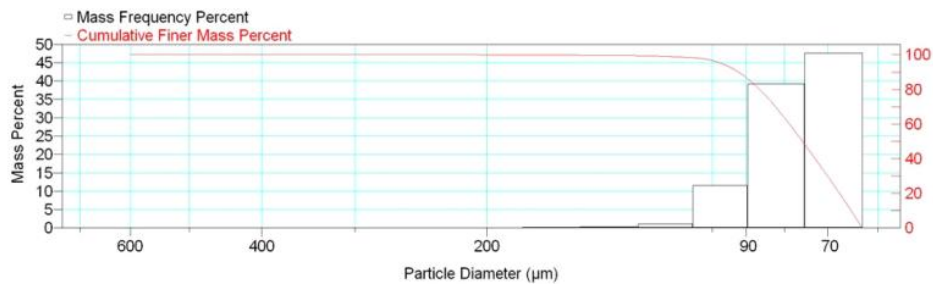
Reported: 01/03/10 19:34:15  
Liquid Visc: 0.7225 cp

Sample Density: 2.650 g/cm<sup>3</sup>  
Liquid Density: 0.9941 g/cm<sup>3</sup>

## Report by Size Class

High Diameter (µm)	Low Diameter (µm)	Average Diameter (µm)	Cumulative Mass Finer (Percent)	Mass Frequency (Percent)
710.0	600.0	652.7	100.0	0.0
600.0	500.0	547.7	100.0	0.0
500.0	425.0	461.0	100.0	0.0
425.0	355.0	388.4	100.0	0.0
355.0	300.0	326.3	100.0	0.0
300.0	250.0	273.9	100.0	0.0
250.0	212.0	230.2	100.0	0.0
212.0	180.0	195.3	99.9	0.1
180.0	150.0	164.3	99.7	0.2
150.0	125.0	136.9	99.4	0.3
125.0	106.0	115.1	98.3	1.1
106.0	90.00	97.67	86.8	11.5
90.00	75.00	82.16	47.6	39.2
75.00	63.00	68.74	0.0	47.6

Mass Frequency vs Diameter



## Summary Report

Full scale pump speed: 3  
Bubble detection: Medium  
Starting Size: 63.00 µm  
Ending Size: 0.50 µm

Stir time: 30 secs  
Stir speed: Low  
Probe time: 30 secs

Sample: TT-23-08 300 cm  
 Operator: Clint Edrington  
 Submitter: Clint Edrington  
 File Name: C:\EDRING~1\TIGER&~1\SANDFR~1\TT-23-08\23\_300CM.SMP  
 Material/Liquid: silicate mud/water/Water

Reported: 01/03/10 19:34:15  
 Liquid Visc: 0.7225 cp

Sample Density: 2.650 g/cm<sup>3</sup>  
 Liquid Density: 0.9941 g/cm<sup>3</sup>

## Summary Report

Parameter 1 0.000

Parameter 2 0.000

Parameter 3 0.000

## Mass Distribution Arithmetic Statistics

Mean	78.36	Std. Dev.	12.09
Median	75.71	Coef. Var.	0.154
Mode	68.74	Skewness	2.515
		Kurtosis	14.400

## Selected Percentiles

Percent Finer	Diameter (µm)
100.0	600.3
80.0	86.39
60.0	78.80
40.0	72.82
20.0	67.54

## Selected Sizes

Diameter (µm)	Percent Finer
500.0	100.0
250.0	100.0
125.0	99.4
88.00	83.3
63.00	0.0

Peak Number	% of Dist. *	Mean	Mode	Median	Standard Deviation	Skewness	Kurtosis
1	100.0	78.36	68.74	75.71	12.09	2.515	14.400

\* Peaks must comprise at least 5.00 % of the distribution.



Micromeritics

WIN5100 V2.03

Page 1

Sample: TT-23-08 340 cm  
Operator: Clint Edrington  
Submitter: Clint Edrington  
File Name: C:\EDRING~1\TIGER&~1\SANDFR~1\TT-23-08\23\_340CM.SMP  
Material/Liquid: silicate mud/water/Water

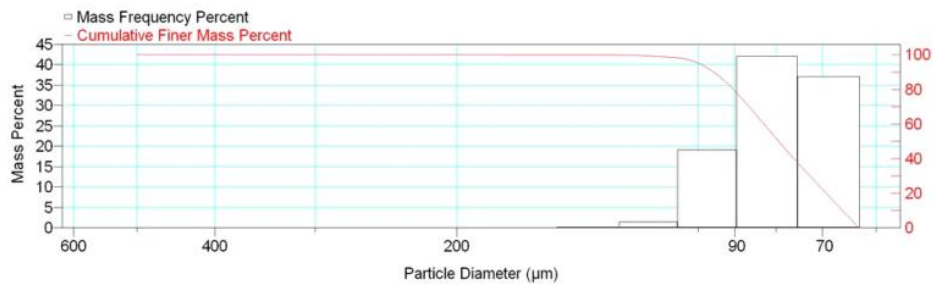
Reported: 01/03/10 19:36:18  
Liquid Visc: 0.7225 cp

Sample Density: 2.650 g/cm<sup>3</sup>  
Liquid Density: 0.9941 g/cm<sup>3</sup>

Report by Size Class

High Diameter (μm)	Low Diameter (μm)	Average Diameter (μm)	Cumulative Mass Finer (Percent)	Mass Frequency (Percent)
600.0	500.0	547.7	100.0	0.0
500.0	425.0	461.0	100.0	0.0
425.0	355.0	388.4	100.0	0.0
355.0	300.0	326.3	100.0	0.0
300.0	250.0	273.9	100.0	0.0
250.0	212.0	230.2	100.0	0.0
212.0	180.0	195.3	100.0	0.0
180.0	150.0	164.3	99.9	0.1
150.0	125.0	136.9	99.7	0.2
125.0	106.0	115.1	98.2	1.5
106.0	90.00	97.67	79.1	19.1
90.00	75.00	82.16	37.1	42.0
75.00	63.00	68.74	0.0	37.1

Mass Frequency vs Diameter



Summary Report

Full scale pump speed: 3  
Bubble detection: Medium  
Starting Size: 63.00 μm  
Ending Size: 0.50 μm

Stir time: 30 secs  
Stir speed: Low  
Probe time: 30 secs

Parameter 1 0.000

Parameter 2 0.000

Parameter 3 0.000

Sample: TT-23-08 340 cm  
 Operator: Clint Edrington  
 Submitter: Clint Edrington  
 File Name: C:\EDRING~1\TIGER&~1\SANDFR~1\TT-23-08\23\_340CM.SMP  
 Material/Liquid: silicate mud/water/Water

Reported: 01/03/10 19:36:18  
 Liquid Visc: 0.7225 cp

Sample Density: 2.650 g/cm<sup>3</sup>  
 Liquid Density: 0.9941 g/cm<sup>3</sup>

## Summary Report

## Mass Distribution Arithmetic Statistics

Mean	80.83	Std. Dev.	11.83
Median	79.39	Coef. Var.	0.146
Mode	82.16	Skewness	1.084
		Kurtosis	2.731

## Selected Percentiles

Percent Finer	Diameter (µm)
100.0	553.2
80.0	90.38
60.0	82.81
40.0	76.00
20.0	69.28

## Selected Sizes

Diameter (µm)	Percent Finer
500.0	100.0
250.0	100.0
125.0	99.7
88.00	74.2
63.00	0.0

Peak Number	% of Dist.*	Mean	Mode	Median	Standard Deviation	Skewness	Kurtosis
1	100.0	80.83	82.16	79.39	11.83	1.084	2.731

\* Peaks must comprise at least 5.00 % of the distribution.

Micromeritics

WIN5100 V2.03

Page 1

Sample: TT-24-08 5 cm  
Operator: Clint Edrington  
Submitter: Clint Edrington  
File Name: C:\EDRING~1\TIGER&~1\SANDFR~1\TT-24-08\24\_5CM.SMP  
Material/Liquid: silicate mud/water/Water

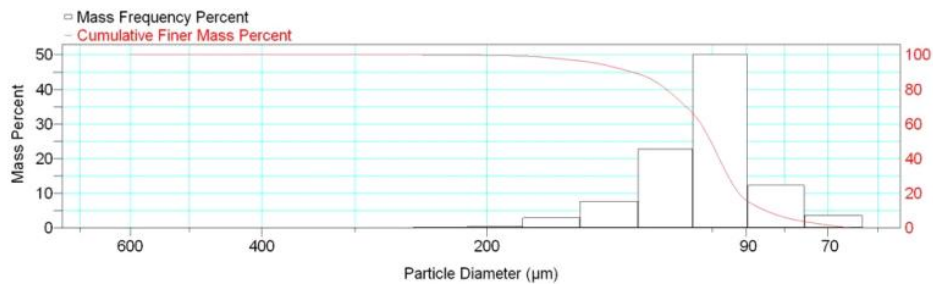
Reported: 01/03/10 19:42:28  
Liquid Visc: 0.7225 cp

Sample Density: 2.650 g/cm<sup>3</sup>  
Liquid Density: 0.9941 g/cm<sup>3</sup>

Report by Size Class

High Diameter (μm)	Low Diameter (μm)	Average Diameter (μm)	Cumulative Mass Finer (Percent)	Mass Frequency (Percent)
710.0	600.0	652.7	100.0	0.0
600.0	500.0	547.7	100.0	0.0
500.0	425.0	461.0	100.0	0.0
425.0	355.0	388.4	100.0	0.0
355.0	300.0	326.3	100.0	0.0
300.0	250.0	273.9	100.0	0.0
250.0	212.0	230.2	99.8	0.2
212.0	180.0	195.3	99.3	0.5
180.0	150.0	164.3	96.4	2.9
150.0	125.0	136.9	88.7	7.7
125.0	106.0	115.1	65.9	22.8
106.0	90.00	97.67	15.9	50.0
90.00	75.00	82.16	3.6	12.3
75.00	63.00	68.74	0.0	3.6

Mass Frequency vs Diameter



Summary Report

Full scale pump speed: 3  
Bubble detection: Medium  
Starting Size: 63.00 μm  
Ending Size: 0.50 μm

Stir time: 30 secs  
Stir speed: Low  
Probe time: 30 secs

Sample: TT-24-08 5 cm  
 Operator: Clint Edrington  
 Submitter: Clint Edrington  
 File Name: C:\EDRING~1\TIGER&~1\SANDFR~1\TT-24-08\24\_5CM.SMP  
 Material/Liquid: silicate mud/water/Water

Reported: 01/03/10 19:42:28  
 Liquid Visc: 0.7225 cp

Sample Density: 2.650 g/cm<sup>3</sup>  
 Liquid Density: 0.9941 g/cm<sup>3</sup>

## Summary Report

Parameter 1 0.000

Parameter 2 0.000

Parameter 3 0.000

## Mass Distribution Arithmetic Statistics

Mean	104.4	Std. Dev.	20.35
Median	100.4	Coef. Var.	0.195
Mode	97.67	Skewness	1.634
		Kurtosis	5.140

## Selected Percentiles

Percent Finer	Diameter (µm)
100.0	651.9
80.0	115.1
60.0	103.5
40.0	97.79
20.0	92.06

## Selected Sizes

Diameter (µm)	Percent Finer
500.0	100.0
250.0	100.0
125.0	88.7
88.00	13.4
63.00	0.0

Peak Number	% of Dist. *	Mean	Mode	Median	Standard Deviation	Skewness	Kurtosis
1	100.0	104.4	97.67	100.4	20.35	1.634	5.140

\* Peaks must comprise at least 5.00 % of the distribution.

# Micromeritics

WIN5100 V2.03

Page 1

Sample: TT-24-08 50 cm  
Operator: Clint Edrington  
Submitter: Clint Edrington  
File Name: C:\EDRING~1\TIGER&~1\SANDFR~1\TT-24-08\24\_50CM.SMP  
Material/Liquid: silicate mud/water/Water

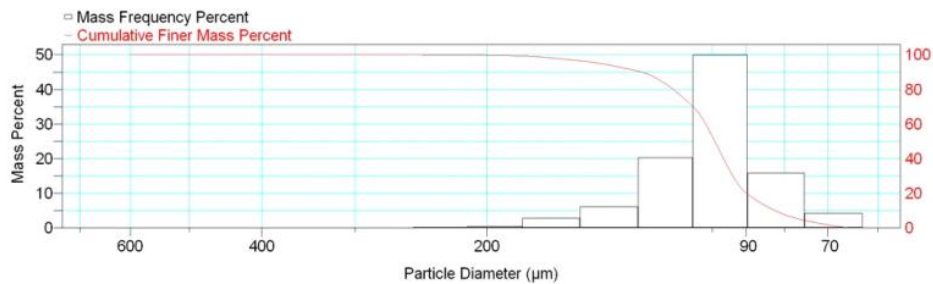
Reported: 01/03/10 19:44:27  
Liquid Visc: 0.7225 cp

Sample Density: 2.650 g/cm<sup>3</sup>  
Liquid Density: 0.9941 g/cm<sup>3</sup>

## Report by Size Class

High Diameter (µm)	Low Diameter (µm)	Average Diameter (µm)	Cumulative Mass Finer (Percent)	Mass Frequency (Percent)
710.0	600.0	652.7	100.0	0.0
600.0	500.0	547.7	100.0	0.0
500.0	425.0	461.0	100.0	0.0
425.0	355.0	388.4	100.0	0.0
355.0	300.0	326.3	100.0	0.0
300.0	250.0	273.9	100.0	0.0
250.0	212.0	230.2	99.8	0.2
212.0	180.0	195.3	99.3	0.5
180.0	150.0	164.3	96.5	2.8
150.0	125.0	136.9	90.3	6.2
125.0	106.0	115.1	70.0	20.3
106.0	90.00	97.67	20.1	49.9
90.00	75.00	82.16	4.2	15.9
75.00	63.00	68.74	0.0	4.2

Mass Frequency vs Diameter



## Summary Report

Full scale pump speed: 3  
Bubble detection: Medium  
Starting Size: 63.00 µm  
Ending Size: 0.50 µm

Stir time: 30 secs  
Stir speed: Low  
Probe time: 30 secs

Sample: TT-24-08 50 cm  
 Operator: Clint Edrington  
 Submitter: Clint Edrington  
 File Name: C:\EDRING~1\TIGER&~1\SANDFR~1\TT-24-08\24\_50CM.SMP  
 Material/Liquid: silicate mud/water/Water

Reported: 01/03/10 19:44:27  
 Liquid Visc: 0.7225 cp

Sample Density: 2.650 g/cm<sup>3</sup>  
 Liquid Density: 0.9941 g/cm<sup>3</sup>

## Summary Report

Parameter 1 0.000

Parameter 2 0.000

Parameter 3 0.000

## Mass Distribution Arithmetic Statistics

Mean	102.6	Std. Dev.	20.34
Median	99.14	Coef. Var.	0.198
Mode	97.67	Skewness	1.735
		Kurtosis	5.656

## Selected Percentiles

Percent Finer	Diameter (µm)
100.0	651.9
80.0	112.7
60.0	102.0
40.0	96.54
20.0	89.94

## Selected Sizes

Diameter (µm)	Percent Finer
500.0	100.0
250.0	100.0
125.0	90.3
88.00	17.1
63.00	0.0

Peak Number	% of Dist. *	Mean	Mode	Median	Standard Deviation	Skewness	Kurtosis
1	100.0	102.6	97.67	99.14	20.34	1.735	5.656

\* Peaks must comprise at least 5.00 % of the distribution.

Micromeritics

WIN5100 V2.03

Page 1

Sample: TT-25-08 10 cm  
Operator: Clint Edrington  
Submitter: Clint Edrington  
File Name: C:\EDRING~1\TIGER&~1\SANDFR~1\TT-25-08\25\_10CM.SMP  
Material/Liquid: silicate mud/water/Water

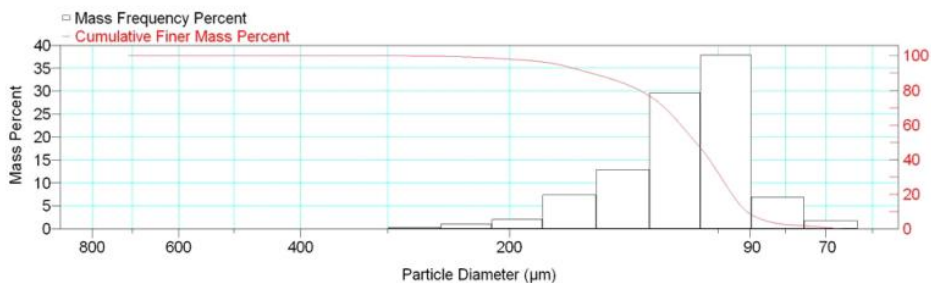
Reported: 01/04/10 11:12:25  
Liquid Visc: 0.7225 cp

Sample Density: 2.650 g/cm<sup>3</sup>  
Liquid Density: 0.9941 g/cm<sup>3</sup>

Report by Size Class

High Diameter (µm)	Low Diameter (µm)	Average Diameter (µm)	Cumulative Mass Finer (Percent)	Mass Frequency (Percent)
850.0	710.0	776.9	100.0	0.0
710.0	600.0	652.7	100.0	0.0
600.0	500.0	547.7	100.0	0.0
500.0	425.0	461.0	100.0	0.0
425.0	355.0	388.4	100.0	0.0
355.0	300.0	326.3	100.0	0.0
300.0	250.0	273.9	99.7	0.3
250.0	212.0	230.2	98.6	1.1
212.0	180.0	195.3	96.5	2.1
180.0	150.0	164.3	89.1	7.4
150.0	125.0	136.9	76.2	12.9
125.0	106.0	115.1	46.6	29.6
106.0	90.00	97.67	8.7	37.9
90.00	75.00	82.16	1.8	6.9
75.00	63.00	68.74	0.0	1.8

Mass Frequency vs Diameter



Summary Report

Full scale pump speed: 3  
Bubble detection: Medium  
Starting Size: 63.00 µm  
Ending Size: 0.50 µm

Stir time: 30 secs  
Stir speed: Low  
Probe time: 30 secs

Sample: TT-25-08 10 cm  
 Operator: Clint Edrington  
 Submitter: Clint Edrington  
 File Name: C:\EDRING~1\TIGER&~1\SANDFR~1\TT-25-08\25\_10CM.SMP  
 Material/Liquid: silicate mud/water/Water

Reported: 01/04/10 11:12:25  
 Liquid Visc: 0.7225 cp

Sample Density: 2.650 g/cm<sup>3</sup>  
 Liquid Density: 0.9941 g/cm<sup>3</sup>

## Summary Report

Parameter 1	0.000	Parameter 2	0.000	Parameter 3	0.000		
Mass Distribution Arithmetic Statistics							
Mean	115.3	Std. Dev.		28.74			
Median	107.8	Coef. Var.		0.249			
Mode	97.67	Skewness		1.816			
		Kurtosis		4.828			
Selected Percentiles			Selected Sizes				
Percent Finer	Diameter (µm)		Diameter (µm)	Percent Finer			
100.0	714.1		500.0	100.0			
80.0	129.9		250.0	99.7			
60.0	113.2		125.0	76.2			
40.0	103.0		88.00	6.6			
20.0	95.56		63.00	0.0			
Peak Number	% of Dist.*	Mean	Mode	Median	Standard Deviation	Skewness	Kurtosis
1	100.0	115.3	97.67	107.8	28.74	1.816	4.828

\* Peaks must comprise at least 5.00 % of the distribution.



# Micromeritics

WIN5100 V2.03

Page 1

Sample: TT-25-08 50 cm  
Operator: Clint Edrington  
Submitter: Clint Edrington  
File Name: C:\EDRING~1\TIGER&~1\SANDFR~1\TT-25-08\25\_50CM.SMP  
Material/Liquid: silicate mud/water/Water

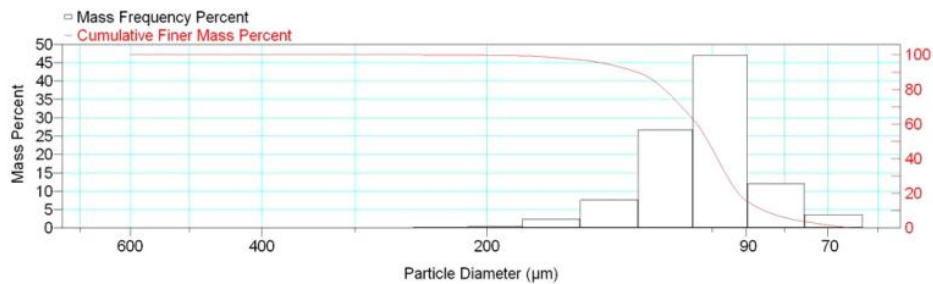
Reported: 01/04/10 11:14:48  
Liquid Visc: 0.7225 cp

Sample Density: 2.650 g/cm<sup>3</sup>  
Liquid Density: 0.9941 g/cm<sup>3</sup>

## Report by Size Class

High Diameter (µm)	Low Diameter (µm)	Average Diameter (µm)	Cumulative Mass Finer (Percent)	Mass Frequency (Percent)
710.0	600.0	652.7	100.0	0.0
600.0	500.0	547.7	100.0	0.0
500.0	425.0	461.0	100.0	0.0
425.0	355.0	388.4	100.0	0.0
355.0	300.0	326.3	100.0	0.0
300.0	250.0	273.9	100.0	0.0
250.0	212.0	230.2	99.8	0.2
212.0	180.0	195.3	99.4	0.4
180.0	150.0	164.3	97.0	2.4
150.0	125.0	136.9	89.4	7.6
125.0	106.0	115.1	62.7	26.7
106.0	90.00	97.67	15.7	47.0
90.00	75.00	82.16	3.6	12.1
75.00	63.00	68.74	0.0	3.6

Mass Frequency vs Diameter



## Summary Report

Full scale pump speed: 3  
Bubble detection: Medium  
Starting Size: 63.00 µm  
Ending Size: 0.50 µm

Stir time: 30 secs  
Stir speed: Low  
Probe time: 30 secs

Sample: TT-25-08 50 cm  
 Operator: Clint Edrington  
 Submitter: Clint Edrington  
 File Name: C:\EDRING~1\TIGER&~1\SANDFR~1\TT-25-08\25\_50CM.SMP  
 Material/Liquid: silicate mud/water/Water

Reported: 01/04/10 11:14:48  
 Liquid Visc: 0.7225 cp

Sample Density: 2.650 g/cm<sup>3</sup>  
 Liquid Density: 0.9941 g/cm<sup>3</sup>

## Summary Report

Parameter 1 0.000

Parameter 2 0.000

Parameter 3 0.000

## Mass Distribution Arithmetic Statistics

Mean	104.6	Std. Dev.	19.72
Median	101.3	Coef. Var.	0.188
Mode	97.67	Skewness	1.526
		Kurtosis	5.268

## Selected Percentiles

Percent Finer	Diameter (µm)
100.0	651.9
80.0	115.8
60.0	104.8
40.0	98.36
20.0	92.18

## Selected Sizes

Diameter (µm)	Percent Finer
500.0	100.0
250.0	100.0
125.0	89.4
88.00	13.1
63.00	0.0

Peak Number	% of Dist. *	Mean	Mode	Median	Standard Deviation	Skewness	Kurtosis
1	100.0	104.6	97.67	101.3	19.72	1.526	5.268

\* Peaks must comprise at least 5.00 % of the distribution.

Micromeritics

WIN5100 V2.03

Page 1

Sample: TT-25-08 100 cm  
Operator: Clint Edrington  
Submitter: Clint Edrington  
File Name: C:\EDRING~1\TIGER&~1\SANDFR~1\TT-25-08\25\_100CM.SMP  
Material/Liquid: silicate mud/water/Water

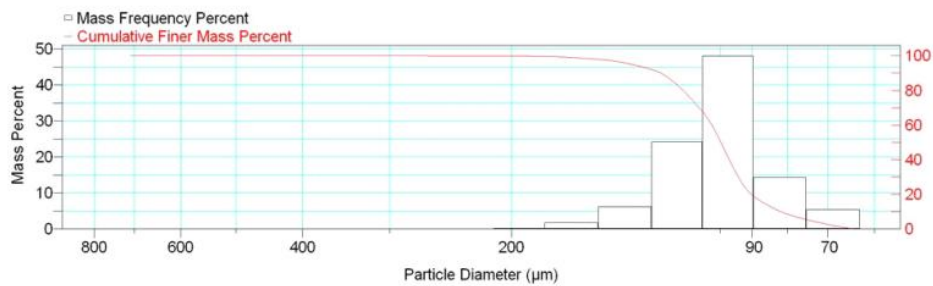
Reported: 01/04/10 11:16:50  
Liquid Visc: 0.7225 cp

Sample Density: 2.650 g/cm<sup>3</sup>  
Liquid Density: 0.9941 g/cm<sup>3</sup>

Report by Size Class

High Diameter ( $\mu\text{m}$ )	Low Diameter ( $\mu\text{m}$ )	Average Diameter ( $\mu\text{m}$ )	Cumulative Mass Finer (Percent)	Mass Frequency (Percent)
850.0	710.0	776.9	100.0	0.0
710.0	600.0	652.7	100.0	0.0
600.0	500.0	547.7	100.0	0.0
500.0	425.0	461.0	100.0	0.0
425.0	355.0	388.4	100.0	0.0
355.0	300.0	326.3	100.0	0.0
300.0	250.0	273.9	99.9	0.1
250.0	212.0	230.2	99.8	0.1
212.0	180.0	195.3	99.6	0.2
180.0	150.0	164.3	97.9	1.7
150.0	125.0	136.9	91.8	6.1
125.0	106.0	115.1	67.6	24.2
106.0	90.00	97.67	19.6	48.0
90.00	75.00	82.16	5.3	14.3
75.00	63.00	68.74	0.0	5.3

Mass Frequency vs Diameter



Summary Report

Full scale pump speed: 3  
Bubble detection: Medium  
Starting Size: 63.00  $\mu\text{m}$   
Ending Size: 0.50  $\mu\text{m}$

Stir time: 30 secs  
Stir speed: Low  
Probe time: 30 secs

Sample: TT-25-08 100 cm  
 Operator: Clint Edrington  
 Submitter: Clint Edrington  
 File Name: C:\EDRING~1\TIGER&~1\SANDFR~1\TT-25-08\25\_100CM.SMP  
 Material/Liquid: silicate mud/water/Water

Reported: 01/04/10 11:16:50  
 Liquid Visc: 0.7225 cp

Sample Density: 2.650 g/cm<sup>3</sup>  
 Liquid Density: 0.9941 g/cm<sup>3</sup>

## Summary Report

Parameter 1	0.000	Parameter 2	0.000	Parameter 3	0.000		
Mass Distribution Arithmetic Statistics							
Mean	102.2	Std. Dev.		19.22			
Median	99.81	Coef. Var.		0.188			
Mode	97.67	Skewness		1.800			
		Kurtosis		9.663			
Selected Percentiles			Selected Sizes				
Percent Finer	Diameter (µm)		Diameter (µm)	Percent Finer			
100.0	714.1		500.0	100.0			
80.0	113.2		250.0	99.9			
60.0	102.9		125.0	91.8			
40.0	97.06		88.00	16.8			
20.0	90.26		63.00	0.0			
Peak Number	% of Dist.*	Mean	Mode	Median	Standard Deviation	Skewness	Kurtosis
1	100.0	102.2	97.67	99.81	19.22	1.800	9.663

\* Peaks must comprise at least 5.00 % of the distribution.

Micromeritics

WIN5100 V2.03

Page 1

Sample: TT-25-08 150 cm  
Operator: Clint Edrington  
Submitter: Clint Edrington  
File Name: C:\EDRING~1\TIGER&~1\SANDFR~1\TT-25-08\25\_150CM.SMP  
Material/Liquid: silicate mud/water/Water

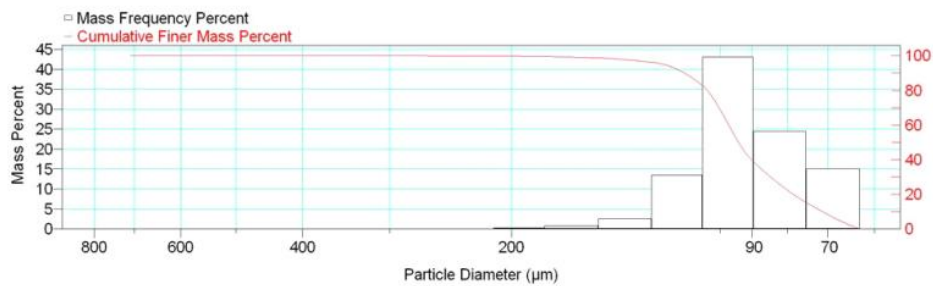
Reported: 01/04/10 11:18:52  
Liquid Visc: 0.7225 cp

Sample Density: 2.650 g/cm<sup>3</sup>  
Liquid Density: 0.9941 g/cm<sup>3</sup>

Report by Size Class

High Diameter (μm)	Low Diameter (μm)	Average Diameter (μm)	Cumulative Mass Finer (Percent)	Mass Frequency (Percent)
850.0	710.0	776.9	100.0	0.0
710.0	600.0	652.7	100.0	0.0
600.0	500.0	547.7	100.0	0.0
500.0	425.0	461.0	100.0	0.0
425.0	355.0	388.4	100.0	0.0
355.0	300.0	326.3	100.0	0.0
300.0	250.0	273.9	99.9	0.1
250.0	212.0	230.2	99.8	0.1
212.0	180.0	195.3	99.5	0.3
180.0	150.0	164.3	98.7	0.8
150.0	125.0	136.9	96.1	2.6
125.0	106.0	115.1	82.6	13.5
106.0	90.00	97.67	39.5	43.1
90.00	75.00	82.16	15.0	24.5
75.00	63.00	68.74	0.0	15.0

Mass Frequency vs Diameter



Summary Report

Full scale pump speed: 3  
Bubble detection: Medium  
Starting Size: 63.00 μm  
Ending Size: 0.50 μm

Stir time: 30 secs  
Stir speed: Low  
Probe time: 30 secs

Sample: TT-25-08 150 cm  
 Operator: Clint Edrington  
 Submitter: Clint Edrington  
 File Name: C:\EDRING~1\TIGER&~1\SANDFR~1\TT-25-08\25\_150CM.SMP  
 Material/Liquid: silicate mud/water/Water

Reported: 01/04/10 11:18:52  
 Liquid Visc: 0.7225 cp

Sample Density: 2.650 g/cm<sup>3</sup>  
 Liquid Density: 0.9941 g/cm<sup>3</sup>

## Summary Report

Parameter 1	0.000	Parameter 2	0.000	Parameter 3	0.000		
Mass Distribution Arithmetic Statistics							
Mean	94.04	Std. Dev.		19.11			
Median	94.14	Coef. Var.		0.203			
Mode	97.67	Skewness		2.110			
		Kurtosis		12.604			
Selected Percentiles			Selected Sizes				
Percent Finer	Diameter (µm)		Diameter (µm)	Percent Finer			
100.0	714.1		500.0	100.0			
80.0	104.4		250.0	99.9			
60.0	97.24		125.0	96.1			
40.0	90.27		88.00	35.9			
20.0	78.50		63.00	0.0			
Peak Number	% of Dist.*	Mean	Mode	Median	Standard Deviation	Skewness	Kurtosis
1	100.0	94.04	97.67	94.14	19.11	2.110	12.604

\* Peaks must comprise at least 5.00 % of the distribution.

# Micromeritics

WIN5100 V2.03

Page 1

Sample: TT-25-08 200 cm  
Operator: Clint Edrington  
Submitter: Clint Edrington  
File Name: C:\EDRING~1\TIGER&~1\SANDFR~1\TT-25-08\25\_200CM.SMP  
Material/Liquid: silicate mud/water/Water

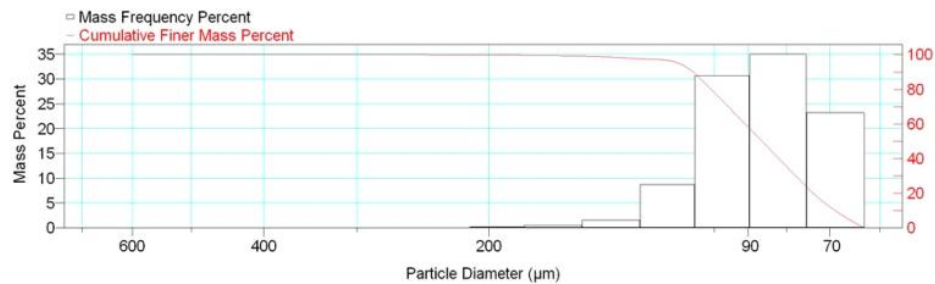
Reported: 01/04/10 11:21:34  
Liquid Visc: 0.7225 cp

Sample Density: 2.650 g/cm<sup>3</sup>  
Liquid Density: 0.9941 g/cm<sup>3</sup>

## Report by Size Class

High Diameter (µm)	Low Diameter (µm)	Average Diameter (µm)	Cumulative Mass Finer (Percent)	Mass Frequency (Percent)
710.0	600.0	652.7	100.0	0.0
600.0	500.0	547.7	100.0	0.0
500.0	425.0	461.0	100.0	0.0
425.0	355.0	388.4	100.0	0.0
355.0	300.0	326.3	100.0	0.0
300.0	250.0	273.9	100.0	0.0
250.0	212.0	230.2	99.9	0.1
212.0	180.0	195.3	99.7	0.2
180.0	150.0	164.3	99.2	0.5
150.0	125.0	136.9	97.6	1.6
125.0	106.0	115.1	88.9	8.7
106.0	90.00	97.67	58.2	30.7
90.00	75.00	82.16	23.2	35.0
75.00	63.00	68.74	0.0	23.2

Mass Frequency vs Diameter



## Summary Report

Full scale pump speed: 3  
Bubble detection: Medium  
Starting Size: 63.00 µm  
Ending Size: 0.50 µm

Stir time: 30 secs  
Stir speed: Low  
Probe time: 30 secs

Sample: TT-25-08 200 cm  
 Operator: Clint Edrington  
 Submitter: Clint Edrington  
 File Name: C:\EDRING~1\TIGER&~1\SANDFR~1\TT-25-08\25\_200CM.SMP  
 Material/Liquid: silicate mud/water/Water

Reported: 01/04/10 11:21:34  
 Liquid Visc: 0.7225 cp

Sample Density: 2.650 g/cm<sup>3</sup>  
 Liquid Density: 0.9941 g/cm<sup>3</sup>

## Summary Report

Parameter 1 0.000

Parameter 2 0.000

Parameter 3 0.000

## Mass Distribution Arithmetic Statistics

Mean	88.34	Std. Dev.	17.36
Median	86.24	Coef. Var.	0.196
Mode	82.16	Skewness	1.803
		Kurtosis	8.074

## Selected Percentiles

Percent Finer	Diameter (µm)
100.0	651.9
80.0	100.9
60.0	90.85
40.0	81.89
20.0	73.68

## Selected Sizes

Diameter (µm)	Percent Finer
500.0	100.0
250.0	100.0
125.0	97.6
88.00	53.9
63.00	0.0

Peak Number	% of Dist. *	Mean	Mode	Median	Standard Deviation	Skewness	Kurtosis
1	100.0	88.34	82.16	86.24	17.36	1.803	8.074

\* Peaks must comprise at least 5.00 % of the distribution.



# Micromeritics

WIN5100 V2.03

Page 1

Sample: TT-25-08 250 cm  
Operator: Clint Edrington  
Submitter: Clint Edrington  
File Name: C:\EDRING~1\TIGER&~1\SANDFR~1\TT-25-08\25\_250CM.SMP  
Material/Liquid: silicate mud/water/Water

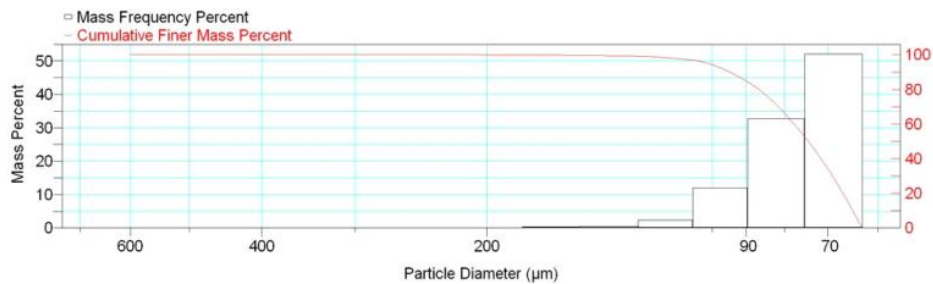
Reported: 01/04/10 11:23:30  
Liquid Visc: 0.7225 cp

Sample Density: 2.650 g/cm<sup>3</sup>  
Liquid Density: 0.9941 g/cm<sup>3</sup>

## Report by Size Class

High Diameter (μm)	Low Diameter (μm)	Average Diameter (μm)	Cumulative Mass Finer (Percent)	Mass Frequency (Percent)
710.0	600.0	652.7	100.0	0.0
600.0	500.0	547.7	100.0	0.0
500.0	425.0	461.0	100.0	0.0
425.0	355.0	388.4	100.0	0.0
355.0	300.0	326.3	100.0	0.0
300.0	250.0	273.9	100.0	0.0
250.0	212.0	230.2	100.0	0.0
212.0	180.0	195.3	99.9	0.1
180.0	150.0	164.3	99.6	0.3
150.0	125.0	136.9	99.1	0.5
125.0	106.0	115.1	96.8	2.3
106.0	90.00	97.67	84.8	12.0
90.00	75.00	82.16	52.1	32.7
75.00	63.00	68.74	0.0	52.1

Mass Frequency vs Diameter



## Summary Report

Full scale pump speed: 3  
Bubble detection: Medium  
Starting Size: 63.00 μm  
Ending Size: 0.50 μm

Stir time: 30 secs  
Stir speed: Low  
Probe time: 30 secs

Sample: TT-25-08 250 cm  
 Operator: Clint Edrington  
 Submitter: Clint Edrington  
 File Name: C:\EDRING~1\TIGER&~1\SANDFR~1\TT-25-08\25\_250CM.SMP  
 Material/Liquid: silicate mud/water/Water

Reported: 01/04/10 11:23:30  
 Liquid Visc: 0.7225 cp

Sample Density: 2.650 g/cm<sup>3</sup>  
 Liquid Density: 0.9941 g/cm<sup>3</sup>

## Summary Report

Parameter 1 0.000

Parameter 2 0.000

Parameter 3 0.000

## Mass Distribution Arithmetic Statistics

Mean	78.42	Std. Dev.	13.48
Median	74.34	Coef. Var.	0.172
Mode	68.74	Skewness	2.464
		Kurtosis	11.275

## Selected Percentiles

Percent Finer	Diameter (µm)
100.0	600.3
80.0	86.63
60.0	77.66
40.0	71.50
20.0	66.83

## Selected Sizes

Diameter (µm)	Percent Finer
500.0	100.0
250.0	100.0
125.0	99.1
88.00	82.1
63.00	0.0

Peak Number	% of Dist. *	Mean	Mode	Median	Standard Deviation	Skewness	Kurtosis
1	100.0	78.42	68.74	74.34	13.48	2.464	11.275

\* Peaks must comprise at least 5.00 % of the distribution.

Micromeritics

WIN5100 V2.03

Page 1

Sample: TT-26-08 5 cm  
Operator: Clint Edrington  
Submitter: Clint Edrington  
File Name: C:\EDRING~1\TIGER&~1\SANDFR~1\TT-26-08\26\_5CM.SMP  
Material/Liquid: silicate mud/water/Water

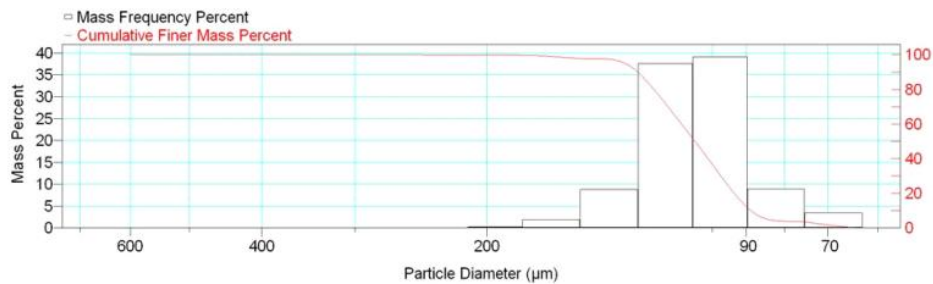
Reported: 01/04/10 11:49:05  
Liquid Visc: 0.7225 cp

Sample Density: 2.650 g/cm<sup>3</sup>  
Liquid Density: 0.9941 g/cm<sup>3</sup>

Report by Size Class

High Diameter (μm)	Low Diameter (μm)	Average Diameter (μm)	Cumulative Mass Finer (Percent)	Mass Frequency (Percent)
710.0	600.0	652.7	100.0	0.0
600.0	500.0	547.7	100.0	0.0
500.0	425.0	461.0	100.0	0.0
425.0	355.0	388.4	100.0	0.0
355.0	300.0	326.3	100.0	0.0
300.0	250.0	273.9	100.0	0.0
250.0	212.0	230.2	99.9	0.1
212.0	180.0	195.3	99.7	0.2
180.0	150.0	164.3	97.8	1.9
150.0	125.0	136.9	89.0	8.8
125.0	106.0	115.1	51.4	37.6
106.0	90.00	97.67	12.3	39.1
90.00	75.00	82.16	3.4	8.9
75.00	63.00	68.74	0.0	3.4

Mass Frequency vs Diameter



Summary Report

Full scale pump speed: 3  
Bubble detection: Medium  
Starting Size: 63.00 μm  
Ending Size: 0.50 μm

Stir time: 30 secs  
Stir speed: Low  
Probe time: 30 secs

Sample: TT-26-08 5 cm  
 Operator: Clint Edrington  
 Submitter: Clint Edrington  
 File Name: C:\EDRING~1\TIGER&~1\SANDFR~1\TT-26-08\26\_5CM.SMP  
 Material/Liquid: silicate mud/water/Water

Reported: 01/04/10 11:49:05  
 Liquid Visc: 0.7225 cp

Sample Density: 2.650 g/cm<sup>3</sup>  
 Liquid Density: 0.9941 g/cm<sup>3</sup>

## Summary Report

Parameter 1 0.000

Parameter 2 0.000

Parameter 3 0.000

## Mass Distribution Arithmetic Statistics

Mean	106.9	Std. Dev.	18.32
Median	105.4	Coef. Var.	0.171
Mode	97.67	Skewness	0.958
		Kurtosis	3.588

## Selected Percentiles

Percent Finer	Diameter (µm)
100.0	651.9
80.0	119.6
60.0	109.9
40.0	101.2
20.0	93.38

## Selected Sizes

Diameter (µm)	Percent Finer
500.0	100.0
250.0	100.0
125.0	89.0
88.00	8.7
63.00	0.0

Peak Number	% of Dist. *	Mean	Mode	Median	Standard Deviation	Skewness	Kurtosis
1	100.0	106.9	97.67	105.4	18.32	0.958	3.588

\* Peaks must comprise at least 5.00 % of the distribution.

# Micromeritics

WIN5100 V2.03

Page 1

Sample: TT-26-08 50 cm  
Operator: Clint Edrington  
Submitter: Clint Edrington  
File Name: C:\EDRING~1\TIGER&~1\SANDFR~1\TT-26-08\26\_50CM.SMP  
Material/Liquid: silicate mud/water/Water

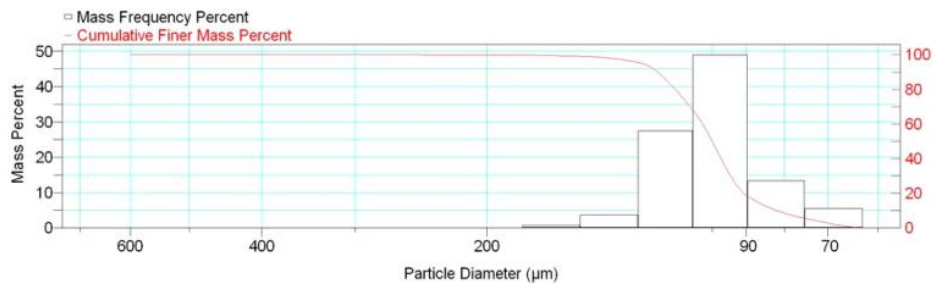
Reported: 01/04/10 11:51:32  
Liquid Visc: 0.7225 cp

Sample Density: 2.650 g/cm<sup>3</sup>  
Liquid Density: 0.9941 g/cm<sup>3</sup>

## Report by Size Class

High Diameter (μm)	Low Diameter (μm)	Average Diameter (μm)	Cumulative Mass Finer (Percent)	Mass Frequency (Percent)
710.0	600.0	652.7	100.0	0.0
600.0	500.0	547.7	100.0	0.0
500.0	425.0	461.0	100.0	0.0
425.0	355.0	388.4	100.0	0.0
355.0	300.0	326.3	100.0	0.0
300.0	250.0	273.9	100.0	0.0
250.0	212.0	230.2	99.9	0.1
212.0	180.0	195.3	99.8	0.1
180.0	150.0	164.3	99.1	0.7
150.0	125.0	136.9	95.4	3.7
125.0	106.0	115.1	67.9	27.5
106.0	90.00	97.67	18.9	49.0
90.00	75.00	82.16	5.5	13.4
75.00	63.00	68.74	0.0	5.5

Mass Frequency vs Diameter



## Summary Report

Full scale pump speed: 3  
Bubble detection: Medium  
Starting Size: 63.00 μm  
Ending Size: 0.50 μm

Stir time: 30 secs  
Stir speed: Low  
Probe time: 30 secs

Sample: TT-26-08 50 cm  
 Operator: Clint Edrington  
 Submitter: Clint Edrington  
 File Name: C:\EDRING~1\TIGER&~1\SANDFR~1\TT-26-08\26\_50CM.SMP  
 Material/Liquid: silicate mud/water/Water

Reported: 01/04/10 11:51:32  
 Liquid Visc: 0.7225 cp

Sample Density: 2.650 g/cm<sup>3</sup>  
 Liquid Density: 0.9941 g/cm<sup>3</sup>

## Summary Report

Parameter 1 0.000

Parameter 2 0.000

Parameter 3 0.000

## Mass Distribution Arithmetic Statistics

Mean	100.9	Std. Dev.	16.32
Median	99.97	Coef. Var.	0.162
Mode	97.67	Skewness	1.045
		Kurtosis	5.744

## Selected Percentiles

Percent Finer	Diameter (µm)
100.0	651.9
80.0	112.0
60.0	102.9
40.0	97.26
20.0	90.68

## Selected Sizes

Diameter (µm)	Percent Finer
500.0	100.0
250.0	100.0
125.0	95.4
88.00	16.2
63.00	0.0

Peak Number	% of Dist. *	Mean	Mode	Median	Standard Deviation	Skewness	Kurtosis
1	100.0	100.9	97.67	99.97	16.32	1.045	5.744

\* Peaks must comprise at least 5.00 % of the distribution.

# Micromeritics

WIN5100 V2.03

Page 1

Sample: TT-26-08 100 cm  
Operator: Clint Edrington  
Submitter: Clint Edrington  
File Name: C:\EDRING~1\TIGER&~1\SANDFR~1\TT-26-08\26\_100CM.SMP  
Material/Liquid: silicate mud/water/Water

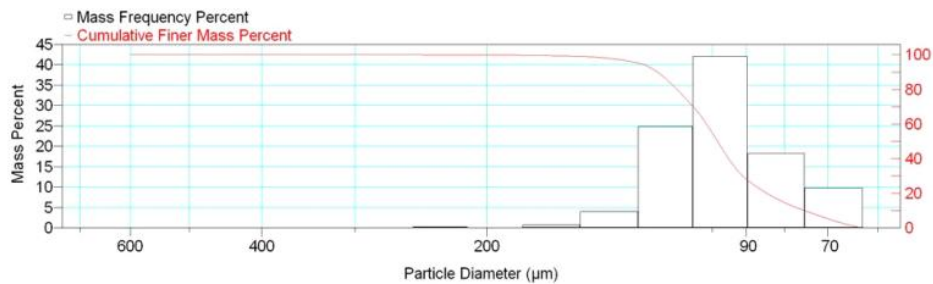
Reported: 01/04/10 11:53:27  
Liquid Visc: 0.7225 cp

Sample Density: 2.650 g/cm<sup>3</sup>  
Liquid Density: 0.9941 g/cm<sup>3</sup>

## Report by Size Class

High Diameter (µm)	Low Diameter (µm)	Average Diameter (µm)	Cumulative Mass Finer (Percent)	Mass Frequency (Percent)
710.0	600.0	652.7	100.0	0.0
600.0	500.0	547.7	100.0	0.0
500.0	425.0	461.0	100.0	0.0
425.0	355.0	388.4	100.0	0.0
355.0	300.0	326.3	100.0	0.0
300.0	250.0	273.9	100.0	0.0
250.0	212.0	230.2	99.8	0.2
212.0	180.0	195.3	99.7	0.1
180.0	150.0	164.3	99.0	0.7
150.0	125.0	136.9	95.0	4.0
125.0	106.0	115.1	70.1	24.9
106.0	90.00	97.67	28.1	42.0
90.00	75.00	82.16	9.8	18.3
75.00	63.00	68.74	0.0	9.8

Mass Frequency vs Diameter



## Summary Report

Full scale pump speed: 3  
Bubble detection: Medium  
Starting Size: 63.00 µm  
Ending Size: 0.50 µm

Stir time: 30 secs  
Stir speed: Low  
Probe time: 30 secs

Sample: TT-26-08 100 cm  
 Operator: Clint Edrington  
 Submitter: Clint Edrington  
 File Name: C:\EDRING~1\TIGER&~1\SANDFR~1\TT-26-08\26\_100CM.SMP  
 Material/Liquid: silicate mud/water/Water

Reported: 01/04/10 11:53:27  
 Liquid Visc: 0.7225 cp

Sample Density: 2.650 g/cm<sup>3</sup>  
 Liquid Density: 0.9941 g/cm<sup>3</sup>

## Summary Report

Parameter 1 0.000

Parameter 2 0.000

Parameter 3 0.000

## Mass Distribution Arithmetic Statistics

Mean	98.74	Std. Dev.	18.39
Median	98.32	Coef. Var.	0.186
Mode	97.67	Skewness	1.168
		Kurtosis	5.841

## Selected Percentiles

Percent Finer	Diameter (µm)
100.0	651.9
80.0	111.4
60.0	101.7
40.0	95.00
20.0	84.47

## Selected Sizes

Diameter (µm)	Percent Finer
500.0	100.0
250.0	100.0
125.0	95.0
88.00	25.0
63.00	0.0

Peak Number	% of Dist. *	Mean	Mode	Median	Standard Deviation	Skewness	Kurtosis
1	99.8	98.48	97.67	98.29	17.44	0.559	1.507

\* Peaks must comprise at least 5.00 % of the distribution.



# Micromeritics

WIN5100 V2.03

Page 1

Sample: TT-27-08 5 cm  
Operator: Clint Edrington  
Submitter: Clint Edrington  
File Name: C:\EDRING~1\TIGER&~1\SANDFR~1\TT-27-08\27\_5CM.SMP  
Material/Liquid: silicate mud/water/Water

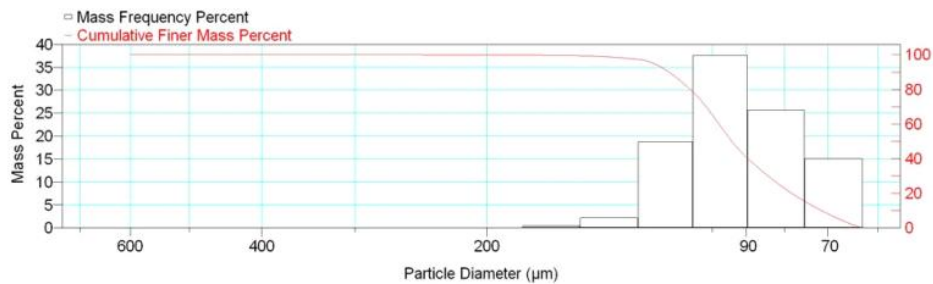
Reported: 01/04/10 11:56:40  
Liquid Visc: 0.7225 cp

Sample Density: 2.650 g/cm<sup>3</sup>  
Liquid Density: 0.9941 g/cm<sup>3</sup>

## Report by Size Class

High Diameter (μm)	Low Diameter (μm)	Average Diameter (μm)	Cumulative Mass Finer (Percent)	Mass Frequency (Percent)
710.0	600.0	652.7	100.0	0.0
600.0	500.0	547.7	100.0	0.0
500.0	425.0	461.0	100.0	0.0
425.0	355.0	388.4	100.0	0.0
355.0	300.0	326.3	100.0	0.0
300.0	250.0	273.9	100.0	0.0
250.0	212.0	230.2	99.9	0.1
212.0	180.0	195.3	99.8	0.1
180.0	150.0	164.3	99.4	0.4
150.0	125.0	136.9	97.2	2.2
125.0	106.0	115.1	78.4	18.8
106.0	90.00	97.67	40.8	37.6
90.00	75.00	82.16	15.1	25.7
75.00	63.00	68.74	0.0	15.1

Mass Frequency vs Diameter



## Summary Report

Full scale pump speed: 3  
Bubble detection: Medium  
Starting Size: 63.00 μm  
Ending Size: 0.50 μm

Stir time: 30 secs  
Stir speed: Low  
Probe time: 30 secs

Sample: TT-27-08 5 cm  
 Operator: Clint Edrington  
 Submitter: Clint Edrington  
 File Name: C:\EDRING~1\TIGER&~1\SANDFR~1\TT-27-08\27\_5CM.SMP  
 Material/Liquid: silicate mud/water/Water

Reported: 01/04/10 11:56:40  
 Liquid Visc: 0.7225 cp

Sample Density: 2.650 g/cm<sup>3</sup>  
 Liquid Density: 0.9941 g/cm<sup>3</sup>

## Summary Report

Parameter 1 0.000

Parameter 2 0.000

Parameter 3 0.000

## Mass Distribution Arithmetic Statistics

Mean	93.95	Std. Dev.	17.62
Median	94.07	Coef. Var.	0.188
Mode	97.67	Skewness	1.036
		Kurtosis	4.549

## Selected Percentiles

Percent Finer	Diameter (µm)
100.0	651.9
80.0	107.0
60.0	97.87
40.0	89.57
20.0	78.24

## Selected Sizes

Diameter (µm)	Percent Finer
500.0	100.0
250.0	100.0
125.0	97.2
88.00	37.1
63.00	0.0

Peak Number	% of Dist. *	Mean	Mode	Median	Standard Deviation	Skewness	Kurtosis
1	100.0	93.95	97.67	94.07	17.62	1.036	4.549

\* Peaks must comprise at least 5.00 % of the distribution.

Micromeritics

WIN5100 V2.03

Page 1

Sample: TT-27-08 349 cm  
Operator: Clint Edrington  
Submitter: Clint Edrington  
File Name: C:\EDRING~1\TIGER&~1\SANDFR~1\TT-27-08\27\_349CM.SMP  
Material/Liquid: silicate mud/water/Water

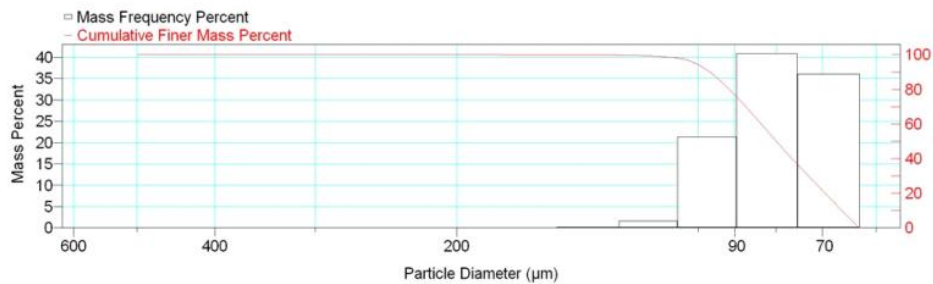
Reported: 01/04/10 11:58:59  
Liquid Visc: 0.7225 cp

Sample Density: 2.650 g/cm<sup>3</sup>  
Liquid Density: 0.9941 g/cm<sup>3</sup>

Report by Size Class

High Diameter (µm)	Low Diameter (µm)	Average Diameter (µm)	Cumulative Mass Finer (Percent)	Mass Frequency (Percent)
600.0	500.0	547.7	100.0	0.0
500.0	425.0	461.0	100.0	0.0
425.0	355.0	388.4	100.0	0.0
355.0	300.0	326.3	100.0	0.0
300.0	250.0	273.9	100.0	0.0
250.0	212.0	230.2	100.0	0.0
212.0	180.0	195.3	100.0	0.0
180.0	150.0	164.3	99.9	0.1
150.0	125.0	136.9	99.7	0.2
125.0	106.0	115.1	98.1	1.6
106.0	90.00	97.67	76.8	21.3
90.00	75.00	82.16	36.0	40.8
75.00	63.00	68.74	0.0	36.0

Mass Frequency vs Diameter



Summary Report

Full scale pump speed: 3  
Bubble detection: Medium  
Starting Size: 63.00 µm  
Ending Size: 0.50 µm

Stir time: 30 secs  
Stir speed: Low  
Probe time: 30 secs

Parameter 1 0.000

Parameter 2 0.000

Parameter 3 0.000

Sample: TT-27-08 349 cm  
 Operator: Clint Edrington  
 Submitter: Clint Edrington  
 File Name: C:\EDRING~1\TIGER&~1\SANDFR~1\TT-27-08\27\_349CM.SMP  
 Material/Liquid: silicate mud/water/Water

Reported: 01/04/10 11:58:59  
 Liquid Visc: 0.7225 cp

Sample Density: 2.650 g/cm<sup>3</sup>  
 Liquid Density: 0.9941 g/cm<sup>3</sup>

## Summary Report

Mass Distribution Arithmetic Statistics			
Mean	81.35	Std. Dev.	12.07
Median	79.92	Coef. Var.	0.148
Mode	82.16	Skewness	0.987
		Kurtosis	2.260

Selected Percentiles		Selected Sizes	
Percent Finer	Diameter (µm)	Diameter (µm)	Percent Finer
100.0	553.2	500.0	100.0
80.0	91.40	250.0	100.0
60.0	83.48	125.0	99.7
40.0	76.42	88.00	71.9
20.0	69.48	63.00	0.0

Peak Number	% of Dist.*	Mean	Mode	Median	Standard Deviation	Skewness	Kurtosis
1	100.0	81.35	82.16	79.92	12.07	0.987	2.260

\* Peaks must comprise at least 5.00 % of the distribution.

Micromeritics

WIN5100 V2.03

Page 1

Sample: TT-28-08 4 cm  
Operator: Clint Edrington  
Submitter: Clint Edrington  
File Name: C:\EDRING~1\TIGER&~1\SANDFR~1\TT-28-08\28\_4CM.SMP  
Material/Liquid: silicate mud/water/Water

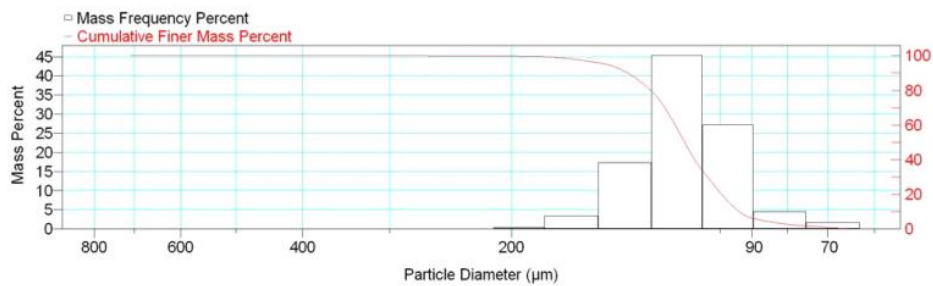
Reported: 01/04/10 12:02:41  
Liquid Visc: 0.7225 cp

Sample Density: 2.650 g/cm<sup>3</sup>  
Liquid Density: 0.9941 g/cm<sup>3</sup>

Report by Size Class

High Diameter (µm)	Low Diameter (µm)	Average Diameter (µm)	Cumulative Mass Finer (Percent)	Mass Frequency (Percent)
850.0	710.0	776.9	100.0	0.0
710.0	600.0	652.7	100.0	0.0
600.0	500.0	547.7	100.0	0.0
500.0	425.0	461.0	100.0	0.0
425.0	355.0	388.4	100.0	0.0
355.0	300.0	326.3	100.0	0.0
300.0	250.0	273.9	99.9	0.1
250.0	212.0	230.2	99.8	0.1
212.0	180.0	195.3	99.4	0.4
180.0	150.0	164.3	96.0	3.4
150.0	125.0	136.9	78.7	17.3
125.0	106.0	115.1	33.4	45.3
106.0	90.00	97.67	6.2	27.2
90.00	75.00	82.16	1.7	4.5
75.00	63.00	68.74	0.0	1.7

Mass Frequency vs Diameter



Summary Report

Full scale pump speed: 3  
Bubble detection: Medium  
Starting Size: 63.00 µm  
Ending Size: 0.50 µm

Stir time: 30 secs  
Stir speed: Low  
Probe time: 30 secs

Sample: TT-28-08 4 cm  
 Operator: Clint Edrington  
 Submitter: Clint Edrington  
 File Name: C:\EDRING~1\TIGER&~1\SANDFR~1\TT-28-08\28\_4CM.SMP  
 Material/Liquid: silicate mud/water/Water

Reported: 01/04/10 12:02:41  
 Liquid Visc: 0.7225 cp

Sample Density: 2.650 g/cm<sup>3</sup>  
 Liquid Density: 0.9941 g/cm<sup>3</sup>

## Summary Report

Parameter 1	0.000	Parameter 2	0.000	Parameter 3	0.000		
Mass Distribution Arithmetic Statistics							
Mean	114.1	Std. Dev.		19.90			
Median	112.6	Coef. Var.		0.174			
Mode	115.1	Skewness		1.249			
		Kurtosis		5.975			
Selected Percentiles			Selected Sizes				
Percent Finer	Diameter (µm)		Diameter (µm)	Percent Finer			
100.0	714.1		500.0	100.0			
80.0	126.0		250.0	99.9			
60.0	116.2		125.0	78.7			
40.0	108.9		88.00	5.3			
20.0	99.56		63.00	0.0			
Peak Number	% of Dist.*	Mean	Mode	Median	Standard Deviation	Skewness	Kurtosis
1	100.0	114.1	115.1	112.6	19.90	1.249	5.975

\* Peaks must comprise at least 5.00 % of the distribution.

Micromeritics

WIN5100 V2.03

Page 1

Sample: TT-28-08 51 cm  
Operator: Clint Edrington  
Submitter: Clint Edrington  
File Name: C:\EDRING~1\TIGER&~1\SANDFR~1\TT-28-08\28\_51CM.SMP  
Material/Liquid: silicate mud/water/Water

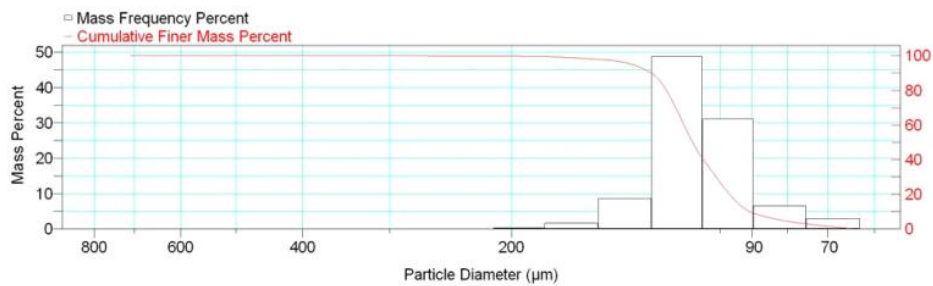
Reported: 01/04/10 12:05:40  
Liquid Visc: 0.7225 cp

Sample Density: 2.650 g/cm<sup>3</sup>  
Liquid Density: 0.9941 g/cm<sup>3</sup>

Report by Size Class

High Diameter (µm)	Low Diameter (µm)	Average Diameter (µm)	Cumulative Mass Finer (Percent)	Mass Frequency (Percent)
850.0	710.0	776.9	100.0	0.0
710.0	600.0	652.7	100.0	0.0
600.0	500.0	547.7	100.0	0.0
500.0	425.0	461.0	100.0	0.0
425.0	355.0	388.4	100.0	0.0
355.0	300.0	326.3	100.0	0.0
300.0	250.0	273.9	99.9	0.1
250.0	212.0	230.2	99.8	0.1
212.0	180.0	195.3	99.5	0.3
180.0	150.0	164.3	97.9	1.6
150.0	125.0	136.9	89.3	8.6
125.0	106.0	115.1	40.5	48.8
106.0	90.00	97.67	9.4	31.1
90.00	75.00	82.16	2.9	6.5
75.00	63.00	68.74	0.0	2.9

Mass Frequency vs Diameter



Summary Report

Full scale pump speed: 3  
Bubble detection: Medium  
Starting Size: 63.00 µm  
Ending Size: 0.50 µm

Stir time: 30 secs  
Stir speed: Low  
Probe time: 30 secs

Sample: TT-28-08 51 cm  
 Operator: Clint Edrington  
 Submitter: Clint Edrington  
 File Name: C:\EDRING~1\TIGER&~1\SANDFR~1\TT-28-08\28\_51CM.SMP  
 Material/Liquid: silicate mud/water/Water

Reported: 01/04/10 12:05:40  
 Liquid Visc: 0.7225 cp

Sample Density: 2.650 g/cm<sup>3</sup>  
 Liquid Density: 0.9941 g/cm<sup>3</sup>

## Summary Report

Parameter 1	0.000	Parameter 2	0.000	Parameter 3	0.000		
Mass Distribution Arithmetic Statistics							
Mean	109.4	Std. Dev.		18.22			
Median	109.6	Coef. Var.		0.167			
Mode	115.1	Skewness		1.472			
		Kurtosis		9.925			
Selected Percentiles			Selected Sizes				
Percent Finer	Diameter (µm)		Diameter (µm)	Percent Finer			
100.0	714.1		500.0	100.0			
80.0	119.6		250.0	99.9			
60.0	112.8		125.0	89.3			
40.0	105.8		88.00	8.2			
20.0	97.00		63.00	0.0			
Peak Number	% of Dist.*	Mean	Mode	Median	Standard Deviation	Skewness	Kurtosis
1	100.0	109.4	115.1	109.6	18.22	1.472	9.925

\* Peaks must comprise at least 5.00 % of the distribution.



Micromeritics

WIN5100 V2.03

Page 1

Sample: TT-29-08 2 cm  
Operator: Clint Edrington  
Submitter: Clint Edrington  
File Name: C:\EDRING~1\TIGER&~1\SANDFR~1\TT-29-08\29\_2CM.SMP  
Material/Liquid: silicate mud/water/Water

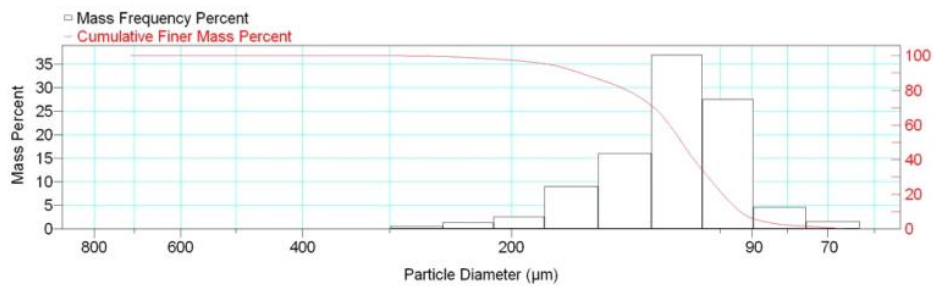
Reported: 01/04/10 12:08:28  
Liquid Visc: 0.7225 cp

Sample Density: 2.650 g/cm<sup>3</sup>  
Liquid Density: 0.9941 g/cm<sup>3</sup>

Report by Size Class

High Diameter (μm)	Low Diameter (μm)	Average Diameter (μm)	Cumulative Mass Finer (Percent)	Mass Frequency (Percent)
850.0	710.0	776.9	100.0	0.0
710.0	600.0	652.7	100.0	0.0
600.0	500.0	547.7	100.0	0.0
500.0	425.0	461.0	100.0	0.0
425.0	355.0	388.4	100.0	0.0
355.0	300.0	326.3	100.0	0.0
300.0	250.0	273.9	99.5	0.5
250.0	212.0	230.2	98.1	1.4
212.0	180.0	195.3	95.5	2.6
180.0	150.0	164.3	86.5	9.0
150.0	125.0	136.9	70.5	16.0
125.0	106.0	115.1	33.6	36.9
106.0	90.00	97.67	6.1	27.5
90.00	75.00	82.16	1.5	4.6
75.00	63.00	68.74	0.0	1.5

Mass Frequency vs Diameter



Summary Report

Full scale pump speed: 3  
Bubble detection: Medium  
Starting Size: 63.00 μm  
Ending Size: 0.50 μm

Stir time: 30 secs  
Stir speed: Low  
Probe time: 30 secs

Sample: TT-29-08 2 cm  
 Operator: Clint Edrington  
 Submitter: Clint Edrington  
 File Name: C:\EDRING~1\TIGER&~1\SANDFR~1\TT-29-08\29\_2CM.SMP  
 Material/Liquid: silicate mud/water/Water

Reported: 01/04/10 12:08:28  
 Liquid Visc: 0.7225 cp

Sample Density: 2.650 g/cm<sup>3</sup>  
 Liquid Density: 0.9941 g/cm<sup>3</sup>

## Summary Report

Parameter 1	0.000	Parameter 2	0.000	Parameter 3	0.000		
Mass Distribution Arithmetic Statistics							
Mean	120.5	Std. Dev.		30.16			
Median	113.7	Coef. Var.		0.250			
Mode	115.1	Skewness		1.738			
		Kurtosis		4.534			
Selected Percentiles			Selected Sizes				
Percent Finer	Diameter (µm)		Diameter (µm)	Percent Finer			
100.0	714.1		500.0	100.0			
80.0	136.2		250.0	99.5			
60.0	118.4		125.0	70.5			
40.0	109.2		88.00	4.9			
20.0	99.19		63.00	0.0			
Peak Number	% of Dist.*	Mean	Mode	Median	Standard Deviation	Skewness	Kurtosis
1	100.0	120.5	115.1	113.7	30.16	1.738	4.534

\* Peaks must comprise at least 5.00 % of the distribution.

Micromeritics

WIN5100 V2.03

Page 1

Sample: TT-29-08 20 cm  
Operator: Clint Edrington  
Submitter: Clint Edrington  
File Name: C:\EDRING~1\TIGER&~1\SANDFR~1\TT-29-08\29\_20CM.SMP  
Material/Liquid: silicate mud/water/Water

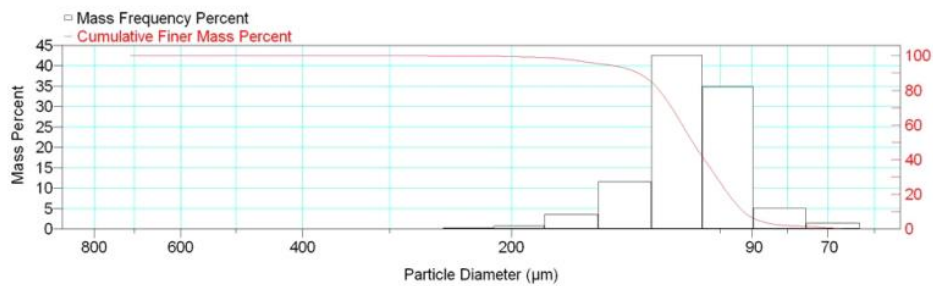
Reported: 01/04/10 12:10:26  
Liquid Visc: 0.7225 cp

Sample Density: 2.650 g/cm<sup>3</sup>  
Liquid Density: 0.9941 g/cm<sup>3</sup>

Report by Size Class

High Diameter (µm)	Low Diameter (µm)	Average Diameter (µm)	Cumulative Mass Finer (Percent)	Mass Frequency (Percent)
850.0	710.0	776.9	100.0	0.0
710.0	600.0	652.7	100.0	0.0
600.0	500.0	547.7	100.0	0.0
500.0	425.0	461.0	100.0	0.0
425.0	355.0	388.4	100.0	0.0
355.0	300.0	326.3	100.0	0.0
300.0	250.0	273.9	99.9	0.1
250.0	212.0	230.2	99.7	0.2
212.0	180.0	195.3	99.0	0.7
180.0	150.0	164.3	95.4	3.6
150.0	125.0	136.9	83.9	11.5
125.0	106.0	115.1	41.4	42.5
106.0	90.00	97.67	6.5	34.9
90.00	75.00	82.16	1.4	5.1
75.00	63.00	68.74	0.0	1.4

Mass Frequency vs Diameter



Summary Report

Full scale pump speed: 3  
Bubble detection: Medium  
Starting Size: 63.00 µm  
Ending Size: 0.50 µm

Stir time: 30 secs  
Stir speed: Low  
Probe time: 30 secs

Sample: TT-29-08 20 cm  
 Operator: Clint Edrington  
 Submitter: Clint Edrington  
 File Name: C:\EDRING~1\TIGER&~1\SANDFR~1\TT-29-08\29\_20CM.SMP  
 Material/Liquid: silicate mud/water/Water

Reported: 01/04/10 12:10:26  
 Liquid Visc: 0.7225 cp

Sample Density: 2.650 g/cm<sup>3</sup>  
 Liquid Density: 0.9941 g/cm<sup>3</sup>

## Summary Report

Parameter 1	0.000	Parameter 2	0.000	Parameter 3	0.000		
Mass Distribution Arithmetic Statistics							
Mean	111.9	Std. Dev.		20.50			
Median	109.6	Coef. Var.		0.183			
Mode	115.1	Skewness		1.756			
		Kurtosis		7.410			
Selected Percentiles			Selected Sizes				
Percent Finer	Diameter (µm)		Diameter (µm)	Percent Finer			
100.0	714.1		500.0	100.0			
80.0	122.4		250.0	99.9			
60.0	113.5		125.0	83.9			
40.0	105.4		88.00	4.8			
20.0	97.31		63.00	0.0			
Peak Number	% of Dist.*	Mean	Mode	Median	Standard Deviation	Skewness	Kurtosis
1	100.0	111.9	115.1	109.6	20.50	1.756	7.410

\* Peaks must comprise at least 5.00 % of the distribution.

Micromeritics

WIN5100 V2.03

Page 1

Sample: TT-30-08 8 cm  
Operator: Clint Edrington  
Submitter: Clint Edrington  
File Name: C:\EDRING~1\TIGER&~1\SANDFR~1\TT-30-08\30\_8CM.SMP  
Material/Liquid: silicate mud/water/Water

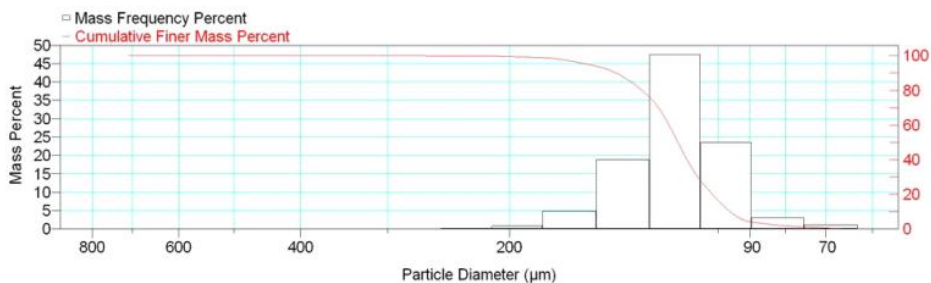
Reported: 01/04/10 12:13:12  
Liquid Visc: 0.7225 cp

Sample Density: 2.650 g/cm<sup>3</sup>  
Liquid Density: 0.9941 g/cm<sup>3</sup>

Report by Size Class

High Diameter (µm)	Low Diameter (µm)	Average Diameter (µm)	Cumulative Mass Finer (Percent)	Mass Frequency (Percent)
850.0	710.0	776.9	100.0	0.0
710.0	600.0	652.7	100.0	0.0
600.0	500.0	547.7	100.0	0.0
500.0	425.0	461.0	100.0	0.0
425.0	355.0	388.4	100.0	0.0
355.0	300.0	326.3	100.0	0.0
300.0	250.0	273.9	99.9	0.1
250.0	212.0	230.2	99.7	0.2
212.0	180.0	195.3	98.9	0.8
180.0	150.0	164.3	94.0	4.9
150.0	125.0	136.9	75.2	18.8
125.0	106.0	115.1	27.7	47.5
106.0	90.00	97.67	4.1	23.6
90.00	75.00	82.16	1.1	3.0
75.00	63.00	68.74	0.0	1.1

Mass Frequency vs Diameter



Summary Report

Full scale pump speed: 3  
Bubble detection: Medium  
Starting Size: 63.00 µm  
Ending Size: 0.50 µm

Stir time: 30 secs  
Stir speed: Low  
Probe time: 30 secs

Sample: TT-30-08 8 cm  
 Operator: Clint Edrington  
 Submitter: Clint Edrington  
 File Name: C:\EDRING~1\TIGER&~1\SANDFR~1\TT-30-08\30\_8CM.SMP  
 Material/Liquid: silicate mud/water/Water

Reported: 01/04/10 12:13:12  
 Liquid Visc: 0.7225 cp

Sample Density: 2.650 g/cm<sup>3</sup>  
 Liquid Density: 0.9941 g/cm<sup>3</sup>

## Summary Report

Parameter 1	0.000	Parameter 2	0.000	Parameter 3	0.000		
Mass Distribution Arithmetic Statistics							
Mean	117.0	Std. Dev.		20.87			
Median	114.4	Coef. Var.		0.178			
Mode	115.1	Skewness		1.432			
		Kurtosis		5.671			
Selected Percentiles			Selected Sizes				
Percent Finer	Diameter (µm)		Diameter (µm)	Percent Finer			
100.0	714.1		500.0	100.0			
80.0	128.9		250.0	99.9			
60.0	117.8		125.0	75.2			
40.0	111.0		88.00	3.6			
20.0	102.0		63.00	0.0			
Peak Number	% of Dist.*	Mean	Mode	Median	Standard Deviation	Skewness	Kurtosis
1	100.0	117.0	115.1	114.4	20.87	1.432	5.671

\* Peaks must comprise at least 5.00 % of the distribution.

Micromeritics

WIN5100 V2.03

Page 1

Sample: TT-30-08 50 cm  
Operator: Clint Edrington  
Submitter: Clint Edrington  
File Name: C:\EDRING~1\TIGER&~1\SANDFR~1\TT-30-08\30\_50CM.SMP  
Material/Liquid: silicate mud/water/Water

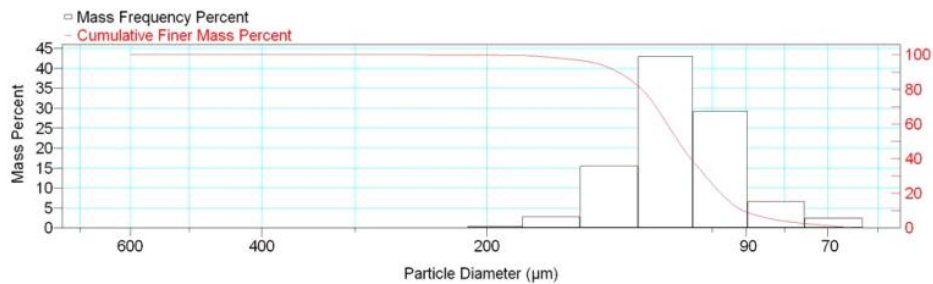
Reported: 01/04/10 12:15:08  
Liquid Visc: 0.7225 cp

Sample Density: 2.650 g/cm<sup>3</sup>  
Liquid Density: 0.9941 g/cm<sup>3</sup>

Report by Size Class

High Diameter (μm)	Low Diameter (μm)	Average Diameter (μm)	Cumulative Mass Finer (Percent)	Mass Frequency (Percent)
710.0	600.0	652.7	100.0	0.0
600.0	500.0	547.7	100.0	0.0
500.0	425.0	461.0	100.0	0.0
425.0	355.0	388.4	100.0	0.0
355.0	300.0	326.3	100.0	0.0
300.0	250.0	273.9	100.0	0.0
250.0	212.0	230.2	99.9	0.1
212.0	180.0	195.3	99.5	0.4
180.0	150.0	164.3	96.7	2.8
150.0	125.0	136.9	81.2	15.5
125.0	106.0	115.1	38.3	42.9
106.0	90.00	97.67	9.1	29.2
90.00	75.00	82.16	2.5	6.6
75.00	63.00	68.74	0.0	2.5

Mass Frequency vs Diameter



Summary Report

Full scale pump speed: 3  
Bubble detection: Medium  
Starting Size: 63.00 μm  
Ending Size: 0.50 μm

Stir time: 30 secs  
Stir speed: Low  
Probe time: 30 secs

Sample: TT-30-08 50 cm  
 Operator: Clint Edrington  
 Submitter: Clint Edrington  
 File Name: C:\EDRING~1\TIGER&~1\SANDFR~1\TT-30-08\30\_50CM.SMP  
 Material/Liquid: silicate mud/water/Water

Reported: 01/04/10 12:15:08  
 Liquid Visc: 0.7225 cp

Sample Density: 2.650 g/cm<sup>3</sup>  
 Liquid Density: 0.9941 g/cm<sup>3</sup>

## Summary Report

Parameter 1 0.000

Parameter 2 0.000

Parameter 3 0.000

## Mass Distribution Arithmetic Statistics

Mean	111.9	Std. Dev.	19.61
Median	111.0	Coef. Var.	0.175
Mode	115.1	Skewness	0.782
		Kurtosis	2.503

## Selected Percentiles

Percent Finer	Diameter (µm)
100.0	651.9
80.0	124.1
60.0	114.8
40.0	106.8
20.0	97.35

## Selected Sizes

Diameter (µm)	Percent Finer
500.0	100.0
250.0	100.0
125.0	81.2
88.00	7.7
63.00	0.0

Peak Number	% of Dist. *	Mean	Mode	Median	Standard Deviation	Skewness	Kurtosis
1	100.0	111.9	115.1	111.0	19.61	0.782	2.503

\* Peaks must comprise at least 5.00 % of the distribution.



Micromeritics

WIN5100 V2.03

Page 1

Sample: TT-30-08 213 cm  
Operator: Clint Edrington  
Submitter: Clint Edrington  
File Name: C:\EDRING~1\TIGER&~1\SANDFR~1\TT-30-08\30\_213CM.SMP  
Material/Liquid: silicate mud/water/Water

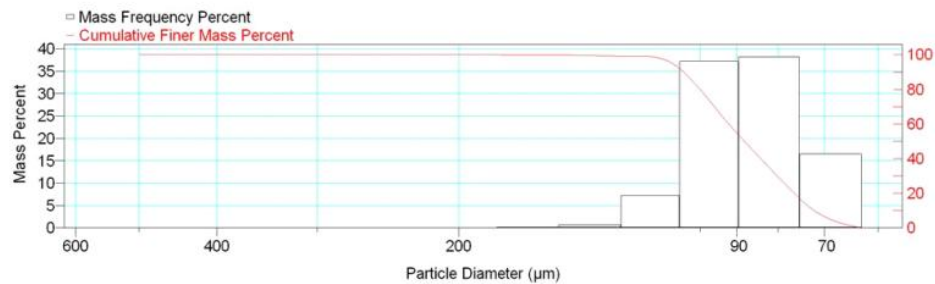
Reported: 01/04/10 12:17:05  
Liquid Visc: 0.7225 cp

Sample Density: 2.650 g/cm<sup>3</sup>  
Liquid Density: 0.9941 g/cm<sup>3</sup>

Report by Size Class

High Diameter (μm)	Low Diameter (μm)	Average Diameter (μm)	Cumulative Mass Finer (Percent)	Mass Frequency (Percent)
600.0	500.0	547.7	100.0	0.0
500.0	425.0	461.0	100.0	0.0
425.0	355.0	388.4	100.0	0.0
355.0	300.0	326.3	100.0	0.0
300.0	250.0	273.9	100.0	0.0
250.0	212.0	230.2	100.0	0.0
212.0	180.0	195.3	100.0	0.0
180.0	150.0	164.3	99.8	0.2
150.0	125.0	136.9	99.1	0.7
125.0	106.0	115.1	91.9	7.2
106.0	90.00	97.67	54.7	37.2
90.00	75.00	82.16	16.5	38.2
75.00	63.00	68.74	0.0	16.5

Mass Frequency vs Diameter



Summary Report

Full scale pump speed: 3  
Bubble detection: Medium  
Starting Size: 63.00 μm  
Ending Size: 0.50 μm

Stir time: 30 secs  
Stir speed: Low  
Probe time: 30 secs

Parameter 1 0.000

Parameter 2 0.000

Parameter 3 0.000

Sample: TT-30-08 213 cm  
 Operator: Clint Edrington  
 Submitter: Clint Edrington  
 File Name: C:\EDRING~1\TIGER&~1\SANDFR~1\TT-30-08\30\_213CM.SMP  
 Material/Liquid: silicate mud/water/Water

Reported: 01/04/10 12:17:05      Sample Density: 2.650 g/cm<sup>3</sup>  
 Liquid Visc: 0.7225 cp      Liquid Density: 0.9941 g/cm<sup>3</sup>

## Summary Report

## Mass Distribution Arithmetic Statistics

Mean	88.64	Std. Dev.	13.78
Median	88.07	Coef. Var.	0.156
Mode	82.16	Skewness	0.711
		Kurtosis	1.657

## Selected Percentiles

Percent Finer	Diameter (µm)
100.0	553.2
80.0	100.1
60.0	92.13
40.0	84.07
20.0	76.35

## Selected Sizes

Diameter (µm)	Percent Finer
500.0	100.0
250.0	100.0
125.0	99.1
88.00	49.8
63.00	0.0

Peak Number	% of Dist.*	Mean	Mode	Median	Standard Deviation	Skewness	Kurtosis
1	100.0	88.64	82.16	88.07	13.78	0.711	1.657

\* Peaks must comprise at least 5.00 % of the distribution.

Micromeritics

WIN5100 V2.03

Page 1

Sample: TT-31-08 5 cm  
Operator: Clint Edrington  
Submitter: Clint Edrington  
File Name: C:\EDRING~1\TIGER&~1\SANDFR~1\TT-31-08\31\_5CM.SMP  
Material/Liquid: silicate mud/water/Water

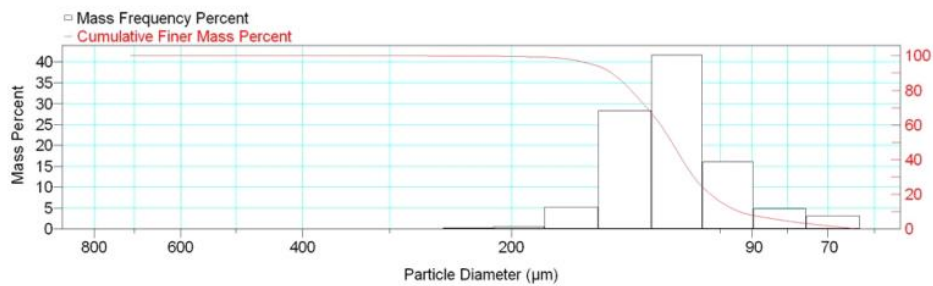
Reported: 01/04/10 12:20:10  
Liquid Visc: 0.7225 cp

Sample Density: 2.650 g/cm<sup>3</sup>  
Liquid Density: 0.9941 g/cm<sup>3</sup>

Report by Size Class

High Diameter (μm)	Low Diameter (μm)	Average Diameter (μm)	Cumulative Mass Finer (Percent)	Mass Frequency (Percent)
850.0	710.0	776.9	100.0	0.0
710.0	600.0	652.7	100.0	0.0
600.0	500.0	547.7	100.0	0.0
500.0	425.0	461.0	100.0	0.0
425.0	355.0	388.4	100.0	0.0
355.0	300.0	326.3	100.0	0.0
300.0	250.0	273.9	99.9	0.1
250.0	212.0	230.2	99.7	0.2
212.0	180.0	195.3	99.2	0.5
180.0	150.0	164.3	94.0	5.2
150.0	125.0	136.9	65.7	28.3
125.0	106.0	115.1	24.0	41.7
106.0	90.00	97.67	7.9	16.1
90.00	75.00	82.16	3.1	4.8
75.00	63.00	68.74	0.0	3.1

Mass Frequency vs Diameter



Summary Report

Full scale pump speed: 3  
Bubble detection: Medium  
Starting Size: 63.00 μm  
Ending Size: 0.50 μm

Stir time: 30 secs  
Stir speed: Low  
Probe time: 30 secs

Sample: TT-31-08 5 cm  
 Operator: Clint Edrington  
 Submitter: Clint Edrington  
 File Name: C:\EDRING~1\TIGER&~1\SANDFR~1\TT-31-08\31\_5CM.SMP  
 Material/Liquid: silicate mud/water/Water

Reported: 01/04/10 12:20:10  
 Liquid Visc: 0.7225 cp

Sample Density: 2.650 g/cm<sup>3</sup>  
 Liquid Density: 0.9941 g/cm<sup>3</sup>

## Summary Report

Parameter 1	0.000	Parameter 2	0.000	Parameter 3	0.000		
Mass Distribution Arithmetic Statistics							
Mean	118.8	Std. Dev.		22.33			
Median	117.5	Coef. Var.		0.188			
Mode	115.1	Skewness		0.676			
		Kurtosis		3.536			
Selected Percentiles			Selected Sizes				
Percent Finer	Diameter (µm)		Diameter (µm)	Percent Finer			
100.0	714.1		500.0	100.0			
80.0	134.5		250.0	99.9			
60.0	121.9		125.0	65.7			
40.0	113.5		88.00	7.2			
20.0	103.3		63.00	0.0			
Peak Number	% of Dist.*	Mean	Mode	Median	Standard Deviation	Skewness	Kurtosis
1	100.0	118.8	115.1	117.5	22.33	0.676	3.536

\* Peaks must comprise at least 5.00 % of the distribution.

Micromeritics

WIN5100 V2.03

Page 1

Sample: TT-31-08 50 cm  
Operator: Clint Edrington  
Submitter: Clint Edrington  
File Name: C:\EDRING~1\TIGER&~1\SANDFR~1\TT-31-08\31\_50CM.SMP  
Material/Liquid: silicate mud/water/Water

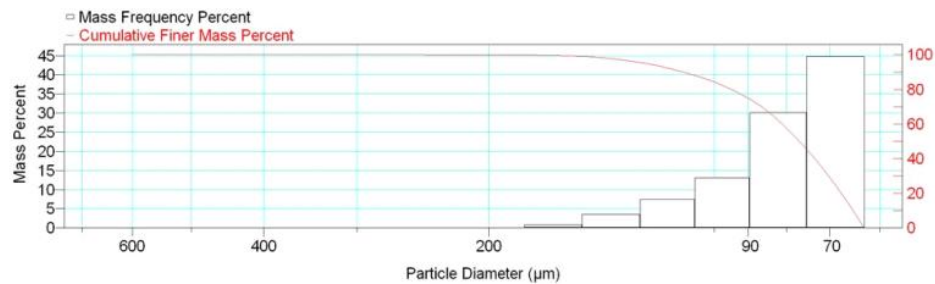
Reported: 01/04/10 12:22:15  
Liquid Visc: 0.7225 cp

Sample Density: 2.650 g/cm<sup>3</sup>  
Liquid Density: 0.9941 g/cm<sup>3</sup>

Report by Size Class

High Diameter (μm)	Low Diameter (μm)	Average Diameter (μm)	Cumulative Mass Finer (Percent)	Mass Frequency (Percent)
710.0	600.0	652.7	100.0	0.0
600.0	500.0	547.7	100.0	0.0
500.0	425.0	461.0	100.0	0.0
425.0	355.0	388.4	100.0	0.0
355.0	300.0	326.3	100.0	0.0
300.0	250.0	273.9	100.0	0.0
250.0	212.0	230.2	99.9	0.1
212.0	180.0	195.3	99.8	0.1
180.0	150.0	164.3	99.0	0.8
150.0	125.0	136.9	95.4	3.6
125.0	106.0	115.1	88.0	7.4
106.0	90.00	97.67	74.9	13.1
90.00	75.00	82.16	44.8	30.1
75.00	63.00	68.74	0.0	44.8

Mass Frequency vs Diameter



Summary Report

Full scale pump speed: 3  
Bubble detection: Medium  
Starting Size: 63.00 μm  
Ending Size: 0.50 μm

Stir time: 30 secs  
Stir speed: Low  
Probe time: 30 secs

Sample: TT-31-08 50 cm  
 Operator: Clint Edrington  
 Submitter: Clint Edrington  
 File Name: C:\EDRING~1\TIGER&~1\SANDFR~1\TT-31-08\31\_50CM.SMP  
 Material/Liquid: silicate mud/water/Water

Reported: 01/04/10 12:22:15  
 Liquid Visc: 0.7225 cp

Sample Density: 2.650 g/cm<sup>3</sup>  
 Liquid Density: 0.9941 g/cm<sup>3</sup>

## Summary Report

Parameter 1 0.000

Parameter 2 0.000

Parameter 3 0.000

## Mass Distribution Arithmetic Statistics

Mean	83.51	Std. Dev.	19.68
Median	76.93	Coef. Var.	0.236
Mode	68.74	Skewness	2.036
		Kurtosis	6.022

## Selected Percentiles

Percent Finer	Diameter (µm)
100.0	651.9
80.0	94.87
60.0	81.09
40.0	73.35
20.0	67.58

## Selected Sizes

Diameter (µm)	Percent Finer
500.0	100.0
250.0	100.0
125.0	95.4
88.00	72.4
63.00	0.0

Peak Number	% of Dist. *	Mean	Mode	Median	Standard Deviation	Skewness	Kurtosis
1	100.0	83.51	68.74	76.93	19.68	2.036	6.022

\* Peaks must comprise at least 5.00 % of the distribution.

Micromeritics

WIN5100 V2.03

Page 1

Sample: TT-31-08 100 cm  
Operator: Clint Edrington  
Submitter: Clint Edrington  
File Name: C:\EDRING~1\TIGER&~1\SANDFR~1\TT-31-08\31\_100CM.SMP  
Material/Liquid: silicate mud/water/Water

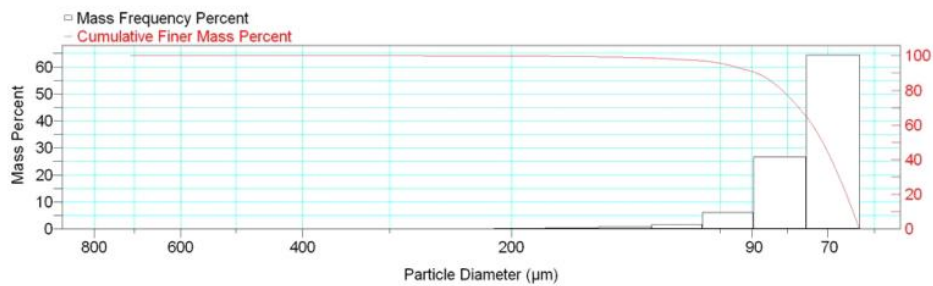
Reported: 01/04/10 12:24:08  
Liquid Visc: 0.7225 cp

Sample Density: 2.650 g/cm<sup>3</sup>  
Liquid Density: 0.9941 g/cm<sup>3</sup>

Report by Size Class

High Diameter ( $\mu\text{m}$ )	Low Diameter ( $\mu\text{m}$ )	Average Diameter ( $\mu\text{m}$ )	Cumulative Mass Finer (Percent)	Mass Frequency (Percent)
850.0	710.0	776.9	100.0	0.0
710.0	600.0	652.7	100.0	0.0
600.0	500.0	547.7	100.0	0.0
500.0	425.0	461.0	100.0	0.0
425.0	355.0	388.4	100.0	0.0
355.0	300.0	326.3	100.0	0.0
300.0	250.0	273.9	99.9	0.1
250.0	212.0	230.2	99.9	0.0
212.0	180.0	195.3	99.7	0.2
180.0	150.0	164.3	99.4	0.3
150.0	125.0	136.9	98.6	0.8
125.0	106.0	115.1	97.0	1.6
106.0	90.00	97.67	90.9	6.1
90.00	75.00	82.16	64.3	26.6
75.00	63.00	68.74	0.0	64.3

Mass Frequency vs Diameter



Summary Report

Full scale pump speed: 3  
Bubble detection: Medium  
Starting Size: 63.00  $\mu\text{m}$   
Ending Size: 0.50  $\mu\text{m}$

Stir time: 30 secs  
Stir speed: Low  
Probe time: 30 secs

Sample: TT-31-08 100 cm  
 Operator: Clint Edrington  
 Submitter: Clint Edrington  
 File Name: C:\EDRING~1\TIGER&~1\SANDFR~1\TT-31-08\31\_100CM.SMP  
 Material/Liquid: silicate mud/water/Water

Reported: 01/04/10 12:24:08  
 Liquid Visc: 0.7225 cp

Sample Density: 2.650 g/cm<sup>3</sup>  
 Liquid Density: 0.9941 g/cm<sup>3</sup>

## Summary Report

Parameter 1	0.000	Parameter 2	0.000	Parameter 3	0.000		
Mass Distribution Arithmetic Statistics							
Mean	76.11	Std. Dev.		14.76			
Median	71.16	Coef. Var.		0.194			
Mode	68.74	Skewness		5.084			
		Kurtosis		44.989			
Selected Percentiles			Selected Sizes				
Percent Finer	Diameter (µm)		Diameter (µm)	Percent Finer			
100.0	714.1		500.0	100.0			
80.0	81.39		250.0	99.9			
60.0	73.66		125.0	98.6			
40.0	69.14		88.00	89.5			
20.0	65.80		63.00	0.0			
Peak Number	% of Dist.*	Mean	Mode	Median	Standard Deviation	Skewness	Kurtosis
1	99.9	75.91	68.74	71.15	13.37	3.648	20.614

\* Peaks must comprise at least 5.00 % of the distribution.



Micromeritics

WIN5100 V2.03

Page 1

Sample: TT-31-08 150 cm  
Operator: Clint Edrington  
Submitter: Clint Edrington  
File Name: C:\EDRING~1\TIGER&~1\SANDFR~1\TT-31-08\31\_150CM.SMP  
Material/Liquid: silicate mud/water/Water

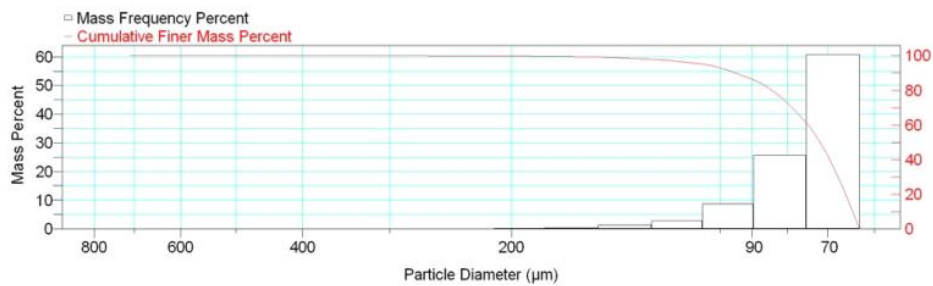
Reported: 01/04/10 12:26:27  
Liquid Visc: 0.7225 cp

Sample Density: 2.650 g/cm<sup>3</sup>  
Liquid Density: 0.9941 g/cm<sup>3</sup>

Report by Size Class

High Diameter ( $\mu\text{m}$ )	Low Diameter ( $\mu\text{m}$ )	Average Diameter ( $\mu\text{m}$ )	Cumulative Mass Finer (Percent)	Mass Frequency (Percent)
850.0	710.0	776.9	100.0	0.0
710.0	600.0	652.7	100.0	0.0
600.0	500.0	547.7	100.0	0.0
500.0	425.0	461.0	100.0	0.0
425.0	355.0	388.4	100.0	0.0
355.0	300.0	326.3	100.0	0.0
300.0	250.0	273.9	99.9	0.1
250.0	212.0	230.2	99.8	0.1
212.0	180.0	195.3	99.6	0.2
180.0	150.0	164.3	99.2	0.4
150.0	125.0	136.9	97.9	1.3
125.0	106.0	115.1	95.1	2.8
106.0	90.00	97.67	86.4	8.7
90.00	75.00	82.16	60.8	25.6
75.00	63.00	68.74	0.0	60.8

Mass Frequency vs Diameter



Summary Report

Full scale pump speed: 3  
Bubble detection: Medium  
Starting Size: 63.00  $\mu\text{m}$   
Ending Size: 0.50  $\mu\text{m}$

Stir time: 30 secs  
Stir speed: Low  
Probe time: 30 secs

Sample: TT-31-08 150 cm  
 Operator: Clint Edrington  
 Submitter: Clint Edrington  
 File Name: C:\EDRING~1\TIGER&~1\SANDFR~1\TT-31-08\31\_150CM.SMP  
 Material/Liquid: silicate mud/water/Water

Reported: 01/04/10 12:26:27  
 Liquid Visc: 0.7225 cp

Sample Density: 2.650 g/cm<sup>3</sup>  
 Liquid Density: 0.9941 g/cm<sup>3</sup>

## Summary Report

Parameter 1	0.000	Parameter 2	0.000	Parameter 3	0.000		
Mass Distribution Arithmetic Statistics							
Mean	77.88		Std. Dev.	17.11			
Median	71.79		Coef. Var.	0.220			
Mode	68.74		Skewness	4.239			
			Kurtosis	30.212			
Selected Percentiles			Selected Sizes				
Percent Finer	Diameter (µm)		Diameter (µm)	Percent Finer			
100.0	714.1		500.0	100.0			
80.0	84.21		250.0	99.9			
60.0	74.71		125.0	97.9			
40.0	69.55		88.00	84.7			
20.0	65.97		63.00	0.0			
Peak Number	% of Dist.*	Mean	Mode	Median	Standard Deviation	Skewness	Kurtosis
1	100.0	77.88	68.74	71.79	17.11	4.239	30.212

\* Peaks must comprise at least 5.00 % of the distribution.

Micromeritics

WIN5100 V2.03

Page 1

Sample: TT-31-08 203 cm  
Operator: Clint Edrington  
Submitter: Clint Edrington  
File Name: C:\EDRING~1\TIGER&~1\SANDFR~1\TT-31-08\31\_203CM.SMP  
Material/Liquid: silicate mud/water/Water

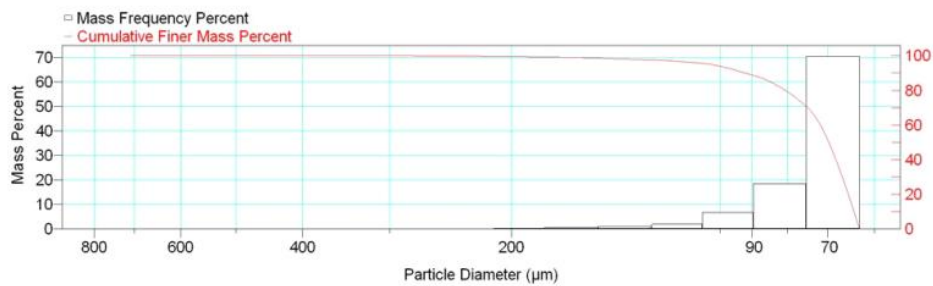
Reported: 01/04/10 12:28:40  
Liquid Visc: 0.7225 cp

Sample Density: 2.650 g/cm<sup>3</sup>  
Liquid Density: 0.9941 g/cm<sup>3</sup>

Report by Size Class

High Diameter (µm)	Low Diameter (µm)	Average Diameter (µm)	Cumulative Mass Finer (Percent)	Mass Frequency (Percent)
850.0	710.0	776.9	100.0	0.0
710.0	600.0	652.7	100.0	0.0
600.0	500.0	547.7	100.0	0.0
500.0	425.0	461.0	100.0	0.0
425.0	355.0	388.4	100.0	0.0
355.0	300.0	326.3	100.0	0.0
300.0	250.0	273.9	99.8	0.2
250.0	212.0	230.2	99.6	0.2
212.0	180.0	195.3	99.3	0.3
180.0	150.0	164.3	98.6	0.7
150.0	125.0	136.9	97.5	1.1
125.0	106.0	115.1	95.6	1.9
106.0	90.00	97.67	88.9	6.7
90.00	75.00	82.16	70.5	18.4
75.00	63.00	68.74	0.0	70.5

Mass Frequency vs Diameter



Summary Report

Full scale pump speed: 3  
Bubble detection: Medium  
Starting Size: 63.00 µm  
Ending Size: 0.50 µm

Stir time: 30 secs  
Stir speed: Low  
Probe time: 30 secs

Sample: TT-31-08 203 cm  
 Operator: Clint Edrington  
 Submitter: Clint Edrington  
 File Name: C:\EDRING~1\TIGER&~1\SANDFR~1\TT-31-08\31\_203CM.SMP  
 Material/Liquid: silicate mud/water/Water

Reported: 01/04/10 12:28:40  
 Liquid Visc: 0.7225 cp

Sample Density: 2.650 g/cm<sup>3</sup>  
 Liquid Density: 0.9941 g/cm<sup>3</sup>

## Summary Report

Parameter 1	0.000	Parameter 2	0.000	Parameter 3	0.000		
Mass Distribution Arithmetic Statistics							
Mean	76.56		Std. Dev.	19.19			
Median	69.73		Coef. Var.	0.251			
Mode	68.74		Skewness	5.121			
			Kurtosis	36.511			
Selected Percentiles			Selected Sizes				
Percent Finer	Diameter (µm)		Diameter (µm)	Percent Finer			
100.0	714.1		500.0	100.0			
80.0	80.58		250.0	99.8			
60.0	71.73		125.0	97.5			
40.0	68.10		88.00	87.7			
20.0	65.37		63.00	0.0			
Peak Number	% of Dist.*	Mean	Mode	Median	Standard Deviation	Skewness	Kurtosis
1	100.0	76.56	68.74	69.73	19.19	5.121	36.511

\* Peaks must comprise at least 5.00 % of the distribution.

Micromeritics

WIN5100 V2.03

Page 1

Sample: TT-31-08 359 cm  
Operator: Clint Edrington  
Submitter: Clint Edrington  
File Name: C:\EDRING~1\TIGER&~1\SANDFR~1\TT-31-08\31\_359CM.SMP  
Material/Liquid: silicate mud/water/Water

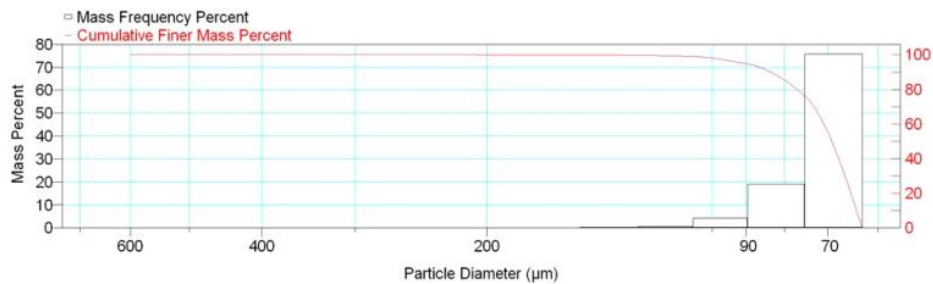
Reported: 01/04/10 12:30:56  
Liquid Visc: 0.7225 cp

Sample Density: 2.650 g/cm<sup>3</sup>  
Liquid Density: 0.9941 g/cm<sup>3</sup>

Report by Size Class

High Diameter (μm)	Low Diameter (μm)	Average Diameter (μm)	Cumulative Mass Finer (Percent)	Mass Frequency (Percent)
710.0	600.0	652.7	100.0	0.0
600.0	500.0	547.7	100.0	0.0
500.0	425.0	461.0	100.0	0.0
425.0	355.0	388.4	100.0	0.0
355.0	300.0	326.3	100.0	0.0
300.0	250.0	273.9	100.0	0.0
250.0	212.0	230.2	100.0	0.0
212.0	180.0	195.3	99.9	0.1
180.0	150.0	164.3	99.9	0.0
150.0	125.0	136.9	99.6	0.3
125.0	106.0	115.1	99.0	0.6
106.0	90.00	97.67	94.8	4.2
90.00	75.00	82.16	75.8	19.0
75.00	63.00	68.74	0.0	75.8

Mass Frequency vs Diameter



Summary Report

Full scale pump speed: 3  
Bubble detection: Medium  
Starting Size: 63.00 μm  
Ending Size: 0.50 μm

Stir time: 30 secs  
Stir speed: Low  
Probe time: 30 secs

Sample: TT-31-08 359 cm  
 Operator: Clint Edrington  
 Submitter: Clint Edrington  
 File Name: C:\EDRING~1\TIGER&~1\SANDFR~1\TT-31-08\31\_359CM.SMP  
 Material/Liquid: silicate mud/water/Water

Reported: 01/04/10 12:30:56  
 Liquid Visc: 0.7225 cp

Sample Density: 2.650 g/cm<sup>3</sup>  
 Liquid Density: 0.9941 g/cm<sup>3</sup>

## Summary Report

Parameter 1 0.000

Parameter 2 0.000

Parameter 3 0.000

## Mass Distribution Arithmetic Statistics

Mean	73.11	Std. Dev.	9.650
Median	69.15	Coef. Var.	0.132
Mode	68.74	Skewness	4.173
		Kurtosis	32.571

## Selected Percentiles

Percent Finer	Diameter (µm)
100.0	600.3
80.0	77.00
60.0	70.85
40.0	67.69
20.0	65.20

## Selected Sizes

Diameter (µm)	Percent Finer
500.0	100.0
250.0	100.0
125.0	99.6
88.00	93.9
63.00	0.0

Peak Number	% of Dist. *	Mean	Mode	Median	Standard Deviation	Skewness	Kurtosis
1	99.9	72.99	68.74	69.14	8.846	2.823	11.093

\* Peaks must comprise at least 5.00 % of the distribution.

# Micromeritics

WIN5100 V2.03

Page 1

Sample: TT-31-08 399 cm  
Operator: Clint Edrington  
Submitter: Clint Edrington  
File Name: C:\EDRING~1\TIGER&~1\SANDFR~1\TT-31-08\31\_399CM.SMP  
Material/Liquid: silicate mud/water/Water

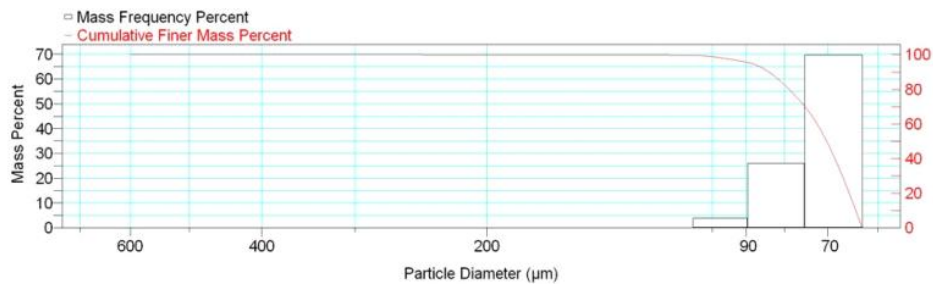
Reported: 01/04/10 12:32:50  
Liquid Visc: 0.7225 cp

Sample Density: 2.650 g/cm<sup>3</sup>  
Liquid Density: 0.9941 g/cm<sup>3</sup>

## Report by Size Class

High Diameter (μm)	Low Diameter (μm)	Average Diameter (μm)	Cumulative Mass Finer (Percent)	Mass Frequency (Percent)
710.0	600.0	652.7	100.0	0.0
600.0	500.0	547.7	100.0	0.0
500.0	425.0	461.0	100.0	0.0
425.0	355.0	388.4	100.0	0.0
355.0	300.0	326.3	100.0	0.0
300.0	250.0	273.9	100.0	0.0
250.0	212.0	230.2	99.9	0.1
212.0	180.0	195.3	99.9	0.0
180.0	150.0	164.3	99.9	0.0
150.0	125.0	136.9	99.8	0.1
125.0	106.0	115.1	99.6	0.2
106.0	90.00	97.67	95.7	3.9
90.00	75.00	82.16	69.7	26.0
75.00	63.00	68.74	0.0	69.7

Mass Frequency vs Diameter



## Summary Report

Full scale pump speed: 3  
Bubble detection: Medium  
Starting Size: 63.00 μm  
Ending Size: 0.50 μm

Stir time: 30 secs  
Stir speed: Low  
Probe time: 30 secs

Sample: TT-31-08 399 cm  
 Operator: Clint Edrington  
 Submitter: Clint Edrington  
 File Name: C:\EDRING~1\TIGER&~1\SANDFR~1\TT-31-08\31\_399CM.SMP  
 Material/Liquid: silicate mud/water/Water

Reported: 01/04/10 12:32:50  
 Liquid Visc: 0.7225 cp

Sample Density: 2.650 g/cm<sup>3</sup>  
 Liquid Density: 0.9941 g/cm<sup>3</sup>

## Summary Report

Parameter 1 0.000

Parameter 2 0.000

Parameter 3 0.000

## Mass Distribution Arithmetic Statistics

Mean	73.68	Std. Dev.	9.492
Median	70.25	Coef. Var.	0.129
Mode	68.74	Skewness	5.665
		Kurtosis	75.480

## Selected Percentiles

Percent Finer	Diameter (µm)
100.0	651.9
80.0	78.82
60.0	72.34
40.0	68.49
20.0	65.53

## Selected Sizes

Diameter (µm)	Percent Finer
500.0	100.0
250.0	100.0
125.0	99.8
88.00	94.6
63.00	0.0

Peak Number	% of Dist. *	Mean	Mode	Median	Standard Deviation	Skewness	Kurtosis
1	99.9	73.52	68.74	70.24	8.101	1.957	5.651

\* Peaks must comprise at least 5.00 % of the distribution.



Micromeritics

WIN5100 V2.03

Page 1

Sample: TT-32-08 12 cm  
Operator: Clint Edrington  
Submitter: Clint Edrington  
File Name: C:\EDRING~1\TIGER&~1\SANDFR~1\TT-32-08\32\_12CM.SMP  
Material/Liquid: silicate mud/water/Water

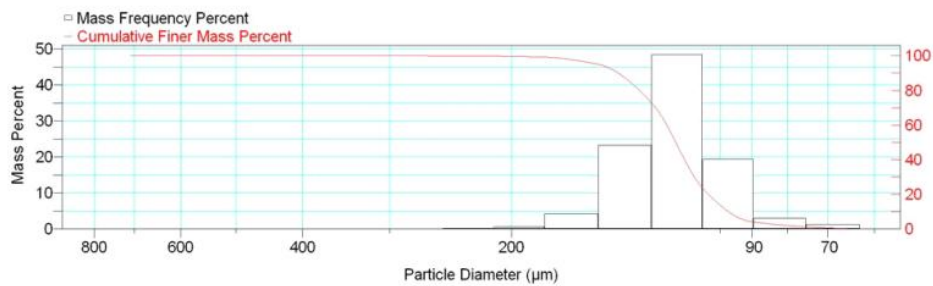
Reported: 01/04/10 12:35:39  
Liquid Visc: 0.7225 cp

Sample Density: 2.650 g/cm<sup>3</sup>  
Liquid Density: 0.9941 g/cm<sup>3</sup>

Report by Size Class

High Diameter (µm)	Low Diameter (µm)	Average Diameter (µm)	Cumulative Mass Finer (Percent)	Mass Frequency (Percent)
850.0	710.0	776.9	100.0	0.0
710.0	600.0	652.7	100.0	0.0
600.0	500.0	547.7	100.0	0.0
500.0	425.0	461.0	100.0	0.0
425.0	355.0	388.4	100.0	0.0
355.0	300.0	326.3	100.0	0.0
300.0	250.0	273.9	99.9	0.1
250.0	212.0	230.2	99.7	0.2
212.0	180.0	195.3	99.2	0.5
180.0	150.0	164.3	95.0	4.2
150.0	125.0	136.9	71.8	23.2
125.0	106.0	115.1	23.4	48.4
106.0	90.00	97.67	4.1	19.3
90.00	75.00	82.16	1.2	2.9
75.00	63.00	68.74	0.0	1.2

Mass Frequency vs Diameter



Summary Report

Full scale pump speed: 3  
Bubble detection: Medium  
Starting Size: 63.00 µm  
Ending Size: 0.50 µm

Stir time: 30 secs  
Stir speed: Low  
Probe time: 30 secs

Sample: TT-32-08 12 cm  
 Operator: Clint Edrington  
 Submitter: Clint Edrington  
 File Name: C:\EDRING~1\TIGER&~1\SANDFR~1\TT-32-08\32\_12CM.SMP  
 Material/Liquid: silicate mud/water/Water

Reported: 01/04/10 12:35:39  
 Liquid Visc: 0.7225 cp

Sample Density: 2.650 g/cm<sup>3</sup>  
 Liquid Density: 0.9941 g/cm<sup>3</sup>

## Summary Report

Parameter 1	0.000	Parameter 2	0.000	Parameter 3	0.000		
Mass Distribution Arithmetic Statistics							
Mean	118.2	Std. Dev.		20.07			
Median	115.9	Coef. Var.		0.170			
Mode	115.1	Skewness		1.248			
		Kurtosis		5.967			
Selected Percentiles			Selected Sizes				
Percent Finer	Diameter (µm)		Diameter (µm)	Percent Finer			
100.0	714.1		500.0	100.0			
80.0	130.8		250.0	99.9			
60.0	119.5		125.0	71.8			
40.0	112.6		88.00	3.6			
20.0	104.0		63.00	0.0			
Peak Number	% of Dist.*	Mean	Mode	Median	Standard Deviation	Skewness	Kurtosis
1	100.0	118.2	115.1	115.9	20.07	1.248	5.967

\* Peaks must comprise at least 5.00 % of the distribution.

Micromeritics

WIN5100 V2.03

Page 1

Sample: TT-32-08 55 cm  
Operator: Clint Edrington  
Submitter: Clint Edrington  
File Name: C:\EDRING~1\TIGER&~1\SANDFR~1\TT-32-08\32\_55CM.SMP  
Material/Liquid: silicate mud/water/Water

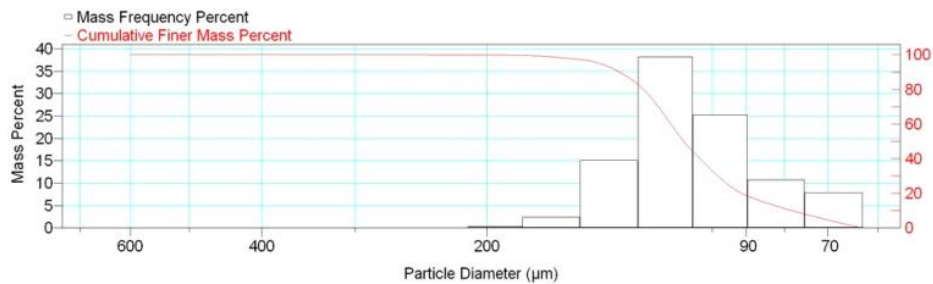
Reported: 01/04/10 12:37:54  
Liquid Visc: 0.7225 cp

Sample Density: 2.650 g/cm<sup>3</sup>  
Liquid Density: 0.9941 g/cm<sup>3</sup>

Report by Size Class

High Diameter (µm)	Low Diameter (µm)	Average Diameter (µm)	Cumulative Mass Finer (Percent)	Mass Frequency (Percent)
710.0	600.0	652.7	100.0	0.0
600.0	500.0	547.7	100.0	0.0
500.0	425.0	461.0	100.0	0.0
425.0	355.0	388.4	100.0	0.0
355.0	300.0	326.3	100.0	0.0
300.0	250.0	273.9	100.0	0.0
250.0	212.0	230.2	99.9	0.1
212.0	180.0	195.3	99.6	0.3
180.0	150.0	164.3	97.2	2.4
150.0	125.0	136.9	82.1	15.1
125.0	106.0	115.1	43.9	38.2
106.0	90.00	97.67	18.7	25.2
90.00	75.00	82.16	7.9	10.8
75.00	63.00	68.74	0.0	7.9

Mass Frequency vs Diameter



Summary Report

Full scale pump speed: 3  
Bubble detection: Medium  
Starting Size: 63.00 µm  
Ending Size: 0.50 µm

Stir time: 30 secs  
Stir speed: Low  
Probe time: 30 secs

Sample: TT-32-08 55 cm  
 Operator: Clint Edrington  
 Submitter: Clint Edrington  
 File Name: C:\EDRING~1\TIGER&~1\SANDFR~1\TT-32-08\32\_55CM.SMP  
 Material/Liquid: silicate mud/water/Water

Reported: 01/04/10 12:37:54  
 Liquid Visc: 0.7225 cp

Sample Density: 2.650 g/cm<sup>3</sup>  
 Liquid Density: 0.9941 g/cm<sup>3</sup>

## Summary Report

Parameter 1 0.000

Parameter 2 0.000

Parameter 3 0.000

## Mass Distribution Arithmetic Statistics

Mean	108.3	Std. Dev.	21.92
Median	109.1	Coef. Var.	0.202
Mode	115.1	Skewness	0.429
		Kurtosis	1.242

## Selected Percentiles

Percent Finer	Diameter (µm)
100.0	651.9
80.0	123.4
60.0	113.5
40.0	103.8
20.0	91.38

## Selected Sizes

Diameter (µm)	Percent Finer
500.0	100.0
250.0	100.0
125.0	82.1
88.00	17.1
63.00	0.0

Peak Number	% of Dist. *	Mean	Mode	Median	Standard Deviation	Skewness	Kurtosis
1	100.0	108.3	115.1	109.1	21.92	0.429	1.242

\* Peaks must comprise at least 5.00 % of the distribution.

Micromeritics

WIN5100 V2.03

Page 1

Sample: TT-32-08 110 cm  
Operator: Clint Edrington  
Submitter: Clint Edrington  
File Name: C:\EDRING~1\TIGER&~1\SANDFR~1\TT-32-08\32\_110CM.SMP  
Material/Liquid: silicate mud/water/Water

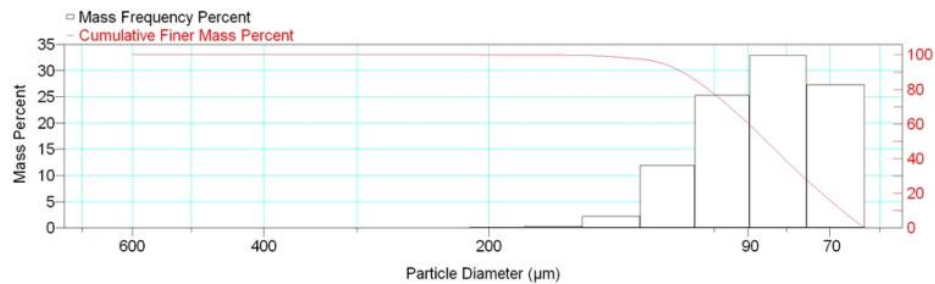
Reported: 01/04/10 12:40:10  
Liquid Visc: 0.7225 cp

Sample Density: 2.650 g/cm<sup>3</sup>  
Liquid Density: 0.9941 g/cm<sup>3</sup>

Report by Size Class

High Diameter (µm)	Low Diameter (µm)	Average Diameter (µm)	Cumulative Mass Finer (Percent)	Mass Frequency (Percent)
710.0	600.0	652.7	100.0	0.0
600.0	500.0	547.7	100.0	0.0
500.0	425.0	461.0	100.0	0.0
425.0	355.0	388.4	100.0	0.0
355.0	300.0	326.3	100.0	0.0
300.0	250.0	273.9	100.0	0.0
250.0	212.0	230.2	100.0	0.0
212.0	180.0	195.3	99.9	0.1
180.0	150.0	164.3	99.6	0.3
150.0	125.0	136.9	97.4	2.2
125.0	106.0	115.1	85.5	11.9
106.0	90.00	97.67	60.2	25.3
90.00	75.00	82.16	27.3	32.9
75.00	63.00	68.74	0.0	27.3

Mass Frequency vs Diameter



Summary Report

Full scale pump speed: 3  
Bubble detection: Medium  
Starting Size: 63.00 µm  
Ending Size: 0.50 µm

Stir time: 30 secs  
Stir speed: Low  
Probe time: 30 secs

Sample: TT-32-08 110 cm  
 Operator: Clint Edrington  
 Submitter: Clint Edrington  
 File Name: C:\EDRING~1\TIGER&~1\SANDFR~1\TT-32-08\32\_110CM.SMP  
 Material/Liquid: silicate mud/water/Water

Reported: 01/04/10 12:40:10  
 Liquid Visc: 0.7225 cp

Sample Density: 2.650 g/cm<sup>3</sup>  
 Liquid Density: 0.9941 g/cm<sup>3</sup>

## Summary Report

Parameter 1 0.000

Parameter 2 0.000

Parameter 3 0.000

## Mass Distribution Arithmetic Statistics

Mean	87.91	Std. Dev.	17.47
Median	85.05	Coef. Var.	0.199
Mode	82.16	Skewness	1.091
		Kurtosis	2.013

## Selected Percentiles

Percent Finer	Diameter (µm)
100.0	600.3
80.0	101.8
60.0	89.90
40.0	80.57
20.0	71.76

## Selected Sizes

Diameter (µm)	Percent Finer
500.0	100.0
250.0	100.0
125.0	97.4
88.00	56.2
63.00	0.0

Peak Number	% of Dist. *	Mean	Mode	Median	Standard Deviation	Skewness	Kurtosis
1	100.0	87.91	82.16	85.05	17.47	1.091	2.013

\* Peaks must comprise at least 5.00 % of the distribution.

Micromeritics

WIN5100 V2.03

Page 1

Sample: TT-33-08 4 cm  
Operator: Clint Edrington  
Submitter: Clint Edrington  
File Name: C:\EDRING~1\TIGER&~1\SANDFR~1\TT-33-08\33\_4CM.SMP  
Material/Liquid: silicate mud/water/Water

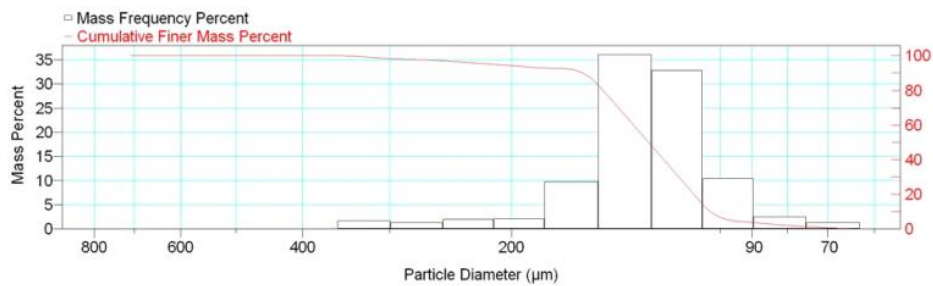
Reported: 01/04/10 12:43:02  
Liquid Visc: 0.7225 cp

Sample Density: 2.650 g/cm<sup>3</sup>  
Liquid Density: 0.9941 g/cm<sup>3</sup>

Report by Size Class

High Diameter (µm)	Low Diameter (µm)	Average Diameter (µm)	Cumulative Mass Finer (Percent)	Mass Frequency (Percent)
850.0	710.0	776.9	100.0	0.0
710.0	600.0	652.7	100.0	0.0
600.0	500.0	547.7	100.0	0.0
500.0	425.0	461.0	100.0	0.0
425.0	355.0	388.4	100.0	0.0
355.0	300.0	326.3	98.3	1.7
300.0	250.0	273.9	97.0	1.3
250.0	212.0	230.2	95.0	2.0
212.0	180.0	195.3	92.9	2.1
180.0	150.0	164.3	83.1	9.8
150.0	125.0	136.9	47.0	36.1
125.0	106.0	115.1	14.2	32.8
106.0	90.00	97.67	3.8	10.4
90.00	75.00	82.16	1.3	2.5
75.00	63.00	68.74	0.0	1.3

Mass Frequency vs Diameter



Summary Report

Full scale pump speed: 3  
Bubble detection: Medium  
Starting Size: 63.00 µm  
Ending Size: 0.50 µm

Stir time: 30 secs  
Stir speed: Low  
Probe time: 30 secs

Sample: TT-33-08 4 cm  
 Operator: Clint Edrington  
 Submitter: Clint Edrington  
 File Name: C:\EDRING~1\TIGER&~1\SANDFR~1\TT-33-08\33\_4CM.SMP  
 Material/Liquid: silicate mud/water/Water

Reported: 01/04/10 12:43:02  
 Liquid Visc: 0.7225 cp

Sample Density: 2.650 g/cm<sup>3</sup>  
 Liquid Density: 0.9941 g/cm<sup>3</sup>

## Summary Report

Parameter 1	0.000	Parameter 2	0.000	Parameter 3	0.000		
Mass Distribution Arithmetic Statistics							
Mean	134.2	Std. Dev.		40.22			
Median	126.9	Coef. Var.		0.300			
Mode	136.9	Skewness		2.562			
		Kurtosis		8.787			
Selected Percentiles			Selected Sizes				
Percent Finer	Diameter (µm)		Diameter (µm)	Percent Finer			
100.0	776.9		500.0	100.0			
80.0	147.6		250.0	97.0			
60.0	133.4		125.0	47.0			
40.0	120.7		88.00	3.4			
20.0	109.2		63.00	0.0			
Peak Number	% of Dist.*	Mean	Mode	Median	Standard Deviation	Skewness	Kurtosis
1	98.3	130.9	136.9	126.4	31.56	1.808	5.560

\* Peaks must comprise at least 5.00 % of the distribution.



Micromeritics

WIN5100 V2.03

Page 1

Sample: TT-33-08 50 cm  
Operator: Clint Edrington  
Submitter: Clint Edrington  
File Name: C:\EDRING~1\TIGER&~1\SANDFR~1\TT-33-08\33\_50CM.SMP  
Material/Liquid: silicate mud/water/Water

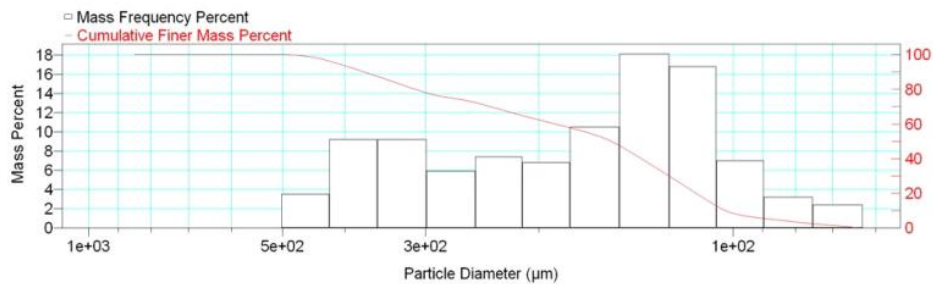
Reported: 01/04/10 12:45:49  
Liquid Visc: 0.7225 cp

Sample Density: 2.650 g/cm<sup>3</sup>  
Liquid Density: 0.9941 g/cm<sup>3</sup>

Report by Size Class

High Diameter (μm)	Low Diameter (μm)	Average Diameter (μm)	Cumulative Mass Finer (Percent)	Mass Frequency (Percent)
1000	850.0	922.0	100.0	0.0
850.0	710.0	776.9	100.0	0.0
710.0	600.0	652.7	100.0	0.0
600.0	500.0	547.7	100.0	0.0
500.0	425.0	461.0	96.5	3.5
425.0	355.0	388.4	87.3	9.2
355.0	300.0	326.3	78.1	9.2
300.0	250.0	273.9	72.2	5.9
250.0	212.0	230.2	64.8	7.4
212.0	180.0	195.3	58.0	6.8
180.0	150.0	164.3	47.5	10.5
150.0	125.0	136.9	29.4	18.1
125.0	106.0	115.1	12.6	16.8
106.0	90.00	97.67	5.6	7.0
90.00	75.00	82.16	2.4	3.2
75.00	63.00	68.74	0.0	2.4

Mass Frequency vs Diameter



Summary Report

Full scale pump speed: 3  
Bubble detection: Medium  
Starting Size: 63.00 μm

Stir time: 30 secs  
Stir speed: Low  
Probe time: 30 secs

Sample: TT-33-08 50 cm  
 Operator: Clint Edrington  
 Submitter: Clint Edrington  
 File Name: C:\EDRING~1\TIGER&~1\SANDFR~1\TT-33-08\33\_50CM.SMP  
 Material/Liquid: silicate mud/water/Water

Reported: 01/04/10 12:45:49      Sample Density: 2.650 g/cm<sup>3</sup>  
 Liquid Visc: 0.7225 cp      Liquid Density: 0.9941 g/cm<sup>3</sup>

## Summary Report

Ending Size: 0.50 µm

Parameter 1 0.000      Parameter 2 0.000      Parameter 3 0.000

## Mass Distribution Arithmetic Statistics

Mean	200.9	Std. Dev.	105.7
Median	154.5	Coef. Var.	0.526
Mode	136.9	Skewness	0.920
		Kurtosis	-0.332

## Selected Percentiles

Percent Finer	Diameter (µm)
100.0	922.0
80.0	311.2
60.0	188.8
40.0	138.8
20.0	114.1

## Selected Sizes

Diameter (µm)	Percent Finer
500.0	100.0
250.0	72.2
125.0	29.4
88.00	5.2
63.00	0.0

Peak Number	% of Dist. *	Mean	Mode	Median	Standard Deviation	Skewness	Kurtosis
1	64.8	132.4	136.9	128.8	32.70	0.283	-0.445
2	20.1	231.2	230.2	227.9	31.14	0.235	-1.372
3	27.8	352.7	326.3	347.2	58.71	0.320	-0.795

\* Peaks must comprise at least 5.00 % of the distribution.

Micromeritics

WIN5100 V2.03

Page 1

Sample: TT-33-08 100 cm  
Operator: Clint Edrington  
Submitter: Clint Edrington  
File Name: C:\EDRING~1\TIGER&~1\SANDFR~1\TT-33-08\33\_100CM.SMP  
Material/Liquid: silicate mud/water/Water

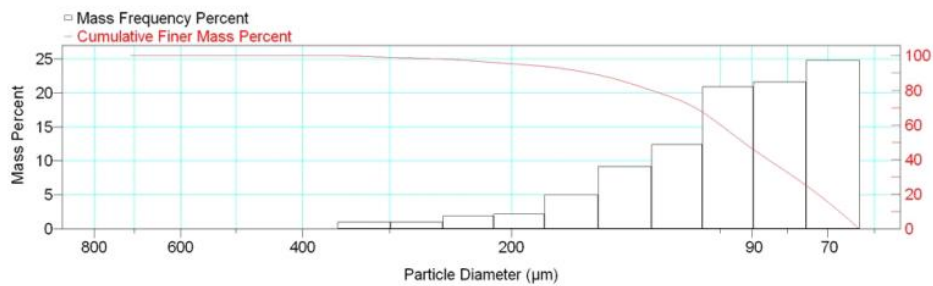
Reported: 01/04/10 12:48:11  
Liquid Visc: 0.7225 cp

Sample Density: 2.650 g/cm<sup>3</sup>  
Liquid Density: 0.9941 g/cm<sup>3</sup>

Report by Size Class

High Diameter (µm)	Low Diameter (µm)	Average Diameter (µm)	Cumulative Mass Finer (Percent)	Mass Frequency (Percent)
850.0	710.0	776.9	100.0	0.0
710.0	600.0	652.7	100.0	0.0
600.0	500.0	547.7	100.0	0.0
500.0	425.0	461.0	100.0	0.0
425.0	355.0	388.4	100.0	0.0
355.0	300.0	326.3	99.0	1.0
300.0	250.0	273.9	98.0	1.0
250.0	212.0	230.2	96.1	1.9
212.0	180.0	195.3	93.9	2.2
180.0	150.0	164.3	88.9	5.0
150.0	125.0	136.9	79.7	9.2
125.0	106.0	115.1	67.3	12.4
106.0	90.00	97.67	46.4	20.9
90.00	75.00	82.16	24.8	21.6
75.00	63.00	68.74	0.0	24.8

Mass Frequency vs Diameter



Summary Report

Full scale pump speed: 3  
Bubble detection: Medium  
Starting Size: 63.00 µm  
Ending Size: 0.50 µm

Stir time: 30 secs  
Stir speed: Low  
Probe time: 30 secs

Sample: TT-33-08 100 cm  
 Operator: Clint Edrington  
 Submitter: Clint Edrington  
 File Name: C:\EDRING~1\TIGER&~1\SANDFR~1\TT-33-08\33\_100CM.SMP  
 Material/Liquid: silicate mud/water/Water

Reported: 01/04/10 12:48:11  
 Liquid Visc: 0.7225 cp

Sample Density: 2.650 g/cm<sup>3</sup>  
 Liquid Density: 0.9941 g/cm<sup>3</sup>

## Summary Report

Parameter 1	0.000	Parameter 2	0.000	Parameter 3	0.000		
Mass Distribution Arithmetic Statistics							
Mean	105.0	Std. Dev.		44.55			
Median	92.62	Coef. Var.		0.424			
Mode	68.74	Skewness		2.368			
		Kurtosis		7.026			
Selected Percentiles			Selected Sizes				
Percent Finer	Diameter (µm)		Diameter (µm)	Percent Finer			
100.0	776.9		500.0	100.0			
80.0	125.6		250.0	98.0			
60.0	99.91		125.0	79.7			
40.0	85.27		88.00	43.7			
20.0	72.27		63.00	0.0			
Peak Number	% of Dist.*	Mean	Mode	Median	Standard Deviation	Skewness	Kurtosis
1	46.4	74.99	68.74	74.06	6.694	0.138	-1.981
2	74.2	114.1	82.16	101.4	38.64	1.912	3.963

\* Peaks must comprise at least 5.00 % of the distribution.

Micromeritics

WIN5100 V2.03

Page 1

Sample: TT-33-08 150 cm  
Operator: Clint Edrington  
Submitter: Clint Edrington  
File Name: C:\EDRING~1\TIGER&~1\SANDFR~1\TT-33-08\33\_150CM.SMP  
Material/Liquid: silicate mud/water/Water

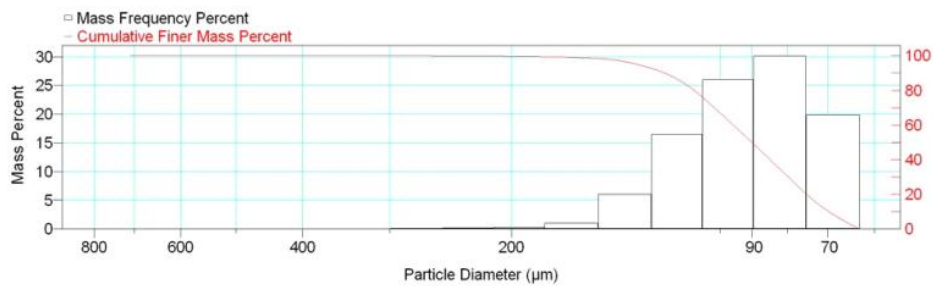
Reported: 01/04/10 12:50:50  
Liquid Visc: 0.7225 cp

Sample Density: 2.650 g/cm<sup>3</sup>  
Liquid Density: 0.9941 g/cm<sup>3</sup>

Report by Size Class

High Diameter (µm)	Low Diameter (µm)	Average Diameter (µm)	Cumulative Mass Finer (Percent)	Mass Frequency (Percent)
850.0	710.0	776.9	100.0	0.0
710.0	600.0	652.7	100.0	0.0
600.0	500.0	547.7	100.0	0.0
500.0	425.0	461.0	100.0	0.0
425.0	355.0	388.4	100.0	0.0
355.0	300.0	326.3	100.0	0.0
300.0	250.0	273.9	99.9	0.1
250.0	212.0	230.2	99.7	0.2
212.0	180.0	195.3	99.4	0.3
180.0	150.0	164.3	98.4	1.0
150.0	125.0	136.9	92.4	6.0
125.0	106.0	115.1	75.9	16.5
106.0	90.00	97.67	49.9	26.0
90.00	75.00	82.16	19.8	30.1
75.00	63.00	68.74	0.0	19.8

Mass Frequency vs Diameter



Summary Report

Full scale pump speed: 3  
Bubble detection: Medium  
Starting Size: 63.00 µm  
Ending Size: 0.50 µm

Stir time: 30 secs  
Stir speed: Low  
Probe time: 30 secs

Sample: TT-33-08 150 cm  
 Operator: Clint Edrington  
 Submitter: Clint Edrington  
 File Name: C:\EDRING~1\TIGER&~1\SANDFR~1\TT-33-08\33\_150CM.SMP  
 Material/Liquid: silicate mud/water/Water

Reported: 01/04/10 12:50:50  
 Liquid Visc: 0.7225 cp

Sample Density: 2.650 g/cm<sup>3</sup>  
 Liquid Density: 0.9941 g/cm<sup>3</sup>

## Summary Report

Parameter 1	0.000	Parameter 2	0.000	Parameter 3	0.000		
Mass Distribution Arithmetic Statistics							
Mean	93.91	Std. Dev.		22.49			
Median	90.06	Coef. Var.		0.240			
Mode	82.16	Skewness		1.778			
		Kurtosis		7.264			
Selected Percentiles			Selected Sizes				
Percent Finer	Diameter (µm)		Diameter (µm)	Percent Finer			
100.0	714.1		500.0	100.0			
80.0	109.1		250.0	99.9			
60.0	95.81		125.0	92.4			
40.0	84.76		88.00	46.2			
20.0	75.09		63.00	0.0			
Peak Number	% of Dist.*	Mean	Mode	Median	Standard Deviation	Skewness	Kurtosis
1	100.0	93.91	82.16	90.06	22.49	1.778	7.264

\* Peaks must comprise at least 5.00 % of the distribution.

# Micromeritics

WIN5100 V2.03

Page 1

Sample: TT-33-08 351 cm  
Operator: Clint Edrington  
Submitter: Clint Edrington  
File Name: C:\EDRING~1\TIGER&~1\SANDFR~1\TT-33-08\33\_351CM.SMP  
Material/Liquid: silicate mud/water/Water

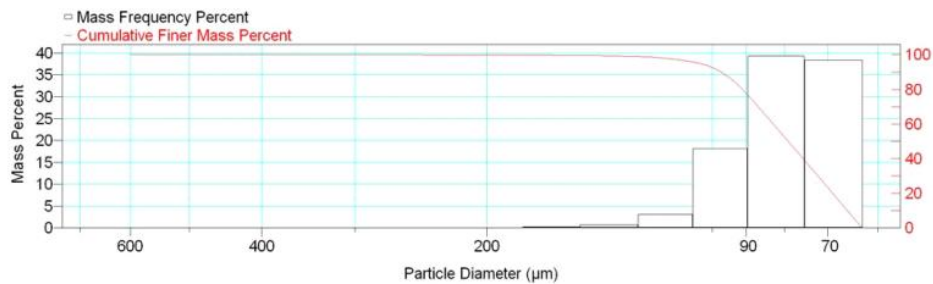
Reported: 01/04/10 12:52:59  
Liquid Visc: 0.7225 cp

Sample Density: 2.650 g/cm<sup>3</sup>  
Liquid Density: 0.9941 g/cm<sup>3</sup>

## Report by Size Class

High Diameter (µm)	Low Diameter (µm)	Average Diameter (µm)	Cumulative Mass Finer (Percent)	Mass Frequency (Percent)
710.0	600.0	652.7	100.0	0.0
600.0	500.0	547.7	100.0	0.0
500.0	425.0	461.0	100.0	0.0
425.0	355.0	388.4	100.0	0.0
355.0	300.0	326.3	100.0	0.0
300.0	250.0	273.9	100.0	0.0
250.0	212.0	230.2	99.9	0.1
212.0	180.0	195.3	99.8	0.1
180.0	150.0	164.3	99.6	0.2
150.0	125.0	136.9	98.9	0.7
125.0	106.0	115.1	95.8	3.1
106.0	90.00	97.67	77.7	18.1
90.00	75.00	82.16	38.4	39.3
75.00	63.00	68.74	0.0	38.4

Mass Frequency vs Diameter



## Summary Report

Full scale pump speed: 3  
Bubble detection: Medium  
Starting Size: 63.00 µm  
Ending Size: 0.50 µm

Stir time: 30 secs  
Stir speed: Low  
Probe time: 30 secs

Sample: TT-33-08 351 cm  
 Operator: Clint Edrington  
 Submitter: Clint Edrington  
 File Name: C:\EDRING~1\TIGER&~1\SANDFR~1\TT-33-08\33\_351CM.SMP  
 Material/Liquid: silicate mud/water/Water

Reported: 01/04/10 12:52:59  
 Liquid Visc: 0.7225 cp

Sample Density: 2.650 g/cm<sup>3</sup>  
 Liquid Density: 0.9941 g/cm<sup>3</sup>

## Summary Report

Parameter 1 0.000

Parameter 2 0.000

Parameter 3 0.000

## Mass Distribution Arithmetic Statistics

Mean	81.64	Std. Dev.	14.67
Median	79.08	Coef. Var.	0.180
Mode	82.16	Skewness	2.577
		Kurtosis	15.862

## Selected Percentiles

Percent Finer	Diameter (µm)
100.0	651.9
80.0	91.03
60.0	82.82
40.0	75.55
20.0	68.97

## Selected Sizes

Diameter (µm)	Percent Finer
500.0	100.0
250.0	100.0
125.0	98.9
88.00	73.0
63.00	0.0

Peak Number	% of Dist. *	Mean	Mode	Median	Standard Deviation	Skewness	Kurtosis
1	100.0	81.64	82.16	79.08	14.67	2.577	15.862

\* Peaks must comprise at least 5.00 % of the distribution.



Micromeritics

WIN5100 V2.03

Page 1

Sample: TT-33-08 406 cm  
Operator: Clint Edrington  
Submitter: Clint Edrington  
File Name: C:\EDRING~1\TIGER&~1\SANDFR~1\TT-33-08\33\_406CM.SMP  
Material/Liquid: silicate mud/water/Water

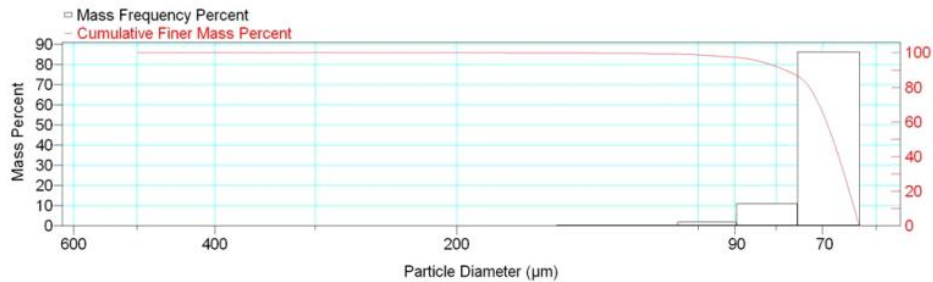
Reported: 01/04/10 12:55:04  
Liquid Visc: 0.7225 cp

Sample Density: 2.650 g/cm<sup>3</sup>  
Liquid Density: 0.9941 g/cm<sup>3</sup>

Report by Size Class

High Diameter (µm)	Low Diameter (µm)	Average Diameter (µm)	Cumulative Mass Finer (Percent)	Mass Frequency (Percent)
600.0	500.0	547.7	100.0	0.0
500.0	425.0	461.0	100.0	0.0
425.0	355.0	388.4	100.0	0.0
355.0	300.0	326.3	100.0	0.0
300.0	250.0	273.9	100.0	0.0
250.0	212.0	230.2	100.0	0.0
212.0	180.0	195.3	100.0	0.0
180.0	150.0	164.3	99.9	0.1
150.0	125.0	136.9	99.6	0.3
125.0	106.0	115.1	99.2	0.4
106.0	90.00	97.67	97.3	1.9
90.00	75.00	82.16	86.3	11.0
75.00	63.00	68.74	0.0	86.3

Mass Frequency vs Diameter



Summary Report

Full scale pump speed: 3  
Bubble detection: Medium  
Starting Size: 63.00 µm  
Ending Size: 0.50 µm

Stir time: 30 secs  
Stir speed: Low  
Probe time: 30 secs

Parameter 1 0.000

Parameter 2 0.000

Parameter 3 0.000

Sample: TT-33-08 406 cm  
 Operator: Clint Edrington  
 Submitter: Clint Edrington  
 File Name: C:\EDRING~1\TIGER&~1\SANDFR~1\TT-33-08\33\_406CM.SMP  
 Material/Liquid: silicate mud/water/Water

Reported: 01/04/10 12:55:04      Sample Density: 2.650 g/cm<sup>3</sup>  
 Liquid Visc: 0.7225 cp      Liquid Density: 0.9941 g/cm<sup>3</sup>

## Summary Report

Mass Distribution Arithmetic Statistics			
Mean	71.25	Std. Dev.	7.816
Median	67.95	Coef. Var.	0.110
Mode	68.74	Skewness	5.179
		Kurtosis	38.929

Selected Percentiles		Selected Sizes	
Percent Finer	Diameter (µm)	Diameter (µm)	Percent Finer
100.0	553.2	500.0	100.0
80.0	72.68	250.0	100.0
60.0	69.21	125.0	99.6
40.0	66.83	88.00	96.9
20.0	64.82	63.00	0.0

Peak Number	% of Dist.*	Mean	Mode	Median	Standard Deviation	Skewness	Kurtosis
1	100.0	71.25	68.74	67.95	7.816	5.179	38.929

\* Peaks must comprise at least 5.00 % of the distribution.

Micromeritics

WIN5100 V2.03

Page 1

Sample: TT-34-08 0 cm  
Operator: Clint Edrington  
Submitter: Clint Edrington  
File Name: C:\EDRING~1\TIGER&~1\SANDFR~1\TT-34-08\34\_0CM.SMP  
Material/Liquid: silicate mud/water/Water

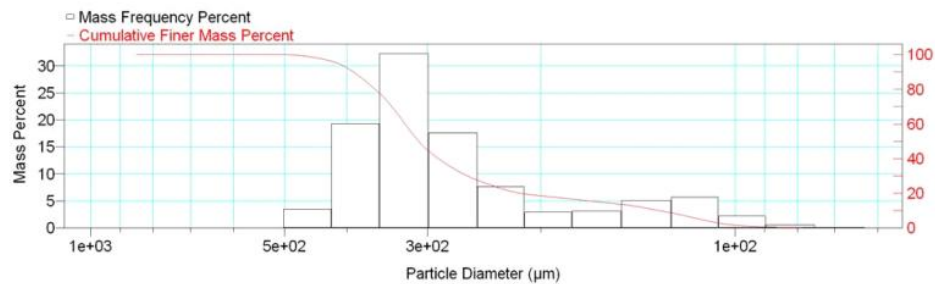
Reported: 01/04/10 13:08:51  
Liquid Visc: 0.7225 cp

Sample Density: 2.650 g/cm<sup>3</sup>  
Liquid Density: 0.9941 g/cm<sup>3</sup>

Report by Size Class

High Diameter ( $\mu\text{m}$ )	Low Diameter ( $\mu\text{m}$ )	Average Diameter ( $\mu\text{m}$ )	Cumulative Mass Finer (Percent)	Mass Frequency (Percent)
1000	850.0	922.0	100.0	0.0
850.0	710.0	776.9	100.0	0.0
710.0	600.0	652.7	100.0	0.0
600.0	500.0	547.7	100.0	0.0
500.0	425.0	461.0	96.5	3.5
425.0	355.0	388.4	77.2	19.3
355.0	300.0	326.3	44.9	32.3
300.0	250.0	273.9	27.3	17.6
250.0	212.0	230.2	19.6	7.7
212.0	180.0	195.3	16.7	2.9
180.0	150.0	164.3	13.6	3.1
150.0	125.0	136.9	8.5	5.1
125.0	106.0	115.1	2.8	5.7
106.0	90.00	97.67	0.6	2.2
90.00	75.00	82.16	0.1	0.5
75.00	63.00	68.74	0.0	0.1

Mass Frequency vs Diameter



Summary Report

Full scale pump speed: 3  
Bubble detection: Medium  
Starting Size: 63.00  $\mu\text{m}$

Stir time: 30 secs  
Stir speed: Low  
Probe time: 30 secs

Sample: TT-34-08 0 cm  
 Operator: Clint Edrington  
 Submitter: Clint Edrington  
 File Name: C:\EDRING~1\TIGER&~1\SANDFR~1\TT-34-08\34\_0CM.SMP  
 Material/Liquid: silicate mud/water/Water

Reported: 01/04/10 13:08:51      Sample Density: 2.650 g/cm<sup>3</sup>  
 Liquid Visc: 0.7225 cp      Liquid Density: 0.9941 g/cm<sup>3</sup>

## Summary Report

Ending Size: 0.50 µm

Parameter 1 0.000      Parameter 2 0.000      Parameter 3 0.000

## Mass Distribution Arithmetic Statistics

Mean	289.4	Std. Dev.	91.69
Median	309.8	Coef. Var.	0.317
Mode	326.3	Skewness	-0.536
		Kurtosis	-0.429

## Selected Percentiles

Percent Finer	Diameter (µm)
100.0	922.0
80.0	361.9
60.0	325.3
40.0	288.4
20.0	215.8

## Selected Sizes

Diameter (µm)	Percent Finer
500.0	100.0
250.0	27.3
125.0	8.5
88.00	0.5
63.00	0.0

Peak Number	% of Dist. *	Mean	Mode	Median	Standard Deviation	Skewness	Kurtosis
1	16.7	127.3	115.1	124.4	23.03	0.132	-0.675
2	86.4	316.2	326.3	320.5	66.29	-0.170	-0.118

\* Peaks must comprise at least 5.00 % of the distribution.

Micromeritics

WIN5100 V2.03

Page 1

Sample: TT-34-08 50 cm  
Operator: Clint Edrington  
Submitter: Clint Edrington  
File Name: C:\EDRING~1\TIGER&~1\SANDFR~1\TT-34-08\34\_50CM.SMP  
Material/Liquid: silicate mud/water/Water

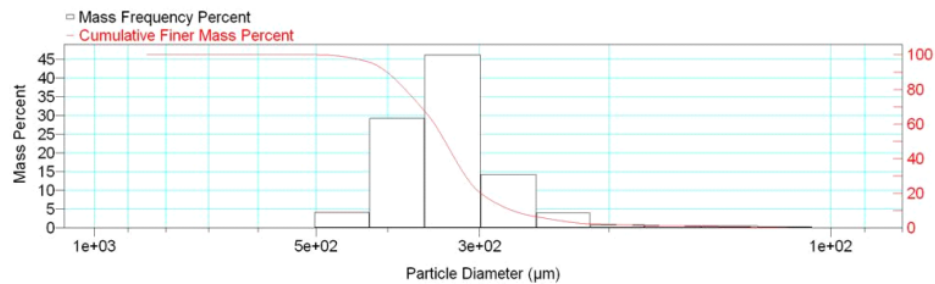
Reported: 01/04/10 13:11:30  
Liquid Visc: 0.7225 cp

Sample Density: 2.650 g/cm<sup>3</sup>  
Liquid Density: 0.9941 g/cm<sup>3</sup>

Report by Size Class

High Diameter (μm)	Low Diameter (μm)	Average Diameter (μm)	Cumulative Mass Finer (Percent)	Mass Frequency (Percent)
1000	850.0	922.0	100.0	0.0
850.0	710.0	776.9	100.0	0.0
710.0	600.0	652.7	100.0	0.0
600.0	500.0	547.7	100.0	0.0
500.0	425.0	461.0	95.9	4.1
425.0	355.0	388.4	66.7	29.2
355.0	300.0	326.3	20.5	46.2
300.0	250.0	273.9	6.3	14.2
250.0	212.0	230.2	2.3	4.0
212.0	180.0	195.3	1.5	0.8
180.0	150.0	164.3	0.9	0.6
150.0	125.0	136.9	0.4	0.5
125.0	106.0	115.1	0.1	0.3
106.0	90.00	97.67	0.0	0.1

Mass Frequency vs Diameter



Summary Report

Full scale pump speed: 3  
Bubble detection: Medium  
Starting Size: 63.00 μm  
Ending Size: 0.50 μm

Stir time: 30 secs  
Stir speed: Low  
Probe time: 30 secs

Sample: TT-34-08 50 cm  
 Operator: Clint Edrington  
 Submitter: Clint Edrington  
 File Name: C:\EDRING~1\TIGER&~1\SANDFR~1\TT-34-08\34\_50CM.SMP  
 Material/Liquid: silicate mud/water/Water

Reported: 01/04/10 13:11:30  
 Liquid Visc: 0.7225 cp

Sample Density: 2.650 g/cm<sup>3</sup>  
 Liquid Density: 0.9941 g/cm<sup>3</sup>

## Summary Report

Parameter 1 0.000

Parameter 2 0.000

Parameter 3 0.000

## Mass Distribution Arithmetic Statistics

Mean	334.9	Std. Dev.	56.72
Median	334.3	Coef. Var.	0.169
Mode	326.3	Skewness	-0.475
		Kurtosis	1.395

## Selected Percentiles

Percent Finer	Diameter (µm)
100.0	922.0
80.0	378.6
60.0	345.5
40.0	324.1
20.0	298.9

## Selected Sizes

Diameter (µm)	Percent Finer
500.0	100.0
250.0	6.3
125.0	0.4
88.00	0.0
63.00	0.0

Peak Number	% of Dist. *	Mean	Mode	Median	Standard Deviation	Skewness	Kurtosis
1	100.0	334.9	326.3	334.3	56.72	-0.475	1.395

\* Peaks must comprise at least 5.00 % of the distribution.

Micromeritics

WIN5100 V2.03

Page 1

Sample: TT-35-08 0 cm  
Operator: Clint Edrington  
Submitter: Clint Edrington  
File Name: C:\EDRING~1\TIGER&~1\SANDFR~1\TT-35-08\35\_0CM.SMP  
Material/Liquid: silicate mud/water/Water

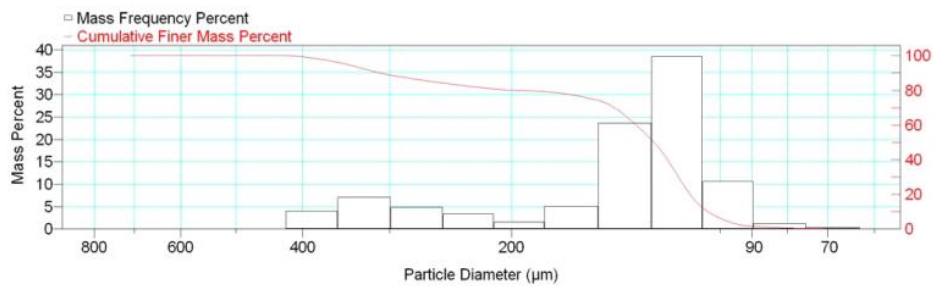
Reported: 01/04/10 13:14:49  
Liquid Visc: 0.7225 cp

Sample Density: 2.650 g/cm<sup>3</sup>  
Liquid Density: 0.9941 g/cm<sup>3</sup>

Report by Size Class

High Diameter (µm)	Low Diameter (µm)	Average Diameter (µm)	Cumulative Mass Finer (Percent)	Mass Frequency (Percent)
850.0	710.0	776.9	100.0	0.0
710.0	600.0	652.7	100.0	0.0
600.0	500.0	547.7	100.0	0.0
500.0	425.0	461.0	100.0	0.0
425.0	355.0	388.4	96.0	4.0
355.0	300.0	326.3	88.9	7.1
300.0	250.0	273.9	84.1	4.8
250.0	212.0	230.2	80.8	3.3
212.0	180.0	195.3	79.3	1.5
180.0	150.0	164.3	74.2	5.1
150.0	125.0	136.9	50.6	23.6
125.0	106.0	115.1	12.1	38.5
106.0	90.00	97.67	1.5	10.6
90.00	75.00	82.16	0.3	1.2
75.00	63.00	68.74	0.0	0.3

Mass Frequency vs Diameter



Summary Report

Full scale pump speed: 3  
Bubble detection: Medium  
Starting Size: 63.00 µm  
Ending Size: 0.50 µm

Stir time: 30 secs  
Stir speed: Low  
Probe time: 30 secs

Sample: TT-35-08 0 cm  
 Operator: Clint Edrington  
 Submitter: Clint Edrington  
 File Name: C:\EDRING~1\TIGER&~1\SANDFR~1\TT-35-08\35\_0CM.SMP  
 Material/Liquid: silicate mud/water/Water

Reported: 01/04/10 13:14:49  
 Liquid Visc: 0.7225 cp

Sample Density: 2.650 g/cm<sup>3</sup>  
 Liquid Density: 0.9941 g/cm<sup>3</sup>

## Summary Report

Parameter 1	0.000	Parameter 2	0.000	Parameter 3	0.000		
Mass Distribution Arithmetic Statistics							
Mean	158.9	Std. Dev.		79.16			
Median	124.6	Coef. Var.		0.498			
Mode	115.1	Skewness		1.684			
		Kurtosis		1.572			
Selected Percentiles			Selected Sizes				
Percent Finer	Diameter (µm)		Diameter (µm)	Percent Finer			
100.0	850.0		500.0	100.0			
80.0	197.6		250.0	84.1			
60.0	132.3		125.0	50.6			
40.0	119.2		88.00	1.3			
20.0	110.6		63.00	0.0			
Peak Number	% of Dist.*	Mean	Mode	Median	Standard Deviation	Skewness	Kurtosis
1	80.8	123.1	115.1	119.4	20.28	0.977	1.903
2	20.7	301.4	326.3	306.7	58.95	-0.076	-0.963

\* Peaks must comprise at least 5.00 % of the distribution.



Micromeritics

WIN5100 V2.03

Page 1

Sample: TT-35-08 50 cm  
Operator: Clint Edrington  
Submitter: Clint Edrington  
File Name: C:\EDRING~1\TIGER&~1\SANDFR~1\TT-35-08\35\_50CM.SMP  
Material/Liquid: silicate mud/water/Water

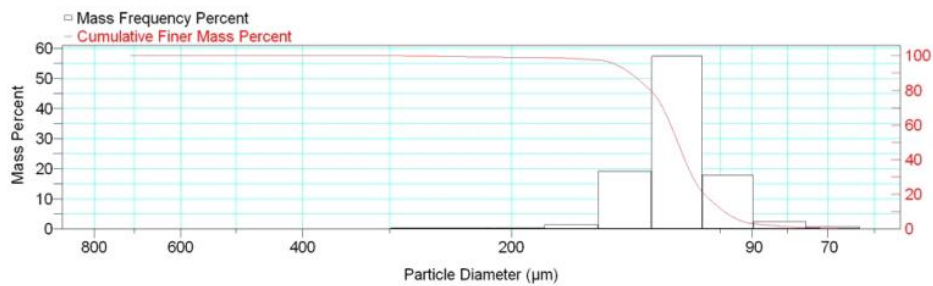
Reported: 01/04/10 13:17:51  
Liquid Visc: 0.7225 cp

Sample Density: 2.650 g/cm<sup>3</sup>  
Liquid Density: 0.9941 g/cm<sup>3</sup>

Report by Size Class

High Diameter (μm)	Low Diameter (μm)	Average Diameter (μm)	Cumulative Mass Finer (Percent)	Mass Frequency (Percent)
850.0	710.0	776.9	100.0	0.0
710.0	600.0	652.7	100.0	0.0
600.0	500.0	547.7	100.0	0.0
500.0	425.0	461.0	100.0	0.0
425.0	355.0	388.4	100.0	0.0
355.0	300.0	326.3	100.0	0.0
300.0	250.0	273.9	99.6	0.4
250.0	212.0	230.2	99.2	0.4
212.0	180.0	195.3	98.9	0.3
180.0	150.0	164.3	97.5	1.4
150.0	125.0	136.9	78.4	19.1
125.0	106.0	115.1	21.0	57.4
106.0	90.00	97.67	3.1	17.9
90.00	75.00	82.16	0.7	2.4
75.00	63.00	68.74	0.0	0.7

Mass Frequency vs Diameter



Summary Report

Full scale pump speed: 3  
Bubble detection: Medium  
Starting Size: 63.00 μm  
Ending Size: 0.50 μm

Stir time: 30 secs  
Stir speed: Low  
Probe time: 30 secs

Sample: TT-35-08 50 cm  
 Operator: Clint Edrington  
 Submitter: Clint Edrington  
 File Name: C:\EDRING~1\TIGER&~1\SANDFR~1\TT-35-08\35\_50CM.SMP  
 Material/Liquid: silicate mud/water/Water

Reported: 01/04/10 13:17:51  
 Liquid Visc: 0.7225 cp

Sample Density: 2.650 g/cm<sup>3</sup>  
 Liquid Density: 0.9941 g/cm<sup>3</sup>

## Summary Report

Parameter 1	0.000	Parameter 2	0.000	Parameter 3	0.000		
Mass Distribution Arithmetic Statistics							
Mean	117.1	Std. Dev.		19.74			
Median	115.2	Coef. Var.		0.169			
Mode	115.1	Skewness		2.926			
		Kurtosis		19.290			
Selected Percentiles			Selected Sizes				
Percent Finer	Diameter (µm)		Diameter (µm)	Percent Finer			
100.0	714.1		500.0	100.0			
80.0	126.2		250.0	99.6			
60.0	117.9		125.0	78.4			
40.0	112.5		88.00	2.7			
20.0	105.4		63.00	0.0			
Peak Number	% of Dist.*	Mean	Mode	Median	Standard Deviation	Skewness	Kurtosis
1	99.2	116.0	115.1	115.1	15.52	0.559	2.536

\* Peaks must comprise at least 5.00 % of the distribution.

Micromeritics

WIN5100 V2.03

Page 1

Sample: TT-35-08 94 cm  
Operator: Clint Edrington  
Submitter: Clint Edrington  
File Name: C:\EDRING~1\TIGER&~1\SANDFR~1\TT-35-08\35\_94CM.SMP  
Material/Liquid: silicate mud/water/Water

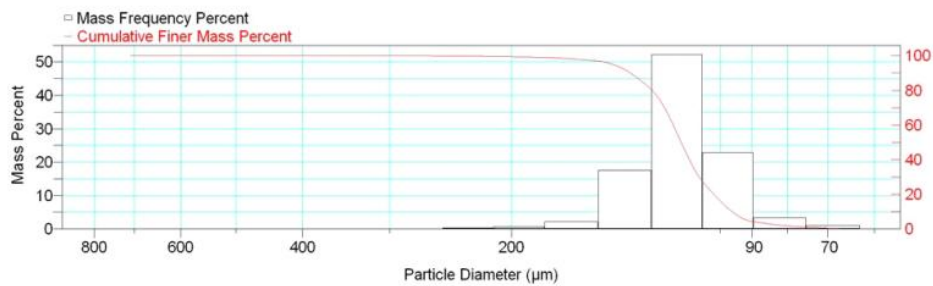
Reported: 01/04/10 13:20:13  
Liquid Visc: 0.7225 cp

Sample Density: 2.650 g/cm<sup>3</sup>  
Liquid Density: 0.9941 g/cm<sup>3</sup>

Report by Size Class

High Diameter (μm)	Low Diameter (μm)	Average Diameter (μm)	Cumulative Mass Finer (Percent)	Mass Frequency (Percent)
850.0	710.0	776.9	100.0	0.0
710.0	600.0	652.7	100.0	0.0
600.0	500.0	547.7	100.0	0.0
500.0	425.0	461.0	100.0	0.0
425.0	355.0	388.4	100.0	0.0
355.0	300.0	326.3	100.0	0.0
300.0	250.0	273.9	99.9	0.1
250.0	212.0	230.2	99.6	0.3
212.0	180.0	195.3	99.0	0.6
180.0	150.0	164.3	96.9	2.1
150.0	125.0	136.9	79.4	17.5
125.0	106.0	115.1	27.2	52.2
106.0	90.00	97.67	4.3	22.9
90.00	75.00	82.16	1.0	3.3
75.00	63.00	68.74	0.0	1.0

Mass Frequency vs Diameter



Summary Report

Full scale pump speed: 3  
Bubble detection: Medium  
Starting Size: 63.00 μm  
Ending Size: 0.50 μm

Stir time: 30 secs  
Stir speed: Low  
Probe time: 30 secs

Sample: TT-35-08 94 cm  
 Operator: Clint Edrington  
 Submitter: Clint Edrington  
 File Name: C:\EDRING~1\TIGER&~1\SANDFR~1\TT-35-08\35\_94CM.SMP  
 Material/Liquid: silicate mud/water/Water

Reported: 01/04/10 13:20:13  
 Liquid Visc: 0.7225 cp

Sample Density: 2.650 g/cm<sup>3</sup>  
 Liquid Density: 0.9941 g/cm<sup>3</sup>

## Summary Report

Parameter 1	0.000	Parameter 2	0.000	Parameter 3	0.000		
Mass Distribution Arithmetic Statistics							
Mean	115.4	Std. Dev.		19.10			
Median	113.9	Coef. Var.		0.165			
Mode	115.1	Skewness		1.764			
		Kurtosis		9.523			
Selected Percentiles			Selected Sizes				
Percent Finer	Diameter (µm)		Diameter (µm)	Percent Finer			
100.0	714.1		500.0	100.0			
80.0	125.5		250.0	99.9			
60.0	116.9		125.0	79.4			
40.0	110.9		88.00	3.7			
20.0	102.2		63.00	0.0			
Peak Number	% of Dist.*	Mean	Mode	Median	Standard Deviation	Skewness	Kurtosis
1	100.0	115.4	115.1	113.9	19.10	1.764	9.523

\* Peaks must comprise at least 5.00 % of the distribution.

Micromeritics

WIN5100 V2.03

Page 1

Sample: TT-36-08 4 cm  
Operator: Clint Edrington  
Submitter: Clint Edrington  
File Name: C:\EDRING~1\TIGER&~1\SANDFR~1\TT-36-08\36\_4CM.SMP  
Material/Liquid: silicate mud/water/Water

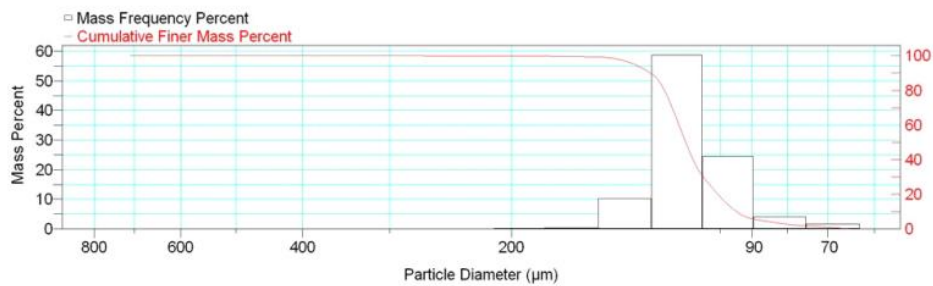
Reported: 01/04/10 13:23:16  
Liquid Visc: 0.7225 cp

Sample Density: 2.650 g/cm<sup>3</sup>  
Liquid Density: 0.9941 g/cm<sup>3</sup>

Report by Size Class

High Diameter (μm)	Low Diameter (μm)	Average Diameter (μm)	Cumulative Mass Finer (Percent)	Mass Frequency (Percent)
850.0	710.0	776.9	100.0	0.0
710.0	600.0	652.7	100.0	0.0
600.0	500.0	547.7	100.0	0.0
500.0	425.0	461.0	100.0	0.0
425.0	355.0	388.4	100.0	0.0
355.0	300.0	326.3	100.0	0.0
300.0	250.0	273.9	99.9	0.1
250.0	212.0	230.2	99.9	0.0
212.0	180.0	195.3	99.7	0.2
180.0	150.0	164.3	99.3	0.4
150.0	125.0	136.9	89.0	10.3
125.0	106.0	115.1	30.3	58.7
106.0	90.00	97.67	5.8	24.5
90.00	75.00	82.16	1.7	4.1
75.00	63.00	68.74	0.0	1.7

Mass Frequency vs Diameter



Summary Report

Full scale pump speed: 3  
Bubble detection: Medium  
Starting Size: 63.00 μm  
Ending Size: 0.50 μm

Stir time: 30 secs  
Stir speed: Low  
Probe time: 30 secs

Sample: TT-36-08 4 cm  
 Operator: Clint Edrington  
 Submitter: Clint Edrington  
 File Name: C:\EDRING~1\TIGER&~1\SANDFR~1\TT-36-08\36\_4CM.SMP  
 Material/Liquid: silicate mud/water/Water

Reported: 01/04/10 13:23:16  
 Liquid Visc: 0.7225 cp

Sample Density: 2.650 g/cm<sup>3</sup>  
 Liquid Density: 0.9941 g/cm<sup>3</sup>

## Summary Report

Parameter 1	0.000	Parameter 2	0.000	Parameter 3	0.000		
Mass Distribution Arithmetic Statistics							
Mean	111.5	Std. Dev.		15.46			
Median	112.2	Coef. Var.		0.139			
Mode	115.1	Skewness		1.295			
		Kurtosis		13.885			
Selected Percentiles			Selected Sizes				
Percent Finer	Diameter (µm)		Diameter (µm)	Percent Finer			
100.0	714.1		500.0	100.0			
80.0	120.4		250.0	99.9			
60.0	114.7		125.0	89.0			
40.0	109.5		88.00	5.1			
20.0	100.8		63.00	0.0			
Peak Number	% of Dist.*	Mean	Mode	Median	Standard Deviation	Skewness	Kurtosis
1	99.9	111.3	115.1	112.2	14.59	0.195	2.959

\* Peaks must comprise at least 5.00 % of the distribution.

Micromeritics

WIN5100 V2.03

Page 1

Sample: TT-36-08 50 cm  
Operator: Clint Edrington  
Submitter: Clint Edrington  
File Name: C:\EDRING~1\TIGER&~1\SANDFR~1\TT-36-08\36\_50CM.SMP  
Material/Liquid: silicate mud/water/Water

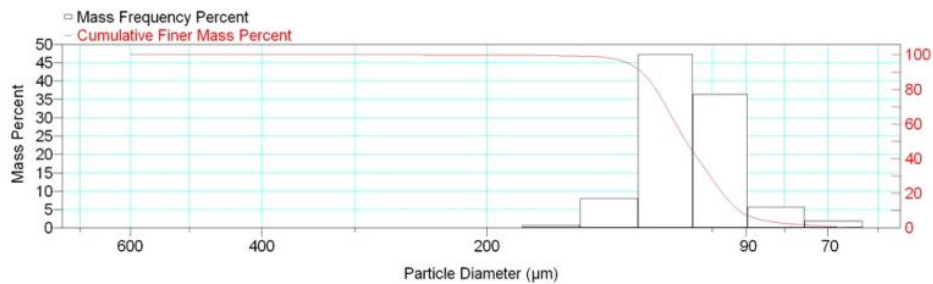
Reported: 01/04/10 13:25:23  
Liquid Visc: 0.7225 cp

Sample Density: 2.650 g/cm<sup>3</sup>  
Liquid Density: 0.9941 g/cm<sup>3</sup>

Report by Size Class

High Diameter (μm)	Low Diameter (μm)	Average Diameter (μm)	Cumulative Mass Finer (Percent)	Mass Frequency (Percent)
710.0	600.0	652.7	100.0	0.0
600.0	500.0	547.7	100.0	0.0
500.0	425.0	461.0	100.0	0.0
425.0	355.0	388.4	100.0	0.0
355.0	300.0	326.3	100.0	0.0
300.0	250.0	273.9	100.0	0.0
250.0	212.0	230.2	99.9	0.1
212.0	180.0	195.3	99.8	0.1
180.0	150.0	164.3	99.1	0.7
150.0	125.0	136.9	91.1	8.0
125.0	106.0	115.1	43.9	47.2
106.0	90.00	97.67	7.5	36.4
90.00	75.00	82.16	1.8	5.7
75.00	63.00	68.74	0.0	1.8

Mass Frequency vs Diameter



Summary Report

Full scale pump speed: 3  
Bubble detection: Medium  
Starting Size: 63.00 μm  
Ending Size: 0.50 μm

Stir time: 30 secs  
Stir speed: Low  
Probe time: 30 secs

Sample: TT-36-08 50 cm  
 Operator: Clint Edrington  
 Submitter: Clint Edrington  
 File Name: C:\EDRING~1\TIGER&~1\SANDFR~1\TT-36-08\36\_50CM.SMP  
 Material/Liquid: silicate mud/water/Water

Reported: 01/04/10 13:25:23  
 Liquid Visc: 0.7225 cp

Sample Density: 2.650 g/cm<sup>3</sup>  
 Liquid Density: 0.9941 g/cm<sup>3</sup>

## Summary Report

Parameter 1 0.000

Parameter 2 0.000

Parameter 3 0.000

## Mass Distribution Arithmetic Statistics

Mean	108.3	Std. Dev.	15.50
Median	108.4	Coef. Var.	0.143
Mode	115.1	Skewness	0.842
		Kurtosis	5.274

## Selected Percentiles

Percent Finer	Diameter (µm)
100.0	651.9
80.0	118.9
60.0	111.8
40.0	104.4
20.0	96.81

## Selected Sizes

Diameter (µm)	Percent Finer
500.0	100.0
250.0	100.0
125.0	91.1
88.00	5.9
63.00	0.0

Peak Number	% of Dist. *	Mean	Mode	Median	Standard Deviation	Skewness	Kurtosis
1	100.0	108.3	115.1	108.4	15.50	0.842	5.274

\* Peaks must comprise at least 5.00 % of the distribution.



Micromeritics

WIN5100 V2.03

Page 1

Sample: TT-36-08 80 cm  
Operator: Clint Edrington  
Submitter: Clint Edrington  
File Name: C:\EDRING~1\TIGER&~1\SANDFR~1\TT-36-08\36\_80CM.SMP  
Material/Liquid: silicate mud/water/Water

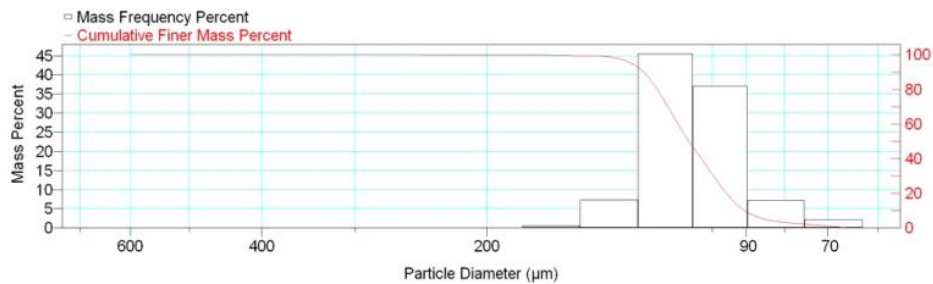
Reported: 01/04/10 13:27:24  
Liquid Visc: 0.7225 cp

Sample Density: 2.650 g/cm<sup>3</sup>  
Liquid Density: 0.9941 g/cm<sup>3</sup>

Report by Size Class

High Diameter (μm)	Low Diameter (μm)	Average Diameter (μm)	Cumulative Mass Finer (Percent)	Mass Frequency (Percent)
710.0	600.0	652.7	100.0	0.0
600.0	500.0	547.7	100.0	0.0
500.0	425.0	461.0	100.0	0.0
425.0	355.0	388.4	100.0	0.0
355.0	300.0	326.3	100.0	0.0
300.0	250.0	273.9	100.0	0.0
250.0	212.0	230.2	99.9	0.1
212.0	180.0	195.3	99.9	0.0
180.0	150.0	164.3	99.3	0.6
150.0	125.0	136.9	92.0	7.3
125.0	106.0	115.1	46.5	45.5
106.0	90.00	97.67	9.4	37.1
90.00	75.00	82.16	2.2	7.2
75.00	63.00	68.74	0.0	2.2

Mass Frequency vs Diameter



Summary Report

Full scale pump speed: 3  
Bubble detection: Medium  
Starting Size: 63.00 μm  
Ending Size: 0.50 μm

Stir time: 30 secs  
Stir speed: Low  
Probe time: 30 secs

Sample: TT-36-08 80 cm  
 Operator: Clint Edrington  
 Submitter: Clint Edrington  
 File Name: C:\EDRING~1\TIGER&~1\SANDFR~1\TT-36-08\36\_80CM.SMP  
 Material/Liquid: silicate mud/water/Water

Reported: 01/04/10 13:27:24  
 Liquid Visc: 0.7225 cp

Sample Density: 2.650 g/cm<sup>3</sup>  
 Liquid Density: 0.9941 g/cm<sup>3</sup>

## Summary Report

Parameter 1 0.000

Parameter 2 0.000

Parameter 3 0.000

## Mass Distribution Arithmetic Statistics

Mean	107.3	Std. Dev.	15.46
Median	107.4	Coef. Var.	0.144
Mode	115.1	Skewness	0.645
		Kurtosis	4.537

## Selected Percentiles

Percent Finer	Diameter (µm)
100.0	651.9
80.0	118.4
60.0	111.1
40.0	103.4
20.0	95.66

## Selected Sizes

Diameter (µm)	Percent Finer
500.0	100.0
250.0	100.0
125.0	92.0
88.00	7.3
63.00	0.0

Peak Number	% of Dist. *	Mean	Mode	Median	Standard Deviation	Skewness	Kurtosis
1	99.9	107.1	115.1	107.4	14.97	0.181	1.032

\* Peaks must comprise at least 5.00 % of the distribution.

Micromeritics

WIN5100 V2.03

Page 1

Sample: TT-37-08 12 cm  
Operator: Clint Edrington  
Submitter: Clint Edrington  
File Name: C:\EDRING~1\TIGER&~1\SANDFR~1\TT-37-08\37\_12CM.SMP  
Material/Liquid: silicate mud/water/Water

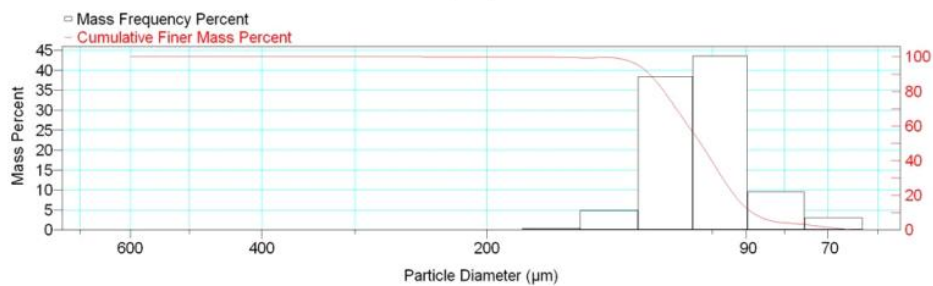
Reported: 01/04/10 14:38:01  
Liquid Visc: 0.7225 cp

Sample Density: 2.650 g/cm<sup>3</sup>  
Liquid Density: 0.9941 g/cm<sup>3</sup>

Report by Size Class

High Diameter (μm)	Low Diameter (μm)	Average Diameter (μm)	Cumulative Mass Finer (Percent)	Mass Frequency (Percent)
710.0	600.0	652.7	100.0	0.0
600.0	500.0	547.7	100.0	0.0
500.0	425.0	461.0	100.0	0.0
425.0	355.0	388.4	100.0	0.0
355.0	300.0	326.3	100.0	0.0
300.0	250.0	273.9	100.0	0.0
250.0	212.0	230.2	99.9	0.1
212.0	180.0	195.3	99.9	0.0
180.0	150.0	164.3	99.5	0.4
150.0	125.0	136.9	94.6	4.9
125.0	106.0	115.1	56.2	38.4
106.0	90.00	97.67	12.6	43.6
90.00	75.00	82.16	3.1	9.5
75.00	63.00	68.74	0.0	3.1

Mass Frequency vs Diameter



Summary Report

Full scale pump speed: 3  
Bubble detection: Medium  
Starting Size: 63.00 μm  
Ending Size: 0.50 μm

Stir time: 30 secs  
Stir speed: Low  
Probe time: 30 secs

Sample: TT-37-08 12 cm  
 Operator: Clint Edrington  
 Submitter: Clint Edrington  
 File Name: C:\EDRING~1\TIGER&~1\SANDFR~1\TT-37-08\37\_12CM.SMP  
 Material/Liquid: silicate mud/water/Water

Reported: 01/04/10 14:38:01  
 Liquid Visc: 0.7225 cp

Sample Density: 2.650 g/cm<sup>3</sup>  
 Liquid Density: 0.9941 g/cm<sup>3</sup>

## Summary Report

Parameter 1 0.000

Parameter 2 0.000

Parameter 3 0.000

## Mass Distribution Arithmetic Statistics

Mean	104.3	Std. Dev.	15.24
Median	103.6	Coef. Var.	0.146
Mode	97.67	Skewness	0.701
		Kurtosis	5.106

## Selected Percentiles

Percent Finer	Diameter (µm)
100.0	651.9
80.0	115.9
60.0	107.6
40.0	100.1
20.0	93.31

## Selected Sizes

Diameter (µm)	Percent Finer
500.0	100.0
250.0	100.0
125.0	94.6
88.00	9.5
63.00	0.0

Peak Number	% of Dist. *	Mean	Mode	Median	Standard Deviation	Skewness	Kurtosis
1	99.9	104.2	97.67	103.5	14.72	0.179	0.973

\* Peaks must comprise at least 5.00 % of the distribution.

Micromeritics

WIN5100 V2.03

Page 1

Sample: TT-37-08 50 cm  
Operator: Clint Edrington  
Submitter: Clint Edrington  
File Name: C:\EDRING~1\TIGER&~1\SANDFR~1\TT-37-08\37\_50CM.SMP  
Material/Liquid: silicate mud/water/Water

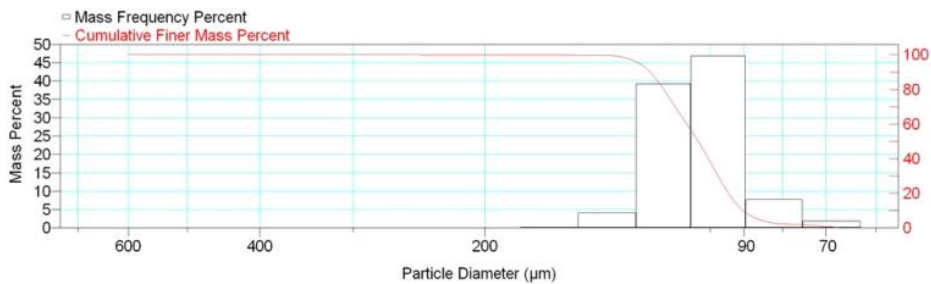
Reported: 01/04/10 14:40:47  
Liquid Visc: 0.7225 cp

Sample Density: 2.650 g/cm<sup>3</sup>  
Liquid Density: 0.9941 g/cm<sup>3</sup>

Report by Size Class

High Diameter (µm)	Low Diameter (µm)	Average Diameter (µm)	Cumulative Mass Finer (Percent)	Mass Frequency (Percent)
710.0	600.0	652.7	100.0	0.0
600.0	500.0	547.7	100.0	0.0
500.0	425.0	461.0	100.0	0.0
425.0	355.0	388.4	100.0	0.0
355.0	300.0	326.3	100.0	0.0
300.0	250.0	273.9	100.0	0.0
250.0	212.0	230.2	99.9	0.1
212.0	180.0	195.3	99.9	0.0
180.0	150.0	164.3	99.7	0.2
150.0	125.0	136.9	95.6	4.1
125.0	106.0	115.1	56.3	39.3
106.0	90.00	97.67	9.5	46.8
90.00	75.00	82.16	1.8	7.7
75.00	63.00	68.74	0.0	1.8

Mass Frequency vs Diameter



Summary Report

Full scale pump speed: 3  
Bubble detection: Medium  
Starting Size: 63.00 µm  
Ending Size: 0.50 µm

Stir time: 30 secs  
Stir speed: Low  
Probe time: 30 secs

Sample: TT-37-08 50 cm  
 Operator: Clint Edrington  
 Submitter: Clint Edrington  
 File Name: C:\EDRING~1\TIGER&~1\SANDFR~1\TT-37-08\37\_50CM.SMP  
 Material/Liquid: silicate mud/water/Water

Reported: 01/04/10 14:40:47  
 Liquid Visc: 0.7225 cp

Sample Density: 2.650 g/cm<sup>3</sup>  
 Liquid Density: 0.9941 g/cm<sup>3</sup>

## Summary Report

Parameter 1 0.000

Parameter 2 0.000

Parameter 3 0.000

## Mass Distribution Arithmetic Statistics

Mean	104.7	Std. Dev.	13.91
Median	103.7	Coef. Var.	0.133
Mode	97.67	Skewness	0.871
		Kurtosis	6.973

## Selected Percentiles

Percent Finer	Diameter (µm)
100.0	651.9
80.0	115.3
60.0	107.5
40.0	100.5
20.0	94.43

## Selected Sizes

Diameter (µm)	Percent Finer
500.0	100.0
250.0	100.0
125.0	95.6
88.00	6.8
63.00	0.0

Peak Number	% of Dist. *	Mean	Mode	Median	Standard Deviation	Skewness	Kurtosis
1	99.9	104.6	97.67	103.7	13.34	0.183	0.966

\* Peaks must comprise at least 5.00 % of the distribution.

Micromeritics

WIN5100 V2.03

Page 1

Sample: TT-37-08 100 cm  
Operator: Clint Edrington  
Submitter: Clint Edrington  
File Name: C:\EDRING~1\TIGER&~1\SANDFR~1\TT-37-08\37\_100CM.SMP  
Material/Liquid: silicate mud/water/Water

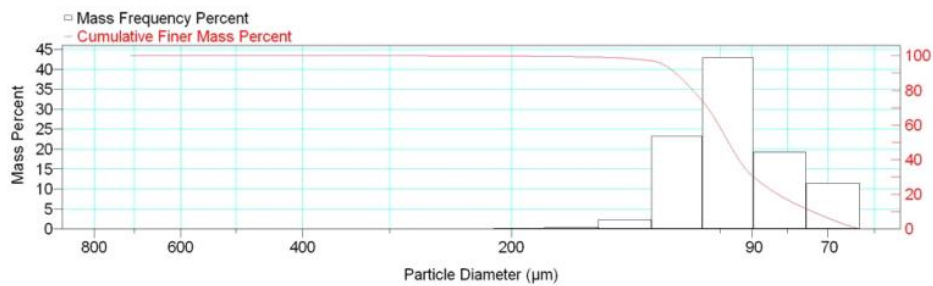
Reported: 01/04/10 14:42:53  
Liquid Visc: 0.7225 cp

Sample Density: 2.650 g/cm<sup>3</sup>  
Liquid Density: 0.9941 g/cm<sup>3</sup>

Report by Size Class

High Diameter (µm)	Low Diameter (µm)	Average Diameter (µm)	Cumulative Mass Finer (Percent)	Mass Frequency (Percent)
850.0	710.0	776.9	100.0	0.0
710.0	600.0	652.7	100.0	0.0
600.0	500.0	547.7	100.0	0.0
500.0	425.0	461.0	100.0	0.0
425.0	355.0	388.4	100.0	0.0
355.0	300.0	326.3	100.0	0.0
300.0	250.0	273.9	99.9	0.1
250.0	212.0	230.2	99.8	0.1
212.0	180.0	195.3	99.6	0.2
180.0	150.0	164.3	99.2	0.4
150.0	125.0	136.9	96.9	2.3
125.0	106.0	115.1	73.6	23.3
106.0	90.00	97.67	30.7	42.9
90.00	75.00	82.16	11.4	19.3
75.00	63.00	68.74	0.0	11.4

Mass Frequency vs Diameter



Summary Report

Full scale pump speed: 3  
Bubble detection: Medium  
Starting Size: 63.00 µm  
Ending Size: 0.50 µm

Stir time: 30 secs  
Stir speed: Low  
Probe time: 30 secs

Sample: TT-37-08 100 cm  
 Operator: Clint Edrington  
 Submitter: Clint Edrington  
 File Name: C:\EDRING~1\TIGER&~1\SANDFR~1\TT-37-08\37\_100CM.SMP  
 Material/Liquid: silicate mud/water/Water

Reported: 01/04/10 14:42:53  
 Liquid Visc: 0.7225 cp

Sample Density: 2.650 g/cm<sup>3</sup>  
 Liquid Density: 0.9941 g/cm<sup>3</sup>

## Summary Report

Parameter 1	0.000	Parameter 2	0.000	Parameter 3	0.000		
Mass Distribution Arithmetic Statistics							
Mean	97.12	Std. Dev.		18.26			
Median	97.32	Coef. Var.		0.188			
Mode	97.67	Skewness		1.733			
		Kurtosis		12.511			
Selected Percentiles			Selected Sizes				
Percent Finer	Diameter (µm)		Diameter (µm)	Percent Finer			
100.0	714.1		500.0	100.0			
80.0	109.5		250.0	99.9			
60.0	100.5		125.0	96.9			
40.0	94.03		88.00	27.6			
20.0	82.61		63.00	0.0			
Peak Number	% of Dist.*	Mean	Mode	Median	Standard Deviation	Skewness	Kurtosis
1	100.0	97.12	97.67	97.32	18.26	1.733	12.511

\* Peaks must comprise at least 5.00 % of the distribution.



Micromeritics

WIN5100 V2.03

Page 1

Sample: TT-37-08 150 cm  
Operator: Clint Edrington  
Submitter: Clint Edrington  
File Name: C:\EDRING~1\TIGER&~1\SANDFR~1\TT-37-08\37\_150CM.SMP  
Material/Liquid: silicate mud/water/Water

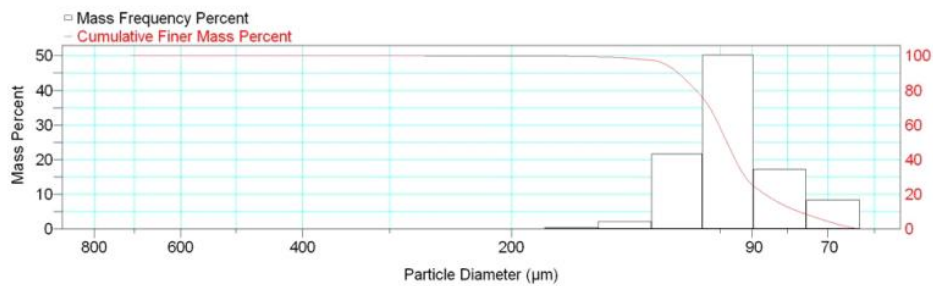
Reported: 01/04/10 14:44:47  
Liquid Visc: 0.7225 cp

Sample Density: 2.650 g/cm<sup>3</sup>  
Liquid Density: 0.9941 g/cm<sup>3</sup>

Report by Size Class

High Diameter (µm)	Low Diameter (µm)	Average Diameter (µm)	Cumulative Mass Finer (Percent)	Mass Frequency (Percent)
850.0	710.0	776.9	100.0	0.0
710.0	600.0	652.7	100.0	0.0
600.0	500.0	547.7	100.0	0.0
500.0	425.0	461.0	100.0	0.0
425.0	355.0	388.4	100.0	0.0
355.0	300.0	326.3	100.0	0.0
300.0	250.0	273.9	99.9	0.1
250.0	212.0	230.2	99.9	0.0
212.0	180.0	195.3	99.8	0.1
180.0	150.0	164.3	99.4	0.4
150.0	125.0	136.9	97.3	2.1
125.0	106.0	115.1	75.7	21.6
106.0	90.00	97.67	25.5	50.2
90.00	75.00	82.16	8.3	17.2
75.00	63.00	68.74	0.0	8.3

Mass Frequency vs Diameter



Summary Report

Full scale pump speed: 3  
Bubble detection: Medium  
Starting Size: 63.00 µm  
Ending Size: 0.50 µm

Stir time: 30 secs  
Stir speed: Low  
Probe time: 30 secs

Sample: TT-37-08 150 cm  
 Operator: Clint Edrington  
 Submitter: Clint Edrington  
 File Name: C:\EDRING~1\TIGER&~1\SANDFR~1\TT-37-08\37\_150CM.SMP  
 Material/Liquid: silicate mud/water/Water

Reported: 01/04/10 14:44:47  
 Liquid Visc: 0.7225 cp

Sample Density: 2.650 g/cm<sup>3</sup>  
 Liquid Density: 0.9941 g/cm<sup>3</sup>

## Summary Report

Parameter 1	0.000	Parameter 2	0.000	Parameter 3	0.000		
Mass Distribution Arithmetic Statistics							
Mean	97.73	Std. Dev.		16.35			
Median	97.81	Coef. Var.		0.167			
Mode	97.67	Skewness		1.671			
		Kurtosis		14.776			
Selected Percentiles			Selected Sizes				
Percent Finer	Diameter (µm)		Diameter (µm)	Percent Finer			
100.0	714.1		500.0	100.0			
80.0	108.4		250.0	99.9			
60.0	100.5		125.0	97.3			
40.0	95.17		88.00	22.5			
20.0	86.19		63.00	0.0			
Peak Number	% of Dist.*	Mean	Mode	Median	Standard Deviation	Skewness	Kurtosis
1	99.9	97.56	97.67	97.80	15.38	0.540	2.529

\* Peaks must comprise at least 5.00 % of the distribution.

Micromeritics

WIN5100 V2.03

Page 1

Sample: TT-37-08 200 cm  
Operator: Clint Edrington  
Submitter: Clint Edrington  
File Name: C:\EDRING~1\TIGER&~1\SANDFR~1\TT-37-08\37\_200CM.SMP  
Material/Liquid: silicate mud/water/Water

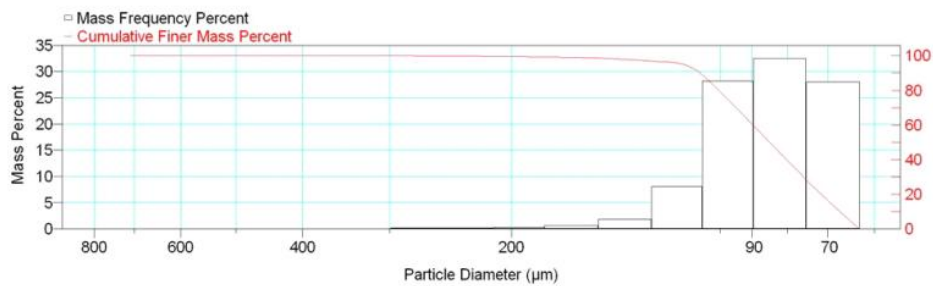
Reported: 01/04/10 14:46:40  
Liquid Visc: 0.7225 cp

Sample Density: 2.650 g/cm<sup>3</sup>  
Liquid Density: 0.9941 g/cm<sup>3</sup>

Report by Size Class

High Diameter (μm)	Low Diameter (μm)	Average Diameter (μm)	Cumulative Mass Finer (Percent)	Mass Frequency (Percent)
850.0	710.0	776.9	100.0	0.0
710.0	600.0	652.7	100.0	0.0
600.0	500.0	547.7	100.0	0.0
500.0	425.0	461.0	100.0	0.0
425.0	355.0	388.4	100.0	0.0
355.0	300.0	326.3	100.0	0.0
300.0	250.0	273.9	99.8	0.2
250.0	212.0	230.2	99.6	0.2
212.0	180.0	195.3	99.3	0.3
180.0	150.0	164.3	98.6	0.7
150.0	125.0	136.9	96.8	1.8
125.0	106.0	115.1	88.7	8.1
106.0	90.00	97.67	60.5	28.2
90.00	75.00	82.16	28.0	32.5
75.00	63.00	68.74	0.0	28.0

Mass Frequency vs Diameter



Summary Report

Full scale pump speed: 3  
Bubble detection: Medium  
Starting Size: 63.00 μm  
Ending Size: 0.50 μm

Stir time: 30 secs  
Stir speed: Low  
Probe time: 30 secs

Sample: TT-37-08 200 cm  
 Operator: Clint Edrington  
 Submitter: Clint Edrington  
 File Name: C:\EDRING~1\TIGER&~1\SANDFR~1\TT-37-08\37\_200CM.SMP  
 Material/Liquid: silicate mud/water/Water

Reported: 01/04/10 14:46:40  
 Liquid Visc: 0.7225 cp

Sample Density: 2.650 g/cm<sup>3</sup>  
 Liquid Density: 0.9941 g/cm<sup>3</sup>

## Summary Report

Parameter 1	0.000	Parameter 2	0.000	Parameter 3	0.000		
Mass Distribution Arithmetic Statistics							
Mean	88.03		Std. Dev.	20.71			
Median	84.87		Coef. Var.	0.235			
Mode	82.16		Skewness	3.073			
			Kurtosis	18.891			
Selected Percentiles			Selected Sizes				
Percent Finer	Diameter (µm)		Diameter (µm)	Percent Finer			
100.0	714.1		500.0	100.0			
80.0	100.5		250.0	99.8			
60.0	89.75		125.0	96.8			
40.0	80.27		88.00	56.5			
20.0	71.54		63.00	0.0			
Peak Number	% of Dist.*	Mean	Mode	Median	Standard Deviation	Skewness	Kurtosis
1	100.0	88.03	82.16	84.87	20.71	3.073	18.891

\* Peaks must comprise at least 5.00 % of the distribution.

Micromeritics

WIN5100 V2.03

Page 1

Sample: TT-38-08 7 cm  
Operator: Clint Edrington  
Submitter: Clint Edrington  
File Name: C:\EDRING~1\TIGER&~1\SANDFR~1\TT-38-08\38\_7CM.SMP  
Material/Liquid: silicate mud/water/Water

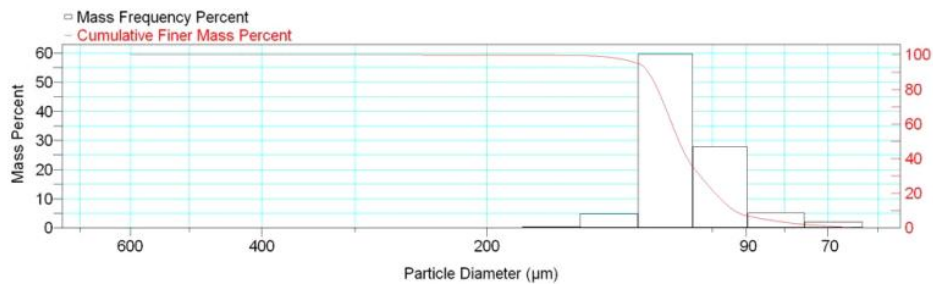
Reported: 01/04/10 14:54:15  
Liquid Visc: 0.7225 cp

Sample Density: 2.650 g/cm<sup>3</sup>  
Liquid Density: 0.9941 g/cm<sup>3</sup>

Report by Size Class

High Diameter (μm)	Low Diameter (μm)	Average Diameter (μm)	Cumulative Mass Finer (Percent)	Mass Frequency (Percent)
710.0	600.0	652.7	100.0	0.0
600.0	500.0	547.7	100.0	0.0
500.0	425.0	461.0	100.0	0.0
425.0	355.0	388.4	100.0	0.0
355.0	300.0	326.3	100.0	0.0
300.0	250.0	273.9	100.0	0.0
250.0	212.0	230.2	99.9	0.1
212.0	180.0	195.3	99.9	0.0
180.0	150.0	164.3	99.5	0.4
150.0	125.0	136.9	94.6	4.9
125.0	106.0	115.1	35.0	59.6
106.0	90.00	97.67	7.1	27.9
90.00	75.00	82.16	2.0	5.1
75.00	63.00	68.74	0.0	2.0

Mass Frequency vs Diameter



Summary Report

Full scale pump speed: 3  
Bubble detection: Medium  
Starting Size: 63.00 μm  
Ending Size: 0.50 μm

Stir time: 30 secs  
Stir speed: Low  
Probe time: 30 secs

Sample: TT-38-08 7 cm  
 Operator: Clint Edrington  
 Submitter: Clint Edrington  
 File Name: C:\EDRING~1\TIGER&~1\SANDFR~1\TT-38-08\38\_7CM.SMP  
 Material/Liquid: silicate mud/water/Water

Reported: 01/04/10 14:54:15  
 Liquid Visc: 0.7225 cp

Sample Density: 2.650 g/cm<sup>3</sup>  
 Liquid Density: 0.9941 g/cm<sup>3</sup>

## Summary Report

Parameter 1 0.000

Parameter 2 0.000

Parameter 3 0.000

## Mass Distribution Arithmetic Statistics

Mean	109.0	Std. Dev.	13.87
Median	110.7	Coef. Var.	0.127
Mode	115.1	Skewness	0.358
		Kurtosis	6.933

## Selected Percentiles

Percent Finer	Diameter (µm)
100.0	651.9
80.0	118.2
60.0	113.1
40.0	107.9
20.0	99.07

## Selected Sizes

Diameter (µm)	Percent Finer
500.0	100.0
250.0	100.0
125.0	94.6
88.00	6.2
63.00	0.0

Peak Number	% of Dist. *	Mean	Mode	Median	Standard Deviation	Skewness	Kurtosis
1	99.9	108.9	115.1	110.7	13.34	-0.321	1.792

\* Peaks must comprise at least 5.00 % of the distribution.

# Micromeritics

WIN5100 V2.03

Page 1

Sample: TT-38-08 50 cm  
Operator: Clint Edrington  
Submitter: Clint Edrington  
File Name: C:\EDRING~1\TIGER&~1\SANDFR~1\TT-38-08\38\_50CM.SMP  
Material/Liquid: silicate mud/water/Water

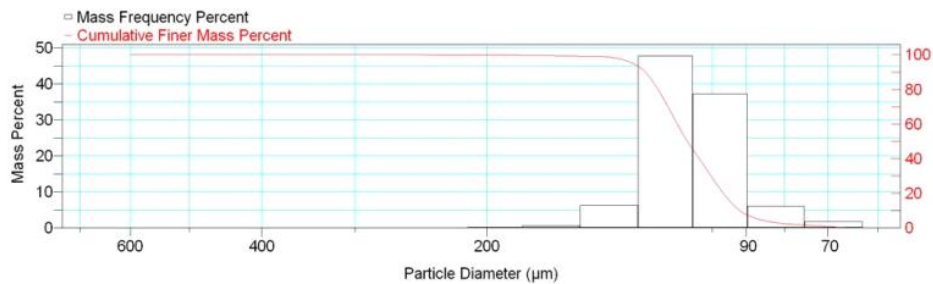
Reported: 01/04/10 14:56:12  
Liquid Visc: 0.7225 cp

Sample Density: 2.650 g/cm<sup>3</sup>  
Liquid Density: 0.9941 g/cm<sup>3</sup>

## Report by Size Class

High Diameter (µm)	Low Diameter (µm)	Average Diameter (µm)	Cumulative Mass Finer (Percent)	Mass Frequency (Percent)
710.0	600.0	652.7	100.0	0.0
600.0	500.0	547.7	100.0	0.0
500.0	425.0	461.0	100.0	0.0
425.0	355.0	388.4	100.0	0.0
355.0	300.0	326.3	100.0	0.0
300.0	250.0	273.9	100.0	0.0
250.0	212.0	230.2	99.9	0.1
212.0	180.0	195.3	99.7	0.2
180.0	150.0	164.3	99.1	0.6
150.0	125.0	136.9	92.8	6.3
125.0	106.0	115.1	45.0	47.8
106.0	90.00	97.67	7.7	37.3
90.00	75.00	82.16	1.7	6.0
75.00	63.00	68.74	0.0	1.7

Mass Frequency vs Diameter



## Summary Report

Full scale pump speed: 3  
Bubble detection: Medium  
Starting Size: 63.00 µm  
Ending Size: 0.50 µm

Stir time: 30 secs  
Stir speed: Low  
Probe time: 30 secs

Sample: TT-38-08 50 cm  
 Operator: Clint Edrington  
 Submitter: Clint Edrington  
 File Name: C:\EDRING~1\TIGER&~1\SANDFR~1\TT-38-08\38\_50CM.SMP  
 Material/Liquid: silicate mud/water/Water

Reported: 01/04/10 14:56:12  
 Liquid Visc: 0.7225 cp

Sample Density: 2.650 g/cm<sup>3</sup>  
 Liquid Density: 0.9941 g/cm<sup>3</sup>

## Summary Report

Parameter 1 0.000

Parameter 2 0.000

Parameter 3 0.000

## Mass Distribution Arithmetic Statistics

Mean	107.8	Std. Dev.	15.24
Median	107.9	Coef. Var.	0.141
Mode	115.1	Skewness	1.018
		Kurtosis	6.645

## Selected Percentiles

Percent Finer	Diameter (µm)
100.0	651.9
80.0	118.1
60.0	111.3
40.0	104.0
20.0	96.55

## Selected Sizes

Diameter (µm)	Percent Finer
500.0	100.0
250.0	100.0
125.0	92.8
88.00	6.0
63.00	0.0

Peak Number	% of Dist. *	Mean	Mode	Median	Standard Deviation	Skewness	Kurtosis
1	100.0	107.8	115.1	107.9	15.24	1.018	6.645

\* Peaks must comprise at least 5.00 % of the distribution.



Micromeritics

WIN5100 V2.03

Page 1

Sample: TT-38-08 100 cm  
Operator: Clint Edrington  
Submitter: Clint Edrington  
File Name: C:\EDRING~1\TIGER&~1\SANDFR~1\TT-38-08\38\_100CM.SMP  
Material/Liquid: silicate mud/water/Water

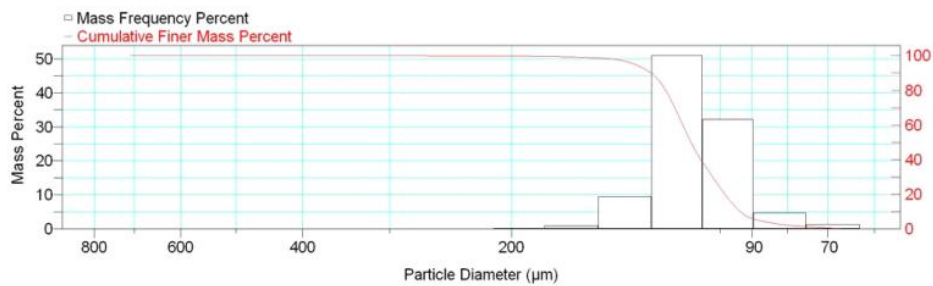
Reported: 01/04/10 14:58:01  
Liquid Visc: 0.7225 cp

Sample Density: 2.650 g/cm<sup>3</sup>  
Liquid Density: 0.9941 g/cm<sup>3</sup>

Report by Size Class

High Diameter (µm)	Low Diameter (µm)	Average Diameter (µm)	Cumulative Mass Finer (Percent)	Mass Frequency (Percent)
850.0	710.0	776.9	100.0	0.0
710.0	600.0	652.7	100.0	0.0
600.0	500.0	547.7	100.0	0.0
500.0	425.0	461.0	100.0	0.0
425.0	355.0	388.4	100.0	0.0
355.0	300.0	326.3	100.0	0.0
300.0	250.0	273.9	99.9	0.1
250.0	212.0	230.2	99.8	0.1
212.0	180.0	195.3	99.6	0.2
180.0	150.0	164.3	98.7	0.9
150.0	125.0	136.9	89.2	9.5
125.0	106.0	115.1	38.2	51.0
106.0	90.00	97.67	6.0	32.2
90.00	75.00	82.16	1.3	4.7
75.00	63.00	68.74	0.0	1.3

Mass Frequency vs Diameter



Summary Report

Full scale pump speed: 3  
Bubble detection: Medium  
Starting Size: 63.00 µm  
Ending Size: 0.50 µm

Stir time: 30 secs  
Stir speed: Low  
Probe time: 30 secs

Sample: TT-38-08 100 cm  
 Operator: Clint Edrington  
 Submitter: Clint Edrington  
 File Name: C:\EDRING~1\TIGER&~1\SANDFR~1\TT-38-08\38\_100CM.SMP  
 Material/Liquid: silicate mud/water/Water

Reported: 01/04/10 14:58:01  
 Liquid Visc: 0.7225 cp

Sample Density: 2.650 g/cm<sup>3</sup>  
 Liquid Density: 0.9941 g/cm<sup>3</sup>

## Summary Report

Parameter 1	0.000	Parameter 2	0.000	Parameter 3	0.000		
Mass Distribution Arithmetic Statistics							
Mean	110.3	Std. Dev.		16.49			
Median	110.2	Coef. Var.		0.150			
Mode	115.1	Skewness		1.778			
		Kurtosis		13.599			
Selected Percentiles			Selected Sizes				
Percent Finer	Diameter (µm)		Diameter (µm)	Percent Finer			
100.0	714.1		500.0	100.0			
80.0	119.9		250.0	99.9			
60.0	113.3		125.0	89.2			
40.0	106.8		88.00	5.0			
20.0	98.46		63.00	0.0			
Peak Number	% of Dist.*	Mean	Mode	Median	Standard Deviation	Skewness	Kurtosis
1	100.0	110.3	115.1	110.2	16.49	1.778	13.599

\* Peaks must comprise at least 5.00 % of the distribution.

Micromeritics

WIN5100 V2.03

Page 1

Sample: TT-38-08 133 cm  
Operator: Clint Edrington  
Submitter: Clint Edrington  
File Name: C:\EDRING~1\TIGER&~1\SANDFR~1\TT-38-08\38\_133CM.SMP  
Material/Liquid: silicate mud/water/Water

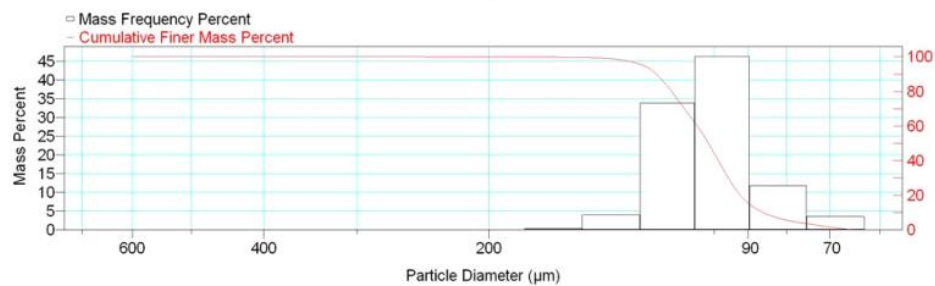
Reported: 01/04/10 15:00:00  
Liquid Visc: 0.7225 cp

Sample Density: 2.650 g/cm<sup>3</sup>  
Liquid Density: 0.9941 g/cm<sup>3</sup>

Report by Size Class

High Diameter (μm)	Low Diameter (μm)	Average Diameter (μm)	Cumulative Mass Finer (Percent)	Mass Frequency (Percent)
710.0	600.0	652.7	100.0	0.0
600.0	500.0	547.7	100.0	0.0
500.0	425.0	461.0	100.0	0.0
425.0	355.0	388.4	100.0	0.0
355.0	300.0	326.3	100.0	0.0
300.0	250.0	273.9	100.0	0.0
250.0	212.0	230.2	99.9	0.1
212.0	180.0	195.3	99.9	0.0
180.0	150.0	164.3	99.5	0.4
150.0	125.0	136.9	95.5	4.0
125.0	106.0	115.1	61.7	33.8
106.0	90.00	97.67	15.4	46.3
90.00	75.00	82.16	3.6	11.8
75.00	63.00	68.74	0.0	3.6

Mass Frequency vs Diameter



Summary Report

Full scale pump speed: 3  
Bubble detection: Medium  
Starting Size: 63.00 μm  
Ending Size: 0.50 μm

Stir time: 30 secs  
Stir speed: Low  
Probe time: 30 secs

Sample: TT-38-08 133 cm  
 Operator: Clint Edrington  
 Submitter: Clint Edrington  
 File Name: C:\EDRING~1\TIGER&~1\SANDFR~1\TT-38-08\38\_133CM.SMP  
 Material/Liquid: silicate mud/water/Water

Reported: 01/04/10 15:00:00  
 Liquid Visc: 0.7225 cp

Sample Density: 2.650 g/cm<sup>3</sup>  
 Liquid Density: 0.9941 g/cm<sup>3</sup>

## Summary Report

Parameter 1 0.000

Parameter 2 0.000

Parameter 3 0.000

## Mass Distribution Arithmetic Statistics

Mean	102.7	Std. Dev.	15.28
Median	101.7	Coef. Var.	0.149
Mode	97.67	Skewness	0.784
		Kurtosis	5.347

## Selected Percentiles

Percent Finer	Diameter (µm)
100.0	651.9
80.0	114.0
60.0	105.3
40.0	98.69
20.0	92.23

## Selected Sizes

Diameter (µm)	Percent Finer
500.0	100.0
250.0	100.0
125.0	95.5
88.00	12.5
63.00	0.0

Peak Number	% of Dist.*	Mean	Mode	Median	Standard Deviation	Skewness	Kurtosis
1	99.9	102.5	97.67	101.7	14.74	0.250	1.034

\* Peaks must comprise at least 5.00 % of the distribution.

Micromeritics

WIN5100 V2.03

Page 1

Sample: TT-39-08 5 cm  
Operator: Clint Edrington  
Submitter: Clint Edrington  
File Name: C:\EDRING~1\TIGER&~1\SANDFR~1\TT-39-08\39\_5CM.SMP  
Material/Liquid: silicate mud/water/Water

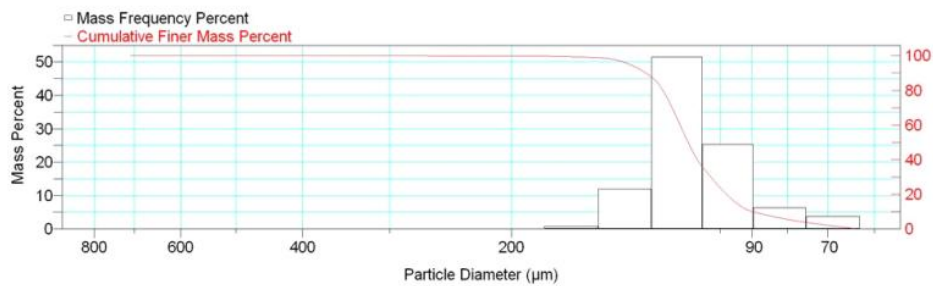
Reported: 01/04/10 15:03:06  
Liquid Visc: 0.7225 cp

Sample Density: 2.650 g/cm<sup>3</sup>  
Liquid Density: 0.9941 g/cm<sup>3</sup>

Report by Size Class

High Diameter (µm)	Low Diameter (µm)	Average Diameter (µm)	Cumulative Mass Finer (Percent)	Mass Frequency (Percent)
850.0	710.0	776.9	100.0	0.0
710.0	600.0	652.7	100.0	0.0
600.0	500.0	547.7	100.0	0.0
500.0	425.0	461.0	100.0	0.0
425.0	355.0	388.4	100.0	0.0
355.0	300.0	326.3	100.0	0.0
300.0	250.0	273.9	99.9	0.1
250.0	212.0	230.2	99.8	0.1
212.0	180.0	195.3	99.7	0.1
180.0	150.0	164.3	98.9	0.8
150.0	125.0	136.9	87.0	11.9
125.0	106.0	115.1	35.5	51.5
106.0	90.00	97.67	10.1	25.4
90.00	75.00	82.16	3.7	6.4
75.00	63.00	68.74	0.0	3.7

Mass Frequency vs Diameter



Summary Report

Full scale pump speed: 3  
Bubble detection: Medium  
Starting Size: 63.00 µm  
Ending Size: 0.50 µm

Stir time: 30 secs  
Stir speed: Low  
Probe time: 30 secs

Sample: TT-39-08 5 cm  
 Operator: Clint Edrington  
 Submitter: Clint Edrington  
 File Name: C:\EDRING~1\TIGER&~1\SANDFR~1\TT-39-08\39\_5CM.SMP  
 Material/Liquid: silicate mud/water/Water

Reported: 01/04/10 15:03:06  
 Liquid Visc: 0.7225 cp

Sample Density: 2.650 g/cm<sup>3</sup>  
 Liquid Density: 0.9941 g/cm<sup>3</sup>

## Summary Report

Parameter 1	0.000	Parameter 2	0.000	Parameter 3	0.000		
Mass Distribution Arithmetic Statistics							
Mean	110.2	Std. Dev.		17.97			
Median	111.3	Coef. Var.		0.163			
Mode	115.1	Skewness		0.996			
		Kurtosis		9.092			
Selected Percentiles			Selected Sizes				
Percent Finer	Diameter (µm)		Diameter (µm)	Percent Finer			
100.0	714.1		500.0	100.0			
80.0	121.0		250.0	99.9			
60.0	114.3		125.0	87.0			
40.0	108.0		88.00	9.1			
20.0	97.96		63.00	0.0			
Peak Number	% of Dist.*	Mean	Mode	Median	Standard Deviation	Skewness	Kurtosis
1	100.0	110.2	115.1	111.3	17.97	0.996	9.092

\* Peaks must comprise at least 5.00 % of the distribution.

Micromeritics

WIN5100 V2.03

Page 1

Sample: TT-39-08 50 cm  
Operator: Clint Edrington  
Submitter: Clint Edrington  
File Name: C:\EDRING~1\TIGER&~1\SANDFR~1\TT-39-08\39\_50CM.SMP  
Material/Liquid: silicate mud/water/Water

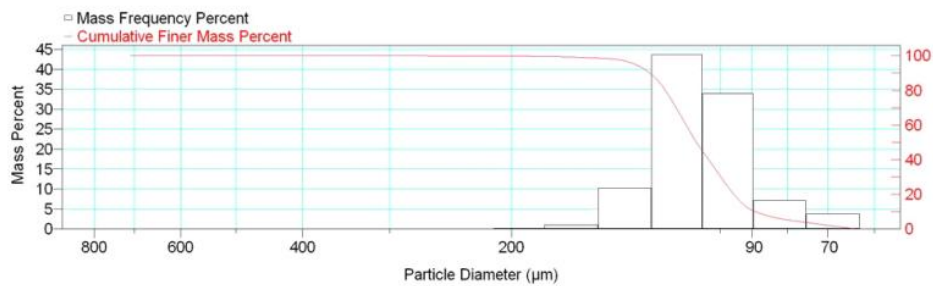
Reported: 01/04/10 15:05:55  
Liquid Visc: 0.7225 cp

Sample Density: 2.650 g/cm<sup>3</sup>  
Liquid Density: 0.9941 g/cm<sup>3</sup>

Report by Size Class

High Diameter (µm)	Low Diameter (µm)	Average Diameter (µm)	Cumulative Mass Finer (Percent)	Mass Frequency (Percent)
850.0	710.0	776.9	100.0	0.0
710.0	600.0	652.7	100.0	0.0
600.0	500.0	547.7	100.0	0.0
500.0	425.0	461.0	100.0	0.0
425.0	355.0	388.4	100.0	0.0
355.0	300.0	326.3	100.0	0.0
300.0	250.0	273.9	99.9	0.1
250.0	212.0	230.2	99.8	0.1
212.0	180.0	195.3	99.6	0.2
180.0	150.0	164.3	98.6	1.0
150.0	125.0	136.9	88.4	10.2
125.0	106.0	115.1	44.7	43.7
106.0	90.00	97.67	10.8	33.9
90.00	75.00	82.16	3.7	7.1
75.00	63.00	68.74	0.0	3.7

Mass Frequency vs Diameter



Summary Report

Full scale pump speed: 3  
Bubble detection: Medium  
Starting Size: 63.00 µm  
Ending Size: 0.50 µm

Stir time: 30 secs  
Stir speed: Low  
Probe time: 30 secs

Sample: TT-39-08 50 cm  
 Operator: Clint Edrington  
 Submitter: Clint Edrington  
 File Name: C:\EDRING~1\TIGER&~1\SANDFR~1\TT-39-08\39\_50CM.SMP  
 Material/Liquid: silicate mud/water/Water

Reported: 01/04/10 15:05:55  
 Liquid Visc: 0.7225 cp

Sample Density: 2.650 g/cm<sup>3</sup>  
 Liquid Density: 0.9941 g/cm<sup>3</sup>

## Summary Report

Parameter 1	0.000	Parameter 2	0.000	Parameter 3	0.000		
Mass Distribution Arithmetic Statistics							
Mean	108.3	Std. Dev.		18.37			
Median	108.2	Coef. Var.		0.170			
Mode	115.1	Skewness		1.291			
		Kurtosis		9.152			
Selected Percentiles			Selected Sizes				
Percent Finer	Diameter (µm)		Diameter (µm)	Percent Finer			
100.0	714.1		500.0	100.0			
80.0	120.0		250.0	99.9			
60.0	112.0		125.0	88.4			
40.0	104.0		88.00	9.2			
20.0	95.67		63.00	0.0			
Peak Number	% of Dist.*	Mean	Mode	Median	Standard Deviation	Skewness	Kurtosis
1	100.0	108.3	115.1	108.2	18.37	1.291	9.152

\* Peaks must comprise at least 5.00 % of the distribution.



Micromeritics

WIN5100 V2.03

Page 1

Sample: TT-39-08 100 cm  
Operator: Clint Edrington  
Submitter: Clint Edrington  
File Name: C:\EDRING~1\TIGER&~1\SANDFR~1\TT-39-08\39\_100CM.SMP  
Material/Liquid: silicate mud/water/Water

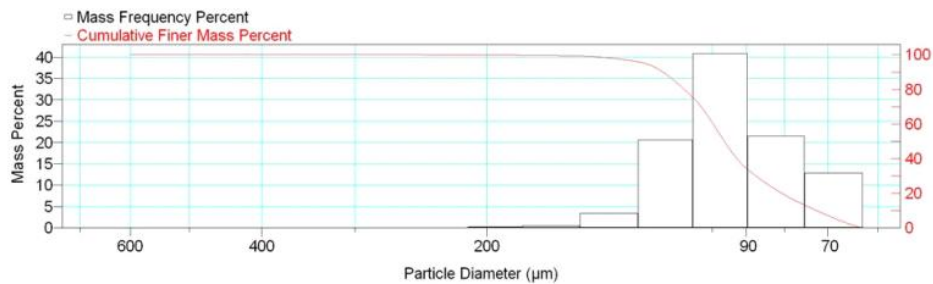
Reported: 01/04/10 15:07:46  
Liquid Visc: 0.7225 cp

Sample Density: 2.650 g/cm<sup>3</sup>  
Liquid Density: 0.9941 g/cm<sup>3</sup>

Report by Size Class

High Diameter (µm)	Low Diameter (µm)	Average Diameter (µm)	Cumulative Mass Finer (Percent)	Mass Frequency (Percent)
710.0	600.0	652.7	100.0	0.0
600.0	500.0	547.7	100.0	0.0
500.0	425.0	461.0	100.0	0.0
425.0	355.0	388.4	100.0	0.0
355.0	300.0	326.3	100.0	0.0
300.0	250.0	273.9	100.0	0.0
250.0	212.0	230.2	99.9	0.1
212.0	180.0	195.3	99.7	0.2
180.0	150.0	164.3	99.2	0.5
150.0	125.0	136.9	95.8	3.4
125.0	106.0	115.1	75.2	20.6
106.0	90.00	97.67	34.4	40.8
90.00	75.00	82.16	12.9	21.5
75.00	63.00	68.74	0.0	12.9

Mass Frequency vs Diameter



Summary Report

Full scale pump speed: 3  
Bubble detection: Medium  
Starting Size: 63.00 µm  
Ending Size: 0.50 µm

Stir time: 30 secs  
Stir speed: Low  
Probe time: 30 secs

Sample: TT-39-08 100 cm  
 Operator: Clint Edrington  
 Submitter: Clint Edrington  
 File Name: C:\EDRING~1\TIGER&~1\SANDFR~1\TT-39-08\39\_100CM.SMP  
 Material/Liquid: silicate mud/water/Water

Reported: 01/04/10 15:07:46  
 Liquid Visc: 0.7225 cp

Sample Density: 2.650 g/cm<sup>3</sup>  
 Liquid Density: 0.9941 g/cm<sup>3</sup>

## Summary Report

Parameter 1 0.000

Parameter 2 0.000

Parameter 3 0.000

## Mass Distribution Arithmetic Statistics

Mean	96.19	Std. Dev.	18.21
Median	96.25	Coef. Var.	0.189
Mode	97.67	Skewness	1.055
		Kurtosis	4.513

## Selected Percentiles

Percent Finer	Diameter (µm)
100.0	651.9
80.0	108.9
60.0	99.64
40.0	92.64
20.0	80.65

## Selected Sizes

Diameter (µm)	Percent Finer
500.0	100.0
250.0	100.0
125.0	95.8
88.00	31.1
63.00	0.0

Peak Number	% of Dist. *	Mean	Mode	Median	Standard Deviation	Skewness	Kurtosis
1	100.0	96.19	97.67	96.25	18.21	1.055	4.513

\* Peaks must comprise at least 5.00 % of the distribution.

Micromeritics

WIN5100 V2.03

Page 1

Sample: TT-39-08 305 cm  
Operator: Clint Edrington  
Submitter: Clint Edrington  
File Name: C:\EDRING~1\TIGER&~1\SANDFR~1\TT-39-08\39\_305CM.SMP  
Material/Liquid: silicate mud/water/Water

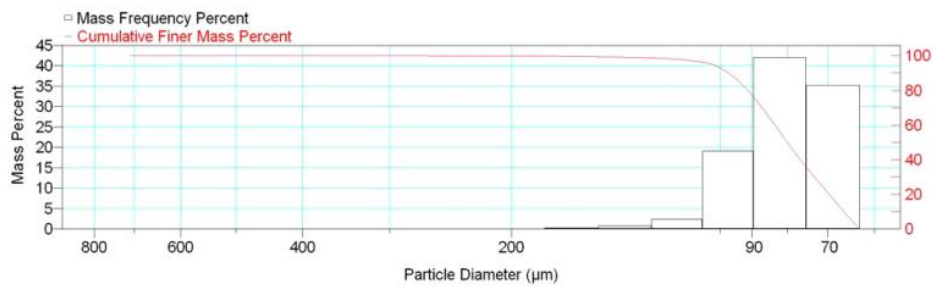
Reported: 01/04/10 15:10:15  
Liquid Visc: 0.7225 cp

Sample Density: 2.650 g/cm<sup>3</sup>  
Liquid Density: 0.9941 g/cm<sup>3</sup>

Report by Size Class

High Diameter (μm)	Low Diameter (μm)	Average Diameter (μm)	Cumulative Mass Finer (Percent)	Mass Frequency (Percent)
850.0	710.0	776.9	100.0	0.0
710.0	600.0	652.7	100.0	0.0
600.0	500.0	547.7	100.0	0.0
500.0	425.0	461.0	100.0	0.0
425.0	355.0	388.4	100.0	0.0
355.0	300.0	326.3	100.0	0.0
300.0	250.0	273.9	99.9	0.1
250.0	212.0	230.2	99.8	0.1
212.0	180.0	195.3	99.7	0.1
180.0	150.0	164.3	99.4	0.3
150.0	125.0	136.9	98.7	0.7
125.0	106.0	115.1	96.3	2.4
106.0	90.00	97.67	77.2	19.1
90.00	75.00	82.16	35.2	42.0
75.00	63.00	68.74	0.0	35.2

Mass Frequency vs Diameter



Summary Report

Full scale pump speed: 3  
Bubble detection: Medium  
Starting Size: 63.00 μm  
Ending Size: 0.50 μm

Stir time: 30 secs  
Stir speed: Low  
Probe time: 30 secs

Sample: TT-39-08 305 cm  
 Operator: Clint Edrington  
 Submitter: Clint Edrington  
 File Name: C:\EDRING~1\TIGER&~1\SANDFR~1\TT-39-08\39\_305CM.SMP  
 Material/Liquid: silicate mud/water/Water

Reported: 01/04/10 15:10:15  
 Liquid Visc: 0.7225 cp

Sample Density: 2.650 g/cm<sup>3</sup>  
 Liquid Density: 0.9941 g/cm<sup>3</sup>

## Summary Report

Parameter 1	0.000	Parameter 2	0.000	Parameter 3	0.000		
Mass Distribution Arithmetic Statistics							
Mean	82.27	Std. Dev.		15.75			
Median	80.06	Coef. Var.		0.191			
Mode	82.16	Skewness		3.886			
		Kurtosis		33.359			
Selected Percentiles			Selected Sizes				
Percent Finer	Diameter (µm)		Diameter (µm)	Percent Finer			
100.0	714.1		500.0	100.0			
80.0	91.28		250.0	99.9			
60.0	83.44		125.0	98.7			
40.0	76.69		88.00	72.4			
20.0	69.70		63.00	0.0			
Peak Number	% of Dist.*	Mean	Mode	Median	Standard Deviation	Skewness	Kurtosis
1	100.0	82.27	82.16	80.06	15.75	3.886	33.359

\* Peaks must comprise at least 5.00 % of the distribution.

Micromeritics

WIN5100 V2.03

Page 1

Sample: TT-39-08 350 cm  
Operator: Clint Edrington  
Submitter: Clint Edrington  
File Name: C:\EDRING~1\TIGER&~1\SANDFR~1\TT-39-08\39\_350CM.SMP  
Material/Liquid: silicate mud/water/Water

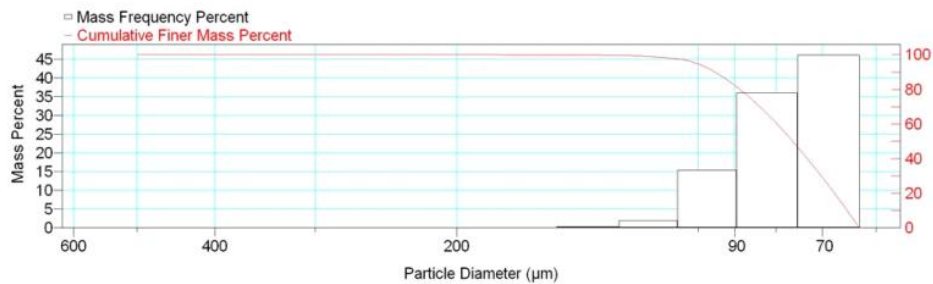
Reported: 01/04/10 15:12:12  
Liquid Visc: 0.7225 cp

Sample Density: 2.650 g/cm<sup>3</sup>  
Liquid Density: 0.9941 g/cm<sup>3</sup>

Report by Size Class

High Diameter (μm)	Low Diameter (μm)	Average Diameter (μm)	Cumulative Mass Finer (Percent)	Mass Frequency (Percent)
600.0	500.0	547.7	100.0	0.0
500.0	425.0	461.0	100.0	0.0
425.0	355.0	388.4	100.0	0.0
355.0	300.0	326.3	100.0	0.0
300.0	250.0	273.9	100.0	0.0
250.0	212.0	230.2	100.0	0.0
212.0	180.0	195.3	100.0	0.0
180.0	150.0	164.3	99.9	0.1
150.0	125.0	136.9	99.6	0.3
125.0	106.0	115.1	97.6	2.0
106.0	90.00	97.67	82.2	15.4
90.00	75.00	82.16	46.1	36.1
75.00	63.00	68.74	0.0	46.1

Mass Frequency vs Diameter



Summary Report

Full scale pump speed: 3  
Bubble detection: Medium  
Starting Size: 63.00 μm  
Ending Size: 0.50 μm

Stir time: 30 secs  
Stir speed: Low  
Probe time: 30 secs

Parameter 1 0.000

Parameter 2 0.000

Parameter 3 0.000

Sample: TT-39-08 350 cm  
 Operator: Clint Edrington  
 Submitter: Clint Edrington  
 File Name: C:\EDRING~1\TIGER&~1\SANDFR~1\TT-39-08\39\_350CM.SMP  
 Material/Liquid: silicate mud/water/Water

Reported: 01/04/10 15:12:12  
 Liquid Visc: 0.7225 cp

Sample Density: 2.650 g/cm<sup>3</sup>  
 Liquid Density: 0.9941 g/cm<sup>3</sup>

## Summary Report

Mass Distribution Arithmetic Statistics			
Mean	79.27	Std. Dev.	12.21
Median	76.25	Coef. Var.	0.154
Mode	68.74	Skewness	1.395
		Kurtosis	3.374

Selected Percentiles		Selected Sizes	
Percent Finer	Diameter (µm)	Diameter (µm)	Percent Finer
100.0	553.2	500.0	100.0
80.0	88.74	250.0	100.0
60.0	79.75	125.0	99.6
40.0	73.13	88.00	78.7
20.0	67.62	63.00	0.0

Peak Number	% of Dist.*	Mean	Mode	Median	Standard Deviation	Skewness	Kurtosis
1	100.0	79.27	68.74	76.25	12.21	1.395	3.374

\* Peaks must comprise at least 5.00 % of the distribution.

Micromeritics

WIN5100 V2.03

Page 1

Sample: TT-39-08 400 cm  
Operator: Clint Edrington  
Submitter: Clint Edrington  
File Name: C:\EDRING~1\TIGER&~1\SANDFR~1\TT-39-08\39\_400CM.SMP  
Material/Liquid: silicate mud/water/Water

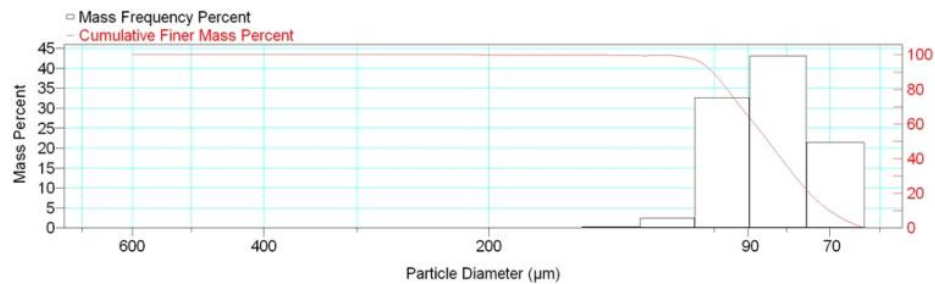
Reported: 01/04/10 15:14:19  
Liquid Visc: 0.7225 cp

Sample Density: 2.650 g/cm<sup>3</sup>  
Liquid Density: 0.9941 g/cm<sup>3</sup>

Report by Size Class

High Diameter (μm)	Low Diameter (μm)	Average Diameter (μm)	Cumulative Mass Finer (Percent)	Mass Frequency (Percent)
710.0	600.0	652.7	100.0	0.0
600.0	500.0	547.7	100.0	0.0
500.0	425.0	461.0	100.0	0.0
425.0	355.0	388.4	100.0	0.0
355.0	300.0	326.3	100.0	0.0
300.0	250.0	273.9	100.0	0.0
250.0	212.0	230.2	100.0	0.0
212.0	180.0	195.3	99.9	0.1
180.0	150.0	164.3	99.8	0.1
150.0	125.0	136.9	99.5	0.3
125.0	106.0	115.1	97.1	2.4
106.0	90.00	97.67	64.5	32.6
90.00	75.00	82.16	21.4	43.1
75.00	63.00	68.74	0.0	21.4

Mass Frequency vs Diameter



Summary Report

Full scale pump speed: 3  
Bubble detection: Medium  
Starting Size: 63.00 μm  
Ending Size: 0.50 μm

Stir time: 30 secs  
Stir speed: Low  
Probe time: 30 secs

Sample: TT-39-08 400 cm  
 Operator: Clint Edrington  
 Submitter: Clint Edrington  
 File Name: C:\EDRING~1\TIGER&~1\SANDFR~1\TT-39-08\39\_400CM.SMP  
 Material/Liquid: silicate mud/water/Water

Reported: 01/04/10 15:14:19  
 Liquid Visc: 0.7225 cp

Sample Density: 2.650 g/cm<sup>3</sup>  
 Liquid Density: 0.9941 g/cm<sup>3</sup>

## Summary Report

Parameter 1 0.000

Parameter 2 0.000

Parameter 3 0.000

## Mass Distribution Arithmetic Statistics

Mean	85.49	Std. Dev.	12.67
Median	84.65	Coef. Var.	0.148
Mode	82.16	Skewness	1.187
		Kurtosis	6.619

## Selected Percentiles

Percent Finer	Diameter (µm)
100.0	600.3
80.0	95.99
60.0	88.24
40.0	81.28
20.0	74.49

## Selected Sizes

Diameter (µm)	Percent Finer
500.0	100.0
250.0	100.0
125.0	99.5
88.00	59.4
63.00	0.0

Peak Number	% of Dist. *	Mean	Mode	Median	Standard Deviation	Skewness	Kurtosis
1	99.9	85.38	82.16	84.63	12.19	0.628	1.655

\* Peaks must comprise at least 5.00 % of the distribution.



# Micromeritics

WIN5100 V2.03

Page 1

Sample: TT-40-08 10 cm  
Operator: Clint Edrington  
Submitter: Clint Edrington  
File Name: C:\EDRING~1\TIGER&~1\SANDFR~1\TT-40-08\40\_10CM.SMP  
Material/Liquid: silicate mud/water/Water

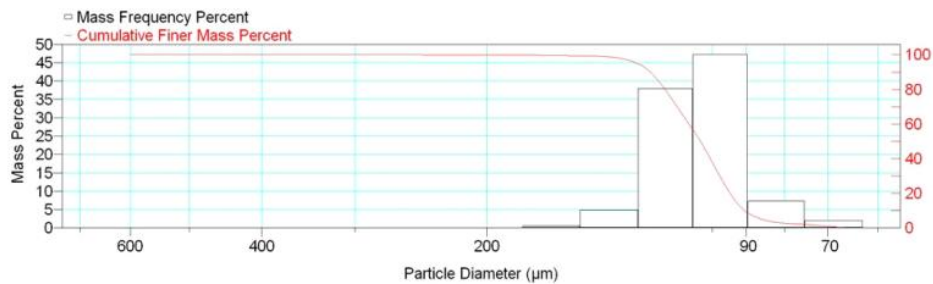
Reported: 01/04/10 15:17:36  
Liquid Visc: 0.7225 cp

Sample Density: 2.650 g/cm<sup>3</sup>  
Liquid Density: 0.9941 g/cm<sup>3</sup>

## Report by Size Class

High Diameter (µm)	Low Diameter (µm)	Average Diameter (µm)	Cumulative Mass Finer (Percent)	Mass Frequency (Percent)
710.0	600.0	652.7	100.0	0.0
600.0	500.0	547.7	100.0	0.0
500.0	425.0	461.0	100.0	0.0
425.0	355.0	388.4	100.0	0.0
355.0	300.0	326.3	100.0	0.0
300.0	250.0	273.9	100.0	0.0
250.0	212.0	230.2	99.9	0.1
212.0	180.0	195.3	99.8	0.1
180.0	150.0	164.3	99.3	0.5
150.0	125.0	136.9	94.4	4.9
125.0	106.0	115.1	56.5	37.9
106.0	90.00	97.67	9.3	47.2
90.00	75.00	82.16	2.0	7.3
75.00	63.00	68.74	0.0	2.0

Mass Frequency vs Diameter



## Summary Report

Full scale pump speed: 3  
Bubble detection: Medium  
Starting Size: 63.00 µm  
Ending Size: 0.50 µm

Stir time: 30 secs  
Stir speed: Low  
Probe time: 30 secs

Sample: TT-40-08 10 cm  
 Operator: Clint Edrington  
 Submitter: Clint Edrington  
 File Name: C:\EDRING~1\TIGER&~1\SANDFR~1\TT-40-08\40\_10CM.SMP  
 Material/Liquid: silicate mud/water/Water

Reported: 01/04/10 15:17:36  
 Liquid Visc: 0.7225 cp

Sample Density: 2.650 g/cm<sup>3</sup>  
 Liquid Density: 0.9941 g/cm<sup>3</sup>

## Summary Report

Parameter 1 0.000

Parameter 2 0.000

Parameter 3 0.000

## Mass Distribution Arithmetic Statistics

Mean	105.1	Std. Dev.	14.83
Median	103.6	Coef. Var.	0.141
Mode	97.67	Skewness	1.130
		Kurtosis	7.019

## Selected Percentiles

Percent Finer	Diameter (µm)
100.0	651.9
80.0	115.6
60.0	107.4
40.0	100.5
20.0	94.60

## Selected Sizes

Diameter (µm)	Percent Finer
500.0	100.0
250.0	100.0
125.0	94.4
88.00	6.9
63.00	0.0

Peak Number	% of Dist. *	Mean	Mode	Median	Standard Deviation	Skewness	Kurtosis
1	100.0	105.1	97.67	103.6	14.83	1.130	7.019

\* Peaks must comprise at least 5.00 % of the distribution.

Micromeritics

WIN5100 V2.03

Page 1

Sample: TT-40-08 50 cm  
Operator: Clint Edrington  
Submitter: Clint Edrington  
File Name: C:\EDRING~1\TIGER&~1\SANDFR~1\TT-40-08\40\_50CM.SMP  
Material/Liquid: silicate mud/water/Water

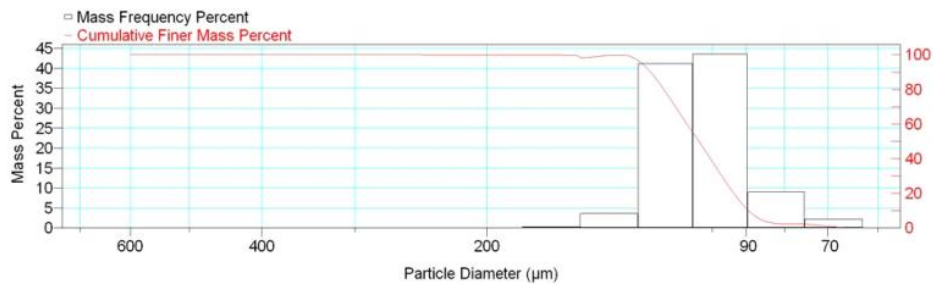
Reported: 01/04/10 15:19:45  
Liquid Visc: 0.7225 cp

Sample Density: 2.650 g/cm<sup>3</sup>  
Liquid Density: 0.9941 g/cm<sup>3</sup>

Report by Size Class

High Diameter (μm)	Low Diameter (μm)	Average Diameter (μm)	Cumulative Mass Finer (Percent)	Mass Frequency (Percent)
710.0	600.0	652.7	100.0	0.0
600.0	500.0	547.7	100.0	0.0
500.0	425.0	461.0	100.0	0.0
425.0	355.0	388.4	100.0	0.0
355.0	300.0	326.3	100.0	0.0
300.0	250.0	273.9	100.0	0.0
250.0	212.0	230.2	99.9	0.1
212.0	180.0	195.3	99.9	0.0
180.0	150.0	164.3	99.6	0.3
150.0	125.0	136.9	96.0	3.6
125.0	106.0	115.1	54.8	41.2
106.0	90.00	97.67	11.2	43.6
90.00	75.00	82.16	2.2	9.0
75.00	63.00	68.74	0.0	2.2

Mass Frequency vs Diameter



Summary Report

Full scale pump speed: 3  
Bubble detection: Medium  
Starting Size: 63.00 μm  
Ending Size: 0.50 μm

Stir time: 30 secs  
Stir speed: Low  
Probe time: 30 secs

Sample: TT-40-08 50 cm  
 Operator: Clint Edrington  
 Submitter: Clint Edrington  
 File Name: C:\EDRING~1\TIGER&~1\SANDFR~1\TT-40-08\40\_50CM.SMP  
 Material/Liquid: silicate mud/water/Water

Reported: 01/04/10 15:19:45  
 Liquid Visc: 0.7225 cp

Sample Density: 2.650 g/cm<sup>3</sup>  
 Liquid Density: 0.9941 g/cm<sup>3</sup>

## Summary Report

Parameter 1 0.000

Parameter 2 0.000

Parameter 3 0.000

## Mass Distribution Arithmetic Statistics

Mean	104.6	Std. Dev.	14.29
Median	104.1	Coef. Var.	0.137
Mode	97.67	Skewness	0.740
		Kurtosis	6.406

## Selected Percentiles

Percent Finer	Diameter (µm)
100.0	651.9
80.0	116.0
60.0	108.1
40.0	100.5
20.0	93.53

## Selected Sizes

Diameter (µm)	Percent Finer
500.0	100.0
250.0	100.0
125.0	96.0
88.00	7.4
63.00	0.0

Peak Number	% of Dist. *	Mean	Mode	Median	Standard Deviation	Skewness	Kurtosis
1	99.9	104.4	97.67	104.1	13.73	0.095	1.023

\* Peaks must comprise at least 5.00 % of the distribution.

Micromeritics

WIN5100 V2.03

Page 1

Sample: TT-40-08 100 cm  
Operator: Clint Edrington  
Submitter: Clint Edrington  
File Name: C:\EDRING~1\TIGER&~1\SANDFR~1\TT-40-08\40\_100CM.SMP  
Material/Liquid: silicate mud/water/Water

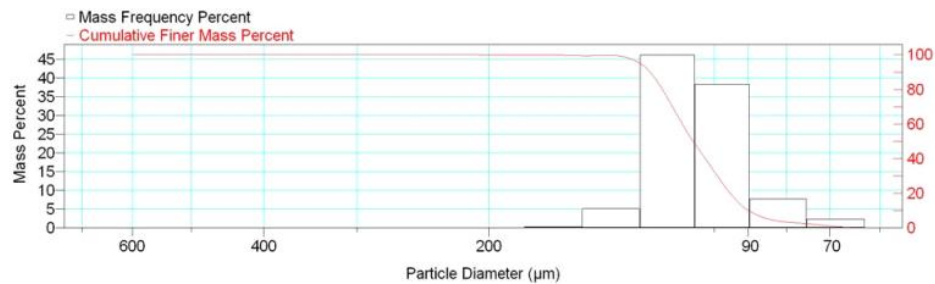
Reported: 01/04/10 15:21:34  
Liquid Visc: 0.7225 cp

Sample Density: 2.650 g/cm<sup>3</sup>  
Liquid Density: 0.9941 g/cm<sup>3</sup>

Report by Size Class

High Diameter (μm)	Low Diameter (μm)	Average Diameter (μm)	Cumulative Mass Finer (Percent)	Mass Frequency (Percent)
710.0	600.0	652.7	100.0	0.0
600.0	500.0	547.7	100.0	0.0
500.0	425.0	461.0	100.0	0.0
425.0	355.0	388.4	100.0	0.0
355.0	300.0	326.3	100.0	0.0
300.0	250.0	273.9	100.0	0.0
250.0	212.0	230.2	100.0	0.0
212.0	180.0	195.3	99.9	0.1
180.0	150.0	164.3	99.6	0.3
150.0	125.0	136.9	94.5	5.1
125.0	106.0	115.1	48.4	46.1
106.0	90.00	97.67	10.1	38.3
90.00	75.00	82.16	2.4	7.7
75.00	63.00	68.74	0.0	2.4

Mass Frequency vs Diameter



Summary Report

Full scale pump speed: 3  
Bubble detection: Medium  
Starting Size: 63.00 μm  
Ending Size: 0.50 μm

Stir time: 30 secs  
Stir speed: Low  
Probe time: 30 secs

Sample: TT-40-08 100 cm  
 Operator: Clint Edrington  
 Submitter: Clint Edrington  
 File Name: C:\EDRING~1\TIGER&~1\SANDFR~1\TT-40-08\40\_100CM.SMP  
 Material/Liquid: silicate mud/water/Water

Reported: 01/04/10 15:21:34  
 Liquid Visc: 0.7225 cp

Sample Density: 2.650 g/cm<sup>3</sup>  
 Liquid Density: 0.9941 g/cm<sup>3</sup>

## Summary Report

Parameter 1 0.000

Parameter 2 0.000

Parameter 3 0.000

## Mass Distribution Arithmetic Statistics

Mean	106.1	Std. Dev.	14.45
Median	106.7	Coef. Var.	0.136
Mode	115.1	Skewness	0.193
		Kurtosis	2.065

## Selected Percentiles

Percent Finer	Diameter (µm)
100.0	600.3
80.0	117.2
60.0	110.3
40.0	102.7
20.0	95.14

## Selected Sizes

Diameter (µm)	Percent Finer
500.0	100.0
250.0	100.0
125.0	94.5
88.00	7.8
63.00	0.0

Peak Number	% of Dist. *	Mean	Mode	Median	Standard Deviation	Skewness	Kurtosis
1	100.0	106.1	115.1	106.7	14.45	0.193	2.065

\* Peaks must comprise at least 5.00 % of the distribution.

Micromeritics

WIN5100 V2.03

Page 1

Sample: TT-40-08 150 cm  
Operator: Clint Edrington  
Submitter: Clint Edrington  
File Name: C:\EDRING~1\TIGER&~1\SANDFR~1\TT-40-08\40\_150CM.SMP  
Material/Liquid: silicate mud/water/Water

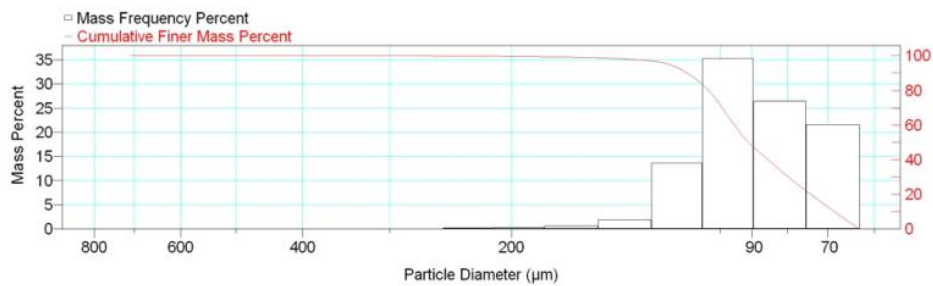
Reported: 01/04/10 15:23:23  
Liquid Visc: 0.7225 cp

Sample Density: 2.650 g/cm<sup>3</sup>  
Liquid Density: 0.9941 g/cm<sup>3</sup>

Report by Size Class

High Diameter ( $\mu\text{m}$ )	Low Diameter ( $\mu\text{m}$ )	Average Diameter ( $\mu\text{m}$ )	Cumulative Mass Finer (Percent)	Mass Frequency (Percent)
850.0	710.0	776.9	100.0	0.0
710.0	600.0	652.7	100.0	0.0
600.0	500.0	547.7	100.0	0.0
500.0	425.0	461.0	100.0	0.0
425.0	355.0	388.4	100.0	0.0
355.0	300.0	326.3	100.0	0.0
300.0	250.0	273.9	99.9	0.1
250.0	212.0	230.2	99.7	0.2
212.0	180.0	195.3	99.4	0.3
180.0	150.0	164.3	98.8	0.6
150.0	125.0	136.9	96.9	1.9
125.0	106.0	115.1	83.3	13.6
106.0	90.00	97.67	48.0	35.3
90.00	75.00	82.16	21.6	26.4
75.00	63.00	68.74	0.0	21.6

Mass Frequency vs Diameter



Summary Report

Full scale pump speed: 3  
Bubble detection: Medium  
Starting Size: 63.00  $\mu\text{m}$   
Ending Size: 0.50  $\mu\text{m}$

Stir time: 30 secs  
Stir speed: Low  
Probe time: 30 secs

Sample: TT-40-08 150 cm  
 Operator: Clint Edrington  
 Submitter: Clint Edrington  
 File Name: C:\EDRING~1\TIGER&~1\SANDFR~1\TT-40-08\40\_150CM.SMP  
 Material/Liquid: silicate mud/water/Water

Reported: 01/04/10 15:23:23  
 Liquid Visc: 0.7225 cp

Sample Density: 2.650 g/cm<sup>3</sup>  
 Liquid Density: 0.9941 g/cm<sup>3</sup>

## Summary Report

Parameter 1	0.000	Parameter 2	0.000	Parameter 3	0.000		
Mass Distribution Arithmetic Statistics							
Mean	91.58	Std. Dev.		19.98			
Median	91.08	Coef. Var.		0.218			
Mode	97.67	Skewness		2.240			
		Kurtosis		12.943			
Selected Percentiles			Selected Sizes				
Percent Finer	Diameter (µm)		Diameter (µm)	Percent Finer			
100.0	714.1		500.0	100.0			
80.0	104.0		250.0	99.9			
60.0	95.41		125.0	96.9			
40.0	85.41		88.00	44.5			
20.0	74.07		63.00	0.0			
Peak Number	% of Dist.*	Mean	Mode	Median	Standard Deviation	Skewness	Kurtosis
1	100.0	91.58	97.67	91.08	19.98	2.240	12.943

\* Peaks must comprise at least 5.00 % of the distribution.



Micromeritics

WIN5100 V2.03

Page 1

Sample: TT-40-08 200 cm  
Operator: Clint Edrington  
Submitter: Clint Edrington  
File Name: C:\EDRING~1\TIGER&~1\SANDFR~1\TT-40-08\40\_200CM.SMP  
Material/Liquid: silicate mud/water/Water

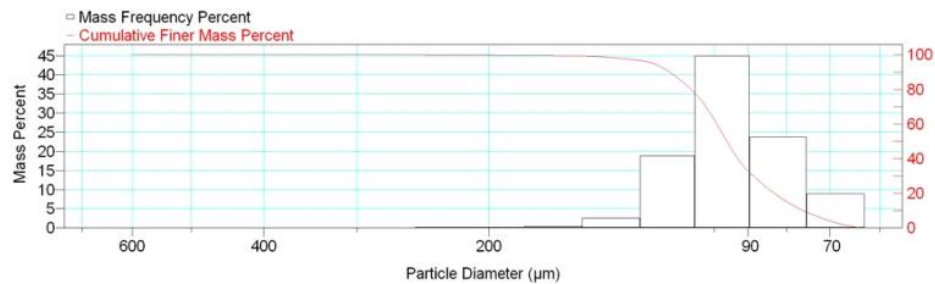
Reported: 01/04/10 15:25:15  
Liquid Visc: 0.7225 cp

Sample Density: 2.650 g/cm<sup>3</sup>  
Liquid Density: 0.9941 g/cm<sup>3</sup>

Report by Size Class

High Diameter (μm)	Low Diameter (μm)	Average Diameter (μm)	Cumulative Mass Finer (Percent)	Mass Frequency (Percent)
710.0	600.0	652.7	100.0	0.0
600.0	500.0	547.7	100.0	0.0
500.0	425.0	461.0	100.0	0.0
425.0	355.0	388.4	100.0	0.0
355.0	300.0	326.3	100.0	0.0
300.0	250.0	273.9	100.0	0.0
250.0	212.0	230.2	99.8	0.2
212.0	180.0	195.3	99.6	0.2
180.0	150.0	164.3	99.2	0.4
150.0	125.0	136.9	96.6	2.6
125.0	106.0	115.1	77.7	18.9
106.0	90.00	97.67	32.7	45.0
90.00	75.00	82.16	8.9	23.8
75.00	63.00	68.74	0.0	8.9

Mass Frequency vs Diameter



Summary Report

Full scale pump speed: 3  
Bubble detection: Medium  
Starting Size: 63.00 μm  
Ending Size: 0.50 μm

Stir time: 30 secs  
Stir speed: Low  
Probe time: 30 secs

Sample: TT-40-08 200 cm  
 Operator: Clint Edrington  
 Submitter: Clint Edrington  
 File Name: C:\EDRING~1\TIGER&~1\SANDFR~1\TT-40-08\40\_200CM.SMP  
 Material/Liquid: silicate mud/water/Water

Reported: 01/04/10 15:25:15  
 Liquid Visc: 0.7225 cp

Sample Density: 2.650 g/cm<sup>3</sup>  
 Liquid Density: 0.9941 g/cm<sup>3</sup>

## Summary Report

Parameter 1 0.000

Parameter 2 0.000

Parameter 3 0.000

## Mass Distribution Arithmetic Statistics

Mean	96.45	Std. Dev.	17.31
Median	96.11	Coef. Var.	0.180
Mode	97.67	Skewness	1.606
		Kurtosis	8.924

## Selected Percentiles

Percent Finer	Diameter (µm)
100.0	651.9
80.0	107.4
60.0	99.16
40.0	92.93
20.0	83.06

## Selected Sizes

Diameter (µm)	Percent Finer
500.0	100.0
250.0	100.0
125.0	96.6
88.00	28.8
63.00	0.0

Peak Number	% of Dist. *	Mean	Mode	Median	Standard Deviation	Skewness	Kurtosis
1	100.0	96.45	97.67	96.11	17.31	1.606	8.924

\* Peaks must comprise at least 5.00 % of the distribution.

# Micromeritics

WIN5100 V2.03

Page 1

Sample: TT-40-08 250 cm  
Operator: Clint Edrington  
Submitter: Clint Edrington  
File Name: C:\EDRING~1\TIGER&~1\SANDFR~1\TT-40-08\40\_250CM.SMP  
Material/Liquid: silicate mud/water/Water

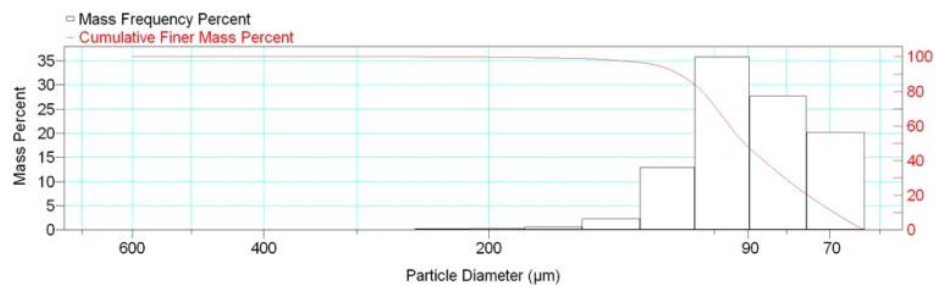
Reported: 01/04/10 15:27:41  
Liquid Visc: 0.7225 cp

Sample Density: 2.650 g/cm<sup>3</sup>  
Liquid Density: 0.9941 g/cm<sup>3</sup>

## Report by Size Class

High Diameter (μm)	Low Diameter (μm)	Average Diameter (μm)	Cumulative Mass Finer (Percent)	Mass Frequency (Percent)
710.0	600.0	652.7	100.0	0.0
600.0	500.0	547.7	100.0	0.0
500.0	425.0	461.0	100.0	0.0
425.0	355.0	388.4	100.0	0.0
355.0	300.0	326.3	100.0	0.0
300.0	250.0	273.9	100.0	0.0
250.0	212.0	230.2	99.8	0.2
212.0	180.0	195.3	99.5	0.3
180.0	150.0	164.3	98.9	0.6
150.0	125.0	136.9	96.6	2.3
125.0	106.0	115.1	83.7	12.9
106.0	90.00	97.67	47.9	35.8
90.00	75.00	82.16	20.2	27.7
75.00	63.00	68.74	0.0	20.2

Mass Frequency vs Diameter



## Summary Report

Full scale pump speed: 3  
Bubble detection: Medium  
Starting Size: 63.00 μm  
Ending Size: 0.50 μm

Stir time: 30 secs  
Stir speed: Low  
Probe time: 30 secs

Sample: TT-40-08 250 cm  
 Operator: Clint Edrington  
 Submitter: Clint Edrington  
 File Name: C:\EDRING~1\TIGER&~1\SANDFR~1\TT-40-08\40\_250CM.SMP  
 Material/Liquid: silicate mud/water/Water

Reported: 01/04/10 15:27:41  
 Liquid Visc: 0.7225 cp

Sample Density: 2.650 g/cm<sup>3</sup>  
 Liquid Density: 0.9941 g/cm<sup>3</sup>

## Summary Report

Parameter 1		0.000		Parameter 2		0.000		Parameter 3		0.000	
Mass Distribution Arithmetic Statistics											
Mean	91.64			Std. Dev.			19.09				
Median	91.07			Coef. Var.			0.208				
Mode	97.67			Skewness			1.752				
				Kurtosis			7.886				
Selected Percentiles						Selected Sizes					
Percent Finer		Diameter (µm)				Diameter (µm)		Percent Finer			
100.0		651.9				500.0		100.0			
80.0		103.7				250.0		100.0			
60.0		95.28				125.0		96.6			
40.0		85.76				88.00		44.2			
20.0		74.88				63.00		0.0			
Peak Number	% of Dist. *	Mean	Mode	Median	Standard Deviation	Skewness	Kurtosis				
1	100.0	91.64	97.67	91.07	19.09	1.752	7.886				

\* Peaks must comprise at least 5.00 % of the distribution.

Micromeritics

WIN5100 V2.03

Page 1

Sample: TT-41-08 0 cm  
Operator: Clint Edrington  
Submitter: Clint Edrington  
File Name: C:\EDRING~1\TIGER&~1\SANDFR~1\TT-41-08\41\_0CM.SMP  
Material/Liquid: silicate mud/water/Water

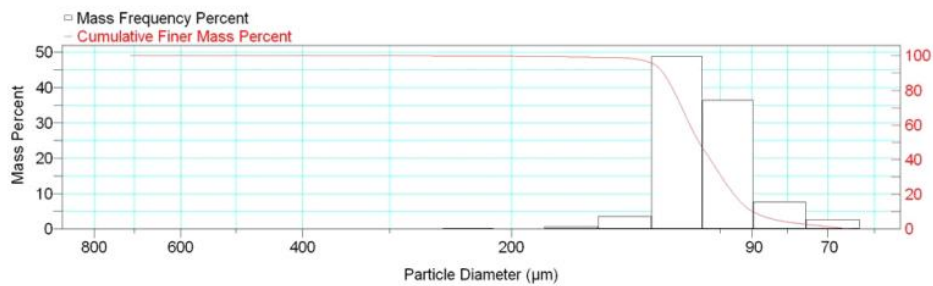
Reported: 01/04/10 15:39:06  
Liquid Visc: 0.7225 cp

Sample Density: 2.650 g/cm<sup>3</sup>  
Liquid Density: 0.9941 g/cm<sup>3</sup>

Report by Size Class

High Diameter (µm)	Low Diameter (µm)	Average Diameter (µm)	Cumulative Mass Finer (Percent)	Mass Frequency (Percent)
850.0	710.0	776.9	100.0	0.0
710.0	600.0	652.7	100.0	0.0
600.0	500.0	547.7	100.0	0.0
500.0	425.0	461.0	100.0	0.0
425.0	355.0	388.4	100.0	0.0
355.0	300.0	326.3	100.0	0.0
300.0	250.0	273.9	99.9	0.1
250.0	212.0	230.2	99.7	0.2
212.0	180.0	195.3	99.6	0.1
180.0	150.0	164.3	99.0	0.6
150.0	125.0	136.9	95.4	3.6
125.0	106.0	115.1	46.6	48.8
106.0	90.00	97.67	10.2	36.4
90.00	75.00	82.16	2.6	7.6
75.00	63.00	68.74	0.0	2.6

Mass Frequency vs Diameter



Summary Report

Full scale pump speed: 3  
Bubble detection: Medium  
Starting Size: 63.00 µm  
Ending Size: 0.50 µm

Stir time: 30 secs  
Stir speed: Low  
Probe time: 30 secs

Sample: TT-41-08 0 cm  
 Operator: Clint Edrington  
 Submitter: Clint Edrington  
 File Name: C:\EDRING~1\TIGER&~1\SANDFR~1\TT-41-08\41\_0CM.SMP  
 Material/Liquid: silicate mud/water/Water

Reported: 01/04/10 15:39:06  
 Liquid Visc: 0.7225 cp

Sample Density: 2.650 g/cm<sup>3</sup>  
 Liquid Density: 0.9941 g/cm<sup>3</sup>

## Summary Report

Parameter 1	0.000	Parameter 2	0.000	Parameter 3	0.000		
Mass Distribution Arithmetic Statistics							
Mean	106.6	Std. Dev.		16.33			
Median	107.3	Coef. Var.		0.153			
Mode	115.1	Skewness		2.030			
		Kurtosis		18.033			
Selected Percentiles			Selected Sizes				
Percent Finer	Diameter (µm)		Diameter (µm)	Percent Finer			
100.0	714.1		500.0	100.0			
80.0	116.8		250.0	99.9			
60.0	110.6		125.0	95.4			
40.0	103.3		88.00	8.4			
20.0	95.59		63.00	0.0			
Peak Number	% of Dist.*	Mean	Mode	Median	Standard Deviation	Skewness	Kurtosis
1	99.7	106.2	115.1	107.3	14.44	0.212	2.663

\* Peaks must comprise at least 5.00 % of the distribution.

# Micromeritics

WIN5100 V2.03

Page 1

Sample: TT-41-08 50 cm  
Operator: Clint Edrington  
Submitter: Clint Edrington  
File Name: C:\EDRING~1\TIGER&~1\SANDFR~1\TT-41-08\41\_50CM.SMP  
Material/Liquid: silicate mud/water/Water

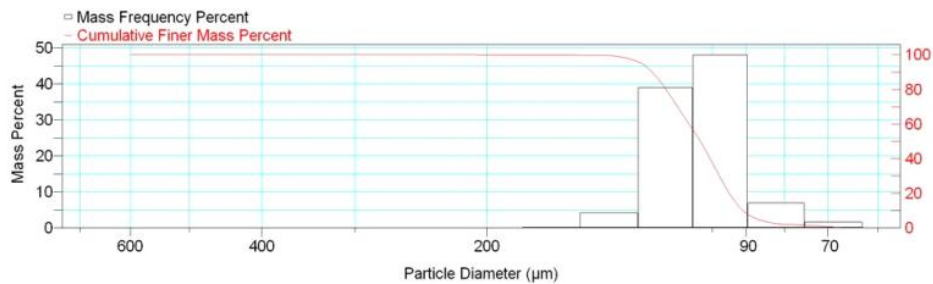
Reported: 01/04/10 15:40:53  
Liquid Visc: 0.7225 cp

Sample Density: 2.650 g/cm<sup>3</sup>  
Liquid Density: 0.9941 g/cm<sup>3</sup>

## Report by Size Class

High Diameter (μm)	Low Diameter (μm)	Average Diameter (μm)	Cumulative Mass Finer (Percent)	Mass Frequency (Percent)
710.0	600.0	652.7	100.0	0.0
600.0	500.0	547.7	100.0	0.0
500.0	425.0	461.0	100.0	0.0
425.0	355.0	388.4	100.0	0.0
355.0	300.0	326.3	100.0	0.0
300.0	250.0	273.9	100.0	0.0
250.0	212.0	230.2	100.0	0.0
212.0	180.0	195.3	99.9	0.1
180.0	150.0	164.3	99.7	0.2
150.0	125.0	136.9	95.5	4.2
125.0	106.0	115.1	56.5	39.0
106.0	90.00	97.67	8.5	48.0
90.00	75.00	82.16	1.6	6.9
75.00	63.00	68.74	0.0	1.6

Mass Frequency vs Diameter



## Summary Report

Full scale pump speed: 3  
Bubble detection: Medium  
Starting Size: 63.00 μm  
Ending Size: 0.50 μm

Stir time: 30 secs  
Stir speed: Low  
Probe time: 30 secs

Sample: TT-41-08 50 cm  
 Operator: Clint Edrington  
 Submitter: Clint Edrington  
 File Name: C:\EDRING~1\TIGER&~1\SANDFR~1\TT-41-08\41\_50CM.SMP  
 Material/Liquid: silicate mud/water/Water

Reported: 01/04/10 15:40:53  
 Liquid Visc: 0.7225 cp

Sample Density: 2.650 g/cm<sup>3</sup>  
 Liquid Density: 0.9941 g/cm<sup>3</sup>

## Summary Report

Parameter 1 0.000

Parameter 2 0.000

Parameter 3 0.000

## Mass Distribution Arithmetic Statistics

Mean	104.8	Std. Dev.	13.44
Median	103.7	Coef. Var.	0.128
Mode	97.67	Skewness	0.514
		Kurtosis	2.755

## Selected Percentiles

Percent Finer	Diameter (µm)
100.0	600.3
80.0	115.2
60.0	107.4
40.0	100.6
20.0	94.81

## Selected Sizes

Diameter (µm)	Percent Finer
500.0	100.0
250.0	100.0
125.0	95.5
88.00	6.1
63.00	0.0

Peak Number	% of Dist. *	Mean	Mode	Median	Standard Deviation	Skewness	Kurtosis
1	100.0	104.8	97.67	103.7	13.44	0.514	2.755

\* Peaks must comprise at least 5.00 % of the distribution.



# Micromeritics

WIN5100 V2.03

Page 1

Sample: TT-41-08 105 cm  
Operator: Clint Edrington  
Submitter: Clint Edrington  
File Name: C:\EDRING~1\TIGER&~1\SANDFR~1\TT-41-08\41\_105CM.SMP  
Material/Liquid: silicate mud/water/Water

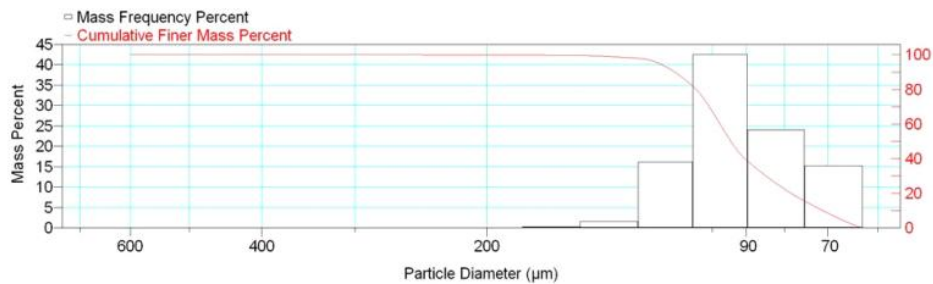
Reported: 01/04/10 15:42:47  
Liquid Visc: 0.7225 cp

Sample Density: 2.650 g/cm<sup>3</sup>  
Liquid Density: 0.9941 g/cm<sup>3</sup>

## Report by Size Class

High Diameter (µm)	Low Diameter (µm)	Average Diameter (µm)	Cumulative Mass Finer (Percent)	Mass Frequency (Percent)
710.0	600.0	652.7	100.0	0.0
600.0	500.0	547.7	100.0	0.0
500.0	425.0	461.0	100.0	0.0
425.0	355.0	388.4	100.0	0.0
355.0	300.0	326.3	100.0	0.0
300.0	250.0	273.9	100.0	0.0
250.0	212.0	230.2	99.9	0.1
212.0	180.0	195.3	99.8	0.1
180.0	150.0	164.3	99.5	0.3
150.0	125.0	136.9	97.9	1.6
125.0	106.0	115.1	81.7	16.2
106.0	90.00	97.67	39.2	42.5
90.00	75.00	82.16	15.2	24.0
75.00	63.00	68.74	0.0	15.2

Mass Frequency vs Diameter



## Summary Report

Full scale pump speed: 3  
Bubble detection: Medium  
Starting Size: 63.00 µm  
Ending Size: 0.50 µm

Stir time: 30 secs  
Stir speed: Low  
Probe time: 30 secs

Sample: TT-41-08 105 cm  
 Operator: Clint Edrington  
 Submitter: Clint Edrington  
 File Name: C:\EDRING~1\TIGER&~1\SANDFR~1\TT-41-08\41\_105CM.SMP  
 Material/Liquid: silicate mud/water/Water

Reported: 01/04/10 15:42:47  
 Liquid Visc: 0.7225 cp

Sample Density: 2.650 g/cm<sup>3</sup>  
 Liquid Density: 0.9941 g/cm<sup>3</sup>

## Summary Report

Parameter 1 0.000

Parameter 2 0.000

Parameter 3 0.000

## Mass Distribution Arithmetic Statistics

Mean	93.43	Std. Dev.	16.77
Median	94.36	Coef. Var.	0.180
Mode	97.67	Skewness	1.070
		Kurtosis	5.679

## Selected Percentiles

Percent Finer	Diameter (µm)
100.0	651.9
80.0	105.0
60.0	97.57
40.0	90.43
20.0	78.42

## Selected Sizes

Diameter (µm)	Percent Finer
500.0	100.0
250.0	100.0
125.0	97.9
88.00	35.7
63.00	0.0

Peak Number	% of Dist. *	Mean	Mode	Median	Standard Deviation	Skewness	Kurtosis
1	100.0	93.43	97.67	94.36	16.77	1.070	5.679

\* Peaks must comprise at least 5.00 % of the distribution.

# Micromeritics

WIN5100 V2.03

Page 1

Sample: TT-41-08 150 cm  
Operator: Clint Edrington  
Submitter: Clint Edrington  
File Name: C:\EDRING~1\TIGER&~1\SANDFR~1\TT-41-08\41\_150CM.SMP  
Material/Liquid: silicate mud/water/Water

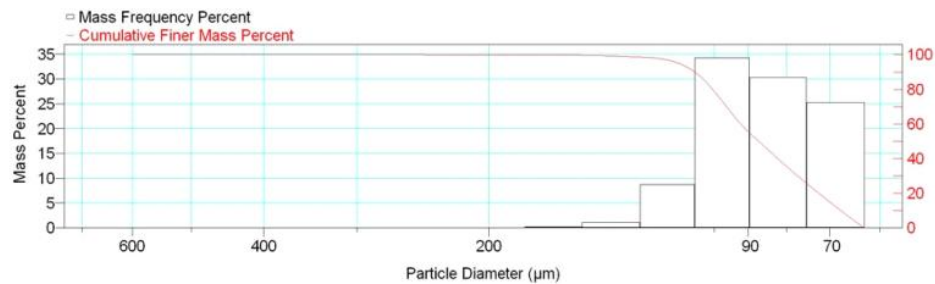
Reported: 01/04/10 15:44:33  
Liquid Visc: 0.7225 cp

Sample Density: 2.650 g/cm<sup>3</sup>  
Liquid Density: 0.9941 g/cm<sup>3</sup>

## Report by Size Class

High Diameter (μm)	Low Diameter (μm)	Average Diameter (μm)	Cumulative Mass Finer (Percent)	Mass Frequency (Percent)
710.0	600.0	652.7	100.0	0.0
600.0	500.0	547.7	100.0	0.0
500.0	425.0	461.0	100.0	0.0
425.0	355.0	388.4	100.0	0.0
355.0	300.0	326.3	100.0	0.0
300.0	250.0	273.9	100.0	0.0
250.0	212.0	230.2	99.9	0.1
212.0	180.0	195.3	99.9	0.0
180.0	150.0	164.3	99.7	0.2
150.0	125.0	136.9	98.6	1.1
125.0	106.0	115.1	89.9	8.7
106.0	90.00	97.67	55.6	34.3
90.00	75.00	82.16	25.3	30.3
75.00	63.00	68.74	0.0	25.3

Mass Frequency vs Diameter



## Summary Report

Full scale pump speed: 3  
Bubble detection: Medium  
Starting Size: 63.00 μm  
Ending Size: 0.50 μm

Stir time: 30 secs  
Stir speed: Low  
Probe time: 30 secs

Sample: TT-41-08 150 cm  
 Operator: Clint Edrington  
 Submitter: Clint Edrington  
 File Name: C:\EDRING~1\TIGER&~1\SANDFR~1\TT-41-08\41\_150CM.SMP  
 Material/Liquid: silicate mud/water/Water

Reported: 01/04/10 15:44:33  
 Liquid Visc: 0.7225 cp

Sample Density: 2.650 g/cm<sup>3</sup>  
 Liquid Density: 0.9941 g/cm<sup>3</sup>

## Summary Report

Parameter 1 0.000

Parameter 2 0.000

Parameter 3 0.000

## Mass Distribution Arithmetic Statistics

Mean	87.87	Std. Dev.	16.08
Median	87.11	Coef. Var.	0.183
Mode	97.67	Skewness	1.284
		Kurtosis	6.403

## Selected Percentiles

Percent Finer	Diameter (µm)
100.0	651.9
80.0	100.4
60.0	92.10
40.0	82.15
20.0	72.42

## Selected Sizes

Diameter (µm)	Percent Finer
500.0	100.0
250.0	100.0
125.0	98.6
88.00	51.7
63.00	0.0

Peak Number	% of Dist. *	Mean	Mode	Median	Standard Deviation	Skewness	Kurtosis
1	99.9	87.72	97.67	87.09	15.44	0.694	0.854

\* Peaks must comprise at least 5.00 % of the distribution.

Micromeritics

WIN5100 V2.03

Page 1

Sample: TT-41-08 200 cm  
Operator: Clint Edrington  
Submitter: Clint Edrington  
File Name: C:\EDRING~1\TIGER&~1\SANDFR~1\TT-41-08\41\_200CM.SMP  
Material/Liquid: silicate mud/water/Water

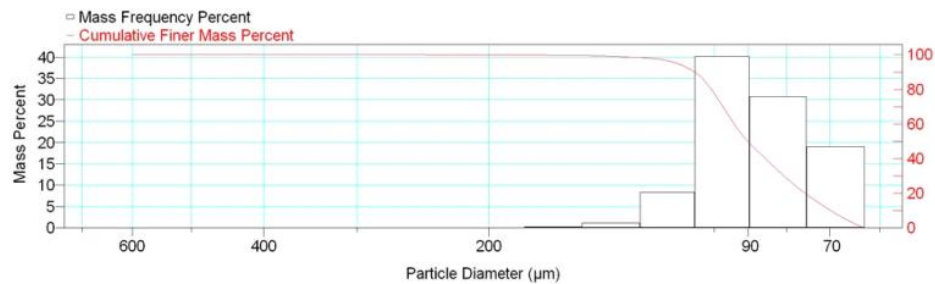
Reported: 01/04/10 15:47:11  
Liquid Visc: 0.7225 cp

Sample Density: 2.650 g/cm<sup>3</sup>  
Liquid Density: 0.9941 g/cm<sup>3</sup>

Report by Size Class

High Diameter (μm)	Low Diameter (μm)	Average Diameter (μm)	Cumulative Mass Finer (Percent)	Mass Frequency (Percent)
710.0	600.0	652.7	100.0	0.0
600.0	500.0	547.7	100.0	0.0
500.0	425.0	461.0	100.0	0.0
425.0	355.0	388.4	100.0	0.0
355.0	300.0	326.3	100.0	0.0
300.0	250.0	273.9	100.0	0.0
250.0	212.0	230.2	99.9	0.1
212.0	180.0	195.3	99.8	0.1
180.0	150.0	164.3	99.5	0.3
150.0	125.0	136.9	98.3	1.2
125.0	106.0	115.1	89.9	8.4
106.0	90.00	97.67	49.7	40.2
90.00	75.00	82.16	19.0	30.7
75.00	63.00	68.74	0.0	19.0

Mass Frequency vs Diameter



Summary Report

Full scale pump speed: 3  
Bubble detection: Medium  
Starting Size: 63.00 μm  
Ending Size: 0.50 μm

Stir time: 30 secs  
Stir speed: Low  
Probe time: 30 secs

Sample: TT-41-08 200 cm  
 Operator: Clint Edrington  
 Submitter: Clint Edrington  
 File Name: C:\EDRING~1\TIGER&~1\SANDFR~1\TT-41-08\41\_200CM.SMP  
 Material/Liquid: silicate mud/water/Water

Reported: 01/04/10 15:47:11  
 Liquid Visc: 0.7225 cp

Sample Density: 2.650 g/cm<sup>3</sup>  
 Liquid Density: 0.9941 g/cm<sup>3</sup>

## Summary Report

Parameter 1 0.000

Parameter 2 0.000

Parameter 3 0.000

## Mass Distribution Arithmetic Statistics

Mean	89.78	Std. Dev.	15.97
Median	90.14	Coef. Var.	0.178
Mode	97.67	Skewness	1.498
		Kurtosis	8.364

## Selected Percentiles

Percent Finer	Diameter (µm)
100.0	651.9
80.0	100.8
60.0	93.98
40.0	85.39
20.0	75.55

## Selected Sizes

Diameter (µm)	Percent Finer
500.0	100.0
250.0	100.0
125.0	98.3
88.00	45.5
63.00	0.0

Peak Number	% of Dist. *	Mean	Mode	Median	Standard Deviation	Skewness	Kurtosis
1	100.0	89.78	97.67	90.14	15.97	1.498	8.364

\* Peaks must comprise at least 5.00 % of the distribution.

# Micromeritics

WIN5100 V2.03

Page 1

Sample: TT-41-08 250 cm  
Operator: Clint Edrington  
Submitter: Clint Edrington  
File Name: C:\EDRING~1\TIGER&~1\SANDFR~1\TT-41-08\41\_250CM.SMP  
Material/Liquid: silicate mud/water/Water

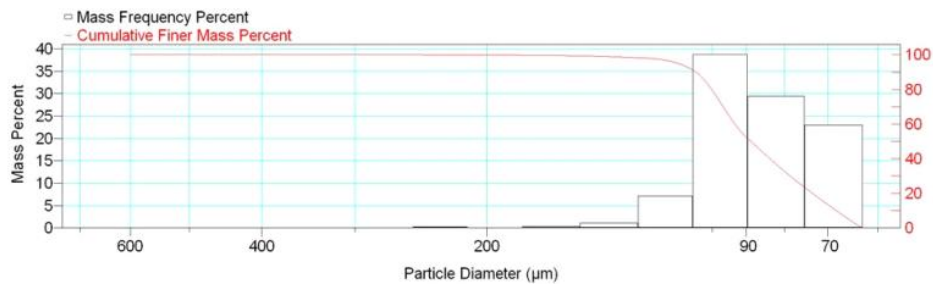
Reported: 01/04/10 15:49:02  
Liquid Visc: 0.7225 cp

Sample Density: 2.650 g/cm<sup>3</sup>  
Liquid Density: 0.9941 g/cm<sup>3</sup>

## Report by Size Class

High Diameter (µm)	Low Diameter (µm)	Average Diameter (µm)	Cumulative Mass Finer (Percent)	Mass Frequency (Percent)
710.0	600.0	652.7	100.0	0.0
600.0	500.0	547.7	100.0	0.0
500.0	425.0	461.0	100.0	0.0
425.0	355.0	388.4	100.0	0.0
355.0	300.0	326.3	100.0	0.0
300.0	250.0	273.9	100.0	0.0
250.0	212.0	230.2	99.8	0.2
212.0	180.0	195.3	99.7	0.1
180.0	150.0	164.3	99.3	0.4
150.0	125.0	136.9	98.2	1.1
125.0	106.0	115.1	91.1	7.1
106.0	90.00	97.67	52.4	38.7
90.00	75.00	82.16	23.0	29.4
75.00	63.00	68.74	0.0	23.0

Mass Frequency vs Diameter



## Summary Report

Full scale pump speed: 3  
Bubble detection: Medium  
Starting Size: 63.00 µm  
Ending Size: 0.50 µm

Stir time: 30 secs  
Stir speed: Low  
Probe time: 30 secs

Sample: TT-41-08 250 cm  
 Operator: Clint Edrington  
 Submitter: Clint Edrington  
 File Name: C:\EDRING~1\TIGER&~1\SANDFR~1\TT-41-08\41\_250CM.SMP  
 Material/Liquid: silicate mud/water/Water

Reported: 01/04/10 15:49:02  
 Liquid Visc: 0.7225 cp

Sample Density: 2.650 g/cm<sup>3</sup>  
 Liquid Density: 0.9941 g/cm<sup>3</sup>

## Summary Report

Parameter 1 0.000

Parameter 2 0.000

Parameter 3 0.000

## Mass Distribution Arithmetic Statistics

Mean	88.76	Std. Dev.	16.88
Median	88.75	Coef. Var.	0.190
Mode	97.67	Skewness	1.971
		Kurtosis	11.720

## Selected Percentiles

Percent Finer	Diameter (µm)
100.0	651.9
80.0	100.2
60.0	93.20
40.0	83.66
20.0	73.41

## Selected Sizes

Diameter (µm)	Percent Finer
500.0	100.0
250.0	100.0
125.0	98.2
88.00	48.6
63.00	0.0

Peak Number	% of Dist. *	Mean	Mode	Median	Standard Deviation	Skewness	Kurtosis
1	99.8	88.47	97.67	88.70	15.66	1.049	3.623

\* Peaks must comprise at least 5.00 % of the distribution.



Micromeritics

WIN5100 V2.03

Page 1

Sample: TT-42-08 8 cm  
Operator: Clint Edrington  
Submitter: Clint Edrington  
File Name: C:\EDRING~1\TIGER&~1\SANDFR~1\TT-42-08\42\_8CM.SMP  
Material/Liquid: silicate mud/water/Water

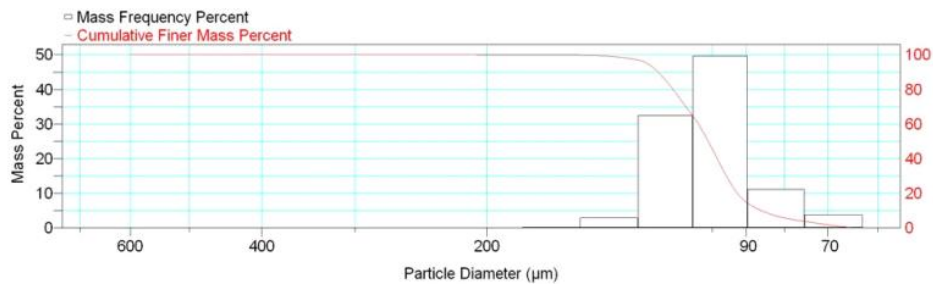
Reported: 01/04/10 15:54:17  
Liquid Visc: 0.7225 cp

Sample Density: 2.650 g/cm<sup>3</sup>  
Liquid Density: 0.9941 g/cm<sup>3</sup>

Report by Size Class

High Diameter (µm)	Low Diameter (µm)	Average Diameter (µm)	Cumulative Mass Finer (Percent)	Mass Frequency (Percent)
710.0	600.0	652.7	100.0	0.0
600.0	500.0	547.7	100.0	0.0
500.0	425.0	461.0	100.0	0.0
425.0	355.0	388.4	100.0	0.0
355.0	300.0	326.3	100.0	0.0
300.0	250.0	273.9	100.0	0.0
250.0	212.0	230.2	100.0	0.0
212.0	180.0	195.3	99.9	0.1
180.0	150.0	164.3	99.7	0.2
150.0	125.0	136.9	96.8	2.9
125.0	106.0	115.1	64.4	32.4
106.0	90.00	97.67	14.8	49.6
90.00	75.00	82.16	3.7	11.1
75.00	63.00	68.74	0.0	3.7

Mass Frequency vs Diameter



Summary Report

Full scale pump speed: 3  
Bubble detection: Medium  
Starting Size: 63.00 µm  
Ending Size: 0.50 µm

Stir time: 30 secs  
Stir speed: Low  
Probe time: 30 secs

Sample: TT-42-08 8 cm  
 Operator: Clint Edrington  
 Submitter: Clint Edrington  
 File Name: C:\EDRING~1\TIGER&~1\SANDFR~1\TT-42-08\42\_8CM.SMP  
 Material/Liquid: silicate mud/water/Water

Reported: 01/04/10 15:54:17  
 Liquid Visc: 0.7225 cp

Sample Density: 2.650 g/cm<sup>3</sup>  
 Liquid Density: 0.9941 g/cm<sup>3</sup>

## Summary Report

Parameter 1 0.000

Parameter 2 0.000

Parameter 3 0.000

## Mass Distribution Arithmetic Statistics

Mean	101.9	Std. Dev.	14.19
Median	101.2	Coef. Var.	0.139
Mode	97.67	Skewness	0.369
		Kurtosis	2.468

## Selected Percentiles

Percent Finer	Diameter (µm)
100.0	600.3
80.0	112.8
60.0	104.3
40.0	98.42
20.0	92.51

## Selected Sizes

Diameter (µm)	Percent Finer
500.0	100.0
250.0	100.0
125.0	96.8
88.00	12.2
63.00	0.0

Peak Number	% of Dist. *	Mean	Mode	Median	Standard Deviation	Skewness	Kurtosis
1	100.0	101.9	97.67	101.2	14.19	0.369	2.468

\* Peaks must comprise at least 5.00 % of the distribution.

Micromeritics

WIN5100 V2.03

Page 1

Sample: TT-42-08 59 cm  
Operator: Clint Edrington  
Submitter: Clint Edrington  
File Name: C:\EDRING~1\TIGER&~1\SANDFR~1\TT-42-08\42\_59CM.SMP  
Material/Liquid: silicate mud/water/Water

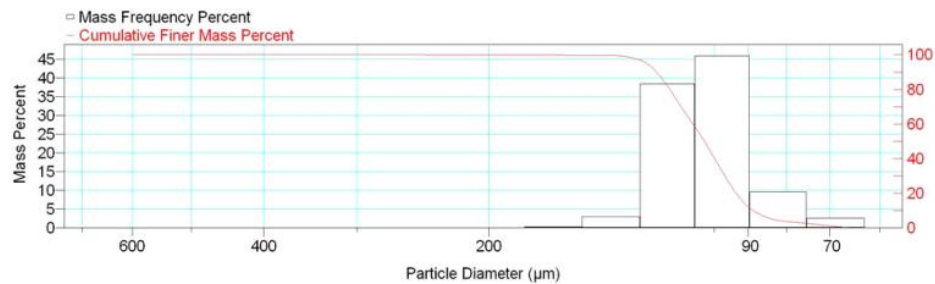
Reported: 01/04/10 15:56:36  
Liquid Visc: 0.7225 cp

Sample Density: 2.650 g/cm<sup>3</sup>  
Liquid Density: 0.9941 g/cm<sup>3</sup>

Report by Size Class

High Diameter (μm)	Low Diameter (μm)	Average Diameter (μm)	Cumulative Mass Finer (Percent)	Mass Frequency (Percent)
710.0	600.0	652.7	100.0	0.0
600.0	500.0	547.7	100.0	0.0
500.0	425.0	461.0	100.0	0.0
425.0	355.0	388.4	100.0	0.0
355.0	300.0	326.3	100.0	0.0
300.0	250.0	273.9	100.0	0.0
250.0	212.0	230.2	99.9	0.1
212.0	180.0	195.3	99.9	0.0
180.0	150.0	164.3	99.6	0.3
150.0	125.0	136.9	96.6	3.0
125.0	106.0	115.1	58.1	38.5
106.0	90.00	97.67	12.2	45.9
90.00	75.00	82.16	2.6	9.6
75.00	63.00	68.74	0.0	2.6

Mass Frequency vs Diameter



Summary Report

Full scale pump speed: 3  
Bubble detection: Medium  
Starting Size: 63.00 μm  
Ending Size: 0.50 μm

Stir time: 30 secs  
Stir speed: Low  
Probe time: 30 secs

Sample: TT-42-08 59 cm  
 Operator: Clint Edrington  
 Submitter: Clint Edrington  
 File Name: C:\EDRING~1\TIGER&~1\SANDFR~1\TT-42-08\42\_59CM.SMP  
 Material/Liquid: silicate mud/water/Water

Reported: 01/04/10 15:56:36  
 Liquid Visc: 0.7225 cp

Sample Density: 2.650 g/cm<sup>3</sup>  
 Liquid Density: 0.9941 g/cm<sup>3</sup>

## Summary Report

Parameter 1 0.000

Parameter 2 0.000

Parameter 3 0.000

## Mass Distribution Arithmetic Statistics

Mean	103.7	Std. Dev.	14.26
Median	103.0	Coef. Var.	0.138
Mode	97.67	Skewness	0.767
		Kurtosis	6.689

## Selected Percentiles

Percent Finer	Diameter (µm)
100.0	651.9
80.0	114.6
60.0	106.8
40.0	99.80
20.0	93.42

## Selected Sizes

Diameter (µm)	Percent Finer
500.0	100.0
250.0	100.0
125.0	96.6
88.00	9.2
63.00	0.0

Peak Number	% of Dist. *	Mean	Mode	Median	Standard Deviation	Skewness	Kurtosis
1	99.9	103.5	97.67	103.0	13.69	0.104	1.100

\* Peaks must comprise at least 5.00 % of the distribution.

Micromeritics

WIN5100 V2.03

Page 1

Sample: TT-42-08 115 cm  
Operator: Clint Edrington  
Submitter: Clint Edrington  
File Name: C:\EDRING~1\TIGER&~1\SANDFR~1\TT-42-08\42\_115CM.SMP  
Material/Liquid: silicate mud/water/Water

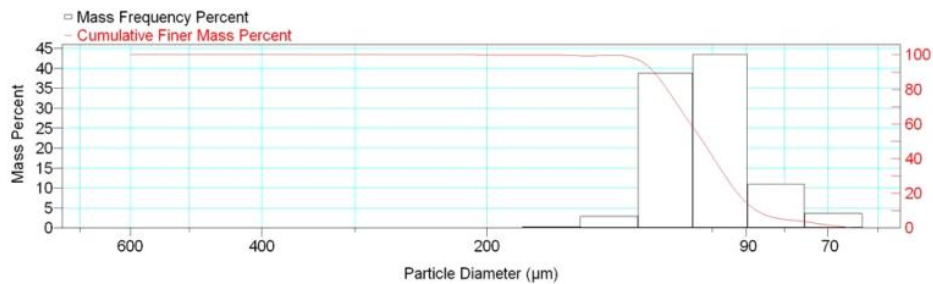
Reported: 01/04/10 15:58:31  
Liquid Visc: 0.7225 cp

Sample Density: 2.650 g/cm<sup>3</sup>  
Liquid Density: 0.9941 g/cm<sup>3</sup>

Report by Size Class

High Diameter (μm)	Low Diameter (μm)	Average Diameter (μm)	Cumulative Mass Finer (Percent)	Mass Frequency (Percent)
710.0	600.0	652.7	100.0	0.0
600.0	500.0	547.7	100.0	0.0
500.0	425.0	461.0	100.0	0.0
425.0	355.0	388.4	100.0	0.0
355.0	300.0	326.3	100.0	0.0
300.0	250.0	273.9	100.0	0.0
250.0	212.0	230.2	100.0	0.0
212.0	180.0	195.3	99.9	0.1
180.0	150.0	164.3	99.6	0.3
150.0	125.0	136.9	96.7	2.9
125.0	106.0	115.1	58.0	38.7
106.0	90.00	97.67	14.6	43.4
90.00	75.00	82.16	3.6	11.0
75.00	63.00	68.74	0.0	3.6

Mass Frequency vs Diameter



Summary Report

Full scale pump speed: 3  
Bubble detection: Medium  
Starting Size: 63.00 μm  
Ending Size: 0.50 μm

Stir time: 30 secs  
Stir speed: Low  
Probe time: 30 secs

Sample: TT-42-08 115 cm  
 Operator: Clint Edrington  
 Submitter: Clint Edrington  
 File Name: C:\EDRING~1\TIGER&~1\SANDFR~1\TT-42-08\42\_115CM.SMP  
 Material/Liquid: silicate mud/water/Water

Reported: 01/04/10 15:58:31  
 Liquid Visc: 0.7225 cp

Sample Density: 2.650 g/cm<sup>3</sup>  
 Liquid Density: 0.9941 g/cm<sup>3</sup>

## Summary Report

Parameter 1 0.000

Parameter 2 0.000

Parameter 3 0.000

## Mass Distribution Arithmetic Statistics

Mean	103.1	Std. Dev.	14.57
Median	102.9	Coef. Var.	0.141
Mode	97.67	Skewness	0.233
		Kurtosis	2.154

## Selected Percentiles

Percent Finer	Diameter (µm)
100.0	600.3
80.0	114.8
60.0	106.8
40.0	99.42
20.0	92.41

## Selected Sizes

Diameter (µm)	Percent Finer
500.0	100.0
250.0	100.0
125.0	96.7
88.00	11.2
63.00	0.0

Peak Number	% of Dist. *	Mean	Mode	Median	Standard Deviation	Skewness	Kurtosis
1	100.0	103.1	97.67	102.9	14.57	0.233	2.154

\* Peaks must comprise at least 5.00 % of the distribution.

Micromeritics

WIN5100 V2.03

Page 1

Sample: TT-42-08 160 cm  
Operator: Clint Edrington  
Submitter: Clint Edrington  
File Name: C:\EDRING~1\TIGER&~1\SANDFR~1\TT-42-08\42\_160CM.SMP  
Material/Liquid: silicate mud/water/Water

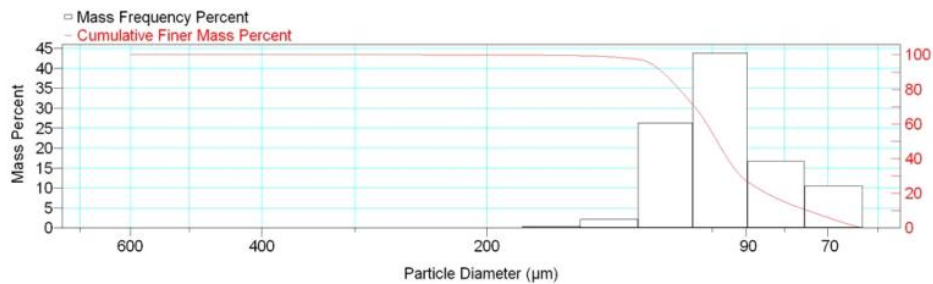
Reported: 01/04/10 16:01:17  
Liquid Visc: 0.7225 cp

Sample Density: 2.650 g/cm<sup>3</sup>  
Liquid Density: 0.9941 g/cm<sup>3</sup>

Report by Size Class

High Diameter (μm)	Low Diameter (μm)	Average Diameter (μm)	Cumulative Mass Finer (Percent)	Mass Frequency (Percent)
710.0	600.0	652.7	100.0	0.0
600.0	500.0	547.7	100.0	0.0
500.0	425.0	461.0	100.0	0.0
425.0	355.0	388.4	100.0	0.0
355.0	300.0	326.3	100.0	0.0
300.0	250.0	273.9	100.0	0.0
250.0	212.0	230.2	99.9	0.1
212.0	180.0	195.3	99.8	0.1
180.0	150.0	164.3	99.4	0.4
150.0	125.0	136.9	97.2	2.2
125.0	106.0	115.1	71.0	26.2
106.0	90.00	97.67	27.2	43.8
90.00	75.00	82.16	10.5	16.7
75.00	63.00	68.74	0.0	10.5

Mass Frequency vs Diameter



Summary Report

Full scale pump speed: 3  
Bubble detection: Medium  
Starting Size: 63.00 μm  
Ending Size: 0.50 μm

Stir time: 30 secs  
Stir speed: Low  
Probe time: 30 secs

Sample: TT-42-08 160 cm  
 Operator: Clint Edrington  
 Submitter: Clint Edrington  
 File Name: C:\EDRING~1\TIGER&~1\SANDFR~1\TT-42-08\42\_160CM.SMP  
 Material/Liquid: silicate mud/water/Water

Reported: 01/04/10 16:01:17  
 Liquid Visc: 0.7225 cp

Sample Density: 2.650 g/cm<sup>3</sup>  
 Liquid Density: 0.9941 g/cm<sup>3</sup>

## Summary Report

Parameter 1 0.000

Parameter 2 0.000

Parameter 3 0.000

## Mass Distribution Arithmetic Statistics

Mean	97.97	Std. Dev.	16.92
Median	98.44	Coef. Var.	0.173
Mode	97.67	Skewness	0.771
		Kurtosis	4.723

## Selected Percentiles

Percent Finer	Diameter (µm)
100.0	651.9
80.0	110.6
60.0	101.6
40.0	95.31
20.0	84.52

## Selected Sizes

Diameter (µm)	Percent Finer
500.0	100.0
250.0	100.0
125.0	97.2
88.00	24.4
63.00	0.0

Peak Number	% of Dist. *	Mean	Mode	Median	Standard Deviation	Skewness	Kurtosis
1	100.0	97.97	97.67	98.44	16.92	0.771	4.723

\* Peaks must comprise at least 5.00 % of the distribution.



# Micromeritics

WIN5100 V2.03

Page 1

Sample: TT-42-08 210 cm  
Operator: Clint Edrington  
Submitter: Clint Edrington  
File Name: C:\EDRING~1\TIGER&~1\SANDFR~1\TT-42-08\42\_210CM.SMP  
Material/Liquid: silicate mud/water/Water

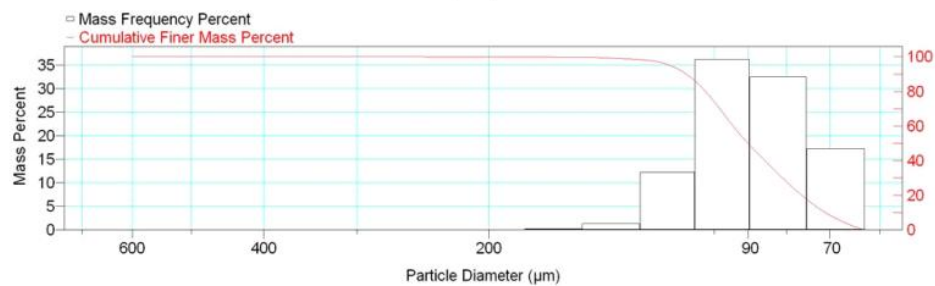
Reported: 01/04/10 16:03:14  
Liquid Visc: 0.7225 cp

Sample Density: 2.650 g/cm<sup>3</sup>  
Liquid Density: 0.9941 g/cm<sup>3</sup>

## Report by Size Class

High Diameter (μm)	Low Diameter (μm)	Average Diameter (μm)	Cumulative Mass Finer (Percent)	Mass Frequency (Percent)
710.0	600.0	652.7	100.0	0.0
600.0	500.0	547.7	100.0	0.0
500.0	425.0	461.0	100.0	0.0
425.0	355.0	388.4	100.0	0.0
355.0	300.0	326.3	100.0	0.0
300.0	250.0	273.9	100.0	0.0
250.0	212.0	230.2	99.9	0.1
212.0	180.0	195.3	99.8	0.1
180.0	150.0	164.3	99.6	0.2
150.0	125.0	136.9	98.3	1.3
125.0	106.0	115.1	86.0	12.3
106.0	90.00	97.67	49.8	36.2
90.00	75.00	82.16	17.3	32.5
75.00	63.00	68.74	0.0	17.3

Mass Frequency vs Diameter



## Summary Report

Full scale pump speed: 3  
Bubble detection: Medium  
Starting Size: 63.00 μm  
Ending Size: 0.50 μm

Stir time: 30 secs  
Stir speed: Low  
Probe time: 30 secs

Sample: TT-42-08 210 cm  
 Operator: Clint Edrington  
 Submitter: Clint Edrington  
 File Name: C:\EDRING~1\TIGER&~1\SANDFR~1\TT-42-08\42\_210CM.SMP  
 Material/Liquid: silicate mud/water/Water

Reported: 01/04/10 16:03:14  
 Liquid Visc: 0.7225 cp

Sample Density: 2.650 g/cm<sup>3</sup>  
 Liquid Density: 0.9941 g/cm<sup>3</sup>

## Summary Report

Parameter 1 0.000

Parameter 2 0.000

Parameter 3 0.000

## Mass Distribution Arithmetic Statistics

Mean	90.64	Std. Dev.	16.34
Median	90.09	Coef. Var.	0.180
Mode	97.67	Skewness	1.344
		Kurtosis	6.881

## Selected Percentiles

Percent Finer	Diameter (µm)
100.0	651.9
80.0	102.7
60.0	94.30
40.0	85.51
20.0	76.32

## Selected Sizes

Diameter (µm)	Percent Finer
500.0	100.0
250.0	100.0
125.0	98.3
88.00	45.5
63.00	0.0

Peak Number	% of Dist. *	Mean	Mode	Median	Standard Deviation	Skewness	Kurtosis
1	100.0	90.64	97.67	90.09	16.34	1.344	6.881

\* Peaks must comprise at least 5.00 % of the distribution.

# Micromeritics

WIN5100 V2.03

Page 1

Sample: TT-42-08 260 cm  
Operator: Clint Edrington  
Submitter: Clint Edrington  
File Name: C:\EDRING~1\TIGER&~1\SANDFR~1\TT-42-08\42\_260CM.SMP  
Material/Liquid: silicate mud/water/Water

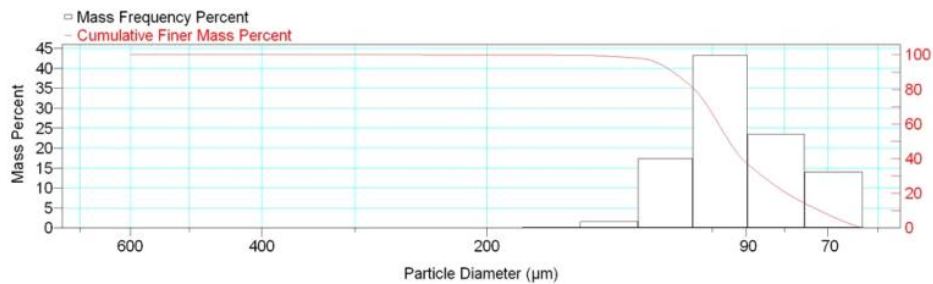
Reported: 01/04/10 16:05:35  
Liquid Visc: 0.7225 cp

Sample Density: 2.650 g/cm<sup>3</sup>  
Liquid Density: 0.9941 g/cm<sup>3</sup>

## Report by Size Class

High Diameter (μm)	Low Diameter (μm)	Average Diameter (μm)	Cumulative Mass Finer (Percent)	Mass Frequency (Percent)
710.0	600.0	652.7	100.0	0.0
600.0	500.0	547.7	100.0	0.0
500.0	425.0	461.0	100.0	0.0
425.0	355.0	388.4	100.0	0.0
355.0	300.0	326.3	100.0	0.0
300.0	250.0	273.9	100.0	0.0
250.0	212.0	230.2	99.9	0.1
212.0	180.0	195.3	99.8	0.1
180.0	150.0	164.3	99.6	0.2
150.0	125.0	136.9	98.0	1.6
125.0	106.0	115.1	80.7	17.3
106.0	90.00	97.67	37.5	43.2
90.00	75.00	82.16	14.0	23.5
75.00	63.00	68.74	0.0	14.0

Mass Frequency vs Diameter



## Summary Report

Full scale pump speed: 3  
Bubble detection: Medium  
Starting Size: 63.00 μm  
Ending Size: 0.50 μm

Stir time: 30 secs  
Stir speed: Low  
Probe time: 30 secs

Sample: TT-42-08 260 cm  
 Operator: Clint Edrington  
 Submitter: Clint Edrington  
 File Name: C:\EDRING~1\TIGER&~1\SANDFR~1\TT-42-08\42\_260CM.SMP  
 Material/Liquid: silicate mud/water/Water

Reported: 01/04/10 16:05:35  
 Liquid Visc: 0.7225 cp

Sample Density: 2.650 g/cm<sup>3</sup>  
 Liquid Density: 0.9941 g/cm<sup>3</sup>

## Summary Report

Parameter 1 0.000

Parameter 2 0.000

Parameter 3 0.000

## Mass Distribution Arithmetic Statistics

Mean	93.98	Std. Dev.	16.54
Median	94.88	Coef. Var.	0.176
Mode	97.67	Skewness	1.005
		Kurtosis	5.687

## Selected Percentiles

Percent Finer	Diameter (µm)
100.0	651.9
80.0	105.6
60.0	98.02
40.0	91.23
20.0	79.40

## Selected Sizes

Diameter (µm)	Percent Finer
500.0	100.0
250.0	100.0
125.0	98.0
88.00	34.0
63.00	0.0

Peak Number	% of Dist. *	Mean	Mode	Median	Standard Deviation	Skewness	Kurtosis
1	100.0	93.98	97.67	94.88	16.54	1.005	5.687

\* Peaks must comprise at least 5.00 % of the distribution.

# Micromeritics

WIN5100 V2.03

Page 1

Sample: TT-43-08 2-5 cm  
Operator: Clint Edrington  
Submitter: Clint Edrington  
File Name: C:\EDRING~1\TIGER&~1\SANDFR~1\TT-43-08\43\_2-5CM.SMP  
Material/Liquid: silicate mud/water/Water

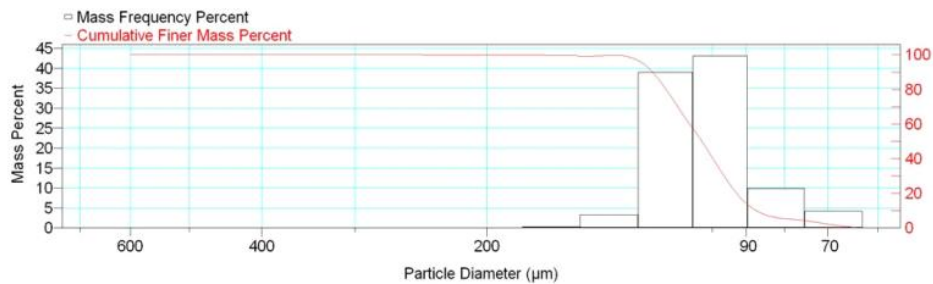
Reported: 01/04/10 16:09:17  
Liquid Visc: 0.7225 cp

Sample Density: 2.650 g/cm<sup>3</sup>  
Liquid Density: 0.9941 g/cm<sup>3</sup>

## Report by Size Class

High Diameter (µm)	Low Diameter (µm)	Average Diameter (µm)	Cumulative Mass Finer (Percent)	Mass Frequency (Percent)
710.0	600.0	652.7	100.0	0.0
600.0	500.0	547.7	100.0	0.0
500.0	425.0	461.0	100.0	0.0
425.0	355.0	388.4	100.0	0.0
355.0	300.0	326.3	100.0	0.0
300.0	250.0	273.9	100.0	0.0
250.0	212.0	230.2	99.9	0.1
212.0	180.0	195.3	99.8	0.1
180.0	150.0	164.3	99.5	0.3
150.0	125.0	136.9	96.2	3.3
125.0	106.0	115.1	57.2	39.0
106.0	90.00	97.67	14.1	43.1
90.00	75.00	82.16	4.2	9.9
75.00	63.00	68.74	0.0	4.2

Mass Frequency vs Diameter



## Summary Report

Full scale pump speed: 3  
Bubble detection: Medium  
Starting Size: 63.00 µm  
Ending Size: 0.50 µm

Stir time: 30 secs  
Stir speed: Low  
Probe time: 30 secs

Sample: TT-43-08 2-5 cm  
 Operator: Clint Edrington  
 Submitter: Clint Edrington  
 File Name: C:\EDRING~1\TIGER&~1\SANDFR~1\TT-43-08\43\_2-5CM.SMP  
 Material/Liquid: silicate mud/water/Water

Reported: 01/04/10 16:09:17  
 Liquid Visc: 0.7225 cp

Sample Density: 2.650 g/cm<sup>3</sup>  
 Liquid Density: 0.9941 g/cm<sup>3</sup>

## Summary Report

Parameter 1 0.000

Parameter 2 0.000

Parameter 3 0.000

## Mass Distribution Arithmetic Statistics

Mean	103.4	Std. Dev.	15.35
Median	103.2	Coef. Var.	0.148
Mode	97.67	Skewness	0.706
		Kurtosis	6.038

## Selected Percentiles

Percent Finer	Diameter (µm)
100.0	651.9
80.0	115.2
60.0	107.2
40.0	99.71
20.0	92.70

## Selected Sizes

Diameter (µm)	Percent Finer
500.0	100.0
250.0	100.0
125.0	96.2
88.00	10.9
63.00	0.0

Peak Number	% of Dist. *	Mean	Mode	Median	Standard Deviation	Skewness	Kurtosis
1	100.0	103.4	97.67	103.2	15.35	0.706	6.038

\* Peaks must comprise at least 5.00 % of the distribution.

Micromeritics

WIN5100 V2.03

Page 1

Sample: TT-43-08 50 cm  
Operator: Clint Edrington  
Submitter: Clint Edrington  
File Name: C:\EDRING~1\TIGER&~1\SANDFR~1\TT-43-08\43\_50CM.SMP  
Material/Liquid: silicate mud/water/Water

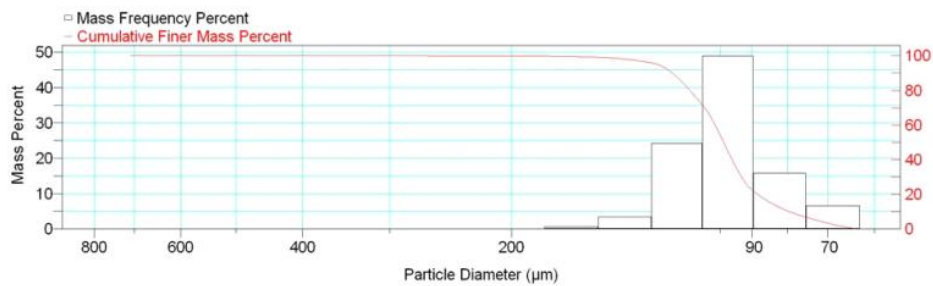
Reported: 01/04/10 16:11:21  
Liquid Visc: 0.7225 cp

Sample Density: 2.650 g/cm<sup>3</sup>  
Liquid Density: 0.9941 g/cm<sup>3</sup>

Report by Size Class

High Diameter (µm)	Low Diameter (µm)	Average Diameter (µm)	Cumulative Mass Finer (Percent)	Mass Frequency (Percent)
850.0	710.0	776.9	100.0	0.0
710.0	600.0	652.7	100.0	0.0
600.0	500.0	547.7	100.0	0.0
500.0	425.0	461.0	100.0	0.0
425.0	355.0	388.4	100.0	0.0
355.0	300.0	326.3	100.0	0.0
300.0	250.0	273.9	99.9	0.1
250.0	212.0	230.2	99.8	0.1
212.0	180.0	195.3	99.7	0.1
180.0	150.0	164.3	99.1	0.6
150.0	125.0	136.9	95.7	3.4
125.0	106.0	115.1	71.4	24.3
106.0	90.00	97.67	22.4	49.0
90.00	75.00	82.16	6.6	15.8
75.00	63.00	68.74	0.0	6.6

Mass Frequency vs Diameter



Summary Report

Full scale pump speed: 3  
Bubble detection: Medium  
Starting Size: 63.00 µm  
Ending Size: 0.50 µm

Stir time: 30 secs  
Stir speed: Low  
Probe time: 30 secs

Sample: TT-43-08 50 cm  
 Operator: Clint Edrington  
 Submitter: Clint Edrington  
 File Name: C:\EDRING~1\TIGER&~1\SANDFR~1\TT-43-08\43\_50CM.SMP  
 Material/Liquid: silicate mud/water/Water

Reported: 01/04/10 16:11:21  
 Liquid Visc: 0.7225 cp

Sample Density: 2.650 g/cm<sup>3</sup>  
 Liquid Density: 0.9941 g/cm<sup>3</sup>

## Summary Report

Parameter 1	0.000	Parameter 2	0.000	Parameter 3	0.000		
Mass Distribution Arithmetic Statistics							
Mean	99.69	Std. Dev.		17.33			
Median	98.87	Coef. Var.		0.174			
Mode	97.67	Skewness		1.890			
		Kurtosis		14.228			
Selected Percentiles			Selected Sizes				
Percent Finer	Diameter (µm)		Diameter (µm)	Percent Finer			
100.0	714.1		500.0	100.0			
80.0	110.6		250.0	99.9			
60.0	101.7		125.0	95.7			
40.0	96.17		88.00	19.5			
20.0	88.38		63.00	0.0			
Peak Number	% of Dist.*	Mean	Mode	Median	Standard Deviation	Skewness	Kurtosis
1	100.0	99.69	97.67	98.87	17.33	1.890	14.228

\* Peaks must comprise at least 5.00 % of the distribution.



# Micromeritics

WIN5100 V2.03

Page 1

Sample: TT-43-08 94 cm  
Operator: Clint Edrington  
Submitter: Clint Edrington  
File Name: C:\EDRING~1\TIGER&~1\SANDFR~1\TT-43-08\43\_94CM.SMP  
Material/Liquid: silicate mud/water/Water

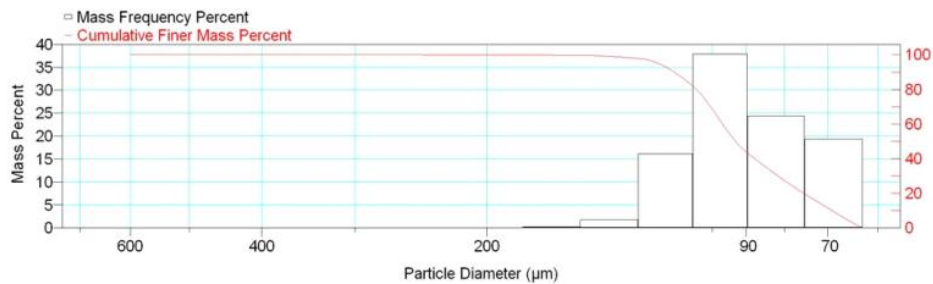
Reported: 01/04/10 16:13:26  
Liquid Visc: 0.7225 cp

Sample Density: 2.650 g/cm<sup>3</sup>  
Liquid Density: 0.9941 g/cm<sup>3</sup>

## Report by Size Class

High Diameter (μm)	Low Diameter (μm)	Average Diameter (μm)	Cumulative Mass Finer (Percent)	Mass Frequency (Percent)
710.0	600.0	652.7	100.0	0.0
600.0	500.0	547.7	100.0	0.0
500.0	425.0	461.0	100.0	0.0
425.0	355.0	388.4	100.0	0.0
355.0	300.0	326.3	100.0	0.0
300.0	250.0	273.9	100.0	0.0
250.0	212.0	230.2	99.9	0.1
212.0	180.0	195.3	99.8	0.1
180.0	150.0	164.3	99.6	0.2
150.0	125.0	136.9	97.8	1.8
125.0	106.0	115.1	81.7	16.1
106.0	90.00	97.67	43.8	37.9
90.00	75.00	82.16	19.4	24.4
75.00	63.00	68.74	0.0	19.4

Mass Frequency vs Diameter



## Summary Report

Full scale pump speed: 3  
Bubble detection: Medium  
Starting Size: 63.00 μm  
Ending Size: 0.50 μm

Stir time: 30 secs  
Stir speed: Low  
Probe time: 30 secs

Sample: TT-43-08 94 cm  
 Operator: Clint Edrington  
 Submitter: Clint Edrington  
 File Name: C:\EDRING~1\TIGER&~1\SANDFR~1\TT-43-08\43\_94CM.SMP  
 Material/Liquid: silicate mud/water/Water

Reported: 01/04/10 16:13:26  
 Liquid Visc: 0.7225 cp

Sample Density: 2.650 g/cm<sup>3</sup>  
 Liquid Density: 0.9941 g/cm<sup>3</sup>

## Summary Report

Parameter 1 0.000

Parameter 2 0.000

Parameter 3 0.000

## Mass Distribution Arithmetic Statistics

Mean	92.15	Std. Dev.	17.42
Median	93.00	Coef. Var.	0.189
Mode	97.67	Skewness	1.018
		Kurtosis	4.707

## Selected Percentiles

Percent Finer	Diameter (µm)
100.0	651.9
80.0	105.0
60.0	96.78
40.0	87.69
20.0	75.39

## Selected Sizes

Diameter (µm)	Percent Finer
500.0	100.0
250.0	100.0
125.0	97.8
88.00	40.5
63.00	0.0

Peak Number	% of Dist. *	Mean	Mode	Median	Standard Deviation	Skewness	Kurtosis
1	100.0	92.15	97.67	93.00	17.42	1.018	4.707

\* Peaks must comprise at least 5.00 % of the distribution.

# Micromeritics

WIN5100 V2.03

Page 1

Sample: TT-43-08 150 cm  
Operator: Clint Edrington  
Submitter: Clint Edrington  
File Name: C:\EDRING~1\TIGER&~1\SANDFR~1\TT-43-08\43\_150CM.SMP  
Material/Liquid: silicate mud/water/Water

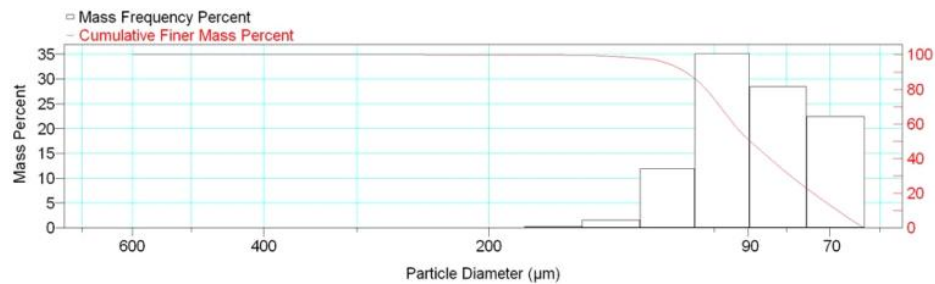
Reported: 01/04/10 16:15:39  
Liquid Visc: 0.7225 cp

Sample Density: 2.650 g/cm<sup>3</sup>  
Liquid Density: 0.9941 g/cm<sup>3</sup>

## Report by Size Class

High Diameter (µm)	Low Diameter (µm)	Average Diameter (µm)	Cumulative Mass Finer (Percent)	Mass Frequency (Percent)
710.0	600.0	652.7	100.0	0.0
600.0	500.0	547.7	100.0	0.0
500.0	425.0	461.0	100.0	0.0
425.0	355.0	388.4	100.0	0.0
355.0	300.0	326.3	100.0	0.0
300.0	250.0	273.9	100.0	0.0
250.0	212.0	230.2	99.9	0.1
212.0	180.0	195.3	99.9	0.0
180.0	150.0	164.3	99.6	0.3
150.0	125.0	136.9	98.0	1.6
125.0	106.0	115.1	86.1	11.9
106.0	90.00	97.67	51.0	35.1
90.00	75.00	82.16	22.5	28.5
75.00	63.00	68.74	0.0	22.5

Mass Frequency vs Diameter



## Summary Report

Full scale pump speed: 3  
Bubble detection: Medium  
Starting Size: 63.00 µm  
Ending Size: 0.50 µm

Stir time: 30 secs  
Stir speed: Low  
Probe time: 30 secs

Sample: TT-43-08 150 cm  
 Operator: Clint Edrington  
 Submitter: Clint Edrington  
 File Name: C:\EDRING~1\TIGER&~1\SANDFR~1\TT-43-08\43\_150CM.SMP  
 Material/Liquid: silicate mud/water/Water

Reported: 01/04/10 16:15:39  
 Liquid Visc: 0.7225 cp

Sample Density: 2.650 g/cm<sup>3</sup>  
 Liquid Density: 0.9941 g/cm<sup>3</sup>

## Summary Report

Parameter 1		0.000		Parameter 2		0.000		Parameter 3		0.000	
Mass Distribution Arithmetic Statistics											
Mean	89.78			Std. Dev.			16.92				
Median	89.46			Coef. Var.			0.188				
Mode	97.67			Skewness			1.151				
				Kurtosis			5.003				
Selected Percentiles						Selected Sizes					
Percent Finer		Diameter (µm)				Diameter (µm)		Percent Finer			
100.0		651.9				500.0		100.0			
80.0		102.5				250.0		100.0			
60.0		94.10				125.0		98.0			
40.0		84.17				88.00		47.3			
20.0		73.65				63.00		0.0			
Peak Number	% of Dist.*	Mean	Mode	Median	Standard Deviation	Skewness	Kurtosis				
1	99.9	89.64	97.67	89.43	16.34	0.670	0.777				

\* Peaks must comprise at least 5.00 % of the distribution.

Micromeritics

WIN5100 V2.03

Page 1

Sample: TT-43-08 200 cm  
Operator: Clint Edrington  
Submitter: Clint Edrington  
File Name: C:\EDRING~1\TIGER&~1\SANDFR~1\TT-43-08\43\_200CM.SMP  
Material/Liquid: silicate mud/water/Water

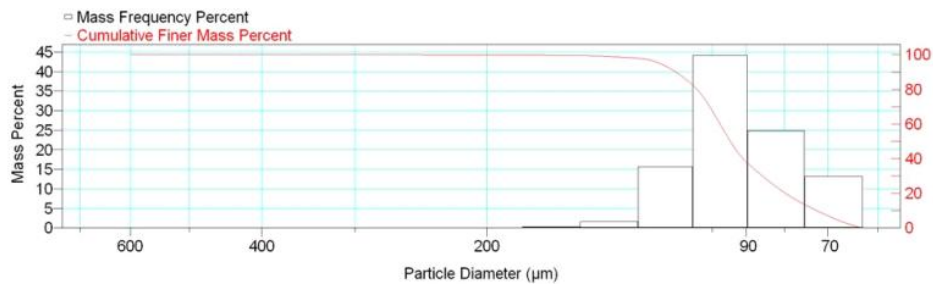
Reported: 01/04/10 16:17:35  
Liquid Visc: 0.7225 cp

Sample Density: 2.650 g/cm<sup>3</sup>  
Liquid Density: 0.9941 g/cm<sup>3</sup>

Report by Size Class

High Diameter (μm)	Low Diameter (μm)	Average Diameter (μm)	Cumulative Mass Finer (Percent)	Mass Frequency (Percent)
710.0	600.0	652.7	100.0	0.0
600.0	500.0	547.7	100.0	0.0
500.0	425.0	461.0	100.0	0.0
425.0	355.0	388.4	100.0	0.0
355.0	300.0	326.3	100.0	0.0
300.0	250.0	273.9	100.0	0.0
250.0	212.0	230.2	99.9	0.1
212.0	180.0	195.3	99.8	0.1
180.0	150.0	164.3	99.5	0.3
150.0	125.0	136.9	97.9	1.6
125.0	106.0	115.1	82.3	15.6
106.0	90.00	97.67	38.1	44.2
90.00	75.00	82.16	13.2	24.9
75.00	63.00	68.74	0.0	13.2

Mass Frequency vs Diameter



Summary Report

Full scale pump speed: 3  
Bubble detection: Medium  
Starting Size: 63.00 μm  
Ending Size: 0.50 μm

Stir time: 30 secs  
Stir speed: Low  
Probe time: 30 secs

Sample: TT-43-08 200 cm  
 Operator: Clint Edrington  
 Submitter: Clint Edrington  
 File Name: C:\EDRING~1\TIGER&~1\SANDFR~1\TT-43-08\43\_200CM.SMP  
 Material/Liquid: silicate mud/water/Water

Reported: 01/04/10 16:17:35  
 Liquid Visc: 0.7225 cp

Sample Density: 2.650 g/cm<sup>3</sup>  
 Liquid Density: 0.9941 g/cm<sup>3</sup>

## Summary Report

Parameter 1 0.000

Parameter 2 0.000

Parameter 3 0.000

## Mass Distribution Arithmetic Statistics

Mean	93.77	Std. Dev.	16.36
Median	94.50	Coef. Var.	0.174
Mode	97.67	Skewness	1.144
		Kurtosis	6.372

## Selected Percentiles

Percent Finer	Diameter (µm)
100.0	651.9
80.0	104.7
60.0	97.56
40.0	90.91
20.0	79.76

## Selected Sizes

Diameter (µm)	Percent Finer
500.0	100.0
250.0	100.0
125.0	97.9
88.00	34.3
63.00	0.0

Peak Number	% of Dist. *	Mean	Mode	Median	Standard Deviation	Skewness	Kurtosis
1	100.0	93.77	97.67	94.50	16.36	1.144	6.372

\* Peaks must comprise at least 5.00 % of the distribution.

Micromeritics

WIN5100 V2.03

Page 1

Sample: TT-44-08 4 cm  
Operator: Clint Edrington  
Submitter: Clint Edrington  
File Name: C:\EDRING~1\TIGER&~1\SANDFR~1\TT-44-08\44\_4CM.SMP  
Material/Liquid: silicate mud/water/Water

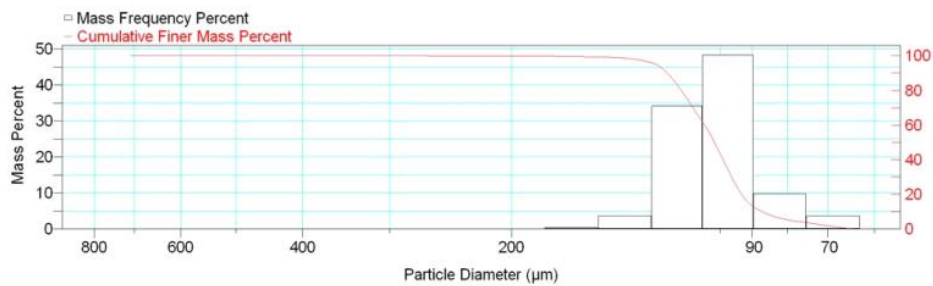
Reported: 01/04/10 16:20:38  
Liquid Visc: 0.7225 cp

Sample Density: 2.650 g/cm<sup>3</sup>  
Liquid Density: 0.9941 g/cm<sup>3</sup>

Report by Size Class

High Diameter ( $\mu\text{m}$ )	Low Diameter ( $\mu\text{m}$ )	Average Diameter ( $\mu\text{m}$ )	Cumulative Mass Finer (Percent)	Mass Frequency (Percent)
850.0	710.0	776.9	100.0	0.0
710.0	600.0	652.7	100.0	0.0
600.0	500.0	547.7	100.0	0.0
500.0	425.0	461.0	100.0	0.0
425.0	355.0	388.4	100.0	0.0
355.0	300.0	326.3	100.0	0.0
300.0	250.0	273.9	99.9	0.1
250.0	212.0	230.2	99.8	0.1
212.0	180.0	195.3	99.7	0.1
180.0	150.0	164.3	99.3	0.4
150.0	125.0	136.9	95.7	3.6
125.0	106.0	115.1	61.6	34.1
106.0	90.00	97.67	13.3	48.3
90.00	75.00	82.16	3.6	9.7
75.00	63.00	68.74	0.0	3.6

Mass Frequency vs Diameter



Summary Report

Full scale pump speed: 3  
Bubble detection: Medium  
Starting Size: 63.00  $\mu\text{m}$   
Ending Size: 0.50  $\mu\text{m}$

Stir time: 30 secs  
Stir speed: Low  
Probe time: 30 secs

Sample: TT-44-08 4 cm  
 Operator: Clint Edrington  
 Submitter: Clint Edrington  
 File Name: C:\EDRING~1\TIGER&~1\SANDFR~1\TT-44-08\44\_4CM.SMP  
 Material/Liquid: silicate mud/water/Water

Reported: 01/04/10 16:20:38  
 Liquid Visc: 0.7225 cp

Sample Density: 2.650 g/cm<sup>3</sup>  
 Liquid Density: 0.9941 g/cm<sup>3</sup>

## Summary Report

Parameter 1	0.000	Parameter 2	0.000	Parameter 3	0.000		
Mass Distribution Arithmetic Statistics							
Mean	103.2	Std. Dev.		16.08			
Median	102.0	Coef. Var.		0.156			
Mode	97.67	Skewness		1.985			
		Kurtosis		17.382			
Selected Percentiles			Selected Sizes				
Percent Finer	Diameter (µm)		Diameter (µm)	Percent Finer			
100.0	714.1		500.0	100.0			
80.0	113.9		250.0	99.9			
60.0	105.3		125.0	95.7			
40.0	99.10		88.00	10.9			
20.0	93.17		63.00	0.0			
Peak Number	% of Dist.*	Mean	Mode	Median	Standard Deviation	Skewness	Kurtosis
1	100.0	103.2	97.67	102.0	16.08	1.985	17.382

\* Peaks must comprise at least 5.00 % of the distribution.



Micromeritics

WIN5100 V2.03

Page 1

Sample: TT-44-08 50 cm  
Operator: Clint Edrington  
Submitter: Clint Edrington  
File Name: C:\EDRING~1\TIGER&~1\SANDFR~1\TT-44-08\44\_50CM.SMP  
Material/Liquid: silicate mud/water/Water

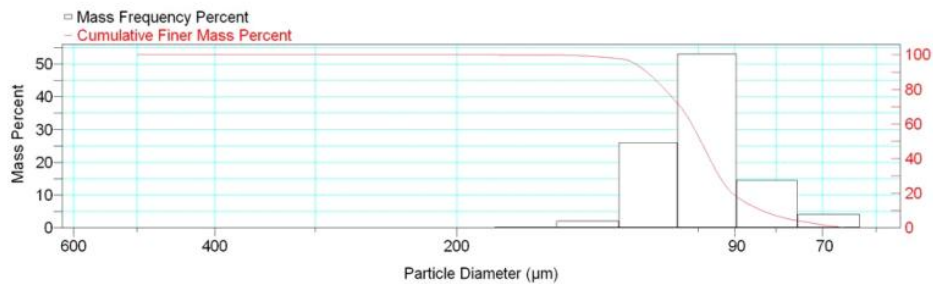
Reported: 01/04/10 16:24:18  
Liquid Visc: 0.7225 cp

Sample Density: 2.650 g/cm<sup>3</sup>  
Liquid Density: 0.9941 g/cm<sup>3</sup>

Report by Size Class

High Diameter (µm)	Low Diameter (µm)	Average Diameter (µm)	Cumulative Mass Finer (Percent)	Mass Frequency (Percent)
600.0	500.0	547.7	100.0	0.0
500.0	425.0	461.0	100.0	0.0
425.0	355.0	388.4	100.0	0.0
355.0	300.0	326.3	100.0	0.0
300.0	250.0	273.9	100.0	0.0
250.0	212.0	230.2	100.0	0.0
212.0	180.0	195.3	100.0	0.0
180.0	150.0	164.3	99.8	0.2
150.0	125.0	136.9	97.7	2.1
125.0	106.0	115.1	71.8	25.9
106.0	90.00	97.67	18.7	53.1
90.00	75.00	82.16	4.1	14.6
75.00	63.00	68.74	0.0	4.1

Mass Frequency vs Diameter



Summary Report

Full scale pump speed: 3  
Bubble detection: Medium  
Starting Size: 63.00 µm  
Ending Size: 0.50 µm

Stir time: 30 secs  
Stir speed: Low  
Probe time: 30 secs

Parameter 1 0.000

Parameter 2 0.000

Parameter 3 0.000

Sample: TT-44-08 50 cm  
 Operator: Clint Edrington  
 Submitter: Clint Edrington  
 File Name: C:\EDRING~1\TIGER&~1\SANDFR~1\TT-44-08\44\_50CM.SMP  
 Material/Liquid: silicate mud/water/Water

Reported: 01/04/10 16:24:18  
 Liquid Visc: 0.7225 cp

Sample Density: 2.650 g/cm<sup>3</sup>  
 Liquid Density: 0.9941 g/cm<sup>3</sup>

## Summary Report

## Mass Distribution Arithmetic Statistics

Mean	99.70	Std. Dev.	13.61
Median	99.24	Coef. Var.	0.137
Mode	97.67	Skewness	0.224
		Kurtosis	1.113

## Selected Percentiles

Percent Finer	Diameter (µm)
100.0	553.2
80.0	110.1
60.0	101.9
40.0	96.77
20.0	90.72

## Selected Sizes

Diameter (µm)	Percent Finer
500.0	100.0
250.0	100.0
125.0	97.7
88.00	15.7
63.00	0.0

Peak Number	% of Dist.*	Mean	Mode	Median	Standard Deviation	Skewness	Kurtosis
1	100.0	99.70	97.67	99.24	13.61	0.224	1.113

\* Peaks must comprise at least 5.00 % of the distribution.

# Micromeritics

WIN5100 V2.03

Page 1

Sample: TT-44-08 103 cm  
Operator: Clint Edrington  
Submitter: Clint Edrington  
File Name: C:\EDRING~1\TIGER&~1\SANDFR~1\TT-44-08\44\_103CM.SMP  
Material/Liquid: silicate mud/water/Water

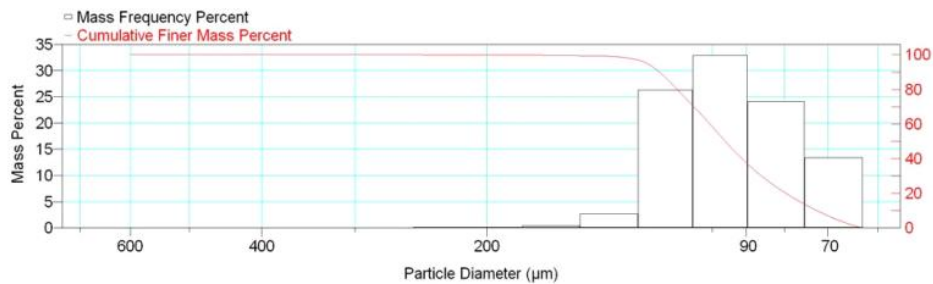
Reported: 01/04/10 16:26:19  
Liquid Visc: 0.7225 cp

Sample Density: 2.650 g/cm<sup>3</sup>  
Liquid Density: 0.9941 g/cm<sup>3</sup>

## Report by Size Class

High Diameter (µm)	Low Diameter (µm)	Average Diameter (µm)	Cumulative Mass Finer (Percent)	Mass Frequency (Percent)
710.0	600.0	652.7	100.0	0.0
600.0	500.0	547.7	100.0	0.0
500.0	425.0	461.0	100.0	0.0
425.0	355.0	388.4	100.0	0.0
355.0	300.0	326.3	100.0	0.0
300.0	250.0	273.9	100.0	0.0
250.0	212.0	230.2	99.9	0.1
212.0	180.0	195.3	99.8	0.1
180.0	150.0	164.3	99.4	0.4
150.0	125.0	136.9	96.7	2.7
125.0	106.0	115.1	70.4	26.3
106.0	90.00	97.67	37.5	32.9
90.00	75.00	82.16	13.4	24.1
75.00	63.00	68.74	0.0	13.4

Mass Frequency vs Diameter



## Summary Report

Full scale pump speed: 3  
Bubble detection: Medium  
Starting Size: 63.00 µm  
Ending Size: 0.50 µm

Stir time: 30 secs  
Stir speed: Low  
Probe time: 30 secs

Sample: TT-44-08 103 cm  
 Operator: Clint Edrington  
 Submitter: Clint Edrington  
 File Name: C:\EDRING~1\TIGER&~1\SANDFR~1\TT-44-08\44\_103CM.SMP  
 Material/Liquid: silicate mud/water/Water

Reported: 01/04/10 16:26:19  
 Liquid Visc: 0.7225 cp

Sample Density: 2.650 g/cm<sup>3</sup>  
 Liquid Density: 0.9941 g/cm<sup>3</sup>

## Summary Report

Parameter 1 0.000

Parameter 2 0.000

Parameter 3 0.000

## Mass Distribution Arithmetic Statistics

Mean	96.20	Std. Dev.	18.29
Median	96.01	Coef. Var.	0.190
Mode	97.67	Skewness	0.786
		Kurtosis	3.247

## Selected Percentiles

Percent Finer	Diameter (µm)
100.0	651.9
80.0	111.3
60.0	100.7
40.0	91.28
20.0	79.65

## Selected Sizes

Diameter (µm)	Percent Finer
500.0	100.0
250.0	100.0
125.0	96.7
88.00	33.8
63.00	0.0

Peak Number	% of Dist. *	Mean	Mode	Median	Standard Deviation	Skewness	Kurtosis
1	100.0	96.20	97.67	96.01	18.29	0.786	3.247

\* Peaks must comprise at least 5.00 % of the distribution.

# Micromeritics

WIN5100 V2.03

Page 1

Sample: TT-44-08 150 cm  
Operator: Clint Edrington  
Submitter: Clint Edrington  
File Name: C:\EDRING~1\TIGER&~1\SANDFR~1\TT-44-08\44\_150CM.SMP  
Material/Liquid: silicate mud/water/Water

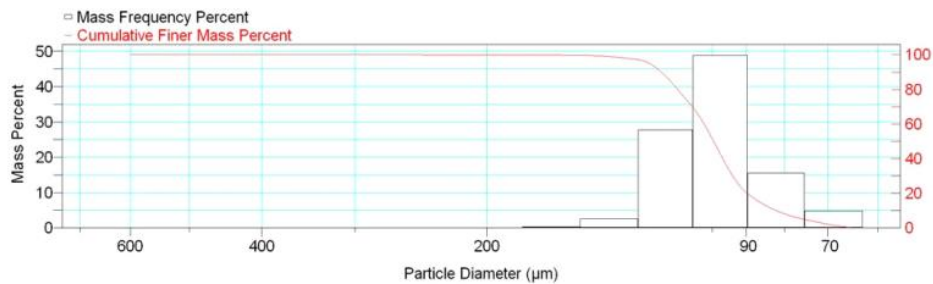
Reported: 01/04/10 16:28:13  
Liquid Visc: 0.7225 cp

Sample Density: 2.650 g/cm<sup>3</sup>  
Liquid Density: 0.9941 g/cm<sup>3</sup>

## Report by Size Class

High Diameter (μm)	Low Diameter (μm)	Average Diameter (μm)	Cumulative Mass Finer (Percent)	Mass Frequency (Percent)
710.0	600.0	652.7	100.0	0.0
600.0	500.0	547.7	100.0	0.0
500.0	425.0	461.0	100.0	0.0
425.0	355.0	388.4	100.0	0.0
355.0	300.0	326.3	100.0	0.0
300.0	250.0	273.9	100.0	0.0
250.0	212.0	230.2	99.9	0.1
212.0	180.0	195.3	99.9	0.0
180.0	150.0	164.3	99.6	0.3
150.0	125.0	136.9	97.0	2.6
125.0	106.0	115.1	69.3	27.7
106.0	90.00	97.67	20.4	48.9
90.00	75.00	82.16	4.8	15.6
75.00	63.00	68.74	0.0	4.8

Mass Frequency vs Diameter



## Summary Report

Full scale pump speed: 3  
Bubble detection: Medium  
Starting Size: 63.00 μm  
Ending Size: 0.50 μm

Stir time: 30 secs  
Stir speed: Low  
Probe time: 30 secs

Sample: TT-44-08 150 cm  
 Operator: Clint Edrington  
 Submitter: Clint Edrington  
 File Name: C:\EDRING~1\TIGER&~1\SANDFR~1\TT-44-08\44\_150CM.SMP  
 Material/Liquid: silicate mud/water/Water

Reported: 01/04/10 16:28:13  
 Liquid Visc: 0.7225 cp

Sample Density: 2.650 g/cm<sup>3</sup>  
 Liquid Density: 0.9941 g/cm<sup>3</sup>

## Summary Report

Parameter 1 0.000

Parameter 2 0.000

Parameter 3 0.000

## Mass Distribution Arithmetic Statistics

Mean	100.0	Std. Dev.	15.08
Median	99.51	Coef. Var.	0.151
Mode	97.67	Skewness	0.841
		Kurtosis	5.960

## Selected Percentiles

Percent Finer	Diameter (µm)
100.0	651.9
80.0	111.2
60.0	102.5
40.0	96.74
20.0	89.76

## Selected Sizes

Diameter (µm)	Percent Finer
500.0	100.0
250.0	100.0
125.0	97.0
88.00	17.2
63.00	0.0

Peak Number	% of Dist. *	Mean	Mode	Median	Standard Deviation	Skewness	Kurtosis
1	99.9	99.92	97.67	99.49	14.51	0.248	0.976

\* Peaks must comprise at least 5.00 % of the distribution.

# Micromeritics

WIN5100 V2.03

Page 1

Sample: TT-44-08 200 cm  
Operator: Clint Edrington  
Submitter: Clint Edrington  
File Name: C:\EDRING~1\TIGER&~1\SANDFR~1\TT-44-08\44\_200CM.SMP  
Material/Liquid: silicate mud/water/Water

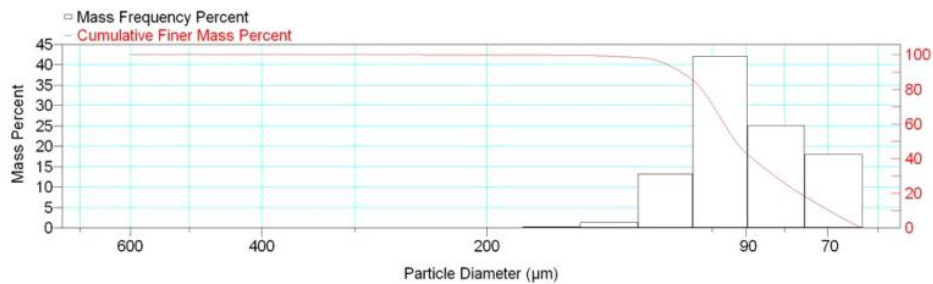
Reported: 01/04/10 16:30:26  
Liquid Visc: 0.7225 cp

Sample Density: 2.650 g/cm<sup>3</sup>  
Liquid Density: 0.9941 g/cm<sup>3</sup>

## Report by Size Class

High Diameter (μm)	Low Diameter (μm)	Average Diameter (μm)	Cumulative Mass Finer (Percent)	Mass Frequency (Percent)
710.0	600.0	652.7	100.0	0.0
600.0	500.0	547.7	100.0	0.0
500.0	425.0	461.0	100.0	0.0
425.0	355.0	388.4	100.0	0.0
355.0	300.0	326.3	100.0	0.0
300.0	250.0	273.9	100.0	0.0
250.0	212.0	230.2	99.9	0.1
212.0	180.0	195.3	99.8	0.1
180.0	150.0	164.3	99.6	0.2
150.0	125.0	136.9	98.3	1.3
125.0	106.0	115.1	85.1	13.2
106.0	90.00	97.67	43.1	42.0
90.00	75.00	82.16	18.0	25.1
75.00	63.00	68.74	0.0	18.0

Mass Frequency vs Diameter



## Summary Report

Full scale pump speed: 3  
Bubble detection: Medium  
Starting Size: 63.00 μm  
Ending Size: 0.50 μm

Stir time: 30 secs  
Stir speed: Low  
Probe time: 30 secs

Sample: TT-44-08 200 cm  
 Operator: Clint Edrington  
 Submitter: Clint Edrington  
 File Name: C:\EDRING~1\TIGER&~1\SANDFR~1\TT-44-08\44\_200CM.SMP  
 Material/Liquid: silicate mud/water/Water

Reported: 01/04/10 16:30:26  
 Liquid Visc: 0.7225 cp

Sample Density: 2.650 g/cm<sup>3</sup>  
 Liquid Density: 0.9941 g/cm<sup>3</sup>

## Summary Report

Parameter 1 0.000

Parameter 2 0.000

Parameter 3 0.000

## Mass Distribution Arithmetic Statistics

Mean	91.75	Std. Dev.	16.50
Median	93.00	Coef. Var.	0.180
Mode	97.67	Skewness	1.133
		Kurtosis	6.248

## Selected Percentiles

Percent Finer	Diameter (µm)
100.0	651.9
80.0	103.2
60.0	96.32
40.0	88.23
20.0	76.33

## Selected Sizes

Diameter (µm)	Percent Finer
500.0	100.0
250.0	100.0
125.0	98.3
88.00	39.6
63.00	0.0

Peak Number	% of Dist. *	Mean	Mode	Median	Standard Deviation	Skewness	Kurtosis
1	100.0	91.75	97.67	93.00	16.50	1.133	6.248

\* Peaks must comprise at least 5.00 % of the distribution.



Micromeritics

WIN5100 V2.03

Page 1

Sample: TT-44-08 250 cm  
Operator: Clint Edrington  
Submitter: Clint Edrington  
File Name: C:\EDRING~1\TIGER&~1\SANDFR~1\TT-44-08\44\_250CM.SMP  
Material/Liquid: silicate mud/water/Water

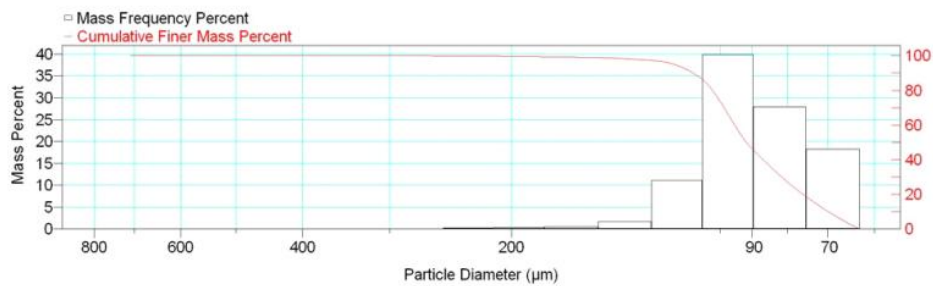
Reported: 01/04/10 16:32:18  
Liquid Visc: 0.7225 cp

Sample Density: 2.650 g/cm<sup>3</sup>  
Liquid Density: 0.9941 g/cm<sup>3</sup>

Report by Size Class

High Diameter ( $\mu\text{m}$ )	Low Diameter ( $\mu\text{m}$ )	Average Diameter ( $\mu\text{m}$ )	Cumulative Mass Finer (Percent)	Mass Frequency (Percent)
850.0	710.0	776.9	100.0	0.0
710.0	600.0	652.7	100.0	0.0
600.0	500.0	547.7	100.0	0.0
500.0	425.0	461.0	100.0	0.0
425.0	355.0	388.4	100.0	0.0
355.0	300.0	326.3	100.0	0.0
300.0	250.0	273.9	99.9	0.1
250.0	212.0	230.2	99.7	0.2
212.0	180.0	195.3	99.4	0.3
180.0	150.0	164.3	98.9	0.5
150.0	125.0	136.9	97.2	1.7
125.0	106.0	115.1	86.1	11.1
106.0	90.00	97.67	46.2	39.9
90.00	75.00	82.16	18.3	27.9
75.00	63.00	68.74	0.0	18.3

Mass Frequency vs Diameter



Summary Report

Full scale pump speed: 3  
Bubble detection: Medium  
Starting Size: 63.00  $\mu\text{m}$   
Ending Size: 0.50  $\mu\text{m}$

Stir time: 30 secs  
Stir speed: Low  
Probe time: 30 secs

Sample: TT-44-08 250 cm  
 Operator: Clint Edrington  
 Submitter: Clint Edrington  
 File Name: C:\EDRING~1\TIGER&~1\SANDFR~1\TT-44-08\44\_250CM.SMP  
 Material/Liquid: silicate mud/water/Water

Reported: 01/04/10 16:32:18  
 Liquid Visc: 0.7225 cp

Sample Density: 2.650 g/cm<sup>3</sup>  
 Liquid Density: 0.9941 g/cm<sup>3</sup>

## Summary Report

Parameter 1	0.000	Parameter 2	0.000	Parameter 3	0.000		
Mass Distribution Arithmetic Statistics							
Mean	91.72	Std. Dev.		19.02			
Median	91.73	Coef. Var.		0.207			
Mode	97.67	Skewness		2.501			
		Kurtosis		15.934			
Selected Percentiles			Selected Sizes				
Percent Finer	Diameter (µm)		Diameter (µm)	Percent Finer			
100.0	714.1		500.0	100.0			
80.0	102.6		250.0	99.9			
60.0	95.36		125.0	97.2			
40.0	86.79		88.00	42.3			
20.0	76.03		63.00	0.0			
Peak Number	% of Dist.*	Mean	Mode	Median	Standard Deviation	Skewness	Kurtosis
1	100.0	91.72	97.67	91.73	19.02	2.501	15.934

\* Peaks must comprise at least 5.00 % of the distribution.

Micromeritics

WIN5100 V2.03

Page 1

Sample: TT-45-08 6 cm  
Operator: Clint Edrington  
Submitter: Clint Edrington  
File Name: C:\EDRING~1\TIGER&~1\SANDFR~1\TT-45-08\45\_6CM.SMP  
Material/Liquid: silicate mud/water/Water

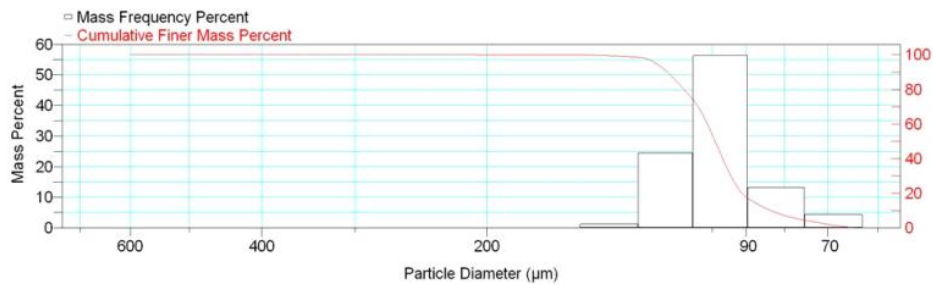
Reported: 01/04/10 18:29:22  
Liquid Visc: 0.7225 cp

Sample Density: 2.650 g/cm<sup>3</sup>  
Liquid Density: 0.9941 g/cm<sup>3</sup>

Report by Size Class

High Diameter (µm)	Low Diameter (µm)	Average Diameter (µm)	Cumulative Mass Finer (Percent)	Mass Frequency (Percent)
710.0	600.0	652.7	100.0	0.0
600.0	500.0	547.7	100.0	0.0
500.0	425.0	461.0	100.0	0.0
425.0	355.0	388.4	100.0	0.0
355.0	300.0	326.3	100.0	0.0
300.0	250.0	273.9	100.0	0.0
250.0	212.0	230.2	100.0	0.0
212.0	180.0	195.3	99.9	0.1
180.0	150.0	164.3	99.8	0.1
150.0	125.0	136.9	98.5	1.3
125.0	106.0	115.1	74.0	24.5
106.0	90.00	97.67	17.7	56.3
90.00	75.00	82.16	4.4	13.3
75.00	63.00	68.74	0.0	4.4

Mass Frequency vs Diameter



Summary Report

Full scale pump speed: 3  
Bubble detection: Medium  
Starting Size: 63.00 µm  
Ending Size: 0.50 µm

Stir time: 30 secs  
Stir speed: Low  
Probe time: 30 secs

Sample: TT-45-08 6 cm  
 Operator: Clint Edrington  
 Submitter: Clint Edrington  
 File Name: C:\EDRING~1\TIGER&~1\SANDFR~1\TT-45-08\45\_6CM.SMP  
 Material/Liquid: silicate mud/water/Water

Reported: 01/04/10 18:29:22  
 Liquid Visc: 0.7225 cp

Sample Density: 2.650 g/cm<sup>3</sup>  
 Liquid Density: 0.9941 g/cm<sup>3</sup>

## Summary Report

Parameter 1		0.000		Parameter 2		0.000		Parameter 3		0.000	
Mass Distribution Arithmetic Statistics											
Mean	99.28			Std. Dev.			13.22				
Median	99.03			Coef. Var.			0.133				
Mode	97.67			Skewness			0.391				
				Kurtosis			3.361				
Selected Percentiles						Selected Sizes					
Percent Finer		Diameter (µm)				Diameter (µm)		Percent Finer			
100.0		600.3				500.0		100.0			
80.0		109.0				250.0		100.0			
60.0		101.4				125.0		98.5			
40.0		96.76				88.00		15.0			
20.0		91.22				63.00		0.0			
Peak Number	% of Dist.*	Mean	Mode	Median	Standard Deviation	Skewness	Kurtosis				
1	99.9	99.19	97.67	99.02	12.87	0.030	0.979				

\* Peaks must comprise at least 5.00 % of the distribution.

Micromeritics

WIN5100 V2.03

Page 1

Sample: TT-45-08 50 cm  
Operator: Clint Edrington  
Submitter: Clint Edrington  
File Name: C:\EDRING~1\TIGER&~1\SANDFR~1\TT-45-08\45\_50CM.SMP  
Material/Liquid: silicate mud/water/Water

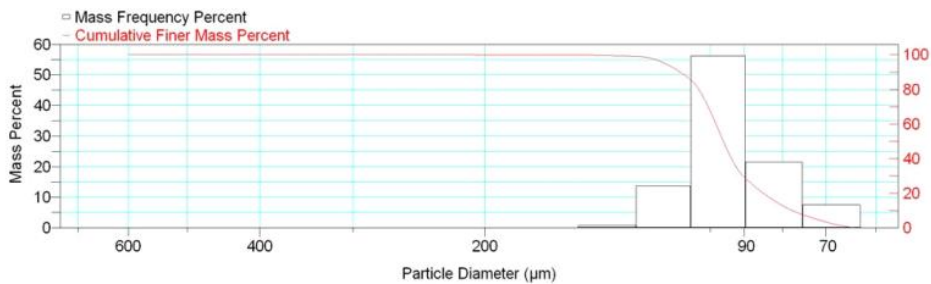
Reported: 01/04/10 18:31:30  
Liquid Visc: 0.7225 cp

Sample Density: 2.650 g/cm<sup>3</sup>  
Liquid Density: 0.9941 g/cm<sup>3</sup>

Report by Size Class

High Diameter (µm)	Low Diameter (µm)	Average Diameter (µm)	Cumulative Mass Finer (Percent)	Mass Frequency (Percent)
710.0	600.0	652.7	100.0	0.0
600.0	500.0	547.7	100.0	0.0
500.0	425.0	461.0	100.0	0.0
425.0	355.0	388.4	100.0	0.0
355.0	300.0	326.3	100.0	0.0
300.0	250.0	273.9	100.0	0.0
250.0	212.0	230.2	100.0	0.0
212.0	180.0	195.3	99.9	0.1
180.0	150.0	164.3	99.8	0.1
150.0	125.0	136.9	99.0	0.8
125.0	106.0	115.1	85.3	13.7
106.0	90.00	97.67	29.1	56.2
90.00	75.00	82.16	7.5	21.6
75.00	63.00	68.74	0.0	7.5

Mass Frequency vs Diameter



Summary Report

Full scale pump speed: 3  
Bubble detection: Medium  
Starting Size: 63.00 µm  
Ending Size: 0.50 µm

Stir time: 30 secs  
Stir speed: Low  
Probe time: 30 secs

Sample: TT-45-08 50 cm  
 Operator: Clint Edrington  
 Submitter: Clint Edrington  
 File Name: C:\EDRING~1\TIGER&~1\SANDFR~1\TT-45-08\45\_50CM.SMP  
 Material/Liquid: silicate mud/water/Water

Reported: 01/04/10 18:31:30  
 Liquid Visc: 0.7225 cp

Sample Density: 2.650 g/cm<sup>3</sup>  
 Liquid Density: 0.9941 g/cm<sup>3</sup>

## Summary Report

Parameter 1 0.000

Parameter 2 0.000

Parameter 3 0.000

## Mass Distribution Arithmetic Statistics

Mean	95.02	Std. Dev.	13.26
Median	95.97	Coef. Var.	0.139
Mode	97.67	Skewness	0.529
		Kurtosis	3.903

## Selected Percentiles

Percent Finer	Diameter (µm)
100.0	600.3
80.0	103.5
60.0	98.22
40.0	93.60
20.0	84.83

## Selected Sizes

Diameter (µm)	Percent Finer
500.0	100.0
250.0	100.0
125.0	99.0
88.00	25.4
63.00	0.0

Peak Number	% of Dist. *	Mean	Mode	Median	Standard Deviation	Skewness	Kurtosis
1	99.9	94.92	97.67	95.96	12.88	0.128	1.074

\* Peaks must comprise at least 5.00 % of the distribution.

Micromeritics

WIN5100 V2.03

Page 1

Sample: TT-45-08 98 cm  
Operator: Clint Edrington  
Submitter: Clint Edrington  
File Name: C:\EDRING~1\TIGER&~1\SANDFR~1\TT-45-08\45\_98CM.SMP  
Material/Liquid: silicate mud/water/Water

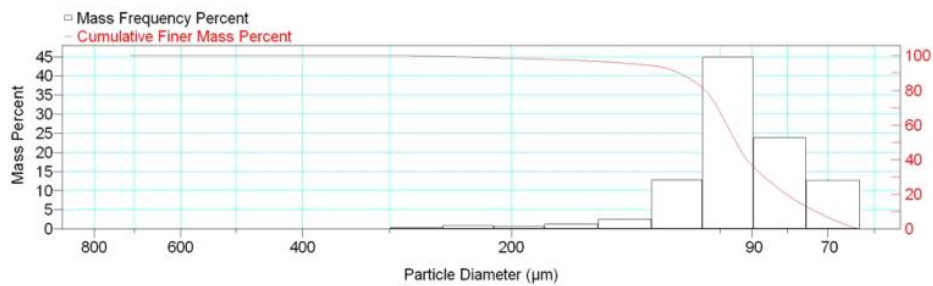
Reported: 01/04/10 18:33:53  
Liquid Visc: 0.7225 cp

Sample Density: 2.650 g/cm<sup>3</sup>  
Liquid Density: 0.9941 g/cm<sup>3</sup>

Report by Size Class

High Diameter (µm)	Low Diameter (µm)	Average Diameter (µm)	Cumulative Mass Finer (Percent)	Mass Frequency (Percent)
850.0	710.0	776.9	100.0	0.0
710.0	600.0	652.7	100.0	0.0
600.0	500.0	547.7	100.0	0.0
500.0	425.0	461.0	100.0	0.0
425.0	355.0	388.4	100.0	0.0
355.0	300.0	326.3	100.0	0.0
300.0	250.0	273.9	99.6	0.4
250.0	212.0	230.2	98.7	0.9
212.0	180.0	195.3	98.0	0.7
180.0	150.0	164.3	96.7	1.3
150.0	125.0	136.9	94.2	2.5
125.0	106.0	115.1	81.4	12.8
106.0	90.00	97.67	36.5	44.9
90.00	75.00	82.16	12.7	23.8
75.00	63.00	68.74	0.0	12.7

Mass Frequency vs Diameter



Summary Report

Full scale pump speed: 3  
Bubble detection: Medium  
Starting Size: 63.00 µm  
Ending Size: 0.50 µm

Stir time: 30 secs  
Stir speed: Low  
Probe time: 30 secs

Sample: TT-45-08 98 cm  
 Operator: Clint Edrington  
 Submitter: Clint Edrington  
 File Name: C:\EDRING~1\TIGER&~1\SANDFR~1\TT-45-08\45\_98CM.SMP  
 Material/Liquid: silicate mud/water/Water

Reported: 01/04/10 18:33:53  
 Liquid Visc: 0.7225 cp

Sample Density: 2.650 g/cm<sup>3</sup>  
 Liquid Density: 0.9941 g/cm<sup>3</sup>

## Summary Report

Parameter 1	0.000	Parameter 2	0.000	Parameter 3	0.000		
Mass Distribution Arithmetic Statistics							
Mean	96.97	Std. Dev.		25.44			
Median	94.92	Coef. Var.		0.262			
Mode	97.67	Skewness		3.206			
		Kurtosis		15.725			
Selected Percentiles			Selected Sizes				
Percent Finer	Diameter (µm)		Diameter (µm)	Percent Finer			
100.0	714.1		500.0	100.0			
80.0	105.1		250.0	99.6			
60.0	97.83		125.0	94.2			
40.0	91.60		88.00	32.9			
20.0	80.31		63.00	0.0			
Peak Number	% of Dist.*	Mean	Mode	Median	Standard Deviation	Skewness	Kurtosis
1	98.7	95.03	97.67	94.72	19.06	1.675	6.001

\* Peaks must comprise at least 5.00 % of the distribution.



# Micromeritics

WIN5100 V2.03

Page 1

Sample: TT-45-08 150 cm  
Operator: Clint Edrington  
Submitter: Clint Edrington  
File Name: C:\EDRING~1\TIGER&~1\SANDFR~1\TT-45-08\45\_150CM.SMP  
Material/Liquid: silicate mud/water/Water

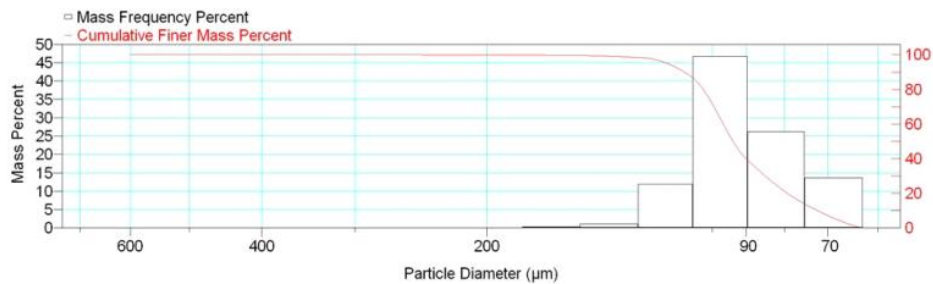
Reported: 01/04/10 18:35:55  
Liquid Visc: 0.7225 cp

Sample Density: 2.650 g/cm<sup>3</sup>  
Liquid Density: 0.9941 g/cm<sup>3</sup>

## Report by Size Class

High Diameter (µm)	Low Diameter (µm)	Average Diameter (µm)	Cumulative Mass Finer (Percent)	Mass Frequency (Percent)
710.0	600.0	652.7	100.0	0.0
600.0	500.0	547.7	100.0	0.0
500.0	425.0	461.0	100.0	0.0
425.0	355.0	388.4	100.0	0.0
355.0	300.0	326.3	100.0	0.0
300.0	250.0	273.9	100.0	0.0
250.0	212.0	230.2	99.9	0.1
212.0	180.0	195.3	99.8	0.1
180.0	150.0	164.3	99.5	0.3
150.0	125.0	136.9	98.4	1.1
125.0	106.0	115.1	86.5	11.9
106.0	90.00	97.67	39.8	46.7
90.00	75.00	82.16	13.6	26.2
75.00	63.00	68.74	0.0	13.6

Mass Frequency vs Diameter



## Summary Report

Full scale pump speed: 3  
Bubble detection: Medium  
Starting Size: 63.00 µm  
Ending Size: 0.50 µm

Stir time: 30 secs  
Stir speed: Low  
Probe time: 30 secs

Sample: TT-45-08 150 cm  
 Operator: Clint Edrington  
 Submitter: Clint Edrington  
 File Name: C:\EDRING~1\TIGER&~1\SANDFR~1\TT-45-08\45\_150CM.SMP  
 Material/Liquid: silicate mud/water/Water

Reported: 01/04/10 18:35:55  
 Liquid Visc: 0.7225 cp

Sample Density: 2.650 g/cm<sup>3</sup>  
 Liquid Density: 0.9941 g/cm<sup>3</sup>

## Summary Report

Parameter 1 0.000

Parameter 2 0.000

Parameter 3 0.000

## Mass Distribution Arithmetic Statistics

Mean	92.61	Std. Dev.	15.65
Median	93.73	Coef. Var.	0.169
Mode	97.67	Skewness	1.310
		Kurtosis	8.173

## Selected Percentiles

Percent Finer	Diameter (µm)
100.0	651.9
80.0	102.7
60.0	96.59
40.0	90.10
20.0	79.29

## Selected Sizes

Diameter (µm)	Percent Finer
500.0	100.0
250.0	100.0
125.0	98.4
88.00	35.9
63.00	0.0

Peak Number	% of Dist. *	Mean	Mode	Median	Standard Deviation	Skewness	Kurtosis
1	100.0	92.61	97.67	93.73	15.65	1.310	8.173

\* Peaks must comprise at least 5.00 % of the distribution.

Micromeritics

WIN5100 V2.03

Page 1

Sample: TT-45-08 206 cm  
Operator: Clint Edrington  
Submitter: Clint Edrington  
File Name: C:\EDRING~1\TIGER&~1\SANDFR~1\TT-45-08\45\_206CM.SMP  
Material/Liquid: silicate mud/water/Water

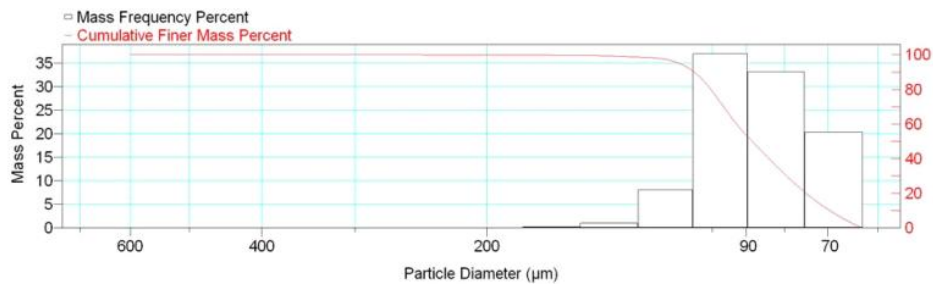
Reported: 01/04/10 18:37:39  
Liquid Visc: 0.7225 cp

Sample Density: 2.650 g/cm<sup>3</sup>  
Liquid Density: 0.9941 g/cm<sup>3</sup>

Report by Size Class

High Diameter (μm)	Low Diameter (μm)	Average Diameter (μm)	Cumulative Mass Finer (Percent)	Mass Frequency (Percent)
710.0	600.0	652.7	100.0	0.0
600.0	500.0	547.7	100.0	0.0
500.0	425.0	461.0	100.0	0.0
425.0	355.0	388.4	100.0	0.0
355.0	300.0	326.3	100.0	0.0
300.0	250.0	273.9	100.0	0.0
250.0	212.0	230.2	99.9	0.1
212.0	180.0	195.3	99.8	0.1
180.0	150.0	164.3	99.6	0.2
150.0	125.0	136.9	98.6	1.0
125.0	106.0	115.1	90.5	8.1
106.0	90.00	97.67	53.5	37.0
90.00	75.00	82.16	20.3	33.2
75.00	63.00	68.74	0.0	20.3

Mass Frequency vs Diameter



Summary Report

Full scale pump speed: 3  
Bubble detection: Medium  
Starting Size: 63.00 μm  
Ending Size: 0.50 μm

Stir time: 30 secs  
Stir speed: Low  
Probe time: 30 secs

Sample: TT-45-08 206 cm  
 Operator: Clint Edrington  
 Submitter: Clint Edrington  
 File Name: C:\EDRING~1\TIGER&~1\SANDFR~1\TT-45-08\45\_206CM.SMP  
 Material/Liquid: silicate mud/water/Water

Reported: 01/04/10 18:37:39  
 Liquid Visc: 0.7225 cp

Sample Density: 2.650 g/cm<sup>3</sup>  
 Liquid Density: 0.9941 g/cm<sup>3</sup>

## Summary Report

Parameter 1 0.000

Parameter 2 0.000

Parameter 3 0.000

## Mass Distribution Arithmetic Statistics

Mean	88.82	Std. Dev.	15.73
Median	88.39	Coef. Var.	0.177
Mode	97.67	Skewness	1.541
		Kurtosis	8.786

## Selected Percentiles

Percent Finer	Diameter (µm)
100.0	651.9
80.0	100.4
60.0	92.73
40.0	83.92
20.0	74.86

## Selected Sizes

Diameter (µm)	Percent Finer
500.0	100.0
250.0	100.0
125.0	98.6
88.00	49.1
63.00	0.0

Peak Number	% of Dist. *	Mean	Mode	Median	Standard Deviation	Skewness	Kurtosis
1	100.0	88.82	97.67	88.39	15.73	1.541	8.786

\* Peaks must comprise at least 5.00 % of the distribution.

Micromeritics

WIN5100 V2.03

Page 1

Sample: TT-45-08 250 cm  
Operator: Clint Edrington  
Submitter: Clint Edrington  
File Name: C:\EDRING~1\TIGER&~1\SANDFR~1\TT-45-08\45\_250CM.SMP  
Material/Liquid: silicate mud/water/Water

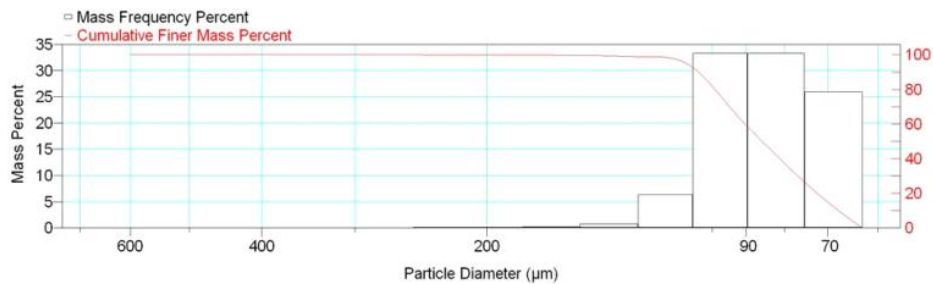
Reported: 01/04/10 18:39:35  
Liquid Visc: 0.7225 cp

Sample Density: 2.650 g/cm<sup>3</sup>  
Liquid Density: 0.9941 g/cm<sup>3</sup>

Report by Size Class

High Diameter (μm)	Low Diameter (μm)	Average Diameter (μm)	Cumulative Mass Finer (Percent)	Mass Frequency (Percent)
710.0	600.0	652.7	100.0	0.0
600.0	500.0	547.7	100.0	0.0
500.0	425.0	461.0	100.0	0.0
425.0	355.0	388.4	100.0	0.0
355.0	300.0	326.3	100.0	0.0
300.0	250.0	273.9	100.0	0.0
250.0	212.0	230.2	99.9	0.1
212.0	180.0	195.3	99.8	0.1
180.0	150.0	164.3	99.6	0.2
150.0	125.0	136.9	98.8	0.8
125.0	106.0	115.1	92.5	6.3
106.0	90.00	97.67	59.2	33.3
90.00	75.00	82.16	25.9	33.3
75.00	63.00	68.74	0.0	25.9

Mass Frequency vs Diameter



Summary Report

Full scale pump speed: 3  
Bubble detection: Medium  
Starting Size: 63.00 μm  
Ending Size: 0.50 μm

Stir time: 30 secs  
Stir speed: Low  
Probe time: 30 secs

Sample: TT-45-08 250 cm  
 Operator: Clint Edrington  
 Submitter: Clint Edrington  
 File Name: C:\EDRING~1\TIGER&~1\SANDFR~1\TT-45-08\45\_250CM.SMP  
 Material/Liquid: silicate mud/water/Water

Reported: 01/04/10 18:39:35  
 Liquid Visc: 0.7225 cp

Sample Density: 2.650 g/cm<sup>3</sup>  
 Liquid Density: 0.9941 g/cm<sup>3</sup>

## Summary Report

Parameter 1 0.000

Parameter 2 0.000

Parameter 3 0.000

## Mass Distribution Arithmetic Statistics

Mean	86.79	Std. Dev.	15.68
Median	85.68	Coef. Var.	0.181
Mode	82.16	Skewness	1.678
		Kurtosis	9.522

## Selected Percentiles

Percent Finer	Diameter (µm)
100.0	651.9
80.0	99.10
60.0	90.38
40.0	81.20
20.0	72.36

## Selected Sizes

Diameter (µm)	Percent Finer
500.0	100.0
250.0	100.0
125.0	98.8
88.00	55.0
63.00	0.0

Peak Number	% of Dist. *	Mean	Mode	Median	Standard Deviation	Skewness	Kurtosis
1	100.0	86.79	82.16	85.68	15.68	1.678	9.522

\* Peaks must comprise at least 5.00 % of the distribution.

Micromeritics

WIN5100 V2.03

Page 1

Sample: TT-45-08 300 cm  
Operator: Clint Edrington  
Submitter: Clint Edrington  
File Name: C:\EDRING~1\TIGER&~1\SANDFR~1\TT-45-08\45\_300CM.SMP  
Material/Liquid: silicate mud/water/Water

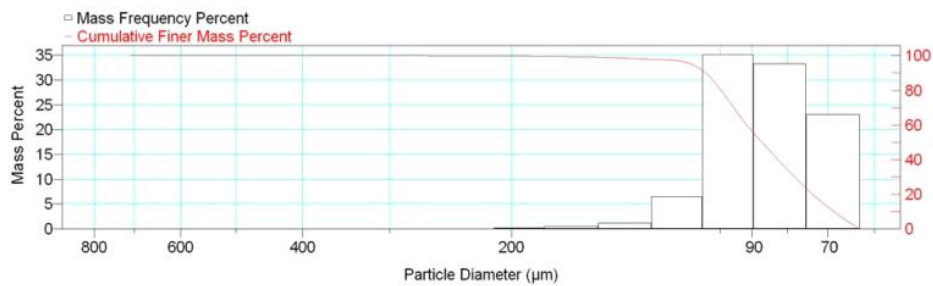
Reported: 01/04/10 18:41:31  
Liquid Visc: 0.7225 cp

Sample Density: 2.650 g/cm<sup>3</sup>  
Liquid Density: 0.9941 g/cm<sup>3</sup>

Report by Size Class

High Diameter (μm)	Low Diameter (μm)	Average Diameter (μm)	Cumulative Mass Finer (Percent)	Mass Frequency (Percent)
850.0	710.0	776.9	100.0	0.0
710.0	600.0	652.7	100.0	0.0
600.0	500.0	547.7	100.0	0.0
500.0	425.0	461.0	100.0	0.0
425.0	355.0	388.4	100.0	0.0
355.0	300.0	326.3	100.0	0.0
300.0	250.0	273.9	99.9	0.1
250.0	212.0	230.2	99.8	0.1
212.0	180.0	195.3	99.6	0.2
180.0	150.0	164.3	99.1	0.5
150.0	125.0	136.9	97.9	1.2
125.0	106.0	115.1	91.4	6.5
106.0	90.00	97.67	56.3	35.1
90.00	75.00	82.16	23.0	33.3
75.00	63.00	68.74	0.0	23.0

Mass Frequency vs Diameter



Summary Report

Full scale pump speed: 3  
Bubble detection: Medium  
Starting Size: 63.00 μm  
Ending Size: 0.50 μm

Stir time: 30 secs  
Stir speed: Low  
Probe time: 30 secs

Sample: TT-45-08 300 cm  
 Operator: Clint Edrington  
 Submitter: Clint Edrington  
 File Name: C:\EDRING~1\TIGER&~1\SANDFR~1\TT-45-08\45\_300CM.SMP  
 Material/Liquid: silicate mud/water/Water

Reported: 01/04/10 18:41:31  
 Liquid Visc: 0.7225 cp

Sample Density: 2.650 g/cm<sup>3</sup>  
 Liquid Density: 0.9941 g/cm<sup>3</sup>

## Summary Report

Parameter 1	0.000	Parameter 2	0.000	Parameter 3	0.000		
Mass Distribution Arithmetic Statistics							
Mean	88.29	Std. Dev.		17.69			
Median	87.07	Coef. Var.		0.200			
Mode	97.67	Skewness		2.715			
		Kurtosis		19.052			
Selected Percentiles			Selected Sizes				
Percent Finer	Diameter (µm)		Diameter (µm)	Percent Finer			
100.0	714.1		500.0	100.0			
80.0	99.71		250.0	99.9			
60.0	91.65		125.0	97.9			
40.0	82.58		88.00	52.0			
20.0	73.60		63.00	0.0			
Peak Number	% of Dist.*	Mean	Mode	Median	Standard Deviation	Skewness	Kurtosis
1	100.0	88.29	97.67	87.07	17.69	2.715	19.052

\* Peaks must comprise at least 5.00 % of the distribution.



Micromeritics

WIN5100 V2.03

Page 1

Sample: TT-45-08 350 cm  
Operator: Clint Edrington  
Submitter: Clint Edrington  
File Name: C:\EDRING~1\TIGER&~1\SANDFR~1\TT-45-08\45\_350CM.SMP  
Material/Liquid: silicate mud/water/Water

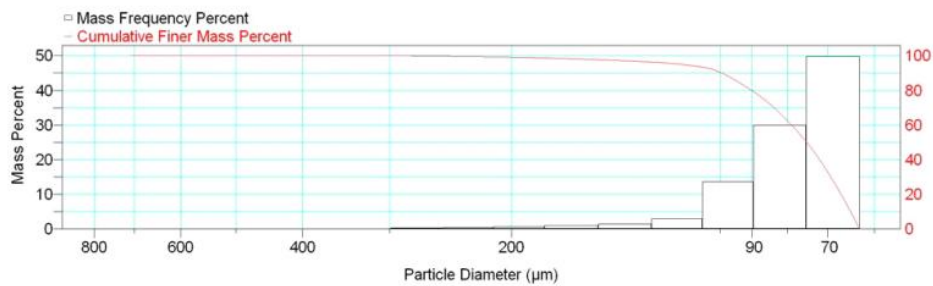
Reported: 01/04/10 18:43:33  
Liquid Visc: 0.7225 cp

Sample Density: 2.650 g/cm<sup>3</sup>  
Liquid Density: 0.9941 g/cm<sup>3</sup>

Report by Size Class

High Diameter (µm)	Low Diameter (µm)	Average Diameter (µm)	Cumulative Mass Finer (Percent)	Mass Frequency (Percent)
850.0	710.0	776.9	100.0	0.0
710.0	600.0	652.7	100.0	0.0
600.0	500.0	547.7	100.0	0.0
500.0	425.0	461.0	100.0	0.0
425.0	355.0	388.4	100.0	0.0
355.0	300.0	326.3	100.0	0.0
300.0	250.0	273.9	99.7	0.3
250.0	212.0	230.2	99.3	0.4
212.0	180.0	195.3	98.7	0.6
180.0	150.0	164.3	97.7	1.0
150.0	125.0	136.9	96.3	1.4
125.0	106.0	115.1	93.4	2.9
106.0	90.00	97.67	79.8	13.6
90.00	75.00	82.16	49.8	30.0
75.00	63.00	68.74	0.0	49.8

Mass Frequency vs Diameter



Summary Report

Full scale pump speed: 3  
Bubble detection: Medium  
Starting Size: 63.00 µm  
Ending Size: 0.50 µm

Stir time: 30 secs  
Stir speed: Low  
Probe time: 30 secs

Sample: TT-45-08 350 cm  
 Operator: Clint Edrington  
 Submitter: Clint Edrington  
 File Name: C:\EDRING~1\TIGER&~1\SANDFR~1\TT-45-08\45\_350CM.SMP  
 Material/Liquid: silicate mud/water/Water

Reported: 01/04/10 18:43:33  
 Liquid Visc: 0.7225 cp

Sample Density: 2.650 g/cm<sup>3</sup>  
 Liquid Density: 0.9941 g/cm<sup>3</sup>

## Summary Report

Parameter 1	0.000	Parameter 2	0.000	Parameter 3	0.000		
Mass Distribution Arithmetic Statistics							
Mean	81.98	Std. Dev.		23.20			
Median	75.07	Coef. Var.		0.283			
Mode	68.74	Skewness		4.109			
		Kurtosis		23.364			
Selected Percentiles			Selected Sizes				
Percent Finer	Diameter (µm)		Diameter (µm)	Percent Finer			
100.0	714.1		500.0	100.0			
80.0	90.16		250.0	99.7			
60.0	78.91		125.0	96.3			
40.0	71.91		88.00	77.1			
20.0	66.97		63.00	0.0			
Peak Number	% of Dist.*	Mean	Mode	Median	Standard Deviation	Skewness	Kurtosis
1	100.0	81.98	68.74	75.07	23.20	4.109	23.364

\* Peaks must comprise at least 5.00 % of the distribution.

# Micromeritics

WIN5100 V2.03

Page 1

Sample: TT-45-08 400 cm  
Operator: Clint Edrington  
Submitter: Clint Edrington  
File Name: C:\EDRING~1\TIGER&~1\SANDFR~1\TT-45-08\45\_400CM.SMP  
Material/Liquid: silicate mud/water/Water

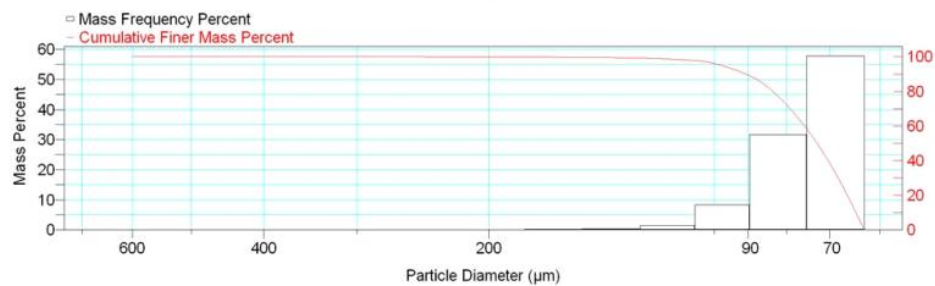
Reported: 01/04/10 18:45:36  
Liquid Visc: 0.7225 cp

Sample Density: 2.650 g/cm<sup>3</sup>  
Liquid Density: 0.9941 g/cm<sup>3</sup>

## Report by Size Class

High Diameter (μm)	Low Diameter (μm)	Average Diameter (μm)	Cumulative Mass Finer (Percent)	Mass Frequency (Percent)
710.0	600.0	652.7	100.0	0.0
600.0	500.0	547.7	100.0	0.0
500.0	425.0	461.0	100.0	0.0
425.0	355.0	388.4	100.0	0.0
355.0	300.0	326.3	100.0	0.0
300.0	250.0	273.9	100.0	0.0
250.0	212.0	230.2	99.9	0.1
212.0	180.0	195.3	99.8	0.1
180.0	150.0	164.3	99.6	0.2
150.0	125.0	136.9	99.2	0.4
125.0	106.0	115.1	97.8	1.4
106.0	90.00	97.67	89.4	8.4
90.00	75.00	82.16	57.8	31.6
75.00	63.00	68.74	0.0	57.8

Mass Frequency vs Diameter



## Summary Report

Full scale pump speed: 3  
Bubble detection: Medium  
Starting Size: 63.00 μm  
Ending Size: 0.50 μm

Stir time: 30 secs  
Stir speed: Low  
Probe time: 30 secs

Sample: TT-45-08 400 cm  
 Operator: Clint Edrington  
 Submitter: Clint Edrington  
 File Name: C:\EDRING~1\TIGER&~1\SANDFR~1\TT-45-08\45\_400CM.SMP  
 Material/Liquid: silicate mud/water/Water

Reported: 01/04/10 18:45:36  
 Liquid Visc: 0.7225 cp

Sample Density: 2.650 g/cm<sup>3</sup>  
 Liquid Density: 0.9941 g/cm<sup>3</sup>

## Summary Report

Parameter 1 0.000

Parameter 2 0.000

Parameter 3 0.000

## Mass Distribution Arithmetic Statistics

Mean	76.81	Std. Dev.	13.08
Median	72.78	Coef. Var.	0.170
Mode	68.74	Skewness	3.921
		Kurtosis	30.098

## Selected Percentiles

Percent Finer	Diameter (µm)
100.0	651.9
80.0	83.42
60.0	75.69
40.0	70.34
20.0	66.32

## Selected Sizes

Diameter (µm)	Percent Finer
500.0	100.0
250.0	100.0
125.0	99.2
88.00	87.3
63.00	0.0

Peak Number	% of Dist. *	Mean	Mode	Median	Standard Deviation	Skewness	Kurtosis
1	100.0	76.81	68.74	72.78	13.08	3.921	30.098

\* Peaks must comprise at least 5.00 % of the distribution.

Micromeritics

WIN5100 V2.03

Page 1

Sample: TT-46-08 16 cm  
Operator: Clint Edrington  
Submitter: Clint Edrington  
File Name: C:\EDRING~1\TIGER&~1\SANDFR~1\TT-46-08\46\_16CM.SMP  
Material/Liquid: silicate mud/water/Water

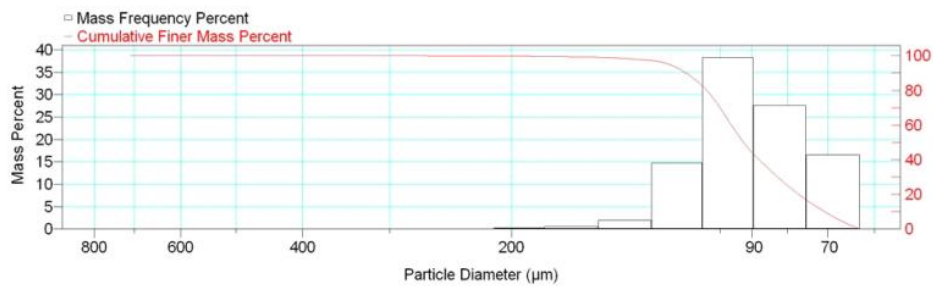
Reported: 01/04/10 18:48:37  
Liquid Visc: 0.7225 cp

Sample Density: 2.650 g/cm<sup>3</sup>  
Liquid Density: 0.9941 g/cm<sup>3</sup>

Report by Size Class

High Diameter (µm)	Low Diameter (µm)	Average Diameter (µm)	Cumulative Mass Finer (Percent)	Mass Frequency (Percent)
850.0	710.0	776.9	100.0	0.0
710.0	600.0	652.7	100.0	0.0
600.0	500.0	547.7	100.0	0.0
500.0	425.0	461.0	100.0	0.0
425.0	355.0	388.4	100.0	0.0
355.0	300.0	326.3	100.0	0.0
300.0	250.0	273.9	99.9	0.1
250.0	212.0	230.2	99.8	0.1
212.0	180.0	195.3	99.6	0.2
180.0	150.0	164.3	99.1	0.5
150.0	125.0	136.9	97.1	2.0
125.0	106.0	115.1	82.4	14.7
106.0	90.00	97.67	44.1	38.3
90.00	75.00	82.16	16.5	27.6
75.00	63.00	68.74	0.0	16.5

Mass Frequency vs Diameter



Summary Report

Full scale pump speed: 3  
Bubble detection: Medium  
Starting Size: 63.00 µm  
Ending Size: 0.50 µm

Stir time: 30 secs  
Stir speed: Low  
Probe time: 30 secs

Sample: TT-46-08 16 cm  
 Operator: Clint Edrington  
 Submitter: Clint Edrington  
 File Name: C:\EDRING~1\TIGER&~1\SANDFR~1\TT-46-08\46\_16CM.SMP  
 Material/Liquid: silicate mud/water/Water

Reported: 01/04/10 18:48:37  
 Liquid Visc: 0.7225 cp

Sample Density: 2.650 g/cm<sup>3</sup>  
 Liquid Density: 0.9941 g/cm<sup>3</sup>

## Summary Report

Parameter 1	0.000	Parameter 2	0.000	Parameter 3	0.000		
Mass Distribution Arithmetic Statistics							
Mean	92.80	Std. Dev.		18.61			
Median	92.63	Coef. Var.		0.201			
Mode	97.67	Skewness		2.061			
		Kurtosis		13.302			
Selected Percentiles			Selected Sizes				
Percent Finer	Diameter (µm)		Diameter (µm)	Percent Finer			
100.0	714.1		500.0	100.0			
80.0	104.6		250.0	99.9			
60.0	96.38		125.0	97.1			
40.0	87.89		88.00	40.2			
20.0	77.14		63.00	0.0			
Peak Number	% of Dist.*	Mean	Mode	Median	Standard Deviation	Skewness	Kurtosis
1	100.0	92.80	97.67	92.63	18.61	2.061	13.302

\* Peaks must comprise at least 5.00 % of the distribution.

Micromeritics

WIN5100 V2.03

Page 1

Sample: TT-46-08 71 cm  
Operator: Clint Edrington  
Submitter: Clint Edrington  
File Name: C:\EDRING~1\TIGER&~1\SANDFR~1\TT-46-08\46\_71CM.SMP  
Material/Liquid: silicate mud/water/Water

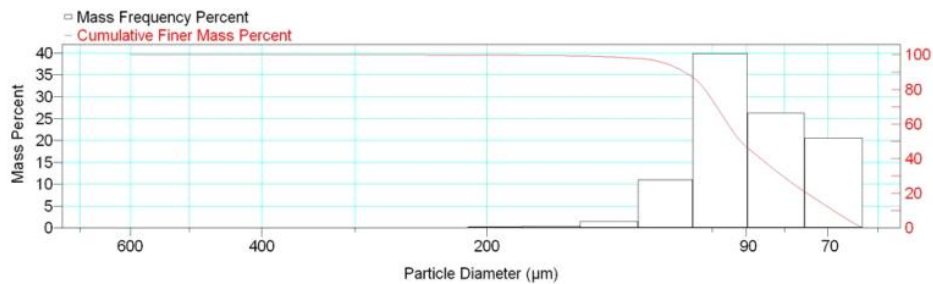
Reported: 01/04/10 18:50:46  
Liquid Visc: 0.7225 cp

Sample Density: 2.650 g/cm<sup>3</sup>  
Liquid Density: 0.9941 g/cm<sup>3</sup>

Report by Size Class

High Diameter (μm)	Low Diameter (μm)	Average Diameter (μm)	Cumulative Mass Finer (Percent)	Mass Frequency (Percent)
710.0	600.0	652.7	100.0	0.0
600.0	500.0	547.7	100.0	0.0
500.0	425.0	461.0	100.0	0.0
425.0	355.0	388.4	100.0	0.0
355.0	300.0	326.3	100.0	0.0
300.0	250.0	273.9	100.0	0.0
250.0	212.0	230.2	99.9	0.1
212.0	180.0	195.3	99.7	0.2
180.0	150.0	164.3	99.3	0.4
150.0	125.0	136.9	97.8	1.5
125.0	106.0	115.1	86.8	11.0
106.0	90.00	97.67	46.9	39.9
90.00	75.00	82.16	20.6	26.3
75.00	63.00	68.74	0.0	20.6

Mass Frequency vs Diameter



Summary Report

Full scale pump speed: 3  
Bubble detection: Medium  
Starting Size: 63.00 μm  
Ending Size: 0.50 μm

Stir time: 30 secs  
Stir speed: Low  
Probe time: 30 secs

Sample: TT-46-08 71 cm  
 Operator: Clint Edrington  
 Submitter: Clint Edrington  
 File Name: C:\EDRING~1\TIGER&~1\SANDFR~1\TT-46-08\46\_71CM.SMP  
 Material/Liquid: silicate mud/water/Water

Reported: 01/04/10 18:50:46  
 Liquid Visc: 0.7225 cp

Sample Density: 2.650 g/cm<sup>3</sup>  
 Liquid Density: 0.9941 g/cm<sup>3</sup>

## Summary Report

Parameter 1 0.000

Parameter 2 0.000

Parameter 3 0.000

## Mass Distribution Arithmetic Statistics

Mean	90.73	Std. Dev.	17.28
Median	91.53	Coef. Var.	0.190
Mode	97.67	Skewness	1.443
		Kurtosis	7.017

## Selected Percentiles

Percent Finer	Diameter (µm)
100.0	651.9
80.0	102.3
60.0	95.23
40.0	86.09
20.0	74.64

## Selected Sizes

Diameter (µm)	Percent Finer
500.0	100.0
250.0	100.0
125.0	97.8
88.00	43.4
63.00	0.0

Peak Number	% of Dist. *	Mean	Mode	Median	Standard Deviation	Skewness	Kurtosis
1	100.0	90.73	97.67	91.53	17.28	1.443	7.017

\* Peaks must comprise at least 5.00 % of the distribution.



# Micromeritics

WIN5100 V2.03

Page 1

Sample: TT-46-08 112 cm  
Operator: Clint Edrington  
Submitter: Clint Edrington  
File Name: C:\EDRING~1\TIGER&~1\SANDFR~1\TT-46-08\46\_112CM.SMP  
Material/Liquid: silicate mud/water/Water

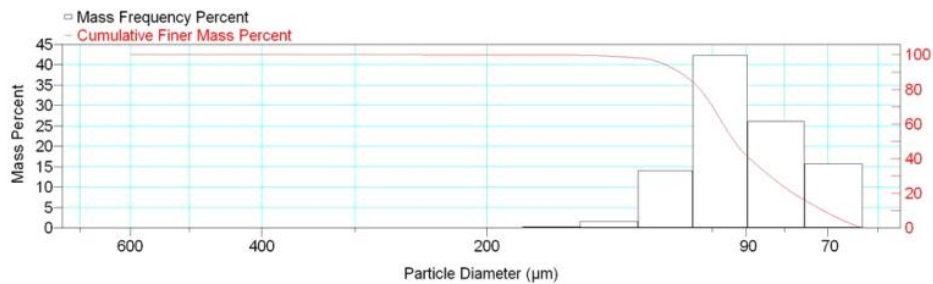
Reported: 01/04/10 18:52:37  
Liquid Visc: 0.7225 cp

Sample Density: 2.650 g/cm<sup>3</sup>  
Liquid Density: 0.9941 g/cm<sup>3</sup>

## Report by Size Class

High Diameter (µm)	Low Diameter (µm)	Average Diameter (µm)	Cumulative Mass Finer (Percent)	Mass Frequency (Percent)
710.0	600.0	652.7	100.0	0.0
600.0	500.0	547.7	100.0	0.0
500.0	425.0	461.0	100.0	0.0
425.0	355.0	388.4	100.0	0.0
355.0	300.0	326.3	100.0	0.0
300.0	250.0	273.9	100.0	0.0
250.0	212.0	230.2	99.9	0.1
212.0	180.0	195.3	99.9	0.0
180.0	150.0	164.3	99.7	0.2
150.0	125.0	136.9	98.1	1.6
125.0	106.0	115.1	84.1	14.0
106.0	90.00	97.67	41.8	42.3
90.00	75.00	82.16	15.7	26.1
75.00	63.00	68.74	0.0	15.7

Mass Frequency vs Diameter



## Summary Report

Full scale pump speed: 3  
Bubble detection: Medium  
Starting Size: 63.00 µm  
Ending Size: 0.50 µm

Stir time: 30 secs  
Stir speed: Low  
Probe time: 30 secs

Sample: TT-46-08 112 cm  
 Operator: Clint Edrington  
 Submitter: Clint Edrington  
 File Name: C:\EDRING~1\TIGER&~1\SANDFR~1\TT-46-08\46\_112CM.SMP  
 Material/Liquid: silicate mud/water/Water

Reported: 01/04/10 18:52:37  
 Liquid Visc: 0.7225 cp

Sample Density: 2.650 g/cm<sup>3</sup>  
 Liquid Density: 0.9941 g/cm<sup>3</sup>

## Summary Report

Parameter 1 0.000

Parameter 2 0.000

Parameter 3 0.000

## Mass Distribution Arithmetic Statistics

Mean	92.42	Std. Dev.	16.13
Median	93.36	Coef. Var.	0.175
Mode	97.67	Skewness	0.977
		Kurtosis	5.362

## Selected Percentiles

Percent Finer	Diameter (µm)
100.0	651.9
80.0	103.7
60.0	96.63
40.0	89.05
20.0	77.84

## Selected Sizes

Diameter (µm)	Percent Finer
500.0	100.0
250.0	100.0
125.0	98.1
88.00	38.0
63.00	0.0

Peak Number	% of Dist. *	Mean	Mode	Median	Standard Deviation	Skewness	Kurtosis
1	99.9	92.28	97.67	93.35	15.54	0.423	0.549

\* Peaks must comprise at least 5.00 % of the distribution.

Micromeritics

WIN5100 V2.03

Page 1

Sample: TT-46-08 385 cm  
Operator: Clint Edrington  
Submitter: Clint Edrington  
File Name: C:\EDRING~1\TIGER&~1\SANDFR~1\TT-46-08\46\_385CM.SMP  
Material/Liquid: silicate mud/water/Water

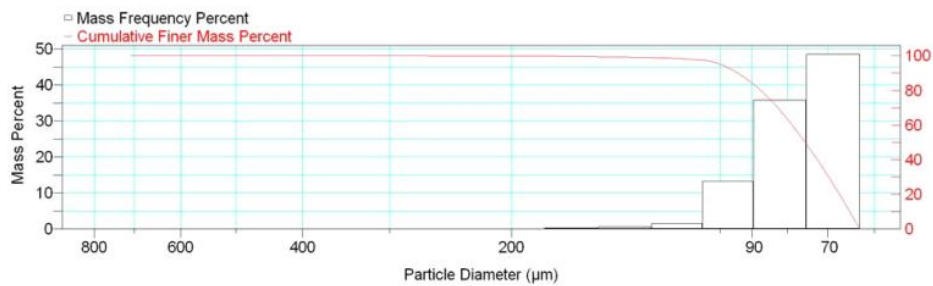
Reported: 01/04/10 18:54:47  
Liquid Visc: 0.7225 cp

Sample Density: 2.650 g/cm<sup>3</sup>  
Liquid Density: 0.9941 g/cm<sup>3</sup>

Report by Size Class

High Diameter ( $\mu\text{m}$ )	Low Diameter ( $\mu\text{m}$ )	Average Diameter ( $\mu\text{m}$ )	Cumulative Mass Finer (Percent)	Mass Frequency (Percent)
850.0	710.0	776.9	100.0	0.0
710.0	600.0	652.7	100.0	0.0
600.0	500.0	547.7	100.0	0.0
500.0	425.0	461.0	100.0	0.0
425.0	355.0	388.4	100.0	0.0
355.0	300.0	326.3	100.0	0.0
300.0	250.0	273.9	99.9	0.1
250.0	212.0	230.2	99.8	0.1
212.0	180.0	195.3	99.7	0.1
180.0	150.0	164.3	99.4	0.3
150.0	125.0	136.9	98.9	0.5
125.0	106.0	115.1	97.4	1.5
106.0	90.00	97.67	84.2	13.2
90.00	75.00	82.16	48.5	35.7
75.00	63.00	68.74	0.0	48.5

Mass Frequency vs Diameter



Summary Report

Full scale pump speed: 3  
Bubble detection: Medium  
Starting Size: 63.00  $\mu\text{m}$   
Ending Size: 0.50  $\mu\text{m}$

Stir time: 30 secs  
Stir speed: Low  
Probe time: 30 secs

Sample: TT-46-08 385 cm  
 Operator: Clint Edrington  
 Submitter: Clint Edrington  
 File Name: C:\EDRING~1\TIGER&~1\SANDFR~1\TT-46-08\46\_385CM.SMP  
 Material/Liquid: silicate mud/water/Water

Reported: 01/04/10 18:54:47  
 Liquid Visc: 0.7225 cp

Sample Density: 2.650 g/cm<sup>3</sup>  
 Liquid Density: 0.9941 g/cm<sup>3</sup>

## Summary Report

Parameter 1	0.000	Parameter 2	0.000	Parameter 3	0.000		
Mass Distribution Arithmetic Statistics							
Mean	79.17	Std. Dev.		15.27			
Median	75.47	Coef. Var.		0.193			
Mode	68.74	Skewness		4.551			
		Kurtosis		41.130			
Selected Percentiles			Selected Sizes				
Percent Finer	Diameter (µm)		Diameter (µm)	Percent Finer			
100.0	714.1		500.0	100.0			
80.0	87.44		250.0	99.9			
60.0	78.79		125.0	98.9			
40.0	72.49		88.00	81.0			
20.0	67.31		63.00	0.0			
Peak Number	% of Dist.*	Mean	Mode	Median	Standard Deviation	Skewness	Kurtosis
1	100.0	79.17	68.74	75.47	15.27	4.551	41.130

\* Peaks must comprise at least 5.00 % of the distribution.

Micromeritics

WIN5100 V2.03

Page 1

Sample: TT-47-08 12 cm  
Operator: Clint Edrington  
Submitter: Clint Edrington  
File Name: C:\EDRING~1\TIGER&~1\SANDFR~1\TT-47-08\47\_12CM.SMP  
Material/Liquid: silicate mud/water/Water

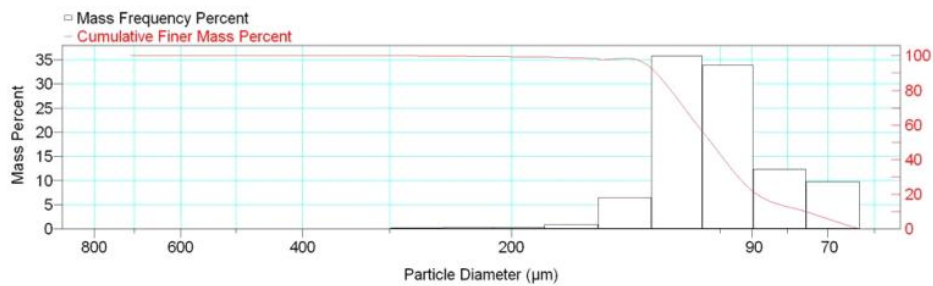
Reported: 01/04/10 18:57:34  
Liquid Visc: 0.7225 cp

Sample Density: 2.650 g/cm<sup>3</sup>  
Liquid Density: 0.9941 g/cm<sup>3</sup>

Report by Size Class

High Diameter (µm)	Low Diameter (µm)	Average Diameter (µm)	Cumulative Mass Finer (Percent)	Mass Frequency (Percent)
850.0	710.0	776.9	100.0	0.0
710.0	600.0	652.7	100.0	0.0
600.0	500.0	547.7	100.0	0.0
500.0	425.0	461.0	100.0	0.0
425.0	355.0	388.4	100.0	0.0
355.0	300.0	326.3	100.0	0.0
300.0	250.0	273.9	99.8	0.2
250.0	212.0	230.2	99.5	0.3
212.0	180.0	195.3	99.2	0.3
180.0	150.0	164.3	98.3	0.9
150.0	125.0	136.9	91.8	6.5
125.0	106.0	115.1	56.0	35.8
106.0	90.00	97.67	22.1	33.9
90.00	75.00	82.16	9.8	12.3
75.00	63.00	68.74	0.0	9.8

Mass Frequency vs Diameter



Summary Report

Full scale pump speed: 3  
Bubble detection: Medium  
Starting Size: 63.00 µm  
Ending Size: 0.50 µm

Stir time: 30 secs  
Stir speed: Low  
Probe time: 30 secs

Sample: TT-47-08 12 cm  
 Operator: Clint Edrington  
 Submitter: Clint Edrington  
 File Name: C:\EDRING~1\TIGER&~1\SANDFR~1\TT-47-08\47\_12CM.SMP  
 Material/Liquid: silicate mud/water/Water

Reported: 01/04/10 18:57:34  
 Liquid Visc: 0.7225 cp

Sample Density: 2.650 g/cm<sup>3</sup>  
 Liquid Density: 0.9941 g/cm<sup>3</sup>

## Summary Report

Parameter 1	0.000	Parameter 2	0.000	Parameter 3	0.000		
Mass Distribution Arithmetic Statistics							
Mean	103.4	Std. Dev.		21.72			
Median	103.1	Coef. Var.		0.210			
Mode	115.1	Skewness		1.771			
		Kurtosis		10.762			
Selected Percentiles			Selected Sizes				
Percent Finer	Diameter (µm)		Diameter (µm)	Percent Finer			
100.0	714.1		500.0	100.0			
80.0	117.8		250.0	99.8			
60.0	108.0		125.0	91.8			
40.0	98.71		88.00	19.3			
20.0	88.56		63.00	0.0			
Peak Number	% of Dist.*	Mean	Mode	Median	Standard Deviation	Skewness	Kurtosis
1	100.0	103.4	115.1	103.1	21.72	1.771	10.762

\* Peaks must comprise at least 5.00 % of the distribution.

Micromeritics

WIN5100 V2.03

Page 1

Sample: TT-47-08 179 cm  
Operator: Clint Edrington  
Submitter: Clint Edrington  
File Name: C:\EDRING~1\TIGER&~1\SANDFR~1\TT-47-08\47\_179CM.SMP  
Material/Liquid: silicate mud/water/Water

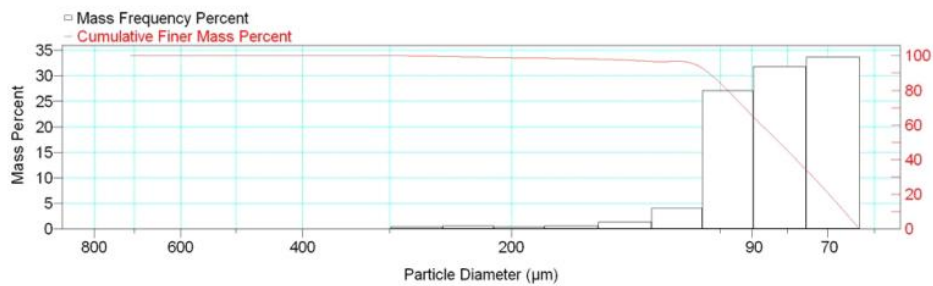
Reported: 01/04/10 18:59:53  
Liquid Visc: 0.7225 cp

Sample Density: 2.650 g/cm<sup>3</sup>  
Liquid Density: 0.9941 g/cm<sup>3</sup>

Report by Size Class

High Diameter ( $\mu\text{m}$ )	Low Diameter ( $\mu\text{m}$ )	Average Diameter ( $\mu\text{m}$ )	Cumulative Mass Finer (Percent)	Mass Frequency (Percent)
850.0	710.0	776.9	100.0	0.0
710.0	600.0	652.7	100.0	0.0
600.0	500.0	547.7	100.0	0.0
500.0	425.0	461.0	100.0	0.0
425.0	355.0	388.4	100.0	0.0
355.0	300.0	326.3	100.0	0.0
300.0	250.0	273.9	99.6	0.4
250.0	212.0	230.2	99.0	0.6
212.0	180.0	195.3	98.6	0.4
180.0	150.0	164.3	98.0	0.6
150.0	125.0	136.9	96.7	1.3
125.0	106.0	115.1	92.6	4.1
106.0	90.00	97.67	65.5	27.1
90.00	75.00	82.16	33.7	31.8
75.00	63.00	68.74	0.0	33.7

Mass Frequency vs Diameter



Summary Report

Full scale pump speed: 3  
Bubble detection: Medium  
Starting Size: 63.00  $\mu\text{m}$   
Ending Size: 0.50  $\mu\text{m}$

Stir time: 30 secs  
Stir speed: Low  
Probe time: 30 secs

Sample: TT-47-08 179 cm  
 Operator: Clint Edrington  
 Submitter: Clint Edrington  
 File Name: C:\EDRING~1\TIGER&~1\SANDFR~1\TT-47-08\47\_179CM.SMP  
 Material/Liquid: silicate mud/water/Water

Reported: 01/04/10 18:59:53  
 Liquid Visc: 0.7225 cp

Sample Density: 2.650 g/cm<sup>3</sup>  
 Liquid Density: 0.9941 g/cm<sup>3</sup>

## Summary Report

Parameter 1	0.000	Parameter 2	0.000	Parameter 3	0.000		
Mass Distribution Arithmetic Statistics							
Mean	86.50		Std. Dev.	23.68			
Median	82.27		Coef. Var.	0.274			
Mode	68.74		Skewness	4.005			
			Kurtosis	23.767			
Selected Percentiles			Selected Sizes				
Percent Finer	Diameter (µm)		Diameter (µm)	Percent Finer			
100.0	714.1		500.0	100.0			
80.0	97.58		250.0	99.6			
60.0	87.18		125.0	96.7			
40.0	77.69		88.00	61.6			
20.0	69.69		63.00	0.0			
Peak Number	% of Dist.*	Mean	Mode	Median	Standard Deviation	Skewness	Kurtosis
1	99.0	84.88	68.74	82.03	17.23	2.076	8.401

\* Peaks must comprise at least 5.00 % of the distribution.



# Micromeritics

WIN5100 V2.03

Page 1

Sample: TT-47-08 230 cm  
Operator: Clint Edrington  
Submitter: Clint Edrington  
File Name: C:\EDRING~1\TIGER&~1\SANDFR~1\TT-47-08\47\_230CM.SMP  
Material/Liquid: silicate mud/water/Water

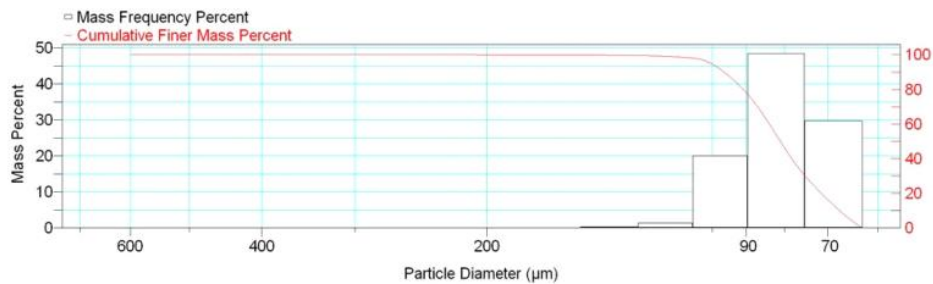
Reported: 01/04/10 19:01:41  
Liquid Visc: 0.7225 cp

Sample Density: 2.650 g/cm<sup>3</sup>  
Liquid Density: 0.9941 g/cm<sup>3</sup>

## Report by Size Class

High Diameter (μm)	Low Diameter (μm)	Average Diameter (μm)	Cumulative Mass Finer (Percent)	Mass Frequency (Percent)
710.0	600.0	652.7	100.0	0.0
600.0	500.0	547.7	100.0	0.0
500.0	425.0	461.0	100.0	0.0
425.0	355.0	388.4	100.0	0.0
355.0	300.0	326.3	100.0	0.0
300.0	250.0	273.9	100.0	0.0
250.0	212.0	230.2	100.0	0.0
212.0	180.0	195.3	99.9	0.1
180.0	150.0	164.3	99.8	0.1
150.0	125.0	136.9	99.5	0.3
125.0	106.0	115.1	98.1	1.4
106.0	90.00	97.67	78.1	20.0
90.00	75.00	82.16	29.7	48.4
75.00	63.00	68.74	0.0	29.7

Mass Frequency vs Diameter



## Summary Report

Full scale pump speed: 3  
Bubble detection: Medium  
Starting Size: 63.00 μm  
Ending Size: 0.50 μm

Stir time: 30 secs  
Stir speed: Low  
Probe time: 30 secs

Sample: TT-47-08 230 cm  
 Operator: Clint Edrington  
 Submitter: Clint Edrington  
 File Name: C:\EDRING~1\TIGER&~1\SANDFR~1\TT-47-08\47\_230CM.SMP  
 Material/Liquid: silicate mud/water/Water

Reported: 01/04/10 19:01:41  
 Liquid Visc: 0.7225 cp

Sample Density: 2.650 g/cm<sup>3</sup>  
 Liquid Density: 0.9941 g/cm<sup>3</sup>

## Summary Report

Parameter 1 0.000

Parameter 2 0.000

Parameter 3 0.000

## Mass Distribution Arithmetic Statistics

Mean	82.10	Std. Dev.	12.06
Median	81.03	Coef. Var.	0.147
Mode	82.16	Skewness	1.742
		Kurtosis	10.019

## Selected Percentiles

Percent Finer	Diameter (µm)
100.0	600.3
80.0	90.87
60.0	83.83
40.0	78.24
20.0	71.44

## Selected Sizes

Diameter (µm)	Percent Finer
500.0	100.0
250.0	100.0
125.0	99.5
88.00	73.1
63.00	0.0

Peak Number	% of Dist. *	Mean	Mode	Median	Standard Deviation	Skewness	Kurtosis
1	99.9	81.98	82.16	81.02	11.52	1.079	3.335

\* Peaks must comprise at least 5.00 % of the distribution.

Micromeritics

WIN5100 V2.03

Page 1

Sample: TT-47-08 300 cm  
Operator: Clint Edrington  
Submitter: Clint Edrington  
File Name: C:\EDRING~1\TIGER&~1\SANDFR~1\TT-47-08\47\_300CM.SMP  
Material/Liquid: silicate mud/water/Water

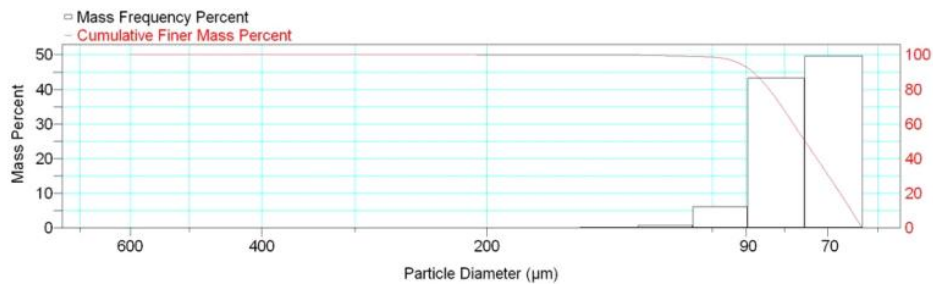
Reported: 01/04/10 19:03:30  
Liquid Visc: 0.7225 cp

Sample Density: 2.650 g/cm<sup>3</sup>  
Liquid Density: 0.9941 g/cm<sup>3</sup>

Report by Size Class

High Diameter (μm)	Low Diameter (μm)	Average Diameter (μm)	Cumulative Mass Finer (Percent)	Mass Frequency (Percent)
710.0	600.0	652.7	100.0	0.0
600.0	500.0	547.7	100.0	0.0
500.0	425.0	461.0	100.0	0.0
425.0	355.0	388.4	100.0	0.0
355.0	300.0	326.3	100.0	0.0
300.0	250.0	273.9	100.0	0.0
250.0	212.0	230.2	100.0	0.0
212.0	180.0	195.3	99.9	0.1
180.0	150.0	164.3	99.9	0.0
150.0	125.0	136.9	99.7	0.2
125.0	106.0	115.1	99.0	0.7
106.0	90.00	97.67	92.9	6.1
90.00	75.00	82.16	49.7	43.2
75.00	63.00	68.74	0.0	49.7

Mass Frequency vs Diameter



Summary Report

Full scale pump speed: 3  
Bubble detection: Medium  
Starting Size: 63.00 μm  
Ending Size: 0.50 μm

Stir time: 30 secs  
Stir speed: Low  
Probe time: 30 secs

Sample: TT-47-08 300 cm  
 Operator: Clint Edrington  
 Submitter: Clint Edrington  
 File Name: C:\EDRING~1\TIGER&~1\SANDFR~1\TT-47-08\47\_300CM.SMP  
 Material/Liquid: silicate mud/water/Water

Reported: 01/04/10 19:03:30  
 Liquid Visc: 0.7225 cp

Sample Density: 2.650 g/cm<sup>3</sup>  
 Liquid Density: 0.9941 g/cm<sup>3</sup>

## Summary Report

Parameter 1 0.000

Parameter 2 0.000

Parameter 3 0.000

## Mass Distribution Arithmetic Statistics

Mean	76.89	Std. Dev.	10.14
Median	75.08	Coef. Var.	0.132
Mode	68.74	Skewness	2.712
		Kurtosis	20.809

## Selected Percentiles

Percent Finer	Diameter (µm)
100.0	600.3
80.0	83.88
60.0	77.80
40.0	72.40
20.0	67.40

## Selected Sizes

Diameter (µm)	Percent Finer
500.0	100.0
250.0	100.0
125.0	99.7
88.00	89.7
63.00	0.0

Peak Number	% of Dist. *	Mean	Mode	Median	Standard Deviation	Skewness	Kurtosis
1	99.9	76.77	68.74	75.07	9.427	1.430	4.021

\* Peaks must comprise at least 5.00 % of the distribution.

Micromeritics

WIN5100 V2.03

Page 1

Sample: TT-47-08 357 cm  
Operator: Clint Edrington  
Submitter: Clint Edrington  
File Name: C:\EDRING~1\TIGER&~1\SANDFR~1\TT-47-08\47\_357CM.SMP  
Material/Liquid: silicate mud/water/Water

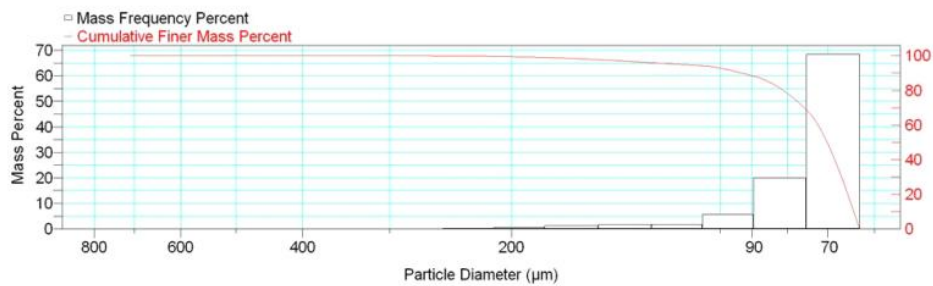
Reported: 01/04/10 19:05:17  
Liquid Visc: 0.7225 cp

Sample Density: 2.650 g/cm<sup>3</sup>  
Liquid Density: 0.9941 g/cm<sup>3</sup>

Report by Size Class

High Diameter (µm)	Low Diameter (µm)	Average Diameter (µm)	Cumulative Mass Finer (Percent)	Mass Frequency (Percent)
850.0	710.0	776.9	100.0	0.0
710.0	600.0	652.7	100.0	0.0
600.0	500.0	547.7	100.0	0.0
500.0	425.0	461.0	100.0	0.0
425.0	355.0	388.4	100.0	0.0
355.0	300.0	326.3	100.0	0.0
300.0	250.0	273.9	99.9	0.1
250.0	212.0	230.2	99.6	0.3
212.0	180.0	195.3	99.0	0.6
180.0	150.0	164.3	97.7	1.3
150.0	125.0	136.9	95.9	1.8
125.0	106.0	115.1	94.2	1.7
106.0	90.00	97.67	88.5	5.7
90.00	75.00	82.16	68.5	20.0
75.00	63.00	68.74	0.0	68.5

Mass Frequency vs Diameter



Summary Report

Full scale pump speed: 3  
Bubble detection: Medium  
Starting Size: 63.00 µm  
Ending Size: 0.50 µm

Stir time: 30 secs  
Stir speed: Low  
Probe time: 30 secs

Sample: TT-47-08 357 cm  
 Operator: Clint Edrington  
 Submitter: Clint Edrington  
 File Name: C:\EDRING~1\TIGER&~1\SANDFR~1\TT-47-08\47\_357CM.SMP  
 Material/Liquid: silicate mud/water/Water

Reported: 01/04/10 19:05:17  
 Liquid Visc: 0.7225 cp

Sample Density: 2.650 g/cm<sup>3</sup>  
 Liquid Density: 0.9941 g/cm<sup>3</sup>

## Summary Report

Parameter 1	0.000	Parameter 2	0.000	Parameter 3	0.000		
Mass Distribution Arithmetic Statistics							
Mean	77.78	Std. Dev.		21.39			
Median	70.12	Coef. Var.		0.275			
Mode	68.74	Skewness		4.181			
		Kurtosis		22.038			
Selected Percentiles			Selected Sizes				
Percent Finer	Diameter (µm)		Diameter (µm)	Percent Finer			
100.0	714.1		500.0	100.0			
80.0	81.16		250.0	99.9			
60.0	72.28		125.0	95.9			
40.0	68.38		88.00	87.4			
20.0	65.48		63.00	0.0			
Peak Number	% of Dist.*	Mean	Mode	Median	Standard Deviation	Skewness	Kurtosis
1	100.0	77.78	68.74	70.12	21.39	4.181	22.038

\* Peaks must comprise at least 5.00 % of the distribution.

Micromeritics

WIN5100 V2.03

Page 1

Sample: TT-48-08 7 cm  
Operator: Clint Edrington  
Submitter: Clint Edrington  
File Name: C:\EDRING~1\TIGER&~1\SANDFR~1\TT-48-08\48\_7CM.SMP  
Material/Liquid: silicate mud/water/Water

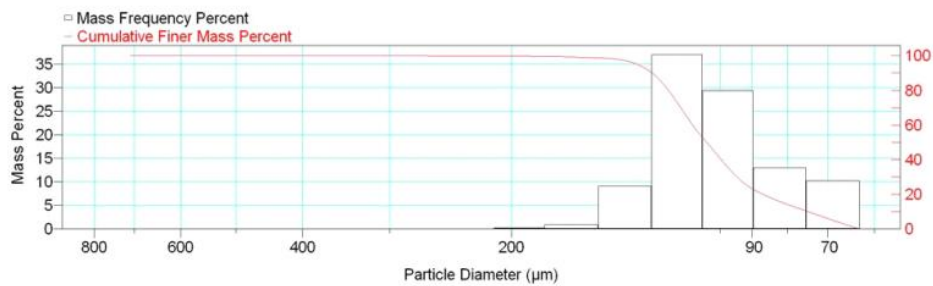
Reported: 01/04/10 19:08:31  
Liquid Visc: 0.7225 cp

Sample Density: 2.650 g/cm<sup>3</sup>  
Liquid Density: 0.9941 g/cm<sup>3</sup>

Report by Size Class

High Diameter (μm)	Low Diameter (μm)	Average Diameter (μm)	Cumulative Mass Finer (Percent)	Mass Frequency (Percent)
850.0	710.0	776.9	100.0	0.0
710.0	600.0	652.7	100.0	0.0
600.0	500.0	547.7	100.0	0.0
500.0	425.0	461.0	100.0	0.0
425.0	355.0	388.4	100.0	0.0
355.0	300.0	326.3	100.0	0.0
300.0	250.0	273.9	99.9	0.1
250.0	212.0	230.2	99.8	0.1
212.0	180.0	195.3	99.6	0.2
180.0	150.0	164.3	98.7	0.9
150.0	125.0	136.9	89.6	9.1
125.0	106.0	115.1	52.6	37.0
106.0	90.00	97.67	23.2	29.4
90.00	75.00	82.16	10.2	13.0
75.00	63.00	68.74	0.0	10.2

Mass Frequency vs Diameter



Summary Report

Full scale pump speed: 3  
Bubble detection: Medium  
Starting Size: 63.00 μm  
Ending Size: 0.50 μm

Stir time: 30 secs  
Stir speed: Low  
Probe time: 30 secs

Sample: TT-48-08 7 cm  
 Operator: Clint Edrington  
 Submitter: Clint Edrington  
 File Name: C:\EDRING~1\TIGER&~1\SANDFR~1\TT-48-08\48\_7CM.SMP  
 Material/Liquid: silicate mud/water/Water

Reported: 01/04/10 19:08:31  
 Liquid Visc: 0.7225 cp

Sample Density: 2.650 g/cm<sup>3</sup>  
 Liquid Density: 0.9941 g/cm<sup>3</sup>

## Summary Report

Parameter 1	0.000	Parameter 2	0.000	Parameter 3	0.000		
Mass Distribution Arithmetic Statistics							
Mean	103.8	Std. Dev.		20.96			
Median	104.6	Coef. Var.		0.202			
Mode	115.1	Skewness		0.922			
		Kurtosis		5.560			
Selected Percentiles			Selected Sizes				
Percent Finer	Diameter (µm)		Diameter (µm)	Percent Finer			
100.0	714.1		500.0	100.0			
80.0	118.8		250.0	99.9			
60.0	109.6		125.0	89.6			
40.0	99.71		88.00	21.2			
20.0	86.81		63.00	0.0			
Peak Number	% of Dist.*	Mean	Mode	Median	Standard Deviation	Skewness	Kurtosis
1	100.0	103.8	115.1	104.6	20.96	0.922	5.560

\* Peaks must comprise at least 5.00 % of the distribution.



Micromeritics

WIN5100 V2.03

Page 1

Sample: TT-48-08 45 cm  
Operator: Clint Edrington  
Submitter: Clint Edrington  
File Name: C:\EDRING~1\TIGER&~1\SANDFR~1\TT-48-08\48\_45CM.SMP  
Material/Liquid: silicate mud/water/Water

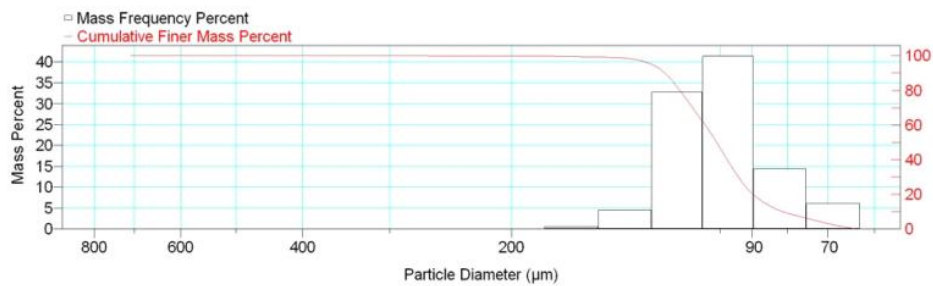
Reported: 01/04/10 19:11:17  
Liquid Visc: 0.7225 cp

Sample Density: 2.650 g/cm<sup>3</sup>  
Liquid Density: 0.9941 g/cm<sup>3</sup>

Report by Size Class

High Diameter ( $\mu\text{m}$ )	Low Diameter ( $\mu\text{m}$ )	Average Diameter ( $\mu\text{m}$ )	Cumulative Mass Finer (Percent)	Mass Frequency (Percent)
850.0	710.0	776.9	100.0	0.0
710.0	600.0	652.7	100.0	0.0
600.0	500.0	547.7	100.0	0.0
500.0	425.0	461.0	100.0	0.0
425.0	355.0	388.4	100.0	0.0
355.0	300.0	326.3	100.0	0.0
300.0	250.0	273.9	99.9	0.1
250.0	212.0	230.2	99.8	0.1
212.0	180.0	195.3	99.7	0.1
180.0	150.0	164.3	99.2	0.5
150.0	125.0	136.9	94.7	4.5
125.0	106.0	115.1	61.9	32.8
106.0	90.00	97.67	20.5	41.4
90.00	75.00	82.16	6.1	14.4
75.00	63.00	68.74	0.0	6.1

Mass Frequency vs Diameter



Summary Report

Full scale pump speed: 3  
Bubble detection: Medium  
Starting Size: 63.00  $\mu\text{m}$   
Ending Size: 0.50  $\mu\text{m}$

Stir time: 30 secs  
Stir speed: Low  
Probe time: 30 secs

Sample: TT-48-08 45 cm  
 Operator: Clint Edrington  
 Submitter: Clint Edrington  
 File Name: C:\EDRING~1\TIGER&~1\SANDFR~1\TT-48-08\48\_45CM.SMP  
 Material/Liquid: silicate mud/water/Water

Reported: 01/04/10 19:11:17  
 Liquid Visc: 0.7225 cp

Sample Density: 2.650 g/cm<sup>3</sup>  
 Liquid Density: 0.9941 g/cm<sup>3</sup>

## Summary Report

Parameter 1	0.000	Parameter 2	0.000	Parameter 3	0.000		
Mass Distribution Arithmetic Statistics							
Mean	101.9	Std. Dev.		17.81			
Median	101.2	Coef. Var.		0.175			
Mode	97.67	Skewness		1.514			
		Kurtosis		11.614			
Selected Percentiles			Selected Sizes				
Percent Finer	Diameter (µm)		Diameter (µm)	Percent Finer			
100.0	714.1		500.0	100.0			
80.0	114.4		250.0	99.9			
60.0	105.1		125.0	94.7			
40.0	97.75		88.00	17.3			
20.0	89.71		63.00	0.0			
Peak Number	% of Dist.*	Mean	Mode	Median	Standard Deviation	Skewness	Kurtosis
1	100.0	101.9	97.67	101.2	17.81	1.514	11.614

\* Peaks must comprise at least 5.00 % of the distribution.

Micromeritics

WIN5100 V2.03

Page 1

Sample: TT-48-08 106 cm  
Operator: Clint Edrington  
Submitter: Clint Edrington  
File Name: C:\EDRING~1\TIGER&~1\SANDFR~1\TT-48-08\48\_106CM.SMP  
Material/Liquid: silicate mud/water/Water

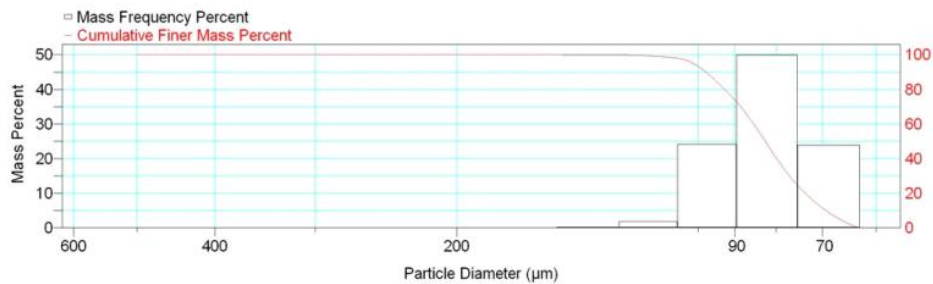
Reported: 01/04/10 19:13:12  
Liquid Visc: 0.7225 cp

Sample Density: 2.650 g/cm<sup>3</sup>  
Liquid Density: 0.9941 g/cm<sup>3</sup>

Report by Size Class

High Diameter ( $\mu\text{m}$ )	Low Diameter ( $\mu\text{m}$ )	Average Diameter ( $\mu\text{m}$ )	Cumulative Mass Finer (Percent)	Mass Frequency (Percent)
600.0	500.0	547.7	100.0	0.0
500.0	425.0	461.0	100.0	0.0
425.0	355.0	388.4	100.0	0.0
355.0	300.0	326.3	100.0	0.0
300.0	250.0	273.9	100.0	0.0
250.0	212.0	230.2	100.0	0.0
212.0	180.0	195.3	100.0	0.0
180.0	150.0	164.3	100.0	0.0
150.0	125.0	136.9	99.8	0.2
125.0	106.0	115.1	98.0	1.8
106.0	90.00	97.67	73.8	24.2
90.00	75.00	82.16	23.9	49.9
75.00	63.00	68.74	0.0	23.9

Mass Frequency vs Diameter



Summary Report

Full scale pump speed: 3  
Bubble detection: Medium  
Starting Size: 63.00  $\mu\text{m}$   
Ending Size: 0.50  $\mu\text{m}$

Stir time: 30 secs  
Stir speed: Low  
Probe time: 30 secs

Parameter 1 0.000

Parameter 2 0.000

Parameter 3 0.000

Sample: TT-48-08 106 cm  
 Operator: Clint Edrington  
 Submitter: Clint Edrington  
 File Name: C:\EDRING~1\TIGER&~1\SANDFR~1\TT-48-08\48\_106CM.SMP  
 Material/Liquid: silicate mud/water/Water

Reported: 01/04/10 19:13:12      Sample Density: 2.650 g/cm<sup>3</sup>  
 Liquid Visc: 0.7225 cp      Liquid Density: 0.9941 g/cm<sup>3</sup>

## Summary Report

## Mass Distribution Arithmetic Statistics

Mean	83.41	Std. Dev.	11.19
Median	82.48	Coef. Var.	0.134
Mode	82.16	Skewness	0.590
		Kurtosis	0.548

## Selected Percentiles

Percent Finer	Diameter (µm)
100.0	505.0
80.0	92.71
60.0	85.28
40.0	79.80
20.0	73.55

## Selected Sizes

Diameter (µm)	Percent Finer
500.0	100.0
250.0	100.0
125.0	99.8
88.00	68.6
63.00	0.0

Peak Number	% of Dist.*	Mean	Mode	Median	Standard Deviation	Skewness	Kurtosis
1	100.0	83.41	82.16	82.48	11.19	0.590	0.548

\* Peaks must comprise at least 5.00 % of the distribution.

# Micromeritics

WIN5100 V2.03

Page 1

Sample: TT-48-08 155 cm  
Operator: Clint Edrington  
Submitter: Clint Edrington  
File Name: C:\EDRING~1\TIGER&~1\SANDFR~1\TT-48-08\48\_155CM.SMP  
Material/Liquid: silicate mud/water/Water

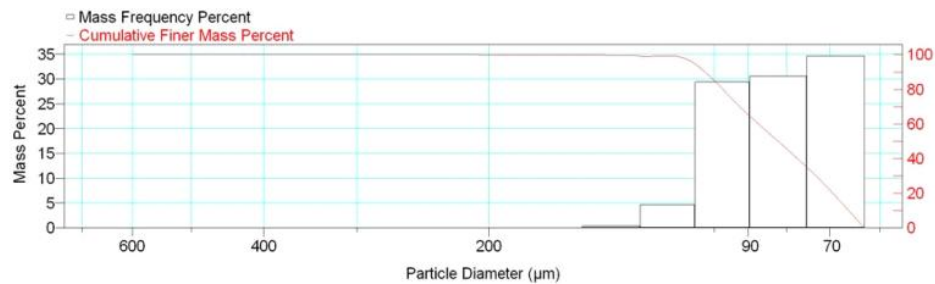
Reported: 01/04/10 19:14:54  
Liquid Visc: 0.7225 cp

Sample Density: 2.650 g/cm<sup>3</sup>  
Liquid Density: 0.9941 g/cm<sup>3</sup>

## Report by Size Class

High Diameter (µm)	Low Diameter (µm)	Average Diameter (µm)	Cumulative Mass Finer (Percent)	Mass Frequency (Percent)
710.0	600.0	652.7	100.0	0.0
600.0	500.0	547.7	100.0	0.0
500.0	425.0	461.0	100.0	0.0
425.0	355.0	388.4	100.0	0.0
355.0	300.0	326.3	100.0	0.0
300.0	250.0	273.9	100.0	0.0
250.0	212.0	230.2	100.0	0.0
212.0	180.0	195.3	99.9	0.1
180.0	150.0	164.3	99.8	0.1
150.0	125.0	136.9	99.4	0.4
125.0	106.0	115.1	94.7	4.7
106.0	90.00	97.67	65.3	29.4
90.00	75.00	82.16	34.7	30.6
75.00	63.00	68.74	0.0	34.7

Mass Frequency vs Diameter



## Summary Report

Full scale pump speed: 3  
Bubble detection: Medium  
Starting Size: 63.00 µm  
Ending Size: 0.50 µm

Stir time: 30 secs  
Stir speed: Low  
Probe time: 30 secs

Sample: TT-48-08 155 cm  
 Operator: Clint Edrington  
 Submitter: Clint Edrington  
 File Name: C:\EDRING~1\TIGER&~1\SANDFR~1\TT-48-08\48\_155CM.SMP  
 Material/Liquid: silicate mud/water/Water

Reported: 01/04/10 19:14:54  
 Liquid Visc: 0.7225 cp

Sample Density: 2.650 g/cm<sup>3</sup>  
 Liquid Density: 0.9941 g/cm<sup>3</sup>

## Summary Report

Parameter 1 0.000

Parameter 2 0.000

Parameter 3 0.000

## Mass Distribution Arithmetic Statistics

Mean	84.03	Std. Dev.	14.57
Median	82.08	Coef. Var.	0.173
Mode	68.74	Skewness	1.101
		Kurtosis	3.641

## Selected Percentiles

Percent Finer	Diameter (µm)
100.0	600.3
80.0	97.29
60.0	87.20
40.0	77.33
20.0	69.37

## Selected Sizes

Diameter (µm)	Percent Finer
500.0	100.0
250.0	100.0
125.0	99.4
88.00	61.5
63.00	0.0

Peak Number	% of Dist. *	Mean	Mode	Median	Standard Deviation	Skewness	Kurtosis
1	65.3	75.03	68.74	74.14	6.697	0.126	-1.984
2	65.2	91.99	82.16	91.04	10.90	1.284	3.542

\* Peaks must comprise at least 5.00 % of the distribution.

# Micromeritics

WIN5100 V2.03

Page 1

Sample: TT-48-08 200 cm  
Operator: Clint Edrington  
Submitter: Clint Edrington  
File Name: C:\EDRING~1\TIGER&~1\SANDFR~1\TT-48-08\48\_200CM.SMP  
Material/Liquid: silicate mud/water/Water

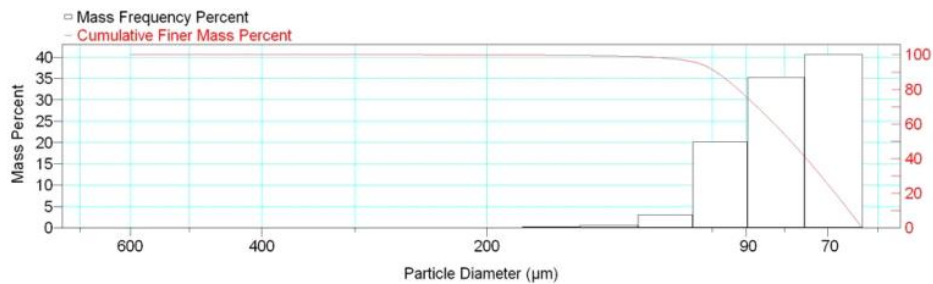
Reported: 01/04/10 19:16:54  
Liquid Visc: 0.7225 cp

Sample Density: 2.650 g/cm<sup>3</sup>  
Liquid Density: 0.9941 g/cm<sup>3</sup>

## Report by Size Class

High Diameter (µm)	Low Diameter (µm)	Average Diameter (µm)	Cumulative Mass Finer (Percent)	Mass Frequency (Percent)
710.0	600.0	652.7	100.0	0.0
600.0	500.0	547.7	100.0	0.0
500.0	425.0	461.0	100.0	0.0
425.0	355.0	388.4	100.0	0.0
355.0	300.0	326.3	100.0	0.0
300.0	250.0	273.9	100.0	0.0
250.0	212.0	230.2	99.9	0.1
212.0	180.0	195.3	99.8	0.1
180.0	150.0	164.3	99.5	0.3
150.0	125.0	136.9	98.9	0.6
125.0	106.0	115.1	95.9	3.0
106.0	90.00	97.67	75.8	20.1
90.00	75.00	82.16	40.6	35.2
75.00	63.00	68.74	0.0	40.6

Mass Frequency vs Diameter



## Summary Report

Full scale pump speed: 3  
Bubble detection: Medium  
Starting Size: 63.00 µm  
Ending Size: 0.50 µm

Stir time: 30 secs  
Stir speed: Low  
Probe time: 30 secs

Sample: TT-48-08 200 cm  
 Operator: Clint Edrington  
 Submitter: Clint Edrington  
 File Name: C:\EDRING~1\TIGER&~1\SANDFR~1\TT-48-08\48\_200CM.SMP  
 Material/Liquid: silicate mud/water/Water

Reported: 01/04/10 19:16:54  
 Liquid Visc: 0.7225 cp

Sample Density: 2.650 g/cm<sup>3</sup>  
 Liquid Density: 0.9941 g/cm<sup>3</sup>

## Summary Report

Parameter 1 0.000

Parameter 2 0.000

Parameter 3 0.000

## Mass Distribution Arithmetic Statistics

Mean	81.65	Std. Dev.	15.06
Median	78.41	Coef. Var.	0.184
Mode	68.74	Skewness	2.498
		Kurtosis	14.739

## Selected Percentiles

Percent Finer	Diameter (µm)
100.0	651.9
80.0	92.24
60.0	82.49
40.0	74.79
20.0	68.43

## Selected Sizes

Diameter (µm)	Percent Finer
500.0	100.0
250.0	100.0
125.0	98.9
88.00	71.9
63.00	0.0

Peak Number	% of Dist. *	Mean	Mode	Median	Standard Deviation	Skewness	Kurtosis
1	100.0	81.65	68.74	78.41	15.06	2.498	14.739

\* Peaks must comprise at least 5.00 % of the distribution.



# Micromeritics

WIN5100 V2.03

Page 1

Sample: TT-48-08 240 cm  
Operator: Clint Edrington  
Submitter: Clint Edrington  
File Name: C:\EDRING~1\TIGER&~1\SANDFR~1\TT-48-08\48\_240CM.SMP  
Material/Liquid: silicate mud/water/Water

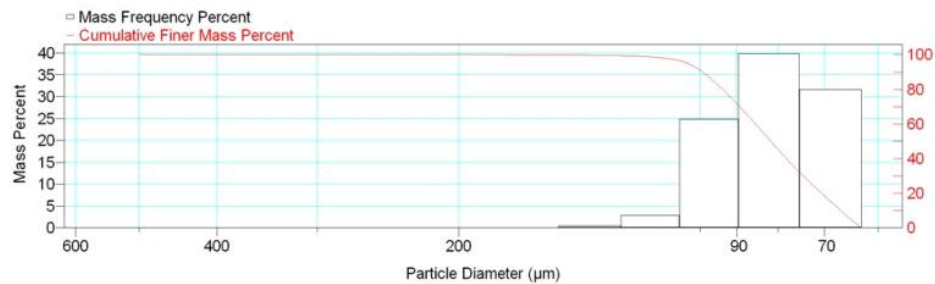
Reported: 01/04/10 19:18:46  
Liquid Visc: 0.7225 cp

Sample Density: 2.650 g/cm<sup>3</sup>  
Liquid Density: 0.9941 g/cm<sup>3</sup>

## Report by Size Class

High Diameter (µm)	Low Diameter (µm)	Average Diameter (µm)	Cumulative Mass Finer (Percent)	Mass Frequency (Percent)
600.0	500.0	547.7	100.0	0.0
500.0	425.0	461.0	100.0	0.0
425.0	355.0	388.4	100.0	0.0
355.0	300.0	326.3	100.0	0.0
300.0	250.0	273.9	100.0	0.0
250.0	212.0	230.2	100.0	0.0
212.0	180.0	195.3	100.0	0.0
180.0	150.0	164.3	99.9	0.1
150.0	125.0	136.9	99.4	0.5
125.0	106.0	115.1	96.5	2.9
106.0	90.00	97.67	71.6	24.9
90.00	75.00	82.16	31.7	39.9
75.00	63.00	68.74	0.0	31.7

Mass Frequency vs Diameter



## Summary Report

Full scale pump speed: 3  
Bubble detection: Medium  
Starting Size: 63.00 µm  
Ending Size: 0.50 µm

Stir time: 30 secs  
Stir speed: Low  
Probe time: 30 secs

Parameter 1 0.000

Parameter 2 0.000

Parameter 3 0.000

Sample: TT-48-08 240 cm  
 Operator: Clint Edrington  
 Submitter: Clint Edrington  
 File Name: C:\EDRING~1\TIGER&~1\SANDFR~1\TT-48-08\48\_240CM.SMP  
 Material/Liquid: silicate mud/water/Water

Reported: 01/04/10 19:18:46  
 Liquid Visc: 0.7225 cp

Sample Density: 2.650 g/cm<sup>3</sup>  
 Liquid Density: 0.9941 g/cm<sup>3</sup>

## Summary Report

## Mass Distribution Arithmetic Statistics

Mean	83.08	Std. Dev.	13.02
Median	81.64	Coef. Var.	0.157
Mode	82.16	Skewness	0.956
		Kurtosis	1.907

## Selected Percentiles

Percent Finer	Diameter (µm)
100.0	553.2
80.0	93.82
60.0	85.31
40.0	78.07
20.0	70.56

## Selected Sizes

Diameter (µm)	Percent Finer
500.0	100.0
250.0	100.0
125.0	99.4
88.00	66.9
63.00	0.0

Peak Number	% of Dist.*	Mean	Mode	Median	Standard Deviation	Skewness	Kurtosis
1	100.0	83.08	82.16	81.64	13.02	0.956	1.907

\* Peaks must comprise at least 5.00 % of the distribution.

# Micromeritics

WIN5100 V2.03

Page 1

Sample: TT-48-08 300 cm  
Operator: Clint Edrington  
Submitter: Clint Edrington  
File Name: C:\EDRING~1\TIGER&~1\SANDFR~1\TT-48-08\48\_300CM.SMP  
Material/Liquid: silicate mud/water/Water

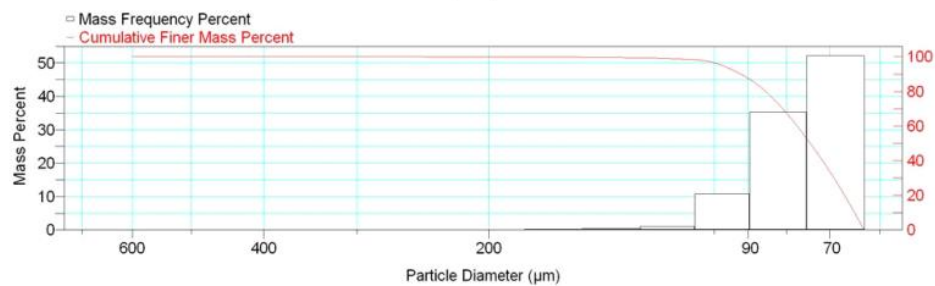
Reported: 01/04/10 19:20:59  
Liquid Visc: 0.7225 cp

Sample Density: 2.650 g/cm<sup>3</sup>  
Liquid Density: 0.9941 g/cm<sup>3</sup>

## Report by Size Class

High Diameter (μm)	Low Diameter (μm)	Average Diameter (μm)	Cumulative Mass Finer (Percent)	Mass Frequency (Percent)
710.0	600.0	652.7	100.0	0.0
600.0	500.0	547.7	100.0	0.0
500.0	425.0	461.0	100.0	0.0
425.0	355.0	388.4	100.0	0.0
355.0	300.0	326.3	100.0	0.0
300.0	250.0	273.9	100.0	0.0
250.0	212.0	230.2	99.9	0.1
212.0	180.0	195.3	99.9	0.0
180.0	150.0	164.3	99.7	0.2
150.0	125.0	136.9	99.3	0.4
125.0	106.0	115.1	98.3	1.0
106.0	90.00	97.67	87.5	10.8
90.00	75.00	82.16	52.2	35.3
75.00	63.00	68.74	0.0	52.2

Mass Frequency vs Diameter



## Summary Report

Full scale pump speed: 3  
Bubble detection: Medium  
Starting Size: 63.00 μm  
Ending Size: 0.50 μm

Stir time: 30 secs  
Stir speed: Low  
Probe time: 30 secs

Sample: TT-48-08 300 cm  
 Operator: Clint Edrington  
 Submitter: Clint Edrington  
 File Name: C:\EDRING~1\TIGER&~1\SANDFR~1\TT-48-08\48\_300CM.SMP  
 Material/Liquid: silicate mud/water/Water

Reported: 01/04/10 19:20:59  
 Liquid Visc: 0.7225 cp

Sample Density: 2.650 g/cm<sup>3</sup>  
 Liquid Density: 0.9941 g/cm<sup>3</sup>

## Summary Report

Parameter 1 0.000

Parameter 2 0.000

Parameter 3 0.000

## Mass Distribution Arithmetic Statistics

Mean	77.69	Std. Dev.	12.58
Median	74.35	Coef. Var.	0.162
Mode	68.74	Skewness	3.375
		Kurtosis	26.663

## Selected Percentiles

Percent Finer	Diameter (µm)
100.0	651.9
80.0	85.33
60.0	77.43
40.0	71.60
20.0	66.90

## Selected Sizes

Diameter (µm)	Percent Finer
500.0	100.0
250.0	100.0
125.0	99.3
88.00	84.7
63.00	0.0

Peak Number	% of Dist. *	Mean	Mode	Median	Standard Deviation	Skewness	Kurtosis
1	99.9	77.54	68.74	74.34	11.63	2.062	8.187

\* Peaks must comprise at least 5.00 % of the distribution.

# Micromeritics

WIN5100 V2.03

Page 1

Sample: TT-48-08 350 cm  
Operator: Clint Edrington  
Submitter: Clint Edrington  
File Name: C:\EDRING~1\TIGER&~1\SANDFR~1\TT-48-08\48\_350CM.SMP  
Material/Liquid: silicate mud/water/Water

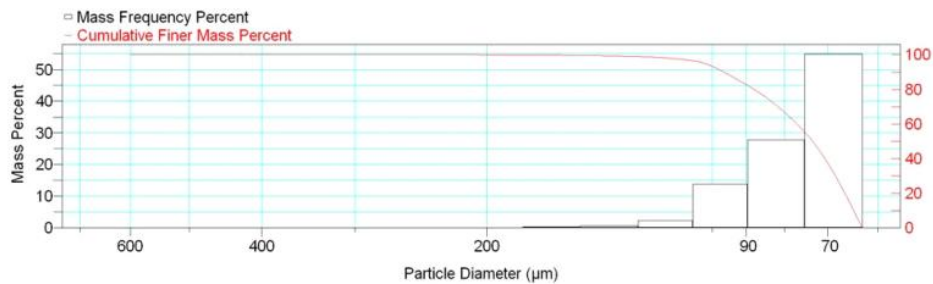
Reported: 01/04/10 19:22:53  
Liquid Visc: 0.7225 cp

Sample Density: 2.650 g/cm<sup>3</sup>  
Liquid Density: 0.9941 g/cm<sup>3</sup>

## Report by Size Class

High Diameter (µm)	Low Diameter (µm)	Average Diameter (µm)	Cumulative Mass Finer (Percent)	Mass Frequency (Percent)
710.0	600.0	652.7	100.0	0.0
600.0	500.0	547.7	100.0	0.0
500.0	425.0	461.0	100.0	0.0
425.0	355.0	388.4	100.0	0.0
355.0	300.0	326.3	100.0	0.0
300.0	250.0	273.9	100.0	0.0
250.0	212.0	230.2	100.0	0.0
212.0	180.0	195.3	99.9	0.1
180.0	150.0	164.3	99.6	0.3
150.0	125.0	136.9	98.9	0.7
125.0	106.0	115.1	96.5	2.4
106.0	90.00	97.67	82.7	13.8
90.00	75.00	82.16	54.9	27.8
75.00	63.00	68.74	0.0	54.9

Mass Frequency vs Diameter



## Summary Report

Full scale pump speed: 3  
Bubble detection: Medium  
Starting Size: 63.00 µm  
Ending Size: 0.50 µm

Stir time: 30 secs  
Stir speed: Low  
Probe time: 30 secs

Sample: TT-48-08 350 cm  
 Operator: Clint Edrington  
 Submitter: Clint Edrington  
 File Name: C:\EDRING~1\TIGER&~1\SANDFR~1\TT-48-08\48\_350CM.SMP  
 Material/Liquid: silicate mud/water/Water

Reported: 01/04/10 19:22:53  
 Liquid Visc: 0.7225 cp

Sample Density: 2.650 g/cm<sup>3</sup>  
 Liquid Density: 0.9941 g/cm<sup>3</sup>

## Summary Report

Parameter 1 0.000

Parameter 2 0.000

Parameter 3 0.000

## Mass Distribution Arithmetic Statistics

Mean	78.47	Std. Dev.	14.09
Median	73.34	Coef. Var.	0.180
Mode	68.74	Skewness	2.345
		Kurtosis	9.640

## Selected Percentiles

Percent Finer	Diameter (µm)
100.0	600.3
80.0	87.84
60.0	77.00
40.0	70.62
20.0	66.42

## Selected Sizes

Diameter (µm)	Percent Finer
500.0	100.0
250.0	100.0
125.0	98.9
88.00	80.2
63.00	0.0

Peak Number	% of Dist. *	Mean	Mode	Median	Standard Deviation	Skewness	Kurtosis
1	100.0	78.47	68.74	73.34	14.09	2.345	9.640

\* Peaks must comprise at least 5.00 % of the distribution.

Micromeritics

WIN5100 V2.03

Page 1

Sample: TT-49-08 0 cm  
Operator: Clint Edrington  
Submitter: Clint Edrington  
File Name: C:\EDRING~1\TIGER&~1\SANDFR~1\TT-49-08\49\_0CM.SMP  
Material/Liquid: silicate mud/water/Water

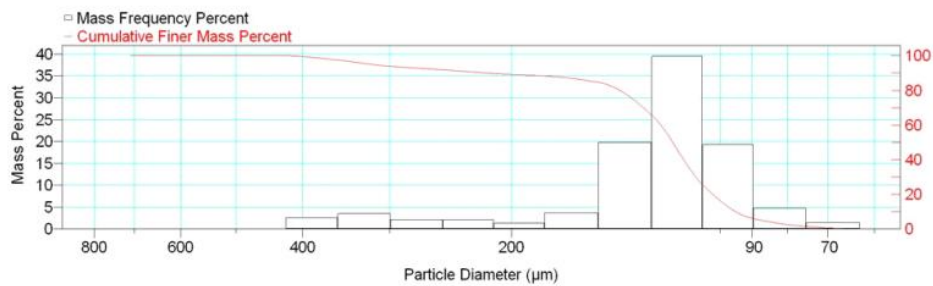
Reported: 01/04/10 19:26:41  
Liquid Visc: 0.7225 cp

Sample Density: 2.650 g/cm<sup>3</sup>  
Liquid Density: 0.9941 g/cm<sup>3</sup>

Report by Size Class

High Diameter (µm)	Low Diameter (µm)	Average Diameter (µm)	Cumulative Mass Finer (Percent)	Mass Frequency (Percent)
850.0	710.0	776.9	100.0	0.0
710.0	600.0	652.7	100.0	0.0
600.0	500.0	547.7	100.0	0.0
500.0	425.0	461.0	100.0	0.0
425.0	355.0	388.4	97.4	2.6
355.0	300.0	326.3	93.9	3.5
300.0	250.0	273.9	91.8	2.1
250.0	212.0	230.2	89.7	2.1
212.0	180.0	195.3	88.4	1.3
180.0	150.0	164.3	84.7	3.7
150.0	125.0	136.9	64.9	19.8
125.0	106.0	115.1	25.4	39.5
106.0	90.00	97.67	6.1	19.3
90.00	75.00	82.16	1.4	4.7
75.00	63.00	68.74	0.0	1.4

Mass Frequency vs Diameter



Summary Report

Full scale pump speed: 3  
Bubble detection: Medium  
Starting Size: 63.00 µm  
Ending Size: 0.50 µm

Stir time: 30 secs  
Stir speed: Low  
Probe time: 30 secs

Sample: TT-49-08 0 cm  
 Operator: Clint Edrington  
 Submitter: Clint Edrington  
 File Name: C:\EDRING~1\TIGER&~1\SANDFR~1\TT-49-08\49\_0CM.SMP  
 Material/Liquid: silicate mud/water/Water

Reported: 01/04/10 19:26:41  
 Liquid Visc: 0.7225 cp

Sample Density: 2.650 g/cm<sup>3</sup>  
 Liquid Density: 0.9941 g/cm<sup>3</sup>

## Summary Report

Parameter 1	0.000	Parameter 2	0.000	Parameter 3	0.000		
Mass Distribution Arithmetic Statistics							
Mean	137.0	Std. Dev.		65.12			
Median	117.1	Coef. Var.		0.475			
Mode	115.1	Skewness		2.525			
		Kurtosis		5.862			
Selected Percentiles			Selected Sizes				
Percent Finer	Diameter (µm)		Diameter (µm)	Percent Finer			
100.0	850.0		500.0	100.0			
80.0	139.6		250.0	91.8			
60.0	121.9		125.0	64.9			
40.0	112.9		88.00	5.3			
20.0	102.5		63.00	0.0			
Peak Number	% of Dist.*	Mean	Mode	Median	Standard Deviation	Skewness	Kurtosis
1	89.7	116.9	115.1	114.9	21.23	0.801	1.831
2	5.5	238.6	273.9	237.5	30.72	-0.094	-1.406
3	8.2	332.6	326.3	331.4	43.46	0.039	-1.281

\* Peaks must comprise at least 5.00 % of the distribution.



Micromeritics

WIN5100 V2.03

Page 1

Sample: TT-49-08 30 cm  
Operator: Clint Edrington  
Submitter: Clint Edrington  
File Name: C:\EDRING~1\TIGER&~1\SANDFR~1\TT-49-08\49\_30CM.SMP  
Material/Liquid: silicate mud/water/Water

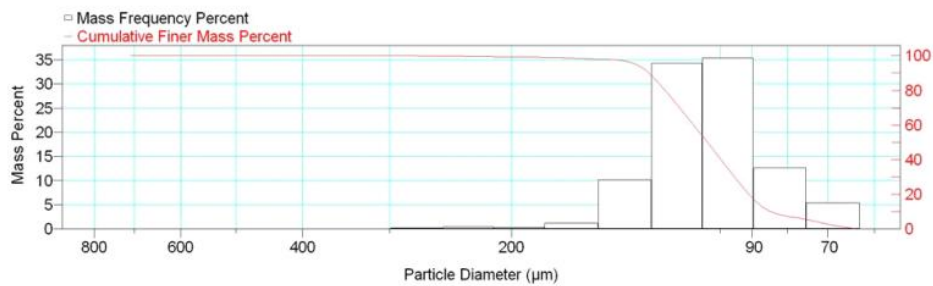
Reported: 01/04/10 19:28:58  
Liquid Visc: 0.7225 cp

Sample Density: 2.650 g/cm<sup>3</sup>  
Liquid Density: 0.9941 g/cm<sup>3</sup>

Report by Size Class

High Diameter (μm)	Low Diameter (μm)	Average Diameter (μm)	Cumulative Mass Finer (Percent)	Mass Frequency (Percent)
850.0	710.0	776.9	100.0	0.0
710.0	600.0	652.7	100.0	0.0
600.0	500.0	547.7	100.0	0.0
500.0	425.0	461.0	100.0	0.0
425.0	355.0	388.4	100.0	0.0
355.0	300.0	326.3	100.0	0.0
300.0	250.0	273.9	99.8	0.2
250.0	212.0	230.2	99.4	0.4
212.0	180.0	195.3	99.1	0.3
180.0	150.0	164.3	97.9	1.2
150.0	125.0	136.9	87.7	10.2
125.0	106.0	115.1	53.4	34.3
106.0	90.00	97.67	18.0	35.4
90.00	75.00	82.16	5.4	12.6
75.00	63.00	68.74	0.0	5.4

Mass Frequency vs Diameter



Summary Report

Full scale pump speed: 3  
Bubble detection: Medium  
Starting Size: 63.00 μm  
Ending Size: 0.50 μm

Stir time: 30 secs  
Stir speed: Low  
Probe time: 30 secs

Sample: TT-49-08 30 cm  
 Operator: Clint Edrington  
 Submitter: Clint Edrington  
 File Name: C:\EDRING~1\TIGER&~1\SANDFR~1\TT-49-08\49\_30CM.SMP  
 Material/Liquid: silicate mud/water/Water

Reported: 01/04/10 19:28:58  
 Liquid Visc: 0.7225 cp

Sample Density: 2.650 g/cm<sup>3</sup>  
 Liquid Density: 0.9941 g/cm<sup>3</sup>

## Summary Report

Parameter 1	0.000	Parameter 2	0.000	Parameter 3	0.000		
Mass Distribution Arithmetic Statistics							
Mean	106.1	Std. Dev.		21.91			
Median	104.3	Coef. Var.		0.206			
Mode	97.67	Skewness		1.907			
		Kurtosis		10.468			
Selected Percentiles			Selected Sizes				
Percent Finer	Diameter (µm)		Diameter (µm)	Percent Finer			
100.0	714.1		500.0	100.0			
80.0	120.2		250.0	99.8			
60.0	109.3		125.0	87.7			
40.0	99.76		88.00	14.3			
20.0	90.94		63.00	0.0			
Peak Number	% of Dist.*	Mean	Mode	Median	Standard Deviation	Skewness	Kurtosis
1	99.4	105.3	97.67	104.2	19.07	0.562	1.430

\* Peaks must comprise at least 5.00 % of the distribution.

Micromeritics

WIN5100 V2.03

Page 1

Sample: TT-49-08 50 cm  
Operator: Clint Edrington  
Submitter: Clint Edrington  
File Name: C:\EDRING~1\TIGER&~1\SANDFR~1\TT-49-08\49\_50CM.SMP  
Material/Liquid: silicate mud/water/Water

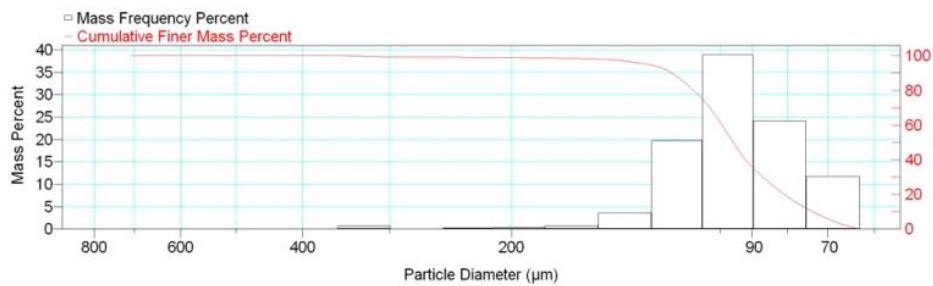
Reported: 01/04/10 19:32:00  
Liquid Visc: 0.7225 cp

Sample Density: 2.650 g/cm<sup>3</sup>  
Liquid Density: 0.9941 g/cm<sup>3</sup>

Report by Size Class

High Diameter ( $\mu\text{m}$ )	Low Diameter ( $\mu\text{m}$ )	Average Diameter ( $\mu\text{m}$ )	Cumulative Mass Finer (Percent)	Mass Frequency (Percent)
850.0	710.0	776.9	100.0	0.0
710.0	600.0	652.7	100.0	0.0
600.0	500.0	547.7	100.0	0.0
500.0	425.0	461.0	100.0	0.0
425.0	355.0	388.4	100.0	0.0
355.0	300.0	326.3	99.3	0.7
300.0	250.0	273.9	99.2	0.1
250.0	212.0	230.2	99.0	0.2
212.0	180.0	195.3	98.7	0.3
180.0	150.0	164.3	98.0	0.7
150.0	125.0	136.9	94.4	3.6
125.0	106.0	115.1	74.7	19.7
106.0	90.00	97.67	35.8	38.9
90.00	75.00	82.16	11.7	24.1
75.00	63.00	68.74	0.0	11.7

Mass Frequency vs Diameter



Summary Report

Full scale pump speed: 3  
Bubble detection: Medium  
Starting Size: 63.00  $\mu\text{m}$   
Ending Size: 0.50  $\mu\text{m}$

Stir time: 30 secs  
Stir speed: Low  
Probe time: 30 secs

Sample: TT-49-08 50 cm  
 Operator: Clint Edrington  
 Submitter: Clint Edrington  
 File Name: C:\EDRING~1\TIGER&~1\SANDFR~1\TT-49-08\49\_50CM.SMP  
 Material/Liquid: silicate mud/water/Water

Reported: 01/04/10 19:32:00  
 Liquid Visc: 0.7225 cp

Sample Density: 2.650 g/cm<sup>3</sup>  
 Liquid Density: 0.9941 g/cm<sup>3</sup>

## Summary Report

Parameter 1	0.000	Parameter 2	0.000	Parameter 3	0.000		
Mass Distribution Arithmetic Statistics							
Mean	98.20	Std. Dev.		27.62			
Median	95.83	Coef. Var.		0.281			
Mode	97.67	Skewness		4.602			
		Kurtosis		33.292			
Selected Percentiles			Selected Sizes				
Percent Finer	Diameter (µm)		Diameter (µm)	Percent Finer			
100.0	776.9		500.0	100.0			
80.0	109.3		250.0	99.2			
60.0	99.47		125.0	94.4			
40.0	91.97		88.00	32.1			
20.0	80.91		63.00	0.0			
Peak Number	% of Dist.*	Mean	Mode	Median	Standard Deviation	Skewness	Kurtosis
1	99.3	96.59	97.67	95.70	19.97	1.994	11.289

\* Peaks must comprise at least 5.00 % of the distribution.

Micromeritics

WIN5100 V2.03

Page 1

Sample: TT-49-08 105 cm  
Operator: Clint Edrington  
Submitter: Clint Edrington  
File Name: C:\EDRING~1\TIGER&~1\SANDFR~1\TT-49-08\49\_105CM.SMP  
Material/Liquid: silicate mud/water/Water

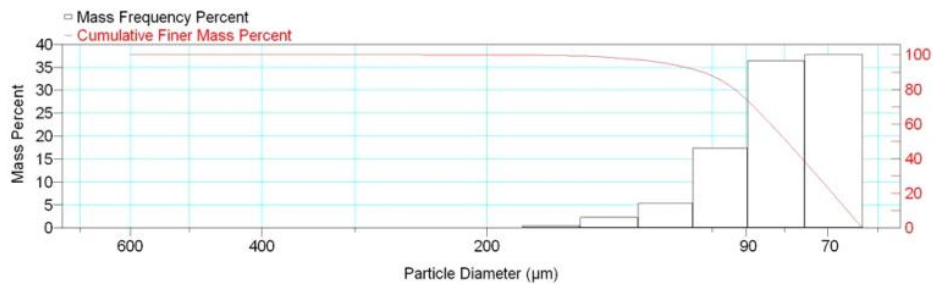
Reported: 01/04/10 19:34:10  
Liquid Visc: 0.7225 cp

Sample Density: 2.650 g/cm<sup>3</sup>  
Liquid Density: 0.9941 g/cm<sup>3</sup>

Report by Size Class

High Diameter (μm)	Low Diameter (μm)	Average Diameter (μm)	Cumulative Mass Finer (Percent)	Mass Frequency (Percent)
710.0	600.0	652.7	100.0	0.0
600.0	500.0	547.7	100.0	0.0
500.0	425.0	461.0	100.0	0.0
425.0	355.0	388.4	100.0	0.0
355.0	300.0	326.3	100.0	0.0
300.0	250.0	273.9	100.0	0.0
250.0	212.0	230.2	99.9	0.1
212.0	180.0	195.3	99.8	0.1
180.0	150.0	164.3	99.3	0.5
150.0	125.0	136.9	97.0	2.3
125.0	106.0	115.1	91.6	5.4
106.0	90.00	97.67	74.2	17.4
90.00	75.00	82.16	37.8	36.4
75.00	63.00	68.74	0.0	37.8

Mass Frequency vs Diameter



Summary Report

Full scale pump speed: 3  
Bubble detection: Medium  
Starting Size: 63.00 μm  
Ending Size: 0.50 μm

Stir time: 30 secs  
Stir speed: Low  
Probe time: 30 secs

Sample: TT-49-08 105 cm  
 Operator: Clint Edrington  
 Submitter: Clint Edrington  
 File Name: C:\EDRING~1\TIGER&~1\SANDFR~1\TT-49-08\49\_105CM.SMP  
 Material/Liquid: silicate mud/water/Water

Reported: 01/04/10 19:34:10  
 Liquid Visc: 0.7225 cp

Sample Density: 2.650 g/cm<sup>3</sup>  
 Liquid Density: 0.9941 g/cm<sup>3</sup>

## Summary Report

Parameter 1 0.000

Parameter 2 0.000

Parameter 3 0.000

## Mass Distribution Arithmetic Statistics

Mean	83.50	Std. Dev.	17.44
Median	79.48	Coef. Var.	0.209
Mode	68.74	Skewness	2.203
		Kurtosis	8.877

## Selected Percentiles

Percent Finer	Diameter (µm)
100.0	651.9
80.0	93.26
60.0	83.52
40.0	75.78
20.0	69.01

## Selected Sizes

Diameter (µm)	Percent Finer
500.0	100.0
250.0	100.0
125.0	97.0
88.00	70.1
63.00	0.0

Peak Number	% of Dist. *	Mean	Mode	Median	Standard Deviation	Skewness	Kurtosis
1	100.0	83.50	68.74	79.48	17.44	2.203	8.877

\* Peaks must comprise at least 5.00 % of the distribution.

Micromeritics

WIN5100 V2.03

Page 1

Sample: TT-49-08 150 cm  
Operator: Clint Edrington  
Submitter: Clint Edrington  
File Name: C:\EDRING~1\TIGER&~1\SANDFR~1\TT-49-08\49\_150CM.SMP  
Material/Liquid: silicate mud/water/Water

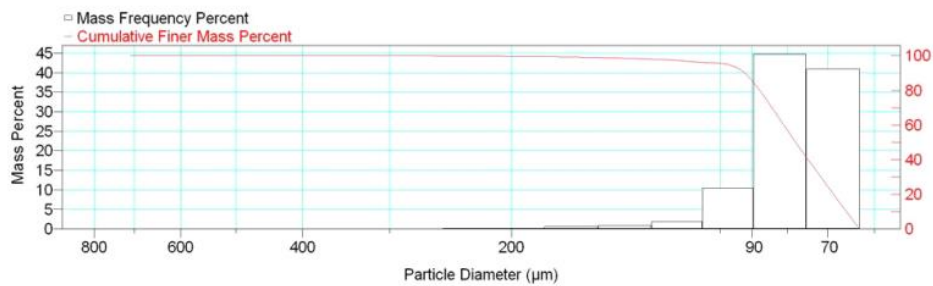
Reported: 01/04/10 19:36:31  
Liquid Visc: 0.7225 cp

Sample Density: 2.650 g/cm<sup>3</sup>  
Liquid Density: 0.9941 g/cm<sup>3</sup>

Report by Size Class

High Diameter (µm)	Low Diameter (µm)	Average Diameter (µm)	Cumulative Mass Finer (Percent)	Mass Frequency (Percent)
850.0	710.0	776.9	100.0	0.0
710.0	600.0	652.7	100.0	0.0
600.0	500.0	547.7	100.0	0.0
500.0	425.0	461.0	100.0	0.0
425.0	355.0	388.4	100.0	0.0
355.0	300.0	326.3	100.0	0.0
300.0	250.0	273.9	99.9	0.1
250.0	212.0	230.2	99.7	0.2
212.0	180.0	195.3	99.5	0.2
180.0	150.0	164.3	98.9	0.6
150.0	125.0	136.9	98.0	0.9
125.0	106.0	115.1	96.1	1.9
106.0	90.00	97.67	85.6	10.5
90.00	75.00	82.16	40.9	44.7
75.00	63.00	68.74	0.0	40.9

Mass Frequency vs Diameter



Summary Report

Full scale pump speed: 3  
Bubble detection: Medium  
Starting Size: 63.00 µm  
Ending Size: 0.50 µm

Stir time: 30 secs  
Stir speed: Low  
Probe time: 30 secs

Sample: TT-49-08 150 cm  
 Operator: Clint Edrington  
 Submitter: Clint Edrington  
 File Name: C:\EDRING~1\TIGER&~1\SANDFR~1\TT-49-08\49\_150CM.SMP  
 Material/Liquid: silicate mud/water/Water

Reported: 01/04/10 19:36:31  
 Liquid Visc: 0.7225 cp

Sample Density: 2.650 g/cm<sup>3</sup>  
 Liquid Density: 0.9941 g/cm<sup>3</sup>

## Summary Report

Parameter 1	0.000	Parameter 2	0.000	Parameter 3	0.000		
Mass Distribution Arithmetic Statistics							
Mean	80.62		Std. Dev.	17.06			
Median	77.85		Coef. Var.	0.212			
Mode	82.16		Skewness	4.568			
			Kurtosis	34.466			
Selected Percentiles			Selected Sizes				
Percent Finer	Diameter (µm)		Diameter (µm)	Percent Finer			
100.0	714.1		500.0	100.0			
80.0	87.78		250.0	99.9			
60.0	80.97		125.0	98.0			
40.0	74.71		88.00	80.6			
20.0	68.64		63.00	0.0			
Peak Number	% of Dist.*	Mean	Mode	Median	Standard Deviation	Skewness	Kurtosis
1	100.0	80.62	82.16	77.85	17.06	4.568	34.466

\* Peaks must comprise at least 5.00 % of the distribution.



Micromeritics

WIN5100 V2.03

Page 1

Sample: TT-49-08 180 cm  
Operator: Clint Edrington  
Submitter: Clint Edrington  
File Name: C:\EDRING~1\TIGER&~1\SANDFR~1\TT-49-08\49\_180CM.SMP  
Material/Liquid: silicate mud/water/Water

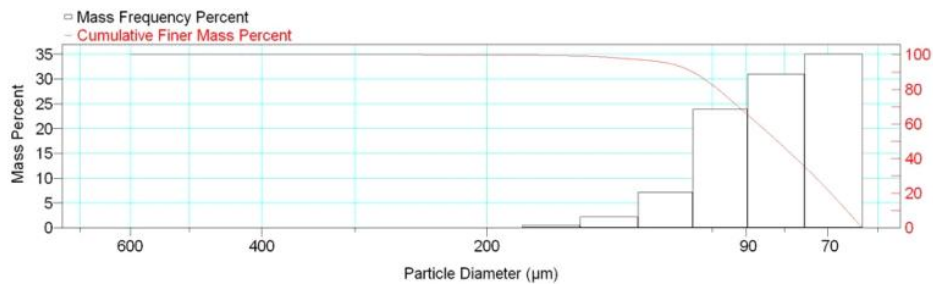
Reported: 01/04/10 19:38:17  
Liquid Visc: 0.7225 cp

Sample Density: 2.650 g/cm<sup>3</sup>  
Liquid Density: 0.9941 g/cm<sup>3</sup>

Report by Size Class

High Diameter (μm)	Low Diameter (μm)	Average Diameter (μm)	Cumulative Mass Finer (Percent)	Mass Frequency (Percent)
710.0	600.0	652.7	100.0	0.0
600.0	500.0	547.7	100.0	0.0
500.0	425.0	461.0	100.0	0.0
425.0	355.0	388.4	100.0	0.0
355.0	300.0	326.3	100.0	0.0
300.0	250.0	273.9	100.0	0.0
250.0	212.0	230.2	99.9	0.1
212.0	180.0	195.3	99.8	0.1
180.0	150.0	164.3	99.3	0.5
150.0	125.0	136.9	97.1	2.2
125.0	106.0	115.1	89.9	7.2
106.0	90.00	97.67	66.0	23.9
90.00	75.00	82.16	35.0	31.0
75.00	63.00	68.74	0.0	35.0

Mass Frequency vs Diameter



Summary Report

Full scale pump speed: 3  
Bubble detection: Medium  
Starting Size: 63.00 μm  
Ending Size: 0.50 μm

Stir time: 30 secs  
Stir speed: Low  
Probe time: 30 secs

Sample: TT-49-08 180 cm  
 Operator: Clint Edrington  
 Submitter: Clint Edrington  
 File Name: C:\EDRING~1\TIGER&~1\SANDFR~1\TT-49-08\49\_180CM.SMP  
 Material/Liquid: silicate mud/water/Water

Reported: 01/04/10 19:38:17  
 Liquid Visc: 0.7225 cp

Sample Density: 2.650 g/cm<sup>3</sup>  
 Liquid Density: 0.9941 g/cm<sup>3</sup>

## Summary Report

Parameter 1 0.000

Parameter 2 0.000

Parameter 3 0.000

## Mass Distribution Arithmetic Statistics

Mean	85.42	Std. Dev.	17.96
Median	81.70	Coef. Var.	0.210
Mode	68.74	Skewness	1.815
		Kurtosis	6.828

## Selected Percentiles

Percent Finer	Diameter (µm)
100.0	651.9
80.0	98.17
60.0	86.77
40.0	77.11
20.0	69.36

## Selected Sizes

Diameter (µm)	Percent Finer
500.0	100.0
250.0	100.0
125.0	97.1
88.00	62.3
63.00	0.0

Peak Number	% of Dist. *	Mean	Mode	Median	Standard Deviation	Skewness	Kurtosis
1	100.0	85.42	68.74	81.70	17.96	1.815	6.828

\* Peaks must comprise at least 5.00 % of the distribution.

Micromeritics

WIN5100 V2.03

Page 1

Sample: TT-49-08 205 cm  
Operator: Clint Edrington  
Submitter: Clint Edrington  
File Name: C:\EDRING~1\TIGER&~1\SANDFR~1\TT-49-08\49\_205CM.SMP  
Material/Liquid: silicate mud/water/Water

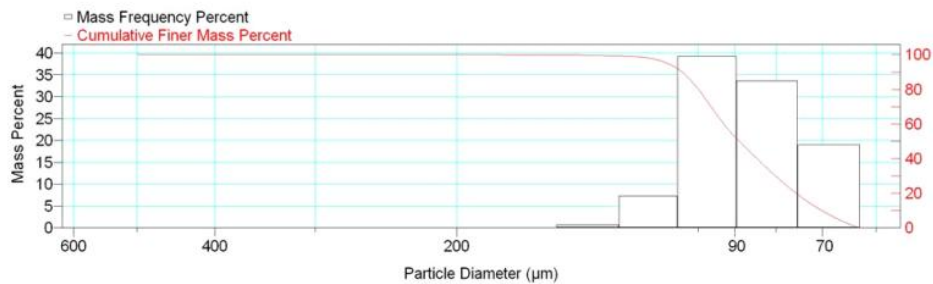
Reported: 01/04/10 19:40:58  
Liquid Visc: 0.7225 cp

Sample Density: 2.650 g/cm<sup>3</sup>  
Liquid Density: 0.9941 g/cm<sup>3</sup>

Report by Size Class

High Diameter (μm)	Low Diameter (μm)	Average Diameter (μm)	Cumulative Mass Finer (Percent)	Mass Frequency (Percent)
600.0	500.0	547.7	100.0	0.0
500.0	425.0	461.0	100.0	0.0
425.0	355.0	388.4	100.0	0.0
355.0	300.0	326.3	100.0	0.0
300.0	250.0	273.9	100.0	0.0
250.0	212.0	230.2	100.0	0.0
212.0	180.0	195.3	100.0	0.0
180.0	150.0	164.3	99.9	0.1
150.0	125.0	136.9	99.2	0.7
125.0	106.0	115.1	91.9	7.3
106.0	90.00	97.67	52.6	39.3
90.00	75.00	82.16	19.0	33.6
75.00	63.00	68.74	0.0	19.0

Mass Frequency vs Diameter



Summary Report

Full scale pump speed: 3  
Bubble detection: Medium  
Starting Size: 63.00 μm  
Ending Size: 0.50 μm

Stir time: 30 secs  
Stir speed: Low  
Probe time: 30 secs

Parameter 1 0.000

Parameter 2 0.000

Parameter 3 0.000

Sample: TT-49-08 205 cm  
 Operator: Clint Edrington  
 Submitter: Clint Edrington  
 File Name: C:\EDRING~1\TIGER&~1\SANDFR~1\TT-49-08\49\_205CM.SMP  
 Material/Liquid: silicate mud/water/Water

Reported: 01/04/10 19:40:58  
 Liquid Visc: 0.7225 cp

Sample Density: 2.650 g/cm<sup>3</sup>  
 Liquid Density: 0.9941 g/cm<sup>3</sup>

## Summary Report

## Mass Distribution Arithmetic Statistics

Mean	88.58	Std. Dev.	13.95
Median	88.84	Coef. Var.	0.157
Mode	97.67	Skewness	0.484
		Kurtosis	0.697

## Selected Percentiles

Percent Finer	Diameter (µm)
100.0	553.2
80.0	99.96
60.0	92.92
40.0	84.46
20.0	75.49

## Selected Sizes

Diameter (µm)	Percent Finer
500.0	100.0
250.0	100.0
125.0	99.2
88.00	48.1
63.00	0.0

Peak Number	% of Dist.*	Mean	Mode	Median	Standard Deviation	Skewness	Kurtosis
1	100.0	88.58	97.67	88.84	13.95	0.484	0.697

\* Peaks must comprise at least 5.00 % of the distribution.

Micromeritics

WIN5100 V2.03

Page 1

Sample: TT-50-08 0 cm  
Operator: Clint Edrington  
Submitter: Clint Edrington  
File Name: C:\EDRING~1\TIGER&~1\SANDFR~1\TT-50-08\50\_0CM.SMP  
Material/Liquid: silicate mud/water/Water

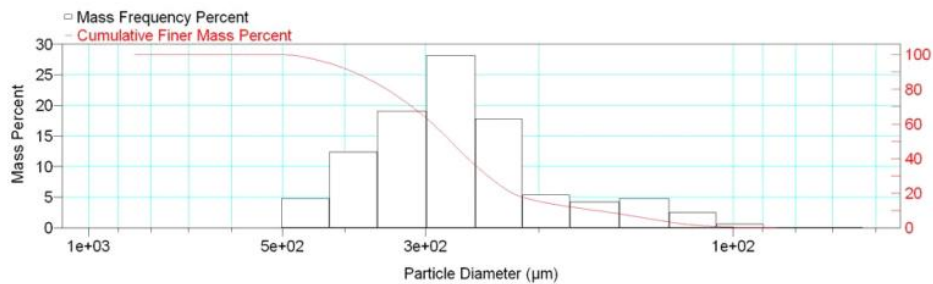
Reported: 01/04/10 19:44:49  
Liquid Visc: 0.7225 cp

Sample Density: 2.650 g/cm<sup>3</sup>  
Liquid Density: 0.9941 g/cm<sup>3</sup>

Report by Size Class

High Diameter (μm)	Low Diameter (μm)	Average Diameter (μm)	Cumulative Mass Finer (Percent)	Mass Frequency (Percent)
1000	850.0	922.0	100.0	0.0
850.0	710.0	776.9	100.0	0.0
710.0	600.0	652.7	100.0	0.0
600.0	500.0	547.7	100.0	0.0
500.0	425.0	461.0	95.2	4.8
425.0	355.0	388.4	82.8	12.4
355.0	300.0	326.3	63.7	19.1
300.0	250.0	273.9	35.5	28.2
250.0	212.0	230.2	17.7	17.8
212.0	180.0	195.3	12.3	5.4
180.0	150.0	164.3	8.1	4.2
150.0	125.0	136.9	3.3	4.8
125.0	106.0	115.1	0.8	2.5
106.0	90.00	97.67	0.2	0.6
90.00	75.00	82.16	0.1	0.1
75.00	63.00	68.74	0.0	0.1

Mass Frequency vs Diameter



Summary Report

Full scale pump speed: 3  
Bubble detection: Medium  
Starting Size: 63.00 μm

Stir time: 30 secs  
Stir speed: Low  
Probe time: 30 secs

Sample: TT-50-08 0 cm  
 Operator: Clint Edrington  
 Submitter: Clint Edrington  
 File Name: C:\EDRING~1\TIGER&~1\SANDFR~1\TT-50-08\50\_0CM.SMP  
 Material/Liquid: silicate mud/water/Water

Reported: 01/04/10 19:44:49      Sample Density: 2.650 g/cm<sup>3</sup>  
 Liquid Visc: 0.7225 cp      Liquid Density: 0.9941 g/cm<sup>3</sup>

## Summary Report

Ending Size: 0.50 µm

Parameter 1 0.000      Parameter 2 0.000      Parameter 3 0.000

## Mass Distribution Arithmetic Statistics

Mean	278.5	Std. Dev.	82.37
Median	274.4	Coef. Var.	0.296
Mode	273.9	Skewness	0.120
		Kurtosis	-0.176

## Selected Percentiles

Percent Finer	Diameter (µm)
100.0	922.0
80.0	344.7
60.0	292.2
40.0	257.8
20.0	219.7

## Selected Sizes

Diameter (µm)	Percent Finer
500.0	100.0
250.0	35.5
125.0	3.3
88.00	0.2
63.00	0.0

Peak Number	% of Dist. *	Mean	Mode	Median	Standard Deviation	Skewness	Kurtosis
1	12.2	139.5	136.9	139.5	21.20	-0.301	-0.811
2	91.9	291.9	273.9	281.3	71.59	0.509	-0.156

\* Peaks must comprise at least 5.00 % of the distribution.

# Micromeritics

WIN5100 V2.03

Page 1

Sample: TT-50-08 50 cm  
Operator: Clint Edrington  
Submitter: Clint Edrington  
File Name: C:\EDRING~1\TIGER&~1\SANDFR~1\TT-50-08\50\_50CM.SMP  
Material/Liquid: silicate mud/water/Water

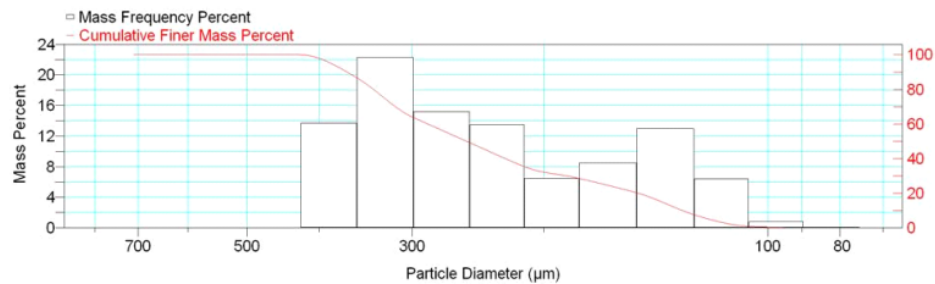
Reported: 01/04/10 19:47:53  
Liquid Visc: 0.7225 cp

Sample Density: 2.650 g/cm<sup>3</sup>  
Liquid Density: 0.9941 g/cm<sup>3</sup>

## Report by Size Class

High Diameter (μm)	Low Diameter (μm)	Average Diameter (μm)	Cumulative Mass Finer (Percent)	Mass Frequency (Percent)
850.0	710.0	776.9	100.0	0.0
710.0	600.0	652.7	100.0	0.0
600.0	500.0	547.7	100.0	0.0
500.0	425.0	461.0	100.0	0.0
425.0	355.0	388.4	86.3	13.7
355.0	300.0	326.3	64.0	22.3
300.0	250.0	273.9	48.8	15.2
250.0	212.0	230.2	35.3	13.5
212.0	180.0	195.3	28.8	6.5
180.0	150.0	164.3	20.3	8.5
150.0	125.0	136.9	7.3	13.0
125.0	106.0	115.1	0.9	6.4
106.0	90.00	97.67	0.1	0.8
90.00	75.00	82.16	0.0	0.1

Mass Frequency vs Diameter



## Summary Report

Full scale pump speed: 3  
Bubble detection: Medium  
Starting Size: 63.00 μm  
Ending Size: 0.50 μm

Stir time: 30 secs  
Stir speed: Low  
Probe time: 30 secs

Sample: TT-50-08 50 cm  
 Operator: Clint Edrington  
 Submitter: Clint Edrington  
 File Name: C:\EDRING~1\TIGER&~1\SANDFR~1\TT-50-08\50\_50CM.SMP  
 Material/Liquid: silicate mud/water/Water

Reported: 01/04/10 19:47:53  
 Liquid Visc: 0.7225 cp

Sample Density: 2.650 g/cm<sup>3</sup>  
 Liquid Density: 0.9941 g/cm<sup>3</sup>

## Summary Report

Parameter 1 0.000

Parameter 2 0.000

Parameter 3 0.000

## Mass Distribution Arithmetic Statistics

Mean	251.4	Std. Dev.	89.00
Median	253.7	Coef. Var.	0.354
Mode	326.3	Skewness	-0.016
		Kurtosis	-1.237

## Selected Percentiles

Percent Finer	Diameter (µm)
100.0	850.0
80.0	338.3
60.0	286.1
40.0	225.1
20.0	149.1

## Selected Sizes

Diameter (µm)	Percent Finer
500.0	100.0
250.0	48.8
125.0	7.3
88.00	0.1
63.00	0.0

Peak Number	% of Dist. *	Mean	Mode	Median	Standard Deviation	Skewness	Kurtosis
1	35.3	149.3	136.9	143.7	28.04	0.314	-0.872
2	71.2	296.9	326.3	301.4	61.49	0.005	-1.094

\* Peaks must comprise at least 5.00 % of the distribution.



Micromeritics

WIN5100 V2.03

Page 1

Sample: TT-50-08 100 cm  
Operator: Clint Edrington  
Submitter: Clint Edrington  
File Name: C:\EDRING~1\TIGER&~1\SANDFR~1\TT-50-08\50\_100CM.SMP  
Material/Liquid: silicate mud/water/Water

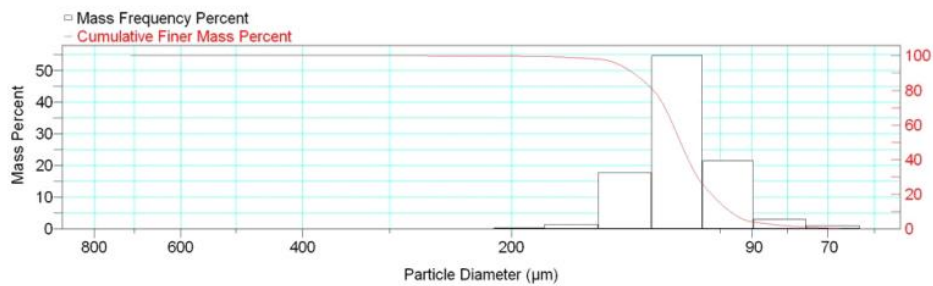
Reported: 01/04/10 19:51:13  
Liquid Visc: 0.7225 cp

Sample Density: 2.650 g/cm<sup>3</sup>  
Liquid Density: 0.9941 g/cm<sup>3</sup>

Report by Size Class

High Diameter (μm)	Low Diameter (μm)	Average Diameter (μm)	Cumulative Mass Finer (Percent)	Mass Frequency (Percent)
850.0	710.0	776.9	100.0	0.0
710.0	600.0	652.7	100.0	0.0
600.0	500.0	547.7	100.0	0.0
500.0	425.0	461.0	100.0	0.0
425.0	355.0	388.4	100.0	0.0
355.0	300.0	326.3	100.0	0.0
300.0	250.0	273.9	99.9	0.1
250.0	212.0	230.2	99.8	0.1
212.0	180.0	195.3	99.5	0.3
180.0	150.0	164.3	98.1	1.4
150.0	125.0	136.9	80.3	17.8
125.0	106.0	115.1	25.6	54.7
106.0	90.00	97.67	4.1	21.5
90.00	75.00	82.16	1.0	3.1
75.00	63.00	68.74	0.0	1.0

Mass Frequency vs Diameter



Summary Report

Full scale pump speed: 3  
Bubble detection: Medium  
Starting Size: 63.00 μm  
Ending Size: 0.50 μm

Stir time: 30 secs  
Stir speed: Low  
Probe time: 30 secs

Sample: TT-50-08 100 cm  
 Operator: Clint Edrington  
 Submitter: Clint Edrington  
 File Name: C:\EDRING~1\TIGER&~1\SANDFR~1\TT-50-08\50\_100CM.SMP  
 Material/Liquid: silicate mud/water/Water

Reported: 01/04/10 19:51:13  
 Liquid Visc: 0.7225 cp

Sample Density: 2.650 g/cm<sup>3</sup>  
 Liquid Density: 0.9941 g/cm<sup>3</sup>

## Summary Report

Parameter 1	0.000	Parameter 2	0.000	Parameter 3	0.000		
Mass Distribution Arithmetic Statistics							
Mean	115.0	Std. Dev.		17.23			
Median	114.1	Coef. Var.		0.150			
Mode	115.1	Skewness		1.462			
		Kurtosis		10.208			
Selected Percentiles			Selected Sizes				
Percent Finer	Diameter (µm)		Diameter (µm)	Percent Finer			
100.0	714.1		500.0	100.0			
80.0	124.8		250.0	99.9			
60.0	117.0		125.0	80.3			
40.0	111.2		88.00	3.6			
20.0	102.9		63.00	0.0			
Peak Number	% of Dist.*	Mean	Mode	Median	Standard Deviation	Skewness	Kurtosis
1	100.0	115.0	115.1	114.1	17.23	1.462	10.208

\* Peaks must comprise at least 5.00 % of the distribution.

# Micromeritics

WIN5100 V2.03

Page 1

Sample: TT-50-08 157 cm  
Operator: Clint Edrington  
Submitter: Clint Edrington  
File Name: C:\EDRING~1\TIGER&~1\SANDFR~1\TT-50-08\50\_157CM.SMP  
Material/Liquid: silicate mud/water/Water

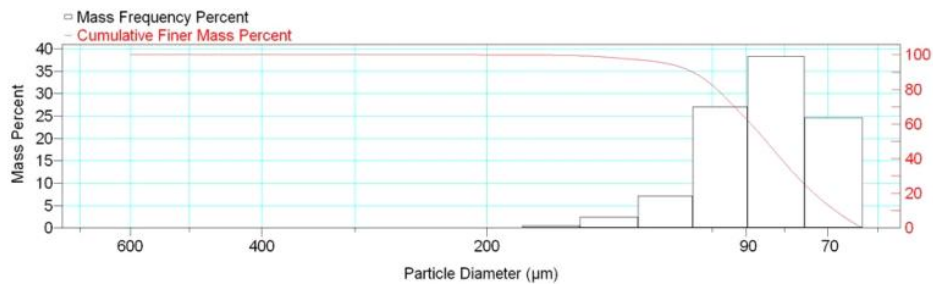
Reported: 01/04/10 19:52:57  
Liquid Visc: 0.7225 cp

Sample Density: 2.650 g/cm<sup>3</sup>  
Liquid Density: 0.9941 g/cm<sup>3</sup>

## Report by Size Class

High Diameter (µm)	Low Diameter (µm)	Average Diameter (µm)	Cumulative Mass Finer (Percent)	Mass Frequency (Percent)
710.0	600.0	652.7	100.0	0.0
600.0	500.0	547.7	100.0	0.0
500.0	425.0	461.0	100.0	0.0
425.0	355.0	388.4	100.0	0.0
355.0	300.0	326.3	100.0	0.0
300.0	250.0	273.9	100.0	0.0
250.0	212.0	230.2	100.0	0.0
212.0	180.0	195.3	99.9	0.1
180.0	150.0	164.3	99.4	0.5
150.0	125.0	136.9	97.0	2.4
125.0	106.0	115.1	89.9	7.1
106.0	90.00	97.67	62.9	27.0
90.00	75.00	82.16	24.6	38.3
75.00	63.00	68.74	0.0	24.6

Mass Frequency vs Diameter



## Summary Report

Full scale pump speed: 3  
Bubble detection: Medium  
Starting Size: 63.00 µm  
Ending Size: 0.50 µm

Stir time: 30 secs  
Stir speed: Low  
Probe time: 30 secs

Sample: TT-50-08 157 cm  
 Operator: Clint Edrington  
 Submitter: Clint Edrington  
 File Name: C:\EDRING~1\TIGER&~1\SANDFR~1\TT-50-08\50\_157CM.SMP  
 Material/Liquid: silicate mud/water/Water

Reported: 01/04/10 19:52:57  
 Liquid Visc: 0.7225 cp

Sample Density: 2.650 g/cm<sup>3</sup>  
 Liquid Density: 0.9941 g/cm<sup>3</sup>

## Summary Report

Parameter 1 0.000

Parameter 2 0.000

Parameter 3 0.000

## Mass Distribution Arithmetic Statistics

Mean	87.22	Std. Dev.	16.71
Median	84.61	Coef. Var.	0.192
Mode	82.16	Skewness	1.445
		Kurtosis	3.858

## Selected Percentiles

Percent Finer	Diameter (µm)
100.0	600.3
80.0	98.53
60.0	88.69
40.0	80.86
20.0	73.06

## Selected Sizes

Diameter (µm)	Percent Finer
500.0	100.0
250.0	100.0
125.0	97.0
88.00	58.4
63.00	0.0

Peak Number	% of Dist. *	Mean	Mode	Median	Standard Deviation	Skewness	Kurtosis
1	100.0	87.22	82.16	84.61	16.71	1.445	3.858

\* Peaks must comprise at least 5.00 % of the distribution.

Micromeritics

WIN5100 V2.03

Page 1

Sample: TT-50-08 200 cm  
Operator: Clint Edrington  
Submitter: Clint Edrington  
File Name: C:\EDRING~1\TIGER&~1\SANDFR~1\TT-50-08\50\_200CM.SMP  
Material/Liquid: silicate mud/water/Water

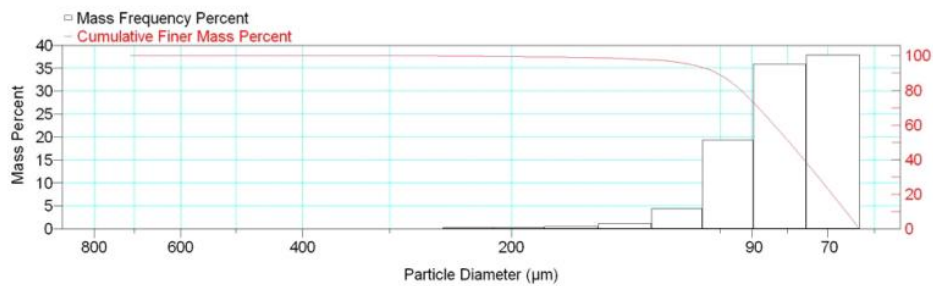
Reported: 01/04/10 19:55:17  
Liquid Visc: 0.7225 cp

Sample Density: 2.650 g/cm<sup>3</sup>  
Liquid Density: 0.9941 g/cm<sup>3</sup>

Report by Size Class

High Diameter ( $\mu\text{m}$ )	Low Diameter ( $\mu\text{m}$ )	Average Diameter ( $\mu\text{m}$ )	Cumulative Mass Finer (Percent)	Mass Frequency (Percent)
850.0	710.0	776.9	100.0	0.0
710.0	600.0	652.7	100.0	0.0
600.0	500.0	547.7	100.0	0.0
500.0	425.0	461.0	100.0	0.0
425.0	355.0	388.4	100.0	0.0
355.0	300.0	326.3	100.0	0.0
300.0	250.0	273.9	99.9	0.1
250.0	212.0	230.2	99.6	0.3
212.0	180.0	195.3	99.3	0.3
180.0	150.0	164.3	98.8	0.5
150.0	125.0	136.9	97.6	1.2
125.0	106.0	115.1	93.2	4.4
106.0	90.00	97.67	73.8	19.4
90.00	75.00	82.16	37.9	35.9
75.00	63.00	68.74	0.0	37.9

Mass Frequency vs Diameter



Summary Report

Full scale pump speed: 3  
Bubble detection: Medium  
Starting Size: 63.00  $\mu\text{m}$   
Ending Size: 0.50  $\mu\text{m}$

Stir time: 30 secs  
Stir speed: Low  
Probe time: 30 secs

Sample: TT-50-08 200 cm  
 Operator: Clint Edrington  
 Submitter: Clint Edrington  
 File Name: C:\EDRING~1\TIGER&~1\SANDFR~1\TT-50-08\50\_200CM.SMP  
 Material/Liquid: silicate mud/water/Water

Reported: 01/04/10 19:55:17  
 Liquid Visc: 0.7225 cp

Sample Density: 2.650 g/cm<sup>3</sup>  
 Liquid Density: 0.9941 g/cm<sup>3</sup>

## Summary Report

Parameter 1	0.000	Parameter 2	0.000	Parameter 3	0.000		
Mass Distribution Arithmetic Statistics							
Mean	83.58	Std. Dev.		19.27			
Median	79.50	Coef. Var.		0.231			
Mode	68.74	Skewness		3.587			
		Kurtosis		22.704			
Selected Percentiles			Selected Sizes				
Percent Finer	Diameter (µm)		Diameter (µm)	Percent Finer			
100.0	714.1		500.0	100.0			
80.0	93.34		250.0	99.9			
60.0	83.63		125.0	97.6			
40.0	75.75		88.00	69.7			
20.0	68.97		63.00	0.0			
Peak Number	% of Dist.*	Mean	Mode	Median	Standard Deviation	Skewness	Kurtosis
1	100.0	83.58	68.74	79.50	19.27	3.587	22.704

\* Peaks must comprise at least 5.00 % of the distribution.

Micromeritics

WIN5100 V2.03

Page 1

Sample: TT-50-08 248 cm  
Operator: Clint Edrington  
Submitter: Clint Edrington  
File Name: C:\EDRING~1\TIGER&~1\SANDFR~1\TT-50-08\50\_248CM.SMP  
Material/Liquid: silicate mud/water/Water

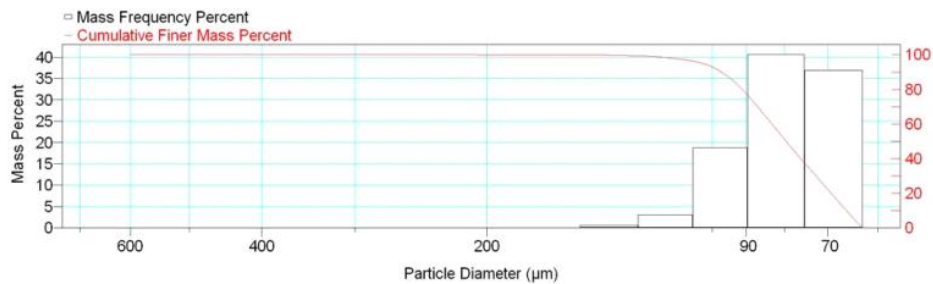
Reported: 01/04/10 19:57:21  
Liquid Visc: 0.7225 cp

Sample Density: 2.650 g/cm<sup>3</sup>  
Liquid Density: 0.9941 g/cm<sup>3</sup>

Report by Size Class

High Diameter (µm)	Low Diameter (µm)	Average Diameter (µm)	Cumulative Mass Finer (Percent)	Mass Frequency (Percent)
710.0	600.0	652.7	100.0	0.0
600.0	500.0	547.7	100.0	0.0
500.0	425.0	461.0	100.0	0.0
425.0	355.0	388.4	100.0	0.0
355.0	300.0	326.3	100.0	0.0
300.0	250.0	273.9	100.0	0.0
250.0	212.0	230.2	100.0	0.0
212.0	180.0	195.3	99.9	0.1
180.0	150.0	164.3	99.9	0.0
150.0	125.0	136.9	99.3	0.6
125.0	106.0	115.1	96.3	3.0
106.0	90.00	97.67	77.5	18.8
90.00	75.00	82.16	36.9	40.6
75.00	63.00	68.74	0.0	36.9

Mass Frequency vs Diameter



Summary Report

Full scale pump speed: 3  
Bubble detection: Medium  
Starting Size: 63.00 µm  
Ending Size: 0.50 µm

Stir time: 30 secs  
Stir speed: Low  
Probe time: 30 secs

Sample: TT-50-08 248 cm  
 Operator: Clint Edrington  
 Submitter: Clint Edrington  
 File Name: C:\EDRING~1\TIGER&~1\SANDFR~1\TT-50-08\50\_248CM.SMP  
 Material/Liquid: silicate mud/water/Water

Reported: 01/04/10 19:57:21  
 Liquid Visc: 0.7225 cp

Sample Density: 2.650 g/cm<sup>3</sup>  
 Liquid Density: 0.9941 g/cm<sup>3</sup>

## Summary Report

Parameter 1 0.000

Parameter 2 0.000

Parameter 3 0.000

## Mass Distribution Arithmetic Statistics

Mean	81.55	Std. Dev.	13.22
Median	79.59	Coef. Var.	0.162
Mode	82.16	Skewness	1.575
		Kurtosis	6.328

## Selected Percentiles

Percent Finer	Diameter (µm)
100.0	600.3
80.0	91.11
60.0	83.17
40.0	76.09
20.0	69.29

## Selected Sizes

Diameter (µm)	Percent Finer
500.0	100.0
250.0	100.0
125.0	99.3
88.00	72.7
63.00	0.0

Peak Number	% of Dist. *	Mean	Mode	Median	Standard Deviation	Skewness	Kurtosis
1	99.9	81.44	82.16	79.57	12.72	1.078	1.509

\* Peaks must comprise at least 5.00 % of the distribution.



# Micromeritics

WIN5100 V2.03

Page 1

Sample: TT-52-08 7 cm  
Operator: Clint Edrington  
Submitter: Clint Edrington  
File Name: C:\EDRING~1\TIGER&~1\SANDFR~1\TT-52-08\52\_7CM.SMP  
Material/Liquid: silicate mud/water/Water

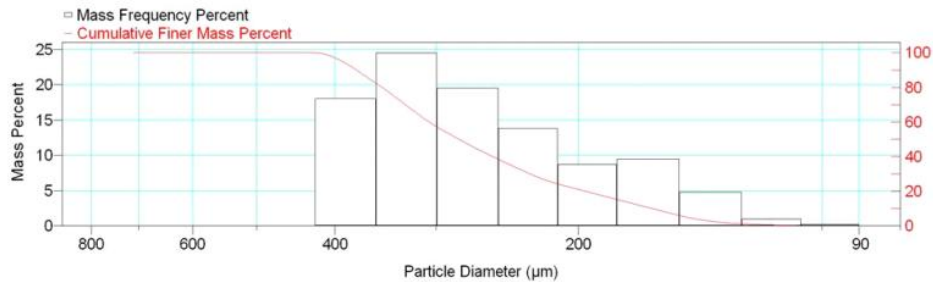
Reported: 01/04/10 20:05:38  
Liquid Visc: 0.7225 cp

Sample Density: 2.650 g/cm<sup>3</sup>  
Liquid Density: 0.9941 g/cm<sup>3</sup>

## Report by Size Class

High Diameter (µm)	Low Diameter (µm)	Average Diameter (µm)	Cumulative Mass Finer (Percent)	Mass Frequency (Percent)
850.0	710.0	776.9	100.0	0.0
710.0	600.0	652.7	100.0	0.0
600.0	500.0	547.7	100.0	0.0
500.0	425.0	461.0	100.0	0.0
425.0	355.0	388.4	82.0	18.0
355.0	300.0	326.3	57.5	24.5
300.0	250.0	273.9	38.0	19.5
250.0	212.0	230.2	24.2	13.8
212.0	180.0	195.3	15.5	8.7
180.0	150.0	164.3	6.0	9.5
150.0	125.0	136.9	1.2	4.8
125.0	106.0	115.1	0.2	1.0
106.0	90.00	97.67	0.0	0.2

Mass Frequency vs Diameter



## Summary Report

Full scale pump speed: 3  
Bubble detection: Medium  
Starting Size: 63.00 µm  
Ending Size: 0.50 µm

Stir time: 30 secs  
Stir speed: Low  
Probe time: 30 secs

Parameter 1 0.000

Parameter 2 0.000

Parameter 3 0.000

Sample: TT-52-08 7 cm  
 Operator: Clint Edrington  
 Submitter: Clint Edrington  
 File Name: C:\EDRING~1\TIGER&~1\SANDFR~1\TT-52-08\52\_7CM.SMP  
 Material/Liquid: silicate mud/water/Water

Reported: 01/04/10 20:05:38  
 Liquid Visc: 0.7225 cp

Sample Density: 2.650 g/cm<sup>3</sup>  
 Liquid Density: 0.9941 g/cm<sup>3</sup>

## Summary Report

Mass Distribution Arithmetic Statistics			
Mean	275.6	Std. Dev.	78.66
Median	281.1	Coef. Var.	0.285
Mode	326.3	Skewness	-0.161
		Kurtosis	-1.017

Selected Percentiles		Selected Sizes	
Percent Finer	Diameter (µm)	Diameter (µm)	Percent Finer
100.0	850.0	500.0	100.0
80.0	349.9	250.0	38.0
60.0	306.0	125.0	1.2
40.0	255.3	88.00	0.0
20.0	196.0	63.00	0.0

Peak Number	% of Dist.*	Mean	Mode	Median	Standard Deviation	Skewness	Kurtosis
1	100.0	275.6	326.3	281.1	78.66	-0.161	-1.017

\* Peaks must comprise at least 5.00 % of the distribution.

Micromeritics

WIN5100 V2.03

Page 1

Sample: TT-52-08 76 cm  
Operator: Clint Edrington  
Submitter: Clint Edrington  
File Name: C:\EDRING~1\TIGER&~1\SANDFR~1\TT-52-08\52\_76CM.SMP  
Material/Liquid: silicate mud/water/Water

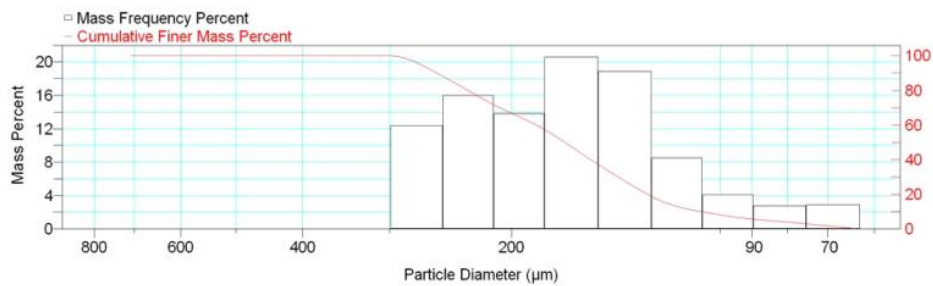
Reported: 01/04/10 20:08:40  
Liquid Visc: 0.7225 cp

Sample Density: 2.650 g/cm<sup>3</sup>  
Liquid Density: 0.9941 g/cm<sup>3</sup>

Report by Size Class

High Diameter (µm)	Low Diameter (µm)	Average Diameter (µm)	Cumulative Mass Finer (Percent)	Mass Frequency (Percent)
850.0	710.0	776.9	100.0	0.0
710.0	600.0	652.7	100.0	0.0
600.0	500.0	547.7	100.0	0.0
500.0	425.0	461.0	100.0	0.0
425.0	355.0	388.4	100.0	0.0
355.0	300.0	326.3	100.0	0.0
300.0	250.0	273.9	87.6	12.4
250.0	212.0	230.2	71.6	16.0
212.0	180.0	195.3	57.8	13.8
180.0	150.0	164.3	37.2	20.6
150.0	125.0	136.9	18.3	18.9
125.0	106.0	115.1	9.8	8.5
106.0	90.00	97.67	5.7	4.1
90.00	75.00	82.16	2.9	2.8
75.00	63.00	68.74	0.0	2.9

Mass Frequency vs Diameter



Summary Report

Full scale pump speed: 3  
Bubble detection: Medium  
Starting Size: 63.00 µm  
Ending Size: 0.50 µm

Stir time: 30 secs  
Stir speed: Low  
Probe time: 30 secs

Sample: TT-52-08 76 cm  
 Operator: Clint Edrington  
 Submitter: Clint Edrington  
 File Name: C:\EDRING~1\TIGER&~1\SANDFR~1\TT-52-08\52\_76CM.SMP  
 Material/Liquid: silicate mud/water/Water

Reported: 01/04/10 20:08:40  
 Liquid Visc: 0.7225 cp

Sample Density: 2.650 g/cm<sup>3</sup>  
 Liquid Density: 0.9941 g/cm<sup>3</sup>

## Summary Report

Parameter 1	0.000	Parameter 2	0.000	Parameter 3	0.000		
Mass Distribution Arithmetic Statistics							
Mean	175.6	Std. Dev.		56.33			
Median	167.6	Coef. Var.		0.321			
Mode	164.3	Skewness		0.210			
		Kurtosis		-0.814			
Selected Percentiles			Selected Sizes				
Percent Finer	Diameter (µm)		Diameter (µm)	Percent Finer			
100.0	714.1		500.0	100.0			
80.0	231.2		250.0	87.6			
60.0	184.2		125.0	18.3			
40.0	153.8		88.00	5.3			
20.0	127.3		63.00	0.0			
Peak Number	% of Dist.*	Mean	Mode	Median	Standard Deviation	Skewness	Kurtosis
1	5.7	75.33	68.74	74.77	6.709	0.035	-1.999
2	68.7	149.6	164.3	150.1	31.98	-0.193	-0.751
3	42.2	231.6	230.2	228.7	30.91	0.220	-1.355

\* Peaks must comprise at least 5.00 % of the distribution.

Micromeritics

WIN5100 V2.03

Page 1

Sample: TT-52-08 90 cm  
Operator: Clint Edrington  
Submitter: Clint Edrington  
File Name: C:\EDRING~1\TIGER&~1\SANDFR~1\TT-52-08\52\_90CM.SMP  
Material/Liquid: silicate mud/water/Water

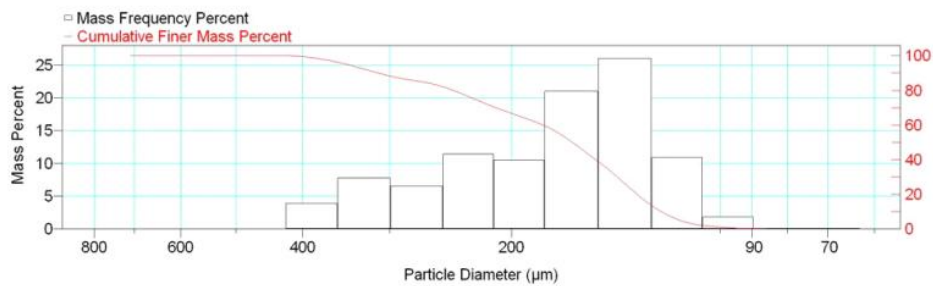
Reported: 01/04/10 20:11:08  
Liquid Visc: 0.7225 cp

Sample Density: 2.650 g/cm<sup>3</sup>  
Liquid Density: 0.9941 g/cm<sup>3</sup>

Report by Size Class

High Diameter (μm)	Low Diameter (μm)	Average Diameter (μm)	Cumulative Mass Finer (Percent)	Mass Frequency (Percent)
850.0	710.0	776.9	100.0	0.0
710.0	600.0	652.7	100.0	0.0
600.0	500.0	547.7	100.0	0.0
500.0	425.0	461.0	100.0	0.0
425.0	355.0	388.4	96.1	3.9
355.0	300.0	326.3	88.3	7.8
300.0	250.0	273.9	81.8	6.5
250.0	212.0	230.2	70.4	11.4
212.0	180.0	195.3	59.9	10.5
180.0	150.0	164.3	38.9	21.0
150.0	125.0	136.9	12.9	26.0
125.0	106.0	115.1	2.0	10.9
106.0	90.00	97.67	0.2	1.8
90.00	75.00	82.16	0.1	0.1
75.00	63.00	68.74	0.0	0.1

Mass Frequency vs Diameter



Summary Report

Full scale pump speed: 3  
Bubble detection: Medium  
Starting Size: 63.00 μm  
Ending Size: 0.50 μm

Stir time: 30 secs  
Stir speed: Low  
Probe time: 30 secs

Sample: TT-52-08 90 cm  
 Operator: Clint Edrington  
 Submitter: Clint Edrington  
 File Name: C:\EDRING~1\TIGER&~1\SANDFR~1\TT-52-08\52\_90CM.SMP  
 Material/Liquid: silicate mud/water/Water

Reported: 01/04/10 20:11:08  
 Liquid Visc: 0.7225 cp

Sample Density: 2.650 g/cm<sup>3</sup>  
 Liquid Density: 0.9941 g/cm<sup>3</sup>

## Summary Report

Parameter 1	0.000	Parameter 2	0.000	Parameter 3	0.000		
Mass Distribution Arithmetic Statistics							
Mean	189.7	Std. Dev.		72.75			
Median	163.5	Coef. Var.		0.383			
Mode	136.9	Skewness		1.161			
		Kurtosis		0.523			
Selected Percentiles			Selected Sizes				
Percent Finer	Diameter (µm)		Diameter (µm)	Percent Finer			
100.0	850.0		500.0	100.0			
80.0	242.9		250.0	81.8			
60.0	180.3		125.0	12.9			
40.0	151.3		88.00	0.2			
20.0	131.8		63.00	0.0			
Peak Number	% of Dist.*	Mean	Mode	Median	Standard Deviation	Skewness	Kurtosis
1	70.3	149.4	136.9	146.0	26.39	0.250	-0.698
2	28.4	227.3	230.2	223.4	29.62	0.424	-1.101
3	18.2	320.9	326.3	317.4	42.19	0.384	-1.042

\* Peaks must comprise at least 5.00 % of the distribution.

Micromeritics

WIN5100 V2.03

Page 1

Sample: TT-52-08 150 cm  
Operator: Clint Edrington  
Submitter: Clint Edrington  
File Name: C:\EDRING~1\TIGER&~1\SANDFR~1\TT-52-08\52\_150CM.SMP  
Material/Liquid: silicate mud/water/Water

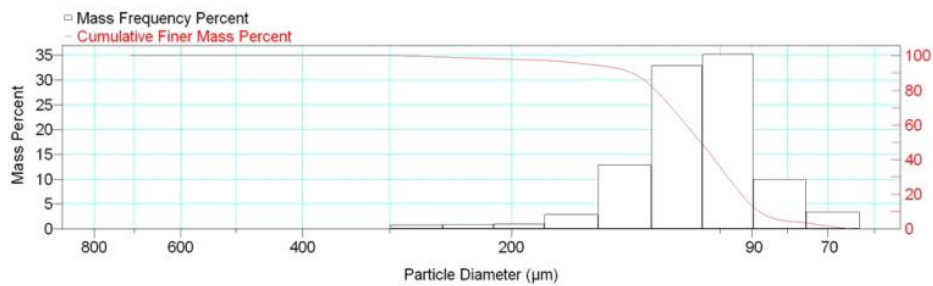
Reported: 01/04/10 20:13:06  
Liquid Visc: 0.7225 cp

Sample Density: 2.650 g/cm<sup>3</sup>  
Liquid Density: 0.9941 g/cm<sup>3</sup>

Report by Size Class

High Diameter ( $\mu\text{m}$ )	Low Diameter ( $\mu\text{m}$ )	Average Diameter ( $\mu\text{m}$ )	Cumulative Mass Finer (Percent)	Mass Frequency (Percent)
850.0	710.0	776.9	100.0	0.0
710.0	600.0	652.7	100.0	0.0
600.0	500.0	547.7	100.0	0.0
500.0	425.0	461.0	100.0	0.0
425.0	355.0	388.4	100.0	0.0
355.0	300.0	326.3	100.0	0.0
300.0	250.0	273.9	99.2	0.8
250.0	212.0	230.2	98.3	0.9
212.0	180.0	195.3	97.3	1.0
180.0	150.0	164.3	94.4	2.9
150.0	125.0	136.9	81.5	12.9
125.0	106.0	115.1	48.6	32.9
106.0	90.00	97.67	13.4	35.2
90.00	75.00	82.16	3.4	10.0
75.00	63.00	68.74	0.0	3.4

Mass Frequency vs Diameter



Summary Report

Full scale pump speed: 3  
Bubble detection: Medium  
Starting Size: 63.00  $\mu\text{m}$   
Ending Size: 0.50  $\mu\text{m}$

Stir time: 30 secs  
Stir speed: Low  
Probe time: 30 secs

Sample: TT-52-08 150 cm  
 Operator: Clint Edrington  
 Submitter: Clint Edrington  
 File Name: C:\EDRING~1\TIGER&~1\SANDFR~1\TT-52-08\52\_150CM.SMP  
 Material/Liquid: silicate mud/water/Water

Reported: 01/04/10 20:13:06  
 Liquid Visc: 0.7225 cp

Sample Density: 2.650 g/cm<sup>3</sup>  
 Liquid Density: 0.9941 g/cm<sup>3</sup>

## Summary Report

Parameter 1	0.000	Parameter 2	0.000	Parameter 3	0.000		
Mass Distribution Arithmetic Statistics							
Mean	111.5	Std. Dev.		28.15			
Median	106.7	Coef. Var.		0.253			
Mode	97.67	Skewness		2.494			
		Kurtosis		10.277			
Selected Percentiles			Selected Sizes				
Percent Finer	Diameter (µm)		Diameter (µm)	Percent Finer			
100.0	714.1		500.0	100.0			
80.0	123.9		250.0	99.2			
60.0	111.9		125.0	81.5			
40.0	101.9		88.00	10.2			
20.0	93.24		63.00	0.0			
Peak Number	% of Dist.*	Mean	Mode	Median	Standard Deviation	Skewness	Kurtosis
1	100.0	111.5	97.67	106.7	28.15	2.494	10.277

\* Peaks must comprise at least 5.00 % of the distribution.



Micromeritics

WIN5100 V2.03

Page 1

Sample: TT-52-08 182 cm  
Operator: Clint Edrington  
Submitter: Clint Edrington  
File Name: C:\EDRING~1\TIGER&~1\SANDFR~1\TT-52-08\52\_182CM.SMP  
Material/Liquid: silicate mud/water/Water

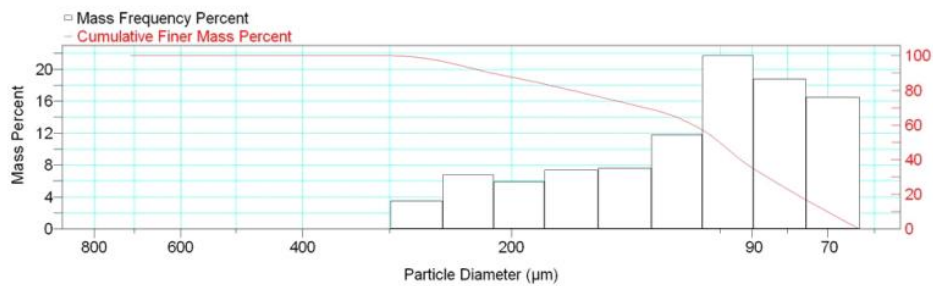
Reported: 01/04/10 20:15:19  
Liquid Visc: 0.7225 cp

Sample Density: 2.650 g/cm<sup>3</sup>  
Liquid Density: 0.9941 g/cm<sup>3</sup>

Report by Size Class

High Diameter (µm)	Low Diameter (µm)	Average Diameter (µm)	Cumulative Mass Finer (Percent)	Mass Frequency (Percent)
850.0	710.0	776.9	100.0	0.0
710.0	600.0	652.7	100.0	0.0
600.0	500.0	547.7	100.0	0.0
500.0	425.0	461.0	100.0	0.0
425.0	355.0	388.4	100.0	0.0
355.0	300.0	326.3	100.0	0.0
300.0	250.0	273.9	96.5	3.5
250.0	212.0	230.2	89.7	6.8
212.0	180.0	195.3	83.8	5.9
180.0	150.0	164.3	76.4	7.4
150.0	125.0	136.9	68.8	7.6
125.0	106.0	115.1	57.0	11.8
106.0	90.00	97.67	35.3	21.7
90.00	75.00	82.16	16.5	18.8
75.00	63.00	68.74	0.0	16.5

Mass Frequency vs Diameter



Summary Report

Full scale pump speed: 3  
Bubble detection: Medium  
Starting Size: 63.00 µm  
Ending Size: 0.50 µm

Stir time: 30 secs  
Stir speed: Low  
Probe time: 30 secs

Sample: TT-52-08 182 cm  
 Operator: Clint Edrington  
 Submitter: Clint Edrington  
 File Name: C:\EDRING~1\TIGER&~1\SANDFR~1\TT-52-08\52\_182CM.SMP  
 Material/Liquid: silicate mud/water/Water

Reported: 01/04/10 20:15:19  
 Liquid Visc: 0.7225 cp

Sample Density: 2.650 g/cm<sup>3</sup>  
 Liquid Density: 0.9941 g/cm<sup>3</sup>

## Summary Report

Parameter 1	0.000	Parameter 2	0.000	Parameter 3	0.000		
Mass Distribution Arithmetic Statistics							
Mean	120.9	Std. Dev.		54.49			
Median	100.2	Coef. Var.		0.451			
Mode	97.67	Skewness		1.284			
		Kurtosis		0.704			
Selected Percentiles			Selected Sizes				
Percent Finer	Diameter (µm)		Diameter (µm)	Percent Finer			
100.0	714.1		500.0	100.0			
80.0	163.8		250.0	96.5			
60.0	109.4		125.0	68.8			
40.0	93.51		88.00	32.9			
20.0	77.72		63.00	0.0			
Peak Number	% of Dist.*	Mean	Mode	Median	Standard Deviation	Skewness	Kurtosis
1	89.7	106.6	97.67	96.75	35.90	1.101	0.321
2	16.2	226.9	230.2	223.9	29.05	0.442	-1.019

\* Peaks must comprise at least 5.00 % of the distribution.

Micromeritics

WIN5100 V2.03

Page 1

Sample: TT-52-08 235 cm  
Operator: Clint Edrington  
Submitter: Clint Edrington  
File Name: C:\EDRING~1\TIGER&~1\SANDFR~1\TT-52-08\52\_235CM.SMP  
Material/Liquid: silicate mud/water/Water

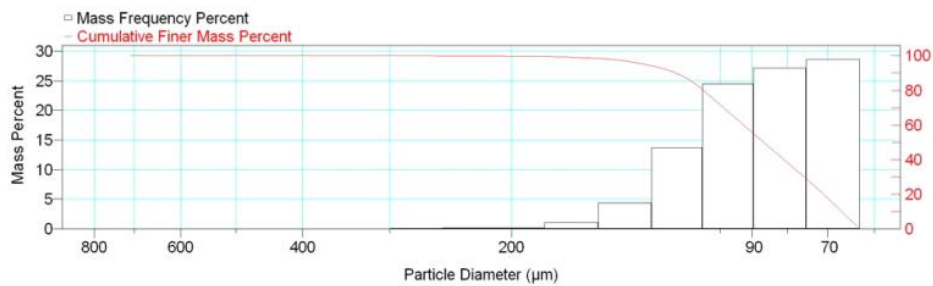
Reported: 01/04/10 20:17:33  
Liquid Visc: 0.7225 cp

Sample Density: 2.650 g/cm<sup>3</sup>  
Liquid Density: 0.9941 g/cm<sup>3</sup>

Report by Size Class

High Diameter (μm)	Low Diameter (μm)	Average Diameter (μm)	Cumulative Mass Finer (Percent)	Mass Frequency (Percent)
850.0	710.0	776.9	100.0	0.0
710.0	600.0	652.7	100.0	0.0
600.0	500.0	547.7	100.0	0.0
500.0	425.0	461.0	100.0	0.0
425.0	355.0	388.4	100.0	0.0
355.0	300.0	326.3	100.0	0.0
300.0	250.0	273.9	99.9	0.1
250.0	212.0	230.2	99.7	0.2
212.0	180.0	195.3	99.5	0.2
180.0	150.0	164.3	98.4	1.1
150.0	125.0	136.9	94.0	4.4
125.0	106.0	115.1	80.3	13.7
106.0	90.00	97.67	55.8	24.5
90.00	75.00	82.16	28.6	27.2
75.00	63.00	68.74	0.0	28.6

Mass Frequency vs Diameter



Summary Report

Full scale pump speed: 3  
Bubble detection: Medium  
Starting Size: 63.00 μm  
Ending Size: 0.50 μm

Stir time: 30 secs  
Stir speed: Low  
Probe time: 30 secs

Sample: TT-52-08 235 cm  
 Operator: Clint Edrington  
 Submitter: Clint Edrington  
 File Name: C:\EDRING~1\TIGER&~1\SANDFR~1\TT-52-08\52\_235CM.SMP  
 Material/Liquid: silicate mud/water/Water

Reported: 01/04/10 20:17:33  
 Liquid Visc: 0.7225 cp

Sample Density: 2.650 g/cm<sup>3</sup>  
 Liquid Density: 0.9941 g/cm<sup>3</sup>

## Summary Report

Parameter 1		0.000		Parameter 2		0.000		Parameter 3		0.000	
Mass Distribution Arithmetic Statistics											
Mean	90.66			Std. Dev.			22.35				
Median	86.57			Coef. Var.			0.246				
Mode	68.74			Skewness			1.930				
				Kurtosis			8.099				
Selected Percentiles						Selected Sizes					
Percent Finer		Diameter (µm)				Diameter (µm)		Percent Finer			
100.0		714.1				500.0		100.0			
80.0		105.8				250.0		99.9			
60.0		92.56				125.0		94.0			
40.0		80.95				88.00		52.4			
20.0		70.97				63.00		0.0			
Peak Number	% of Dist.*	Mean	Mode	Median	Standard Deviation	Skewness	Kurtosis				
1	55.8	75.28	68.74	74.65	6.708	0.050	-1.997				
2	71.4	99.45	82.16	95.26	20.73	2.513	12.123				

\* Peaks must comprise at least 5.00 % of the distribution.

Micromeritics

WIN5100 V2.03

Page 1

Sample: TT-52-08 279 cm  
Operator: Clint Edrington  
Submitter: Clint Edrington  
File Name: C:\EDRING~1\TIGER&~1\SANDFR~1\TT-52-08\52\_279CM.SMP  
Material/Liquid: silicate mud/water/Water

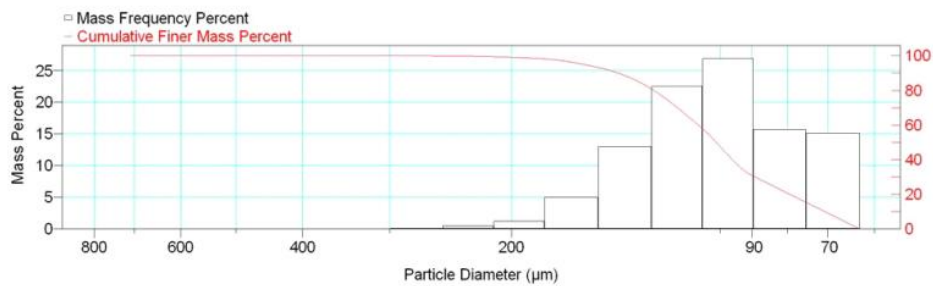
Reported: 01/04/10 20:19:28  
Liquid Visc: 0.7225 cp

Sample Density: 2.650 g/cm<sup>3</sup>  
Liquid Density: 0.9941 g/cm<sup>3</sup>

Report by Size Class

High Diameter (μm)	Low Diameter (μm)	Average Diameter (μm)	Cumulative Mass Finer (Percent)	Mass Frequency (Percent)
850.0	710.0	776.9	100.0	0.0
710.0	600.0	652.7	100.0	0.0
600.0	500.0	547.7	100.0	0.0
500.0	425.0	461.0	100.0	0.0
425.0	355.0	388.4	100.0	0.0
355.0	300.0	326.3	100.0	0.0
300.0	250.0	273.9	99.9	0.1
250.0	212.0	230.2	99.4	0.5
212.0	180.0	195.3	98.2	1.2
180.0	150.0	164.3	93.2	5.0
150.0	125.0	136.9	80.2	13.0
125.0	106.0	115.1	57.7	22.5
106.0	90.00	97.67	30.8	26.9
90.00	75.00	82.16	15.1	15.7
75.00	63.00	68.74	0.0	15.1

Mass Frequency vs Diameter



Summary Report

Full scale pump speed: 3  
Bubble detection: Medium  
Starting Size: 63.00 μm  
Ending Size: 0.50 μm

Stir time: 30 secs  
Stir speed: Low  
Probe time: 30 secs

Sample: TT-52-08 279 cm  
 Operator: Clint Edrington  
 Submitter: Clint Edrington  
 File Name: C:\EDRING~1\TIGER&~1\SANDFR~1\TT-52-08\52\_279CM.SMP  
 Material/Liquid: silicate mud/water/Water

Reported: 01/04/10 20:19:28  
 Liquid Visc: 0.7225 cp

Sample Density: 2.650 g/cm<sup>3</sup>  
 Liquid Density: 0.9941 g/cm<sup>3</sup>

## Summary Report

Parameter 1	0.000	Parameter 2	0.000	Parameter 3	0.000		
Mass Distribution Arithmetic Statistics							
Mean	105.2		Std. Dev.		28.83		
Median	101.4		Coef. Var.		0.274		
Mode	97.67		Skewness		1.194		
			Kurtosis		2.610		
Selected Percentiles			Selected Sizes				
Percent Finer	Diameter (µm)		Diameter (µm)		Percent Finer		
100.0	714.1		500.0		100.0		
80.0	124.8		250.0		99.9		
60.0	107.6		125.0		80.2		
40.0	96.09		88.00		28.8		
20.0	79.39		63.00		0.0		
Peak Number	% of Dist.*	Mean	Mode	Median	Standard Deviation	Skewness	Kurtosis
1	30.8	75.58	82.16	75.26	6.709	-0.039	-1.998
2	84.9	111.7	97.67	105.9	26.46	1.536	3.801

\* Peaks must comprise at least 5.00 % of the distribution.

# Micromeritics

WIN5100 V2.03

Page 1

Sample: TT-52-08 345 cm  
Operator: Clint Edrington  
Submitter: Clint Edrington  
File Name: C:\EDRING~1\TIGER&~1\SANDFR~1\TT-52-08\52\_345CM.SMP  
Material/Liquid: silicate mud/water/Water

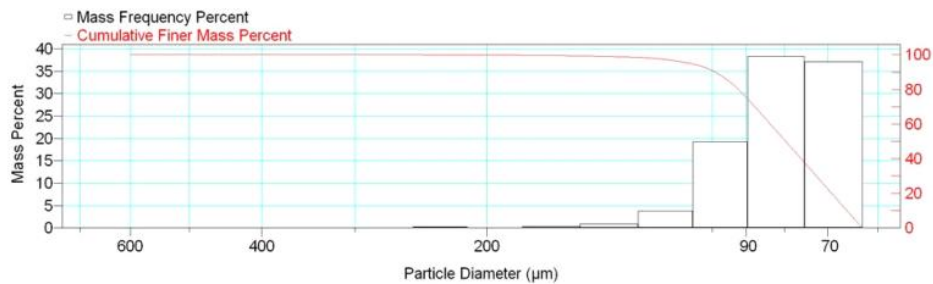
Reported: 01/04/10 20:21:24  
Liquid Visc: 0.7225 cp

Sample Density: 2.650 g/cm<sup>3</sup>  
Liquid Density: 0.9941 g/cm<sup>3</sup>

## Report by Size Class

High Diameter (µm)	Low Diameter (µm)	Average Diameter (µm)	Cumulative Mass Finer (Percent)	Mass Frequency (Percent)
710.0	600.0	652.7	100.0	0.0
600.0	500.0	547.7	100.0	0.0
500.0	425.0	461.0	100.0	0.0
425.0	355.0	388.4	100.0	0.0
355.0	300.0	326.3	100.0	0.0
300.0	250.0	273.9	100.0	0.0
250.0	212.0	230.2	99.8	0.2
212.0	180.0	195.3	99.7	0.1
180.0	150.0	164.3	99.3	0.4
150.0	125.0	136.9	98.4	0.9
125.0	106.0	115.1	94.6	3.8
106.0	90.00	97.67	75.4	19.2
90.00	75.00	82.16	37.1	38.3
75.00	63.00	68.74	0.0	37.1

Mass Frequency vs Diameter



## Summary Report

Full scale pump speed: 3  
Bubble detection: Medium  
Starting Size: 63.00 µm  
Ending Size: 0.50 µm

Stir time: 30 secs  
Stir speed: Low  
Probe time: 30 secs

Sample: TT-52-08 345 cm  
 Operator: Clint Edrington  
 Submitter: Clint Edrington  
 File Name: C:\EDRING~1\TIGER&~1\SANDFR~1\TT-52-08\52\_345CM.SMP  
 Material/Liquid: silicate mud/water/Water

Reported: 01/04/10 20:21:24  
 Liquid Visc: 0.7225 cp

Sample Density: 2.650 g/cm<sup>3</sup>  
 Liquid Density: 0.9941 g/cm<sup>3</sup>

## Summary Report

Parameter 1 0.000

Parameter 2 0.000

Parameter 3 0.000

## Mass Distribution Arithmetic Statistics

Mean	82.64	Std. Dev.	16.27
Median	79.71	Coef. Var.	0.197
Mode	82.16	Skewness	2.887
		Kurtosis	17.437

## Selected Percentiles

Percent Finer	Diameter (µm)
100.0	651.9
80.0	92.17
60.0	83.59
40.0	76.03
20.0	69.20

## Selected Sizes

Diameter (µm)	Percent Finer
500.0	100.0
250.0	100.0
125.0	98.4
88.00	70.7
63.00	0.0

Peak Number	% of Dist. *	Mean	Mode	Median	Standard Deviation	Skewness	Kurtosis
1	99.8	82.35	82.16	79.67	14.88	1.885	7.020

\* Peaks must comprise at least 5.00 % of the distribution.



Micromeritics

WIN5100 V2.03

Page 1

Sample: TT-53-08 7 cm  
Operator: Clint Edrington  
Submitter: Clint Edrington  
File Name: C:\EDRING~1\TIGER&~1\SANDFR~1\TT-53-08\53\_7CM.SMP  
Material/Liquid: silicate mud/water/Water

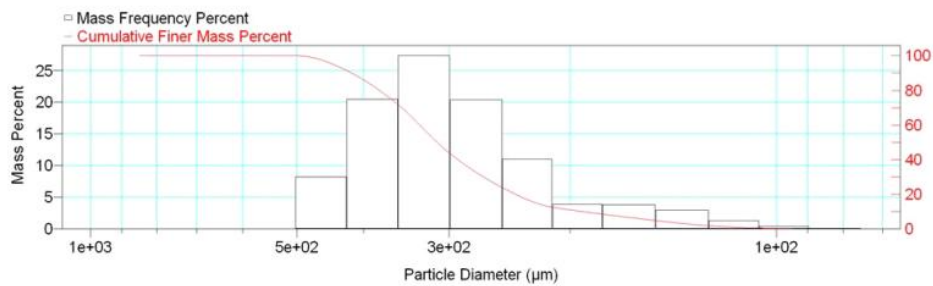
Reported: 01/04/10 20:24:40  
Liquid Visc: 0.7225 cp

Sample Density: 2.650 g/cm<sup>3</sup>  
Liquid Density: 0.9941 g/cm<sup>3</sup>

Report by Size Class

High Diameter (μm)	Low Diameter (μm)	Average Diameter (μm)	Cumulative Mass Finer (Percent)	Mass Frequency (Percent)
1000	850.0	922.0	100.0	0.0
850.0	710.0	776.9	100.0	0.0
710.0	600.0	652.7	100.0	0.0
600.0	500.0	547.7	100.0	0.0
500.0	425.0	461.0	91.8	8.2
425.0	355.0	388.4	71.3	20.5
355.0	300.0	326.3	43.9	27.4
300.0	250.0	273.9	23.5	20.4
250.0	212.0	230.2	12.5	11.0
212.0	180.0	195.3	8.6	3.9
180.0	150.0	164.3	4.8	3.8
150.0	125.0	136.9	1.8	3.0
125.0	106.0	115.1	0.5	1.3
106.0	90.00	97.67	0.1	0.4
90.00	75.00	82.16	0.0	0.1

Mass Frequency vs Diameter



Summary Report

Full scale pump speed: 3  
Bubble detection: Medium  
Starting Size: 63.00 μm  
Ending Size: 0.50 μm

Stir time: 30 secs  
Stir speed: Low  
Probe time: 30 secs

Sample: TT-53-08 7 cm  
 Operator: Clint Edrington  
 Submitter: Clint Edrington  
 File Name: C:\EDRING~1\TIGER&~1\SANDFR~1\TT-53-08\53\_7CM.SMP  
 Material/Liquid: silicate mud/water/Water

Reported: 01/04/10 20:24:40  
 Liquid Visc: 0.7225 cp

Sample Density: 2.650 g/cm<sup>3</sup>  
 Liquid Density: 0.9941 g/cm<sup>3</sup>

## Summary Report

Parameter 1	0.000	Parameter 2	0.000	Parameter 3	0.000		
Mass Distribution Arithmetic Statistics							
Mean	308.0		Std. Dev.	84.32			
Median	312.3		Coef. Var.	0.274			
Mode	326.3		Skewness	-0.197			
			Kurtosis	-0.341			
Selected Percentiles			Selected Sizes				
Percent Finer	Diameter (µm)		Diameter (µm)	Percent Finer			
100.0	922.0		500.0	100.0			
80.0	379.2		250.0	23.5			
60.0	331.0		125.0	1.8			
40.0	291.3		88.00	0.1			
20.0	240.0		63.00	0.0			
Peak Number	% of Dist.*	Mean	Mode	Median	Standard Deviation	Skewness	Kurtosis
1	100.0	308.0	326.3	312.3	84.32	-0.197	-0.341

\* Peaks must comprise at least 5.00 % of the distribution.

Micromeritics

WIN5100 V2.03

Page 1

Sample: TT-53-08 52 cm  
Operator: Clint Edrington  
Submitter: Clint Edrington  
File Name: C:\EDRING~1\TIGER&~1\SANDFR~1\TT-53-08\53\_52CM.SMP  
Material/Liquid: silicate mud/water/Water

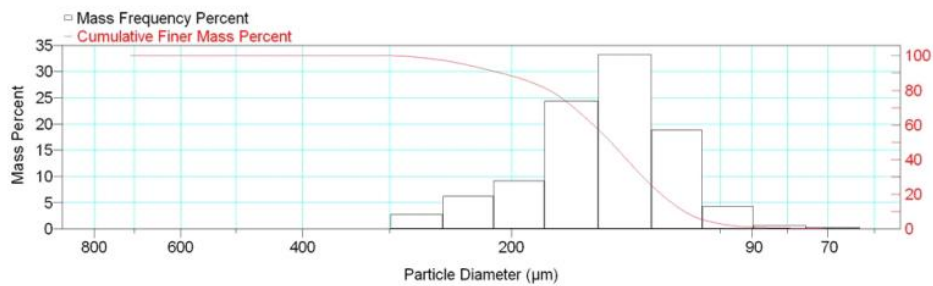
Reported: 01/04/10 20:26:48  
Liquid Visc: 0.7225 cp

Sample Density: 2.650 g/cm<sup>3</sup>  
Liquid Density: 0.9941 g/cm<sup>3</sup>

Report by Size Class

High Diameter (µm)	Low Diameter (µm)	Average Diameter (µm)	Cumulative Mass Finer (Percent)	Mass Frequency (Percent)
850.0	710.0	776.9	100.0	0.0
710.0	600.0	652.7	100.0	0.0
600.0	500.0	547.7	100.0	0.0
500.0	425.0	461.0	100.0	0.0
425.0	355.0	388.4	100.0	0.0
355.0	300.0	326.3	100.0	0.0
300.0	250.0	273.9	97.2	2.8
250.0	212.0	230.2	91.0	6.2
212.0	180.0	195.3	81.8	9.2
180.0	150.0	164.3	57.4	24.4
150.0	125.0	136.9	24.2	33.2
125.0	106.0	115.1	5.3	18.9
106.0	90.00	97.67	1.0	4.3
90.00	75.00	82.16	0.3	0.7
75.00	63.00	68.74	0.0	0.3

Mass Frequency vs Diameter



Summary Report

Full scale pump speed: 3  
Bubble detection: Medium  
Starting Size: 63.00 µm  
Ending Size: 0.50 µm

Stir time: 30 secs  
Stir speed: Low  
Probe time: 30 secs

Sample: TT-53-08 52 cm  
 Operator: Clint Edrington  
 Submitter: Clint Edrington  
 File Name: C:\EDRING~1\TIGER&~1\SANDFR~1\TT-53-08\53\_52CM.SMP  
 Material/Liquid: silicate mud/water/Water

Reported: 01/04/10 20:26:48  
 Liquid Visc: 0.7225 cp

Sample Density: 2.650 g/cm<sup>3</sup>  
 Liquid Density: 0.9941 g/cm<sup>3</sup>

## Summary Report

Parameter 1	0.000	Parameter 2	0.000	Parameter 3	0.000		
Mass Distribution Arithmetic Statistics							
Mean	152.2	Std. Dev.		38.98			
Median	143.7	Coef. Var.		0.256			
Mode	136.9	Skewness		1.110			
		Kurtosis		1.255			
Selected Percentiles			Selected Sizes				
Percent Finer	Diameter (µm)		Diameter (µm)	Percent Finer			
100.0	714.1		500.0	100.0			
80.0	176.3		250.0	97.2			
60.0	152.5		125.0	24.2			
40.0	136.4		88.00	0.9			
20.0	121.6		63.00	0.0			
Peak Number	% of Dist.*	Mean	Mode	Median	Standard Deviation	Skewness	Kurtosis
1	100.0	152.2	136.9	143.7	38.98	1.110	1.255

\* Peaks must comprise at least 5.00 % of the distribution.

Micromeritics

WIN5100 V2.03

Page 1

Sample: TT-53-08 100 cm  
Operator: Clint Edrington  
Submitter: Clint Edrington  
File Name: C:\EDRING~1\TIGER&~1\SANDFR~1\TT-53-08\53\_100CM.SMP  
Material/Liquid: silicate mud/water/Water

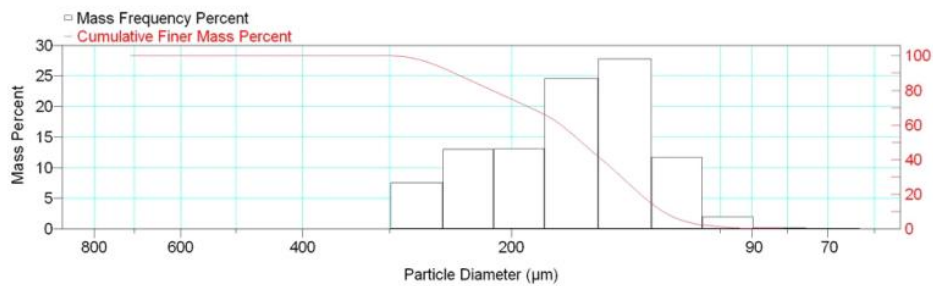
Reported: 01/04/10 20:28:50  
Liquid Visc: 0.7225 cp

Sample Density: 2.650 g/cm<sup>3</sup>  
Liquid Density: 0.9941 g/cm<sup>3</sup>

Report by Size Class

High Diameter ( $\mu\text{m}$ )	Low Diameter ( $\mu\text{m}$ )	Average Diameter ( $\mu\text{m}$ )	Cumulative Mass Finer (Percent)	Mass Frequency (Percent)
850.0	710.0	776.9	100.0	0.0
710.0	600.0	652.7	100.0	0.0
600.0	500.0	547.7	100.0	0.0
500.0	425.0	461.0	100.0	0.0
425.0	355.0	388.4	100.0	0.0
355.0	300.0	326.3	100.0	0.0
300.0	250.0	273.9	92.5	7.5
250.0	212.0	230.2	79.5	13.0
212.0	180.0	195.3	66.4	13.1
180.0	150.0	164.3	41.8	24.6
150.0	125.0	136.9	14.0	27.8
125.0	106.0	115.1	2.3	11.7
106.0	90.00	97.67	0.3	2.0
90.00	75.00	82.16	0.1	0.2
75.00	63.00	68.74	0.0	0.1

Mass Frequency vs Diameter



Summary Report

Full scale pump speed: 3  
Bubble detection: Medium  
Starting Size: 63.00  $\mu\text{m}$   
Ending Size: 0.50  $\mu\text{m}$

Stir time: 30 secs  
Stir speed: Low  
Probe time: 30 secs

Sample: TT-53-08 100 cm  
 Operator: Clint Edrington  
 Submitter: Clint Edrington  
 File Name: C:\EDRING~1\TIGER&~1\SANDFR~1\TT-53-08\53\_100CM.SMP  
 Material/Liquid: silicate mud/water/Water

Reported: 01/04/10 20:28:50  
 Liquid Visc: 0.7225 cp

Sample Density: 2.650 g/cm<sup>3</sup>  
 Liquid Density: 0.9941 g/cm<sup>3</sup>

## Summary Report

Parameter 1	0.000	Parameter 2	0.000	Parameter 3	0.000		
Mass Distribution Arithmetic Statistics							
Mean	170.2	Std. Dev.		46.47			
Median	158.5	Coef. Var.		0.273			
Mode	136.9	Skewness		0.736			
		Kurtosis		-0.298			
Selected Percentiles			Selected Sizes				
Percent Finer	Diameter (µm)		Diameter (µm)	Percent Finer			
100.0	714.1		500.0	100.0			
80.0	213.3		250.0	92.5			
60.0	169.8		125.0	14.0			
40.0	148.1		88.00	0.3			
20.0	130.3		63.00	0.0			
Peak Number	% of Dist.*	Mean	Mode	Median	Standard Deviation	Skewness	Kurtosis
1	100.0	170.2	136.9	158.5	46.47	0.736	-0.298

\* Peaks must comprise at least 5.00 % of the distribution.

Micromeritics

WIN5100 V2.03

Page 1

Sample: TT-53-08 165 cm  
Operator: Clint Edrington  
Submitter: Clint Edrington  
File Name: C:\EDRING~1\TIGER&~1\SANDFR~1\TT-53-08\53\_165CM.SMP  
Material/Liquid: silicate mud/water/Water

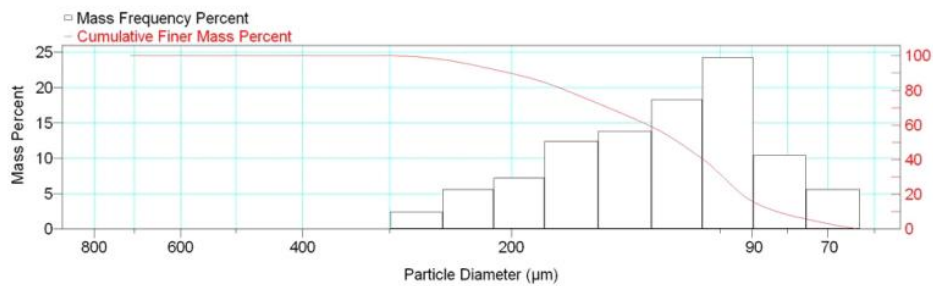
Reported: 01/04/10 20:30:32  
Liquid Visc: 0.7225 cp

Sample Density: 2.650 g/cm<sup>3</sup>  
Liquid Density: 0.9941 g/cm<sup>3</sup>

Report by Size Class

High Diameter ( $\mu\text{m}$ )	Low Diameter ( $\mu\text{m}$ )	Average Diameter ( $\mu\text{m}$ )	Cumulative Mass Finer (Percent)	Mass Frequency (Percent)
850.0	710.0	776.9	100.0	0.0
710.0	600.0	652.7	100.0	0.0
600.0	500.0	547.7	100.0	0.0
500.0	425.0	461.0	100.0	0.0
425.0	355.0	388.4	100.0	0.0
355.0	300.0	326.3	100.0	0.0
300.0	250.0	273.9	97.6	2.4
250.0	212.0	230.2	92.0	5.6
212.0	180.0	195.3	84.8	7.2
180.0	150.0	164.3	72.4	12.4
150.0	125.0	136.9	58.6	13.8
125.0	106.0	115.1	40.3	18.3
106.0	90.00	97.67	16.0	24.3
90.00	75.00	82.16	5.6	10.4
75.00	63.00	68.74	0.0	5.6

Mass Frequency vs Diameter



Summary Report

Full scale pump speed: 3  
Bubble detection: Medium  
Starting Size: 63.00  $\mu\text{m}$   
Ending Size: 0.50  $\mu\text{m}$

Stir time: 30 secs  
Stir speed: Low  
Probe time: 30 secs

Sample: TT-53-08 165 cm  
 Operator: Clint Edrington  
 Submitter: Clint Edrington  
 File Name: C:\EDRING~1\TIGER&~1\SANDFR~1\TT-53-08\53\_165CM.SMP  
 Material/Liquid: silicate mud/water/Water

Reported: 01/04/10 20:30:32  
 Liquid Visc: 0.7225 cp

Sample Density: 2.650 g/cm<sup>3</sup>  
 Liquid Density: 0.9941 g/cm<sup>3</sup>

## Summary Report

Parameter 1	0.000	Parameter 2	0.000	Parameter 3	0.000		
Mass Distribution Arithmetic Statistics							
Mean	130.0	Std. Dev.		47.56			
Median	114.8	Coef. Var.		0.366			
Mode	97.67	Skewness		1.115			
		Kurtosis		0.718			
Selected Percentiles			Selected Sizes				
Percent Finer	Diameter (µm)		Diameter (µm)	Percent Finer			
100.0	714.1		500.0	100.0			
80.0	166.9		250.0	97.6			
60.0	127.2		125.0	58.6			
40.0	105.7		88.00	14.0			
20.0	93.09		63.00	0.0			
Peak Number	% of Dist.*	Mean	Mode	Median	Standard Deviation	Skewness	Kurtosis
1	100.0	130.0	97.67	114.8	47.56	1.115	0.718

\* Peaks must comprise at least 5.00 % of the distribution.



Micromeritics

WIN5100 V2.03

Page 1

Sample: TT-53-08 265 cm  
Operator: Clint Edrington  
Submitter: Clint Edrington  
File Name: C:\EDRING~1\TIGER&~1\SANDFR~1\TT-53-08\53\_265CM.SMP  
Material/Liquid: silicate mud/water/Water

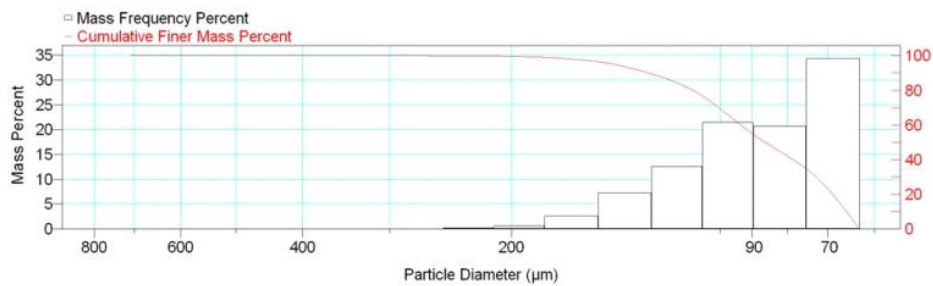
Reported: 01/04/10 20:32:39  
Liquid Visc: 0.7225 cp

Sample Density: 2.650 g/cm<sup>3</sup>  
Liquid Density: 0.9941 g/cm<sup>3</sup>

Report by Size Class

High Diameter (µm)	Low Diameter (µm)	Average Diameter (µm)	Cumulative Mass Finer (Percent)	Mass Frequency (Percent)
850.0	710.0	776.9	100.0	0.0
710.0	600.0	652.7	100.0	0.0
600.0	500.0	547.7	100.0	0.0
500.0	425.0	461.0	100.0	0.0
425.0	355.0	388.4	100.0	0.0
355.0	300.0	326.3	100.0	0.0
300.0	250.0	273.9	99.9	0.1
250.0	212.0	230.2	99.7	0.2
212.0	180.0	195.3	99.1	0.6
180.0	150.0	164.3	96.5	2.6
150.0	125.0	136.9	89.2	7.3
125.0	106.0	115.1	76.6	12.6
106.0	90.00	97.67	55.1	21.5
90.00	75.00	82.16	34.4	20.7
75.00	63.00	68.74	0.0	34.4

Mass Frequency vs Diameter



Summary Report

Full scale pump speed: 3  
Bubble detection: Medium  
Starting Size: 63.00 µm  
Ending Size: 0.50 µm

Stir time: 30 secs  
Stir speed: Low  
Probe time: 30 secs

Sample: TT-53-08 265 cm  
 Operator: Clint Edrington  
 Submitter: Clint Edrington  
 File Name: C:\EDRING~1\TIGER&~1\SANDFR~1\TT-53-08\53\_265CM.SMP  
 Material/Liquid: silicate mud/water/Water

Reported: 01/04/10 20:32:39  
 Liquid Visc: 0.7225 cp

Sample Density: 2.650 g/cm<sup>3</sup>  
 Liquid Density: 0.9941 g/cm<sup>3</sup>

## Summary Report

Parameter 1	0.000	Parameter 2	0.000	Parameter 3	0.000		
Mass Distribution Arithmetic Statistics							
Mean	92.33		Std. Dev.		26.44		
Median	86.16		Coef. Var.		0.286		
Mode	68.74		Skewness		1.664		
			Kurtosis		4.398		
Selected Percentiles			Selected Sizes				
Percent Finer	Diameter (µm)		Diameter (µm)		Percent Finer		
100.0	714.1		500.0		100.0		
80.0	109.5		250.0		99.9		
60.0	93.45		125.0		89.2		
40.0	78.59		88.00		52.4		
20.0	68.87		63.00		0.0		
Peak Number	% of Dist.*	Mean	Mode	Median	Standard Deviation	Skewness	Kurtosis
1	55.1	73.78	68.74	71.68	6.499	0.513	-1.736
2	65.6	104.7	97.67	98.48	24.91	1.865	5.640

\* Peaks must comprise at least 5.00 % of the distribution.

Micromeritics

WIN5100 V2.03

Page 1

Sample: TT-53-08 310 cm  
Operator: Clint Edrington  
Submitter: Clint Edrington  
File Name: C:\EDRING~1\TIGER&~1\SANDFR~1\TT-53-08\53\_310CM.SMP  
Material/Liquid: silicate mud/water/Water

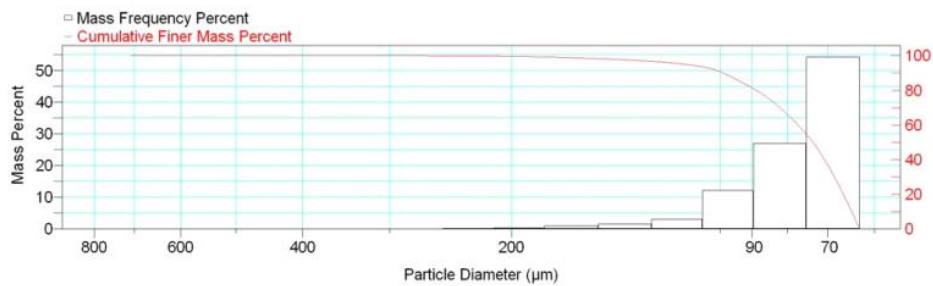
Reported: 01/04/10 20:34:37  
Liquid Visc: 0.7225 cp

Sample Density: 2.650 g/cm<sup>3</sup>  
Liquid Density: 0.9941 g/cm<sup>3</sup>

Report by Size Class

High Diameter ( $\mu\text{m}$ )	Low Diameter ( $\mu\text{m}$ )	Average Diameter ( $\mu\text{m}$ )	Cumulative Mass Finer (Percent)	Mass Frequency (Percent)
850.0	710.0	776.9	100.0	0.0
710.0	600.0	652.7	100.0	0.0
600.0	500.0	547.7	100.0	0.0
500.0	425.0	461.0	100.0	0.0
425.0	355.0	388.4	100.0	0.0
355.0	300.0	326.3	100.0	0.0
300.0	250.0	273.9	99.9	0.1
250.0	212.0	230.2	99.7	0.2
212.0	180.0	195.3	99.3	0.4
180.0	150.0	164.3	98.3	1.0
150.0	125.0	136.9	96.7	1.6
125.0	106.0	115.1	93.6	3.1
106.0	90.00	97.67	81.4	12.2
90.00	75.00	82.16	54.3	27.1
75.00	63.00	68.74	0.0	54.3

Mass Frequency vs Diameter



Summary Report

Full scale pump speed: 3  
Bubble detection: Medium  
Starting Size: 63.00  $\mu\text{m}$   
Ending Size: 0.50  $\mu\text{m}$

Stir time: 30 secs  
Stir speed: Low  
Probe time: 30 secs

Sample: TT-53-08 310 cm  
 Operator: Clint Edrington  
 Submitter: Clint Edrington  
 File Name: C:\EDRING~1\TIGER&~1\SANDFR~1\TT-53-08\53\_310CM.SMP  
 Material/Liquid: silicate mud/water/Water

Reported: 01/04/10 20:34:37  
 Liquid Visc: 0.7225 cp

Sample Density: 2.650 g/cm<sup>3</sup>  
 Liquid Density: 0.9941 g/cm<sup>3</sup>

## Summary Report

Parameter 1	0.000	Parameter 2	0.000	Parameter 3	0.000		
Mass Distribution Arithmetic Statistics							
Mean	80.42	Std. Dev.		20.13			
Median	73.52	Coef. Var.		0.250			
Mode	68.74	Skewness		3.664			
		Kurtosis		20.327			
Selected Percentiles			Selected Sizes				
Percent Finer	Diameter (µm)		Diameter (µm)	Percent Finer			
100.0	714.1		500.0	100.0			
80.0	88.72		250.0	99.9			
60.0	77.26		125.0	96.7			
40.0	70.73		88.00	79.1			
20.0	66.46		63.00	0.0			
Peak Number	% of Dist.*	Mean	Mode	Median	Standard Deviation	Skewness	Kurtosis
1	100.0	80.42	68.74	73.52	20.13	3.664	20.327

\* Peaks must comprise at least 5.00 % of the distribution.

Micromeritics

WIN5100 V2.03

Page 1

Sample: TT-54-08 3 cm  
Operator: Clint Edrington  
Submitter: Clint Edrington  
File Name: C:\EDRING~1\TIGER&~1\SANDFR~1\TT-54-08\54\_3CM.SMP  
Material/Liquid: silicate mud/water/Water

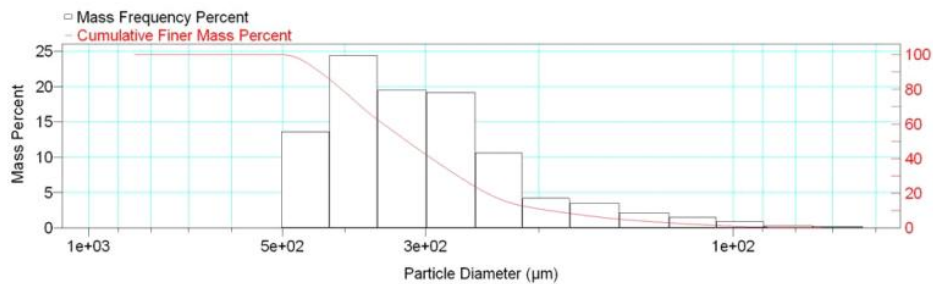
Reported: 01/04/10 20:37:49  
Liquid Visc: 0.7225 cp

Sample Density: 2.650 g/cm<sup>3</sup>  
Liquid Density: 0.9941 g/cm<sup>3</sup>

Report by Size Class

High Diameter (μm)	Low Diameter (μm)	Average Diameter (μm)	Cumulative Mass Finer (Percent)	Mass Frequency (Percent)
1000	850.0	922.0	100.0	0.0
850.0	710.0	776.9	100.0	0.0
710.0	600.0	652.7	100.0	0.0
600.0	500.0	547.7	100.0	0.0
500.0	425.0	461.0	86.4	13.6
425.0	355.0	388.4	62.0	24.4
355.0	300.0	326.3	42.5	19.5
300.0	250.0	273.9	23.3	19.2
250.0	212.0	230.2	12.7	10.6
212.0	180.0	195.3	8.5	4.2
180.0	150.0	164.3	5.0	3.5
150.0	125.0	136.9	2.9	2.1
125.0	106.0	115.1	1.4	1.5
106.0	90.00	97.67	0.5	0.9
90.00	75.00	82.16	0.2	0.3
75.00	63.00	68.74	0.0	0.2

Mass Frequency vs Diameter



Summary Report

Full scale pump speed: 3  
Bubble detection: Medium  
Starting Size: 63.00 μm

Stir time: 30 secs  
Stir speed: Low  
Probe time: 30 secs

Sample: TT-54-08 3 cm  
 Operator: Clint Edrington  
 Submitter: Clint Edrington  
 File Name: C:\EDRING~1\TIGER&~1\SANDFR~1\TT-54-08\54\_3CM.SMP  
 Material/Liquid: silicate mud/water/Water

Reported: 01/04/10 20:37:49  
 Liquid Visc: 0.7225 cp

Sample Density: 2.650 g/cm<sup>3</sup>  
 Liquid Density: 0.9941 g/cm<sup>3</sup>

## Summary Report

Ending Size: 0.50 µm

Parameter 1 0.000

Parameter 2 0.000

Parameter 3 0.000

## Mass Distribution Arithmetic Statistics

Mean	317.9	Std. Dev.	93.21
Median	320.4	Coef. Var.	0.293
Mode	388.4	Skewness	-0.277
		Kurtosis	-0.549

## Selected Percentiles

Percent Finer	Diameter (µm)
100.0	922.0
80.0	405.1
60.0	349.1
40.0	293.4
20.0	241.0

## Selected Sizes

Diameter (µm)	Percent Finer
500.0	100.0
250.0	23.3
125.0	2.9
88.00	0.5
63.00	0.0

Peak Number	% of Dist. *	Mean	Mode	Median	Standard Deviation	Skewness	Kurtosis
1	100.0	317.9	388.4	320.4	93.21	-0.277	-0.549

\* Peaks must comprise at least 5.00 % of the distribution.

Micromeritics

WIN5100 V2.03

Page 1

Sample: TT-54-08 56 cm  
Operator: Clint Edrington  
Submitter: Clint Edrington  
File Name: C:\EDRING~1\TIGER&~1\SANDFR~1\TT-54-08\54\_56CM.SMP  
Material/Liquid: silicate mud/water/Water

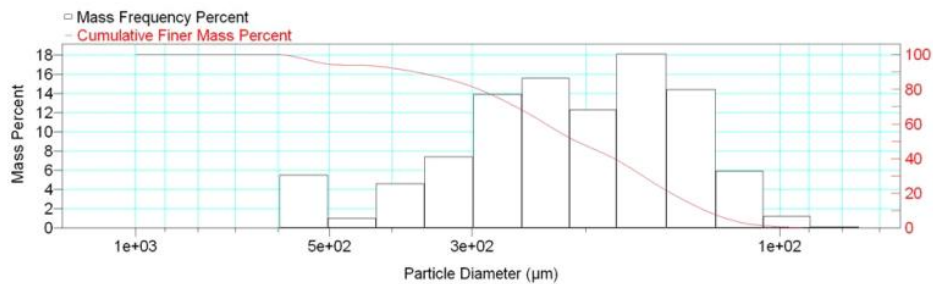
Reported: 01/04/10 20:40:29  
Liquid Visc: 0.7225 cp

Sample Density: 2.650 g/cm<sup>3</sup>  
Liquid Density: 0.9941 g/cm<sup>3</sup>

Report by Size Class

High Diameter (µm)	Low Diameter (µm)	Average Diameter (µm)	Cumulative Mass Finer (Percent)	Mass Frequency (Percent)
1180	1000	1086	100.0	0.0
1000	850.0	922.0	100.0	0.0
850.0	710.0	776.9	100.0	0.0
710.0	600.0	652.7	100.0	0.0
600.0	500.0	547.7	94.5	5.5
500.0	425.0	461.0	93.5	1.0
425.0	355.0	388.4	88.9	4.6
355.0	300.0	326.3	81.5	7.4
300.0	250.0	273.9	67.6	13.9
250.0	212.0	230.2	52.0	15.6
212.0	180.0	195.3	39.7	12.3
180.0	150.0	164.3	21.6	18.1
150.0	125.0	136.9	7.2	14.4
125.0	106.0	115.1	1.3	5.9
106.0	90.00	97.67	0.1	1.2
90.00	75.00	82.16	0.0	0.1

Mass Frequency vs Diameter



Summary Report

Full scale pump speed: 3  
Bubble detection: Medium  
Starting Size: 63.00 µm

Stir time: 30 secs  
Stir speed: Low  
Probe time: 30 secs

Sample: TT-54-08 56 cm  
 Operator: Clint Edrington  
 Submitter: Clint Edrington  
 File Name: C:\EDRING~1\TIGER&~1\SANDFR~1\TT-54-08\54\_56CM.SMP  
 Material/Liquid: silicate mud/water/Water

Reported: 01/04/10 20:40:29  
 Liquid Visc: 0.7225 cp

Sample Density: 2.650 g/cm<sup>3</sup>  
 Liquid Density: 0.9941 g/cm<sup>3</sup>

## Summary Report

Ending Size: 0.50 µm

Parameter 1 0.000 Parameter 2 0.000 Parameter 3 0.000

## Mass Distribution Arithmetic Statistics

Mean	232.3	Std. Dev.	106.7
Median	206.9	Coef. Var.	0.459
Mode	164.3	Skewness	1.465
		Kurtosis	1.923

## Selected Percentiles

Percent Finer	Diameter (µm)
100.0	1010
80.0	292.9
60.0	230.8
40.0	180.6
20.0	147.4

## Selected Sizes

Diameter (µm)	Percent Finer
500.0	94.5
250.0	67.6
125.0	7.2
88.00	0.1
63.00	0.0

Peak Number	% of Dist. *	Mean	Mode	Median	Standard Deviation	Skewness	Kurtosis
1	52.0	156.8	164.3	156.9	27.73	-0.106	-0.885
2	54.8	263.9	230.2	248.6	62.77	1.016	0.547
3	6.5	534.4	547.7	536.6	31.30	-1.919	1.682

\* Peaks must comprise at least 5.00 % of the distribution.



Micromeritics

WIN5100 V2.03

Page 1

Sample: TT-54-08 100 cm  
Operator: Clint Edrington  
Submitter: Clint Edrington  
File Name: C:\EDRING~1\TIGER&~1\SANDFR~1\TT-54-08\54\_100CM.SMP  
Material/Liquid: silicate mud/water/Water

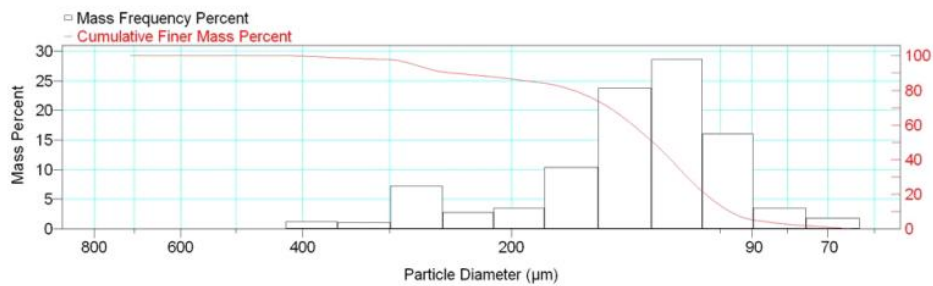
Reported: 01/04/10 20:42:54  
Liquid Visc: 0.7225 cp

Sample Density: 2.650 g/cm<sup>3</sup>  
Liquid Density: 0.9941 g/cm<sup>3</sup>

Report by Size Class

High Diameter (μm)	Low Diameter (μm)	Average Diameter (μm)	Cumulative Mass Finer (Percent)	Mass Frequency (Percent)
850.0	710.0	776.9	100.0	0.0
710.0	600.0	652.7	100.0	0.0
600.0	500.0	547.7	100.0	0.0
500.0	425.0	461.0	100.0	0.0
425.0	355.0	388.4	98.8	1.2
355.0	300.0	326.3	97.7	1.1
300.0	250.0	273.9	90.5	7.2
250.0	212.0	230.2	87.7	2.8
212.0	180.0	195.3	84.2	3.5
180.0	150.0	164.3	73.8	10.4
150.0	125.0	136.9	50.0	23.8
125.0	106.0	115.1	21.4	28.6
106.0	90.00	97.67	5.3	16.1
90.00	75.00	82.16	1.8	3.5
75.00	63.00	68.74	0.0	1.8

Mass Frequency vs Diameter



Summary Report

Full scale pump speed: 3  
Bubble detection: Medium  
Starting Size: 63.00 μm  
Ending Size: 0.50 μm

Stir time: 30 secs  
Stir speed: Low  
Probe time: 30 secs

Sample: TT-54-08 100 cm  
 Operator: Clint Edrington  
 Submitter: Clint Edrington  
 File Name: C:\EDRING~1\TIGER&~1\SANDFR~1\TT-54-08\54\_100CM.SMP  
 Material/Liquid: silicate mud/water/Water

Reported: 01/04/10 20:42:54  
 Liquid Visc: 0.7225 cp

Sample Density: 2.650 g/cm<sup>3</sup>  
 Liquid Density: 0.9941 g/cm<sup>3</sup>

## Summary Report

Parameter 1	0.000	Parameter 2	0.000	Parameter 3	0.000		
Mass Distribution Arithmetic Statistics							
Mean	143.7	Std. Dev.		58.92			
Median	125.0	Coef. Var.		0.410			
Mode	115.1	Skewness		1.894			
		Kurtosis		3.618			
Selected Percentiles			Selected Sizes				
Percent Finer	Diameter (µm)		Diameter (µm)	Percent Finer			
100.0	850.0		500.0	100.0			
80.0	162.9		250.0	90.5			
60.0	133.7		125.0	50.0			
40.0	117.9		88.00	4.7			
20.0	105.0		63.00	0.0			
Peak Number	% of Dist.*	Mean	Mode	Median	Standard Deviation	Skewness	Kurtosis
1	90.5	127.9	115.1	121.4	32.23	1.119	1.608
2	11.1	268.1	273.9	268.0	26.83	0.316	0.208

\* Peaks must comprise at least 5.00 % of the distribution.

Micromeritics

WIN5100 V2.03

Page 1

Sample: TT-55-08 3 cm  
Operator: Clint Edrington  
Submitter: Clint Edrington  
File Name: C:\EDRING~1\TIGER&~1\SANDFR~1\TT-55-08\55\_3CM.SMP  
Material/Liquid: silicate mud/water/Water

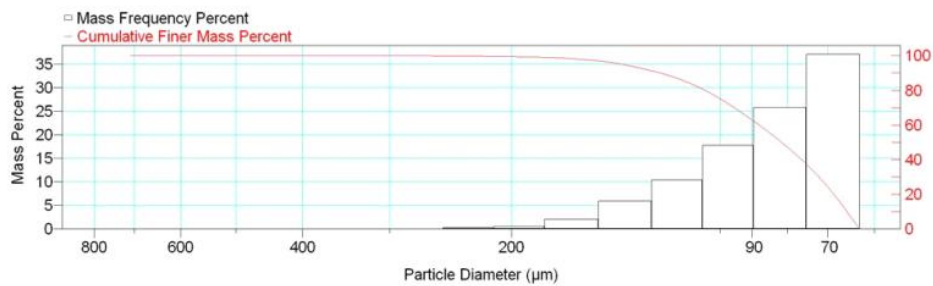
Reported: 01/04/10 20:46:14  
Liquid Visc: 0.7225 cp

Sample Density: 2.650 g/cm<sup>3</sup>  
Liquid Density: 0.9941 g/cm<sup>3</sup>

Report by Size Class

High Diameter (µm)	Low Diameter (µm)	Average Diameter (µm)	Cumulative Mass Finer (Percent)	Mass Frequency (Percent)
850.0	710.0	776.9	100.0	0.0
710.0	600.0	652.7	100.0	0.0
600.0	500.0	547.7	100.0	0.0
500.0	425.0	461.0	100.0	0.0
425.0	355.0	388.4	100.0	0.0
355.0	300.0	326.3	100.0	0.0
300.0	250.0	273.9	99.9	0.1
250.0	212.0	230.2	99.6	0.3
212.0	180.0	195.3	99.1	0.5
180.0	150.0	164.3	97.0	2.1
150.0	125.0	136.9	91.1	5.9
125.0	106.0	115.1	80.7	10.4
106.0	90.00	97.67	62.9	17.8
90.00	75.00	82.16	37.1	25.8
75.00	63.00	68.74	0.0	37.1

Mass Frequency vs Diameter



Summary Report

Full scale pump speed: 3  
Bubble detection: Medium  
Starting Size: 63.00 µm  
Ending Size: 0.50 µm

Stir time: 30 secs  
Stir speed: Low  
Probe time: 30 secs

Sample: TT-55-08 3 cm  
 Operator: Clint Edrington  
 Submitter: Clint Edrington  
 File Name: C:\EDRING~1\TIGER&~1\SANDFR~1\TT-55-08\55\_3CM.SMP  
 Material/Liquid: silicate mud/water/Water

Reported: 01/04/10 20:46:14  
 Liquid Visc: 0.7225 cp

Sample Density: 2.650 g/cm<sup>3</sup>  
 Liquid Density: 0.9941 g/cm<sup>3</sup>

## Summary Report

Parameter 1	0.000	Parameter 2	0.000	Parameter 3	0.000		
Mass Distribution Arithmetic Statistics							
Mean	89.53		Std. Dev.	25.57			
Median	81.60		Coef. Var.	0.286			
Mode	68.74		Skewness	2.036			
			Kurtosis	6.427			
Selected Percentiles			Selected Sizes				
Percent Finer	Diameter (µm)		Diameter (µm)	Percent Finer			
100.0	714.1		500.0	100.0			
80.0	105.1		250.0	99.9			
60.0	87.92		125.0	91.1			
40.0	76.36		88.00	60.1			
20.0	68.61		63.00	0.0			
Peak Number	% of Dist.*	Mean	Mode	Median	Standard Deviation	Skewness	Kurtosis
1	100.0	89.53	68.74	81.60	25.57	2.036	6.427

\* Peaks must comprise at least 5.00 % of the distribution.

Micromeritics

WIN5100 V2.03

Page 1

Sample: TT-55-08 99 cm  
Operator: Clint Edrington  
Submitter: Clint Edrington  
File Name: C:\EDRING~1\TIGER&~1\SANDFR~1\TT-55-08\55\_99CM.SMP  
Material/Liquid: silicate mud/water/Water

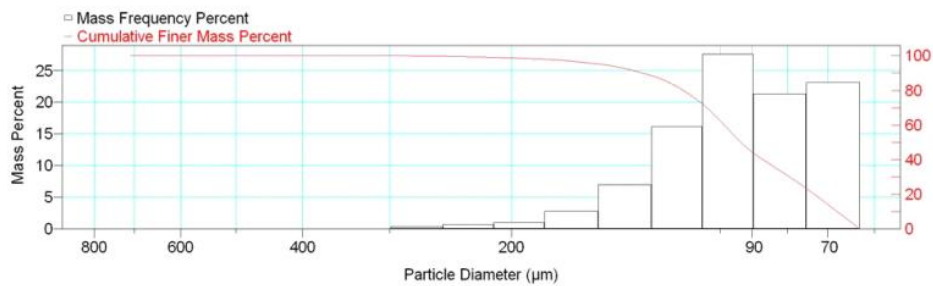
Reported: 01/04/10 20:48:12  
Liquid Visc: 0.7225 cp

Sample Density: 2.650 g/cm<sup>3</sup>  
Liquid Density: 0.9941 g/cm<sup>3</sup>

Report by Size Class

High Diameter (µm)	Low Diameter (µm)	Average Diameter (µm)	Cumulative Mass Finer (Percent)	Mass Frequency (Percent)
850.0	710.0	776.9	100.0	0.0
710.0	600.0	652.7	100.0	0.0
600.0	500.0	547.7	100.0	0.0
500.0	425.0	461.0	100.0	0.0
425.0	355.0	388.4	100.0	0.0
355.0	300.0	326.3	100.0	0.0
300.0	250.0	273.9	99.7	0.3
250.0	212.0	230.2	99.0	0.7
212.0	180.0	195.3	98.0	1.0
180.0	150.0	164.3	95.2	2.8
150.0	125.0	136.9	88.2	7.0
125.0	106.0	115.1	72.0	16.2
106.0	90.00	97.67	44.4	27.6
90.00	75.00	82.16	23.1	21.3
75.00	63.00	68.74	0.0	23.1

Mass Frequency vs Diameter



Summary Report

Full scale pump speed: 3  
Bubble detection: Medium  
Starting Size: 63.00 µm  
Ending Size: 0.50 µm

Stir time: 30 secs  
Stir speed: Low  
Probe time: 30 secs

Sample: TT-55-08 99 cm  
 Operator: Clint Edrington  
 Submitter: Clint Edrington  
 File Name: C:\EDRING~1\TIGER&~1\SANDFR~1\TT-55-08\55\_99CM.SMP  
 Material/Liquid: silicate mud/water/Water

Reported: 01/04/10 20:48:12  
 Liquid Visc: 0.7225 cp

Sample Density: 2.650 g/cm<sup>3</sup>  
 Liquid Density: 0.9941 g/cm<sup>3</sup>

## Summary Report

Parameter 1	0.000	Parameter 2	0.000	Parameter 3	0.000		
Mass Distribution Arithmetic Statistics							
Mean	97.56		Std. Dev.		28.94		
Median	93.44		Coef. Var.		0.297		
Mode	97.67		Skewness		2.034		
			Kurtosis		6.823		
Selected Percentiles			Selected Sizes				
Percent Finer	Diameter (µm)		Diameter (µm)		Percent Finer		
100.0	714.1		500.0		100.0		
80.0	113.1		250.0		99.7		
60.0	98.72		125.0		88.2		
40.0	86.78		88.00		41.6		
20.0	73.22		63.00		0.0		
Peak Number	% of Dist.*	Mean	Mode	Median	Standard Deviation	Skewness	Kurtosis
1	44.4	75.18	68.74	74.48	6.704	0.081	-1.993
2	76.9	106.2	97.67	99.54	27.66	2.401	8.362

\* Peaks must comprise at least 5.00 % of the distribution.

Micromeritics

WIN5100 V2.03

Page 1

Sample: TT-55-08 148 cm  
Operator: Clint Edrington  
Submitter: Clint Edrington  
File Name: C:\EDRING~1\TIGER&~1\SANDFR~1\TT-55-08\55\_148CM.SMP  
Material/Liquid: silicate mud/water/Water

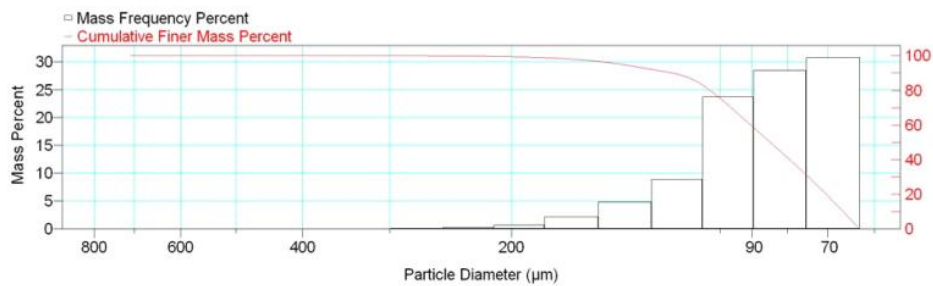
Reported: 01/04/10 20:51:00  
Liquid Visc: 0.7225 cp

Sample Density: 2.650 g/cm<sup>3</sup>  
Liquid Density: 0.9941 g/cm<sup>3</sup>

Report by Size Class

High Diameter (µm)	Low Diameter (µm)	Average Diameter (µm)	Cumulative Mass Finer (Percent)	Mass Frequency (Percent)
850.0	710.0	776.9	100.0	0.0
710.0	600.0	652.7	100.0	0.0
600.0	500.0	547.7	100.0	0.0
500.0	425.0	461.0	100.0	0.0
425.0	355.0	388.4	100.0	0.0
355.0	300.0	326.3	100.0	0.0
300.0	250.0	273.9	99.9	0.1
250.0	212.0	230.2	99.6	0.3
212.0	180.0	195.3	98.9	0.7
180.0	150.0	164.3	96.7	2.2
150.0	125.0	136.9	91.9	4.8
125.0	106.0	115.1	83.0	8.9
106.0	90.00	97.67	59.3	23.7
90.00	75.00	82.16	30.8	28.5
75.00	63.00	68.74	0.0	30.8

Mass Frequency vs Diameter



Summary Report

Full scale pump speed: 3  
Bubble detection: Medium  
Starting Size: 63.00 µm  
Ending Size: 0.50 µm

Stir time: 30 secs  
Stir speed: Low  
Probe time: 30 secs

Sample: TT-55-08 148 cm  
 Operator: Clint Edrington  
 Submitter: Clint Edrington  
 File Name: C:\EDRING~1\TIGER&~1\SANDFR~1\TT-55-08\55\_148CM.SMP  
 Material/Liquid: silicate mud/water/Water

Reported: 01/04/10 20:51:00  
 Liquid Visc: 0.7225 cp

Sample Density: 2.650 g/cm<sup>3</sup>  
 Liquid Density: 0.9941 g/cm<sup>3</sup>

## Summary Report

Parameter 1	0.000	Parameter 2	0.000	Parameter 3	0.000		
Mass Distribution Arithmetic Statistics							
Mean	90.50	Std. Dev.		24.99			
Median	84.72	Coef. Var.		0.276			
Mode	68.74	Skewness		2.189			
		Kurtosis		7.520			
Selected Percentiles			Selected Sizes				
Percent Finer	Diameter (µm)		Diameter (µm)	Percent Finer			
100.0	714.1		500.0	100.0			
80.0	103.5		250.0	99.9			
60.0	90.41		125.0	91.9			
40.0	79.43		88.00	55.8			
20.0	70.36		63.00	0.0			
Peak Number	% of Dist.*	Mean	Mode	Median	Standard Deviation	Skewness	Kurtosis
1	100.0	90.50	68.74	84.72	24.99	2.189	7.520

\* Peaks must comprise at least 5.00 % of the distribution.



Micromeritics

WIN5100 V2.03

Page 1

Sample: TT-55-08 200 cm  
Operator: Clint Edrington  
Submitter: Clint Edrington  
File Name: C:\EDRING~1\TIGER&~1\SANDFR~1\TT-55-08\55\_200CM.SMP  
Material/Liquid: silicate mud/water/Water

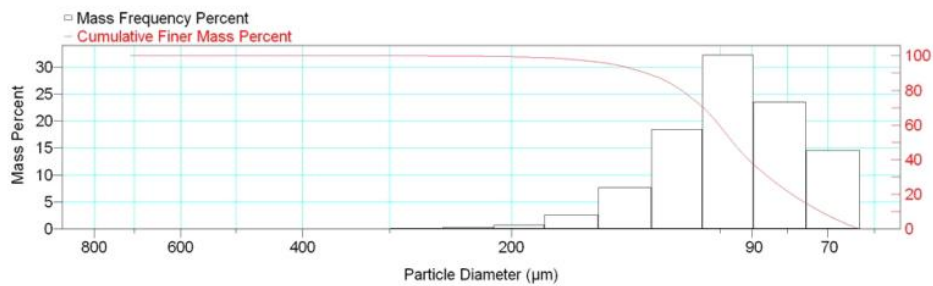
Reported: 01/04/10 20:53:42  
Liquid Visc: 0.7225 cp

Sample Density: 2.650 g/cm<sup>3</sup>  
Liquid Density: 0.9941 g/cm<sup>3</sup>

Report by Size Class

High Diameter (μm)	Low Diameter (μm)	Average Diameter (μm)	Cumulative Mass Finer (Percent)	Mass Frequency (Percent)
850.0	710.0	776.9	100.0	0.0
710.0	600.0	652.7	100.0	0.0
600.0	500.0	547.7	100.0	0.0
500.0	425.0	461.0	100.0	0.0
425.0	355.0	388.4	100.0	0.0
355.0	300.0	326.3	100.0	0.0
300.0	250.0	273.9	99.9	0.1
250.0	212.0	230.2	99.6	0.3
212.0	180.0	195.3	98.9	0.7
180.0	150.0	164.3	96.3	2.6
150.0	125.0	136.9	88.6	7.7
125.0	106.0	115.1	70.2	18.4
106.0	90.00	97.67	38.0	32.2
90.00	75.00	82.16	14.5	23.5
75.00	63.00	68.74	0.0	14.5

Mass Frequency vs Diameter



Summary Report

Full scale pump speed: 3  
Bubble detection: Medium  
Starting Size: 63.00 μm  
Ending Size: 0.50 μm

Stir time: 30 secs  
Stir speed: Low  
Probe time: 30 secs

Sample: TT-55-08 200 cm  
 Operator: Clint Edrington  
 Submitter: Clint Edrington  
 File Name: C:\EDRING~1\TIGER&~1\SANDFR~1\TT-55-08\55\_200CM.SMP  
 Material/Liquid: silicate mud/water/Water

Reported: 01/04/10 20:53:42  
 Liquid Visc: 0.7225 cp

Sample Density: 2.650 g/cm<sup>3</sup>  
 Liquid Density: 0.9941 g/cm<sup>3</sup>

## Summary Report

Parameter 1	0.000	Parameter 2	0.000	Parameter 3	0.000		
Mass Distribution Arithmetic Statistics							
Mean	99.05	Std. Dev.		24.83			
Median	95.86	Coef. Var.		0.251			
Mode	97.67	Skewness		1.656			
		Kurtosis		5.435			
Selected Percentiles			Selected Sizes				
Percent Finer	Diameter (µm)		Diameter (µm)	Percent Finer			
100.0	714.1		500.0	100.0			
80.0	113.8		250.0	99.9			
60.0	100.4		125.0	88.6			
40.0	91.12		88.00	34.6			
20.0	78.85		63.00	0.0			
Peak Number	% of Dist.*	Mean	Mode	Median	Standard Deviation	Skewness	Kurtosis
1	100.0	99.05	97.67	95.86	24.83	1.656	5.435

\* Peaks must comprise at least 5.00 % of the distribution.

Micromeritics

WIN5100 V2.03

Page 1

Sample: TT-55-08 322 cm  
Operator: Clint Edrington  
Submitter: Clint Edrington  
File Name: C:\EDRING~1\TIGER&~1\SANDFR~1\TT-55-08\55\_322CM.SMP  
Material/Liquid: silicate mud/water/Water

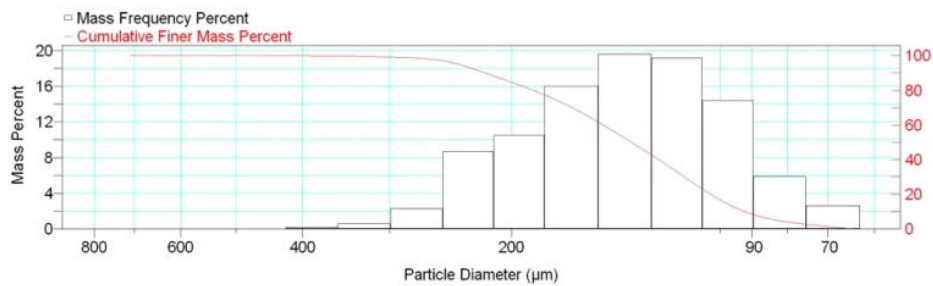
Reported: 01/04/10 20:56:08  
Liquid Visc: 0.7225 cp

Sample Density: 2.650 g/cm<sup>3</sup>  
Liquid Density: 0.9941 g/cm<sup>3</sup>

Report by Size Class

High Diameter (μm)	Low Diameter (μm)	Average Diameter (μm)	Cumulative Mass Finer (Percent)	Mass Frequency (Percent)
850.0	710.0	776.9	100.0	0.0
710.0	600.0	652.7	100.0	0.0
600.0	500.0	547.7	100.0	0.0
500.0	425.0	461.0	100.0	0.0
425.0	355.0	388.4	99.8	0.2
355.0	300.0	326.3	99.2	0.6
300.0	250.0	273.9	96.9	2.3
250.0	212.0	230.2	88.2	8.7
212.0	180.0	195.3	77.7	10.5
180.0	150.0	164.3	61.7	16.0
150.0	125.0	136.9	42.1	19.6
125.0	106.0	115.1	22.9	19.2
106.0	90.00	97.67	8.5	14.4
90.00	75.00	82.16	2.6	5.9
75.00	63.00	68.74	0.0	2.6

Mass Frequency vs Diameter



Summary Report

Full scale pump speed: 3  
Bubble detection: Medium  
Starting Size: 63.00 μm  
Ending Size: 0.50 μm

Stir time: 30 secs  
Stir speed: Low  
Probe time: 30 secs

Sample: TT-55-08 322 cm  
 Operator: Clint Edrington  
 Submitter: Clint Edrington  
 File Name: C:\EDRING~1\TIGER&~1\SANDFR~1\TT-55-08\55\_322CM.SMP  
 Material/Liquid: silicate mud/water/Water

Reported: 01/04/10 20:56:08  
 Liquid Visc: 0.7225 cp

Sample Density: 2.650 g/cm<sup>3</sup>  
 Liquid Density: 0.9941 g/cm<sup>3</sup>

## Summary Report

Parameter 1	0.000	Parameter 2	0.000	Parameter 3	0.000		
Mass Distribution Arithmetic Statistics							
Mean	145.5	Std. Dev.	50.46				
Median	134.3	Coef. Var.	0.347				
Mode	136.9	Skewness	1.025				
		Kurtosis	1.249				
Selected Percentiles			Selected Sizes				
Percent Finer	Diameter (µm)		Diameter (µm)	Percent Finer			
100.0	850.0		500.0	100.0			
80.0	186.0		250.0	96.9			
60.0	147.5		125.0	42.1			
40.0	122.7		88.00	7.4			
20.0	103.2		63.00	0.0			
Peak Number	% of Dist.*	Mean	Mode	Median	Standard Deviation	Skewness	Kurtosis
1	100.0	145.5	136.9	134.3	50.46	1.025	1.249

\* Peaks must comprise at least 5.00 % of the distribution.

## **VITA**

Clint Edrington was born and raised on the Mississippi Gulf Coast, where he attended grade school and graduated from Saint Stanislaus High School. After earning his Bachelor of Science in geophysics from the University of New Orleans, Clint traveled upriver to Louisiana State University where he earned a Master of Science in geology. Clint then moved one building over to pursue a PhD in geological oceanography, focusing on the depositional history of the early Mississippi Delta. Clint will graduate in May, 2013. He now lives in Houston, Texas, working for Fugro GeoConsulting.